MendelNet

Conference Brno 2020

Editors:

Radim Cerkal

Natálie Březinová Belcredi

Lenka Prokešová

Proceedings of 27th International PhD Students Conference

11 November 2020, Brno, Czech Republic

Mendel University in Brno
Faculty of AgriSciences

MendelNet 2020

Proceedings of 27th International PhD Students Conference
11 November 2020, Brno, Czech Republic

Editors: Radim Cerkal, Natálie Březinová Belcredi, Lenka Prokešová

The MendelNet 2020 conference would not have been possible without the generous support of The Special Fund for a Specific University Research according to the Act on the Support of Research, Experimental Development and Innovations and the **support of**:

BIOMIN Czech s.r.o.

kontroluje.me

PELERO CZ o.s.

Profi Press s.r.o.

Research Institute of Brewing and Malting, Plc.

All contributions of the present volume were peer-reviewed by two independent reviewers. Acceptance was granted when both reviewers' recommendations were positive.

ISBN 978-80-7509-765-1

Scientific Committee:

Assoc. Prof. Ing. Radim Cerkal, Ph.D. (Chair)
Prof. Ing. Radovan Pokorný, Ph.D.
Prof. Ing. Gustav Chládek, CSc.
Assoc. Prof. Ing. Radovan Kopp, Ph.D.
Assoc. Prof. Ing. Josef Suchomel, Ph.D.
Prof. Dr. Ing. Milada Šťastná
Assoc. Prof. Ing. Šárka Nedomová, Ph.D.
Assoc. Prof. Ing. Pavel Hanáček, Ph.D.
Prof. MVDr. Zbyšek Sládek, Ph.D.
Assoc. Prof. Ing. Vojtěch Kumbár, Ph.D.
Assoc. Prof. Mgr. Markéta Vaculovičová, Ph.D.
Assoc. Prof. RNDr. Ondřej Zítka, Ph.D.

Organizing Committee:

Ing. Natálie Březinová Belcredi, Ph.D. (Chair)
Assoc. Prof. Ing. Hana Středová, Ph.D.
Ing. Lucie Melišová, Ph.D.
Ing. Lenka Prokešová
Mgr. Patrik Vacek

PREFACE

Each year, the editors of the volume you are about to read are tasked with the responsibility of putting a coherent form to the proceedings from MendelNet, the international PhD Students Conference of the Faculty of AgriSciences of Mendel University in Brno.

The event which reached, this year, on November 11, 2020, its 27th edition, is traditionally aimed at both under and postgraduate students from the Czech Republic, Europe and beyond, and proudly welcomes the participants of various professional and cultural backgrounds. And while this time the people could not gather on-site due to globally-imposed COVID-19 restrictions, the conference swiftly transformed itself into a virtual and fascinating beehive of results, opinions and brand new research paths and ideas.

Here in Brno, under the spell of great genetician J. G. Mendel and the guidance of skilled senior researchers and supervisors, students can introduce, defend and discuss their scientific results while those who do not feel confident enough to present and pen their paper in English are invited to join as spectators and follow-up discussion participants.

The best submissions are, after rigorous peer-review process, collected here and range from plant and animal production to fisheries and hydrobiology to wildlife research while agroecology and rural development, food technology, plant and animal biology, techniques and technology and applied chemistry and biochemistry also belong to the core areas being investigated.

The collection as varied and huge as this can succeed only as a team effort, both on authors' and editors' side, so we would like to express our thanks and gratitude to all committees and reviewers both for their outstanding work and invaluable comments and advice. The final volume is, as always, sent to Clarivate Analytics to be considered for an inclusion in Conference Proceedings Citation Index.

The Editors

TABLE OF CONTENTS

PLANT PRODUCTION

Effect of humic substances on yield and grain quality of spring barley
DUFKOVA R., KOURILOVA V., HRIVNA L., MACO R., SNUPIKOVA N. 15

Responses of winter wheat (*Triticum aestivum* L.) to drought
FRANTOVA N., SMUTNA P., HOLKOVA L., ELZNER P., RABEK M. 21

Estimation of crop nutritional status by UAV survey for site specific crop management
HORNIACEK I., LUKAS V., NEUDERT L., DUFFKOVA R., SMUTNY V. 26

Invasive plant species in the vegetation of landfills
HURAJOVA E., CERNY M., VYKYDALOVA L., WINKLER J. 32

Polyphenols content and seed vigor interaction in spring barley (*Hordeum vulgare* L.)
JOVANOVIC I., ALBA MEJIA J.E., STREDA T. 38

Assessment of spatial heterogeneity of winter wheat canopy stand by Sentinel-2 satellite imagery
MEZERA J., LUKAS V., ELBL J., NEUDERT L., SMUTNY V. 44

The influence of pyrethroid cypermethrin on non-target species *Harmonia axyridis* ladybird
NECASOVA A., PRAZANOVA Z., HRUDOVA E., SEIDENGLANZ M. 50

Influence of the addition of vermicompost and earthworms to the soil on the yield and quality of radish phytomass
NEUPAUER J., KOVACIK P. 55

The influence of age of pheromone lures on *Grapholita funebrana* on their efficiency
PRAZANOVA Z., NECASOVA A., SEFROVA H. 59

The interactive effects of elevated CO_2 concentration, nitrogen nutrition and timing of drought stress on wheat grain yield and quality in two genotypes with contrasting length of vegetation
SIMOR J., KLEM K. 64

The effect of soil application of superabsorbent polymers saturated with nutrients on selected growth parameters of maize in drought conditions
SKOLNIKOVA M., SKARPA P., KLOFAC D., ANTOSOVKY J., MIKUSOVA D. 68

Effect of different irrigation rations on fruit yield and annual increments of "Gala" apple
VASTIK L., MASAN V., BURG P., HIC P. 74

ANIMAL PRODUCTION

Total haemolymph protein and hypopharyngeal glands in the honeybee
BABICA O., MUSILA J., FUZIK T., PLEVKA P., PRIDAL A. 81

Analysis of weight, size, bone strength and blood biochemical parameters depending on dietary intake of organic and inorganic selenium in layers diet
BAHOLET D., NOVOTNY J., ROZTOCILOVA A., ONDRUSIKOVA S., NEDOMOVA S., MRKVICOVA E., PAVLATA L., STASTNIK O. 86

Analysis of the performance of the best dressage and show jumping horses in the world
BRUDNAKOVA M., SOBOTKOVA E. 91

Occurrence of *Helicobacter pylori* in bulk milk samples of raw cow's milk in Moravia
GRONDELOVA A., STASTKOVA Z., NAVRATILOVA P., BEDNAROVA I., FURMANCIKOVA P., NECASOVA D. 97

The use of hemp herb in diet for growing rabbits
HORAKOVA L., STASTNIK O., PAVLATA L., MRKVICOVA E. 102

Evaluation of vital activities in relation to selected parameters of meat performance at Czech Fleckvieh Simmental fattening bulls
JENIK D., FALTA D., KOPEC T., CHLADEK G. 107

Fermented rapeseed meal as a feed additive and its effect on the performance of broiler chickens – a pilot study
KONKOL D., SZMIGIEL I., LUKASZEWICZ M., KRASOWSKA A., KORCZYNSKI M. 111

Evaluating and comparing descendants of stallions from the Dark Ronald line in Czech Warmblood breeding according to basic body measurements
KUBIKOVA Z., JISKROVA I., KUBISTOVA B. 116

Utilization of Duroc boars in production of piglets
LUJKA J., NEVRKLA P., HADAS Z. 122

Total haemolymph protein in honeybee workers as a marker for the evaluation of colony condition?
MUSILA J., BABICA O., LACKOVA Z., PROUZA J., FUZIK T., ZITKA O., PLEVKA P., PRIDAL A. 127

The influence of different sources of selenium on blood glutathione peroxidase activity in laying hens
NOVOTNY J., ROZTOCILOVA A., STASTNIK O., BAHOLET D., MRKVICOVA E., PAVLATA L. 133

The influence of different feed particle size on the performance parameters of laying hens
NOVOTNY J., ROZTOCILOVA A., STASTNIK O., UMLASKOVA B., MRKVICOVA E., PAVLATA L. 137

Evaluation of pregnancy rate and length of pregnancy after artificial insemination in Zwartbles sheep
PESAN V., HOSEK M., FILIPCIK R. 142

The influence of parent stock age on embryonic development of broiler chicken at oviposition
PESANOVA TESAROVA M., LICHOVNIKOVA M. 147

Survival rate in the honeybee workers (*Apis mellifera* L.) additively fed with polypore mycelial extract
PROUZA J., MUSILA J., LONDYNOVA M., PLEVKA P., PRIDAL A. 151

Acaricidal activity of active substances of essential oils against poultry red mites (*Dermanyssus gallinae*)
RADSETOULALOVA I., LICHOVNIKOVA M. 155

Nutritional evaluation of selected varieties of sorghum
RIHACEK M., PAVLATA L., DOLEZAL P., STASTNIK O., MRKVICOVA E., RABEK M., SMUTNY V. 159

The effect of organic and inorganic selenium supplementation on egg production and egg quality of laying hens
ROZTOCILOVA A., NOVOTNY J., MRKVICOVA E., PAVLATA L., STASTNIK O. 165

Effect of different calcium content in feed mixture on eggs quality and blood biochemical parametrs of laying hens
ROZTOCILOVA A., NOVOTNY J., STASTNIK O., PAVLATA L., MRKVICOVA E. 170

The influence of pigs housing system on back fat thickness
SKLENAR J., SLADEK L., VECERA M., CHLADEK G. 175

Effect of incubation temperature on hatching characteristics and post-hatch performance in broiler chickens
SKOUPA M., OPAVSKA T., LICHOVNIKOVA M., FOLTYN M. 178

Effect of different particle sizes in layer diets on feed consumption, live weight and digestive viscosity
ZALESAKOVA D., NOVOTNY J., ROZTOCILOVA A., KUMBAR V., MRKVICOVA E., PAVLATA L., STASTNIK O. 183

FISHERIES AND HYDROBIOLOGY

The effects of microplastic on haematological and biochemical parameters in fish
HOLLEROVA A., HODKOVICOVA N., FALDYNA M., BLAHOVA J. 190

Effects of diclofenac and ibuprofen on fish embryos
MEDKOVA D., SEHONOVA P., BLAHOVA J., POSTULKOVA E., SVOBODOVA Z., MARES J. 195

WILDLIFE RESEARCH

Interesting findings of beetles (Coleoptera) from Cerová vrchovina Upland in Slovakia
BALAZS A., KOPECKY T., BEZDEK J. 200

Habitat preferences of Eurasian Skylark (*Alauda arvensis*)
DVORAKOVA D., SIPOS J., SUCHOMEL J. 205

Importance of active conservation management for spider communities in National Nature Monument Kukle
HULEJOVA P., SIPOS J., KOSULIC O. 211

Diversity of bees (Apoidea) and their pesticide contamination in two different types of agricultural management
HYBL M., MRAZ P., SIPOS J. 216

Influence of agroecosystems on the occurrence of common starling (*Sturnus vulgaris*) in the South Moravian Region
SKOPALOVA G., SIPOS J., SUCHOMEL J. 222

AGROECOLOGY AND RURAL DEVELOPMENT

Used palm oil as material in the soap production
ANTONIC B., TESIKOVA K., JANCIKOVA S., DORDEVIC D., TREMLOVA B. 227

Evaluation of spatio-temporal distribution of erosion control effectiveness of winter wheat using phenological and rain gauge stations network
BRYCHTA J., PODHRAZSKA J., HAJKOVA L. 232

Effect of different soil-processing operations in the inter-row of vineyards on soil washdown
CIZKOVA A., VAIDOVA M., ZATLOUKAL P., BURG P. 237

Identification of vegetation barriers to model their influence on the effects of wind erosion in the Czech Republic
KUCERA J., PODHRAZSKA J. 243

Influence of windbreak on the surrounding environment
KUCERA J., PODHRAZSKA J., STREDA T., SZTURC J. 249

Effect of soil amendments on fire affected soil – a pilot scale pot experiment
MARTINEZ BARROSO P., VAVERKOVA M.D. 255

Current occurrence of endangered *Pedicularis palustris* L. in the Bohemian-Moravian Highlands and its relation to well-performed management
OULEHLA J., JIROUSEK M. 261

How can the weight of *Sinapis alba* L. biomass be affected by adding biochar to the soil irrigated with leachates?
SOURKOVA M., ADAMCOVA D., VAVERKOVA M.D., ZLOCH J. 266

Analysis of tourist's satisfaction with cultural tourism: Case study South Moravia
TUZOVA K., STASTNA M. 271

Reconstruction of historic land-use using historical property records – study site of the Jakubovice cadastral area
ULRICH O., OPPELTOVA P. 277

Effect of biochar doses on soil pH and organic matter
ZACHOVALOVA M., JANDAK J. 283

FOOD TECHNOLOGY

Characteristics of sorption isotherms for fermented meat products
BAUER J., RICHTR P., BENO F., KORANDOVA R., POHUNEK V. 290

The effect of the malt used on the viscosity of the wort
BLSAKOVA L., GREGOR T., KUMBAR V. 296

Influence of feed fortification with selenium on rheological parameters of liquid egg products
DOSTALOVA M., KUMBAR V., ONDRUSIKOVA S., STASTNIK O., NEDOMOVA S. 301

The temperature influence on the rheological behaviour of chocolate
DUFKOVA R., KOURILOVA V., HRIVNA L., KUMBAR V. 307

Microbiological quality of sushi from restaurants
FURMANCIKOVA P., HULANKOVA R. 313

Effects of flavouring methods on the colour of olive oil
KACALOVA T., JAROSOVA A., BRETTFELDOVA T. 318

The effect of the cocoa solids content on the rheological behaviour of chocolate
KOURILOVA V., DUFKOVA R., HRIVNA L., KUMBAR V. 324

Effect of milk chocolate production technology and storage conditions on its stability
KOURILOVA V., DUFKOVA R., HRIVNA L., NEDOMOVA S. 330

The effect of the homogenization process on the viscoelastic properties of processed cheese sauce with furcellaran addition
KUROVA V., SALEK R.N., SVAJDOVA N., GAL R., BUNKA F. 335

Preparation of gelatine from poultry bones residue
MARTINEK J., GAL R., MOKREJS P., PAVLACKOVA J. 341

Influence of extraction time and temperature on the yield, gel strength and viscosity of chicken skin gelatine
MRAZEK P., GAL R., MOKREJS P., ORSAVOVA J., JANACOVA D. 347

Sensory evaluation of hen's eggs with the addition of organic and inorganic selenium to the diet of laying hens
ONDRUSIKOVA S., NEDOMOVA S., STASTNIK O., PAVLATA L., MRKVICOVA E. 353

Relationship between pH values and electrical conductivity, their usability in chicken breast meat evaluation as marker post mortal quality
OVCHYNNIKOVA O., GROSSOVA L., SNUPIKOVA N., STASTNIK O., JUZL M. 359

Potential use of cod liver oil in a pig diet: effects on the chemical, physical and sensory parameters of a bologna sausage
PIECHOWICZOVA M., KOMPRDA T., MATEJOVICOVA M., JUZL M., NEDOMOVA S., POPELKOVA V., VYMAZALOVA P., ONDRUSIKOVA S. 365

The use of chicken collagen hydrolyzate as a functional polymer in cosmetics
POLASTIKOVA A., PAVLACKOVA J., GAL R., MOKREJS P., ORSAVOVA J. 371

The nature of virgin fruit seed oils and their oxidative stability after three months of storage
SINKOVA A., MASAN V., VASTIK L., BUKOVSKA P. 377

PLANT BIOLOGY

Plant species suitable for landfills recultivation
CERNY M., HURAJOVA E., KADLCEK L., WINKLER J. 384

Genetic analysis of selected genes active in chickpea seed dormancy and germination testing
SEDLAKOVA V., HANACEK P., GRULICHOVA M., SMYKAL P. 390

Growth, morphological and biochemical response of *Pisum sativum* roots to non-steroidal anti-inflammatory drug naproxen
SVOBODNIKOVA L., KUMMEROVA M., ZEZULKA S., BABULA P., SENDECKA K. 396

ANIMAL BIOLOGY

Pathogens of bee brood present in the diet do not influence the immunity of nurse bees (*Apis mellifera*)
DOSTALKOVA S., DANIHLIK J., PETRIVALSKY M. 403

Optimization of mitochondrial DNA testing for biodiversity studies in invertebrates
MIFKOVA T., WIJACKI J., BULAWA T., URBAN T. 409

Effect of the digestive process of the Greater wax moth (*Galleria mellonella*) on the causative agents of American Foulbrood (*Paenibacillus larvae*)
MRAZ P., HYBL M., KOPECKY M., SIPOS J., RYBA S., CURN V. 413

Survivability of sperm in insemination doses of Warmblood stallions using different types of extender
SOUSKOVA K., FILIPCIK R., MAMICA O., HAVLICKOVA T. 419

Study of selected signaling pathways genes that play an important role in bone metabolism in laying hens
STEINEROVA M., HORECKY C., KNOLL A., NEDOMOVA S., PAVLIK A. 424

Bull sperm capacitation treatment and oocyte-sperm co-culture system affect *in vitro* bovine embryo development
TRAVNICKOVA I., HULINSKA P., SLADEK Z., MACHATKOVA M. 430

The use of molecular-genetic methods and bioinformatics tools to identify the representatives of the order Coleoptera occurring on decaying cadavers
WRZECIONKOVA N.E., WIJACKI J., KNOLL A., MIFKOVA T. 435

Novel method for morphometry analysis of bursa of Fabricius
ZMRHAL V., SKOUPA M., SVORADOVA A., SLAMA P., LICHOVNIKOVA M. 439

TECHNIQUES AND TECHNOLOGY

Influence of DMLS method topology on mechanical properties of alloy AlSi10Mg
DVORAKOVA J., DVORAK K., CERNY M. 445

Properties of the ecological energy carrier in the tractor's transmission–hydraulic system during the simulation of the operating load in laboratory conditions
JANOUSKOVA R., MICHALIDES M., KOZUCH P., FERIANCOVA P. 451

Time series analysis of three-point hitch control by ploughing
KUCIN M., FAJMAN M. 457

Design of laboratory test hydraulic equipment for testing hydrostatic transducers and hydraulic fluids
NOSIAN J., JANOUSKOVA R., MICHALIDES M., KOZUCH P. 462

Development of a new device for fire prevention in waste management facilities
ROUS R., HENEK DLABOLOVA D., CHOVANEC J., ONDRACKA T. 468

Influence of phase structures on cutting surface quality and cutting tool degradation
SMAK R., VOTAVA J., POLCAR A. 474

Determination of the Young's modulus of samples made from waste materials
SMUTNY L., SOTNAR M., AL-SHANTIR O., MARECEK J. 480

Mathematical models for temperature dependent viscosity of biobutanol and gasoline blends
TROST D., POLCAR A., DOSTAL P., JELINEK J., CUPERA J., KUMBAR V. 486

Evaluation of energy potential in compost with proportion of grape marc
ZATLOUKAL P., CIZKOVA A., ZEMANEK P., MASAN V. 492

Drawbar pull increase of off-road car with special driving wheels
ZUBCAK T., KOLLAROVA K., MATEJKOVA E. 498

APPLIED CHEMISTRY AND BIOCHEMISTRY

Workflow for targeted and semi-targeted quantitation of polar metabolites in *Solanum tuberosum* leaf via a high-resolution orbitrap GC-MS and Skyline, a freely-available open-source tool
BERKA M., MENSIKOVA S., GREPLOVA M., BERKOVA V., BRZOBOHATY B., CERNY M. 505

Bacterial growth and biofilm formation on titanium materials with specific surface treatment
FIALOVA T., VRCHOVECKA K., PAVKOVA-GOLDBERGOVA M., DOLEZELIKOVA K., KOSARISTANOVA L., SVEC P., SMERKOVA K. 511

Antimicrobial activity of PLGA nanoparticles
KOSARISTANOVA L., VYMAZALOVA P., POPELKOVA V., KOMPRDA T. 517

Optimization of cryosection thickness of *Danio rerio* for MALDI-MSI
KOUDELKOVA Z., DO T., GURAN R., PRIBORSKY J., POSTULKOVA E., RADOJCIC M., KOPP R., MARES J., ZITKA O. 522

Monitoring the disassembly process of human ferritins as tools for cancer nanotherapy
KRATOCHVIL Z., TAKACSOVA P., CHAROUSOVA M. 527

Optimization of assay for total protein in the haemolymph of the honeybee (*Apis mellifera* L.)
MUSILA J., LACKOVA Z., VLADEK A., PRIDAL A., ZITKA O. 530

Construction of experimental device suitable for the separation of heavy metals from wastewater
ONDRACKA T., KOUKALOVA L., KULOVANA E., KOUTNY T., KOIS J., POSPICHAL J., JOHN J. 536

Behaviour of pesticides during the denitrification process
PANIKOVA K., BILKOVA Z., MALA J. 542

Identification of volatile compounds associated with sepsis progression by mass spectrometry
PAVELICOVA K., ZEMANKOVA K., VANICKOVA L.P., VACULOVICOVA M. 548

Optimization of Metafectene-mediated transfection of metallothionein down-regulating siRNA in triple-negative breast cancer cells
PETRLAK F., SUBRTOVA H., SMIDOVA V. 553

Synthesis of poly(lactic-co-glycolic) acid nanoparticles with incorporated fish oil
POPELKOVA V., VYMAZALOVA P., KOMPRDA T., SABLIOV C., ASTETE C.E. 557

Tyrosine kinase inhibitors differentially deregulate expression of metallothionein sub/isoforms in triple-negative breast cancer cells
SMIDOVA V., PETRLAK F., SUBRTOVA H. 562

Comparative analysis of metallothionein expression profile in hepatocellular carcinoma cell lines
SUBRTOVA H., SPLICHAL Z., SMIDOVA V., PETRLAK F. 567

Palladium-loaded PLGA-chitosan NPs as efficient catalysts for bioorthogonal chemistry
TAKACSOVA P., PEKARIK V. 572

Development of electrochemical biosensor for direct histamine detection by using selective peptides as biorecognition element
VANOVA V., MILOSAVLJEVIC V., HYNEK D., RICHTERA L., ADAM V. 578

Molecularly imprinted polymers as a recognition element for pesticide detection
VODOVA M., NEJDL L., BEZDEKOVA J., PAVELICOVA K., ZEMANKOVA K., ASSI N., SEDLACKOVA E., LUKLOVA M., VACULOVICOVA M. 584

Synthesis of PLGA nanoparticles with entrapped antibiotic mupirocin
VYMAZALOVA P., POPELKOVA V., KOMPRDA T., SABLIOV C., ASTETE C.E. 589

In vitro anti-microbial activity of titanium dioxide nanoparticles
YOUNIS A.B., KOSARISTANOVA L., DOLEZELIKOVA K., SMERKOVA K. 594

MALDI MSI of MeLiM melanoma: search for prognostic miomarker in skin cancer
ZEMANKOVA K., PAVELICOVA K., BEZDEKOVA J., VANICKOVA L., VACULOVICOVA M. 599

Optimized assembly of functionalized-neuroblastoma targeting EcLHFRT nanocarriers
ZIVOTSKA H., KAPOLKOVA K. 603

PLANT PRODUCTION

Effect of humic substances on yield and grain quality of spring barley

Renata Dufkova, Veronika Kourilova, Ludek Hrivna, Roman Maco, Nikol Snupikova
Department of Food Technology
Mendel University in Brno
Zemedelska 1, 613 00 Brno
CZECH REPUBLIC

renca.dufkova@seznam.cz

Abstract: The effect of foliar application with humic substances was tested on the malting barley yield and grain quality of the Bojos variety using the Lignohumate MAX product from 2017 to 2019. Lignohumate MAX was applied twice together with two levels of nitrogen nutrition (N_1 – 75 kg/ha N, N_2 – 94 kg/ha N) during the growing season. The grain yield was increased with a positive effect on the quality after the application of humic substances. The proportion of malting usable grain, bulk density, starch content in the grain was increased but the content of nitrogen substances was decreased. The application of the N_1 nitrogen dose in combination with humic substances proved a higher effect in the year with extremely dry weather. The combination of the N_2 nitrogen dose and humic substances showed to be more effective in 2017 and 2019. The highest decrease in nitrogen content was detected in the variant 3 by up to 1.0% using a lower nitrogen dose in 2019. In 2017, the highest increase in starch content was repeatedly detected in the variant 3 using a lower level of nitrogen nutrition. The increase reached up to 2.0% in comparison with the control.

Key Words: malting barley, Lignohumate MAX, foliar nutrition, grain yield, grain quality

INTRODUCTION

The quality and grain yield is influenced by a number of factors in malting barley. The influence of the pre-crop, the incorporation of post-harvest residues, the conditions and sowing date, seed rate or plant nutrition during the vegetation can be included in the most important factors (Richter et al. 2006). Last but not least, the yield and grain quality are significantly affected by weather conditions during the vegetation especially with sufficient moisture. Adverse windy weather conditions are often limiting factors. The more frequent occurrence of dry periods may be critical for grain yield and quality because of an average length of malting barley vegetation from 100 to 120 days (Prugar et al. 2008).

Humic acid may be reduced the amount of viruses transmitted to the soil. Humic acid can also improve soil health, nutrient uptake by plants, mineral availability, crop quality and may reduce the amount of applied fertilizer. Humic acid fertilizers may increase crop yields or stimulate plant enzymes, hormones and can improve soil fertility (Mayhew 2004). Humic and fulvic acids are applied either directly to the soil environment or to vegetation. The foliar nutrition term means a process in which nutrients are applied to the leaf surface by gentle spraying and the plant subsequently receives and uses them. This way can lead to support the plant activity and to supply part of the nutrient requirements. The intake, transport and subsequent use of nutrients are influenced by a number of factors in foliar plant nutrition. The most limiting factors of foliar fertilizer application are weather conditions, especially precipitation leading to rinse the applied fertilizer from the leaf surface. On the contrary, the water can evaporate quickly in a very dry environment and the applied fertilizer dries out (often immediately after the application) and therefore the applied substance cannot affect. Lignohumate MAX is a widely used product to treat plant growth during vegetation. This product is a highly concentrated aqueous solution composed of humic and fulvic acids and their salts. Fulvic acids and their salts predominate in the composition of Lignohumate MAX produced by hydrolytic-oxidative decomposition of technical lignosulfonates (Mráz 2001, Amagro Humic Substances 2008, Vaněk et al. 2007).

MATERIALS AND METHODS

The application of Lignohumate MAX was tested in foliar nutrition of spring barley during three years (from 2017 to 2019). Field small-plot experiments were established on the lands belonging to the Agrospol Velká Bystřice Company. The lands are located in a slightly warm and slightly humid climate region. The soil is medium-heavy and the soil type is brown soil. Table 1 shows the weather conditions during the vegetation of three years.

Barley was grown on the pre-crop of sugar beet and post-harvest residues (sugar beet tops) were plowed by medium plowing in all years of the experiment. Both N-fertilizers and K-fertilizers were applied before the sowing. The LAV 27 fertilizer in the amount up to 200 kg/ha was applied. Respectively, the amounts of 54 kg/ha N and 100 kg/ha potassium salt (up to 60% K_2O) were used (the fertilizers were applied according to the fertilization plan of the agricultural company). The Bojos barley variety was sown at a sowing rate of 3.7 MGS/ha. The additional fertilization with nitrogen was added during the vegetation according to the plan shown in Table 2. The terms of Lignohumate MAX application by spraying on the leaf are also described in the Table 2. Each variant was performed in 4 replicates.

Table 1 The course of weather conditions for 2017, 2018 and 2019, Velká Bystřice

Year	Month	Average temperature [°C]	The norm [°C]	Variation from the norm [°C]	Precipitation [mm]	The norm [mm]	Precipitation [%]
2017	January	-5.7	-2.0	-3.7	19.7	22.0	89.5
	February	1.4	-0.3	1.7	11.5	18.0	63.9
	March	7.3	3.9	3.4	30.8	25.0	123.2
	April	8.8	8.9	-0.1	56.8	33.0	172.1
	May	16.0	14.3	1.7	41.3	61.0	67.7
	June	20.4	17.1	3.3	64.1	70.0	91.6
	July	20.7	18.9	1.8	104.8	71.0	147.6
2018	January	2.1	-2.0	4.1	28.5	22.0	129.5
	February	-2.2	-0.3	-1.9	20.0	18.0	111.1
	March	2.2	3.9	-1.7	44.4	25.0	177.6
	April	15.3	8.9	6.4	17.4	33.0	52.7
	May	19.2	14.3	4.9	20.5	61.0	33.6
	June	20.4	17.1	3.3	44.5	70.0	63.6
	July	21.6	18.9	2.7	27.0	71.0	38.0
2019	January	-1.7	-2.0	0.3	17.0	22.0	77.3
	February	1.7	-0.3	2.0	29.2	18.0	162.2
	March	7.2	3.9	3.3	14.9	25.0	59.6
	April	12.0	8.9	3.1	21.8	33.0	66.1
	May	13.1	14.3	-1.2	77.2	61.0	126.6
	June	22.8	17.1	5.7	88.7	70.0	126.7
	July	21.1	18.9	2.2	79.9	71.0	112.5

Table 2 The experiment scheme for 2017, 2018 and 2019, Velká Bystřice

Variant	The total dose of N [kg/ha]	The term of treatment and the dose of Lignohumate MAX [l/ha]	
		The end of tillering	The end of shooting
1	94	-	-
2	94	0.4	0.4
3	75	0.4	0.4

Standard agrotechnical interventions were performed on all variants of the experiment during the vegetation which meant the application of fungicides and morphoregulators. The harvest was carried

out on August 8, 2017 in the first year of the experiment. In the following year, the harvest was performed on July 28, 2018 and the harvest term was established on August 6, 2019 in the last year of the experiment. A small-plot Wintersteiger combine harvester with automatic weighing and sampling device was used for harvesting. A sample from each replicate (1.2 kg) was taken for further analysis. The yield, grading, bulk density of the grain, weight of a thousand grains were determined for individual grain samples. Furthermore, the content of N-substances and starch was determined (Basařová et al. 1992). The vegetation was not lying flat at the harvest time in all experimental years.

The obtained results were evaluated using MS Excel 2010 and Statistica 12 (multiple factor analysis of variance followed by Tuckey testing).

RESULTS AND DISCUSSION

The harvesting results are presented in Figure 1. In 2017, grain yields were conclusive the highest ($p > 0.95$). The highest yield was determined in variant 2 with the full dose application of nitrogen and Lignohumate MAX. The increase in yield was determined to be about 505 kg/ha compared to the control one (variant 1). In 2018, grain yields were conclusive the lowest ($p > 0.95$) due to the persistent drought (Table 1). The highest yield was found out in variant 3. The lowest yield was detected in the control. The application of Lignohumate MAX product increased the grain yield by about 157–252 kg/ha. The grain yield was not affected by a higher nitrogen dose probably also due to the drought. In 2019, the highest grain yield was established in variant 2. In the same year, the lowest grain yield was determined in variant 3. Although the differences in yields between the individual years were substantial, the application of humic substances proved a favourable effect on grain yield especially by using full nitrogen nutrition. The increase in grain yield after the addition of humic substances was also noted by Wali et al. (2018). Procházka et al. (2018) stated that the application of humic substances proved to be important in stress conditions and contributed to higher production stability. This finding corresponded with our results. This fact was confirmed mainly in the extremely unfavourable precipitation (persistent drought) in 2018.

In 2017, the high-quality harvest was also evidenced by the fact that the values of grading of barley grain over the 2.8 mm ranged above the level of 90% in all variants. The highest values were recorded in variant 3 (Figure 2). However, the decisive factor was the amount of grain over the 2.5 mm that is $\sum_{2.5 + 2.8\ mm}$. This finding proved a very high level from the point of view of malting processing. This fact is also evident from the grading (Figure 4) showed to be very low and ranged from 1.07 to 1.47%.

In 2018, the grain harvest in terms of the quality could be evaluated as a favourable year despite the great drought. The grading of barley grain over the 2.8 mm were detected in a high level and ranged from 79.9 to 83.6% (Figure 2). The high grain quality was also confirmed by the total sum of grading reached up higher than 2.5 mm ($\sum_{2.5 + 2.8\ mm}$). This fact was also confirmed by the low grading not to exceed up to 1.44% (see Figure 4). The yield of grading over the 2.5 mm was found out higher due to the higher yield in both variants with the application of Lignohumate MAX compared to the control.

Figure 1 Grain yield of barley (effect of variant x year) [t/ha]

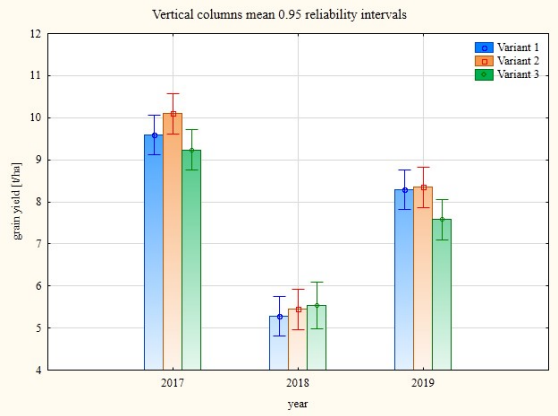

Figure 2 The grading of barley grain x > 2.8 mm (effect of variant x year) [%]

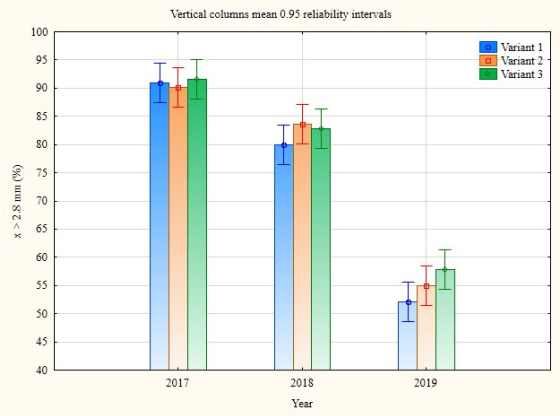

Figure 3 The grading of barley grain 2.5 mm < x < 2.8 mm (effect of variant x year) [%]

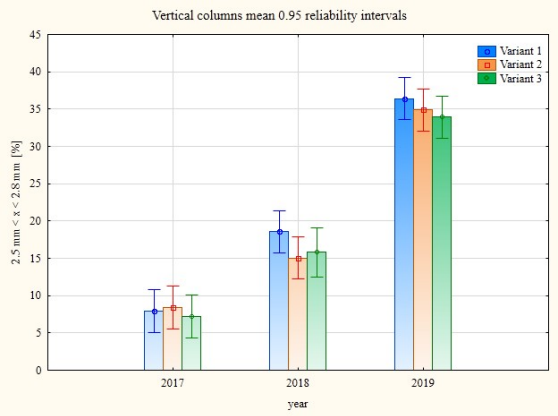

Figure 4 The grading of barley grain x < 2.5 mm (effect of variant x year) [%]

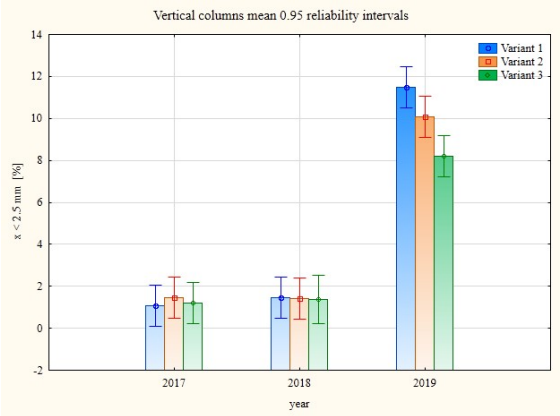

In 2019, the harvest did not reach the same qualities as in previous years and grading was conclusive the worst ($p > 0.95$) and ranged from 8.2 to 11.5%. The grading decreased after the application of Lignohumate MAX (Figure 4). The grading of barley grain over the 2.8 mm ranged from 52.1 to 57.9% and proved to be significantly higher after the application of Lignohumate MAX. In the Czech Republic (crop 2017) the average values of grading over the 2.5 mm were 88.2% (Hartman 2018), in 2018 the average values were 92.1% and in 2019 83.5% (Hartman and Psota 2019, Hartman and Psota 2020).

The balance and fullness of the malting barley grain were characterized by the grading of barley grain over the 2.5 mm. The high proportion of grading over the 2.5 mm affected the malt yield. The basic value should range above 80% (Kosař et al. 2000). All variants performed this requirement in our experiment. The values were supported as a result of the application of Lignohumate MAX.

Thousand grain weight of barley was conclusive marked ($p < 0.95$) by considerable year-on-year variability (Figure 5). In 2017 and 2018, the application of Lignohumate MAX contributed to the higher weight of thousand grain weight. In 2019, the values were balanced. According to Psota and Vejražka (2006), thousand grain weight of barley should be at least in the range of 38–42 g which was confirmed with our results.

The application of Lignohumate MAX proved a positive effect on the bulk density of the grain in all experimental years (Figure 6). Conclusive the highest bulk density of grain was reached in 2017 ($p > 0.95$) because the values achieved above the level of 69 kg/hl. Conclusive the lowest values were recorded in 2019 ($p > 0.95$). Although the bulk density did not reach the requirements of 72–74 kg/hl considered as the optimal values as Psota and Vejražka (2006) reported. Despite these findings, the achieved results can be assessed as satisfactory.

Figure 5 Thousand grain weight of barley (effect of variant x year) [g]

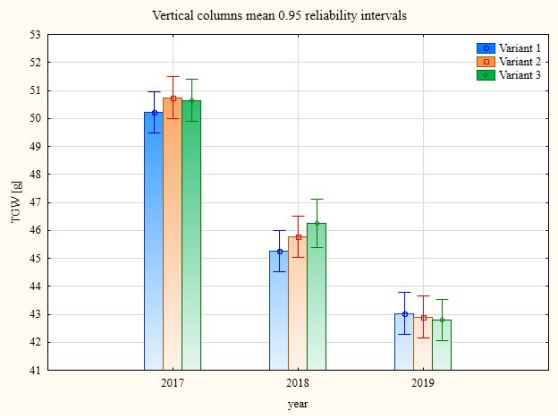

Figure 6 Specific weight of barley (effect of variant x year) [kg/hl]

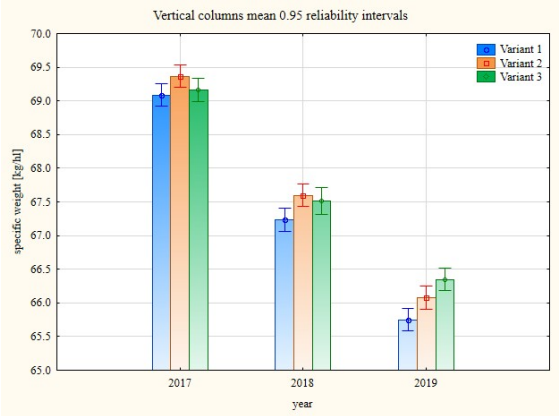

The application of Lignohumate MAX proved a positive effect on the nitrogen content of the grain (Figure 7). In 2017 and 2018, the application of Lignohumate MAX contributed

to the nitrogen content reduction below 12% as this limit is required by malting houses (ČSN 461100-5). According to Hartman (2018), the average nitrogen content in the Czech Republic in 2017 was 12.2%. In 2018 the average nitrogen content was 12.48% and in 2019 11.43% (Hartman and Psota 2019, Hartman and Psota 2020).

In 2018, the starch content reached a lower level and ranged from 61.1 to 62.7%. The effect of drought showed a negative effect. In 2017 and 2019, the starch content was detected at a high level. The application of the tested product contributed to a higher starch content compared to the control (Figure 8). In 2017 the average starch content in the Czech Republic was 62.6% and in 2018 62.2% (Hartman 2018, Hartman and Psota 2019). According to Hartman and Psota (2020), the average starch content in 2019 was 62.56%. The starch content should be in the range of 63–64% in the dry matter for quality barley. The starch content depends not only on the protein content but also on the plant condition and the sunlight length at the end of the vegetation (Kosař et al. 2000).

Figure 7 Content of N-substances in barley grain (effect of variant x year) [%]

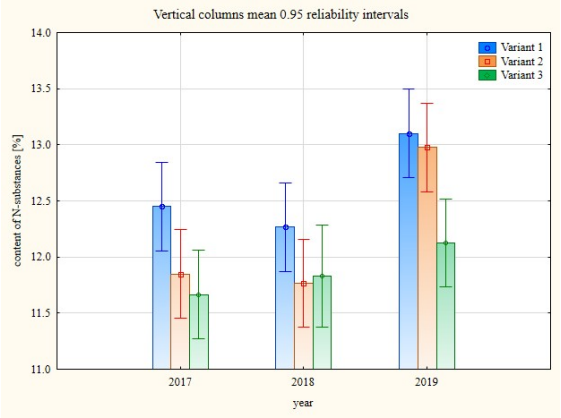

Figure 8 Content of starch in barley grain (effect of variant x year) [%]

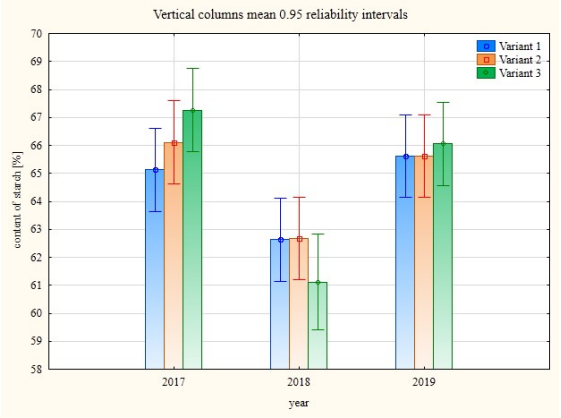

CONCLUSION

A negative course of windy conditions significantly affected the experiment in 2018. A deficit of precipitation confirmed the negative course of weather conditions in the key period that means in the months of April–June. This fact proved a conclusive effect on the grain yield ($p > 0.95$) but the grain quality was not detected so negatively. In 2019, the results again confirmed that the course of weather conditions can play a crucial role in the yield and quality of the production. Although the barley crop was not significantly stressed, sufficient moisture and heat promoted a mineralization and released more nitrogen accumulated in the grain.

The application of Lignohumate MAX showed a positive effect on grain yield and its technological quality. The bulk density of the grain was increased. Thousand grain weight of barley and the content of nitrogenous substances and mostly starch were also favourably affected.

ACKNOWLEDGEMENTS

The research was financially supported by the Internal Grant Agency AF-IGA2020-IP050.

REFERENCES

Amagro Humic Substances. ©2008. Výrobky. [Online]. Available at: https://amagro.com/lignohumat-max.html. [2020-09-02].

Basařová, G. et al. 1992. Pivovarsko-sladařská analytika 1. 1st ed., Praha: Merkanta s.r.o.

Hartman, I. 2018. Quality of malting barley grain in the Czech Republic, crop 2017. Kvasný průmysl [Online], 64(6): 297–301. Available at: https://kvasnyprumysl.cz/pdfs/kpr/2018/06/03.pdf. [2020-10-30].

Hartman, I., Psota, V. 2019. Sladovnický ječmen v roce 2018. In Proceedings of Sladovnický ječmen 2019 [Online]. Libčany, Vsisko, Černá Hora, Czech Republic, 28–30 January, Praha: Česká zemědělská

univerzita v Praze, pp. 5–8. Available at: http://konference.agrobiologie.cz/2019-01-28/03-Hartman-Psota_SLADOVNICKY_JECMEN_V_ROCE_2018.pdf. [2020-10-30].

Hartman, I., Psota, V. 2020. Sladovnický ječmen v roce 2019. In Proceedings of Sladovnický ječmen 2020 [Online]. Černá Hora, Vsisko, Bezno, Perknov, Czech Republic, 20–23 January, Praha: Česká zemědělská univerzita v Praze, pp. 23–26. Available at: http://konference.agrobiologie.cz/2020-01-20/08-Hartman-Psota_SLADOVNICKY_JECMEN_V_ROCE_2019.pdf. [2020-10-30].

Kosař, K. et al. 2000. Technologie výroby sladu a piva. 1st ed., Praha: Výzkumný ústav pivovarský a sladařský.

Mayhew, L. 2004. Humic substances in biological agriculture. Acres U.S.A. [Online], 34(1–2): 80–88. Available at: http://www.jssagri.com/Content/ModuleData/Upload/Resource/Humic-Substances-(Dr-Mayhew).pdf. [2020-08-29].

Mráz, J. 2001. Listová výživa - nedostatečně využívané intenzifikační opatření. Agro, 6(4): 36–67.

Procházka, P. et al. 2018. Use of biologically active substances in hops. Plant, Soil and Environment Journal [Online], 64(12): 626–632. Available at: https://www.agriculturejournals.cz/publicFiles/655_2018-PSE.pdf. [2020-08-20].

Prugar, J. et al. 2008. Kvalita rostlinných produktů na prahu 3. tisíciletí. Praha: Výzkumný ústav pivovarský a sladařský ve spolupráci s Komisí jakosti rostlinných produktů ČAZV.

Psota, V., Vejražka, K. 2006. Fyzikální vlastnosti obilek ječmene a zrn sladu. Kvasný průmysl [Online], 52(5): 148–150. Available at: https://kvasnyprumysl.cz/pdfs/kpr/2006/05/02.pdf. [2020-08-26].

Richter, R. et al. 2006. Výživa a hnojení ječmene jarního. In Ječmen - formy a užitkové směry v ČR. Praha: Profi Press s.r.o., pp. 59–84.

ÚNMZ. 2006. Obiloviny potravinářské – Část 5: Ječmen sladovnický. ČSN 461100-5 (461100). Praha: Úřad pro technickou normalizaci, metrologii a státní zkušebnictví.

Vaněk, V. et al. 2007. Výživa polních a zahradních plodin. Praha: Profi Press s.r.o.

Wali, A.M. et al. 2018. Responses of barley (Hordeum vulgare) Cultivars to humic acid, mineral and biofertilization under calcareous soil conditions. Middle East Journal of Agriculture [Online], 7(1): 71–82. Available at: http://www.curresweb.com/mejar/mejar/2018/71-82.pdf. [2020-08-24].

Responses of winter wheat (*Triticum aestivum* L.) to drought

Nicole Frantova[1], Pavlina Smutna[1], Ludmila Holkova[1], Petr Elzner[1], Michal Rabek[2]
[1]Department of Crop Science, Breeding and Plant Medicine
[2]Department of Agrosystems and Bioclimatology
Mendel University in Brno
Zemedelska 1, 613 00 Brno
CZECH REPUBLIC

nicole.frantova@mendelu.cz

Abstract: Six winter and one facultative wheat varieties were observed at two different localities Obora and drier Písky in Žabčice, South Moravia, during growing season 2019/2020. The effect of drought was observed on ear formation and yield components of chosen varieties. Drought affected the ear formation e.g. number of fertile spikelets per ear, number of fertile florets per ear, number of grains per ear and the yield components such as number of fertile tillers and thousand grain weight. All these traits were generally lower at the plants grown in drier location Písky. The most sensitive varieties to drought with the highest differences between yields of these two localities were Bohemia and Balitus, on the contrary, the least sensitive varieties were IS Conditor and Tybalt. Timing of drought stress led to the reduction of the yield components and the yield itself. The weather played a crucial role and in the year 2020, precipitation came during flowering time which was beneficial for later varieties. The recommendation to sow early varieties on dry locality is not always valid, especially in the conditions of Czech Republic where drought is unpredictable.

Key Words: Triticum aestivum, yield components, yield formation, abiotic stress

INTRODUCTION

Wheat (*Triticum aestivum* L.) is a plant from the *Poaceae* family and belongs to the major and the most valuable cereal. In the climate of central Europe, three forms of wheat can be grown: spring, winter and facultative.

Plants are frequently exposed to various unfavourable conditions that adversely affect their growth and productivity (Cavatte et al. 2012). Extreme growth conditions can hinder normal growth and development, which might be even fatal in extreme cases (Lämke and Bäurle 2017). The major losses in crop plants are caused by abiotic stresses (Jenks and Hasegawa 2005) like drought, flooding, radiation, extremes in temperatures, salinity, etc. The sensitivity of plants to abiotic stress depends on the intensity and duration of stress, other stress factors involved, plant species and developmental stage (Dragičević 2015).

Drought can occur at any time during development of wheat. If water stress occurs at the stage of pre-anthesis, consequently days to anthesis are reduced; when drought occurs at stage of post-anthesis, time to grain-filling is reduced. Post-anthesis drought stress is the most harmful to grain yield due to its impact on grain weight. When drought occurs at flowering stage or later, the number of grains per ear and grain weight can be affected (Sallam et al. 2019). Long-lasting drought limits the number of grains more than grain size (Dolferus et al. 2011).

As Shavrukov et al. (2017) suggest, a shorter vegetative stage and early flowering can play a crucial role for minimizing exposure of plants to drought stress during flowering and grain filling. There is a tendency of growing earlier flowering cultivars in countries with Mediterranean type of climate where drought is regular.

The objective of this experiment was to evaluate the response of selected varieties on limited water availability based on comparison of quantitative changes of ears. Timing of stress was specified by phenological stages of plant development.

MATERIAL AND METHODS

Location

Winter wheat was grown at the Field research station in Žabčice (49°00'50.3"N, 16°36'03.6"E) on two localities Obora and Písky. The average annual precipitation is about 480 mm, the average annual temperature is proximately 9 °C. The two localities vary at the level of groundwater, the level of soil moisture, the soil type and soil texture. The locality Obora is situated close to the station in 179 m.a.s.l. with higher groundwater level and higher clay content, the locality Písky is situated at 218 m.a.s.l. with lower groundwater level and higher content of sandy particle being regularly exposed to drought. The weather conditions were recorded (rain precipitation, temperature above ground, temperature of soil and soil moisture) and based on these observation (data not given), we can assume that drought occurred on the locality Písky from April to May (2020).

Varieties

Six winter wheat varieties with diverse earliness were chosen (from earliest to latest): Bohemia, Balitus, IS Conditor, RGT Sacramento, Tobak, Tonnage, and one facultative variety Tybalt. These varieties were grown in small plots of size 10.3 m^2 in three replications for each locality during growing season 2019/2020.

Plant material assessments

Plant samples were taken for ear analyses in two terms, at the stage of 60–71 Zadoks scale (28th May 2020) for the count of fertile florets on 10 ears per variety and at the stage of 82–87 Zadoks scale (15th June 2020) for the number of fertile spikelets and grains per ear on 30 ears per variety. The number of fertile tillers from 1 m^2 were evaluated prior to harvest. After harvest in July, the yield in t/ha and thousand grain weight were measured.

Statistical Data Analysis

The collected data for the two localities and 7 varieties were processed and analysed using the software Statistica 12.0 (Tibco Software, USA). ANOVA was used for the statistical data analysis, where $p>0.05$ was chosen as the level of statistical significance.

RESULTS AND DISCUSSION

The effect of drought was observed on ear formation and yield components of chosen varieties. The average values of the yield components and yield itself is given in Table 1.

A highly statistical significant difference was found for number of fertile tillers between the drier locality Písky (averagely 606 fertile tillers/m^2) and the less stressful locality Obora (averagely 924 fertile tillers/m^2), lesser number of fertile tillers was also observed in the study made by Destro et al. (2001), where plants had lesser number of fertile tillers from the non-irrigated area. However a highly statistical significant difference was not found in number of tillers among varieties nor interaction between locality and varieties in our study (Table 2).

From the varieties grown in Obora, the highest number of tillers was recorded in Tonnage and Tybalt; from Písky, the highest number was found in Bohemia and Tybalt, the lowest number from drier locality was in Balitus and RGT Sacramento (Table 1). Lesser number of fertile tillers in Písky means that higher number of tillers wilted and died due to drought, death of tillers in water stress condition is one of mechanisms how to save water for the main stem (Blum et al. 1990).

A higher number of fertile spikelets per ear from the locality Obora was observed and statistical differences were found between the localities, varieties and interaction between locality and variety (Table 2). This finding suggests that drought negatively affected the number of fertile spikelets. The average number of fertile florets per ear was higher at Obora than at Písky (54.8 and 52.3) and the number of developed grains per ear responded to this ratio (41.6 and 38.8). However, the genotype dependent differences were observed on both localities (Table 1). The reaction of varieties Balitus, Tobak and Tonnage to drought at Písky locality manifested in development of higher number of fertile florets, but the final number of grains per ear was lower than in other varieties with the exception of RGT Sacramento. The effects of genotype on stress reaction were reported by Dreccer et al. (2014) who suggested that sugar metabolism can affect the number of fertile florets.

Thousand grain weight (TGW) was in average higher at Písky (46 g) than at Obora (42 g). Varieties RGT Sacramento and Tonnage had low TGW at Obora in comparison with Písky locality, which can be related to the highest number of grains per ear and tillers density in Obora (Table 1). With lesser number of tillers, the varieties Balitus, IS Conditor, Tobak and Tonnage developed fewer grains but bigger in size at the locality Písky. Two varieties Bohemia and Tobak had lower TGW number in Písky, which corresponds with the result of Mirbahar et al. (2009), where the wheat plants not irrigated had reduced all traits as shorter spikes, shorter plants, fewer grains per spike, etc. If stress lasts throughout the whole development of wheat, the main yield components will be reduced. However, in the experiment made by Zhiqiang et al. (2011), plants exhibited a stronger compensation ability on yield traits when rewatering came after drought. Our results confirm that, the wheat plants were affected by drought until May in Písky, after that, drought stress stopped in stage of flowering and compensation mechanism was manifested mainly in the size of grain.

As all the main yield components were affected by drought (Figure 1), the yield itself was statistically different between the localities and varieties. The biggest difference between yield from Obora and Písky was recorded in Bohemia and Balitus (about 6 t/ha, 45% and 46%), the smallest difference was observed for varieties IS Conditor and Tybalt (about 4 t/ha, 62% for both). Bohemia and Balitus as the earliest varieties were the most affected by drought stress in Písky, fewer fertile tillers and fewer grains per ear caused reduction in the yield of Balitus, the yield reduction of Bohemia was caused by heterogenity of wheat ears in canopy.

Table 1 Mean numbers for the main yield components and the yield

Variety	Locality	No. of Fertile Tillers (Mean)	Fertile Spikelets per Ear (Mean)	Fertile Florets per Ear (Mean)	Grains per Ear (Mean)	TGW (Mean)	Yield t/ha (Mean)
Bohemia	Obora	802.6 ± 45	16.9 ± 0.4	51.1 ± 9.3	35.9 ± 4.8	45.35 ± 1.80	10.78 ± 0.65
Balitus	Obora	885.3 ± 48	17.3 ± 0.6	46.4 ± 4.5	44.3 ± 1.0	38.66 ± 2.39	11.95 ± 0.41
IS Conditor	Obora	949.3 ± 208	15.4 ± 0.2	58.0 ± 8.2	36.2 ± 0.2	37.84 ± 2.63	9.87 ± 0.93
RGT Sacramento	Obora	872.0 ± 121	15.1 ± 0.5	58.1 ± 7.4	42.1 ± 1.0	36.23 ± 0.55	11.37 ± 0.67
Tobak	Obora	869.3 ± 102	17.4 ± 0.3	51.6 ± 5.1	47.7 ± 3.0	43.25 ± 2.39	10.46 ± 0.44
Tonnage	Obora	1034.6 ± 150	17.9 ± 1.1	58.6 ± 7.7	49.8 ± 4.6	36.98 ± 1.79	10.33 ± 0.32
Tybalt	Obora	1053.3 ± 95	17.1 ± 1.8	59.8 ± 3.1	35.0 ± 10.1	40.70 ± 0.83	9.77 ± 0.85
Bohemia	Písky	654.0 ± 52	15.5 ± 1.0	47.4 ± 8.8	39.6 ± 4.3	45.06 ± 0.96	4.85 ± 0.24
Balitus	Písky	510.0 ± 40	14.1 ± 0.7	61.7 ± 6.3	37.8 ± 2.5	44.89 ± 0.52	5.51 ± 0.22
IS Conditor	Písky	646.0 ± 94	15.6 ± 0.5	44.7 ± 6.2	46.8 ± 2.0	39.89 ± 0.59	6.16 ± 0.20
RGT Sacramento	Písky	550.0 ± 64	13.1 ± 1.3	43.2 ± 5.1	31.6 ± 6.8	43.89 ± 1.38	6.07 ± 0.45
Tobak	Písky	626.0 ± 140	15.1 ± 1.6	51.7 ± 7.4	38.2 ± 11.3	42.05 ± 0.57	6.58 ± 0.35
Tonnage	Písky	576.0 ± 49	14.2 ± 1.1	60.0 ± 10.7	35.7 ± 6.2	44.70 ± 0.85	6.37 ± 0.41
Tybalt	Písky	682.0 ± 221	16.3 ± 1.1	57.1 ± 7.8	41.8 ± 5.9	44.67 ± 0.84	6.06 ± 0.21

Table 2 ANOVA for the main yield components and the yield

	DF	No. of Fertile Tillers (MS)	No of Fertile Tillers (p)	Fertile Spikelets per Ear (MS)	Fertile Spikelets per Eat (p)	Fertile Florets per Ear (MS)	Fertile Florets per Ear (p)
Locality	1	1209856.4	0.000	43.6	0.000	293.3	0.000
Variety	6	25518.8	0.110	4.7	0.002	206.1	0.053
Loc.*Variety	6	17256.3	0.292	3.1	0.025	452.2	0.000
Error	35	13495.8		1.1		53.7	

Legend: DF = Degree of Freedom, MS = Mean Square, Loc = Locality

Table 3 ANOVA for the main yield components and the yield – continue

	DF	Grains per Ear (MS)	Grains per Ear (p)	TGW (MS)	TGW (p)	Yield t/ha (MS)	Yield t/ha (p)
Locality	1	92.0	0.105	83567.3	0.000	265.3	0.000
Variety	6	42.1	0.298	167.3	0.000	1.0	0.002
Loc.*Variety	6	159.7	0.001	29.3	0.000	2.3	0.000
Error	35	33.2		23.1		0.2	

Figure 1 Drought damage percentage of the main yield components and the yield

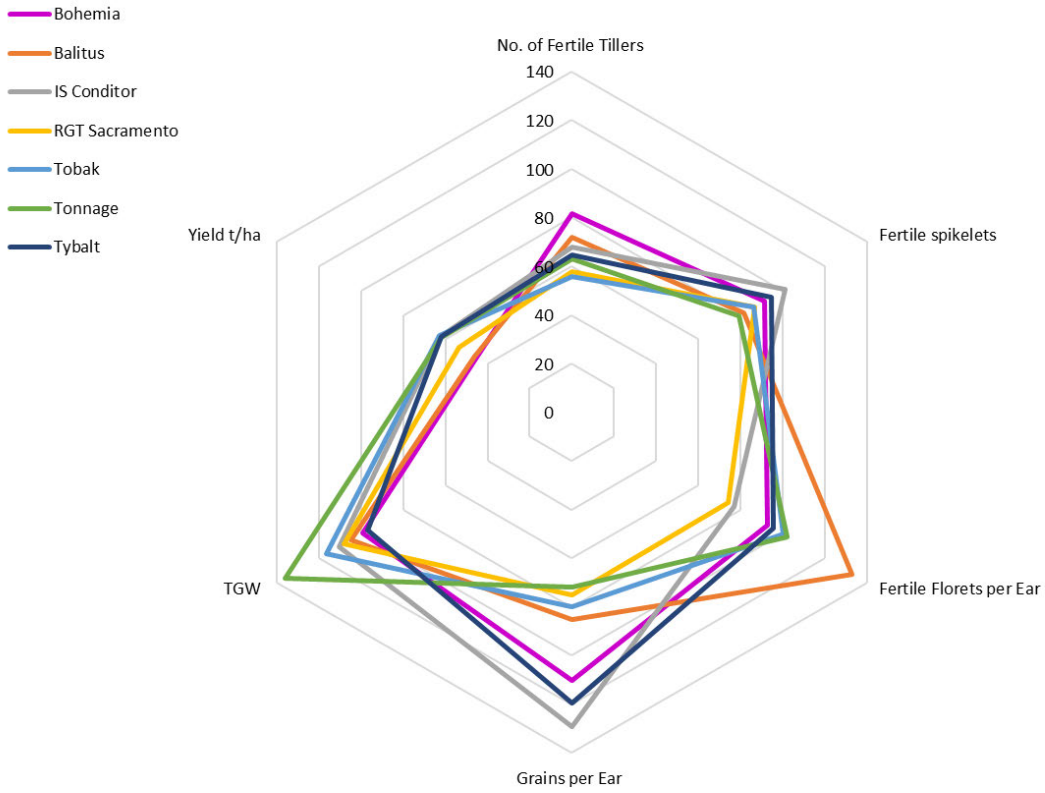

Legend: The values of the parameters measured at the locality Písky are expressed in % in relation to the values of the parameters from the locality Obora.

From Figure 1 it is obvious that the varieties grown in drier locality showed higher variability in analysed traits. It seemed, that varieties have noticeable compensation ability e.g. in Tonnage, Tobak and Conditor these abilities mean developing higher number of grains per ear and bigger grains according to results of TGW. There was not found a connection between number of fertile florets per ear and number of grains per ear. Compensation mechanisms were not the same at the each varieties.

CONCLUSION

Drought-tolerant variety should not reduce yield under drought stress conditions, the chosen varieties grown on two contrasting localities showed differences in yield. The lowest reduction in yield from varieties grown in Písky was in IS Conditor and Tybalt, the highest reduction was in Bohemia and Balitus. The highest yield from Písky locality was recorded in later varieties Tobak and Tonnage with longer vegetation period, this can be explained by the weather conditions and the compensation ability of these varieties to develop bigger grains or more grains per ear. According to our evaluation, drought altered the number of grains, the number of fertile florets, the number of fertile spikelets per ear, thousand grain weight and the number of fertile tillers compared with plants from less stressful locality. The weather played a crucial role too and in the year 2020 precipitation came in the time of flowering which was beneficial for later varieties with slower development in comparison with earlier ones. The recommendation to sow early varieties on similar locality as Písky is not always valid, especially in the conditions of Czech Republic where drought is more unpredictable.

ACKNOWLEDGEMENTS

The research was funded by the project QK1910269 (Adaptation potential of common wheat in response to drought and extreme temperatures) of the National Agency for Agricultural Research (NAZV).

REFERENCES

Blum, A. et al. 1990. Wheat recovery from drought stress at the tillering developmental stage. Field Crops Research [Online], 24(1): 67–85. Available at: https://www.sciencedirect.com/science/article/abs/pii/0378429090900224. [2020-09-13].

Cavatte, P.C. et al. 2012. The Physiology of Abiotic Stresses. In Plant Breeding for Abiotic Stress Tolerance [Online]. Berlin: Springer-Verlag, pp. 21–51. Available at: https://www.researchgate.net/publication/278710629_The_Physiology_of_Abiotic_Stresses. [2020-09-13].

Destro, D. et al. 2001. Main stem and tiller contribution to wheat cultivars yield under different irrigation regimes. Brazilian archives of biology and technology [Online], 44(4): 325–330. Available at: https://www.scielo.br/pdf/babt/v44n4/a01v44n4.pdf. [2020-09-13].

Dolferus, R. et al. 2011. Abiotic stress and control of grain number in cereals. Plant Science [Online], 181(4): 331–341. Available at: https://pubmed.ncbi.nlm.nih.gov/21889038/. [2020-09-13].

Dragičević, V. 2015. Thermodynamics of Abiotic Stress and Stress Tolerance of Cultivated Plants. In Recent Advances in Thermo and Fluid Dynamics [Online]. Intech, pp. 195–221. Available at: https://www.intechopen.com/books/recent-advances-in-thermo-and-fluid-dynamics/thermodynamics-of-abiotic-stress-and-stress-tolerance-of-cultivated-plants. [2020-09-13].

Dreccer, M.F. et al. 2014. More fertile florets and grains per spike can be achieved at higher temperature in wheat lines with high spike biomass and sugar content at booting. Functional Plant Biology [Online], 41(5): 482–495. Available at: https://europepmc.org/article/agr/ind500745637. [2020-09-13].

Jenks, M.A., Hasegawa, P.M. 2005. Plant Abiotic Stress. 1st ed., USA: Blackwell Publishing Ltd.

Lämke, J., Bäurle, I. 2017. Epigenetic and chromatin-based mechanisms in environmental stress adaptation and stress memory in plants. Genome Biology [Online], 18(124): 1–11. Available at: https://genomebiology.biomedcentral.com/articles/10.1186/s13059-017-1263-6. [2020-09-13].

Mirbahar, A.A. et al. 2009. Effect of water stress on yield and yield components of wheat (*Triticum aestivum* L.) varieties. Pakistan Journal of Botany [Online], 41(3): 1303–1310. Available at: https://www.researchgate.net/publication/251715109_Effect_of_water_stress_on_yield_and_yield_components_of_wheat_Triticum_aestivum_L_varieties. [2020-09-13].

Sallam, A. et al. 2019. Drought Stress Tolerance in Wheat and Barley: Advances in Physiology, Breeding and Genetics Research. International Journal of Molecular Sciences [Online], 20(13): 1–36. Available at: https://www.ncbi.nlm.nih.gov/pmc/articles/PMC6651786/. [2020-09-13].

Shavrukov, Y. 2017. Early Flowering as a Drought Escape Mechanism in Plants: How Can It Aid Wheat Production? Frontiers in Plant Science [Online], 8(1950): 1–8. Available at: https://www.frontiersin.org/articles/10.3389/fpls.2017.01950/full. [2020-09-13].

Zhiqiang, W. et al. 2011. Studies on Compensation Effects of Rewatering on Winter Wheat Suffering from Droughts During Spring Under Different Soil Fertility Conditions. Zhongguo Nongye Kexue (Scientia Agricultura Sinica) [Online], 44(8): 1628–1636. Available at: https://jglobal.jst.go.jp/en/detail?JGLOBAL_ID=201402278558186720. [2020-09-13].

Estimation of crop nutritional status by UAV survey for site specific crop management

Igor Horniacek[1], Vojtech Lukas[1], Lubomir Neudert[1], Renata Duffkova[2], Vladimir Smutny[1]
[1]Department of Agrosystems and Bioclimatology
Mendel University in Brno
Zemedelska 1, 613 00 Brno
[2]Research Institute for Soil and Water Conservation
Zabovreska 250, 156 27 Praha
CZECH REPUBLIC

igor.horniacek@mendelu.cz

Abstract: This study is focused on the evaluation of UAV multispectral imaging for the diagnosis of nutritional status of winter wheat in precision agriculture. A field experiment was conducted in 2018 on two plots with the total area of 36 ha and 2019 at one plot with area 41.38 ha in ZD Kojcice (Pelhrimov, Czech Republic). During the vegetation period the field survey was carried out in stem elongation (BBCH 31) and heading (BBCH 51), both important vegetation stages for application of nitrogen fertilizers. The plant samples were taken on 56 and 53 sampling points distributed across the high – and low yielded zones and later analyzed for nitrogen content in plant tissues and total amount of above-ground biomass (fresh, dry). Simultaneously, unmanned aerial imaging was carried out by multispectral cameras Micasense RedEdge or Parrot Sequoia and the images were processed in photogrammetric software to create seamless ortho-mosaic in individual spectral bands (G, R, RE, NIR). A set of vegetation indices (NDVI, GNDVI, NDRE, NRERI, SAVI, MSAVI, EVI, EVI2, etc.) was calculated from these data and the mean value estimated by zonal statistics from 2m buffer zone around each sampling points. The statistical evaluation by correlation and regression analysis showed significant relationship between crop parameters and vegetation indices from UAV survey, thus it can be said that traditional field monitoring could be replaced by UAV survey even at a low number of calibration points. From the set of vegetation indices, NDVI showed better correlation values to estimate the amount of plant biomass, while the most sensitive vegetation index for estimation of nitrogen content in plants was NDRE index.

Key Words: precision agriculture, remote sensing, vegetation index, UAV

INTRODUCTION

Precision farming is the way of agriculture management which uses new technologies to increase efficiency of food production. It is a progressive, constantly evolving area, through which the approaches, methods and technologies already used are modified used in the management of agricultural production processes. It includes big ones amount of technical means and program inputs. An important feature of precision agriculture is the consistent use of a systems approach and intellect, given the overall higher level and complexity of the whole process (Nozdrovicky 2008).

One of the most important mapping technique in precision agriculture is remote sensing, which is based on the measurement of reflection of visible and near-infrared light from crops or soil. Remote sensing primarily does not require direct contact between the sensor and the crops. It is usually achieved using cameras mounted on remotely piloted aircraft systems (RPAS), aircrafts and satellites (Mulla and Khosla 2015).

The development of unmanned aerial survey by UAV taken remote sensing and precision agriculture one step further. The use of the UAV system for crop monitoring offers great possibilities for collecting data from fields in a fast, simple and inexpensive way compared to known conventional monitoring methods. The ability of UAV to fly at low altitudes, it results in ultra-high spatial

resolution of the recorded images. In addition, the UAVs are relatively simple to operate and are much cheaper than fully manned aircraft. In addition, they are more efficient than terrestrial systems because they can cover a large field in a short time and in a non-destructive way, which is very important for subsequent monitoring and work with vegetation (Tsouros et al. 2019).

The aim of this study was to verify the use of unmanned aerial multispectral imaging for estimation of agronomic relevant crop parameters of cereal crop stand to improve the efficiency of crop management practices.

MATERIAL AND METHODS

Experimental area

Data for the study were collected in 2018 and 2019 in the locality of Kojcice (Pelhrimov, Czech Republic, 49.473N, 15.254E) in three selected fields with winter wheat and spring barley. In 2018, these were the fields "Kazy" with an area of 10.2 ha, elevation 550 m a.s.l. and an average slope of 2.75 ° and "Vrcha" with an area of 26.2 ha, elevation 515 m a.s.l. and an average slope of 4.35 °, both with winter wheat crop. In 2019, the study was carried out on the field with spring barley "Mokriny-Stetky" with an area of 41.3 ha, elevation 530 m a.s.l. and an average slope of 2.6 °.

Plant sampling

Field monitoring consists of sampling plants in irregular sampling grid and their subsequent analysis in the laboratory. Data processing in the laboratory focuses on the evaluation of the values of aboveground biomass of the canopy (dry) and nitrogen concentrations in plants. This evaluation takes place in terms of two important vegetation stages, namely – stem elongation (BBCH 31) and heading (BBCH 51). A total of 109 sampling points were distributed in the monitored fields in 2018 and 2019. In 2018, there were 23 sampling points in the field “Kazy” and 33 sampling points in the field “Vrcha”, in 2019, totally 53 sampling points were sampled in the spring barley crop at “Mokriny-Stetky” field. Plant samples were taken from two 0.5 x 0.5 m squares per sampling point. Plant samples were analysed in the laboratory to estimate the nitrogen content [%] and the total amount of above-ground dry biomass [t/ha]. These two parameters were an input for calculation of Nitrogen nutrition Index (NNI) based on the calculation of Lemaire (2008). NNI represents the nitrogen status of the plants, NNI <1 indicates the under-fertilization of N, NNI >1 over-fertilization of nitrogen (Klem 2014).

Unmanned remote survey by UAV

Simultaneously with plant sampling a multispectral aerial imaging by UAV was realized by company Skymaps s.r.o. (Brno, Czech Republic) with Micasense RedEdge-M (2018) and Parrot Sequioa (2019) multispectral cameras. Both camera records images in visible (RGB), red-edge (RE) and near-infrared (NIR) spectrum, but also measures incoming radiance by Downwelling Light Sensor (DLS) to normalize lighting conditions. The images were processed by photorametric software to obtain the resulting orthomosaic with a spatial resolution of 18 cm per pixel. A set of eight broadband vegetation indices was calculated from raster data in ESRI ArcGIS, this study involve mainly three of them: NDVI, GNDVI and NDRE. Due to the high spatial resolution of images, average value of all pixel values inside of 2 m buffer zone around each sampling point was calculated. Statistical evaluation of relationship between plant parameters and aerial survey was done by correlation analysis and calculation of regression equation in Excel software statistical package.

RESULTS AND DISCUSSION

Descriptive statistics of the results of laboratory analysis of plant samples taken from the monitored fields (Kazy, Vrcha, Mokriny-Stetky) and phenology stages (BBCH 33 and 51) are shown in Table 1. Coefficients of variability (CV) indicate the highest variability in the field "Mokriny-Stetky", which also corresponds to the higher area of this field (41.3 ha) compared

to the fields "Kazy" (10.2 ha) and "Vrcha" (26.2 ha). Higher variability of plant parameters was reached in heading stage (BBCH 51), mainly for the aboveground biomass, with the increase up to 7% of CV at field Kazy and 1% at the field Vrcha. The average value of NNI was on observed fields similar for both crop growth vegetation stages, the range of values could be considered at the same level. This is valid for winter wheat (2018), where nutrition status indicated by NNI increased in heading stage (BBCH 51). In case of spring barley, NNI decreased in BBCH 51, which corresponds with the requirement for lower concentration of nitrogen in the grain for keeping high quality of grain for malting purposes.

Table 1 Descriptive statistics of monitored localities

Mokriny-Stetky 2019	*BBCH 31*			*BBCH 51*		
	Biom_D [t/ha]	*N [%]*	*NNI*	*Biom_D [t/ha]*	*N [%]*	*NNI*
Average	2.21	2.76	0.72	691.02	1.25	0.55
Median	2.17	2.74	0.72	683.14	1.21	0.54
Std.	0.49	0.49	0.12	119.77	0.20	0.09
Min.	0.68	2.05	0.51	344.58	0.95	0.40
Max.	3.31	4.93	1.03	952.30	2.06	0.78
Count	51.00	51	51	53.00	53.00	53.00
CV [%]	22.56	17.64	17.13	17.33	15.68	16.81
Vrcha 2018	*BBCH 31*			*BBCH 51*		
	Biom_D [t/ha]	*N [%]*	*NNI*	*Biom_D [t/ha]*	*N [%]*	*NNI*
Average	1.83	2.85	0.69	7.39	1.94	0.88
Median	1.76	2.81	0.70	7.68	1.87	0.90
Std.	0.39	0.35	0.13	1.68	0.24	0.17
Min.	1.03	2.17	0.47	4.14	1.55	0.63
Max.	2.71	3.86	1.06	9.84	2.39	1.18
Count	33.00	33.00	33.00	33.00	33.00	33.00
CV [%]	21.39	12.19	18.14	22.79	12.33	19.01
Kazy 2018	*BBCH 31*			*BBCH 51*		
	Biom_D [t/ha]	*N [%]*	*NNI*	*Biom_D [t/ha]*	*N [%]*	*NNI*
Average	1.69	3.10	0.73	6.53	2.28	0.98
Median	1.69	3.11	0.75	6.38	2.27	0.95
Std.	0.23	0.16	0.07	1.14	0.18	0.13
Min.	1.31	2.77	0.63	5.10	1.97	0.76
Max.	2.05	3.34	0.86	9.48	2.65	1.29
Count	23.00	23.00	23.00	23.00	23.00	23.00
CV[%]	13.89	5.25	9.42	17.41	8.07	13.68

The relationship between the monitored crop parameters and the indices calculated from the remote sensing was established based on the evaluation by correlation analysis (Table 2). The sensitivity of individual vegetation indices to crop parameters, mainly the NNI index, changes in crop growth between vegetation stages and differences between the observed fields were monitored.

In the first sampling period (BBCH 31), the highest correlation between vegetation indices and NNI was achieved using the NDRE index (Kazy. R = 0.60), (Mokriny-Stetky. R = 0.70) and the simple ratio index (SRI) at the site (Vrcha. R = 0.64). The values of correlation coefficients with other crop parameters show the different sensitivity of vegetation indices in relation to the amount of aboveground biomass or nitrogen content. However, we can see that the sensitivity of vegetation indices is not uniform between the monitored localities.

In the second sampling period (BBCH 51) reached the highest values the index EVI2 (Kazy. R = 0.774), NRERI (Vrcha. R = 0.813) and NDRE (Mokriny-Stetky. R = 0567). High values of correlation analysis at all three monitored localities in the second term were achieved by the GNDVI index and can therefore be recommended for a comprehensive diagnosis of plant nutrition status in fields in the main vegetation stage. Also, Wang et al. (2019) in their study show that NDRE and CIRE were both able to explain 67% of the NNI variability across the whole stage better than the remaining five vegetation indices. The NDVI, NDRE and GNDVI values were very similar with low standard deviation, while the remaining indices showed greater mutual differences and standard deviation.

Table 2 Correlation coefficients between crop parameters and vegetation indices calculated from unmanned aerial survey. Colored background shows the level of correlation (minimal-maximal values as red-green gradient).

Mokriny-Stetky 2019	*BBCH 31*			*BBCH 51*		
	Biom_D [t/ha]	*N* [%]	*NNI*	*Biom_D* [t/ha]	*N* [%]	*NNI*
EVI2	0.34	0.07	0.33	0.36	0.23	0.41
GNDVI	0.71	0.19	0.69	0.62	0.26	0.56
MSAVI2	0.58	0.10	0.51	0.50	0.19	0.44
NDRE	0.68	0.23	0.70	0.58	0.29	0.57
NDVI	0.71	0.03	0.54	0.55	0.11	0.39
NRERI	0.63	0.25	0.69	0.56	0.30	0.57
SAVI	0.38	0.08	0.36	0.39	0.22	0.41
SRI	0.74	0.13	0.66	0.61	0.18	0.49
Vrcha 2018	*BBCH 31*			*BBCH 51*		
	Biom_D [t/ha]	*N* [%]	*NNI*	*Biom_D* [t/ha]	*N* [%]	*NNI*
EVI2	0.33	0.17	0.30	0.68	0.53	0.69
GNDVI	-0.15	-0.07	0.15	0.78	0.60	0.70
MSAVI2	0.35	0.30	0.40	0.69	0.53	0.69
NDRE	0.39	0.19	0.35	0.61	0.54	0.78
NDVI	0.39	0.34	0.45	0.68	0.50	0.70
NRERI	0.10	-0.07	0.01	0.62	0.54	0.81
SAVI	0.32	0.18	0.31	0.64	0.54	0.68
SRI	0.58	0.47	0.64	0.79	0.59	0.74
Kazy 2018	*BBCH 31*			*BBCH 51*		
	Biom_D [t/ha]	*N* [%]	*NNI*	*Biom_D* [t/ha]	*N* [%]	*NNI*
EVI2	-0.17	-0.43	-0.35	0.79	0.69	0.77
GNDVI	-0.02	-0.35	-0.21	0.81	0.60	0.76
MSAVI2	-0.03	-0.35	-0.22	0.80	0.66	0.77
NDRE	0.54	0.43	0.60	0.76	0.59	0.73
NDVI	0.35	-0.11	0.17	0.77	0.55	0.72
NRERI	0.31	0.49	0.48	0.77	0.57	0.67
SAVI	-0.18	-0.43	-0.36	0.75	0.50	0.77
SRI	0.35	-0.10	0.18	0.66	0.50	0.76

Figure 1 shows aerial photographs from an unmanned survey converted to the vegetation index NDVI, which document the imbalances of stands on the monitored fields. Schirrmann et al. (2016) described that UAV systems can include information about the canopy volume of the wheat crops estimated from point clouds calculated by the overlapped UAV imagery in addition to the spectral information contained in the image tone which might be well suited to estimate biophysical crop parameters. The images are from the BBCH 51 period, for 2018 taken with a multispectral sensor Micasense RedEdge and for 2019 a sensor Parrot Sequoia. In the pictures, the points of plant collection are marked with crosses.

Figure 1 Maps of the experimental sites "Kazy" (above left), "Vrcha“ (above right) and" Mokriny-Stetky"(bellow), collected from an unmanned aerial survey, white crosses represent sampling points

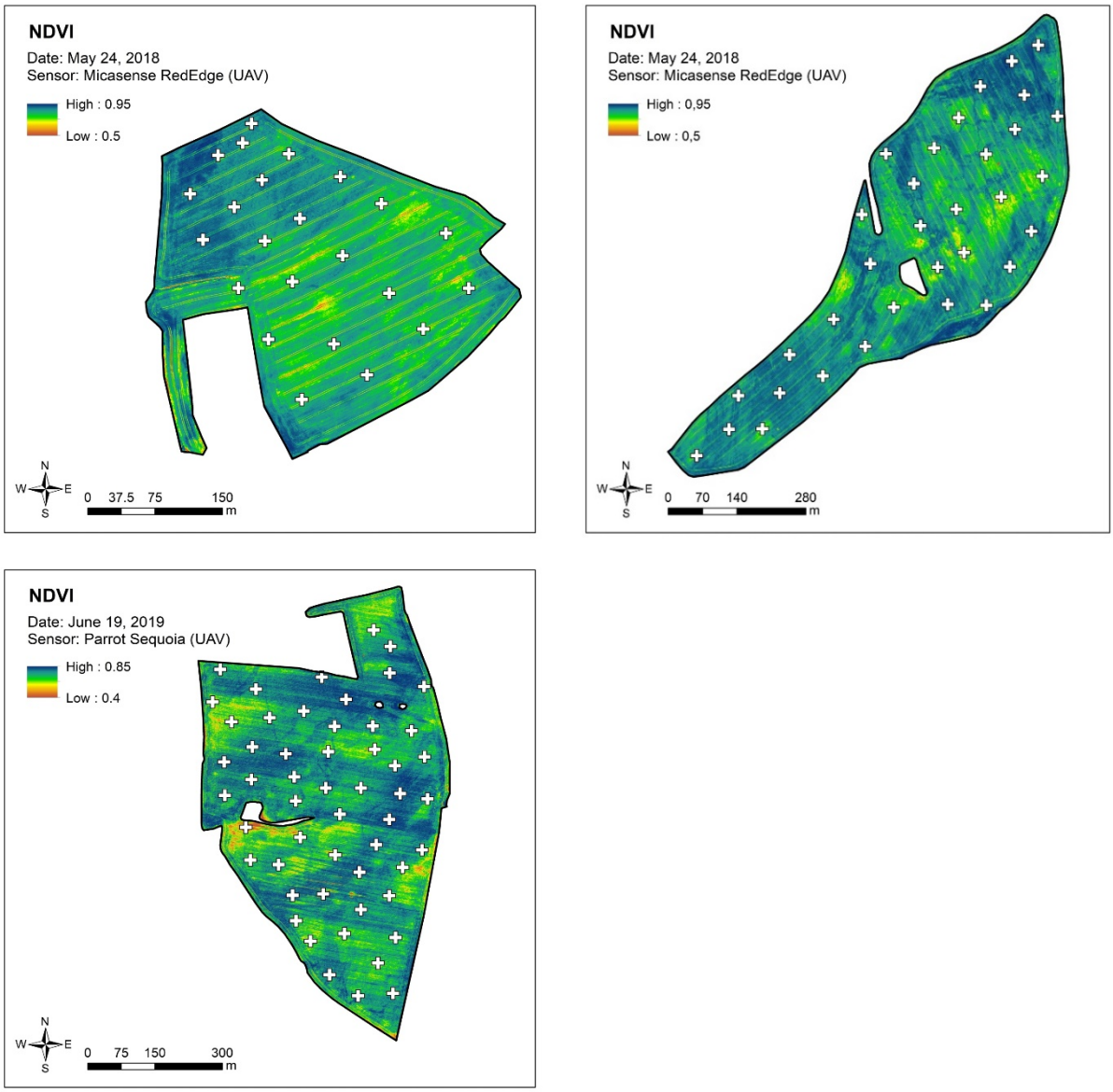

CONCLUSIONS

The results of this study showed that multispectral imaging by using unmanned aerial survey is appropriated for identification of nitrogen status within the fields. The relationship between crop parameters and vegetation indices was not consistent in vegetation stages and also in all fields. Higher correlation coefficients in early period of observation (BBCH 31) were achieved by NDRE index (for field Kazy, Mokriny-Stetky) or SRI (in case of field Vrcha). while in the stage of heading (BBCH 51) higher sensitivity to changes in NNI was detected by GNDVI vegetation index. These results prove that in case of aerial imaging by common multispectral cameras, calculation of set of vegetation indices is useful. Especially the calculation from the red-edge part of electromagnetic spectrum which promises high sensitivity to the chlorophyll content, thus also the N-status of plants. High spatial resolution of RPAS imagery provides very detailed information of crop damages or other local problematic areas of the field, which could be useful for field inspection. However, in most cases such level of spatial details is usually not needed for variable rate application in site-specific crop management because of the limited section control of fertilizers applicators (spreaders and sprayers).

ACKNOWLEDGEMENTS

This study was supported by Internal Grant Agency of Faculty of AgriSciences at Mendel University in Brno as the research project AF-IGA2020_IP063.

REFERENCES

Klem, K. et al. 2014. Využití měření spektrální odrazivosti a odvozených specializovaných vegetačních indexů v pěstební technologii jarního ječmene. Methodology for agricultural practice. Kroměříž, Brno, Havlíčkův Brod: Agrotest fyto, s.r.o., Centrum výzkumu globální změny AV ČR, v.v.i., GRYF HB, spol. s r.o., Mendelova univerzita v Brně.

Lemaire, G. et al. 2008. Diagnosis tool for plant and crop N status in vegetative stage: Theory and practices for crop N management. European Journal of Agronomy, 28(4): 614–624.

Mulla, D., Khosla, R. 2015. Historical Evolution and Recent Advances in Precision Farming. In Soil-Specific Farming. CRC Press, pp. 1–35.

Nozdrovicky, L. 2008. Presné pôdohospodárstvo: Implementácia s podporou informačných technológií a techniky. Nitra: Slovenská poľnohospodárska univerzita.

Schirrmann, M. et al. 2016. Monitoring Agronomic Parameters of Winter Wheat Crops with Low-Cost UAV Imagery. Remote Sensing, 19(13).

Tsouros, D. et al. 2019. A Review on UAV-Based Applications for Precision Agriculture. Information, 10(11): 349.

Wang, H. et al. 2019. Estimating the nitrogen nutrition index in grass seed crops using a UAV-mounted multispectral camera. International Journal of Remote Sensing, 40(7): 2467–2482.

Invasive plant species in the vegetation of landfills

Erika Hurajova, Martin Cerny, Lucie Vykydalova, Jan Winkler
Department of Plant Biology
Mendel University in Brno
Zemedelska 1, 613 00 Brno
CZECH REPUBLIC

xhurajo1@node.mendelu.cz

Abstract: The aim of the paper was to determine the species composition of vegetation in a landfill, belonging to Zdounky-Nětčice. Monitoring took place in July 2020. Three sections with different types of waste were compared in the landfill: municipal waste, biodegradable waste and inert waste. The evaluation of vegetation was carried out using phytocenological images. Furthermore, the influence of the type of waste on the representation of invasive plant species was evaluated. A total of 73 plant species were found. There were 11 invasive species: *Amaranthus powelli, Amaranthus retroflexus, Arrhenatherum elatius, Atriplex sagittata, Beta vulgaris, Conyza canadensis, Echinochloa crus-galli, Eragrostis minor, Helianthus tuberosus, Portulaca oleracea* and *Sisymbrium loeselii*.

Key Words: invasive plants, vegetation, landfills, waste

INTRODUCTION

There are 1454 non-native species in the flora of the Czech Republic at present, of which 350 are archaeophytes and 1104 neophytes. Their numbers have been increasing over the last 200 years. Of the non-native species, 4% behave invasively. Invasive species include 11 archaeophytes and 50 neophytes (Pyšek et al. 2012).

Invasive species have become a global problem that decreases biodiversity and threatens ecosystem stability (Callaway and Ridenour 2004, Davis 2003).

Human activities such as agriculture, forestry, transport, recreation and construction activity support the spread of invasive plant species to new habitats (Pyšek et al. 2012). In the last few decades, human activity has intensified. Therefore, we can assume that the penetration of neophytes into new habitats is greater today than in the past. In general, neophytes' invasive success is associated with warmer habitats and nutrient depletion (Chytrý et al. 2005, Rai and Singh 2020).

Moreover, anthropogenic activities degrade the soil, which becomes to show conditions unfavourable for the environment and ecosystems worldwide (Bai et al. 2013, Chen et al. 2015). Human activities are also connected with the misuse of soil, water and vegetation resources (Liu et al. 2014, Wong et al. 2015). One of anthropogenic activities that changes natural ecosystems and underestimated for tens of years is landfilling (Wong et al. 2015).

Landfilling is the most used and worldwide spread method of municipal solid waste (MSW) disposal (Koda et al. 2017). The disposal of MSW in landfills entails a number of environmental risks. It raises concerns about harmful impacts on human health, e.g. pollution of air, soil and groundwater, risk of fires and explosions, bad odours, or vegetation (Nannoni et al. 2015, Adamcová et al. 2017). Vegetation conditions can influence the growth and activity of methanotrophs in various ways, and vegetation coverage and diversity are critical determinants of soil-mediated methane oxidation (Reay et al. 2005).

The type of waste, supply of bio-waste (seeds, fruits, vegetative parts), neighboring habitats and sufficient nutrients creates specific conditions maintaining the occurrence of invasive plants in the landfill. The aim of the study is to monitor the species composition of vegetation of landfills. Furthermore, to determine the influence of landfill waste types on the representation of invasive plant species. Subsequently, invasive plant species were selected, which can spread from the monitored landfill further into the landscape. Last but not least, invasive plant species were selected, which can be spread from the monitored landfill further into the landscape.

MATERIAL AND METHODS

Characterization of research locality Zdounky

The fieldwork was conducted on the municipal solid waste landfill (MSW) in cadastral area of Zdounky-Nětčice (Zlín Region, Czech Republic). The landfill is surrounded by a thin line of trees and arable land behind it. According to Quitt (1971), the entire region lies in the warm zone T2.

A multi-layer composite liner protects the bottom and all sides and the upper part of the landfill. Leachate and landfill gas collection system is incorporated to catch the wastewater and gases. In terms of maintenance, the landfill is classified in the S-category - other waste, sub-category S-OO3. The landfill's designed area is 70 700 m^2 in five stages with a total volume of 907 000 m^3. The facility receives the waste from an area of ca. 75 000 residents. The annually deposited amount of waste is ca. 40 000 10^3 kg, of which 50% are from the communal sphere. Three variants were distinguished within the actively used landfill: municipal waste, biodegradable waste, and inert waste (consisting mainly of bricks, concrete, and other construction waste).

Methodology for evaluating vegetation

The composition of the vegetation was carried out by the method of phytocenological plots. Monitoring took place in July 2020. The size of the phytocenological images was 25 m^2. The cover of the species found was estimated as a percentage. The scientific names of individual plant species, their origin, and invasive status were taken from the database of Czech flora and vegetation Pladias (2020).

The land with the landfill was divided into three parts according to the type of waste, 5 phytocenological images were recorded for each. The biowaste is stored in the first part of the landfill. Mixed municipal waste is stored in the second part and inert waste (construction waste material) is stored in the third part of the landfill.

The obtained data on the occurrence of plant species were subsequently processed using multivariate analysis of ecological data. Canonical correspondence analysis (CCA) was used. There were 999 permutations when testing the validity using the Monte-Carlo test. The data were processed using the computer program Canoco 5.0 (Ter Braak and Šmilauer 2012).

RESULTS AND DISCUSSION

Results of vegetation monitoring

Based on the monitoring, 73 plant species were found, representing 14 neophytes, 38 archaeophytes and 21 apophytes. There were 9 casual species, 11 invasive species, 21 native species and 32 naturalized species. Table 1 shows the average cover of plant species found in landfills with different types of waste.

Table 1 The list and average coverage of species in the observed variants of waste

Species	Abbreviations	Origin in the Czech Republic	Invasion status	Variants (average coverage in %)		
				Municipal waste (Waste)	Biodegradable waste (Bio_waste)	Inert waste (Inert_wa)
Aethusa cynapium	*Aet cyna*	**native**	**native**	0.0	1.0	0.0
Agrostis capillaris	*Agr capi*	**native**	**native**	0.6	0.8	1.4
Amaranthus albus	*Ama albu*	**neophyte**	**naturalized**	0.0	0.0	0.8
Amaranthus powelli	*Ama powe*	**neophyte**	**invasive**	0.0	0.0	1.2
Amaranthus retroflexus	*Ama retr*	**neophyte**	**invasive**	0.0	5.0	2.4
Anagallis arvensis	*Ana arve*	**archaeophyte**	**naturalized**	0.0	0.0	0.6
Arrhenatherum elatius	*Arr elat*	**archaeophyte**	**invasive**	0.0	1.6	0.0
Artemisia vulgaris	*Art vulg*	**native**	**native**	1.2	0.0	0.0
Atriplex prostrata	*Atr pros*	**native**	**native**	0.0	2.4	0.0
Atriplex sagittata	*Atr sagi*	**archaeophyte**	**invasive**	3.0	3.2	3.0
Avena fatua	*Ave fatu*	**archaeophyte**	**naturalized**	1.0	0.8	0.0
Ballota nigra	*Bal nigr*	**archaeophyte**	**naturalized**	0.0	5.8	0.0
Beta vulgaris	*Bet vulg*	**archaeophyte**	**invasive**	0.0	1.0	0.0
Bidens tripartitus	*Bid trip*	**native**	**native**	0.0	1.2	0.0

Table 1 The list and average coverage of species in the observed variants of waste – continue

Species	Abbreviations	Origin in the Czech Republic	Invasion status	Variants (average coverage in %)		
				Municipal waste (Waste)	Biodegradable waste (Bio_waste)	Inert waste (Inert_wa)
Bromus hordeaceus	*Bro hord*	**archaeophyte**	**naturalized**	0.8	0.0	0.0
Bromus sterilis	*Bro ster*	**archaeophyte**	**naturalized**	0.0	0.0	0.4
Bromus japonicus	*Bro japo*	**archaeophyte**	**naturalized**	0.0	0.0	0.4
Calystegia sepium	*Cal sepi*	**native**	**native**	0.0	1.2	0.0
Cannabis sativa	*Can sati*	**archaeophyte**	**casual**	0.0	0.8	0.0
Capsella bursa-pastoris	*Cap bursa*	**archaeophyte**	**naturalized**	0.0	0.0	1.0
Carduus acanthoides	*Car acan*	**archaeophyte**	**naturalized**	0.0	2.0	0.0
Citrullus lanatus	*Cit lana*	**archaeophyte**	**casual**	0.0	2.0	0.0
Commelina communis	*Com comm*	**neophyte**	**casual**	0.2	0.0	0.0
Conyza canadensis	*Con cana*	**neophyte**	**invasive**	1.0	0.6	0.0
Cucurbita maxima	*Cuc maxi*	**neophyte**	**casual**	1.8	0.0	0.0
Daucus carota	*Dau caro*	**native**	**native**	1.0	0.0	0.0
Descurainia sophia	*Des soph*	**archaeophyte**	**naturalized**	0.0	2.6	0.0
Digitaria sanguinalis	*Dig sang*	**archaeophyte**	**naturalized**	1.4	4.0	0.0
Echinochloa crus-galli	*Ech crus*	**archaeophyte**	**invasive**	1.8	4.8	0.0
Elytrigia repens	*Ely repe*	**native**	**native**	0.0	3.0	0.0
Eragrostis minor	*Era mino*	**archaeophyte**	**invasive**	0.0	0.2	0.0
Euphorbia helioscopia	*Eup heli*	**archaeophyte**	**naturalized**	0.2	0.0	0.0
Geranium pusillum	*Ger pusi*	**archaeophyte**	**naturalized**	0.0	1.0	0.0
Helianthus annuus	*Hel annu*	**neophyte**	**casual**	0.8	0.0	0.0
Helianthus tuberosus	*Hel tube*	**neophyte**	**invasive**	0.8	0.0	0.0
Hordeum murinum	*Hor muri*	**archaeophyte**	**naturalized**	0.0	3.0	2.2
Chelidonium majus	*Che maju*	**archaeophyte**	**naturalized**	0.0	0.6	0.0
Chenopodium album	*Che albu*	**native**	**native**	3.2	2.4	1.0
Chenopodium glaucum	*Che glau*	**native**	**native**	0.6	0.0	0.0
Chenopodium hybridum	*Che hybr*	**native**	**native**	0.0	1.0	0.0
Chenopodium pedunculare	*Che pedu*	**archaeophyte**	**naturalized**	0.0	0.0	0.2
Chenopodium polyspermum	*Che poly*	**native**	**native**	0.0	1.6	1.0
Ipomoea purpurea	*Ipo purp*	**neophyte**	**casual**	0.6	0.0	0.0
Lactuca serriola	*Lac serr*	**archaeophyte**	**naturalized**	0.0	1.8	0.0
Lolium perenne	*Lol pere*	**native**	**native**	0.0	1.6	0.0
Malva sylvestris	*Mal sylv*	**archaeophyte**	**naturalized**	0.0	1.0	0.0
Melilotus albus	*Mel albu*	**archaeophyte**	**naturalized**	1.8	3.0	2.0
Myosotis arvensis	*Myo arve*	**archaeophyte**	**naturalized**	0.0	0.0	0.4
Nicandra physalodes	*Nic phys*	**neophyte**	**casual**	0.0	0.6	0.0
Panicum miliaceum	*Pan mili*	**archaeophyte**	**naturalized**	0.6	0.0	0.0
Papaver rhoeas	*Pap rhoe*	**archaeophyte**	**naturalized**	0.0	0.0	0.6
Persicaria lapathifolia	*Per lapa*	**native**	**native**	0.0	1.0	0.0
Phalaris canariensis	*Pha cana*	**neophyte**	**casual**	0.0	0.8	0.0
Physalis alkekengi	*Phy alke*	**archaeophyte**	**naturalized**	0.0	1.0	0.0
Plantago lanceolata	*Pla lanc*	**native**	**native**	0.6	0.8	0.0
Plantago major	*Pla majo*	**native**	**native**	0.6	0.4	0.0
Poa compressa	*Poa comp*	**native**	**native**	0.4	0.6	0.0
Polygonum aviculare	*Pol avic*	**native**	**native**	1.0	1.8	2.0
Portulaca oleracea	*Por oler*	**archaeophyte**	**invasive**	1.2	1.6	2.0
Senecio vulgaris	*Sen vulg*	**archaeophyte**	**naturalized**	0.6	1.2	0.0
Setaria pumila	*Set pumi*	**archaeophyte**	**naturalized**	0.0	2.6	0.0
Setaria viridis	*Set viri*	**archaeophyte**	**naturalized**	1.0	0.0	0.8
Sisymbrium loeselii	*Sis loes*	**neophyte**	**invasive**	0.0	5.8	1.0
Solanum lycopersicum	*Sol lyco*	**neophyte**	**casual**	0.0	2.2	0.0
Solanum nigrum	*Sol nigr*	**archaeophyte**	**naturalized**	1.4	2.4	1.0
Sonchus oleraceus	*Son oler*	**archaeophyte**	**naturalized**	0.0	0.2	0.6
Tanacetum vulgare	*Tan vulg*	**archaeophyte**	**naturalized**	0.4	0.0	0.0
Trifolium hybridum	*Tri hybr*	**neophyte**	**naturalized**	0.0	1.8	0.0
Trifolium medium	*Tri medi*	**native**	**native**	0.0	1.0	0.0
Tripleurospermum inodorum	*Tri inod*	**archaeophyte**	**naturalized**	1.2	1.0	1.0
Urtica dioica	*Urt dioi*	**native**	**native**	0.0	0.6	0.0
Verbascum densiflorum	*Ver dens*	**native**	**native**	0.0	1.0	0.0

Processing the results of vegetation monitoring

The cover of the found plant species on individual parts of the landfill was processed by DCA analysis. The length of the calculated gradient, determined by DCA, was 3.72. Based on this calculation, the canonical correspondence analysis CCA was chosen for further processing. The CCA analysis defines the spatial arrangement of individual plant species in the monitored variants, which are then graphically expressed using an ordination diagram (Figure 1).

The results of the CCA analysis, which evaluated the cover of plant species in the monitored variants, is significant at the level of significance $\alpha = 0.001$ for all canonical axes. Based on the CCA analysis (Figure 1), it is possible to divide the found plant species into six groups.

The first group of species was represented mainly in vegetation of the landfill with municipal waste: *Aethusa cynapium, Arrhenatherum elatius, Atriplex patula*, *Atriplex prostrata*, *Ballota nigra*, *Beta vulgaris*, *Bidens tripartitus*, *Calystegia sepium*, *Cannabis sativa*, *Carduus acanthoides*, *Citrullus lanatus*, *Descurainia sophia*, *Elytrigia repens*, *Eragrostis minor*, *Geranium pusillum*, *Chelidonium majus*, *Chenopodium hybridum*, *Lactuca serriola*, *Lolium perenne*, *Malva sylvestris*, *Nicandra physalodes, Persicaria lapathifolia*, *Phalaris canariensis, Setaria pumila*, *Solanum lycopersicum*, *Sisymbrium loeselii*, *Trifolium hybridum*, *Trifolium medium*, *Urtica dioica*, *Verbascum densiflorum.*

The second group of species was represented mainly in the vegetation of the landfill with inert waste: *Amaranthus albus*, *Amaranthus powelli*, *Anagallis arvensis*, *Bromus japonicus*, *Bromus sterilis*, *Capsella bursa-pastoris*, *Chenopodium pedunculare*, *Myosotis arvensis*, *Papaver rhoeas.*

The third group of species was represented mainly in the vegetation in the landfill with biodegradable waste: *Artemisia vulgaris*, *Bromus hordeaceus*, *Commelina communis*, *Cucurbita maxima*, *Daucus carota, Euphorbia helioscopia*, *Helianthus annuus*, *Helianthus tuberosus*, *Chenopodium glaucum*, *Ipomoea purpurea*, *Panicum miliaceum, Tanacetum vulgare.*

The fourth group of species was represented in the vegetation at the landfill with municipal waste and biodegradable waste: *Avena fatua*, *Digitaria sanguinalis*, *Echinochloa crus-galli*, *Conyza canadensis*, *Plantago lanceolata, Plantago major, Poa compressa*, *Senecio vulgaris.*

The fifth group of species was represented in the vegetation at the landfill with municipal waste and inert waste: *Agrostis capillaris, Amaranthus retroflexus*, *Hordeum murinum*, *Chenopodium polyspermum*, *Polygonum aviculare*, *Portulaca oleracea*, *Sonchus oleraceus.*

The sixth group of species was affected by several other factors: *Atriplex sagittata, Chenopodium album, Melilotus albus, Physalis alkekengi, Setaria viridis, Solanum nigrum, Tripleurospermum inodorum.*

Figure 1 Similarities of plant species composition on phytosociological plots with respect to analysed categorical factor (type of waste)

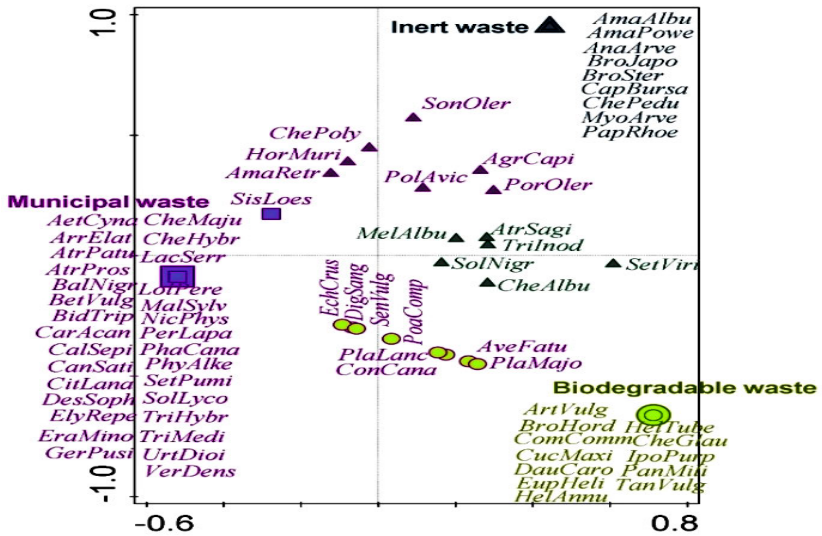

Legend: Municipal waste – part of a landfill with the storage of mixed municipal waste; Biodegradable waste – part of a landfill with biowaste disposal, Inert waste – part of a landfill with storage of construction waste.

The results show that landfills are suitable habitats for invasive plant species. Invasive species, according to Chytrý et al. (2005) are most commonly found in ruderal habitats. According to Davis (2003), invasive species contribute to the decline of native species at the habitat. According to Rai and Singh (2020), invasive species affect biodiversity. According to these authors, invasive species often have an impact on human health (they contain toxins or cause allergic reactions). According to Adamcová et al. (2017), invasive species can accumulate heavy metals: Co, Cu, Fe, Hg and Pb. According to Rai and Singh (2020), invasive species can be used as a source of bioenergy.

CONCLUSION

Invasive plant species are part of the vegetation of a municipal waste landfill. From our results, it is evident that a number of species with invasive status were recorded at the monitored landfill. The most important plant species found include: *Amaranthus powelli*, *Amaranthus retroflexus*, *Arrhenatherum elatius*, *Atriplex sagittata*, *Beta vulgaris*, *Conyza canadensis*, *Echinochloa crus-galli*, *Eragrostis minor*, *Helianthus tuberosus*, *Portulaca oleracea* and *Sisymbrium loeselii*. From a phytosanitary point of view, landfills can be a source of diaspores of invasive plant species. Municipal landfills can pose a threat to the ecosystem and allow the spread of new species of plants and weeds.

ACKNOWLEDGEMENTS

This work was created with the financial support of project IGA AF-IGA2020-IP004 Study of synantropic vegetation of municipal waste dumps.

REFERENCES

Adamcová, D. et al. 2017. Environmental assessment of the effects of a municipal landfill on the content and distribution of heavy metals in Tanacetum vulgare L. Chemosphere [Online], 185: 1011–1018. Available at: https://doi.org/10.1016/j.chemosphere.2017.07.060. [2020-08-24].

Bai, X.Y. et al. 2013. Assessing spatial–temporal evolution processes of karst rocky desertification land: indications for restoration strategies. Land Degradation & Development [Online], 24: 47–56. https://onlinelibrary.wiley.com/doi/10.1002/ldr.1102. [2020-08-21].

Callaway, R.M., Ridenour W.M. 2004. Novel weapons: invasive success and the evolution of increased competitive ability. Frontiers in Ecology and the Environment [Online], 2(8): 436–443. Available at: https://esajournals.onlinelibrary.wiley.com/doi/10.1890/1540-9295%282004%29002%5B0436%3ANWISAT%5D2.0.CO%3B2. [2020-08-23].

Chen, X.W. et al. 2015. Ecological performance of the restored south east new territories (SENT) landfill in Hong Kong (2000–2012). Land Degradation & Development [Online], 27 (6): 1664–1676. Available at: https://doi.org/10.1002/ldr.2366. [2020-08-24].

Chytrý, M. et al. 2005. Invasions by alien plants in the Czech Republic: a quantitative assesment across habitats. Preslia [Online], 77(4): 339–354. Available at: https://www.sci.muni.cz/botany/chytry/Chytry_etal2005_Preslia.pdf. [2020-08-24].

Davis, M.A. 2003. Biotic globalization: does competition from introduced species threaten biodiversity? Bioscience [Online], 53(5): 481–489. Available at: https://academic.oup.com/bioscience/article/53/5/481/241416. [2020-08-23].

Koda, E. et al. A. 2017. Levels of organic pollution indicators in groundwater at the old landfill and waste management site. Applied Science [Online], 7 (6): 638. Available at: https://doi.org/10.3390/app7060638. [2020-08-24].

Liu, Z. et al. 2014. Land use and climate changes and their impacts on runoff in the Yarlung Zangbo river basin, China. Land Degradation & Development [Online], 25: 203–215. Available at: https://doi.org/10.1002/ldr.1159. [2020-08-21].

Nannoni, F. et al. 2015. Heavy element accumulation in Evernia prunastri lichen transplants around a municipal solid waste landfill in central. Waste Manage [Online], 43: 353–362. Available at: https://doi.org/10.1016/j.wasman.2015.06.013. [2020-08-24].

Pladias © 2020: Department of Botany and Zoology Faculty of Science Masaryk University. Database of the Czech Flora and Vegetation. 2018. [Online]. Available at: https://pladias.cz/en/. [2020-08-23].

Pyšek, P. et al. 2012. Plant invasions in the Czech Republic: current state, introduction dynamics, invasive species and invaded habitats. Preslia [Online], 84(3): 575–629. Available at: http://www.ibot.cas.cz/invasions/pdf/Pysek,%20Chytry,%20Pergl,%20Sadlo,%20Wild-Plant%20invasions%20in%20the%20Czech%20Republic_Preslia2012.pdf. [2020-08-23].

Quitt, E. 1971. Klimatické oblasti Československa. 1st ed., Praha: Academia.

Rai, P.K., Singh, J.S. 2020. Invasive alien plant species: Their impact on environment, ecosystem services and human health. Ecological Indicators [Online], 111: 106020. Available at: https://doi.org/10.1016/j.ecolind.2019.106020. [2020-08-24].

Reay, D.S. et al. 2005. Effect of tree species on methane and ammonium oxidation capacity in forest soils. Soil Biology and Biochemistry [Online], 37(4):719–730. Available at: https://www.sciencedirect.com/science/article/abs/pii/S0038071704003797. [2020-08-24].

Ter Braak, C.J.F., Šmilauer, P. 2012: Canoco reference manual and user's guide: software for ordination (version 5.0). Microcomputer Power, Ithaca.

Wong, M.H. et al. 2015. Comparison of pioneer and native woodland species growing on top of an engineered landfill, Hong Kong: restoration programme. Land Degradation & Development [Online], 27(3): 500–510. Available at: https://doi.org/10.1002/ldr.2380. [2020-08-21].

Polyphenols content and seed vigor interaction in spring barley (*Hordeum vulgare* L.)

Ivana Jovanovic, Jhonny Edison Alba-Mejia, Tomas Streda
Department of Crop Science, Breeding and Plant Medicine
Mendel University in Brno
Zemedelska 1, 613 00 Brno
CZECH REPUBLIC

ivana.jovanovic@mendelu.cz

Abstract: Drought and cold stress are main factors influencing germination of barley in spring. The aim of this work was to investigate whether higher content of polyphenols in seeds affects vigor and germination ability. For the purpose of this study ten varieties from different growing areas were selected while seed vigor was determined by two different methods. The first method was conventional germination method, where seeds were placed on filter paper in germinated trays whereas the second method was that barley kernels were placed in Petri dishes without filter paper under the same environmental conditions. Effect of drought and cold stress was simultaneously monitored. Drought stress was performed with addition of polyethylene glycol (PEG) solution with osmotic potential of - 0.2 MPa and for the cold stress seeds were germinated at 10 °C. Evaluated parameters were root length and surface area performed with WinRhizo (Régent Instruments Inc., Quebec, Kanada) software while the content of total polyphenols in the grains was determined spectrophotometrically from the previously prepared extract.

Key Words: spring barley, total polyphenols, seed vigor, drought stress, cold stress

INTRODUCTION

Polyphenols in barley form a very wide group of substances with different molecular weights and different physicochemical properties with positive and negative impacts on grain quality (Basařová et al. 2015). Similar to other cereals, in barley, phenolic compounds are found in three different forms including free (soluble), soluble- conjugated (esterified) and bound phenolics (insoluble/unextractable) which are covalently bound to cell wall materials such as lignin, arabinoxylans, cellulose, hemicellulose and structural protein (Fernandez-Orozco et al. 2010). The majority of the free phenolics in barley are flavanols that are usually found in their monomeric form as catechin and epicatechin as well as in their polymeric form as proanthocyanidins (Verardo et al. 2008). Ferulic and coumaric acid, the major phenolic acids in barley grains, are mainly found in the outer layers (husk, pericarp, testa, and aleurone), but also can be detected in the endosperm (Kim et al. 2007).

Total phenolic compounds (TPCs) represent the entire spectrum of polyphenol compounds contained in the phenolic acids and flavonoids (Mikyška et al. 2019). Moreover, the amount and composition of polyphenols depend, like most other substances in barley grain, on the genetic characteristics of the variety, the cultivation locality and climate conditions of the harvest year (Gangopadhyay et al. 2015). Although there is a meaningful insight into the different polyphenols present in barley extracts, the identities of the individual phenolic compound which are the strongest contributors to the antioxidant capacity of barley are still unknown (Gangopadhyay et al. 2016). Some of them have been considered as possible germination inhibitors. Furthermore, during germination grain breakdown increases which is accompanied by the release of phenolic substances from the cell walls and an increase in the proportion of free phenolic substances (Basařová et al. 2015).

The influence of germination on total phenolic contents has been investigated in many seeds. Recent studies indicate that germination can change the level of total phenolics in germinated seeds and sprouts while having a distinct impact on bound phenolics (Gan et al. 2017). Nevertheless, a major limitation of these approaches is the difficulty in quantifying TPCs in the product dry matter. Dry matter content can vary with sprouting and germination conditions, like light, temperature, and humidity

(Singhal et al. 2012). Thus, the quantification on the dry matter is important for assessment and comparison of the nutritional content in different products especially when the moisture contents are different (Niroula et al. 2019).

In addition, the TPCs play a significant role in the regulation of plant metabolic processes as well as lignin synthesis. In some species, an increase in total phenolic content correlated with enhanced seedling vigor (Burguieres et al. 2007). In barley, their amount ranges from about 0.1 to 0.6% of dry matter (Basařová et al. 2015). The aim of this study was to explain the effect and the relationship of phenolic compounds on the germination and seed vigor of ten different varieties of barley grain.

MATERIALS AND METHODS

Plant material

Common barley seeds were provided by Research Institute of Brewing and Malting. Ten varieties of spring barley were selected from four growing stations in the Czech Republic. Growing stations were chosen based on habitat conditions for development and growth of the crop. Two of them belongs to the corn production area, which is a drier area of South Moravia region and they are Lednice and Úherský Ostroh. The other one belongs to the beet production area, which in our case was growing station Čáslav. The last one belongs to the cereal production area and that was growing station Chrastava. Čáslav and Chrastava are growing stations with the best conditions for growing spring barley. Chosen varieties were: Malz (Chrastava), Laureatte (Čáslav), Spitfire (Uherský Ostroh), Francin (Chrastava), KWS Amadora (Lednice), Bojos (Chrastava), Accordine (Chrastava), Laudis 550 (Chrastava), Manta (Lednice), KWS Irina (Uherský Ostroh).

Determination of germination and seed vigor processes

Fifty barley seeds were placed on a filter paper previously moistened with polyethylene glycol solution (PEG-6000) with osmotic potential of -0.2 MPa for simulating water deficit. Also, six seeds of each variety were chosen and placed in Petri dishes, with 10 ml of PEG inside. Thereupon, each of them was placed in the climate box under 10 °C. Seed vigor process was monitored after seven, eleven and fourteen days in order to observe how the kernels would behave under cold and drought conditions. After seven, eleven and fourteen days, kernels from germination trays and Petri dishes were counted. Each germinated seed from Petri dishes has been scanned and analyzed in WinRhizo (Régent Instruments Inc., Quebec, Kanada) root detection program.

Preparation of the extract

Twenty grams of barley from each variety was ground finely on a 1 mm sieve barley grinder. After that, 5 g of ground barley was weighed into a 200 ml tall beaker. Then, 100 ml of 75% dimethylformamide solution was added. Shortly afterwards, the mixer head has been immersed in the beaker and mixed for ninety seconds. The mixture was supposed to be left from twelve to fifteen minutes and the whole procedure is repeated three times in each sample. After the last mixing, the solution has been poured into a centrifuge tube. Samples were centrifuged at 3000 rpm for 10 min. From the centrifuged solution was pipetted 25 ml of the solution into a 100 ml volumetric flask and made up to the mark line with deionized water. The solution was poured into a centrifuge tube and for the last time samples were centrifuged at 15000 rpm for 30 min. The pure solution has been used for the determination of the polyphenols content.

Determination of polyphenols

Twenty ml of extract has been pipetted into a 50 ml volumetric flask, then 16 ml of ethylene-diaminetetraacetic sodium hydroxide (CMC/EDTA) was added. To the solution was also added 0.10 ml ammonium ferric citrate and content was shaken. Then, 0.10 ml of ammonium solution was added, made up to the mark line with deionized water and mixed thoroughly. The absorbance was measured spectrophotometrically in 10 mm cuvette at a wavelength of 525 nm against a blank solution.

Preparation of a blank solution

Twenty ml of extract has been pipetted into a 50 ml volumetric flask. After that, 0.10 ml ammonium ferric citrate was added. The solution was mixed thoroughly and made up to the mark line with deionized water. Then it was let to stand for 10 min and the clarity of the solution was observed.

Calculation and evaluation of polyphenol content

The calculation was performed according to the formula for calculating the content of polyphenols in the original solution.

Pp = (Ah – Ak) * 2,52

where Pp is a polyphenols content in the original solution (%); Ah is the absorbance of the main solution (%) and Ak is the absorbance of the blank solution (at 525 nm wavelength)

After that, it was necessary to make a recalculation to the dry matter of the sample. That has been done according to the following formula:

$$Ps = \frac{Pp*100}{100-V}$$

where Ps is a polyphenols content in dry matter of the sample (%) and V is the content of the water in barley kernels

In order to obtain the water content of the barley kernels, it was necessary to determine the percentage of moisture for each variety.

Correlation in Excel

Correlation between gained parameters have been provided by Excel "correlation" function. This function calculates level of significance based on Pearson correlation coefficient r. The Pearson correlation coefficient r (a value between -1 and +1) indicates how strongly variables are related to each other. Critical value of Pearson correlation coefficient r on the level of significance 0.005 for ten samples was 0.632.

RESULTS AND DISCUSSION

As already mentioned, two different methods were selected to determine seed vigor and germination in ten varieties of spring barley – germination in germination trays with filter paper and germination in Petri dish without filter paper. Furthermore, length of root and surface area of germinated kernels grown in Petri dishes was analyzed in WinRhizo software. For all variants, the number of germinated and non-germinated kernels was evaluated after 7, 11 and 14 days. It was found that the selected methods do not correlate with each other, as expected.

Table 1 Correlation between the length (Len) of the roots analyzed in WinRhizo program, their surface area (SA) after seven, eleven and fourteen days

	7 days Len	11 days Len	14 days Len	7 days SA	11 days SA	14 days SA
7 days Len	-	0.871	0.803	-	-	-
11 days Len	-	-	0.979	-	-	-
14 days Len	-	-	-	-	-	-
7 days SA	-	-	-	-	0.760	0.534
11 days SA	-	-	-	-	-	0.920
14 days SA	-	-	-	-	-	-

As it is shown in Table 1 highly significant correlation was observed among length of roots in germinated seeds in all tested periods (7 and 11; 7 and 14; 11 and 14 days). Moreover, from the surface area values, correlation was observed only in the case of 7 and 11 days and 11 and 14 days. Interestingly, correlation among 7 and 14 days was not detected due to the water deficit, as previously published by Shahriari et al. 2014, Silviera et al. 2020.

Germination of seeds is commonly done in germination trays on filter paper. However, in the studies related to drought stress i.e. usage of PEG, Petri dishes without filter paper might be

a useful tool since filter paper can cause the problems with breaking the root architecture during samples manipulation. Although, it was expected that these two approaches will correlate and that no differences will appear, unexpectedly the correlation among them was not observed (Table 2). Moreover, correlation was not recorded among germinated seeds in Petri dishes.

Table 2 Correlation between germinated barley kernels on filter paper (F.P.) in germination trays and Petri dishes (P.D.) after seven, eleven and fourteen days

Days / Treatment	7 days P.D.	11 days P.D.	14 days P.D.
7 days F.P.	0.256	-	-
11 days F.P.	-	0.519	-
14 days F.P.	-	-	-0.207
7 days P.D.	-	0.523	0.314
11 days P.D.	0.523	-	0.346
14 days P.D.	0.314	0.346	-

Table 3 Correlation between germinated barley kernels on filter paper (F.P.) after seven, eleven and fourteen days

Days / Treatment	14 days F.P.	11 days F.P.
7 days F.P.	0.507	0.867
11 days F.P.	0.667	-

Highly significant correlation was detected among kernels placed on filter paper (Table 3). Correlation was determined in kernels between 7 and 11 and 11 and 14 days under drought and cold stress. The development and size of the kernels was not affected by stress conditions (Steiner et al. 2019).

Table 4 Correlation between total polyphenols content, germinated barley kernels on filter paper (F.P.) and Petri dishes (P.D.), length of the roots (Len), their surface area (SA) analyzed in WinRhizo program (W.R.)

Days / Treatment	r
7 days F.P.	0.463
11 days F.P.	0.323
14 days F.P.	0.013
7 days P.D.	0.297
11 days P.D.	0.311
14 days P.D.	0.632
7 days Len (W.R.)	0.232
11 days Len (W.R.)	0.110
14 days Len (W.R.)	0.211
7 days SA (W.R.)	0.309
11 days SA (W.R.)	0.216
14 days SA (W.R.)	0.167

All analyzed barley varieties contained average level of polyphenols (data not shown). The level of total polyphenols was found to be in the range of 0.01–0.2% dry matter, with an average 0.1%. Obtained results are in compliance with findings of Basařová et al. (2015) where level of polyphenols in barley ranged from 0.1–0.6%.

As it is shown in Table 4, no correlation was seen between almost all tested parameters and polyphenols content. However, correlation was observed in case of germinated seeds in Petri dish at the end of experimental period (14 days). Reason for this is unknown, but we can assume that polyphenolic content increase with the length of the experiment since it is known that germination

modifies the quantitive and qualitative phenolic compounds and these changes mainly depends on the germination conditions (Lopez-Amorós et al. 2006, Tarzi et al. 2012, Chon 2013).

CONCLUSION

Based on this research it could be concluded that methods, germination in germination trays with filter paper and germination in Petri dish without filter paper did not correlate among each other. Therefore, highly significant correlation among length of roots in germinated seeds in all tested periods was confirmed. Highly significant correlation was also detected among kernels placed on filter paper. On the other hand, there is no certainty that the results obtained from correlation between seed vigor testing methods and total polyphenolic content depend only on the kernels germination conditions. Hence, the research should be continued in order to perceive all disadvantages and assumptions in pre-screening study.

ACKNOWLEDGEMENTS

The work was supported by the project from Czech Ministry of Agriculture QK1910197 „The strategy for minimizing the impact of drought on sustainable production and barley malting quality“.

REFERENCES

Basařová, G. et al. 2015. Sladařství: Teorie a praxe výroby sladu. 1st ed., Praha, CZ: Havlíček Brain Team.

Burguieres, E. et al. 2007. Effect of vitamin C and folic acid on seed vigour response and phenolic-linked antioxidant activity. Bioresource Technology, 98(7): 1393–1404.

Chon, S-U. 2013. Total Polyphenols and Bioactivity of Seeds and Sprouts in Several Legumes. Current Pharmaceutical Design, 19(34): 6112–6124.

Fernandez-Orozco, R. et al. 2010. Effects of environment and genotype on phenolic acids in wheat in the HEALTHGRAIN diversity screen. Journal of Agricultural and Food Chemistry, 58(17): 9341–9352.

Gan, R.Y. et al. 2017. Bioactive compounds and bioactivities of germinated edible seeds and sprouts: An updated review. Trends in Food Science & Technology, 59: 1–14.

Gangopadhyay, N. et al. 2015. A review of extraction and analysis of bioactives in oat and barley and scope for use of novel food processing technologies. Molecules, 20(6): 10884–10909.

Gangopadhyay, N. et al. 2016. Antioxidant-guided isolation and mass spectrometric identification of the major polyphenols in barley (*Hordeum vulgare*) grain. Food Chemistry, 210: 212–220.

Kim, M.J. et al. 2007. Relationship between phenolic compounds, anthocyanins content and antioxidant activity in colored barley germplasm. Journal of Agricultural and Food Chemistry, 55(12): 4802–4809.

Lopez-Amorós, M.L. et al. 2006. Effect of germination on legume compounds and their antioxidant activity. Journal of Food Composition and Analysis, 19(4): 277–283.

Mikyška, A. et al. 2019. Influence of barley variety and growing locality on the profile of flavonoid polyphenols in malt. Kvasny Prumysl, 65(5): 149–157.

Niroula, A. et al. 2019. Total phenolic contents and antioxidant activity profile of selected cereal sprouts and grasses. International Journal of Food Properties, 22(1): 427–437.

Shahriari, S. et al. 2014. Germination at low osmotic potential as a selection criteria for drought stress tolerance in sweet corn. African Journal of Biotechnology, 13(2): 294–300.

Silviera, N.M. et al. 2020. Germination and initial growth of common bean plants under water deficit as affected by seed treatment with S-nitrosoglutathione and calcium chloride. Theoretical and Experimental Plant Physiology, 32(1): 49–62.

Singhal, A. et al. 2012. WHEATGRASS: An alternative household nutritional food security. International Research Journal of Pharmacy, 3(7): 246–250.

Steiner, F. et al. 2019. Does seed size affect the germination rate and seedling growth of peanut under salinity and water stress? Pesquisa Agropecuária Tropical, 49(e54353): 1–9.

Tarzi, B.G. et al. 2012. The Effect of Germination on Phenolic Content and Antioxidant Activity of Chickpea. Iranian Journal of Pharmaceutical Research, 11(4): 1137–1143.

Verardo, V. et al. 2008. Distribution of bound hydroxycinnamic acids and their glycosyl esters in barley (*Hordeum vulgare* L.) air-classified flour: Comparative study between reversed phase-high performance chromatography-mass spectrometry (RP-HPLC/MS) and spectrophotometric analysis. Journal of Agricultural and Food Chemistry, 56(24): 11900–11905.

Assessment of spatial heterogeneity of winter wheat canopy stand by Sentinel-2 satellite imagery

Jiri Mezera, Vojtech Lukas, Jakub Elbl, Lubomir Neudert, Vladimir Smutny
Department of Agrosystems and Bioclimatology
Mendel University in Brno
Zemedelska 1, 613 00 Brno
CZECH REPUBLIC

jiri.mezera@mendelu.cz

Abstract: Evaluation of cereal plant status and other biophysical parameters, such as nitrogen uptake (Nupt), nitrogen content and total amount of aboveground biomass, is important information for decision support in agronomy for correct treatment of crop management practices. This information could be provided in precision agriculture by remote sensing as an efficient method for the monitoring of crop within field heterogeneity. The aim of this study was to verify the use of satellite images for estimation of agronomic relevant crop parameters of winter wheat, such as nitrogen uptake, amount of above-ground biomass and nitrogen content. Input data were obtained from field trials with winter wheat realized in 2017–2020 at five locations (Otnice, Dolni Dubnany, Zdounky, Rasovice a Kardasova Recice) with total area of 528 ha. The field survey was carried out in sampling grid to estimate total amount of aboveground biomass, nitrogen concentration in plants and nitrogen uptake during vegetation stage BBCH 31–45. Besides the plant sampling, the values of vegetation indices from Sentinel-2 multispectral imagery were obtained to characterise spectral response of plants. The relationship between crop parameters and Sentinel satellite indices was evaluated using the Spearman correlation coefficient. The high correlation coefficient between Nupt and biomass showed a large influence of the amount of aboveground biomass on the consumption of nitrogen. The highest correlation coefficient of vegetation indices to the crop parameters at all localities was achieved by REIP index, which corresponds with the higher sensitivity of the red-edge bands to the chlorophyll content. The results vary among the localities, the highest values for all vegetation indices were reached for the locality Rasovice, on the contrary, the lowest for the locality Zdounky. The most consistent results for all localities were achieved for the vegetation indices NRERI, REIP and RENDVI, which thus appear to be the most universal indices for the diagnosis of plant nutritional status and its within field heterogeneity by satellite multispectral imaging.

Key Words: precision agriculture, crop sensing, Sentinel-2, vegetation indices

INTRODUCTION

Achieving the expected yield and at the same time reducing the burden on the environment by nitrogen losses is only possible by harmonizing the requirements of individual crops and nitrogen fertilization. Various tools are used to determine the nutritional status of the stand. Plants inorganic analyses represent the destructive methods of diagnosing nutritional status, which is based on the estimation of the concentrations of individual nutrients and their mutual proportions in different vegetation stages. By evaluating the results of these analyses, it is possible to optimize fertilization and thus ensure the achievement of the required yield and quality of production. Inorganic analysis of plants is time consuming, although accurate conventional method (Ryant and Dryšlová 2015).

An alternative can be non-destructive methods based on monitoring of spectral parameters and its relation to the content of chlorophyll or total nitrogen in the leaves. The spectral response is obtained by measurement of the amount of radiation passing through the leaf (transmittance) or radiation reflected from the vegetation (reflectance). There are already available sensing systems installed on the agricultural machinery, such as Fritzmeier ISARIA, Yara N-Sensor, Trimble GreenSeeker and others. Another category of reflectance survey is the remote sensing by satellite monitoring, such as free available data from Sentinel-2. The two satellites Sentinel-2 (A/B) routinely deliver multispectral images of the Earth in 13 spectral bands from visible to short-wave infrared part

of spectrum with spatial resolution 10, 20 and 60 m per pixel (Adan 2017). The presence of red-edge bands aims on the more precise detection chlorophyll content in plants by improved calculation of vegetation indices (Frampton et al. 2013). Above all, these satellites are able to provide us actual satellite images every 4–6 day in the condition of the middle Europe (Söderström et al. 2016). The aim of the study was to verify the use of satellite images for estimation of agronomic relevant crop parameters of winter wheat, such as amount of above-ground biomass, nitrogen content and nitrogen uptake.

MATERIAL AND METHODS

Study area

Data were obtained from eight experimental fields in 2017–2020 in five locations in Czech Republic – Otnice, Dolni Dubnany, Zdounky, Rasovice and Kardasova Recice. The total area of the observation was 528 ha, the overview of field trials is mentioned in Table 1.

Table 1 Description od localities

Locality	Sample term	Satellite term	Area [ha]	Altitude [m a.s.l.]	Slope [°]	District	Coordinates
Otnice_1	26.04.2017	01.05.2017	70.81	238	4.66	Vyskov	49.086N, 16.814E
Otnice_2	19.05.2017	18.05.2017	70.81	238	4.66	Vyskov	49.086N, 16.814E
Dolni Dubnany	18.05.2017	18.05.2017	40.45	305	2.58	Znojmo	49.055N, 16.226E
Zdounky	06.05.2019	08.05.2019	95.84	275	6.45	Kromeriz	49.297N, 17.393E
Rasovice	28.04.2020	25.04.2020	153	277–323	3.37–4.13	Vyskov	49.120N, 16.948E
Kardasova Recice	04.05.2020	08.05.2020	96.55	446–456	0.97–2.65	Jindrich. Hradec	49.184N, 14.853E

Plant sampling

Field survey consists of plant sampling and its laboratory analysis. The aboveground biomass of canopy (dry) and nitrogen concentration in plants were assessed by plant sampling realized in important vegetation stages - in stem elongation (BBCH 31) and also in booting (BBCH 45 – Otnice only). The number of sampling points at each locality differs from 20 to 26 (see count in Table 3). Plant samples were taken from 0.5 x 0.5 m squares per each sampling point localised by DGPS (Differential Global Positioning System). Plant samples were analysed in laboratory for estimation of nitrogen content [%] and total amount of aboveground dry biomass [t/ha]. A Nitrogen uptake (Nupt, [kg/ha]) was calculated from these two parameters as multiplication of N concentration by dry biomass.

Remote sensing by satellite platform Sentinel-2

The Sentinel-2 images were selected to be cloudless and taken near to the date of plant sampling. The datasets were downloaded from ESA open hub database as surface reflectance product (L2A, Copernicus 2020) and filtered through a cloud mask derived with L2A scene classification dataset by sen2cor algorithm (Lantzanakis et al. 2016). Set of ten vegetation indices was calculated from multispectral bands by the automatized workflow in ArcGIS (see the list in Table 2).

Table 2 List of Sentinel-2 vegetation indices used in the study (Sentinel Hub 2020, Klem et al. 2014)

CIRE	Chlorophyll index using red-edge and NIR
EVI	Enhanced Vegetation Index
IRECI	Inverted Red-Edge Chlorophyll Index
NDMI	Normalized Difference Moisture Index
NDRE	Normalized Difference Red Edge Index
NDVI	Normalized Difference Vegetation Index
NRERI	Normalized Red Edge Index
REIP	Red Edge Inflection Point
RENDVI	Red Edge NDVI
SCI	Soil Composition Index

The results of crop mapping by plant sampling and datasets from Sentinel-2 were processed in Geographic Information System ArcMap 10.6.1 (ESRI, Redlands, USA). For each sampling point, the pixel value of Sentinel-2 vegetation indices was obtained by overlay analysis. The data was then exported to Microsoft Excel (Microsoft Corporation, Redmond, USA) and subsequently to Statistica 12 (Tibco, USA) for correlation and regression analysis.

RESULTS AND DISCUSSION

Basic statistical characteristics of results from laboratory analysis of plant samples taken from five locations and vegetation stages (BBCH 31 and 45) are shown in Table 3. High values of the coefficient of variation (CV) indicate high variability within the fields, the highest CV was reached for Nupt in Kardasova Recice (33.14%).

Table 3 Basic statistics of plant sampling results

	Location	Count	Average	Median	Minimum	Maximum	Std	CV (%)
N [%]	Otnice_1	20	3.92	3.89	3.18	4.92	0.45	11.44
Biomass [t/ha]	Otnice_1	20	2.07	2.07	0.50	3.12	0.61	29.38
Nupt [kg/ha]	Otnice_1	20	81.01	74.03	23.06	122.76	26.75	33.02
N [%]	Otnice_2	20	2.88	2.88	2.15	3.58	0.40	13.78
Biomass [t/ha]	Otnice_2	20	5.56	5.73	3.94	6.64	0.84	15.05
Nupt [kg/ha]	Otnice_2	20	159.36	151.75	115.34	215.01	29.78	18.69
N [%]	Dol. Dubnany	26	2.63	2.52	1.97	3.66	0.42	16.07
Biomass [t/ha]	Dol. Dubnany	26	5.20	5.36	2.43	6.60	1.12	21.54
Nupt [kg/ha]	Dol. Dubnany	26	134.86	138.73	86.36	188.21	29.34	21.75
N [%]	Zdounky	20	2.70	2.73	2.10	3.37	0.31	11.32
Biomass [t/ha]	Zdounky	20	7.26	7.27	4.98	9.38	0.99	13.59
Nupt [kg/ha]	Zdounky	20	196.71	204.84	108.03	282.39	35.52	18.06
N [%]	Rasovice	21	2.45	2.53	2.02	3.01	0.29	11.69
Biomass [t/ha]	Rasovice	21	7.53	7.59	3.79	10.44	1.83	24.24
Nupt [kg/ha]	Rasovice	21	186.58	200.48	81.97	275.52	55.37	29.67
N [%]	Kardas. Recice	21	3.02	3.04	2.03	3.77	0.39	12.89
Biomass [t/ha]	Kardas. Recice	21	4.38	4.32	2.63	7.30	1.25	28.56
Nupt [kg/ha]	Kardas. Recice	21	132.58	126.07	66.86	241.58	43.93	33.14

Legend: Std – standard deviation; CV – coefficient of variation; N – nitrogen content; Nupt – nitrogen uptake; Otnice_1/Otnice_2 – first / second plant sampling (BBCH 31 / BBCH 45)

The plant analysis in two phenological stages in Otnice allowed to observe dilution effect of nitrogen in plants – with increasing amount of biomass is decreasing the nitrogen content in plants (from 3.92 N% to 2.88 N%). However, calculation of Nitrogen uptake showed increase from 81 kg/ha N to 159 kg/ha N. The overall range of Nupt varied from 20 to 280 kg/ha N.

The relationship between crop parameters and Sentinel satellite indices was evaluated using the Spearman correlation coefficient (Table 4). Attention was paid to the sensitivity of individual vegetation indices to the crop parameters, mainly on the nitrogen uptake as the main indicator of the nutritional status of the plants, and differences between all observed locations. The high correlation coefficient between Nupt and biomass showed a large influence of the amount of biomass on the consumption of N. When evaluating the relationship among vegetation indices, biomass and Nupt for all localities, the highest values of correlation coefficient were achieved for red-edge vegetation index REIP. Although the vegetation index NDVI is the most frequently used in most publications, in our study the lowest values of the correlation coefficient were obtained for it, all other evaluated indices were more sensitive to the amount of biomass and to Nupt than the NDVI index.

Table 4 Correlation coefficients between crop parameters and vegetation indices for individual sites. Red values represent statistically significant results at 95% of probability.

	Location	Nupt [kg/ha]	CIRE	EVI	IRECI	NDMI	NDRE	NDVI	NRERI	REIP	RENDVI	SCI
N [%]	Otnice_1	0.385	0.364	0.221	0.295	0.093	0.364	0.379	0.442	0.412	0.448	-0.093
Biomass [t/ha]	Otnice_1	0.916	0.611	0.714	0.627	0.659	0.611	0.597	0.633	0.614	0.609	-0.659
Nupt [kg/ha]	Otnice_1	**1.000**	**0.764**	**0.811**	**0.749**	**0.699**	**0.764**	**0.762**	**0.809**	**0.788**	**0.789**	**-0.699**
N [%]	Otnice_2	0.532	0.241	0.523	0.392	0.289	0.241	0.443	0.392	0.036	0.390	-0.289
Biomass [t/ha]	Otnice_2	0.650	0.498	0.406	0.481	0.326	0.498	0.072	0.472	0.602	0.466	-0.326
Nupt [kg/ha]	Otnice_2	**1.000**	**0.681**	**0.747**	**0.749**	**0.582**	**0.681**	**0.444**	**0.756**	**0.564**	**0.741**	**-0.582**
N [%]	D. Dubn.	0.309	0.037	-0.131	-0.086	-0.205	0.037	0.002	-0.031	-0.080	-.0.056	0.205
Biomass [t/ha]	D. Dubn.	0.739	0.627	0.734	0.692	0.737	0.627	0.649	0.708	0.686	0.719	-0.737
Nupt [kg/ha]	D. Dubn.	**1.000**	**0.741**	**0.707**	**0.701**	**0.651**	**0.741**	**0.725**	**0.756**	**0.681**	**0.746**	**-0.651**
N [%]	Zdounky	0.700	0.375	0.156	0.201	0.183	0.375	0.073	0.402	0.422	0.361	-0.183
Biomass [t/ha]	Zdounky	0.594	0.242	0.071	0.057	0.179	0.242	-0.015	0.513	0.543	0.529	-0.179
Nupt [kg/ha]	Zdounky	**1.000**	**0.436**	**0.277**	**0.233**	**0.296**	**0.436**	**0.120**	**0.608**	**0.614**	**0.582**	**-0.296**
N [%]	Rasovice	0.662	0.542	0.537	0.488	0.521	0.542	0.609	0.594	0.440	0.581	-0.521
Biomass [t/ha]	Rasovice	0.919	0.869	0.894	0.865	0.868	0.869	0.804	0.821	0.696	0.803	-0.868
Nupt [kg/ha]	Rasovice	**1.000**	**0.875**	**0.888**	**0.858**	**0.861**	**0.875**	**0.830**	**0.845**	**0.679**	**0.826**	**-0.861**
N [%]	K. Recice	0.297	0.099	0.198	0.155	0.166	0.099	0.212	0.222	0.035	0.222	-0.166
Biomass [t/ha]	K. Recice	0.856	0.799	0.714	0.739	0.723	0.799	0.734	0.701	0.764	0.701	-0.723
Nupt [kg/ha]	K. Recice	**1.000**	**0.808**	**0.745**	**0.768**	**0.751**	**0.808**	**0.782**	**0.730**	**0.781**	**0.730**	**-0.751**

Legend: N – nitrogen content; Nupt – nitrogen uptake

Figure 1 Sentinel-2 REIP image of the experimental fields, black crosses represent sampling points

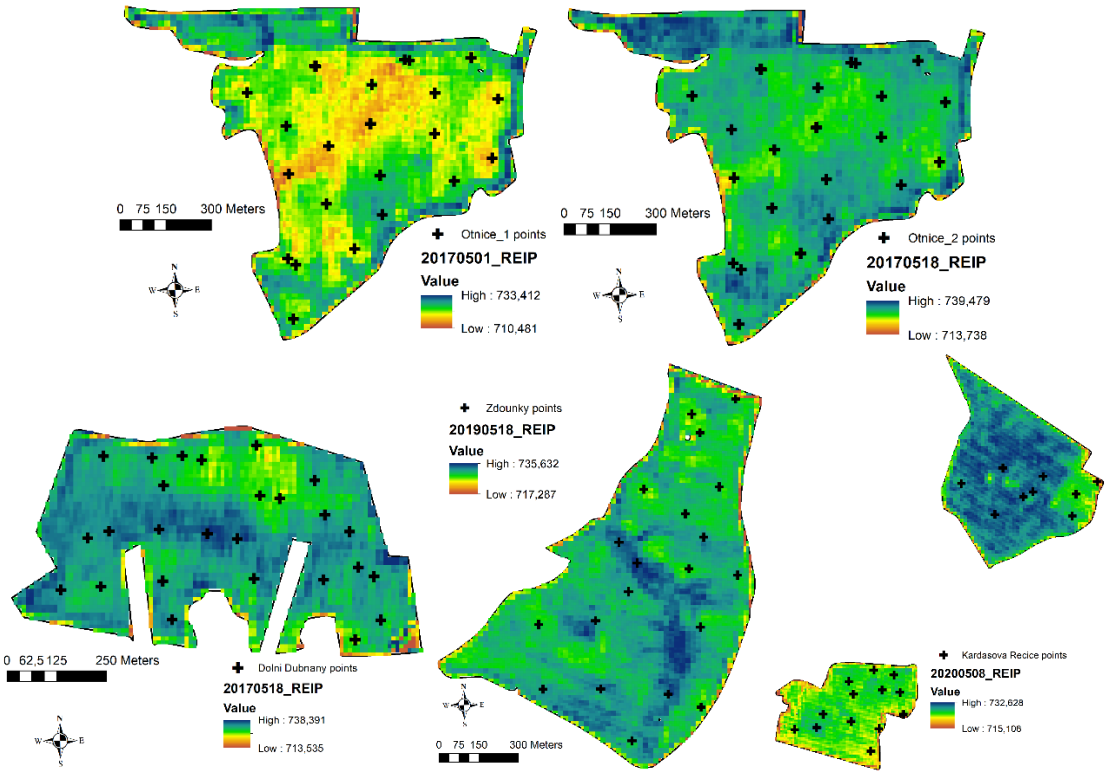

The evaluation of the sensitivity of vegetation indices to the observed crop parameters for individual localities proved also high effect of biomass on Nupt among all localities. Overall,

the highest values of correlation coefficients for all vegetation indices were reached for the locality Rasovice, on the contrary, the lowest values were reached for the locality Zdounky, where a large part is not even statistically significant. Exclusion of the Zdounky locality in the evaluation selected CIRE, EVI, NDRE and NRERI indices as the most sensitive. Including low values of the correlation coefficient for the Zdounky locality, the best results were achieved for the NRERI and RENDVI indices. Both indices appear to be the most universal across all localities and can thus be recommended for a comprehensive diagnosis of plant nutrition in the vegetation phase from stem elongation to booting. The map results of REIP are shown in Figure 1.

Figure 2 Scatterplot of vegetation index REIP (left) and NDVI (right) and Nupt

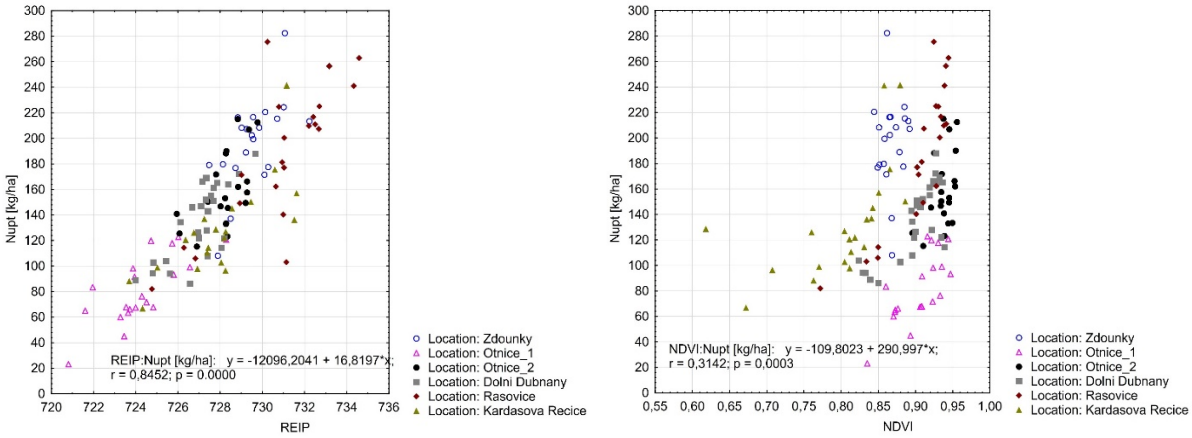

More detailed results of the analysis of relationship between vegetation index (REIP, NDVI) and Nupt across all sites is documented by scatter plots (Figure 2). Individual localities are distinguished by classification of point clusters. For the Otnice locality, there is a noticeable increase in vegetation and an increasing value of vegetation indices between the two samples. For the REIP index, almost all points had linear distribution, so a universal regression equation can be used. Different situation was observed by NDVI, which showed exponential distribution with ride-side cumulation of values (up to NDVI = 0.95). As reported by Li et al. (2008), the relationship between vegetation indices and stand parameters changes during the vegetation period, which is reflected in the lower sensitivity of vegetation indices at a higher leaf area index (LAI). This is known as the saturation effect of NDVI and it is typical behavior of NDVI values at a higher LAI of vegetation.

CONCLUSIONS

The relationship between vegetation indices from the Sentinel-2 satellite and diagnostics of the nutritional status of the winter wheat crop stand was investigated in this study. High values of correlation coefficients between vegetation indices and nitrogen uptake were found. The most consistent results for all localities were achieved for the vegetation indices NRERI, REIP and RENDVI, which thus appear to be the most universal indices for the evaluation of plant nutritional diagnostics. The relationship between crop parameters and vegetation indices was not the same across all studied localities. The best values were achieved for the Rasovice locality, on the contrary the lowest values for the Zdounky locality. These results proved that in case of Sentinel-2 multispectral imagery, calculation of set of vegetation indices is useful, at least from the red-edge part of electromagnetic spectrum. However, the availability and subsequent quality of the captured scenes of Sentinel-2 depends on the presence of clouds in the satellite scene. High occurrence of cloud cover decreases the usability of the data for reliable estimation of crop status within the fields.

ACKNOWLEDGEMENTS

This study was supported by Internal Grant Agency of Faculty of AgriSciences at Mendel University in Brno as the research project AF-IGA2020-IP054.

REFERENCES

Adan, M.S. et al. 2017. Integrating Sentinel-2 derived vegetation indices and terrestrial laser scanner to estimate above-ground biomass/carbon in ayer hitam tropical forest Malaysia. Thesis, University of Twente, Netherlands. Available at: webapps.itc.utwente.nl/librarywww/papers_2017/msc/nrm/adan.pdf. [2020-08-26].

Frampton, W.J. et al. 2013. Evaluating the capabilities of Sentinel-2 for quantitative estimation of biophysical variables in vegetation. ISPRS Journal of Photogrammetry and Remote Sensing, 82: 83–92.

Klem, K. et al. 2014. Využití měření spektrální odrazivosti a odvozených specializovaných vegetačních indexů v pěstební technologii jarního ječmene. Methodology for agricultural practice. Kroměříž, Brno, Havlíčkův Brod.

Lantzanakis, G. et al. 2016. Comparison of physically and image based atmospheric correction methods for Sentinel-2 satellite imagery. In Proceedings of Fourth International Conference on Remote Sensing and Geoinformation of the Environment (RSCy2016). Paphos, Cyprus, 4–8 April.

Li, F. et al. 2008. Estimating N status of winter wheat using a handheld spectrometer in the North China Plain. Field Crops Research, 106(1): 77–85.

Ryant, P., Dryšlová, T. 2015. Optimalizace výživy rostlin. In PRECIZNÍ ZEMĚDĚLSTVÍ: Technologie a metody v rostlinné produkci. Brno, pp. 111–137.

Sentinel Hub. 2020. Sentinel 2 EO products [Online]. Ljubljana: Laboratory for geographical information systems, Ltd. Available at: https://www.sentinel-hub.com/develop/documentation/eo_products/Sentinel2EOproducts. [2020-08-25].

Söderström, M. et al. 2016. CropSAT – A public satellite-based decision support system for variable-rate nitrogen fertilization in Scandinavia. In Proceedings of 13th International Conference on Precision Agriculture (ICPA). St Louis, USA, pp. 1–8.

The influence of pyrethroid cypermethrin on non-target species *Harmonia axyridis* ladybird

Aneta Necasova[1], Zaneta Prazanova[1], Eva Hrudova[1], Marek Seidenglanz[2]
[1]Department of Crop Science, Breeding and Plant Medicine
Mendel University in Brno
Zemedelska 1, 613 00 Brno
[2]AGRITEC, Research, Breeding and Services, Ltd.
Zemedelska 16, 787 01, Sumperk
CZECH REPUBLIC

aneta.necasova@mendelu.cz

Abstract: This study deals with the influence of insecticide active ingredients on selected non-target organisms. Aphidophagous harlequin ladybird (*Harmonia axyridis)* was the tested species, a non-native species that occurs in large populations across the Czech Republic, even in agrocenosis. The objective was to find out if this useful insect was affected by plant protection products (PPP), as was the case with pests of agricultural crops, and whether the development of resistance against selected active ingredients (AI) of insecticides occurred here as well. During the 2020 vegetation season, individual harlequin ladybirds were collected at selected sites and subsequently tested in a laboratory for sensitivity to cypermethrin AI in different concentrations. The efficiency of this AI was evaluated, and from the values acquired, the percentage mortality at the registered dose was calculated. Results were further processed using the specialised POLO PLUS 2.0 software, which calculates values of lethal doses of LD50, LD90 and LD95. As the results show, the mortality increase was recorded due to the increasing dose of the tested AI. From the calculated mortality values and lethal dose, it was found that harlequin ladybird populations are sensitive to the affect of cypermethrin, and thus, the negative influence of this PPP on non-target organisms was verified.

Key Words: Harmonia axyridis, resistance, natural enemy, active ingredient, insecticide

INTRODUCTION

Harlequin ladybird (*Harmonia axyridis* [Pallas, 1773]) is a predatory beetle that belongs to the Coccinellidae family (Poutsma 2008). This family is significant mainly because of its diversity and ability to adapt to different habitats (Ali et al. 2018). The harlequin ladybird comes from East Asia and is quite variable in terms of elytron colouring (Nedvěd 2014). Even though the harlequin ladybird is an invasive species, it is being introduced and used in biological plant protection against insect pests throughout the world. The first population of this ladybird was introduced for biological protection in the USA in 1916 (Brown et al. 2008). In the Czech Republic, the first individuals were introduced for use in hop gardens in 2003 (Nedvěd 2014). Its extension was recorded throughout the whole country during 2006–2009 (Panigaj et al. 2014). Currently, the harlequin ladybird, because of its preference for woody plants, is used mainly in orchards as a natural predator for aphids and used less in field crops and greenhouses. Thanks to its natural link to woody plants and people's homes, one of the most common biotopes of this species are ornamental shrubs and trees (Nedvěd 2014). In the case of aphid overgrowth, it can be used on cereals (Honěk et al. 2017). In a heterogeneous environment, the harlequin ladybird can coexist with other predator species (Osawa 2011).

Due to the intensive production of monocultural crops, the risk of pest occurrence increases. This fact leads to an increased need for chemical treatment of vegetation by plant protection products (PPP). In the case of insect pests, this means insecticides. Recently, synthetic agents have been used for insecticide protection of plants. Zimmer et al. (2014) state that the most used group of insecticide agents are synthetic pyrethroids. The increasing need for treatment with these products also causes an increase in plant protection costs. The reason is that PPP, especially ones with the same active ingredient (AI), are applied repeatedly and, in some cases, inaccurately (Stará et al. 2009). The result

is a negative effect on the quality of the environment and on natural enemies of agricultural crops pests, which are also limited by these interventions.

The diversity of population in nature, so-called genetic variability within a population, influences the emergence of resistance. Resistance is defined as an organism's ability to resist adverse influences or a characteristic that allows them to persist against adverse conditions (Petráčková and Kraus 2001). Resistance is an ability inherited or acquired by a process called mutation. According to the Insecticide Resistance Action Committee (IRAC, 2020), resistance can appear within 2–20 years after the introduction or first use of an active ingredients of insecticide. Resistance then results in the inefficiency of an insecticide (Stará et al. 2009). The level of resistance should be monitored, especially in the case of useful organisms. It is the only way to determine the level of the negative influence of PPP on these organisms and effectively support their occurrence at the same time.

MATERIAL AND METHODS

Sampling of *Harmonia axyridis* imagoes

The collection of harlequin ladybirds took place at selected areas during the 2020 vegetation season. The selected areas were numbered: 1 – Ořechov (Brno–venkov), 2 – Brno-Chrlice and 3 – Těšany (Brno–venkov) (Figure 1). Localities of individual populations had to be at least five kilometres apart. The foliage-beating method was chosen for the collection of individuals. The number of individuals was set to be sufficient for testing the chosen AI. According to Nedvěd (2014), beetles should be placed in glass bottles. A small number of plants infested with aphids that served as food to avoid cannibalism within individuals were also placed in these bottles. Absorbent paper was inserted into bottles to absorb surplus moisture. The samples thus prepared were then transported to a laboratory in a thermobox, so they were not subjected to temperatures higher than 20 °C.

Figure 1 Geographical location of areas

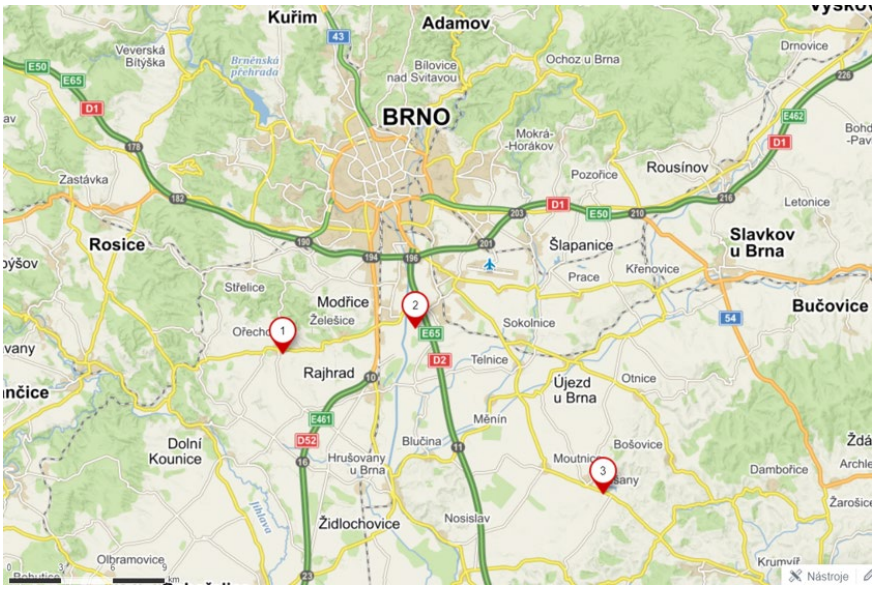

Laboratory testing

The IRAC method No. 011 for pyrethroids using the adult-vial-test was used for laboratory testing.

The cypermethrin AI was selected for testing. Dosages were derived from the doses registered for the winter rape plant (*Brassica napus* var. *napus*). The reason for selecting this crop was that rape is very frequently sown, and thus, it is often treated against pests. Additionally, pyrethroids are among the most common AIs.

One millilitre of an AI's solution was applied to each glass vial using a dosing pipette. Acetone was used as a solvent. The AI was applied in various concentrations, namely, 0% (control dose, acetone only), 1.33% dose (= 0.33 g cypermethrin/ha), 4% dose (= 1 g cypermethrin/ha), 20% dose (= 5 g

cypermethrin/ha), 100% dose (= 25 g cypermethrin/ha → registered out-of-field dose in the Czech Republic) and 500% dose (= 125 g cypermethrin/ha). Three repetitions were performed for each dose. The whole inner surface of each vial was covered with an AI using a laboratory roller. Imagoes were inserted into prepared vials using soft entomological tweezers: five individuals into each vial. The vials were then closed with a ventilated lid, and subsequently, the vials were placed for 24 hours into a thermostat at 20 °C. Two hundred and seventy specimens of *Harmonia axyridis* were tested during the experiment in total. The progress of the laboratory testing is illustrated in Figure 2.

Figure 2 Use of adult-vial-test during testing by IRAC methods

RESULTS AND DISCUSSION

The efficiency of the AI used on individuals was assessed after 24 hours. The number of live, dead and tremor individuals was evaluated. The mortality percentage was assessed at 100% dose of the AI cypermethrin, which is shown in Table 1. From these values, it is clear that tested individuals were sensitive to the selected AI. In cooperation with the Agritec Plant Research s.r.o. company, Šumperk, the results of laboratory tests executed at Mendel University in Brno were further processed using specialised software, POLO PLUS 2.0. This program calculated the values of lethal doses – LD50, LD90 and LD95. All data are stated in Table 2.

Table 1 Mortality assessment for the active ingredient cypermethrin

Active substance	**Locality**	**Replicate 1**				**Replicate 2**				**Replicate 3**				**Mortality (%)**
		Total amount	Dead	Alive	% mortality	Total amount	Dead	Alive	% mortality	Total amount	Dead	Alive	% mortality	
Cypermethrin	1	5	4	1	80	5	5	0	100	5	5	0	100	93.33
	2	5	5	0	100	5	5	0	100	5	5	0	100	100
	3	5	5	0	100	5	5	0	100	5	5	0	100	100

Table 2 Evaluation of the adult-vial-test for cypermethrin

Locality	Active substance (preparation)	Registered dose (g/ha)	Mortality (%)	LD 50 (g/ha)	LD 90 (g/ha)	LD 95 (g/ha)
1	Cypermethrin	25	93.33	0.908	9.028	17.314
2	Cypermethrin	25	100	0.099	1.500	3.238
3	Cypermethrin	25	100	0.706	4.106	6.763

In Figure 3 the mortality growth (y) against the increase in dose (x) of an active ingredient is given.

Figure 3 Mortality growth (y) against the increase in dose (x) for cypermethrin in real quantities and transformed (log = decimal logarithm) values

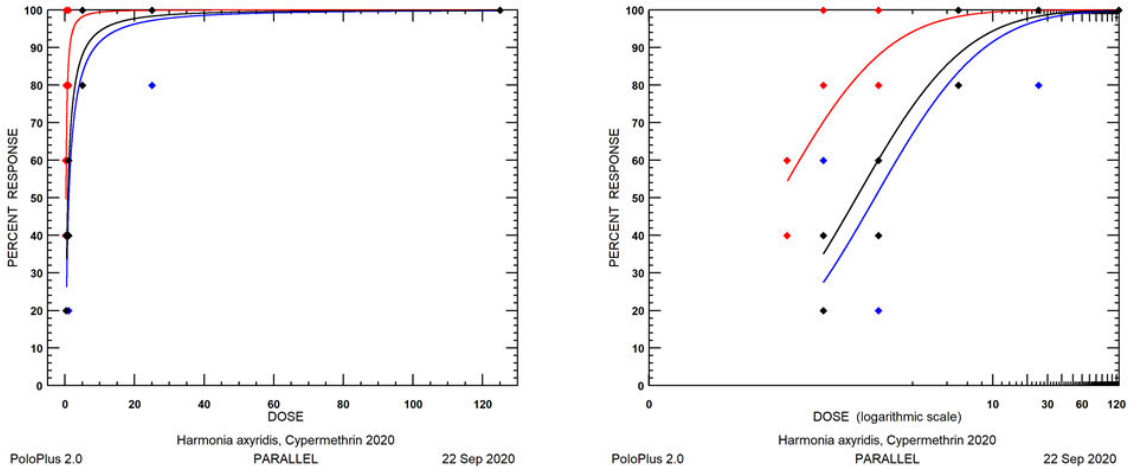

Based on the monitored mortality and calculation of lethal doses, it can be stated that tested populations of the harlequin ladybird (*Harmonia axyridis*) were sensitive to the influence of the cypermethrin pyrethroid. Rodrigues et al. (2013) monitored the reaction of *Hippodamia convergens* populations of lambda-cyhalothrin pyrethroid, and their results confirmed that resistance is a genetically conditioned feature. Costa et al. (2018) also tested field populations of *Eriopis connexa* for lambda-cyhalothrin pyrethroid, and 50% of their tested samples showed resistance against this AI. All these authors confirmed that the resistance of the above stated AI was ten times higher after 54.5 generations of selection.

The problem of pest resistance against insecticides, namely to pyrethroid AIs, is commonly monitored within the Czech Republic (e.g. Seidenglanz et al. 2017), as well as abroad (e.g. Joseph et al. 2017). However, in terms of natural predators, it is still monitored only rarely, and there is a lack of data about it.

CONCLUSION

The submitted study clearly shows that monitored populations of the harlequin ladybird are negatively affected by the AIs from the pyrethroids group. The repeated application of plant protection products can subsequently cause resistance to used active ingredient. In the case of agricultural crops pests, this phenomenon is a significant problem in practice. In the case of natural predators, however, the opposite is true because the selection of resistant populations guarantees that there always will be individuals in vegetation that will be able to suppress survivor pests so that they can slow down their subsequent overgrowth.

ACKNOWLEDGEMENTS

This research was financially supported by grant No. AF-IGA2020-IP055.

REFERENCES

Ali, M. et al. 2018. An annotated checklist of Coccinellidae with four new records from Pakistan (Coleoptera, Coccinellidae). ZooKeys [Online], 803: 93–120. Available at: https://zookeys.pensoft.net/article/22543/. [2020-08-27].

Brown, P.M.J. et al. 2008. *Harmonia axyridis* in Europe: spread and distribution of a non-native coccinellid. Biological Control, 53(1): 5–21.

Costa, P. et al. 2018. Field-evolved resistance to λ-cyhalothrin in the lady beetle *Eriopis connexa*. Bulletin of Entomological Research, 108(3): 380–387.

Honěk, A. et al. 2017. Mšice na obilninách: biologie, prognóza a regulace. Certified methodology. Praha: Výzkumný ústav rostlinné výroby, v.v.i.

IRAC (Insecticide Resistance Action Committee) Test Methods. 2020. [Online]. Available at: https://www.irac-online.org/. [2020-08-27].

Joseph, S.H. et al. 2017. Outlook of pyrethroid insecticides for pest management in the Salinas Valley of California. Journal of Integrated Pest Management, 8(1): 1–11.

Nedvěd, O. 2014. Slunéčko východní (*Harmonia axyridis*) – pomocník v biologické ochraně nebo ohrožení biodiverzity? Certifikovaná metodika pro praxi. 2nd ed., České Budějovice: Jihočeská univerzita v Českých Budějovicích.

Osawa, N. 2011. Ecology of *Harmonia axyridis* in natural habitats within its native range. Biological Control, 56(4): 613–621.

Panigaj, L. et al. 2014. The invasion history, distribution and colour pattern forms of the harlequin ladybird beetle *Harmonia axyridis* (Pall.) (Coleoptera, Coccinellidae) in Slovakia, Central Europe. ZooKeys [Online], 412: 89–102. Available at: https://zookeys.pensoft.net/articles.php?id=3822. [2020-08-27].

Petráčková, V., Kraus, J. 2001. Akademický slovník cizích slov A–Ž. 1st ed., Praha: Nakladatelství Akademie Věd ČR.

Poutsma, J. et al. 2008. Predicting the potential geographical distribution of the harlequin ladybird, *Harmonia axyridis*, using the CLIMEX model. Biological Control, 53: 103–125.

Rodrigues, A.R.S. et al. 2013. Pyrethroid resistance and its inheritance in a field population of *Hippodamia convergens* (Guérin-Méneville) (Coleoptera: Coccinellidae). Pesticide Biochemistry and Physiology, 105(2): 135–143.

Seidenglanz, M. et al. 2017. Negative correlations between the susceptibilities of Czech and Slovak pollen beetle populations to lambda-cyhalothrin and chlorpyrifos-ethyl in 2014 and 2015. Plant Protection Science, 53(2): 108–117.

Stará, J. et al. 2009. Metodika hodnocení rezistence blýskáčka řepkového k insekticidům. Methodology for practice. Praha: Výzkumný ústav rostlinné výroby, v.v.i.

Zimmer, C. et al. 2014. Baseline susceptibility and insecticide resistance monitoring in European populations of *Meligethes aeneus* and *Ceutorhynchus assimilis* collected in winter oilseed rape. Entomologia Experimentalis et Applicata, 150(3): 279–288.

Influence of the addition of vermicompost and earthworms to the soil on the yield and quality of radish phytomass

Jakub Neupauer, Peter Kovacik
Department of Agrochemistry and Plant Nutrition
Slovak University of Agriculture in Nitra
Tr. A. Hlinku 2, 949 76 Nitra
SLOVAK REPUBLIC

xneupauer@uniag.sk

Abstract: Positive and negative findings on the impact of vermicomposts and earthworms on the quantity and quality of crops force researchers around the world to look for the causes of these different findings. In the present experiment were investigated: A) the effect of adding vermicompost to the soil and B) the influence of earthworms number (genus *Eisenia fetida*) in the soil substrate on the dynamics of changes in the weight of radish phytomass (*Raphanus sativus*) and on selected qualitative parameters of roots and leaves. The obtained results show that the tenth proportion of vermicompost from the total weight of soil substrate caused the statistically significant increase in yield of the radish roots and leaves, reducing the total polyphenols content in roots and increasing the total polyphenols content in the leaves. The addition of vermicompost to the soil also led to an increase in the content of N, S and nitrates in the roots and leaves of radish. Earthworms had a negative impact on the radish yield and a positive impact on qualitative parameters such as total polyphenols content, nitrate content and sulphur content.

Key Words: earthworms, vermicompost, total polyphenols, nitrates, nutrients

INTRODUCTION

The laic public accepted the opinion that the presence of earthworms in soil has significantly positive impact on plants. However, the worldwide findings confirm that the earthworms can influence the quantity and quality of the cultivated crops in both positive and negative way (Doan et al. 2013, Elmer 2016, Kováčik et al. 2018a). Their impact on the crops has not been researched sufficiently until now. The objective of our experiment was to acquire the answer to the question how the single vermicompost application and vermicompost application along with earthworms of genus *Eisenia fetida* influence the quantity and quality of radish phytomass (*Raphanus sativus*).

The knowledge of vermicompost application on the yield quantity, on the phytomass formation of the grown crops is usually positive (Jami et al. 2020), which is related to the significant contents of the available macronutrients and micronutrients in vermicomposts (Goswami et al. 2017). On the contrary, the impacts on the qualitative parameters are often opposite. The positive impact on the content of total antioxidants, carotenes, lycopene, carbohydrates, vitamin C, proteins, dry matter, iron and zinc in the cultivated plants was recorded by Shankar et al. (2009), Sinha et al. (2011), Ghosh et al. (2013). Reversely, the decrease of vitamin C content, the total polyphenols and the total antioxidant activity in carrot roots was detected by Kováčik et al. (2018a). The result of influence of vermicompost application on the yield parameter of the cultivated crops depends on the quality of vermicompost, its application dose, date and way of application (Lacko-Bartošová et al. 2005).

MATERIAL AND METHODS

The pot experiment was carried out in the vegetation cage located in the area of the Slovak University of Agriculture in Nitra, Slovakia. Soil (20 kg – treatment 1) and soil (18 kg) with vermicompost (2 kg) mixed in the rate 9:1 (treatments 2, 3, 4) was in spring 2017 put into the pots. Then ten and twenty individuals of adult earthworms (*Eisenia fetida*) were placed to the pots of treatment 3 (10 ind.) and treatment 4 (20 ind.). The agrochemical parameters of the used soil (Haplic Luvisol) and the soil mixed with vermicompost (S+V) are indicated in the Table 1. For the indication of the given

parameters, the following analytical methods were used: N-NH_4^+ by colorimetrically with Nessler's agent; N-NO_3^- by colorimetrically with phenol – 2.4 disulphonic acid. N_{in} = N–NH_4^+ + N–NO_3^-. The contents of available P, K were determined by Mehlich 3 extraction procedure (Mehlich 1984). Content of P by colorimetrically, K by flame photometrycally, S by spectrophotometrically, C_{ox} by spectrophotometrically after the oxidation (Tyurin 1966) and pH/KCl potentiometrically.

The experiment was established according to the method of random arrangement of pots with the quadruple repetition. The model crop was radish (*Raphanus sativus*, L) cultivar Granát. During growth season three samplings of plant material were accomplished. Total polyphenols content (TPC) was determined by the method according to Lachman et al. (2003**)** and expressed as mg of gallic acid equivalent per kg fresh mater. In order to determine nitrates was used ion-selective electrode of the type 07-35 and reference electrode of the type RCE 101. Both qualitative parameters were measured only in plants from the third sampling (May 9).

Table 1 Agrochemical properties of the soil and growing medium used in the experiment

Substrate		N_{min}	P	K	S	pH_{KCl}	C_{ox}
Description	Mark	mg/kg					**%**
Soil	S	13.2	22	156	1.3	6.97	0.92
Soil + vermicompost (9:1)	S+V	91.7	88	3,925	938	6.99	4.91

RESULTS AND DISCUSSION

The tenth proportion of vermicompost in the cultivation substrate (tr. 2) in comparison with the soil without vermicompost (tr. 1) increased the weight of radish roots and leaves on 27th day after the beginning of germination, i.e. 24th April (Table 2). The presence of earthworms in soil and also their number during the whole radish growing season had the negative impact on the weight radish roots and leaves. In the treatments 3 and 4 the weight of roots and leaves was lower than in the treatment 2. The determined facts are presumably related to the ability of earthworms to attack the root hairs, which was evident with the younger plants.

The application of vermicompost into soil (tr. 2) decreased the content of the total polyphenols in roots and increased the contents of TPC in radish leaves, which is a negative effect, because in the Slovak Republic there a radish root is predominantly being consumed (Table 3). The addition of vermicompost into soil increased the content of nitrates in both radish roots and leaves. The decrease of polyphenols and the growth of nitrates in roots after the application of vermicompost is the confirmation that fertilizing by the fertilizers containing nitrogen results mostly in the deterioration of the quality of cultivated crops (Bielek and Kudejarov 1991).

The inoculation of soil by earthworms (tr. 3 and 4 versus tr. 2) increased the content of the total polyphenols (TPC) and decreased the content of nitrates in both roots and leaves, which means the positive impact of earthworms on the stated qualitative parameters of radish.

Partly different results were presented by Kováčik et al. (2018a), who during the cultivation of carrots found that the effect of earthworms on the content of total polyphenols in the roots was insignificant and conversely, the effect on the content of the TPC in leaves was significant and positive.

In particular, the nitrogen and sulphur content significantly contribute to protein creation. Sulphur is present also in the vegetable oils, vitamins and the secondary metabolites (allines, glucosinolates). Therefore, the N and S contents in radish plants can be considered as a qualitative parameter (Lu et al. 2011, Karmakar et al. 2013, Kováčik et al. 2018b).

Due to the significant content of available nitrogen and sulphur in vermicompost (Table 1), after its addition to the soil (var. 2 versus var. 1), the contents of N and S was increased, both in the roots and leaves of radish (Table 4).

The presence of earthworms in the soil, regardless of their number (var. 3 and 4 versus var. 2), caused an increase the N and S contents in radish plants. The reason for the finding is that the activity of earthworms increases the content of available nutrients in the soil (Tripathi and Bhardwaj 2004, Garg et al. 2006, Kováčik and Ryant 2019).

Table 2 Impact of treatments on the dynamics of the changes in the weight of the radish roots and leaves (fresh matter)

Treatment		Date								
		April 24			May 3			May 9		
		g/10 ind.								
n	mark	roots	leaves	r/l	roots	leaves	r/l	roots	leaves	r/l
1	S	2.0 b	14.5 a	0.13	20.0 a	15.7 a	1.5	27.8 a	18.2 a	1.50
2	S+$V_{9:1}$	2.8 c	20.9 b	0.14	148.7 c	83.6 c	1.8	185.8 c	104.2 c	1.78
3	S+$V_{9:1}$ +EW_{10}	1.9 ab	17.2 a	0.11	106.1 b	59.2 b	1.8	142.0 b	71.0 b	2.00
4	S+$V_{9:1}$+EW_{20}	1.5 a	15.4 a	0.10	95.2 b	56.4 b	1.7	127.9 b	68.6 b	1.86
LSD $_{0.05}$		0.43	3.02		12.68	4.02		20.52	4.46	

Legend: n – number; April 24, May 3 and May 9 i.e. in 27/39, 36/48, 42/54 days after germination/sowing; ind. – individuals; $LSD_{0.05}$ – least significant difference at the level $\alpha \leq 0.05$

Table 3 Impact of vermicompost and earthworms on the content of total polyphenols and nitrates in radish plants (fresh matter)

Treatment		TPC		$NaNO_3$	
		roots	leaves	roots	leaves
n	mark	mg/kg			
1	S	545.20 c	284.31 a	570 a	1,138 a
2	S+$V_{9:1}$	462.81 a	299.60 b	1,480 c	1,262 c
3	S+$V_{9:1}$+EW_{10}	480.02 ab	325.66 c	815 b	1,014 b
4	S+$V_{9:1}$+EW_{20}	496.40 b	341.52 d	816 b	1,014 b
LSD $_{0.05}$		20.65	13.03	55.83	58.41

Legend: TPC – total polyphenol content; n. – number; $LSD_{0.05}$ – least significant difference at the level $\alpha \leq 0.05$

Increasing the number of earthworms in the container from 10 individuals to 20 (var. 3 versus var. 4) did not have an unambiguous effect on the N and S content in the radish plants. The N : S ratios (2.36 – 3.24 : 1) indicated sufficient sulphur in both leaves and roots. For field plants, the ratio N : S > 20 : 1 and for garden plants N : S > 10 : 1 are given as ratios indicating a lack of sulphur (Kováčik and Ryant 2019).

Table 4 Impact of vermicompost on nitrogen and sulphur content in radish roots and leaves (dry matter)

Treatment		Roots			Leaves		
		N	S	N : S	N	S	N : S
n	mark	mg/kg			mg/kg		
1	S	11,774 a	3,701 a	3.18	29,988 a	9,989 a	3.00
2	S+$V_{9:1}$	12,950 b	3,916 b	3.31	30,630 b	12,963 b	2.36
3	S+$V_{9:1}$+EW_{10}	13,195 c	4,216 c	3.13	34,468 c	13,477 c	2.56
4	S+$V_{9:1}$+EW_{20}	13,670 d	4,220 c	3.24	34,282 c	13,309 c	2.58
LSD $_{0.05}$		224.21	109.83		545.62	195.63	

Legend: n. – number; $LSD_{0.05}$ – least significant difference at the level $\alpha \leq 0.05$

CONCLUSIONS

The results show that the tenth proportion of vermicompost from the total weight of soil substrate caused the statistically significant increase in yield of the radish roots and leaves, reducing the total polyphenols content in roots and increasing the total polyphenols content in the leaves. Vermicompost (a nitrogen-containing fertilizer) increased the nitrate, nitrogen and sulphur content of both the radish

roots and leaves. The impact of earthworms was negative on the root and leaves weight, however there was the positive impact on the content of total polyphenols, nitrogen and sulphur in the aboveground and underground radish phytomass. Earthworms had a negative impact on the quantitative parameters of the radish yield and a positive impact on qualitative parameters of yield.

ACKNOWLEDGMENTS
This research was supported by the project VEGA no. 1/0378/20.

REFERENCES

Bielek, P., Kudejarov, V.N. 1991. Nitrogen cycle in the present agriculture. Bratislava: Príroda.

Doan, T.T. et al. 2013. Interactions between compost, vermicompost and earthworms influence plant growth and yield: A one-year greenhouse experiment. Scientia Horticulturae, 160: 148–154.

Elmer, W.H. 2016. Effect of leaf mold mulch, biochar, and earthworms on mycorrhizal colonization and yield of asparagus affected by *Fusarium crown* and root rot. Plant Disease [Online], 100: 2507–2512. Available at: https://apsjournals.apsnet.org/doi/10.1094/PDIS-10-15-1196-RE. [2020-09-10].

Garg, P. et al. 2006. Vermicomposting of different types of waste using *Eisenia foetida*: A comparative study. Bioresource Technology, 97: 391–395.

Ghosh, B.C. et al. 2013. Effect of varying soil and vermicompost mixtures on growing media and yield and quality of sweet corn. International Conference on Food and Agricultural Sciences, 55: 38–42.

Goswami, L. et al. 2017. Application of drum compost and vermicompost to improve soil health, growth, and yield parameters for tomato and cabbage plants. Journal of Environmental Management, 200: 243–252.

Jami, N. et al. 2020. Investigating the use of different levels of Mycorrhiza and Vermicompost on quantitative and qualitative yield of saffron (*Crocus sativus* L.). Scientia Horticulture, 262: 109027.

Karmakar, K. et al. 2013. Chemical composition of some leafy vegetables of Bangladesh. Dhaka University Journal of Science, 61(2): 199–201.

Kováčik, P. 2018a. Determination of the carrot (*Daucus Carota* L.) yields parameters by vermicompost and earthworms (*Eisenia foetida*). Slovak Journal of Food Sciences, 12(1): 520–526.

Kováčik, P. 2018b. Impact of vermicompost as component of growing medium on phytomass formation of radish (*Raphanus sativus* L.). Agriculture [Online], 64(3): 106–115. Available at: https://content.sciendo.com/view/journals/agri/64/3/article-p106.xml?product=sciendo. [2020-09-08].

Kováčik, P., Ryant, P. 2019. Agrochémia (princípy a prax). 1st ed., Nitra: Slovenská poľnohospodárska univerzita.

Lacko-Bartošová, M. et al. 2005. Udržateľné a ekologické poľnohospodárstvo. 1. vyd. Nitra: Slovenská poľnohospodárska univerzita.

Lu, H.J. et al. 2011. Growth and yield responses of crops and macronutrient balance influenced by commercial organic manure used as a partial substitute for chemical fertilizers in an intensive vegetable cropping system. Physics and Chemistry of the Earth, 36: 387–394.

Mehlich, A. 1984. Mehlich 3 soil test extractant: A modification of Mehlich 2 extractant. Communication in Soil Science and Plant Analysis [Online], 15(12): 1409–1416. Available at: https://www.tandfonline.com/doi/abs/10.1080/00103628409367568. [2020-09-15].

Shankar, K.S. 2009. Effect of organic farming on nutritional profile, quality characteristics and toxic parameters of spinach crop. Indian Journal of Dryland Agricultural Research and Development, (24)2: 66–73.

Sinha, R.K. 2011. Organic farming by vermiculture: Producing safe, nutritive and protective foods by earthworms (Charles Darwin's Friends of Farmers). American Journal of Experimental Agriculture, 1(4): 363–399.

Tripathi, G., Bhardwaj, P. 2004. Comparative studies on biomass production life cycles and composting efficiency of *Eisenia foetida* (Savigny) and *Lampito mauritii* (Kinberg). Bioresource Technology, 92: 275–283.

Tyurin, I.V. 1966. K metodike analiza deja sravníteľnogo izučenja sostava počvennogo pereg noja ili gumusa. Voprosy genezisa i plodorodija počv. Moskva: Nauka.

The influence of age of pheromone lures on *Grapholita funebrana* on their efficiency

Zaneta Prazanova, Aneta Necasova, Hana Sefrova
Department of Crop Science, Breeding and Plant Medicine
Mendel university in Brno
Zemedelska 1, 613 00 Brno
CZECH REPUBLIC

xprazano@mendelu.cz

Abstract: In 2020 (May to August), we compared the efficiency of pheromone lures of different age from the Propher s.r.o. company on *Grapholita funebrana.* The monitoring took place at a co-operative farm in Starý Lískovec. In total, five green delta traps from the Propher company were used together with pheromone lures from 2014, 2017, 2018, 2019 and 2020. *Grapholita funebrana* was recorded in all traps, and 113 imagoes were caught in total. Most imagoes (43) flew to the 2020 pheromone. On the contrary, fewest imagoes (3) flew to the 2014 pheromone. 394 individuals of non-target species were recorded in total. Most imagoes of non-target species, 140 in total, flew to the 2018 pheromone lure, and fewest (27) to the 2019 pheromone lure. Based on the monitoring, the influence of the age of pheromone lures on their efficiency was proved.

Key Words: Grapholita funebrana, monitoring, pheromone lure

INTRODUCTION

More and more pressure is being placed on growers to take less drastic plant protection measures. Essentially, it is about reducing the use of chemical substances to the minimal level necessary. One of the considerate approaches to plant protection is using synthetic, usually sexual, pheromones (Hrdý and Pultar 1998). Currently, nine pheromone-based products for plant protection and 17 products based on semiochemicals are registered in the Czech Republic (CISTA 2020).

Pheromone specificity is given by the chemical structure of individual ingredients, its mutual ratio and the presence of inhibitors (Hrdý et al. 1979, 1993, Hrdý 2006). Pheromones find practical use especially in plant protection against moths from the Tortricidae family. Pheromones do not affect non-target species adversely (Witzgall et al. 2010).

Tortricidae caterpillars cause great damage in agriculture and forestry and attack leaves, shoots or fruits. *Grapholita funebrana* Treitschke, 1835, is the main plum pest. The first-generation caterpillars are evolving on unripe fruits and have lesser economic impact. Serious damages are caused by the second-generation caterpillars that cause worminess of ripening fruits (Šefrová 2003, Hrdý 2006).

Pheromone lures are made of gum or rubber; therefore, they represent additional waste that burdens the environment. At the same time, lures are relatively expensive plant protection products, thus the usage of older pheromones may save costs at agricultural holdings. Effective monitoring and signalization of *Grapholita funebrana* in orchards may help improve the business's economy.

MATERIALS AND METHODS

Defining the study areas

Monitoring of *Grapholita funebrana* took place at a plum orchard in Starý Lískovec in Brno from May to August 2020. The orchard lies at an altitude of 270 m, within an area of approximate 2 ha. Regular treatments with synthetic insecticides against Tenthredinidae are performed here. The orchard is surrounded by apricot and apple orchards. A spectrum of the following varieties is grown here: 'Haganta', 'Top End', 'Top First'. Meteorological data are monitored here by an automatic

meteorological station. The characteristics of the study area are stated in Table 1; the climate conditions characteristic of the area are stated in Table 2.

Table 1 Description of study area Starý Lískovec (https://www.google.cz/maps, https://www.jablka.cz/)

Study area	Starý Lískovec
Coordinates	49°09'31.4"N, 16°34'25.1"E
Fauna square	6865
Altitude	270 m
Area	2 ha
Type of fruit tree	plum

Table 2 Climatic conditions characteristic of the study area Starý Lískovec according to Quitt (1971)

Climatic region	T2
Number of summer days	50–60
Number of days with average temperature of 10 °C or more	160–170
Number of frosty days	100–110
Number of icy days	30–40
Average air temperature in January	-2– -3
Average air temperature in April	8–9
Average air temperature in July	18–19
Average air temperature in October	7–9
Average number of days with precipitation of 1 mm and more	80–100
Sum of precipitation in vegetation period	350–400
Sum of precipitation in winter period	200–300
Number of days with snow cover	40–50
Number of cloudy days	120–140
Number of bright days	40–50

Material

Green delta-type pheromone lures from the Propher s.r.o. company were used for the monitoring (Figure 1). Green glue plates, which are inserted inside the traps, have an area of 246 cm^2. A pheromone lure of different ages was inserted into each *Grapholita funebrana* trap with the active substance of (E)-dodec-8-en-1-yl acetate (0.0012 g/kg), (Z)-dodec-8-en-1-ol (0.0204 g/kg), Chemstop Ecofix (20–25%) and dodecyl acetate (0.2784 g/kg). All pheromone lures used were supplied by the Propher s.r.o. company. These were lures from 2014, 2017, 2018, 2019 and 2020 (Figure 1).

Monitoring

The traps were hung in the orchard in Starý Lískovec on 24th April 2020. The traps were placed on trees at the height of approximately 160 cm above the ground. Five green traps were hung in total. The traps were at least 50 m from each other. The glue plates were checked at least once per week and replaced according to need. Each pheromone lure was replaced after four weeks. Collected glue plates were placed into a box and transported to an entomological laboratory where they were subjected to further examination (Figure 1). To determine the tortrix moths, Razowski's monograph (2001) was used.

Figure 1 Green delta-type lures, pheromones of Grapholita funebrana and laboratory works

RESULTS AND DISCUSSION

Grapholita funebrana

Grapholita funebrana presence was recorded in all traps. The first catch was recorded by the beginning of May, in the week of 4th May to 10th May 2020. Jakubíková et al. (2016), as well as Hrdý et al. (1993), present similar findings. 133 imagoes of this species were collected in total (Figure 2). Most individuals of the target species were recorded on the 2020 pheromone lure (43 imagoes), which represent almost half (47.25%) of the total number of collected species on the given lure. On the contrary, the fewest individuals of *Grapholita funebrana* were recorded on the 2014 lure (3 imagoes), which represents 2.13% of the total number of recorded species on the 2014 lure. This assumption has been met. However, comparing to the 2020 lure, a percentage of almost the same number of *Grapholita funebrana* imagoes (44.9%) flew to the 2019 lure. Thus, even this older lure can be used for monitoring in the orchard (Table 3).

Table 3 Percentage share of Grapholita funebrana imagoes from the total number of collected individuals of all trapped species

Pheromone lure	%
GF 2014	2.13
GF 2017	18.00
GF 2018	20.45
GF 2019	44.90
GF 2020	47.25

Figure 2 Numbers of Grapholita funebrana species with using the different old pheromone lures for tortricid moths

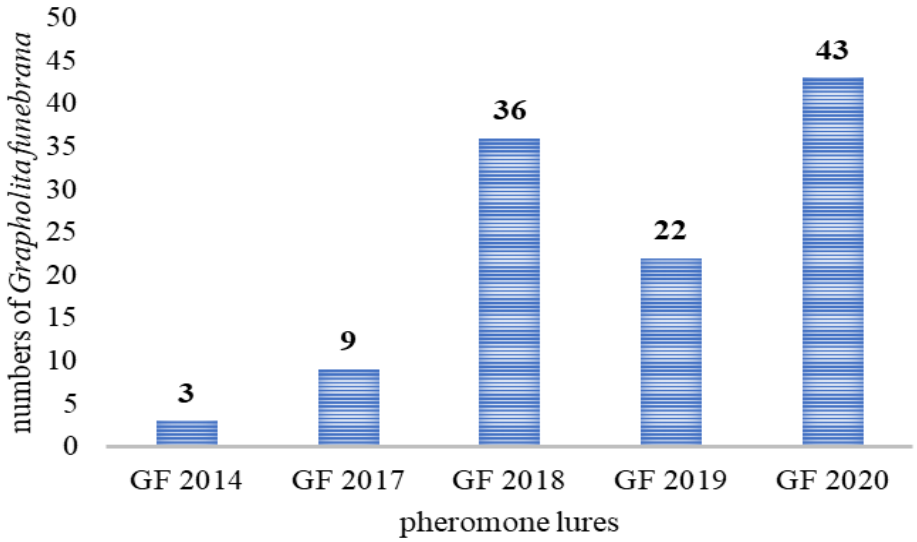

Non-target species

In total, 394 individuals of non-target species were collected (Figure 3). Most non-target species were caught into traps with lures from 2018 (140 imagoes) and 2014 (138 imagoes). On the 2014 lure, almost 100% of all collected species (97.87%) were non-target species. All lures always attracted more than 50% individuals of non-target species (Table 4) comparing to the target species. Fewest individuals of non-target species flew to the trap with the 2019 lures (27 imagoes). However, in terms of percentual ratio of individuals on one trap, fewest individuals flew to the 2020 lure (52.75%). Almost all imagoes of the non-target species were from the Tortricidae family. Several authors identified more than 58 non-target species on the *Grapholita funebrana* lure, from which most belong to the Tortricidae family (Hrdý et al. 1979, 1993, 1997, Velcheva 2000, Hrudová 2005, Hluchý 2011, Jakubíková et al. 2016, Pražanová 2018).

Table 4 Percentage share of non-target imagoes from the total number of collected individuals of all trapped species

Pheromone lure	%
GF 2014	97.87
GF 2017	82.00
GF 2018	79.55
GF 2019	55.10
GF 2020	52.75

Figure 3 Numbers of non-target lepidoptera species in traps with using the different pheromone lures for tortricid moths

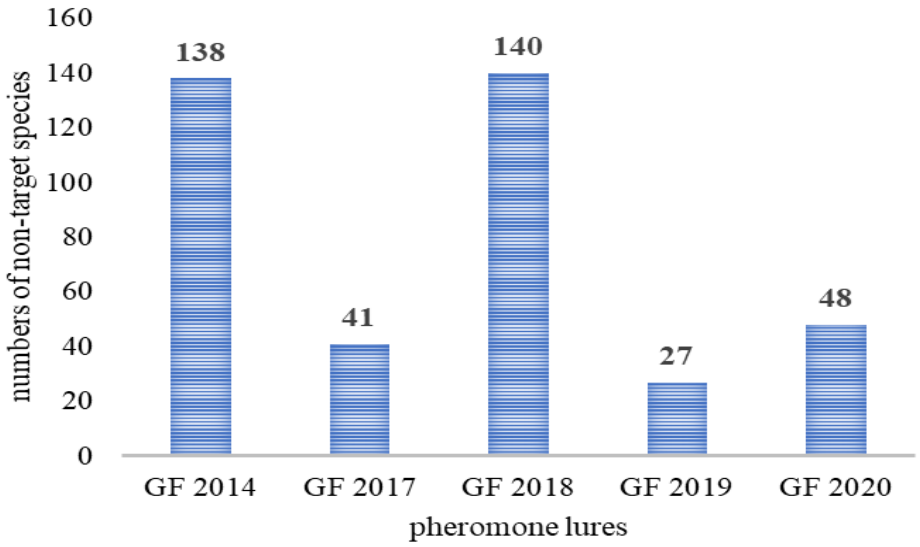

CONCLUSION

The occurrence of *Grapholita funebrana* was recorded in traps with all pheromone lures of various age. Based on the monitoring, the 2020 pheromone lure was the most effective one (43 target/48 non-target imagoes). On the contrary, the 2014 lure seemed to be the least suitable for further use (3 target/138 non-target imagoes). Year-old pheromones, stored in cold, can be also used for the monitoring of the target pest in an orchard.

ACKNOWLEDGEMENTS

The research was financially supported through grant No. AF-IGA2020-IP027.

REFERENCES

CISTA (Central Institute for Supervising and Testing in Agriculture), The register of plant protection products. 2020. [Online]. Available at: http://eagri.cz/public/app/eagriapp/POR/. [2020-09-21].

Hluchý, Š. 2011. Necílové druhy obalečů (Tortricidae) ve feromonových lapácích v ochraně jabloňových sadů, jejich letová dynamika a bionomie. Diploma thesis (in Czech) Mendel University in Brno.

Hrdý, I. 2006. Feromony v integrované ochraně rostlin V. Obaleči a makadlovka na broskvoních a švestkách. Živa, (5): 161–168.

Hrdý, I., Pultar, O. 1998. Feromonové lapáky – systémy pro monitorování hmyzích škůdců. Agro, 3(9): 19–21.

Hrdý, I. et al. 1979. Sexual pheromone activity of 8-dodecenyl and 11-tetradecenyl acetates for males of several lepidopteran species in field trials. Acta Entomologica Bohemoslovaca, 76(2): 65–84.

Hrdý, I. et al. 1993. Distribution of the fruit tree pests *Cydia molesta*, *Cydia funebrana* and *Anarsia lineatella* (Lepidoptera: Tortricidae, Gelechiidae) in former Czechoslovakia as recorded by pheromone traps. Acta Societatis Zoologicae Bohemicae, 58(1–2): 53–60.

Hrdý, I. et al. 1997. Výskyt potenciálních škůdců sadů, obaleče slivoňového, *Cydia lobarzewskii* a obaleče trnkového, *C. janthinana* (Lepidoptera: Tortricidae) v České republice a poznámky k dalším druhům podle úlovků do feromonových lapáků. Klapalekiana, 33: 155–172.

Hrudová, E. 2005. Nontarget lepidoptera species found in the pheromone traps for selected tortricid species in 2002 and 2003. Acta Universitatis Agriculturae et Silviculturae Mendelianae Brunensis, 53(1): 35–44.

Jakubíková, K. et al. 2016. Target and non-target moth species captured by pheromone traps for some fruit tortricid moths (Lepidoptera). Acta Universitatis Agriculturae et Silviculturae Mendelianae Brunensis, 64(5): 1561–1568.

Pražanová, Ž. 2018. Reakce cílových a necílových druhů na feromony motýlů v arboretu Mendelovy univerzity v Brně. Diploma thesis (in Czech), Mendel University in Brno.

Quitt, E. 1971. Klimatické oblasti Československa. Studia Geographica 16. Geografický ústav ČSAV. Praha: Academia.

Razowski, J. 2001. Die Tortriciden (Lepidoptera, Tortricidae) Mitteleuropas. Bestimmung – Verbreitung – Flugstandort – Lebensweise der Raupen. Bratislava: F. Slamka.

Šefrová, H. 2003. Změny ve škodlivosti druhů řádu Lepidoptera na polních, zahradních a okrasných rostlinách v průběhu 20. století. Acta Universitatis Agriculturae et Silviculturae Mendelianae Brunensis, 51(5): 7–18.

Velcheva, N. 2000. Faunal investigations on the species of leaf rollers attracted by synthetic pheromones intended for the plum (*Grapholita funebrana*) and oriental (*G. molesta*) fruit moths. Plant Science, 37: 181–187.

Witzgall, P. et al. 2010. Sex pheromones and their impact on pest management. Journal of Chemical Ecology, 36(1): 80–100.

The interactive effects of elevated CO_2 concentration, nitrogen nutrition and timing of drought stress on wheat grain yield and quality in two genotypes with contrasting length of vegetation

Jan Simor[1], Karel Klem[1,2]
[1]Department of Agrosystems and Bioclimatology
Mendel University in Brno
Zemedelska 1, 613 00 Brno
[2]CzechGlobe – Global Change Research Institute, CAS
Belidla 986/4a, 603 00 Brno
CZECH REPUBLIC

jan.simor@gmail.com

Abstract: Ongoing climate change brings not only long-term effects which are represented mainly by elevated atmospheric CO_2 concentration and gradual increase in mean temperature, but also by increasing the extremity of the weather, which means, for example, higher frequency, higher intensity and longer periods of drought. In this study, the effect of elevated CO_2 concentration in combination with nitrogen nutrition and drought was studied in two contrasting genotypes of winter wheat in terms of vegetation length. The results showed that drought in the period after heading generally had a greater effect on yield, while drought before the start of heading had a greater impact on gluten content in grain. The elevated CO_2 concentration partly alleviated the negative effect of the late drought. Conversely, under early drought, elevated CO_2 concentration led to a partial amplification of the drought effect on yield. Although a greater effect on gluten content was observed under the early drought, the combination of late drought and elevated CO_2 concentration showed a higher impact than under the combination with early drought. The application of nitrogen partly mitigated the negative effect of drought on gluten content in both droughts. The response of the varieties to the experimental factors are very similar, although it is evident that the late variety Tobak shows slightly higher sensitivity to early drought. It is clear from the results that the timing of drought determines not only the yield reduction and the impact on quality but also the interactions with other factors such as atmospheric CO_2 concentration, nitrogen nutrition or genotype.

Key Words: winter wheat, elevated carbon dioxide, nitrogen nutrition, drought stress, grain quality

INTRODUCTION

Climate change is one of the world's most significant problems today. This phenomenon is not a question of a distant future, but it is actually affecting our lives. Crops growth and development are influenced continuously by changing environmental conditions related to climate change causing numerous biotic and abiotic stresses. Winter wheat represents about 30% of the world's cereal area, with over 220 million ha cultivated worldwide under abiotic stress conditions (Cossani and Reynolds 2012). Between the abiotic stresses, drought belongs to most frequent across world regions, which often synchronizes with higher (or extreme) temperature leading increasing severity of drought stress (Barnabas et al. 2008) and could cause a negative impact on crop production (Field et al. 2012). Raising the CO_2 concentration in the atmosphere is another factor which is related to climate change. Anthropogenic activities between the pre-industrial period and year 2000 caused an increase in CO_2 concentration by 90 ppm (House et al. 2002). The current state (August 2020) of CO_2 concentration in the atmosphere is 413 ppm, with an average increase of more than 2 ppm per year (NOAA 2020). These factors determine the growth and yield of crops significantly and thus can result in food shortage and compromise food security of the world (Mosley 2015). For this reason, understanding the interactions between the effect of elevated CO_2 concentration, drought stress and its timing, nitrogen nutrition and also other factors associated with climate change is crucial for predicting future food security.

It is expected that not only the yield but also crop quality is affected by climate change. However, a relatively small amount of work has been performed on the combined effect of climate change variables on crop quality. Crop quality is thought to be a complex subject involving crop growth, CO_2 assimilation, biosynthesis and partitioning of carbohydrates, proteins and secondary metabolites. It has been shown, that CO_2 enrichment increases significantly starch and reduces protein content in grain cereals (Erbs et al. 2010), which both determine the basic qualitative parameters, mainly the baking quality of wheat. The positive effect of EC on yield is enhanced in combination with nitrogen nutrition (Reedy and Hodges 2000).

The aim of this study was to analyze impacts of climate change factors (represented by elevated CO_2 concentration and drought stress) and nitrogen nutrition on the yield and relative gluten content in two contrasting genotypes of winter wheat in terms of length of vegetation season.

MATERIAL AND METHODS

The multifactorial field experiment was carried out in Open Top Chamber (OTC) facility in experimental station Domanínek near Bystřice nad Pernštejnem (Figure 1). The experiment consists of 24 OTCs, in which two winter wheat genotypes with the contrasting length of vegetation (Tobak – late, Avenue – very early) were sown on October 10, 2017. The sowing density was 3.5 million of germinable seeds per hectare. The plants were at the growth stages mid of tillering (DC 23–25) and beginning of stem elongation (DC 31) fertilized twice with nitrogen (calcium saltpeter) at dose 100 kg/ha (N+ treatment) or left unfertilized with nitrogen (N-treatment). From the growth stage end of tillering (DC 25–26) the plants were also exposed to two levels of CO_2 concentration: ambient (AC, ca 400 ppm), elevated (EC, ca 700 ppm). Three water availability treatments were used. During stem elongation (from DC 32 to DC 45) the treatment "early drought" (ED) was applied for 21 days. Between heading and beginning of grain filling (DC 51–72) the plants were exposed to "late drought" (LD) for another 21 days. The last treatment was regularly irrigated during the whole season by 20 mm of water every week.

At the end of each drought treatment, the detailed morphological and physiological measurements were performed. Then the harvest was conducted manually, the above-ground biomass determined and the grain threshed using small plot research harvester to determine grain yield.

Figure 1 Open top chambers for manipulation of CO_2 concentration and water availability (left) and view inside the chamber with plots unfertilized and fertilized with N (right).

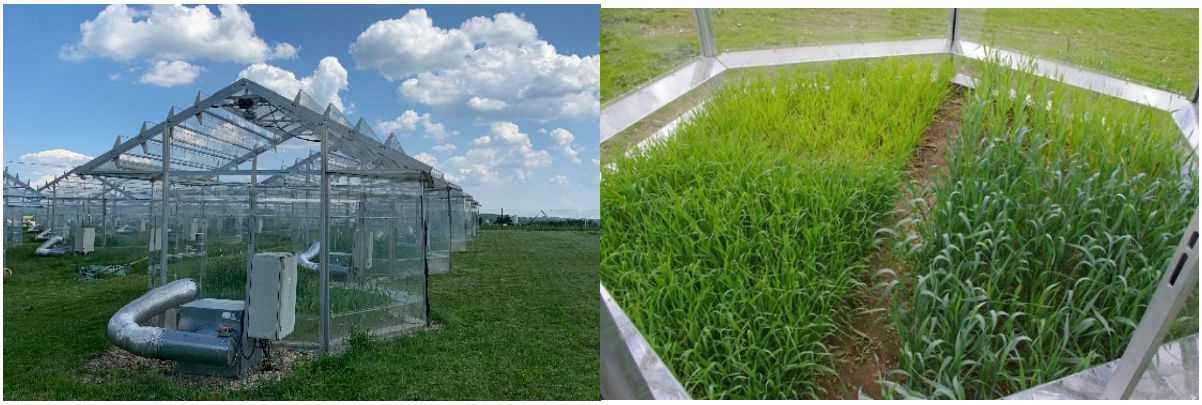

RESULTS AND DISCUSSION

The results show the dominant effect of nitrogen nutrition and also CO_2 concentration on grain yield (Figure 2). At the same time, it is evident that the effect of elevated CO_2 concentration is higher at a higher level of nitrogen nutrition. In contrast, the effect of drought on yield was lower, with a higher decrease in grain yield observed in late drought (LD), while in the case of early drought (ED) the effect was less pronounced. Thus, the reaction of both varieties, early variety Avenue and late variety Tobak to most factors studied was similar, although the variety Tobak showed a generally higher level of grain yield. In the case of late drought, the mitigating effect of the increased CO_2 concentration is also noticeable, especially for variants fertilized with nitrogen (N +). The most studies show

that increase of production parameters by elevated CO_2 concentration is conditioned by sufficient nitrogen availability (reviewed by Leakey et al. 2009, Poorter and Navas 2003). Elevated CO_2 concentration also leads to improved water use efficiency and enhanced drought tolerance of plants however such effect helps only under short term drought stress (Allen et al. 2011, Wullschleger et al. 2002).

Figure 2 The interactive effects of acclimation to elevated CO_2 concentration, N nutrition and drought timing on wheat grain yield in two winter wheat genotypes (Tobak and Avenue)

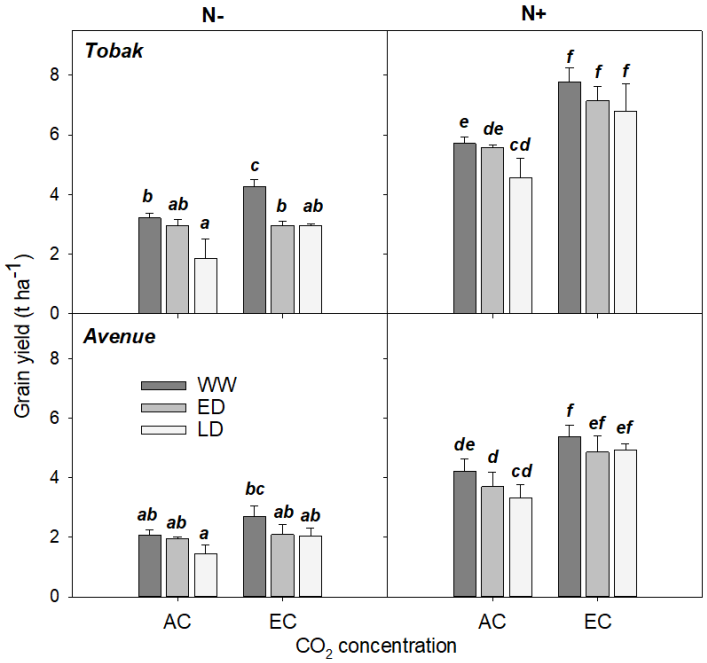

The means (columns) and standard deviations (error bars) are presented (n=3). (AC) – ambient CO_2 concentration (400 ppm), (EC) – elevated CO_2 concentration (700 ppm), (N-) – no N fertilisation, (N+) – N fertilisation (200 kg/ha N), WW – well-watered, ED – early drought during stem elongation, LD – late drought between heading and beginning of grain filling.

Figure 3 The interactive effects of acclimation to elevated CO_2 concentration, N nutrition and drought timing on relative gluten content in two winter wheat genotypes (Tobak and Avenue)

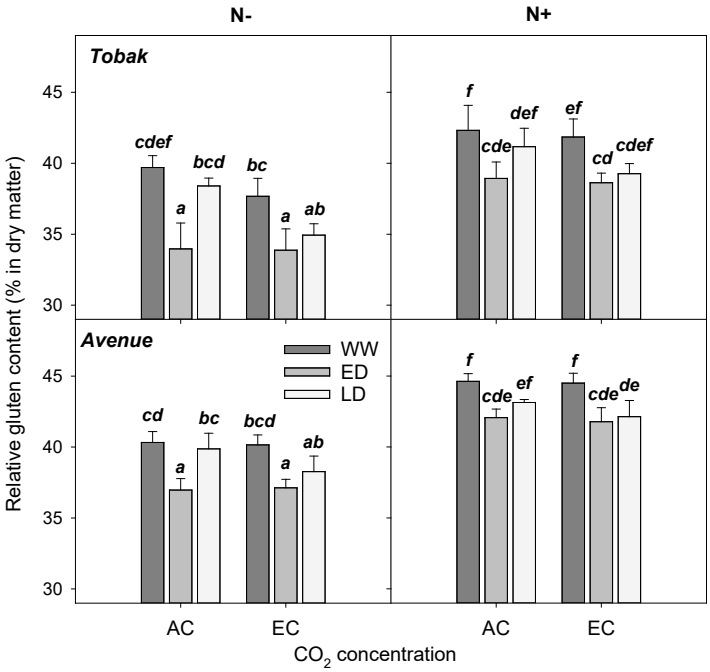

The means (columns) and standard deviations (error bars) are presented (n=3). (AC) – ambient CO_2 concentration (400 ppm), (EC) – elevated CO_2 concentration (700 ppm), (N-) – no N fertilization, (N+) – N fertilization (200 kg/ha N), WW – well-watered, ED – early drought during stem elongation, LD – late drought between heading and beginning of grain filling.

Relative gluten content in grain was mostly affected by nitrogen nutrition, which increases gluten content, and also by early drought (ED), which significantly reduced gluten content (Figure 3). Late drought, on the contrary, had an only small effect on gluten content, and this was more pronounced

under elevated CO_2 concentration (EC). EC led to reduction of relative gluten content; however, such an effect is relatively small and mostly statistically insignificant. Gluten content was also higher in variety Avenue. Fernando et al. (2014) found that the effect of elevated CO_2 concentration on grain protein content is mainly associated with dilution in higher yield. Similar results of CO_2 effect on protein content were also demonstrated by Erbs et al. (2010).

CONCLUSION

In our experiment, we found that the timing of drought plays a key role in terms of the effect on winter wheat yield and quality. While yield is more significantly affected by late drought, the impact on gluten content was generally higher under early drought. We also found a slight mitigating effect of elevated CO_2 concentration on late drought response. In addition, nitrogen generally reduced the negative impact of drought on gluten content.

ACKNOWLEDGEMENTS

This study was supported by research projects IGA – AF-IGA2020-IP036 (Climate change impact on yield and quality parameters of winter wheat). KK was supported by the project SustES-Adaptation strategies for sustainable ecosystem services and food security under adverse environmental conditions" project no. CZ.02.1.01/0.0/0.0/16_019/0000797.

REFERENCES

Allen, Jr.L.H. et al. 2011. Elevated CO_2 increases water use efficiency by sustaining photosynthesis of water-limited maise and sorghum. Journal of Plant Physiology, 168(16): 1909–1918.

Barnabas, B. et al. 2008. The effect of drought and heat stress on reproductive processes in cereals. Plant Cell & Environment, 31: 11–38.

Cossani, C.M., Reynolds, M.P. 2012. Physiological traits for improving heat tolerance in wheat. Plant Physiology, 160(4): 1710–1718.

Erbs, M. et al. 2010. Effects of free-air CO_2 enrichment and nitrogen supply on grain quality parameters and elemental composition of wheat and barley grown in a crop rotation. Agriculture, Ecosystems & Environment, 136(1–2): 59–68.

Fernando, N. et al. 2014. Elevated CO_2 alters grain quality of two bread wheat cultivars grown under different environmental conditions. Agriculture, Ecosystems & Environment, 185: 24–33.

Field, C.B. et al. 2012. Managing the Risks of Extreme Events and Disasters to Advance Climate Change Adaptation: Special Report of the Intergovernmental Panel on Climate Change. Cambridge University Press, 545–553.

House, J.I. et al. 2002. Maximum impacts of future reforestation or deforestation on atmospheric CO_2. Global Change Biology, 8(11): 1047–1052.

Leakey, A.D. et al. 2009. Elevated CO_2 effects on plant carbon, nitrogen, and water relations: six important lessons from FACE. Journal of Experimental Botany, 60(10): 2859–2876.

Mosley, L.M. 2015. Drought impacts on the water quality of freshwater systems; review and integration. Earth-Science Reviews, 140: 203–214.

NOAA (National and Oceanic Administration), 2020. Recent Global CO_2 [Online]. Available at: http://www.esrl.noaa.gov/gmd/ccgg/trends/global.html. [2020-09-11].

Poorter, H., Navas, M.L. 2003. Plant growth and competition at elevated CO_2: on winners, losers and functional groups. New Phytologist, 157(2): 175–198.

Wullschleger, S.D. et al. 2002. Plant water relations at elevated CO_2 – implications for water-limited environments. Plant, Cell & Environment, 25(2): 319–331.

The effect of soil application of superabsorbent polymers saturated with nutrients on selected growth parameters of maize in drought conditions

Marie Skolnikova, Petr Skarpa, Daniel Klofac, Jiri Antosovky, Dominika Mikusova
Department of Agrochemistry, Soil Science, Microbiology and Plant Nutrition
Mendel University in Brno
Zemedelska 1, 613 00 Brno
CZECH REPUBLIC

mar.skolnikova@seznam.cz

Abstract: Superabsorbent polymers (SAP) seem to be suitable for optimization soil moisture conditions due to their ability to repeatably bound and release water and solutions with dissolved nutrients. Application of SAP contributes to better water management in soil and can prevent nutrients losses caused by leaching or volatilization. In this work, we focused on determination of the effect of SAP saturated with nutrients on maize selected growth parameters of maize in drought conditions. The results showed that soil application of SAP and fertilizers (SAP + NP or NPK fertilizer) had positive impact on observed growth parameters. In well-watered conditions, the highest increase of chlorophyll content in leaves was found after application of SAP + NP fertilizer, the increase was about 9.2% in compare to variant with NP fertilizer in term 30 days after sowing (DAS). Root electric capacitance (REC), which describes size of root system, was higher about 8% after application of SAP + NP than after application of NP fertilizer in drought conditions (term 58 DAS). SAP in combination with fertilizers had positive effect on dry matter production in well-watered conditions, it was higher than variants with only NP or NPK fertilization in term 58 DAS.

Key Words: superabsorbent polymers, fertilization, maize, drought stress

INTRODUCTION

The area affected by drought have been increasing in recent years. The main causes are irregular precipitation and lower soil ability to retain the water as consequences of intensive cultivation. Such a soils have higher surface runoff during torrential rain which leads to erosion of upper layers and deterioration in soil quality. Drought stress became regular phenomenon and we try to find the ways how to reduce the impact of this stress on plants. Application of preparations with ability to hold water and reduce soil vapor seems to be suitable for optimization of soil moisture conditions. Soil additives which improve water management in soil are important possibility how to solve these problems. These preparations could combine water holding with controlled nutrients release, organically bounded nutrients for soil or plants protective preparations release.

Superabsorbent polymers (SAP) is repeatably able to bound and release up to five hundred more of their weight which makes SAP suitable for improve moisture conditions in soil (Horie et al. 2004). The main advantages of SAP application on soil are elevation of water capacity and/or absorption nutrients in light, sandy soils (Abd El-Rehim et al. 2004). Utilization of SAP also could contribute to lower level of irrigation and better soil structure which lead to lower soil compaction and erosion. Hou et al. (2018) described strong effect of SAP application on decrease of soil density together with increase of soil water retention and porosity.

Not only good moisture conditions are important for optimal plant grow and development, but sufficient amount of nutrients also plays an important role. Unfortunately, approximately 40–70% of nitrogen, 80–90% of phosphorus and 50–70% of potassium from commonly used fertilizers are not utilized by plants due to losses as leaching, volatilization, immobilization in soil, etc. (Ni et al. 2009, Wang and Wang 2009). Superabsorbent polymers can absorb some nutrients to their structures and postpone nutrients dissolving (Akhter et al. 2004). Islam et al. (2011) mentioned that SAP could absorb water solutions with dissolved nutrients in huge volume. The releasing of nutrients is particularly

influenced by diffusion characteristic of polymer, soil compartments, type of used SAP or nutrient form. SAP saturated with controlled release nutrients should enhanced the effectivity of fertilization as well as to reduce their losses (Liang et al. 2009). The aim of presented experiment was to determine the effect of soil application of SAP saturated with nutrients on selected growth parameters of maize in drought conditions.

MATERIAL AND METHODS

Vegetation pots experiment was established into growth chambers of the Department of Agrochemistry, Soil Science, Microbiology and Plant Nutrition, Faculty of AgriSciences, MENDELU in controlled temperature, humidity and light mode (12 h day length, photosynthetic photo flux density of 350 µmol/m^2/s, temperature of 20/10 °C (day/night) and relative humidity of 55/70%. Maize variety SY Dartona was used as a modal crop and it was seed on December 8, 2019. Pots were filled with 2.5 kg of brown soil. The selected agrochemical soil properties are shown in Table 1.

Table 1 Physicochemical parameters of the soil

Soil parameters	Value
pH ($CaCl_2$)	5.7
cox	0.80%
clay	20%
silt	27%
sand	53%
CEC	164 mmol/kg
N tot	0.19%
N-NH_4^+ (K_2SO_4)	1.48 mg/kg
N-NO_3^-(K_2SO_4)	17.2 mg/kg
P (Mehlich 3)	113 mg/kg
K (Mehlich 3)	306 mg/kg
Ca (Mehlich 3)	1766 mg/kg
Mg (Mehlich 3)	132 mg/kg

Superabsorbent polymers (SAP) containing selected nutrients/fertilizer and commonly commercial fertilizers were placed to the soil under seed ("starter fertilizer") according to Table 1. The irrigation was uniform in term from maize emergence to December 17, 2019 – 9 days after sowing (DAS). After that plants were divided into two groups (irrigation regime), the treatment consisted of excess water application. The first group had complete water application (100% soil moisture), the second group was under drought stress and had limited water application (25% soil moisture). Two plants were cultivated per pot and all variants (Table 2) were conducted in four repetitions.

Table 2 Variants of vegetation pots experiment

Variants	Dose of nutrients per pot (g)			SAP or fertilizer dose per pot (g)
	N	P_2O_5	K_2O	
Control	0	0	0	0.00
SAP	0	0	0	0.40
NP fertilizer	0.32	0.60	0	2.67
SAP + NP fertilizer	0.32	0.60	0	5.33
NPK fertilizer	0.32	0.13	0.40	2.67
SAP + NPK fertilizer	0.32	0.13	0.40	5.33

Legend: NPK fertilizer was YaraMila COMPLEX 12+11+18 and contains 12% N, 11% P_2O_5, 18% K_2O, NP fertilizer was Amofos and contains 52% P_2O_5 and 12% N, SAP contains Potassium polyacrylate + biodegradable binder.

The content of chlorophyll in leaves which is involved by nitrogen content was determined by Yara N tester (YARA International ASA, Germany). The size of root system was evaluated

by measuring root electrical capacitance (REC) according to Chloupek (1977) and Dalton (1995) and it was measured by LCR meter ELC–131D (Escort Instruments Corp., Taiwan) at frequency of 1 kHz in nanofarads (nF). The monitored parameters were detected in period of 14 days (January 7–30 DAS, January 21–44 DAS and February 4, 2020 – 58 DAS). The content of dry matter was determined in two terms, January 21, 2020 (44 DAS) and February 4, 2020 (58 DAS). Plant samples were crushed and dried to constant weight at the temperature of 105 °C. The results were statistically evaluated by ANOVA analysis of variance and follow-up tests according to Tukey at 95% ($p<0.05$) level of significance in program Statistica 12 CZ (StatSoft CR, Czech Republic).

RESULTS AND DISCUSSION

Fertilizers application had already influenced nitrogen content (hence chlorophyll content) in first term (30 DAS) of N-tester measuring (Table 3). The differences of N-tester values between control and variants with combination of SAP and fertilizers in well-watered conditions were increased in time. The highest difference between application of fertilizer and combination of fertilizer with SAP in well-watered conditions was found on variant SAP + NP fertilizer (higher about 9.2% in term 30 DAS). Similar trend was observed on variants growing in drought conditions. We also determinated the lack of nitrogen on control variant (not fertilized).

Table 3 N-tester values for well-watered variants (3 terms of measuring)

Variants	30 DAS			40 DAS			58 DAS		
	N tester value	rel. %	rel. %	N tester value	rel. %	rel. %	N tester value	rel. %	rel. %
Control	456	100.0	100.0	387	100.0	100.0	304	100.0	100.0
SAP	469	102.9	102.9	399	103.1	103.1	375	123.4	123.4
NP fertilizer	501	109.9	100.0	538	139.0	100.0	511	168.1	100.0
SAP + NP fertilizer	547	120.0	109.2	555	143.4	103.2	516	169.7	101.0
NPK fertilizer	562	123.2	100.0	535	138.2	100.0	546	179.6	100.0
SAP + NPK fertilizer	567	124.3	100.9	558	144.2	104.3	523	172.0	95.8

Application of SAP with fertilizers promoted chlorophyll content, the highest increase of chlorophyll content in drought conditions was observed on variant SAP + NPK, N-tester value was about 93% higher than control and about 5.6% than variant with only NPK (term 58 DAS). Application of SAP without fertilizers had less positive effect on chlorophyll content than SAP with nutrients, nevertheless N-values was about 62% higher than control in term 58 DAS (Table 4). Khadem et al. (2010) also described higher chlorophyll increased after application of SAP with nutrients.

Table 4 N-tester values for variants under drought stress (3 terms of measuring)

Variants	30 DAS			40 DAS			58 DAS		
	N tester value	rel. %	rel. %	N tester value	rel. %	rel. %	N tester value	rel. %	rel. %
Control	554	100.0	100.0	438	100.0	100.0	294	100.0	100.0
SAP	549	99.1	99.1	453	103.4	103.4	475	161.6	161.6
NP fertilizer	612	110.5	100.0	562	128.3	100.0	531	180.6	100.0
SAP + NP fertilizer	643	116.1	105.1	549	125.3	97.7	516	175.5	97.2
NPK fertilizer	630	113.7	100.0	552	126.0	100.0	537	182.7	100.0
SAP + NPK fertilizer	643	116.1	102.1	549	125.3	99.5	567	192.9	105.6

REC measuring was done in two terms (30 DAS and 58 DAS). The differences between well-watered and drought variants are obvious from Figure 1 and 2, drought had negative impact on the size of root system. Combination of SAP with fertilizers had significant effect on REC

in well-watered conditions in term 30 DAS, the significantly highest REC in well-watered conditions had variant SAP + NP fertilizer, it was about 48% higher than variant with only NP fertilizer. SAP with fertilizers did not enhance REC in drought conditions in term 30 DAS in compare to NP or NPK application.

Figure 1 Root electrical capacitance of maize in 30 days after sowing

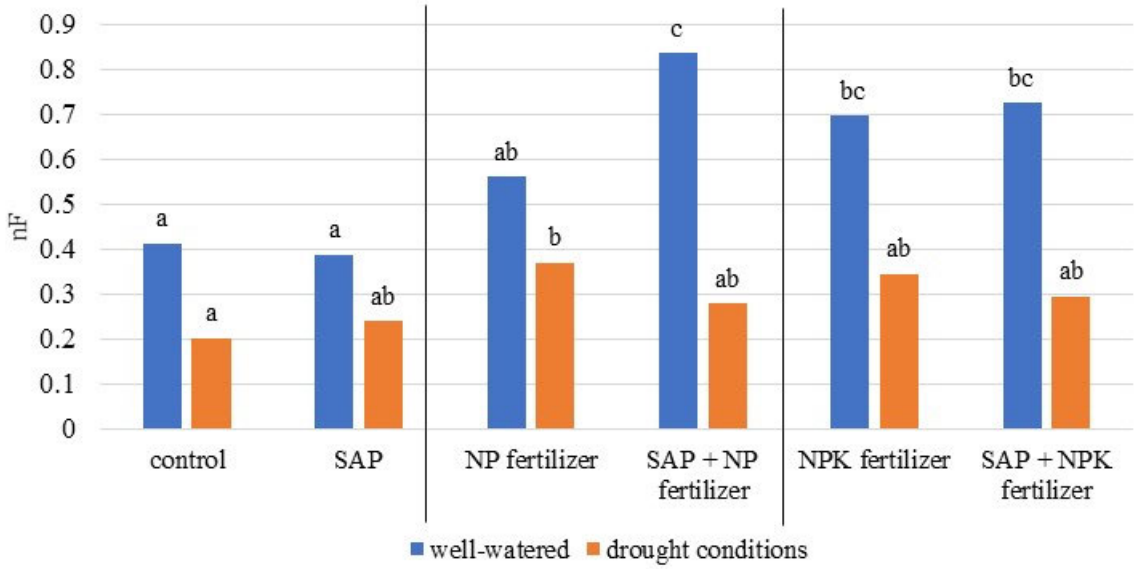

Legends: Statistically evaluated within groups of irrigation regime (well-watered/drought conditions), same letters are not significantly different (P<0.05) according to LSD test.

Application of SAP with fertilizers influenced also REC of plants cultivated in drought conditions in term of 58 days after sowing, variant SAP + NP fertilizer had significantly higher REC than control (about 39%). REC of variant SAP + NPK was about 54% higher than control (Figure 2). Combination of SAP + NP fertilizer enhanced REC in drought conditions (about 8% higher than variant with NP fertilizer) contrary to SAP + NPK variant which showed positive effect on REC in well-watered conditions (about 14.6% higher that NPK fertilized variant).

Figure 2 Root electrical capacitance of maize in 58 days after sowing

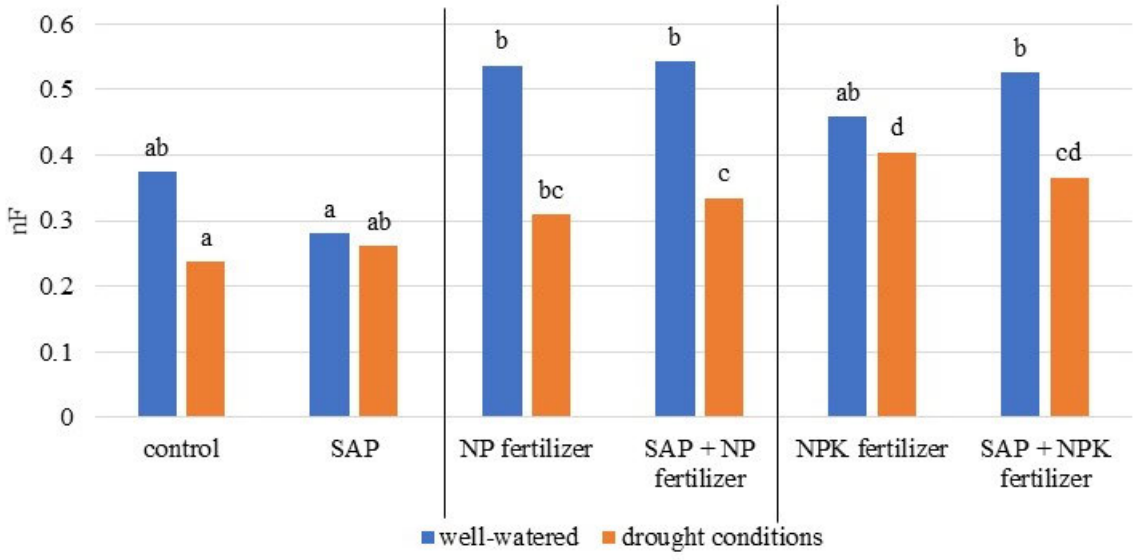

Legends: Statistically evaluated within groups of irrigation regime (well-watered/drought conditions), same letters are not significantly different (P<0.05) according to LSD test.

Dry matter weight production was determinated in two terms as presents Table 5. It was significantly influenced by combination of SAP and NP or NPK in well-watered conditions, these variants had suitable conditions for utilization of applied fertilizers. Dry matter weight of variants SAP + NP and SAP + NPK was about 80% higher than control variant in term 58 DAS. Relative increase of dry matter production was even determined after SAP application without fertilizers in drought conditions (increase about 5.2–8.8%). The effect of SAP with nutrients on dry matter production was not found in drought conditions, nevertheless, we determined increase after SAP + NP (about 8%) or SAP + NPK (about 22%) fertilizer application in contrast to NP or NPK application in well-watered conditions. SAP application has potential to increase crop yield, Hou et al. (2018) mentioned significantly increased potatoes yield, Bečka et al. (2018) observed the effect of SAP on oilseed rape or Verma et al. (2019) used SAP in flower cultivation.

Table 5 Weight of above-ground maize biomass (in dry matter weight)

Variants	30 DAS				58 DAS			
	well-watered		drought conditions		well-watered		drought conditions	
	weight (g)	rel. %	weight (g)	rel. %	weight (g)	rel. %	weight (g)	rel. %
Control	0.85^{a}	100.0	0.32^{a}	100.0	1.48^{ab}	100.0	0.54^{a}	100.0
SAP	0.73^{a}	85.7	0.34^{a}	105.2	1.37^{b}	92.2	0.59^{a}	108.8
NP fertilizer	1.33^{b}	156.9	0.59^{b}	184.7	2.48^{c}	167.4	1.03^{a}	189.9
SAP + NP fertilizer	1.42^{b}	167.7	0.46^{ab}	143.5	2.67^{c}	180.1	0.90^{a}	165.9
NPK fertilizer	1.54^{b}	181.3	0.51^{ab}	158.5	2.19^{bc}	148.1	1.02^{a}	187.6
SAP + NPK fertilizer	1.41^{b}	166.0	0.49^{ab}	154.7	2.67^{c}	180.6	0.86^{a}	159.0

Legends: Means with same letter are not significantly different (P<0.05).

CONCLUSION

Occurrence of drought became regular in recent years and we need to find the ways how to get over the negative impact of this abiotic stress on plants cultivation. Application of superabsorbent polymers could contribute to alleviation this stress. Application of SAP had positive effect on maize growth parameters. We observed positive impact of SAP with NP or NPK fertilizer application (compare to application of NP or NPK fertilizer) on monitored parameters especially in well-watered conditions, nevertheless application of SAP + NP increased REC in comparison to variant with NP fertilization in drought conditions (term 58 days after sowing). Dry matter weigh was enhanced after application of SAP with nutrients in contrast to application of NP or NPK fertilizers in well-watered conditions. Kinetics clarification of nutrients releasing from enriched SAP would contribute to explanation of their effect on plants production.

ACKNOWLEDGEMENTS

The research was supported by grant no. AF-IGA2020-TP007.

REFERENCES

Abd El-Rehim, H.A. et al. 2004. Radiation synthesis of hydrogels to enhance sandy soils water retention and increase plant performance. Journal of Applied Polymer Science [Online], 93(3): 1360–1371. Available at: https://onlinelibrary.wiley.com/doi/full/10.1002/app.20571. [2020-09-15].

Akhter, J. et al. 2004. Effects of Hydrogel Amendment on Water Storage of Sandy Loam and Loam Soils and Seedling Growth of Barley, Wheat and Chickpea. Plant Soil Environment [Online], 50(10): 463–469. Available at: https://agris.fao.org/agris-search/search.do?recordID=CZ2005000199. [2020-09-15].

Bečka, D. et al. 2018. Performance Comparison of Winter Oilseed Rape Varieties in the Slovakia in 2017/18. In Proceedings of Prosperous Oil Crops, Prague, 4–6 December 2018. Prague: Czech University of Life Sciences Prague, Faculty of Agrobiology, Food and Natural Resources, pp. 32–35.

Chloupek, O. 1977. Evaluation of the size of a plant's root system using its electrical capacitance. Plant and Soil, 48(2): 525–532.

Dalton, F.N. 1995. In-situ root extent measurements by electrical capacitance methods. Plant and Soil, 173(1): 157–165.

Horie, K. et al. 2004. Definition of terms relating to reactions of polymers and to functional polymeric materials: IUPAC Recommendations 2003. Pure Applied Chemistry [Online], 76(4): 889–906. Available at: http://old.iupac.org/publications/pac/2004/pdf/7604x0889.pdf. [2020-09-17].

Hou, X.Q. et al. 2018. Superabsorbent polymers influence soil physical properties and increase potato tuber yield in a dry-farming region. Journal of Soils and Sediments [Online], 18(3): 816–826. Available at: http://dx.doi.org/10.1007/s11368-017-1818-x. [2020-09-16].

Islam, M.R. et al. 2011. Effects of water-saving superabsorbent polymer on antioxidant enzyme activities and lipid peroxidation in corn (*Zea mays* L.) under drought stress. Journal of the Science of Food and Agriculture [Online], 91(5): 813–819. Available at: https://onlinelibrary.wiley.com/doi/full/10.1002/jsfa.4252. [2020-09-15].

Khadem, S.A. et al. 2010. Effect of animal manure and super absorbent polymer on corn leaf relative water content, cell membrane stability and leaf chlorophyll content under dry condition. Australian Journal of Crop Science [Online], 4(8): 642–647. Available at: https://profdoc.um.ac.ir/articles/a/1018397.pdf. [2020-09-15].

Liang, R. et al. 2009. Synthesis of Wheat Straw-G-Poly (Acrylic Acid) Superabsorbent Composites and Release of Urea from It. Carbohydrate Polymers [Online], 77(2): 181–187. Available at: https://www.sciencedirect.com/science/article/pii/S014486170800578X. [2020-09-17].

Ni, B. et al. 2009. Multifunctional Slow-Release Urea Fertilizer from Ethylcellulose and superabsorbent Coated Formulations. Chemical Engineering Journal [Online], 155(3): 892–898. Available at: https://www.sciencedirect.com/science/article/pii/S138589470900597X. [2020-09-17].

Verma, A.K. et al. 2019. Conditioning effects of biodegradable superabsorbent polymer and vermi-products on media properties and growth of gerbera. Ecological Engineering [Online], 132: 23–30. Available at: https://krishi.icar.gov.in/jspui/bitstream/123456789/29459/1/Conditioning%20effects%20of%20biodegradable%20superabsorbent%20polymer%20and%20vermiproducts.pdf. [2020-09-16].

Wang, W., Wang, A. 2009. Synthesis, Swelling Behaviors, and Slow-Release Characteristics of a Guar Gum-g-Poly (sodium acrylate)/Sodium Humate Superabsorbent. Journal of Applied Polymer Science [Online], 112: 2102–2111. Available at: http://www.emec.licp.cas.cn/kycg/2009/201207/W020110416394432417241.pdf. [2020-09-17].

Effect of different irrigation rations on fruit yield and annual increments of "Gala" apple

Lukas Vastik[1], Vladimir Masan[1], Patrik Burg[1], Pavel Hic[2]
[1]Department of Horticultural Machinery
[2]Department of Post-Harvest Technology of Horticultural Products
Mendel University in Brno
Zemedelska 1, 613 00 Brno
CZECH REPUBLIC

xvastik@mendelu.cz

Abstract: The consequences of a changing climate are clearly causing changes in the entire climate system of the Earth. In Europe, this results in changes in precipitation conditions and the number of precipitation days during the year and a deepening of the dry season in the summer months. Climate change is also strongly influenced by fruit growing and the use of irrigation water, which may be scarce during this period. Therefore, there is an effort to save with it. During the experiment, five methods of irrigation were monitored in the orchard: IR + F-2.1 (irrigation with fertigation, drip flow 2.1 l/h), IR + F-1.6 (irrigation with fertigation, drip flow 1.6 l/h), IR + F-1 (irrigation with fertigation, drip flow 1 l/h), IR-2.1 (irrigation without fertigation, drip flow 2.1 l/h) and NON-IR (without irrigation and fertigation). The research points to the system of irrigation and fertigation at different irrigation doses and their influence on fruit yield and the length of annual increments in Gala apple. When it comes to Gala apple, the difference in fruit weight between IR + F-2.1 variants was statistically demonstrated; IR + F-1.6 and non-irrigated variant. The highest weight was measured for the IR + F-2.1 variant, namely 147 g, and the lowest for the NON-IR variant, 132 g. Differences in fruit weight during irrigation with and without fertigation were not statistically detectable. The largest fruit diameter was achieved with the IR + F-2.1 and IR + F-1.6 variants (67.5 mm) and the lowest with the NON-IR (64 mm). Differences in fruit diameter were not demonstrated between irrigated variants with and without fertigation. The demonstrably longest annual increments were found for the IR + F-2.1 (677.3 mm) and IR + F-1.6 (568.9 mm) variants and demonstrably the shortest for the NON-IR variant (436.0 mm).

Key Words: drip flow, irrigation, fertigation, apple tree, orchard

INTRODUCTION

Apples represent the most common cultivated type of pome fruit that requires intensive care. "Gala" is one of the world's most widely grown apple varieties. It is widely popular thanks to its red skin colour, juiciness and sugar content. The popularity of this variety is added by clones that have been selected for their more pronounced colour, taste and easier storage. The most famous clones include "Gala Schniga", "Gala Schniga Schnico Red", "Gala Galaxy", "Royal Gala", "Gala Galaval", "Red Gala 95" and "Gala Mondial" (FAO 2020).

Intensive care of fruit plantations is necessary for achieving the highest possible yields. Typical for intensive orchards is a dense tree clip (3,600 pcs/ha), a regular cut, for example in the shape of a slender spindle, and the importance is placed on fruit picking, which is either chemical when flowering or mechanical after the so-called "June drop" (Radivojevic et al. 2020). Irrigation with fertigation is an integral part of intensive care in orchards. Drip irrigation is the most used irrigation system for fruit orchards. The water reaches directly to the root system of the trees and does not irrigate the surroundings unnecessarily, while the clamps and the flow rate of the drips can be selected. Drip irrigation saves up to 39% of water compared to spray irrigation (Fallahi 2017) and with efficient use of fertilizers, water consumption can be further reduced while maintaining the quality parameters of apples (Neilsen et al. 2008).

The irrigation period begins when the trees sprout and ends approximately two weeks before harvest, with the most important irrigation period being during fruit growth and the differentiation

of flower buds. Irrigation just before harvest has a negative effect on the length of storage and the quality of stored fruit (Wang et al. 2019).

The aim of this experiment was to evaluate five variants of drip irrigation and its effect on fruit weight and diameter, as well as annual increments.

MATERIAL AND METHODS

Characteristics of opinion and cultivated variety

The experiment builds on previous measurements, which were performed in the Plantex company fruit orchard and are described in the article by Mašán et al. (2018). The orchard is located in the village of Veselé, 10 km south of Piešťany (latitude: 48°33'4.25" N, longitude: 17°43'57.78" E). The experiment examined 15-year-old Gala apples, a Schniga clone inoculated on M9 rootstocks. The trees were grown in the shape of a slender spindle. The tree strip was maintained with herbicides and the intercrop was grassed and mowed regularly. The trees were planted in a clip 3.6 × 1 m.

Irrigation and fertigation program

Irrigation and fertigation were performed by using the drip irrigation, which is attached to the bottom row of the wire. Droppers are located in the pipeline, so-called *in-line*. The distance between the drippers is 0.75 m. The diameter of the drip hose is 22 mm and the flow rate of the drip tray is 2.1 l/h of water. Five methods of irrigation were monitored in the experiment: IR + F-2.1 (irrigation with fertigation, drip flow 2.1 l/h), IR + F-1.6 (irrigation with fertigation, drip flow 1.6 l/h), IR + F-1 (irrigation with fertigation, drip flow 1 l/h), IR-2.1 (irrigation without fertigation, drip flow 2.1 l/h), while this variant was removed from irrigation during fertigation of other variants and the last one, NON-IR (without irrigation and fertigation; Table 1). Fully water-soluble fertilizers from Haifa Chemicals company (Israel) were used for fertigation: ammonium sulfate, iron chelate 6% EDDHA, Humifirst, KNO3 Multi K, K2SO4 Solupotasse, MKP. Irrigation and fertigation were controlled by an automatic irrigation system.

Table 1 The amount of natural precipitation and irrigation benefits for 2019 (ALA 2019)

Month	Precipitation (mm)	Variant IR+F-2.1 (mm)		Variant IR+F-1.6 (mm)		Variant IR+F-1 (mm)		Variant IR-2.1 (mm)	
		No precipitation	With precipitation	No precipitation	With precipitation	No precipitation	With precipitation	No precipitation	With precipitation
I.	57.1	0	57.1	0	57.1	0	57.1	0	57.1
II.	28.9	0	28.9	0	28.9	0	28.9	0	28.9
III.	40.8	0	40.8	0	40.8	0	40.8	0	40.8
IV.	26.5	94.5	121	72	98.5	45	71.5	77.7	104.2
V.	141.1	31.5	172.6	24	165.1	15	156.1	27.3	168.4
VI.	12.3	131.3	143.6	100	112.3	62.5	74.8	114.5	126.8
VII.	54.4	163.8	218.2	124.8	179.2	78	132.4	147	201.4
VIII.	89.7	176.4	266.1	134.4	224.1	84	173.7	142.8	232.5
IX.	48.6	65.1	113.7	49.6	98.2	31	79.6	52.5	101.1
X.	22.8	12.6	35.4	9.6	32.4	6	28.8	8.4	31.2
XI.	74.5	0	74.5	0	74.5	0	74.5	0	74.5
XII.	107.1	0	107.1	0	107.1	0	107.1	0	107.1
∑	703.8	675.2	1 379	514.4	1 218.2	321.5	1 025.	570.2	1 274

Evoluetion of the experiment

Fruit weight was measured on an accurate scale KERN PCB 1000-2 (England). The resulting weight of the apples was recorded and averaged. For weighing, 100 apples were randomly selected.

The diameter of the fruit was measured by plastic fruit gauges used in the orchard. In the scales, circular holes are cut in. The diameter of the holes is gradually increased by 5 mm. The resulting diameter of the apples was written down in the table and then averaged. For weighing, 100 apples were randomly selected.

Measurement of the length of annual increments was performed at the end of vegetation. For each variant, 100 randomly selected shoots were measured. The selection of measured shoots was carried out evenly, between the wires of the supporting structure. The length of the shoot was measured from the terminal bud scale scar from the previous vegetation to the terminal shoot bud. The measurement of the length of the annual increments was performed by using a tape measure.

Statistical analysis

100 apples were selected for statistical analysis and data were reported as mean ± standard deviation. SHD assay and one-way ANOVA with interaction ($P < 0.05$) were used to determine differences. Statistical analyses were performed with "Statistica 12.0" software (StatSoft Inc., USA).

RESULTS AND DISCUSSION

Fruit weight

The highest fruit weight of 147 g was determined at the IR + F-2.1 variant. By reducing the irrigation dose, the fruit weight decreased, with the IR + F-1.6 variant the average fruit weight was 145 g and with the IR + F-1 variant it was reduced to 140 g. In the IR-2.1 variant, the average weight of the apples was 138 g despite the higher irrigation dose. The reason for the lower weight of the fruit is the absence of fertigation during the growing season. The expected lowest fruit weight was found for the NON-IR variant 132 g (Figure 1 A). Wang et al. (2019) reports more than 60 g higher weight for the IR + F-2.1 variant, almost the same weight for the IR + F-1.6 variant and approximately 20 grams lower for the IR + F-1 variant. Campi and García (2011) report an average fruit weight of 122 g in the non-irrigated variant. The results point to the need for irrigation and fertilization during the growing season in order to maximize yield. The difference in variants was not proven, mainly due to the fact that the results are from the first year after the establishment of the experiment. The soil has a residual supply of nutrients from the previous period, which slightly affects the results in the first year. In the following years of monitoring the experiment, the gradual reduction of fruit weight at lower irrigation doses is assumed (Robinson 2006).

Fruit diameter

Fruit diameter (Figure 1 B) plays an important role in sorting apples and dividing them into the quality classes according to which they are bought. According to the ČSN 46 3010 standard, apples of a diameter of 70+ mm with dyed flesh of at least 80% belong to the premium quality, apples of diameter 55–69 mm with dyed flesh of at least 40% belong to the I. class quality and the II. class includes apples below 55 mm in size and less than 40% dyed flesh (Table 2). The company's profit then depends on the share of individual quality classes. Apples of premium quality are the most valuable for the producer. The largest diameter of fruits was found in the variant IR + F-2.1 and IR + F-1.6 with a diameter of 67.5 mm. For the IR + F-1 variant, a fruit diameter of 65.9 mm was measured. This was followed by the IR-2.1 variant with a fruit diameter of 65.6 mm and the smallest diameter was measured with the NON-IR variant at 64 mm. The representation of quality classes was approximately the same (Table 2). The share of apples in the premium quality was the largest in the IR + F-1.6 variant, namely 46%. In I. class, the largest proportion was 61% in variant IR+F-1 and in II. class was the largest proportion of apples in the NON-IR variant, namely 24%. Wang et al. (2019) in the first variant states a fruit diameter 20 mm larger, in the second variant it states a similar fruit diameter. Fruit diameter in variant IR + F-1 was similar to fruit diameter reported in Mert et al. (2007) and Yildirim et al. (2016). The difference in fruit diameter was demonstrated only between the IR + F-2.1 variants; IR + F-1.6 and NON-IR. The results for the IR + F-2.1 and IR + F-1.6 variants indicate the importance and need for fruit thinning. If the trees on poorly executed thinning fruit, then it affects the diameter of the fruit. It is recommended to load the tree with 100–120 pieces of apples.

Length of annual increments

The annual increments are basic vegetative supporting element for flowers. Their length affects the number of flowers and the subsequent load on the number of fruits. According to Webster et al. (2000), the length of annual increments depends on several factors. First is the amount of nitrogen and irrigation dose and the amount of precipitation during vegetative growth (May–June). Another factor

is rust. If trees are cut too deep in the spring, their vegetative growth is significantly more lush. Root pruning also plays an important role in the length of annual increments. The demonstrably longest average annual increments were found for the IR + F-2.1 variant (577.3 mm) and for the IR + F-1.6 variant (568.9 mm). For the IR-2.1 variant, the average length of the annual increments was 493.2 mm. This results in the remaining nutrient supply from the previous year and a higher irrigation dose that helps nutrient intake. Subsequently, for the IR + F-1 variant, namely 474.9 mm. The demonstrably most beautiful average annual increments were measured with the NON-IR 436.0 mm variant (Figure 2). Neilsen and Neilsen (2002) report the longest increments in the first variant of IR + F-2.1, but with a larger difference caused by higher doses of nitrogen during vegetative growth. Another factor that affected the length of annual growth was the higher total precipitation during the month of May, when the growth of shoots is intense. The shortest annual increments were as long as Iancu et al. (2011) state. Longer annual increments have a positive effect on the content of organic matter in the soil and the return of depleted nutrients back to the soil, as they mulch in the middle row after cutting.

Figure 1 Impact of irrigation on "Gala" apple fruit weight and diameter

A) Fruit weight *B) Fruit diameter*

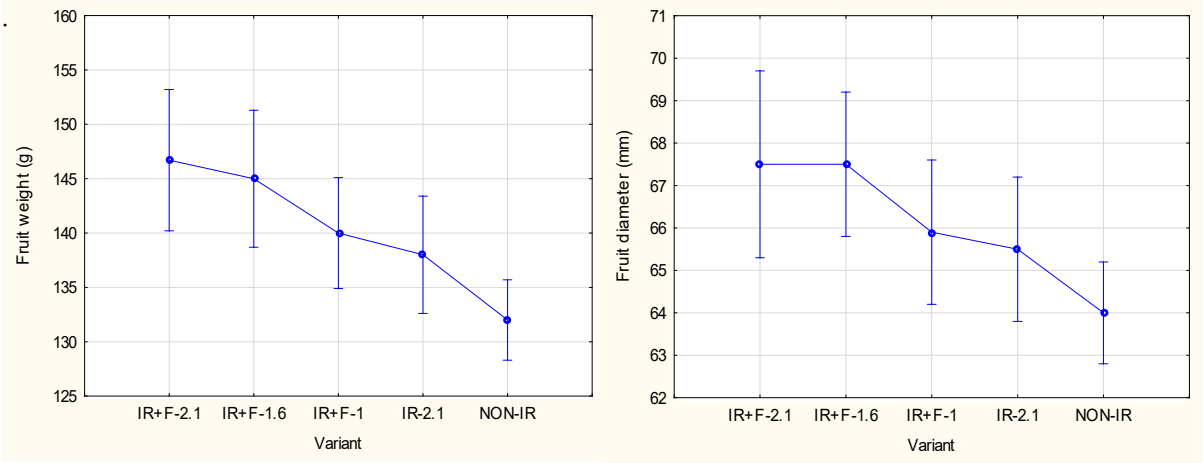

Figure 2 Impact of irrigation on length of annual increments on "Gala" apple

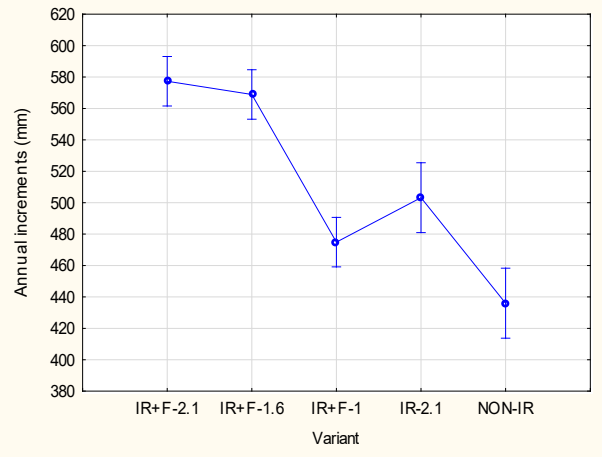

Table 2 Proportion of quality classes for individual irrigation variants on "Gala" apple

Variant	IR+F-2.1	IR+F-1.6	IR+F-1	IR-2.1	NON-IR
Premium quality (%)	41	46	30	24	17
I. class (%)	56	52	61	58	59
II. class (%)	3	2	9	18	24

CONCLUSION

Drip irrigation is an integral part of irrigation in orchards. Thanks to it, it is possible to achieve higher yields, better fruit quality and keep the trees in the best possible vitality. Current trend is to try to optimize costs while ensuring the best quality of fruit. The highest fruit weight was found for variant IR + F-2.1 147 g. The weight of the fruit gradually decreased with decreasing irrigation dose, the lowest weight being found for the NON-IR variant (132 g). The difference was shown only between the IR + F-2.1 variants; IR + F-1.6 and NON-IR. The largest fruit diameter was found in variants IR + F-2.1 and IR + F-1.6, namely 67.5 mm. The smallest diameter was achieved by the NON-IR variant (64 mm). Both in terms of fruit weight and average, the difference was shown only between the IR + F-2.1 variants; IR + F-1.6 and NON-IR. The demonstrably longest annual increments were measured for variants IR + F-2.1 (577.3 mm) and IR + F-1.6 (568.9 mm). While the demonstrably shortest increments were measured with the NON-IR variant (436.0 mm). The results of the experiment pointed out the importance of irrigation. As this is the first year of the experiment, larger differences in the individual variants can be expected in the following years. The minimal and unprovable differences show results between variants IR + F-2.1 and IR + F-1.6. This results in an unnecessarily high irrigation dose and water waste in the IR + F-2.1 variant. Drip irrigation with a flow rate of 1.6 l/h points to more gentle and economical irrigation and fertigation. In order to obtain the most relevant results, it is appropriate to perform measurements in multiannual repetitions.

ACKNOWLEDGEMENTS

This paper was supported by the project CZ.02.1.01/0.0/0.0/16_017/0002334 Research Infrastructure for Young Scientists, this is co-financed from Operational Programme Research, Development and Education.

REFERENCES

ALA. 2019. Amet. [Online]. Available at: http://a.la-a.la/chart/chart.php?probe=11359336. [2020-07-09].

Campi, P., García, C. 2011. Effects of irrigation management and nitrogen fertilization on the yield and quality of 'Gala' apple. Acta Horticulturae [Online], 889(29): 249–255. Available at: https://doi.org/10.17660/ActaHortic.2011.889.29. [2020-07-02].

Czech Standards Institute. 1995. Fresh Fruits. Red chokeberries, Apples, Pears, Rowanberries, Quinces, Medlars. CSN 46 3010 (463010). Praha: Czech Standards Institute.

Fallahi, E. 2017. Long-Term Influence of Irrigation Systems on Postharvest Fruit Quality Attributes in Mature 'Autumn Rose Fuji' Apple Trees. International Journal of Fruit Science [Online], 18(2): 177–187. Available at: https://doi.org/10.1080/15538362.2017.1389329. [2020-07-02].

Food and Agriculture Organization of the United Nations. 2020. Statistics Database. [Online]. Available at: http://www.fao.org/faostat/en/#search/Gala%20Apple. [2020-07-02].

Iancu, M. et al. 2011. Influence of the groundcover management system and drip irrigation on behavior of the 'Golden Spur' apple cultivar grafted on MM106 rootstock. Acta Horticulturae [Online], 889(31): 265–271. Available at: https://doi.org/10.17660/ActaHortic.2011.889.31. [2020-07-09].

Mašán, V. et al. 2018. Effects of Irrigation and Fertigation on Yield and Quality Parameters of 'Gala' and 'Fuji' Apple. Acta Universitatis Agriculturae et Silviculturae Mendelianae Brunensis [Online], 66(5): 1183–1190. Available at: https://acta.mendelu.cz/66/5/1183/. [2020-08-14].

Mert, C. et al. 2007. The King Fruit versus Lateral Fruit Thinning Effects on Yield and Fruit Quality in Apple. International Journal of Fruit Science [Online], 7(1): 37–46. Available at: https://doi.org/10.1300/J492v07n01_04. [2020-07-10].

Neilsen, D., Neilsen, G.H. 2002. Efficient Use of Nitrogen and Water in High-density Apple Orchards. HortTechnology [Online], 12(1): 19–25. Available at: https://doi.org/10.21273/HORTTECH.12.1.19. [2020-07-09].

Neilsen, D. et al. 2008. Drainage losses of water, N and P from microirrigation systems in a young, high density apple planting. Acta Horticulturae [Online], 792(55): 483–490. Available at: https://doi.org/10.17660/ActaHortic.2008.792.55. [2020-07-03].

Radivojevic, D. et al. 2020. Comparison of metamitron efficiency for postbloom thinning of young 'Gala' and 'Golden Delicious' apple trees. Turkish Journal of Agriculture and Forestry [Online], 44(1): 83–94. Available at: http://journals.tubitak.gov.tr/agriculture/issues/tar-20-44-1/tar-44-1-9-1902-22.pdf. [2020-07-02].

Robinson, T.L. 2006. Interaction of fertilization, rootstock and irrigation on growth, thinning efficiency, yield and fruit quality of 'empire' apple. Acta Horticulturae [Online], 721(4): 41–48. Available at: https://doi.org/10.17660/ActaHortic.2006.721.4. [2020-07-10].

Wang, Y. et al. 2019. Effects of soil water stress on fruit yield, quality and their relationship with sugar metabolism in 'Gala' apple. Scientia Horticulturae [Online], 258: 108753. Available at: https://doi.org/10.1016/j.scienta.2019.108753. [2020-07-02].

Webster, A.D. et al. 2000. Interactions between root restriction, irrigation and rootstock treatments on the growth and cropping of 'Queen Cox' apple trees: Effects on orchard growth and cropping. The Journal of Horticultural Science and Biotechnology [Online], 75(2): 181–189. Available at: https://doi.org/10.1080/14620316.2000.11511220. [2020-07-02].

Yildirim, F. et al. 2016. Interaction of Crop Load and Irrigation on Yield, Fruit Size, Color and Stem-end Splitting Ratio of Apple c.v. 'Gala, Galaxy'. Erwerbs-Obstbau [Online], 58(2): 103–111. Available at: https://doi.org/10.1007/s10341-015-0262-6. [2020-07-09].

ANIMAL PRODUCTION

Total haemolymph protein and hypopharyngeal glands in the honeybee

Ondrej Babica[1], Jan Musila[1], Tibor Fuzik[2], Pavel Plevka[2], Antonin Pridal[1]
[1]Department of Zoology, Fisheries, Hydrobiology and Apidology
Mendel University in Brno
Zemedelska 1, 613 00 Brno
[2]Central European Institute of Technology
Masaryk University
Kamenice 5, 625 00 Brno
CZECH REPUBLIC

apridal@mendelu.cz

Abstract: The development of the hypopharyngeal glands (HG) of honeybees depends on nutrition, which influences also the total concentration haemolymph proteins (THP). The objective of this study was to compare the size of hypopharyngeal glands and the total haemolymph protein in the honeybee workers. Unaffected natural ontogenesis of HG development and THP content was measured in four colonies of different strength. Correlation between HG and THP without age or colony sorting was weak. The moderately positive correlation between HG and THP was found in freshly emerged workers. Strong dependence was confirmed between the mean values of HG and THP of all colonies together sorted according to age of workers.

Key Words: Apis mellifera, colony, haemolymph protein, hypopharyngeal gland, superorganism

INTRODUCTION

The honeybee is a social insect forming superorganism (a honeybee colony) with well-defined anatomical, physiological and behavioural cohort differentiation (Moritz and Southwick 2012). Worker honeybee cohorts are involved in age-dependent division of labour and ontogenesis of their physiological markers (Crailsheim 1986). Physiologically young workers, the hive bees, posse bigger hypopharyngeal glands and whole body weight, higher protein levels in the haemolymph, higher antioxidant ability and enzymatic activity (Halberstadt 1967, Fluri et al. 1982, González-Santoyo and Córdoba-Aguilar 2012) than physiologically old workers, the foragers rapidly approaching their death, which have high titre of juvenile hormone (Amdam and Omholt 2002). In addition, distinction of duties and lifespan between the summer and winter workers are typical for temperate climate regions (Fluri et al. 1982). The winter honeybee workers prepare to overwinter under temperate climates by entering a distinct physiological and behavioural state (Doeke et al. 2015). Workers developed within spring/summer show significantly faster physiological ageing/shorter lifespan than workers developed in autumn (Fluri et al. 1982).

The fitness of bee workers is not outwardly apparent due to external skeleton (Snodgrass 1925) as it is considerably easily evaluable in vertebrates with internal skeleton (Ullman-Culleré and Foltz 1999). As a worker bee condition decreases with the physiological ageing it may be determinable by biochemical parameters (Kunert and Crailsheim 1988). The total protein in worker haemolymph and the hypopharyngeal gland size are easily assayed age dependent parameters for evaluating the worker physiological status (Fluri et al. 1982, Kunc et al. 2019).

The regular development of the hypopharyngeal glands depends on nutrition and on the existence of a social system (Crailsheim and Stolberg 1989). The nutrition influences the total haemolymph protein content (De Jong et al. 2009). Therefore, the aim of this study was to compare the size of hypopharyngeal glands and the total haemolymph protein in the honeybee workers and to find whether there is dependence between these two physiological parameters that would be useful for determination of honeybee worker condition. These hypotheses were established: Does the total

haemolymph protein content in the worker correlate with its hypopharyngeal glands size? Do the honeybees of equal age have similar values of the total protein and hypopharyngeal gland size?

MATERIAL AND METHODS

The field experiment was realized on 4 bee colonies (1 apiary) in the spring 2020 (May, June). Bees of known age were collected and sampled to measure their total haemolymph protein content and hypopharyngeal gland size.

Evaluation of colonies

Strength of all colonies involved in the experiment [n = 20] was assessed according to their overall condition on April 15th 2020. The colonies were divided into 4 groups with respect to number of bee-occupied frames (combs), supers and brood area [dm^2]. The colonies were scored with grades 1–10: a) very week colonies with no growth potential and with less than 3 occupied inter-frames gaps (grades 1–3, the colonies were excluded), b) weak colonies with substandard development (grades 4–5), c) good condition colonies with standard growth (grades 6–7), d) strong colonies with above standard development and growth abilities (grades 8–10). Four colonies were selected for the experiment: colony No 1 (grade 4, weak condition), colonies No 2 (grade 6) and No 3 (grade 7) both of good condition and colony No 4 (grade 8, strong condition).

Marking and sampling of the bee workers

In each of the experimental colonies a comb with the oldest stadium of the sealed brood was isolated on April 24th 2020 into plastic net bag and returned back to the colony for 24 hours. Emerged workers were marked by colour pen (brand POSCA) and both the comb and marked workers were returned back to the maternal colony. The first sampling was made at the marking of workers and the other ones at weekly intervals until the marked workers vanished from the colony; totally 5 sampling dates with workers up to 4week-old. A sample with 10 workers from each of the experimental colonies was collected into a plastic vial and cooled to 4 °C directly after sampling.

Haemolymph collection

Haemolymph was collected as soon as the cooled workers became motionless. The haemolymph was collected individually from every worker using micro-capillary pipette by incision between 3rd and 4th abdominal tergites in volume 1 µl. The haemolymph sample was immediately pippeted into 1.5 ml Eppendorf tube containing 49 µl of phosphate buffer (pH = 7) and homogenized.

Hypopharyngeal glands

Each of the workers was decapitated and the head was put into 0.5 ml Eppendorf tube containing 30 µl of 75% ethyl alcohol. The head samples were stored at room temperature until dissection. The hypopharyngeal gland dissection was performed by cutting off the forehead part of the cuticle by micro-scalpel. The cuticle and the tracheal sacs were removed by tweezers. The size of hypopharyngeal gland was scored on a scale:1 = almost invisible shrunken gland, 2 = oval shaped pseudoacini spread within a one layer, 3 = oval shaped pseudoacini spread within more than one layer, 4 = polygonally shaped pseudoacini filling fully space between brain and frontal cuticle with regular convex formation of the gland on its surface. Transitional forms were scored with a semi-degree, e.g. gland between the 2nd and the 3rd size was scored with degree 2.5.

Total protein quantification

The protein concentrations were estimated by Bradford assay in micro-titration plates. Briefly: 5 µl of protein sample (50× diluted haemolymph) was mixed with 250 µl of Bradford reagent (Sigma-Aldrich, Merck). After 5 min of incubation at room temperature, the absorbance at 595 nm was measured using FUOstar Omega plate reader (BMG Labtech). Concentrations were calculated using calibration curve. The calibration curve for each measured plate was done using bovine serum albumin (Sigma Aldrich) as standard. Each measurement was performed in triplicate.

Statistical evaluation

The abscissae around means in charts represent the standard deviation. The data were evaluated by regression analysis and Pearson's correlation.

RESULTS AND DISCUSSION

Regression analysis between the total haemolymph protein (THP) and the hypopharyngeal gland (HG) size in all of the sampled workers (all individuals from all colonies) is depicted in Figure 1. The analysis showed only medium positive correlation (r = 0.412). The workers with the 4th degree of HG size showed THP values in range of 5 to 33 µg/µl. The workers with smaller HG showed this THP range in approx. 3–18 µg/µl.

Figure 1 Regression analysis between the total protein contents and the hypopharyngeal glands sizes of all sampled worker honeybees

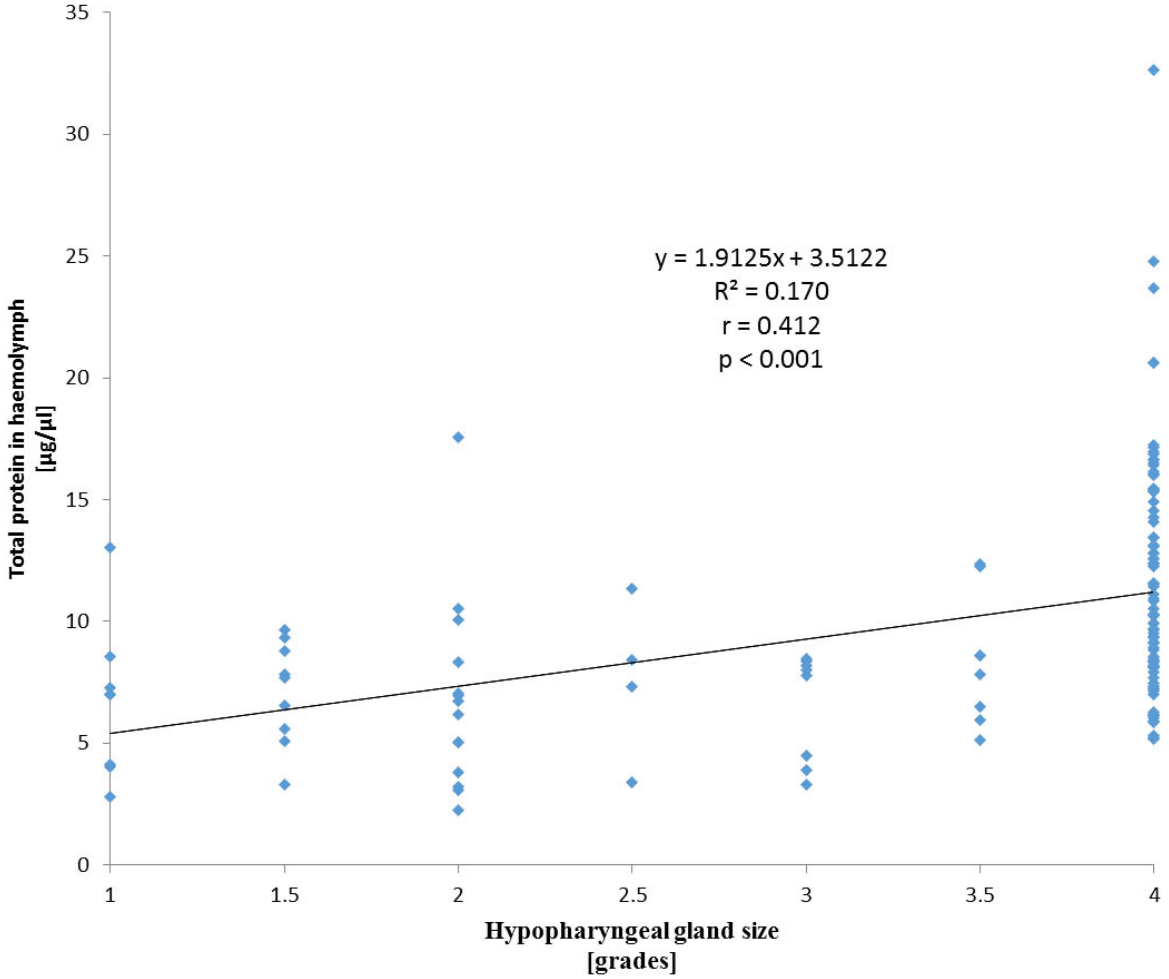

The correlation coefficients in the emerged workers and workers older than two weeks are summarized in Table 1. The dependence of middle importance was detected only in the freshly emerged workers. The older analysable samples of workers showed only weak dependence. The correlation in one- or two-week-old workers was not possible to calculate due to the fact that workers had HGs developed to 4th degree.

Table 1 Correlation between THP and HG size according to the worker age

Age of workers	Up to 24 hours old (n = 40)	3week-old (n = 40)	4week-old (n = 40)
r total haemolymph protein - hypopharyngeal gland size	0.58 p < 0.001	0.26 p < 0.105	0.17 p < 0.294

The analysis of ontogenetic changes according to the worker age expressed as a mean value for the experimental colonies together is depicted in Figure 2. Dependence between these mean values

(n_{yz} = 5) was very high and positive (r = 0.703, p = 0.185). The premise that workers with well-developed HG have concurrently high protein concentration in haemolymph is based on the fact that the injection of high doses of juvenile hormone into adult honeybee worker causes size reduction of HG and lowers the THP concentration (Rutz et al. 1976). However, the premise was confirmed by the results only up to the colony level instead of the individual level. This finding is in accordance with the superorganism postulates (Moritz and Southwick 2012) and points to the existing integrity in the honeybee colony (Crailsheim and Stolberg 1989). Since, there were lower levels of THP in workers with smaller HG we suppose that the workers with the low level of THP and fully sized HG could show only low secretion activity in their HGs as it was found by Brouwers (1982). However, three- or four-week-old workers did not show this dependence in our experiment. There are probably other factors involved in the investigated relationship because the size of HG is concurrently closely related physiological parameter to labour-division and age of the summer workers (Pridal et al. 1997). One of them may be a fact a shrunken HG produces proteins too, mainly enzymes (Sasagawa et al. 1989).

Figure 2 Ontogenetic course of changes in THP and HG

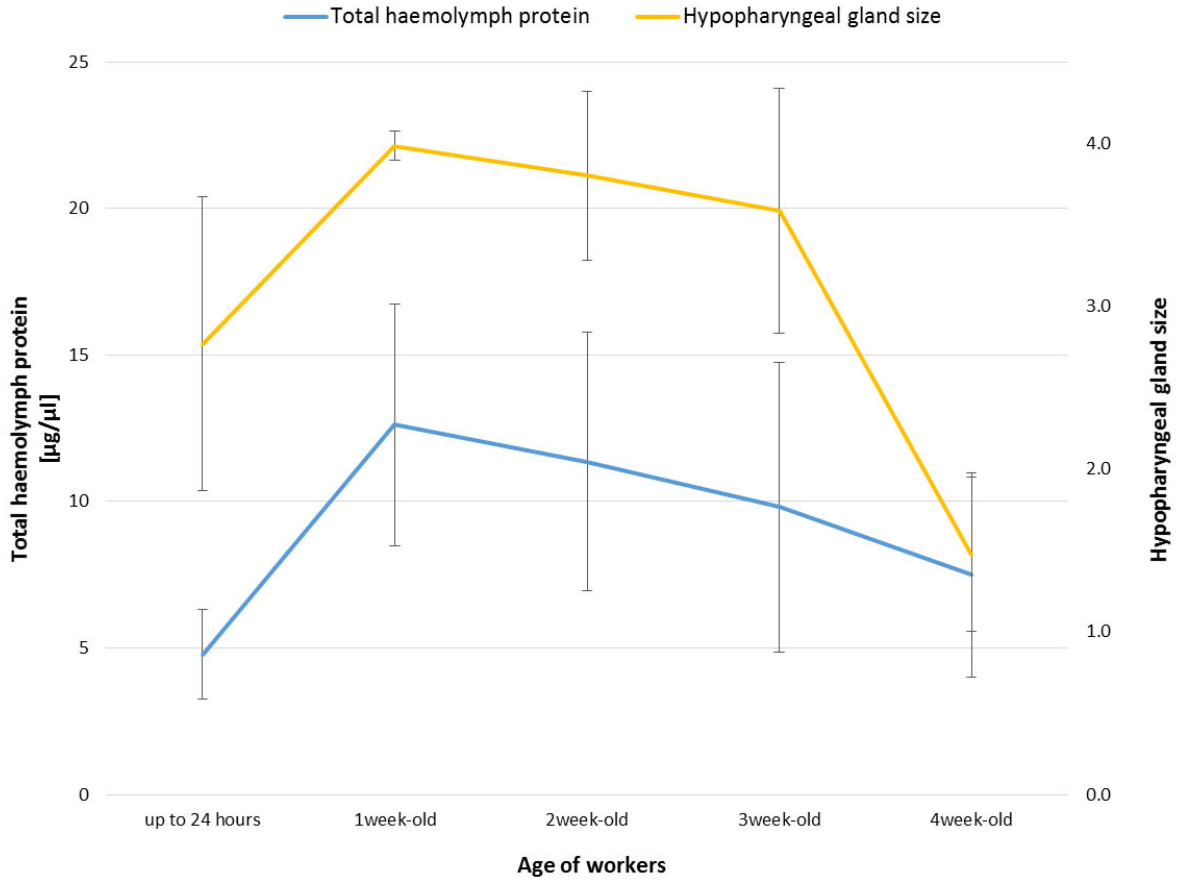

CONCLUSION

The hypopharyngeal gland size and the total haemolymph protein are physiological parameters related probably only at the honeybee colony level. The size of HG and THP were increasing from emerging of worker to age of the hive worker and then decrease to age of the forage only on average. This premised relationship at the level of the individual workers was not detected in spite of the size of HG is concurrently closely related to labour-division and age in the summer workers. Thus, the physiological context between development of HG and THP is not still fully understood. The given findings are in accordance with the superorganism postulates of the honeybee colony.

ACKNOWLEDGEMENTS
The research was financially supported from the donations by elitbau, Ltd.

REFERENCES

Amdam, G.V., Omholt, S.W. 2002. The regulatory anatomy of honeybee lifespan. Journal of theoretical biology, 216(2): 209–228.

Brouwers, E.V.M. 1982. Measurement of hypopharyngeal gland activity in the honeybee. Journal of Apicultural Research, 20(4): 193–198.

Crailsheim, K., 1986. Dependence of protein metabolism on age and season in the honeybee (Apis mellifica carnica Pollm). Journal of Insect Physiology, 32(7): 629–634.

Crailsheim, K., Stolberg, E. 1989. Influence of diet, age and colony condition upon intestinal proteolytic activity and size of the hypopharyngeal glands in the honeybee (Apis mellifera L). Journal of Insect Physiology, 35(8): 595–602

De Jong, D. et al. 2009. Pollen substitutes increase honey bee haemolymph protein levels as much as or more than does pollen. Journal of Apicultural Research, 48(1): 34–37.

Doeke, M.A. et al. 2015. Overwintering honey bees: biology and management. Current Opinion in Insect Science, 10: 185–193.

Fluri, P. et al. 1982. Changes in weight of the pharyngeal gland and haemolymph titres of juvenile hormone, protein and vitellogenin in worker honey bees. Journal of Insect Physiology, 28(1): 61–68.

González-Santoyo, I., Córdoba-Aguilar, A. 2012. Phenoloxidase: a key component of the insect immune system. Entomologia Experimentalis et Applicata, 142(1): 1–16.

Halberstadt, K. 1967. Über die Proteine, der Hypopharynxdrüse der Bienenarbeiterin. II. Elektrophoretische Untersuchung der Sekretproteine bei Schwarmbienen und Arbeiterinnen aus brutschwachen Völkern (1). Les Annales de l'Abeille, INRA Editions, 10(2): 119–132.

Kunc, M. et al. 2019. The Year of the Honey Bee (Apis mellifera L.) with Respect to Its Physiology and Immunity: A Search for Biochemical Markers of Longevity. Insects, 10(8): 244.

Kunert, K., Crailsheim, K. 1988. Seasonal changes in carbohydrate, lipid and protein content in emerging worker honeybees and their mortality. Journal of Apicultural Research, 27(1): 13–21.

Moritz, R., Southwick, E.E. 2012. Bees as superorganisms: an evolutionary reality. 1st ed., Berlin, Heidelberg: Springer-Verlag.

Pridal, A. et al. 1997. Condition of hypopharyngeal glands and ovaries of honeybee workers (Apis mellifera L.) during growth and swarming of colonies. Acta universitatis agriculturae et silviculturae Mendelianae Brunensis (Brno), 45(3–4): 51–58.

Rutz, W. et al. 1976. The function of juvenile hormone in adult worker honeybees, Apis mellifera. Journal of Insect Physiology, 22(11): 1485–1491.

Sasagawa, H. et al. 1989. Hormonal control of the division of labor in adult honeybees (Apis mellifera L.) I. Effect of methoprene on corpora allata and hypopharyngeal gland, and its a-glucosidase activity. Applied Entomology and Zoology, 24(1): 66–77.

Snodgrass, R.E. 1925. Anatomy and physiology of the honeybee. 1st ed., New York, London: McGraw-Hill Book Company Inc.

Ullman-Culleré, M.H., Foltz, C.J. 1999. Body condition scoring: a rapid and accurate method for assessing health status in mice. Comparative Medicine, 49(3): 319–323.

Analysis of weight, size, bone strength and blood biochemical parameters depending on dietary intake of organic and inorganic selenium in layers diet

Daria Baholet[1], Jakub Novotny[1], Andrea Roztocilova[1], Sylvie Ondrusikova[2], Sarka Nedomova[2], Eva Mrkvicova[1], Leos Pavlata[1], Ondrej Stastnik[1]
[1]Department of Animal Nutrition and Forage Production
[2]Department of Food Technology
Mendel University in Brno
Zemedelska 1, 613 00 Brno
CZECH REPUBLIC

xbaholet@mendelu.cz

Abstract: The aim of the research was to determine the effects of organic (*Saccharomyces cerevisiae* CNCM I-3060) and inorganic (sodium selenite – Na_2SeO_3) selenium supplemented in layer diets and its effect on the bone weight, strength and biochemical blood parameters. In both experimental groups (Organic and Inorganic, respectively) selenium was supplied with its natural content in the feed plus selenium was added that its total content was 0.31 mg/kg in both groups. In the bones were analysed parameters as width, length, strength and weight. Biochemical analysis of blood samples was performed, analysing ALT, AST, GGT, ALP, LD, CK, Tbili and Urea activities. The results show that there is no statically significant effect either from the organic form of selenium than inorganic form.

Key Words: sodium selenite, *Saccharomyces cerevisiae*, hens, dietary additives

INTRODUCTION

The role of trace elements to increase poultry productivity is important in the production environment. The level and the source of trace elements play an important role in ration formulations and optimizing product quality, production level, health status and antioxindant status. of birds and trerefore influence the economic returns (Attia 2010, Urbankova 2018). Selenium (Se) is an important natural antioxidant that is essential in many metabolic processes in the body. It is found in two forms, inorganic and organic. Inorganic selenium refers to different minerals such as selenite, selenate and selenide, and organic selenium is related to amino acids such as methionine and cysteine (Combs and Combs 1986). Deficiency of Se causes reduced fertility (Hefnawy and Tórtora-Pérez 2010). Some researches indicate Se yeast might be a superior organic source of selenium compared to other selenite sources of Se (Asadi 2017).

Selenium deficiency can results in higher damage of membrane structures, impaired reproduction and rapid organism aging (Horky 2016). The most common and practical delivery of selenium can be refilling to the mineral feed. Form of addition is particulate mineral mixtures with selenium either in inorganic form such as sodium selenite or in organic form as selenomethionine from *Saccharomyces cerevisiae*.

The aim of this experiment was to evaluate the influence of inorganic or organic selenium supplementation to layer hens.

MATERIAL AND METHODS

Characterization of the experimental design

The experiment was performed with the approval of the Ethics Committee at the Faculty of AgriSciences, Mendel university in Brno, Czech Republic in accordance with the Act No. 246/1992 Coll. on the protection of animals against cruelty. The experiment was performed at the experimental laboratory of Mendel university in Brno. Throughout the experiment, microclimatic conditions were maintained at 23 ± 1 °C, 60% humidity, and the light regime were controlled according

to the requirements to produce Lohmann hens (Lohmann Tierzucht 2020). The lighting system was set at a 16-h light and 8-h dark light cycle. A conventional deep litter system was used with wood shavings as the bedding material. The Lohman Brown- Classic hens were at the age of 33 weeks at the beginning of the study and lasted till 41st weeks of age.

Layers were divided into three equal groups with four repetitions. The animals had access to water and feed *ad libitum.* Control group (n28) was fed with a diet without addition of selenium (selenium was supplied only with its natural content in the feed). First experimental group (Organic; n=28) was fed with organic source of selenium (*Saccharomyces cerevisiae* CNCM I-3060) and the second experimental group (Inorganic; n=28) was fed with inorganic source of selenium (sodium selenite – Na_2SeO_3). In both experimental groups (Organic and Inorganic, respectively) selenium was supplied with its natural content in the feed plus selenium was added that its total content was 0.31 mg/kg in both groups. The three isocaloric and isonitrogenous diets were formulated according to the recommended nutrient content for Lohmann Brown-Classic hens (Lohmann Tierzucht 2020).

The chemical compositions of diets were determined for dry matter, crude protein, crude fat, crude fibre, and ash according to the EC Commission Regulation (Commission Regulation 152/2009). Composition and chemical composition of diets are shown in Table 1 and Table 2, respectively.

Table 1 Composition of diets (%)

Components	Control	Organic	Inorganic
Maize	33.339	33.339	33.339
Soybean meal	31.000	31.000	31.000
Wheat	19.000	19.000	19.000
Limestone grit	5.400	5.400	5.400
Rapeseed oil	4.000	4.000	4.000
Premix*	3.000	3.000	3.000
Limestone milled	2.500	2.500	2.500
Monocalcium phosphate	1.300	1.300	1.300
Sodium chloride	0.300	0.300	0.300
DL-Methionine	0.160	0.160	0.160
L-Threonine	0.001	0.001	0.001
Sodium selenite	0.000	0.000	0.001
Saccharomyces cerevisiae	0.000	0.010	0.000

*Legend: *Premix contains (per kg): L-Lysine 13 g; DL-Methionine 45 g; Calcium 295 g; Phosphorus 67 g; Sodium 46 g; copper 300 mg; iron 2,300 mg; zinc 1,800 mg; manganese 2,400 mg; iodine 30 mg; retinol 330,000 IU (international units); calciferol 100,000 IU; tocopherol 500 mg; phylloquinone 40 mg; thiamine 40 mg; riboflavin 120 mg; pyridoxin 54 mg; cobalamin 400 ug; biotin 3 mg; niacinamid 420 mg; folic acid 30 mg; calcium pantothenate 250 mg; cholin chloride 6,000 mg.*

Table 2 Chemical analysis of diets

	Control	Organic	Inorganic
Dry matter (%)	100	100	100
ME_N (MJ/kg)	11.47	11.47	11.47
Crude protein (%)	20.76	20.8	20.8
Ether extract (%)	6.27	6.5	6.34
Crude fibre (%)	2.21	1.55	1.97
Crude ash (%)	16.41	16.39	16.93
Ca (%)	4.57	4.57	4.57
P (%)	0.67	0.67	0.67
Se (mg/kg)	0.09	0.31	0.31

Legend: ME_N – Apparent metabolizable energy

The health status of animals was evaluated daily and live weight was measured regularly during the trial. One death was recorded during the trial. At the end of the experiment all hens were weighed, and 8 birds were randomly selected from each group and slaughtered by decapitation.

Blood (n=8 per group) was collected into the heparinized tubes and centrifuged for 15 minutes at 3,000 rpm. The separated blood plasma was frozen (-20 °C) until biochemical examination.

The biochemical profile of blood plasma was analysed with the use of Ellipse (AMS Spa, Italy) analyser. The blood parameters related to hepatocyte damage were selected, it was showed functional activity of liver, respectively. The individual parameters were analysed using individual tests produced by Erba Lachema (Brno, CZ): albumin; AST – aspartate aminotransferase; GGT – gamma glutamyl transferase; ALP – alkaline phosphatase; ALT – alanine aminotransferase, LD – lactate dehydrogenase, Tbili – total bilirubin, CK – creatine kinase and Urea.

Femur and tibia bones (n=8 per group) were demuscled and measured (via sliding scale) and weighed. The strength of bones was measured by TIRATEST 27025 testing machine (TIRA Maschinenbau GmbH, Germany). The bone strength was evaluated using a three-point bending test.

Statistical analysis

Data has been processed by Microsoft Excel (USA) and Statistica version 12.0 (USA). One-way analysis of variance (ANOVA) was used. To ensure evidential differences Scheffé´s test was applied and $P < 0.05$ was regarded as statistically significant difference.

RESULTS AND DISCUSSION

Bone parameters analysis

The results from bone analysis are showed in the Figures 1 and 2. In the bones were analysed parameters as width, length, strength, and weight to prove the influence of different form of selenium on these parameters. From these results we can constate no influence of organic or inorganic selenium on the measured parameters in bones. Selenium level, source and the interaction between the level and the source of Se had no significant effect on the tibia and thing bones parameters compared with that in hens fed the control diet (Figure 1, 2). Similar conclusion was constated in the study of (Attia 2010). The mechanism by which Se affects the bone formation is not known at present, for example the Se presence in human bones is about 16% of total body Se (Zachara et al. 2001). More research on this topic is necessary.

Figure 1 Tibia bones parameters

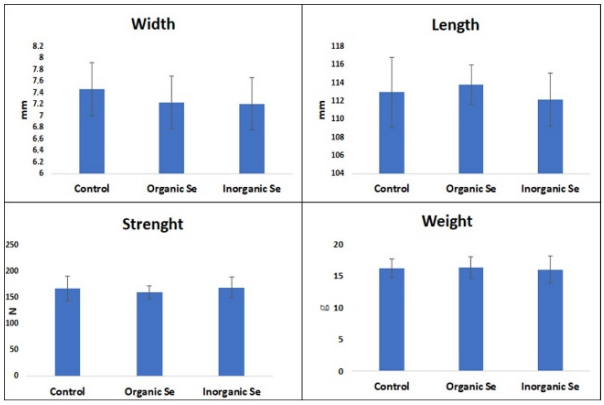

Figure 2 Femur bones parameters

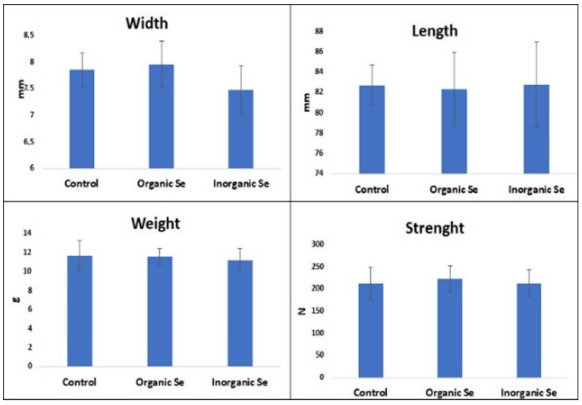

Legend: There were found no statistically significant differences (P >0.05).

Biochemical analysis of blood samples

Results of the biochemical analysis are presented in Figure1 and 2. The ALT, AST, GGT, ALP, LD, CK, Tbili and Urea activities indicate liver tissue status. The urea indicates nitrogen metabolism of the organism. All these parameters interfere with metabolism of liver and have influence to it. This argument is confirmed by the study of Dufour et al. (2000), which state the concentration of AST and ALT in the blood reflects the extent of the tissue damage.

This study deals also with the possible toxicity of selenium included in feed mixture, that may affect liver enzymes. This effect was not discovered in our experiment. This phenomenon may be due to relatively short time of feeding selenium mixture. In accordance with our findings, Abadi et al. (2014). Moreover, absorption of inorganic Se from food is relatively low if compared to organic Se, thus

resulting in production of animal foodstuffs containing low concentration of selenium (Payne et al. 2005, Yoon et al. 2007).

Figure 3 Biochemical parameters in layer blood samples

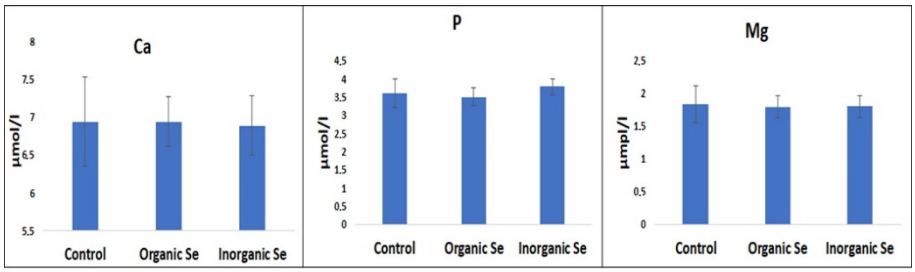

Legend: Ca – calcium, P – phosphorus, Mg – magnesium. There were found no statistically significant differences (P >0.05).

Figure 4 Biochemical parameters in layer blood samples

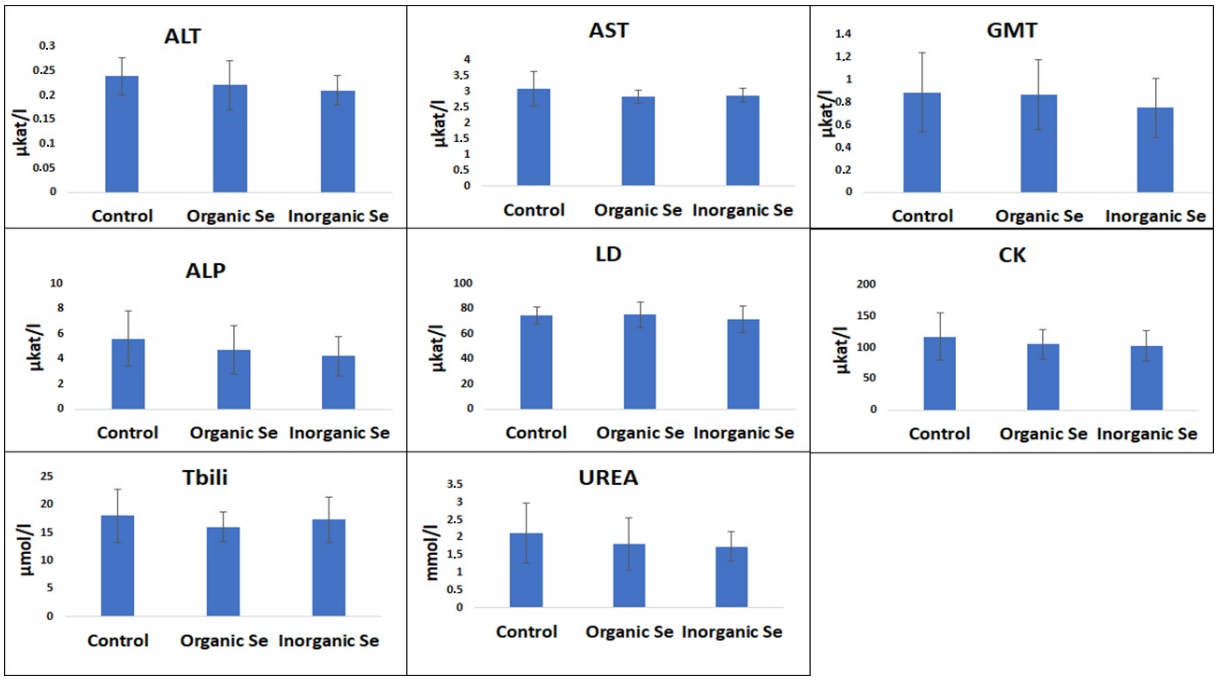

Legend: ALT – alanine aminotransferase, AST – aspartate aminotransferase, GMT – gamma-glutamyl transferase, ALP – alkaline phosphatase, LD – lactate dehydrogenase, CK – creatine kinase, Tbili – total bilirubin, Urea; There were found no statistically significant differences (P >0.05).

CONCLUSION

In conclusion based on biochemical characteristics and performance of bones the organic (*Saccharomyces cerevisiae* CNCM I-3060) and inorganic (sodium selenite – Na_2SeO_3) selenium supplemented in layer diets does not affect the animal positively either negatively.

ACKNOWLEDGEMENTS

The research was financially supported by the Internal Grant Agency of Faculty of AgriSciences no. AF-IGA2020-TP012.

REFERENCES

Abadi, M.H.M.G. et al. 2014. Efficacy of wheat based vs. corn based diet formulated based on digestible amino acid method on performances, carcass traits, blood parameters, immunity response, jejunum histomorphology, cecal microflora and excreta moisture in broiler chickens. Iranian Journal of Applied Animal Science, 4(1): 105–110.

Asadi, F. et al. 2017. Comparision of different Selenium Sources and Vitamin E in Laying Hen Diet and Their Influences on Egg Selenium and Cholesterol Content, Quality and Oxidative Stability. Iranian Journal of Applied Animal Science, 7(1): 83–89.

Attia, Y.A. et al. 2010. Effect of inorganic or organic selenium supplementation on productive performance, egg quality and some physiological traits of dual-purpose breeding hens. Czech Journal Animal Science, 55(11): 505–519.

Combs, G.F., Combs, S.B. 1986. The role of selenium in Nutrition. New York, USA: Academic Press.

Commission regulation (EC) 152/2009. Laying down the methods of sampling and analysis for the official control of feed. Brussels: The commission of the European Communities.

Dufour, D.R. et al. 2000. Diagnosis and monitoring of hepatic injury. II. Recommendations for use of laboratory tests in screening, diagnosis, and monitoring. Clinical Chemistry, 46(12): 2050–068.

Hefnawy, A.E.G., Tórtora-Pérez, J.L. 2010. The Importance of selenium and the effect of its deficiency in animal health. Small Ruminant Research, 89: 185–192.

Horky P. et al. 2016. Electrochemical Methods for Study of Influence of Selenium Nanoparticles on Antioxidant Status of Rats. International Journal of Electrochemical Science [Online]. Available at: http://www.electrochemsci.org/papers/vol11/110402799.pdf. [2020-9-10].

Lohmann Tierzucht 2020. Management guide [Online]. Available at: http://www.ltz.de/en/e-guide/new_e-guide/HTML/. [2020-09-10].

Payne, R.L. et al. 2005. Effect of inorganic versus organic selenium on hen production and egg selenium concentration. Poultry Science, 84(2): 232–237.

Urbankova, L. et al. 2018. Antioxidant status of rats' blood and liver affected by sodium selenite and selenium nanoparticles. Biochemistry, Biophysics and Molecular Biology [Online]. Available at: https://peerj.com/articles/4862/. [2020-8-20].

Yoon, I. et al. 2007. Effect of Source and Concentration of Selenium on Growth Performance and Selenium Retention in Broiler Chickens. Poultry Science, 86(4): 727–730.

Zachara, B.A. et al. 2001. Tissue level, distribution, and total body selenium content in healthy and diseased humans in Poland. Archives of Environmental Health, 56(5): 461–466.

Analysis of the performance of the best dressage and show jumping horses in the world

Michaela Brudnakova, Eva Sobotkova
Department of Animal Breeding
Mendel University in Brno
Zemedelska 1, 613 00 Brno
CZECH REPUBLIC

michaela.brudnakova@mendelu.cz

Abstract: In this article we focused on the comparing the performance between the best dressage and showjumping horses in the world. We collected the database of the best 500 horses in showjumpig and also dressage which competed in Federation Equestre Internationale (FEI) dressage and jumping shows. Data used in the research has been gathered from the official website of FEI. We focused on the specifics factors: age, sex, breed and auxiliary points (AAP) reached through the season. We processed the data in statistic program STATISTICA 2012. Then we tested statistically significant factors using Scheffe´s test. As a statistically high significant ($p<0.001$) factors were demonstrated factors such as breed. We found out, that according to auxiliary points the most successful sex are geldings in both of the disciplines. In showjumping they gained 708.6 AAP and in dressage 1347.9 AAP. The most successful breed in average values is Westphalian (914.3 AAP) in showjumping and statistically highly significant ($p<0.001$) Trakhennen (1555.9 AAP) in dressage. According to the age group the most successful is category of the horses 7–13 years old in showjumping and the oldest category of horses in dressage competition (1347.7 AAP). The most important breeders in showjumping in the year 2019 are Chacco Blue (22 descendants), Cassal Ask (13) and Diamand de Semilly (12). The most important breeders in dressage are Broere Jazz (14 descendants), Glocks Johnson Tn (14) and Sandro Hit (14).

Key Words: dressage, showjumping, performance, pedigree, ranking

INTRODUCTION

The breeding programmes of sport horses are run with the aim to breed horses which can compete successfully at the highest levels of competition in dressage and show jumping (Rovere et al. 2017). The goal of show jumping is for combinations to jump over all the fences on the course in a test of the rider's skill and the horse's power, scope, speed, athleticism and carefulness and also dressage with its popularity rapidly grows each year (Federation Equestre Internationale 2020a, 2020b). Horse and rider perform a "test" consisting of difficult moves and gait changes. Considerable training is required to master even the simplest of movements required during a dressage test. Riders cannot use voice commands and the horse–rider pair is scored on how well it performs the test (Rovere et al. 2016). Kearsley (2008) said that it is possible to predict the performance of a horse at the advanced level based on its performance at novice or even pre novice level. Breeders and horse trainers have been concerned with the problem of assessing the utility value of young horses in particular their suitability for breeding, sport and recreational uses (Janicki 2015). The main aim of this research is to point out the influence of the age, sex and breed on the performance of the best dressage and show jumping horses in the world. In the research we also focused on the pedigree of horses. The evaluation of the foundation sires due the amount of the auxiliary points of their descendants from the database is also the part of the research. We focused on the sires which have minimum 5 descendants and more.

MATERIAL AND METHODS

Data used in this article was taken from the official websites of Federation Equestre Internationale from the year 2019. We analysed 500 horses of each discipline and we compared them. The performance was evaluated according to the number of points from particular competitions within the given year (season). Formula for calculating of auxiliary points is officially provided in accordance to FEI world

performance rating (Federation Equestre Internationale 2020a, 2020b). Data were processed by the statistic program STATISTICA 2012 and we also used multi-factor Analysis of Variance (ANOVA) and Scheffe´s test. We divided individual horses into the groups according the age, sex, breed. Except for the statistics, we also composed the special sire ranking. It consists of fathers of our horses from the database.

RESULTS AND DISCUSSION

In time period from January 1, 2019 to December 31, 2019. 1000 the most successful horses competed in the world FEI competitions in show jumping and dressage. In the population of 500 the most successful horses which competed under FEI, geldings were the sex group with the highest amount of horses in both disciplines (show jumping 263 horses/ dressage 324 horses), followed by mares in show jumping (150) and stallions in dressage (90) there was the lowest amount of stallions in show jumping (87) and mares in dressage (87).

On the opposite site, geldings had the best performance results in both of the disciplines (show jumping 708.6 AAP/ dressage 1347.9 AAP). In the case of the breed we can see that in the population of the best 500 horses in the world is in show jumping competition the most successful Westphalian breed (914.3 AAP) and on the opposite site in dressage is the Trakhenen breed (1555.9 AAP). This difference is presented in Figure 1 and Figure 2.

Table 1 Descriptive statistics of dressage discipline according to auxiliary points (AAP)

Number of horses	Average	Median	Modus	Minimum	Maximum	Coefficient of variation
500	1305.9	1289	1045	579	2888	37.01

From Table 1 we can see that dressage horses reached in average (1305.9 AAP) more points like show jumping horses (690 AAP). Dressage horses gained more points in minimum and maximum also. Coefficient of variation is also smaller in dressage discipline so it means that population of dressage horses was more established.

*Table 2 ANOVA statistics of dressage discipline ($p<0.001$**)*

Factors	Points
Sex	-
Breed	**
Age	-

When we compare ANOVA statistics between show jumping and dressage competition we can see, that in the dressage horse population there was statistically highly significant factor breed. Unfortunately, we didn't prove any other factor, so in the next comparison we will work only with average values. In the show jumping competition we didn't prove any of the factors, so we will use just average values.

Table 3 Descriptive statistics of show jumping discipline according to auxiliary points (AAP)

Number of horses	Average	Median	Modus	Minimum	Maximum	Coefficient of variation
500	690	590	multiple	400	1495	56.5

*Table 4 ANOVA statistics of show jumping discipline ($p<0.001$**)*

Factors	Points
Sex	-
Breed	-
Age	-

Scheffe's test

In the dressage discipline was the most successful sex the group of stallions (1366 AAP*)*. In the other research were geldings shown as more trainable than mares and stallions more rideable than mares when assessed in a dressage scenario. It seems likely that mares may perform worse than males. The results showed that sex has an effect on behavioral reactivity of horses. Thus, it is important to consider the horses sex during selection for a particular type of riding (Budzynska 2014). The stallions were also shown to perform better than mares in dressage also in the other researches (Hanousek et al. 2018). Gelding obtained the smallest number of AAP in dressage discipline.

Figure 1 Success of each sex in dressage discipline

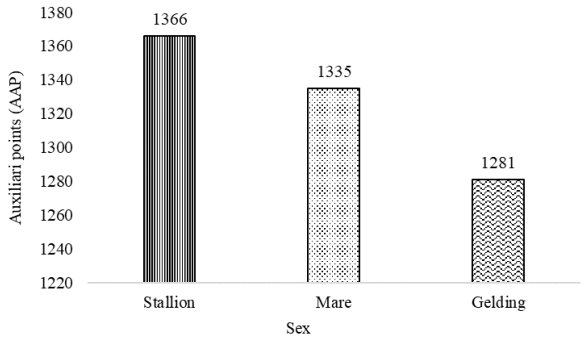

*Figure 2 Success of each sex in show jumping discipli*ne

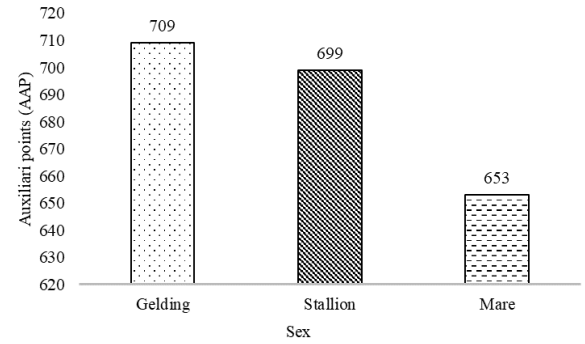

Geldings reached the best ranking in show jumping (709 AAP). They provided better performance than stallions and mares. In the other research, mares and gelding incurred fewer penalty points than stallions. It was the only area in which the mares have performed significantly better than either stallions or geldings, and stallions are generally considered to be faster than mares (Hanousek et al. 2018). The main reason is the effect of ovarian activity and particularly the state of estrus has been considered an important factor in reduced athletic performance (Pryor 2005).

Figure 3 List of the best dressage horse breeds in the year 2019

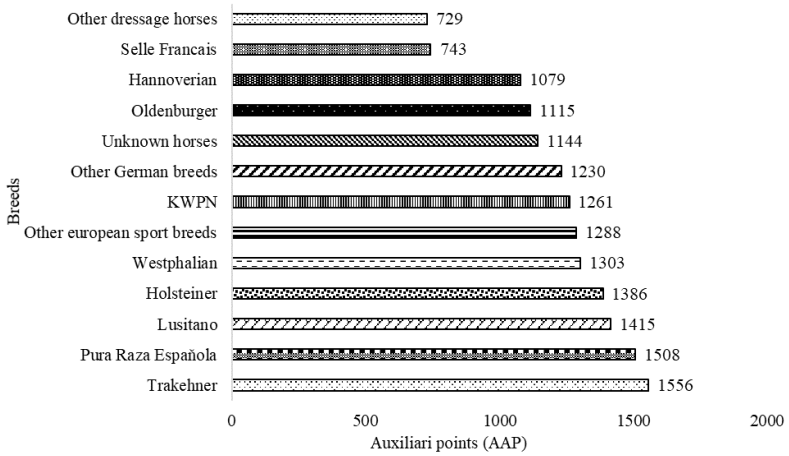

In Figure 3 dressage competitions provided the best performance results Trakehnen *(*1556 AAP), PRE (1508 AAP) and Lusitano horses (1415 AAP). On the other site, the worst performance results had shown other dressage horses (729 AAP), Selle francais horse breed (743 AAP) and Hannoverian breed (1079). The breed Zangersheide is in the dressage discipline missing.

Figure 4 List of the best show jumping horse breeds of the year 2019

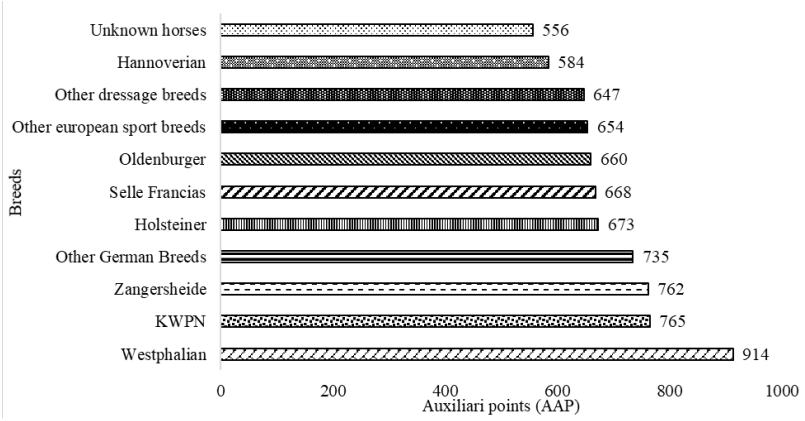

In the show jumping competition had the best results breeds: Westphalian horse breed (914 AAP), KWPN (914 AAP) and Zangersheide breed (762 AAP). In the year 2018 were on the list of the best show jumping breeds: Zangersheide (570.3 AAP), Holsteiner (565.9 AAP) and Other European sport breeds (524.9 AAP) (Brudnakova and Sobotkova 2018). The group of horses with the lowest amount of AAP were horses with unknown pedigree (556 AAP), Hannoverian breed (584 AAP) which is on the list of the best dressage horse one of the most successful and Other dressage breeds (647 AAP). The other research showed that breed has an impact on scores obtained during stationary and field tests, and, as a result, on the utility scores obtained by individual animals and their usability when breeding animals for particular sporting events (Drewka et al. 2013a). The most successful age group in dressage competition is group of the oldest horses 17 and more years (1348 AAP). In my opinion, this group is experienced the most and is therefore the most successful. And the age group with the lowest amount of AAP is the group of middle aged horses (1258 AAP). It was found that performance in the competition on average increase with age and stallions and geldings have on average a higher performance than mares (Rovere et al. 2016). In the other research where they were working with a young mares which were preparing for a performance test they realized that 4 years old horses had the highest amount of points which might indicate their higher level of training and development (Drewka et al. 2013b).

Pedigree

Figure 5 The most common foundation sires in pedigree of dressage horses

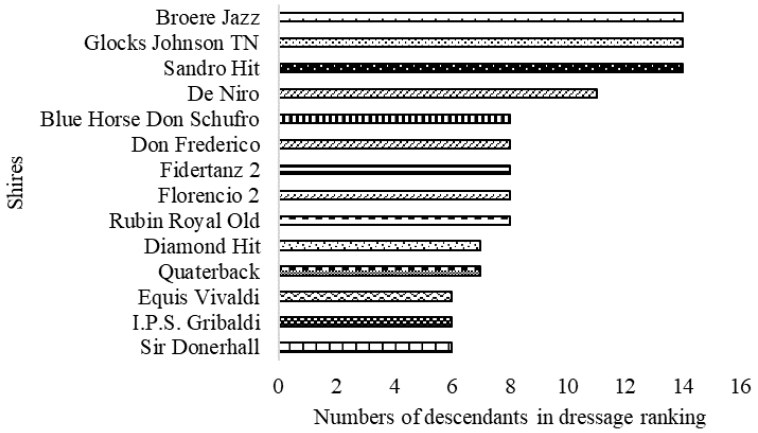

In the pedigree of the best dressage horses in the world were the most common these foundation sires. More than 5 descendants had also sire like Blue Horse Hotline, Blue Horse Zack, Dancier, Dimaggio, Glocks Romanov, Rousseau, San Amour and Stedinger.

Figure 6 The most common foundation sires in pedigree of show jumping horses

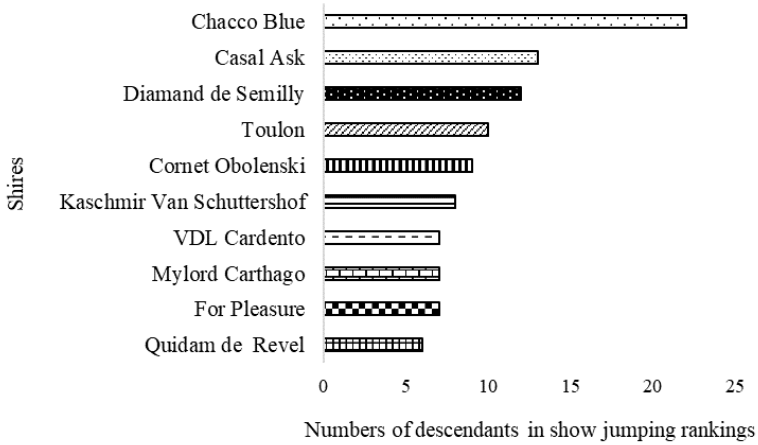

In pedigree of the best show jumping horses in the world were the most these foundation sires. More than 5 descendants had sire like Clinton and Nabab de Reye.

CONCLUSION

The main aim of this research was to find out and compare the best performance of the horses in dressage and show jumping and compare their pedigree. For this comparison we used the most important factors such a breed, sex and the age of horses. We also worked with the pedigree of concrete horses. We were comparing the foundation sires which had more than 5 descendants in the list of the best show jumping or dressage horses in the world. We used statistics analysis ANOVA and we proved that factor breed in population of dressage horses has statistically highly significant impact on performance of the horses. We dint prove like significant any of the other factors. After ANOVA analysis we used the Scheffes test and found out that the most successful breed in dressage is Trakehner (1556 AAP) and in the show jumping it is Wesphalian horse (914 AAP). On the other side the breeds which were not so successful in dressage are Other dressage horses (729 AAP) and Zangersheide breed is completely missing. In the show jumping were the breeds with lover performance results Unknown horses (556 AAP). Zangersheide breed was one of the most successful show jumping breeds. The sex with the highest amount of auxiliary points in dressage is group of stallions (136 6AAP), mares (1335 AAP) and the lowest amount of auxiliary points had geldings (1281 AAP). On the opposite site in the show jumping was the most successful sex group, the group of geldings (709 AAP), stallions (699 AAP) and the lowest amount of auxiliary points had mares (653 AAP). The age group with the highest amount of auxiliary points were the oldest horses (1348 AAP), the age group of 7–14 years old horses (1325 AAP) and the lowest amount of auxiliary points had the group of the youngest horses (1258 AAP). The foundation sires which had the highest number of descendants in a list of the best 500 dressage horses in the world were Glocks Johnson TN (14), Broere Jazz (14) and Sandro Hit (14). In show jumping were the results different. The most used were foundation sires like Chacco Blue (22), Cassal Ask (12) and Diamand de Semilly (12). I hope that this research will help to breeders and owners of the sport horses in our country with a breeding and choosing the best stallions for their mares.

REFERENCES

Brudnakova, M., Sobotkova, E. 2018. Comparison of the performance between the best jumping horses in the Czech Republic and the world. In Proceedings of 25th International PhD Students Conference MendelNet 2018. Brno, Czech Republic, 7–8 November. Brno: Mendel University in Brno, Faculty of AgriSciences, pp. 104–107.

Budzynska, M. et al. 2014. Behavioral and psychological reactivity of mares and stallions evaluated in performance tests. Acta Veterinaria, 64(3): 327–337.

Drewka, M. et al. 2013a. The effect of age on results obtained by mares during stationary and field performance tests conducted in Poland in the years 2001–2010. Journal of Central European Agriculture, 14(4): 1374–1383.

Drewka, M. et al. 2013b. The effect of the breed of Warmblood mares on results obtained during stationary and field performance tests in Poland in the years 2001–2010. Journal of Central European Agriculture, 14(4): 1394–1401.

Federation Equestre Internationale. 2020a. Rankings and Standing page in show jumping [Online]. Available at: https://data.fei.org/Ranking/Search.aspx?rankingCode=S_WR_RH.

Federation Equestre Internationale. 2020b. Rankings and Standing page in dressage [Online]. Available at: https://data.fei.org/Ranking/Search.aspx?rankingCode=D_WR.

Hanousek, K. et al. 2018. Effect of horse sex status on British Eventing competition performance: an observation study between 1998 and 2016. The Veterinary Record, 182(23): 666.

Janicki, B. et al. 2015. Assessment of performance traits in breeding horses in context of the operation of training stations in Poland. Journal of Central European Agriculture, 16(1): 197–207.

Kearsley, C.G.S. et al. 2008. Use of competition data for genetic evaluations of eventing horses in Britain: Analysis of the dressage, showjumping and crosscountry phases of eventing competition. Livestock Science, 118(1–2): 72–81.

Pryor, P. et al. 2005. Management of Estrus in the performance Mare. Clinical Techniques in Equine Practice, 4(3): 197–209.

Rovere, G. et al. 2016. Analysis of competition performance in dressage and show jumping of Dutch Warmblood horses. Animal Breeding and Genetics, 133(6): 503–512.

Rovere, G. et al. 2017. Genetic correlations between dressage, show jumping and studbook-entry inspections traits in a process of specialization in Dutch Warmblood horses. Journal Animal Breeding and Genetics, 134(2): 162–171.

Occurrence of *Helicobacter pylori* in bulk milk samples of raw cow's milk in Moravia

Aneta Grondelova, Zora Stastkova, Pavlina Navratilova, Ivana Bednarova, Petra Furmancikova, Daniela Necasova
Department of Animal Origin Food & Gastronomic Sciences
University of Veterinary and Pharmaceutical Sciences Brno
Palackeho tr. 1946/1, 612 42 Brno
CZECH REPUBLIC

H19348@vfu.cz

Abstract: The aim of the study was to determine the frequency of occurrence of *Helicobacter pylori* in raw cow's milk originating from the Moravian region in the Czech Republic. A total of 68 bulk samples of raw cow's milk were examined for the presence of *H. pylori* using the classical culture method and the Nested polymerase chain reaction (Nested-PCR). *H. pylori* was not isolated using the culture method in any of the examined samples. Using the Nested-PCR method, *H. pylori* DNA was detected in 31 (46%) samples. On the basis of the obtained results, the applied culture method appears to be unsuitable for monitoring the occurrence of *H. pylori* in raw cow's milk. On the contrary, the Nested-PCR method showed a high sensitivity to the detection of *H. pylori* in the samples. This study showed that raw cow's milk from the Moravian region can be a source of *Helicobacter pylori* bacteria.

Key Words: raw milk, *Helicobacter pylori*, culture method, Nested polymerase chain reaction

INTRODUCTION

Consumption of raw milk poses a risk to human health due to the possible presence of pathogenic microorganisms causing serious human diseases. Some authors state that the risk of foodborne illness for consumers may be considered real and even high, in the case of frequent consumption of raw milk (Verraes et al. 2014, EFSA 2015).

The EFSA statement also implies that raw milk in the European Union may be a source of zoonotic agents occurring in dairy livestock populations, in particular *Campylobacter* spp., *Salmonella* spp., shigatoxin-producing *E. coli* (STEC), *B. cereus*, *Brucella abortus*, *Brucella melitensis*, *L. monocytogenes*, *Mycobacterium bovis*, *Staphylococcus aureus*, *Yersinia enterocolitica*, *Yersinia pseudotuberculosis*, *Corynebacterium* spp., *Streptococcus suis* subsp. *zooepidemicus*, the parasites *Toxoplasma gondii*, and *Cryptosporidium parvum*, as well as tick-borne encephalitis virus (TBEV). The EFSA statement, based on the statistics on the incidence of foodborne illness in EU Member States in 2007–2013, further indicates that 27 epidemics were related to raw milk consumption. Most of them (21) were attributed to *Campylobacter* spp., 1 was caused by *Salmonella* Typhimurium, two by STEC, and 3 by TBEV (EFSA 2015). As mentioned by Verraes et al. (2014) in the summary, a number of pathogenic microorganisms were detected in milk. The authors dwell on the relatively high frequency of positive findings of *Helicobacter pylori* in raw milk.

H. pylori is a gram-negative, microaerophilic bacterium colonizing the human gastric mucosa. The prevalence of *H. pylori* infection is high; it is estimated to affect more than 50% of the world's population. The *H. pylori* infection has been associated with chronic gastritis, duodenal and gastric ulcer, the development of adenocarcinoma and gastric lymphoma MALT (Mucosa-Associated Lymphoid Tissue). The majority of infected individuals (70%) are asymptomatic (Zamani et al. 2017).

Despite the high incidence of infection, the reservoirs and transmission pathways of *H. pylori* have not been completely clarified. Transmission from person to person by the oral-oral or oral-faecal route is considered highly likely. Another accepted hypothesis is that human infection may also occur through contaminated food or water. On the basis of the microbiological and epidemiological properties of *H. pylori*, it has been classified as a foodborne pathogen. *H. pylori* has been detected in drinking

water, seawater, vegetables and foodstuffs of animal origin. It has the capacity to survive for a relatively long time in foodstuffs such as milk, vegetables and ready-to-eat foods. The foodstuff becomes a vehicle for *H. pylori* infection; in the case of primary food contamination (animal reservoir) or secondary food contamination as a result of non-compliance with hygienic processing conditions (human reservoir) (Quaglia et al. 2007, Quaglia and Dambrosio 2018). According to literature sources, foodstuffs of animal origin, especially raw milk, are considered the most likely source of infection when transmitted by food, as *H. pylori* DNA has been largely isolated from raw milk samples (Zamani et al. 2017).

In the Czech Republic, it is primarily packaged heat-treated cow's milk that is consumed, but since 2003, direct sales of raw milk from the farm have been permitted in the Czech Republic, and since 2009, sales of raw milk from milk vending machines have also expanded. Consumers are advised to consume milk only after heat treatment, but some consumers do not follow the recommendations. A study on the detection of *H. pylori* in raw milk has not yet been published in the Czech Republic.

Various methods are used to detect *H. pylori* in foodstuffs and water. Cultivation is one of the time-consuming methods used to detect *H. pylori*. Selective media, usually based on Brain heart agar or Columbia agar, are used to isolate this bacterium from food. Selective media tend to be complemented with antibiotic supplements (vancomycin, colistin, trimethoprim, polymyxin, etc.) to suppress the growth of contaminating microflora and enriched with growth supplements (blood, serum, coal, yolk emulsion, etc.) to support the growth of *H. pylori* (Quaglia and Dambrosio 2018). In addition to classical culture methods, other methods have been included, such as immuno-separation (IMS), epifluorescence microscopy, autoradiography, or fluorescence in situ hybridization assay (FISH). Molecular-biological methods enabling specific sequence amplification of the DNA of the microorganism together with molecular typing of strains show high sensitivity. In order to identify *H. pylori* in foodstuffs, the multiplex touchdown PCR (MT-PCR), Nested-PCR, quantitative real time PCR, and reverse transcription PCR (RT-PCR) have been developed (Quaglia and Dambrosio 2018).

The principle of the Nested-PCR method is based on the use of two pairs of primers, external and internal. After the reaction with the outer primer pairs, the resulting product serves as a template for the reaction with the inner primers. Owing to these two consecutive reactions, the probability of the amplification of a specific section of the DNA is significantly increased (Pelt-Verkuil et al. 2008).

The aim of the study was to determine the frequency of the occurrence of *Helicobacter pylori* in raw cow's milk originating from the Moravian region in the Czech Republic, using the classical culture method and the Nested polymerase chain reaction.

MATERIAL AND METHODS

Samples

In July 2020, bulk samples of cow's milk (n = 68) were obtained on the collection lines of two milk processing companies which take milk from dairy farms in the Moravia region of the Czech Republic. This means that one bulk sample came from one dairy farm located in the Moravia region. The samples were collected automatically (using the auto-sampler) when receiving milk on the farm into sterile sample containers. The samples were transported and stored at 4–6 °C. The examination of the samples in the laboratory took place within 24 hours after the collection.

Cultivation method

For the purposes of the direct cultivation of the samples, the Helicobacter agar was used, containing the following ingredients: Brain Heart Infusion Broth (Cat. No. CM0983, Oxoid LTD., Hampshire, UK), Norit® A (Cat. No. 30890, SERVA Electrophoresis GmbH, Heidelberg, Germany), Starch from Potato (Cat. No. S2004, Sigma-Aldrich, Co., St. Louis, USA), Yeast Extract (Cat. No. LP0021, Oxoid LTD., Hampshire, UK), and Agar Bacteriological (Cat. No. LP0011, Oxoid LTD., Hampshire, UK), as well as defibrinated horse blood, horse serum, enrichment agent A (Cat. No. 15, Dulab s.r.o., Dubné, CR), and the antibiotics mixture: vancomycin (30 000 units/ml) (Code: 0166265, Mylan Pharmaceuticals s.r.o., Prague, CR), colistin (30 000 units/ml) (Code: 0218400, Teva Pharmaceuticals, s.r.o., Prague, CR) and trimethoprim (1500 units/ml) (Cat. No. T-7883, Sigma-Aldrich, Co., St. Louis, USA). 50 µl of the milk sample was cultivated in Petri dishes with Helicobacter

agar. The Petri dishes were incubated at 37 °C for the period of 9 days in an anaerostat, under microaerophilic conditions (5% O_2, 15% CO_2 and 80% N_2) generated using a CampyGen™ 2.5L generator (Cat. No. CN0025A, Oxoid LTD., Hampshire, UK). At the end of the incubation, suspected colonies (resembling small, clear, transparent, and domed colonies) were subjected to the UREASAtest50 urease test (Cat. No. Ut0050, TestLine Clinical Diagnosis s.r.o., Brno, CZ) to demonstrate the urease activity of *H. pylori*.

Nested-PCR

The *H. pylori* DNA was extracted from the milk using QIAamp® DNA Blood Mini Kit (Cat. No. 51104, QIAGEN GmbH, Hilden, Germany) according to the instructions provided by the manufacturer.

Oligonucleotide primers (Cat. No. 1000-020, Generi Biotech s.r.o., Hradec Králové, CR) as published by Quaglia et al. (2009) were used throughout this investigation. Outer oligonucleotide primers designated Hp 1 (5′-AAGCTTTTAGGGGTGTTAGGGGTTT-3′) and Hp 2 (5′-AAGCTTACTTTCTAACACTAAACGC-3′) were used to amplify *H. pylori glmM* gene at 294 bp region and internal primers designated Hp 3 (5′-CTTTCTTCTCAAGCGGTTGTC-3′) and Hp 4 (5′-CAAGCCATCGCCGGTTTTAGC-3′) were used to amplify a 252 bp region. The reaction mixture was prepared from the PPP Master mix (Cat. No. P125, Top-Bio s.r.o., Vestec, CR), PCR H_2O (Cat. No. P242, Top-Bio s.r.o., Vestec, CR), Hp 1 and Hp 2 (0.5 µM). 2 µl of the extracted DNA were added to 23 µl of this mixture. The Nested-PCR was performed according to the Quaglia et al. (2007) under the following conditions: 95 °C for 2 minutes, followed by 33 cycles (94 °C for 1 min, 61 °C for 2 min, and 72 °C for 1.5 min), the final synthesis 72 °C for 5 minutes, and cooling to 6 °C. Once the amplification was completed, 2 µl of the final product from the first reaction were added to the second reaction mixture of the same composition as in the first reaction, only with the difference of the primers added (Hp 3 and Hp 4). The amplification conditions of the second reaction were as follows: 95 °C for 2 minutes, followed by 30 cycles (94 °C for 1 min, 62 °C for 2 min, and 72 °C for 1.5 min), with the final synthesis at 72 °C for 5 minutes. The samples were cooled again to 6 °C. For the purposes of detecting the PCR products, electrophoretic separation in ethidium bromide-stained 1.5% agarose gel, followed by visualization under UV light. Electrophoresis was performed at 120 V, 90 mA and 60 minutes. A 100–4000 bp DNA Ladder (Lonza Rockland, Inc., Rockland, USA) was used as a marker. The *H. pylori* DNA derived from a human gastric mucosa sample was used as a positive testing sample. The *H. pylori* strain was provided by the Microbiology Department of the St. Anne's University Hospital, Brno.

RESULTS AND DISCUSSION

A total of 68 bulk samples of raw cow's milk from farms in the Moravian region were examined for the presence of *H. pylori* bacteria. The classical culture method and the molecular biological Nested-PCR were used to detect the bacterium.

The culture method did not demonstrate the presence of *H. pylori* in any of the examined samples. Tabatabaei (2012) reached the same results. Out of the 20 raw cow's milk samples taken from the area of south-western Iran, the presence of *Helicobacter* was not demonstrated in a single sample. The authors of another study also failed to isolate *H. pylori* in milk samples from the central region of Algeria using the culture method (Guessoum et al. 2018). In their study, Fujimura et al. (2002) also addressed the detection of *H. pylori* in raw cow's milk. They detected bacterial colonies in one of three samples from different parts of Japan. El-Gohary et al. (2015) examined the presence of *H. pylori* in cow's milk from the province of Dakahlia in Egypt. Out of the 36 samples examined, 9 were positive. Differences in the presence of *H. pylori* in the samples may be due to different geographical distribution of the bacterium and hygienic conditions during milk production. The capacity to isolate *H. pylori* from milk using the culture method depends on the capacity to convert *H. pylori* to a cocoid, viable non-culturable form (VNC), which, however, remains metabolically active. This transformation may occur under conditions unfavourable for bacterial growth (Quaglia et al. 2008). In our case, it could have been unfavourable conditions between sampling and examination (transport of the samples to the laboratory and storage at refrigerated temperatures and under aerobic conditions). The culture method cannot be used to detect the VNC, which may result in false negative results. Another reason

why *H. pylori* bacteria were not detected by the culture method may have consisted in an overgrown contaminating microflora, due to which it is not possible to identify small colonies of *H. pylori* after the cultivation. Selective media for culturing *H. pylori* may also pose a problem, as they are primarily developed for culturing microorganisms from clinical specimens whose microflora is different from food microflora (Quaglia and Dambrosio 2018).

Using the Nested-PCR method, it was demonstrated that 31 (46%) bulk samples of raw cow's milk originating from the Moravian region were positive for the presence of *H. pylori* bacteria (see Figure 1). Similar results were obtained by Quaglia et al. (2008), detecting *H. pylori* in 55 samples from a set of 110 samples originating in southern Italy, i.e. in 50%. The Nested-PCR method was also used in study to detect *H. pylori* by Osman et al. (2015). They detected 22% (11/50) positive raw cow's milk samples originating from Sudan.

Figure 1 Agarose 1.5% gel electrophoresis of selected Nested polymerase chain reaction (PCR) products from milk samples

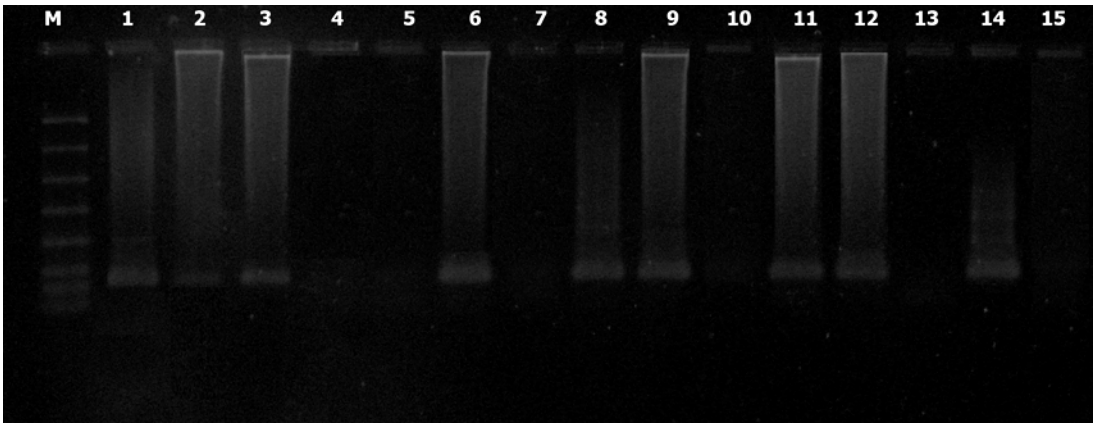

Legend: Lanes 1–13 raw milk, 14 positive control, 15 negative control, M – molecular size marker. The Nested PCR products (252 bp) were found in lanes 1, 2, 3, 6, 8, 9, 11 and 12

Some authors have used the PCR method itself or its modification to examine raw cow's milk. Fujimura et al. (2002) used the semi-nested PCR method to detect the presence of *H. pylori* in 72.2% (13/18) of milk samples from different regions of Japan. Talaei et al. (2015) examined the prevalence of *H. pylori* in raw cow's milk originating from western Iran using the PCR method. In their study, 12 of the 75 samples were positive, i.e. 16%. Also, the team of the authors Mousavi et al. (2014) found that out of 120 raw cow's milk samples, 20 (16.6%) were positive. The high sensitivity of these molecular methods allows detecting even a small number of bacterial cells, including VNC forms, in contrast to the culture method. The authors Quaglia et al. (2008) and Osman et al. (2015) agree that the Nested-PCR method in particular is highly sensitive and specific for the detection of *H. pylori* in milk from cows, sheep and goats. The Nested-PCR method showed to be more sensitive and specific than other methods described for *H. pylori* detection samples, such as immuno-separation, followed by the PCR, semi-nested PCR, autoradiography and ATP bioluminescence (Quaglia et al. 2009). The multiplex touchdown PCR method (MT-PCR) is proved to be highly specific; the Nested-PCR technique showed to be more sensitive (3 CFU/mL vs. 15 CFU/mL). Finally, the Nested-PCR method for the detection of *H. pylori* from raw milk might represents a rapid and sensitive screening tool to be employed in routine milk sanitary examinations (Quaglia and Dambrosio 2018).

CONCLUSION

The results obtained in the present study show that the Nested-PCR method is highly sensitive and allows the detection of *H. pylori* in raw cow's milk in contrast to the culture method. The results of the study showed the presence of the *H. pylori* DNA in 46% of bulk samples of raw cow's milk originating from various dairy cattle farms in the Moravian region of the Czech Republic. This high percentage proves that raw cow's milk is a source of *H. pylori* bacteria and may pose a risk to the consumer.

ACKNOWLEDGEMENTS
The research was financially supported by the Internal Grant Agency of the University of Veterinary and Pharmaceutical Sciences Brno [Grant no. 224/2020/FVHE].

REFERENCES

EFSA. 2015. Scientific Opinion on the public health risks related to the consumption of raw drinking milk. EFSA Journal [Online], 13(1): 3940. Available at: https://doi.org/10.2903/j.efsa.2015.3940. [2015-01-13].

El-Gohary, A.H. et al. 2015. Epidemiological study on *H. pylori* in cattle and its milk with special reference to its zoonotic importance. Biology and Medicine (Aligarh), 7(5): 1–5.

Fujimura, S. et al. 2002. Detection of *Helicobacter pylori* in cow's milk. Letters in Applied Microbiology, 35(6): 504–507.

Guessoum, M. et al. 2018. First-time serological and molecular detection of *Helicobacter pylori* in milk from Algerian local-breed cows. Veterinary World [Online], 11(9): 1326–1330. Available at: www.veterinaryworld.org/Vol.11/September-2018/20.pdf. [2019-10-25].

Mousavi, S. et al. 2014. Virulence factors and antibiotic resistance of *Helicobacter pylori* isolated from raw milk and unpasteurized dairy products in Iran. Journal of Venomous Animals and Toxins including Tropical Diseases [Online], 20(51): 1–7. Available at: http://www.jvat.org/content/20/1/51. [2019-10-21].

Osman, E.Y. et al. 2015. Detection of *Helicobacter pylori glmM* gene in bovine milk using Nested polymerase chain reaction. Veterinary World [Online], 8(7): 913–917. Available at: www.veterinaryworld.org/Vol.8/July-2015/17.pdf. [2019-12-03].

Pelt-Verkuil, E. et al. 2008. Ensuring PCR Quality – Laboratory Organization, PCR Optimization and Controls. In Principles and technical aspects of PCR amplification. Dordrecht: Springer, pp. 190.

Quaglia, N.C. et al. 2007. Survival of Helicobacter pylori in artificially contaminated ultrahigh temperature and pasteurized milk. Food Microbiology [Online], 24(3): 296–300. Available at: https://doi.org/10.1016/j.fm.2006.04.008. [2019-10-11].

Quaglia, N.C. et al. 2008. High occurrence of *Helicobacter pylori* in raw goat, sheep and cow milk inferred by glmMgene: a risk of food-borne infection? International Journal of Food Microbiology [Online], 124(1): 43–47. Available at: https://doi.org/10.1016/j.ijfoodmicro.2008.02.011. [2019-10-18].

Quaglia, N.C. et al. 2009. Evaluation of a Nested-PCR assay based on the phosphoglucosamine mutase gene (glmM) for the detection of *Helicobacter pylori* from raw milk. Food Microbiology [Online], 20(2): 119–123. Available at: https://doi.org/10.1016/j.foodcont.2008.02.010. [2019-10-17].

Quaglia, N.C., Dambrosio, A. 2018. *Helicobacter pylori*: A foodborne pathogen? World Journal of Gastroenterology [Online], 24(31): 3472–3487. Available at: https://www.wjgnet.com/1007-9327/full/v24/i31/3472.htm. [2019-10-18].

Tabatabaei, M. 2012. Application of molecular and cultural methods for identification of *Helicobacter* spp. in different animal sources. Global Veterinaria, 8(3): 292–297.

Talaei, R. et al. 2015. Milk of livestock as a possible transmission route of *Helicobacter pylori* infection. Gastroenterol Hepatol Bed Bench, 8(1): S30–S36.

Verraes, C. et al. 2014. A review of the microbiological hazards of raw milk from animal species other than cows. International Dairy Journal [Online], 39(1): 121–130. Available at: https://doi.org/10.1016/j.idairyj.2014.05.010. [2020-08-10].

Zamani, M. et al. 2017. Role of food in environmental transmission of *Helicobacter pylori*. Caspian Journal of Internal Medicine [Online], 8(3): 146–152. Available at: https://www.ncbi.nlm.nih.gov/pmc/articles/PMC5596183/. [2020-10-18].

The use of hemp herb in diet for growing rabbits

Lucie Horakova, Ondrej Stastnik, Leos Pavlata, Eva Mrkvicova
Department of Animal Nutrition and Forage Production
Mendel University in Brno
Zemedelska 1, 613 00 Brno
CZECH REPUBLIC

xhorak34@mendelu.cz

Abstract: The aim of the present study was to evaluate the effect of hemp herb in a diet for growing Californian rabbits. It was evaluated average weight gain, feed consumption and health condition of the fattened rabbits. The experiment took place on rabbits divided into two groups from age 60 to 151 days. The rabbits in control group (n=10) were fed a diet without hemp herb. The rabbits in experimental group (n=10) received a diet with the addition of 10% hemp herb. At the end of the experiment was not found statistically significant differences ($P > 0.05$) in live weight between control group and experimental group. Final average live weight of rabbits in experimental and control groups were 3.33 kg and 3.46 kg, respectively. No differences were found in feed intake, feed conversion ratio and mean weight gain, as well. In our experiment, no positive effect of dietary administered hemp herb on the rabbit health was found.

Key Words: Cannabis sativa, cannabidiol, rabbit nutrition, Californian rabbits, health

INTRODUCTION

Rabbit husbandry is currently gaining more and more popularity. The main reason is their dietary, white, easily digestible meat, which is characterized by a favorable content of phosphorus and calcium, as well as other necessary microelements (zinc, cobalt and copper) and low content of fat, cholesterol and sodium (MZE 2018). Hemp (*Cannabis sativa* L.) is a multi-purpose crop, the use of which ranges from the textile industry to the food industry (Petříková and Weger 2015). It is characterized by its favorable growth properties and almost zero THC (tetrahydrocannabinol) content (Petříková 2006). The cannabis plant has anti-inflammatory effects and has a beneficial effect on the digestive tract. In the past, humans fed it to their livestock, including rabbits (Dupal 2010). Today's research seeks to demonstrate other beneficial effects of this non-traditional feed. This plant could contribute to the health of rabbits, especially their digestive tract and possibly improve growth in young rabbits (Váňa 2004). According to Nissen et al. (2010) *Cannabis* shows good anti-microbial activity. The results to date show a promising inhibitory activity of *Cannabis* sown against gram-positive pathogens such as *Clostridium* spp. and *Enterococcus* spp. (Sturm et al. 1980, Mcfarland 2006). The aim of the present study was to evaluate the dietary effect of hemp herb in the growing Californian rabbits on their health status, average weight gain and feed consumption.

MATERIAL AND METHODS

Husbandry conditions

All animals were treated in accordance with Act No. 246/1992 Coll. about protection of animals against cruelty, as amended. The technology of rabbits housing complied with Decree No. 208/2004 Coll., On minimum standards for the protection of livestock. The rabbits were housed in outdoor hutches with a wooden floor. Rabbits had available drip drinkers and ceramic feed bowls.

Animals and diets

A total of 20 kits were born and fed on colostrum and breast milk. At the beginning of the experiment (at the 60th day of age) the rabbits were separated from the mother and divided into two groups. Subsequently, young rabbits were placed in hutch of one, two and three individuals, depending on sex and feeding group. The experiment lasted for 91 days (from 60 to 151 days of rabbits age). Twenty male and female rabbits were divided into two groups equally. The control group (n=10)

was fed the diet without hemp herb. The experimental group (n=10) received the diet with the addition of 10% hemp herb. The form of diets was pelleted. The experimental and control diets (Table 1) were based on the nutrient requirements of rabbits (Zeman et al. 2003, Volek 2017). The experimental diets were given to animals without anticoccidials because it was investigated whether *Cannabis* or other biologically active substances will work against coccidiosis. The hemp herb contained flowers with a proportion of seeds and the upper part of the stem of technical hemp. The hemp herb (Carmagnola variety) contained (in dry matter) 18.5% of crude protein, 28.9% crude fiber, 6.9% ether extract and 16.4% of ash. Cannabinoids were measured according to the method of Lalge et al. (2016). The cannabinoids content was only 0.15% of cannabidiol (CBD), THC and cannabinol (CBN) content were below the limit of detection in hemp herb.

Table 1 Composition and chemical composition of used diets (as fed)

Component	Unit	Experimental group	Control group
Alfalfa meal	%	40	50
Winter barley	%	20	20
Premix RabMix Adi*	%	1	1
Soybean meal	%	8	8
Rapeseed oil	%	3	3
Wheat bran	%	15	15
Maize	%	3	3
Hemp herb	%	10	0
Dry matter	**g/kg**	**880**	**880**
Crude protein	g/kg	152.1	146.8
Ether extract	g/kg	50.7	45.6
Crude fiber	g/kg	116.2	105.6
ADFom	g/kg	135.4	128.7
aNDFom	g/kg	215.9	205.0
ADL	g/kg	30.8	26.7
Ash	g/kg	66.8	60.7
Nitrogen-free extract	g/kg	416.4	407.4
DE	MJ/kg	10.34	10.45

*Legend: *Premix added to 1 kg of feed: 0.48 g calcium, 5 mg phosphorus, 1.92 g sodium, 47 mg zinc, 47 mg iron, 13.5 mg copper, 43.5 mg manganese, 0.62 mg cobalt, 0.95 mg iodine, 0.15 mg selenium, 1.25 g DL-methionine, 1.25 g methionine + cysteine, 0.25 g L-threonine, 12 500 IU retinol, 1.880 IU calciferol, 50.5 mg tocopherol, 2.5 mg thiamine, 2 mg phylloquinone, 6 mg riboflavin, 3.9 mg pyridoxine, 20 mcg cobalamine, 15 mg pantothenic acid, 2.4 mg folic acid, 157 mg choline, 200 mcg biotin, 0.15 mg betain, 4 mg butylhydroxytoluen, 4 mg butylhydroxyanisol, 5 mg etoxyquine0.2 g adiCox AP. DE = digestible energy, ADFom = acid detergent fibre, aNDFom = neutral detergent fibre, ADL = acidic detergent lignin.*

Prior to the start of the experiment, all individuals were weighed on an Angyu electronic hanging scale. The following weighing always took place once per week in the afternoon. Temperature and relative humidity were written down every day at the morning. During the experiment, one rabbit from the control group and four rabbits from the experimental group died.

In the evening, the rest of the feed and a new feed were weighed. The next morning, rest of the feed were checked for a possible increase in the daily ration. Feed conversion ratio were calculated based on feed consumption and rabbit weight data. Rabbits had *ad libitum* access to water and feed throughout the day. The health status of all individuals was checked daily. The experiment was ended at 151st day of rabbit's age.

Statistical analysis

Data has been processed by Microsoft Excel (USA). The StatSoft Statistica version 12 (USA) was used to evaluate the data, in which one-factor analysis of variance (ANOVA) was used. The Scheffé´s test was used to determine the significant differences, where $P < 0.05$ was considered as a statistically significant difference.

RESULTS AND DISCUSSION

Health condition and mortality of rabbits

One rabbit from the control group and four rabbits from the experimental group died during the experiment. Most mortality were recorded in the second week of the experiment (67 day of age), when one rabbit (male) from the control group and two (females) rabbits from the experimental group died. Two other rabbits (females) in the experimental group died two weeks later (81 day of age). The rabbits showed symptoms of coccidiosis before death. The symptoms manifested were diarrhea, weight loss and growth retardation and worsened feed conversion. Inflammation of the mucosa with whitish spots was found during the autopsy.

Evaluation of rabbits live weight

The live weight of the rabbits was evaluated every week (Table 2). No statistically significant differences were found ($P > 0.05$) in live weight of rabbits during the trail. At the beginning of the experiment, both groups of rabbits had a similar mean weight, differing by 24 g, when the rabbit´s from the experimental group achieved higher live weights.

Table 2 Average live weight (g) of rabbits during the experiment

Week of experiment	Group	Control group			Experimental group		
	n	9			6		
	Day of age	Mean	±	Standard error	Mean	±	Standard error
1	60	1,203	±	231.1	1,227	±	79.6
2	67	1,309	±	252.3	1,313	±	102.4
3	74	1,394	±	279.9	1,368	±	137.4
4	81	1,475	±	306.4	1,428	±	183.2
5	88	1,733	±	311.9	1,704	±	200.1
6	95	2,000	±	299.2	1,956	±	231.4
7	102	2,259	±	199.3	2,181	±	243.1
8	109	2,446	±	197.8	2,394	±	272.7
9	116	2,614	±	213.9	2,626	±	313.4
10	123	2,737	±	189.7	2,773	±	292.0
11	130	2,994	±	190.8	3,010	±	302.7
12	137	3,123	±	197.4	3,107	±	278.9
13	144	3,283	±	204.6	3,215	±	274.6
14	151	3,462	±	217.9	3,334	±	263.4

Legend: n – number of rabbits per group. There were found no statistically significant differences (P > 0.05).

At the end of the experiment, the rabbit´s in the control group had a higher total average live weight compared to the experimental group (difference was 128 g). According to Zadina (2003), California rabbits should achieve live weigh 1.3 kg in the second month of life. However, not all rabbits reached this value in our experiment. According to the Zadina (2003), rabbits should reach a live weight of 3.1 kg in the fifth month of life. All rabbit´s from our experiment reached this weight, but most of them weighed much more at the same age, which could be due to the composition of the diets and different housing conditions than those reported by Zadina (2003). Figure 1 contains statistics of daily average weight gain for each group depending on gender.

Evaluation of feed consumption and conversion

Statistical analysis did not show significant differences between the control and experimental groups. Average daily feed consumption varied between 140–150 g/rabbit/day. Volek (2017) states that the average daily consumption during fattening should be between 130–150 g/rabbit/day. On the other hand, Zita et al. (2011) reported lower feed consumption – 123 g/rabbit. Mach et al. (2011) stated an average daily feed consumption of 182 g/rabbit. However, it is necessary to take into account the different length of fattening, housing conditions and different breeds were used in these experiments. Figure 1 shows the average daily feed consumption of the control and experimental groups. This Figure shows that there were no differences between the groups ($P > 0.05$), except for the differences occurred

between days 120 and 140. In this period of rabbits age the experimental group had a higher feed consumption which probably worsened the result of freed conversion.

Figure 1 Average daily feed consumption in the control and experimental groups

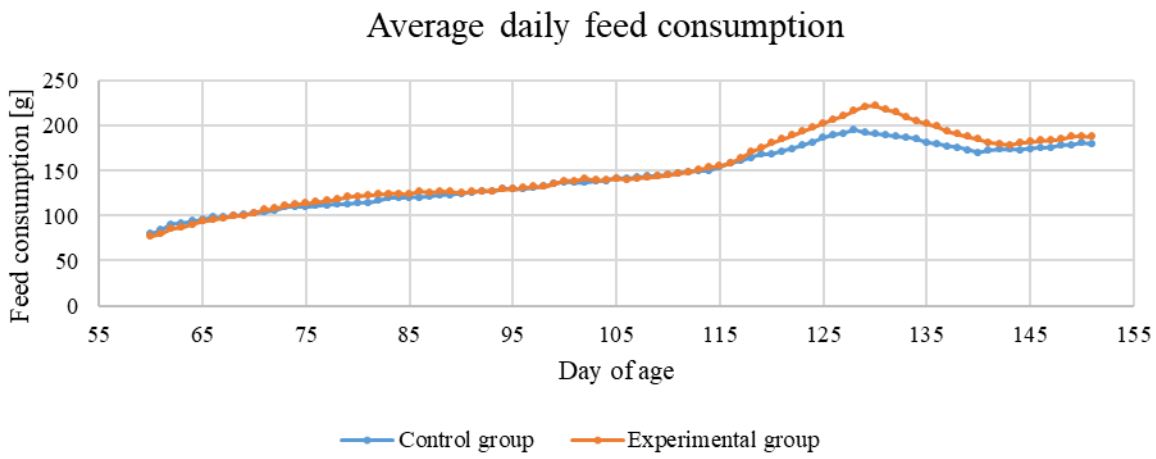

Legend: There were found no statistically significant differences (P > 0.05).

The calculated feed conversion ratio (FCR) was not different between groups. But tendency for its higher value was in the experimental group. However, the weight gain was 18 g higher in the control group. Table 3 shows the average feed intake, weight gain, feed conversion ratio per rabbit for the whole experiment of the control and experimental groups.

Table 3 Mean values in the control and experimental groups (per 1 rabbit)

Group	**Control group**	**Experimental group**
n	9	6
	Mean ± Standard error	Mean ± Standard error
Total feed intake (g)	13,213.4 ± 1,395.3	13,811.7 ± 1,520.1
Weight gain (g)	2,148.4 ± 213.6	2,129.8 ± 231.3
Feed conversion ratio	6.2 ± 0.9	6.5 ± 0.4
Average daily feed intake (g)	143.6 ± 15.2	150.1 ± 16.5

Legend: n – number of rabbits per group. There were found no statistically significant differences (P > 0.05).

The resulting value of feed conversion ratio in the experiment over the 91 days of its duration exceeded 6. According to Volek (2017), feed conversion ratio has decreased from 3.8 to 3.4 over the last 15 years. The worse conversion in the experiment could be due to the gradual fattening and the fact that some rabbits became ill with coccidiosis and thus significantly lost weight. It is now known that in young and fast-growing rabbits, the conversion be worse with age and has worsened sharply in recent weeks of fattening. Another fact is that females from the age of 14 store higher amounts of fat and their feed conversion worsened rapidly. Zita et al. (2011) in their experiment found feed conversion ratio value of 3.62 and Mach et al. (2011) to 4.5. Chrastinova (1993) reports a FCR value of 3.65. The diets were administered without anticoccidials because it was investigated whether hemp herb will or will not work against coccidiosis. This hypothesis was not confirmed – the rabbits in our trial showed the coccidiosis and low weight gain and some of them even died.

CONCLUSION

At the end of the experiment, no significant differences in mean weight were found between the control and experimental groups of rabbits. No differences between assessed groups were found in feed intake, feed conversion ratio and mean weight gain as well. In our experiment, the positive effect of hemp herb and its active substances on the health of rabbits was not found. A disease was found in rabbits - coccidiosis, which caused lower feed intake, slow growth and finally a higher mortality. Based on the results, it can be stated that hemp herb does not prevent against development of coccidiosis. It would be appropriate to preventively cure the rabbits before experiment and repeat the experiment with higher number of animals.

ACKNOWLEDGEMENTS
Authors gratefully thank to reviewers.

REFERENCES

Česká republika. 1992. Zákon č. 246/1992 Sb., o ochraně zvířat proti týrání. Ministerstvo zemědělství. Available at: http://eagri.cz/public/web/mze/legislativa/pravni-predpisy-mze/tematicky-prehled/Legislativa-MZe_uplna-zneni_zakon-1992-246-viceoblasti.html

Česká republika. 2004. Vyhláška č. 208/2004 Sb., o minimálních standardech pro ochranu hospodářských zvířat. Available at: http://eagri.cz/public/web/mze/legislativa/pravni-predpisy-mze/tematicky-prehled/Legislativa-MZe_uplna-zneni_Vyhlaska-2004-208-ochranazvirat.html

Chrastinová, L. 1993. Spotreba krmiva rastúcích králikov do 85. dňa veku. In Proceedings of „Chov brojlerových králikov". Nitra, Slovakia, 25 April. Nitra: VÚŽV.

Dupal, L. 2010. Kniha o marihuaně. 3. ed., Praha: Maťa. Matamata.

Lalge, A.B. et al. 2016. GC-FID analysis of food samples made of 115 hemp. In Proceedings of International PhD Students Conference MendelNet 2016 [Online]. Brno, Czech Republic, 9–10 November, Brno: Mendel University in Brno, Faculty of AgriSciences, pp. 600–604. Available at: https://mendelnet.cz/pdfs/mnt/2016/01/107.pdf [2020-09-02].

Mach, K. et al. 2011. Užitkovost finálních hybridů brojlerového králíka v závislosti na věku a živé hmotnosti při ukončení výkrmu. In Proceedings of Sborník referátů XI. Celostátního semináře: nové směry v intenzivních a zájmových chovech králíků. Praha, Czech Republic, 16 November. Praha: VÚŽV, v.v.i., pp. 76–79.

Mcfarland, L.V. 2006. Meta-analysis of probiotics for the prevention of antibiotic associated diarrhea and the treatment of Clostridium difficile disease. American Journal of Gastroenterology, 101(4): 812–822.

Ministerstvo Zemědělství ČR. 2018. Králíci – situační a výhledová zpráva. 1. ed. Praha: MZE. Available at: http://eagri.cz/public/web/file/612397/Kralici.pdf

Nissen, L. et al. 2010. Characterization and antimicrobial activity of essential oils of industrial hemp varieties (Cannabis sativa L.). Fitoterapia, 81(5): 413–419.

Petříková, V. 2006. Energetické plodiny. 1. ed., Praha: Profi Press.

Petříková, V., Weger, J. 2015. Pěstování rostlin pro energetické a technické využití: biomasa, bioplyn, krmiva. 1. ed., Praha: Profi Press.

Sturm, R. et al. 1980. Neonatal necrotizing enterocolitis associated with penicillin-resistant, toxigenic Clostridium butyricum. Pediatrics, 60(6): 928–931.

Váňa, P. 2004. Léčba zvířat podle bylináře Pavla. 1. ed., Praha: Eminent.

Volek, Z. 2017. Základy výživy a krmení brojlerových králíků. 1. vyd., Praha: Výzkumný ústav živočišné výroby.

Zadina, J. 2003. Vzorník plemen králíků. 1. ed., Brno: Print Typia, spol. s.r.o.

Zeman, L. et al. 2003. Potřeba živin a tabulky výživné hodnoty krmiv pro králíky. 2. ed., Brno: Mendelova zemědělská a lesnická univerzita v Brně.

Zita, L. et al. 2011. Porovnání užitkovosti brojlerových králíků Hyla a Hyplus. In Sborník referátů XI. celostátního semináře „Nové směry v intenzivních a zájmových chovech králíků", Praha, Czech Republic, 16 November. Praha: VÚŽV, v.v.i., pp. 70–76.

Evaluation of vital activities in relation to selected parameters of meat performance at Czech Fleckvieh Simmental fattening bulls

David Jenik, Daniel Falta, Tomas Kopec, Gustav Chladek
Department of Animal Breeding
Mendel University in Brno
Zemedelska 1, 613 00 Brno
CZECH REPUBLIC

xjenik@mendelu.cz

Abstract: Monitoring of vital activities („Eating“, „Rumination“) of cattle is currently being increasingly used for dairy cows mainly due to reproductive and welfare indicators. In contrast, they are used sporadically for growing categories (fattening bulls). Therefore, these categories need to monitor vital activities and quantify their relationship not only to welfare but also to meat performance. The experiment was carried out on 11 bulls of the Czech Fleckvieh Simmental cattle. The monitoring of vital activities was carried out in 12 weeks (from 6 to 18 weeks) of average daily gain (ADG) of 1.554 kg. Subsequently was used data from the abattoir according to EU evaluation system SEUROP, specifically carcass conformation, and fatness. The parameter „Eating“ showed an average value of 276.5 minutes for U-grade, resp. 235.3 minutes for R-grade. As far as fatness is concerned, bulls classified in 2nd class reported 269.0 minutes, resp. 255.3 minutes in 3rd class. There were found correlation coefficients for carcass conformation r = 0.376, resp. for fatness r = 0.125. It was also found that the parameter „Eating“ correlates with the average daily gain r = 0.359. The „Rumination" parameter showed an average value of 520.8 minutes for the U-grade and just 484.3 minutes for the R-grade. Regarding carcass fattening, bulls classified in 2nd class ruminate on average 508.1 minutes, while in 3rd class 518.0 minutes on average. Correlation coefficients were generally at a lower level of conformation r = 0.28, resp. for fatness r = 0.08. The findings confirmed that there is a positive relationship between vital activities and meat performance at the period of the beginning of the fattening bulls.

Key Words: bull, eating, rumination, SEUROP, abattoir

INTRODUCTION

Meat performance is the second most important performance of cattle. Also, the formation of a by-product of manure and other livestock fertilizers contributes to higher soil fertility and thus better yields in crop production (Chládek and Ingr 2001).

Beef has the second-largest share of meat production and consumption in the world after pork. This is mainly due to the countries of the Middle East, which, for religious reasons, do not eat pork and thus replace it with beef. Nevertheless, beef consumption has been declining for the last 30 years. The low purchase price of meat and the import of cheaper food from other countries causes the unprofitability of many farms. Due to these problems and staff shortages, livestock numbers are declining every year. That is why it is necessary to look for new technologies and systems that will increase work efficiency and reduce costs (Chládek and Falta 2006, Geuder et al. 2012).

The two most important breeds bred in our country are Czech Fleckvieh and Holstein cattle. While Holstein cattle is only focused on milk yield and meat is considered here as a by-product, Czech spotted cattle are a breed focused on combined (dual-purpose) efficiency. Although cows of this breed do not match the milk yield of Holstein cattle, their milk yield is still relatively high. Besides, bulls can produce good growths, so it is possible to sell them well as calves or young fattening bulls. In terms of meat efficiency, the Czech Fleckvieh breed is the most numerous breed used for meat production (Strapák et al. 2013).

MATERIAL AND METHODS

The first part of the experiment took place from 6 to 18 weeks of age on a calf on a farm at the village of Křižínkov in the South Moravian Region (468 m above sea level) in the old K-96 stable, where there was free housing with deep bedding. For 12 weeks, calves were examined daily using the SRC system Eating (Animal State Eating) and Rumination (Animal State Rumination). Feeding took place ad libitum with the establishment twice a day and regular feeding. The composition of the feed ration was compiled using a feed system from typical components for the area (Doležal 1996, Zeman 2006, Beauchemin 1991).

The second part of the experiment involved the transport of already fattened bulls to a slaughterhouse at the age of 23 months on average. It was originally planned to carry out the whole experiment on 14 bulls, but one bull died and two were eliminated due to slaughter in slaughterhouses other than the remaining 11 evaluated bulls of the Czech spotted breed. For each bull sent to the slaughterhouse from which the report was received, stating the date of slaughter, the carcass weight weight, the conformation class, the fattening class, and the weight conversion to live weight, which was carried out classically by a coefficient of 1.78. As the weights of calves at birth were not known, an average calf weight at birth of 40 kg was entered. The average daily gain was calculated as the difference in live weight at slaughter and at birth and was divided by feeding days. Furthermore, the relationship between the data obtained from calves ("Eating", "Rumination") and the resulting fleshiness and fatness of carcass weight were investigated. All these data were entered into a spreadsheet in MS Excel. Subsequently, the individual pieces were classified according to the season in which they were born. Using mathematical analysis, the averages of individual monitored categories were calculated, divided into groups according to the seasons and the average of all pieces regardless of the season. I combined the given values into one table and interpreted the results.

The effects of the Eating and Rumination on the carcass conformation and fatness were tested by the analysis of variance (ANOVA, post hoc analysis using Scheffe test) and Pearson correlation coefficients were estimated using program Statistica CZ. Statistical significance was tested at the level of significance $\alpha = 0.05$ (marked *).

RESULTS A DISCUSSION

The default set of 11 bulls is described in the Table 1, in which the detected parameters in conventional SI system units are given. The average age of bulls at slaughter was 682 days with a minimum of 671 and a maximum of 701 days. The average weight of carcass weight was 449.35 kg. The activity of these bulls was monitored during the experiment using cervical responders (Brehme et al. 2008), which were recorded by Eating and Rumination. The average Eating value of the whole set was 265.27 and for rumination 510.82.

Table 1 Base dataset

Bull	Eating (min)	Rumination (min)	Carcass weight (kg)	Body weight at slaughtering (kg)	SEUROP	Fatness	Age at slaughter (days)	Daily gain from birth to slaughtering (g/day)
1	177	429	430.20	765.76	R	3	701	1035.32
2	215	442	489.20	870.78	U	2	701	1185.14
3	231	463	414.50	737.81	R	2	675	1033.79
4	237	479	429.00	763.62	U	2	671	1078.42
5	265	489	450.60	802.07	U	2	695	1096.50
6	268	493	433.50	771.63	U	2	673	1087.12
7	269	516	451.20	803.14	U	2	679	1123.92
8	282	535	506.50	901.57	U	3	672	1282.10
9	298	561	429.60	764.69	R	2	683	1061.04
10	307	590	492.70	877.01	U	3	678	1234.53
11	369	622	415.90	740.30	U	2	683	1025.33

To evaluate the effect of chewing time and eating on selected parameters of meat yield, the effect of classification of bulls at slaughter according to carcass conformation and fatness was tested using the analysis of variance in the program STATISTICA CZ. In both cases, the differences in the mean values of eating and chewing were statistically inconclusive (Table 2). This can also be caused by a small number of evaluated bulls

Table 2 Effect of carcass conformation and fatness on Eating and Rumination

	Level	Nr. of animals	Eating (min)			Rumination (min)		
			Mean	SD	SE	Mean	SD	SE
SEUROP	R	3	235.30	60.62	35.00	484.30	68.54	39.57
	U	8	276.50	46.48	16.43	520.80	59.76	21.13
Fatness	2	8	269.00	48.17	17.03	508.10	58.16	20.56
	3	3	255.30	68.98	39.83	518.00	81.84	47.25

Legend: SD – standard deviation, SE – standard error of the mean

Despite an inconclusive result, a positive effect on the resulting meatiness can be observed in animals with a longer eating and chewing time in the observed period. Bulls classified in the meatiness class U achieved on average higher values of Eating (276.5 minutes) and Rumination (520.8 minutes) in the observed period. A higher intensity of Eating in class 2 (269 minutes) and a higher intensity of Rumination in class 3 (518 minutes) were observed in fatness. The relationship of Rumination to the animal condition was discussed by Soriani et al. (2012). Fattened bulls of this breed are usually classified in fatness classes 2 and 3, this indicator is secondary for breeders unless they are extreme values (eg 1 and 5), which are penalized in the slaughterhouse. Classification into groups 2 or 3, which is shown by our group, is desirable for breeders, slaughterhouses, and the final consumer. In the case of classification R, resp. high values of standard deviation (60.62 minutes and 68.98 minutes, respectively) are observed compared to classification U, resp. fatness 2 (46.48 minutes and 48.17 minutes, respectively). This is due to the low number of observations in the case of classification R, resp. fattening 3. The relatively high values of the standard error of mean correspond to this. Eating and Rumination has been analyzed by several authors (Couderc et al. 2006, De Ondarza 2015).

Table 3 Pearson correlation coefficient between Carcass traits, Eating, and Rumination

	Eating	Rumination	Carcass weight	SEUROP	Fatness	Daily gain
Eating	1.00	0.96*	0.00	0.38	-0.12	0.09
Rumination		1.00	0.08	0.28	0.08	0.16
Carcass weight			1.00	0.49	0.54	0.98*
SEUROP				1.00	-0.08	0.52
Fatness					1.00	0.53
Daily gain						1.00

*Legend: Pearson correlations coefficients denoted by * were significantly non-zero at $\alpha = 0.05$.*

In the Table 3 shows the correlation coefficients for Eating, Rumination, Carcass weight, Carcass conformation, fatness, and Daily Gain. As expected, a very high correlation coefficient is based between Carcass weight and daily gain. Also, a high correlation coefficient is between Eating and Rumination activity. Due to the small number of evaluated bulls, the other correlation coefficients are not statistically demonstrably non-zero, so it is not possible to infer a relationship between these properties. Nevertheless, a correlation coefficient of 0.38 between Carcass conformation and Eating can be observed. It follows from the above that it is necessary to continue research.

CONCLUSION

The experiment was carried out on 11 bulls of the Czech Fleckvieh cattle. The monitoring of vital activities was carried out in 12 weeks. The parameter „Eating“ showed an average value of 276.5 minutes for U-grade, resp. 235.3 minutes for R-grade. As far as fatness is concerned, bulls

classified in 2nd class reported 269.0 minutes, resp. 255.3 minutes in 3rd class. From the above results, it can be stated that especially in the case of Carcass conformation, better classification of Czech Fleckvieh bulls, which showed higher activity of Eating and Rumination, is evident. However, no association Eating and rumination on fatness . The research was performed on a limited number of animals and the initial results indicate the need to continue collecting data. This positive trend, especially in the case of Carcass conformation, indicates the importance of the use of collars in fattening bulls and can lead not only to better monitoring of bulls' health but also to better meat performance parameters of slaughtered bulls and thus to an overall increase in bull fattening efficiency.

REFERENCES

Beauchemin, K.A. 1991. Ingestion and mastication of feed by dairy cattle. Veterinary Clinics of North America: Food Animal Practice, 7(2): 439–463.

Brehme, U. et al. 2008. ALT pedometer-New sensor-aided measurement system for improvement in oestrus detection. Computers and Electronics in Agriculture, 62(1): 73–80.

Chládek, G., Falta, D. 2006. Beef performance of Holstein calves slaughtered at 300 kg of live weight. Acta Universitatis Agriculturae et Silviculturae Mendelianae Brunensis, 54(4): 13–20.

Chládek, G., Ingr, I. 2001. Meat production and quality of Holstein bulls fattened to 405–480 kg of live weight. Czech Journal of Animal Science, 46(8): 370–374.

Couderc, J.J. et al. 2006. Silage chop length and hay supplementation on milk yield, chewing activity, and ruminal digestion by dairy cows. Journal of Dairy Science, 89(9): 3599–3608.

De Ondarza, M.B. 2015. Prežúvanie je oknom k zdraviu kravy. Slovenská holsteinská asociácia-Maxi info, august 2015, [Online], (8): 18–19. Available at: https://www.holstein.sk/files/infomagazin/maxiinfo-08-2015-web.pdf. [2020-09-17].

Doležal, O. 1996. Technologie a technika chovu skotu. Praha: SCHČSS.

Geuder, U. et al. 2012. Mast-, Schlachtleistung und Fleischqualität bayerischer Rinderrassen. Züchtungskunde, 84(6): 485–499.

Soriani, N. et al. 2012. Relationships between rumination time, metabolic conditions, and health status in dairy cows during the transition period. Journal of Animal Science, 90(12): 4544–4554.

Strapák, P. et al. 2013. Chov hovädzieho dobytka. 1. vyd., Nitra: Slovenská poľnohospodárska univerzita.

Zeman, L. 2006. Výživa a krmení hospodářských zvířat. Praha: Profi Press.

Fermented rapeseed meal as a feed additive and its effect on the performance of broiler chickens – a pilot study

Damian Konkol[1], Ida Szmigiel[2], Marcin Lukaszewicz[2], Anna Krasowska[2], Mariusz Korczynski[1]
[1]Department of Environment Hygiene and Animal Welfare
Wroclaw University of Environmental and Life Sciences
Chelmonskiego 38C, 51-650 Wroclaw
[2]Department of Biotransformation
University of Wroclaw
F. Joliot-Curie 14a, 50-383 Wroclaw
POLAND

damian.konkol@upwr.edu.pl

Abstract: This study examined the influence of fermented rapeseed meal on the performance of broiler chickens. Forty-eight 21-day old Ross 308 broilers were used in this experiment. The birds were placed in metabolic cages and randomly assigned to 4 experimental groups. Group I was a negative control and received no additive. Group II was a positive control and received 3% additive of unfermented rapeseed meal. Group III received a 3% additive of rapeseed meal fermented with the *Bacillus subtilis* 67 bacterial strain. Group IV received a 3% additive of rapeseed meal fermented with *B. subtilis* 87Y. The birds were weighed on 30, 37 and 44 days of age. On this basis, the live body weight of birds and daily gains were monitored. The feed intake was weighed daily – on this basis the feed conversion ratio was calculated. The obtained results did not show any statistically significant effect of the used additives on the performance of broiler chickens.

Key Words: rapeseed meal, Bacillus subtilis, broilers, fermentation

INTRODUCTION

Rapeseed meal is a feed material with huge economic potential. It can be used to feed all species of farm animals and is the second-most used raw protein material worldwide (after soybean meal). The protein content of rapeseed meal is 33.9–36% of dry matter (Blair and Scougall 1975, Bell and Jeffers 1976, Bell 1984). This protein contains less lysine than soybean meal protein, however is more rich in sulfur-containing amino acids (Khajali and Slominski 2012).

Rapeseed meal also has disadvantages, including high levels of anti-nutritional compounds, such as: glucosinolates, tannins, phytic acid, sinapine, and erucic acid. These compounds can negatively affect the health and productivity of farm animals, including poultry (Verlag and Issn 1981, Butler et al. 1982, Tripathi and Mishra 2007, Mejicanos et al. 2016).

Rapeseed meal is a good substitute for soybean meal due to its high availability in Europe, competitive costs compared, and the possibility of diversifying protein sources in the feed. Given the problems associated with the use of rapeseed meal, research and developments efforts are needed to overcome the drawbacks of this feed material. Given the growing market for functional food, the prohibition of antibiotics in farm animals nutrition and the restrictive feed policy (mainly in the EU), new feed preparations are in great demand. These new preparations should optimize the production process, animal health and the quality of the animal origin products. This possibility is provided by the use of food-grade bacteria for the biotransformation of rapeseed meal. For example, *Bacillus subtilis* var. natto produces biosurfactants (surfactins), biopolymers (levan) as well as several enzymes (xylanases, cellulases, lipases, proteases or phytases) through a solid state fermentation process that can make rapeseed meal more useful in animal nutrition (Konkol et al. 2019).

The aim of this study was to determine the effect of fermented rapeseed meal on the performance of broiler chickens.

MATERIAL AND METHODS

Fermentation of rapeseed meal by Bacillus subtilis 87Y and 67 strains in 50 kg SSF bioreactor

Fermentation of the rapeseed meal was performed using *Bacillus subtilis* 87Y and *B. subtilis* 67 strains, isolated from the earthworm, *Eisenia fetida* (Szmigiel et al. 2019). Bacterial inoculum with optical density OD_{600} = 0.1 was prepared by resuspending *B. subtilis* precultures in minimal MIM1 medium (sucrose 60 g/L, urea 2.3 g/L, $MgSO_4$ 0.5 g/L, Na_2HPO_4 8.4 g/L, NaH_2PO_4 3.9 g/L, $FeSO_4$ 1.2 mg/L, $CuSO_4$ 1.6 mg/L, $MnSO_4$ 5 mg/L, pH = 7.0). RSM was pasteurised for 8 min in 80 °C, then mixed with prepared inoculum in 1:1 ratio (m/v) to maintain 50% humidity. Fermentation was performed with 20 rpm shaking, 50 L/min aeration for 24 h in 37 °C. After 24 h, RSM was immediately dried using a fluid bed drier.

Broiler chickens population and experimental design

The research was carried out at the Agricultural Experimental Station "Swojec" (Wroclaw University of Environmental and Life Sciences). A total of forty-eight 21-day old Ross 308 broiler chickens (978.58 g of live weight, males) were used for the study. The birds were kept in controlled microclimatic conditions, which were in accordance with the line manufacturer's recommendations. The setpoint for temperature was 32 °C for day 1, after that slowly reduced to 22 °C till day 21 and remained constant until day 44. The 10 min of light was provided every 6 h during the first week of life and then for 18 h every 6 h, except for the last 3 days when the light was provided for 24 h. In 21 days of life, the chickens were placed in metabolic cages. The birds were divided into 4 experimental groups with each group consisting of 12 birds. Each group consisted of 4 replicates, while each replication consisted of 3 birds. Group I was a negative control (NC) and received no additive. Group II was a positive control (PC) and received 3% additive of unfermented rapeseed meal. Group III (67) received a 3% additive of rapeseed meal fermented with the bacterium *B. subtilis* 67. Group IV (87Y) received a 3% additive of rapeseed meal fermented with *B. subtilis* 87Y. Rapeseed meal was used in this study only as an additive, it was not used as a substitution of other feed components. Addition of 3% fermented rapeseed meal (FRSM) did not significantly change the content of feed mixture (according to Smulikowska and Rutkowski 2005).

Nutrition

The birds were fed in accordance with Poultry Nutritional Standards (Smulikowska and Rutkowski 2005). Table 1 presents the composition of the basal diet. The feed was provided in the form of pellets. Birds received food and water *ad libitum*. Table 2 presents chemical composition of feeds used in the experiment.

Table 1 Composition of the basal diet

Component	Amount (kg of component / 1000 kg of complete feed mixture)
Maize	361.87
Wheat	300.00
Soybean meal 45	217.00
Animal fat	30.00
Sunflower seed cake	25.00
Sunflower meal	15.00
Medium chain fatty acids	12.00
Guar 60	10.00
Chalk	7.30
Dicalcium phosphate	7.00
L-methionine 99	2.40
Salt	2.10
L-lysine SO4	2.00
Premix	2.00

Table 1 Composition of the basal diet – continue

Component	Amount (kg of component / 1000 kg of complete feed mixture)
L-lysine 98	1.70
Sodium bicarbonate (NAHCO3)	1.20
L-Threonine	1.10
Choline chloride 75%	0.67
Sacox 120/ Kokcisan/Salinomax	0.58
Mycofix select 5.E	0.50
L-valine	0.44
Hiphos Liquid (L) (phytase)	0.08
Hostazym (xylanase)	0.06

Table 2 Chemical composition of feeds

Composition	NC	PC	67	87Y
Dry matter (g/kg)	902.17	903.99	902.04	903.25
Ash (% DM)	3.79	4.07	4.04	4.11
Crude fat (% DM)	5.94	6.00	6.15	6.07
Crude protein (% DM)	20.17	20.29	20.75	20.57
Crude fibre (% DM)	3.09	3.45	3.54	3.48
Metabolic energy (MJ/kg DM)	17.85	18.44	18.01	18.41

Legend: NC – negative control; PC – positive control; 67 - 3% addition of rapeseed meal fermented with the Bacillus subtilis 67 bacterial strain; 87Y - 3% addition of rapeseed meal fermented with B. subtilis 87Y.

Performance of broiler chickens

The birds were weighed on 30, 37, and 44 days of age. On this basis, the live body weight of birds and daily gains were monitored. The feed intake was weighed daily – on this basis the feed conversion ratio was calculated.

Statistical analyses

The mean and standard error of the means (SEM) were calculated for production parameters (live body weight, daily gains, FCR). Data normality was assessed using the Shapiro-Wilk test. If the data distribution was normal, a one-way analysis of variance was performed, followed by the Tukey post hoc test. If the data distribution was not normal, the Kruskal-Wallis test was carried out. Differences were considered statistically significant when $P<0.05$. Data were analysed using Statistica ver. 13.1.

RESULTS AND DISCUSSION

Table 3 presents performance of broiler chickens used in the experiment. In this study, production parameters were monitored only to ensure that the additives would not adversely affect the performance of the birds. The production parameters of the tested birds did not go beyond the standards presented in the line manufacturer's instructions. Slight decreases in performance may have been a result of keeping the birds in non-standard conditions (metabolic cages).

Used additives had no significant effect on body mass, daily gains, and feed conversion ratio. Similar results were obtained by Xu et al. (2012) who showed that the weight gain and FCR of birds fed 5% additive of rapeseed meal fermented with *Lactobacillus fermentum* and *B. subtilis* did not differ significantly from birds that did not receive the additive. Conversely, Chiang et al. (2010) found that fermented rapeseed meal significantly improved weight gain and FCR compared to birds fed unfermented rapeseed meal. Despite the fact that Chiang et al. (2010) used 10% of additive, they also used for fermentation *B. subtilis* in addition to other microorganisms, such as *L. fermentum, Enterococcus faecium* and *Saccharomyces cerevisiae*. This, however, increased the cost of feed,

which may lead to low profitability. Therefore, from an economic point of view, it seems more beneficial to use bacterial monocultures in the fermentation of rapeseed meal.

Table 3 Performance of broiler chickens used in the experiment

Day 30						
Parameter	NC	PC	67	87Y	SEM	p-value
Live body weight (g)	Mean 1617.50	Mean 1706.25	Mean 1697.50	Mean 1698.75	38.54	0.859
Daily gains (g, day 21 to 30)	84.42	75.68	74.89	76.75	3.28	0.760
FCR (kg of feed/kg of gain, day 21 to 30)	1.58	1.49	1.52	1.49	0.03	0.815
Day 37						
Parameter	NC	PC	67	87Y	SEM	p-value
Live body weight (g)	Mean 2242.50	Mean 2275.00	Mean 2236.25	Mean 2250.00	36.59	0.987
Daily gains (g, day 31 to 37)	89.28	81.24	76.95	78.74	5.34	0.881
FCR (kg of feed/kg of gain, day 31 to 37)	1.60	1.59	1.60	1.60	0.02	0.998
Day 44						
Parameter	NC	PC	67	87Y	SEM	p-value
Live body weight (g)	Mean 2946.25	Mean 2892.50	Mean 2945.00	Mean 2881.25	51.17	0.963
Daily gains (g, day 38 to 44)	100.53	88.21	101.24	90.17	7.38	0.909
FCR (kg of feed/kg of gain, day 38 to 44)	1.57	1.60	1.59	1.61	0.02	0.973

Legend: NC – negative control; PC – birds receiving 3% addition of URSM; 67 – birds receiving 3% addition of FRSM by B. subtilis 67; 87Y – birds receiving 3% addition of FRSM by B. subtilis 87Y.

CONCLUSION

The aim of this study was to investigate the effect of fermented rapeseed meal on the performance of broiler chickens. By examining growth rates, it was shown that the addition of fermented rapeseed meal does not affect the production parameters of broiler chickens.

ACKNOWLEDGEMENTS

The research was financially supported by the POIR.01.02.00-00-0064/17 and POIR.02.01.00-IZ.00-00-001/19 (NCBR).

REFERENCES

Bell, J.M. 1984. Nutrients and toxicants in rapeseed meal: a review. Journal of Animal Science, 58(4): 996–1010.

Bell, J.M., Jeffers, H.F. 1976. Variability in the chemical composition of rapeseed meal. Canadian Journal of Animal Science, 56(2): 269–273.

Blair, R., Scougall, R. 1975. Chemical composition, nutritive values of rapeseed meal. Feedstuffs, 10: 26–27.

Butler, E.J. et al. 1982. Problems which limit the use of rapeseed meal as a protein source in poultry diets. Journal of the Science of Food and Agriculture, 33(9): 866–875.

Chiang, G. et al. 2010. Effects of feeding solid-state fermented rapeseed meal on performance, nutrient digestibility, intestinal ecology and intestinal morphology of broiler chickens. Asian-Australasian Journal of Animal Science, 23(2): 263–271.

Gill, J.K. et al. 1981. Changes in composition and enzyme activities of mitochondrial and post-mitochondrial fractions of tissues of rats given mustard oil diet with carnitine and/or fish oil. Z Ern&hrungswiss, 20(3): 188–193.

Khajali, F., Slominski, B.A. 2012. Factors that affect the nutritive value of canola meal for poultry. Poultry Science, 91(10): 2564–2575.

Konkol, D. et al. 2019. Biotransformation of rapeseed meal leading to production of polymers, biosurfactants and fodder. Bioorganic Chemistry, 93: 102865.

Mejicanos, G. et al. 2016. Recent advances in canola meal utilization in swine nutrition. Journal of Animal Feed Science and Technology, 58: 7.

Smulikowska, S., Rutkowski, A. 2005. Normy Żywienia Drobiu. 4th ed., Jabłonna, Poland: Instytut Fizjologii i Żywienia Zwierząt im. Jana Kielanowskiego PAN.

Szmigiel, I. et al. 2019. The influence of Bacillus subtilis 87Y isolated from Eisenia fetida on the growth of pathogenic and probiotic microorganisms. Biomass Conversion and Biorefinery, 1–8.

Tripathi, M.K., Mishra, A.S. 2007. Glucosinolates in animal nutrition: a review. Animal Feed Science and Technology, 132(1): 1–27.

Xu, F.Z. et al. 2012. Effects of replacing soybean meal with fermented rapeseed meal on performance, serum biochemical variables and intestinal morphology of broilers. Asian-Australasian Journal of Animal Science, 25(12): 1734–1741.

Evaluating and comparing descendants of stallions from the Dark Ronald line in Czech Warmblood breeding according to basic body measurements

Zuzana Kubikova, Iva Jiskrova, Barbora Kubistova
Department of Animal Breeding
Mendel University in Brno
Zemedelska 1, 613 00 Brno
CZECH REPUBLIC

x.kubiko6@mendelu.cz

Abstract: The aim of this study was to evaluate the influence of the Dark Ronald stallion line in the breeding of the Czech Warmblood. To evaluate the importance of the line, the offspring of stallions authorized to act as stud horses in the breeding of the Czech Warmblood were used. The values of the basic body measurements of their offspring (SHW, THW, ChC and CBC) were used to evaluate the quality of the stallions. A total of 6 breeding stallions were compared: two representatives of the Holsteiner horse (2765 CASSILIUS, 2666 PORTER), one Russian Holsteiner (2782 BALLAST), one Slovak Warmblood (794 CORSÁR), one Dutch Warmblood (2745 OSCAR) and one representative of the Zweibrücker breed (662 CARBIDO). The group for comparison consisted of 284 offspring of the Czech Warmblood breed from these sires. Evaluation by the GLM model detected statistically significant differences between the basic body measurements of the individual groups of offspring. The influence of the dams on the basic body measurements of offspring was taken into account by a graphical comparison of the massiveness and boniness indices. It was found that the stallion 2782 BALLAST significantly affects the massiveness of his offspring, but the dam has a greater influence on boniness than the sire. Furthermore, it was found that mares are statistically significantly more massive than stallions, but that they have a smaller cannon bone circumference. It was found that the progeny of 2666 PORTER is the most balanced, while in other stallions it is highly variable, and the greatest, statistically significant influence of the sire can be observed in the stallion 2782 BALLAST.

Key Words: stallion, offspring, line, Czech Warmblood

INTRODUCTION

The main trend in contemporary horse breeding is the production of high-quality athletes capable of the best possible performance. Breeders One of the main assessment criteria in horse breeding is sporting performance, and individual breeders' associations try to respond to this demand in their breeding programmes (Czech Warmblood Horse Association 2017). The right choice of horses for breeding is therefore extremely important. Cross-breeding is used to correct the traits of certain breeds. This phenomenon can be seen relatively frequently in warmblood breeding, since the use of English Thoroughbred stud horses to increase constitutional hardness is common. Unfortunately, however, this refinement also entails a negative aspect: the lightening of the frame, which is definitely not desirable for a sport horse (Dušek 2011).

Sobotková and Oravcová (2014) state that the Czech Warmblood should be a noble, sound and easy-to-ride horse which is suitable for all FEI equestrian disciplines due to its character, temperament, stride and elastic movement and good health. At the same time, however, it should be suitable for recreational and carriage riding. An adult Czech Warmblood horse has a medium build with good lines, a solid foundation and no apparent defects or diseases of a genetic nature. The breed standard gives the range for stick height at withers as 161−167 cm for mares and 162−170 cm for stallions (Czech Warmblood Horse Breeders Association 2017). According to Dušek (2011), the variability of conformation in the Czech Warmblood has been affected by the relatively short period of improvement and the use of a large number of breeds. The aim of the current breeders' association

should therefore be to place greater emphasis on the conformation of breeding stock. Individuals for breeding should be free of exterior defects, have a strong constitution and be in good health. Saastamoinen and Barrey (2000) say that the conformation plays an important role in the breeding programme of Horse Breeders Association to achieve better soundness and locomotion and thus, in practical selection, individuals with serious weaknesses and conformational defects should be culled.

Dark Ronald was an English Thoroughbred stallion who was sold to the German stud in 1913 (Eurodressage 2020). Peters (2005) reports that Dark Ronald was a good racer but had far greater significance as a stud horse. Although he only physically stood in England and Germany, his influence has been global and he has influenced the breeding of many warmblood breeds. Dark Ronald was sired by Bay Ronald and was the founder of one of the two Thoroughbred lines which have long dominated warmblood breeding in Germany. His Thoroughbred sons Son-in-Law and Dark Legend went on to play an important role in the pedigrees of showjumpers throughout Europe and North America (Birdsall 2017). According to Peters (2005), Dark Ronald had good conformation and a powerful frame, was well-muscled and was fairly low at the withers, which became typical of this line.

MATERIAL AND METHODS

The underlying database was created from data provided on the website of the Association of Czech Warmblood Breeders. Six stud horses classified within the Dark Ronald line were selected and the relevant data on the stud horses and their offspring were collected. The database contains a total of 284 descendants, with the following data being recorded for each of them: name, year of birth, year of measuring, sex, sire's data, and body measurements: stick height at withers (SHW), tape height at withers (THW), chest circumference (ChC) and cannon bone circumference (CBC). The database of descendants was created in the programme Microsoft Office Excel 2010. The data acquired were then statistically processed using the GLM linear model in the statistical programme Statistica. Each stud horse was assigned an internal identification number from 1 to 6 solely for the purposes of statistical processing. The effect of the sire, year of birth and sex on the values of the basic body measurements was observed. It was also necessary to separate sex numerically into groups 1 (stallions and geldings) and 2 (mares). In addition, hippometric indices were calculated: a massiveness index and a boniness index for offspring, sires and dams. The indices were subsequently graphically processed, compared and evaluated.

Distribution of stud horses

1) 2765 CASSILIUS
2) 2782 BALLAST
3) 662 CARBIDO
4) 794 CORSÁR
5) 2666 PORTER
6) 2745 OSCAR

Model equation:

$y_{ijk} = \mu + p_i + q_j + r_k + e_{ijk}$

where:

y_{ijk} is the observed effect (SHW, THW, ChC and CBC)

μ is the total average of the set

p_i is the fixed effect of the i-th group of sires (i = 1,…, 6)

q_j is the fixed effect of the j-th year of birth (j = 1,…, 20)

r_k is the fixed effect of the k-th sex (k = 1,2)

$e_{ijk\ is}$ the random effect

Based on the results of the general linear model, the differences between values were established by subsequent testing using the Scheffe method. The test was conducted at a significance level of $P \leq 0.01$.

Hippometric indices

Formula for the massiveness index: $\frac{\text{Ch C}}{\text{SW H}} * 100$

Formula for the boniness index: $\frac{\text{CB C}}{\text{SW H}} * 100$

RESULTS AND DISCUSSION

Table 1 Results of statistical significance of variance analysis by GLM

Body measurement	Sire	Year of birth	Sex
SHW	-	*	-
ChC	**	-	**
CBC	-	-	*

Evaluation by the GLM model in Table 1 revealed high statistical significance of the observed effects of sire and sex for the basic body measurement of chest circumference. Another two statistically significant effects were noted with tape height at withers and cannon bone circumference. A highly significant influence of the sire could only be proven statistically in the case of chest circumference. This confirms that the transfer of sires' phenotypic traits to offspring exhibits a degree of heritability, but according to these results it primarily affects massiveness. The effect of the year of birth emerged as statistically significant for the attribute SHW. This result can be explained by the fact that more descendants with an above-average stick height at withers were born in one of the year groups. The highly significant statistical result for the effect of sex on chest circumference can be rated very positively since the conformation of stallions and mares should be different. When assessing the influence of sex on cannon bone circumference, a statistically significant effect was recorded. Cannon bone circumference is an important breed attribute subject to Czech Warmblood standards. That is why the assessment and observation of this measurement is extremely important, as it indicates the strength of the skeleton, which is highly desirable. At present it is essential that stud horses with the ability to pass on a powerful frame to their offspring are included in breeding, as the influence of a wide range of different breeds in Czech Warmblood breeding has resulted in it becoming lighter, which is definitely undesirable for the breed. It can therefore be said that the importance of observing this attribute has been confirmed and statistically proven.

Results of effect of sires on chest circumference

Table 2 Results of comparison of stud horses according to offspring ChC by Scheffe testing

Name	No. of offspring	Average ChC	662 Carbido	2666 Porter	2745 Oscar
2765 Cassilius	53	191.02 cm	-	-	-
2782 Ballast	72	195.08 cm	*	*	*
662 Carbido	50	190.44 cm	-	-	-
794 Corsár	37	190.95 cm	-	-	-
2666 Porter	50	189.58 cm	-	-	-
2745 Oscar	22	188.68 cm	-	-	-

The evaluation by Scheffe subsequent testing in Table 2 showed that offspring by the stud horse 2782 Ballast have a statistically significantly higher chest circumference than offspring by the stallions 662 Carbido, 2666 Porter and 2745 Oscar. According to the average values, it can be stated that the group of offspring by 2782 Ballast achieves the highest value from the whole assessed set, with a difference of 6.4 cm compared to the group by 2745 Oscar, which has the lowest average group value. At the same time, the group by 2782 Ballast greatly surpasses the group of offspring with the second highest average value, that of 2765 Cassilius, the difference being 4.06 cm. Based on these results, it can be stated that offspring by the stud horse 2782 Ballast exhibit statistically significant massiveness, which is rated very positively. Furthermore, it was found that 86%

of the descendants of the stud horse 2782 Ballast had their measurements taken at the age of three, when they were entered in the stud book, as did 86% of the offspring by 2745 Oscar. With the stud horse 2666 Porter, as many as 90% of offspring were measured at three years old, and with offspring by 662 Carbido the figure was 74%. It can therefore be said that the age of measuring did not substantially affect the values of chest circumference in the observed set.

Table 3 Results of comparison of effect of stud horses according to massiveness indices of sire, offspring and dams

Name	No. of offspring	% of offspring greater than sire	% of offspring greater than dams	% of dams greater than sire
2765 Cassilius	53	45	39.6	64
2782 Ballast	72	33	54	27.7
662 Carbido	50	49	43	60.7
794 Corsár	37	72.9	48	86
2666 Porter	50	74	20	98
2745 Oscar	22	18	27	31

As is shown by Table 3 above, according to a comparison of the massiveness indices of the sires, offspring and dams, the sires have an influence on the massiveness of offspring only in the groups by 2782 Ballast and 2745 Oscar. The massiveness of the other groups is influenced more by the dams than the sires. It can therefore be said that the stud horse 2782 Ballast greatly influences the ChC measurement and related massiveness of his offspring. If we take into account the fact that offspring by 2745 Oscar have a statistically significantly smaller ChC than offspring by 2748 Ballast and at the same time this group achieves the smallest average values of all the groups, it is thus apparent that the dams mated with the stallion 2745 Oscar were of a lighter frame and less massive.

Results of effect of sex on chest and cannon bone circumference

Table 4 Results of comparison of sex by offspring ChC according to Scheffe testing

Sex	Number	Average ChC	Stallions
Mares	270	192 cm	**
Stallions	14	186 cm	

Table 4 shows that the mares have a statistically highly significantly larger chest circumference than the stallions. This can be regarded as desirable since the body of mares should in general be more capacious for breeding purposes. Baban et al. (2009) assert that a larger chest circumference together with a larger cannon bone circumference positively affects the length and speed of the stride. This is desirable in sport horses and, as Rustin et al. (2009) state, conformation and gaits are among the most important criteria for selecting horses for breeding. When comparing the average values of stallions with the obtained results of a study of stallions of Polish warmbloods (Pietrzak et al. 2016), it was found that Czech warmbloods have an average of 4.49 cm smaller chest circumference.

Table 5 Results of comparison of sex according to offspring CBC by Scheffe testing

Sex	Number	Average CBC	Mares
Mares	270	20.65 cm	
Stallions	14	21.22 cm	*

From Table 5 it is clear that mares have a statistically significantly smaller cannon bone circumference than stallions. This can be rated very positively as stallions should have a more powerful conformation than mares and therefore the cannon bone circumference should also be larger. The average values can be regarded as very good since in both groups of sexes they meet the breed standard for the Czech Warmblood, which according to Czech Warmblood Horse Breeders Association (2017) is 19.5−22 for mares and 21−22.5 for stallions. Novotná et al. (2017) mention that there is a moderately high phenotypic correlation between refinement and cannon bone circumference.

This is also confirmed by these results, as the more refined and lighter mares have a smaller cannon bone circumference than stallions, which should have clear secondary sex characteristics including a larger cannon bone circumference. In comparison with the stallions of the Polish Warmblood (Pietrzak et al. 2016), the stallions in the monitored group have a cannon bone circumference 0.21 cm smaller on average.

Table 6 Results of comparison of effect of stud horses according to boniness indices of sire, offspring and dams

Name	No. of offspring	% of offspring greater than sire	% of offspring greater than dams	% of dams greater than sire
2765 Cassilius	53	20.7	28	37.7
2782 Ballast	72	2.7	48.6	11
662 Carbido	50	18	70	12
794 Corsár	37	2.7	16	37.8
2666 Porter	50	52	30	72
2745 Oscar	22	77	50	81.8

When the boniness indices of sires, offspring and dams in Table 6 were compared, it was found that the stud horse 662 Carbido had the greatest influence on the boniness of his offspring. A total of 70% of offspring by this stallion achieve a greater boniness index than their dams and 18% even surpass the sires; with these offspring, the influence of the dam can be seen in three cases out of nine where the dams surpass the sires. Another stud horse that substantially influences the boniness of his offspring is 2782 Ballast. In this case we can see that 48.6% of the descendants have a greater boniness index than the dams, and only 11% of the dams have a greater index than the sire. At the other end of the scale, the stallions 2666 Porter and 2745 Oscar have the smallest influence on the boniness of their offspring. In the case of offspring by 2666 Porter, 72% of the dams and 52% of the descendants have a greater index than the sire, and 30% of the offspring even surpassed their dams. With the group by 2745 Oscar, the effect of the sire on the boniness index is even smaller. Nearly 82% of the dams and 77% of the descendants have a greater index than the sire, and as many as 50% of the offspring surpassed their dams. According to Černohorská et al. (2013), the influence of the sire line on the conformation of offspring has not been proven in rearing facilities for testing young horses. However, according to these results, it can be said that within the Dark Ronald line the stud horse 2782 Ballast has a statistically significant effect on the chest circumference, massiveness and boniness of his offspring in comparison with the other stud horses from the line.

CONCLUSION

The aim of this work was to evaluate the influence of the Dark Ronald line in the breeding of the Czech Warmblood. With THW, no statistical significance of the observed effects was found. In the case of the attribute SHW, the effect of the year of birth is significant. With the measurement ChC, a statistically highly significantly larger chest circumference was demonstrated in offspring by 2782 Ballast than in the offspring of the stallions 662 Carbido, 2666 Porter and 2745 Oscar. The hippometric indices of massiveness and boniness revealed that the massiveness of offspring is mainly influenced by 2782 Ballast and 2745 Oscar and the boniness by 2782 Ballast and 662 Carbido. With CBC the effect of sex is significant: it was found that stallions have larger CBC than mares, which is rated very positively with regard to secondary sex characteristics. According to the results obtained, it can be said that within Czech Warmblood breeding the greatest influence on the conformation of offspring from the Dark Ronald line comes from the stud horse 2782 Ballast. This stud horse has not played an active role in breeding since 2011; nevertheless, he has left behind many high-quality mares and stud horses which breeders should continue to include in breeding, making use of their genotypic traits, which are also very well reflected in the phenotype of conformation.

REFERENCES

Baban, M. et al. 2009. Phenotypic Correlations of Stride Traits and Body Measurements in Lipizzaner Stallions and Mares. Journal of Equine Veterinary Science, 29(7): 513–518.

Birdsall, P. 2017. Sire Lines Of International Jumpers The Dark Ronald Line. Sporthorse-data Passionate about Pedigrees [Online]. Available at: https://sporthorse-data.com/articles/2017/01/01/sire-lines-international-jumpers-dark-ronald-line. [2020-07-27].

Czech Warmblood Horse Breeders Association, 2017. Řád plemenné knihy ČT. Svaz chovatelů českého teplokrevníka [Online]. Available at: http://www.schct.cz/cz/svaz/rad-pk.html. [2020-07-27].

Černohorská, H. et al. 2013. Analysis of lines and breeds of sires in the breeding of the Czech warmblood horses based on grading their off spring in rearing facilities for testing young horses (RFT). Acta Universitatis Agriculturae et Silviculturae Mendelianae Brunensis, 61(6): 1605–1612.

Dušek, J. et al. 2011. Česká teplokrevná plemena. In Chov koní. Praha: Nakladatelství Brázda, pp. 114–115.

Eurodressage, 2020. Dark Ronald xx, Not Origin Horse for Warmblood Fragile Foal Syndrome (WFFS) [Online]. Available at: https://www.eurodressage.com/2020/07/07/dark-ronald-xx-not-origin-horse-warmblood-fragile-foal-syndrome-wffs. [2020-07-27].

Novotná, A. et al. 2017. Estimation of genetic parameters for linear type traits in the population of sport horses in the Czech Republic. Livestock Science, 202(8): 1–6.

Peters, A. 2005. Dark Ronald. Thoroughbred Heritage [Online]. Available at: https://www.tbheritage.com/Portraits/DarkRonald.html. [2020-07-27].

Pietrzak, S. et al. 2016. Effect of some factors on performance value assessment of stallions during performance tests. Annals of Animal Science, 16(4): 1175–1184.

Rustin, M. et al. 2009. Multi-trait animal model estimation of genetic parameters for linear type and gait traits in the Belgian warmblood horse. Journal of Animal Breeding and Genetics, 126(5): 378–386.

Saastamoinen, M., Barrey, E. 2000. Conformation, locomotion and physiological traits. In The Genetics of the Horse. Wallingford, UK: CABI, pp. 439–472.

Sobotková, E., Oravcová, I. 2014. Czech Warmblood. Horse Husbandry [Online]. Available at: https://web2.mendelu.cz/af_291_projekty2/vseo/stranka.php?kod=487. [2020-08-03].

Utilization of Duroc boars in production of piglets

Jan Lujka, Pavel Nevrkla, Zdenek Hadas
Department of Animal Breeding
Mendel University in Brno
Zemedelska 1, 613 00 Brno
CZECH REPUBLIC

honza.lujka@gmail.com

Abstract: The study was designed to evaluate the effect of three terminal boars, originating from the Duroc breed, on reproductive parameters of sows and losses of piglets from birth to weaning and also to evaluate the effect of these boars on individual weight of piglets at the time of birth and weaning and on average daily gain from birth to weaning. Boars of the Duroc x Large White $_{\text{sire line}}$ (D x LW_{SL}), Danish Duroc (DD) and Norwegian Duroc (ND) were included in the experiment. Evaluation of the effect of the selected boars on reproductive parameters in sows and losses of piglets showed no statistically significant differences. Observation of the effect of boars on birth weight of piglets revealed a statistically significant difference ($P \leq 0.05$) between the piglets after the D x LW_{SL} boar (individual birth weight 1.47 kg) and the piglets after the DD boar (1.32 kg) and the ND boar (1.35 kg). Evaluation of individual weight at weaning showed statistically significant differences ($P<0.05$) between the piglets after the ND boar (7.96 kg) and after the DD boar (7.21 kg). The statistically highest ($P<0.05$) average daily gain was achieved by the piglets after the ND boar (235.96 g) on the contrary, the lowest was recorded in the piglets after the DD boar (210.02 g). Although Boars included in the experiment was coming from the same breed, differences were observable.

Key Words: boar, sow, Duroc, reproduction, growth of piglets

INTRODUCTION

The ability to produce viable piglets of a good quality is an elementary condition for breeding of pigs for slaughter. Reproductive parameters such as litter size, losses of piglets and birth weight are characterized by low heredity (Andersen et al. 2009). Oliviero et al. (2010) state that these parameters are most affected by breeding technologies. However, it has been proven that they are significantly influenced also by genetic factors (Vanderhaeghe et al. 2010). Genetic variance between the pig breeds used in commercial meat production is significant, which can be used in various breeding combinations for more pronounced heterosis effect (Su et al. 2007). Marandu et al. (2015) add that unlike in the reproductive performance parameters in sows, the heredity of birth weight in piglets is very favourable, with coefficient of 0.31. It is therefore important to emphasize selection of suitable parents for final slaughter hybrids. Studies focused on the effect of terminal boars on the numbers of piglets born, the numbers of piglets reared and growth ability of piglets before weaning are not frequent, despite of their significant effect on these parameters (McClann et al. 2008).

In the Czech Republic and worldwide, the breed of Duroc is utilized among others. This breed originating from America (Sambraus 2006) is used in production of slaughter pigs mainly for its solid constitution and resistance together with meat of a very good quality with good intramuscular fat content and fine muscle fibres (SCHP 2017). For these characteristics it is included in hybridization programs of many breeding companies, where it is used on paternal position in production of final hybrids. This study compares the effect of the D x LWSL, DD and ND boars on the total number of piglets, the numbers of live-born and stillborn piglets, the losses of piglets from birth to weaning and the growth ability of piglets before weaning on a production farm.

MATERIAL AND METHODS

Animals and analyses

A total of 19 F1 sows of the Large White x Landrace hybrids combinations were included in the experiment. All the sows were observed on their third parity and the observation was performed during one shift. The sows were inseminated with the doses of selected terminal boars. The boars came from the same insemination station and preparation of the insemination doses was equal. The sows were divided into groups while each group was inseminated with semen of a different boar. The boar of Duroc x Large White $_{\text{sire line}}$ (D x LW_{SL}) was used for insemination of 5 sows. The Danish Duroc (DD) boar was used for insemination of 8 sows. The remaining 6 sows were inseminated with the Norwegian Duroc (ND) boar. Intracervical insemination method was used for all the sows. Reinsemination was performed 12 hours after the insemination. Insemination and reinsemination were done by one operator. After farrowing, selected reproductive parameters were evaluated for each sow, namely total number of piglets, numbers of live-born and stillborn piglets, numbers of mummified and non-viable piglets and losses of piglets from birth to weaning per litter. All reared piglets were included in evaluation of growth ability of piglets, expressed as average daily gain in grams. A total of 235 piglets were evaluated. The piglets were weighed within 24 hours after birth and at the time of weaning at average age of 28 days. A hanging scale with accuracy of 0.01 kg was used for weighing of the piglets. The number of piglets after the D x LW_{SL} boar was 63, while 103 piglets were after the DD boar and 69 piglets after the ND boar.

Housing and feeding

The observed sows were housed in conventional stables of a production farm. At the time of insemination, they were kept in individual boxes. The boxes consisted of concrete floor and grates and were equipped with a feeding unit and a drinker. The sows were transferred to group pens 30 days after insemination. The pens were differentiated to a bed with concrete floor and dunging place with grates. The pens were equipped with automatic feeding units and pin drinkers in an amount corresponding to the number of sows. One week before the expected farrowing, the sows were transferred to the farrowing house to individual pens with farrowing boxes. The pens were equipped with heated nests, feeders and drinkers for piglets. Ventilation in stable was automatic. The housing was in compliance with COUNCIL DIRECTIVE 2008/120/EC. The sows were given moistened feed ration in amount that corresponded to their condition and the number of piglets in case of lactating sows.

Statistical analysis

The data were statistically analysed in the form of mean and SEM using the single-factor ANOVA and HSD test for unequal n in the STATISTICA cz 12 software. The differences between means were considered highly statistically significant (**) when $P < 0.01$ and statistically significant (^{*,a,b,c}) when $P < 0.05$. Correlations of the observed parameters were determined by calculation of Pearson's correlation coefficients.

RESULTS AND DISCUSSION

Table 1 presents the results of the evaluated effect of terminal boars on reproductive parameters and losses of piglets from birth to weaning. No significant differences were observed among the evaluated groups, however, differences in the absolute values of selected reproductive parameters in sows inseminated with the selected boars are evident. The values in the table show the highest total number of piglets after the D x LW_{SL} boar (16.00), on the contrary, the lowest total number of piglets was recorded in sows inseminated with the ND boar (13.33). The highest number of live-born piglets was also observed after insemination with the D x LW_{SL} boar (14.40) and the lowest after the ND boar (11.83). The highest number of stillborn piglets was found after insemination with the ND boar (1.33), while the lowest value was observed after the DD boar (0.88). Mummified foetuses were observed only after insemination with the DD boar (0.63). The highest number of non-viable piglets was found after insemination with the DD boar (1.25) and the lowest number after the ND boar (0.17). The highest number of reared piglets was recorded in sows inseminated with the DD boar (12.88), the lowest number of piglets were reared after the ND boar (11.50). The highest losses of piglets were recorded after the D x LW_{SL} boar (1.80), the lowest losses were observed after the ND boar (0.33).

Fertility rate is usually related to hybrid combination of sows, with different fertility rates found in different hybrid combinations (Sonderman and Luebbe 2008). According to King et al. (1998), reproductive parameters in sows are also significantly influenced by breeding management. Haley et al. (1995) state that the effect of breed or hybrid combination used on the paternal position is much more limited than the effect of sows. Some authors came to different conclusion, such as McClann et al. (2008) who described that the breed in the terminal position affects some reproductive parameters in sows. Apart from that, fertility is also influenced by selection of a boar within breed (Roca et al. 2015).

Table 1 The effect of terminal boar on selected reproductive parameters in sows and losses of piglets per litter

Parameters	Terminal boar			SEM	P - value
	D x LW_{SL}	DD	ND		
Total number of piglets (pcs)	16.00	15.50	13.33	0.74	0.79
Live-born piglets (pcs)	14.40	13.38	11.83	0.63	0.87
Stillborn piglets (pcs)	1.20	0.88	1.33	0.31	0.55
Mummified foetuses (pcs)	0.00	0.63	0.00	0.09	0.38
Non-viable piglets (pcs)	0.40	1.25	0.17	0.21	0.83
Reared piglets (pcs)	12.60	12.88	11.50	0.59	0.95
Losses of piglets (pcs)	1.80	0.50	0.33	0.19	0.79

Legend: D x LWSL – Duroc x Large White sire line; DD – Danish Duroc; ND – Norwegian Duroc; Non-viable piglets – Piglets that died within 6 hours after birth for no evident reason.

Table 2 shows results of the evaluated effect of the terminal boar on growth ability of piglets. The significantly highest birth weight ($P<0.05$) was observed in the piglets after the D x LW_{SL} (1.47 kg). Birth weight of the piglets after the DD and ND boars was very similar (DD 1.32 kg, ND 1.35 kg). Evaluation of weaning weight revealed statistically significant differences ($P<0.05$) between the piglets after the ND boar (7.96 kg) and the piglets after the DD boar (7.21 kg). The significantly highest ($P<0.05$) average daily gain was found in the piglets after the ND boar (235.96 g), while the lowest value was recorded after the DD boar (210.02 g).

Fix et al. (2010) state that mortality of piglets increases with decreasing birth weight. Piglets with a low birth weight lag behind their siblings with their daily gains, which leads to lower quality at weaning. This is manifested by slower growth in later breeding categories and consequently leads to economic losses. According to Rohe and Kalm (2000), birth weight is influenced by breed or hybrid combination. Kabalin et al. (2012) consider the total number of piglets in litter to be an elementary factor affecting birth weight of piglets and subsequent growth, however, they also admit the effect of terminal boar. Čechová (2006) studied the effect of four terminal boars of different breeds of which the highest birth weight was recorded in piglets after the LW_{SL} boar, while the lowest weight was found in piglets after the Duroc boar which, however, reached relatively high weaning weight. This finding is supported by Magowan et al. (2011) who add that this trend was recorded also for hybrid terminal boars with utilization of the Duroc boar. Those results also correspond to the findings of the present experiment, where piglets of the D x LW_{SL} hybrid combination showed the highest birth weight, while the highest weaning weight was observed in the piglets after the ND boar.

Table 2 The effect of terminal boar on growth of piglets

Parameters	Terminal boar			SEM	p - value
	D x LW_{SL}	DD	ND		
Individual birth weight (kg)	1.47^{a}	1.32^{b}	1.35^{b}	0.02	<0.01
Individual weaning weight (kg)	7.70	7.21^{a}	7.96^{b}	0.08	0.04
Average daily gain from birth to weaning (g/day)	222.45	210.02^{a}	235.96^{b}	2.58	0.03

Legend: a, b – statistically significant differences ($P \leq 0.05$); D x LWSL – Duroc x Large White sire line; DD – Danish Duroc; ND – Norwegian Duroc

Table 3 presents coefficients of phenotypic correlations between the reproductive parameters in sows and productive parameters in piglets. The total numbers of piglets and numbers of live-born piglets are in a moderate negative correlation ($P < 0.01$) with birth weight of piglets and weaning weight of piglets. The number of non-viable piglets is in significant moderate negative correlation ($P < 0.05$) with birth weight of piglets. Other moderate but significant negative correlations ($P < 0.01$) were found between the total numbers of piglets and live-born piglets and the average daily gain from birth to weaning. Kabalin et al. (2012) proved that piglets from larger litters are characterized by slower growth than the piglets from smaller litters. Johansen et al. (2004) note that milk fat is an important source of energy for piglets during first days of their lives, due to their low body fat content after birth. In this respect, sows need to produce as much milk as possible with an adequate content of fat milk. The piglets from large litters usually grow more slowly, since there is less milk available on average for each of the piglets.

Table 3 Coefficients of phenotypic correlation between reproductive parameters in sows and growth parameters in piglets

Parameter	TN	LB	SB	MF	NV	RP	LP
Individual weight of piglets (kg)							
Birth	-0.49**	-0.48**	-0.14	-0.12	-0.33*	-0.45**	-0.19
Weaning	-0.46**	-0.49**	-0.21	-0.20	-0.09	-0.48**	-0.08
Average daily gain (g/day)							
Birth – Weaning	-0.39**	-0.42**	-0.22	-0.22	-0.04	-0.42**	-0.02

Legend: TN – total number of piglets/litter, LB – number of live-born piglets/litter, SB – number of stillborn piglets/litter, MF – number of mummified foetuses/litter, NV – number of non-viable piglets/litter, RP – number of reared piglets/litter, LP – losses of piglets/litter; (*) indicates correlation of values at P < 0.05, (**) indicates correlation of values at P < 0.01.

CONCLUSION

The experiment revealed no statistically significant effect of the observed terminal boars on the selected reproductive parameters in sows. However, the effect of these boars on individual birth weight and weaning weight of piglets was proven and it influenced also the growth ability of piglets which was expressed as a significant difference in mean daily gain from birth to weaning.

REFERENCES

Andersen, I.L. et al. 2009. Drying and warming immediately after birth may reduce piglet mortality in loose-housed sows. Animal, 3(4): 592–597.

Čechová, M. 2006. Analysis of some factors influencing the birth weight of piglets. Slovak Journal of Animal Science, 39(3): 139–144.

Fix, J.S. et al. 2010. Effect of piglet birth weight on survival and quality of commercial market swine. Livestock Science, 132(1): 98–106.

Haley, C.S. et al. 1995. Comparative farrowing to weaning performance in Meishan ang Large White pigs and crosses. Animal Science, 60(2): 259–267.

Johansen, M. et al. 2004. Factors associated with suckling piglet average daily gain. Preventive Veterinary Medicine, 63(1–2): 91–102.

Kabalin, A.E. et al. 2012. Influence of birth mass on losses and weight gain of Large Yorkshire piglets during preweaning period. Macedonian Journal of Animal Science, 2(3): 273–276.

King, V.L. et al. 1998. Management factors associated with swine breeding-herd productivity in the United States. Preventive Veterinary Medicine, 35(4): 255–264.

Magowan, E. et al. 2011. Effect of Breed, Finish Weight and Sex on Pork Meat and Eating Quality and Fatty Acid Profile. Agri-Food and Bioscience Institute, UK [Online] 28. Available at: https://www.afbini.gov.uk/sites/afbini.gov.uk/files/publications/%5Bcurrent-domain%3Amachine-name%5D/finishing%20weight%20of%20pork%20sex.pdf. [2020-08-03].

Marandu, N. et al. 2015. Effect of within-litter birth weight variation on piglet survival and pre-weaning weight gain in a commercial herd. Journal of Agriculture and Rural Development in the Tropics and Subtropics, 116(2): 123–129.

McClann, M. et al. 2008. The effect of boar breed type on reproduction, production performance and carcass and meat quality in pigs. Irish Journal of Agricultural and Food Research, 47(2): 171–185.

Oliviero, C. et al. 2010. Environmental and sow-related factors affecting the duration of farrowing. Animal Reproduction Science, 119(1–2): 85–91.

Roca, J. et al. 2015. Boar differences in artificial insemination outcomes: can they be minimized? Reproduction in Domestic Animals, 50(2): 48–55.

Rohe, R., Kalm E. 2000. Estimation of genetic and environmental risk factors associated with pre-weaning mortality in piglets using generalized linear mixed models. Animal Science, 70(2): 227–240.

Sambraus, H.H. 2006: Atlas plemen hospodářských zvířat. 1st ed., Praha, CR: Brázda.

Sonderman, J.P., Luebbe, J.J. 2008. Semen production and fertility issues related to differences in genetic lines of boars. Theriogenology. 70(8): 1380–1383.

Su, G. et al. 2007. Selection for litter size at day five to improve litter size at weaning and piglet survival rate. Journal of Animal Science, 85(6): 1385–1392.

Svaz chovatelů prasat, z.s. 2017. Svaz chovatelů prasat v Čechách a na Moravě, Českomoravská společnost chovatelů, Ročenka/Yearbook 2017. 21. [Online] Available at: https://www.schpcm.cz/publikace/rocenka_2017_cz.pdf. [2020-08-03].

Vanderhaeghe, C. et al. 2010. Longitudinal field study to assess sow level risk factors associated with stillborn piglets. Animal Reproduction Science, 120(1–4): 78–83.

Total haemolymph protein in honeybee workers as a marker for the evaluation of colony condition?

Jan Musila[1], Ondrej Babica[1], Zuzana Lackova[2], Jan Prouza[1,3], Tibor Fuzik[4], Ondrej Zitka[2], Pavel Plevka[4], Antonin Pridal[1]
[1]Department of Zoology, Fisheries, Hydrobiology and Apidology
[2]Department of Chemistry and Biochemistry
Mendel University in Brno
Zemedelska 1, 613 00 Brno
[3]Department of Experimental Biology
Masaryk University
Kotlarska 2, 611 37 Brno
[4]Central European Institute of Technology
Kamenice 5, 625 00 Brno
CZECH REPUBLIC

apridal@mendelu.cz

Abstract: The winter loses of honeybee colonies have been increasing in recent decades. Successful overwintering depends on abundance of the long-living bees in the colony. This study verified whether the total haemolymph protein content in the pooled sample from workers (TP) could be a useful marker to determine the overall colony condition and predict winter survivability. Here we show that the values of TP in autumnal workers did not correlate with the winter survival of colonies. The average TP did not differ between the collapsed and survived colonies. In the early spring, the average TP among apiaries did not differ in spite of very different health conditions of individual apiaries. These results do not support the hypothesis that TP assayed in the pooled sample prepared from unknown-aged workers is a reliable marker for prediction of the overwintering ability or the overall condition of colonies.

Key Words: Apis mellifera, condition, colony, haemolymph, protein

INTRODUCTION

Winter colony loses have been considered to be the most serious issue of recent beekeeping (Stokstad 2007, van Engelsdorp et al. 2009, Williams et al. 2010). This loses are caused multifactorially: diseases (Genersch et al. 2010), sublethal intoxication (Di Prisco et al. 2013) or malnutrition (Zhang et al. 2020). Devastating consequences arise mainly due to weakening and damage of winter bees (van Dooremalen et al. 2012). Overwintering is closely dependent on the number of long-living bees and their condition within wintering colony (Döke et al. 2015). There is a demanding issue to find predictive markers for the honey bee colony collapse (Dainat et al. 2012, Aurori et al. 2014, Steinmann et al. 2015). There were studied following physiological parameters in honey bee workers; a) in body: weight, storage proteins, size of hypopharyngeal glands, total antioxidant status, glutathione, activity of enzymes (superoxide dismutase, peroxidase, catalase, glutathione S-transferase), b) in haemolymph: total protein, vitellogenin, titre of juvenile hormone, lipids, carbohydrates, antibacterial activity, activity of phenoloxidase and number of haemocytes and c) a gene expression e.g. methyl farnesoate epoxidase (Fluri et al. 1981, Kunert and Crailsheim 1988, Otis et al. 2004, Farjan et al. 2012, Steinmann et al. 2015, Kunc et al. 2019).

Kunc et al. (2019) emphasised that the distinction of the summer and winter bees is important for prediction of the success of overwintering. The total haemolymph protein is basic physiological parameter correlating with several other physiological parameters (Kunc et al. 2019) in which their determination is more difficult (e.g. vitellogenin). Kunc et al. (2019) mentioned that their study was performed on only one colony, therefore, future experiments would involve efforts to measure

the parameters on a large number of colonies to correlate the results of analyses to the success of overwintering rate.

Therefore, following experiments on a large number of colonies were aimed on the total haemolymph protein in honeybee workers as a predictive marker of overwintering ability. The hypotheses were as follow: Is total haemolymph protein in autumn a predictive marker for overwintering of colony and its further growth in spring? Does the total haemolymph protein in early spring correlate with the strength of the colony?

MATERIAL AND METHODS

The experiments were carried out: a) in autumn 2019 at three apiaries in Lysicko region totally with 19 colonies and b) in early spring 2020 at three apiaries in Brno city, Brno – countryside region and Opava region totally with 59 colonies; totally 78 colonies of *Apis mellifera*.

Evaluation of colonies

The colonies included in the autumnal experiment were evaluated with respect to their ability to survive winter (survived/collapsed) in the early spring (March 2020) and then in spring (May 2020) with respect to their overall condition reflecting the ability to grow (strength of the colony). The colony strength was assessed according to number of occupied frames, supers and surface of brood area [dm^2]. Thus the colony population was divided into two groups: 1) colonies with good condition having standard spring growth and abilities to build combs and 2) weak colonies whose hive space had to be reduced in early spring and with substandard growth and limited abilities to build new combs.

The colonies included in the early spring experiment were evaluated in March 2020 with respect to their overall condition after winter period. The colony condition were scored with grades 1–10 (the grade 10 described a colony with excellent condition – occupied maximum frames and supers, had the largest areas of brood).

Haemolymph collection

The haemolymph for the autumnal experiment was collected on 23th October 2019 and for the early spring experiment on 18th March 2020. Twenty workers from each experimental colony (*Apis mellifera*) were sampled to plastic vials. The bees were taken from the broodless comb that was located straight next to the first brood comb of the brood nest (Kunc et al. 2019). The plastic vials with bees were cooled up to 4 °C and transported to laboratory for haemolymph collection. Haemolymph was collected from each sampled worker by micro-capillary pipette by incision between the 3rd and 4th abdominal tergites in volume 1 µl to create pooled haemolymph sample of total volume 20 µl representing a colony. For quantification of protein, 1 µl of haemolymph representatively taken from the pooled sample was mixed with phenylthiourea and phosphate buffer (pH = 7) to prevent haemolymph melanisation and to improve stability of the haemolymph proteins.

Total protein quantification

Bovine serum albumin (BSA) was used as a standard and to validate the method. Validation of the method using the BSA standard always took place before each determination (the standard was always prepared fresh). Ready-to-use protein reagent Dry Reagent Concentration (BIO-RAD, California, USA) was purchased. This reagent was diluted 1:4 with MilliQ water before analysis (the reagent was always prepared fresh). Determination procedure: 10 µl of the sample was pipetted into a 96 well microtiter plate Nunc Immuno (Fisher Scientific, Pardubice, Czech Republic). Subsequently, 200 µl of diluted protein reagent was added to 10 µl of the sample. Followed by incubation for 5 min at room temperature and absorbance measurement at 595 nm using instrument Infinite M200Pro (Tecan, Männedorf, Switzerland). Each sample was analysed three-times (triplet).

Statistical evaluation

The abscissae around means in charts represent the standard deviation. Relations between the total protein and overwintering/early spring condition were evaluated by Spearman's/Pearson's correlation or regression analysis. The statistical significance of differences of the mean values was analysed by t-test (two groups) or ANOVA (more than two groups) with post-hoc analysis by Tukey's test. A difference with p-value above 0.05 ($p > 0.05$) was considered statistically insignificant.

RESULTS

Autumn

Relationship analysis between the total haemolymph protein in autumnal workers and the winter survival resulted only in low and positive coefficient of correlation ($r = 0.348$, $p = 0.144$). There was a tendency of colonies with a higher content of the protein in haemolymph to overwinter successfully, however, this dependence was weak. This tendency according to individual colonies is depicted in Figure 1. Both extreme values of the total protein belonged to the collapsed colonies. The collapsed colonies are crowded namely in the central and the right parts of the chart, i.e. with middle and low protein content. However, the survived colonies are evenly distributed over entire width of the chart. The survived colonies with weak early spring condition had, paradoxically a high protein content in autumn (yellow columns, the left part in Figure 1).

Figure 1 Total autumnal protein content in individual colonies in descending order with colour marking their overwintering ability and early spring development

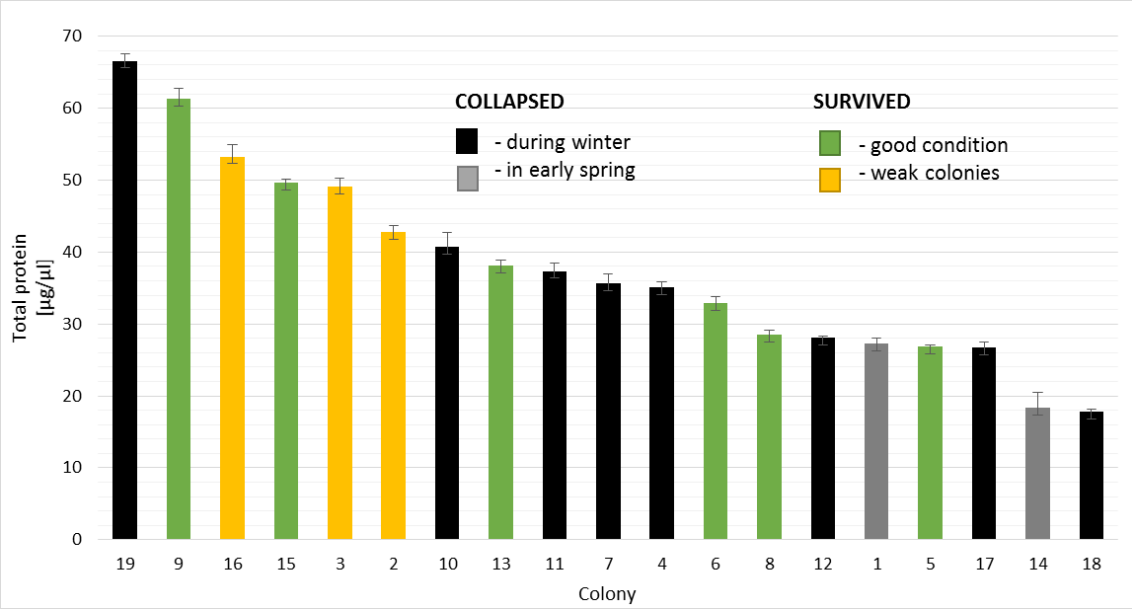

Figure 2 Average total autumnal protein content in collapsed and survived colonies

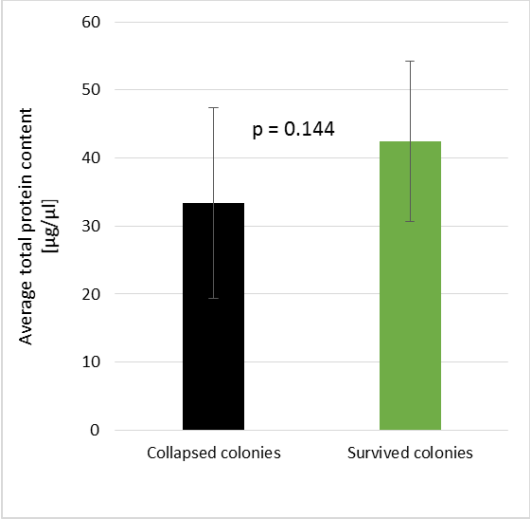

The average total haemolymph protein in the collapsed and the survived colonies differed insignificantly (Figure 2) and in the collapsed colonies was lower only by 9.1 µg/µl in comparison with the survived colonies.

Early spring

The apiary at Brno-city showed more than half winter losses in the early spring 2020. The Opava region apiary had only low losses about 15%. The best overwintering result showed colonies at Brno – countryside region. There were predominantly colonies with the excellent condition, without deaths or need to outlay any colony. There were only two colonies showing conspicuous weakening.

Regression analysis between the total haemolymph protein in early spring workers and the condition of overwintered colonies showed almost zero and negative dependence (Figure 3).

Figure 3 Regression analysis between of the total protein content and colony condition in early spring

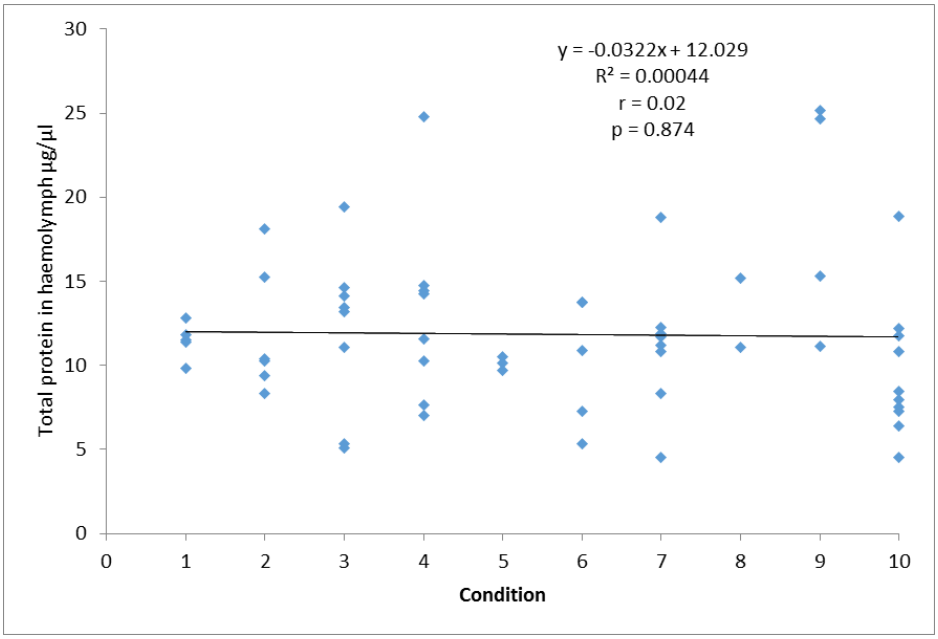

Despite that the average total protein in the early spring workers differed among apiaries insignificantly ($F_{0.95}$ (2,56) = 2.085; p = 0.134) the average condition of the early spring colonies differed significantly ($F_{0.95}$ (2,56) = 25.620; p < 0.001) (Figure 4).

Figure 4 The average total protein content and average colony condition by apiaries in early spring

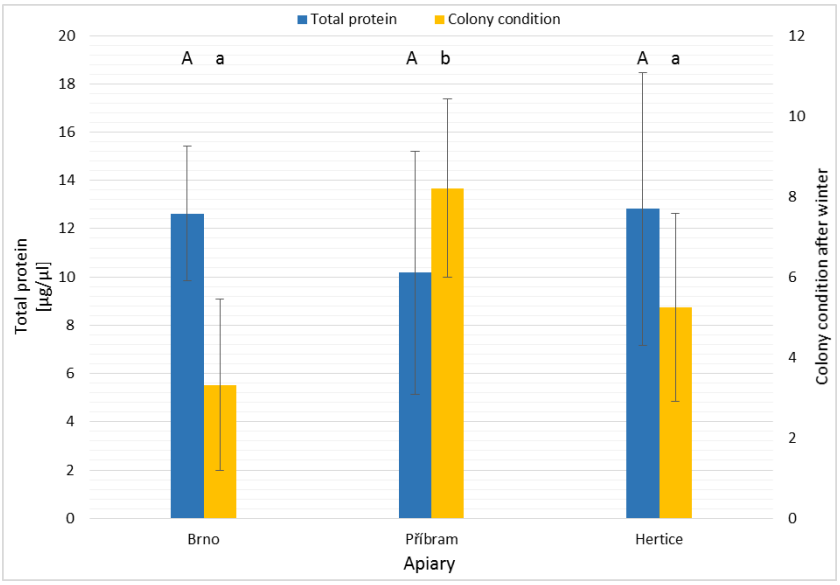

Legend: capitals letters = total protein; small letters = colony condition; different letters = p < 0.05 (Tukey's test)

The haemolymph protein content in the early spring workers did not correspond with the colony condition in any way. This result is supported at example of four selected colonies with extreme combinations of both values (Figure 5). These examples show that there were colonies with

excellent/insufficient condition and at the same time with very low/very high level of the protein in haemolymph.

DISCUSSION

The colony No 19 with the highest level of protein in haemolymph in October 2019 died within the winter 2019/2020. Moreover, the weak colonies (No 2, 3 and 16) had the total haemolymph protein content higher than average in comparison with the rest of the experimental colonies. Although, the total protein was somewhat lower in the collapsed colonies, the difference with the survived colonies was not significant. The results of overwintering did not correspond with autumnal levels of protein in the worker bee haemolymph. Therefore, we decided to assay the protein level in many colonies located in several apiaries also at the first inspection of colonies in early spring 2020. Even in this case, it was not possible to find any significant differences. There was no correlation between the overall colony condition and the protein level. Even differences in the protein level among apiaries in the early spring were insignificant in spite of the strikingly different rate of collapses among apiaries.

Figure 5 The total protein content and condition colonies with extreme values in early spring

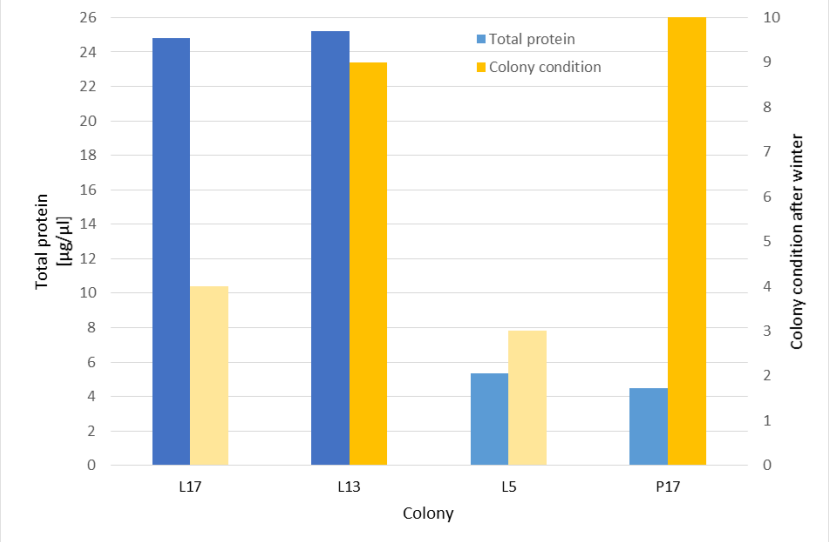

Legend: lighter shade of colour = low value, darker shade of colour = high value

Content of the total haemolymph protein from the pooled sample of haemolymph of honey bee workers did not correlate with the overall condition of a colony either in autumn or in spring. This result is not in conflict with results by Fluri et al. (1982) or Kunc et al. (2019). However, the total haemolymph protein content is not a predictive marker for 'potential overwintering problems' with regard to the applicated sampling of bees as it was proposed by Kunc et al. (2019). Besides other, they proposed sampling in October and compare measured results with their data, since, this approach might provide useful insight into the readiness of long-living bees which are necessary for successful overwintering and beekeepers could estimate proportion of long-living workers in the colony and so predict potential overwintering problems. However, their data did not involve estimation of proportion of long-living workers in the colony. Kunc et al. (2019) sampled worker bees from the comb without brood and adjacent to brood chamber to avoid the sampling of freshly emerged adults. There were sampled probably no freshly emerged imagoes, however, workers of all ages. The following question arises: Where or how were the workers sampled in the winter period without brood?

It is known that physiology in honeybee workers is age-related (Crailsheim 1990, Huang and Robinson 1995, Crailsheim and Leonhard 1997) and interpretation of physiological parameters without known age of a bee is rather complicated. Therefore, it can be presumed that a physiological parameter, e.g. total haemolymph protein, should be compared only in the same age colony cohorts. A simple average value of any physiological parameter obtained from several workers has lower importance for an explanation than values for each worker bee separately, and knowledge about the structure of workers in a colony as it was analogically proposed e.g. by Oliver (2012).

CONCLUSION

The total protein assayed from the pooled sample of haemolymph collected from workers of unknown age is not appropriate predictive maker for a capability of the honeybee colony to overwinter or evaluation of its overall condition. However, the total haemolymph protein is not disqualified as an applicable physiological parameter in the case of haemolymph collection from workers of known age with respect to the complex structure of the honeybee colony.

ACKNOWLEDGEMENTS

The research was financially supported from the donations by elitbau, Ltd. We are grateful to Jiri Krenovsky for providing his apiaries for experiments.

REFERENCES

Aurori, C.M. et al. 2014. What is the main driver of ageing in long-lived winter honeybees: Antioxidant enzymes, innate immunity, or vitellogenin? Journals of Gerontology Series A: Biomedical Sciences and Medical Sciences, 69(6): 633–639.

Crailsheim, K. 1990. The protein balance of the honey bee worker. Apidologie, 21(5): 417–429.

Crailsheim, K., Leonhard, B. 1997. Amino acids in honeybee worker haemolymph. Amino Acids, 13(2): 141–153.

Dainat, B. et al. 2012. Predictive markers of honey bee colony collapse. PLoS one, 7(2): e32151.

Di Prisco, G. et al. 2013. Neonicotinoid clothianidin adversely affects insect immunity and promotes replication of a viral pathogen in honey bees. PNAS, 110(46): 18466–18471.

Döke, M.A. et al. 2015. Overwintering honey bees: Biology and management. Current Opinion in Insect Science, 10: 185–193.

Farjan, M. et al. 2012. Supplementation of the honey bee diet with vitamin C: The effect on the antioxidative system of Apis mellifera carnica brood at different stages. Journal of Apicultural Research, 51(3): 263–270.

Fluri, P. et al. 1982. Changes in weight of the pharyngeal gland and haemolymph titres of juvenile hormone, protein and vitellogenin in worker honey bees. Journal of Insect Physiology, 28(1): 61–68.

Genersch, E. et al. 2010. The German bee monitoring project: a long term study to understand periodically high winter losses of honeybee colonies. Apidologie, 41(3): 332–352.

Huang, Z.Y., Robinson, G.E. 1995. Seasonal changes in juvenile hormone titers and rates of biosynthesis in honey bees. Journal of Comparative Physiology B, 165(1): 18–28.

Kunc, M. et al. 2019. The Year of the Honey Bee (Apis mellifera L.) with Respect to Its Physiology and Immunity: A Search for Biochemical Markers of Longevity. Insects, 10(8): 244.

Kunert, K., Crailsheim, K. 1988. Seasonal changes in carbohydrate, lipid and protein content in emerging worker honeybees and their mortality. Journal of Apicultural Research, 27(1): 13–21.

Oliver, R. 2012. Sick Bees: Part 15, An Improved Method for Nosema Sampling. American Bee Journal, 152(1): 65–70.

Otis, G.W. et al. 2004. Storage proteins in winter honey bees. Apiacta, 38: 352–357.

Steinmann, N. et al. 2015. Overwintering is associated with reduced expression of immune genes and higher susceptibility to virus infection in honey bees. PLoS ONE, 10(6): e0129956.

Stokstad, E. 2007. The case of empty hives. Science, 316(5827): 970–972.

vanDooremalen, C. et al. 2012. Winter survival of individual honey bees and honey bee colonies depends on level of Varroa destructor infestation. PLoS ONE, 7: e36285.

van Engelsdorp, D. et al. 2009. Colony collapse disorder: A descriptive study. PLoS ONE, 4: e6481.

Williams, G.R. et al. 2010. Colony collapse disorder in context. BioEssays, 32(10): 845–846.

Zhang, G. et al. 2020. Honey Bee (Hymenoptera: Apidea) Pollen Forage in a Highly Cultivated Agroecosystem: Limited Diet Diversity and Its Relationship to Virus Resistance. Journal of Economic Entomology, 113(3): 1062–1072.

The influence of different sources of selenium on blood glutathione peroxidase activity in laying hens

Jakub Novotny, Andrea Roztocilova, Ondrej Stastnik, Daria Baholet, Eva Mrkvicova, Leos Pavlata
Department of Animal Nutrition and Forage Production
Mendel University in Brno
Zemedelska 1, 613 00 Brno
CZECH REPUBLIC

jakub.novotny@mendelu.cz

Abstract: The influence of different forms of selenium (organic and inorganic source) on blood glutathione peroxidase activity in laying hens Lohmann Brown-Classic was evaluated. The hens were divided into 3 equal groups (Control, Organic, Inorganic). The content of selenium in the Control group´s diet (0.08 mg/kg Se) was only with its natural content in the feed. The Organic group (0.27 mg/kg Se) was fed with an organic source of selenium (selenium-enriched *Saccharomyces cerevisiae* CNCM I-3060) and the Inorganic group (0.27 mg/kg Se) was fed with an inorganic source of selenium (sodium selenite – Na_2SeO_3). There were not found any statistically significant differences ($P < 0.05$) between the groups. Based on our trial an addition of selenium in different forms has no effect on glutathione peroxidase activity in whole blood of laying hens.

Key Words: poultry, nutrition, *Saccharomyces cerevisiae,* sodium selenite, organic selenium

INTRODUCTION

A biological active form of selenium was found in 1973 as an integral part of the glutathione peroxidase (GPx) and others like iodothyronine deiodinases, selenophosphate synthase or thioredoxin reductase (Rotruck et al. 1973). Selenium is an essential nutrient, functions as cofactor for the antioxidant enzymes, i.e., glutathione peroxidase, certain forms of thioredoxin peroxidase (Ferguson et al. 2012). Selenoenzymes´ activity depends on intake of Se in food. More than 0.1 mg/kg of Se in diet has a positive effect on immunity (Song et al. 2006). GPx keeps low levels of H_2O_2 and else hydroperoxides in cells to protect tissues from peroxidation damages (Kim and Mahan 2003). A deficiency of Se usually combined with a low vitamin E causes several issues. A low Se in poultry causes reduced growth, muscular dystrophy, mild hemorrhage and others (Thomson and Scott 1970, Bartholomew et al. 1998).

An organic Se increases Se content in eggs and improves quality of eggs in comparison with other sources of selenium (Payne et al. 2005, Asadi et al. 2017). As a source of organic Se is a Se yeast because of its better absorption and utilization by the animals (Delezie et al. 2014). Some studies showed that there were no differences in the activity of blood GPx in chicks fed organic Se (Se-enriched yeast) and sodium selenite (Kuricova et al. 2003, Payne and Southern 2005). Opposite effect found Mahmoud and Edens (2003). In their experiment chickens (in thermoneutral environment and after heat distress) fed Se-enriched yeast had higher GPx activity in blood than inorganic Se.

MATERIAL AND METHODS

Animals and experimental conditions

The total of 84 LOHMANN BROWN-CLASSIC laying hens aged 33 weeks were divided into 3 equal groups (n=28) named Control, Organic and Inorganic. A conventional deep litter system was used with wood shavings as the bedding material. Temperature, lighting regime and humidity were set according to the requirements for the production of Lohmann hens (Lohmann Tierzucht 2020). Live weight was measured regularly. Health status was monitored – one death was recorded during the trial. The layers had free access to water and were fed *ad libitum*. At the end of the trial (41 weeks of age) all hens were weighed and 8 birds from each group were randomly selected and slaughtered by decapitation.

Blood was collected and evaluated. Before the trial, the hens were fed commercial feed mixture ratios with addition of 0.3 mg/kg Se in inorganic form (sodium selenite).

Experimental groups and diets

The tree isoenergic and isonitrogenous diets were formulated according to the recommended nutrient content for Lohmann Brown-Classic hens (Lohmann Tierzucht 2020). Table 1 shows the composition of diets.

Table 1 Composition of used diets (g/kg)

Component	Control	Organic	Inorganic
Maize	333.39	333.39	333.39
Soybean meal	310.00	310.00	310.00
Wheat	190.00	190.00	190.00
Limestone grit	54.00	54.00	54.00
Rapeseed oil	40.00	40.00	40.00
Premix*	30.00	30.00	30.00
Limestone milled	25.00	25.00	25.00
Monocalcium phosphate	13.00	13.00	13.00
Sodium chloride	3.00	3.00	3.00
Methionine	1.60	1.60	1.60
Threonine	0.01	0.01	0.01
Sodium selenite	0.00	0.00	0. 01
Saccharomyces cerevisiae	0.00	0.10	0.00

*Legend: *Premix contains (per kg): L-lysine 13 g; DL-Methionine 45 g; calcium 295 g; phosphorus 67 g; sodium 46 g; copper 300 mg; iron 2,300 mg; zinc 1,800 mg; manganese 2,400 mg; iodine 30 mg; retinol 3300,000 IU (international units); calciferol 100,000 IU; tocopherol 500 mg; phylloquinone 40 mg; thiamine 40 mg; riboflavin 120 mg; pyridoxin 54 mg; cobalamin 400 µg; biotin 3 mg; niacinamid 420 mg; folic acid 30 mg; calcium pantothenate 250 mg; cholin chloride 6,000 mg.*

The control group was fed diets without the addition of selenium. Selenium was supplied only with its natural content in the feed. The first experimental group – Organic was fed with organic source of selenium (selenium-enriched *Saccharomyces cerevisiae* CNCM I-3060). The second experimental group – Inorganic was fed with inorganic source of selenium (sodium selenite – Na_2SeO_3). In both experimental groups (Organic and Inorganic, respectively) selenium was supplied with its natural content in the feed plus selenium was added (in organic or inorganic form). The chemical compositions of the diets (Table 2) were determined for dry matter (DM), crude protein, crude fat, crude fibre, and ash according to the EC Commission Regulation (Commission Regulation 152/2009).

Table 2 Chemical analysis of used diets

	Control	Organic	Inorganic
Dry matter (g/kg)	880	880	880
ME_N (MJ/kg)	11.47	11.47	11.47
Crude protein (g/kg)	182.72	183.03	183.03
Ether extract (g/kg)	55.21	57.21	55.82
Ash (g/kg)	144.41	144.22	149.02
Ca (g/kg)	40.24	40.24	40.24
P (g/kg)	5.94	5.94	5.94
Se (mg/kg)	0.08	0.27	0.27

Legend: ME_N – Apparent metabolize energy

Sample collection

Blood was collected into heparinized tubes. Whole blood was frozen (-20 °C) until biochemical examination. The glutathione peroxidase activity was determined using standardized biochemical

methods using Ransel Randox commercial sets on the Ellipse automatic biochemical analyzer (AMS Spa, Italy) in whole blood samples. GPx in whole blood is an indicator of a long-term supply of selenium. It´s decrease occurs after depletion of body reserves. Decrease or increase in activity occurs in connection with the replacement of the erythrocyte population (Gerlof 1992).

Statistical analysis

Data has been processed by Microsoft Excel (USA) and StatSoft Statistica 12 (USA). It was used one-way analysis of variance (ANOVA). For evaluate statistically differences between groups was used the Sheffé´s test and $P < 0.05$ was regarded a level of statistically significant difference.

RESULTS AND DISCUSSION

GPx activity values in blood are shown in Figure 1. The absolute values of GPx activity in groups with Se addition (Organic and Inorganic) were higher than the Control group. There were found no statistically significant differences between the groups ($P > 0.05$).

Figure 1 GPx activity in blood (mean ± standard error)

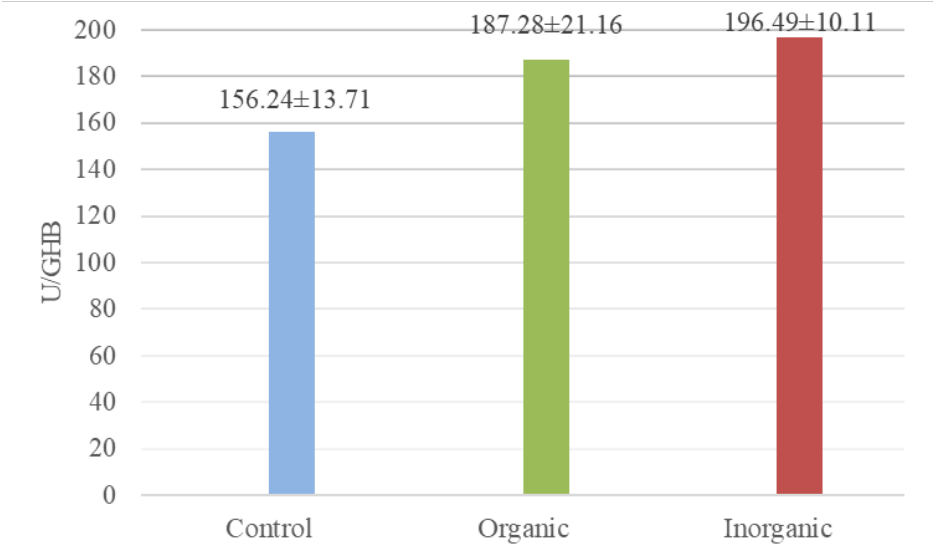

Legend: There was not found statistically significant differences (P > 0.05)

Our results correspond with results of Kuricova et al. (2003) and Payne and Southern (2005). Kuricova et al. (2003) used level of Se in diets 0.12 mg/kg for control group and 0.2 mg/kg and 0.7 mg/kg in dry matter for experimental groups. Levels of Se in Payne and Southern (2005) trial were 0.12 ppm as control and 0.46 ppm in both experimental groups (organic and inorganic form of Se). They said that activity of blood GPx in chicks fed organic Se in the form of Se-enriched yeast and sodium selenite was not different. Nevertheless, GPx activity increased significantly ($P < 0.05$) with the higher supplementation in the diet of broilers and laying hens. Plasma Se concentration of chickens fed Se-enriched yeast increased significantly ($P < 0.05$) compared with chickens fed inorganic Se. The same result found by Mahmoud and Ednens (2003). In their experiment chickens (in thermoneutral environment and after heat distress) fed Se-enriched yeast (0.46 mg/kg) had higher GPx activity in blood than inorganic Se (0.46 mg/kg).

During the experiment, despite a significant reduction in Se intake, there was no significant decrease, respectively difference in GPx activity between the Control group and both experimental groups. This may be because GPx responds only to a long-term deficiency. Our trial lasted 8 weeks. The hens could use selenium reserves in internal organs.

CONCLUSION

In the trial GPx blood activity was evaluated depending on the level and forms of selenium. There were not found statistically significant differences ($P < 0.05$) between the Control group with no addition of selenium, the Organic group with an addition of organic source of Se (selenium-enriched

Saccharomyces cerevisiae CNCM I-3060) and the Inorganic group with an addition of inorganic source of Se (sodium selenite Na_2SeO_3). According to our trial there is no differences in blood GPx activity between diets with organic source of Se (0.27 mg/kg) and inorganic sources of Se (0.27 mg/kg). 8 weeks long trial did not make the differences between control and experimental groups. However, there is a clear trend of higher GPx activity in the subsidized groups, but without the results for the organic form of selenium being better than inorganic one. Some long-term experiments with the higher content of Se in diets would be done to find out some differences in blood GPx activity.

ACKNOWLEDGEMENTS

The research was financially supported by the Internal Grant Agency of Faculty of AgriSciences (Mendel University in Brno) no. AF-IGA2020-TP012.

REFERENCES

Asadi, F. et al. 2017. Comparison of Different Selenium Sources and Vitamin E in Laying Hen Diet and Their Influence on Egg Selenium and Cholesterol Content, Quality and Oxidative Stability. Iranian Journal of Applied Animal Science, 7(1): 83–89.

Bartholomew, A. et al. 1998. Changes in blood chemistry hematology and histology caused by a selenium/vitamin E deficiency and recovery in chicks. Biological Trace Element Research, 62: 7–16.

Commission regulation (EC) 152/2009. Laying down the methods of sampling and analysis for the official control of feed. Brussels: The commission of the European Communities.

Delezie, E. et al. 2014. Comparing responses to different selenium sources and dosages in laying hens. Poultry Science, 93(12): 3083–3090.

Ferguson, L.R. et al. 2012. Selenium and its´ role in the maintenance of genomic stability. Mutation Research, 733(1–2): 100–110.

Gerlof, B.J. 1992. Effect of selenium supplementation on diary cattle. Journal of Animal Science, 70(12): 3943–3940.

Kim Y.Y, Mahan D.C. 2003. Biological Aspects of Selenium in Farm Animals. Asian-Australasian Journal of Animal Science, 16(3): 435–444.

Kuricova, S.K. et al. 2003. Chicken selenium status when fed a diet supplemention with Se-Yeast. Acta Veterinaria, 72: 339–346.

Lohmann Tierzucht 2020. Management guide for Lohmann Brown–Classic layers. Lohmann Tierzucht. GMBH. Cuxhaven, Germany.

Mahmoud, K., Edens, F.W. 2003. Influence of selenium sources on age-related and mild heat stress-related changes of blood and liver glutathione redox cycle in broilers chickens (*Gallus domesticus*). Comporative Biochemistry and Physiology. Part B: Biochemistry and Molecular Biology, 136(4): 921–934.

Payne, R.L., Southern, L.L. 2005. Comparison of inorganic and organic selenium sources for broilers. Poultry Science, 84(6): 989–902.

Payne, R.L. et al. 2005. Effect of inorganic versus organic selenium on hen production and egg selenium concentration. Poultry Science, 84(2): 232–237.

Rotruck, J.T. et al. 1973. Selenium. Biochemical role as a component of glutathione peroxidase. Science, 179(4073): 588–590.

Song, Z.Y. et al. 2006. Effects of dietary iodine and selenium on the activities of blood lymphocytes in laying hens. Asian–Australasian Journal of Animal Science, 19(5): 713–719.

Thomson, J.N., Scott, M.L. 1970. Impaired lipid and vitamin E absorption related to atrophy to pancreas in selenium-deficient chicks. The Journal of Nutrition, 100(7): 799–809.

The influence of different feed particle size on the performance parameters of laying hens

Jakub Novotny, Andrea Roztocilova, Ondrej Stastnik, Barbora Umlaskova, Eva Mrkvicova, Leos Pavlata
Department of Animal Nutrition and Forage Production
Mendel University in Brno
Zemedelska 1, 613 00 Brno
CZECH REPUBLIC

jakub.novotny@mendelu.cz

Abstract: The influence of different feed particle size in laying hen´s diet on performance parameters were evaluated. Hens were divided into two different groups based on the structure of particles (coarse and fine). Geometric Mean Diameter (GMD) and Geometric Standard deviation (GSD) of particles size were calculated. The coarse group (GMD 1,339.92 µm; GSD 1,3362.19 µm) had a positive effect on eggshell quality ($P < 0.05$) in comparison with the fine group (GMD 572.03 µm; GSD 389.10 µm). There were found no statistically significant differences ($P > 0.05$) in body weight, egg production, laying intensity and feed conversion ratio between different feeding groups. The higher daily feed intake ($P < 0.05$) was noticed in laying hens fed coarse feed mixture. Based on our results seems hens rather consume diet with coarse particles. The coarse feed mixture also had a positive effect on the selected eggshell quality traits.

Key Words: poultry nutrition, Geometric Mean Diameter, Geometric Standard Deviation, eggshell quality, egg quality

INTRODUCTION

The physical structure of the diet is determined by the size and shape of its particles (Amerah et al. 2007). The particle size is determined by dry sieving of representative sample (Baker and Herrman 2002). The sample is sieving usually for 10 minutes on the set of sieves. The amount of particles retained on individual sieves is determined. GMD (Geometric Mean Diameter, also d_{gw}) and GSD (Geometric Standard Deviation, also S_{gw}) is used to describe particle size (Lentle et al. 2006). GMD indicates the trough particle size (in mm or µm) and GSD is the indicator of particle size uniformity. The higher uniformity of particles size means the lower GSD (Amerah et al. 2007). Wolf et al. (2012) described the specific particle size as coarse (> 1.4 mm), medium (0.8–1.4 mm), fine (0.8–0.4 mm) and very fine (< 0.4 mm). The feed particle size can affect the intake of diet. The higher intake was found in laying hens fed coarse feed mixture (Safaa et al. 2009). The same result found Amerah et al. (2007) in broilers chickens. Many studies claim that the structure of the compound feed does not affect the egg quality in any way (Ruhnke et al. 2015, Hafeez et al. 2015, Koçer et al. 2016, Herrera et al. 2017, Ege et al. 2019). The aim of this study is determined the influence of different feed particle size in laying hen´s diet on performance parameters.

MATERIAL AND METHODS

Animals and diets

The total of 20 laying hens of LOHMANN BROWN CLASSIC layer were divided into 2 different experimental groups (coarse group and fine group – 10 hens per feeding group). The hens were placed in an individual balance cages each representing a single experimental unit. The lighting program was set on 16 hours of light and 8 hours of dark. The temperature was maintained at 20 °C. The hens were fed by two different diets (coarse and fine). The daily feed intake and the egg production was recorded. The body weight was measured once a month. The laying hens were fed *ad libitum*. The trial lasted from 17 to 36 week of age. In the experiment the commercial feed mixture was used. The coarse group was fed by the mixture with no change. For the fine group, the feed mixture was ground with the hammer

mill using the 3 mm sieve. This caused different particle size of diets. Diets (coarse and fine) contained corn, wheat, calcium carbonite, soybean extracted meal (toasted), barley, dark distilled offal, peeled sunflower extracted meal, rapeseed extracted meal, peas, wheat bran, corn extract, vinasse, animal fat, vegetable fat and oil, sodium chloride and calcium dihydrogen phosphate. Table 1 shows the chemical compositions of used diets.

Table 1 Chemical composition of used diets in 88% dry matter

	COARSE	FINE
Crude protein (%)	14.63	14.92
Crude fibre (%)	3.23	3.08
Ether extract (%)	3.18	3.15
Ash (%)	12.58	13.11

The structure of diets was evaluated by dry sieving on a separator (Retch AS 200 Control) using a representative sample of 100 g for 10 minutes. The amplitude was set on 1.8 mm/g. The samples were passed through the set of sieves with different mesh size (3 mm–0.3 mm). The amount of particles on each sieve was determined and the GSD and GMD were calculated.

Egg parameters

Eggs quality analysis was performed weekly. The egg weight, eggshell weight, eggshell thickness, eggshell strength, eggshell weight ratio, Haugh units, weight of yolk were monitored. The weight of egg, yolk and shell were determined using a laboratory scale. The strength of the eggshell was determined by using Egg Force Reader (ORKA Food Technology**,** USA). The thickness of eggshell was monitored on 3 different places – in the centre of shell and on the blunt and sharp of the peak shell. The arithmetic mean was calculated. The laying intensity (%) was calculated as $\frac{total\ number\ of\ eggs}{number\ of\ feeding\ days} * 100$. The feed conversion ratio (FCR) was calculated as $\frac{feed\ consumption}{egg\ mass}$.

Statistical analysis

Data has been processed by Microsoft Excel (USA) and StatSoft Statistica 12 (USA). It was used one-way analysis of variance (ANOVA). For evaluated differences between groups was used the Sheffé´s test. $P < 0.05$ was a significance level determinate statistically significant difference.

RESULTS AND DISCUSSION

Diets analysis

Coarse and fine feed mixture were determined by dry sieving and the representation of particles is shown in Figure 1. The coarse mixture contains most of particles bigger than 1.5 mm (60%), 10% of particles from 1 mm to 1.5 mm and 30% smaller than 1 mm. The fine mixture has about 20%

Figure 1 Particle size distribution

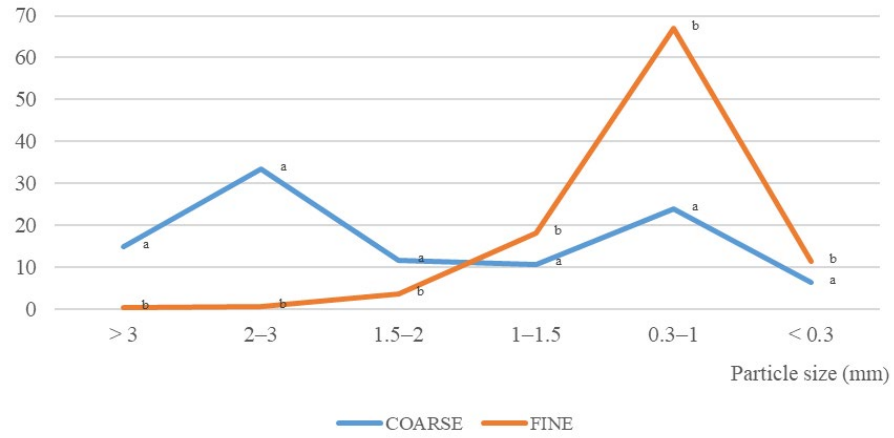

Legend: ^{a,b} means differ significantly at $P < 0.05$

of particles bigger than 1 mm. The rest of particles (about 80%) was smaller than 1 mm. On each sieve there were found the statistically significant differences ($P < 0.05$) between amount of particles for coarse and fine diet. According the weight fraction on individual sieves the GMD and GSD were calculated (see Figure 2).

Figure 2 GMD and GSD of diets

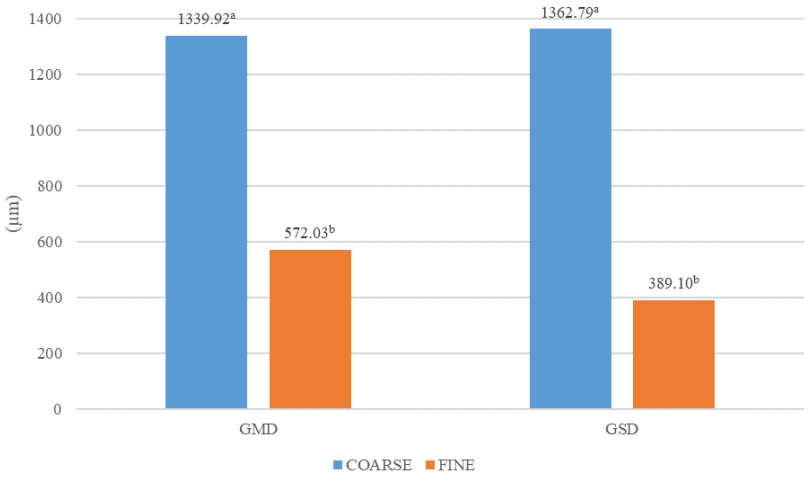

Legend: [a,b] means differ significantly at P < 0.05; GMD – Geometric Mean Diameter; GSD – Geometric Standard Deviation

There were found statistically significant differences between GMD for coarse and fine diet ($P < 0.05$). Ege et al. (2019) carried out a similar experiment. In their trial the GDM values were 1096 vs. 707 µm for coarse and fine, respectively. The GSD as a homogeneity indicator of diet also showed the statistically significant differences ($P < 0.05$). The value of fine mixture was lower than value of coarse mixture (389.10 vs. 1362.79 µm, respectively). This means the fine feed mixture is more homogenous than coarse.

Feed consumption, egg production and qualitative analyses and live body weight

Table 2 shows values for feed consumption and egg production. There were no statistically significant differences in numbers of eggs and laying intensity between groups ($P > 0.05$). The average daily feed intake corresponds to the instructions for LOHMANN BROWN CLASSIC layer which is 110–120 g (LOHMANN TIERZUCHT 2019). There were found the statistically significant differences between groups ($P < 0.05$). The same result found out Safaa et al. (2009) in their trial. The mean weight of one egg is 54.62 g in coarse group and 55.75 g in fine group ($P > 0.05$).

Table 2 Feed consumption, egg production

	n	Feed consumption		Number of eggs per trial	Laying intensity	Feed conversion ratio
		(kg/bird/trial)	(g/bird/day)		(%)	
		Mean ± SE		Mean ± SE	Mean ± SE	Mean ± SE
Coarse	10	14.625 ± 563.06	121.88 ± 0.81[a]	111.2 ± 0.84	91.75 ± 0.87	2.45 ± 0.12
Fine	10	13.3156 ± 643.80	110.95 ± 0.69[b]	112.7 ± 1.51	93.08 ± 1.38	2.16 ± 0.13

Legend: [a,b] means differ significantly at P < 0.05; n – number of cases; SE – standard error

In qualitative analyses of eggs there were found statistically significant differences ($P < 0.05$) in its values (see Table 3). In the similar trial (Safaa et al. 2009) were not found the statistically significant differences on egg quality of laying hens from 20 to 48 weeks of age. In that trial were used diets based on corn (GMD from 935 through 1,126 to 1,411 µm) and wheat (GMD from 1,078 through 1,192 to 1,339 µm). Other studies claim that the structure of the feed mixtures does not affect the egg parameters in any way (Ruhnke et al. 2015, Hafeez et al. 2015, Koçer et al. 2016, Herrera et al. 2017).

Table 3 Qualitative analyses of eggs

	COARSE	FINE
n	180	180
	Mean ± SE	Mean ± SE
Eggshell weight (g)	5.86 ± 0.06	5.83 ± 0.06
Eggshell strength (N)	40.16 ± 0.23[a]	39.29 ± 0.36[b]
Eggshell thickness (µm)	406.69 ± 2.19[a]	395.05± 2.80[b]
Eggshell weight ratio (%)	10.47 ± 0.08[a]	10.25 ± 0.08[b]
Haugh units	98.81 ± 0.33	97.66 ± 0.58
Yolk weight (g)	13.48 ± 0.12	13.76 ± 0.12

Legend: [a,b] means differ significantly at P < 0.05; n – number of cases; SE – standard error

The differences of eggshell parameters can be caused by different level of feed intake. The Coarse group had a higher feed intake, therefore higher intake of minerals necessary to create eggshell and it could be the reason of the higher eggshell strength and eggshell thickness.

Figure 3 Live weight of hens during the trial

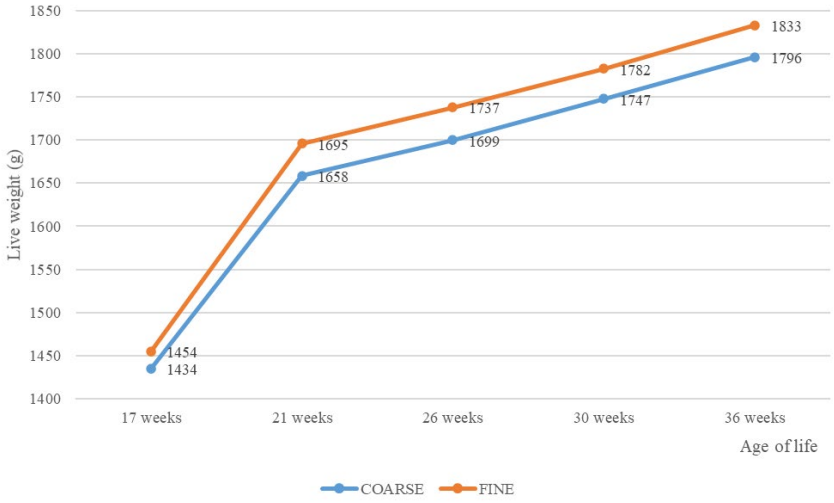

Legend: There was not found statistically significant differences (P > 0.05)

The body weight (Figure 3) of hens was lower in the coarse group throughout the experiment, but there were not found the statistically significant differences between groups (P > 0.05). The monthly weight gains were similar in both groups (Figure 3). Both groups had lower mean body weight comparing with the instructions for LOHMANN BROWN CLASSIC hens. The average body weight of the hen aged 34 weeks should be about 1,931 g (LOHMANN TIERZUCHT 2019).

CONCLUSION

In the trial feed consumption, body weight and egg quality parameters were evaluated. The diets with different particle size (coarse and fine) had no influence on body weight and egg production. The differences (P < 0.05) were found in daily feed intake and eggshell strength, eggshell thickness, and eggshell weight ratio. The higher feed intake was found in the coarse group as well as the eggshell parameters. It seems hen´s rather consume diet with coarse particles. Many studies claim that the structure of the compound feed does not affect the egg quality in any way which is contrary to our results (Ruhnke et al. 2015, Hafeez et al. 2015, Koçer et al. 2016, Herrera et al. 2017, Ege et al. 2019). But more studies would be needed to confirm the results.

ACKNOWLEDGEMENTS

The research was financially supported by the Internal Grant Agency of Faculty of AgriSciences (Mendel University in Brno) no. AF-IGA2020-IP064.

REFERENCES

Amerah, A. et al. 2007. Feed particle size: Implications on the digestion and performance of poultry. World´s Poultry Science Journal, 63(3): 439–455.

Baker, S., Herrman, T. 2002. Particle size. MF–2051 Feed Manufakturing [Online]. Available at: https://bookstore.ksre.ksu.edu/pubs/MF2051.pdf. [2020-08-20].

Ege, G. et al. 2019. Influence of feed particle size and feed form on productive performance, egg quality, gastrointestinal tract traits, digestive enzymes, intestinal morphology, and nutrient digestibility of laying hens reared in enriched cages. Poultry Science, 98(9): 3787–3801.

Hafeez, A. et al. 2015. Implication of milling methods, thermal treatment, and particle size of feed in layers on mineral digestibility and retention of minerals in egg contents. Poultry Science, 94(2): 240–248.

Herrera, J. et al. 2017. Influence of particle size of the main cereal of the diet on egg production, gastrointestinal tract traits, and body measurement of brown laying hens1. Poultry Science, 96(2): 440–448.

Koçer, B. et al. 2016. Effects of feed particle size and physical form of the diet on performance, egg quality and size of the digestive organs in laying hens. European Poultry Science, 80.

Lentle, R.G. et al. 2006. Influence of feed particle size on the efficiency of broiler chickens fed wheat-based diets. The Journal of Poultry Science, 43(2): 135–142.

Lohmann Tierzucht 2019. Management guide for Lohmann Brown–Classic layers. Lohmann Tierzucht. GMBH. Cuxhaven, Germany.

Ruhnke, I. et al. 2015. The effect of particle size, milling method, and thermal treatment of feed on performance, apparent ileal digestibility, and pH of the digesta in laying hens. Poultry Science, 94(4): 692–699.

Safaa, H.M. 2009. Effect of main cereal of the diet and particle size of the cereal on productive performance and egg quality of brown egg-laying hens in early phase of production. Poultry Science, 88(3): 608–614.

Wolf, P. et al. 2012. Einfluss der Partikelgröße im Futter auf die Nährstoffverdaulichkeit und Leistung beim Schwein. Übersichten zur Tierernährung, 40: 21–44.

Evaluation of pregnancy rate and length of pregnancy after artificial insemination in Zwartbles sheep

Vojtech Pesan, Martin Hosek, Radek Filipcik
Department of Animal Breeding
Mendel University in Brno
Zemedelska 1, 613 00 Brno
CZECH REPUBLIC

vojtech.pesan@mendelu.cz

Abstract: The oestrus cycle synchronization and artificial insemination are some of the most frequently used biotechnical methods of reproduction. They are used mainly to achieve easier breeding and shortening of the lambing period. An exact determination of the lambing period (according to the length of the pregnancy) is essential for the breeding process optimization, namely it allows a precise timing of the lambing period. The experiment monitors forty eight Zwartbles ewes, whose oestrus cycles were first synchronized with the use of hormonal intravaginal sponges Ovigest. The subsequent intracervical insemination was done using fresh, diluted and chilled semen from rams of the Zbyšek and Zachari lineages extracted into an artificial vagina. The pregnancy rates after insemination and after the subsequent breeding of the barren ewes in a harem were determined according to the pregnancy detection and the subsequent lambing times. The overall pregnancy length in the artificially inseminated animals was determined through marking the exact date and time of insemination and the lambing period of each animal. The pregnancy rate after insemination was 63.6% for ram Zbyšek and 23.1% for ram Zachari. The overall pregnancy rate after insemination was 41.7%, and after the subsequent natural breeding of the barren ewes in harems the overall pregnancy rate was 93.8%. The pregnancy periods generally ranged between 141 and 147 days and the lambing itself took place between the 144th and 146th day in 70% of the cases.

Key Words: insemination, pregnancy rate, reproduction, sheep, synchronization of Oestrus, Zwartbles

INTRODUCTION

Similary to other ruminants, sheep breeding is usually done through natural breeding or artificial insemination (Louda and Hegedüšová 2009). Both the natural breeding with prior oestrus cycle synchronization and artificial insemination (with or without prior oestrus cycle synchronization) are amongst the most often used biotechnical methods used in sheep breeding. These methods can assure decrease of the work load and time restraints of the breeding process, they can assure a better record keeping and health monitoring of the animals, as well as shortening of the lambing period, which subsequently leads to a better balance in the flock (Čunát et al. 2013, Sándor et al. 2011).

The methods used for oestrus cycle synchronization can be divided into the artificial (additives in the feed, intravaginal sponges, subcutaneous implants), and natural ones (light regimen control, flushing, the ram effect); (Čunát et al. 2013, Horák et al. 2012, Louda and Ježková 2002). For better efficiency, these individual methods can be combined (for example the ram effect + flushing, the ram effect + intravaginal sponges, flushing + intravaginal sponges); (Čunát et al. 2013, Říha 1999).

The artificial insemination is performed using fresh, chilled, diluted semen. Previously extracted doses stored in liquid nitrogen for a longer period of time are used only rarely, since this method of conservation leads to a rapid decrease of fertility of the insemination dose after its defrosting (Louda et al. 2001, Ntemka et al. 2018). In the Czech Republic, frozen insemination doses are currently created only for certain gene reserve programs for the Valachian sheep and Šumavská sheep breeds. Rarely, they are imported from abroad on demand of the breeder or created from top-level rams of domestic origin (Čunát et al. 2013; Louda and Hegedüšová 2009).

Insemination methods are further divided according to the place of the semen insertion - generally, the deeper into the sexual apparatus of the ewe it is inserted, the higher probability of pregnancy, but also the higher price and difficulty of the method. These methods are thus divided into intravaginal, intracervical, and intrauterine ones (Čunát et al. 2013, Sándor et al. 2011).

The insemination doses are created from sperm extracted at the day of insemination. Semen is usually extracted into an artificial vagina after a jump on an ewe in heat. To eliminate the time restraint and to eliminate the need of an ewe being present, an electroejaculator can be used. The extracted semen is then macroscopically and microscopically evaluated. For the dilution, commercial thinners, as well as milk-based thinners, can be used (Čunát et al. 2013). The milk used for dilution was pasteurized (min. 95 °C for 10 minutes) to inactivate lactein, an antibacterial agent that would act as toxic towards the semen in its active state (Salamon and Maxwell 2000).

Subsequently, it is crucial to know the exact data concerning the pregnancy length. This data allows for an estimation of lambing times, and thanks to the estimated number of expected lambs, the care for the new-borns can be optimized and complications, which usually arise due to the bad lambing times management, can be eliminated.

The pregnancy lengths vary. Vaněk and Štolc (2002), Kuchtík (2015) state that the pregnancy can last between 143 and 157 days, while the average pregnancy length is somewhere between 147 and 150 days according to them. Gajdošík and Polách (1984) state that the upper limit is one day shorter (156 days). The average of 147 days of pregnancy with a deviation within a few days is stated in the works of Tzanidakis et al. (2014) and Gootwine (2016).

The correct choice and application of biotechnical methods is crucial for optimization of reproduction outcomes. The aim of this work is to evaluate the pregnancy lengths of individual sheep.

MATERIAL AND METHODS

This experiment focused on 48 Zwartbles breed sheep from private farm belonging to dr. HOSEK in the MOHELNO, CZECH REPUBLIC. All of the sheep were of age ranging between 2 and 8 years, with an average body condition score (BCS) of 3. The experiment itself took place between September 2019 and April 2020. The synchronization of the oestrus cycle using intravaginal sponges, insemination doses extraction and dilution, the insemination itself and the pregnancy scanning all took place in September 2019. In April 2020, the experiment ended with the lambing.

The rams, as well as the ewes, were fed grass silage and hay ad libitum. Additionally, 400 g of grains and 200 g of fodder potatoes per animal were fed to the animals one month before and one and a half month after the insemination, serving as a flushing.

For the oestrus cycle synchronization performed in 2019, only intravaginal sponges Ovigest (60 mg medroxyprogesterone acetate/sponge, Laboratorios Hipra, Spain) were used. These hormonal progesterone preparations or synthetic progestogens obstruct the oestrus cycle. Using a specialized applicator, these sponges were inserted inside the ewes' vaginas for fourteen days. After removal of the sponges, each ewe was injected with a lyophilized serum gonadotropin PMSG (0.2 ml/ewe = Sergon 200 IU, Bioveta Ivanovice, CZ), which works similarly to the hormone-stimulating follicles (FSH) and the luteinizing hormone (LH). 56–60 hours after this injection, the ewes were inseminated.

Two rams, one from the Zbyšek (ZBS 0001 – 7 years) and one from the Zachari (ZAC0001 – 8 months) lineages were used for the ID (insemination dose) creation. An ewe was fixed to a fixing pad and the semen was extracted into an artificial vagina (Minitübe, Germany) in one jump (two jumps in case of a lower amount of extracted semen) on the day of insemination.

The semen was then macroscopically and microscopically evaluated and the degree of dilution was determined due to the observed sperm concentration and motility. For the dilution, pasteurized cow milk with 3.5% fat content was used in a 1:1–2 (milk:semen) ratio. The diluted semen was then placed in small labelled plastic containers and cooled down to 3 °C in a cooling box.

The insemination itself was performed 56 to 60 hours after removal of the intravaginal sponges and PMSG application. The ewes were divided into two groups and the insemination took place on October 11, 2019, from 13:00 to 14:30 and on October 13, 2019, from 12:20 to 14:40.

Each ewe was fixed to a fixing pad by a collar and, for better access, the tail was fixed as well. Each ewe was then evaluated due to its oestrus symptoms (the colour and amount of mucus, blood perfusion, stiffness and openness of cervix, overall activity, etc.).

The insemination itself was performed with a plastic tube fixed to a plastic syringe. The diluted semen was drawn into the syringe in a 0,4 ml amount. During the time of insemination, the ID was not

taken out from the cooling box to assure its viability, to reduce temperature changes and to eliminate possible contamination.

Before the insemination, the outer genitalia were cleaned and disinfected. The vagina and cervix were inspected using a 12cm long sheep vaginal speculum and a LED torch. Excess mucus was removed where needed. The ID was then inserted through the speculum 1 to 2 cm deep into the cervix.

Several days after the insemination, the ewes were put into groups (harems) with the rams whose semen was used for the insemination. This was done to assure an increase in the pregnancy rate in the ewes in which the artificial insemination was not successful.

The pregnancy scanning took place on the 43rd and 83rd day after insemination using OVI-SCAN (BCF technology, Scotland) and, along with the data on pregnant/barren ewes, the number of foetuses in the uterus was noted.

Due to marking the exact day and time of insemination and lambing in individual ewes, the overall pregnancy durations were subsequently calculated.

STATISTICA 12.0 software and MS Excel 2016 were used for statistical assessment of the data.

RESULTS AND DISCUSSION

Figure 1 shows the pregnancy rates after insemination/breeding with the individual ram lineages. The pregnancy rate after insemination was 63.6% for ram Zbyšek (ZBS 0001) – 14 pregnant sheep out of the 22 inseminated – which was an above-average outcome compared to the 60% presented by Kuchtík et al. (2007) as an average for the Czech Republic. On the other hand, with ram Zachari (ZAC 0001) the pregnancy rate after artificial insemination was only 23.1% – 6 pregnant ewes out of the 26 inseminated), which is a very below-average outcome caused by the worsened quality of the IDs. The overall pregnancy rate after artificial insemination was thus 41.7%, which is a below-average outcome.

Figure 1 Comparison of the pregnancy rates after insemination and the overall pregnancy rates in individual rams

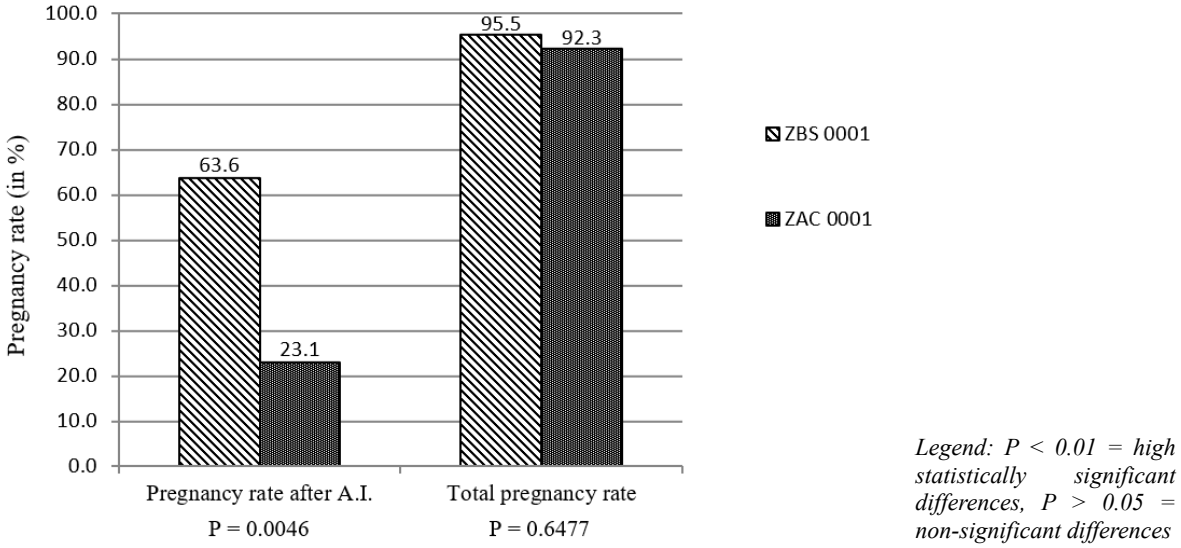

Legend: P < 0.01 = high statistically significant differences, P > 0.05 = non-significant differences

After the insemination itself and after letting the barren ewes naturally breed in the next oestrus cycle, the ewes were put into harems with the rams whose semen was used for the insemination, to assure an increase in the pregnancy rate. The subsequent overall pregnancy rate was 95.5% with ram Zbyšek and 92.3% with ram Zachari. The overall pregnancy rate was thus 93.8% (45 pregnant ewes out of 48 used in the experiment). This can be considered a relatively good outcome, since Louda and Hegedušová (2009) state the average pregnancy rate in natural breeding to be 95%.

Vallejo et al. (2019) states in his study that the pregnancy rates at sheep after oestrus synchronization done with hormonal preparations and after subsequent intracervical insemination were

between 45% and 65%. He also states that after the follow-up ten days of natural breeding of the barren sheep in a harem the overall pregnancy rate reached more than 80%.

Within the individual rams, a highly statistically provable difference was noted in the individual pregnancy rates. On the contrary, within the data on overall pregnancy rates, there was no notable statistical deviation.

Figure 2 Length of pregnancy in sheep lambing in 2020

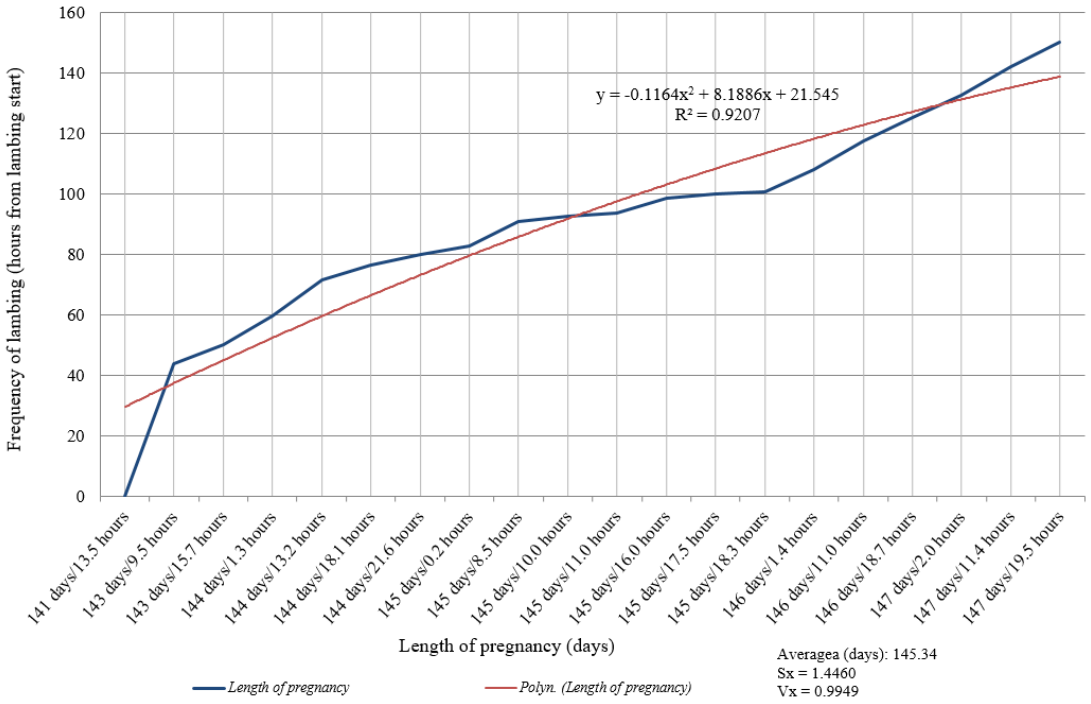

Figure 2 show the lengths of pregnancy in individual sheep inseminated on October 11, 2019 between 13:00 and 14:30 and October 13, 2019 between 12:20 and 14:40. During these phases a total of 48 ewes were inseminated. After the insemination, the pregnancy rate was 41.7%, that is 20 ewes (in which an exact pregnancy duration could be determined after lambing, which is shown in Figure 2), which can be considered a below-average outcome compared to the average pregnancy rates after artificial insemination (Kuchtík et al. 2007, Louda and Hegedüšová 2009). This average rate after insemination is usually 60% (Kuchtík et al. 2007).

The first lambing took place 141 days and 13.5 hours after the insemination. The last lambing took place 147 days and 19.5 hours after the insemination. The lambing thus took place within a 150 hour span (6 days and 6 hours). In Figure 2 and Table 1 we can observe that the most frequent lambing times came in the middle of day 144 and lasted until the middle of day 146 of pregnancy.

Table 1 Frequency of lambing according to pregnancy lenght

	Days range after insemination						
	141.0–141.9	142.0–142.9	143.0–143.9	144.0–144.9	145.0–145.9	146.0–146.9	147.0–147.9
Number of lambing sheep	1	-	2	4	7	3	3
(%)	5	-	10	20	35	15	15

The pregnancy length in ewes that were lambing in 2019/2020 (as seen in Figure 2 and Table 1) varied between 141 and 147 days. However, very little ewes go into lambing during the two threshold days and these cases are considered an exception. In comparison with the average pregnancy lengths in sheep mentioned in the introduction (143–157 days), the average pregnancy length observed in this research was approximately 145 days, which is two days less than stated by e.g. Ingoldby and Jackson (2016).

The pregnancy length can be influenced by a number of factors, such as the breed, the feed composition, microclimatic and macroclimatic conditions, sex or the number of foetuses. For this reason, to gain more exact data, it is necessary to replicate this research and carry it out again on a larger number of animals and, subsequently, to evaluate the influence of these factors on the pregnancy length itself.

CONCLUSION

Within this research, the pregnancy length in Zwartbles breed sheep was determined to last between 141 and 147 days, while majority of the animals went into lambing between days 144 and 146.

These numbers are lower than the average pregnancy lenghts usually stated for sheep in general, without taking the breed into consideration.

The pregnancy rate after insemination was 63.6% for ram Zbyšek and 23.1% for ram Zachari. The total pregnancy rate after insemination was 41.7% and the overall pregnancy rate after insemination and natural breeding in a harem was 93.8%.

The results of this research will be used for its replication and broadening, mainly for an even more exact determination of the lambing times and better time management for the lambing times preparations.

REFERENCES

Čunát, L. et al. 2013. Využití inseminace ovcí v chovatelské praxi. Certified methodology. Praha: Česká zemědělská univerzita v Praze.

Gajdošík, M., Polách, A. 1984. Chov oviec. 1st ed., Bratislava: Príroda.

Gootwine, W. 2016. Husbandry of Dairy Sciences: Sheep: Reproductive Management. Encyclopedia of Dairy Sciences [Online], 1(1): 887–892. Available at:

https://www.researchgate.net/publication/310573090_Sheep_Reproductive_Management. [2020-08-08].

Horák, F. et al. 2012. Chováme ovce. 1st ed., Praha: Brázda.

Ingoldby, L., Jackson, P. 2001. Induction od parturition in sheep. In Practice, 23(4): 228–231.

Kuchtík, J. et al. 2007. Chov ovcí. 1st ed., Brno: Mendelova zemědělská a lesnická univerzita v Brně.

Kuchtík, J. 2015. Březost a porod ovcí. Chodzvirat.cz [Online]. Available at:

http://www.chovzvirat.cz/clanek/728-brezost-a-porod-ovci/. [2020-08-20].

Louda, F., Hegedüšová, Z. 2009. Inseminace ovcí – intenzifikační faktor šlechtitelské práce. Certified methodology. Rapotín: Agrovýzkum Rapotín.

Louda, F., Ježková, A. 2002. Biotechnické metody v reprodukci ovcí a koz. Náš chov [Online], Available at: https://naschov.cz/biotechnicke-metody-v-reprodukci-ovci-a-koz/. [2020-08-17].

Louda, F. et al. 2001. Inseminace hospodářských zvířat. 1st ed., Praha: Česká zemědělská univerzita v Praze.

Ntemka, A. et al. 2018. Current status and advances in ram semen cryopreservation. Journal of the Hellenic Veterinary Medical Society, 69(2): 911–924.

Říha, J. 1999. Biotechnologie v chovu a šlechtění hospodářských zvířat. 1st ed., Rapotín: Asociace chovatelů masných plemen.

Sándor, K. et al. 2011. Artificial Insemination of Sheep - Possibilities, Realities and Technique at the Farm Level In Artificial Insemination in Farm Animals, Iran: IntechOpen, pp. 27–50.

Salamon. S., Maxwell, W.M.C. 2000. Storage of ram semen. Animal Reproduction Science, 62(1–3): 77–111.

Tzanidakis, N. et al. 2014. Dairy sheep breeding. LowInputBreeds technical note [Online], 1(1): 1–6. Available at: http://www.lowinputbreeds.org/publications/lib-technical-notes.html. [2020-08-20].

Vallejo, D.A. et al. 2019. Pregnancy rates in hair sheep after Ovsynch synchronization and a combined intracervical fixed-time artificial insemination and 10-day mating period. Veterinary World, 12(11): 1779–1783.

Vaněk, D., Štolc, L. 2002. Chov skotu a ovcí: (přednášky pro Bc). 1st ed., Praha: Česká zemědělská univerzita, Agronomická fakulta.

The influence of parent stock age on embryonic development of broiler chicken at oviposition

Martina Pesanova Tesarova, Martina Lichovnikova
Department of Animal Breeding
Mendel University in Brno
Zemedelska 1, 613 00 Brno
CZECH REPUBLIC

martina.tesarova@mendelu.cz

Abstract: This study focuses on the degree of embryonic development determination after oviposition, based on the age of the parent stock of broiler chicken. In this experiment parent stock of the ROSS 308 hybrid from 23 to week age of was used. The hatching eggs were collected to determinated degree of embryonic development every 3 or 4 weeks from this age, until the parent stock reached the age of 45 weeks. In each monitored week of age of the parent flock, 60 hatching eggs were collected. Total of 480 hatching eggs were used in this experiment. After determining the degree of embryonic development over a period of time, the results show a statistically significant ($P<0.05$) increase at the stage of embryonic development with the older age of the parent flock.

Key Words: embryonic development, embryonic degree, broiler

INTRODUCTION

Depending on the ever-increasing market interest and its varying intervals of day-old broiler chick and the large capacity of commercial hatcheries for broiler chickens production in hatchery practice becomes a necessity to store hatching eggs (Van de Ven 2004). The process of long-term storage is an integral part of hatching practice, but it has a number of negative effects on the embryonic development of chickens and their subsequent hatchability and viability (Fasenko et al. 2001, Lapão et al. 1999, Tona et al. 2003, Whitehead et al. 1985). This negative effect can be caused by the processes that take place in the egg during long-term storage, such as and depletion of cellular reserves (Arora and Kosin 1968, Walsh et al. 1995), increasing the pH of the white and yolk (Lapão et al. 1999), mechanical tensioning of the yolk membrane and its increased fragility (Fromm 1966). One way to eliminate these negative effects of storage is preheating the hatching eggs before and during the long-term storage process. This method of eliminating the negative effect of long-term storage is based on shifting the stage of embryonic development of the embryo by raising the storage temperature above physiological zero. This is therefore the temperature at which the embryo begins to develop again. After shifting the stage of embryonic development, the embryo is more resistant to the negative effects of storage (Fasenko et al. 2001). For the application of the hatching egg preheating method, the degree of embryonic development after laying of the hatching egg is crucial. The stage of embryonic development is necessary information because if the XIV developmental stage according to the methodology (Eyal-Giladi and Kochav 1976) or degree 2 according to Hamburger and Hamilton (1951) is exceeded, preheating already has a negative effect on hatchability (Tesařová 2018). Most eggs after laying are in stage X (Eyal-Giladi and Kochav 1976, Sellier et al. 2006), but in some cases the eggs may be in stage 11 (Sellier et al. 2006, Tesařová 2018). The embryonic stage of development after egg laying can be influenced by a number of factors, one of which may be the age of the parent stock, the length of egg formation and persistence of laying which increases with increasing age of the parent stock (Fasenko et al. 1992).

MATERIAL AND METHODS

Hatching eggs at the age of the parent flock of 23 weeks were used in this experiment. Hatching eggs were extracted to determine the degree of embryonic development every three or four weeks from this age until the parent stock reached the age of 45 weeks. The hatching eggs were collected from the breeding farm in Velké Albrechtice.

For each part of the experiment, 60 hatching eggs were collected. The hatching eggs were transported to the laboratory at constant temperature of 15 °C. Blastoderm extraction was performed within 72 hours after laying at constant temperature of 7 °C. Altogether, 230 hatching eggs were used in this experiment.

Blastoderm insulation

Blastoderm from hatching eggs were isolated according by methodology Gupta and Bakst (1993) and subsequently determined according to the methodology for determining the degree of embryonic development Eyal-Giladi and Kochav (1976) or Hamburger and Hamilton (1951).

Embryos were isolated at stages X, XI and XII in this experiment. Stage X is defined as state when observation both from the upper and lower surfaces reveals that the formation of the area pellucida has been completed and there is a clearly demarcated border between it and the area opaca. Stage XI is indicated as observation of the upper surface of the blastoderm reveals a smooth thin layer through which deeper concentrations of cells may be seen. From the ventral side stage XI is defined by the formation Koller's sickle (Eyal-Giladi and Kochav 1976). The first step in this experiment was egg broken, and the egg yolk was separated from the egg white. Then, the blastoderm was found and the excess white in its vicinity on the ventral side was removed with cellulose wadding. A ring cut from a filter paper was placed around the dried blastoderm. The ring was then cut out and turned so that the blastoderm was in the middle of the aperture. The blastoderm prepared in such way was then placed into a Petri dish with PBS (Phosphate-buffered saline).

Cleaning and Determination of the degree of Embryo

The blastoderm was cleaned in the PBS under a microscope using a hair loop attached on a small stick. The excess yolk was slowly pushed away with the hair loop until the blastoderm was uncovered. After full cleaning, the blastoderm was released from the paper ring using a plastic pipette with more PBS. Picture of the embryo was taken with a Dino Capture camera and, subsequently, the degree of development was determined.

However, during each of the cycles, not all 60 samples were successfully isolated and evaluated. Altogether, 230 blastoderms were isolated and evaluated in this experiment. Because some of the eggs were unfertilized and due to the difficulty of blastoderm isolating it was impossible to achieve 100% success rate.

Statistical Methods

The observed characteristics were expressed as a mean and the significance of the difference between the means was tested by one-way analysis of variance and the Tukey-HSD test was used for subsequent testing.

RESULTS

The results of the determination of stages of embryonic development are shown in Table 1. The stage was very similar in all weeks of age. Only at age 45 weeks the embryo development was significantly higher than at weeks 26, 30 and 36 ($P<0.05$). Among other weeks there was no observed statistically significant differences. Almost all the fertile eggs were thus laid at the X stage.

DISCUSSION

Sellier et al. (2006) compared the embryonic development degree in chicken, duck, turkey and quail, every six hours within the first 72 hours after laying in a temperature between 15 °C and 18 °C. Their study showed that the hatching eggs are in the X degree immediately after laying, but in 12.5% of the tested hatching eggs that were stored for 72 hours, the degree was boosted to XI degree. This shows that it is fundamental to determine the embryonic development degree immediately after oviposition.

Similar data was concluded by Tesařová (2018), who determined the embryonic development degree in a broiler chicken ROSS 308 of the parent stock age of 30, 45 and 58 weeks. Most of the hatching eggs were in the X degree, but in all three groups eggs in the XI degree were observed.

These data are consistent with the results of Tesařová and Lichovníková (2019), which report a statistically significant influence (P<0.05) effect of the age of the parent stock on the degree of embryonic development after oviposition in 44th (10.8), 50th (10.1), 52nd (10.4), 59th (10.2), 61th(10.1) weeks of age parental stock.

Table 1 Determination of the stage of embryonic development based on the parent stock age

Age of the parent stock (weeks)	Number of determined embryos	Stage of embryonic development	SE	v_x	Standard deviation
23	23	10.13^{ab}	0.095	0.0452	0.46
26	26	10.00^{a}	0.000	0.0000	0.00
30	26	9.96^{a}	0.039	0.0197	0.20
33	31	10.06^{ab}	0.045	0.0248	0.25
36	29	10.00^{a}	0.000	0.0000	0.00
39	32	10.13^{ab}	0.059	0.0332	0.34
42	39	10.26^{ab}	0.088	0.0535	0.55
45	24	10.33^{b}	0.115	0.0546	0.56

Legend: Different upper indexes (a, b) state the statistically provable variances (P<0.05), v_x –coefficient of variation, SE – standard error

Lukaszewicz et al. (2017) state that the development of the goose embryo at the time of laying is identical to that of the chicken. For an experiment was used hatching eggs from hybrid combination White Koluda. The determination of the degree of embryos was made according by methodology Eyal-Giladi's and Kochav's (1976). From 135 isolated blastoderms it was determined that 35.6% was in degree X, 24.4% was in degree XI and 8.2% was in degree IX.

Lukaszewicz et al. (2019) supposed that age of parental stock has an influence on embryonic degree after laid. It has been found that geese have a much greater extent of embryonic development than chickens. The greater extent of embryonic development in geese was found from the degree VI according by methodology Eyal-Giladi and Kochav (1976) to the 2. degree according by methodology Hamburger and Hamilton (1951). Confirmed at the beginning of laying in the younger parent stock the embryos were in the stage VI–XI. Eggs at the end of laying was observed more progress embryonic degree XI–XIII. Some were even observed the beginning of formation primitive streak.

CONCLUSION

The final data show that the age of the parental stock affects the embryonic development degrees after oviposition. The degrees get higher with the rising age of the parent stock of a meat type hybrid.

ACKNOWLEDGEMENTS

The research was financially supported by the grant no. AF-IGA2020-IP083.

REFERENCES

Arora, K.L., Kosin, I.L. 1968. The response of the early chicken embryo to pre-incubation temperature as evidenced from its gross morphology and mitotic pattern. Physiological Zoology, 41(1): 104–112.

Eyal-Giladi, H., Kochav, S. 1976. From cleavage to primitive streak formation: A complementary normal table and a new look at the first stages of the development of the chick. Developmental Biology, 49(2): 321–337.

Fasenko, G.M. et al. 1992. Relationship of hen age and egg sequence position with fertility, hatchability, viability, and preincubation embryonic development in broiler breeders. Poultry Science, 71(8): 1374–1383.

Fasenko, G.M. et al. 2001. Prestorage incubation of long-term stored broiler breeder eggs: 1. Effects on hatchability. Poultry Science, 80(10): 1406–1411.

Fromm, D. 1966. The influence of ambient pH on moisture content and yolk index of the hen's yolk. Poultry Science, 45(2): 374–379.

Gupta, S.K., Bakst, M.R. 1993. Turkey embryo staging from cleavage through hypoblast formation. Journal of Morphology, 217(3): 313–325.

Hamburger, V., Hamilton, H.L. 1951. A series of normal stages in the development of the chick embryo. Journal of Morphology, 88(1): 49–92.

Lapão, C. et al. 1999. Effects of broiler breeder age and length of egg storage on albumen characteristics and hatchability. Poultry Science, 78(5): 640–645.

Lukaszewicz, E. et al. 2017. Goose embryonic development from oviposition through 16 hours of incubation. Poultry Science, 96(6): 1934–1938.

Lukaszewicz, E. et al. 2019. Stage of goose embryo development at oviposition depending on genotype, flock age, and period of laying. Poultry Science, 98(10): 5152–5156.

Sellier, N. et al. 2006. Comparative staging of embryo development in chicken, turkey, duck, goose, guinea fowl, and japanese quail assessed from five hours after fertilization through seventy-two hours of Incubation. The Journal of Applied Poultry Research, 15(2): 219–228.

Tesařová, M. 2018. Vliv preinkubace vajec během dlouhodobého skladování na líhnivost kuřat masného typu. Diploma thesis (in Czech), Mendel University in Brno.

Tesařová, M., Lichovníková, M. 2019. The effect of parent stock age on embryo development at oviposition. In Proceedings of 26th International PhD Students Conference MendelNet 2019 [Online]. Brno, Czech Republic, 6–7 November, Brno: Mendel University in Brno, Faculty of AgriSciences, pp. 196–199. Available at: https://mendelnet.cz/pdfs/mnt/2019/01/34.pdf. [2020-08-20].

Tona, K. et al. 2003. Effects of egg storage time on spread of hatch, chick quality, and chick juvenile growth. Poultry Science, 82(5): 736–741.

Van de Ven, L. 2004. Storage of hatching eggs in the production process. International Hatchery Practice, 18(8): 27–31.

Walsh, T. et al. 1995. Effects of temperature and carbon dioxide on albumen characteristics, weight loss, and early embryonic mortality of long stored hatching eggs. Poultry Science, 74(9): 1403–1410.

Whitehead, C. et al. 1985. Influence of egg storage on hatchability, embryonic development and vitamin status in hatching broiler chicks. British Poultry Science, 26(2): 221–228.

Survival rate in the honeybee workers (*Apis mellifera* L.) additively fed with polypore mycelial extract

Jan Prouza[1, 2], Jan Musila[2], Marketa Londynova[3], Pavel Plevka[3], Antonin Pridal[2]
[1]Department of Experimental Biology
Masaryk University
Kotlarska 2, 611 37 Brno
[2]Department of Zoology, Fisheries, Hydrobiology and Apidology
Mendel University in Brno
Zemedelska 1, 613 00 Brno
[3]Central European Institute of Technology
Masaryk University
Kamenice 5, 625 00 Brno
CZECH REPUBLIC

apridal@mendelu.cz

Abstract: The deteriorating health status of honeybee colonies is considered to be the result of the interaction among several stress factors, in particular pathogens, pesticides and malnutrition. Secondary metabolites from mushrooms were shown to have the potential to mitigate the impact of some of these stressors. However, possible side effects mushroom extracts must be evaluated. The aim of this experiment was to test the survival rate in worker bees fed by mycelial extract from *Fomes fomentarius*. 1% (v/v) extract was well ingested by honeybees and did not cause them any harm. There was no difference in the survival rates in the experimental and control groups. These results did not confirm the previously reported effect of mycelial extracts on the substantially increasing bee longevity. Potential variability of the mycelial extracts is discussed.

Key Words: Fomes fomentarius, mycelium, extract, *Apis mellifera*, survival

INTRODUCTION

Mushrooms are rich source of specific pharmaceutical substances (Grienke et al. 2014). The health of honeybee colonies has been getting worse in the last decades due to several stress factors. It means especially pathogens (Nazzi and Pennacchio 2014) with emphasis on the bee viruses (Genersch and Aubert 2010) causing covert infections (Benaets et al. 2017). The reduction of *Varroa destructor* population, as a vector of the bee viruses, is only indirect and uncertain method how to prevent the virus infections (Roth et al. 2020). However, acaricides have side effects and are source of additional stresses (Tihelka 2018).

Stamets et al. (2018) had shown that mycelial extracts from Polyporales probably act as an antiviral substance. They determined that the extracts from *Fomes fomentarius* and *Ganoderma resinaceum* are highly effective against two bee viruses (DWV and LSV). There are also other mushrooms with an antiviral potential: *Fomitopsis officinalis*, *F. pinicola*, *Ganoderma applanatum* and outside of Polyporales group also *Schizophyllum commune* or *Inonotus obliquus* (Stamets 2018). The mushrooms are attractive for bees. It was repeatedly observed in case of many mushrooms, e.g. *Xerocomus* sp., *Sepedonium* sp. and *Hypomyces chrysospermus* (Takahashi et al. 2019). The explanations why bees are lured by mushrooms are rather speculative. In the case of *Zygosaccharomyces* sp., this yeast was found as a source of steroids important for development of bee brood (Paludo et al. 2018).

It is expected that mycelial mushroom extracts containing p-coumaric acid can be involved in activating the expression of cytochrome P450 detoxifying path or induction of antimicrobial bee proteins (Mao et al. 2013, Gong and Diao 2017). That is why the mycelial extracts were tested as a hopeful matter for support of bee immunity (Stamets 2018).

In summary, the antiviral effect of the mycelial extracts was demonstrated (Stamets et al. 2018) and the extracts were tested in a beekeeper practice (Pătruică et al. 2017, Stevanovic et al. 2018). There are only limited results about possible side effects of the mycelial extracts (Stamets 2018), therefore, we tested the mycelial extract from *Fomes fomentarius* in a cage experiment with the aim to evaluate a survival rate in the honeybee workers.

MATERIAL AND METHODS

Cultivation and mycelial extraction

The extract was prepared from polypore mushroom (Polyporales) *Fomes fomentarius* (collected as the basidiocarp in a birch forest Kurimska Nova Ves, Czech Republic, N49°20'52", E16°17'6"). Cultivation procedure was carried out according the method by Stamets et al. (2018). The method was not described in all details, therefore, temperature 24 °C and humidity 60–70% were chosen, inspired by Masaryková et al. (2009). Mycelium from basidiocarp of *F. fomentarius* was isolated by cultivation of dissected cube from trama with an edge of about 1 cm. Uninfected part of the mycelium grown from trama was aseptically transferred on 2% malt yeast agar (HiMedia Laboratories GmbH, Germany) for cultivation of the pure mycelial culture. The extraction of the mycelium was carried out also according the methodology by Stamets et al. (2018) with only one difference, i.e. the fresh mycelium was directly extracted without its freezing.

Cage experiment – founding and supplementation

For the cage experiment, a large box was filled with approximately 2000 workers honey bees pooled from multiple colonies and catched on a brood comb. Each cage (n = 3 per treatment, triplicate) was randomly populated with 60 worker bees. In the experimental cages, the worker bees were maintained in the incubator with 32 °C and 60% RH with *ad libitum* sources of candy (honey and powdered beet sugar in proportions 1:4) given in a plastic tube to prevent sticking of bees. The water was supplied in a drinker (6 ml) with 1% (v/v) of the mycelial extract in the experimental group and only pure water was supplied in the control group. The drinkers were changed and newly filled every 3rd day of the experiment to prevent any decomposition of the content. The solution rests in the drinkers was recorded and so the total intake of water was measured. Dead bees were counted and removed from a cage once per day over the course of the experiment. The experiment was stopped 15th day when a first cage collapsed, i.e. more than 50% bees were dead.

Statistical evaluation

The survival curves for 14 days of experiment were fitted by the Kaplan-Meier method. Significance of a difference between the survival curves was tested by log-rank test which compares observed number of the events with events what would be expected under null hypotheses (i.e. identical survival curves). The difference of intake of the water/solution was evaluated by t-test. Statistical analysis was performed using the SAS software.

RESULTS AND DISCUSSION

The content of the drinkers was sucked by bees by the same intensity among all cages during the whole experiment ($p = 0.893$). The survival rate was similar in both groups (Figure 1) and the differences were insignificant (Table 1).

Table 1 The log-rank test comparing survival curves

Treatment	Degrees of freedom	Chi-square statistic	p-value
Control/Experimental	1	0.23	0.63

The results showed that the 1% (v/v) mycelial extract from *Fomes fomentarius* had no adverse effect on caged worker bees. Stamets (2018) mentioned that the extracts at 100% are far too potent and toxic. Even, the 10% extracts had some toxicity. However, when further diluted to 1% or 0.1% or less, longevity substantially increased. However, the preferred effective dose varies from species to species. Our results did not confirm any increase of honeybee worker longevity or any other apparent potentially beneficial effect (e.g. increased water or feed intake). The neutral effect of the extract could

have several causes. The experimental bees were of an unknown health status, i.e. they were not tested for presence of viruses or pesticides. Therefore, the bee health could somehow interact with the extract's effect (Stamets 2018). Further, our result can be interpreted only in respect to the used strain of *Fomes fomentarius*. It was shown that there are several distinct internal transcribed spacer lineages/sublineages of *Fomes fomentarius* which differ among continents (Gaper et al. 2016).

Figure 1 Survival rate by Kaplan-Meier survival analyses

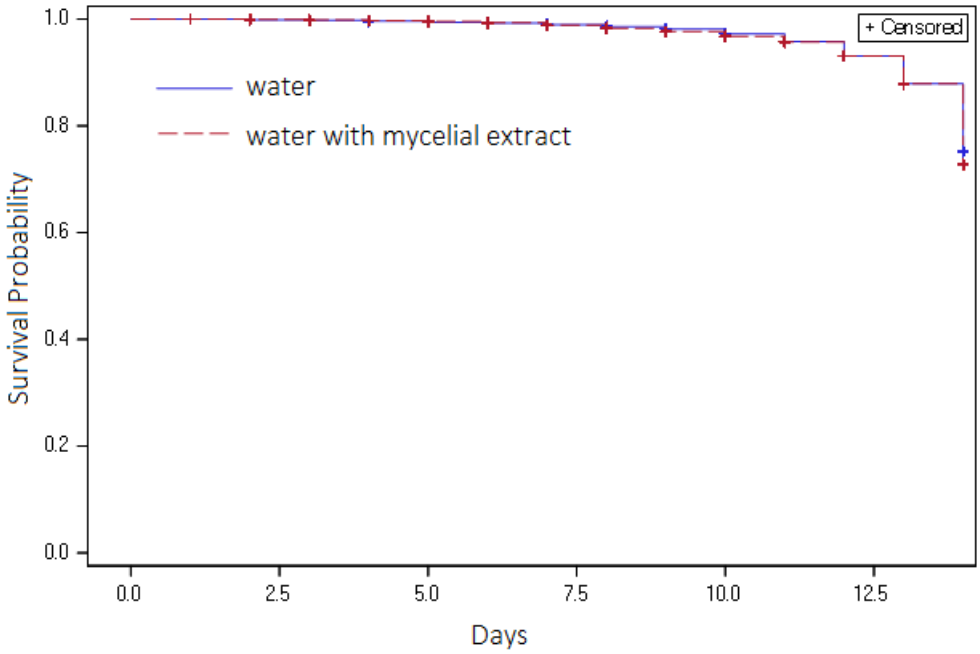

Polyphenols, which are considered to be beneficial to bees in the diet, are often synthesized as protection against extreme environmental conditions (Mao et al. 2013, Gong and Diao 2017). Content of polyphenols differs not only among *F. fomentarius* strains (Gaper et al. 2016) but there are the effects of cultivation conditions, substrates or UV rays (Stamets 2018). The intraspecific variability of bioactive compounds in dependence on cultivation performance parameters has already been demonstrated in *Pleurotus ostreatus* (Koutrotsios et al. 2017). Therefore, the partial finding on the mycelial extract effects must be interpreted with respect of the taxonomy, the cultivation conditions, and the extraction methods. These parameters are important for improvement of biotechnological applications

CONCLUSION

The tested mycelial extract did not cause any change in water or feed intake of honeybees. The survival rates of worker bees were the same in the experimental group additively watered with the extract and the control group. The extract is safe for further testing of potential biological effects.

ACKNOWLEDGEMENTS

The research was financially supported from the donations by elitbau, Ltd. We are grateful for consultations with Svetlana Gaperova (Dept. of Biology and Ecology, Matej Bel University in Banska Bystrica), Dagmar Palovcikova (Dept. of Forest Protection and Wildlife Management of Mendel University in Brno), and with Jan Mlecka (beekeeper) about general details on laboratory cultivation of mushrooms and collection of biological material.

REFERENCES

Benaets, K. et al. 2017. Covert deformed wing virus infections have long-term deleterious effects on honeybee foraging and survival. Proceedings of the Royal Society B: Biological Sciences, 284(1848): 20162149.

Gaper, J. et al. 2016. Medicinal Value and Taxonomy of the Tinder Polypore, Fomes fomentarius (Agaricomycetes): A Review. International Journal of Medicinal Mushrooms, 18(10): 851–859.

Genersch, E., Aubert, M. 2010. Emerging and re-emerging viruses of the honey bee (*Apis mellifera* L.). Veterinary Research, 41(6): 54.

Gong, Y., Diao, Q. 2017. Current knowledge of detoxification mechanisms of xenobiotic in honey bees. Ecotoxicology, 26(1): 1–12.

Grienke, U. et al. 2014. European medicinal polypores – A modern view on traditional uses. Journal of Ethnopharmacology, 154(3): 564–583.

Koutrotsios, G. et al. 2017. Bioactive compounds and antioxidant activity exhibit high intraspecific variability in Pleurotus ostreatus mushrooms and correlate well with cultivation performance parameters. World Journal of Microbiology and Biotechnology, 33(5): 98.

Mao, W. et al. 2013. Honey constituents up-regulate detoxification and immunity genes in the western honey bee Apis mellifera. Proceedings of the National Academy of Sciences, 110(22): 8842–8846.

Masaryková, M. et al. 2009. Microscopy analyses of horse chestnut wood decay by fungus *Fomes fomentarius*. Acta Facultatis Xylologiae, 51(2): 5−15.

Nazzi, F., Pennacchio, F. 2014. Disentangling multiple interactions in the hive ecosystem. Trends in Parasitology, 30(12): 556–561.

Paludo, C.R. et al. 2018. Stingless Bee Larvae Require Fungal Steroid to Pupate. Scientific Reports, 8(1): 1122.

Pătruică, S. et al. 2017. The effect of using medicinal plant extracts upon the health of bee colonies. Romania Biotechnological Letters, 22(6): 13182–13185.

Roth, M.A. et al. 2020. Biology and Management of *Varroa destructor* (Mesostigmata: Varroidae) in *Apis mellifera* (Hymenoptera). Journal of Integrated Pest Management, 11(1): 1–8.

Stamets, P.E. 2018. Integrative fungal solutions for protecting bees. U.S. Patent 20180243356. Available at: https://patents.google.com/patent/US20180243356A1/en. [2020-09-01].

Stamets, P.E. et al. 2018. Extracts of Polypore Mushroom Mycelia Reduce Viruses in Honey Bees. Scientific Reports, 8(1): 1–6.

Stevanovic, J. et al. 2018. The effect of *Agaricus brasiliensis* extract supplementation on honey bee colonies. Anais da Academia Brasileira de Ciências, 90(1): 219–229.

Takahashi, J. et al. 2019. Asian Honey Bee *Apis cerana* Foraging on Mushrooms. Bee World, 96(1): 10–11.

Tihelka, E. 2018. Effects of synthetic and organic acaricides on honey bee health: A review. Slovenian Veterinary Research, 55(3): 119–140.

Acaricidal activity of active substances of essential oils against poultry red mites (*Dermanyssus gallinae*)

Iva Radsetoulalova, Martina Lichovnikova
Department of Animal Breeding
Mendel University in Brno
Zemedelska 1, 613 00 Brno
CZECH REPUBLIC

iva.radsetoulalova@mendelu.cz

Abstract: The main objective of this study was to monitor mortality of poultry red mites (*Dermanyssus gallinae,* PRM), caused by selected active substances of plant essential oils (eugenol, linalool, cinnamaldehyde, limonene, eucalyptol, menthol). The second objective was to define the lethal doses (LD_{50}; LD_{90}) of these active substances. The acaricidal activity of these active substances against poultry house-collected red mites was examined 24 hours after treatment using direct contact method – by glass vial bioassay. The tested concentrations of active substances of essential oils were from 1 to 0.0005 µL/cm^2. Active substances of essentials oils were dissolved in water and Tween 20. Only adult PRM were used for the tests. The average mortality in the negative control was 2.5%. All used active substances caused mortality of PRM. The highest estimated mortality was observed with eugenol (85%), the LD_{50} was estimated to be 4.3 µg/cm^2 for this substance, followed by cinnamaldehyde (79%), the LD_{50} of which was estimated to be 11.6 µg/cm^2 and menthol (74%), the LD_{50} was estimated to be 17.8 µg/cm^2. Linalool, limonene and eucalyptol were generally less effective. The results of these performed experiments suggest that active substances like eugenol and cinnamaldehyde and menthol in merit further study as potential PRM control agents. Active substances of essential oils may be effective natural botanical pesticides against PRM.

Key Words: eugenol, linalool, cinnamaldehyde, limonene, eucalyptol, menthol

INTRODUCTION

The poultry red mite (*Dermanyssus Gallinae*, PRM) is obligatory hematophagous ectoparasite of birds. It feeds blood of its host, but it lives and develops out of host's body – it is a pseudoparasite. Its hosts are hens, especially egg-laying hens, turkeys, ducks and pigeons from domestic poultry, wild birds, rodents and humans too. It feeds on its host in periods once every 2–4 days (Sparagano et al. 2014), but no longer that two hours, mostly during the dark. All development stages of PRM feed blood except larva stage and adult males feed only sometimes. PRM doesn´t attack a human intentionally. It worse digests of mammalian blood. However, its faeces and little hairs on its cuticle are strong allergens. Mainly workers in poultry houses can have eczema even dermatitis in strong infestations. PRM makes huge colonies number hundreds of thousands of mites in several layers (Dohnal 2009, Sparagano et al. 2014). In poultry houses with cages technologies are these mites all year, but its extreme concentrations occur during warm and wet seasons (Sparagano et al. 2014).

High incidence of PRM is one of an economic problem in egg-laying hens today. These parasites are found up to 95% flocks across the Europe, in USA, Japan and China. The cost expends on fight with PRM and production losses are calculated on 360 million EUR per year (Teuling 2017). PRM has very fast life cycle (7–10 days) and some of them are resistant against commercial acaricides against these mites. Next problem is restricted choice of admissible chemical preparations against PRM. Adult PRM can survive from 6 to 8 months without feed in bird's droppings or feathers even longer. It may be one of the origins of the infestation in new flock in poultry house (Dohnal 2009, Sparagano et al. 2014). These problems have highlighted the need to monitor infestation on poultry houses, development of selective PRM control alternative methods for fighting this parasite (Sparagano et al. 2014).

Plant essential or ethereal or aromatic oils are biological active substances of aromatic plants – aromatic hydrocarbons. Essential oils obtained from aromatic plant by water or steam distillation

or by carbon dioxide during supercritical extraction. It is chemical complex mixture of 20–80 monoterpenes, which are contained in different concentrations. From one to five main active substances in essential oil are typical for given plant species (George et al. 2009, Pavela 2011). Essential oils worked on pests both directly and indirectly – may bring acute or chronic toxicity (are neurotoxic), have repellence and anti-oviposition effects connect with inhibition growth grubs, restriction fertility of adults (Pavela 2011).

Pesticides based on essential oils with complex chemistry have the advantage, that for their manifold active substances, resistance formed very difficult on them (Miresmailli et al. 2006). However, their relative lack standardization and consequent inconsistent efficiency lead to restricted using as PRM control. Differences in chemistry among apparently same plant essential oils may be consequence many factors, like kind of plant or its part, geographic origin of plant, climatic conditions of environment, method and harvest days of plant, storage, method extraction of oil or obtain results (George et al. 2009, Isman 2006). This problem could be at least in part solve isolating active substances derived from plant extracts. Active substances could be far developed for usage like acaricides (Sparagano et al. 2014). Disadvantage essential oils is their little persistence in environment. They have little or no harmful effects on non-target organisms (mammalians, birds and fishes) (Isman 2006, Pavela 2011). It seems essential oils with its acaricidal effect could be an alternative to commercial pesticides.

MATERIAL AND METHODS

The acaricidal effectiveness of selected active substances of plant essential oils against PRM were tested via in vitro direct contact method – by glass vial bioassay. All chemicals were of reagent grade. For tests were used following active substances: eugenol ($C_{10}H_{12}O_2$) – active substance of clove bud essential oil, linalool ($C_{10}H_{18}O$) – active substance of lavender essential oil, cinnamaldehyde (C_9H_8O) – active substance of cinnamon essential oil, limonene ($C_{10}H_{16}$) – active substance of essential oil of citrus fruits, eucalyptol ($C_{10}H_{18}O$) – active substance of rosemary essential oil and menthol ($C_{10}H_{20}O$) – active substance of peppermint essential oil. These substances were bought from Sigma-Aldrich, Inc., Prague. Each active substance was diluted in Tween 20 (essential oil : Tween 1:1), than it was diluted with water to final concentrations: 1; 0.5; 0.4; 0.25; 0.2; 0.1; 0.08; 0.06; 0.03; 0.02; 0.015; 0.01; 0.008; 0.005; 0.004; 0.003; 0.002; 0.001 and 0.0005 µL/cm^2.

Solution was applied on two circles of filter paper on top of each other (Whatman No. 1; 25 mm diameter) at the bottom of the glass vial (area of the bottom is 4.9 cm^2, volume of vial is 10 ml) at tested concentration in amount of 50 µL solution. After application vials were opened and filter papers were allowed to air-dry for 50 minutes before adding ten adult PRM. The solvent of solution was then evaporated and active substances were spread equally on filter papers. Ten movable adult PRM were placed on the impregnated filter papers at the bottom of the glass vials with an entomological tweezer. Each glass vial was then closed with lid (Hubert et al. 2015, Rádsetoulalová et al. 2017). All glass vials were stored at laboratory temperature in container with water, that mites were not escaped to surroundings.

Colonies of PRM used in these tests were collected in poultry houses with enriched cages in the Czech Republic in 2020. There were used PRM traps – plastic containers filled with rolled cardboard attached to the constructions. After 3–5 days the containers with PRM were closed by lids and transferred to the laboratory. Adult PRM were tested within three days after collection (Rádsetoulalová et al. 2017).

Always six repetitions per each concentration and active substance and negative control were used. Negative control contained no active substance on filter paper, only solvent (Tween : water 1:1). The mortality of the PRM was measured 24h after the treatment. PRM were considered dead, if they did not move after they were prodded with entomological tweezer. Mite mortality was assessed under magnification (× 2.5 illuminated bench magnifier) (Hubert et al. 2015, Rádsetoulalová et al. 2017).

The percentage mortality of PRM under each treatment was calculated (100 x dead mites / total mites). Data were processed using software MS Excel, XLSTAT-Dose. The effect of in vitro method in each active substance on PRM mortality was statistically analysed using one way analysis of variance and subsequently LSD test was applied to evaluate significant difference among the substances using

software Unistat 5.1 (Unistat Ltd, ENGLAND). Lethal dose (LD) values of LD_{50} and LD_{90} were calculated for each active substance using probit analysis.

RESULTS AND DISCUSSION

Comparison of the acaricidal activity of six active substances of essential oils at a dose from 1 to 0.0005 µL/cm^2 with solvents of Tween 20 with water, via direct contact method – by glass vial bioassay, against adult PRM by in vitro method is shown in Table 1. All used active substances caused mortality of PRM after 24h contact. The mean mortality in negative control was 2.5%. The most effective active substances were eugenol and cinnamaldehyde and menthol, their estimated mortality of PRM were more than 70%. Limonene and eucalyptol were generally less effective.

Table 1 Influence of active substances to mortality (%) of PRM

Active substance	Estimated mortality ± SE (%)
Eugenol	85.23 ± 1.91^{d}
Linalool	63.44 ± 2.93^{b}
Cinnamaldehyde	79.34 ± 2.52^{c}
Limonene	35.26 ± 2.3^{a}
Eucalyptol	38.11 ± 2.09^{a}
Menthol	74.42 ± 5.36^{c}

Legend: a, b – the values marked with different letters make statistically significant difference between the active substances of essential oils at specific concentrations; SE – standard error of mean

Table 2 shown lethal doses (LD_{50} and LD_{90}), which expressed concentration of active substance (µg/cm^2), where gotten up to 50% and 90% mortality of population PRM including 95% confidence intervals. Coefficient determination R^2 (Nagelkerke) is range between 0 and 1, it shows how well the model fits the data. If the value of coefficient is closer to 1, the fitting of the data is higher (Hubert et al. 2015).

The lethal doses were evaluated for eugenol, linalool, cinnamaldehyde, limonene, eucalyptol and menthol. The highest lethal doses values were observed in limonene, where for LD_{50} it was needed 1685.43 (1381.5/2148.693) µg/cm^2 and for LD_{90} it was needed 5977.29 (4883.142/7751.136) µg/cm^2. The least lethal doses values were observed in eugenol, where for LD_{50} it was needed 4.268 (3.201/5.335) µg/cm^2 and for LD_{90} it was needed 25.608 (22.407/28.809) µg/cm^2. It is mean, that eugenol is the most effective active substance from tested active substances.

Table 2 Estimation of lethal dose values (µg/cm^2) of active substances against PRM

Active substance	R^2	LD_{50}	LD_{90}
Eugenol	0.31	4.268 (3.201/5.335)	25.608 (22.407/28.809)
Linalool	0.52	34.8 (32.19/38.28)	89.6 (83.52/97.4)
Cinnamaldehyde	0.48	11.55 (9.45/13.65)	42 (38.85/46.2)
Limonene	0.05	1685.43 (1381.5/2148.693)	5977.29 (4883.142/7751.136)
Eucalyptol	0.18	595.294 (519.514/689.598)	1904.604 (1669.686/2223.772)
Menthol	0.86	17.8 (16.91/18.69)	23.14 (21.36/24.92)

Legend: For LD_{50} and LD_{90} values is given fit and 95% confidence interval in brackets

The results of this study confirmed the acaricidal effect of essential oils and their active components on PRM, as previously observed (Rádsetoulalová et. al. 2017, 2020). Clove bud essential oil contains at least 11 components and eugenol represents 49–57% of them (Wenqiang et al. 2007). In this study eugenol showed the highest acaricidal effect against PRM. Lee et al. (2019) estimated the LD_{50} for eugenol only 0.7 µg/cm^2 vs. 4.268 µg/cm^2 in this study. Cinnamon bark essential oil contains about 12 compounds, the majority (98%) is represented by cinnamaldehyde (Singh et al. 2007). The LD_{50} and LD_{90} for cinnamaldehyde in this study were 11.55 and 42 µg/cm^2. Lee et al. (2019) estimated the LD_{50} for cinnamaldehyde it was only 0.6 µg/cm^2. Lavender essential oil contains of over 300 chemical compounds and content of linalool is highly variable, from 9.3% to 68.8% (Prusinowska and Smigielski 2014). Limonene represents about 26% of components in lemon peel essential oil (Vekiari et al. 2002). Limonen showed the lowest acaricidal effect against PRM in this study.

CONCLUSION

The results of these experiments suggest that main active substances of plant essential oils have higher potential as PRM control agents. Eugenol was found to be the most effective of active substances. Eugenol and cinnamaldehyde and menthol were deemed appropriate candidates for testing acaricidal effects in vivo with poultry.

The interest about new pesticides against PRM currently increased. It is for increased resistance of pests against commercial chemical products. However, for development alternative products based on essential oils and they consequent using in practice, is necessary standardization their chemistry, for there are not big differences between their efficiency. The solution may be isolating active substances of plant essential oils and their consequent tested for using like acaricides. Essential oils have no or little negative effect on nontarget organisms like mammals and fish. They may be used like alternative or supplementary attention of poultry houses and in organic farming too. There is not prove their negative effect on egg and meat quality.

ACKNOWLEDGEMENTS

The research was financially supported by the grant No. AF-IGA2020-IP069.

REFERENCES

Dohnal, K. 2009. Nezvaný host Dermanyssus gallinae alias čmelík kuří. Drůbežář, 9: 9–13.

George, D.R. et al. 2009. Mode of action and variability in efficacy of plant essential oils showing toxicity against the poultry red mite, Dermanyssus gallinae. Veterinary Parasitology, 161(3–4): 276–282.

Hubert, J. et al. 2015. Certifikovaná metodika pro hodnocení účinnosti akaricidních látek na skladištní roztoče a pro identifikaci rezistence. Praha: Výzkumný ústav rostlinné výroby, v.v.i.

Isman, M.B. 2006. Botanical insecticides, deterrents, and repellents in modern agriculture and an increasingly regulated world. Annual Review of Entomology, 51(1): 45–66.

Lee, S.J. et al. 2019. Toxicity and effects of essential oils and their components on Dermanyssus Gallinae (Acari: Dermanyssidae). Experimental and Applied Acarology, 78(1): 65–78.

Miresmailli, S. et al. 2006. Comparative toxicity of Rosmarinus officinalis L. essential oil and blends of its major constituents against Tetranychus urticae Koch (Acari: Tetranychidae) on two different host plants. Pest Management Science, 62(4): 366–371.

Pavela, R. 2011. Aromatické rostliny. In Botanické pesticidy. České Budějovice: Kurent, pp. 36–37.

Prusinowska, R., Smigielski, K.B. 2014. Composition, biological properties and therapeutic effects of lavender (Lavandula Angustifolia L.). A Review. Herba Polonica, 60(2): 56–66.

Rádsetoulalová, I. et al. 2017. Acaricidal activity of plant essential oils against poultry red mite (Dermanyssus Gallinae). In Proceedings of International PhD Students Conference MendelNet 2017 [Online]. Brno, Czech Republic, 8 November, Brno: Mendel University in Brno, Faculty of AgriSciences, pp. 260–265. Available at: https://mendelnet.cz/pdfs/mnt/2017/01/81.pdf. [2020-08-22].

Rádsetoulalová, I. et al. 2020. Active components of essential oils as acaricides against Dermanyssus Gallinae. British Poultry Science, 61(2): 169–172.

Singh, G. et al. 2007. A comparison of chemical, antioxidant and antimicrobial studies of cinnamon leaf and bark volatile oils, oleoresins and their constituents. Food and Chemical Toxicology, 45(9): 1650–1661.

Sparagano, O.A.E. et al. 2014. Significance and Control of the Poultry Red Mite, Dermanyssus gallinae. Annual Review of Entomology, 59(4): 447–66.

Teuling, M. 2017. The battle against red mites. Poultry World [Online]. Available at: https://www.poultryworld.net/Health/Articles/2017/10/The-battle-against-red-mites-197077E/ [2020-08-22].

Vekiari, S.A. et al. 2002. Composition and seasonal variation of the essential oil from leaves and peel of a cretan lemon variety. Journal of Agricultural Food Chemistry, 50(1): 147–153.

Wenqiang, G. et al. 2007. Comparison of essential oils of clove buds extracted with supercritical carbon dioxide and other three traditional extraction methods. Food Chemistry, 101(4): 1558–1564.

Nutritional evaluation of selected varieties of sorghum

Michal Rihacek[1], Leos Pavlata[1], Petr Dolezal[1], Ondrej Stastnik[1], Eva Mrkvicova[1], Michal Rabek[2], Vladimir Smutny[2]
[1]Department of Animal Nutrition and Forage Production
[2]Department of Agrosystems and Bioclimatology
Mendel University in Brno
Zemedelska 1, 613 00 Brno
CZECH REPUBLIC

rihacek.michal@seznam.cz

Abstract: The alternation of warm and dry periods results in slowing down of vegetation growth, drying of soils, which leads to high losses of plant production. Consequently, it is so difficult to ensure sufficient production of the required amount of forage. One of the many alternatives is to use plants tolerating dry and hot conditions, such as sorghum. This article is focused on the comparison of 8 varieties of forage sorghum, for which the basic nutritional parameters were determined and expressed in dry matter: crude protein, acid detergent fibre, neutral detergent fibre and digestibility of dry matter and organic matter by *in vitro* pepsin cellulase method. The mean content of crude protein reached 9.6 to 11.3% of dry matter. Acid detergent fibre shows range from 27.3 to 36.4%. The neutral detergent fibre concentrations were from 48.5 to 56.7%. Range of digestibility of dry matter reached 41.9 to 55.3%. Nutri Honey BMR variety had the highest digestibility of dry matter (55.3%). Nutri Honey BMR and Sweet Caroline varieties had the highest digestibility of the organic matter (50.0%) while Ruzrok variety proved to be the one with the lowest digestibility of organic matter with value 36.2%.

Key Words: nutritional value, acid detergent fibre, neutral detergent fibre, digestibility, ruminants nutrition

INTRODUCTION

Sorghum belong to the one of the most widespread cereal in the world, mostly cultivated in arid and semi-arid regions (Ratnavathi et al. 2012). Sorghum is C4 plant adapted to drought-prone areas with hot semi-arid conditions (Vittal et al. 2010). Nowadays according to Doležal et al. (2009) traditional varieties are replaced by new hybrids with more suitable nutritional and agronomical properties. Based on the digestibility of organic matter in the later stages of plant development, forage varieties of sorghum can be divided into traditional varieties and BMR (Brown Mid Rib) varieties. These varieties are characterized by increasing digestibility in later vegetation stages as well as reduction of lignin content in their cell walls (Hermuth et al. 2012).

Grain sorghum is usually grown for grain, which is used as food, especially for people who are intolerant to gluten (celiac disease) (Al-Naggar et al. 2018). It can also be used as a forage (green biomass or silage) (Hermuth et al. 2012). Nutritional value of sorghum grain is high due to 4–21.1% protein, 2.1–7.6% fat, 1.0–3.4% crude fibre, 1.3–3.3% ash, 57.0–80.6% total carbohydrates, 55.6–75.2% starch. (Ratnavathi et al. 2019). The higher content of starch in grain hybrid silages increase energy concentration, similar to maize.

MATERIAL AND METHODS

Experimental location characteristics

Sorghums were grown in the Field Experimental Station in Žabčice. The Field Experimental Station is situated approximately 25 km south of the city of Brno, in the dry area of southern Moravia in the Czech Republic, at the altitude of 179 m a.s.l. The average annual temperature is 9.2 °C, and the thirty-year average of annual rainfall is 480 mm. Two sites were used for the experiment, Obora and Písky, differed in soil quality. While Obora is location characterized by heavier soils with higher

groundwater level (fluvisol), Písky is location with lighter, sandy and dry soils (chernozem). All varieties were grown in both localities. Our results present the average of both sites.

Sorghum varieties

For the experiment 8 following sorghum varieties were tested: *Sorghum bicolor* x *Sorghum sudanense* (KWS Freya, Nutri Honey, Nutri Honey BMR), *Sorghum bicolor* x *Sorghum bicolor* (KWS Tarzan, Ruzrok). As for sorghum grains varieties we used Sweet Susana, Sweet Caroline and Express. Seeds of these varieties were provided by SEED Service and KWS companies.

Experimental design

Our values are averages from analyzes that have been done repeatedly during two growing seasons (2017 and 2018) and two sites (Obora and Písky). Fertilization was applied in both localities in the rate 120 kg of N (in urea 46% N). The rows distance was 45 cm and the sowing depth 3 cm. The harvest date was determined based on the value of the dry matter from samples of plants (28% of dry matter and above). Harvest area was always 5 meters in one row and repeated for 3 times. The dimensions and size of the harvest area were 2.25 m^2 (5 m x 0.45). From each variety, 2 kg of fresh matter was taken. Above-ground biomass from all varieties was harvested and chopped. Then these samples were pre-dried in oven (65 °C for 24 hours) and grinded through a 1 mm sieve. This modified samples were analysed for basic laboratory parameters – crude protein, acid-detergent fibre (ADF), neutral detergent fibre (NDF) and digestibility of dry matter and organic matter using *in vitro* pepsin by cellulase method. The analyses were performed according to the relevant standards.

Statistical analyses

The results of the experiment were processed using Microsoft Office (USA) and STATISTICA version 12 (USA). Gathered values were tested using by one-way analyses of variance (ANOVA) and post-hoc Sheff´s test, where $P < 0.05$ was considered as statistically significant difference.

RESULTS AND DISCUSSION

Based on the results achieved from laboratory analyses, attention was focused primarily on the comparison of selected sorghum varieties in terms of nutrient composition. The large variance between the achieved values for individual varieties can be caused by the influence of dry matter or the habitat.

Table 1 Overview of the results of crude protein (% of dry matter)

Varieties	n	Mean	Standard deviation	Minimum	Maximum
Express	16	11.3	1.8	8.1	14.8
KWS Freya	16	9.7	2.1	6.8	14.3
KWS Tarzan	16	9.6	2.3	6.1	15.7
Nutri Honey	16	9.6	1.8	6.3	13.2
Nutri Honey BMR	16	11.2	2.9	6.2	15.6
Ruzrok	16	9.7	1.8	6.4	13.1
Sweet Caroline	16	11.2	3.1	7.6	16.8
Sweet Susana	16	11.1	2.3	7.3	16.0

Legend: n – number of samples. There are found no statistically significant differences (P>0.05).

Crude protein

An overview of the results of crude proteins in selected varieties of sorghum are displayed in Table 1. Our results did not show statistically significant differences. The highest content of crude protein was recorded by grain varieties Express (11.3%), Sweet Caroline (11.2%) and Sweet Susana (11.1%). Similar values reached hybrid of sorghum and Sudan grass Nutri Honey BMR (11.2%). KWS Tarzan and Nutri Honey varieties achieved lower mean values of crude protein (9.6%). Baholet et al. (2018) in their experiment reach similar values (7.1–14.1%). According to Hibberd et al. (1982) the optimal content of crude protein in sorghum is 11.1–16.5%. This was also confirmed by Rajčáková

(2005), who determined the content of crude protein in the range of 13.1–18.6%. However, the values of crude protein even within one variety ranged from 6.2 to 16.8% in dry matter. Large differences were influenced by the location and time of sampling. The content of crude protein can also be increased by fertilization.

Wheeler and McKinlay (1998) stated that during vegetation the crude protein of sorghum rapidly decreases, while the fibre content increases, thus reducing the energy value of the feed. Loučka and Homolka (2013) observed the effect of the course of vegetation on the nutritional value of sorghum harvested from July to September. They found out an increase in fibre content from 21.1% in dry matter to 29.9% and a decrease in crude protein from 22.7% in dry matter to 9.1%.

Neutral detergent fibre

According to the achieved results in Table 2 among the varieties, our results did not show a significant statistical difference (P>0.05). If the NDF content is too high, the feed volume needed for good animal's performance is increased and the potential intake of dry matter by animals is reduced. This is also confirmed by Rajčáková (2005), who monitored the nutrient content of the Sudan sorghum hybrid grown in various sites in South Slovakia. NDF content ranged between 541–553 g/kg dry matter. Amer et al. (2012) compared the feed rations of silage from sugar sorghum and alfalfa silage in dairy cows. The sorghum feed contained 58% more NDF. They concluded that replacing alfalfa silage with sorghum silage had negative effects on milk yield.

According to Oba and Allen (2000), the digestibility of neutral detergent fibre is an important indicator of forage quality in practice. Reducing digestibility of NDF by 1% results in a reduction of silage intake by about 0.5 kg, and thus a reduction the milk yield of cows by up to 0.25 l FCM. Di Marco et al. (2009) examined the digestibility of NDF in silages prepared from grain, sweet and BMR hybrid sorghum. They found out that the digestibility of NDF was higher in sweet sorghum (53.3%) compared to other silages (45.3%). According to Fritz et al. (1990) and Grant et al. (1995) BMR sorghum hybrids and Sudan grass hybrids have a higher extent of NDF digestion than other varieties. Dann et al. (2008) found out NDF content in BMR sorghum silage is higher than maize silage. In vitro digestibility of NDF for BMR sorghum silage was approximately 10% higher than that of the maize hybrid.

Table 2 Overview of the results of neutral detergent fibre (% of dry matter)

Varieties	n	Mean	Standard deviation	Minimum	Maximum
Express	16	48.5	9.8	32.7	62.1
KWS Freya	16	55.6	5.7	44.3	66.4
KWS Tarzan	16	56.7	4.9	46.5	63.7
Nutri Honey	16	50.1	6.0	34.8	58.3
Nutri Honey BMR	16	52.2	6.6	39.2	62.3
Ruzrok	16	55.3	5.6	44.9	63.1
Sweet Caroline	16	50.8	5.7	40.5	57.5
Sweet Susana	16	50.0	7.9	33.4	61.3

Legend: n – number of samples. There were found no statistically significant differences (P>0.05).

Acid detergent fibre

Table 3 shows significantly different values among varieties in the acid detergent fibre content. The lowest acid detergent fibre content was in the Express (27.3%), Nutri Honey BMR (29.1%), Sweet Caroline (29.4%), Sweet Caroline (29.4%) varieties. This varieties were statistically different against varieties that had a much higher content of ADF – KWS Freya (35.0%), KWS Tarzan (36.4%) and Ruzrok (35.8%). According to Přikryl (2014), the differences in nutritional values in the ADF content of sorghum are 30–40% compared to maize with 20–25%.

Table 3 Overview of the results of acid detergent fibre (% of dry matter)

Varieties	n	Mean	Standard deviation	Minimum	Maximum
Express	16	27.3[a]	5.6	19.3	36.0
KWS Freya	16	35.0[bc]	3.4	28.8	39.8
KWS Tarzan	16	36.4[c]	3.7	29.1	42.6
Nutri Honey	16	31.3[ac]	3.7	23.5	36.5
Nutri Honey BMR	16	29.1[a]	5.4	18.7	38.0
Ruzrok	16	35.8[c]	3.5	29.6	42.9
Sweet Caroline	16	29.4[ab]	3.4	23.9	34.7
Sweet Susana	16	29.8[ab]	4.8	21.4	42.2

Legend: n – number of samples. [a, b, c, d, e] – different letters in the column means statistically significant differences (P<0.05) among varieties.

Digestibility of dry matter

The highest mean digestibility of dry matter (Table 4) had varieties Nutri Honey BMR (55.3%) and Sweet Caroline (55.0%). The lowest digestibility of dry matter was observed in Ruzrok and KWS Freya varieties (41.9% and 44.95, respectively).

Table 4 Overview of the results of in vitro digestibility of dry matter (%)

Varieties	n	Mean	Standard deviation	Minimum	Maximum
Express	16	52.8[cd]	7.0	40.7	66.1
KWS Freya	16	45.0[ab]	6.2	34.0	57.4
KWS Tarzan	16	47.3[abc]	3.9	41.7	54.4
Nutri Honey	16	50.1[bcd]	3.4	42.6	54.4
Nutri Honey BMR	16	55.3[d]	4.3	47.4	61.8
Ruzrok	16	41.9[a]	6.7	29.6	54.9
Sweet Caroline	16	55.0[d]	4.2	46.5	62.2
Sweet Susana	16	52.9[cd]	4.6	43.5	63.8

Legend: n – number of samples. [a, b, c, d] – different letters in the column means statistically significant differences (P<0.05) among varieties.

Table 5 Overview of the results of in vitro digestibility of organic matter (%)

Varieties	n	Mean	Standard deviation	Minimum	Maximum
Express	16	47.2[bcd]	8.1	33.8	58.5
KWS Freya	16	39.3[ab]	6.7	28.5	51.5
KWS Tarzan	16	41.7[abe]	3.8	36.5	49.1
Nutri Honey	16	44.2[bcd]	3.4	38.4	49.5
Nutri Honey BMR	16	50.0[cd]	5.4	40.3	59.5
Ruzrok	16	36.2[a]	7.7	20.5	50.7
Sweet Caroline	16	50.0[d]	5.0	38.3	60.1
Sweet Susana	16	48.1[cde]	5.4	35.0	61.8

Legend: n – number of samples. [a, b, c, d, e] – different letters in the column means statistically significant differences (P<0.05) among varieties.

Digestibility of organic matter

The highest mean digestibility of organic matter (Table 5) was proved in Nutri Honey BMR and Sweet Caroline (50.0%). Ruzrok was the variety with the lowest digestibility of organic matter with value 36.2%. Except KWS Freya, where the mean digestibility was 39.3%, the other tested varieties were above 40%. According to Přikryl (2014) the average digestibility of organic matter is in the range

of 45–60%. According to Sriagtula et al. (2017) the digestibility of organic matter was affected by mutant lines of sorghum. In their study BMR sorghum achieved higher digestibility of organic matter (66.59%). Traditional varieties without BMR mutation contained lower digestibility of organic matter (60.59%).

CONCLUSION

Sorghum is not a comparable crop to silage maize in the term of forage quality. But it can be an alternative and reserve source of feed justified in dry areas, when there is a shortage of feed and especially silage maize of good quality. The differences between grain and biomass types of sorghum are due to the higher content of starch in the former ones, which is the main carrier of energy.

ACKNOWLEDGEMENTS

This publication has been summarizing with project "MendelFarm – Integrated plant protection in a company operating in dry conditions" 9. F. m – Demonstrační farmy. Supported by Ministry of Agriculture of the Czech Republic.

REFERENCES

Al-Naggar, A.M.M. et al. 2018. Agronomic and yield characteristic of grain sorghum as influenced by environment factors and genotype. Annual Research a Review in Biology, 26: 1–14.

Amer, S. et al. 2012. Effects of feeding sweet sorghum silage on milk production of lactating dairy cows. Journal of Dairy Science, 95(2):859–863.

Baholet, D. et al. 2018. Comparison of nutrient composition of sorghum varieties depending on different soil types. In Proceedings of 25th International PhD Students Conference MendelNet 2018 [Online]. Brno, Czech Republic, 7–8 November, Brno: Mendel University in Brno, Faculty of AgriSciences, pp. 100–103. Available at: https://mnet.mendelu.cz/mendelnet2018/mnet_2018_full.pdf [2020-09-10].

Dann, H.M. et al. 2008. Comparison of Brown Midrib Sorghum-Sudangrass with Corn Silage on Lactational Performance and Nutrient Digestibility in Holstein Dairy Cow. Journal of Dairy Science, 91: 663–672.

Di Marco, O.N. et al. 2009. Digestibility of forage silages form grain, sweet and bmr sorghum types: Comparison of in vivo, in situ and in vitro data. Animal Feed Science and Technology, 153(3–4): 161–168.

Doležal, P. et al. 2009. Uplatnění vícesečných čiroků ve výživě a krmení zvířat (I. část). Krmivářství, 13(2): 45–46.

Fritz, J.O. et al. 1990. Digestion Kinetics and Cell Wall Composition of Brown Midrib SorghumX Sudangrass Morphological Components. Crop Science, 30(1): 213–219.

Grant, R.J. et al. 1995. Brown midrib sorghum silage for midlactation dairy cows. Journal of Dairy Science, 78(9): 1970–1980.

Hermuth, J. et al. 2012. Čirok obecný Sorghum bicolor (L.) Moench, možnosti využití v podmínkách České republiky: Methodology for Practice [Online]. Praha-Ruzyně: Výzkumný ústav rostlinné výroby, v.v.i. Available at: http://invenio.nusl.cz/record/124035/files/nusl-124035_1.pdf [2020-09-14].

Hibberd, C.A. et al. 1982. Nutritive characteristics of different varieties of sorghum and corn grains. Journal of Animal Science, 55(3): 665–672.

Loučka, R., Homolka, P. 2013. Silážování čiroku. In: Hodnocení krmiv pro dojnice. Pohořelice: Agro Digest s.r.o., pp. 350–354.

Oba, M., Allen, M.S. 2000. Effects of brown midrib 3 mutation in corn silage on productivity of dairy cows fed two concentrations of dietary neutral detergent fiber: 1. Feeding behaviour and nutrient utilization. Journal of Dairy Science, 83(6): 1333–1341.

Přikryl, J. 2014. Čirok nebo kukuřice. Úroda, 62(4): 13.

Rajčáková, L. 2005. Pestovanie ciroku sudánského v suchom postihovaných oblastiach. Krmivářství, 9(4): 36–37.

Ratnavathi, C.V. 2019. Grain Structure, Quality, and Nutrition. In Breeding Sorghum for Diverse End Uses. Duxford, United Kingdon: Woodhead Publishing, pp. 193–207.

Ratnavathi, C.V. et al. 2012. Natural occurrence of aflatoxin B1 in sorghum grown in different geographical regions of India. Journal of Science of Food and Agriculture, 92(12): 2416–2420.

Sriagtula, R. et al. 2017. Nutrient changes and in vitro digestibility in generative stage of M10–BMR sorghum mutant lines. Media Peternakan, 40(2): 111–117.

Vittal, R. et al. 2010. Genetic diversity among Sorghum bicolor L. Moench genotypes as revealed by prolamines and SSR markers. Journal of Biotech Research [Online], 2(1): 101–111. Available at: https://www.researchgate.net/publication/46033552_Genetic_diversity_among_Sorghum_bicolor_L_Moench_genotypes_as_revealed_by_prolamines_and_SSR_markers. [2020-09-2].

Wheeler, B., McKinlay, J. 1998. Forage Sorghum-Sudan Grass Factsheet. OMAFRA Ontario.

The effect of organic and inorganic selenium supplementation on egg production and egg quality of laying hens

Andrea Roztocilova, Jakub Novotny, Eva Mrkvicova, Leos Pavlata, Ondrej Stastnik
Department of Animal Nutrition and Forage Production
Mendel University in Brno
Zemedelska 1, 613 00 Brno
CZECH REPUBLIC

xroztoc1@mendelu.cz

Abstract: The aim of our study was to evaluate the effect of organic and inorganic selenium supplementation in feed mixture for hens to eggs production and egg quality. The study was conducted on 84 Lohman Brown-Classic hens. They were kept on conventional deep litter system. The experimental period started from hens age 33 weeks and lasted to 41st weeks of age. The hens were randomly divided into 3 groups. The Control group (n=28) was fed diets without the addition of selenium. The first experimental group (Organic; n=28) was fed with organic source of selenium. The second experimental group (Inorganic; n=28) was fed with inorganic source of selenium. The selenium was supplied with its natural content in the feed plus selenium was added that its total content was 0.31 mg/kg. No significant differences ($P>0.05$) were observed during the study between the evaluated groups in egg production and egg quality, but significant differences ($p<0.05$) were recorded in feed consumption between groups. The lowest feed consumption per group and day was found in Organic group.

Key Words: poultry nutrition, *Saccharomyces cerevisiae*, sodium selenite, selenomethionine

INTRODUCTION

Selenium (Se) is an essential trace element for animal health, because it is important element for many biological functions. Selenium is present in all tissues in animals organism, especially in blood, liver and muscles. Selenium is involved in the process of lipid digestion and absorption of tocopherols (Papp et al. 2010). Selenium have protective properties mainly due to its anti-oxidative activities and prevention of carcinogenic factors and free radicals (Kieliszek and Błażejak 2016). The nutrients in eggs are results a feature of the diet. It is possible to enhance the levels of vitamin E and selenium in eggs by adding Se to the feed of laying hens (Payne et al. 2005). Supplement the diets of laying hens with appropriate contain of Se to enhance the Se concentration of carcass meat and eggs start be a common practice in modern poultry nutrition (US Food and Drug Administration 2002, Kieliszek and Błażejak 2016). It is important to include an appropriate amount of selenium in the feed ration, as selenium and vitamin E deficiency causes exudative diathesis in poultry, manifested by oedema under the skin, bruising in the muscles and growth retardation. Only registered producers of feed premixes are allowed to supply selenium to animal feed rations. Higher doses of Se may be toxic for animals (Zelenka 2014). Selenium is added to the feed ration of poultry in the form of sodium selenite, sodium selenate or in the form of organic *Saccharomyces cerevisiae*, or in industrially produced selenomethionine or selenocysteine (Zelenka 2014). It was shown that addition of organic selenium to laying hens' diets can improve the quality of stored eggs (Wakebe 1998). The aim of this study was to evaluate the influence of feeding with contain of 0.31 mg/kg inorganic and organic selenium on egg production and egg quality.

MATERIAL AND METHODS

Animals and diets

The trial was performed with 84 Lohmann Brown-Classic hens. A conventional deep litter system was used with wood shavings as the bedding material. The study started when the hens were at the age of 33 weeks and lasted till 41st weeks of age. Room temperature, humidity and lighting system were set

and controlled according to the requirements for the production of Lohmann hens (Lohmann 2020). Lighting regime was set at a 16 hours light and 8 hours dark with a maximum light intensity of 20 luxuries. The layers were randomly divided into three equal groups with four repetitions. In one repetition were 7 hens. The control group (Control; n=28) was fed diets without the addition of selenium (Se). Se was supplied only with its natural content in the feed. The first experimental group (Organic; n=28) was fed with organic source of selenium (*Saccharomyces cerevisiae* CNCM I-3060) and the second experimental group (Inorganic; n=28) was fed with inorganic source of selenium (sodium selenite – Na_2SeO_3). In both experimental groups (Organic and Inorganic, respectively) selenium was supplied with its natural content in the feed and selenium was added that its total content was 0.31 mg/kg in both groups (Table 2).

This three diets were formulated according to the recommended nutrient content for Lohmann Brown-Classic hens so that they are isocaloric and isonitrogenous (Lohmann 2020). The chemical compositions of diets were determined for dry matter, crude protein, crude fat, crude fibre, and ash according to the EC Commission Regulation (Commission Regulation 152/2009). Composition of diets is shown in Table 1 and chemical composition of diets shows Table 2.

Table 1 Composition of feed diets (g/kg)

Component (g/kg)	Control	Organic	Inorganic
Maize	333.390	333.390	333.390
Soybean meal	310.000	310.000	310.000
Wheat	190.000	190.000	190.000
Limestone grit	54.000	54.000	54.000
Rapeseed oil	40.000	40.000	40.000
Premix*	30.000	30.000	30.000
Limestone milled	25.000	25.000	25.000
Monocalcium phosphate	13.000	13.000	13.000
Sodium chloride	3.000	3.000	3.000
Methionine	1.600	1.600	1.600
Threonine	0.010	0.010	0.010
Selenium	0.000	0.100	0.007

*Legend: *Premix contains (per kg): L-lysine 13 g; DL-methionine 45 g; calcium 295 g; phosphorus 67 g; sodium 46 g; copper 300 mg; iron 2.300 mg; zinc 1.800 mg; manganese 2.400 mg; iodine 30 mg; retinol 330.000 IU (international units); calciferol 100,000 IU; tocopherol 500 mg; phylloquinone 40 mg; thiamine 40 mg; riboflavin 120 mg; pyridoxin 54 mg; cobalamin 400 ug; biotin 3 mg; niacinamid 420 mg; folic acid 30 mg; calcium pantothenate 250 mg; cholin chloride 6,000 mg.*

Table 2 Chemical composition of feed mixtures in 88% dry matter

	Control	Organic	Inorganic
Dry Matter (%)	88.00	88.00	88.00
ME_N (MJ/kg) *	11.47	11.47	11.47
Crude protein (%)	18.27	18.30	18.30
Crude fat (%)	5.52	5.72	5.58
Crude Ash (%)	14.44	14.42	14.9
Ca (%)	4.024	4.024	4.024
P (%)	0.594	0.594	0.594
Se (mg/kg)	0.08	0.027	0.027

*Legend: *ME_N – Apparent metabolizable energy; calculated value, Ca-calcium, P-phosphorus, Se-selenium*

The health status of animals was evaluated daily and live weight was measured regularly during the trial. The hens had free access to feed and water.

Performance

The number of laid eggs and its total weight were recorded every day for 56 days during the experiment. The average weight of eggs in each group and the feed consumption per hen and eggs were calculated. Qualitative evaluation of eggs was ranged from 35 weeks to 40 weeks of laying hens age. Three eggs per one cage (one repetition of group) were taken every week for from each group (n=12). During experiment egg weight and shell thickness were determined and albumen index (albumen weight / egg weight ×100), yolk index (yolk weight / egg weight × 100) shell index (shell weight / egg weight × 100) were calculated. Subsequently, Haugh units (HU) were calculated: HU=100 × log (solid albumen height + 7.6–1.7 × egg weight 0.37). The shell was dried at room temperature. The weight of the shell was determined by weighing on a laboratory scale to the nearest 0.01 g, including eggshell membranes. The thickness of the shell was measured at the blunt end, the sharp end and middle of the egg, and the arithmetic mean was calculated from the measured values.

Statistical analysis

The obtained data were processed in Microsoft Excel and StatSoft Statistica, version 12.0. The basic statistical characteristics of the sets of values were calculated from the results of individual groups. One-way analysis of variance (ANOVA) and multi-factor analysis of variance (MANOVA) were used. The Scheffés test was used to determine significant differences, where $P<0.05$ was considered a statistically significant difference.

RESULTS AND DISCUSSION

From our data given in the tables 3 and 4 it can be seen that neither the sources of selenium added by us had a statistically significant ($P>0.05$) effect on the egg performance of laying hens, nor the evaluated qualitative parameters. But in opposite, Gjorgovska et al. (2012) in their study published, that after the addition of organic selenium the percentage increase in egg production. The effect of selenium on laying performance and egg quality should be interesting for many scientists because of egg-laying, and their quality affects the profitability of breeding. Lot of studies concluded that adding selenium increased laying performance and egg qualitative parameters and also their fertility and hatchability (Asadi et al. 2017, Waseem et al. 2016). The source of added selenium is very important because the source determines its subsequent usability and the resulting effect on egg production. For example, Qu et al. (2017) reported in their study that adding selenium nanoparticles in feed of laying hens had no effect on egg performance. However, the results of studies dealt with the effect of different forms of selenium supplementation in hens diet, and their subsequent production are inconsistent.

Table 3 Egg production

Group		Control	Organic	Inorganic
Weeks	Units	8	8	8
		Mean ± standard error		
Average weight of 1 egg	(g)	60.33±0.18	60.35±0.18	60.59±0.20
Feed consumption	(g)	750±6.6^{ab}	728±5.4^{a}	750±8.7^{b}
Feed consumption	(g)	107.4±0.9^{ab}	103.97±0.8^{a}	108.5±1.05^{b}
Feed consumption	(g)	109.76±1.5	105.6±1.4	112.6±3.1
Feed conversion		1.82±0.03	1.75±0.02	1.86±0.05
Laying intensity	(%)	98.02±1.01	98.81±0.88	97.75±1.49

Legend: $^{a, b}$ – different letters by parameters feed consumption per group and day and feed consumption per hen and day means statistically significant differences ($P<0.05$).

Average eggs weight was similar ($p>0.05$) in all evaluated groups. The eggs mean weight ranged from 60.33 g for the control group to 60.59 g for the group fed the inorganic form of Se. Equally

the mean values of laying intensity were very close, ranging from 97.75 to 98.8. The values 109.76 g and 105.6 g of Table 3, it can be seen that there were statistical differences ($p<0.05$) in feed consumption. The differences were both in the consumption of feed per group and in the consumption of feed for the hen. Opposite to our results, for example Payne et al. (2005) described reported no significant influences of organic Se on feed intake. The mean egg mass production reached averaged 59 g without significant differences ($p>0.05$).

Table 4 Selenium effect on egg qualitative parameters

Group	Week	n	Egg weight (g)	HU	Albumen index	Yolk index	Shell index	Shell thickness (mm)
	Mean ± standard error							
Control	35	12	60.39±1.01	96.04±1.70	65.16±0.49	24.62±0.52	10.23±0.10	0.41±0.00
Organic	35	12	60.85±0.60	98.99±0.97	65.45±0.56	24.37±0.50	10.17±0.20	0.41±0.01
Inorganic	35	12	60.89±1.16	94.94±1.43	64.62±0.57	25.21±0.55	10.17±0.17	0.41±0.01
Control	36	12	60.67±1.84	97.32±0.70	64.06±0.52	25.98±0.44	9.96±0.14	0.45±0.01
Organic	36	12	59.99±0.70	93.74±1.27	64.38±0.49	25.30±0.46	10.32±0.15	0.46±0.01
Inorganic	36	12	61.31±1.16	95.13±0.96	65.22±0.51	24.67±0.48	10.12±0.17	0.46±0.01
Control	37	12	65.05±0.84	94.07±1.05	65.18±0.56	24.69±0.58	10.13±0.16	0.48±0.01
Organic	37	12	62.13±0.49	94.21±1.09	65.12±0.49	24.72±0.41	10.16±0.19	0.47±0.01
Inorganic	37	12	64.81±0.81	92.58±1.36	65.47±0.45	24.67±0.40	9.85±0.14	0.47±0.00
Control	38	12	64.10±0.91	94.49±1.30	65.64±0.49	24.42±0.50	9.94±0.15	0.40±0.00
Organic	38	12	62.09±0.71	92.98±1.23	65.23±0.38	24.81±0.28	9.96±0.12	0.40±0.00
Inorganic	38	12	65.05±0.92	93.65±1.27	65.26±0.63	24.98±0.58	9.77±0.12	0.40±0.00
Control	39	12	64.09±0.98	95.45±1.24	65.01±0.72	25.05±0.62	9.94±0.22	0.41±0.01
Organic	39	12	63.57±0.98	93.62±1.29	65.50±0.51	24.66±0.47	9.84±0.16	0.41±0.00
Inorganic	39	12	65.38±0.93	93.05±1.09	65.44±0.37	24.82±0.31	9.74±0.13	0.41±0.01
Control	40	12	64.33±1.09	95.30±1.10	65.63±0.58	24.43±0.60	9.94±0.21	0.42±0.01
Organic	40	12	64.08±0.60	94.51±1.22	64.75±0.61	25.23±0.59	10.01±0.13	0.41±0.01
Inorganic	40	12	64.75±0.82	92.79±1.11	65.44±0.52	24.78±0.44	9.78±0.15	0.40±0.01

Legend: There were no statistically significant differences P>0.05. HU – Haugh Units

The average weight of eggs in individual weeks was in the range from 60.39±1.01g to 64.75±0.82 g without statistically significant differences between the groups Control, Organic and Inorganic. Our results of Haugh units show that the addition of selenium had no effect on them compared with values of Haugh units from eggs by hens feeded by control mixture as in the Patton (2000) study where the supplement of Selen had no effect on Haugh unit values. On the other hand, Ferguson et al. (2012) report improvements to Haug's unit. The shell thickness recorded by us reached higher values 0.40±0.01 mm than in the Renema study (2006), which states a shell thickness of 0.35 ± 0.01 mm. Hanafy et al. (2009) describes that organic Se has the positive impact to enhance yolk index, but our values are without statistical differences ($p>0.05$). According to results described by Arpasova et al. (2012), Se-yeast found to be more effective in enhancing egg breadth and improving shape index; our values do not show significant differences ($p>0.05$). The positive effect of organic selenium addition was also observed by Renema and Sefton (2004), which monitored improved egg shape index in laying hens. Evaluated shell index was without differences ($p>0.05$).

CONCLUSION

The higher feed consumption was found in group of hens receiving diet with inorganic source of selenium. Different sources of selenium had no effect on laying of eggs and egg quality. Similarly, diet without any selenium source (expect natural content in feeds) had no effect on evaluated parameters as well. It can be concluded that organic or inorganic source of selenium can be safely used in the hen's diet.

ACKNOWLEDGEMENTS
The research was financially supported by the Internal Grant Agency of Faculty of AgriSciences no. AF-IGA2020-TP012.

REFERENCES

Arpasova, H. et al. 2012. The effect of various forms and doses of selenium supplementation of the hens diet on selected qualitative parameters and freshness of table eggs. Animal Science and Biotechnologies, 45(1): 11–16.

Asadi, F. et al. 2017. Comparison of different selenium sources and vitamin E in laying hen diet and their influences on egg selenium and cholesterol content, quality and oxidative stability. Iranian Journal Applied Animal Science, 7(1): 83–89.

Commission regulation (EC) 152/2009. Laying down the methods of sampling and analysis for the official control of feed. Brussels: The commission of the European Communities.

Ferguson, L.R. et al. 2012. Selenium and its' role in the maintenance of genomic stability. Mutation Research/Fundamental and Molecular Mechanisms of Mutagenesis, 733(1–2): 100–110.

Gjorgovska, N. et al. 2012. The effect of different levels of selenium in feed on egg production, egg quality and selenium content in yolk. Lucrari Stiintifice-Seria Zootehnie, 57: 270–274.

Hanafy, M.M. et al. 2009. The effect of organic selenium supplementation on productive and physiological performance in a local strain of chicken.1-The effect of organic selenium (Sel-Plex™) on productive, reproductive and physiological traits of bandarah local strain. Egyptian Poultry Science Journal, 29(4): 1061–1084.

Kieliszek, M. Błażejak, S. 2016. Current knowledge on the importance of selenium in food for living organisms: A Review. Molecules, 21(5): 609.

Lohmann, T. 2020: Management guide [Online]. Available at: http://www.ltz.de/en/e-guide/new_e-guide/HTML/. [2020-08-20].

Papp. V. et al. 2010. Selenium and selenoproteins in health and disease. Antioxidants & Redox Signaling, 12(7): 793–795.

Patton, N.D. 2000. Organic Selenium in the Nutrition of Laying Hens: Effects on Egg Selenium Content, Egg Quality and Transfer to Developing Chick Embryos. PhD. Thesis, University of Kentucky.

Payne, R.L. 2005. Effect of inorganic versus organic selenium on hen production and egg selenium concentration. Poultry Science, 84(2): 232–237.

Qu, W. 2017. Effect of Selenium Nanoparticles on Anti-Oxidative Level, Egg Production and Quality and Blood Parameter of Laying Hens Exposed to Deoxynivalenol. Journal of Animal Research Nutrutrition, 2(1): 1–8.

Renema, R.A. 2006. Creating the ideal hatching egg: quality, efficiency and fertility. In Nutritional biotechnology in the feed and food industries: Proceedings of Alltech's 22nd Annual Symposium. Kentucky, USA, 23–26 April, pp. 233–239.

Renema, R.A., Sefton, A.E. 2004. Dietary selenium source can affect egg production, shell quality and fertility traits of broiler breeders. In Proceedings of XXII World's Poultry Congress. Istanbul, Turkey, 8–13 June, pp. 521.

US Food and Drug Administration. 2002. Food additives permitted in feed and drinking water: Selenium yeast. Federal Register, 67: 46850–46851.

Wakebe M. 1998. Organic selenium and egg freshness. Patent 10-23864. Feed for meat chickens and feed for laying hens. Japanese Patent Office, Application Heisei 8-179629.

Waseem, M.Z. et al. 2016. Egg quality, geometry and hatching traits of indigenous Aseel as influenced by organic and inorganic selenium supplementation. Indian Journal of Animals Research, 51(5): 860–867.

Zelenka, J. 2014. Výživa a krmení drůbeže. Olomouc: Agriprint.

Effect of different calcium content in feed mixture on eggs quality and blood biochemical parametrs of laying hens

Andrea Roztocilova, Jakub Novotny, Ondrej Stastnik, Leos Pavlata, Eva Mrkvicova
Department of Animal Nutrition and Forage Production
Mendel University in Brno
Zemedelska 1, 613 00 Brno
CZECH REPUBLIC

xroztoc1@mendelu.cz

Abstract: The aim of present study was to evaluate the effect of different calcium content in feed mixture on eggs quality and blood biochemical parameters of laying hens. The hens (n= 12) were divided into two groups. The first group (L; n=6) was fed by feeding mixture with 2.1% content of calcium, and the second group (H; n=6) was fed by diet content 3.7% of calcium. There were found statistically significant differences ($P < 0.05$) in some eggs qualitative parameters between the groups. Higher values ($P < 0.05$) for the shell strength (40.90 N) and shell thickness (393.4 μm) were found in the second group (H). The content of serum Ca was affected by higher dietary Ca levels. Evaluated blood parameters alkaline phosphatase, lactate dehydrogenase, total protein and uric acid showed statistically significant differences ($P < 0.05$) after different adding levels of calcium in diet. Other monitored parameters (egg mass, feed consumption, feed conversion, alanine aminotransferase, aspartate aminotransferase, gamma-glutamyl transferase, creatine kinase, total bilirubin, glucose, cholesterol, triacylglycerides, albumin, urea, creatinine) were without statistically significant differences ($P > 0.05$) between groups.

Key Words: poultry nutrition, mineral metabolism, egg alkaline phosphatase

INTRODUCTION

Minerals plays important role in the body and ensure or participate in the operation of many vital functions. Minerals are found in all tissues of the body, but in varying amounts due to their location and their role in the relevant tissue. For example, calcium is most contain in bone tissue (Kleyn 2013). Bar (2008) write that 2 to 3 g are excreted daily during the calcification shell by the laying hens. Calcium is obtained to the body by consumption of feed (Kleyn 2013). Calcium deficiency reduces feed intake, slows growth, bones are insufficiently mineralized and muscle bleeding increases. On the other hand, excess calcium has a negative impact on the use of phosphorus, while increasing the requirements for magnesium, iron, manganese, iodine, zinc, copper and deficiency can also lead to decreased appetite, lethargy, convulsions, slow growth, and severe elemental deficits can lead to death (Zelenka 2014, Kleyn 2013). The calcium is store from 90–95% to the eggshell in hens. In laying hens the requirement of calcium content in feed is changing from 1.8% to 3.2% to 3.6% depending on increasing egg production (NRC 1994).

The aim of this study was to evaluate some aspects of calcium metabolism in hens that have been fed with diets with different calcium content from 30th to 40th week of age. It was evaluated qualitative parameters of eggs as eggshell strength and thickness, egg mass production and eggs weight. Furthermore, it was evaluated selected blood biochemical parameters as aspartate aminotransferase (AST), gamma-glutamyl transferase (GGT), alkaline phosphatase (ALP), alanine aminotransferase (ALT), lactate dehydrogenase (LD), cretaine kinase, total bilirubin and others.

MATERIAL AND METHODS

The animal procedures were reviewed and approved by the Animal Care Committee of Mendel University in Brno and by the Ministry of Education, Youth and Sports MSMT-2494/2018-3.

Animals and diets

The study was conducted on twelve LOHMAN BROWN CLASSIC hens. Hens were kept in individual cages and randomly divided to two groups of six hens. The first group (n = 6) was marked as Low (L) because it was fed by diet with 2.1% content of calcium. The second group (n = 6) was marked as High (H) because consumed diet containing 3.7% calcium . These two feed mixtures were formulated (except for calcium content) according to the recommended nutrient content for LOHMANN BROWN CLASSIC hens (Lohmann 2020) and pelleted. The feed was weighted daily. The feed residue was collected and weighted daily as well to calculate total feed consumption. Composition of diets are shown in Table 1 and chemical composition of diets are shown in Table 2. Feed intake was recorded daily for each hen separately. Room temperature, humidity and lighting mode was set and controlled according to technological instructions for LOHMAN BROWN CLASSIC layers (Lohmann 2013). Hens had free access to water. The experimental period lasted from 30th to 40th weeks of animals age. Health status was evaluated daily during the trial.

Egg quality

Individual egg laying was assessed daily and eggs were collected once a week for evaluate qualitative parameters. The feed conversion ratio was calculated (total feed consumption divide egg mass). The egg mass was calculated as number of eggs times average weight of eggs. Strength of the eggs, weight of the shell, percentage of the shell and shell thickness were evaluated. The egg weight and shell weight were determined by weighing using a laboratory scale, egg shell strength was determined destruction method by machine Egg Force Reader. The eggshell thickness was monitored by special device in 3 places: in the equatorial line, on the blunt and sharp peaks of the eggshell. The arithmetic mean was calculated from measured data.

Blood collection and analysis

The blood from right wing vein were taken at the end of experiment. The samples of blood were collected into heparinized tubes. These samples were centrifuged for 10 minutes at 3.000 rpm till 2 hours after collection. The separated blood plasma were frozen (-20 °C) for the next biochemical examination. Evaluated parameters from blood plasma were determined using standardized biochemical methods using Erba Lachema (Czech Republic) commercial sets on the Ellipse automatic biochemical analyser (AMS Spa, Italy).

Table 1 Composition of feed diets (%)

Component (%)	L (2.1%) Ca	H (3.7%) Ca
Maize	40.00	40.00
Soybean meal	23.50	26.00
Wheat	26.67	19.48
Rapeseed oil	2.50	2.80
Premix*	0.20	0.20
Monocalcium phosphate	1.46	1.50
L-Lysine	0.05	0
DL-Methionine	0.20	0.19
Threonine	0.03	0.01
Limestone milled	4.95	9.38
L-Valin	0.04	0.04
Sodium chloride	0.30	0.30
Bicarbonate	0.10	0.10

*Legend: *Premix contains (per kg): copper 7500 mg; iron 30000 mg; zinc 55000 mg; manganese 60000 mg; iodine 1000 mg; selenium 150 mg; retinol 5000000 IU; cholecalciferol 1500000 IU; alphatocoferol 50000 mg; menadione 3000 mg; ascorbic acid 52000 mg; B1 2000 mg; B2 8000 mg; B6 3000 mg; B12 20000 mcg; biotine 200 mg; niacinamide 27500 mg; folic acid 2000 mg; calcium pantothenate 12600 mg; choline chloride 120000 mg;betaine 60000 mg; butylhydroxyanisole 600 mg; butylhydroxytoluene 3000 mg*

Statistical evaluation

The data were processed by Microsoft Excel (USA) and Statistica version 12.0 (USA). A one-way analysis of variance (ANOVA) was used to determine the differences between groups. To ensure the evidential differences, Scheffé´s test was applied and $P < 0.05$ was regarded as a statistically significant difference.

Table 2 Chemical composition of feed mixtures in dry matter

	L (2.1%) Ca	H (3.7%) Ca
Dry Matter (%)	100.00	100.00
ME_N (MJ/kg)*	12.04	11.48
Crude protein (%)	19.31	19.80
Crude fat (%)	5.37	4.93
Crude fiber (%)	2.14	2.13
Crude ash (%)	10.04	13.92
Ca (%)	2.10	3.70

*Legend: *ME_N – Apparent metabolizable energy, Ca – calcium*

RESULTS AND DISCUSSION

The average feed consumption (Table 3) ranged from 108.54 g (H) to 130.06 g (L) without statistically significant difference ($P > 0.05$) between groups. Atteh and Leeson (1983) described the similar result without a statistically significant difference in feed consumption between evaluated groups fed by feed mixture with different calcium levels.

Table 3 Different calcium level effect on egg production, some egg qualitative parameters, feed consumption and feed conversion

GROUP		L (2.1%) Ca	H (3.7%) Ca
n		6	6
		Mean ± standard error	
Average weight of 1 egg	g	61.61 ± 0.474 [a]	58.07 ± 0.472 [b]
Shell strength	N	38.34 ± 0.548 [b]	40.90 ± 0.459 [a]
Shell thickness	µm	369.17 ± 3.197 [b]	393.39 ± 3.43 [a]
Egg mass	kg	4.403 ± 0.108	4.096 ± 0.113
Feed consumption per hen/day	g	130.06 ± 12.4	108.54 ± 13.39
Feed conversion		2.15 ± 0.237	1.89 ± 0.204

Legend: [a,b] – the differences between the groups are statistically significant ($P < 0.05$).. number of eggs evaluated in the group were 60.

In the group with a higher level of calcium, a significantly ($P < 0.05$) higher strength and thickness of the shell was found. In this group was found a lower weight of eggs. In the Table 3 we can see that average weight of one egg is 58.07 g in the group with higher calcium content, and 61.61 g in the group with lower calcium content with statistical differences ($P < 0.05$) between group. Different effect describes Geraldo et al. (2006), which describes in their study that the different calcium level did not affect the egg weight. Similar conclusion describes Cufadar et al. (2011) in their study did not found any significant differences in egg weight among the Ca levels of 3.0%, 3.6%, or 4.2% of diets laying hens.

There were statistically significant differences ($P < 0.05$) between the groups in shell strength (38.34 N (L) vs. 40.90 N (H)) and thickness (369.17 µm (L) vs. 393.39 µm (H)). Jiang et al. (2013) describes the same situation with eggshell that layers fed on a diet with 2.62% Ca had a weaker eggshell breaking strength than those on a diet with 3.7% or 4.4% Ca. But for example Keshavarz and Nakajima (1993) states that increasing levels of dietary calcium from 3.5% to 5.5% did not have any beneficial effects on eggshell qualities in a long-term experiment.

Table 4 Blood biochemical parameters

GROUP	L (2.1%) Ca		H (3.7%) Ca	
n	6		6	
Parameters units	Mean ± standard error			
AST (µkat/l)	2.792 ± 0.157		2.662 ± 0.133	
GGT (µkat/l)	0.678 ± 0.094		0.607 ± 0.078	
ALP (µkat/l)	25.860 ± 5.251	a	10.890 ± 2.966	b
ALT (µkat/l)	0.212 ± 0.097		0.192 ± 0.036	
LD (µkat/l)	6.752 ± 0.431	a	4.775 ± 0.645	b
Creatine kinase (µmol/l)	74.963 ± 9.354		59.317 ± 15.23	
Total bilirubin (µmol/l)	7.733 ± 2.091		10.517 ± 1.034	
Glucose (mmol/l)	13.933 ± 0.373		14.653 ± 0.421	
Cholesterol (mmol/l)	4.525 ± 0.453		5.850 ± 0.546	
Triacylglycerides (mmol/l)	13.718 ± 1.633		16.908 ± 1.387	
Total protein (g/l)	47.717 ± 1.530	b	56.917 ± 1.521	a
Albumin(g/l)	19.800 ± 0.300		20.967 ± 0.495	
Urea (mmol/l)	1.087 ± 0.060		1.113 ± 0.143	
Creatinine (µmol/l)	32.833 ± 1.818		34.067 ± 2.243	
Uric acid (µmol/l)	305.283 ± 26.402	b	523.00 ± 69.86	a
Calcium (mmol/l)	3.060 ± 0.064	b	3.472 ± 0.113	a

Legend: [a,b] – the differences between the groups are statistically significant (P < 0.05). ALT – alanine aminotransferase; AST – aspartate aminotransferase; GGT – gamma-glutamyl transferase; ALP – alkaline phosphatase;LD – lactate dehydrogenase

The values of egg mass production were without a statistically significant difference (P > 0.05). The same results have Keshavarz and Nakajima (1993) which also reported that different levels of ration Ca had no significant effect on egg mass. Our result is different with results of Rostagno et al. (2005), which discuss that higher content of calcium (4.12%) has a positive role on egg mass production.

Parameters in Table 4 show statistically significant differences (P < 0.05) after adding different levels of calcium to diets. In our study was confirmed that higher intake of Ca significantly affected (increased) the concentration of Ca in the blood. Also Frost and Roland (1991) described increased level of plasma ionized Ca with increased dietary Ca level in ratio from 2.75% to 4.25%, but not plasma total calcium. The values of alkaline phosphatase (ALP) are similar as in study of Hurwitz and Griminger (1961) higher for group with low content Ca (2.1%) in fed than group with higher Ca (3.7%). The differences (P < 0.05) were also found for values of uric acid with higher values in second group (H) with higher content Ca (3.7%). Acording to statement Konan et al. (2007) as the blood uric acid content of the birds were influenced by the different calcium levels in the feed, it can be said that there is probably impairment of renal function. The lactate dehydrogenase (LD) and total protein showed statistically differences (P < 0.05) between group. Alkaline phosphatase and lactate dehydrogenase are important enzymes related to bone metabolism. Their activity increases in the blood, after the tissue cells are damaged. Our values of glucose are in normal levels of glucose concentration in the majority of birds, which are between 11.1–27.8 mmol/L (Coles 1997). Next parameters were without statistically differences (P > 0.05).

CONCLUSION

In our experiment, a higher level of calcium had a positive effect on the thickness and strength of the shell, which is important in terms of egg distribution. However, the average egg weight was 5.7% lower. Also in our study was confirmed that higher intake of Ca by feed significantly affected (increased) the concentration of Ca in the blood. According to the results of the evaluated blood parameters, it can be stated that better values were in the group with a higher content (H) of calcium in the feed. The values show that insufficient calcium in the feed is reason for low calcium contain in blood and may cause some diseases for example bone damage. For determine the optimal calcium content in the diets for hens, is needed next studies also deal with qualitative parameters of bones

ACKNOWLEDGEMENTS
The research was financially supported by the individual project of Internal Grant Agency AF-IGA2020-IP084.

REFERENCES

Atteh, J.O., Leeson, S. 1983. Influence of increasing dietary calcium and magnesium levels on performance, mineral metabolism, and egg mineral content of laying hens. Poultry Science, 62(7): 1261–1268.

Bar, A. 2008. Calcium homeostasis and vitamin D metabolism and expression in strongly calcifying laying birds. Comparative Biochemistry and Physiology. Part A: Molecular and Integrative Physiology, 151(4): 477–490.

Coles, B.H. 1997. Library Veterinary Practice: Avian Medicine and Surgery. 2nd ed., Oxford, UK: Wiley-Blackwell Publishing.

Cufadar, Y. et al. 2011. The effect of dietary calcium concentration and particle size on performance, eggshell quality, bone mechanical properties and tibia mineral contents in moulted laying hens. British Poultry Science, 52(6): 761–768.

Frost, T.J., Roland, D.A. 1991. The influence of various calcium, and phosphorus levels on tibia strength, and eggshell quality of pullets during peak production. Poultry Science, 70(4): 963–969.

Geraldo, A. et al. 2006. Níveis de cálcio e granulometrias do calcário para frangas e seus efeitos sobre a produção e qualidade de ovos. Revista Brasileira de Zootecnia, 35(4): 1720–1727.

Hurwitz, S., Griminger, P. 1961. The response of plasma alkaline phosphatase, parathyroids and blood and bone minerals to calcium intake in the fowl. Journal of Nutrition, 73(2): 177–185.

Jiang, S. et al. 2013. Effects of dietary energy and calcium levels on performance, egg shell quality and bone metabolism in hens. The Veterinary Journal, 198(1): 252–258.

Keshavarz, K., Nakajima, S. 1993. Re-evaluation of calcium and phosphorus requirements of laying hens for optimum performance and eggshell quality. Poultry Science, 72(1): 144–153.

Lohmann, T. 2020. Management guide [Online]. Available at: http://www.ltz.de/en/e-guide/new_e-guide/HTML/. [202-07-30].

Kleyn, R. 2013. Minerals. In Chicken nutrition a guide for nutritionists and poultry professionals. England: Context, pp. 69–78.

Konan, N.A. et al. 2007. Acute, subacute toxicity and genotoxic effect of hydroethanolic extract of the cashew (Anacardium occidentale L.). Journal of Ethnopharmacol, 110(1): 30–38.

NRC (National Research Council). 1994. Nutrient Requirements of Poultry. 9th Revised Edition, Washington, DC: The National Academies Press Pub.

Rostagno, H.S. et al. 2005. Tabelas brasileiras de exigências nutricionais para aves e suínos (Composição de alimentos e exigências nutricionais). 3th ed., Viçosa, MG: Universidade Federal de Vicosa Pub.

Zelenka, J. 2014. Minerální látky. In Výživa a krmení drůbeže. Olomouc: Agriprint s.r.o., pp. 34–36.

The influence of pigs housing system on back fat thickness

Jiri Sklenar, Libor Sladek, Milan Vecera, Gustav Chladek
Department of Animal Breeding
Mendel University in Brno
Zemedelska 1, 613 00 Brno
CZECH REPUBLIC

xsklena7@mendelu.cz

Abstract: The aim of experiment was a comparation between back fat thickness and other slaughter indicators. Pigs were fattened up on deep-bed pen or slatted floor pen. There were 499 slaughter pigs, 278 of those were fattened up on slatted floor pen and remaining 221 pigs were fattened up on deep-bed pen. Average back fat thickness for slatted floor pen was 14.14 mm and average value for deep-bed pen was 17.00 mm. Average carcass weight of pigs that were feeded on slatted floor pen was 112.22 kg, for pigs feeded on deep-bed pen the average carcass weight was 120.13 kg.

Key Words: back fat thickness, housing system, carcass weight

INTRODUCTION

Pigs breeding has long tradition in Czechia (Holec and Poláková 2019). The main purpose is to provide sufficient amount of quality pork (Close 2008). The pork is one of the most favorite type of meat in most of the European countries (Holec and Poláková 2019). The most consumed meat per year per person in Czechia is pork (Kvapilík 2009).

Deep-bed pen systems are better for pigs welfare than slatted floor pen systems. Thermal stress is happens to pigs feeded on deep-bed pen. Ecological based farms tend to use deep-bed pen systems lately. The disadvantage of deep-deb pen systems is more fattening of pigs compared to slatted floor pen systems (Lucas et al. 2017).

Studies shows that with increasing slaughter weights the quality of meat and the quality of carcass is decreasing (Latorre et al. 2004).

MATERIAL AND METHODS

Research was performed in pig farm located in Vysočina region in time period April 2017 – December 2019. Pigs were fattened up on slatted floor pen (Technology 1) or deep-bed pen (Technology 2). There were 499 slaughter pigs, 278 of those were fattened up by Technology 1 and remaining 221 pigs were fattened up by Technology 2. Pigs were hybrids (ČBU[1] x ČL[2]) x (D[3]). Sows were hybrids (ČBU x ČL) and as boars were used duroc breed (D).

Pigs were fattened up in groups divided by breeding technologies. Technology 1 group contained 15–25 pigs, Technology 2 group contained 30–40 pigs. Feeding lasted from 3 to 4 months.

Breeding utility has its own slaughterhouse, where the non-invasive ultrasound IS-D-05 is used for determination of back fat thickness.

All results were processed according to common mathematical-statistical methods and evaluated in STATISTICA 12 software.

RESULTS AND DISCUSSION

Table 1 contains the comparation of housing system as per slaughter indicators. The results show that pigs fattened up by Technology 1 had average carcass weight 88.37 kg, muscle deep was 57.26 mm,

[1] ČBU stands for Czech Large White breed (České bílé ušlechtilé prase)
[2] ČL stands for Czech Landrace breed (Česká landrase)
[3] D stands for Duroc breed

back fat thickness was 14.14 mm, average price per 1 kg/ carcass weight was 31.75 CZK. Pigs fattened up by Technology 2 had average carcass weight 94.59 kg, muscle deep was 62.14 mm, back fat thickness was 17.00 mm, average price per 1 kg/ carcass weight was 31.66 CZK. Prices were listed on slaughter classification paper.

Authors Kvapilík et al. (2009) mentions that average back fat thickness was 15.95 mm in their research. In comparison with this experiment, the Technology 1 lean meat content was 1.47% higher, muscle deep 4.69 mm worse and back fat thickness 1.81 mm worse than Kvapilík work. Technology 2 lean meat content was 0.43% worse, muscle deep 0.19 mm higher and back fat thickness 1.05 mm higher than Kvapilík work.

Comparing results to Červená (2016), as pigs were breeded using slatted floor pen and had average back fat thickness 17.00 mm, which is 2.86 more than for Technology 1 in this experiment, but same as Technology 2 results.

Table 1 Technology comparation

	n	Back fat thickness [mm]		Lean meat content [%]		Carcass weight price [CZK/kg]	
		$\bar{x}$	s_x	$\bar{x}$	s_x	$\bar{x}$	s_x
Technology 1	278	14.14^{A}	4.73	57.30^{A}	3.31	31.75	2.04
Technology 2	221	17.00^{B}	4.34	55.40^{B}	3.01	31.66	2.36

	n	Carcass weight [kg]		Slaughter weight [kg]		Muscle deep [mm]	
		$\bar{x}$	s_x	$\bar{x}$	s_x	$\bar{x}$	s_x
Technology 1	278	88.37^{A}	12.11	112.22^{A}	15.38	57.26^{A}	9.36
Technology 2	221	94.59^{B}	12.47	120.13^{B}	15.84	62.14^{B}	10.06

Legend: Various letters stands for statistically significant differences between Technology 1 and Technology 2. A, B: $p \leq 0.01$.

The influence of SEUROP classification to carcass weight, lean meat content, back fat thickness and muscle deep for Technology 1 are given in the Table 2. For Technology 1 results shows that the majority of carcass weight were classified in class E (52.16%). Class R had the highest average weight of carcass (93.7 kg), on the other hand the least average weight of carcass was in class S (79.95 kg). The majority of back fat thickness were classified in class O (32.20 mm), the least height of back fat thickness were classified in class S (8.61 mm). Difference between classes S and R was 23.59 mm.

There is statistically significant difference ($p \leq 0.01$) between carcasses graded in classes S and E and also graded in classes S and U in carcass weight. There is also statistically significant difference ($p \leq 0.05$) between carcasses graded in classes S and R.

In case of the lean meat content and back fat thickness there is statistically significant difference ($p \leq 0.01$) between all classes except carcasses graded in class O. Muscle deep statistical significance ($p \leq 0.01$) is proofable in between classes E and U and classes E and R.

Table 2 The influence of SEUROP classification to carcass weight, lean meat content, back fat thickness and muscle deep in Technology 1

	n	Carcass weight [kg]		Lean meat content [%]		Back fat thickness [mm]		Muscle deep [mm]	
		$\bar{x}$	s_x	$\bar{x}$	s_x	$\bar{x}$	s_x	$\bar{x}$	s_x
S	67	$79.95^{A,a}$	9.90	61.13^{A}	0.57	8.61^{A}	0.88	62.14	10.06
E	145	91.78^{B}	11.89	57.62^{B}	1.30	13.73^{B}	1.90	59.50^{A}	9.17
U	58	88.81^{B}	10.16	53.43^{C}	1.22	19.61^{C}	1.76	53.77^{B}	9.01
R	7	93.70^{b}	14.33	47.67^{D}	1.39	27.74^{D}	1.75	63.12^{B}	10.82
O	1	93.30	-	44.50	-	32.20	-	48.30	-

Legend: Various letters stands for statistically significant differences between letters A, B, C, D: $p \leq 0.01$. A, B: $p \leq 0.05$.

The influence of SEUROP classification to carcass weight, lean meat content, back fat thickness and muscle deep for Technology 2 are given in the Table 3. For Technology 2 results shows that the majority of carcass weight were classified in class E (53.85%). Class U had the highest average

weight of carcass (98.40 kg), on the other hand the least average weight of carcass was in class S (75.47 kg). The majority of back fat thickness were classified in class O (31.90 mm), the least height of back fat thickness were classified in class S (9.22 mm). Difference between classes O and S is 22.68 mm.

There is statistically significant difference ($p \leq 0.01$) between carcasses graded in classes S and E, carcasses graded in classes S and U, carcasses graded in classes S and R, and also carcasses graded in classes U and R in carcass weight.

In case of the lean meat content and back fat thickness there is statistically significant difference ($p \leq 0.01$) between all classes except carcasses graded in classes O and P. Back fat thickness statistical significance ($p \leq 0.01$) is proofable in between all classes except carcasses graded in classes O and P.

Table 3 The influence of SEUROP classification to carcass weight, lean meat content, back fat thickness and muscle deep in Technology 2

	n	Carcass weight [kg]		Lean meat content [%]		Back fat thickness [mm]		Muscle deep [mm]	
		$\bar{x}$	s_x	$\bar{x}$	s_x	$\bar{x}$	s_x	$\bar{x}$	s_x
S	6	75.47^{A}	6.79	60.65^{A}	0.51	9.22^{A}	0.81	62.14	10.06
E	119	92.77^{B}	12.64	57.27^{B}	1.34	14.32^{B}	1.99	62.37	9.55
U	84	98.40^{C}	10.99	53.47^{C}	1.30	19.80^{C}	1.86	63.12	10.82
R	11	$95.57^{B,C}$	11.35	48.01^{D}	1.76	27.52^{D}	2.40	58.35	8.75
O	1	94.10	-	44.80	-	31.90	-	50.60	-

Legend: Various letters stands for statistically significant differences between letters A, B, C, D: $p \leq 0.01$.

CONCLUSION

Comparing Technologies 1 and 2 the outcome is that the value of back fat thickness is higher for deep-bed pen (17.00 mm) than slatted floor pen. Pig fattened up in slatted floor pen had average height of back fat thickness 14.14 mm, which is 2.86 mm worse value compared to deep-bed pen.

Therefore, it seems that the deep-bed pen is more profitable, yet in the majority of conventional pig farms the slatted floor pen systems are commonly used. According to results of this experiment, pig farms should use deep-bed pen systems for better or higher profit.

REFERENCES

Close, W.H. 2008. Trace minerals in pig nutrition: The big three issues from weaning to slaughter production, health and environment. Pig Progress, (9): 22–24.

Červená, M. 2016. Obchodní zatřídění jatečných prasat podle SEUROP systému. Diploma thesis (in Czech), Mendel University in Brno.

Holec, J., Poláková, J. 2019. Zemědělství a potraviny. Praha: Profi Press.

Kvapilík, J. et al. 2009. Results of pig carcass classification according to SEUROP in Czech Republic. Czech Journal Animal Science, 54(5): 217–228.

Latorre, M.A. et al. 2004. The effects of gender and slaughter weight on the growth performance, carcass traits, and meat quality characteristics of heavy pigs. Journal of Animal Science, 82(2): 526–533.

Lucas, D. et al. 2017. Relationship between pig carcass characteristics measured in live pigs or carcasses with Piglog, Fat-oMeat'er and computed tomography. Livestock Science, (197): 88–95.

Effect of incubation temperature on hatching characteristics and post-hatch performance in broiler chickens

Marketa Skoupa[1], Tereza Opavska[1], Martina Lichovnikova[1], Marian Foltyn[2]
[1]Department of Animal Breeding
Mendel University in Brno
Zemedelska 1, 613 00 Brno
[2]Lihen Chropyne
Vykrm Trebic, s.r.o.
Komenskeho 75, 768 11 Chropyne
CZECH REPUBLIC

xskoupa2@mendelu.cz

Abstract: This study was conducted to elucidate the embryonic development, hatchability, and post-hatch growth performance of broiler chickens when eggs were incubated during first 36 hours at 2 different temperatures. Totally, 1200 hatching eggs produced by Ross 308 broiler breeders (55 weeks of age) had been stored for 4 days. The hatching eggs were divided into 2 groups. Control group (CG) was incubated first 36 hours at 38.22 °C (100.8 °F). Experimental group (EG) was incubated first 36 hours at 39.17 °C (102.5 °F). Although the hatchability of fertilized eggs was higher in CG, as with fertility, there was no significant difference between groups. Differences in mean embryonic mortality and late embryonic mortality were statistically significant ($P<0.05$). In CG the mean middle embryonic mortality was 1.76% and the mean late mortality 2.47%, while in EG the mean middle embryonic mortality was 0.71% and the mean late embryonic mortality 4.17%. However, during the whole experimental period, in EG the average weight was statistically significantly ($P<0.05$) below the weight of CG, in uniformity, feed intake and feed conversion there was not statistically significant ($P>0.05$) difference. Temperature setting change in hatching machine at first 36 hours of incubation from standard 100.8 °F to 102.5 °F had negative impact on hatchability and post-hatch growth.

Key Words: fertility, embryonic development, hatchability, feed conversion, feed intake

INTRODUCTION

The embryonic development of a chicken starts already in the oviduct during the formation of the egg and even the diapause (storage period) should not be ignored (Musil and Tuláček 1964). At the oviposition, the egg cools down, cell division stops, and the embryo does not develop further, but gets into a latent stage where the life processes slow down. The embryo begins to develop when the temperature increases above 20 °C (Holoubek 2007). During incubation, the temperature is one of the most important environmental factors (Decuypere and Michels 1992). Birds incubated outside the optimal temperature must utilize resources to survive and their growth and development are reduced (Hill 2001). Early pre-or postnatal ontogeny may have a practical advantage of alleviating of problems that are associated with the thermoregulation control, it means that posthatch performance of broiler chickens may be enhanced by altering standard incubation temperatures (Nichelmann 2002, Yalçin and Siegel 2003). At the beginning of incubation chicken embryo is the most sensitive to suboptimal temperatures (French 1997). For hatchability, chick weight and broiler performance, the first week of embryo development is the most important (Joseph et al. 2006). In several studies the immaturity of the temperature regulation mechanism in young chicks during first week of life was exploited by rapid heat stress response modulated by early age thermal conditioning (Arjona et al. 1990, Yahav and Hurwitz 1996). Due to the fact that posthatch environmental manipulation is complicated, manipulations with temperature during incubation period lead to a better thermal response of the embryo and subsequently thermal response of the growing chicken can be monitored (Dunnington and Siegel 1984).

The trial was conducted to investigate the effects of exposure to higher temperature in hatching compartment during first 36 hours of incubation on hatching characteristics and post-hatch performance in broiler chickens.

MATERIAL AND METHODS

Hatching conditions

A total of 1200 hatching eggs (65 to 69g) produced by commercial flock of 55 weeks of age of Ross 308 broiler breeders were used in 20 repetitions. Prior to incubation eggs were stored for 4 days. The experiment was processed in hatchery Chropyně belonging to company Výkrm Třebíč s.r.o. The incubation was performed in hatching machines Biostreamer 24S from Belgian company Petersime. The eggs were divided into two groups. The temperature in hatching machine at first 36 hours was distinct for both groups. The temperature of the incubator was maintained at 38.22 °C (100.8 °F) during first 36 hours for control group (CG), considered as the standard incubation temperature. The temperature at the beginning of incubation for experimental group (EG) was maintained at 39.17 °C (102.5 °F) that is higher than ordinarily in commerce hatcheries. During whole incubation after the first 36 hours the temperature in hatchery was controlled by OvoScan which scans the eggshell temperature until the 18th day of incubation. On the 7th day of incubation all eggs were candled to discard unfertilized eggs and to determine early embryonic mortality. On the 18th day all the eggs were transferred from the turning trays to hatcher baskets using the hatching machine Biostreamer 8H where the eggs were incubated until the 21st day according to the standard program indicated by the technology producer. The 21st day the hatching was completed, and the chicks were taken out of the incubator. The number of hatched chicks was recorded, and unhatched eggs were broken for macroscopic analysis to classify them as infertile eggs or eggs with dead embryos. The number of infertile eggs was expressed as a percentage of the total number of eggs. The embryonic mortalities per week were expressed as a percentage of the fertile eggs.

Evaluation of chicken growth

To measure production parameters a total of 423 hybrid males were sexed from the hatched chickens and were fattened in experimental room of Mendel University in Brno. The males were divided into two groups of 6 repetitions of each. CG contained 212 chickens and EG contained 211 chickens. The chickens were housed on shaving litter and according to the principles given in the technological instructions for Ross 308 hybrids with controlled environmental conditions. A standard broiler starter diet and water were provided *ad libitum*. The whole experiment lasted from day 0 until the 31st day of age. During the rearing period, the birds were individually weighed at hatch (day 0), 10th, 17th, 24th, and 31st day of age. Feed conversion and uniformity for individual pens were calculated on each weighing day.

Statistical analysis

Individual observed characteristics were expressed by means; characterized by the standard error (SE). The variability of the characteristics were expressed by the coefficient of variation. T-test was used to test for the significance of differences between means within individual characteristics. Unistat 5.1 software (UNISTAT Ltd, ENGLAND) was used for statistical evaluation.

RESULTS AND DISCUSSION

Hatchability of fertilized eggs

The results of hatchability are displayed in Table 1; statistically significant differences were found in middle and late embryonic mortality between the observed groups ($P<0.05$). The mean middle embryonic mortality was 1.76% and the mean late embryonic mortality 2.47% for hatching eggs incubated at standard temperature, while the mean middle mortality was 0.71% and the mean late mortality was 4.17% for hatching eggs incubated at elevated temperatures for the first 36 hours (Table 1).

Table 1 The effect of heat treatment on hatchability of fertilized eggs and embryonic mortality (%)

Indicator	CG	v_x	EG	v_x
	Mean ± SE		Mean ± SE	
Hatchability of fertilized eggs	92.22 ± 1.21[a]	0.04	90.41 ± 1.50[a]	0.49
Early embryonic mortality	3.53 ± 0.77[a]	0.69	4.70 ± 0.85[a]	0.53
Middle embryonic mortality	1.76 ± 0.37[b]	0.66	0.71 ± 0.29[a]	1.29
Late embryonic mortality	2.47 ± 0.35[a]	0.45	4.17 ± 0.72[b]	0.55

Legend: different superscripts (a, b) indicate statistically significant differences between groups (P<0,05); SE - standard error of the mean; v_x - coefficient of variation; CG – control group; EG – experimental group

The results obtained by Nakage et al. (2003) showed that early embryonic mortality increased by low temperature during incubation (less than 35.5 °C) while middle and late embryonic mortality increased at high temperature (more than 36.5 °C). A significant decrease in hatching rate by increasing the temperature by 1 °C (38.8 °C) from day 13 of incubation above the optimum incubation temperature (37.8 °C) was obtained by Givisiez et al. (2000), decreasing the temperature by 1 °C (36.8 °C) had no effect on hatching quality. Increased temperature during incubation causes metabolic disorders associated with cardiovascular development and inhibits the intestinal development (Molenaar et al. 2011, Wineland et al. 2004).

Live weight and uniformity

The average live weight determined in regular intervals is illustrated in Table 2; on the day of hatching the difference in mean live weight of 0.49g proves that an increased temperature of 0.95 °C during the first 36 hours had a negative effect on the weight of day-old chicks (P<0.05). At day 24, the groups differed by 22.5g (P<0.05). At day 31, the average weight of CG was higher by 38.3g than the average weight of EG (P<0.05).

The difference in the average uniformity of the chickens was not statistically significant in any day of observation between the control and experimental group (P>0.05).

Table 2 The effect of heat treatment at the beginning of incubation on chicken weight and uniformity

Age (days)	Live weight (g)				Uniformity (%)			
	CG	v_x	EG	v_x	CG	v_x	EG	v_x
	Mean ± SE		Mean ± SE		Mean ± SE		Mean ± SE	
1	44.76 ± 0.11[b]	0.03	44.27 ± 0.11[a]	0.03	99.5 ± 0.41[a]	0.01	99.0 ± 0.62[a]	0.01
10	320.8 ± 0.00[a]	0.08	319.3 ± 0.00[a]	0.09	77.8 ± 4.47[a]	0.14	76.8 ± 3.16[a]	0.10
17	715.8 ± 0.00[a]	0.10	710.0 ± 0.00[a]	0.10	64.1 ± 3.18[a]	0.12	69.5 ± 3.85[a]	0.13
24	1285.0 ± 0.00[b]	0.10	1262.5 ± 0.01[a]	0.11	67.9 ± 2.16[a]	0.07	65.3 ± 4.37[a]	0.16
31	1988.6 ± 0.01[b]	0.10	1950.3 ± 0.01[a]	0.11	65.6 ± 4.00[a]	0.14	62.9 ± 5.82[a]	0.22

Legend: different superscripts (a, b) indicate statistically significant differences between groups (P<0,05); SE - standard error of the mean; v_x - coefficient of variation; CG – control group; EG – experimental group

Similar to results of present study, Sgavioli et al. (2016) found that chicks hatched from eggs incubated at elevated temperature (39 °C) had lower weight than chicks hatched from eggs incubated at standard temperature of 37.5 °C (P<0.05). In contrast, Ipek et al. (2014) found that average weight of day-old chicks hatched from eggs incubated at elevated temperature (38.9 °C) was higher than average weight of day-old chicks hatched from eggs incubated at standard incubation temperature (37.8 °C). Yahav et al. (2004) showed that the ability of thermoregulation in hatched chicks was positively affected by heat manipulation during embryogenesis by repeated short-term increase of incubation temperature.

According to Wilson (1991), sorting the hatching eggs according to size before incubation would be advantageous to improve the uniformity of chickens. However, Montanhini et al. (2013)

demonstrated that such a procedure does not increase the uniformity of broilers at the end of production period.

Feed conversion ratio and feed intake

The mean values of feed conversion for both monitored groups are displayed in Table 3; the difference between the groups in feed conversion was not statistically significant in any day of observation (P>0.05).

Since no statistically significant difference was found in feed conversion, a statistical evaluation was realised also for cumulative feed intake. However, even in feed intake, no statistically significant difference was found between the groups on any day of observation (P>0.05). Except the 10th day of age, the average feed intake was higher in CG compared to EG (P>0.05).

Table 3 The effect of incubation conditions on feed conversion and cumulative feed intake

Age (days)	Feed conversion				Feed intake (g)			
	CG	v_x	EG	v_x	CG	v_x	EG	v_x
	Mean ± SE		Mean ± SE		Mean ± SE		Mean ± SE	
10	1.27 ± 0.05[a]	0.09	1.29 ± 0.06[a]	0.12	412.0 ± 16.44[a]	0.10	414.5 ± 20.73[a]	0.12
17	1.30 ± 0.02[a]	0.04	1.31 ± 0.03[a]	0.05	944.8 ± 20.35[a]	0.05	944.4 ± 27.75[a]	0.07
24	1.15 ± 0.01[a]	0.02	1.16 ± 0.00[a]	0.01	1498.6 ± 23.78[a]	0.04	1497.6 ± 32.17[a]	0.05
31	1.31 ± 0.00[a]	0.00	1.33 ± 0.01[a]	0.02	2640.4 ± 35.95[a]	0.03	2618.6 ± 32.78[a]	0.03

Legend: different superscripts (a, b) indicate statistically significant differences between groups (P<0,05); SE - standard error of the mean; v_x - coefficient of variation; CG - control group; EG – experimental group

Hulet (2007) reported statistically significantly higher (P<0.05) feed conversion. In chickens hatched from eggs incubated at higher temperature (38.7 °C) compared to chickens hatched from eggs incubated at standard temperature (37.6 °C). However, Leksrisompong et al. (2009) showed in their results lower feed conversion (P<0.05) in chickens hatched from eggs exposed to elevated temperature (39.4 °C) after 16 day of incubation in comparison to chickens hatched from eggs incubated at 37.6 °C. Kadam et al. (2008) concluded that feed conversion in chickens at the first week of age can be improved by providing in amount from 10 to 40 mg of threonine to the yolk sac in ovo. According to Pesti and Bakalli (1996), feed conversion in broiler chickens can be reduced by 3.4% by supplementing the feed mixture (based on corn and soybean meal) with copper (Cupric Sulfate Pentahydrate and Cupric Citrate).

According to Bhanja et al. (2009), feed intake after hatch affects the subsequent weight of chickens. Zelenka (2014) reported that late access to feed after hatch has negative impact on the development of broiler chickens, especially on the gastrointestinal tract.

CONCLUSION

Data from this study showed that the increased temperature by 0.95 °C (1.7 °F) in the first 36 hours of incubation had negative impact on late embryonic mortality (P<0.05). Elevated temperature at the beginning of the incubation significantly affected the weight of day-old broiler chickens and the weight of chickens at 24th and 31st day of age (P<0.05), and although there was no difference in feed conversion between the two groups throughout the experimental period, final weight of broiler chickens hatched from eggs incubated at elevated temperature was reduced (P<0.05). The elevated temperature at the first 36 hours of incubation may have a negative effect on the weight of the broiler chickens. If incubating eggs need to be stored, it is recommended to keep the hatchery temperature as close as possible to 38.22 °C (100.8 °F).

ACKNOWLEDGEMENTS

The research was financially supported by the grant No. AF-IGA2020-IP073.

REFERENCES

Arjona, A. et al. 1990. Neonatally-induced thermotolerance: Physiological responses. Comparative Biochemistry and Physiology Part A: Physiology, 95(3): 393–399.

Bhanja, S.K. et al. 2009. Effect of post hatch feed deprivation on yolk-sac utilization and performance of young broiler chickens. Asian-Australasian Journal of Animal Sciences, 22(8): 1174–1179.

Decuypere, E., Michels, H. 1992. Incubation temperature as a management tool. World´s Poultry Science, 56: 367–377.

Dunnington, E.A., Siegel, P.B. 1984. Thermoregulation in Newly Hatched Chicks. Poultry Science, 63(7): 1303–1313.

French, N. 1997. Modeling incubation temperature: the effects of incubator design, embryonic development, and egg size. Poultry Science, 76: 124–133.

Givisiez, P. et al. 2000. Desempenho e resposta ao estresse calórico gradativo de frangos submetidos a estresse de calor e frio durante a incubação. Revista Brasileira de Ciência Avícola (Suplemento), 2(1).

Hill, D. 2001. Chick length uniformity profiles as a field measurement of chick quality. International Hatchery Practice, Avian Poultry Biology Review, 12: 188.

Holoubek, J. et al. 2007. Základy chovu drůbeže. 2nd ed., Praha: Česká zemědělská univerzita.

Hulet, R.M. 2007. Managing Incubation: Where are we and why? Poultry Science, 86(5): 1017–1019.

Ipek, A. et al. 2014. The effects of different eggshell temperature on embryonic development, hatchability, chick, quality, and first-week broiler performance. Poultry Science, 93(2): 464–472.

Joseph, N.S. et al. 2006. The effects of suboptimal eggshell temperature during incubation on broiler chick quality, live performance, and further processing yield. Poultry Science, 85(5): 932–938.

Kadam, M.M. et al. 2008. Effect of in ovo threonine supplementation on early growth, immunological responses and digestive enzyme activities in broiler chickens. British Poultry Science, 49(6): 736–741.

Leksrisompong, N. et al. 2009. Broiler Incubation. 2. Interaction of incubation and brooding temperatures on broiler chick feed consumption and growth. Poultry Science, 88(6): 1321–1329.

Molenaar, R. et al. 2011. High eggshell temperatures during incubation decrease growth performance and increase the incidence of ascites in broiler chickens. Poultry Science, 90(3): 624–632.

Montanhini, N. et al. 2013. The effect of grouping one-day-old chicks by body weight on the uniformity of broilers. The Journal of Applied Poultry Research, 22(2): 245–250.

Musil, F., Tuláček, F. 1964. Líhnutí drůbeže. 1st ed., Praha: Státní zemědělské nakladatelství.

Nakage, E.S. et al. 2003. Effect of temperature on incubation period, embryonic mortality, hatch rate, egg water loss and partridge chick weight (Rhynchotus rufescens). Brasilian Journal of Poultry Science, 5: 131–135.

Nichelmann, M. 2002. Perinatal development of control systems in birds. Comparative Biochemistry and Physiology Part A: Physiology, 131: 697–699.

Pesti, G.M., Bakalli, R.I. 1996. Studies on the Feeding of Cupric Sulfate Pentahydrate and Cupric Citrate to Broiler Chickens. Poultry Science, 75(9): 1086–1091.

Sgavioli, S. et al. 2016. Effect of High Incubation Temperature on Blood Parameters of Layer Chicks. Brasilian Journal of Poultry Science, 18(2): 41–47.

Wilson, H.R. 1991. Interrelationships of egg size, chick size, posthatching growth and hatchability. World's Poultry Science Journal, 47(1): 5–20.

Wineland, M.J. et al. 2004. Incubator Temperature and Oxygen Concentration at the Plateau Stage Affects Intestinal Maturation of Turkey Embryos. International Journal of Poultry Science, 3(6): 378–385.

Yahav, S. et al. 2004. The effect of thermal manipulations during embryogenesis of broiler chicks (Gallus domesticus) on hatchability, body weight and thermoregulation after hatch. Journal of Thermal Biology, 29(4–5): 245–250.

Yahav, S., Hurwitz, S. 1996. Induction of thermotolerance in male broiler chickens by temperature conditioning at an early age. Poultry Science, 75(3): 402–406.

Yalçın, S., Siegel, P.B. 2003. Developmental Stability of Broiler Embryos in Relation to Length of Egg Storage Prior to Incubation. The Journal of Poultry Science, 40(4): 298–308.

Zelenka, J. 2014. Výživa a krmení drůbeže. 1st ed., Olomouc: Agriprint.

Effect of different particle sizes in layer diets on feed consumption, live weight and digestive viscosity

Dana Zalesakova[1], Jakub Novotny[1], Andrea Roztocilova[1], Vojtech Kumbar[2], Eva Mrkvicova[1], Leos Pavlata[1], Ondrej Stastnik[1]
[1]Department of Animal Nutrition and Forage Production
[2]Department of Technology and Automobile Transport
Mendel University in Brno
Zemedelska 1, 613 00 Brno
CZECH REPUBLIC

xzalesa4@node.mendelu.cz

Abstract: The aim of this study was to evaluate the effects of different particle sizes in layers diets on feed consumption, live weight and digestive viscosity. In the experiment, the effects of different particle sizes were investigated on two groups of laying hens of the Bovans Brown hybrid combination aged from 76 to 80 weeks. The first group (n = 8) was fed a finely ground mash (geometric mean diameter – GMD, 632 μm) and the second group (n = 8) was fed a coarsely ground mash (GMD, 1258 μm) with the same nutritional parameters. The particle sizes of the feed mixtures was analysed and compared with the particle sizes of unaccepted residues using a feed separator. During this experiment were not observed statistically significant differences (P>0.05) between both groups in live weight, feed intake and digestive viscosity.

Key Words: Bovans Brown, hens, poultry nutrition, poultry performance, particle size, physical form of feed mixtures

INTRODUCTION

The different particle size of feed mixtures has been the subject of researches and discussions for decades. The appropriate particle size of feed mixtures participates in fulfilment of the genetic potential of modern laying and meat hybrids combinations of poultry (Flock 1998). It also affects other categories of livestock. The appropriately or inappropriately chosen particle size of feed mixture may affect intensity of feed intake, changes in the growth, development and weight of individual sections of the digestive tract, nutrients digestion (Nir et al. 1994) and parameters of laying (Wahlström et al. 1999).

Particle size of feed mixtures can be divided into coarse (<1.4 mm), medium (0.8–1.4 mm), fine (0.4–0.8 mm) and very fine (<0.4 mm) (Wolf et al. 2012). In feed mixtures, all these fractions are usually present in different proportions. Their amount can be determined by dry sieving of a representative sample on the feed separator. From the amount of particles retained on each sieve, the GMD (geometric mean diameter) and GSD (geometric standard deviation) are calculated, which can more accurately characterize the size and structure of the feed mixture for experimental purposes (Amerah et al. 2007). The composition of the feed is also important in determining the appropriate particle size of the feed mixture, especially with a higher proportion of NSP (non-starch polysaccharides) (Lee et al. 2010). NSP increases viscosity of the digestion, which can be described as the intrinsic resistance of a fluid (Ward 1996). Higher viscosity of the digestion mainly occurs when feeding finely ground feed mixtures (Yasar 2003) which may cause difficult nutrient absorption and other problems (Ward 1996).

The aim of this experiment was to determine how the different feed particle size of the feed mixture will affect the monitored parameters of poultry after peak laying period.

MATERIAL AND METHODS

A total of 16 layers, 77-week-old hybrid Bovans Brown, were chosen for the experiment. The experiment lasted for 21 days – from 77th to 80th weeks of hen's age. Hens were divided into two

groups of 8 with 4 repetitions. Hens were placed in air-conditioned room. The air temperature was maintained at 18–20 °C, the relative humidity was in the range of 60–70%. The light mode was set to 18 hours of light and 6 hours of darkness with gradual dimming and switching on, the light intensity was 5–10 lux. The health of the laying hens was checked regularly.

Non-pelleted feed mixture was used for feeding. Layers were fed *ad libitum* every day and had a constant supply of drinking water. The feed mixture was replenished at the same time every day. Residues of feed mixture were regularly collected, weighed and separated. The experimental feed mixture (coarse) contained coarser particles (wheat and corn were ground on a roller mill). The control feed mixture (fine) contained finer particles (wheat and corn were ground on a hammer mill with a 3 mm sieve). The experiment was divided into a preparatory period and a balance period. The preparatory period lasted 7 days (from 76 weeks of age) during which the animals got used to housing and experimental diets. The balance period lasted 21 days. The composition of the feed mixture met the recommended nutritional requirements of the relevant category according to the recommended nutrient content in feed mixtures for laying hens from 45 weeks (Zelenka 2014). Composition of feed mixture and nutrients content of diets are shown in Table 1 and Table 2.

Table 1 Composition of feed mixture

Components (g/kg)	Finely ground mixture	Coarsely ground mixture
Maize	330	330
Wheat	330	330
Soybean meal	193.8	193.8
Limestone	74.1	74.1
Rapeseed oil	31.7	31.7
Vitamin-mineral premix[1]	30	30
Monocalcium phosphate	5	5
Cr_2O_3	3	3
L-Lysine	1.4	1.4
DL-Methionine	1	1

Legend: [1]Vitamin-mineral premix contains (per kg): 0.39 g lysine; 1.35 g methionine; 8.85 g Ca; 2.01 g P; 1.38 g Na; 9.00 mg Cu; 54.00 mg Zn; 60 mg Fe; 72.00 mg Mn; 0.9 mg I; 0.24 mg Se; 9,900 IU vitamin A; 3,000 IU vitamin D_3; 15.00 mg vitamin E; 1.2 mg B_1; 3.6 mg B_2; 1.62 mg B_6; 12.00 mg B_{12}; 0.09 mg biotin; 0.9 mg folic acid; 12.6 mg niacinamide; 7.5 mg calcium pantothenate; 180 mg choline chloride; 0.3 mg butylhydroxyanisole; 1.5 mg butylhydroxytoluene; 3 mg etoxyquin

Table 2 Nutrients content of diets (as fed)

Analysed composition (per kg)	Finely ground mixture	Coarsely ground mixture
AME_N (MJ)[1]	11.45	11.45
Dry matter (g)	880	880
Crude protein (g)	161.2	164.1
Ether extract (g)	44.6	44.7
Crude fiber (g)	18.0	18.4
Ash (g)	117.2	124.8
Calcium (g)	35.6	33.6
Total phosphorus (g)	62.2	65.4

Legend: [1]AME_N – apparent metabolizable energy.

All layers were weighed three times during the experiment: at 76th, 78th and 80th weeks of age. Both coarse and fine feed mixtures and their unaccepted residues were analysed using a feed separator. The mixtures were separated by a cascade of 5 sieves with screen of different sizes: sieve 1 = 3.0 mm; sieve 2 = 2.0 mm; sieve 3 = 1.5 mm; sieve 4 = 1.0 mm; sieve 5 = 0.3 mm. The separation time was 10 minutes and the amplitude was set at 1.80 mm / g. After shaking, the sieves with separated samples were weighed and the weight of each was recorded. After subtracting the weight of the empty sieves,

the weight of the particles adhering to the individual sieves (including the bottom = 0 mm) was determined. Subsequently, GSD, GMD and dMEAN (discrete mean) were calculated.

At the end of the experiment both groups were weighed and slaughtered by decapitation. Next they were bled, skinned, and eviscerated. Then the digestion was removed from the distal part of the *ileum* to determine viscosity. The digestion was collected in tubes and then centrifuged for 10 minutes at 3,000 rpm. The resulting supernatant was pipetted into eppendorf tubes. The samples were analysed for dynamic viscosity on an RST rheometer (Brookfield, USA) with a constant shear strain rate of 50 s^{-1} and a cone-plate geometrical setting (RCT-50-2; α = 2°), including a temperature duplicator. The measurement was performed in 10 replicates at 40 °C and the sample volume was about 2 ml. The obtained data were evaluated by specialized software Rheo300 (Brookfield, USA). This software allows to program measurements, obtain and process data on rheological and viscosity properties of substances. It also allows statistical evaluation and insertion of suitable mathematical models.

The obtained data were processed in Microsoft Excel and StatSoft Statistica, version 12.0.

RESULTS AND DISCUSSION

Different particle size of experimental feed mixtures and feed residues

Different particle size of experimental feed mixtures and unaccepted residues of feed mixtures were determined in the experiment on a feed separator. Figure 1 shows the average weights of the individual fractions of these experimental mixtures.

Figure 1 The mean weight fractions of experimental feed mixtures

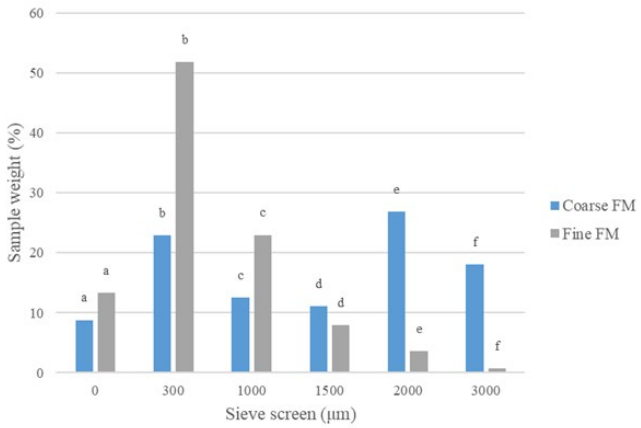

Legend: a:a, b:b, c:c, d:d, e:e, f:f – the same characters indicate a statistically significant differences P<0.05; FM – feed mixture

Based on the determined weights of the feed mixture fractions retained on each sieves, the dMEAN, GMD and GSD of these mixtures were determined, as shown in Table 3.

Table 3 The dMEAN, GMD and GSD values of experimental feed mixtures

	n	dMEAN (mm)	GMD (µm)	GSD (µm)
		Mean ± standard deviation		
Fine	7	1.49 ± 0.01[a]	632.02 ± 11.83[a]	554.95 ± 5.66[a]
Coarse	7	2.91 ± 0.03[b]	1258.18 ± 20.29[b]	1426.19 ± 17.76[b]

Legend: n – number of cases; dMEAN – discrete mean of particle size; GMD – geometric mean diameter; GSD – geometric standard deviation; [a:b] – different characters at a column indicate a statistically significant differences P<0.05

The results show that the values of individual quantities differ significantly for fine and coarse feed mixture. While the dMEAN of finely ground mixture was based on 1.49 mm. the dMEAN of coarsely ground mixture was 2.91 mm, which roughly corresponds to the experiment of Hafeez et al. (2015), where the values of fine versus coarse mixtures were 1.44 mm vs. 2.41 mm. A more generally used value for describing the different particle size of feed and the average particle size relative to the mass representation of the individual fractions is GMD, i.e. the geometric mean diameter of the particles. In our experiment, the GMD of finely ground feed mixture reached

an average value of 632 µm and of coarsely ground feed mixture value of 1258 µm, which is approximately the same as the experiments of other authors who studied the effects of fine and coarser particle structure on poultry performance (Nir et al. 1990: 574 µm vs. 905 µm, Ege et al. 2019: 707 vs. 1096 µm). The GSD, i.e. the geometric standard deviation, in this case relative to mass, determines the extent to which the particle size values deviate from their mean size.

Unaccepted residues of feed mixtures were subjected to the same analysis. The results are shown in Figure 2 and Table 4. According to the scheme of Wolf et al. (2012), in coarse residues of feed mixture compared to coarse feed mixture were almost 4% more coarse particles found and 4% more coarse particles in finely ground mash compared to residues of finely ground feed mixtures. Fine and very fine particles were found to be 3.2% more in coarse feed mixture residues compared to coarse feed mixture and less than 5% more in fine feed mixture residues compared to fine feed mixture. Statistically significant differences ($P<0.05$) are evident between finely ground and coarsely ground feed mixture on all sieves, as well as between fine and coarse feed mixture residues on 0.3, 1, 2 and 3 mm sieves.

Figure 2 The mean weight fractions of unaccepted residues of experimental feed mixtures

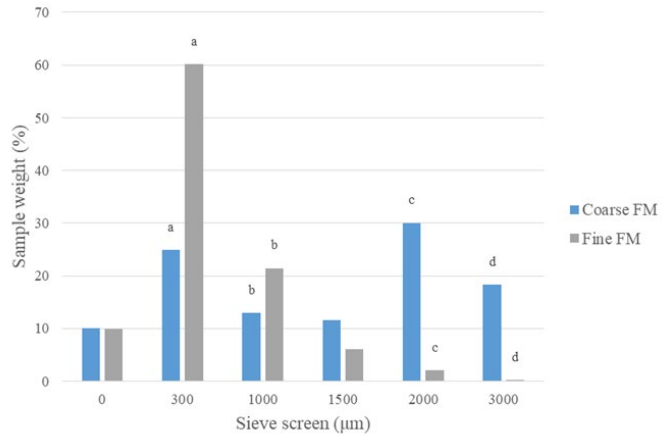

Legend: a:a. b:b. c:c. d:d – the same characters indicate a statistically significant differences P<0.05; FM – feed mixture

Table 4 dMEAN. GMD and GSD of unaccepted residues experimental feed mixture values

	n	dMEAN (mm)	GMD (µm)	GSD (µm)
		Mean ± standard deviation		
Jemná	24	1.41 ± 0.019[a]	625.656 ± 10.337[a]	464.75 ± 9.886[a]
Hrubá	23	3.10 ± 0.211[b]	1263.80 ± 34.331[b]	1440.59 ± 35.770[b]

Legend: n – number of cases; dMEAN – discrete mean; GMD – geometric mean diameter; GSD – geometric standard deviation; [a:b] – different characters at a column indicate a statistically significant differences P<0.05

We found that there was no statistically significant difference ($P>0.05$) between coarse feed mixture and coarse feed mixture residues, as well as between fine feed mixture and fine feed mixture residues. Based on the findings, it can be assumed that the separation, sorting and preference of some fractions of feed mixture compared to others was almost non-existent and their intake by laying hens proceeded at a steady pace. Although some authors mention the preference for larger particles in feed mixtures for poultry (Nir et al. 1994), this has not been proven in our experiment. This can be due to the uniform incorporation of the individual fractions into the feed mixture and the even distribution of the particles of the feed mixtures. It is associated with a lower GSD, also a better uniformity of the particles, which is evident especially in fine mixtures and residues. The time spent selecting and searching for a larger particle is reduced, which saves energy (Amerah et al. 2007).

Feed intake

Feed intake was assessed and evaluated in all laying hens on the basis of continuously collected and weighted unaccepted feed residues. The results are shown in Table 5.

Table 5 Average feed intake of layers

	n	Average feed intake per experiment (g)			Average feed intake per day (g)		
		Mean ± standard deviation					
Fine	8	2,297.13	±	106.41	114.86	±	5.32
Coarse	8	2,433.31	±	178.33	121.67	±	8.92

Legend: n – number of cases; differences between groups are not statistically significant (P>0.05).

According to the Bovans Brown (2018) technology manual, the average feed intake per laying hen at the observed age should be 116 g per day. For laying hens fed finely ground mixture this consumption was slightly lower, for laying hens fed coarsely ground mixture the consumption was higher. Laying hens fed a fine mixture consumed almost 115 g, laying hens fed a coarse mixture then received almost 122 g of feed per day. During the 21 days of the experiment layers consumed almost 2,300 g of the fine mixture and 2,433 g of the coarse mixture. Although there was no statistically significant difference (P>0.05) in our results. Safaa et al. (2009) observed a higher feed intake in laying hens fed coarsely ground cereals. The same findings were reached by Nir et al. (1990) and Amerah et al. (2007). In general, it can be stated that poultry will be more willing to accept feed mixtures with a coarser structure. In addition, some recent research confirms that the weight of gizzard and pancreas increases during intake of coarser mixtures (Ege et al. 2019), which favorably affects intestinal motility (Ferket 2000).

Live weight

The live weight of the laying hens was recorded continuously at 76th. 78th and 80th weeks of age. The results are shown in Figure 3.

Figure 3 Average live weight of laying hens

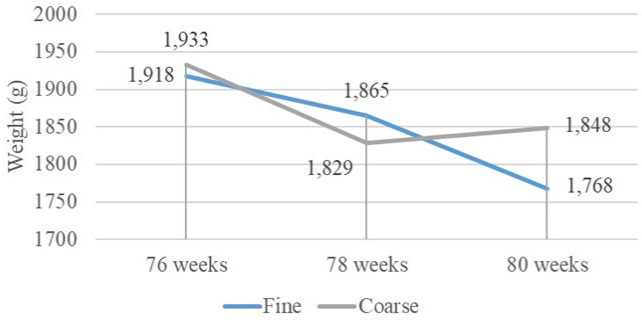

At the beginning of the experiment, the live weight of both groups of layers was almost the same (1,918 g "fine" vs. 1,933 g "coarse"). Over the next few weeks, both groups gradually lost weight. This trend persisted, especially in laying hens fed a finer mixture, which weighted 1,768 g at the end of the experiment. It was 80 g less than laying hens fed a coarser mixture (1,848 g). They had been losing weight until the age of 78 weeks and then their weight started to gradually increase. However, the differences in weights between the two groups were not statistically significant (P>0.05).

According to the Bovans Brown (2018) technology manual, laying hens from 76th to 80th weeks of age should weigh 1,993–1,996 g. In our experiment these results were not obtained, but the gradual weight loss in laying hens at this age may be caused by slower adaptation to the housing and feeding system, which lasted until the end of the balance period. The small weight gain in layers fed a coarser mixture is supported by experiments performed by Nir et al. (1990), Amerah et al. (2007) and others. Therefore, it can be stated that the use of coarser particles in non-pelleted feed mixtures can more effectively support the willingness to eat and positively affect the live weight of poultry.

Viscosity of the digestion

The viscosity of the digestion was measured after the end of the experiment by sampling from the distal part of the ileum. Viscosity of the digestion in layers fed by finely ground feed mixture was 5.55 ± 0.46 mPa·s and the result in layers fed by coarsely ground feed mixture was 6.10 ± 0.74 mPa·s.

Between two groups of layers were no observed statistically significant difference (P>0.05) in the viscosity of digestion. In our experiment, therefore, it does not affect the change in viscosity of the digestion, which would be caused by a different structure of feed mixture. Yasar (2003), on the other hand, found, that poultry fed a fine mixture based on wheat had a high viscosity of the digestion compared to those groups fed medium or coarse wheat particles. The feed composition and especially the higher proportion of NSPs play an important role in increasing the viscosity of digestion, as confirmed by for example Lee et al. (2010).

CONCLUSION

Feed intake, live weight and digestion viscosity were monitored in laying hens after peak laying period. Our experiment did not show any statistically significant differences in parameters between the group fed the fine feed mixture and the group fed the coarse feed mixture.

ACKNOWLEDGEMENTS

The research was financially supported by the Internal Grant Agency of Faculty of AgriSciences (Mendel University in Brno) no. AF-IGA2020-IP064.

REFERENCES

Amerah, A.M. et al. 2007. Feed particle size: Implications on the digestion and performance of poultry. World's Poultry Science Journal, 63(3): 439–455.

Bovans Brown: Technologický návod 2018. Žabčice: INTEGRA. 35 p. Available at: https://www.integrazabcice.cz/documents/320/BOVANS_BROWN_TN_2018_web.pdf [2020-09-10]

Ege, G. et al. 2019. Influence of feed particle size and feed form on productive performance. egg quality. gastrointestinal tract traits. digestive enzymes. intestinal morphology. and nutrient digestibility of laying hens reared in enriched cages. Poultry Science, 98(9): 3787–3801.

Ferket, P. 2000. Feeding whole grains to poultry improves gut health. Feedstuffs. 72(37): 12–13.

Flock, D.K. 1998. Genetic-economic aspects of feed efficiency in laying hens. World's Poultry Science Journal, 54(3): 225–239.

Hafeez, A. et al. 2015. Implication of milling methods. thermal treatment. and particle size of feed in layers on mineral digestibility and retention of minerals in egg contents. Poultry Science, 94(2): 240–248.

Lee, S.Y. et al. 2010. Effects of multiple enzyme (Rovabio® Max) containing carbohydrolases and phytase on growth performance and intestinal viscosity in broiler chicks fed corn-wheat-soybean meal based diets. Asian-Australasian Journal of Animal Sciences, 23(9): 1198–1204.

Nir, I. et al. 1990. Effect of particle size of sorghum grains on feed intake and performance of young broilers. Poultry Science, 69(12): 2177–2184.

Nir, I. et al. 1994. Effect of particle size on performance.: 1. Corn. Poultry Science, 73(1): 45–49.

Safaa, H.M. et al. 2009. Effect of main cereal of the diet and particle size of the cereal on productive performance and egg quality of brown egg-laying hens in early phase of production. Poultry Science, 88(3): 608–614.

Wahlström, A. et al. 1999. Production and egg quality as influenced by mash or crumbled diets fed to laying hens in an aviary system. Poultry Science, 78(12): 1675–1680.

Ward, N. 1996. Intestinal viscosity. broiler performance. Poultry Digest, 55: 12–17.

Wolf, P. et al. 2012. Einfluss der Partikelgröße im Futter auf die Nährstoffverdaulichkeit und Leistung beim Schwein. Übersichten zur Tierernährung, (40): 21–64.

Yasar, S. 2003. Performance. gut size and ileal digesta viscosity of broiler chickens fed with a whole wheat added diet and the diets with different wheat particle sizes. International Journal of Poultry Science, 2(1): 75–82.

Zelenka, J. 2014. Výživa a krmení drůbeže. Olomouc: Agriprint.

FISHERIES AND HYDROBIOLOGY

The effects of microplastic on haematological and biochemical parameters in fish

Aneta Hollerova[1,2], Nikola Hodkovicova[2], Martin Faldyna[2], Jana Blahova[1]
[1] Department of Animal Protection and Welfare & Veterinary Public Health
University of Veterinary and Pharmaceutical Sciences
Palackeho tr. 1, 612 42 Brno
[2] Department of Infectious Diseases and Preventive Medicine
Veterinary Research Institute
Hudcova 296/70, 621 00 Brno
CZECH REPUBLIC

H19003@vfu.cz

Abstract: Microplastics (MPs) are 20 µm to 5 mm large plastic particles that are a frequent contaminant of the aquatic environment. Knowledge of their impact on aquatic organisms are limited. In our assay, we targeted on polyethylene microparticles to assess their impact on the rainbow trout haematological and biochemical parameters. Four groups of fishes were used; the first was the control group, the second group was exposed to 0.5% MPs, the third group was exposed to 2% MPs, and the fourth group was exposed to 5% MPs for 6 week. Our study showed that polyethylene microparticles affect some haematological and biochemical parameters. Leukocytes (significant decline) and haematocrit level (significant increment) after exposure to microplastics compared to control group from haematological parameters were affected. Biochemical parameters (ALT, ammonia, lactate) showed significant decrease after exposure to microplastics compared to control group. This study revealed that MPs may have an important impact on the haematological and biochemical parameters which in turn may influence fish behaviour and endanger their health.

Key Words: aquatic environment, pollution, rainbow trout, plastic, polyethylene

INTODUCTION

Due to low weight and their resistance, plastic polymers can be transported over long distances and the related environmental hazard raises worldwide concerns (Derraik 2002). Up to 10% of plastic fragments end up in the oceans because of the extensive use of plastic materials, increasing production and most importantly improper waste management (Li et al. 2018).

Scientists started to raise questions about where all the disappeared plastic waste had gone, because plastics are well-resistant synthetic polymers. The disappearance of plastics suggests that smaller particles (meso-, micro-, nano-) are generated by fragmentation of larger plastic debris (Eerkes-Medrano et al. 2015). Furthermore, they enter aquatic environment from cosmetics, clothing and many other industrial manufacturing sectors. Microplastics are spread in aquatic, atmospheric and terrestrial environments due to their small size and ubiquity showing their high bioavailability. The presence of these particles has been demonstrated in the digestive tracts of most aquatic organisms at various trophic levels and evidence of negative effects has been found in relation to their effects on oxidative stress, mortality, fertility, immune system and metabolic processes (Cooper and Corcoran 2010, Ryan et al. 2009).

In our study, we tested polyethylene particles with mean size 40–48 µm (Sigma-Aldrich, USA). Their impact on rainbow trout *(Oncorhynchus mykiss)* was tested for six weeks of oral application. Microplastics were mixed into the feed at three tested concentrations" 0.5%, 2% and 5%, and subsequently compared to the control group. The main aim of our experiment was to determine the potential influence of polyethylene microparticles on the haematological and biochemical parameters of rainbow trout.

MATERIAL AND METHODS

Our experiment was conducted in 160 juvenile rainbow trout (average body length 179.6 ± 8.9 mm, average body weight 89.4 ± 0.2 g). Fish were first acclimated for two weeks to laboratory conditions. Subsequently, the fish were allocated into 8 aquariums of 20 fish each; aquaria were connected to the recirculation system. The conditions of the water in every aquarium were monitored every 12 hour and the average parameters were as follow: temperature 17.9 ± 0.1 °C, oxygen saturation 8.3 ± 0.1 mg/L, pH 7.3 ± 0.1, total ammonia < 0.01 mg/L, chlorides 141.7 ± 6.7 mg/L, nitrites < 0.01 mg/L. The test was conducted in duplicate – two aquariums were exposed to 0.5% polyethylene concentration in feed (E1), another two to 2% concentration (E2) and the last two to 5% concentration (E3). Two aquariums served as control (K) and were exposed to 0% concentration of polyethylene. The fish were fed 3 times per day at a total dose of 1.5% of their body weight/day. This dose was adjusted every 2 weeks according to the current weight of the fish. The experimental phase lasted six weeks and a total of three samplings were performed during the course of the experiment – at 2nd and 4th week, and the entire trial was completed at 6th week with final sampling. One fish was culled as part of the experiment, at the highest concentration tested.

A blood sample was taken from each fish into a heparinised syringe for the determination of basic haematological and biochemical parameters. Subsequently, the fish were stunned by a blunt blow to the head, killed by cutting the gill arches, and each piece was individually measured for basic biometric parameters (body mass, liver mass, total length, width, height). The data obtained was submitted for statistical analysis in which always the control group was compared to the experimental group. At first, the data were tested for normality and if achieved, the ANOVA testing was made; otherwise the data were subjected to Mann-Whitney test. In both testing, the statistical significance was considered when * $p<0.05$ and ** $p<0.01$.

The samples of blood were used to determine the number of red blood cells (RBCs) and the number of white blood cells (WBCs). The results were obtained by counting the cells in Burker's hemocytometer after diluting heparinized blood with Natt-Herick solution in a 1:200 ratio. The microhematocrit method, with centrifugation of capillaries containing blood samples, was used to determine haematocrit levels. Furthermore, in our experiment, a photometric method was used with cyanohaemoglobin at 540 nm, which was used to determine haemoglobin (Hb). Subsequently, the mean haemoglobin of erythrocytes (MCH), the mean erythrocyte volume (MCV) and the mean haemoglobin concentration in the body (MCHC) were detected by using the following formulas:

$$MCH\ [pg] = \frac{Hb}{RBC} \times 10 \qquad MCV\ [fl] = \frac{PVC}{RBC} \times 10 \qquad MCHC\ [\%] = \frac{Hb}{PVC} \times 100$$

Blood samples were centrifuged at 800 x g at 4°C for 10 minutes to obtain blood plasma. Subsequently, biochemical parameters were determined from the blood plasma as levels of albumin (ALB), alkaline phosphatase (ALP), alanine aminotransferase (ALT), aspartate aminotransferase (AST), calcium (Ca), cholesterol (CHOL), glucose (GLU), lactate (LACT), lactate dehydrogenase (LDH), phosphorus (PHOS), triglycerides (TG) and total protein (TP). All biochemical analysis were made according to manufacturer´s instruction with using a commercial kit (BioVendor PLC, Czechia) and biochemical analyser Konelab 20i (Thermo Fisher Scientific, Czechia).

RESULTS AND DISCUSSION

There was no statistically significant difference in biometric parameters when evaluating the results of the effect of applying polyethylene microparticles in feed. Out of haematological parameters a statistically significant decrease in leukocytes with increasing concentrations of microparticles were found relative to the length of the experiment.

Haematocrit showed a statistically significant increase in E1, E2 and E3 in the first sampling and E3 in the third sampling in comparison with the control group. Haematological parameters are very important measures which reflect fish health status (Thummabancha et al. 2016). Many studies have shown that haematocrit of fish displayed decreased values after exposure to different pollutants under laboratory conditions (Osman et al. 2018). Significant decrement in haematocrit values may be imputed

to haem-dilution of blood due to the damage of tissues or haemolysis caused by microplastics toxicity (Lal Shah 2010). The decrease of leukocytes may be due to the negative effect of microplastics on lymphoid tissues of the exposed fish (Alkaladi et al. 2015). Furthermore, the uptake of these particles may lead to alteration of the immune system with impact on animal defence and health (Espinosa et al. 2017). The immune system may be interacting due to many potentially toxic chemical substances that microplastics might contain, absorb or release them. They may physically block the digestive organs, which decrease the absorption of nutrients (Cole et al. 2011). The reduction of leukocytes may result from bioaccumulation of the pollutants it the tissues and may be detected after the recovery period (Martins and Guilhermino 2018).

Figure 1 Graphic representation of leukocyte and haematocrit values. K1–3 – control group (first to third sampling), E1 1–3 (experimental group E1, first to third sampling), E2 1–3 (experimental group E2, first to third sampling, E3 1–3 (experimental group E3, first to third sampling)

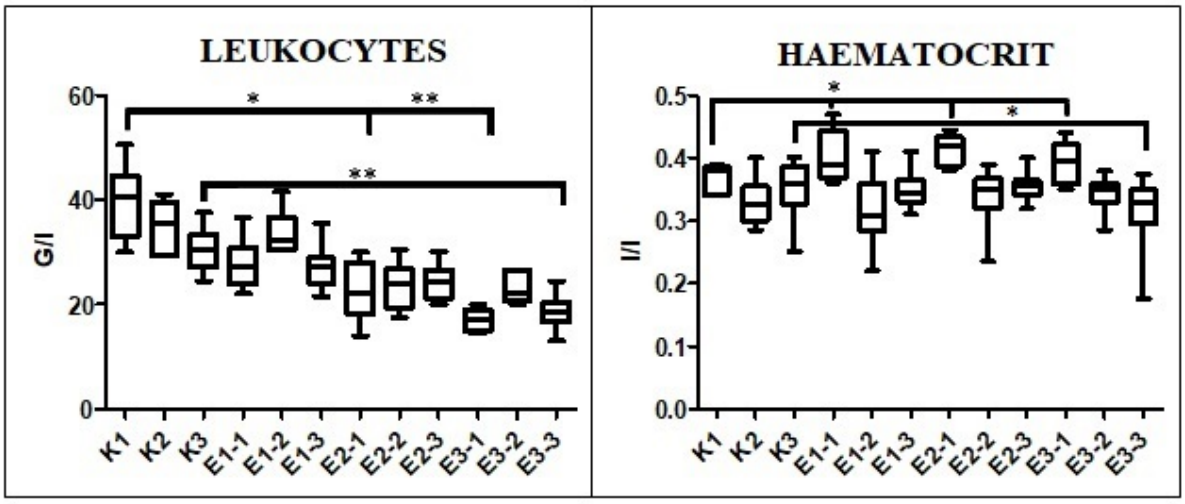

Table 1 Results of biochemical analysis

	First sampling				Second sampling			
	K1	E1–1	E2–1	E3–1	K2	E1–2	E2–2	E3–2
ALT (µkat/l)	0.37 ±0.14	0.47 ±0.15	0.51 ±0.28	0.44 ±0.12	0.41 ±0.14*	0.39 ±0.13	0.29 ±0.07	0.22 ±0.07*
AMON (µmol/l)	1024.0 ±93.9	928.6 ±75.2	755.9 ±71.2	665.0 ±57.8	837.5 ±89.6 **	694.6 ±64.6	612.9 ±83.1	485.5 ±77.1 **
LACT (mmol/l)	5.6 ±1.3**	3.4 ±1.0	4.1 ±1.6	2.3 ±0.8**	4.3 ±1.0	3.4 ±1.0	4.0 ±1.4	3.1 ±1.2
	Third sampling							
	K3	E1–3	E2–3	E3–3				
ALT (µkat/l)	0.33 ±0.14	0.29 ±0.07	0.33 ±0.12	0.33 ±0.08				
AMON (µmol/l)	539.8 ±83.4	467.9 ±73.5	470.6 ±114.3	404.8 ±65.7				
LACT (mmol/l)	3.7 ±1.4	3.9 ±1.1	4.3 ±1.4	3.9 ±1.4				

Legend: ALT – alanine aminotransferase, AMON – ammonia, LACT – lactate. Average ± SD

The biochemical examination found a statistically significant decrease in alanine-aminotransferase levels (ALT), specifically in E3 group as part of the second sampling. In accordance with our results, changes in this parameter were detected in common goby *(Pomatoschistus microps)* after exposures to microplastics and pyrene (Oliveira et al. 2013). This enzyme is present in cells of different organs of body systems. ALT is important for the transamination of amino acids and is also an important serum marker of hepatic damage (Solter et al. 2000). Changes in its levels could be sign of the hepatic system disruption caused by polyethylene, due to ALT is a specific serum marker of hepatic damage (Solter et al. 2000). Ammonia levels almost halved in the E3 group versus control group at the second tome of sampling and there was also statistically significant decrease in values of lactate in the E3 group, in turn during the first sampling. In many studies, an increase values of both parameters are observed (Yin et al. 2019, Qiao et al. 2019). Therefore, further experiment

on these subjects will be needed. Other values of our biochemical analysis did not show statistical significance in compare a check at the same sampling time. The resulting data is presented in Table 1.

CONCLUSION

The aim of this study was to assess the impact of microplastics contaminating fish feed on the non-target rainbow trout (*Onchorhynchus mykiss*) organism. In conclusion, our study demonstrated that polyethylene microparticles caused some changes in haematological and biochemical parameters. Nevertheless, these results need to be completed at least with histopathological analysis and analysis of differential leukocyte count to evaluate their possible harmful effect on trout's organism. These data are currently analysed and will be hereafter published.

ACKNOWLEDGEMENTS

This research was supported by the Internal Grant Agency of the University of Veterinary and Pharmaceutical Sciences Brno [no. 212/2019/FVHE] and by the ERDF/ESF "Profish" [no. CZ.02.1.01/0.0/0.0/16_019/0000869].

REFERENCES

Alkaladi, A. et al. 2015. Hematological and biochemical investigations on the effect of vitamin E and C on *Oreochromis niloticus* exposed to zinc oxide nanoparticles. Saudi Journal of Biological Sciences, 22(5): 556–563.

Cole, M. et al. 2011. Microplastics as contaminants in the marine environment: a review. Marine Pollution Bulletin, 62(12): 2588–2597.

Copper, D.A., Corcoran, P.L. 2010. Effects of mechanical and chemical processes on the degradation of plastic beach debris on the island of Kauai, Hawaii. Marine Pollution Bulletin, 60(5): 650–654.

Derraik, J.G. 2002. The pollution of the marine environment by plastic debris: a review. Marine Pollution Bulletin, 44(9): 842–852.

Eerkes-Medrano, D. et al. 2015. Microplastics in freshwater systems: A review of the emerging threats, identification of knowledge gaps and prioritisation of research needs. Water Research, 75: 63–82.

Espinosa, C. et al. 2017. Effects of dietary polyvinylchloride microparticles on general health, immune status and expression of several genes related to stress in gilthead seabream (*Sparus aurata* L.). Fish Shellfish Immunology, 68: 251–259.

Lal Shah. S. 2010. Hematological changes in *Tinca tinca* after exposure to lethal and sublethal doses of Mercury, Cadmium and Lead. Iranian Journal of Fisheries Sciences, 9(3): 434–443.

Li, J. et al. 2018. Microplastics in freshwater systems: A review on occurrence, environmental effects, and methods for microplastics detection. Water Research, 137: 362–374.

Martins, A., Guilhermino, L 2018. Transgenerational effects and recovery of microplastics exposure in model populations of the freshwater cladoceran *Daphnia magna Straus*. Science of Total Environment, 631–632: 421–428.

Oliveira, M. et al. 2013. Single and combined effects of microplastics and pyrene on juveniles (0+ group) of the common goby *Pomatoschistus microps* (Teleostei, Gobiidae). Ecological Indicators, 34: 641–647.

Osman, A. et al. 2018. Blood Biomarkers in Nile tilapia *Oreochromis niloticus Niloticus* and African Catfish *Clarias gariepinus* to Evaluate Water Quality of the River Nile. Journal of Fisheriessciences.com, 12(1): 001–015.

Qiao, R. et al. 2019. Microplastics induce intestinal inflammation, oxidative stress, and disorders of metabolome and microbiome in zebrafish. Science of the Total Environment, 66: 246–253.

Ryan, P.G. et al. 2009. Monitoring the Abundance of Plastic Debris in the Marine Environment. Philosophical Transactions: Biological Sciences, 364(1526): 1999.

Solter, P. et al. 2000. Decreased Hepatic ALT Synthesis is an Outcome of Subchronic Microcystin-LR Toxicity. Toxicology and Applied Pharmacology, 164: 216–220.

Thummabancha, K. et al. 2016. Analysis of hematologic alterations, immune responses and metallothionein gene expression in Nile tilapia (*Oreochromis niloticus*) exposed to silver nanoparticles. Journal of Immunotoxicology, 13(6): 909–917.

Yin, L. et al. 2019. Impacts of polystyrene microplastics on the behavior and metabolism in a marine demersal teleost, black rockfish (*Sebastes schlegelii*). Journal of Hazardous Materials, 380: 120861.

Effects of diclofenac and ibuprofen on fish embryos

Denisa Medkova[1,2], Pavla Sehonova[2], Jana Blahova[2], Eva Postulkova[1], Zdenka Svobodova[2], Jan Mares[1]
[1]Department of Zoology, Fisheries, Hydrobiology and Apiculture
Mendel University in Brno
Zemedelska 1, 613 00 Brno
[2]Department of Animal Protection and Welfare & Veterinary Public Health
University of Veterinary and Pharmaceutical Sciences
Palackeho tr. 1, 612 42 Brno
CZECH REPUBLIC

H19004@vfu.cz

Abstract: Contamination of aquatic environment results in negative effects on both human and aquatic biota. Diclofenac and ibuprofen are commonly used pharmacologically active substances, which are found in aquatic environment. Occurrence of their residues in the aquatic environment is caused by constantly increasing consumption, discharge in wastewater and its imperfect purification in wastewater treatment plants. The aim of this study was to assess the impact of diclofenac and ibuprofen residues on embryonic stages of zebrafish (*Danio rerio*). The study was performed according to the acute toxicity test on zebrafish embryos guideline no. 236. Six different concentrations of diclofenac and ibuprofen were tested. Lethal and various sublethal effects of diclofenac and ibuprofen were observed at concentrations ranging from 2 000 µg/l to 20 000 µg/l. The most frequently negative effect was observed on the cardiovascular system, where heart edema of embryos occurred. Moreover, the results suggest negative effects on hatching. For example in the end of the experiment at the highest tested concentration of ibuprofen was hatched only 37.14% embryos. Our study showed that the non-steroidal anti-inflammatory drugs (NSAIDs) diclofenac and ibuprofen have a negative effect on the development of fish embryos.

Key Words: toxicity test, malformation, mortality, edema, *Danio rerio*

INTRODUCTION

In the few past decades, water pollution caused by pharmacologically active substances has become a commonly discussed issue. Such a pollution has a potential to negatively affect non-target organisms. The most sensitive to veterinary and human pharmacologically active substances are the early life stages. Various fish species are used as valid model organisms to monitor the quality of effluents, surface water and toxicity of chemicals. The most commonly used fish species are zebrafish (*D. rerio*), common carp (*Cyprinus carpio*), rainbow trout (*Oncorhynchus mykiss*), Japanese rice fish (*Oryzias latipes*), and guppy *(Poecilia reticulata)* (Sehonova et al. 2016).

Diclofenac and ibuprofen belong among the group of non-steroidal anti-inflammatory drugs (NSAIDs), which are used to reduce inflammation, pain and fever. Since ibuprofen and diclofenac are the two most prescribed drugs of the NAIDs group, it is necessary to monitor their effect on non-target fish (Zhang et al. 2020). For example, in Spain the concentrations in surface water were up to 4.6 µg/l and 1.1 µg/l for ibuprofen and diclofenac, respectively (Zhang et al. 2020). The aim of the present study was to evaluate the potential negative effect of diclofenac and ibuprofen residues on zebrafish embryos in order to widen the current level of knowledge concerning the effects of NSAIDs on non-target aquatic biota.

MATERIAL AND METHODS

The experiment was performed according to the Guideline for Test No. 236: Fish Embryo Acute Toxicity (FET) (OECD 2013) for the period of 96 hours with six different concentrations of each test substances and two control groups. Fertilized eggs without obvious irregularities were visually selected using binocular microscope. Fertilized eggs of zebrafish were distributed into microwell

plates with 48 wells on each plate. For each concentration, 18 embryos were used. The test was performed in duplicate. Diclofenac and ibuprofen were tested at concentrations of 0.2 µg/l (environmentally relevant), 2 µg/l, 20 µg/l (wastewater relevant), 200 µg/l, 2 000 µg/l, and 20 000 µg/l. Diclofenac and ibuprofen are insoluble in water, therefore a solvent DMSO was used. The control group was exposed to dilution water prepared according ISO 7346 (ISO, 1996) and second control group was exposed to dilution water prepared according to ISO 7346 with addition of DMSO. In order to ensure that real concentration values did not fall under 80% of the nominal concentration, the tested solutions were renewed every 24 hours. Temperature during the test was 26 °C and photoperiod was 12 hours light/12 hours dark. Water with tested substances was completely changed every day for new water with appropriate concentrations of diclofenac and ibuprofen.

In order to evaluate the toxic effects, four indicators of mortality, in particular coagulation of fertilized eggs, lack of somite formation, lack of detachment of the tail-bud from the yolk sack and the lack of heartbeat, were observed, followed by sub-lethal endpoints observation, such as hatching rate or various developmental malformations (OECD 2013).

Statistical analysis was conducted using Unistat 5.6 (Czech Republic). Cumulative mortality, early ontogeny and hatching data were analyzed using chi-square and contingency tables.

RESULTS AND DISCUSSION

Diclofenac and ibuprofen were described in various studies to have a negative impact on hatching and also physical activity of zebrafish (Xia et al. 2017).

Table 1 Type of the malformation caused by diclofenac on zebrafish (D. rerio) embryos in different concentrations

Concentration	Number	Type of malformation
Control	1x	less pigment
Control	1x	more pigmet
Control DMSO	1x	less pigment
0.2 µg/l	1x	deformation of tail
0.2 µg/l	3x	blood clot
0.2 µg/l	1x	heart edema
2 µg/l	2x	heart edema
20 µg/l	2x	heart edema
20 µg/l	1x	blood clot
200 µg/l	4x	heart edema
2 000 µg/l	10x	heart edema
2 000 µg/l	4x	heart edema and blood clot
2 000 µg/l	5x	blood clot
2 000 µg/l	1x	less pigment
2 000 µg/l	1x	heart edema and deformation of spine
20 000 µg/l	15x	total malformation
20 000 µg/l	11x	heart edema and total malformation
20 000 µg/l	2x	heart edema, blood clot and total malformation
20 000 µg/l	5x	deformation of tail
20 000 µg/l	1x	heart edema and deformation of spine
20 000 µg/l	1x	heart edema and deformation of tail

In our study, only the highest tested concentrations of diclofenac influenced the mortality rate of zebrafish embryos. Significantly higher mortality was observed at 72 hours post fertilization (hpf) in the group exposed to 20 000 µg/l diclofenac compared to the control. Mortality at this concentration was 100% of zebrafish specimen ($p<0.01$). In case of ibuprofen, no significant effects on mortality were observed among groups.

At 48 hpf, exposure to diclofenac at the concentrations of 2 000 µg/l and 20 000 µg/l revealed increased number of malformations in comparison with the control. Malformation rate at the concentration of 2 000 µg/l was 25% of zebrafish specimen ($p<0.05$) and at the concentration of 20 000 µg/l 97.22% of zebrafish specimen ($p<0.01$). At 72 hpf, ibuprofen at the concentration of 20 000 µg/l caused at least one type of malformation to 77.7% of zebrafish specimen ($p<0.01$). The most common malformations were heart edema and blood clot (Table 1 and Table 2). The results of this study and results reported by Zhang et al. (2020) suggest that diclofenac and ibuprofen have negative effects on zebrafish heart.

Figure 1 Heart edema and blood clot in zebrafish embryo at 96 hpf after exposure to 2 000 µg/l of diclofenac (A). Heart edema and blood clot non-hatching zebrafish embryo at 72 hpf after exposure to 20 000 µg/l of ibuprofen (B).

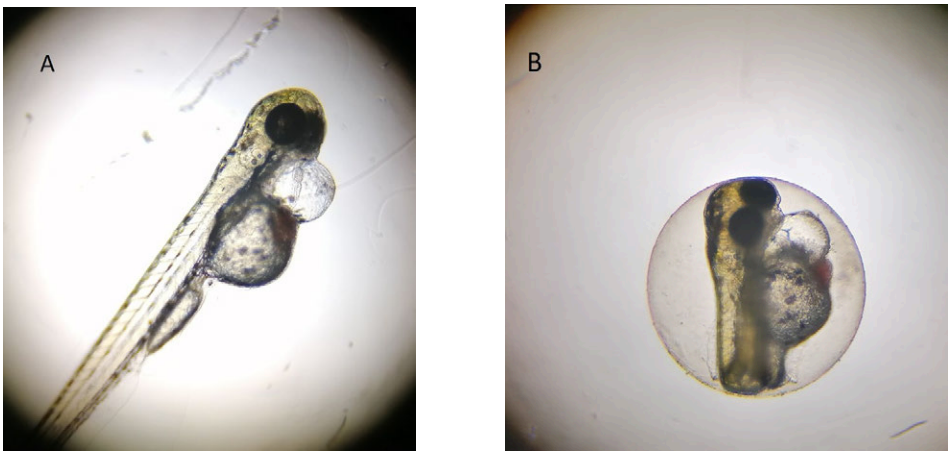

Table 2 Type of the malformation caused by ibuprofen on zebrafish (D. rerio) embryos in different concentrations

Concentration	Number	Type of malformation
Control	1x	less pigment
Control	1x	more pigmet
Control DMSO	1x	less pigment
0.2 µg/l	1x	deformation of tail
2 µg/l	1x	blood clot
2 µg/l	1x	heart edema
20 µg/l	1x	heart edema and blood clot
20 µg/l	2x	heart edema
200 µg/l	1x	heart edema
2 000 µg/l	2x	blood clot
2 000 µg/l	1x	heart edema and blood clot
20 000 µg/l	3x	heart edema and deformation of tail
20 000 µg/l	15x	heart edema
20 000 µg/l	9x	heart edema and blood clot
20 000 µg/l	2x	heart edema, blood clot and less pigment
20 000 µg/l	1x	blood clot
20 000 µg/l	1x	heart edema and lees pigment

Furthermore, diclofenac and ibuprofen were found to affect hatching. At 72 hpf, exposure to diclofenac at the concentration of 0.2 µg/l and 2 µg/l caused that only 25% of embryos were hatched, which was significantly less compared to the control ($p<0.01$). In contrast, ibuprofen affected hatching on at the highest tested concentrations of 2 000 µg/l and 20 000 µg/l ($p<0.01$) in comparison with the control. At 96 hpf at the concentration of 20 000 µg/l was hatched 37.14%, whereas

in the control it was 100% ($p<0.01$). Similarly to the results of our study, Xia et al. (2017) reported delayed hatching at a concentration of 500 µg/l ibuprofen and 500 µg/l and 5 µg/l of diclofenac.

CONCLUSION

In conclusion, the present study demonstrated that diclofenac and ibuprofen negatively affect hatching of zebrafish embryos. Even if no changes such as mortality or malformations were observed at the environmentally relevant concentrations, these substances have the ability to negatively affect development and welfare on fish embryos at high tested experimental concentration. NOEC was determined only for ibuprofen (200 µg/l) since it was not possible to establish it for diclofenac. In case of diclofenac, significant changes has been observed from the lowest tested concentration of 0.2 µg/l (LOEC). LOEC for ibuprofen was determined to be 2 000 µg/l. For this reason, it is important to continuously monitor the concentrations of diclofenac and ibuprofen in surface water.

ACKNOWLEDGEMENTS

This research was supported by project PROFISH – Mendel University in Brno, CZ.02.1.01/0.0/0.0/16_019/0000869.

REFERENCES

ISO 7346. 1996. Waterquality – Determination of the acute lethal toxicity of substances to a freshwaterfish [*Brachydanio rerio* Hamilton-Buchanan (Teleostei, *Cyprinidae*)] – Part 1: Static method.

OECD. 2013. Test No 236: Fish Embryo acute Toxicity (FET) Test. OECD Guidelines for the Testing of Chemicals, Section 2, OECD Publishing, Paris, France.

Sehonova, P. et al. 2016. Embrya ryb jako alternativní modely v toxikologii. Veterinářství, 66(9): 692–696.

Xia L. et al. 2017. Effects of ibuprofen, diclofenac and paracetamol on hatch and motor behavior in developing zebrafish (*Danio rerio*). Chemosphere [Online], 182: 416–425. Available at: http://dx.doi.org/10.1016/j.chemosphere.2017.05.054. [2020-09-10].

Zhang K. et al. 2020. Ibuprofen and diclofenac impair the cardiovascular development of zebrafish (*Danio rerio*) at low concentrations. Environmental Pollution [Online], 258. Available at: https://doi.org/10.1016/j.envpol.2019.113613. [2020-09-10].

WILDLIFE RESEARCH

Interesting findings of beetles (Coleoptera) from Cerová vrchovina Upland in Slovakia

Attila Balazs[1], Tomas Kopecky[2], Jan Bezdek[1]
[1]Department of Zoology, Fisheries, Hydrobiology and Apiculture
Mendel University in Brno
Zemedelska 1, 613 00 Brno
[2]Jamenska 346, 561 64 Jablonne nad Orlici
CZECH REPUBLIC

balazsaeko@gmail.com

Abstract: Entomological research was launched in 2019 and 2020 in Cerová vrchovina Upland. The occurrence of *Variimorda* (*Galeimorda*) *hladili* Horák, 1985 (Mordellidae) in Slovakia is confirmed. The data for three very rare beetle species are presented: *Zonitis flava* Fabricius, 1775 (Meloidae), *Odontosphindus grandis* (Hampe, 1861) (Sphindidae), *Cassida aurora* Weise, 1907 (Chrysomelidae).

Key Words: pasturelands, Insecta, Mordellidae, Meloidae, Sphindidae, Chrysomelidae

INTRODUCTION

At the beginning of the 20th century, rural areas in central Europe were frequently under immense environmental pressure due to human activities. Mistreatment of water resources, in conjunction with the arrival of large-scale agriculture, contributed to the most devastating ones (Azadi et al. 2020). Today, some people are trying to help to the country to recover from its damages, but often, establishments are still looking to benefit when it comes to natural resources.

Despite the various negative changes to land use, such as the abandonment of traditional farming (e.g. cattle grazing and skiving) and replacement of it with modern commercial technologies, insensible forest management regulations (e.g. irrational exploitations of primary forests), mining operations, droughts, and global warming, Cerová vrchovina Upland still offers treasures for entomological researchers (Szirácsik 2010, Dulák and Kovalčík 2010).

Cerová vrchovina Upland is situated in the south of central Slovakia, in the imaginary borders of the Alpine and Pannonian bioregions. In the second half of the 20th century, the most valuable biotopes and geotopes were recognised and declared small protected units, and later in 1989, the Protected Landscape Area, Cerová vrchovina, was established. As a matter of fact, diverse geomorphological relief with major altitudinal inclines enriches the diversity of species with a wide variety of habitats. The shallow soils that are characterised by heliothermic Pannonian flora, on the southern slopes of volcanic hills, strike a sharp contrast with the wet beech forests on the northern slopes. The vast lowlands with their creeks, rivers, and dams, between these highlands, further enhance the biological diversity in this dry Mediterranean-like region (Csiky et al. 2010).

It is clear now that there is a worldwide decline in insect species. As they are the primary consumers of biomass, they react to the environmental alteration immediately. Moreover, countless insect species have complex and delicate ecological requirements; therefore, they respond to these changes sensitively (Bell et al. 2020). To capture the remaining rare insect species of the erstwhile extraordinary diversity of Cerová vrchovina, we launched intensive and long-term research in 2019.

These enhanced efforts, which used several types of collecting approaches never applied before, resulted in the discovery of numerous unusual insect species. Regarding the entomological research in Slovakia, this is currently one of the most researched regions in the country. In this article, we report the most erratic insect species. Some of them are rediscoveries at a national scale, whereas other findings are interesting from a biogeographical point of view.

MATERIAL AND METHODS

Sampling

We conducted a several research expeditions in Cerová vrchovina Upland every season during 2019 and 2020. The study was conducted on various types of habitats including but not limited to pasturelands, orchards, meadows and forests. The collected material was obtained by using a sweeping net. Through the research, an interception trap was used of the dimension 100 cm × 100 cm, its collecting vessel contained salt water. The research was conducted in accordance with permission OU-BB-OSZP1–2019022541–12. If the species determination could not be done right in the field, specimens were taken by the authors for further identification in the laboratory. Hereby listed species were deposited at the authors' personal collections.

Study sites

Locality 1 – **Hegy** (48°14′43.296″N, 19°51′18.396″E, 250 m a.s.l., 7785 DFS). In the north-eastern part of the municipality of Belina village, bellow the Pannonian-Balkan Turkey oak forest there is a sun-exposed hill with rich floristic elements (Figure 1). Here grows *Euonymus europaeus* L., several scrubby *Ulmus minor* Mill. and *Prunus spinosa* L., in the understorey can be found common grass species such as *Brachypodium pinnatum* (L.) P. Beauv., *Brumus erectus* Huds., *Calamagrostis epigejos* (L.) Roth, completed with plants like *Onobrychis viciifolia* Scop., *Astragalus onobrychis* L., 1753 or *Inula ensifolia* L.

Locality 2 – **Nagy Somos** (48°12′47.077″N, 20°2′53.934″E, 270 m a.s.l., 7786 DFS). An overgrowing valley of pastureland with exceptional biological value in the vicinity of Jestice village (Figure 2). Between others here grows on vast area heliophile plants like *Securigera varia* (L.) Lassen 1989, *Lychnis coronaria* (L.) Clairv., *Vicia cracca* L. or *Nonea pulla* (L.) amended with shrubs and trees such as *Junniperus communis* L., *Prunus spinosa* L., *Cerasus avium* L. or *Prunus pyraster* (L.) Burgsd.

Locality 3 – **Sátoros** (48°10′47.285″N, 19°50′54.922″E, 450 m a.s.l., 7885 DFS). Forest on shallow acidic soil, with *Fagus sylvatica* L. mixed mainly with *Quercus petrea* (Matt.) Liebl., *Carpinus betulus* L., 1753 or with *Tilia cordata* Mill (Figure 3). Tree canopy is single layered with underdeveloped shrubs like *Sambucus racemosa* L. or *Rubus idaeus* L. Understorey is comprised by xerophilic plants such as *Melica uniflora* Retz, (L.) *Maianthemum bifolium* F. W. Schmidt or *Luzula luzuloides* (Lam.) Dandy & Wilmott.

Figure 1 Photos of examined localities (1–site 1, 2–site 2, 3–site 3). Photo of locality number 2 taken by J. Pelikán, others by A. Balázs

1 **2** **3**

RESULTS AND DISCUSSION

***Variimorda* (*Galeimorda*) *hladili* Horák, 1985 (Mordellidae)**

Material examined: 1 ♀, Hegy, Belina (locality 1), 7.7.2020, swept off from the vegetation, J. Bezděk lgt. et coll., det. Horák. Confirmed occurrence in Slovakia.

The subgenus *Galeimorda* Horák, 1985 contains following 5 species: *Galeimorda caprai* (Franciscolo 1951), *G. fagniezi* (Méquignon 1946,) *G. krikkeni* (Batten 1977), *G. theryi* (Méquignon, 1946) and finally *G. hladili* Horák, 1985 (Horák 2008). *Variimorda hladili* is the most widespread of them. The species was described in Macedonia (Horák 1985). Since then, it was confirmed from the following countries: Bulgaria, Greece, Crete, Rhodes, Ukraine, Russia and Kazakhstan (Horák

2008). Horák (1989) published the series of 7 specimens from Čenkov which were, however, treated as uncertain and demanding confirmation. Due this fact *Variimorda hladili* was not listed for Slovakia in the Catalogue of Palaearctic Coleoptera (Horák 2008). The specimen collected in Cerová vrchovina confirms the occurrence in Slovakia and it also gives the relevance to the specimens from Čenkov (Figure 4).

***Zonitis flava* Fabricius, 1775 (Meloidae)**

Material examined: 1 ♂, Nagy Somos, Jestice (locality 2), 5.6.2019, swept off from the vegetation, J. Bezděk lgt., det. et coll. Second record for Slovakia.

The genus *Zonitis* Fabricius, 1775 contains 29 species. *Zonitis flava* is distributed in Azerbaijan, Albania, Algeria, Armenia, Austria, Bulgaria, Croatia, Czech Republic, France, Georgia, Greece, Hungary, Italy, Kazakhstan, Portugal, Romania, Slovakia, Spain, Russia, Switzerland, Ukraine, Serbia, Montenegro, Libya, Morocco, Tunisia, Cyprus, Iran, Israel, Jordan, Lebanon, Syria, Turkmenistan, Turkey, Uzbekistan and Xinjiang (Bologna 2008) (Figure 5). First record from Slovakia was published by Tomčík (2019) from Kamenica nad Hronom, Burda.

***Odontosphindus grandis* (Hampe, 1861) (Sphindidae)**

Material examined: 2 spec., Sátoros, Šiatorská Bukovinka, (locality 3), interception trap, exposed from 22.6. until 14.8.2020, Kopecký lgt., det. et coll. Second record for Slovakia.

Four species of the family *Sphindidae* live in Europe, namely: *Aspidiphorus lareyiniei* Jacquelin Du Val, 1859, *Aspidiphorus orbiculatus* (Gyllenhal, 1808), *Sphindus dubius* (Gyllenhal, 1808) and *Odontosphindus grandis* (Hampe, 1861) (Jelínek 2007a). All species of the family develop in the *Mycetozoa*, the development is documented in genera: *Lycogala* sp. (Audisio et al. 2008), *Stemonitis* sp. and *Fuligo septica* (Freeman et al. 2003). Genus *Odontosphindus* Le Conte, 1878 contains three species. Two live in North America (Audisio et al. 2008) and one species *O. grandis* (Hampe, 1861) occurs in Europe (Jelínek 2007a). *O. grandis* is documented from France (Pyrenees and Corsica) (Freeman et al. 2003), Slovakia, Croatia, Bosnia and Herzegovina, Romania, Greece (Jelínek 2007a), Italia (Audisio et al. 2008) and possible occurrence from Hungary, Bulgaria, Serbia, Montenegro, Macedonia and Ukraine presented (Jelínek 2007b). From Slovakia *O. grandis* was recorded for the first time by Jelínek (1976) from Remetské Hámre in Vihorlat Mts.

Figure 4 Photos of examined material (4 – Variimorda hladili, 5 – Zonitis flava, 6 – Cassida aurora)

4 **5** **6**

***Cassida aurora* Weise, 1907 (Chrysomelidae)**

Material examined: 1 spec., Sátoros, Šiatorská Bukovinka, (locality 3), 18.6.2020, sitting on *Rosa* sp. leaf, J. Bezděk, lgt., det. et coll. In Slovakia presently known only from Cerová vrchovina Upland.

The rarest European tortoise beetle confirmed from: Austria, Bulgaria, Croatia, Czech Republic, Greece, Hungary, Italy, Romania, Slovakia, Slovenia, Russia and Ukraine (Figure 6). The species was also confirmed in Poland (Niedojad 2013). The host plants are species of the genera *Achillea* sp.

After the Second World War, *Cassida aurora* was reliably reported from Slovakia only from Cerová vrchovina Upland (Kopecký et al. 2015, present record). The record from Bučany (Majzlan 2012) is doubtful and very probably based on misidentified specimens (Bezděk in press).

CONCLUSION

The Cerová vrchovina Upland is not an unknown area for coleopterists as it was investigated continuously mainly from the 90s of 20th century (e.g. Franc 1995, 1997, Kopecký et al. 2015, Ouda et al. 2013). The Slovakian checklist of beetles counts as much as 6711 species (Majzlan 2019). Therefore, it is still a lot to discover since our database of beetles of Cerová vrchovina Upland is comprised till this time of 1778 species. As the ongoing systematic research has just started, in the future we expect much more unusual findings of beetles. Our international research group of entomologists are building a comprehensive database of insects, consequently, a monograph of the insects of Cerová vrchovina Upland is expected to be published in the future.

ACKNOWLEDGEMENTS

Many thanks go to Associate Professor Josef Suchomel (Mendel University in Brno) for ensuring the institutional background of this research.

REFERENCES

Audisio, P. et al. 2008. Odontosphindus grandis, genere e specie nuovi per la fauna italiana (Coleoptera, Sphindidae). Bollettino dell'Associazione Romana di Entomologia, 63(1–4): 43–46.

Azadi, H. et al. 2020. Impact of agricultural land conversion on climate change. Environment, Development and Sustainability [Online], 22: 4 Available at: https://www.researchgate.net/publication/340743269_Impact_of_agricultural_land_conversion_on_climate_change. [2020-09-14].

Bell, J.R. et al. 2020. Are insects declining and at what rate? An analysis of standardised, systematic catches of aphid and moth abundances across Great Britain. Insect Conservation and Diversity [Online], 13(2): 115–126. Available at: https://onlinelibrary.wiley.com/doi/10.1111/icad.12412. [2020-08-15].

Bezděk, J. in press. Updated checklist of Slovak leaf-beetles (Coleoptera: Orsodacnidae, Megalopodidae, Chrysomelidae), with comments on the occurrence of some species. Klapalekiana.

Bologna, M.A. 2008. Family Meloidae Gyllenhal, 1810. In Catalogue of Palaearctic Coleoptera. Volume 5. Stenstrup: Apollo Books, pp. 370–412.

Csiky, J. et al. 2010. Rastlinstvo. In Chránená krajinná oblasť Karancs-Medves a Chránená krajinná oblasť Cerová vrchovina, Na hranici Novohradu a Gemera. Alföldi Nyomda Zrt. Debrecen: Riaditeľstvo Národného parku Bükk, pp. 115–143.

Dulák, M., Kovalčík, V. 2010. Lesné hospodárstvo na území CHKO Cerová vrchovina od roku 1879. In Chránená krajinná oblasť Karancs-Medves a Chránená krajinná oblasť Cerová vrchovina, Na hranici Novohradu a Gemera. Alföldi Nyomda Zrt. Debrecen: Riaditeľstvo Národného parku Bükk, pp. 249–258.

Franc, V. 1995. O chrobákoch (Coleoptera) Cerovej vrchoviny so zvláštnym zreteľom k bioindikačne významným druhom. [On beetles (Coleoptera) of "Cerová vrchovina" Mts. with special reference to bioindicatively significant species)]. In Rimava 1995 - Odborné výsledky zoologických a mykologických výskumov. Rimavská Sobota: SAŽP, S-CHKO Cerová vrchovina, pp. 52–70.

Franc, V. 1997. O genofondových hodnotách a ochranárskom význame Cerovej vrchoviny vzhľadom na chrobáky (Coleoptera) a pavúky (Araneae). [On genofund values and conservational significance of the Cerová vrchovina Mts. with regard to beetles (Coleoptera) and spiders (Araneae)]. In Poiplie. Banská Bystrica: SAŽP, pp. 43–50.

Freeman, J.C. et al. 2003. *Odontosphindus grandis* Hampe, nouvelle espèce, nouveau genre, nouvelle sous-famille pour la faune de France et pour l'Europe occidentale (Coleoptera, Sphindidae). Bulletin de la Société entomologique de France, 108(3): 221–232.

Horák, J. 1985. Ergebnisse der tschechoslowakisch-iranischen entomologischen Expeditionen nach Iran 1970, 1973 und 1977, Coleoptera: Mordellidae 1 (Stenaliini, Mordellini). Entomologische Abhandlungen, 49(1): 1–25.

Horák, J. 1989. Faunistic records from Czechoslovakia. Acta Entomologica Bohemoslovaca, 86: 477–480.

Horák, J. 2008. Family Mordellidae Latreille, 1802. In Catalogue of Palaearctic Coleoptera. Volume 5. Stenstrup: Apollo Books.

Jelínek, J. 1976. Faunistic records from Czechoslovakia. Acta Entomologica Bohemoslovaca, 73: 61.

Jelínek, J. 2007a. Family Sphindidae Jacquelin du Val 1861, 455. In Catalogue of Palaearctic Coleoptera. Volume 4. Stenstrup. Apollo Books.

Jelínek, J. 2007b. Fauna Europaea: Sphindidae. In Fauna Europaea, Coleoptera 2, Beetles. Fauna Europaea version 1.3 [Online], Available at: http://www.faunaeur.org. [2020-09-14].

Kopecký, T. et al. 2015. Zpráva o výsledku průzkumu Coleoptera – chrobáky Cerové vrchoviny 2012–2014, pp. 1–118.

Majzlan, O. 2012. Beetle (Coleoptera) fauna in the vicinity of the village of Bučany. Naturae Tutela, 16(1): 37–50.

Majzlan, O. 2019. Faunistic notes on beetles (Coleoptera) 14. from Slovakia, Naturae Tutela, 23(2): 209–213.

Niedojad, K. 2013. The first confirmed occurence of *Bruchidius bimaculatus* (Olivier, 1795) and *Cassida aurora* Weise, 1907 and new records of rare Polish leaf beetles (Coleoptera: Chrysomelidae). Wiadomości Entomologiczne, 32(1): 25–33.

Ouda, M. et al. 2013. Dřepčíci (Coleoptera: Chrysomelidae: Galerucinae: Alticini) CHKO Cerová vrchovina – výsledky faunistického průzkumu v letech 2009–2012 (The flea beetles (Coleoptera: Chrysomelidae: Galerucinae: Alticini) of the Cerová vrchovina Protected Landscape Area – results of faunistic research in 2009–2012). Západočeské entomologické listy, 4: 16–43.

Szirácsik, E. 2010. História poľnohospodárstva v oblasti Karancs-Medves. In Chránená krajinná oblasť Karancs-Medves a Chránená krajinná oblasť Cerová vrchovina, Na hranici Novohradu a Gemera. Alföldi Nyomda Zrt. Debrecen: Riaditeľstvo Národného parku Bükk, pp. 259–265.

Tomčík, J. 2019. Blister beetle *Zonitis flava* (Coleoptera: Meloidae) – new species for Slovakia. Entomofauna Carpathica, 31(2): 93–94.

Habitat preferences of Eurasian Skylark (*Alauda arvensis*)

Denisa Dvorakova, Jan Sipos, Josef Suchomel
Department of Zoology, Fisheries, Hydrobiology and Apiculture
Mendel University in Brno
Zemedelska 1, 613 00 Brno
CZECH REPUBLIC

xdvora33@mendelu.cz

Abstract: The article evaluates the importance of habitat classes as living space to Eurasian skylark (*Alauda arvensis* Linnaeus, 1758). From the faunistic database Czech Society for Ornithology (CSO) were gathered 21 110 records concerning the presence and abundance of Eurasian skylark from 2014 to 2019 in the Czech Republic. The data about the occurrences was paired to data containing the Corine land cover classes. The boosted regression trees (BRT) and the Generalized Estimating Equations method (GEE) were used for data analysis. The main result of this study showed that over the last 6 years, the abundance of the skylark has decreased slightly, and the species prefers an agricultural landscape and green areas (parks, lawns etc.) in an urbanized and post-industrial landscape.

Key Words: Eurasian skylark, larks (Alaudidae), habitat preferences, bird mapping

INTRODUCTION

Eurasian Skylark (*Alauda arvensis* Linnaeus, 1758) is a species from Alaudidae family, that breeds in the summer months in the Czech Republic and in autumn they return to the wintering in Mediterranean (Szilassi et al. 2019), but some of the birds stays in the breeding sites (Hudec and Šťastný 2011).

It is generally known that skylark species live in open landscape and as living space they often use agricultural landscape (e.g. crop-fields, meadows or pastures) (Wakeham-Dawson and Smith 1999, Loretto et al. 2019). But in recent decades occurrence of skylark have declined sharply due to agricultural intensification in Europe (Geiger et al. 2014, Piha et al. 2003, Donald et al. 2001, Chamberlain et al. 2000). Some of the studies say that the reason for decreasing of skylark is replacement of the food crops fields by the energy crops (e.g. maize and winter rape) and the associated homogenization of the environment (Csikós and Szilassi 2020).

The main goals of our study were: a) to determine which land cover classes are preferred by Eurasian skylark and b) to sort the different land cover classes according to its importance for the frequency of skylark occurrence.

MATERIAL AND METHODS

Used data

The information about the presence and abundance of Eurasian skylark in the Czech Republic comes from the public ornithological database (AVIF 2014–2019) operated by the Czech Society for Ornithology (CSO) and is freely available for non-commercial or study purposes in CSV format. The dataset from CSO includes point data and additional information (district, day, year etc.). Data about the habitat classes come from Corine land cover (CLC 2018). The CLC classes were simplified and generalized to improve predictive power of statistical models (Table 1). Together we collected 21 110 records of Eurasian skylark occurrences and abundances between 2014–2019.

Data processing

The obtained information was processed into one CSV data file. Data from Corine land cover database were paired to data from ornithological database by using LAT and LON coordinates. Information about a given land cover class at a given coordinate was then generated by using ”Extract

Multi Values to Points" function in the geographical information system ArcMap. This function extracts the data from individual cells that are specific by their coordinates and contain specified raster data in individual pixels of the image. The extracted data was added to the attribute table according to the desired point coordinates (ESRI ArcMap 2019). The final data set was subsequently analysed by two statistical methods.

Table 1 CLC classes and simplified shortcuts used in this study. Shrotcuts mean: AL AgricultureLand, BL BushyLand, GU GreenUrban, M Marshes, MA MinigAreas, MF MixedForest, NA NaturalAgri, OV OrchardsVineyards, PG PasturesGrasslands, UA UrbanAreas, WB WaterBodies.

Classes	AL	BL	GU	M	MA	MF	NA	OV	PG	UA	WB
Airports										1	
Bare rocks		1									
Broad-leaved forest						1					
Complex cultivation patterns							1				
Coniferous forest						1					
Construction sites										1	
Continuous urban fabric										1	
Discontinuous urban fabric										1	
Dump sites										1	
Fruit trees and berry plantations								1			
Green urban areas			1								
Industrial or commercial units										1	
Inland marshes				1							
Land principally occupied by …							1				
Mineral extraction sites					1						
Mixed forest						1					
Moors and heathland		1									
Natural grasslands									1		
Non-irrigated arable land	1										
Pastures									1		
Peat bogs				1							
Road and rail networks and …										1	
Sparsely vegetated areas		1									
Sport and leisure facilities										1	
Transitional woodland-shrub		1									
Vineyards								1			
Water bodies											1
Water courses											1

Used statistical methods

Two approaches were chosen to test the relationship between the abundance of Eurasian skylark and explanatory classes of Corine land cover database. The first approach was the non-parametric method "Boosted regression trees" (BRT), which is based on the interconnection of two statistical methods: decision trees (regression trees) and machine learning (boosting) (Elith et al. 2008). This approach was chosen due to diverse structure of the data (e.g. large amounts of unmeasured data, data recorded at different scales, outliers, correlated environmental factors). The second method of data processing was the regression model based on the Generalized Estimating Equations method (GEE) with Poisson error distribution and log link function. Data from ornithological database were spatially arranged on the basis of repeated measurements in individual districts. Therefore, the repeated measurement from the same districts were nested within clusters by the argument "id" in the GEE method. The result of the BRT model was a list of all factors sorted by relative influence on the abundance of Eurasian skylark (Table 2). The next step was to test the influence of individual environmental factors by using the GEE method (Table 3). Among the most influential factors were selected those that had a high relative effect (calculated by BRT method) and at the same time significantly influenced the abundance of Eurasian skylark (calculated by GEE method). Partial

dependence plot was used for graphical displaying dependence between land cover classes and the abundance of Eurasian skylark. Partial dependence plot shows how the dependent variable partially depend on the explanatory variables after subtracting the influence of covariates (Elith et al. 2008). Data were analyzed in R (R Core Team 2020).

RESULTS AND DISCUSSION

The results of the study based on the two statistical approaches (BRT and GEE) confirmed significant association among land cover classes and skylark abundance (Table 3). The BRT and GEE method showed that year was the variable with the smallest effect on skylarks' abundance, which may mean that skylarks shows a small year-on-year fluctuations in abundance in the Czech Republic (Table 2–3).

Figure 1 The partial dependence bar plot calculated by Boosted regression trees shows which types of environments mostly affected the skylark abundance

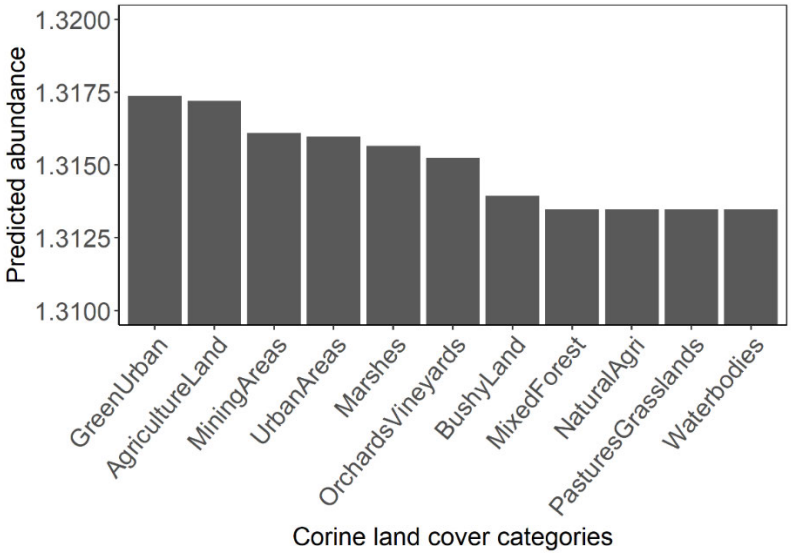

The main result of the analyses showed that the greatest abundance of skylarks occurred in the agriculture land and in the green areas of urbanized and post-industrial landscape (Figure 1). An exact name of the Corine land cover class preferred by skylark is "Non-irrigated arable land" defined as the cultivated land used for agricultural use. In other words, it is classic agriculture land under a crop rotation system (CLC 2018).

Figure 2 Relationship between skylark abundance and years (recorded number of individuals in each year). Regression curves with marked 95% confidence intervals were fitted by a generalized linear model with Poisson error distribution and log link function.

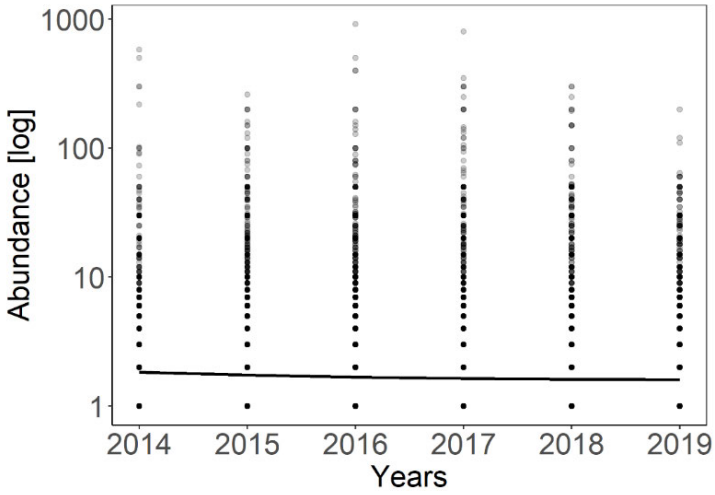

In the study of Loretto et al. (2019) is described that the cereals and crops for green manuring has strong positive effect on the skylarks. On the other hand, the strongest negative impact on skylarks had the intensive crop farming, woody areas and urbanized areas. This is in concordance with part of the results of our research where the low and intermediate intensity of crop farming and diverse farmland showed only small positive effect on the skylarks' abundance in comparison with other land cover classes. In the study of Szilassi et al. (2019) the skylarks mostly preferred permanent crops and pastures, but did not prefer the urban areas, wetlands and heterogenous agriculture land and forests. From this information we can state that a relatively small-sized fields providing small-scale heterogeneity and urbanized areas are not preferred by skylarks (Csikós and Szilassi 2020).

Table 2 Results of the boosted regression trees (BRT) which compares relative impact of explanatory variables on the abundance of Eurasian skylark

Factor	Relative impact
District	71.0835990
Day	26.6174699
Month	0.9669299
Land cover classes	0.8340621
Year	0.4979391

Table 3 Results of the Generalized Estimating Equations method tested by the analysis of deviance

Factor	Df	X2	P (> |Chi|)
Month	1	27.30	< 0.001
Day	1	9.90	< 0.01
Year	1	8.44	< 0.01
Land cover classes	10	334.11	< 0.001
Year: habitat	10	20.74	0.023

Table 4 Summary table showing: number of records, mean abundance and confidence intervals of the skylark in each year, the results show that the year 2019 is significantly different from all other years

Year	Number of records	Mean abundance	Lower confidence interval	Upper confidence interval
2014	1917	4.50	3.65	5.53
2015	3450	3.71	3.33	4.12
2016	3993	3.93	3.36	4.66
2017	3617	4.04	3.45	4.77
2018	3622	3.53	3.14	3.98
2019	3968	2.81	2.62	3.03

In our analyses the urbanized and post-industrial areas had positive effect, so these results are opposite from the other studies. This could be caused by data type used in our models where we used abundance as a dependent variable instead of presence/absence data. Another assumption is that our land cover classes do not contain only post-industrial and urban places adjacent to settlements. Loretto et al. (2019) in their study assumed that habitats in the proximity to settlements lead to increased disturbance due to recreational activities (e.g. walking with dogs or running), which in turn can negatively affect wildlife populations. We thus assume that post-industrial areas far from settlement provide enough habitat quality for skylark survivor. We also modelled pattern of skylark abundance during 6 years. The results showed that the abundance slightly decrease during years (Figure 2, Table 4). The decreasing population of Eurasian skylarks is common much-discussed recent problem;

the possible reason of decreasing is an inappropriate agricultural production (Chamberlain et al. 1999, Geiger et al. 2014, Piha et al. 2003, Wakeham-Dawson and Smith 1999).

CONCLUSION

The studied data sample of the skylark abundance distribution showed that species abundance slightly decreased between the years 2014 to 2019. Based on our results, we can say that skylarks highly preferred a low-diverse agriculture land and green areas (parks, lawns etc.) in an urbanized and post-industrial landscape. We thus conclude that post-industrial and urban areas may not only have negative impact on birds' population but especially post-industrial sites far from settlements could also have a potential as secondary habitats for Eurasian skylark.

ACKNOWLEDGEMENTS

Many thanks to the Czech Society for Ornithology for permission to use the ornithological data.

REFERENCES

AVIF. 2014–2019. Česká společnost ornitologická. Faunistická databáze [Online]. Available at: http://birds.cz/avif/obs_new.php. [2020-07-06].

Chamberlain, D. et al. 1999. Effects of habitat type and management on the abundance of skylarks in the breeding season. Journal of Applied Ecology [Online], 36(6): 856–870. Available at: https://doi.org/10.1046/j.1365-2664.1999.00453.x. [2020-08-20].

Chamberlain, D. et al. 2000. Spatial and temporal distribution of breeding Skylarks Alauda arvensis in relation to crop type in periods of population increase and decrease. Alauda [Online], 88(1): 61–73. Available at: https://www.researchgate.net/publication/279625149_Spatial_and_temporal_distribution_of_breeding_Skylarks_Alauda_arvensis_in_relation_to_crop_type_in_periods_of_population_increase_and_decrease. [2020-08-20].

Corine Land Cover (CLC) 2018. European Environment Agency (EEA) under the framework of the Copernicus programme [Online]. Available at: https://land.copernicus.eu/pan-european/corine-land-cover/clc2018. [2020-08-20].

Csikós, N., Szilassi, P. 2020. Impact of Energy Landscapes on the Abundance of Eurasian Skylark (Alauda arvensis), an Example from North Germany. Sustainability [Online], 12(2): 664. Available at: https://doi.org/10.3390/su12020664. [2020-08-18].

Donald, P.F. et al. 2001. Habitat use and diet of Skylarks Alauda arvensis wintering on lowland farmland in southern Britain. Journal of Applied Ecology [Online], 38(3): 536–547. Available at: https://doi.org/10.1046/j.1365-2664.2001.00618.x. [2020-08-18].

Elith, J. et al. 2008. A working guide to boosted regression trees. Journal of Animal Ecology [Online], 77(4): 802–813. Available at: https://doi.org/10.1111/j.1365-2656.2008.01390.x. [2020-07-27].

ESRI ArcMap. 2019. Environmental Systems Research Institute. Redlands. CA. ArcGIS Desktop release 10.6.1 [Online]. Available at: https://www.esri.com [2020-07-25].

Geiger, F. et al. 2013. Habitat use and diet of Skylarks (*Alauda arvensis*) wintering in an intensive agricultural landscape of the Netherlands. Journal of Ornithology [Online], 155(2): 507–518. Available at: https://doi.org/10.1007/s10336-013-1033-5. [2020-08-15].

Hudec, K., Šťastný K. 2011. Ptáci 3/I, II Fauna ČR. Praha: Academia.

Loretto, M. et al. 2019. Occurrence of Eurasian Skylark Alauda arvensis territories in relation to urban area and heterogeneous farmland. Bird Study [Online], 66(2): 273–278. Available at: https://doi.org/10.1080/00063657.2019.1637816. [2020-08-15].

Piha, M. et al. 2003. Habitat preferences of the Skylark Alauda arvensis in southern Finland. Ornis Fennica. [Online], 80(3): 97–110. Available at: https://www.researchgate.net/publication/232271545. [2020-08-18].

R Core Team. 2020. R Foundation for Statistical Computing. Austria. R: A language and environment for statistical computing [Online]. Available at: https://www.R-project.org/. [2020-08-15].

Szilassi, P. et al. 2019. Recent and predicted changes in habitat of the Eurasian Skylark Alauda arvensis based on the link between the land cover and the field survey based abundance data. Acta Ornithologica [Online], 54(1): 59–71. Available at: https://doi.org/10.3161/00016454AO2019.54.1.006. [2020-07-15].

Wakeham-Dawson, A., Smith, K.W. 1999. Birds and lowland grassland management practices in the UK: an overview. In Proceedings of British Ornithologists' Union Spring Conference [Online]. Southampton, United Kingdom, 27–28 March, Southampton: University of Southampton, pp. 77–88. Available at: https://www.researchgate.net/publication/279749393_Birds_and_lowland_grassland_management_practices_in_the_UK_an_overview. [2020-08-15].

Importance of active conservation management for spider communities in National Nature Monument Kukle

Petra Hulejova[1], Jan Sipos[2], Ondrej Kosulic[1]
[1]Department of Forest Protection and Wildlife Management
[2]Department of Zoology, Fisheries, Hydrobiology and Apiculture
Mendel University in Brno
Zemedelska 3, 613 00 Brno
CZECH REPUBLIC

petra.martina@seznam.cz

Abstract: The objective of the present study was to investigate the impact of active logging interventions on spiders in formerly coppiced oak-hornbeam forests in the Kukle National Nature Monument, which were conserved for overall 80 years without any active conservation management. Ten study plots were selected for the research, which were subsequently divided into five unmanaged plots (control) and five, where active conservation management took place in the last 2–3 years. The spiders were collected using pitfall traps during vegetation season of 2018. We used three pitfall traps per plot, placed five meters from each other across the diagonal of each research plot. A total of 5,445 adult spiders belonging to 17 families, 47 genera and 82 species were captured. Of the 82 species found, 72 were on the plots with active conservation management and 49 on the unmanaged plots. The species richness, conservation value and presence of rare and endangered species was significantly higher in areas under active conservation management. The results show that the forest opening and restoration of the management in the form of a transfer to the coppiced forest with standards had a positive effect on the overall diversity of the spiders in oak woodlands. However, the logging activities should not be applied by large scale clearings.

Key Words: Araneae, biodiversity, active management, NNM Kukle, biomonitoring, ecological restoration

INTRODUCTION

During the second half of the 20th century, a large part of the lowland oak-hornbeam forests was transformed into protected forest for the purpose of nature conservation, which led to their homogenization and strong succession (Hédl et al. 2010). Regular human-induced disturbances that have influenced the overall ecological cycle in selected stands for centuries have been eliminated (Bengtsson et al. 2000). The forest canopy became very dense, reducing the amount of incident light into the undergrowth. As a result of these phenomena, forest heterogeneity has disappeared and biodiversity has been gradually decreasing in various representatives of invertebrates and plants (Hédl et al. 2010, Košulič et al. 2016, Stejskal et al. 2019). Spiders are among the most endangered group of invertebrates associated with light and formerly managed forests (Košulič et al. 2016, Šipoš et al. 2017). However, an important question is whether newly introduced active interventions maintained by selective logging and coppicing may constitute conditions suitable for overall biodiversity of spiders including forest as well as open habitat specialists.

Spiders are an important part of all terrestrial ecosystems (Nyffeler and Birkhoffer 2017, Michalko et al. 2019), with 875 species in the Czech Republic (Kůrka et al. 2015). At the same time, spiders are very important bioindication organisms (Marc et al. 1997). Spiders have demands on the quality of the environment, food, and microclimate (Kůrka et al. 2015).

For this reason, spiders were selected as a model group for assessing reintroduced active conservation management at the Kukle NPP located in South Moravia, Czech Republic. Interventions in protected area were planned as part of a management plan aimed on promoting biodiversity in thermophilic oak forests. We hypothesized that active conservation management will have positive effect on spider diversity and presence of rare and endangered species of spiders.

MATERIAL AND METHODS

Kukle NNM is located in the cadastral area of Boleradice, approximately 2 km east from the village. The average altitude is 400 m a.s.l. The forest type belongs to thermophilous oak forests with dominant representation of *Quercus petraea*, *Quercus pubescens* and *Acer campestre*.

The Kukle NNM was established as protected area in 2013, when no interventions were made in the forest habitats since the end of the WW2. In 2016, active conservation management interventions were carried out and were included as part of the forest management plan. These interventions were carried out in order to convert a part of the area into the middle forest, so that it corresponds with the historical state of the locality.

A total of 10 research plots were selected, which we then divided into 5 plots control without any management and 5 with active management (conservation thinning) conducted over the last two years. A square of 10 x 10 m was selected in each of the areas. We used three pitfall traps per plot, placed five meters from each other across the diagonal of each research plot. The spiders were collected using pitfall traps during vegetation season of 2018. The pitfall traps were installed on 13 April and were collected on the following dates: 18 May, 15 June, 20 July, 19 August, and 21 September. A total of 30 samples / 5 sampling dates were collected, a total of 150 samples were used for evaluation. Material was identified by Petra Hulejova with help of mentor Ondrej Kosulic.

Using the identification keys of Heimer and Nentwig (1991) and Nentwig et al. (2018), only adult spiders were used and determined to the species level. The following indicators were used to evaluate active conservation management in the studied locality: (a) species richness (number of spider species), (b) abundance, (c) conservation value, and (d) abundance of rare and endangered spider species. For the abundance of rare species, we used species only from the Red List (Řezáč et al. 2015), e.g. outside of the categories of common species. To evaluate the correlation of the degree of rarity between the two types of management, spiders were categorized based on their occurrence in the Czech Republic (Buchar and Růžička 2002). It was classified into the following categories: very rare (VR), rare (R), scarce (S), abundant (A) and very abundant (VA).

Statistical analyses were carried out by nested analysis of variance (ANOVA). The treatment was used as a fixed effect variable and the locality as a random effect variable. Further, we used ordination model to show differences between time gradient and intensity of canopy opening in studied plots (RDA analysis). Correlation between the repeated samples in time from the same plot has been solved by the setting of the permutation test. It means that randomization was restricted by randomizing time records within each area. In addition, spiders were also sampled sequentially from May to September therefore we have to maintained the time autocorrelation of individual records by using cyclic shifts.

Univariate analyses were performed using R (R Development Core Team, 2020), and multivariate analyses were evaluated using CANOCO 5 (ter Braak and Šmilauer 2012).

RESULTS AND DISCUSSION

During the arachnological research conducted in the Kukle NNP, a total of 5445 adult spiders belonging to 17 families, 47 genera and 82 species were captured between 13 April and 21 September 2018. Of the total number of non-intervention (control) plots, 49 species were captured, on plots with active conservation management, 73 species. The most dominant families were Gnaphosidae (21 species) and Lycosidae (16 species). The most abundant species were *Pardosa lugubris* with 3,288 individuals and *Trochosa terricola* with 406 individuals, both belonging to the family Lycosidae. The next dominant species were *Drassylus villicus* and *Zelotes apricorum* from the Gnaphosidae family. Of the 82 species identified, 72 were in plots with active conservation management and 49 in the control plots without any conservation management. In general, valuable arachnofauna composition including 24 rare and endangered species belonging to Red List of Czech Spiders (Řezáč et al. 2015) were discovered. The following species are mainly represented by species whose occurrence is typical of open forest-steppe and grasslands at the early stages of succession: *Agroeca cuprea, Arctosa lutetiana, Alopecosa sulzeri, Atypus affinis, Atypus piceus, Callilepis schuszteri, Carrhotus xanthogramma, Cozyptila blackwalli, Drassyllus pumilus, Drassyllus villicus, Episinus truncatus,*

Gnaphosa bicolor, Gnaphosa lucifuga, Haplodrassus minor, Micaria fulgens, Panamomops affinis, Pardosa monticola, Pardosa nigriceps, Scotina celans, Xysticus luctator, Zelotes apricorum, Zelotes aurantiacus, Zelotes erebeus, Zelotes longipes, Zelotes pygmaeus.

The species richness was significantly higher in the plots under active management (Figure 1, $F_{1.8} = 10.21$ P = 0.0127).

Figure 1 Influence of active management on species richness of spiders

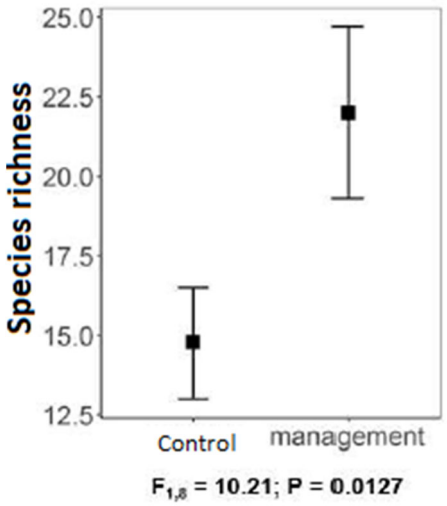

Figure 2 The difference in conservation value between two types of management

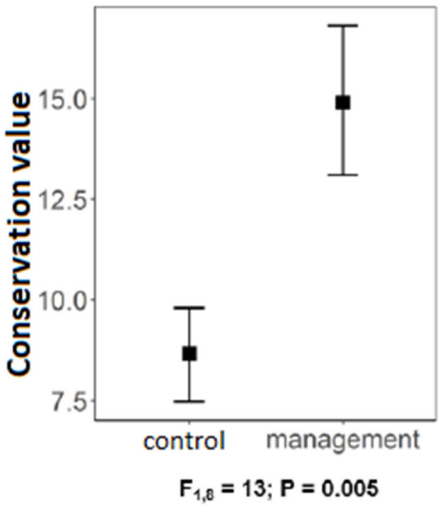

Figure 3 The difference between two types of management in abundance of rare and endangered spider species

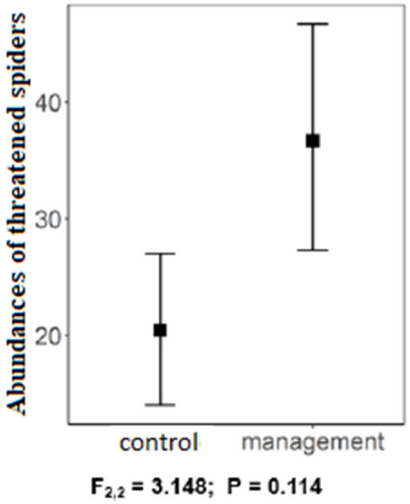

Figure 4 The difference between two types of management in abundance of bound species

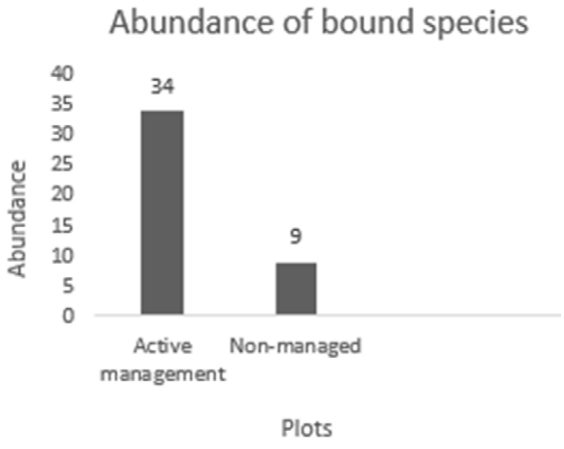

There was a significant difference in the conservation value ($F_{1.8} = 13$, P = 0.005). The value was significantly higher in the plots under active management (Figure 2). The abundance of rare and endangered spider species was not statistically different between the two management types (Figure 3, $F_{2.2} = 3.148$, P = 0.114). That was probably caused of migration of Atypus piceus and Atypus affinis males in mating season. Abundance of bound species on two types of management was significantly higher same as in conservation value, in plots under active management (Figure 4).

On the other hand, the overall increasing trend in the abundance of rare and endangered species is evident. The first three (limited) axes explain 4.52% and the remaining (unlimited) axes explain

3.63% of the variability in the distribution of spiders according above-mentioned categories. Categories are consistent with IUCN categories, but the list of spider endangered is according to the National Red List. The link between rare and endangered spider species to the more open areas under active management is also demonstrated by the ordination diagram (Figure 5), where we found statistically significant correlation between very rare and rare species and species belonging to the Red List category in plots with active management, rather than in non-intervention areas (RDA, pseudo-F = 5.1, P = 0.001).

Figure 5 RDA analysis showing the composition of categories of spiders according to the degree of rarity and conservation category in the Red List depending on the different management methods

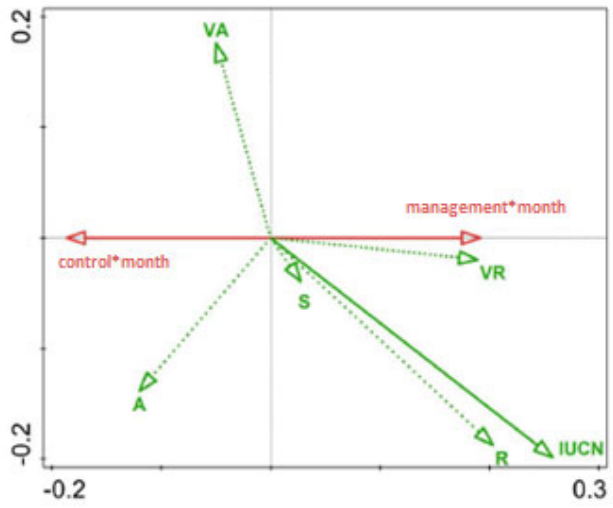

Legend: VR – Very rare, R – rare, S – scarce, A – abundant, VA – very abundant. IUCN – Red List species. The division of categories is explained in the material and methods.

Recently, many authors confirm hypothesis that active management is very important management tool for maintaining biodiversity in formerly managed oak woodlands. Therefore, we suggest that returning and restoration of active management is important in studied location of Kukle, thus it can increase diversity of habitats in homogeneous and dense forests (Hédl et al. 2010, Šebek et al. 2015). However, it is important to monitor these locations in order to find out what changes are taking place and at the same time to remove possible negative phenomena, such as the influence of non-native and invasive plants. In general, however, it is now known that active conservation management is desirable in these types of forests for many organisms, therefore it can prevent the decline of biodiversity in lowland forests that have historically been managed by man and/or natural disturbances (Bengtsson et al. 2000, Spitzer et al. 2008, Hédl et al. 2010, Vodka and Čížek 2013).

CONCLUSION

During the arachnological research, which took place in the protected areas of Kukle NNM in 2018, a total of 5,445 adult spider specimens were captured, classified into 17 families, 47 genera and 82 species. The presented research showed that return to active management can be an appropriate strategy for biodiversity conservation in oak woodlands. However, the logging activities should not be applied by large scale clearings. The strong community changes of spiders highlight the importance of complexity of lowland forests maintained by active interventions. We propose an active forest management in oak forest reserves as suitable conservation tool to prevent the generally observed decline of woodland biodiversity in the landscapes of Central Europe.

ACKNOWLEDGEMENTS

We would like to express our special thanks to the Administration of the Pálava Protected Landscape Area, namely Vladan Riedl for research permits and information on study sites.

The study was financially supported by the Specific University Research Fund of the Faculty of Forestry and Wood Technology, Mendel University in Brno (LDF_PSV_2017004) and by the Grant Agency of the Czech Republic, project 17-09283S.

REFERENCES

Bengtsson, J. et al. 2000. Biodiversity, disturbances, ecosystem function and management of European forests. Forest Ecology and Management, 132(1): 39–50.

Buchar, J., Růžička, V. 2002. Catalogue of Spiders of the Czech Republic. Praha: Peres.

Hédl, R. et al. 2010. Half a century of succession in a temperate oakwood: from species-rich community to mesic forest. Diversity and Distributions, 16(2): 267–276.

Heimer, S., Nentwig, W. 1991. Spinnen Mitteleuropas. Ein Bestimmungsbuch. Berlin/Hamburg: Verlag Paul Parey.

Košulič, O. et al. 2016: Impact of Canopy Openness on Spider Communities: Implications for Conservation Management of Formerly Coppiced Oak Forests. PLoS ONE, 11(2): e0148585.

Kůrka, A. et al. 2015. Pavouci České republiky. Praha: Academia.

Marc, P., Canard, A. 1997. Maintaining Spider Biodiversity in Agroecosystems as a Tool in Pest Control. Agriculture, Ecosystems & Environment, 62(2–3): 229–235.

Michalko, R. et al. 2019. An updated perspective on spiders as generalist predators in biological control. Oecologia, 189: 21–36.

Nentwig, W. et al. 2018. Araneae – Spiders of Europe, version 07.2018. Available at: http://www.araneae.nmbe.ch 10.24436/1

Nyffeler, M., Birkhofer, K. 2017. An estimated 400–800 million tons of prey are annually killed by the global spider community. The Science of Nature, 104: 30.

R Development Core Team, 2020. Language and Environment for Statistical Computing. R Foundation for Statistical Computing, Vienna. http://www.Rproject.org/

Řezáč, M. et al. 2015. Red list of Czech spiders: 3rd edition, adjusted according to evidence-based national conservation priorities. Biologia, 70(5): 1–22.

Spitzer, L. et al. 2008. Does closure of traditionally managed open woodlands threaten epigeic invertebrates? Effects of coppicing and high deer densities. Biological Conservation, 141(3): 827–837.

Stejskal, R. et al. 2019. The effect of coppice restoration in two forest stands in Podyjí national park on weevils (Coleoptera: Curculionoidea). Thayensia, 16: 29–50.

Šebek, P. et al. 2015. Does a minimal intervention approach threaten the biodiversity of protected areas? A multi-taxa short-term response to intervention in temperate oakdominated forests. Forest Ecology and Management, 358: 80–89.

Šipoš, J. et al. 2017. Patterns of functional diversity of two trophic groups after canopy thinning in an abandoned coppice. Folia Geobotanica, 52(1): 45–58.

Ter Braak, C.J.F., Šmilauer, P., 2012. Cannoco 5. Software for multivariate data exploration, testing, and summarization. Netherlands.

Vodka, Š., Čížek, L. 2013. The effects of edge-interior and understoreycanopy gradients on the distribution of saproxylic beetles in a temperate lowland forest. Forest Ecology and Management, 304: 33–41.

Diversity of bees (Apoidea) and their pesticide contamination in two different types of agricultural management

Marian Hybl[1], Petr Mraz[2], Jan Sipos[1]
[1]Department of Zoology, Fisheries, Hydrobiology and Apidology
Mendel University in Brno
Zemedelska 1, 613 00 Brno
[2]Department of Plant Production
University of South Bohemia in Ceske Budejovice
Studentska 1668, 370 05 Ceske Budejovice
CZECH REPUBLIC

Mario.eko@seznam.cz

Abstract: The biodiversity and density of pollinators systematically and drastically decreases. The intensification of agriculture, including a change in land use, increased chemistry and different farm management are considered to be the main causes. In the study differences in land use, biodiversity of apidofauna and chemical contamination of bees by pesticides was compared between the locations with different management. While the locality in conventional regime of agriculture was characterized by intensively farmed rapeseed field and main landscape matrix was formed by arable land, at the locality in organic regime of agriculture was observed flowering strips and major landscape matrix was formed by permanent grassland. At the locality in organic regime, a significantly higher richness and abundance of bees were observed in comparison with the locality in conventional regime. In addition, the analyses of bees from the locality in conventional regime revealed the presence of residues of several pesticides. In contrast, at the locality in organic regime, analyses did not confirm presence of any residues.

Key Words: biodiversity, pesticides, pollinators, contamination

INTRODUCTION

Apoidea are a diverse group comprising solitary, socially or kleptoparasitic species living exclusively on pollen and nectar (Macek et al. 2010). The bee superfamily includes approximately 430 genera and about 16,000 species. The most important agricultural genera in the Czech Republic includes bees (Apis), bumblebees (Bombus) and solitary bees, of which there are 6 genera and about 600 species in the Czech Republic (Straka et al. 2010). Bees are the most important pollinators of agricultural crops and it is estimated that 30% of crop production depends on bee pollination (O'Toole 1993). In addition, many wild plants (estimated at 60–90%) are dependent on insect pollination, with bees making the greatest contribution to pollination (Spivak et al. 2011). Except to improving the qualitative and quantitative characteristics of agricultural production (especially vegetables, fruits and seeds) (Vládek et al. 2018), bee activity also contributes significantly to wider plant biodiversity and improved ecosystem equilibrium (Delaphane and Mayer 2000).

Thus, the decline in the diversity of wild pollinators and the massive collapses of *A. mellifera* colonies are extremely worrying (Biesmeijer et al. 2006). This pollinator crisis is expected to continue to have a far-reaching impact not only on agriculture and the related economy (Gallai et al. 2009), but also on the species diversity of plants associated with them (Biesmeijer et al. 2006) and the overall landscape character (Ricketts et al., 2008). The main factors contributing to the decline of native pollinator species are landscape fragmentation, habitat loss, pesticide use (Cane and Tepedino 2001). In addition to declining wild bee populations in recent years, there have also been severe losses of *A. mellifera* colonies due to pests, diseases and especially pesticide pollution and malnutrition (Matheson et al. 1996, Hýbl et al. 2019).

Pesticide pollution in intensively farmed landscapes is a dangerous phenomenon because these substances accumulate in vegetation, water and soil and cause damage to beneficial organisms such

as bees (Porrini et al. 2002). In agricultural areas, *A. mellifera* colonies are commonly used as bioindicators of environmental pollution. In addition to the state of the colony, chemical pollution of the environment is detected by chemical analyses of bees and bee products, which tells us about the state of the environment. This makes bees a generally accepted bioindicator (Balayiannis and Balayiannis 2008).

The aim of the study is to verify the influence of the intensity of agricultural management on the population of bees (Apoidea), to describe the differences in diversity, abundance, balance and contamination of the bee community in differently managed agricultural localities.

MATERIAL AND METHODS

At both localities, measuring of biodiversity and abundance were done and chemical analyses of bodies of bees (*A. mellifera*) caught at the entrance of hives located in close proximity to the localities was performed.

Study areas

The locality in the ecological regime of agriculture was located near the village of Malonty. The landscape matrix consisted mainly of permanent grasslands, which were also exclusively in the ecological regime of farming. In addition to permanent grassland, there were a large number of significant landscape elements and an inconsiderable part of landscape was occupied by forests. However, the observation and collection of bees took place in flowery belts dividing the field, which was also in mode of organic agriculture. A large part of the landscape was occupied by the development of the village (Figure 1). The average slope of the site is 5 °, the average altitude is 680 meters. In recent years, in addition to cereals, a significant number of clovers have been grown in the locality and its surroundings, and flowering catch crops and buckwheat are also an integral part of sowing procedures, which provide bees with a valuable source of food. The location in the conventional agricultural regime was located near the town of České Budějovice. The landscape matrix consisted mainly of arable land, thus intensively cultivated areas on which most oilseed rape was grown. However, in the immediate vicinity of the monitored locality, there were also more extensively used areas, mainly regularly mown grasslands and commercial forests. There were also several other ecologically important areas in the landscape (borders, draws, tree lines and others). Apart from that, the urban area is also represented to a lesser extent (Figure 1). The monitored field had an area of 1.83 ha, a slope of 2 ° and an average altitude of 520 meters. In recent years, almost only rape, corn, and wheat have been grown in the area.

Figure 1 Graph of land use in radius 1km in observed localities (locality in organic regime in left, locality in conventional regime in right)

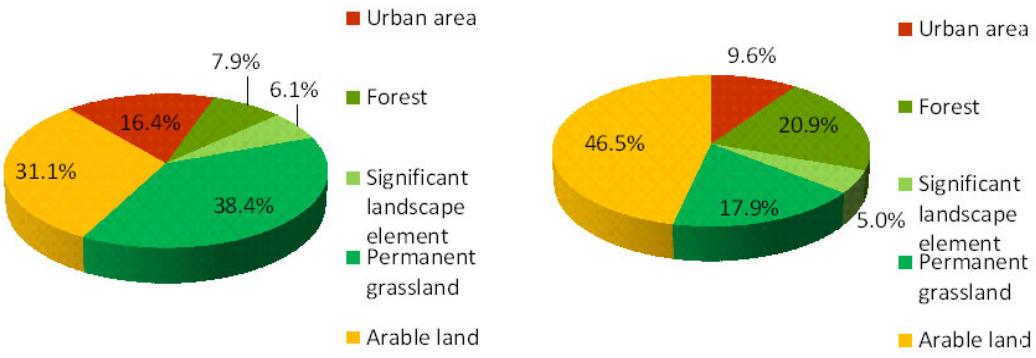

Sampling

Measurement of bee diversity and abundance was based on trapping in the Moericke traps. The principle of the traps lies in the attractiveness of the yellow colour for the bees, which drown after sitting on the surface. Traps were collected regularly every 14 days. Bee diversity was measured throughout the flowering period of rapeseed at the locality in conventional regime. This period also coincided with the flowering of the main blossoming species at the locality in organic regime.

The material was then determined and classified into families and species. Based on this, the Shannon-Weaver diversity index and equitability were calculated.

Analyses of pesticides

The workers of western honey bee (*A. mellifera*) used for pesticide contamination analyses were obtained by capture at a time when the last chemical treatment at rapeseed field had already been provided. On May 9, approximately 1,000 *A. mellifera* individuals were captured at the site in the conventional agricultural regime, and approximately 1,000 *A. mellifera* individuals were also captured at locality in organic farming regime on May 10. The analyses of contamination of bees were performed by the State Research Institute in Prague. Methods used: SOP 10.58 (GC-ECD) and SOP 70.101 (HPLC-MS / MS). Using these methods, the presence and amount of pesticides and their residues were detected.

Statistical analyses

Individual study plots were clustered within fields and each plot was repeatedly sampled over time. Accordingly, due to nested design, the mixed effect model procedure was applied to data analysis. The relationship between species richness and abundance as dependent variables and the agriculture management as explanatory variable was separately evaluated by two linear mixed effect models (LMMs) with Poisson error distribution and link function log. In the LMM model, particular plot was used as random intercept effect and sample date as random slope effect. The significance of the explanatory variables was then tested by Likelihood Ratio Test.

RESULTS

During the monitoring, a total of 310 individuals of bees belonging to 5 families representing 39 species of bees were observed (Figure 3 and 4). At the locality in organic regime, altogether 36 species of bees from 5 families (Apidae, Andrenidae, Colletidae, Halictidae and Megachilidae) were observed. The most abundant group in terms of species and numbers were bees of the family Andrenidae, which numbered 17 species, 147 individuals and accounted for 64.2% of all observed bees. The most abundant species were *Andreana cineraria* (76 individuals, 33.2%), *Andrena Bicolor* (30 individuals, 13.1%) and *A. mellifera* (27 individuals, 11.8%). However, compared to the abundance of solitary bees, a small occurrence of bumblebees was found, including 2 species *of Bombus terrestris* (4 individuals, 1.7%) and *Bombus lucorum* (1 individual, 0.4%). The least numerous family was Megachilidaee represented by 2 species of bees, *Chelostoma florisomne* numbered only one individual, *Chelostoma rapunculi* numbered 3, which together accounted for 1.7% of the total number of captured individuals. In the locality in convetional regime were observed 20 species of bees from 3 families (Apidae, Andrenidae and Halictidae) The most abundant group in terms of species and numbers were bees from the Andrenidae family, which numbered 13 species, 50 individuals that accounted for 61.7% of all caught bees. However, the most abundant species was *A. mellifera* of the genus Apidae, which represented 15 individuals and 18.5% of all bees collected. A significant proportion of bumblebees were also found. Two species were captured, numbering a total of 10 individuals, most of which were *B. Terrestris* and a smaller part of *Bombus lapidarius*, together accounting for 12.3%. The least numerous family was Haliactidae in which, despite the presence of 4 species, only 6 individuals were caught, which gave only 7.5% of the total number. The graphs show a difference in the composition of the pollinator community in the both localities. In the ratio of occurrence and richness of species, localities vary considerably. While the locality in organic agriculture has 5 families representing 36 species, the locality of conventional agriculture has only 3 families including only 20 species. This corresponds to the value of Shannon-Weaver index and equitability, which is about twice as high in the locality in organic regime, compared to the locality in conventional regime. Similarly, in the case of the locality in organic regime, the species richness (χ^2= 4.5717, p = 0.0325) and species abundance (χ^2 = 13.313, p < 0.001) are significantly higher compared to the locality in conventional regime (Figure 4).

The most significant difference between localities was in the presence of pesticides. At the locality in convenctional agriculture, altogether 4 pesticides were detected (Table 2), all of them correspond with pesticides applied on the rapeseed field (Table 1), except for carbendazim (which is a metabolite of thiophanate methyl). In the other hand, at the locality in organic regime, no pesticides were found.

Figure 2 Comparison of the percentage of bee families between different farming systems of over time

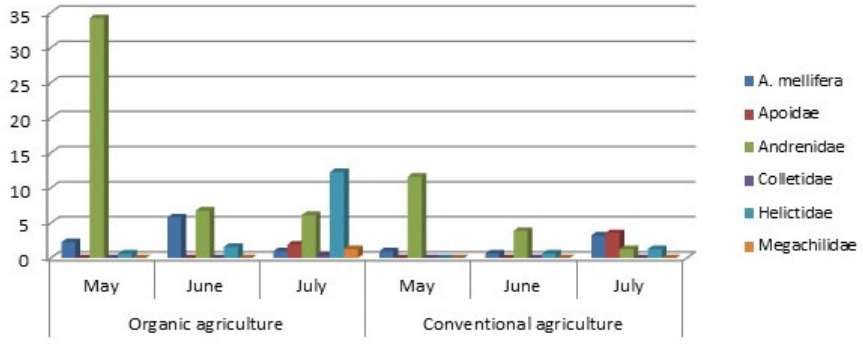

Figure 3 Comparison of species and families richness between different farming systems (in left) and value of Shannon-Weaver index and equitability (in right)

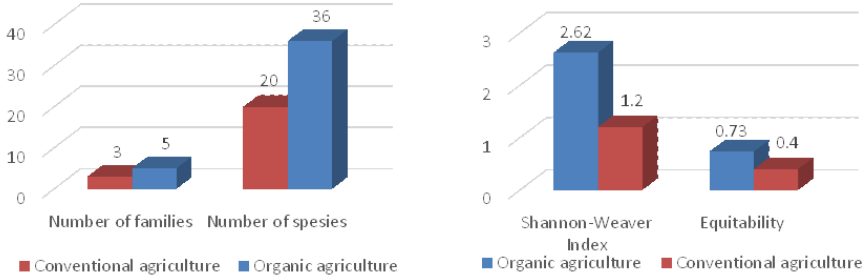

Figure 4 Comparison of species abundance (in left) and species richness (in right) between different farming systems

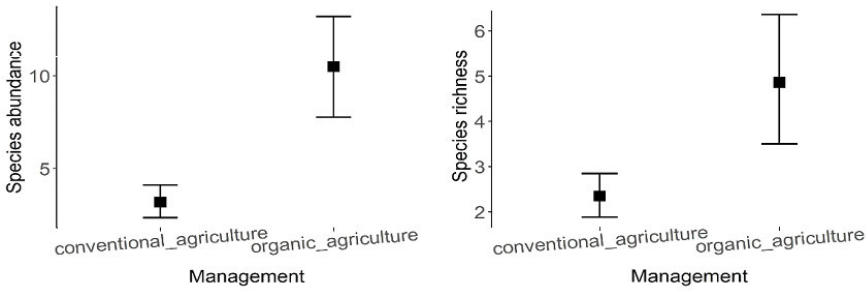

Table 1 Pesticides used on rapeseed field at the locality in the conventional regime

Trade name	Date of application	Amount	Active substances	Function
Succesor 600	21. 08. 2015	1.83 l/ha	pethoxamid 600 g/l	herbicide
Command 36CS	21. 08. 2015	0.145 l/ha	clomazone 360 g/l	herbicide
Groundet	21. 08. 2015	0.3 l/ha	732 g/l paraffin oil	wetting agent
Metarex	26. 08. 2015	4 kg/ha	metaldehyde 40 g/kg	molluscicide
Garland forte	1. 09. 2015	0.6 l/ha	propaquizafop 100 g/l	herbicide
Lynx	2. 10. 2015	0.95 l/ha	tebuconazole 250h/l	fungicide
Nurelle D	4. 4. 2016	0.6 l/ha	chlorpyrifos 500 g/l cypermethrin 50 g/l	insecticide
Bariard	2. 5. 2016	0.3 l/ha	thiacloprid 240 g/l	insecticide
Paroli	2. 5. 2016	3 l/ha	thiophanate methyl 167 g/l iprodione 167 g/l	fungicide

Table 2 Detected pesticides in bee bodies captured at the locality in conventional regime of agriculture

Pesticide	Amount (mg/kg)	Function	Toxicity	LD50 bee	Detected amount per 1 bee
thiophanate-methyl	0.119 (± 50 %)	fungicide	slight	>100 µg	0.0119µg
thiacloprid	0.114 (± 50 %)	insecticide	low	24 µg	0.0114µg
iprodione	0.084 (± 50 %)	fungicide	slight	>100 µg	0.0084µg
carbendazim	0.067 (± 50 %)	fungicide	low	50 µg	0.0067µg

DISCUSSION

When comparing the localities, there is a clear difference in the composition of the pollinator community. In the ratio of occurrence and richness of species, the localities differ considerably (Figure 3 and 4). Higher species diversity and abundance of bees on the locality in the organic regime of agriculture was probably caused by lower farming intensity, i.e., lower environmental chemistry, but higher landscape heterogenity and higher diversity of cultivated plants, which is in agreement with literature (Cane and Tepedino 2001, Porrini et al. 2002). This suggests that the ecological management system is a much more suitable environment for apidofauna compared to the conventional way of management, represented by the locality near České Budějovice. The results of the Shannon-Weaver index and equitability point to a markedly higher equilibrium and stability of the pollinator community in space and time (which is also evident from Figures 2 and 3). However, the higher proportion of bumblebees (Bombus spp.) and *A. mellifera* in the locality in the conventional regime points the ability of generalist bee species to some extent adapt to the anthropogenic environment to take the place of more specialized pollinators and thus replace their pollination service, which is in accordance with literature (Ghazoul 2005).

Although the determined amount of pesticide residues in bee bodies was very low, a negative effect on bee populations cannot be ruled out (Blackuiére 2012), which can be difficult to detect at such low doses (Lambin et al. 2001). Another potential risk, even with such low doses of pesticides, is a possible synergistic effect (Iwasa et al. 2004). In addition to direct toxicity, persistent exposure to pesticides at low doses can disrupt the bees' immune system, making it more susceptible to viral infections to which bees are normally resistant (Di Prisco 2013). Last but not least, the question remains as to the mortality of bees contaminated with a lethal dose and what was the concentration of pesticides in such affected individuals. The presence of natural and semi-natural habitats (Carré et al. 2009) certainly has another effect on the differences in diversity of pollinators in monitored localities, which is again related to the degree of landscape intensification.

CONCLUSION

The locality in the regime of conventional agriculture was characterized by a lower richness and abundance of bees. Furthermore, a lower number of specialists and, conversely, a higher number of generalists were observed in comparison with the locality in the ecological regime of agriculture.

The bee population at the site in the conventional regime was contaminated with pesticides. Residues of several pesticides were detected directly in bodies of bees, in contrast, in bees from the locality in the regime of organic farming, no pesticide residues were detected.

ACKNOWLEDGEMENTS

We are indebted to Martin Šlachta for help with determination of bees and Jiří Peterka (both from University of South Bohemia in České Budějovice) for help with collection of samples.

REFERENCES

Balayiannis, G., Balayiannis, P. 2008. Bee honey as an environmental bioindicator of pesticides occurrence in six agricultural areas of Greece. Archives of Environmental Contamination and Toxicology, 55(3): 462–470.

Biesmeijer, J.C. et al. 2006. Parallel declines in pollinators and insect-pollinated plants in Britain and the Netherlands. Science, 313(5785): 351–354.

Blacquiére, T. et al. 2012. Neonicotinoids in bees: a review on concentrations, side-effects and risk assessment. Ecotoxicology, 21: 973–992.

Cane, J.H., Tepedino, V.J. 2001. Causes and extent of declines among native North American invertebrate pollinators: detection, evidence, and consequences. Conservation Ecology, 5(1): 1.

Carré, G. et al. 2009. Landscape context and habitat type as drivers of bee diversity in European annual crops. Agriculture, Ecosystems and Environment, 133(1–2): 40–47.

Delaphane, K.S., Mayer, D.R. 2000. Crop Pollination by Bees. 1st ed., Washington State University, USA: Cabi Publishing.

Di Prisco, G. et al. 2013. "Neonicotinoid clothianidin adversely affects insect immunity and promotes replication of a viral pathogen in honey bees". Proceedings of the National Academy of Sciences, 110(46): 18466–18471.

Gallai, N. et al. 2009. Economic valuation of the vulnerability of world agriculture confronted with pollinator decline. Ecological Economics, 68(3): 810–821.

Ghazoul, J. 2005. Buzziness as usual? Questioning the global pollination crisis. Trends in Ecology and Evolution, 20(7): 367–373.

Hýbl, M. et al. 2019. Effects of phenolic bioactive substances on reducing mortality of bees (*Apis mellifera*) intoxicated by thiacloprid. In Proceedings of International PhD Students Conference, MendelNet 2019 [Online]. Brno, Czech Republic, 6–7 November, Brno: Mendel University in Brno, Faculty of AgriSciences, pp. 131–135. Available at: https://mendelnet.cz/pdfs/mnt/2019/01/21.pdf [2020-09-16].

Iwasa, T. et al. 2004. Mechanism for the differential toxicity of neonicotinoid insecticides in the honey bee, Apis mellifera. Crop Protection, 23(5): 371–378.

Lambin, M. et al. 2001. Imidacloprid-induced facilitation of the proboscis extension reflex habituation in the honeybee. Archives of Insect Biochemistry and Physiology, 48: 129–134.

Macek, J. 2010. Blanokřídlí České republiky I. - Žahadloví. 1. Vyd., Praha: Academia. Atlas (Academia).

O`Toole, C. et al. 1993. Diversity of native bees and agroecosystems. In Hymenoptera and biodiversity. Wallingford: CAB International, pp. 169–196.

Porrini, C. et al. 2014. Using honey bee as bioindicator of chemicals in Campanian agroecosystems (South Italy). Bulletin of Insectology, 67(1): 137–146.

Spivak, M. 2011. The Plight of the Bees. Environmental Science and Technology, 45(1): 34–38.

Straka, J. et al. 2007. Apoidea: Apiformes (včely). Acta Entomologica Musei Nationalis Pragae, 11: 241–299.

Vládek, A. et al. 2018. Pollination and pollinators of Hascap (Lonicera caeruela). In Proceedings of International PhD Students Conference MendelNet 2018 [Online]. Brno, Czech Republic, 7–8 November, Brno: Mendel University in Brno, Faculty of AgriSciences, pp. 211–216. Available at: http://mendelnet.cz/pdfs/mnt/2018/01/43.pdf. [2020-09-16].

Influence of agroecosystems on the occurrence of common starling (*Sturnus vulgaris*) in the South Moravian Region

Gabriela Skopalova, Jan Sipos, Josef Suchomel
Department of Zoology, Fisheries, Hydrobiology and Apiculture
Mendel University in Brno
Zemedelska 1, 613 00 Brno
CZECH REPUBLIC

xskopal3@mendelu.cz

Abstract: The article evaluates the importance of agroecosystems (vineyards and orchards) for the occurrence of common starling in the South Moravian Region. The data used for the analysis contained 4101 data from the faunistic database Czech Society for Ornithology for the years 2012 to 2018. The data were evaluated by two statistical methods, namely Boosted Regression Trees (BRT) and Generalized Least Squares (GLS). The results showed that the agricultural landscape had the greatest positive effect on the occurrence of common starling. Especially large areas of vineyards and orchards were the most important types of land use for common starling occurrence.

Key Words: starlings (Sturnidae), bird, pest, grapes, vineyard

INTRODUCTION

The common starling belongs to the genus *Sturnus*, which includes five species (Podpěra 2015). In the species *Sturnus vulgaris* itself, a total of 13 subspecies are distinguished (Sotolář 2008), where only one subspecies nests in our territory, namely the European starling – *Sturnus vulgaris vulgaris* Linnaeus, 1758 (Šťastný et al. 2011). The common starling has been present in our nature since time immemorial and its population in the Czech Republic has been growing slightly in recent years (ČSO/JPSP 2020). Its occurrence in the landscape is conditioned by various environmental factors, especially the agricultural landscape itself, in which it seeks food and nesting cavities. However, man, with his intensive agricultural activity, created monocultures, destroyed the bounder, draws, tree alleys and shrubs. In addition to all this, it uses an inexhaustible amount of pesticides and various other chemicals, which results in the starling losing its natural habitat and especially its natural food, which it then looks for in large numbers in orchards and vineyards, where it is then labeled as a pest because it causes significant damage to the crop.

This article shows the proportion of starlings in individual areas of the South Moravian Region at the level of two landscape structures (vineyards and orchards). Using statistical methods, it models the relationship between the occurrence of individual of starlings and the characteristics of its environment.

MATERIAL AND METHODS

Used data

Birds data were obtained from the faunistic database Birds.cz (ČSO), which contains records of the starling occurrence at particular time and space. It is a publicly accessible database with records of observations of various species of birds in the Czech Republic. In the case of this work, data concerning the common starling (*Sturnus vulgaris*) in the South Moravian Region in the period from 1 January 2012 to 31 December 2018, i.e. in the range of 7 years, were used. The resulting data table for analysis, in CSV format, contained 4101 starling observation data (Birds 2020). Other data table, such as the share of agricultural land in the total area (%), vineyards (ha) and orchards (ha), were downloaded from territorial analytical data (ÚAP) from the website of the Czech Statistical Office (ČSÚ 2020).

Data processing

After obtaining all the data, the data from the ČSO and the ČSÚ were first matched according to the unique codes of municipalities using the code list of municipalities (CISOB), which based on the created formula combined the codes of ČSO municipalities with the codes of ČSÚ municipalities to ensure the accuracy of analyzed data. The data were processed in an Excel file. The processed data were then statistically evaluated by two statistical methods (BRT and GLS methods) due to the complex structure of the data, which came from different scales, consisted of different types of variables and contained a large number of environmental factors. The most influential factors were those that had a high relative effect (calculated by BRT method) and at the same time significantly influenced the occurrence of starling (calculated by GLS method).

Used statistical methods

The data were evaluated by two statistical methods, namely the non-parametric method – Boosted Regression Trees (BRT model), the so-called regression tree method. The advantage of this nonparametric method is great robustness against high data complexity. Another method used was the regression method – Generalized Least Squares (GLS method), in contrast to classical regression models, it fits data using generalized least squares, which are weighted using a variance-covariance matrix. This least squares algorithm allows it to cope with heteroskedasticity and the dependence between the measured values. The evidence of the influence of individual environmental factors on the occurrence of starlings was tested using the "likelihood-ratio test" (LRT). First, a list of all factors was created using the BRT model, sorted according to the relative influence on the occurrence of the common starling. Furthermore, these effects of individual environmental factors were tested using the second statistical method GLS and their statistical significance was determined. The influence of individual explanatory factors on the occurrence of starling was shown using a "partial dependence plot", which shows the dependence between the explained and explanatory variable after deducting the influence of all remaining environmental factors.

RESULTS AND DISCUSSION

The results showed that except water bodies, vineyards and orchards were the most preferred types of land use by staring in South Moravia. South Moravia represents special region within the Czech Republic with specific natural conditions that allow it to continue in traditional fields of agricultural production such as viticulture, fruit growing and vegetable growing. South Moravia itself is known mainly for viticulture, where there is more than 90% of the area of vineyards from all over the Czech Republic (JMK Portal 2019).

The common starling feeds on plant and animal food. Animal food is an important source of nutrients and proteins, especially for growing young during the first nesting period in spring (Šťastný et al. 2009). According to Šťastný et al. (2011) the common starling likes pulpy fruits such as cherries, elderberries, and especially grapes, which eat and damage in large flocks. This is happening especially in South Moravia in the South Moravian region (district Břeclav, Hodonín, Znojmo and Brno-venkov), where there are reed stands near the vineyards, serving up to tens of thousands of flocks as lodging places. According to the above-mentioned facts, it is therefore understandable that starlings occur in large numbers mainly in areas with sufficiently large areas of vineyards, which suit them because they represent a rich and easily accessible food offer, especially before departure to wintering grounds.

The starlings also likes to nest in tree cavities it mainly uses carved cavities after large spotted woodpeckers, but also natural tree cavities (Klejdus and Vačkař 2016), which is the reason why the number of starlings in these localities increases with the growing area of orchards. They have enough animal food here, especially for young, as well as plant food. In addition, they have many nesting opportunities here. Of the fruit species of trees, he prefers cherries, apples, apricots, walnuts, pears and some other trees. The larger the area of an orchard, the more food and nesting opportunities it offers to starlings.

Figure 1 The partial dependence plot calculated by Boosted regression trees shows the relationship between the predicted values of starling occurrence and the area of: A) vineyards in hectares (ha) and B) orchards in logarithmic hectares [ha (log)]. The curves show partial dependence of starling occurrence on the particular land use type after subtracting the influence of covariates. The blue curve is then a smoothed variant of the black curve.

A) B)

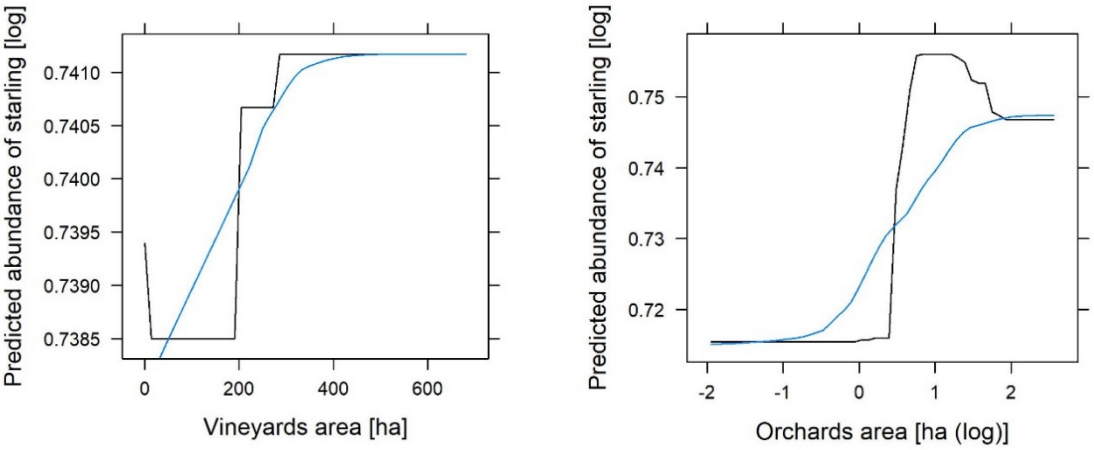

Table 1 Results of the boosted regression trees (BRT) showing the arrangement of the seven individual variables with the greatest impact according to their relative influence on the occurrence of the starling.

Factor	Relative impact
Landscape homogeneity	40.70463
Orchards	14.20086
Landscape heterogeneity	10.90267
Population density	9.085040
Precipitation	7.620945
Water bodies	5.582436
Vineyards	4.097946

Table 2 Results of the likelihood-ratio test (LRT) testing the effect of the explanatory variables with the greatest impact on the occurrence of common starlings. The LRT test compares the most complex model containing all explanatory variables (null model), gradually with individual models reduced by the variable of interest.

Factor	Df	AIC	LRT	p-value
Null model	-	3719.3	-	-
Landscape homogeneity	1	3718.4	1.111	0.29176
Orchards	1	3717.3	0.010	0.91877
Landscape heterogeneity	1	3717.5	0.189	0.66347
Population density	1	3722.2	4.901	0.02683
Precipitation	1	3722.4	5.085	0.02412
Vineyards	1	3737.2	19.941	<0.001

CONCLUSION

The results showed that the starling prefers an open agricultural landscape with a varied mosaic structure and a large area of vineyards and orchards, where it has enough space to find plant and animal food. In addition, the trees in the orchards also offer enough cavities for nesting.

ACKNOWLEDGEMENTS
We thank the Czech Ornithological Society for permission to use ornithological data.

REFERENCES

Birds. 2020. Birds.cz – pozorování ptáků (faunistická databáze ČSO) [Online]. Available at: https://birds.cz/avif/obs_new.php. [2020-02-05].

ČSO/JPSP. 2020. Jednotný program sčítání ptáků – Indexy a trendy 2019 [Online]. Available at: http://jpsp.birds.cz/vysledky.php?taxon=848. [2020-08-15].

ČSÚ. 2020. ČSÚ a územně analytické podklady. Datové vrstvy pro GIS – Obce 2009, 2010, 2011, 2012, 2013, 2014, 2015, 2016, 2017, 2018 [Online]. Available at: https://www.czso.cz/csu/czso/csu_a_uzemne_analyticke_podklady. [2020-02-05].

Klejdus, J., Vačkař J. 2016. Ptáci a stromy. 1st ed., Brno: MVDr. Julius Klejdus.

Podpěra, P. 2015. Špaček obecný *Sturnus vulgaris*, Linnaeus, 1758 – iFauna. cz [Online]. Available at: https://www.ifauna.cz/okrasne-ptactvo/clanky/r/detail/7570/spacek-obecny-sturnus-vulgaris-linnaeus-1758/. [2019-01-24].

Portál JMK. 2019. Základní údaje o Jihomoravském kraji. Portál Jihomoravského kraje [Online]. Available at: https://m.kr-jihomoravsky.cz/Default.aspx?ID=27204&TypeID=2. [2019-11-23].

Sotolář, R. 2008. Causa špaček obecný – *Sturnus vulgaris* Linnaeus. In Proceedings of Národní konference s mezinárodní účastí "Kvalita moravských a českých vín a jejich budoucnost". Sborník příspěvků. Lednice, 11–12 September. MZLU v Brně: Ediční středisko MZLU v Brně, pp. 180–185.

Šťastný, K. et al. 2009. Špaček obecný – *Sturnus vulgaris*. In Atlas hnízdního rozšíření ptáků v České republice: 2001–2003. Praha: Aventinum, pp. 390–391.

Šťastný, K. et al. 2011. 22. čeleď STURNIDAE Rafinesque, 1815 – Špačkovití. In Ptáci – Aves 3/II. Praha: Academia, pp. 888–903.

AGROECOLOGY AND RURAL DEVELOPMENT

Used palm oil as material in the soap production

Bojan Antonic[1], Karolina Tesikova[1], Simona Jancikova[1], Dani Dordevic[1,2], Bohuslava Tremlova[1]

[1]Department of Plant Origin Foodstuffs Hygiene and Technology
University of Veterinary and Pharmaceutical Sciences
Palackeho trida 1946/1, 61242 Brno
CZECH REPUBLIC

[2]Department of Technology and Organization of Public Catering
South Ural State University
Lenin Prospect 76, 454080 Chelyabinsk
RUSSIA

antonicb@vfu.cz

Abstract: The study aimed to describe the possibility of waste frying oil utilization through soap production. For the experiment's purposes, palm oil was chosen as one of the most used ones. The frying of oil was performed in 5 different stages until total polar matter (TPM) reached 6.5, 10, 15, 20 and 24%. The gained oil samples served as raw material for the production of soaps. The soap samples produced from fresh/not fried palm oil represented control samples. Following chemical parameters of produced soaps were tested: pH, moisture content, total alkali content, total fat matter, and malondialdehyde (MDA). Beside MDA, all other tested physicochemical parameters were similar among two soap groups (produced from fried and fresh palm oil). The differences between soaps obtained from fresh and fried palm oil were the most observable within MDA evaluations. Soaps produced from fried palm oil had significantly ($p < 0.05$) the highest MDA value: 1.55 µg/g (obtained in the last stage of frying with 24% TPM). The hardness of the samples ranged from 2087 g to 2740 g; certain statistically significant ($p < 0.05$) differences within experimentally produced soap are observable, though a clear pattern was not found. Obtained results indicated that used/fried palm oil represents a reasonably valuable raw material for the soap production, since physicochemical analysis of soaps produced from fresh and fried palm oil did not exhibit a full distinction between these two products.

Key Words: frying oil, oxidation stability, hydrolytic stability, waste management

INTRODUCTION

The problem with waste management has been increasing together with the growth of the world population (Herva et al. 2014). Frying oils represent an important part of waste as well. During the frying of food at temperatures of 180 ºC or higher, reactions such as hydrolysis, thermal and oxidative decomposition, and polymerization occur. These reactions can result in highly toxic compounds (Park et al. 2016, Panadare 2015). Some part of this waste, produced by industry, restaurants and households, are collected and recycled, but there are still large quantities improperly disposed of into the sewage. Consequently, this material is clogging the drainage systems, and it has a negative effect on the ecosystem (creation of toxic compounds and rancid odours) (Singh-Ackbarali et al. 2017, Azahar et al. 2016). Treatment of such wastes requires a lot of energy due to oil sticking to the cleaning apparatuses and corrosion that occurs on the equipment (Maniak, et al. 2009). On the other hand, waste frying oils can be successfully used as a low-cost material in the production of biodiesel, lubricants, resins, soaps, or can be used as a fermentation substrate (Panadare 2015).

The process of soaps production requires a minimal amount of energy, creates no by-products and it is less harmful to nature in comparison with oils. Using the frying oils for the soap production can be named as the technology with a green prospective (Maotsela et al. 2019, Félix et al. 2017).

Palm oil is one of the most used cooking oils because of its good quality, high content of stable saturated fatty acids and it is free of trans-fats (Oboh et al. 2014). According to the Food and Agricultural

Organisation (FAO), in 2014 the production of this oil was more than 58 million tonnes (FAOSTAT, 2014).

The present study aims to investigate the possibility to use fried palm oil in the soap production, and to evaluate the level of differences in physicochemical properties between soaps obtained from fresh and fried palm oil.

MATERIAL AND METHODS

Preparation of oil and soap samples

The frying palm oil, bottled in Austria, was used for the experimental frying and afterwards for the soap production. French fries (Hearty Food Co., Tesco, Czech Republic) were used to simulate ordinary palm oil use in frying processes. The frying process was conducted in the fryer "CONCEPT FR 2035" The determination of total polar matter (TPM) served as the indicator of oil spoilage during the frying process. TPM value was recorded by TPM meter "testo 270". The fresh (unused) sample was taken as the control one. The description of the samples is given in Table 1. The sampling was done according to TPM values given in Table 1. The soap samples were made using the cold saponification and the recipe consisted of 130 g of oil, 17.52 g of NaOH and 49.40 g of distilled water. The water solution of NaOH was firstly cooled to the room temperature and then mixed with oil using the blender until a pudding-like consistency was achieved. The mixture was then poured into the silicone moulds and left for 24 hours to harden, after which it was pulled out and placed on filter paper to mature in the air for four weeks.

Table 1 Description of oil and soap samples and abbreviations

Sample	Abbreviation	TPM level (%)
Control	0P	5
Sample 1	1P	6.5
Sample 2	2P	10
Sample 3	3P	15
Sample 4	4P	20
Sample 5	5P	24

Analysis of the oil and soap

Oil and soap analysis were done using standard procedures. Oil samples were tested on acid value, peroxide value and malondialdehyde (MDA), while analysis of soap samples included pH, moisture content (dry matter), total alkali, total fat content, MDA, hardness and brittleness.

Acid value (AV) was determined by titration of oil samples dissolved in diethyl ether with KOH solution according to the method from ISO 660:2009 standard. Results are calculated using the formula:

$$AV = (56.11 \times V(KOH) \times c(KOH) / m(sample)) \times 10$$

Determination of peroxide value was done using the method from ISO 3960:2017. The oil sample was mixed with chloroform/glacial acetic acid mixture, added distilled water and 1% starch solution, and titrated with 0.01M $Na_2S_2O_3$ solution. Water was used instead of samples for blank preparation. Calculation of results was done using the formula:

$$PV = 10 \times (V(Na_2S_2O_3) - V(blank)) / m(sample)$$

pH measurements were done in a 1% solution of soap in distilled water (Vivian et al. 2014). The measurements were done using the instrument pH meter Orion 4 star, Thermo Scientific.

Moisture content was done by drying the 5 g of sample in an oven until a constant mass was achieved. The weighing was done on an analytical balance model "ALS 250-4A", Kern. The percentage of moisture was calculated using the following formula:

$$\% \text{ moisture} = (m(sample) - m(dried\ sample))/(m(sample)) \times 100.$$

The total alkali was determined by titration of a mixture containing dissolved 10g of soap in 100 ml of neutralized ethanol and 5 ml of 1 N $H_2SO_{4(aq)}$ with 1N NaOH using the phenolphthalein as the indicator (Vivian et al. 2014). The percentage of total alkali was obtained using the formula:

% Total alkali = (V(Acid)-V(Base))/(m(sample)) x 3.1.

The total fat matter was done by determination of the matter insoluble in alcohol (Vivian et al. 2014). The 10g of soap sample was dissolved in 150 ml of warm neutralized ethanol, filtered and remaining residues on filter dried and weighed. The results were obtained using the formula:

% Total fat matter = (100 – (moisture content + matter insoluble in alcohol)) / 1.085.

The MDA values were obtained using the TBA (thiobarbituric acid) method (Khalifa et al. 2016). The sample of 1.5 g was homogenized with 1 ml of EDTA, 5 ml of 0.8% BHT and 8 ml of 10% TCA and centrifuged for 5 minutes at 3000 RPM. The lower layer was filtered and supplemented with 10% TCA to the 10 ml volumetric flask. 4 ml of this solution was mixed with 1 ml of TBA and incubated 90 minutes at 70°C, then cooled down to room temperature and incubated for another 45 minutes before the measurements were done on 532 nm on spectrophotometer "CE7210", Cecil Instruments. Calculations were done using the standard calibration curve.

Measurement of texture was done on the texturometer TA.XT plus, Stable Microsystems. The hardness and brittleness results were obtained using the fracture wedge A/WEG fixture.

RESULTS AND DISCUSSION

In Table 2 are shown the results for the palm oil samples in several stages of french fries frying process. Acid value (AV), suggests the level of triglycerides decomposition and the quality of free fatty acids (Oladiji et al. 2010, Oboh et al. 2014). From the obtained results for AV, it can be seen a significant ($P < 0.05$) increase for the samples 3P (15% TPM) and 4P (20% TPM), the values were 3.7 (mg KOH/g and 11.15mg KOH/g for 3P and 4P respectively. Between three first samples (0P, 1P and 2P) no significant difference was obtained, and it was below 2.5 mg KOH/g value that was marked as the limit for used frying oil freshness (Park et al. 2016). Though, AV is used as an indicator of the freshness and condition of the used oil; value for samples in the final stage of frying (5P) showed no significant ($P > 0.05$) differences within the first three samples (0P, 1P and 2P). The reason might be in the thermal degradation of acids formed in the previous steps.

Table 2 Results of oil samples analysis

Sample	Acid value (mg KOH/g)	Peroxide value (mEq/kg)	MDA (µg/g)
0P	1.86 ± 0.00^{a}	3.97 ± 0.00^{a}	0.15 ± 0.00^{a}
1P	2.32 ± 0.66	21.56 ± 0.93^{ab}	0.16 ± 0.00^{b}
2P	1.85 ± 0.01^{a}	18.71 ± 0.23^{b}	0.30 ± 0.01^{c}
3P	3.70 ± 0.01^{b}	61.63 ± 1.23^{c}	0.67 ± 0.04^{d}
4P	11.15 ± 0.02^{c}	295.00 ± 16.83	2.42 ± 0.00^{e}
5P	4.64 ± 1.31	58.10 ± 1.59^{c}	1.29 ± 0.00^{f}

Peroxides are known as the primary oil oxidation products (Kaleem et al. 2015). Expected increasing trend in peroxide values (PV) (Table 2), was obtained from 3.97 mEq/kg for fresh sample (0P) to 295.00 mEq/kg for sample 4P. The sample 5P exhibited lower PV in comparison to the sample 4P, and a similar decrease in PV was also reported at some point in work of Oboh et al. 2014. This can be explained by the instability of peroxides that are decomposing to aldehydes and carbonyl compounds (Oboh et al. 2014).

MDA is known as a secondary product of oil oxidation (Gaweł et al. 2004). MDA oil values (Table 2) significantly ($p < 0.05$) increased with each stage of oil frying from 0.15 µg/g (sample 0P) to 2.42 µg/g (sample 4P). The increase of the MDA in heat-treated palm oil was also reported in the work of Oboh, during 20 minutes of frying. The decrease to 1.29 µg/g in sample 5P could be attributed to the further decomposition of MDA.

Chemical analysis of experimentally produced soap samples are presented in Table 3.

Table 3 Results of soap samples chemical analysis

Sample	pH	Moisture content (%)	Total alkali (%)	Total fat matter (%)	MDA (µg/g)
0P	10.13 ± 0.02^{a}	7.07 ±0.16	0.00 ± 0.00^{a}	85.44 ± 0.12^{a}	0.74 ± 0.01^{a}
1P	10.16 ± 0.01^{b}	8.80 ± 1.22	0.01 ± 0.01	83.80 ± 0.91	0.58 ± 0.00^{b}
2P	10.07 ± 0.01^{c}	8.58 ± 1.00	0.00 ± 0.00^{a}	83.93 ± 0.76	0.49 ± 0.01^{c}
3P	10.13 ± 0.01^{a}	7.40 ± 0.06	0.00 ± 0.00^{a}	84.99 ± 0.12^{b}	0.68 ± 0.00^{a}
4P	10.00 ± 0.00^{d}	8.21 ± 0.29	0.03 ± 0.01^{b}	84.09 ± 0.24^{c}	0.58 ± 0.02^{b}
5P	9.97 ± 0.01^{e}	8.04 ± 0.11	0.00 ± 0.00^{a}	84.58 ± 0.08^{c}	1.55 ± 0.00^{d}

The pH values of all soap samples ranged from 9.97 in 5P sample to 10.16 in 1P sample. Statistically significant ($P < 0.05$) difference was obtained between all samples except between samples 0P and 3P. Though, the absolute difference was quite low. The obtained results were in accordance with the study of Sanaguano-Salguero et al. (2018), their results ranged from 9.96 to 11.30. Commercial soaps tested in the work of Tarun et al. (2014) mainly had pH values between 9 and 10.

The moisture content analysis revealed low values for obtained soap samples. The values ranged from 7.07% in 0P sample to 8.80% in 1P sample. No statistically ($P > 0.05$) significant differences were obtained between all the samples. Higher moisture content values were reported by Sanaguano-Salguero et al. (2018), with the range from 24.90% to 43.24% for soaps made from waste frying oils, and from 30% to 35% for tested commercial soaps. Lower moisture content in our study could be explained by the different recipe and different type of oil used for the preparation. The 14% of moisture as a maximum was declared on some of branded commercial soaps' labels (Betsy et al. 2013).

Total alkali content exhibited low values and only above 0.00% for samples 1P (0.01%) and 4P (0.03%). Quality of soap is better if alkali content is lower (Betsy et al. 2013). The important factor for the determination of soap quality is the total fat matter because higher fatty acid concentration positively affects the skin rehydration and supports the cleansing (Betsy et al. 2013). The obtained values for soap samples were similar ranging from 83.80 (1P) to 85.44 (0P), but without significant ($P > 0.05$) differences between them.

The results obtained for MDA in soap samples did not follow the increasing trend which was obtained in oil samples. The lowest value had the sample 2P (0.49 µg/g) while the highest had the sample 5P (1.55 µg/g). The reason for such results might be in reactions that may occur during and after the process of saponification that are still not explained. The fact is supported by not finding studies (in respectful science databases) about malondialdehyde content in soaps.

Textural analysis of soaps has been poorly explained in the literature too. Hardness and brittleness of soap samples are presented in Table 4.

Table 4 Results of soap samples texture analysis

Sample	Hardness (g)	Brittleness (mm)
0P	2740 ± 263^{a}	5.4 ± 0.5
1P	2278 ± 122^{bc}	5.5 ± 0.4
2P	2492 ± 178^{ac}	5.4 ± 0.4
3P	2065 ± 189^{b}	5.7 ± 0.3
4P	2087 ± 207^{b}	5.7 ± 0.3
5P	2693 ± 206^{a}	6.2 ± 0.9

The hardness of all soap samples ranged from 2087 g (sample 3P) to 2740 g (sample 4P). The statistical ($P < 0.05$) difference was not obtained between sample made of fresh oil (0P) and sample made of oil from the last stage of frying (5P), and other samples do not differ much from each other. Thus, it can be concluded that frying of oils did not affect the hardness of the soaps made out of it. Brittleness can be described as a distance the knife travels through the sample dimensions

10 x 10 mm before it breaks. All obtained values for this property were similar and no significant ($P > 0.05$) difference was obtained between them.

CONCLUSION

Frying oils that were used for cooking are mostly disposed of in the sewage that have a negative ecological and economic impact. In the present study, fresh and fried palm oils were used for soap making purposes. Based on the results obtained from the physicochemical analysis, it can be concluded that it was possible to produce soaps with satisfying chemical and textural properties and that the frying did not fully distinguish soaps made from fresh and fried palm oil. Certainly, that future studies will focus on more in depth analysis of soaps produced from used/fried oils. From the ecological point of view fried oil used in the soap production represents green technology that could be applied more in industrial soap production.

ACKNOWLEDGEMENTS

The research was financially supported by the Veterinary and Pharmaceutical University Brno on Project: Internal Grant Agency IGA 228/2020

REFERENCES

Azahar, W.N.A.W. et al. 2016. The potential of waste cooking oil as bio-asphalt for alternative binder–an overview. Jurnal Teknologi, 78(4).

Betsy, K.J. et al. 2013. Determination of alkali content & total fatty matter in cleansing agents. Asian Journal of Science and Applied Technology, 2(1): 8–12.

FAOSTAT. 2014. Food and Agriculture Organization of the United Nations. Available at: http://www.fao.org/faostat/en/#data/QC. [2020-09-15].

Félix, S. et al. 2017. Soap production: A green prospective. Waste management, 66: 190–195.

Gaweł, S. et al. 2004. Malondialdehyde (MDA) as a lipid peroxidation marker. Wiadomosci lekarskie (Warsaw, Poland: 1960), 57(9–10): 453.

Herva, M. et al. 2014. Environmental assessment of the integrated municipal solid waste management system in Porto (Portugal). Journal of Cleaner Production, 70: 183–193.

Kaleem, A. et al. 2015. Investigating changes and effect of peroxide values in cooking oils subject to light and heat. FUUAST Journal of Biology, 5(2): 191–196.

Khalifa, I. et al. 2016. Improving the shelf-life stability of apple and strawberry fruits applying chitosan-incorporated olive oil processing residues coating. Food Packaging and Shelf Life, 9: 10–19.

Maniak, B. et al. 2009. Physicochemical changes of post frying sunflower oil. International Agrophysics, 23(3): 243–248.

Maotsela, T. et al. 2019. Utilization of Waste Cooking Oil and Tallow for Production of Toilet "Bath" Soap. Procedia Manufacturing, 35: 541–545.

Oboh, G. et al. 2014. Effect of thermal oxidation on the physico-chemical properties, malondialdehyde and carotenoid contents of palm oil. Rivista Italiana Delle Sostanze Grasse, 91(1): 59–65.

Oladiji, A.T. et al. 2010. Studies on the physicochemical properties and fatty acid composition of the oil from ripe plantain peel (Musa paradisiaca). African Scientist, 11(1): 73–78.

Panadare, D.C. 2015. Applications of waste cooking oil other than biodiesel: a review. Iranian Journal of Chemical Engineering (IJChE), 12(3): 55–76.

Park, J.M., Kim, J.M. 2016. Monitoring of used frying oils and frying times for frying chicken nuggets using peroxide value and acid value. Korean journal for food science of animal resources, 36(5), 612.

Sanaguano-Salguero, H. et al. 2018. Use of waste cooking oil in the manufacture of soaps. International Journal of Ecology & Development, 33(1): 19–27.

Singh-Ackbarali, D. et al. 2017. Potential of used frying oil in paving material: solution to environmental pollution problem. Environmental Science and Pollution Research, 24(13): 12220–12226.

Tarun, J. et al. 2014. Evaluation of pH of bathing soaps and shampoos for skin and hair care. Indian Journal of Dermatology, 59(5): 442.

Vivian, O. P. et al. 2014. Assessment of the physicochemical properties of selected commercial soaps manufactured and sold in Kenya. Open Journal of Applied Sciences, 4: 433–440.

Evaluation of spatio-temporal distribution of erosion control effectiveness of winter wheat using phenological and rain gauge stations network

Jiri Brychta[1], Jana Podhrazska[1], Lenka Hajkova[2]
[1]Department of Applied and Landscape Ecology
Mendel University in Brno
Zemedelska 1, 613 00 Brno
[2]Department of Biometeorological Applications
Czech Hydrometeorological Institute
Na Sabatce 2050/17, 143 06 Praha
CZECH REPUBLIC

xbrychta@mendelu.cz

Abstract: Erosion control effectiveness of agricultural crops is expressed by C factor in USLE or RUSLE equation. Several methods of its estimation were developed due to lack of data required in original methodology. Calculation respectively mapping of its spatio-temporal distribution became a big challenge in erosion risk modelling and land consolidation process in practice. Field measurements of time variable crops characteristics – effective fall height of rain drops, root mass in topsoil layer of 10 cm width and canopy cover, were performed in several localities of Czech Republic (CR). Growing phases were monitored by network of phenological stations. Using a network of rain gauge and phenological stations were created spatio-temporally distributed maps of erosion control effectiveness of winter wheat. For interpolations were used cokriging methods with meteorological data as covariates. Resulting erosion control effectiveness of winter wheat in evaluated variant reached 81.3–93.4% in compared with black fallow. For practical use were defined average C factor values for each climatic region used in the CR.

Key Words: erosion, winter wheat, USLE, geostatistics, phenology

INTRODUCTION

Water erosion caused by heavy rainfall is one of the most environmental problems in the CR and cause a degradation of topsoil and deterioration of soil properties. The most often used methods for evaluation of water erosion respectively calculating average annual soil loss is USLE (Wischmeier and Smith, 1978) or RUSLE (Renard et al. 1997). One of the factors of these equations is so called crop-management factor C which express protective influence of vegetation cover and agrotechnics. There are several difficulties in application for local conditions due to lack of data required in original methodology. Calculation of C factor in RUSLE requires much more input data in comparison to USLE which does not allow application in CR and similarly in the most states of Europe.

Several different methods of C factor estimation and calculation were developed due to lack of optimal data defined in original methodology. We can divided these methods into several groups – based on: 1) long-term monitoring of runoff plots (Janeček et al. 2012, Wischmeier and Smith 1978), 2) defining subfactor values (Dissmeyer and Foster 1981), 3) simulated rainfall (Garcia-Orenes et al. 2009), 4) land cover classification method and average values (Panagos et al. 2015), 5) satellite multispectral data and vegetation indices (Van der Knijff et al. 2000), 6) regression and correlation analyses with climate data (Toman and Kadlec 2003), 7) Spatial-temporal distributed C factor tool (Brychta et al. 2018).

Due to limited funding sources, calculation respectively mapping of spatio-temporal distribution of C factor values (group 7) became a big challenge in erosion risk modelling and land consolidation process in practice in the sense of optimal allocation of financial expenses for erosion control measures. There has to exit databases with input data for application in engineering practice. The goal

of this research is to evaluate and summarize spatio-temporal C values for winter wheat as the most important field crop grown on a quarter of arable land in the CR.

MATERIAL AND METHODS

Used data for evaluation were obtained from 38 phenological stations and 224 temperature stations for period 2000–2012, 32 rain gauges with continuous recording and 206 rain gauge stations for period 1970–2019. Locations of used stations are shown on Figure 1. Using proposed methodology the erosion control effectiveness of winter wheat was evaluated in the form of spatio-temporal distributed maps (Figure 3–5).

Figure 1 Location of used stations

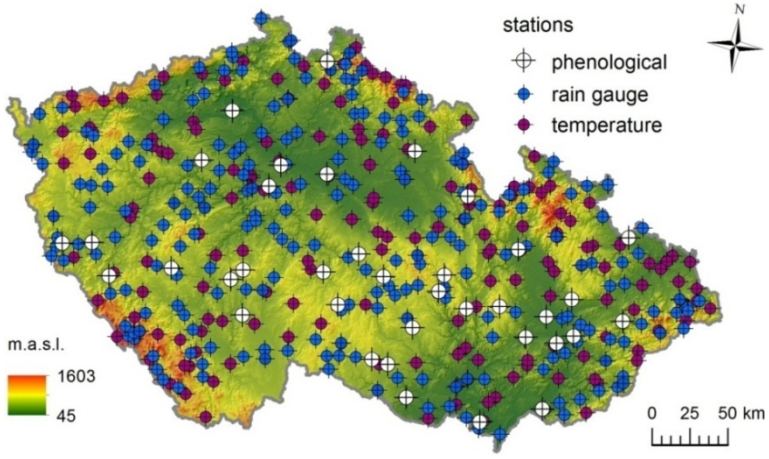

In the first step the percentage occurrence of erosive rainfalls has to be determined. Erosivity of rainfall is determined by R factor according to Wischmeier and Smith (1978) with modification of erosive rainfall determination according to Brychta and Janeček (2019) using equations 1–3:

$$R = E \times i_{30}/100 \quad (1)$$

where: R – rainfall erosivity factor (M/ha×cm/h), E – total kinetic energy of rainfall (J/m2), i_{30} – max 30-min intensity (cm/h). The total kinetic energy of rainfall is:

$$E = \sum_{i=1}^{n} E_i, \quad (2)$$

where: E_i – kinetic energy of rainfall in the i-section (n – number of section):

$$E_i = (206 + 87 \log i_{si}) \times H_{si}, \quad (3)$$

where: i_{si} – intensity of rainfall in the i-section (cm/h), H_{si} – rainfall total in the i-section (cm). Erosive rainfall was considered with total > 12.5 mm AND (simultaneously) intensity > 6.25 mm/15 min separated from other rainfall at least by 6 hours or less if the section was considered as one erosive rainfall. R factor values were calculated for each month. For interpolation were used geostatistical methods Simple Cokriging with covariates of daily rainfall total > 12.5 mm and longitude (Figure 3).

For C factor values calculation was used STD-C factor tool (Brychta et al. 2018). All time-consuming process of C calculation is automated in the tool with innovative procedure of R factor weights determination for each agro-phase using fully distributed monthly R factor maps (Figure 3). The input data of sowing and harvest according to Figure 2 are newly getting from fully distributive maps. The maps were created using interpolation of dates from phenological stations network by Simple Cokriging method with covariates of altitude and average daily effective temperature > 5 °C (Figure 4). Resulting STD-C factor values are calculated according to following equations (4–6):

$$STD\ C = (\sum_{i=4}^{n=10} Ci)/yr, \quad (4)$$

$$Ci = Ri \times Cp, \quad (5)$$

$$Ri = (Rd/Nm) \times Np, \quad (6)$$

where: STD-C – spatial-temporal distributed C factor, i, n – sequential number of months where erosive rainfalls were detected (April–October), Ci – C factor values for each month that occurs in a given agro-phase, yr – number of years, Cp – soil loss ratio (SLR) between given vegetation conditions and black

fallow – continuous regularly tilled bare fallow condition (Wischmeier and Smith 1978) for each agro-phase (according to Figure 2), Ri – R factor weights for each month that occurs in a given phase, Np – number of days that occur in a given month and agro-phase, Rd - percentage distribution of R throughout the year (decimal number – see example for May and July on Figure 3), Nm – number of days in a month (e.g. 31 for August).

Tested crop was winter wheat cultivated in variants of agrotechnology – sowing into ploughed land after cereal and all straw harvested. Soil loss ratio values were determined according to Table 1 (Brychta et al. 2018). Field measurements of time variable crops characteristics – effective fall height of rain drops, root mass in topsoil layer of 10 cm width and canopy cover, were performed in 17 localities of CR according to methodology used in RUSLE (Renard et al. 1997).

Figure 2 The timeline of 5 agro-phases for C factor calculation

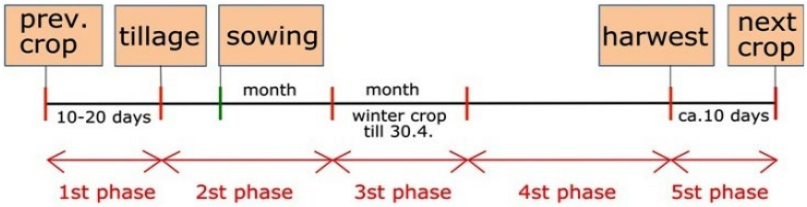

Table 1 C factor values for 5 agro-phases and different pre-crop and used agro-technique

Pre-crop	Agro-technique	C factor for each phenophase (Cp) – SLR					
		1	2	3	4	5	5m
Cereals	Sowing into ploughed land	0.65	0.7	0.45	0.08	0.25	0.04

Legend: m – straw left (not harvested).

RESULTS AND DISCUSSION

Maps of monthly percentage distribution of rainfall erosivity were created for months within which erosive rainfall occur - in CR from April to October. Example of maps for the lowest and the highest values is shown on Figure 3. Even in July exhibits generally the highest number of erosive rainfall there are high spatial variability in range of 8–70% of their occurrence. Similar research were performed by Ballabio et at. (2017) for all Europe. These maps proved the importance of spatio-temporal variability of erosive rainfall occurrence in C factor calculation in compared to currently used average values for CR.

Figure 3 The percentage distribution of rainfall erosivity in April (left) and July (right)

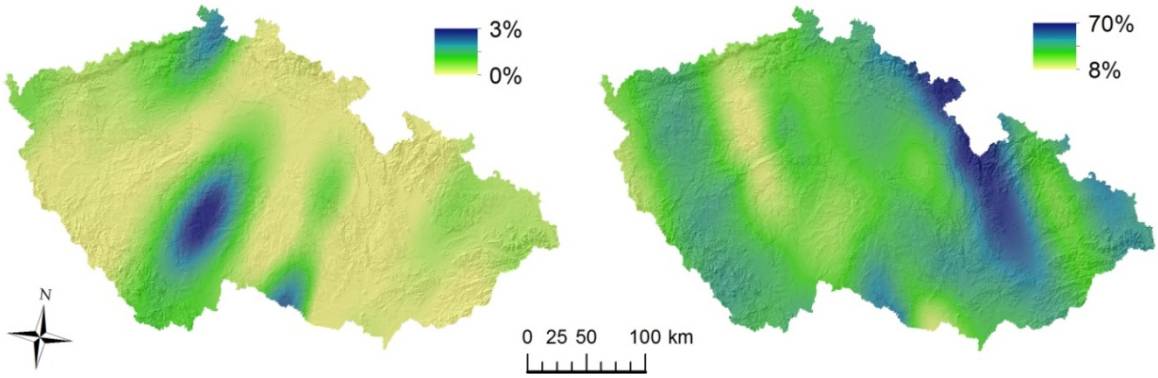

Except spatial variability of rainfall erosivity, also dates of sowing and harvest exhibits spatial variability as shown on created maps on Figure 4. These maps are key for determination of start and end of each agro-phase according to Figure 2 with respect of spatio-temporal variability figured out during 13 year monitoring by phenological stations network. While interpolated sowing dates exhibit high spatial variability, the interpolated harvest dates defines a consistent zones. Resulting calculation of fully

distributed C factor values of winter wheat for given variant is shown on Figure 5 left and average values determined for each climatic regions (classification used in BPEJ map - see details in Toman and Kadlec 2003) on Figure 5 right. Both maps exhibit significant similarities. This is in accordance to research by Toman and Kadlec (2003) who found a relationship of C values and climatic regions.

Figure 4 The spatial variability of dates of sowing (left) and harvest (right)

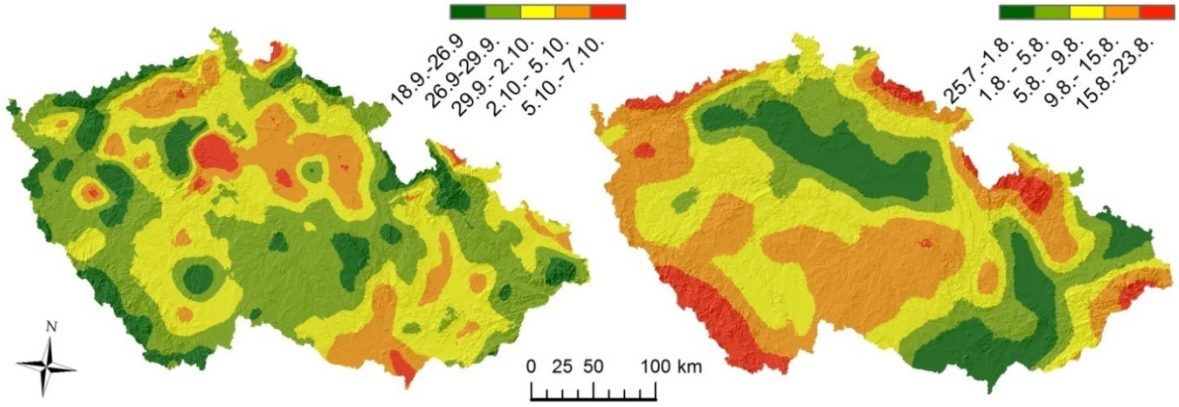

Figure 5 C factor values for winter wheat - fully distributed (right), for climatic regions (left)

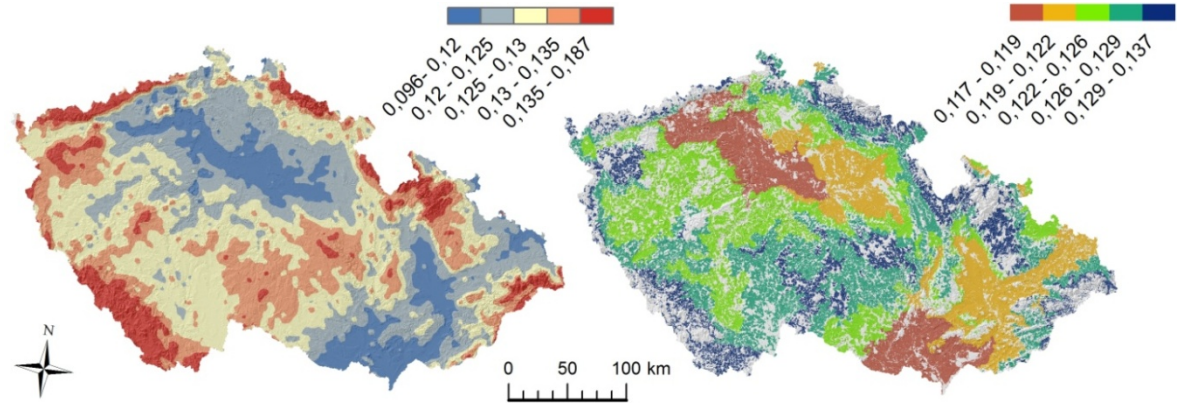

Due to climate change, the need of evaluation soil protection against heavy rainfall in higher time resolution increases. Selected time variable crop properties using in RUSLE (Renard et al. 1997) were collect by field measurements in 17 localities of CR. We can see in chart (Figure 6) average of all collected important temporal variables. The most important point in the sense of soil protection is the beginning of high occurrence erosive rainfalls. According our research, 86.2% of erosive rainfalls fall within June - August period which corresponds to period from 230th age day of crop to ca. 10–20 critical days after harvest (Brychta and Podhrázská, 2020) and 27.27% in August when is often already harvested. Winter wheat in this period reaches over 80% canopy cover and 60 g/m^2 root mass in top soil and relative lower values of effective fall height of rain drops in compare to other crops.

Figure 6 Time variable crop properties (left) and spatial distribution of heading phase (right)

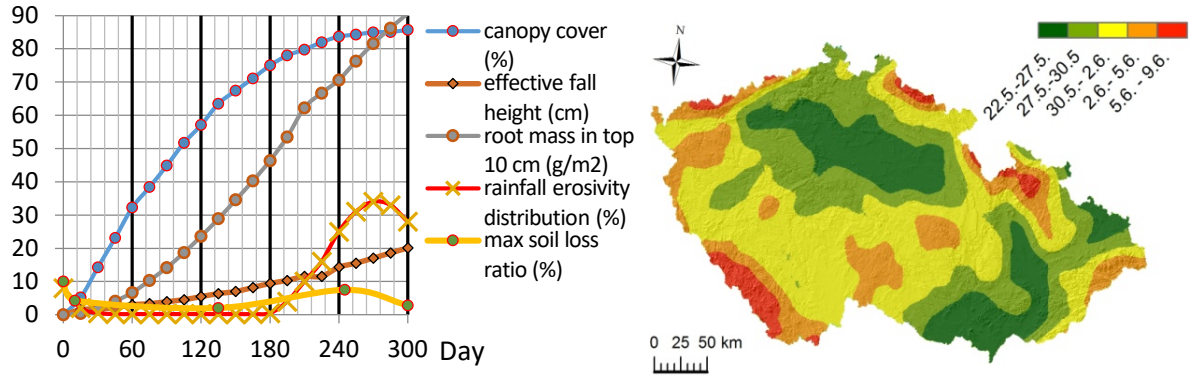

The important pheno-phase is therefore heading (code 55 according BBCH scale) when the canopy cover reaches maximal values. This pheno-phase corresponds to ca. 240th age day of crop but can be spatially variable (Figure 6 left).

CONCLUSION

Erosion control effectiveness of winter wheat in evaluated variant reached 81.3–93.4% in compared with black fallow. For evaluation of its spatio-temporal distribution was created fully distributed maps of sowing (in range 18. 9.–7. 10.) and harvest dates (in range 25. 7.–23. 8.) and rainfall erosivity. The 86.2% of erosive rainfall fall within June – August period which correspond to period from 230th age day (beginning of heading pheno-phase) of crop to harvest and ca. 10–20 critical days after harvest. The values of measured temporally variable crop properties in this period were in range – canopy cover 83–87.5%, root mass in top soil 70.6–90.6 g/m^2 and 14.3–20.1 cm effective fall height of rain drops. Critical period is after harvest which can fall within August with occurrence of 27.3% of erosive rainfalls. The use of control measures like leaving post-harvest residues in the field is a key in this critical period otherwise erosive rainfalls with numerous occurrences during this period can cause significant damages. For practical use of water erosion modelling were defined average C factor values for each climatic region used in the CR.

ACKNOWLEDGEMENTS

The research was financially supported by the Internal Grant Agency of Faculty of AgriSciences, Mendel University in Brno, project AF-IGA2020-IP00.

REFERENCES

Ballabio, C. et al. 2017. Mapping monthly rainfall erosivity in Europe. Science of the Total Environment, 579: 1298–1315.

Brychta, J., Podhrázská J. 2020. Evaluation of the Erosion Control Effectiveness of Winter Cereals in Nongrowing and Snow Melting Period. In Proceedings of Conference Public recreation and landscape protection – with sense hand in hand? Czech Republic, 11–13 May, Brno: Mendel University in Brno, pp. 158–162.

Brychta, J. et al. 2018. Crop-management factor calculation using weights of spatio-temporal distribution of rainfall erosivity. Soil and Water Research, 13(3): 150–160.

Brychta, J., Janeček, M. 2019. Determination of erosion rainfall criteria based on natural rainfall measurement and its impact on spatial distribution of rainfall erosivity in the Czech Republic. Soil and Water Research, 14(3): 153−162.

Dissmeyer, G.E., Foster, G.R. 1981. Estimating the cover-management factor (C) in the Universal Soil Loss Equation for forest condition. Journal of Soil and Water Conservation, 36(4): 235–240.

Garcia-Orenes, F. et al. 2009. Effects of agricultural management on surface soil properties and soil-water losses in eastern Spain. Soil and Tillage Research, 106(1): 117–123.

Janeček et al. 2012. Ochrana zemědělské půdy před erozí. 1st ed. Prague: Czech University of Life Sciences.

Panagos, P. et al. 2015. Estimating the soil erosion cover–management factor at the European scale. Science of the Total Environment, 48: 38–50.

Renard, K.G. et al. 1997. Predicting soil erosion by water: A guide to conservation planning with the Revised universal soil loss equation (RUSLE). USDA Agriculture Handbook No. 703. USDA-ARS. Washington D.C.

Toman, F., Kadlec, M. 2003. Regionalization methods of agricultural land use expressed by C factor and number of runoff curves CN. Soil and Water, 2: 139–150.

Van Der Knijff, J.M. et al. 2000. Soil Erosion Risk Assessment in Europe. European Soil Bureau, Joint Research Centre, Space Applications Institute.

Wischmeier, W.H., Smith, D.D. 1978. Predicting Rainfall Erosion Losses: A Guide to Conservation Planning. Agriculture Handbook no. 537. Washington, U.S.: Government Printing Office.

Effect of different soil-processing operations in the inter-row of vineyards on soil washdown

Alice Cizkova, Michaela Vaidova, Patrik Zatloukal, Patrik Burg
Department of Horticultural Machinery
Mendel University in Brno
Zemedelska 1, 613 00 Brno
CZECH REPUBLIC

alice.cizkova@mendelu.cz

Abstract: The aim of the research was to verify the share of soil particles in the surface runoff of water from the measuring area in the space of the vineyard inter-row during a different processing of the soil surface. The experiments were carried out in 2020 at an experimental site in cadastral region of Rakvice. Prior to the implementation of the experimental measurements, using the method of rainfall simulation, the soil surface in the inter-row of the experimental vineyard was treated with various types of cultivation tools. These were a ploughshare cultivator (var. I), a rotary cultivator (var. II), and a disc stubble cultivator (var. III). The working depth was 40 mm for the ploughshare cultivator, 120 mm for the rotary cultivator and 150 mm for the disc stubble cultivator. The control variant was the soil surface without a prior treatment (var. IV). For rainfall simulations, a rainfall simulator of the RIAE type was used, the simulations were performed using FullJet nozzles with wide square sprays, a working pressure of 1.0 bar and a selected intensity of 60 mm/h. The obtained results indicate that the highest values of surface washdown were found in var. IV, on the contrary, the lowest in var. III. The obtained results thus confirmed the influence of different methods of soil surface treatment on the washing of soil particles in vineyards.

Key Words: vineyard, soil tillage, soil washdown, rainfall simulation, water erosion

INTRODUCTION

Agriculture is based on intensive land use and thus contributes to its highest losses on all continents and in all climatic conditions. Vineyards in particular belong to agricultural crops with a higher degree of susceptibility, especially to water erosion, due to intensive cultivation practices, slope of land and also often lower soil fertility (Novara et al. 2018). Similarly, Biddoccu et al. (2013) state that rainfall, slope of cultivated areas, intensive tillage and its surface properties are together among the most important indicators in analyses focused on the classification of erosion processes in the conditions of European viticulture. According to Gabarrón-Galeote et al. (2013), the increasing reduction of soil water permeability leads to an increase in surface runoff of rainwater and soil erosion. Soil erodibility in vineyards depends on soil properties of a physical, chemical and mineralogical nature (Gabarrón-Galeote et al. 2013). The main process of water erosion is the separation of soil material due to raindrops and its transport through surface runoff, when the most fertile soil layer is lost (Assouline and Ben-Hur 2006). For these reasons, Ries et al. (2013) state that in the field of soil protection, standardization is needed to organize cultivation practices and evaluate experiments using precipitation simulations to assess land vulnerability, risk levels and control soil erosion.

A number of authors (Hůla et al. 2017, Ramos and Martínez-Casasnovas 2006) have addressed the issue of reducing erosive effects on agricultural land. The results of existing work suggest that a positive effect is brought by a suitably chosen method of soil processing, based on the selection of suitable cultivation tools (Novara et al. 2019). The impact of the working tools during tillage leads to varying degrees of cutting, crushing and compacting of the soil and in consequence loosening, turning and moving of the particles. Particularly in rugged and sloping terrain, the wrong choice of cultivation tools can cause surface erosion on the upper sections of the slopes, which in the middle and mostly lower parts of the slopes can turn into much more severe groove or pothole erosion. The treated land thus becomes less fertile due to soil removal (Hůla et al. 2017).

The aim of the work is a variant verification of different methods of tillage in the inter-row of vineyards for the washing of soil particles from the measuring area in the inter-row of vineyards during simulated rainfall.

MATERIALS AND METHODS

Characteristics of the experimental site

Experimental measurements were conducted during the vegetation of year 2020 and followed up on a set of experiments carried out in the previous period in a vineyard in the viticultural sub-region of Velké Pavlovice (Latitude: 48°51′29″N, Longitude: 16°48′48″ E). The inter-row of the vineyard is maintained in the form of black fallow land, and with respect to soil, chernozem, mainly loamy soil with no soil rock fragments is represented at the site. The slope of the land is 17%.

Character of experimental variants

The soil surface in the inter-rows of the vineyard was alternatively treated using a set consisting of a New Holland T4F vineyard tractor aggregated with a ploughshare cultivator OSTRATICKÝ UVPN 1.25 (var. I), a rotary cultivator KUHN EL 42 – 130 (var. II) and a disc stubble cultivator CIME TB 1300 (var. III). The working depth was 40 mm for the ploughshare cultivator, 120 mm for the rotary cultivator and 150 mm for the disc stubble cultivator. The control variant (var. IV) was compromised of inter-rows without conducted cultivation (a no-tillage).

Evaluation of physical properties of soil

At the site, soil samples were taken from a depth of 100–200–300 mm using Kopecky's physical cylinders, sampling was performed in each depth in three repetitions. Analyses of soil samples to determine particular current moisture, reduced bulk density and porosity were performed according to the methodology reported by Pospíšilová et al. (2016). At the same time, soil samples were taken from a depth of 100 and 300 mm for the purpose of determining the soil structure, which was used to determine the structural coefficient, according to the methodology given in Badalíková and Kňákal (2001).

Rainfall simulator and rainfall simulation parameters

A rainfall simulator type RIAE (Research Institute of Agricultural Engineering, p.r.i.) was gradually installed on the surface of each of the experimental variants. The device is equipped with a dosing nozzle FullJet of the type HH 17WSQ, located at a height of 1.0 m above the soil surface, the working pressure for water application was set to 1.0 bar using a manometer. This nozzle produces droplets with a size (VDM = 2 mm) that correspond to the droplet size in natural rainfall. The resulting rain intensity corresponding to a dose of 60 mm/h was determined for these conditions. Each of the experimental variants was rainfall-simulated in two replicates.

Surface runoff and washdown measurement

When measuring the runoff, the time interval from the beginning of rainfall simulation to the beginning of the water runoff was recorded, then the outflowing water was collected in 3-minute intervals together with the soil particles into plastic containers. The total simulation time was 30 minutes, until the surface runoff stabilized, the course of the whole experiment was recorded on the time axis – runoff and rinsing. The resulting surface runoff volume was determined at individual intervals after subtracting the dry weight volume, together with the cumulative volumetric runoff volume. Solids were obtained the day after decantation, drying and subsequent weighing. The weight of the dried samples was then converted to soil volume and cumulative soil volume according to soil density.

Statistical analysis

"Statistics 12.0" software (StatSoft Inc., Tulsa, Oklahoma, USA) was used to evaluate the measured data. The analysis of variance and Tukey's multiple range assay at a significance level $\alpha = 0.05$ was chosen from the statistical methods.

RESULTS AND DISCUSSION

The input values of the basic physical properties of the soil at the experimental site corresponded to the conditions of the site (Table 1).

Table 1 Physical character of soil

Depth (m)	Density (g/cm^3)	Porosity (%)	Volume		Maximum capillary capacity	Minimal air capacity
			Water	Air		
			(% volume)		(% volume)	
0.0–0.1	1.22 ± 0.04	48.88 ± 1.58	36.64 ± 5.55	12.23 ± 4.59	37.73 ± 4.67	11.14 ± 5.51
0.1–0.2	1.34 ± 0.01	52.95 ± 0.28	37.81 ± 4.20	12.96 ± 4.17	40.62 ± 1.59	14.28 ± 1.64
0.2–0.3	1.37 ± 0.03	53.44 ± 1.12	39.57 ± 2.70	13.87 ± 1.58	45.51 ± 2.94	17.93 ± 1.82

The values of reduced bulk density at all sampling depths were in the acceptable range of 1.22–1.37 g/cm^3. Thus, the limit value expressed for this soil type at the level of 1.45 g/cm^3 was not exceeded, by comparison with critical values of selected physical properties of compacted soil Badalíková and Kňákal (2001). The porosity values also correspond to the limit values. For instance, Joel et al. (2002) state that a good condition has a porosity in the range of 46–54%, Kovaříček et al. (2013) state a value of 47.08% for tillage. Values of maximum capillary capacity (critical value above 36%) and minimum values of air capacity, which were not below 10% of volume (Joel et al. 2002).

Soil structure, measured by dry aggregation, is expressed by the coefficient of structure. Values of the structural coefficient less than 1 can be considered critical. Judging by the results given in Table 2 it is clear that overall the values of the structural coefficient were high, so the soil structure in this site appeared to be good.

Table 2 Representation of structural elements

Depth (m)	Structural elements (% weight)							Structurality coefficient
	< 0.25	0.25–0.5	0.5–1.0	1.0–5.0	5.0–10.0	10.0–20.0	>20.0	
0.0–0.15	7.22	9.26	9.88	39.96	14.88	11.96	6.48	2.84
0.15–0.30	6.93	9.77	9.89	39.01	16.41	11.99	6.00	3.01
Average	7.08	9.52	9.89	39.49	15.65	11.98	6.42	2.93

Judging by the values shown in Figure 1, it is obvious that at the selected rainfall simulation intensity (60 mm/h) the highest cumulative surface runoff was measured in the control variant (var. IV) and was (27390.90 ml/m^2). The smallest values were achieved with the variant III cultivated with a disc stubble cultivator (1224.36 ml/m^2). A similar situation was measured in the case of soil particle leaching (Figure 2).

Govers et al. (1999) state that the movement of soil particles by working operations and machines during tillage is one of the little-studied areas of soil erosion research. At the same time, it states that a change in the soil structure after tillage further brings a change in hydraulic conductivity and permeability to water, heat and air. The effect of porosity is evident here. The pores are divided into those that retain water and pores that support water outflow. The intensity of soil treatment therefore reflects the orientation of the soil structure or pores. Lobb et al. (1995) state that there is insufficient description of the influence of individual groups of machines and their implements on the soil with respect to the translocation of soil particles, which can be displaced both in the machine direction and in the transverse direction with consequent erosive vulnerability.

Table 3 shows the cumulative values of surface runoff and dry mater washdown, which were evaluated using analysis of variance. From the obtained results, a statistically significant difference between all evaluated variants is evident. The largest surface runoff occurred in the control variant, the high rate of surface runoff had a direct impact on the rate of soil particle runoff, which many times

exceeded the three remaining evaluated variants. Govers et al. (1999) state that quality soil loosening is associated with better infiltration of water into the soil profile. There is no massive surface runoff or soil runoff. Hůla et al. (2017) states that in uncultivated soils, structural aggregates may be broken, the soil might merge and the permeability of the soil to water can be reduced due to the clogging of larger pores by flooded subtle particles. The result is an increased surface runoff associated with leaching. Similarly, Tippl et al. (2010) state with reference to the experiments carried out at RISWC Prague (Research Institute for Soil and Water Conservation) that disturbance of the soil surface by loosening has a significant effect on increasing soil infiltration capacity, which leads to reduced surface runoff.

Table 3 The surface runoff and dry matter loss – evaluation of variants

Experiment variants	Cumulative values of volume	
	Surface runoff (ml/m^2)	Dry matter washdown (ml/m^2)
Var. I (ploughshare cultivator)	27390.90 ± 109.91^{c}	29.10 ± 0.09^{c}
Var. II (rotary cultivator)	2801.56 ± 57.02^{b}	10.94 ± 0.48^{b}
Var. III (disc stubble cultivator)	1224.36 ± 15.02^{a}	5.64 ± 0.02^{a}
Var. IV (control)	83105.00 ± 63.35^{d}	209.99 ± 1.65^{d}

Legend: Data are expressed as means ± standard deviation, different letters in the same columns represent significant difference ($P < 0.05$).

The obtained results suggest that a suitably chosen method of soil cultivation represents in our conditions an effective procedure to reduce water runoff and soil washdown in the cultivation of vines. Unprotected and at the same time unprocessed soil surface contributes to the formation of surface crust, which limits the intake of water by soil during heavy rain and thus deepens soil erosion.

Figure 1 Surface runoff

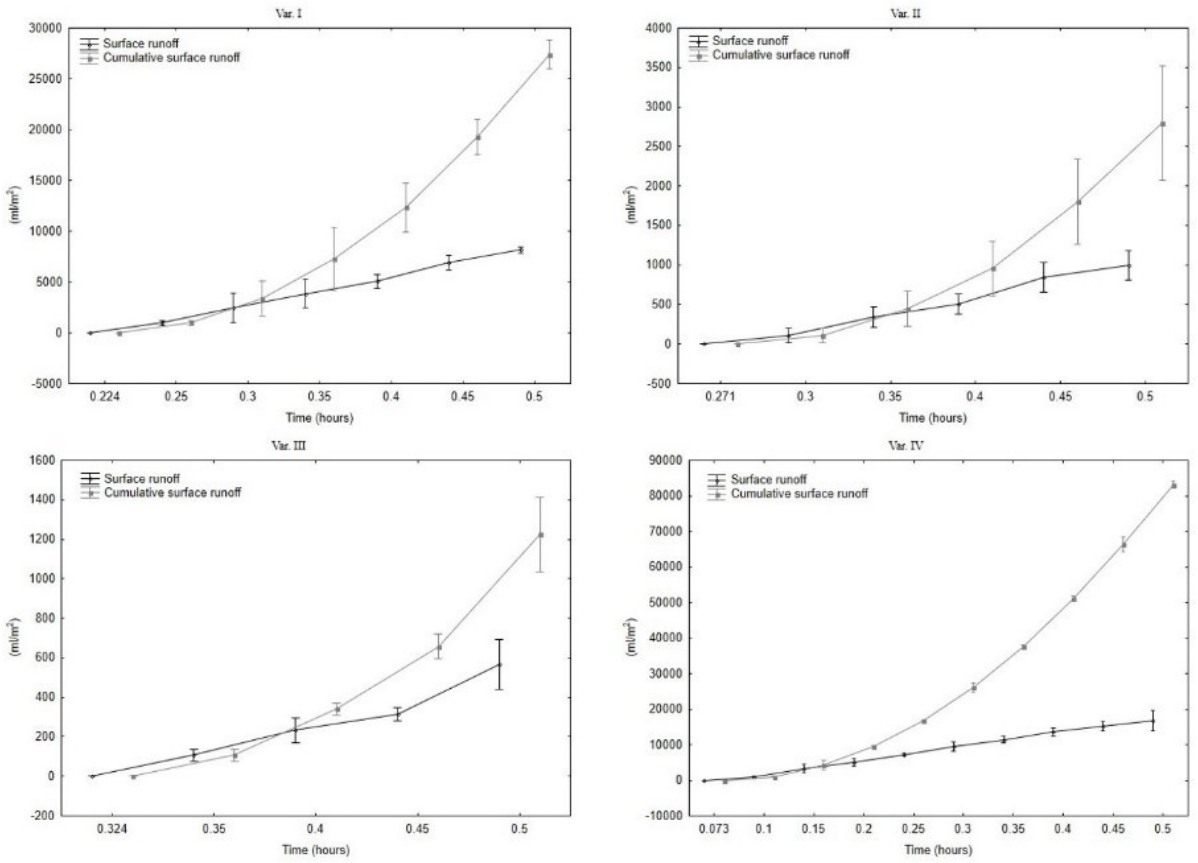

Figure 2 Washdown

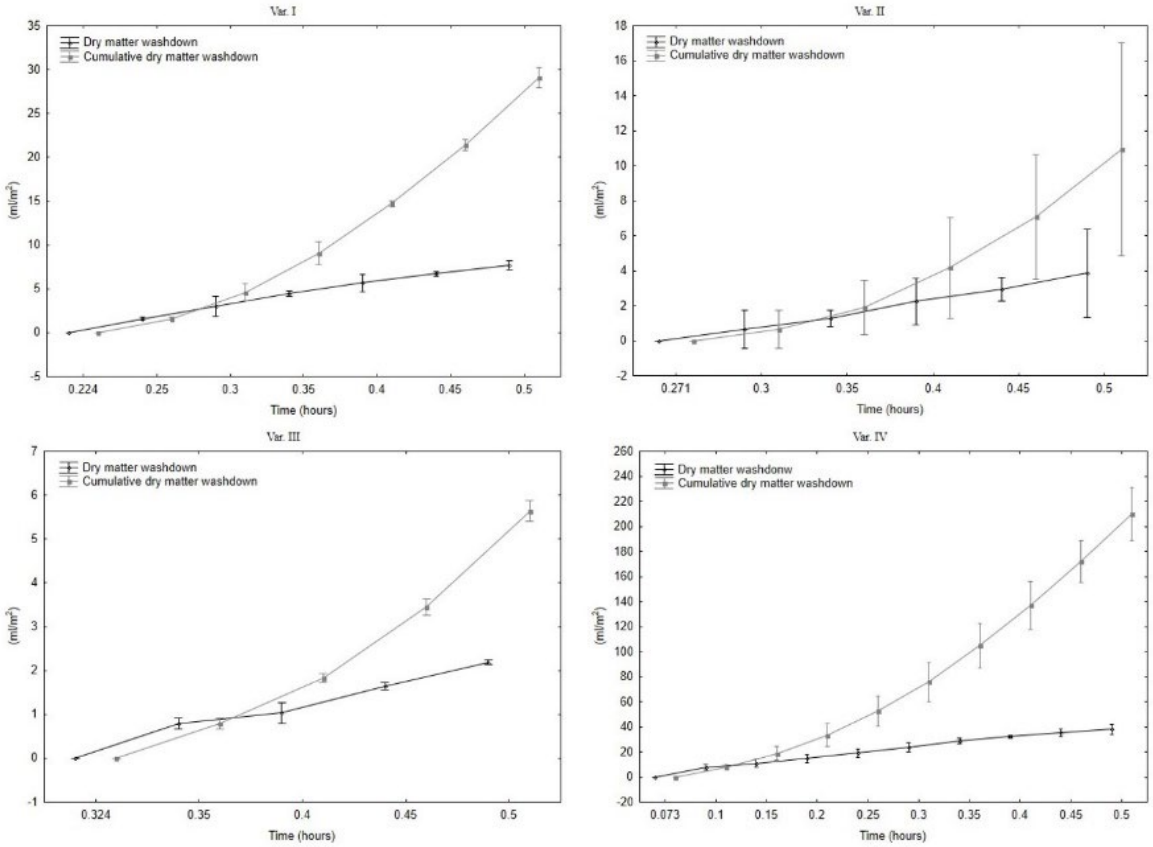

CONCLUSIONS

In particular, water erosion is considered to be the cause of the loss of large amounts of land in the conditions of wine-growing regions. This paper focuses on the evaluation of different variants of tillage in the inter-row of vineyards using different types of mechanization means, whose working tools have the ability to loosen the soil with different intensity and at different depths. The best results were obtained at variant III, cultivated with a disc stubble cultivator (working depth 150 mm) with the lowest soil particle outflow, followed by variant II cultivated with a rotary cultivator (working depth 120 mm). In both variants, the working tools worked at greater depths than in variant I (working depth 40 mm) and control variant IV without tillage. The obtained results suggest that the selection of a suitable type of cultivation tool can be an effective tool in the regulation of erosive effects. The subject of further research should therefore be the evaluation of the types of working tools used acting on the soil, their geometry, adjustment of cultivation machines, including determination of the correct working depth and travel speed of sets performing soil cultivation on sloping land in inter-rows of vineyards.

ACKNOWLEDGEMENTS

This paper was finalized and supported by the project IGA-ZF/2020–DP001 “Evaluation of the impact of soil-processing operations on the vulnerability of vineyard plots to water erosion” and by the project CZ.02.1.01/0.0/0.0/16_017/0002334 Research Infrastructure for Young Scientists, co-financed by Operational Programme Research, Development and Education.

REFERENCES

Assouline, S., Ben-Hur, M. 2006. Effects of rainfall intensity and slope gradient on the dynamics of interrill erosion during soil surface sealing. Catena, 66(3): 211–220.

Badalíková, B., Kňákal, Z. 2001. Vliv zpracování půdy na půdní strukturu. Úroda [Online]. Available at: http://uroda.cz/vliv-zpracovani-pudy-na-pudni-strukturu. [2020-08-02].

Biddoccu, M. et al. 2013. Hillslope vineyard rainfall-runoff measurements in relation to soil infiltration and water content. Procedia Environmental Sciences, 19: 351–360.

Gabarrón-Galeote, M.A. et al. 2013. Seasonal changes in the soil hydrological and erosive response depending on aspect, vegetation type and soil water repellency in different Mediterranean microenvironments. Solid Earth, 4(2): 497–509.

Govers, G. et al. 1999. Tillage erosion and translocation: emergence of a new paradigm in soil erosion research. Soil and Tillage Research, 51(3–4): 167–174.

Hůla, J. et al. 2017. Zpracování půdy po plodinách sklízených v letním období. Mechanizace zemědělství, 67(8): 36–38.

Joel, A. et al. 2002. Measurement of surface water runoff from plots of two different sizes. Hydrological Processes, 16(7): 1467–1478.

Kovaříček, P. et al. 2013. Vliv zapravení kompostu na pórovitost a na vlhkost půdy. Agritech Science, 7(2): 1–5.

Lobb, D.A. et al. 1995. Tillage translocation and tillage erosion on shoulder slope landscape positions measured using 137 Cs as a tracer. Canadian Journal of Soil Science, 75: 211–218.

Novara, A et al. 2018. The impact of soil erosion on soil fertility and vine vigor. A multidisciplinary approach based on field, laboratory and remote sensing approaches. Science of the Total Environment, 622–623: 474–480.

Novara, A. et al. 2019. The Effect of Shallow Tillage on Soil Erosion in a Semi-Arid Vineyard. Agronomy, 9(5): 257.

Pospíšilová, L. et al. 2016. Standardní analytické metody a kritéria hodnocení fyzikálních, agrochemických, biologických a hygienických parametrů půd: původní vědecká práce. 1st ed., Brno: Mendelova univerzita v Brně: Folia Universitatis Agriculturae et Silviculturae Mendelianae Brunensis.

Ramos, M.C., Martínez-Casasnovas, J.A. 2006. Impact of land levelling on soil moisture and runoff variability in vineyards under different rainfall distributions in a Mediterranean climate and its influence on crop productivity. Journal of Hydrology, 321(1–4): 131–146.

Ries, J.B. et al. 2013. Rainfall simulations - constraints, needs and challenges for a future use in soil erosion research. Zeitschrift für Geomorphologie, Supplementary Issuses, 57: 1–10.

Tippl, M. et al. 2010. Vliv vybraných technologií pěstování kukuřice na erozi půdy a povrchový odtok. Agritech Science, 4(2): 1–10.

Identification of vegetation barriers to model their influence on the effects of wind erosion in the Czech Republic

Josef Kucera[1,2], Jana Podhrazska[1,2]
[1]Department of Applied and Landscape Ecology
Mendel University in Brno
Zemedelska 1, 613 00 Brno
[2]Department of Land Consolidation
Research Institute for Soil and Water Conservation, Brno
Lidicka 25, 602 00 Brno
CZECH REPUBLIC

xkucera@node.mendelu.cz

Abstract: Increasing the risk of wind erosion is a very topical issue in the context of climate change. Increasing the incidence of drought and higher temperatures in agriculture-intensive areas increase the risk of wind erosion. Permanent vegetation barriers are effective protection against wind erosion, especially during the period when the soil is not protected by vegetation cover of cultivated crops. The present article presents the creation of a nationwide database of existing vegetation barriers with subsequent use for the modelling of vegetation barrier protective zones and the assessment of the spatial arrangement of liner elements in the landscape. The baseline determining the extent of vegetation barrier identification was the Map of the risk to arable land from wind erosion according to the cadastre. Identification was done for categories 5, 4 and 3 of hazard. Vegetation barriers have been identified from available databases of the Forest management institute information on Czech, Forests of the Czech Republic and ZABAGED. A classification algorithm in the GIS environment has been developed to identify vegetation barriers to model their effect on the effects of wind erosion. Outputs of the classification algorithm were subsequently verified over the current ortho-map. The modelling of the influence of vegetation barriers on the effect of wind erosion represents the creation of protective zones that will be further used for updating the map of the potential vulnerability of the CR including the influence of soil-climatic factors.

Key Words: climate change, windbreak, containment (protection) zones, spatial functions of windbreaks, soil protection

INTRODUCTION

Wind erosion (eolic) is a result of the mechanic activity of wind, which disrupts the soil surface, loosens and removes the soil particles and deposits them in other locations. This event occurs when the wind strength exceeds the threshold value of soil resistance to erosion (Pasák et al. 1984). In intensively managed agricultural land, the surface covered by protective vegetation is gradually reduced, creating conditions for the occurrence of accelerated erosion (Doležal et al. 2017).

Sown crops are damaged by the abrasive effects of sand grains carried by the wind over the soil surface. The negative impact of airborne dust on human health is not negligible either. Wind erosion occurs during dormancy, when the fields are without plant cover, especially at the beginning of the year and in early spring. The largest number of days with wind erosion during the year occurs in March (to 30%), January (23%), February and April (20%). In May, the fields are already largely protected by vegetation (Švehlík 1985).

In the conditions of the Czech Republic, for a certain period, the processes of wind erosion had not attracted particular attention. Wind erosion was perceived as a marginal process compared to water erosion, which affects more than 50% of agricultural land. The surface of the land at risk of wind erosion was estimated at 23% (Podhrázská et al. 2016, Doležal et al. 2017).

The process of wind erosion is a result of an entire complex of interactions including the wind speed, precipitation, surface roughness, soil texture and aggregation, agricultural activities, vegetation cover, and land block size (Janeček et al. 2012).

Windbreaks are an essential permanent measure against the negative effects of wind erosion. In general, these are different wide strips of trees and shrubs facing perpendicular to the prevailing wind direction with anti-erosion and soil-protection functions, e.g. in the land treatment process they are seen as primarily anti-erosion measures, but they are (and should be) also an integrated component of the ecological measures system as important landscaping elements. They can appropriately alter the landscape, make the landscape more accessible to its inhabitants, serve as habitats for natural flora and fauna (Cable 1999).

In literature and practice, the terms windbreak, protective wood belts (PWB) and line element are used for permanent vegetation wind barriers. Windbreak is virtually any permanent woody vegetation of a linear nature used to protect the land from the negative effects of the wind. Line element is any linear woody vegetation on forest or non-forest land in the landscape, their wind protection function may not be a priority. PWB is woody vegetation planted on land intended to fulfil forest functions and to protect against wind erosion (Podhrázská et al. 2008, Středa et al. 2008).

The position of windbreaks in the ecological network tends to be assessed from different perspectives. Primary is the assessment of their effectiveness in terms of protection against wind erosion. Efficiency is determined in part by its external structure, which is characterised by height, length, orientation, continuity, width and section shape. It is also determined by its internal structure, which is a function of the quantity and distribution of free and filled spaces, the area and shape of the individual vegetation elements (Brandle et al. 2004, Podhrázská et al. 2008).

According to their permeability and effectiveness, windbreaks are divided into three principal categories: permeable (porosity ca 60%), semi-permeable, and nonpermeable (porosity ca 20%) (Abel et al. 1997). The windbreak structure is determined by both its outer and inner structure. The outer structure is represented by its width, height, shape, and orientation. The inner structure includes the amount and distribution of leaves, branches, boughs, and trunks of the shrubs or trees (Podhrázská et al. 2011). To assess the windbreak effectiveness, we often use optical porosity (OP) established based on photographs (Kenney 1987, Guan et al. 2003, Podhrázská et al. 2011, Lampartová et al. 2015, Středová et al. 2012, Řeháček et al. 2017).

According to Heisler and DeWalle (1988), low and medium porosity windbreaks have significantly higher efficiency compared to windbreakers with higher porosity. Low porosity windbreaks have more frequent turbulent flows with higher wind speeds on the lee side than mid porosity windbreaks (Cornelis et al. 2000). For the efficiency of a windbreak to reduce wind speed, it is given between 20–35 times its height on the lee side, depending on its optical porosity (Heisler and DeWalle 1988, Abel et al. 1997, Brandle et al. 2004, Janeček et al. 2012). OP is taken as a proportion of the background, visible from the perpendicular direction of the windbreak (Podhrázská et al. 2011, Řeháček et al. 2017). The appearance and function of wind traps are positively influenced by the growth consisting of trees and shrubs in which conifers have been mixed with deciduous woods (Grala et al. 2010).

MATERIAL AND METHODS

A map of areas potentially at risk from wind erosion based on soil-climatic factors (Podhrázská et al. 2016) and a map of the risk to arable land of wind erosion based on cadastre (Doležal et al. 2017) have been used to determine the potential threat of land to wind erosion. The maps were created based on new knowledge about the soil factors in the threat of heavy soils from wind erosion and new climate knowledge aiding the occurrence of wind erosion. The specific impact of meteorological conditions during cold periods of the year has been taken into account to determine the risk factor for heavy soils. These are mainly the number of cycles of thawing and subsequent freezing of the soil surface. The soil risk factor of light soils was taken from the Podhrázská et al. (2008) methodology. For climate data, new knowledge about the risk of occurrence of dries and wind conditions in the Czech Republic has been used. The climate data was compiled from a dedicated database of relevant data from selected weather stations, which was then regionalised and synthesised into a single

layer. By synthesizing a layer of soil and climate factors, a new map has been created of areas potentially at risk of wind erosion on the ground-climatic factors (Doležal et al. 2017), used as a basis for further analyses presented in this study.

Figure 1 Map of the risk to arable land of wind erosion based on cadastre

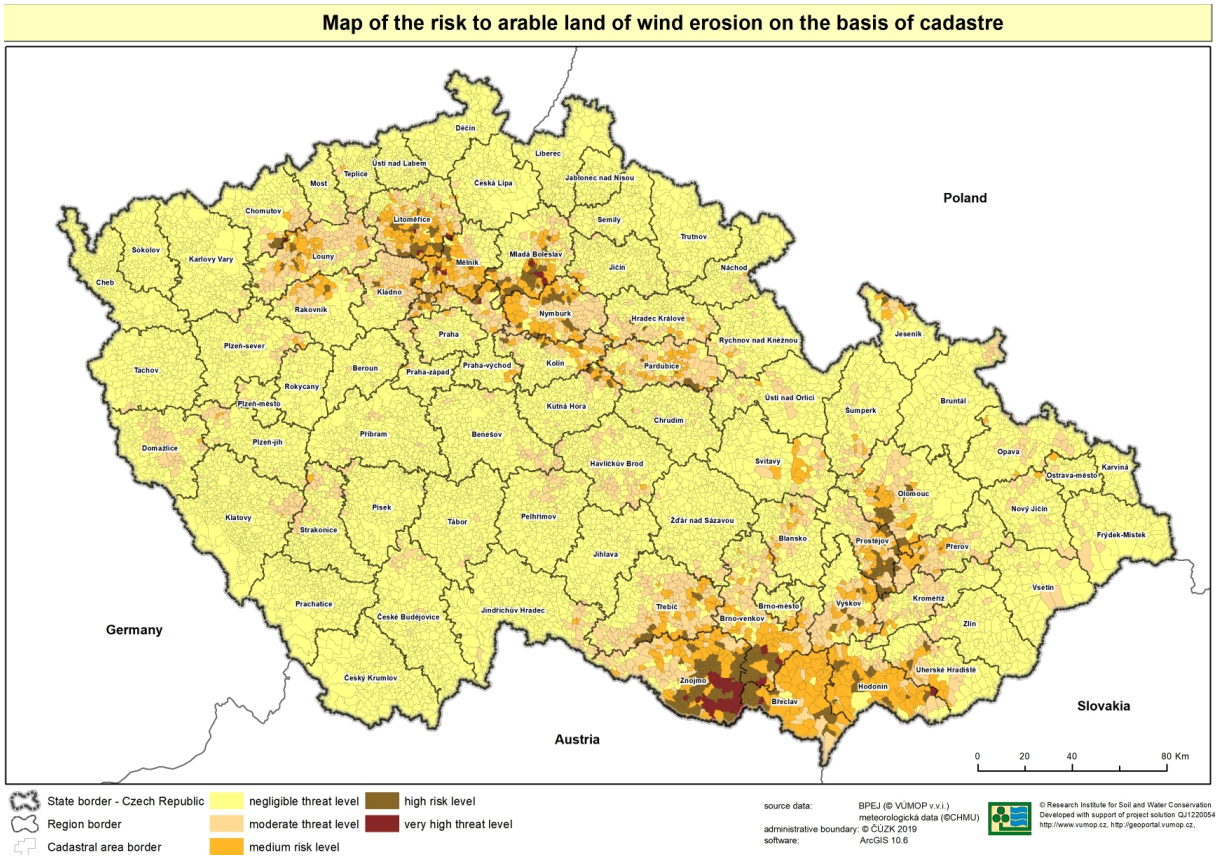

Vegetation Barrier Database

The database of vegetation barriers (windbreaks) was compiled based on information from the Forest management institute information on Czech forests (FMI), based on which it was possible to identify PWB-type elements where these elements are kept as forests with an increased function of soil protection and have been established methodologically. It was also necessary to identify other liner elements having parameters approaching PWB (height, width, density) which are not kept in the database FMI. This was done using database Forests of the Czech Republic and the CR orthophotos. For greater clarity, both PWB and these additionally digitised liner elements are referred to as windbreaks. Line elements digitised from an orthophoto not meeting the above criteria for windbreaks have been identified as other line elements (OLVP) or male forest units (an area less than 15 ha). The categorisation of the elements was therefore carried out according to the following criteria (Podhrázská et al. 2008, Podhrázská et al. 2011, Doležal et al. 2017):

Windbreak (including PWB) – the element's length-to-width ratio is min. 4:1; width of element max. 30 m (in rare cases max. 50 m).

OLVE – the ratio of length to width of an element is min. 4:1; width of element max. 6 m.

Small forest unit – less than 15 ha.

The baseline determining the extent of vegetation barrier identification was the Map of the risk to arable land from wind erosion according to the cadastre (Doležal et al. 2017). The identification was made for risk category 3 (medium risk level), 4 (high risk level), 5 (very high threat level). For the initial categorisation of vegetation barriers, a classification algorithm in the GIS environment has been developed according to these criteria.

For each windbreak, a protection zone can be established in the prevailing wind direction, which is divided into lee side and windward sides and represents an area protected from the effects of wind erosion. The width of such a zone is determined by the predicted efficiency of the wind barrier (see Table 1). Assuming their optimum spatial and species composition, the width of the protection zone can be determined at about 20–30 times the height of the windbreak on the lee side and 5–10 times on the windward side. With an assumed average height of windbreaks of 15 m, the width of the packing zone before and after the windbreak can be determined. Other linear vegetation elements (OLVE – bank stands, alleys, treehouses…) for which the expected efficiency is lower may also be considered, hence the need to reduce the buffer zone.

Outputs of the classification algorithm were subsequently verified over the current CR orthophotos. This verification was carried out for the cadastral area in threat category 4 and 5, taking into account the extent of the territory. Vegetation elements have been categorized into categories assigned a protection zone, according to the methodology of Podhrázská et al. 2008 see Table 1. A sample of the modelled buffer zones was shown in Figure 2.

Table 1 Vegetation barrier with a given protection zone

Vegetation barrier	Protective zone size – windward side [m]	Protection zone size – lee side [m]
Windbreak (including PWB)	100	300
Other linear vegetation elements (OLVE), Small forest units	50	150
Forest	not rated	not rated

RESULTS AND DISCUSSION

Based on the methodology set out in the methodology of Doležal et al. (2017), the level of risk of the territory being threatened by wind erosion per cadastral territory (c.t.) – see Table 2. In the highest fifth category of risk, 34 c.t. were at risk. in the fourth category, 260 c.t. were represented and in the next category 3, 749 c.t. were represented. In total, therefore, the verification of the rating algorithm was done in 1 043 c.t.

Table 2 Summary table of cadastre numbers for the Catastrophe Risk Map of the threat to arable land by wind erosion

Risk category	Count cadastre
1	10,210
2	1,838
3	749
4	260
5	34

A summary of the vegetation barriers identified was given in Table 3. The total database created is 9,613. Of the total 2,2846 windbreaks, 2,209 OLVE and 4,558 small forest units. The database also contains the following attributes for each element: length [m], width [m], azimuth [°], altitude [m a.s.l.].

Table 3 Summary table of vegetation barrier database

Element Name	Number of elements
Windbreaks (including PWB)	2,846
Other linear vegetation elements (OLVE)	2,209
Small forest units	4,558
Total	9,613

Figure 2 Example of modelling protection zones (white colour) windbreaks (red colour)

Identified and categorised vegetation barriers will be further used as a data base for the modelling of buffer zones. The protection zones will then be used to update the map of the potential vulnerability of the CR, including the influence of soil-climatic factors.

The issue of windbreaks (other vegetation barriers) and their irreplaceable function in areas prone to wind erosion is increasingly being discussed. In recent years, attention has turned to their importance for soil protection, mitigating the effects of climate extremes, supporting the extra-productive functions of the landscape and, last but not least, as part of agroforestry systems. Planting treehouses in fields is one form of agroforestry. It is in its beginnings in the Czech Republic, but it is one way to mitigate the effects of climate change on the agricultural landscape (Brown et al. 2018). In addition to environmental benefits, trees can also have economic benefits for farmers. Wood species may also be selected according to the intent to use woody matter.

CONCLUSION

The issue of the threat to land from wind erosion is currently a growing topic of discussion, particularly in the context of droughts and their further spread. Protecting the land with windbreaks is one of the oldest ways to protect the land against wind erosion. Our ancestors were aware of this fact, which is why forest belts have historically been planted in endangered areas to protect against the effects of wind erosion. A particularly important stage in the planting of windbreaks was the period of the 1950s to 1960s, when, especially after collectivization and land tenure, extensive networks of forest protection strips were built there. Over time, the windbreaks ceased to be cared for, with the degradation, drying and growth of invasive species. Currently, efforts are being made to return the liner greenery to the landscape mainly through territorial ecological stability systems, the planting of local bio-corridors and interaction elements implemented by e.g. land improvements. It must always be borne in mind, however, that in the territory of southern Moravia these elements should fulfil not only the function of landscape building but also of anti-erosion, adapting their spatial and functional parameters as well as their species composition.

The state of the landscape is providing conditions for the development of both water and wind erosion processes to an increasing extent. Increasing frequencies of extreme climatic events (floods, droughts, wind storms) are contributing to the expansion of areas affected by erosion processes. The aim of the European Union's Common Agricultural Policy is to ensure the long-term management of natural resources and to ensure sustainable rural development. Maintenance, establishment

and reconstruction of permanent vegetation in the agricultural landscape is an integral part of this policy. Investments in these activities should be targeted, to maximise the effect of eliminating defined risks. The study carried out in the area of interest will help to further refine the Maps of areas potentially at risk from wind erosion based on soil-climatic factors and to further assess the spatial structure of windbreaks to identify the area most at risk in terms of occurrence and potential development of wind erosion.

ACKNOWLEDGEMENTS

The study was supported by the project of National Agency of Agricultural Research (NAAR) Ministry of Agriculture No. QK1710197 and by the Ministry of Agriculture of the Czech Republic, Project No. RO2020.

REFERENCES

Abel, N. et al. 1997. Design principles for farm forestry: A guide to assist farmers to decide where to place trees and farm plantations on farms. 1st ed. Canberra: Rural Industries Research and Development Corporation.

Brandle, J.R. et al. 2004. Windbreaks in North American agricultural systems. Agroforestry Systems 61: 65–78.

Brown, S.E. et al. 2018. Evidence for the impacts of agroforestry on agricultural productivity, ecosystem services, and human well-being in high-income countries: a systematic map protocol. Environmental Evidence, 7(24): 1–16.

Cable, T. 1999. Nonagricultural benefits of windbreaks in Kansas Great Plains. Research, 9(1): 41–53.

Doležal, P. et al. 2017. Řízení rizika větrné eroze. Certifikovaná metodika. 1st ed., Brno CR: Research Institute for Soil and Water Conservation.

Grala, R.K. et al. 2010. Impact of field windbreaks on visual appearance of agricultural lands. Agroforestry Systems, 80(3): 411–422.

Guan, D. et al. 2003. A wind-tunnel study of windbreak drag. Agricultural and Forest Meteorology, 118 (1–2): 75–84.

Heisler, G.M., DeWalle, D.R. 1988. Effects of windbreak structure on wind flow. Agriculture, Ecosystems & Environment, 22/23: 41–69.

Janeček, M. et al. 2012. Ochrana zemědělské půdy před erozí: metodika. 1st ed., Prague CR: Czech University of Life Science.

Kenney, W.A.A. 1987. Method for Estimating Windbreak Porosity Using Digitized Photographic Silhouettes. Agricultural and Forest Meteorology, 39(2–3): 91–94.

Lampartová, I. et al. 2015. Impact of protective shelterbelt microclimate characteristics. Ekológia (Bratislava), 34(2): 101–110.

Pasák, V. et al. 1984. Ochrana půdy před erozí. 1st ed., Prague CR: SZN Prague.

Podhrázská, J. et al. 2008. Optimalizace funkcí větrolamů v zemědělské krajině. 1st ed., Brno CR: Research Institute for Soil and Water Conservation.

Podhrázská, J. et al. 2011. Potenciální ohroženost zemědělské půdy větrnou erozí. 1st ed., Brno CR: Research Institute for Soil and Water Conservation.

Podhrázská, J. et al. 2016. Mapa oblastí potenciálně ohrožených větrnou erozí na podkladu půdně-klimatických faktorů. Brno CR: Research Institute for Soil and Water Conservation.

Řeháček, D. et al. 2017. Effect of Windbreaks on Wind Speed Reduction and Soil Protection against Wind Erosion, Soil and Water Research, 12: 128–135.

Středa, T. et al. 2008. The Efficiency of Windbreaks on The Basis of Wind Field and Optical Porosity Measurement. Acta Universitatis Agriculturae et Silviculturae Mendelianae Brunensis. 4: 281–288.

Středová, H. et al. 2012. Aerodynamic parameters of windbreak based on its optical porosity. Contributions to Geophysics and Geodesy, 42: 213–226.

Švehlík, R. 1985. Větrná eroze půdy na jihovýchodní moravě. Zabraňujeme škodám. 1st ed., Praha CR: State Agricultural Publishing.

Influence of windbreak on the surrounding environment

Josef Kucera[1,3], Jana Podhrazska[1,3], Tomas Streda[2], Jan Szturc[1]
[1]Department of Applied and Landscape Ecology
[2]Department of Crop Science, Breeding and Plant Medicine
Mendel University in Brno
Zemedelska 1, 613 00 Brno
[3]Department of Land Consolidation
Research Institute for Soil and Water Conservation, Brno
Lidicka 25, 602 00 Brno
CZECH REPUBLIC

xkucera@node.mendelu.cz

Abstract: The basic function of windbreaks is to protect the soil from wind erosion, but it also performs many other functions in the landscape. The importance of windbreaks is increasingly also related to the positive impact on its surroundings, especially in connection with the negative effects of drought. The paper focuses on the evaluation of the impact of a windbreak on its surroundings in terms of air and soil temperature. To evaluate the influence of the windbreak on the surrounding microclimate, a line element was selected in the village of Bulhary. Furthermore, the optical porosity was determined Optical porosity was set as the average for the whole period at 19%. It is a semi-permeable windbreak. The mentioned evaluation was performed to determine the spatial parameters of the windbreak in the context of field measurements. Continuous measurements of air temperature were performed at two meters height and soil temperature at 5 cm depth. The measurements were performed using automatic meteorological stations (time step 15 minutes) located in the windbreak (B 2) and outside the windbreak (B 1). The measurement took place on two dates, in May 2018 and in March 2019. The evaluation was performed for individual days of the month when the average temperature was determined for each day of the month. The last step of the evaluation was to determine the temperature differences for the location in the windbreak and outside the windbreak.

Key Words: microclimate, air temperature, soil temperature, windbreak, optical porosity

INTRODUCTION

Janeček et al. (2005) and other authors differentiate three basic categories of windbreaks, according to their permeability. Windbreaks with porosity 60% and more are considered as permeable, windbreaks with the porosity ca 20% and less are considered as nonpermeable and those with the porosity between 20% and 60% are considered as semipermeable. The optical porosity (OP) is often used to assess windbreak effectiveness. OP can be established by using digital images. (Kenney 1987, Guan et al. 2003, Řeháček et al. 2017). Windbreaks with low and medium porosity provide much higher effectiveness than those with higher porosity. In addition to reducing wind speed, windbreaks also affect temperature and humidity (Podhrázská et al. 2008, 2011). They also provide many direct effects on agricultural production with the maximum benefits of ecosystem biodiversity (Brandle and Finch 1991). The windbreak complex reduces air mass exchange, causing a change in temperature modes compared to the unprotected area. The effect of a windbreak on air temperature depends on the time of day and the weather. During the summer season, their influence is greater as the weather gets hotter and drier, the solar radiation stronger. The influence also increases with the increasing daytime air temperature range. It is stated that the average daily air temperature is 1–3 °C higher in the protected area than in the unprotected area (Dumbrovský et al. 1995). For impermeable strips there is an increase in average temperature of up to 6 °C (Krajčírová and Streďanský 1990).

Reducing air mixing usually means an increase in daytime temperature and a decrease at night. The warming influence of the windbreak occurs in the first half of the day, when the temperature of the soil surface increases, the cooling influence starts after about 15 hours and lasts all night (Bodrov 1952).

The difference between open and sheltered areas will be greater the faster the temperature drops and rises in the ground–level air. Wind causes temperatures to level out, so there will be significant warming in the lee of the belt, where air exchange is smaller, on sunny days. In contrast, on the shaded side of the strip, the temperature is lower.

In reduced evaporation (by reducing the wind), heat is retained when the evaporation area is higher as a result of higher soil moisture or snowdrifts, the temperature drops (Brandle et al. 2004).

There is also a change in soil temperature near windbreaks. This is the result of reduced evaporation due to reduced air flow (Cleugh 1998).

An important prerequisite for the good efficiency of windbreak is the appropriate species composition of the wood used. The selected tree species should ensure the necessary efficiency of the windbreak as soon as possible, while respecting the natural conditions of the habitat. At the same time, tree species resistant to wind effects and suitable for windbreak construction (i.e. reaching desired height, ensuring required permeability) must be selected. Dumbrovský et al. (1995).

MATERIAL AND METHODS

Model locality Bulhary

To evaluate the influence of the windbreak on the surrounding microclimate, a line element was selected in the village of Bulhary, see Figure 1 and Figure 2. The windbreak was planted in the 1960s to protect the surrounding land from erosion. The field from point B2 to point B1 was seeded with corn in May 2018. On the other side, winter wheat was sown. The field from point B2 to point of measurement B1 was seeded with winter wheat in March 2019. Corn was planted on the other side.

Figure 1 Location of the interest windbreak in the cadastral area Bulhary

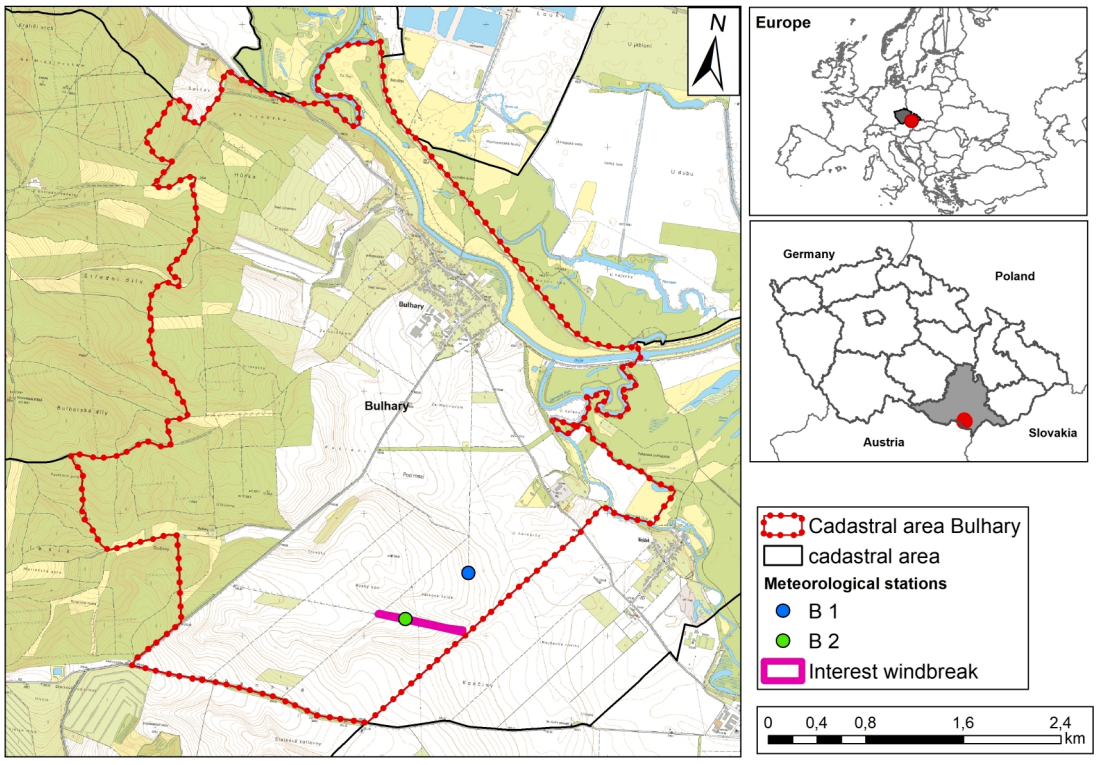

A spatial evaluation was performed for the windbreak, according to the methodological procedure specified in the methodology (Podhrázská et al. 2008), see table 1. The methodology for assessing line elements is based on the categorisation of parameters of individual windbreaks - species composition, age of the stand, functional type and its horizontal and vertical parameters (spaciousness) – Part A. Part A evaluated the following parameters: A1 spatial parameters (quantitative level), criterion – type of linear element, A2 parameters of different representation of woody plants and shrubs species, A3 parameters of horizontal and vertical composition of woody plants and shrubs, A4 parameters

of vertical composition of woody plants and shrubs. Optical porosity was also determined using the windbreak catalogue given in the methodology (Khel et al. 2017). A digital images to assess the optical porosity of the windbreak is shown in Figure 2.

Furthermore, continuous measurement of air temperature at two meters height and soil temperature at 5 cm depth was performed. The measurement was performed using automatic meteorological stations (time step 15 minutes) located in the windbreak (B 2) and outside the windbreak (B 1), see Figure 1. Stations also sensed air and soil moisture. However, these elements were not evaluated for the purposes of the paper. The measurement took place on two dates, in May 2018 and in March 2019.

Figure 2 The windbreak of interest in the cadastral area of Bulhary

RESULTS AND DISCUSSION

Evaluation of the Windbreak

The selected windbreak has an orientation N-E, its width is 14 m and height about 22 m. It is a 6-row windbreak (2 rows of poplars and 4 rows of shrubs). Optical porosity was set as the average for the whole period at 19%. The mentioned evaluation was performed to determine the spatial parameters of the windbreak in the context of field measurements (see Table 1).

Table 1 Example of evaluation of two windbreaks in the area of interest cadastral area Bulhary

The locality of interest / mark of element	Length [m]	Width [m]	Age	Height [m]	Optical porosity av. [%]	Probable way of planting		A1	A2	A3	A4	In sum	Evaluation
						Number of rows	Placement						
Bulhary / Bul	708	14	60	20	19	6 rows	2 rows of trees, 4 rows of shrubs	3	2	2	1	8	2

Field measurement

The following figures present the evaluation of daily average air temperature at 2 m height and soil temperature at 5 cm depth at the Bulhary locality in a windbreak (B 2) and outside a windbreak (B 1) for two measurement dates (May 2018 and March 2019). The evaluation was performed for individual days of the month when the daily average air and soil temperature was determined for each day of the month. The last step of the evaluation was to determine the temperature differences for the location in the windbreak and outside the windbreak. In figure 3 is presented the average air temperature and soil temperature for March 2019. In the windbreak, the average air temperature was 9.41 °C and the average soil temperature was 6.87 °C. Outside the windbreak, the average air

temperature was 10.42 °C and the average soil temperature was 7.73 °C. If we compare the average air temperatures, in the windbreak and outside the windbreak, then in this period the average air temperature was 1.01 °C higher outside the windbreak. The difference in average soil temperatures near the soil surface was 0.86 °C higher outside the windbreak. The figure 3 also shows the value of the length of sunlight in hours. The value of the sunlight length was obtained from the nearest station of the Czech Hydrometeorological Institute in Lednice. The station is about 6 kilometers from the location of interest.

Figure 3 The course of the average daily air temperature and soil temperature for March 2019

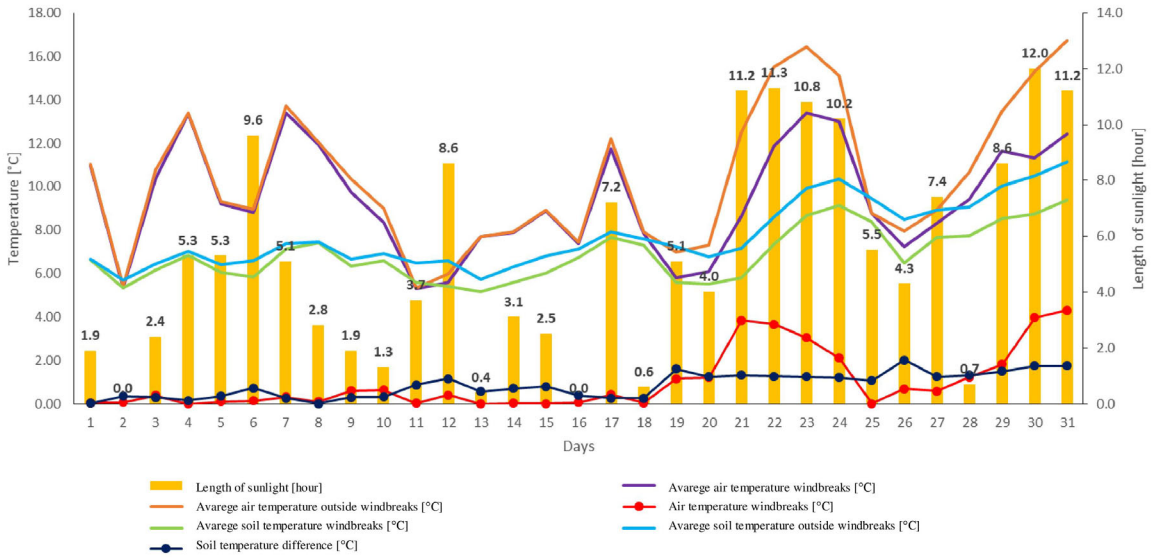

Figure 4 presents the average air temperature and soil temperature for May 2018. In the windbreak, the average air temperature was 20.16 °C and the average soil temperature was 16.51 °C. Outside the windbreak, the average air temperature was 21.56 °C and the average soil temperature was 18.85 °C. The results show that the average air temperature was 1.39 °C higher outside the windbreak. Higher average temperatures were also achieved in the evaluation of the soil temperature. Here, outside the windbreak, the average temperature was 2.34 °C higher. The figure 4 also shows the value of the length of sunlight in hours.

Figure 4 The course of the average daily air temperature and soil temperature for May 2018

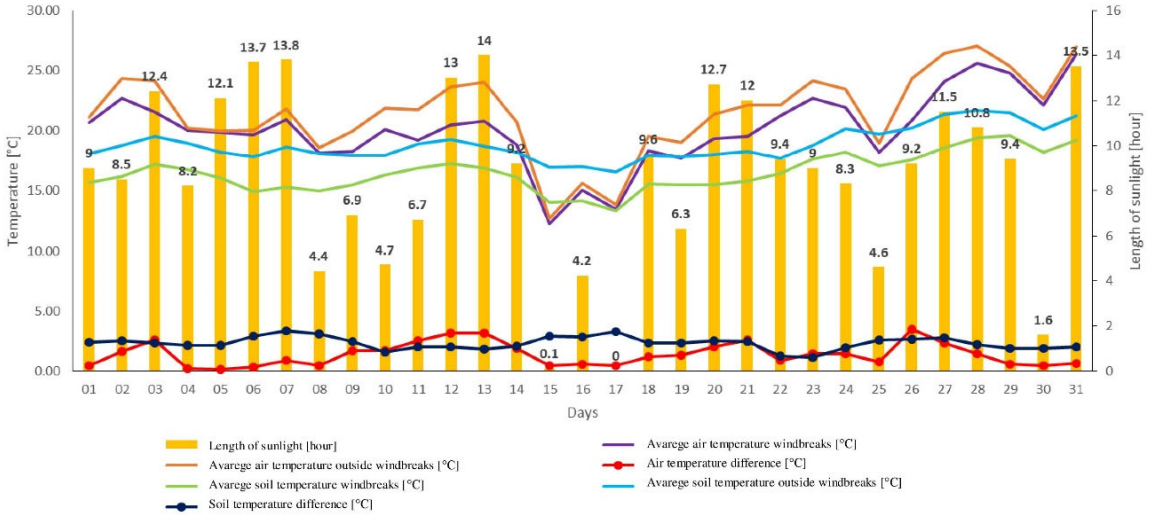

Table 2 presents comparison day and night values air temperature and soil temperature for May 2018 and March 2019. The comparison shows that outside the windbreak, temperatures have always been higher.

Table 2 Comparing day and night averages

Date	Average air temperature windbreaks [°C]	Average air temperature outside windbreaks [°C]	Air temperature difference [°C]	Average soil temperature windbreaks [°C]	Average soil temperature outside windbreaks [°C]	Soil temperature difference [°C]
2019–March–daily	9.41	10.42	1.01	6.87	7.73	0.86
2019–March–night	4.88	5.74	0.86	5.97	6.30	0.34
2018–May–daily	20.16	21.56	1.39	16.51	18.85	2.34
2018–May–night	14.72	15.21	0.49	15.18	17.41	2.24

The following figure 5 showing the detailed course of the temperature during a 22 day (24 hours in steps of 15 minutes) for March 2019. For this day, the sunlight was measured for 11.3 hours.

Figure 5 Graph showing the detailed course of the temperature during a 22 day (24 hours in steps of 15 minutes) for March 2019

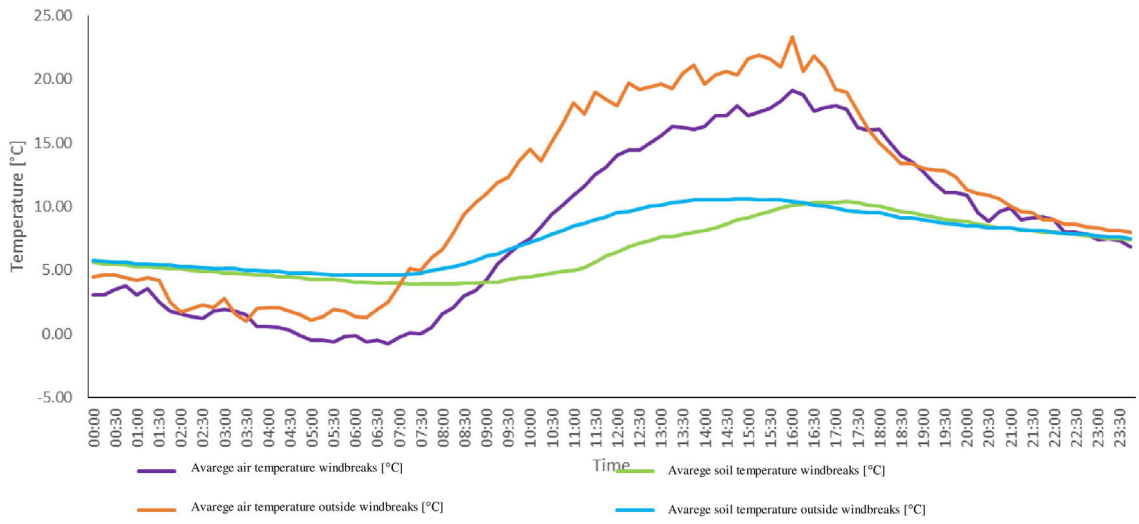

CONCLUSION

When evaluating the measurements from March 2019, it was found, that the average air temperature in this period was 1.01 °C higher outside the windbreak. The difference in average soil temperatures near the surface was also 0.86 °C higher outside the windbreak. In the second evaluated period in May 2018, the average air temperature was 1.39 °C higher outside the windbreak. Higher average temperatures were also achieved in the evaluation of the soil temperature near the surface. Outside the windbreak, the average temperature was 2.34 °C higher. The results for both measurement dates show a clear trend of increasing air and soil temperature outside the windbreak. The comparison shows that outside the windbreak, temperatures have always been higher. However, for more detailed conclusions, a deeper analysis would be needed, using other factors such as wind speed, the length of sunlight.

The issue of windbreaks and their irreplaceable function in areas prone to wind erosion is increasingly being discussed. In recent years, attention has turned to their importance for soil protection, mitigating the effects of climate extremes, supporting the extra-productive functions of the landscape. The aim of this article was to analyse the impact of the windbreak on the soil and air temperatures and thereby contribute to the deepening of knowledge, particularly in the use of windbreak plantings to mitigate climate excretion. The results of the research can also be used to support the planting of windbreaks e.g. on the territory of the Czech Republic in the process of land consolidation.

ACKNOWLEDGEMENTS
The study was supported by the project of National Agency of Agricultural Research (NAAR) Ministry of Agriculture No. QK1710197 and by the Ministry of Agriculture of the Czech Republic, Project No. RO2020.

REFERENCES

Bodrov, V.A. 1952. Les v boji proti suchu. 1st ed., Prague, CR.

Brandle, J.R., Finch, S. 1991. How Windbreaks Work. Papers in Natural Resources. 121

Brandle, J.R. et al. 2004. Windbreaks in North American agricultural systems. Agroforestry Systems, 61: 65–78.

Dumbrovský, M. et al. 1995. Doporučený systém protierozní ochrany v procesu komplexních pozemkových úprav. 1st ed., Prague CR: Research Institute for Soil and Water Conservation.

Cleugh, H.A. 1998. Effects of windbreaks on airflow, microclimates and crop yields. Agroforestry Systems, 41: 55–84.

Guan, D. et al. 2003. A wind tunnel study of windbreak drag. Agricultural and Forest Meteorology, 118(1–2): 75–84.

Janeček, M. et al. 2005. Ochrana zemědělské půdy před erozí: metodika. 1st ed., Prague, CR: Czech University of life Science.

Kenney, W.A.A. 1987. Method for Estimating Windbreak Porosity Using Digitized Photographic Silhouettes. Agricultural and Forest Meteorology, 39(2–3): 91–94.

Khel, T. et al. 2017. Metodika hodnocení účinnosti a realizace větrolamů v krajině jako nástroj pro ochranu půdy ohrožené větrnou erozí. 1st ed., Prague, CR: Research Institute for Soil and Water Conservation.

Krajčírová, Z., Streďanský, J. 1990. Lesotechnické meliorácie, 1st ed., Nitra SK: University of Agricultural in Nitra.

Podhrázská, J. et al. 2008. Optimalizace funkcí větrolamů v zemědělské krajině. 1st ed., Brno, CR: Research Institute for Soil and Water Conservation.

Podhrázská, J. et al. 2011. Potenciální ohroženost zemědělské půdy větrnou erozí. 1st ed., Brno, CR: Research Institute for Soil and Water Conservation.

Řeháček, D. et al. 2017. Effect of Windbreaks on Wind Speed Reduction and Soil Protection against Wind Erosion. Soil and Water Research, 12: 128–135.

Effect of soil amendments on fire affected soil – a pilot scale pot experiment

Petra Martinez Barroso[1], Magdalena Daria Vaverkova[1,2]
[1]Department of Applied and Landscape Ecology
Mendel University in Brno
Zemedelska 1, 613 00 Brno
CZECH REPUBLIC
[2]Institute of Civil Engineering
Warsaw University of Life Sciences – SGGW
Nowoursynowska 159, 02 776 Warsaw
POLAND

xmarti15@mendelu.cz

Abstract: A locality situated in the protected landscape area in Pálava which suffered from a recent intentionally set fire was monitored during a period of 6 months. Pot experiment investigating possibility of soil amendment application to burnt soil was performed with *Brassica juncea* L. The long-term monitoring revealed that the burnt area got revegetated rapidly but with undesirable noxious plant species that endanger local flora biodiversity. Soil amendments used in the pot experiment were not found beneficial for above-ground biomass growth and the plant best prospered in the unamended burnt soil. On the other hand, diatomite and biochar demonstrated a potential of improving soil conditions and so enhanced the root growth. Root mass yield in these two treatments, with diatomite and biochar, were higher than in the unamended burnt soil. The research suggests keeping monitoring the natural recovery of the fire affected area to gain information about the locality ability to cope with the aggressive plant species and further, recommends to carry out chemical analysis of soil, biomass and roots which will complement findings about the fire effects on soil.

Key Words: pot experiment, soil amendments, post-fire management, monitoring, natural revegetation

INTRODUCTION

Fires have always been present and affecting the world´s ecosystems which adapted to this natural disturbance (Doerr and Santín 2016). During the last century fire suppression policies were introduced which together with the migration of people from rural areas to cities led to accumulation of fuel in these areas and created ideal places for high severity fires. Ecosystems loses its capacity to recover after increased occurrence of high severity fires (Pereira et al. 2018). Parameters met during the burning (e.g. the extent, length, and intensity of fire) can affect the soil differently and there is a significant variance between the effects of low and high severity fires (Merino et al. 2018). The soil can be left contaminated with heavy metals, polycyclic aromatic hydrocarbons and other products generated during imperfect combustion. Increased concentration of these substances can deteriorate conditions for post-fire restoration or natural vegetation recovery of the affected area. Although there are many post-fire management techniques, there is still a need to search for new ones that would tackle the issue of a lack of data about contaminants generated during the fire and about its long-term impact on soil. The most frequent techniques are mulching, seedings, counter-felled logs, straw wattles, silt fences, afforestation, and natural revegetation (Robichaud et al. 2000). Soil amendments, also called soil conditioners or improvers, are materials used for supplementing the soil with the aim to enhance its physical quality. Aided phytomanagement combines the application of soil amendments and the use of vegetation and was studied in this research. The fire affected area is a suitable place for colonizing species (Doerr and Santín 2016). In certain cases, depending on pre-fire history of the area, the fire can enhance native biodiversity by clearing away weeds and provoking dormant seeds to germinate. However, in the protected landscape area which has not been adapted to reoccurring fires, it is evident that an introduction of post-fire management technique would be appropriate. The most convenient may appear to be mulching. Mulching suppresses a natural vegetation recovery which can be perceived

as a negative but on the other hand, it does not allow noxious non-native plant species to establish in the fire affected area (Robichaud et al. 2010). Mulching is an expensive method applied mainly in burnt areas where there is a risk of high-value damage of water supplies, roads, and habitats of endangered or protected species.

MATERIAL AND METHODS

Characterization of study locality

The study locality lies in a protected landscape area in Pálava, Stolová hora (48°50´25.1"N, 16°38´07.3"E). There was an intentional fire set in March 2020 in order to clear away shrubs that were impeding in a paragliding launch area. The fire affected approximately 20 x 5 m.

Experimental design

The selected study area was monitored and photographed during a natural post-fire revegetation period (April 2020–September 2020) and a green-house pot experiment with *Brassica juncea* L. (Indian/brown mustard) and following soil amendments: bentonite, diatomite and biochar (Table 1) was carried out parallelly. Samples of burnt soil from the described area were taken from the topsoil (0–15 cm) from 15 different collection points. A composite sample was created by thorough mixture of all the collected subsamples. Air-dried burnt soil was sieved, coarse material removed, and homogenized soil was used to fill the pots, each with a mixture of 291 g of burnt soil and 9 g of soil amendment (bentonite, diatomite, biochar respectively). Application rate 3% w/w was chosen based on previously carried out studies (Radziemska et al. 2017, Martínez Barroso and Vaverková 2020). The soil mixtures were saturated till reaching the water holding capacity and were left for two weeks to allow the reactions of soil amendments with the soil. Implications of soil amendments after their application to soil are described in the Table 1. Variants with burnt and unburnt soil without soil amendments (0% w/w) were set as control samples. Each treatment was prepared in 6 replicates and arranged randomly. 100 seeds of *Brassica juncea* L. (Indian mustard) were sown to each pot. The experiment was performed under greenhouse conditions (23°C, humidity of approximately 60%) and lasted for 6 weeks. After this period above-ground biomass was removed and roots carefully picked from the soil. Roots were washed in water and rinsed by distilled water. After that, all the components were dried. Biomass and roots from individual treatments were weighed and compared to controls. Figure 1 shows gradual colonization of the burnt area by non-native aggressive plant species.

Table 1 Overview of soil amendment treatments

Soil amendment	Application rate	Implications on soil
		Chemical composition
Bentonite	3% w/w	Promotes nutrient and water content retention in sandy soils (Mi et al. 2017)
		SiO_2 – 61.28% w/w; Fe_2O_3 – 17.79% w/w; Al_2O_5 – 13.01% w/w; CaO – 4.54% w/w; Na_2O – 2.70% w/w; MgO – 2.10% w/w; K_2O – 1.24% w/w (Khoeini et al. 2009)
Diatomite	3% w/w	Decreases formation of crust and big aggregates and keeps light textured soils moistened (Aksakal et al. 2013)
		SiO_2 – 54.72% w/w; Fe_2O_3 – 25.50% w/w; Al_2O_5 – 14.82% w/w; C_2O – 4.18% w/w; MgO – 0.79 %w/w (Radziemska et al. 2017)
Biochar	3% w/w	It balances the water and air content in the soil to enhance root growth and releases carbon gradually and so fertilizes over a long period (Glazunova et al. 2018)
		Carbon – 80.97 % d.m.; Nitrogen – 0.61 % d.m.; Cd – 0.5 $mg.kg^{-1}$ d.m.; Cr – 0.1 $mg.kg^{-1}$ d.m.; Cu – 6.8 $mg.kg^{-1}$ d.m. (Malinowski et al. 2018)

Figure 1 Burnt area – a gradual colonization of the burnt area by aggressive plant species

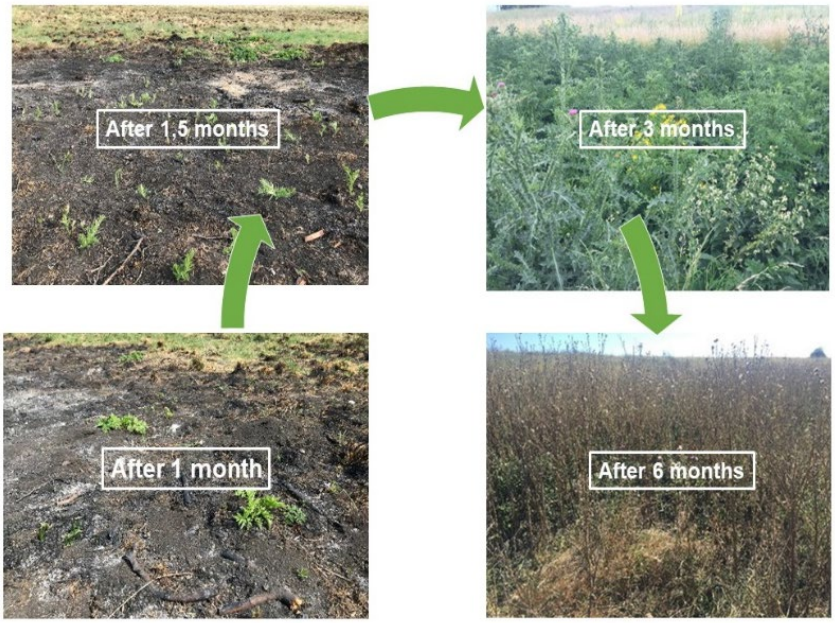

Statistical analysis

Data analysis was carried out with the use of online tool (available at: https://www.statskingdom.com/180Anova1way.html#R). For the characterization of the relation between the biomass and the root yield respectively, and the effects of individual soil amendments (with 6 replicates), a one-way analysis of variance (ANOVA) and a Tukey HSD (honestly significant difference) test were performed.

RESULTS AND DISCUSSION

Pot experiment

Biomass yields obtained from individual treatments of amended samples of burnt soil are displayed in Figure 3. The untreated burnt soil (100% BS) provided the best conditions for the biomass growth which can be explained by a temporary increase of pH and available nutrients experienced by the fire-affected soil (Certini 2005). The vegetation can benefit from these transient soil alterations. A significant difference between biomass harvested from the burnt and the unburnt soil ($p = 1.75^{-7}$; $p < 0.05$) can be attached to the fact of low fertility soils in this area. The fire can be considered as a fertilizing factor in this case. The soil amended with diatomite appears to create good conditions for growth which can be attributed to its capability to keep the soil moistened. During a fire, a water repellent layer is created on the soil surface decreasing the soil permeability (Certini 2005). Diatomite assist to tackle this problem. Biochar and bentonite were the least beneficial for the biomass growth. Although there are known benefits of biochar application, these can turn into challenges when considering biochar application to the unfertilized soils. Biochar can decrease the bioavailability of essential plant nutrients owing to strong adsorbtion (Beesley et al. 2011). A lower effect of bentonite on the biomass growth can be associated to its primary application to sandy soils while in this experiment it has been applied to sandy clay soil.

Effects of the individual soil amendments on the root yield are shown in Figure 4. Biochar had a positive effect on the root growth and the root yield was the second highest after diatomite. Biochar is added to soil to improve the conditions for root growth (Glazunova et al. 2018). The conditions for root growth in the unburnt soil were as unfavourable as for the biomass growth which might have been caused by low fertility of the soil.

Figure 3 Biomass of Brassica juncea L., Stolová hora, Pálava, CR, 2020: means with SEM (standard error of mean, n = 6)

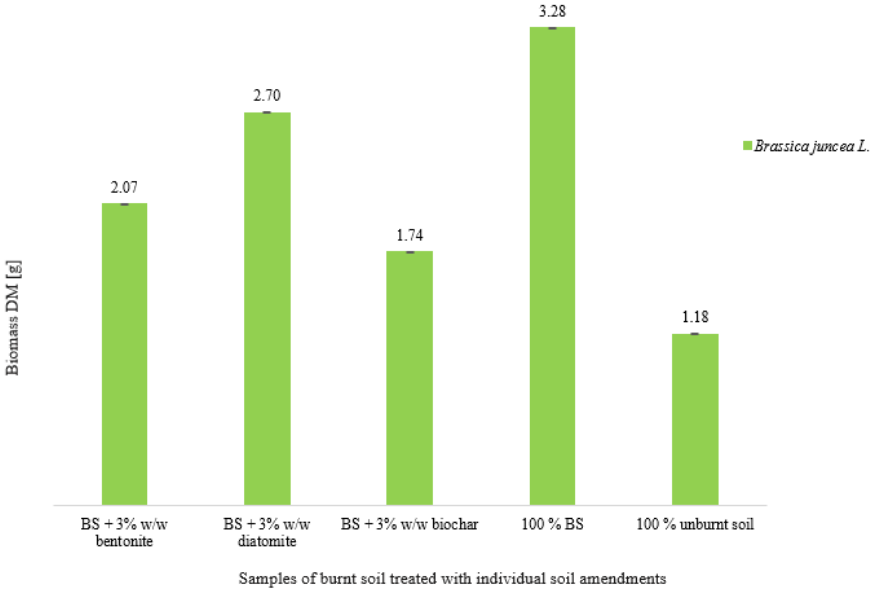

Legend: BS – burnt soil; DM – dry matter

Figure 4 Root mass of Brassica juncea L., Stolová hora, Pálava, CR, 2020: means with SEM (standard error mean, n = 6)

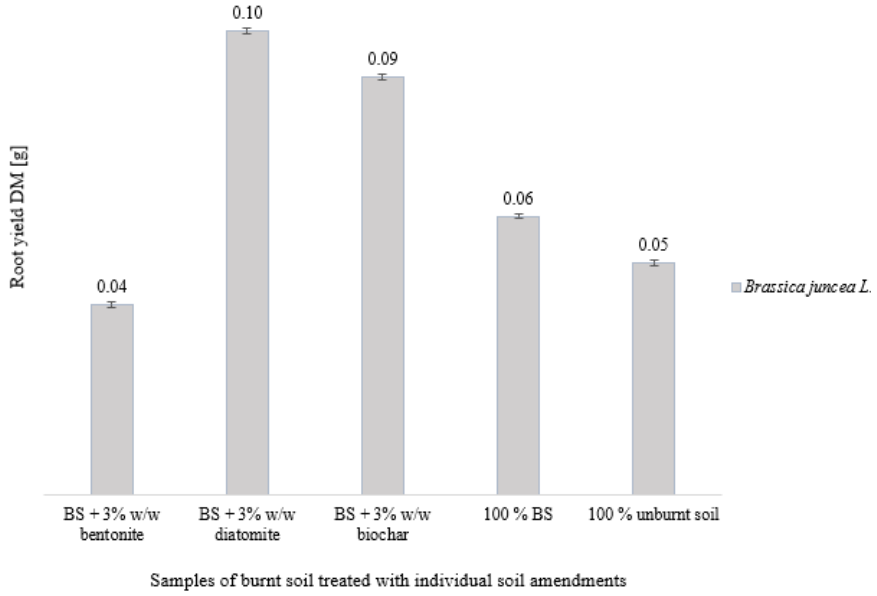

Legend: BS – burnt soil; DM – dry matter

Dependences of biomass and root yield on the effects of individual soil amendments

The results of one-way ANOVA analysis confirm a statistically significant difference between the relation of biomass yield and the effects of individual soil amendments, and between the relation of root yield and the effects of individual soil amendments since p-value of the biomass yield ($p = 1.20^{-36}$), and of the root yield ($p = 1.85^{-12}$) are lower than α ($\alpha = 0.05$). Due to this fact, the Tukey HSD test was performed, and revealed the pairs of means that are significantly different from each other. In the case of biomass yield the statistically significant difference has been validated among all the soil amendments pairs (Table 3). In the case of the root yield a significant difference has been affirmed among the following soil amendments pairs (Table 3):
BS + 3% w/w bentonite – BS + 3% w/w diatomite; BS + 3% w/w bentonite – BS + 3% w/w biochar;

BS + 3% w/w bentonite – 100% BS; BS + 3% w/w diatomite – 100% BS; BS + 3% w/w diatomite – 100% unburnt soil; BS + 3% w/w biochar – 100% BS; BS + 3% w/w biochar – 100% unburnt soil.

Table 2 Tukey HSD test – relation between the biomass yield and the effects of individual soil amendment

Pair	Difference	Standard Error (SE)	Q (SE/difference)	Lower CI	Upper CI	Critical Mean	p-value
x1-x2	0.105	0.0018043	58.193	0.097506	0.112494	0.007494	1.75^{-10}
x1-x3	0.055	0.0018043	30.482	0.047506	0.062494	0.007494	1.75^{-10}
x1-x4	0.202	0.0018043	112.046	0.194673	0.209661	0.007494	1.75^{-10}
x1-x5	0.149	0.0018043	82.302	0.141006	0.155994	0.007494	1.75^{-10}
x2-x3	0.160	0.0018043	88.676	0.152506	0.167494	0.007494	1.75^{-10}
x2-x4	0.0972	0.0018043	53.852	0.089673	0.104661	0.007494	1.75^{-10}
x2-x5	0.254	0.0018043	140.496	0.246006	0.260994	0.007494	1.75^{-10}
x3-x4	0.257	0.0018043	142.528	0.249673	0.264661	0.007494	1.75^{-10}
x3-x5	0.094	0.0018043	51.820	0.086006	0.100994	0.007494	1.75^{-10}
x4-x5	0.351	0.0018043	194.349	0.343173	0.358161	0.007494	1.75^{-10}

Legend: x1 – BS + 3% w/w bentonite, x2 – BS + 3% w/w diatomite, x3 – BS + 3% w/w biochar, x4 – 100% BS, x5 – 100% unburnt soil. Red p-values represent statistically significant differences between concrete pair of means. CI – Confidence Interval

Table 3 Tukey HSD test – relation between the root yield and the effects of individual soil amendment

Pair	Difference	Standard Error (SE)	Q (SE/difference)	Lower CI	Upper CI	Critical Mean	p-value
x1-x2	0.0098	0.000550757	17.854	0.00754588	0.0121209	0.00228749	2.51^{-6}
x1-x3	0.0082	0.000550757	14.828	0.00587918	0.0104542	0.00228749	1.18^{-4}
x1-x4	0.0032	0.000550757	5.749	0.00087918	0.00545416	0.00228749	3.51^{-3}
x1-x5	0.0015	0.000550757	2.723	-0.00078749	0.00378749	0.00228749	3.30^{-1}
x2-x3	0.0017	0.000550757	3.026	-0.00062079	0.00395419	0.00228749	2.35^{-1}
x2-x4	0.0067	0.000550757	12.104	0.00437921	0.00895419	0.00228749	6.41^{-3}
x2-x5	0.0083	0.000550757	15.130	0.00604588	0.0106209	0.00228749	7.80^{-5}
x3-x4	0.0050	0.000550757	9.078	0.00271251	0.00728749	0.00228749	9.42^{-6}
x3-x5	0.0067	0.000550757	12.104	0.00437918	0.00895416	0.00228749	6.41^{-3}
x4-x5	0.0017	0.000550757	3.026	-0.00062082	0.00395416	0.00228749	2.35^{-1}

Legend: x1 – BS + 3% w/w bentonite, x2 – BS + 3% w/w diatomite, x3 – BS + 3% w/w biochar, x4 – 100% BS, x5 – 100% unburnt soil. Red p-values represent statistically significant differences between concrete pair of means, green p-values stands for pairs of means that are not statistically significantly different. CI – Confidence Interval

CONCLUSION

The monitored fire affected area in the protected landscape area has been revegetated in a relative short time. However, the new vegetation comprises exclusively of invasive species (neophytes) of thistles and weeds which are undesirable for this locality because they can endanger local protected and rare species. Therefore, it is recommended to continue with the monitoring of the fire affected area on a long-term basis to obtain important data about the ability of this locality to cope with the introduced invasive species which colonized the area after the fire. Pot experiment provided information about the effectiveness of soils amendments. Although most biomass grew in untreated burnt soil, soil amendments are a promising tool as they had a positive impact on root growth, namely diatomite and biochar. Pot experiment will be complemented with chemical analysis of harvested biomass, roots, burnt soil, and samples of amended burnt soil. This will provide essential information for facilitating an insight into the effects that fire imposes on the soil and for evaluating soil amendment effectiveness as well.

ACKNOWLEDGEMENTS
The research was financially supported by the Internal Agency Faculty of AgriSciences (MENDELU No. AF-IGA2020-IP007).

REFERENCES

Aksakal, E.L. et al. 2013. Effects of diatomite on soil consistency limits and soil compactibility. CATENA [Online], 101: 157–163. Available at: http://www.sciencedirect.com/science/article/pii/S0341816212001841. [2020-09-10].

Beesley, L. et al. 2011. A review of biochars' potential role in the remediation, revegetation and restoration of contaminated soils. Environmental Pollution [Online], 159(12): 3269–3282. Available at: DOI:10.1016/j.envpol.2011.07.023. [2020-22-10].

Doerr, S.H., Santín, C. 2016. Global trends in wildfire and its impacts: perceptions versus realities in a changing world. Philosophical Transactions of the Royal Society B: Biological Sciences [Online], 371: 20150345. Available at: https://royalsocietypublishing.org/doi/10.1098/rstb.2015.0345. [2020-09-11].

Glazunova, D. et al. 2018. Assessing the Potential of Using Biochar as a Soil Conditioner. IOP Conference Series: Earth and Environmental Science [Online], 107: 012059. Available at: https://www.researchgate.net/publication/322842089_Assessing_the_Potential_of_Using_Biochar_as_a_Soil_Conditioner. [2020-09-10].

Khoeini, M. et al. 2009. Investigation of the modification process and morphology of organosilane modified nanoclay. Ceramics – Silikaty [Online], 53: Available at: http://www.ceramics-silikaty.cz/index.php?page=cs_detail_doi&id=435. [2020-22-10].

Lim, J.-M. et al. 2004. Phytoremediation of lead using Indian mustard (Brassica juncea) with EDTA and electrodics. Microchemical Journal [Online], 76/1–2: 3–9. Available at: https://www.sciencedirect.com/science/article/pii/S0026265X03001413. [2020-09-10].

Malinowski, M. et al. 2019. Effect of biochar addition on the OFMSW composting process under real conditions. Waste Management [Online], 84(364–372). Available at: doi:10.1016/j.wasman.2018.12.011. PMID: 30691911. [2020-22-10].

Martínez Barroso, P., Vaverková, M.D. 2020. Fire Effects on Soils – A Pilot Scale Study on the Soils Affected by Wildfires in the Czech Republic. Journal of Ecological Engineering [Online], 21(6): 248–256. Available at: http://www.jeeng.net/Fire-effects-on-soils-A-pilot-scale-study-on-soils-affected-by-wildfires-in-the-Czech,123471,0,2.html [2020-09-06].

Merino, A. et al. 2018. Inferring changes in soil organic matter in post-wildfire soil burn severity levels in a temperate climate. Science of The Total Environment [Online], 627: 622–632. Available at: https://www.researchgate.net/publication/322919321_Inferring_changes_in_soil_organic_matter_in_post-wildfire_soil_burn_severity_levels_in_a_temperate_climate [2020-09-10].

Mi, J. et al. 2017. Effect of bentonite amendment on soil hydraulic parameters and millet crop performance in a semi-arid region. Field Crops Research [Online], 212: 107–114. Available at: http://www.sciencedirect.com/science/article/pii/ S0378429016308814. [2020-09-10].

Pereira, P. et al. 2018. Post-fire soil management. Current Opinion in Environmental Science & Health [Online], 5: 26–32. Available at: http://www.sciencedirect.com/science/article/pii/ S2468584418300217. [2020-09-11].

Robichaud, P.R. et al. 2010. Post-fire treatment effectiveness for hillslope stabilization [Online]. 1st ed, Fort Collins: U.S. Department of Agriculture, Forest Service. Available at: https://www.fs.usda.gov/Internet/FSE_DOCUMENTS/stelprdb5294525.pdf. [2020-09-06].

Current occurrence of endangered *Pedicularis palustris* L. in the Bohemian-Moravian Highlands and its relation to well-performed management

Jan Oulehla[1], Martin Jirousek[2,3]
[1]Department of Applied and Landscape Ecology
[2]Department of Plant Biology
Mendel University in Brno
Zemedelska 1, 613 00 Brno
[3]Department of Botany and Zoology
Masaryk University
Kotlarska 2, 611 37 Brno
CZECH REPUBLIC
jan.oulehla@mendelu.cz

Abstract: A hemiparasitic herbaceous plant species, *Pedicularis palustris*, has historically been abundant in most of the Bohemian-Moravian Highlands. Populations of this wetland species decreased dramatically during the twentieth century, due to the gradual abandonment of the traditional use of the landscape. For this reason, *Pedicularis palustris* is now a critically endangered species within the Czech Republic, with the Bohemian-Moravian Highlands being one of the most important and last refuges of this species in Central Europe. A field survey of the current population size was carried out in 30 localities, where the species was known to be located over the last 20 years. The species was confirmed in only nine of them, whereas in the other locations, the species is probably lost due to the succession of vegetation, climate change or change in land use. The importance of well-performed management was found to be crucial for the survival of the remaining populations.

Key Words: biodiversity, plant extinction, degradation of wetlands, nature protection

INTRODUCTION

Pedicularis palustris is a hemiparasitic plant of the *Orobanchaceae* family that uses water and nutrients by haustoria from a wide range of host plants sharing the same habitats (Těšitel et al. 2015). Monocotyledonous plants like grasses and sedges are considered as main hosts (Hrouda 2000), but *Pedicularis palustris* is also able to parasitise on dicotyledons (Petrů and Lepš 2000). The most suitable habitats for this species are transitional mires, moss rich fens, reed beds and tall-sedge vegetation (Hrouda 2000, Chytrý et al. 2011). Seed propagation takes place autochorously and hydrochorously (PLADIAS), which implies the importance of a quality water regime.

There were two subspecies distinguished in the territory of the Czech Republic. Nominotypical subspecies occurs mainly in the Bohemian-Moravian Highlands, and in parts of the Šumava and Slavkovský les, although the occurrence is extremely rare in the rest of the Czech Republic. In addition to the nominotypical subspecies, the North-European subspecies *Pedicularis palustris* subsp. *opsiantha* was recently recorded in northern Bohemia (Krása 2007, Wild et al. 2019). According to Decree No. 395/1992 Sb. the species is classified as a highly endangered plant, and according to the Red List of Endangered Plants of the Czech Republic, it is classified as critically endangered (Grulich and Chobot 2017). The species is also evaluated as endangered in other central European countries (Niklfeld and Schratt-Ehrendorfer 1999, Eliáš et al. 2015).

In the twentieth century, the species was very abundant in the Bohemian-Moravian Highlands (Rybníček 1974). However, due to the change in landscape management and the adjustment of the water regime by drainage, large populations have been reduced to a critical level (Čech et al. 2014).

The aim of this article is to survey the populations of *Pedicularis palustris* in the whole Bohemian-Moravian Highlands, evaluate their current abundance in particular localities, assess the consequences of changes in abundance, and assess the possible survival of the species in this region.

MATERIAL AND METHODS

The Bohemian-Moravian Highlands are located in the central part of the Czech Republic. A total of 30 localities were visited during the vegetation season of 2020, where the species was known to be located in the last 20 years (2000–2019). Data on historical species distribution were obtained from floristic databases (Wild et al. 2019), literature (Rybníček 1974), and personal communication with local experts (E. Ekrtová, F. Lysák, T. Peterka, K. Juřičková). Abundance data were recorded at the localities, where the species was confirmed. Exact numbers of individuals were recorded on a logarithmic scale (individuals, dozens, hundreds or thousands of individuals). Information related to the local conditions and management practice was also noted.

Both the confirmed and unconfirmed findings are summarised, mapped (ESRI ArcGIS Desktop, Figure 1), and discussed in this paper. Based on a link between current and previous abundance and observed management, we recommend here a form of well-performed management for the survival of *Pedicularis palustris*.

RESULTS AND DISCUSSION

Occurrence of *Pedicularis palustris*

In the Bohemian-Moravian Highlands, the species has occurred in dozens of localities in the second half of the twentieth century (in 40 European mapping quadrates, Čech et al. 2014). Due to the abandonment of the traditional use of landscape and the adjustment of the water regime by drainage, there was a drastic decrease in the population up to 2000. Since 2000, the species have been recorded in the Bohemian-Moravian Highlands in only 23 localities (twelve quadrates of the European mapping network). In most localities, the populations showed a declining tendency.

Our own field survey of *Pedicularis palustris* sites in 2020 confirmed its occurrence in only nine localities in seven mapping quadrates of the European mapping network (Table 1, Figure 1). Stable populations during the last 20 years were found for Řeka, V Lisovech, Chvojnov, Na Oklice, Ratajské rybníky, Vílanecké rašeliniště and Kladinský potok. It should be mentioned here, that in the locality Vílanecké rašeliniště, the habitat including a population of *P. palustris* was restored by removing dense vegetation consisting of tall sedges. In the whole study region, two localities (Chvojnov and Na Oklice) had the most numerous populations. Also, in these locations the species was purposefully supported by appropriate management, which led to an increase in the abundance of the population. At present, the populations of the species exceed a thousand individuals and significantly affect the composition of vegetation and increase biodiversity. Similar numbers of individuals as in the past have been verified on Řeka mire meadow, where variation in the occurrence of individuals within the locality were observed, depending on the disturbances caused by heavy mechanisation during mowing. The occurrence in Kladinský potok can also be described as stable despite drier a habitat compared to other localities.

In the south-eastern subregion of Velké Meziříčí, last populations of *P. palustris* were found 15 years ago, and despite regular mowing management could not be restored (localities: Bohdalov, Těšíkův mlýn). In the north-eastern subregion of the Žďárské vrchy Hills, P. *palustris* was found a few years ago in the localities of Bahna, Mokřadlo, Volákův kopec and Radostínské rašeliniště. The situation in the Žďárské vrchy Hills Protected Landscape Area is critical, as the species is probably preserved in only three localities. Although it is possible that there will be new findings in the future, the probability is rather small due to the size and conspicuousness of the species. The last discovered locality is probably Medlovský rybník Pond from August 2017 (Roleček, personal communication). This locality consists of wetland vegetation on the edge of the pond and is sufficiently humid and slightly disturbed by tourists and fishermen. The example of this locality shows how positively the fluctuation of the water level can affect the distribution of the species. *P. palustris* was not confirmed in either of the localities of the south-western part of the study region (U Zabitého and Chytrov).

Table 1 List of localities with abundance of Pedicularis palustris observed in the field in 2020 and obtained for the previous twenty years. Explanatory notes: "<"population decrease, ">"population increase, "="stable population

Number (*Figure 1*)	Locality	Relative abundance 2000–2019	Relative abundance 2020	Last occurrence	Population
1	Chvojnov	100–1000 pcs	>1000 pcs	-	>
2	Nad Svitákem	<10 pcs	not confirmed	2008 (Juřička J.)	<
3	Na Oklice	10–100 pcs	100–1000 pcs	-	>
4	Kladinský potok	10–100 pcs	10–100 pcs	-	=
5	U Potoků	<10 pcs	not confirmed	-	<
6	Vílanecké rašeliniště	<10 pcs	10–100 pcs	-	>
7	V Lisovech	10–100 pcs	100–1000 pcs	-	>
8	Kaliště	<10 pcs	not confirmed	-	<
9	Chytrov	10–100 pcs	not confirmed	-	<
10	U Zabitého	<10 pcs	not confirmed	2013 (Holá E.)	<
11	U Hájenky	10–100 pcs	<10 pcs	-	<
12	Těšíkův mlýn	10–100 pcs	not confirmed	2010 (Lysák F.)	<
13	Bohdalov	<10 pcs	not confirmed	2002 (Lysák F.)	<
14	Medlovský rybník	no data	10–100 pcs	-	>
15	Radostínské rašeliniště	10–100 pcs	not confirmed	2018 (Peterka T.)	<
16	Řeka	100–1000 pcs	100–1000 pcs	-	=
17	Mokřadlo	10–100 pcs	not confirmed	2019 (Špinar J.)	<
18	Velký Černý	<10 pcs	not confirmed	2015 (Pecharová E.)	<
19	Utopenec	<10 pcs	not confirmed	2018 (Gutzerová N.)	<
20	Volákův kopec	<10 pcs	not confirmed	2013 (Peterka T.)	<
21	Bahna	10–100 pcs	not confirmed	2017 (Peterka T.)	<
22	Ratajské rybníky	100–1000 pcs	10–100 pcs	-	<

Importance of management

The current decline in populations, or extinction, is very evident in the localities in Žďárské vrchy, despite the mowing and removal of organic matter. In contrast, localities from the western part of the territory show a better condition than twenty years ago. The most obvious situation is at the Chvojnov locality, where the degraded part of the locality was revitalised. In the place of reeds or almost ruderal vegetation there are very high-quality moss-rich fens, and the population of *Pedicularis palustris* has expanded to become one of the largest in the Czech Republic. In a larger population, the importance of an ecological engineer (Decleer et al. 2014) in influencing host plants and suppressing competition is seen, which leads to the promotion of biodiversity.

The increase in populations in these localities is linked to the management carried out. In addition to mowing and removing biomass, vegetation around the mother plants is also excavated here. This effect is very significant, for example Petrů and Lepš (2000) have shown that most seedlings occur within 0.3 m of the mother plant, and if plants are left uncut, a rather limited seed shadow is created (Fenner 1992). Several historical records also show the occurrence of the species in ruts from heavy mechanization. This is similar to the Řeka locality, where the species spreads mainly in an intensively mowed meadow out of the main part of the endangered locality.

In addition, important prerequisites for the occurrence of the species are a sufficient seed bank (strict requirement), sufficient moisture and low nutrient content in the locality (Jensen and Schmidt 2000). In such a mode, the species is able to occur without management. When moisture decreases and nutrients increase in the locality, *Pedicularis palustris* cannot compete with higher plants like other hemiparasitic plants, which are bound to nutrient-poor habitats (Těšitel et al. 2015).

Figure 1 Current occurence of Pedicularis palustris in Bohemian-Moravian Highlands

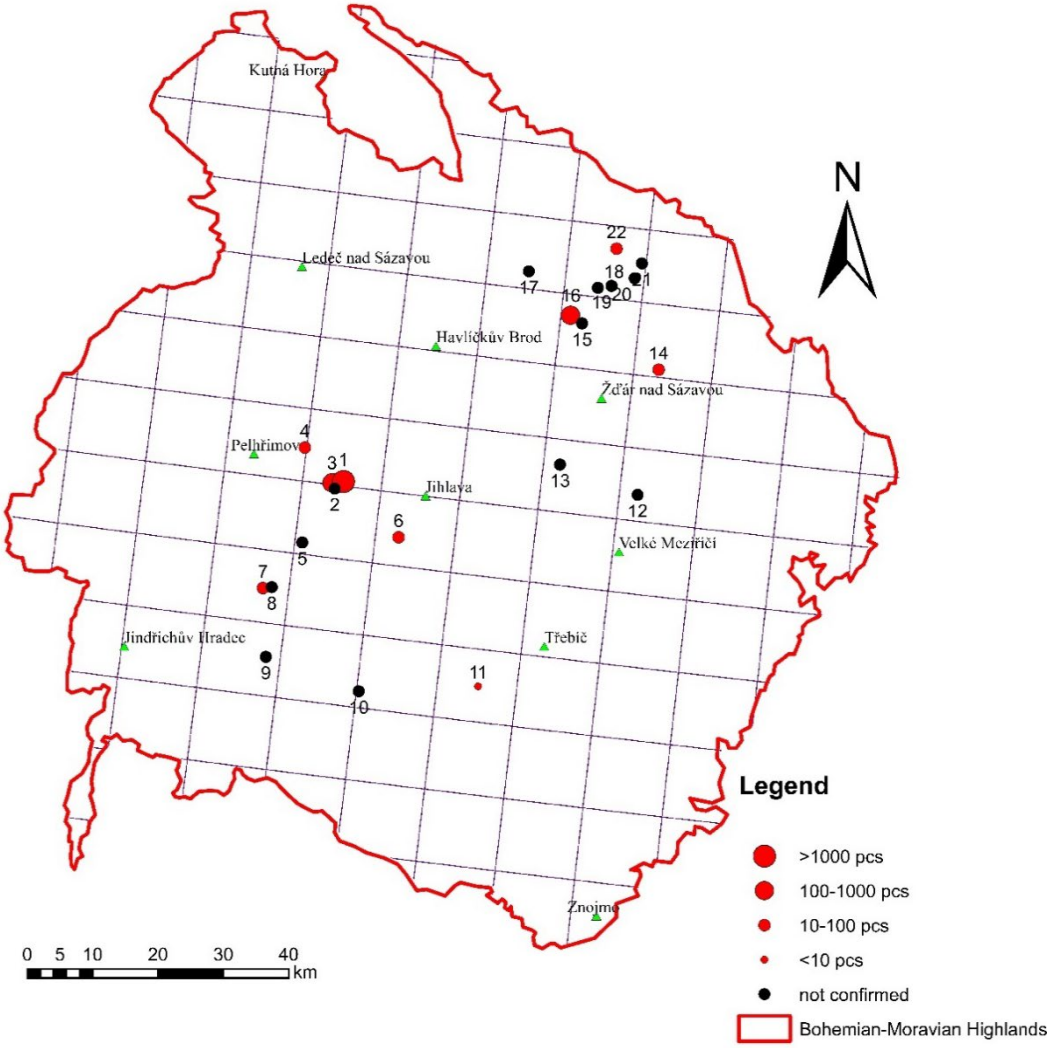

The extent and method of management is fully dependent on change of the two factors mentioned above, which must be replaced and approached for each site individually. While in some localities it is enough to reduce the height of the cut vegetation, in some places management cannot be done without disturbing the surface. In all cases, it is necessary to leave at least part of the mother plants uncut for producing seeds. If the capsules are open, the plants can be mown, and the seeds will be distributed by mowing tools. The disadvantage of this method is the gradual ripening of plants, which lasts from June to August (Hrouda 2000).

Without adequate management, populations in some localities may become extinct during drier seasons, as occurred in the dry episode 2014–2019. Combined with the low lifespan of the seed bank, the future of the species is uncertain without regular management. Consequently, it would be appropriate to undertake greater management interventions in the form of soil removal. Priority should be given to those localities where the last occurrence is reported within a period of less than five years from the present, due to the short lifespan of the seed bank. Positive examples of success are shown by interventions in the localities of Vílanecké rašeliniště, U Hájenky, Chvojnov, Na Oklice and V Lisovech. The following localities are proposed for interventions to restore the population: Bahna, Volákův kopec, Utopenec and Radostínské rašeliniště. All the mentioned localities are mowed, which gives the intended intervention a good precondition for the future state.

CONCLUSION

The updated data on the occurrence of Pedicularis palustris has shown how critical the current situation is. Thanks to the dry period that occurred between 2014–2019, it is possible to understand how

quickly endangered species associated with specific conditions can disappear. Compared to the historical occurrence (2000) in 23 localities in twelve mapping quadrates, the occurrence in 2020 was demonstrated in only nine localities in seven mapping quadrates. The occurrence maps created show a reduction of the population across the whole territory.

During the 2020 season, the water level increased in several localities 0.5 m above the ground surface. Precipitation increased and temperatures decreased compared to the previous five years, which were characterised by extremely low precipitation. However, the benefits for other population trends are questionable due to the submerged flowering plants, which have remained under stagnant water for a relatively long time. In the following years, we will discover whether this year's wetting supported the germination of plants from the seed bank. Localities where negative findings were recorded and the historical occurrence is less than five years old are still suitable for *P. palustris* restoration, with continual mowing together with local soil removal or other surface disturbance benefiting the low-competitive species regenerating from seeds. To preserve the species, it is necessary to practise well-established management because specific examples of occurrence in combination with the chosen method of management demonstrate its positive effect.

ACKNOWLEDGEMENTS

The authors would like to thank Tomáš Peterka, Ester Ekrtová, Filip Lysák, Kamila Juřičková and Jan Roleček for sharing the occurrence data and the description of the management on localities. The research was financially supported by the Mendel University in Brno internal grant agency of the Faculty of AgriSciences (MENDELU AF-IGA2020-IP014).

REFERENCES

Chytrý, M. 2011. Vegetation of the Czech Republic 3. Aquatic and wetland vegetation, Praha: Academia.

Čech, L. et al. 2017. Pedicularis palustris L. - všivec bahenní v Kraji Vysočina. [Online]. Available at: http://www.prirodavysociny.cz/. [2020-09-17].

Decleer, K. et al. 2013. The hemiparasite *Pedicularis palustris*: "ecosystem engineer" for fen-meadow restoration. Journal for Nature Conservation, 21: 65–71.

Eliáš, P. et al. 2015. Red list of ferns and flowering plants of Slovakia. Biologia [Online], 70: 218–228. Available at: http://doi.org/10.1515/biolog-2015-0018. [2020-09-17].

Fenner, M. 1992. Seeds: the ecology of regeneration in plant communities. 2nd ed., Wallingford, UK: CABI Publishing.

Grulich, V., Chobot, K. 2017. Red List of vascular plants of the Czech Republic. Příroda, 35: 75–132.

Hrouda, L. 2000. Pedicularis L. - všivec. In Květena České republiky 6, Praha: Academia, pp. 455–461.

Jensen, K., Schmidt, K. 2000. Genetic structure and AFLP variation of remnant populations in the rare plant *Pedicularis palustris* (*Scrophulariaceae*) and its relation to population size and reproductive components. American Journal of Botany, 87(5): 678–689.

Krása, P. 2007. PEDICULARIS PALUSTRIS L. – všivec bahenní/všivec močiarny. [Online]. Available at: http:// https://botany.cz/cs/pedicularis-palustris/. [2020-09-17].

Niklfeld, H., Schratt-Ehrendorfer, L. 1999. Rote Listen gefährdeter Pflanzen Österreichs. 2nd ed., Graz: Bundesministeriums für Umwelt, Jugend und Familie

Petrů, M., Lepš, J. 2000. Regeneration dynamics in populations of two hemiparasitic species in wet grasslands. In Proceedings IAVS Symposium. Uppsala, January 1999. Uppsala: Opulus Press Uppsala, pp. 329–333.

PLADIAS. 2018. Database of the Czech flora and vegetation. [Online]. Available at: http://www.pladias.cz/. [2020-09-17].

Rybníček, K. 1974. Vegetace ČSSR A6: Die Vegetation der Moore im südlichen Teil der Böhmisch-Mährischen Höhe. 1st ed., Praha: Československá akademie věd.

Těšitel, J. et al. 2015. Habitats and ecological niches of root-hemiparasitic plants: an assessment based on a large database of vegetation plots. Preslia, 87: 87–108

Wild, J. et al. 2019. Plant distribution data for the Czech Republic integrated in the Pladias database. Preslia, 91: 1–24.

How can the weight of *Sinapis alba* L. biomass be affected by adding biochar to the soil irrigated with leachates?

Marketa Sourkova, Dana Adamcova, Magdalena Daria Vaverkova, Jan Zloch
Department of Applied and Landscape Ecology
Mendel University in Brno
Zemedelska 1, 613 00 Brno
CZECH REPUBLIC

xsourkov@mendelu.cz

Abstract: The current method of waste management most frequently used in the Czech Republic is a process called landfilling. This economically favourable and oldest method brings about a range of environmental impacts. One of them is the generation of leachates. Leachates used in these tests were collected once a month from the Bukov municipal solid waste landfill in the period from April to September 2018. The leachates were applied onto the reference soil for 28 days in the shares of 5%, 25% and 50%. For the tests, seeds of white mustard (*Sinapis alba* L.) were used. The developed plant above ground biomass was weighed after the end of the pot experiment. Its values in fresh state ranged from 0.77 g to 6.03 g. After drying up at a constant temperature of 22 °C for 7 days, amount of dry biomass was measured. The values ranged from 0.23 g to 0.49 g. The goal of this research was to define the effect of biochar addition worked into the soil which was irrigated with the leachate shares onto the resulting weight of dry above ground biomass of *Sinapis alba* L. The highest value (0.49 g) of dry biomass was recorded after the addition of biochar into the reference soil.

Key Words: landfill, leachate, nutrients, white mustard, reference soil

INTRODUCTION

Every aspect of our daily life leads to waste generation. The currently ever growing population and the ever increasing population needs and requirements result in the huge amounts of waste which have to be disposed (Costa et al. 2019, Naveen et al. 2017). The method of waste disposal most frequently used in these modern times is called landfilling (Kudelová et al. 1999, Vaverková 2019).

Landfilling is a process during which the municipal solid waste (MSW) is landfilled in a prescribed manner (Tikhe 2019, Greedy 2015). However, landfilling brings also certain risks. This particularly applies to the long-term active state of landfilled waste (Vaverková 2019), in which chemical, physical and biological waste-degrading processes take place (Kuraš 2014). Landfill gas (consisting of CH_4 and CO_2) and dust cause air pollution. Soils and waters are contaminated by chemicals and leachates (Kreith and Tchobanoglous 2002). Leachates generated during the process of landfilling are complex fluids containing soluble inorganic and organic substances (ammonia, phosphates, sulphates, heavy metals etc.) (Naveen et al. 2017, Kamaruddin et al. 2015). Leachates collected from the Bukov MSW landfill were applied onto the reference OECD soil sown with the seeds of *Sinapis alba* L. The OECD artificial soil is a widely used substrate in soil toxicity tests. The substrate was added biochar which was to demonstrate a possible influence on the resulting weight of dry above ground biomass of the tested plant.

Biochar is currently ever more recognized in combating emissions of glasshouse gases (Kookana et al. 2011), in having a favourable effect on crop yields (Saeid and Chojnacka 2019) and enhancing fertility and quality of soils (Spears 2018, Blanco-Canqui 2017, Paustain 2014). Thanks to the content of stable C (carbon), it can isolate it in the soil much longer than its initial organic form (Agegnehu et al. 2017). Biochar is a term for solid organic material produced through a process called pyrolysis (Leng et al. 2019, Weber and Quicker 2018). The process consists in the thermal decomposition of biomass without the access of oxygen (Wang et al. 2017) with the simultaneous creation of several products: bio-oil, syngas, coal and biochar (Song et al. 2016), which can be used to mitigate the climate change (Leng et al. 2019, Laird et al. 2009).

The goal of this study is to determine the effect of biochar supplementation on the biomass weight of *Sinapis alba* L. which grew on the OECD soil watered with leachates.

MATERIAL AND METHODS

Pot experiment preparation and biomass weighing

A mixture used in the pot experiment contained earth, peat and silica sand and no artificial fertilizers (hereinafter substrate), enabling the natural germination of seeds and the growth of plants in line with the European national standard. The experiment was carried out pursuant to Decree ČSN EN 13432 (Appendix E) for the testing of chemical substances 208 Testing the growth of terrestrial plants. The testing was made with the seeds of white mustard (*Sinapis alba* L.).

There were altogether 24 pots used in the test, which were filled with 200 g of substrate. A half of them (12 pots) were added 5% of biochar. Fifty seeds of *Sinapis alba* L. were evenly distributed on the surface. Mixed shares of leachates (5%, 25% and 50%) collected from the MSW landfill in Bukov in the given period were applied onto the substrate for 28 days three times a week. A control sample used to compare the results was substrate onto which distilled water was applied (E SIA). Each test had three replicates. The labelling of individual pots with the applied leachate shares is presented in Table 1.

The experiment was evaluated after the lapse of 28 days from the establishment. The green biomass was dried out for 7 days at a temperature of 22 °C and the dry biomass was weighed by using the Preciosa 4000 C digital scales. A scheme of the experiment is presented in Figure 1.

Figure 1 Pot experiment, Bukov and Brno, Czech Republic, 2020

Legend: 1 – MSW Landfill Bukov; 2 – A sample collected from the accumulation well; 3 – Preparation of aids; 4 – Substrate with the seeds of Sinapis alba L. irrigated with leachate shares; 5 – Pot experiment after 28 days; 6 – Weighing of dry biomass

Table 1 Overview of flowers pots and their labelling

Designation	Addition of biochar	Repeat
Control (E SIA)	-	3×
Control (E SIA)	5%	3×
5% leachate SIA	-	3×
5% leachate SIA	5%	3×
25% leachate SIA	-	3×
25% leachate SIA	5%	3×
50% leachate SIA	-	3×
50% leachate SIA	5%	3×

Legend: Control (E SIA) – control sample, substrate irrigated with distilled H_2O, 3 replicates without biochar and 3 replicates with biochar; 5% leachate SIA – substrate irrigated with a 5% leachate share, 3 replicates without biochar and 3 replicates with biochar; 25% leachate SIA – substrate irrigated with a 25% leachate share, 3 replicates without biochar and 3 replicates with biochar;50% leachate SIA – substrate irrigated with a 5% leachate share, 3 replicates without biochar and 3 replicates with biochar

RESULTS AND DISCUSSION

In each series of three replicates (Control I, Control II and Control III), after its drying out of 7 days the days at a constant temperature of 22 °C, the dry biomass was weighed. The average of all three values was calculated as arithmetic mean.

The values were recorded in Table 2. These average values (Average 5%, 25% and 50%) were used to plot a diagram (Figure 2), in which the initial value for calculation was a blank sample (Average E SIA).

Table 2 Dry biomass weights

Designation without biochar	Dry biomass[g]	Designation with biochar	Dry biomass[g]
Control I (E SIA)	0.26	Control I (E SIA)	0.45
Control II (E SIA)	0.57	Control II (E SIA)	0.39
Control III (E SIA)	0.38	Control III (E SIA)	0.43
Average E SIA	**0.40**	**Average E SIA**	**0.42**
5% leachate SIA I	0.37	5% leachate SIA I	0.33
5% leachate SIA II	0.47	5% leachate SIA II	0.40
5% leachate SIA III	0.30	5% leachate SIA III	0.58
Average 5%	**0.38**	**Average 5%**	**0.44**
25% leachate SIA I	0.27	25% leachate SIA I	0.51
25% leachate SIA II	0.45	25% leachate SIA II	0.54
25% leachate SIA III	0.10	25% leachate SIA III	0.43
Average 25%	**0.27**	**Average 25%**	**0.49**
50% leachate SIA I	0.26	50% leachate SIA I	0.43
50% leachate SIA II	0.18	50% leachate SIA II	0.27
50% leachate SIA III	0.26	50% leachate SIA III	0.26
Average 50%	**0.23**	**Average 50%**	**0.32**

The presented results of the weight of dry biomass derive from the amounts of added leachate and 5% of biochar. The highest average weight of dry biomass was found in the sample of Average 25% with biochar, i.e. in the sample with the leachate share of 5% and the 5% biochar addition 0.49 g, which was a difference of -0.07 g as compared to the control sample (Average E SIA with biochar). The lowest average weight of dry biomass was recorded in the sample of Average 50% without biochar,

i.e. in the sample with the leachate share of 50% without a biochar addition 0.23 g, which was a difference of -0.17 g as compared to the control sample (Average E SIA without biochar).

Figure 2 Biomass weight after drying (dry biomass) (in grams), Brno, Czech Republic, 2020

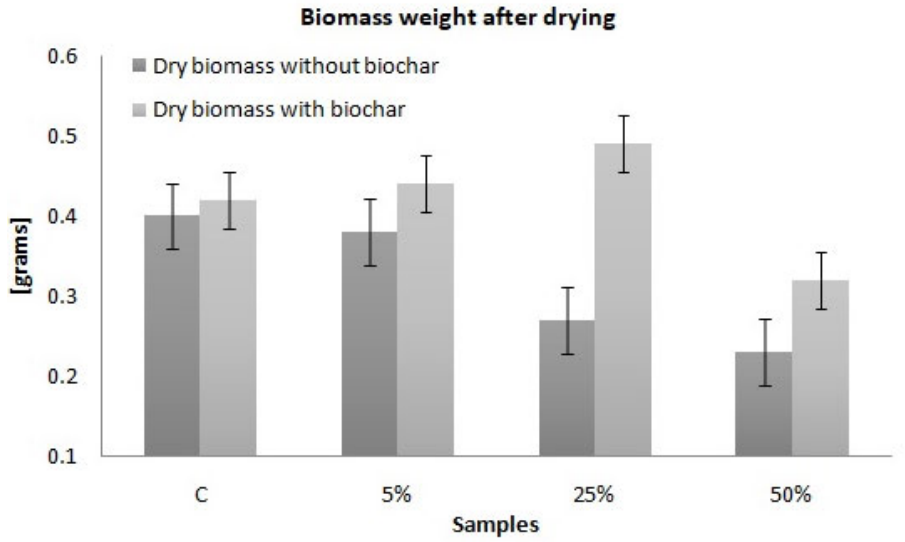

Legend: C – Average E SIA; 5% – Average 5%; 25% – Average 25%; 50% – Average 50%

Increased weight values of dry biomass were found in the samples enriched with 5% of biochar. A comparison of dry biomass weights revealed that the weight of biomass in all samples with the leachate share of 5%, 25% and 50% and biochar addition was higher than biomass weights without biochar. It follows that the presence of biochar in the substrate promotes the uptake of nutrients and growth, which is expressed in the greater biomass weight.

CONCLUSION

Leachates are generated as side products during the landfilling of wastes. Thus, they represent a potential risk to the environment and have an unfavourable impact on human health. The amount of wastes can be minimized if we give up the dominant landfilling and go for more appropriate methods of handling wastes (reuse, recycling, incineration). It is important however to focus primarily on the prevention of their generation.

The effect of biochar addition on the resulting weight of dry biomass of *Sinapis alba* L. was studied in the pot experiment performed in laboratory conditions. The biochar addition was worked into the reference soil which was irrigated with the leachate shares (5%, 25% and 50%). The experiment demonstrated that the higher dry biomass weight (0.49 g) resulted from the 5% biochar addition into the reference soil. Further, it was also demonstrated that the application of biochar into the reference soil can considerably reduce the effect of leachate phytotoxicity and thus promote the uptake of nutrients and the growth of *Sinapis alba* L. plants.

REFERENCES

Agegnehu, G. et al. 2017. The role of biochar and biochar-compost in improving soil quality and crop performance: A review. Applied Soil Ecology [Online], 119: 156–170. Available at: https://linkinghub.elsevier.com/retrieve/pii/S0929139316304954. [2020-08-26].

Blanco-Canqui, H. 2017. Biochar and Soil Physical Properties. Soil Science Society of America Journal [Online], 81(4): 687–711. Available at: http://doi.wiley.com/10.2136/sssaj2017.01.0017. [2020-08-26].

Costa, A.M. et al. 2019. Landfill leachate treatment in Brazil – An overview. Journal of Environmental Management [Online], 232: 110–116. Available at: https://linkinghub.elsevier.com/retrieve/pii/S0301479718312714. [2020-08-29].

Greedy, D. 2015. Landfilling and landfill mining. Waste Management & Research [Online], 34(1): 1–2. Available at: http://journals.sagepub.com/doi/10.1177/0734242X15617878. [2020-08-29].

Kamaruddin, M.A. et al. 2015. Sustainable treatment of landfill leachate. Applied Water Science [Online], 5(2): 113–126. Available at: http://link.springer.com/10.1007/s13201-014-0177-7. [2020-08-29].

Kookana, R.S. et al. 2011. Biochar Application to Soil. Advances in Agronomy [Online], 112: 103–143. Available at: https://linkinghub.elsevier.com/retrieve/pii/B9780123855381000032. [2020-09-05].

Kreith, F., Tchobanoglous, G. 2002. Handbook of solid waste management. 2nd ed., New York: McGraw-Hill.

Kudelová, K. et al. 1999. Odpady. 1st ed., Olomouc: Univerzita Palackého.

Kuraš, M. 2014. Odpady a jejich zpracování. 1st ed., Chrudim: Vodní zdroje Ekomonitor.

Laird, D.A. et al. 2009. Review of the pyrolysis platform for coproducing bio-oil and biochar. Biofuels, Bioproducts and Biorefining [Online], 3(5): 547–562. Available at: http://doi.wiley.com/10.1002/bbb.169. [2020-09-06].

Leng, L. et al. 2019. Biochar stability assessment methods: A review. Science of The Total Environment [Online], 647: 210–222. Available at: https://linkinghub.elsevier.com/retrieve/pii/S0048969718328997. [2020-08-26].

Naveen, B.P. et al. 2017. Physico-chemical and biological characterization of urban municipal landfill leachate. Environmental Pollution [Online], 220: 1–12. Available at: https://www.sciencedirect.com/science/article/pii/S0269749116311150. [2020-09-03].

Paustian, K. 2014. Soil: Carbon Sequestration in Agricultural Systems. Encyclopedia of Agriculture and Food Systems [Online], 140–152. Available at: https://linkinghub.elsevier.com/retrieve/pii/B9780444525123000930. [2020-08-28].

Saeid, A., Chojnacka, K. 2019. Fertlizers. Organic Farming [Online], 91–116. Available at: https://linkinghub.elsevier.com/retrieve/pii/B9780128132722000045. [2020-08-28].

Song, B. et al. 2016. Biomass Pyrolysis for Biochar Production: Kinetics, Energetics and Economics. 1st ed., Cambridge University Press: Cambridge University Press.

Spears, S. ©2018. What is Biochar? Regeneration international [Online], Available at: https://biochar.international/the-biochar-opportunity/what-is-biochar/. [2020-08-26].

Tikhe, A. 2015. Landfilling. [Online], Available at: https://www.slideshare.net/akashtk/landfilling. [2020-09-03].

Vaverková, M.D. 2019. Landfill Impacts on the Environment— Review. Geosciences [Online], 9(10): 1–16. Available at: https://www.mdpi.com/2076-3263/9/10/431. [2020-10-20].

Wang, S. et al. 2017. Lignocellulosic biomass pyrolysis mechanism: A state-of-the-art review. Progress in Energy and Combustion Science [Online], 62: 33–86. Available at: https://linkinghub.elsevier.com/retrieve/pii/S0360128517300266. [2020-09-01].

Weber, K., Quicker, P. 2018. Properties of biochar. Fuel [Online], 217: 240–261. Available at: https://linkinghub.elsevier.com/retrieve/pii/S0016236117316216. [2020-08-30].

Analysis of tourist's satisfaction with cultural tourism: Case study South Moravia

Kristyna Tuzova, Milada Stastna
Department of Applied and Landscape Ecology
Mendel University in Brno
Zemedelska 1, 613 00 Brno
CZECH REPUBLIC

xtuzova@mendelu.cz

Abstract: The study aimed to determine the tourist's satisfaction with cultural tourism in the South Moravian Region. Based on the method of a questionnaire survey with participants in cultural tourism at the local level, data were obtained on the satisfaction of visitors with quality factors and the overall satisfaction with the visit to the site. The data obtained were statistically analyzed to determine if there was a correlation between the age and gender of respondents and their satisfaction. The results of the research show that the gender and age of the respondents do not have a significant effect on factors specific to cultural tourism, but it affects individual and basic factors. According to the results, it was possible to determine which factors have the potential to be developed in the studied area and thus support the number of visitors in the South Moravian Region in the future.

Key Words: culture, tourist, destination, quality, factors

INTRODUCTION

The study deals with the evaluation of tourist's satisfaction with the offer of cultural tourism in the studied area. The first mentions of cultural tourism term appeared in the early 1980s. The World Tourism Organization defines cultural tourism as a "*type of tourism activity in which the visitor's essential motivation is to learn, discover, experience and consume the tangible and intangible cultural attractions/products in a tourism destination"* (UNWTO 2018). In 2018, a UNWTO report highlighted the international importance of a cultural tourism. According to the survey in 2017 involving 43% of UNWTO Member States and 61 international tourism professionals, 89% of local tourism and more than 39% of inbound tourism can be considered cultural tourism, equivalent to approximately 516 million international trips in 2017. This corresponds to an estimate that cultural tourism accounts for 40% of global tourism. (Richard 2018). According to data collected by the Czech Statistical Office (CZSO 2020), the importance of tourism in the South Moravian Region is visible. The South Moravian Region is located in the southwestern part of the Czech Republic and has a total area of 7 188 km^2. The region consists of 7 districts: Blansko, Brno-město, Brno-venkov, Břeclav, Hodonín, Vyškov and Znojmo. There are 673 municipalities and 49 towns in the district. In 2019, the population size was 1 187 667 with a population density of 170 inhabitants per km^2 (CZSO 2020). The research focused on the entire territory of the South Moravian Region, as the respondents visited all districts. In 2019, a total of 2 136 191 guests were accommodated in the South Moravian Region. Almost two-thirds of them were domestic visitors (1 379 775) and one-third foreign visitors (756 416). The average number of overnight stays was two nights: residents spent an average of 2.1 nights and non-residents 1.7 nights. The share of cultural tourism in tourism can only be estimated, but according to the UNWTO, cultural tourism represents approximately 40% of the total volume of tourism, which means that cultural tourism is an important factor in this area. Cultural tourism consists in the fact that the participants are interested in unique experiences, such as discovering local traditions, folklore, visiting cultural and historical monuments and other activities. The quality of the experience gained affects their satisfaction with the visit (Zhang 2020). However, it is important to satisfy tourists, but also to preserve the authenticity of the place within cultural tourism in order to prevent its destruction by excessive tourism (Frey 2019). Positive emotions associated with visiting the destination significantly affect the satisfaction of tourists, their memories, responsible behavior towards the environment and increase the chance of a return visit (Su et al. 2020).

MATERIAL AND METHODS

Main research questions were defined as:

1. What are the most important factors that affect the overall satisfaction of the tourist with the destination?

2. Is there any correlation between tourist's gender and age and their satisfaction with individual quality factors?

To answer scientific questions, it is necessary to know what tourist satisfaction and destination quality factors mean and how they can be evaluated. Tourist satisfaction can be understood basically as a compliance or disagreement with expectations. Tourist satisfaction is based on their experience with the service and it is the result of the interaction between the experience of tourists in the destination and their expectations. (Martin et al. 2019). Overall, satisfaction is perceived as a broad concept, but the quality of services focuses primarily on the dimensions of services, although in practice the conditions of satisfaction and quality can be interchanged (Alegre and Garau 2010). Overall satisfaction can be assessed as the result of the connection between the individual factors of the destination with the overall perception of satisfaction with the visit. In this context, the perception of tourist factors has a decisive influence on the overall satisfaction of tourists with the visit (Marinao 2018). The tourism quality factors are used to evaluate the satisfaction of tourists with visiting the destination. The determination of tourism quality factors is the subject of long-term research by many scientific studies. So far, there is no one universal method that could be used to evaluate the quality of tourism, but the authors use different methods (Ryglová et al. 2017). The definition of quality factors has several interpretations, which are closely related to the high subjectivity of visitors' perception of the quality of the destination. Based on previous research Buhalis (2013), the basic factors of destination quality have been determined as: attractiveness, facilities, support services, accessibility and an available package. According to Middleton and Clarke (2001) the basic factors are: Attraction, amenities, accessibility, the way tourists perceive the destination and the price. The results of previous research show that socio-demographic characteristics may have a different effect in each specific area: different customs, beliefs, development of tourism (Muresan et al. 2019). For this reason the research focused on the influence of respondents' gender and age on satisfaction with quality factors. In this study, the individual and basic and qualitative factors were evaluated, determined on the basis of previous research and the innovation of this research is the inclusion of factors specific to cultural tourism in the research.

Data collection

The data were collected in the form of a questionnaire survey with tourism participants. The questionnaire survey can be characterized as a " *summary of pre-selected questions used to collect primary data".* Using a questionnaire survey, it is possible to verify the established hypothesis in a relatively large sample of the population. When compiling the questionnaire, it is necessary to determine the main goal of the research and to ask comprehensible questions (Vojtíšek 2012). The questionnaire was available on the website: Survio.com from 17. August 2020 to 10. September 2020. To obtain basic data on the respondent: gender and age the analytical (identification and classification) questions were used. Furthermore, the survey continued with the so-called meritorious questions, which examine the opinion and behavior of respondents on the researched topic.

Data processing

The obtained data were further processed by the method of quantitative analysis, which consists of the identification of destination quality factors that most significantly affect the overall satisfaction of the visitors. The data were statistically processed by the method of regression analysis, which allows describing the dependence of one variable (overall satisfaction) on a group of other variables (specific quality factors) while maintaining the requirement of independence of variables. The Mann-Whitney test (M-W test) was used to tests the dependence of the ordinal quantity (evaluation of factor 1-5) on categorical variables with two variations (gender). The Kruskal-Wallis test (K-W test) was used to tests the dependence of the ordinal quantity (evaluation of factor 1–5) on categorical variables with more than two variations (age category). The Spearman correlation coefficient was used to test the dependence of the two ordinal variables.

Data evaluation

The significance of individual quality factors perceived by the visitor was evaluated on a five-point scale, where the number 1 represented a high significance of the evaluated factor and 5 a minor factor. The total satisfaction with a visit was evaluated on the scale (1–10) where 1 means low satisfaction and 10 high satisfaction with visit. The 15 individual quality factors were used in factor analysis (Table 2) and three basic factors of services (Table 3) were chosen based on the theoretical and scientific research and models related to the quality destination, and nine factors (Table 4) were determined as a new quality factors related to cultural tourism. The quality factors with the lowest value in the (3rd column) can be considered as the most significant and the factors with the highest value as the least significant. The (4th and 5th column) shown the median and standard deviation of the individual factors. These values prove that all factors are for the corresponding members. The results of the M-W test of the sample (6th column) shown the dependence of the factors on the gender of the respondents. The results of the K-W test formulas (7th column) shown the dependence of individual factors on the age of the respondents. The strength of the dependence can be evaluated according to the value of the correlation coefficient (correlation column). The closer the value is +1 or -1, the stronger is the dependence, the closer the value is 0, the weaker it is. The Significance column tells us (as well as the last column) whether the correlation coefficient is significant, if there is a demonstrable relationship between gender/age and factors. The strength of the dependence can be evaluated according to the value of the correlation coefficient (correlation column). The closer the value is +1 or -1, the stronger is the dependence, the closer the value is 0, the weaker it is. If the Significance is less than 0.05 (the most frequently chosen level of significance), the correlation coefficient is significant, if it is higher, the coefficient is insignificant. On the Spearman's correlation factor (8th column) and significance (9th column) is shown in the (10th column) the overall satisfaction with visit on each quantity factor. Whether gender and age affect individual factors is shown in the last column (Significant dependent – yes, no).

RESULTS

The table 1 shown the selected characteristics of the survey respondents. The first column shown basic respondents data. The second column shown the individual categories, third column shown the percentage and the fourth column shown the total number of responses.

Table 1 Selected Characteristics of the Survey Respondents

	Category	Percentage (%)	Number
Number of questionnaires	Incomplete	58.21	280
	Complete	41.78	117
Gender	Male	31.6	37
	Female	68.4	80
Age	< 18 years	3.4	4
	18–29 years	28.2	33
	30–39 years	31.6	37
	40–49 years	18.8	22
	50–59 years	12	14
	> 60 years	6	7
Satisfaction	Overall	100	8,19

The total number of respondents to the survey was 280 people, but only 117 successfully completed the questionnaire, which means 42% return of the questionnaire. Other respondents did not complete the questionnaire. Respondents were contacted in person and through an online website. Respondents were selected at random. The sex ratio was two-thirds of women and one-third of men. The age structure of the respondents was diverse. The most respondents were between 18–29, 30–39 and 40–49 years.

Table 2 Selected individual quality factors

Nr	Quality factors	Mean	Median	Std. Dev	M-W Sex	K-W Age	Correlation	Significance	Dependence
1	Natural attractions	2.15	1.00	1.46	No	No	-.217	0.019	Yes
2	Cultural attractions	1.96	1.00	1.43	No	No	-.280	0.002	Yes
3	Accommodation	2.73	2.00	1.57	No	Yes	-.371	0.000	Yes
4	Catering services	2.09	2.00	1.20	Yes	No	-.353	0.000	Yes
5	Transport infrastructure	2.85	3.00	1.12	No	No	-.248	0.007	Yes
6	Public transport services	3.30	3.00	1.65	No	No	-.075	0.423	No
7	Information services	2.40	2.00	1.37	No	No	-.384	0.000	Yes
8	Customer-friendly attitude	2.28	2.00	1.29	No	No	-.252	0.006	Yes
9	Local- friendly attitude	2.05	2.00	1.23	No	No	-.301	0.001	Yes
10	Sense of security	2.03	2.00	1.31	Yes	No	-.238	0.010	Yes
11	Destination cleanliness	2.03	2.00	1.31	Yes	No	-.242	0.008	Yes
12	Uniqueness of a destination	1.91	2.00	1.14	No	No	-.260	0.005	Yes
13	Number of tourist in destination	2.69	3.00	1.16	Yes	No	-.223	0.016	Yes
14	Exclusive services	4.32	5.00	1.27	No	No	-.068	0.463	No
15	Facilities for children's guests	4.09	5.00	1.46	No	No	.108	0.245	No

Considered by the respondents' satisfaction with individual factors as the most important factors are the uniqueness of the destination, cultural attractions, sense of security, destination cleanliness and friendly attitude of locals. On the contrary, respondents see the offer of exclusive services, facilities for children's guests, public transport services, transport infrastructure and accommodation offer as the least important factors of quality. The dependence on gender is evident at the 27% level of significance in 4 factors from the following number 15. The dependence on age is evident at the 7% level of significance in the one factor from the following number 15. A significant effect on the overall satisfaction with the destination visit was recorded for 12 factors out of a total of 15, which represents an overall effect of 80% on the total satisfaction.

Table 3 Basic factors of services

Nr	Quality factors	Mean	Median	Std. Dev	M-W Sex	K-W Age	Correlation	Significance	Dependence
1	Price of services	2.46	2.00	1.13	No	No	-.271	0.003	Yes
2	Availability of services	2.15	2.00	1.26	No	No	-.226	0.014	Yes
3	Quality of services	2.03	2.00	1.14	Yes	Yes	-.350	0.000	Yes

The results show a similar significance of all investigated basic factors. Respondents consider the quality of services as the most important factor and the least significant price of services. In terms of overall significance, these factors are among the most important for the interviewed respondents of all the examined factors. The dependence of gender and age only on the quality of services is shown and all factors had a significant dependence on the overall satisfaction with the visit.

Table 4 Selected important factors of cultural tourism

Nr	Quality factors	Mean	Median	Std. Dev	M-W Sex	K-W Age	Correlation	Significance	Dependence
1	Local and folklore activities	2.88	2.00	1.81	No	No	.048	0.604	No
2	Leisure activities	4.22	5.00	1.35	No	No	-.080	0.388	No
3	Animal activities	4.31	5.00	1.33	No	No	-.023	0.805	No
4	Adrenaline activities	4.55	5.00	1.10	No	No	-.010	0.915	No
5	Gastronomic activities	2.91	2.00	1.68	No	No	-.072	0.440	No
6	Cultural activities	3.46	5.00	1.75	Yes	No	.039	0.673	No
7	Sport activities	3.21	3.00	1.77	Yes	No	-.104	0.262	No
8	Sustainable activities	4.19	5.00	1.43	No	Yes	.054	0.564	No
9	Media tourism activities	4.19	5.00	1.43	No	Yes	-.138	0.139	No

The most important activities for cultural tourism seems to be folklore, gastronomic, sport and cultural activities. At least important activities are considered by the respondents' adrenaline activities, activities connected with animals and leisure activities. The dependence on gender is evident at the 27% level of significance in 2 factors from the following number 9. The dependence on age is evident at the 7% level of significance in the 2 factors from the following number 9. There was no significant effect demonstrated on the gender and age on the overall satisfaction.

DISCUSSION

The result of the study is possible to compare with research done by Ryglová et al. (2015), which deals with tourist's satisfaction in Brno city. The total of 1097 respondents evaluated quality factors depending on the same parameters (age and gender). In the research, a total of 19 quality factors were evaluated. Similar factors are observed in the research (individual and basic factors of quality), but also some factors differed. Within this research, the most important factors were sense of security, destination cleanliness and natural attractions. The least important factors were respecting sustainable development of the destination, additional infrastructure and local transportation. Dependence on gender was proven at significance level in 11 factors (almost 60%) and dependence on age was proven in 16 factors (almost 85%). Compared to our study, differences can be observed, where a higher dependence of factors on gender and age was demonstrated in previous research. According to the significance of individual factors the sense of security, destination cleanliness and low importance of transport have similar importance in this study well. What the expected development will be in the future can only be estimated, as the preferences of tourists differ in space and time, as has been shown when comparing the results with previous research.

CONCLUSION

Understanding of satisfaction is one of the bases for evaluating the performance of a tourist attraction and services. The obtained data can serve as a tool to measure the competitiveness of various types of destinations or to compare changes in the destination over time. The research demonstrated the influence of age and gender on the evaluation of satisfaction with individual factors in general and basic quality factors and was not demonstrated in factors specific to cultural tourism. From the results of the study is obvious that the most important factors that affect the overall satisfaction of the tourist with the destination are the uniqueness of the destination, cultural attractions, sense of security and health. The most important activities for cultural tourism are folklore, gastronomic, sport and cultural activities. Due to the importance of these cultural activities, it would be appropriate to focus on their support and development in a study area.

Based on the results of tourist‘s satisfaction with individual factors and their gender and age significant effect was demonstrated in 80% of all general factors, 100% of basic factors and none of the cultural factors. From the results, it can be concluded that the gender and age of the respondents do not have a significant effect on activities specific to cultural tourism, but it has significant effect on general factors. Based on the results of the study, it is possible to claim that cultural tourism has the potential to make a significant contribution to increasing the sustainability of local society, economic growth, increasing competitiveness, promoting employment and improving the quality of life in the examined locality in the case that it will be properly managed.

ACKNOWLEDGEMENTS

The research was financially supported by the Internal Grant Agency of the Faculty of AgriSciences Mendel University in Brno (no. AF-IGA2020-IP032) Analysis of cultural tourism of rural landscape in the South Moravian Region.

REFERENCES

Alegre, J., Garau, J. 2010. Tourist satisfaction and dissatisfaction. Annals of Tourism Research, 37: 52–73.

Buhalis, D. 2003. eTourism: information technology for Strategic Tourism Management. 1st ed., London: Prentice Hall.

CZSO, 2020. Výběrové šetření cestovního ruchu. [online]. Available at: https://www.czso.cz/csu/vykazy/vyberove_setreni_cestovniho_ruchu. [2020-08-02].

Frey, B.S. 2019. Cultural Tourism. In: Economics of Art and Culture. Zurich: Springer International Publishing, pp. 115–120.

Marinao, E. 2018. Determinants of Satisfaction with the Tourist Destination. In Mobilities, Tourism and Travel Behavior - Contexts and Boundaries. London: IntechOpen. pp. 3–4.

Martin, J.C. et al. 2019. Determining satisfaction of international tourist: A different approach. Journal of Hospitality and Tourism Management, 40: 1–10.

Middleton, V.T.C., Clarke, J.R. 2001. Marketing in Travel and Tourism. 3rd ed., Boston: Butterworth-Heinemann.

Muresan, I.C. et al. 2019. Residents’ Perception of Destination Quality: Key Factors for Sustainable Rural Development. Sustainability, 11(9): 1–3.

Richard, G. 2018. Cultural tourism: A review of recent research and trends. Journal of Hospitality and Tourism Management, 36: 12–21.

Ryglová, K. et al. 2015. Quality as a Competitive Factor of the Destination. Procedia Economics and Finance. [Online], 34: 550–556. Available at: https://doi.org/10.1016/S2212-5671(15)01667-6. [2020-09-05].

Ryglová, K. et al. 2017. Rural Tourism - Evaluating the Quality of Destination. European Countryside [Online], 9(4): 769–788. Available at: https://doi.org/10.1515/euco-2017-0043. [2020-09-06].

Su, L. et al. 2020. From recreation to responsibility: Increasing environmentally responsible behavior in tourism. Journal of Business Research, 109: 557–573.

UNWTO. 2018. Tourism and Culture Synergies [Online]. 1st ed., Madrid: UNWTO. Available at: https://doi.org/10.18111/9789284418978. [2020-08-02].

Vojtíšek, P. 2012. Výzkumné metody Metody a techniky výzkumu a jejich aplikace v absolventských pracích vyšších odborných škol, Praha: Vyšší odborná škola sociálně právní.

Zhang, J. 2020. Diversification of factors influencing qualitative evaluation of a historical and cultural destination. Polish Journal of Sport and Tourism, 27(1): 33–39.

Reconstruction of historic land-use using historical property records – study site of the Jakubovice cadastral area

Ondrej Ulrich, Petra Oppeltova
Department of Applied and Landscape Ecology
Mendel University in Brno
Zemedelska 1, 613 00 Brno
CZECH REPUBLIC

xulrich@mendelu.cz

Abstract: This research aimed to reconstruct historical land-use structure in the small former municipality of Jakubovice located in the Sudetenland (Czech Republic). Written historical property records (Stable Cadastre, Land Register, Uniform Land Registry and the present Cadastre of Real Estate) were used for reconstruction of historical land-use structure. The obtained land-use structure dates from between 1840 and 2020 and the identified land-use changes were put into historical context. The land-use structure development after the Velvet Revolution (1989) indicate to transition from intensive to extensive forms of agriculture. Arable land decreased (-46.12%) mainly at the expanse of permanent grassland (+168.88%) and other areas (+109.44%). The most significant changes to land-use structure occurred during the period of socialist collectivization of agriculture (1950s–1980s) and after the implementation of Complex Land Consolidation in 2010–2011.

Key Words: type of land-use, land-use changes, cadastre, historical property records, Sudetenland

INTRODUCTION

Land-use represents land usage by human society. Development of land-use is characterized by land-use changes, which are based on socio-economic demands and the needs of the human population at a certain time, and are influenced by natural conditions (Petek and Urbanc 2004, Demek et al. 2012, Opršal et al. 2013, Yang et al. 2014, Kolejka et al. 2020). Studying land-use and land-use changes is important for understanding human-environment interactions (Yang et al. 2014, Demek et al. 2012, Frajer and Fiedor 2020) and is used for extensive specific applications and analyses. To identify a historical/traditional/cultural landscape and its relics (Albert 2020, Kolejka et al. 2020) for tracking the spread of diseases in the past (Webster 2020), for rainfall-runoff, flood or erosion simulations (Havlíček et al. 2012, Gao et al. 2020), land-use suitability evaluation (Ziadat and Al-Bakri 2006), or for future prediction of land-use development and its impacts (Tang et al. 2020), for example. Land-use changes are often associated with ecological issues such as soil degradation, alternating of hydrologic cycles, water quality, pollution migration, habitat loss, habitat fragmentation or biodiversity loss. The above-mentioned issues are closely linked to land-use heterogeneity and structure (Demek et al. 2012, Opršal et al. 2013, Yang et al. 2014, Gao et al. 2020, Tello et al. 2020). Land-use changes are mainly caused by intensification of agriculture, urbanization, industrialization, traffic system expansion, gentrification or abandonment of farmland (Opršal et al. 2013, Yang et al. 2014, Frajer and Fiedor 2020, Tang et al. 2020). As the demands of the human population increase, there is rising pressures on the landscape and its productivity (Ziadat and Al-Bakri 2006) and the proper, sustainable management and optimization of a landscape is crucial for meeting the increasing demands of human society (Opršal et al. 2013, Kolejka et al. 2020) and for avoiding negative issues related to land-use changes.

Reconstruction of historical land-use by means of historical sources is a well-known and widely used practice. There are many methods, of varying accuracy. These methods can be classified into two categories. The first category is indirect methods, which include non-spatial data, where land-use can be estimated via an established relationship: historical statistical data (tax records, statistical inventories, number of domestic animals, forest inventories), historical documents (government reports), archival data (chronicles), landscape photographs or paintings and natural archives (sediment layers, pollen, tree rings, etc.). Natural archives are mainly used for reconstruction of a historical landscape on the scale

of thousands or more years (Havlíček et al. 2012, Yang et al. 2014). The second category is direct methods, utilizing spatial information about land-use: aerial or satellite photographs, remote sensing and historical topographic maps (Havlíček et al. 2012). Researchers must be cautious, as historical maps contain errors, inconsistencies, inaccuracies, and each map shows types of land-use based mainly on the map's specific purpose and criteria (Yang et al. 2014, Forejt et al. 2018, Frajer and Fiedor 2020). Despite all the above-mentioned limitations, historical maps (especially cadastral maps), and pictures or paintings are the most crucial material for land-use reconstruction (Petek and Urbanc 2004, Demek et al. 2012, Tang et al. 2014, Forejt et al. 2018, Frajer and Fiedor 2020). For accurate reconstruction of historical land-use, it is important not to depend on just one source of data, so this often requires a multidisciplinary approach and collaboration.

The primary purpose of this research was to reconstruct historical land-use structure in the past 180 years, in the small former municipality of Jakubovice. The written history property records were used for reconstruction of historical land-use structure. The main topics of research were: 1) How did land-use in a small cadastral area in Sudetenland develop? 2) Were changes to land-use abrupt or gradual? 3) Which events caused major changes in land-use structure? The presented article is based on the outcomes of a bachelor's thesis (Ulrich 2016).

MATERIAL AND METHODS

Study site

The Jakubovice cadastral area (3.52 km^2) is in the Lanškroun District of the Pardubice Region (Czech Republic) (Figure 1) and has a primarily agricultural character. The former Jakubovice municipality has a long history and was first mentioned in 1304 under the name of Jacubisdorf, Jacobsdzdorf or Jokelsdorf (Šilar a Jansa 2005). The study site was part of the German-language region called "Schönhengstgau," and most of the municipality's inhabitants were Sudeten Germans. Jakubovice was an independent municipality with a local government until 1972, and then became part of the Dolní Čermná municipality. The Jakubovice cadastral area is in the foothills of the Orlické Mountains with an average altitude of around 450 m.a.s.l. The northern part of the study site consists of a plateau, which slowly descends in a southern-easterly direction, into a wide valley plain. The soils in the study site are mainly stagnosols, cambisols and brown soils. The average annual temperature ranges from 7 to 8 °C, with an average annual rainfall of between 700–800 mm (Ulrich 2016).

Figure 1 Localization of the Jakubovice cadastral area in the Czech Republic

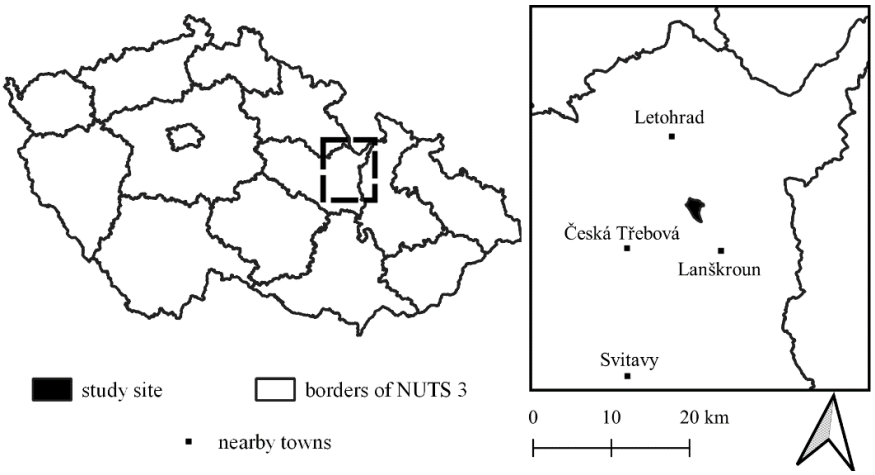

The life of residents of the Jakubovice municipality was difficult, because the municipality suffered one hardship after another. There was massive migration to the USA after 1850 and the Austrian-Prussian war resulted in heavy damage to the municipality in 1866. The Jakubovice municipality was also seriously affected by the First World War, but events after the Second World War had the greatest impact. After the occupation in 1938, most of the population declared themselves German and openly supported fascism. As a result, approximately 95% of the population of Jakubovice was expelled after the Second World War (Šilar and Jansa 2005).

Data collection and processing

Data about historical land-use and area was obtained for each registered plot from written historical property records from the archives of the Cadastral Office in Ústí nad Orlicí. More types of land-use were registered in historical property records and these had to be reclassified into the closest currently registered types of land-use in the Cadastre of Real Estate (e.g.: meadow/pasture → permanent grassland). This had to be carried out to obtain comparable data throughout the entire studied period. Data about land-use was obtained from the written Stable Cadastre (Land Plot Records), Land Register (List of Plots), Uniform Land Registry (List of Plots) and the present-day Cadastre of Real Estate.

RESULTS AND DISCUSSION

Summaries of individual types of land-use for selected years are given in Figure 2. Table 1 shows changes to the area of individual types of land-use over the years as percentage. Figure 3 gives a spatial representation of the land-use structure in the years 1840 and 2020, on which the loss of landscape heterogeneity can be seen.

Figure 2 Development of individual types of land-use in selected years between 1845 and 2020

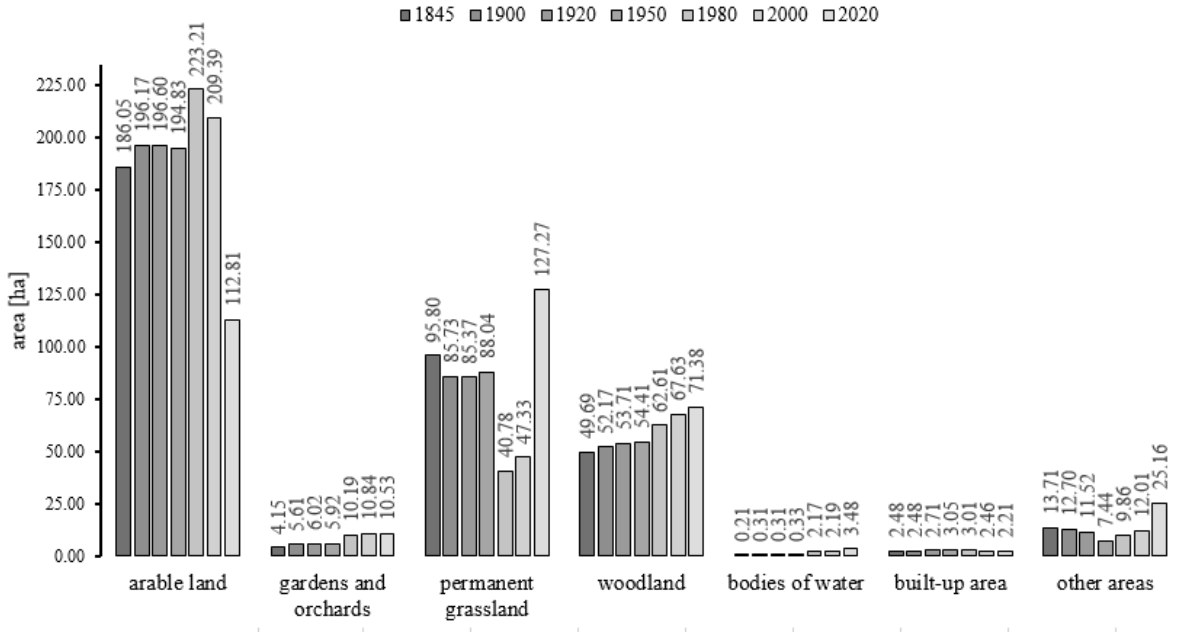

Table 1 Changes in land-use over the years

	1845-1900 [%]	1900-1920 [%]	1920-1950 [%]	1950-1980 [%]	1980-2000 [%]	2000-2020 [%]
Arable land	+5.44	+0.22	-0.90	+14.57	-6.19	-46.12
Gardens and orchards	+35.04	+7.44	-1.77	+72.23	+6.38	-2.84
Permanent grassland	-10.51	-0.42	+3.12	-53.67	+16.06	+168.88
Woodland	+4.98	+2.96	+1.29	+15.09	+8.00	+5.55
Bodies of water	+44.24	0	+7.79	+554.41	+0.93	+58.84
Built-up area	-0.13	+9.30	+12.69	-1.38	-18.37	-10.17
Other areas	-7.39	-9.30	-35.42	+32.58	+21.80	+109.44

In 1845 the study site was primarily used as arable land (52.84%), followed by permanent grassland (27.21%), woodland (14.11%), other areas (3.87%) and gardens and orchards (1.18%). Less than one per cent of the study site was built-up area (0.71%) and bodies of water (0.06%).

In the second half of the 19th century the main driving forces for land-use changes were the Patent of Abolition of Tributary and Forced Labour (1848), the Patent of Unrestricted Divisibility of Plots (1868) and, the Agricultural and the Industrial Revolution (Havlíček et al. 2012, Ulrich 2020).

The Industrial Revolution started establishment of a new industry and transport system, and urbanization has occurred. The use of agricultural machinery was also spreading, which initiated the conversion from extensive to intensive farming systems, which led to an increase in the area of arable land, especially in the alluvial plains (Demek et al. 2012). In 1900, arable land (55.75%, +5.44%), woodland (14.83%, +4.98%), gardens and orchards (1.59%, +35.04%) and bodies of water (0.09%, +44.24%) increased to the detriment of permanent grassland (24.36%, -10.51%), other areas (3.61%, -7.39%) and built-up area (0.70%, -0.13%). The structure of land-use in 1900 shows that the above-mentioned events had only a minor effect and it reflects the fact that the soil within the study site was not fertile enough for intensive agricultural production.

After the World War One land-use structure was affected by the Abolition of Nobility and Titles and the First Land Reform Act, which was intended to confiscate and redistribute the nobility's property (Demek et al. 2012, Kolejka et al. 2020, Ulrich 2020). These events had just a slight impact on land-use structure and only minor changes occurred, chiefly the decline of other areas, indicating removal of road networks. In 1920 there was a slight increase in the areas of arable land (55.87%, +0.22%), woodland (15.27%, +2.96%), gardens and orchards (1.71%, +7.44%) and built-up area (0.77%, +9.30%). The areas of permanent grassland (24.26%, -0.42%) and other areas (3.27%, -9.30%) declined slightly. The area of water bodies remained stable (0.09%).

Figure 3 Spatial representation of land-use in 1840 and 2020. Data for maps was obtained from the Stable Cadastre (left) and the Cadastre of Real Estate (right)

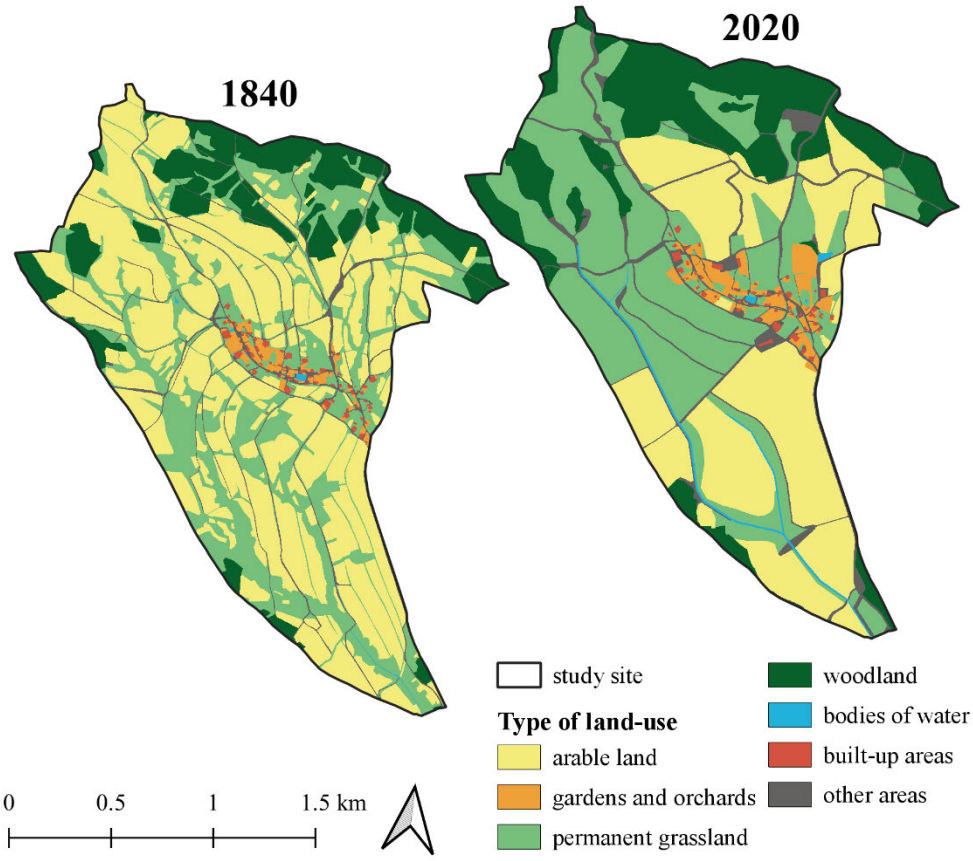

Because the Jakubovice municipality was a part of the Sudetenland, events after World War Two had a serious impact here. The New Land Reform was implemented immediately after World War Two and all land over 50 ha and land that was not used by its owner was confiscated. Practically the entire municipality was also depopulated due to the Expulsion of the Germans (Šilar and Jansa 2005) and the land was redistributed to settlers from the interior of the Czech Republic. The areas of permanent grassland (25.02%, +3.12%), woodland (15.46%, +1.29%), built-up area (0.87%, +12.69%) and bodies of water (0.09%, +7.79%) increased in 1950. In contrast, the areas of arable land (55.37%, -0.90%), other areas (2.11%, -35.42%) and gardens and orchards (1.68%, -1.77%) decreased. Changes

in land-use structure were minor and marginally traced events after the World War Two. There was a small decline in the area of arable land, which indicates the reduction of intensively cultivated land. Other areas also suffered a decline, which could mean the disappearance of the traditional road network. The significant increase in built-up areas represents the construction activities of new settlers.

Year 1980 was at the brink of the end of the Communist regime (1989), which has a serious effect not only on the Czech rural landscape. The Communist regime in the Czech Republic was distinguished by a centralized planned economy and socialist collectivization of agriculture (Kolejka et al. 2020), which was launched fully after 1955 (Demek et al. 2012). The transition from private agricultural production to planned mass production changed the landscape structure (Erlebach 2014). Small fields were replaced by extensive soil blocks managed by newly established cooperative or state farms (Demek et al. 2012, Erlebach 2014). These used large scale agricultural machinery from the 1970s, which subsequently led to the significant homogenization of the rural landscape in the 80s (Kolejka et al. 2020). The massive and rapid expansion of socialist agriculture was based on suppressed property rights, which were surpassed by the right of use (Ulrich, 2020). In 1980, the areas of arable land (63.44%, +14.57%), woodland (17.80%, +15.09%), orchards and gardens (2.90%, +72.23%), other areas (2.80%, +32.58%) and bodies of water (0.62%, +554.41%) had increased at the expense of permanent grassland (11.59%, -53.67%) and built-up area (0.86%, -1.38%). The impact of socialist collectivization struck land-use structure hard at the study site (permanent grassland was ploughed), and the land was consolidated and homogenized. A cooperative farm was established in the Jakubovice municipality in the 60s. After establishment of the cooperative farm, the economic and technical adjustment of the land mainly focused on land drainage, which was carried out in the 70s (Ulrich 2016).

Events after the Velvet Revolution in 1989 brought about many changes, transformation of the central planned economy, market liberalization and many environmentally oriented legislative regulations were issued. This essentially slightly improved the approach to landscape and its protection (Erlebach 2014), but many socialist habits persisted, and more sustainable agriculture and a better environment was not achieved. Furthermore, land privatization after 1990 reinforced the trend of land consolidation from the previous regime (Kolejka et al. 2020). There was an increase in the areas of woodland (19.22%, +8.00%), permanent grassland (13.45%, +3.12%), other areas (3.41%, +21.80%), gardens and orchards (3.08%, +6.38%) and bodies of water (0.62%, +0.93%) in 2000. In contrast, the areas of arable land (59.51%, -6.19%) and built-up area (0.70%, -18.37%) decreased. Changes to land-use showed a trend of receding intensive agricultural production, due to low fertile soil at the study site (stagnosols).

In 2004 the Czech Republic became part of the European Union, which brought new opportunities, challenges and constraints. Subsidies and various environmental programs, which led to more intensive agriculture on fertile soil in the lowlands, and to conversion of less fertile soil into permanent grasslands or forests (Demek et al. 2012, Havlíček et al. 2012, Kolejka et al. 2020), became the dominant driving force for Czech agriculture (Havlíček et al. 2012). The number of private farmers who are concerned about the landscape has increased in the last two decades, but there are still very few of them and extensive fields from socialist times still persist (Demek et al. 2012). In 2020 there was an increase in the areas of permanent grassland (36.07%, +168.88%), woodland (20.23%, +5.55%), other areas (7.13%, +109.44%) and bodies of water (0.99%, +58.84%) at the expense of arable land (31.97%, -46.12%), gardens and orchards (2.98%, -2.84%) and built-up area (0.63%, -10.17%). A massive land-use change took place in 2010 and 2011 due to implementation of Complex Land Consolidation, which primarily lead to grassing over of low fertile arable land on stagnosols.

CONCLUSION

Throughout the past 175 years, the land-use structure of the Jakubovice cadastral area has undergone many land-use changes corresponding to major development trends and events, which formed the Czech landscape. Some events had gradual consequences (e.g. The Agricultural and Industrial Revolution), some had immediate impact on land-use structure (the Expulsion of the Germans). The most significant changes to land-use structure occurred during the socialist collectivization of agriculture (1960s–1970s) and as a result of implementation of the Complex Land

Consolidation in 2010–2011. Based on our findings, it is evident that the landscape is a dynamic system (Petek and Urbanc 2004, Forejt et al. 2018), which is chiefly directed by the demands of human society, resulting in a specific land-use structure.

ACKNOWLEDGEMENTS

I would like to thank Jana Benešová for the opportunity to access the archive of the Cadastral Office in Ústí nad Orlicí and for providing data from the Cadastre of Real Estate. My thanks also to my grandfather Vladimír Jansa, who provided me with historical documents from the dome of the Church of St. Anthony of Padua and helped me obtain historical records.

REFERENCES

Albert, K. 2020. Introducing historical landscape in the cultural heritage conservation through the example of the Tokaj wine region in Hungary. AUC Geographica, 55(1): 112–122.

Demek, J. et al. 2012. Spatial and temporal trends in land-use changes of central European landscapes in the past 170 years: a case study from the south-eastern part of the Czech Republic. Moravian Geographical Reports, 20(3): 2–21.

Erlebach, M. 2014. Land use development in the eastern Giant Mts: the example of the village Babí near Trutnov. Opera Corcontica, 51: 85–96.

Forejt, M. et al. 2018. How reliable is my historical land-use reconstruction? Assessing uncertainties in old cadastral maps. Ecological Indicators, 94(1): 237–245.

Frajer, J., Fiedor, D. 2021. A historical curiosity or a source of accurate spatial information on historical land use? The issue of accuracy of old cadastres in the example of Josephian Cadastre from the Habsburg Empire. Land Use Policy, 100: 1–10.

Gao, Y. et al. 2020. Prediction of hydrological responses to land-use change. Science of the Total Environment, 708: 1–13.

Havlíček, M. et al. 2012. Long-term land use development and changes in streams of the Kyjovka, Svratka and Velička river basins (Czech Republic). Moravian Geographical Reports, 20(1): 28–42.

Kolejka, J. et al. 2020. The Pre-industrial landscape in Moravia. The case study of inventory and analysis of the ancient land use structures in the Czech Republic. Land Use Policy, 97: 1–10.

Opršal, Z. et al. 2013. Land-use Changes and their Relationships of Selected Landscape Parameters in three Cadastral Areas in Moravia (Czech Republic). Moravian Geographical Reports, 21(1): 41–50.

Petek, F., Urbanc, M. 2004. The Franziscean Land Cadastre as a key to understanding the 19th-century cultural landscape in Slovenia. Acta geographica Slovenia, 44(1): 89–113.

Šilar, J., Jansa, V. 2005. 700 let obce Čermná. 1st ed., Čermná, CZ: obec Čermná.

Tang, F. et al. 2020. Land-use change in Changli County, China: Predicting its spatio-temporal evolution in habitat quality. Ecological Indicators, 117: 1–8.

Tello, E. et al. 2020. The Loss of Landscape Ecological Functionality in the Barcelona Province (1956-2009): Could Land-Use History Involve a Legacy for Current Biodiversity? Sustainability, 12: 22–38.

Ulrich, O. 2016. Využití zemědělského půdního fondu v katastrálních územích Anenská Studánka a Jakubovice. Bachelor thesis (in Czech), Mendel University in Brno.

Ulrich, O. 2020. Land-use as a witness of historic changes – study site in the cadastral area of Anenská Studánka. In Conference proceedings of Public recreation and landscape protection – with sense hand in hand? Křtiny, Czech Republic, 11–13 May. Brno: Mendel University in Brno, pp. 260–266.

Webster, E. 2020. Tubercular landscape: land use change and *Mycobacterium* in Melbourne, Australia, 1839-1900. Journal of Historical Geography, 67: 48–60.

Yang, Y. et al. 2020. A review of historical reconstruction methods of land use/land cover. Journal of Geographical Sciences, 24(4): 746–766.

Ziadat, F.M., Al-Bakri, J.T. 2006. Comparing Existing and Potential Land Use for Sustainable Land Utilization. Jordan Journal of Agricultural Sciences, 2(4): 372–386.

Effect of biochar doses on soil pH and organic matter

Marketa Zachovalova, Jiri Jandak
Department of Agrochemistry, Soil Science, Microbiology and Plant Nutrition
Mendel University in Brno
Zemedelska 1, 613 00 Brno
CZECH REPUBLIC

xzachova@mendelu.cz

Abstract: The field trial aiming at the effect of the biochar application on soil organic matter, chemical properties of the soil and on the soil reaction was conducted at the area of the Research grassland station Vatín. The observed variants were as follows: 1) the control without biochar, 2) the biochar dose of 15 t/ha applied to the topsoil, 3) the biochar dose of 30 t/ha applied to the topsoil and 4) the biochar dose of 45 t/ha applied to the topsoil. Biochar is the final product of the decomposition of organic materials under the conditions of heat and the limited access to oxygen. Biochar doses influence physical, chemical and biological properties of the soil. The experiment demonstrated that the biochar doses of 30 t/ha and 45 t/ha increased pH_{H2O} very significantly by more than 0.33. It was confirmed that almost the identical average pH_{H2O} values were at both crop rotations. After 6 months, the application of biochar resulted in a significant increase in pH_{H2O}. The biochar doses of 30 t/ha and 45 t/ha raised pH_{KCl} very significantly by more than 0.41. As far as the effect of the biochar application on organic matter is concerned, the research treatise signified that within the crop rotation L (Livestock production) as well as the crop rotation P (Plant production) the effect of the biochar doses did not manifest, the differences are inconclusive. The average values for the crop rotation P are almost identical for all the biochar variants. However, the average values are slightly higher in the variants with the biochar application within the crop rotation L.

Key Words: biochar, field trial, cambisol, soil pH, organic matter

INTRODUCTION

Biochar can be characterized as pyrogenic carbon which typically originates from carbon-rich materials or biomass, in particular agricultural residues (Inyang et al. 2016, Wang et al. 2017). Pyrolysis, gasification, hydrothermal carbonization and flash carbonization are the methods applied for the production of biochar (Wang et al. 2017). Biochar is produced in the process of the decomposition of organic materials, conditioned by heat and with the minimum access to oxygen (Lorenz and Lal 2014). Biochar has a significant impact on the soil – it makes porosity higher by 14 to 64% and wet aggregate stability by 3 to 226% and makes soil consistency better (Blanco-Canqui 2017). Moreover, it positively influences the crop yield, nutrient cycling and carbon sequestration (Glab et al. 2016). Biochar is known to be a very light material and is typical of its high porosity and the surface area. Its amendment alters some physical properties of the soil such as the bulk density, surface area, penetration resistance and water holding capacity. Furthermore, biochar influences chemical and biological properties of the soil (Mukherjee and Lal 2013). According to Verheijen et al. (2010) biochar pH values are primarily neutral to alkaline (>7) and comparatively homogeneous. The biochar structure and its chemical composition are substantially heterogeneous.

Undoubtedly, one of the most significant factors which have the impact on the plant growth by means of influencing the microbial community and cycle of nutrients is the soil pH. The research conducted by Dai et al. (2017) was focused on the soil pH. Its outcomes revealed that on average the soil pH may be significantly enhanced by 8.78% in soils amended with biochar. Similarly, the study carried out by Scislowska et al. (2015) reports that biochar, irrespective of its origin, significantly increases the pH value of all types of soils (0.1–0.9 units). Juriga and Šimanský (2019) monitored the effects of biochar and its reapplication in the field trial. The soil samples were taken from the plots with the different biochar doses (0, 10 and 20 t/ha) in 2014 and 2018. The results of the experiment confirmed that the first application at the dose of 20 t/ha substantially increased the soil pH values

in H_2O, the soil pH in KCl, the sum of base cations and cation exchange capacity compared to the control samples. The similar outcomes were also ascertained after reapplication of biochar.

A research work by Widowati et al. (2020) with a goal to raise the levels of soil organic matter on dry land confirmed that soil organic matter is instrumental in soil aggregation and makes the soil aggregate stability better. Corn cob biochar with manure enhanced soil organic matter (16.5%) in entisols and rice husk biochar with manure increased soil organic matter (135.3%) compared to the control measurements in inceptisols.

MATERIAL AND METHODS

In 2016, the field trial was carried out at the area of the Research grassland station Vatín where students of the Faculty of AgriSciences, Mendel University in Brno, Czech Republic, do their research experiments. The research station is located in the Bohemian-Moravian Highlands with an altitude of 560 metres above sea level. This area belongs to the climatic region 7 which is moderately warm. The field trial is carried out on Dystric Cambisol, textural class sandy loam.

Sampling of the loose soil samples was performed using a probe rod from the depth of 0–20 cm to determine the soil pH and soil organic matter content**.** The number of the loose soil samples was 8 (spring 2017), 24 (spring 2018), 24 (spring 2019), 24 (autumn 2017), 24 (autumn 2018) and 24 (autumn 2019).

The first crop rotation (corn, spring barley with clover, clover, winter wheat, winter oil seed) reflects the conditions of management in agriculture, including animal production (manure application once per crop rotation and inclusion of red clover in crop rotation). The second crop rotation (corn, spring barley, corn, winter wheat, winter oil seed) corresponds to agricultural production without livestock production. At the beginning of the experiment (5^{th} April 2016), biochar was applied to the individual plots and incorporated into a depth of approximately 20 cm using a rotavator.

Biochar was composed of digestate (80%) and cellulosic fibre. It was produced in the process of termochemical reduction (pyrolysis) and its pH (KCl) was 7.9. The biochar composition was as follows: P (1250 mg/kg), K (11 135 mg/kg), Ca (88 605 mg/kg), Mg (5 630 mg/kg), C (966 350 mg/kg), N (1850 mg/kg), ash (107 005 mg/kg), Na (2 865 mg/kg), Fe (2490 mg/kg), Al (4 885 mg/kg) and Mb (5630 mg/kg).

The following amounts of biochar were applied: 0 t/ha, 15 t/ha, 30 t/ha and 45 t/ha. The size of the plot was 12 m^2.

The soil reaction (pH in H_2O and pH in KCl) was determined according to ISO/DIS 10390. Oxidimetric determination of soil organic carbon was performed using the Walkley-Black method (Jandák et al. 2015).

ANOVA programme (STATISTICA CZ 12) was applied to evaluate the results statistically. Then, they were tested using the Tukey test at a 95% ($P < 0.05$) level of significance.

RESULTS AND DISCUSSION

The effect of biochar doses on soil reaction

The effect of the biochar doses on the active soil reaction (hereinafter referred to as pH_{H2O}) is shown in Figure 1. The dose of 15 t/ha caused an increase in pH_{H2O} by 0.15, this is not a significant difference ($p = 0.179$). The dose of 30 t/ha increased pH_{H2O} in a highly significant way ($p = 0.00005$) by 0.33. The dose of 45 t/ha brought about an almost identical alteration in pH_{H2O} compared to the previous dose. Almost the identical average pH_{H2O} values were determined in both crop rotations (hereinafter referred to as crop rotation L and crop rotation P). The application of biochar resulted in an increase in pH_{H2O} in a significant way ($p = 0.012$) after merely six months. The definitive increase in the pH_{H2O} value (reaching a stable value), as shown in Figure 2, did not occur until 1 year after the application of biochar (45 t/ha).

Figure 1 Effect of biochar doses on active soil reaction within the whole field trial (2017, 2018, 2019)

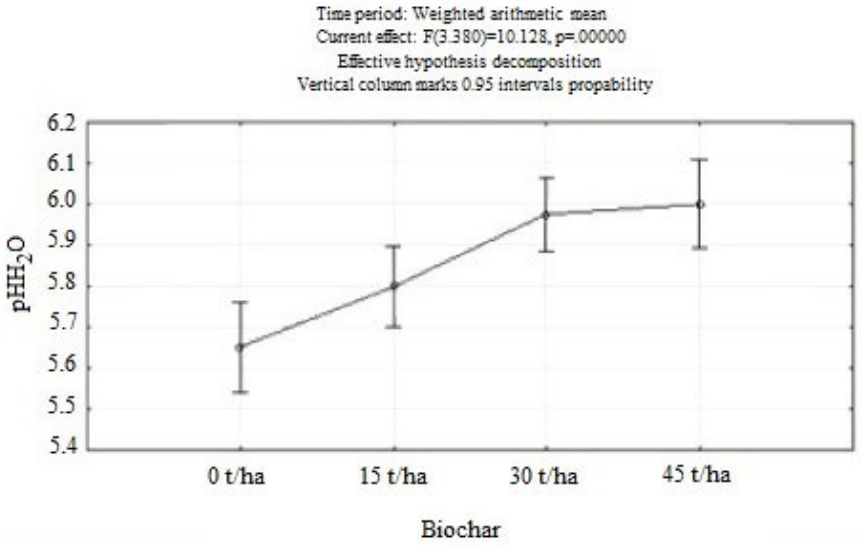

Figure 2 Active soil reaction in particular time periods of soil sampling (2017, 2018, 2019)

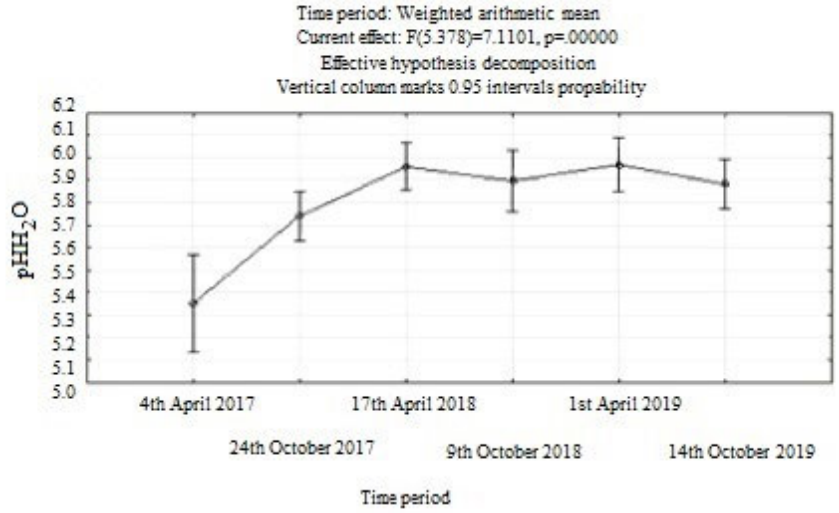

The effect of the biochar doses on the exchangeable soil reaction (hereinafter referred to as pH_{KCl}) was also monitored. The dose of 15 t/ha caused an increase in pH_{KCl} by 0.19, it is a significant difference of p = 0.032. The dose of 30 t/ha enhanced pH_{KCl} in a highly significant way (p = 0.00008) by 0.41. The dose of 45 t/ha also increased pH_{KCl} in a highly significant way (p = 0.000008) by 0.47 (see Figure 3). Even in the instance of pH_{KCl}, the very close average values were determined in both crop rotations. The applied biochar increased the exchangeable soil reaction to a steady value after only six months. However, the significant difference (p = 0.044) is only between the pH_{KCl} values in the first and fifth samples (in April 2019) as evident from the Figure 4.

The effect of biochar doses on organic matter

Farmyard manure was applied at the dose of 30 t/ha on 21st October 2015, the Cox content was 9.90%, thus the Cox rate was 2.97 t/ha. The effect of the biochar doses did not occur in the whole field experiment. The average values are almost identical (in the zero variant the Cox content was 1.49%, after the application of 15 t/ha 1.50%, after the application of 30 t/ha 1.48% and after the application of 45 t/ha 1.46%) and the differences between the amount of the used doses are inconclusive (see Figure 5).

Figure 3 Effect of biochar doses on exchangeable soil reaction within the whole field trial (2017, 2018, 2019)

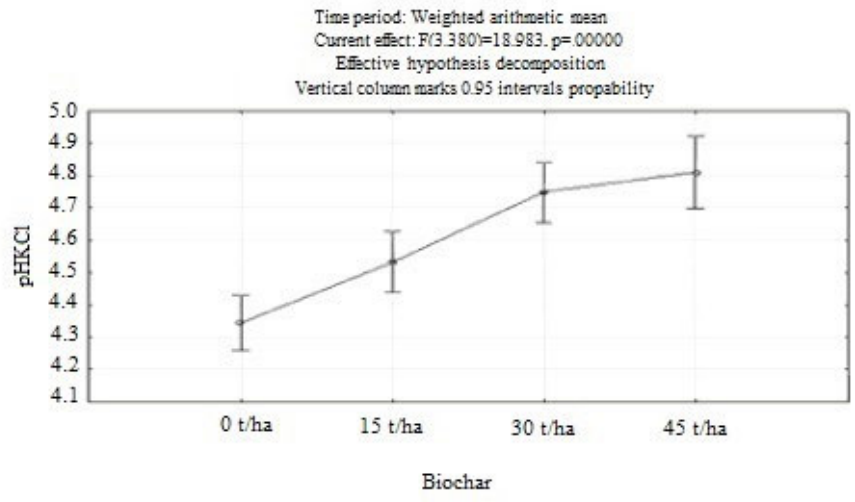

Figure 4 Exchangeable soil reaction in particular time periods of soil sampling (2017, 2018, 2019)

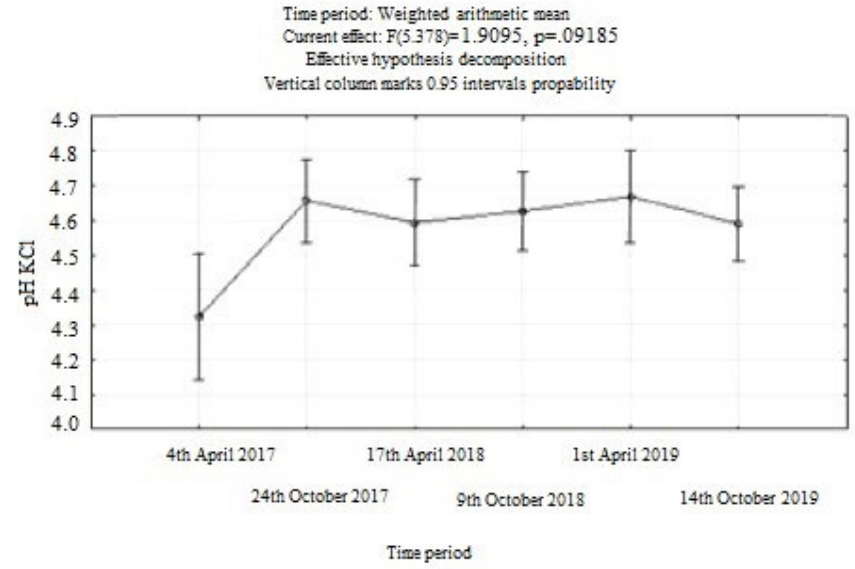

Figure 5 Effect of biochar doses on organic matter (2017, 2018, 2019)

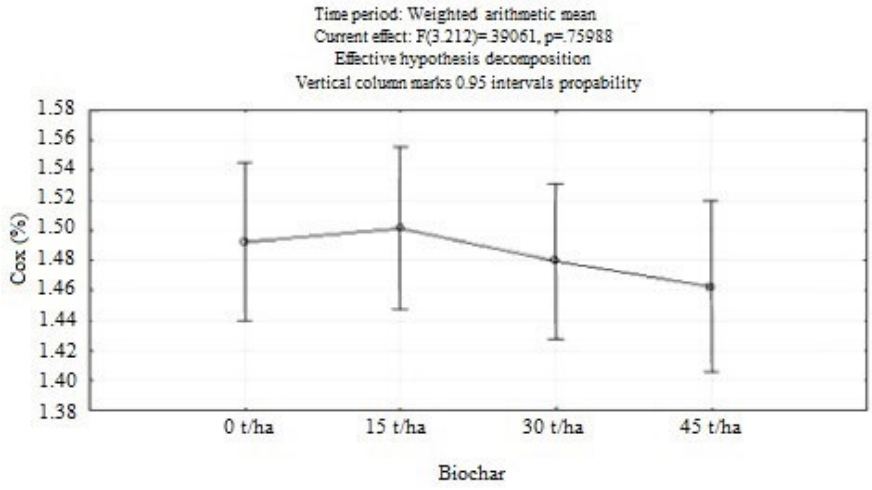

In the crop rotation with the application of manure and clover, which was grown in this variant in 2018, the higher average Cox content of 1.51% was determined. However, it was 1.46% in the market variant of the crop rotation which can be expected in agricultural enterprises without livestock production, but the difference is inconclusive ($p = 0.0585$).

Within the crop rotation P, the effect of biochar doses did not manifest itself again. The average values are almost identical (in the zero variant the Cox content was 1.52%, after the application of 15 t/ha 1.53%, after the application of 30 t/ha 1.48% and after the application of 45 t/ha 1.48%) and the differences between the biochar dose variants are inconclusive.

Within the crop rotation L, the effect of biochar doses did not manifest itself again. The average values are slightly higher in the variants with the biochar application (in the control variant the Cox content was 1.54%, after the application of 15 t/ha 1.57%, after the application of 30 t/ha 1.60% and after the application of 45 t/ha 1.59%). However, the differences between the biochar dose variants are inconclusive.

In their research study, Juriga and Šimanský (2019) reports that biochar may increase the soil pH because of its alkaline nature. These authors observed the significant increase of pH_{H2O} as well as pH_{KCl}. They identified the significant influence of biochar on pH changes in higher biochar doses. Similarly, we may also confirm that the most significant effect on the pH value was at the higher biochar doses of 30 and 45 t/ha within our study performed at the Vatín research grassland station. The same trend was ascertained in the research study by Leal et al. (2013) which states that higher doses of biochar (40 t/ha) enhance the soil pH value in comparison with the control treatment (0 t/ha). Likewise, Sheng and Zhu (2018) and Han et al. (2020) reported that the biochar addition significantly increased the soil pH in the monitored soils amended with biochar. According to the treatise by Pimenta et al. (2019), pH increased with rising doses of biochar. As evident from the outcomes of the above-mentioned research works and our field trial, biochar shows a potential for use as a soil conditioner since pH increases with rising biochar doses.

Dai et al. (2020) investigated the beneficial effect of the biochar application into agricultural soils on plant productivity. They state that on average the soil pH can significantly increase by 8.78% in biochar amended soils. Furthermore, the increased extent of the soil pH positively correlates with the increased amount of plant productivity.

CONCLUSION

Biochar has been widely used in agriculture for its unique capability of changing soil properties. In addition to the physical and hydro-physical properties of the soil, the application of biochar also alters the chemical properties. The biochar doses of 30 t/ha and 45 t/ha increased pH_{H2O} in a highly significant way. It was confirmed that almost the same pH_{H2O} values (5.98 and 6.00) were determined in both crop rotations. The application of biochar enhanced pH_{H2O} in a demonstrable way after 6 months. In the crop rotation with the application of manure and clover, the higher average Cox content of 1.51% was determined while in the market variant of the crop rotation, which may be expected in agricultural enterprises without livestock production, it was 1.46%, but the difference is inconclusive.

REFERENCES

Blanco-Canqui, H. 2017. Biochar and Soil Physical Properties. Soil Science Society of America Journal, 81(4): 687–711.

Dai, Y. et al. 2020. Combined effects of biochar properties and soil conditions on plant growth: A meta-analysis. Science of the Total Environment, 713: 1–11.

Glab, T. et al. 2016. Effect of Biochar Application on Soil Hydrological Properties and Physical Quality of Sandy Soil. Geoderma, 281: 11–20.

Han, L. et al. 2020. Biochar´s stability and effect on the content, composition and turnover of soil organic carbon. Geoderma, 364: 1–17.

Inyang, M.I. et al. 2016. A review of biochar as a low-cost adsorbent for aqueous heavy metal removal. Critical Reviews in Environmental Science and Technology, 46: 406–433.

ISO/DIS 10390. URL: https://www.iso.org/obp/ui/#iso:std:iso:10390:dis:ed-3:v1:en

Jandák, J. et al. 2015. Cvičení z půdoznalství. 1st ed., Brno: Mendelova univerzita v Brně.

Juriga, M., Šimanský, V. 2019. Effects of Biochar and its Reapplication on Soil pH and Sorption Properties of Silt Loam Haplic Luvisol. Acta Horticulturae et Regiotecturae, 2: 65–70.

Leal, O. et al. 2013. Total Organic Carbon, Total Nitrogen and Chemical Characteristics of an Haplic Cambisol after Biochar Incorporation. In Proceedings of the European Science Foundation-Exploratory Workshop "Impact of natural and anthropogenic pyrogenic Carbon in Mediterranean ecosystems. Sevilla, Spain, 5–7 November, CSIC - Instituto de Recursos Naturales y Agrobiología de Sevilla (IRNAS), European Science Foundation, pp. 1–2. Available at: http://digital.csic.es/handle/10261/86093 [2020-08-10].

Lorenz, K., Lal, R. 2014. Biochar Application to Soil for Climate Change Mitigation by Soil Organic Carbon Sequestration. Journal of Plant Nutrition and Soil Science, 177: 651–670.

Mukherjee, A., Lal, R. 2013. Biochar impacts on soil physical properties and greenhouse gas emissions. Agronomy, 3(2): 313–339.

Pimenta, A.S. et al. 2019. Effects of biochar addition on chemical properties of a sandy soil from northeast Brazil. Arabian Journal of Geosciences, 12(3): 1–6.

Scislowska, M. et al. 2015. Biochar to improve the quality and productivity of soils. Journal of Ecological Engineering, 16(3): 31–35.

Sheng, Y., Zhu, L. 2018. Biochar Alters Microbial Community and Carbon Sequestration Potential Across Different Soil pH. Science of the Total Environment, 622-623: 1391–1399.

Verheijen, F. et al. 2010. Biochar Application to Soils – A Critical Scientific Review of Effects on Soil Properties, Processes and Functions. 1st ed., Luxembourg: European Commission Publication Office, Joint Research Centre.

Wang, B. et al. 2017. Recent advances in engineered biochar productions and applications. Critical Reviews in Environmental Science and Technology, 47: 2158–2207.

Widowati, S. et al. 2020. Soil amendment impact to soil organic matter and physical properties on the three soil types after second corn cultivation. Agriculture and Food, 5(1): 150–168.

FOOD TECHNOLOGY

Characteristics of sorption isotherms for fermented meat products

Josef Bauer[1], Premysl Richtr[2], Filip Beno[1], Romana Korandova[3], Vaclav Pohunek[1]
[1]Department of Food Preservation
[2]Department of Chemical Engineering
University of Chemistry and Technology Prague
Technicka 5, 166 28 Prague 6
[3]Department of Food Science
Czech University of Life Sciences Prague
Kamycka 129, 165 21 Prague 6
CZECH REPUBLIC

bauerj@vscht.cz

Abstract: Sorption isotherms were measured by the Dynamic Dewpoint Isotherm (DDI) method for samples of fermented meat products. A total of 600 values were recorded which were processed in the software MATLAB R2019b for six different sorption models (Halsey, Chin, Henderson, Oswin, Smith, and GAB) with statistical parameters: root-mean-square error (RMSE) and coefficient of determination (R^2). Measured experimental data proved that the most suitable model for these types of fermented meat products is GAB model (the values of RMSE $\leq$ 0.0004 and $R^2 \geq$ 0.997 for desorption and RMSE $\leq$ 0.0032 and $R^2 \geq$ 0.884 for adsorption). Experimental data should help to better manage fermentation, drying, and smoking processes during production of fermented meat products.

Key Words: water activity, adsorption isotherm, desorption isotherm, fermented meat products, DDI method

INTRODUCTION

The production of fermented meat products is very difficult due to the fact, that it does not undergo heat treatment. The main problems are hygiene requirements, low microbial contamination of raw materials, technological, and time-consuming production. Microbiological stability of fermented meat products is determined by combination of several factors, also called „barrier effect". These several factors are: low water activity and pH value, salt and sodium nitrite content, the presence of phytoncides in spices, and the presence of competitive microflora in starter culture. The quality of fermented meat products is closely related to fermentation responsible for the product colour, taste, flavour, and shelf-life. These properties are the result of microbiological, biochemical, physico-chemical changes that take place in the production of these products during precisely defined conditions of temperature and relative humidity (Leroy et al. 2006, Costa-Corredor et al. 2010).

The water activity of fermented meat products such as sausages, fermented hams and others is lower compared with fresh meat. Knowledge of this parameter is a very important because of ensuring the required stability against microbiological product spoilage. Because of it is necessary to know the sorption isotherms and their measurement in order to model the processes of drying and fermentation but also the storage process of meat products (Comaposada et al. 2007, Aktaş and Gürses 2005, Muñoz et al. 2009).

Relation between water activity and water content at constant temperature is defined by sorption isotherms. This relationship is completely unique and complex for each product due to the different interactions between water and solids content. The adsorption and desorption are not reversible processes, and therefore we distinguish adsorption and desorption isotherms. Adsorption isotherms can be divided into five types: Type I - Langmuir isotherm, Type II adsorption isotherm of sigmoidal shape, and Types III, IV, V do not have special marking. The sorption isotherms of most foods are nonlinear, sigmoidal in shape (Type II) (Al-Muhtaseb et al. 2002, Kaymak-Ertekin and Gedik 2004).

Sorption isotherm measuring can be divided into three methods: gravimetric, manometric, and hygrometric. The most commonly used are gravimetric methods which can be divided into a dynamic method – Dynamic Dewpoint Isotherm (DDI) and static method - Dynamic Vapor Sorption (DVS). The DDI method is based on measuring of the sorption isotherm using gravimetric analysis and measuring water activity. The principle is the sample humidification (adsorption) and drying of the sample (desorption). The water content is determined by weighing the sample with high measurement accuracy and the dew point is measured to determine the water activity. The advantages of the method are mainly speed, prevention of mould growth during high values of water activity, and large number of data points (Romani et al. 2016, Schmidt and Lee 2012).

MATERIALS AND METHODS

Materials

For this experiment were made two fermented meat products: sausage 1 (Třemšín salám) and sausage 2 (Brdská klobása). The products were made by using: beef (H2), pork (V2, V3, V5, V8) (Uzeniny Příbram a.s.), curing salt (European Salt Company GmbH & Co. KG), spice mixture (ALFA-FOOD s.r.o.), pork bowels 32/34 (KUBIMA s.r.o.), polymer packaging NaloFaser (Kalle CZ s.r.o.), starter culture NOVAFERM (NOVALI, a.s.): original starter culture S2 *Lactobacillus curvatus*, *Staphylococcus carnosus* ($\geq 1.6 \times 10^{10}$ CFU/ml) and A1 *Pediococcus pentosaceus*, *Staphylococcus carnosus*, *Lactobacillus curvatus*, *Kocuria varians* ($\geq 4.4 \times 10^{10}$ CFU/ml), new starter culture F-50 *Lactobacillus curvatus*, *Staphylococcus carnosus* ($\geq 1.5 \times 10^{10}$ CFU/ml) and F-AL-50 *Lactobacillus curvatus*, *Lactobacillus plantarum*, *Staphylococcus carnosus* ($\geq 2.5 \times 10^{10}$ CFU/ml). The recipe of sausage 1 (after drying process) in 100 kg: 65 kg V2, 50 kg V5 (frozen), 20 kg V3 (frozen), 10 kg V8 (frozen), 6 kg H2, 3.75 kg curing salt, 1.8 kg spice mixture, 0.02 kg starter cultures (S2, F-50, F-AL-50). The recipe of sausage 2 (after drying process) in 100 kg: 50 kg V2 (frozen), 50 kg V8 (frozen), 40 kg H2 (4–5 mm), 10 kg V3 (4–5 mm), 3.15 kg curing salt, 2.4 kg spice mixture, 0.02 kg starter culture (A1, F-50, F-AL-50).

Production process

In total were made 3 types of sausage 1 (sample 1 with starter culture A1, sample 2 with starter culture F-50, and sample 3 with starter culture F-AL-50) and 3 types of sausage 2 (sample 4 with starter culture S2, sample 5 with starter culture F-50, and sample 6 with starter culture F-AL-50) in two batches. The production took place in the meat production of the company Uzeniny Příbram, a.s. Frozen meat (-15 °C), followed by starter culture, spice mixture, curing salt, and fresh meat (minced to 5 mm) was placed in a cutter (GEA, Germany) and were cut to a homogeneous mixture. The temperature during cutting of the mixture was controlled and was not higher than -2 °C. An automatic filler (VEMAG, Germany) was used to fill the mixture into the packaging. Fermentation, drying, and smoking processes of the products were made under controlled air flow condition, relative humidity and temperature in smoking chamber. To achieve the required values, the products were placed in a cooling chamber and then packaged (Table 1 and Table 2 show the processes and settings of the smoking chambers).

Table 1 Processes and settings of smoking chamber at sausage 1

Step number	Temperature (°C)	Relative humidity (%)	Convection (%)	Time (hours)	Process
1.	6	-	-	0–48	shaping
2.	24	85	85	48–56	drying
3.	22	85	85	56–64	drying
4.	20	80	85	64–72	drying
5.	18	80	85	72–99	drying
6.	18	80	70	99 ≤	drying

Table 2 Processes and settings of smoking chamber at sausage 2

Step number	Temperature (°C)	Relative humidity (%)	Convection (%)	Time (hours)	Process
1.	24	85	85	0–6.5	drying
2.	24	80	52	6.5–7.5	smoking
3.	22	85	85	7.5–13.5	drying
4.	22	80	52	14–15	smoking
5.	22	80	85	15–21	drying
6.	22	80	52	21.5–23.5	smoking
7.	20	80	85	23.5–99	drying

Physico-chemical analyses

For determination of the dry matter, pH value, water activity, samples were taken in different time intervals: sausage 1 (day 1, 3, 6, 8, 10, 13, 15) and for sausage 2 (day 1, 3, 6, 8, 10). These parameters were measured in two batches, i.e. in total 72 samples of fermented meat products, and each sample was measured three times in a parallel determination from which the average values and standard deviation were calculated. The pH determination was measured using pH meter Portavo 904 X (KNICK, Germany) with needle probe SE 104 N (KNICK, Germany) and the temperature was measured with a temperature probe, which is part of the pH meter. Water activity was measured with a_w meter Aqualab 4 TEV (Decagon Devices, USA) at a temperature of 25 °C. Dry matter determination was performed gravimetrically. Drying took place at a temperature of 105 °C in an oven HS 32 A (ZPA, Czech Republic) to a constant weight loss.

Sorption isotherms

In this work, the AquaLab Vapor Sorption Analyzer (Decagon Devices, USA) was used to measure sorption isotherms and the measurement was performed using the DDI method. The second batch of final products (3 samples of sausage 1 and 3 samples of sausage 2) was used for sorption isotherms measuring. Desorption was measured in the range of water activity 0.95–0.50, and adsorption in the range 0.50–0.80, both at 25 °C. Values were recorded in every 0.01 of the range.

Statistical analysis

The experimental data from sorption isotherms were applied the following six sorption models: Halsey, Chin, Henderson, Oswin, Smith and GAB. The equation are given in Table 3. The experimental data were first evaluated by the Moisture Analysis Toolkit (Decagon Devices, USA) and subsequently transferred to MATLAB R2019b software (MathWorks, USA), where linearized forms of equations were used to calculate constants using nonlinear regression. The models will fit the experimental data well if they have a coefficient of determination (R^2) closely to 1 and a root-mean-square error (RMSE) close to 0.

Table 3 Selected sorption models (Al-Muhtaseb et al. 2002, Sopade 2001)

Author	Equation	Author	Equation
Halsey	$M = -\left(\frac{A}{lna_w}\right)^{\frac{1}{B}}$	Chin	$M = \frac{A}{lna_w} + B$
Henderson	$M = \left[\frac{\ln(1-a_w)}{-A}\right]^{\frac{1}{B}}$	Oswin	$M = A\left(\frac{a_w}{1-a_w}\right)^{B}$
Smith	$M = A - Bln(1-a_w)$	GAB	$\frac{M}{M_m} = \frac{ABa_w}{(1-Ba_w)(1-Ba_w+ABa_w)}$

Legend: Where m is the moisture in g/100 g solids, a_w is water activity, M_m is the monolayer value in g/100 g solids and A, B are constants

RESULTS AND DISCUSSION

Physico-chemical analyses

The water content of meat mixture of sausage 1 was 58.9–59.5% and 36.5–37.2% for final products. Water loss was around 23%. The water content of cut mixture of sausage 2 was 45.3–46.3% and 28.8–30.8% for final products. Water loss was around 17%. The water activity of all cut mixtures was in the range 0.966–0.975 and for final fermented meat products in the range 0.898–0.908. These values of water activity complies the Czech legislative requirement (Vyhláška č. 69/2016 sb.). Influence of the starter cultures on water content and water activity was insignificant. In Table 4 are shown meat products pH values of second batch.

Table 4 pH values for samples of fermented meat products

Days	Sample 1	Sample 2	Sample 3	Sample 4	Sample 5	Sample 6
1.	5.76 ± 0.02	5.67 ± 0.02	5.70 ± 0.03	5.62 ± 0.03	5.64 ± 0.02	5.61 ± 0.01
3.	5.93 ± 0.04	5.89 ± 0.05	5.90 ± 0.02	5.54 ± 0.02	5.64 ± 0.05	5.65 ± 0.01
6.	4.76 ± 0.03	4.78 ± 0.03	4.74 ± 0.02	4.75 ± 0.02	4.76 ± 0.02	4.63 ± 0.03
8.	4.80 ± 0.03	4.77 ± 0.01	4.74 ± 0.02	4.73 ± 0.01	4.78 ± 0.02	4.68 ± 0.03
10.	4.79 ± 0.04	4.78 ± 0.01	4.76 ± 0.03	4.72 ± 0.01	4.75 ± 0.03	4.65 ± 0.02
13.	4.83 ± 0.02	4.8 ± 0.01	4.79 ± 0.02	-	-	-
15.	4.85 ± 0.03	4.86 ± 0.02	4.81 ± 0.02	-	-	-

It is possible to see slight increase in pH value of sausage 1 from day 1 to day 3 of the fermentation process. It caused by that the sausage 1 was placed to smoking chamber after 48 hours and was placed in the cooling chamber (6 °C). The next phase is a fast decreasing of pH values which is common for all samples from day 3 to day 6. The trend of higher acidification can be seen in the final products using the F-AL-50 starter culture than in the samples with standard cultures and the F-50 culture.

Sorption isotherms

For desorption in the range of water activity 0.95–0.5 were recorded 55 values and for adsorption in the range of water activity 0.5–0.8 55 were recorded 45 values in every final fermented meat products (n = 6). A total of 600 values were recorded which were processed in the software MATLAB R2019b for six different models of sorption isotherms. The results of the constants, coefficient of determination (R^2), and root-mean-square error (RMSE) are given in Table 5.

The most suitable model for these types of fermented meat products is the GAB model (the values of RMSE ≤ 0.0004 and $R^2 \geq 0.997$ for desorption and RMSE ≤ 0.0032 and $R^2 \geq 0.884$ for adsorption). The greater inaccuracy of the adsorption parameters was due to the fact that less values were measured due to poorly water adsorption at a water activity ≥ 0.800. The Chin and Smith models are completely unsuitable for the use of moisture modelling for these fermented meat products. The Oswin, Halsey and Henderson models had similar RMSE and R^2 values. In comparison to the literature (Muñoz et al. 2009) where sorption isotherms were measured for similar matrices (pork meat), the RMSE values of desorption in our study was ≤ 0.0004, while in the literature the values are higher, which means a high degree of accuracy of our values. The same phenomenon also occurs in our study for adsorption.

Table 5 The parameters in sorption models for fermented meat products

Sample	Model	Adsorption					Desorption				
		Constants					Constants				
		A	B	M_m	R^2	RMSE	A	B	M_m	R^2	RMSE
1	Halsey	0.964	1.771	-	0.894	0.0803	0.710	2.230	-	0.990	0.0748
	Chin	-5.849	-0.436	-	0.934	0.9764	-2.640	14.848	-	0.933	8.6487
	Hender	0.781	2.537	-	0.856	0.0930	0.696	2.763	-	0.987	0.0846
	Oswin	8.179	0.786	-	0.881	0.0849	11.309	0.650	-	0.994	0.0562

Table 5 The parameters in sorption models for fermented meat products – continue

Sample	Model	Adsorption					Desorption				
		Constants					Constants				
		A	B	M_m	R^2	RMSE	A	B	M_m	R^2	RMSE
	Smith	5.803	18.328	-	0.896	1.228	-20.86	34.304	-	0.971	5.6620
	GAB	-1.468	1.160	2.386	0.884	0.0025	7.232	0.967	6.653	0.999	0.0003
2	Halsey	0.629	2.366	-	0.916	0.0569	0.648	2.543	-	0.998	0.0280
	Chin	-4.818	6.669	-	0.958	0.843	-3.305	16.742	-	0.969	5.7099
	Hender	1.164	2.868	-	0.879	0.0685	0.797	3.0417	-	0.969	0.1113
	Oswin	13.193	0.518	-	0.904	0.0611	15.284	0.588	-	0.997	0.0366
	Smith	1.4621	15.941	-	0.920	1.1567	-17.79	35.971	-	0.958	6.7070
	GAB	-1.720	1.071	3.905	0.918	0.0009	-7.304	0.964	7.399	0.997	0.0004
3	Halsey	1.004	1.651	-	0.897	0.0872	0.746	2.151	-	0.989	0.0802
	Chin	-5.595	-0.916	-	0.935	0.9760	-2.809	13.637	-	0.989	8.1182
	Hender	0.752	2.452	-	0.864	0.1002	0.664	2.705	-	0.990	0.0785
	Oswin	7.370	0.818	-	0.885	0.0919	10.544	0.683	-	0.995	0.0570
	Smith	-5.865	17.409	-	0.899	1.2130	-23.68	35.832	-	0.968	6.0944
	GAB	-1.386	1.173	2.069	0.888	0.0030	3.487	0.967	6.854	0.999	0.0004
4	Halsey	1.013	1.362	-	0.847	0.0886	0.858	1.823	-	0.987	0.0631
	Chin	-4.407	-1.052	-	0.888	0.7450	-3.844	4.503	-	0.977	1.8382
	Hender	0.785	2.164	-	0.808	0.0991	0.698	2.505	-	0.999	0.0117
	Oswin	5.574	0.810	-	0.832	0.0927	8.071	0.753	-	0.994	0.0443
	Smith	-3.778	12.503	-	0.842	0.8843	-9.189	21.396	-	0.995	0.8795
	GAB	-1.045	1.237	1.268	0.928	0.0028	0.921	0.905	9.432	0.999	0.0003
5	Halsey	2.281	-0.713	-	0.927	0.1829	1.179	1.0741	-	0.931	0.2295
	Chin	-4.449	-6.636	-	0.959	0.7018	-3.781	1.042	-	0.961	3.0217
	Hender	0.324	1.106	-	0.901	0.2127	0.478	1.989	-	0.981	0.1194
	Oswin	1.068	1.874	-	0.919	0.1934	4.148	1.050	-	0.948	0.1996
	Smith	-11.01	14.296	-	0.922	0.9681	-16.49	24.347	-	0.997	0.913
	GAB	-1.837	1.259	0.451	0.879	0.0032	2.044	0.925	6.211	0.997	0.0003
6	Halsey	0.894	1.637	-	0.918	0.0785	0.758	2.048	-	0.988	0.0569
	Chin	-4.381	0.650	-	0.957	0.7288	-3.518	7.313	-	0.964	2.4085
	Hender	0.832	2.351	-	0.882	0.0941	0.777	2.652	-	0.998	0.0211
	Oswin	6.980	0.732	-	0.906	0.0841	9.783	0.668	-	0.994	0.0396
	Smith	-3.696	14.129	-	0.922	0.9880	-7.089	21.162	-	0.995	0.9023
	GAB	-1.619	1.134	2.092	0.918	0.0027	1.841	0.917	8.225	0.999	0.0003

CONCLUSION

The measured experimental data in this study should help to meat manufactures and small meat producers which produce fermented meat products to better manage fermentation, drying, and smoking processes. It should provide the ability to determine water content or water activity by using only one of these parameters. The advantages of DDI method are fast measuring (no moulding of the samples) and the possibility to calculate more accurate results from a large amount of data, due to the fact that the values were recorded every 0.01 in the range of water activity. According to the statistical significance of sorption isotherm models, the GAB model is the most suitable for these types of meat products. The influence of the starting culture had an effect only on the pH values but not on the values of the water content and the water activity.

ACKNOWLEDGEMENTS
This work was supported from the grant of Specific university research - grant No A2_FPBT_2020_051.

REFERENCES

Aktaş, N., Gürses, A. 2005. Moisture adsorption properties and adsorption isosteric heat of dehydrated slices of Pastirma (Turkish dry meat product). Meat Science, 71(3): 571–576.

Al-Muhtaseb, A.H. et al. 2002. Moisture sorption isotherm characteristics of food products: A review. Food and Bioproducts Processing, 80(2): 118–128.

Comaposada, J. et al. 2007. Sorption isotherms of salted minced pork and of lean surface of dry-cured hams at the end of the resting period using KCl as substitute for NaCl. Meat Science, 77(4): 643–648.

Costa-Corredor, A. et al. 2010. Simulation of simultaneous water and salt diffusion in dry fermented sausages by the Stefan-Maxwell equation. Journal of Food Engineering, 97(3): 311–318.

Česká republika. 2016. Vyhláška č. 69/2016 Sb., o požadavcích na maso, masné výrobky, produkty rybolovu a akvakultury a výrobky z nich, vejce a výrobky z nich. In: Sbírka zákonů České republiky. 26: 714–759. Also avaible at: http://www.eagri.cz/public/web/mze/ [2020-09-11].

Kaymak-Ertekin, F., Gedik, A. 2004. Sorption isotherms and isosteric heat of sorption for grapes, apricots, apples and potatoes. LWT - Food Science and Technology, 37(4): 429–438.

Leroy, F. et al. 2006. Functional meat starter cultures for improved sausage fermentation. International Journal of Food Microbiology, 106(3): 270–285.

Muñoz, I. et al. 2009. Desorption isotherms of salted minced pork using K-lactate as a substitute for NaCl. Meat Science, 83(4): 642–646.

Romani, S. et al. 2016. Moisture adsorption behaviour of biscuit during storage investigated by using a new Dynamic Dewpoint method. Food Chemistry, 195: 97–103.

Schmidt, S.J., Lee, J.W. 2012. Comparison between water vapor sorption isotherms obtained using the new dynamic dewpoint isotherm method and those obtained using the standard saturated salt slurry method. International Journal of Food Properties, 15(2): 236–248.

Sopade, P.A. 2001. Criteria for an appropriate sorption model based on statistical analysis. International Journal of Food Properties, 4(3): 405–418.

The effect of the malt used on the viscosity of the wort

Lucia Blsakova[1], Tomas Gregor[1], Vojtech Kumbar[2]
[1]Department of Food Technology
[2]Department of Technology and Automobile Transport
Mendel University in Brno
Zemedelska 1, 613 00 Brno
CZECH REPUBLIC

xblsakov@mendelu.cz

Abstract: The aim of this study was to determine the worts viscosity in beer, which affects the lautering process. The course of dynamic viscosity was observed during the mashing process in barley, wheat, and oat worts. Samples were taken in five different phases of mashing. The viscosity was measured at a coaxial cylinder sensor system with precision small samples adapter and standard spindle. The results were recorded in mPa·s. in the range of 4.9 mPa·s. up to 78.8 mPa·s. and then graphically evaluated. A sharp increase during mashing was visible in the proteolysis phase. Higher viscosity in the wort can slow down the lautering, therefore the obtained results can provide a powerful tool to facilitate the malting of different types of malt.

Key Words: beer, dynamic viscosity, wort, mashing, malt

INTRODUCTION

High quality raw materials are the basis of beer brewing since time immemorial. One of them is malt, which provides an extract for beer production. The basic type of malt in our region for beer production is barley. However, malts made from wheat, oats and corn are also used to a lesser extent.

Different technological properties of malts together with different proportions of individual fractions of crushed malt have an effect on the speed of lautering. After mashing the mentioned fractions form a filtration cake called grains, from which the extractives pass into the used boiling water and the concentration of which is referred to as plato degree or specific gravity. As their concentration increases, so does the viscosity.

Viscosity plays an important role in beer production. It is, for example, the initial control of malt, in which the viscosity reveals its quality or in the case of fermentation of wort, filtration or in the case of a hot product (Severa and Los 2008). The viscosity of beer has the nature of a non-Newtonian liquid. Nevertheless, its important properties are still limited in literature (Hlaváč et al. 2016).

In addition to the technological point of view, the viscosity is also chemically affected, and it mainly contains ß-glucans non-starch polysaccharides which are found in the cell wall of the grain endosperm. They are extracted into beer during brewing, where they significantly correlate with its viscosity (Li et al. 2020). The increased level of which is proven to reduce the filterability of beer (Sadosky et al. 2018). Individual types of malts also contain different concentrations of ß-glucans, what significantly affects the viscosity.

MATERIAL AND METHODS

Material

In this experiment, cereals such as spring barley (Malz variety), food wheat (Bohemia), and naked oats (Abel) were used to produce malt.

Malting

These cereals were later malted in the micro-malthouse in the laboratory brewery of Department of Food Technology of Mendel University in Brno for light-type malts with a final curing temperature 80 °C, where the wort was also prepared for research.

Micro-malthouse (Ravoz, Czech Republic) of Mendel University is a technological device that is primarily used for malting cereals (secondarily, for example, as a ripening or drying chamber for food products, air-conditioned baths with defined humidity, etc.). The micro-malthouse consists of three stainless steel cabinets (boxes for steeping, germination, kilning), a control cabinet, a computer with a printer and a device for removing malt. The box for steeping and germination is equipped with heating and cooling and the box for steeping is equipped with heating only. Steeping and germination took place in all cereals at a temperature of 13 °C, germination always took place according to the same temperature program, the final curing temperature was used for light type malt 80 °C.

Production of wort

The production took place in the mashing kettle of the micro-brewery by weighing 20 kg of malt scrap into 40 l of 45 °C hot tap water, maintaining a temperature of 45 °C for 30 minutes with constant stirring. After this time, the temperature was raised to 70 °C over 25 minutes, 30 l of 75 °C water was added from the hot water tank, and the mixture was stirred for 60 minutes. The mixture was further transferred to a straining vat, from where, after 30 minutes of rest, the clear wort was pumped through a layer of spent grain back to mashing kettle, boiled for 10 minutes and, after cooling through a plate cooler, filled into 1 l sterile glass bottles and stored at 5 °C in a refrigerator. The total volume of wort after sparge was 120 l.

Wort samples

All beers were made by infusion and original gravity was 11°P. The wort samples were separated in different stages of brewing base preparation (Table 1).

Table 1 Different stages of wort samples (own construction)

Sample	Phase	Temperature (°C)	Time (min)
1	Mash	40	0
2	Mash	40	5
3	Proteolysis	52	15
4	1. Saccharify stage	62	30
5	2. Saccharify stage	72	30
6	Mash out	90	10

Determination of carbohydrates by HPLC

Samples of wort were analysed by high pressure liquid chromatography, the content of oligosaccharides, maltotriose, maltose, glucose, and fructose were monitored. A Watrex 300x8 mm column with a stationary phase Polymer IEX H 8 µm in conjunction with an LCP 4000 pump (Ecom, Czech Republic) and a RIDK-102 refractometric detector (Laboratory Instruments Prague, Czech Republic) was used for the measurement. Calibration was performed to maltotriose, maltose, glucose, fructose, and glycerol standards (all Sigma-Aldrich, UK). For analysis, carbon dioxide was shaken from the sample and the sample was centrifuged for 5 min at 18,000 RPM. The sample injection onto the column was 5 µl.

Determination of dynamic viscosity

The viscosity measurement was carried out using the DV-3P rotary viscometer (Anton Paar, Austria) equipped with a coaxial cylinder sensor system with precision small samples adapter and standard spindle TR8 according to Anton Paar (number 26 according to Brookfield). Viscosity of samples was measured at rotational speed of spindle 100 RPM (shear strain rate 93 l/s) in the standard room temperature 22 °C.

RESULTS AND DISCUSSION

Based on the obtained data, wort dynamic viscosity data at 100 RPM, which appeared to be the most accurate, were further graphically processed. The measured results are shown in Table 2.

Table 2 Dynamic viscosity of malt at 100 RPM

Type of malt	RPM*	1 (mPa·s)	2 (mPa·s)	3 (mPa·s)	4 (mPa·s)	5 (mPa·s)	6 (mPa·s)
Barley	100	5.5	5.6	28.2	42.8	73.5	5.8
Oat	100	5.1	5.0	11.8	38.7	42.7	5.2
Wheat	100	4.9	9.5	29.4	56.6	78.8	5.4

*Legend: *round per minute; 1 – Mash, 2 – Mash 5min; 3 – Proteolysis, 4 – 1. Saccharify stage, 5 – 2. Saccharify stage, 6 – Mash out*

In Table 2 it is possible to see the measured values of dynamic viscosity during individual technological phases of mashing. The highest viscosity in selected samples was recorded for wheat in phase 5 (2nd saccharify stage). Conversely, the lowest was also detected for wheat in initial phase 1 (mash). Oat malt showed significantly lower values compared to the remaining malts, but the curve of the course of dynamic viscosity was the same (see Figure 1).

However, it was not possible to compare the values measured by us with the results of other authors, as there were no relevant studies dealing with this issue in scientific databases.

Figure 1 Graphical representation of the dynamic viscosity of wort

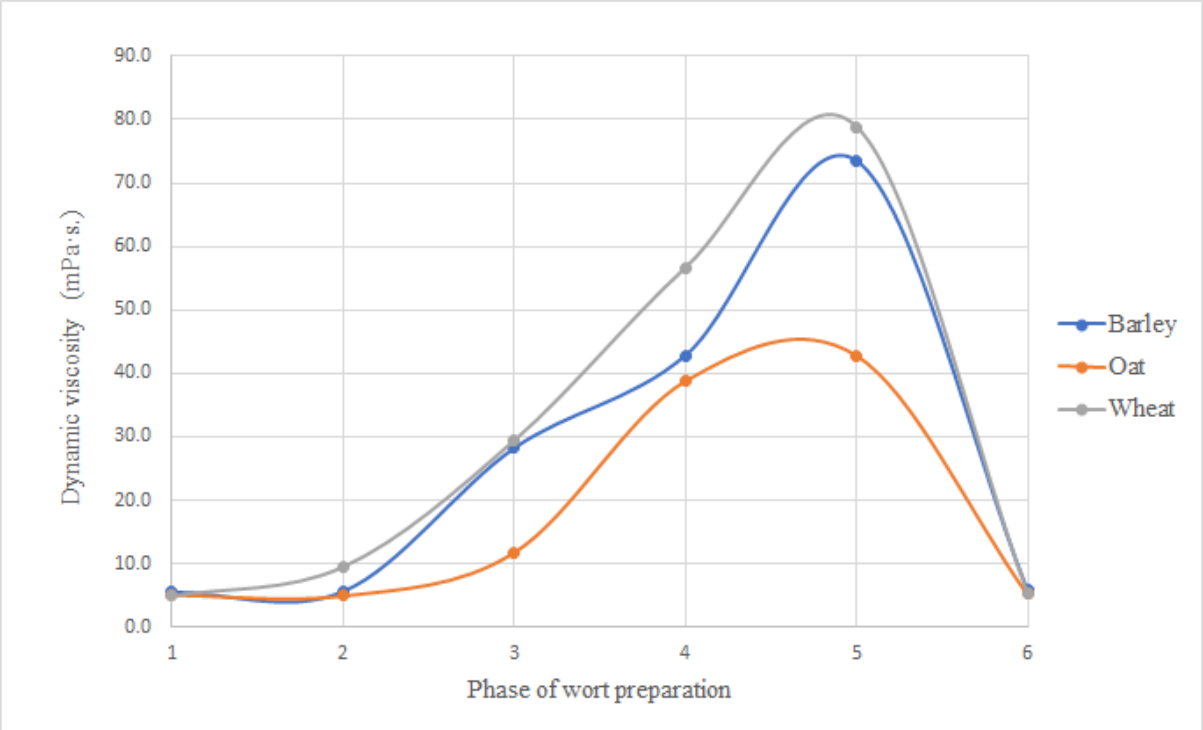

Legend: 1– Mash, 2– Mash 5min; 3– Proteolysis, 4– 1. Saccharify stage, 5– 2. Saccharify stage, 6– Mash out

A sharp increase in dynamic viscosity occurred in phase 2 (mash). This trend continued until phase 5 (2nd saccharify stage), when the viscosity decreased and returned to a value close to phase 1.

Regarding mash from barley, as the most commonly used cereals for beer production, the trend of changes in viscosity was similar to the wheat mash. Jin et al. (2004) measured the dynamic viscosity in wort at 20 °C with 12 original extract in at 1.521 mPa·s. Hlaváč et al. (2016) recorded the dynamic viscosity value of the wort at 50 RPM at 1.35 mPa·s. Their values were significantly lower compared to the resulting value of sweet barley measured in this work. Nielsen and Munck (2003) also recorded the same low dynamic viscosity as the mentioned author, who compared different physical properties of several species of malt and wort. Their values ranged from 1.48 up to 2.16 mPa·s.

The difference in the results can be due to the storage length and method, different types of spindle, the gradation of the beer or the different content of ß-glucans, which increase the dynamic viscosity.

Influence of carbohydrates content in wort on the course of dynamic viscosity

Table 3 shows the results of the chemical analysis of individual worts by high performance liquid chromatography.

Table 3 Result of chemical analysis of carbohydratest by HPLC

	Barley	Oat	Wheat
Oligosaccharide (%)	0.6	1.8	1.5
Maltotriose (%)	0.5	0.5	0,8
Maltose (%)	2.8	1.2	1.2
Glucose (%)	2.5	0.5	1.5
Fructose (%)	0.5	0.1	0.2

The action of amylolytic enzymes breaks down starch into oligosaccharides and later into maltotriose, maltose and glucose, which results in a rapid decrease in the viscosity of the mash (Basařová et al. 2010) which explains its rapid decrease in phase 6 (mash out). At the same time, we can conclude that barley showed a significant decomposition of carbohydrates compared to the values of wort from oats and wheat.

CONCLUSION

This study focused on the effects of the malt used on the viscosity of the wort, which was monitored during the individual mashing phases in the production of beer with original gravity 11°P. The worts were formed from wheat, barley, and oat malt. Subsequently, their different viscosities during the phases were recorded using a rotary viscometer with a coaxial cylinder sensor system. Viscosity was measured at room temperature and 100 RPM. The values obtained ranged from 4.9 mPa·s. up to 78.8 mPa·s. The results of dynamic viscosity obtained by us were significantly higher than reported by other authors in their publications. At the same time, the hypothesis of a decrease in the viscosity of wort due to the decomposition of starch into simpler carbohydrates was confirmed in this work. On the other hand, it has been found that the issue of dynamic viscosity of worts from cereals other than barley is a little explored topic. For this reason, it has not been possible to better compare the viscosity results of worts other than barley, and in the future, it would be appropriate to pay more attention to research in this area as well.

ACKNOWLEDGEMENTS

The research was financially supported by the Internal Grant Agency of the Faculty of AgriSciences no. AF-IGA-2020-TP006 “Modelling of rheological properties of liquid and semi-liquid food raw materials and foods showing non-Newtonian behaviour”.

REFERENCES

Basařová, G. et al. 2010. Pivovarství: teorie a praxe výroby piva. Praha: Publishing VŠCHT.

Hlaváč, P. et al. 2016. Dynamic viscosity and activation energy of wort during fermentation and storing. Acta Technologica Agriculturae [Online], 19(1):6–9. Available at: doi:10.1515/ata-2016-0002. [2020-09-09].

Jin, Y. et al. 2004. Effects of β-Glucans and Environmental Factors on the Viscosities of Wort and Beer. Journal of the Institute of Brewing [Online], 110(2): 104–116. Available at: doi:10.1002/j.2050-0416.2004.tb00189.x. [2020-09-10].

Li, M. et al. 2020. Profiling of carbohydrates in commercial beers and their influence on beer quality. Journal of the Science of Food and Agriculture [Online], 100(7): 3062–3070. Available at: doi:10.1002/jsfa.10337. [2020-09-12].

Nielsen, J.P., Munck, L. 2003. Evaluation of malting barley quality using exploratory data analysis. I. Extraction of information from micro-malting data of spring and winter barley. Journal of Cereal Science [Online], 38(2): 173–180. Available at: doi:10.1016/S0733-5210(03)00023-7. [2020-09-10].

Sadosky, P. et al. 2018. Effect of Arabinoxylans, β-Glucans, and Dextrins on the Viscosity and Membrane Filterability of a Beer Model Solution. Journal of the American Society of Brewing Chemists [Online], 60(4): 153–162 Available at: doi:10.1094/ASBCJ-60-0153. [2020-09-09].

Severa, L., Los, J. 2008. On the influence of temperature on dynamic viscosity of dark beer. Acta Universitatis Agriculturae et Silviculturae Mendelianae Brunensis [Online], 56(2): 303–308. Available at: doi:10.11118/actaun200856020303. [2020-09-09].

Influence of feed fortification with selenium on rheological parameters of liquid egg products

Marie Dostalova[1], Vojtech Kumbar[2], Sylvie Ondrusikova[1], Ondrej Stastnik[3], Sarka Nedomova[1]
[1]Department of Food Technology
[2]Department of Technology and Automobile Transport
[3]Department of Animal Nutrition and Forage Production
Mendel University in Brno
Zemedelska 1, 613 00 Brno
CZECH REPUBLIC

maruskadostalov@seznam.cz

Abstract: The aim of this work was to monitor changes in the rheological properties of liquid egg products depending on organic and inorganic selenium, which was added to the nutrition of laying hens. The viscosity was determined at 21 °C using a rotary viscometer with a coaxial cylinder sensor system and standard spindle at a shear strain rate of 0.279 1/s up to 93 1/s for yolk and from 0.279 1/s up to 186 1/s for albumen and liquid whole egg respectively. Experimental results were modelled using Newton viscosity model for yolk and Ostwald-de Waele model for albumen and liquid whole egg. The obtained flow curves indicate close Newtonian behaviour of liquid yolk and non-Newtonian behaviour (flow index $n < 1$) of liquid albumen and liquid whole eggs.

Key Words: hen eggs, rheological properties, liquid egg products, Ostwald-de Waele, fortification with selenium

INTRODUCTION

Hen eggs are complete food source with components essential to human nutrition. The eggs contain for example high quality proteins, ω-3 fatty acids, vitamins, carotenoids and minerals. Liquid egg products are characterized in the food industry also due to their functional properties, such as emulsifications, foam and gel formation. Traditionally, eggs are marketed as shell eggs, but in recent years, the demand for eggs in the form of egg products has increased. Egg products are products that are created by beating the egg contents out of the shell and are widely used in the processing industry to simplify and streamline production. They are used for commercial, foodservice, but also for home use. These products can be divided into refrigerated liquid, dried and frozen products (Jesús et al. 2013). Egg quality can be affected by the environmental conditions for example temperature, humidity and time of storage as well as the gaseous environment. Storage can modify some characteristics of the egg such as loss of carbon dioxide, water and a subsequent increase in the pH of the albumen, but also comprehensively changes in quality characteristics. The reason for these changes is the shell of egg allows escape of moisture and carbon dioxide resulting in loss of weight. Storage time causes various chemical, physical and biological changes in a food product (Nedomová et al. 2017). Therefore, changes in the rheological properties of the food product during storage are expected (Singh et al. 2014).

The knowledge of the rheological properties is very important for egg liquids owing to an increasing demand for processed egg products because each liquid egg product that is marketed must be pasteurized (Jesús et al. 2013). Pasteurization is carried out using a continuous flow in stainless steel pipes with a constant flow velocity, temperature, and defined conditions (Guilmineau and Kulozik 2007). Information about of the rheological properties of food products is important for the product development, sensory evaluation, quality control and determination of processing method and instruments (Kumbár et al. 2015a). The rheological data are used in engineering calculations involving a wide range of equipment such as pumps, pipelines, mixers, coaters, homogenizers, heat exchangers, shelf life testing, and in the evaluation of food texture by correlation to sensory data (Singh et al. 2014). The variable that characterizes the behaviour in the flow is the viscosity that determines the degree of internal resistance. The viscosity of liquid egg products depends on a number of variables

– egg age, pH, temperature, specific gravity, water content and stress (Kumbár et al. 2015b). The flow behavior of a fluid can be varied from Newtonian to time-dependent non-Newtonian (Kumbár et al. 2015a).

Selenium (Se) is recognized as an essential dietary nutrient for long time for animals and humans. It is important for maintenance growth, of health, physiological functions Utterback et al. (2005) is a component of several major metabolic pathways, the antioxidant defence system and immune functions. Chronic marginal Se deficiency may enhance susceptibility to viral infection, thyroid dysfunction, cancer, cardiovascular disease, and various inflammatory conditions. Food is the main source of selenium in the human diet, but its consumption is still low, therefore, it is necessary to constantly increase their income. Therefore, strategies to increase Se intake have been implemented, for example Se fertilisation of crops and vegetables, human and animal supplementation and education to consume higher-Se foods. Egg's nutrient content can be modified by the diet given to hens (Bargellini et al. 2008). Traditionally, Se has been added to poultry diets via inorganic form, such as sodium selenite and the organic form – selenomethionine (Utterback et al. 2005). Studies Lechevalier-Datin et al. (2017) shows that the enrichment of feed for laying hens with OH-SeMet (hydroxy-selenomethionine) improves the technological properties of egg albumen. Solid albumin from the experimental group had a significantly higher viscosity at this shear stress of 0.1 1/s and 1 1/s. However, the scientific works dealing with this issue is quite unique.

The hypothesis of the thesis was to determine whether the fortification of feed with organic and inorganic selenium will affect the rheological parameters of liquid egg products or not.

MATERIAL AND METHODS

Fortification of hen eggs

Eggs of Lohmann Brown-Classic hybrids were used for our research. The experiment was performed on 84 laying hens using a conventional deep litter system with wood shavings. Our research was started at 33 weeks of age of laying hens and lasted until 41 weeks of age. Laboratory humidity, temperature and light were set according to Lohmann laying hen production recommendations. Laying hens were divided into three groups. The first group being the control, in which the laying hens were fed with the mixture without the addition of selenium. The second group of laying hens was fed a feed mixture with the addition of an organic selenium source (Sel-Plex – *Saccharomyces cerevisiae* CNCM I-3060). The third group of laying hens was fed with a mixture with the addition of an inorganic selenium source (Na_2SeO_3 – Sodium selenite). In all groups selenium was supplied with its natural content in the feed and in second and third group selenium was also added to give a total content of 0.31 mg/kg.

Rheological properties

The eggs (n = 21) were subsequently stored under temperature 4 °C in unchangeable conditions for the period of 0, 14 and 28 days. For the preparation of liquid egg products, the egg was manually broken properly, the individual liquid egg masses separated yolk, albumen and liquid whole egg and further homogenized. All liquids egg products were filtered in order to separate impurities such as chaladza and membranes. The 40 ml of samples for each liquid egg product were prepared (albumen, yolk and liquid whole egg) from each group. The thus prepared liquid eggs products was measured viscosity depend on shear strain rate. The viscosity of each sample was measured out using a rotary viscometer DV-3P (Anton Paar, Austria) equipped with a coaxial cylinder sensor system and measuring the torque of the standard spindle (TR8) immersed in the sample at temperature of 21 °C. For the measurement were used a shear strain rate from 0.279 1/s up to 93 1/s for yolk (Y) and from 0.279 1/s up to 186 1/s for albumen (A) and liquid whole egg (LWE). The power-law (also known as Ostwald-de Waele) model is used for non-Newtonian fluids, the equation takes the form:

$$\tau = K \cdot \dot{\gamma}^n, \qquad (1)$$

where τ [Pa s] is the shear stress, K [Pa·s^n] is a consistency coefficient, $\dot{\gamma}$ [1/s] is the shear strain rate, and n [-] is a flow index. The flow index n indicates the type of liquid (see in Table 1). If n = 1 the Ostwald-de Waele model is reduced to Newton model for Newtonian fluids, an equation is used which takes the form:

$$\tau = \eta \cdot \dot{\gamma}, \qquad (2)$$

where η [Pa·s] is the coefficient of dynamic viscosity.

Table 1 Overview of the type of liquid according to a flow index

Flow index [-]	The type of liquid
$n < 1$	Pseudoplastic fluid
$n = 1$	Newtonian liquid
$n > 1$	Dilatant fluid

RESULTS AND DISCUSSION

The average results of dynamic viscosity of tested liquid egg yolk are shown in Table 2. The highest viscosity values reached the liquid egg yolk with inorganic Se at a shear strain rate of the 0.279 1/s (3134.8 mPa·s for fresh, 2452.4 mPa·s 14 day of storage and 1047.6 mPa·s 28 day of storage). The viscosity of the liquid egg yolk decreases with the storage duration, which is consistent with the study by Kumbár et al. (2015b). The viscosity of liquid albumen and liquid whole eggs is lower than that for liquid egg yolk. The highest viscosity values reached the liquid albumen without Se added to the feed laying hens at a shear strain rate of the 0.279 1/s (784.28 mPa·s for fresh, 1047.6 mPa·s 14 day of storage and 967.8 mPa·s 28 day of storage). The viscosity of albumen and LWE did not change much during egg storage which is consistent with the study by Singh et al. (2014). The increasing of viscosity of the liquid egg products can improve the quality of processing food. For example, increasing the emulsion stability, because the higher the viscosity of the liquid egg products, the faster and more stable it occurs and the formation of a stable sauce or foam (Gouda et al. 2017).

The flow curves of the liquid egg products are shown in Figure 1, 2 and 3. In the Figure 1 are the flow curves of the liquid yolk without Se, with organic Se and with inorganic Se after 14 days of the storage modelled using Newton model (eq. 2). From Figure 1 it can be seen that the flow curve of the liquid yolk is highest in egg yolk with organic Se after 14 days of the storage. According to Table 2 it can be said that the highest the viscosities was reached by the egg yolk without Se (1373.3 and 379.7 mPa·s) for fresh and 28 days of storage. The viscosity of the liquid egg yolk was the highest in eggs without Se for fresh and 28 day of storage, but in eggs for 14 day of storages was the viscosity the lowest in eggs without Se. The viscosity of the liquid egg yolk decreases with the time of the egg storage as described Riscardo et al. (2005). The liquid egg yolk exhibits behaviour the Newtonian liquid (Figure 1).

Figure 1 The flow curves of the liquid yolk without Se, with organic Se and with inorganic Se after 14 days of the storage

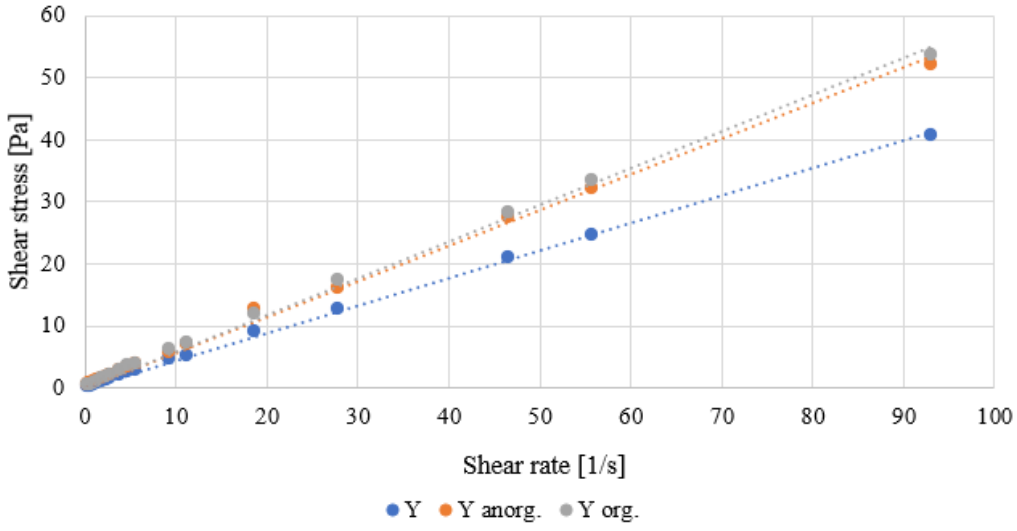

Table 2 Coefficient of Newton model for liquid yolk

Day		Newton model	
		η [mPa·s]	R^2
0	Yolk	1373.3	0.9975
	Yolk org. Se	740.4	0.9983
	Yolk inorg. Se	1108.5	0.9954
14	Yolk	444.3	0.9990
	Yolk org. Se	591.6	0.9985
	Yolk inorg. Se	574.8	0.9979
28	Yolk	379.7	0.9983
	Yolk org. Se	313.7	0.9979
	Yolk inorg. Se	367.4	0.9974

The significant non-Newtonian behaviour modelled using Ostwald-de Waele model (eq. 1) exhibits liquid egg albumen and liquid whole egg, with the same result describing of Kumbár et al. (2015b) and Li et al. (2020). In the Figure 2 are the flow curves of the liquid albumen without Se, with organic Se and with inorganic Se after 14 days of the storage. From Figure 2 it can be seen that the flow curve of the liquid albumen is highest in egg albumen with inorganic Se after 14 days of the storage. The flow index for liquid albumen ranged from 0.5127 (organic Se) to 0.4319 (inorganic Se) for fresh eggs. After 14 days of storage, the flow index of liquid albumen ranged from 0.3669 (inorganic Se) to 0.2132 (without Se). After 28 days of storage, the flow index of liquid albumen ranged from 0.3559 (organic Se) to 0.2027 (without Se). The flow index for the liquid egg albumen was the highest in eggs with organic Se. The flow index of liquid egg albumen decreases with the time of the egg storage. In the Figure 3 are the flow curves of the liquid whole eggs without Se, with organic Se and with inorganic Se for fresh eggs. From Figure 3 it can be seen that the flow curve of the liquid whole eggs is highest in liquid whole egg without Se for fresh eggs. The flow index for liquid whole eggs ranged from 0.3705 (organic Se) to 0.3264 (without Se) for fresh eggs. After 14 days of storage, the flow index of liquid whole eggs ranged from 0.4334 (inorganic Se) to 0.3305 (organic Se). After 28 days of storage, the flow index of liquid whole eggs ranged from 0.5256 (inorganic Se) to 0.4346 (without Se). The flow index for the liquid whole egg was the highest in eggs with inorganic Se. The flow index of liquid whole egg increases with the time of the egg storage. The results in Table 3 and 4 indicating that egg albumen and liquid whole egg exhibit pseudoplastic behaviour in nature as described Strohalm et al. (2000) and Icier and Bozkurt (2011).

Figure 2 The flow curves of the liquid albumen without Se, with organic Se and with inorganic Se after 14 days of the storage

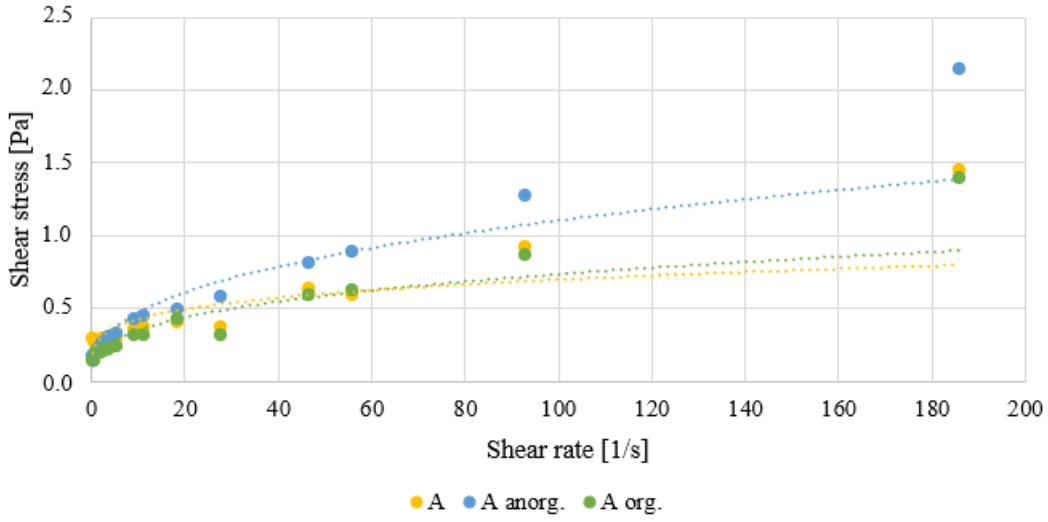

Table 3 Coefficients of the Ostwald-de Waele model for liquid albumen

Day		Ostwald-de Waele model		
		K [mPa·s^n]	n [-]	R^2
0	Albumen	0.2373	0.4481	0.9410
	Albumen org. Se	0.1096	0.5127	0.9762
	Albumen inorg. Se	0.2318	0.4319	0.9763
14	Albumen	0.2625	0.2132	0.7293
	Albumen org. Se	0.1697	0.3191	0.9070
	Albumen inorg. Se	0.2043	0.3669	0.9440
28	Albumen	0.2059	0.2027	0.5942
	Albumen org. Se	0.2634	0.3559	0.8888
	Albumen inorg. Se	0.2156	0.2736	0.7968

Figure 3 The flow curves of the liquid whole eggs without Se, with organic Se and with inorganic Se for fresh eggs

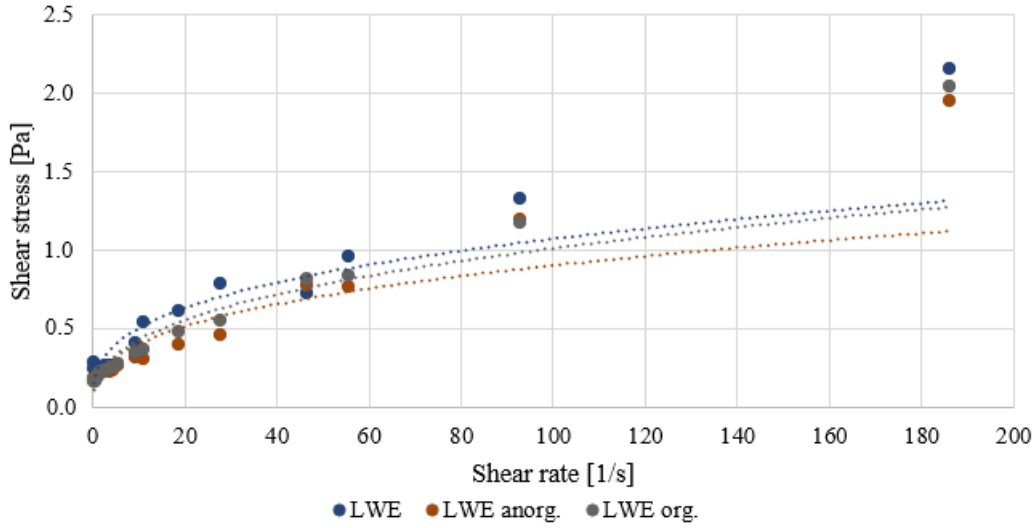

Table 4 Coefficients of the Ostwald-de Waele model for liquid whole eggs

Day		Ostwald-de Waele model		
		K [mPa·s^n]	n [-]	R^2
0	Liquid whole eggs	0.2393	0.3264	0.8238
	Liquid whole eggs org. Se	0.1843	0.3705	0.9202
	Liquid whole eggs inorg. Se	0.1829	0.3476	0.8683
14	Liquid whole eggs	0.1771	0.4087	0.8924
	Liquid whole eggs org. Se	0.2296	0.3305	0.8450
	Liquid whole eggs inorg. Se	0.1834	0.4334	0.9429
28	Liquid whole eggs	0.1889	0.4346	0.9161
	Liquid whole eggs org. Se	0.2152	0.4568	0.8953
	Liquid whole eggs inorg. Se	0.1967	0.5256	0.9279

CONCLUSION

This paper dealt with knowledge of rheological parameters, when these parameters can be used in various software applications and numerical simulation of flow. Experimental data were modelled using Ostwald-de Waele model, but just for liquid albumen and liquid whole eggs, and Newton model for liquid yolk. These findings can be used in the design of industrial equipment and pipelines, tubes, and/or trough for pasteurization, cooling, freezing, drying in the manufacturing industry, because

if the rheological properties of liquid egg masses change there could be a change the flow (different volume and mass flow, different velocity, turbulent flow may occur).

The addition of Selenium in organic and inorganic form did not affect the rheological properties of liquid egg products, which may be considered as a positive benefit. Selenium as an essential element is added to the diet mixture of laying hens to enrich the egg. This enrichment may contribute to an increase in selenium intake in the population in terms of food intake.

ACKNOWLEDGEMENTS

The research was financially supported by the Internal Grant Agency of Faculty of AgriSciences no. AF-IGA-2020-TP006 "Modelling of rheological properties of liquid and semi-liquid food raw materials and foods showing non-Newtonian behaviour" in cooperation with AF-IGA2020-TP012 „The influence of feeding selected phytoaditives on meat quality of broiler chickens".

REFERENCES

Bargellini, A. et al. 2008. Selenium interactions with essential and toxic elements in egg yolk from commercial and fortified eggs. Journal of Trace Elements in Medicine and Biology, 22(3): 234–241.

Gouda, M. et al. 2017. Effects of four natural antioxidant phenyl terpenes on emulsifying and rheological properties of egg yolk. LWT-Food Science and Technology, 83: 59–67.

Guilmineau, F., Kulozik, U. 2007. Influence of a thermal treatment on the functionality of hen's egg yolk in mayonnaise. Journal of Food Engineering, 78(2): 648–654.

Icier, F., Bozkurt, H. 2011. Ohmic heating of liquid whole egg: Rheological behaviour and fluid dynamics. Food and Bioprocess Technology, 4(7): 1253–1263.

Jesús, M. N. de. et al. 2013. Sensory and physico-chemical characteristics of desserts prepared with egg products processed by freeze and spray drying. Food Science and Technology, 33(3): 549–554.

Kumbár, V. et al. 2015a. Fluid dynamics of liquid egg products. Journal of Biological Physics, 41(3): 303–311.

Kumbár, V. et al. 2015b. Effect of egg storage duration on the rheology of liquid egg products. Journal of Food Engineering, 156: 45–54.

Lechevalier-Datin, V. et al. 2017. Effect of organic selenium supplementation on the technological properties of egg white. XVIIth european symposium on the quality of eggs and egg products, Edinburgh, United Kingdom. (hal-01595723).

Li, R. et al. 2020. Rheological, structural and physicochemical characteristics of heat-induced egg albumin/sesbania gum mixed gels. International Journal of Biological Macromolecules, 163: 87–95.

Nedomová, Š. et al. 2017. Mechanical properties of sugar beet root during storage. International Agrophysics, 31(4): 507–513.

Riscardo, M.A. et al. 2005. Rheological characterisation of salad-dressing-type emulsions stabilised by egg yolk/sucrose distearate blends. European Food Research and Technology, 220(3–4): 380–388.

Singh, J. et al. 2014. Effect of storage conditions of egg on rheological properties of liquid whole egg. Journal of Food Science and Technology, 51(3): 543–550.

Strohalm, J. et al. 2000. Influence of high pressure treatment on rheological and other properties of egg white. High Pressure Research, 19(1-6): 137–143.

Utterback, P. L. et al. 2005. Effect of supplementing selenium yeast in diets of laying hens on egg selenium content. Poultry Science, 84(12): 1900–1901.

The temperature influence on the rheological behaviour of chocolate

Renata Dufkova[1], Veronika Kourilova[1], Ludek Hrivna[1], Vojtech Kumbar[2]
[1]Department of Food Technology
[2]Department of Technology and Automobile Transport
Mendel University in Brno
Zemedelska 1, 613 00 Brno
CZECH REPUBLIC

renca.dufkova@seznam.cz

Abstract: Three samples of commercially available dark chocolate with a minimum cocoa content of 50%, 78% and 99% were used to experimentally verify the temperature influence on the rheological behaviour of chocolate. The change in the shear stress with an increasing shear strain rate was measured using an RST rheometer with a cone-plate spindle arrangement at a shear strain rate from 0.01/s to 100/s at temperatures of 36 °C, 38 °C, 40 °C, 42 °C and 44 °C for a 1 minute load. To describe the flow curves at selected temperatures, a mathematical flow model according to Casson was used, which, according to the calculated coefficient of determination R^2, seemed to be the most suitable. The results show that with an increasing chocolate sample temperature, their viscosity decreased, with respect to the shear stress.

Key Words: dark chocolate, viscosity, flow curves, Casson model, cocoa butter

INTRODUCTION

The basic raw materials used to make chocolate include cocoa mass, cocoa butter, sugar and emulsifiers. Milk powder, vegetable fats (other than cocoa butter) and flavourings (Becket 2008) are some of the other raw materials that can be used. Cocoa butter is a natural fat obtained from the seeds of cacao trees and, thanks to its properties, is an essential component of chocolate. Cocoa butter makes up about 55% of the cocoa beans. It is known for its specific physical properties, such as its hardness at room temperature, but its complete melting at body temperature (Momeny et al. 2013, Afoakwa 2010).

The principles of rheology are commonly used to understand and improve the flow behaviour and textural properties of food and to reveal the relationships between the physical properties and the functionality of the material (Arana 2012). The rheological properties are important in the production of chocolate for quality control purposes and may be related to its composition, e.g., a higher content of cocoa butter in chocolate results in a decrease in the flow and viscosity (Servais et al. 2007). General rheology deals with the physical and mathematical description of the behaviour of the substances between three quantities – the stress to which the material is exposed, the final amount of deformation of the material and time, with respect to the combination of time and the deformation. Mathematically, the flow properties of liquids are expressed by the rheological equations of state, which usually express the relationship between the deformation shear stress τ and the deformation of the liquid. They are expressed graphically using flow curves (Kadlec et al. 2013). The flow limit is the point where the shear stress and shear strain rate curve begin to show the deviation of the shear rate from zero. This condition indicates the start of the flow and the corresponding shear stress is considered as the flow limit (Cruz et al. 2014).

Viscosity and yield strength are important rheological properties in chocolate production technologies and for its final quality. It is important when pumping chocolate, mixing it and pouring it into moulds. Viscosity is also important for the sensory perception of the final product when consumed by the consumer. Viscosity is defined as the resistance of a fluid to creep (the energy required to keep the fluid moving) and the flow limit as the minimum amount of energy required for the fluid to begin to flow. For liquids such as water or cocoa butter, the viscosity is the same throughout the flow regardless of the shear rate. These fluids are called Newtonian. However, the vast majority of all fluids are

non-Newtonian, which means that the viscosity changes with the shear rate. This group also includes chocolate, which belongs to the subgroup of pseudoplastic liquids. This means that its viscosity decreases with an increasing shear rate (Afoakwa et al. 2008, Cikrikci et al. 2017, Glicerina et al. 2013, Pandey and Singh 2011, Talbot 2009).

MATERIAL AND METHODS

Table 1 shows the characteristics of the chocolate samples used to measure the change in the shear stress with increasing shear strain rate at 36 °C, 38 °C, 40 °C, 42 °C and 44 °C. All the chocolate samples were from the same commercial manufacturer LINDT & SPRÜNGLI GMBH (Germany). It was a dark chocolate with a minimum cocoa content of 50%, 78% and 99%.

Table 1 The characteristics of the used chocolates

Chocolate with a minimum cocoa solids content of	Ingredients	Nutritional information per 100 g				
		Energy value	Fats Of which are saturated fatty acids	Carbohydrates Of which are sugars	Protein	Salt
50%	cocoa mass, sugar, concentrated butter, cocoa butter and vanilla	2302 kJ 533 kcal	36 g 22 g	48 g 45 g	5.6 g	0.04 g
78%	cocoa mass, cocoa butter, sugar, low-fat cocoa powder, anhydrous milk fat, may contain traces of hazelnuts and other nuts, milk, soybeans	2384 kJ 576 kcal	46 g 29 g	24 g 17 g	10 g	0.05 g
99%	cocoa mass, low-fat cocoa powder, cocoa butter, sugar	2433 kJ 590 kcal	51 g 31 g	8 g 1 g	15 g	0.01 g

The chocolate samples were measured using an RST rheometer (Brookfield, USA) with a cone-plate spindle arrangement (RCT-50-2) equipped with a duplicator to temper the sample. This rheometer is suitable for measuring the flow properties of chocolate. Specialised software Rheo 3000 (Brookfield, USA) was used to evaluate the measured data. Thanks to the software, it is possible to programme the measuring cycles, to obtain and process the obtained data, including the insertion of mathematical models and the statistical evaluation. In our case, the flow curves were modelled using the Casson mathematical flow model, which was adopted by The International Office of Cocoa and Chocolate as the official method for describing the flow properties of chocolates (Servais et al. 2007).

The individual chocolate samples were gradually dissolved at 36 °C on an RTS rheometer plate, which was pressed against a rotating cone followed by the overall tightening of the rheometer mechanism. The temperature of 36 °C was the starting temperature for measuring the shear stress at a shear strain rate ranging from 0.01/s to 100/s for 1 minute. Between the measurements, the temperature was continuously increased by 2 °C to a final measurement temperature of 44 °C.

RESULTS AND DISCUSSION

The measured values of the flow limit, Casson's viscosity and the coefficient of determination according to Casson's model are given in Table 2. To determine which mathematical model is most suitable for a given type of liquid (semi-solid), it is necessary to measure the stable shear stress during the interval of the assessed shear deformation velocity and substitute the resulting values into the mathematical relations of the individual models. The resulting value of the coefficient of determination will then show whether the given calculation model is satisfactory or not (Balmforth et al. 2014).

Casson's model is given by:

$$\sqrt{\tau} = \sqrt{\tau_0} + \sqrt{\eta_c \dot{\gamma}},$$

where τ is the shear stress, τ_0 is the value of the stress at the flow limit, η_c is the value of Casson's viscosity and $\dot{\gamma}$ is the shear strain rate. Casson's model is a very close alternative to Bingham's model. Although this model is based on the Bingham model, all the variables are increased by a certain constant, which makes the transition between the flow limit and the Newtonian region more pronounced (Glicerina et al. 2016). Casson's model can describe the behaviour of plastics. It is also used to characterise dispersion systems in foods and also to characterise the flow properties of chocolates (Rao 2007).

Table 2 Coefficients of the Casson model

Temperature	Casson model								
	Cocoa content 50%			Cocoa content 78%			Cocoa content 99%		
[°C]	τ_0 [Pa]	η_c [Pa/s]	R^2	τ_0 [Pa]	η_c[Pa/s]	R^2	τ_0 [Pa]	η_c [Pa/s]	R^2
36	10.0495	1.2863	0.9935	5.0406	0.5978	0.9935	10.8338	4.0713	0.9980
38	10.0126	1.1244	0.9950	3.7063	0.5832	0.9965	7.5497	3.4816	0.9990
40	10.1931	0.9841	0.9951	3.6089	0.5168	0.9934	6.4432	3.1586	0.9988
42	9.2372	0.9321	0.9950	3.7789	0.4661	0.9940	5.6532	2.9056	0.9987
44	9.6185	0.8240	0.9940	3.0405	0.4670	0.9956	5.8116	2.5817	0.9979

The flow limit τ_0 for all three chocolate samples decreased with an increasing temperature. The higher the temperature, the more thermal energy is contained in the material, and, therefore, less stress is sufficient to initiate the flow of material. Therefore, the flow limit tends to decrease with an increasing temperature, although there may not be any changes in the structure caused by the increased temperature (Balmforth et al. 2014).

The coefficients of determination R^2 ranged from 0.9934 to 0.9990, which indicate a correctly chosen mathematical model for the description of the flow properties of the chocolate.

Figures 1–3 show the flow curves for the individual chocolate samples at five different temperature regimes.

Figure 1 The flow curves (according to Casson's model) for the chocolate with a min. cocoa content of 50%

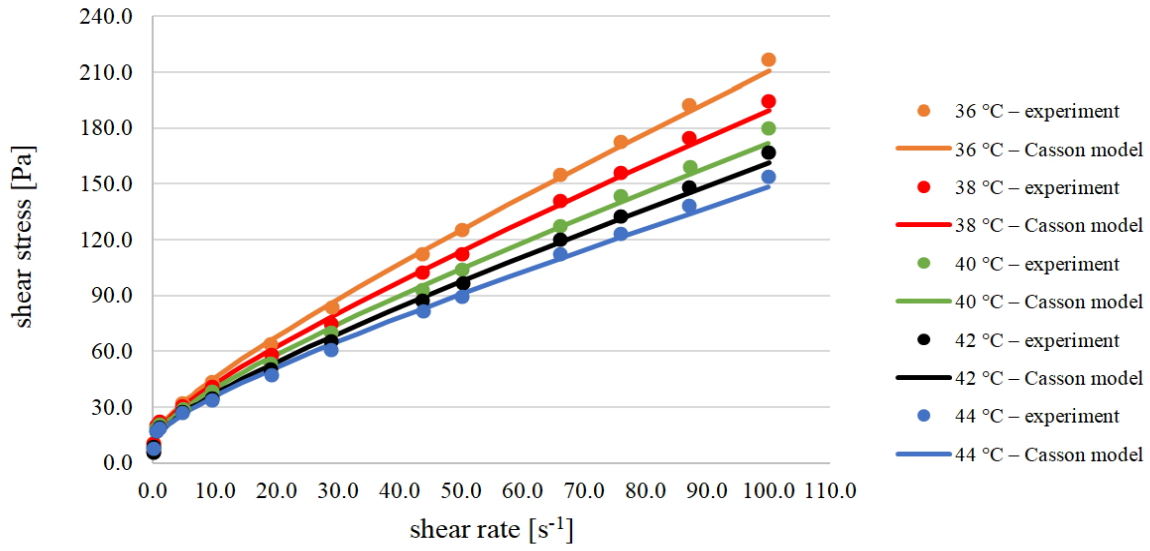

The highest shear stress values were measured in all three chocolate samples at a shear strain rate of 100/s at a temperature of 36 °C. The chocolate with a min. cocoa content of 50% had a shear stress of 216.94 Pa, the 78% chocolate had a shear stress of 106.56 Pa and the 99% chocolate had a value of 529.29 Pa. While the lowest values were measured at 44 °C for all the chocolates at the same shear strain rate. The measured values were as follows: 153.81 Pa for the 50% chocolate, 77.89 Pa for the 78% chocolate and 355.07 Pa for the 99% chocolate. As the temperature rises, the Casson plastic

viscosity value decreases. This phenomenon can be eliminated, especially with dark chocolates, by adding lecithin (Čopíková 1999). If the temperature was low when the chocolate melted, not all the modifications of the cocoa butter would have to dissolve and the viscosity and flow rate could increase (Bourne 2002).

Figure 2 The flow curves (according to Casson's model) for the chocolate with a min. cocoa content of 78%

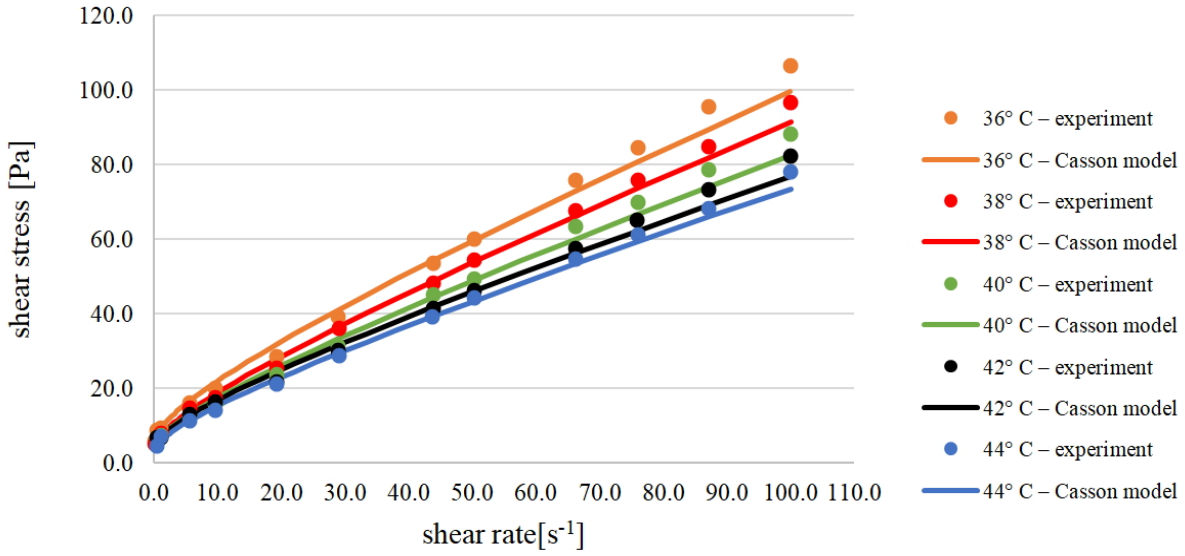

Figure 3 The flow curves (according to Casson's model) for the chocolate with a min. cocoa content of 99%

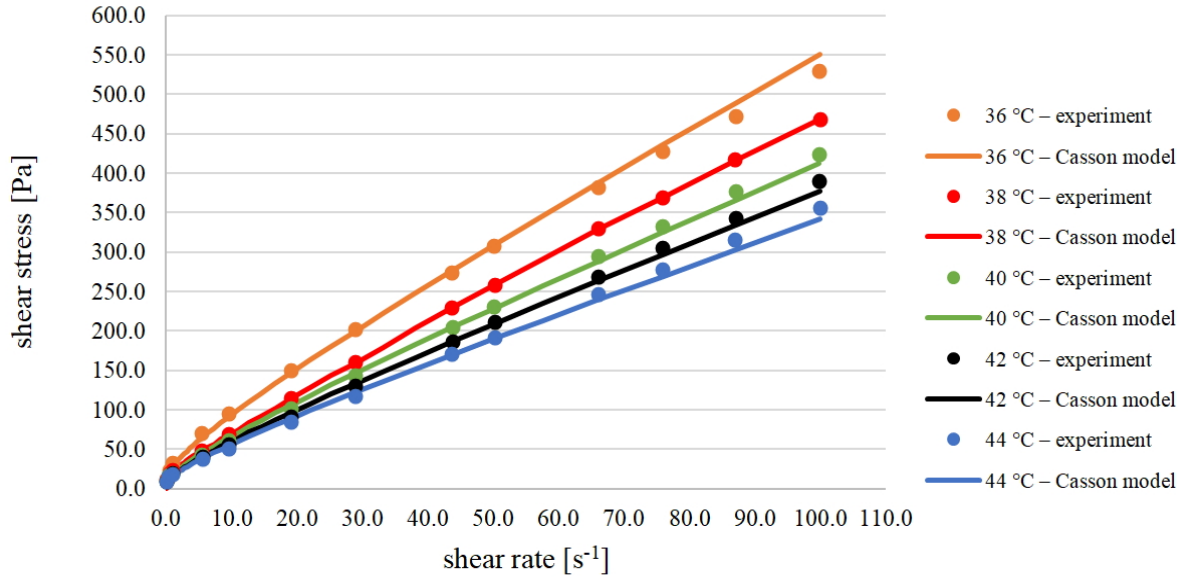

Up to a shear strain rate of 0.1/s, the shear stress values at all temperatures were very similar, then they began to diverge with an increasing shear strain rate depending on the temperature actually used.

CONCLUSION

Knowledge of the rheological properties in food production is important especially for the mathematical calculations of the equipment or processes, e.g., during mixing, kneading, pumping, centrifugation, etc. It is necessary to determine the exact range of shear rates and temperatures in the equipment. At five selected temperatures (36 °C, 38 °C, 40 °C, 42 °C and 44 °C), the change in the shear stress as a function of the shear strain rate was monitored in three dark chocolate samples

with a min. cocoa content of 50%, 78% and 99%. The higher the exposure temperature of the sample, the lower the shear stress value. As a result of the rising temperature, the viscosity decreased, which is closely related to the content of the cocoa butter in the individual chocolate samples.

The high values of the determination coefficient R^2 (0.9934–0.9990) confirmed that the mathematical model according to Casson is suitable for the description of the flow properties of chocolate.

ACKNOWLEDGEMENTS

The research was financially supported by the Internal Grant Agency of the Faculty of AgriSciences no. AF-IGA2020-TP006 "Modelling of rheological properties of liquid and semi-liquid food raw materials and foods showing non-Newtonian behaviour".

REFERENCES

Afoakwa, E. 2010. Chocolate Science and Technology. 1st ed., York, UK: Willey-Blackwell.

Afoakwa, E. et al. 2008. Relationship between rheological, textural and melting properties of dark chocolate as influenced by particle size distribution and composition. European Food Research and Technology [Online], 227(4): 1215–1223. Available at: https://www.researchgate.net/publication/225539470_Relationship_between_rheological_textural_and_melting_properties_of_dark_chocolate_as_influenced_by_particle_size_distribution_and_composition. [2020-08-15].

Arana, I. 2012. Physical properties of food: Novel measurement techniques and applications. 1st ed., Boca Raton: CRC Press.

Balmforth, N.J. et al. 2014. Yielding to Stress: Recent Developments in Viscoplastic Fluid Mechanics. Annual Review of Fluid Mechanics [Online], 46(1): 121–146. Available at: https://www.annualreviews.org/doi/abs/10.1146/annurev-fluid-010313-141424. [2020-08-18].

Becket, S.T. 2008. The Science of Chocolate. 2nd ed., Cambridge: The Royal Society of Chemistry.

Bourne, M. 2002. Food texture and viscosity: concept and measurement. 2nd ed., San Diego: Academic Press.

Cikrikci, S. et al. 2017. Physical characterization of low-calorie chocolate formulations. Journal of Food Measurement and Characterization [Online], 11(1): 41–49. Available at: https://link.springer.com/article/10.1007/s11694-016-9369-1. [2020-08-15].

Cruz, R.M.S. et al. 2014. Methods in food analysis. 1st ed., Boca Raton: CRC Press.

Čopíková, J. 1999. Technologie čokolády a cukrovinek. 1st ed., Praha: VŠCHT.

Glicerina, V. et al. 2016. Microstructural and rheological characteristics of dark, milk and white chocolate. Journal of Food Engineering [Online], 169(1): 165–171. Available at: https://www.sciencedirect.com/science/article/pii/S0260877415003647. [2020-08-17].

Glicerina, V. et al. 2013. Rheological, textural and calorimetric modifications of dark chocolate during process. Journal of Food Engineering [Online], 119(1): 173–179. Available at: https://www.sciencedirect.com/science/article/pii/S0260877413002410. [2020-0807].

Kadlec, P. et al. 2013. Procesy a zařízení v potravinářství a biotechnologiích. 1st ed., Ostrava: Key Publishing.

Momeny, E. et al. 2013. Physicochemical properties and antioxidant activity of a synthetic cocoa butter equivalent obtained through modification of mango seed oil. International Journal of Food Science and Technology [Online], 48(7): 1549–1555. Available at: https://ifst.onlinelibrary.wiley.com/doi/full/10.1111/ijfs.12125. [2020-08-13].

Pandey, A., Singh, G. 2011. Development and storage study of reduced sugar soy containing compound chocolate. Journal of Food Science and Technology [Online], 48(1): 76–82. Available at: https://www.ncbi.nlm.nih.gov/pmc/articles/PMC3551080/. [2020-08-11].

Rao, M.A. 2007. Rheology of Fluid and Semisolid Foods. 2nd ed., Boston: Springer.

Servais, C. et al. 2007. Determination of chocolate viscosity. Journal of Texture Studies [Online], 34(5–6): 467–497. Available at: https://onlinelibrary.wiley.com/doi/pdf/10.1111/j.1745-4603.2003.tb01077.x. [2020-08-11].

Talbot, G. 2009. Science and Technology of Enrobed and Filled Chocolate, Confectionery and Bakery Products. 1st ed., Amsterdam: Elsevier Science.

Microbiological quality of sushi from restaurants

Petra Furmancikova, Radka Hulankova
Department of Animal Origin Food and Gastronomic Sciences
University of Veterinary and Pharmaceutical Sciences Brno
Palackeho tr. 1946/1, 612 42 Brno
CZECH REPUBLIC

furmancikovap@vfu.cz

Abstract: In recent years, sushi has become a very popular foodstuff in many countries, including the Czech Republic. As it is one of the ready-to-eat foods (foods that are not subject to further heat treatment before consumption), care must be taken to ensure the hygiene of their production and the quality of the raw materials. The aim of this study was to obtain and evaluate information on the microbiological load of sushi. A total of 90 Maki and Nigiri sushi samples were analyzed, as well as pickled ginger and wasabi paste, which were purchased at restaurants. All 90 samples were negative for the presence of pathogenic bacteria of interest. The highest numbers of spoilage microorganisms were recorded in Nigiri sushi (with a higher proportion of animal component). Salmon sushi showed higher contamination than shrimp sushi ($P < 0.001$). High average numbers of lactic acid bacteria (6.68 log CFU/g) and a high total number of microorganisms (5.53 log CFU/g) were detected in the wasabi paste, indicating that this paste is not freshly and hygienically prepared and stored in restaurants. For other types of samples, the average numbers of the individual groups of microorganisms determined did not exceed 6 log CFU/g, and overall, the investigated samples can be assessed as microbiologically acceptable.

Key Words: microbiological analysis, RTE food, sushi, food safety and quality

INTRODUCTION

Thanks to the endless possibilities offered by today's world, the structure of the European population has changed significantly in recent years. The wide combination of different world cultures and customs has helped to spread traditional foods and dishes throughout Europe. Not only restaurants but also retail chains try to meet the needs, requirements and wishes of consumers. Thanks to this, sushi has gradually entered to the European market. Sushi has recently become very popular with consumers and has become a kind of trendy food (Tirloni et al. 2017).

Sushi is a traditional Japanese dish consisting mainly of cooked, rice vinegar acidified rice (the size of one bite), which is covered with raw fish or seafood. Rice can also be in the shape of a roll, complemented by raw fish and vegetables, wrapped in a slice of seaweed.

The typical and most common ingredients of animal origin for making sushi are raw salmon, tuna, flounder and boiled shrimp. Eating sushi is one of the few cases where we can encounter on consumption of raw meat (Hoel et al. 2015).

Sushi is one of the RTE foods (ready-to-eat). RTE foods are intended for direct consumption without further cooking. Due to the lack of heat treatment of food before consumption, RTE foods are associated with a potential health risk due to microbial contamination (Ramires et al. 2019). Contamination of these foods by pathogenic microorganisms can occur at all steps of the food chain, so it is very important to follow good hygiene practices in their production, storage and distribution.

In general, the microbial safety of RTE foods depends on many factors. The main factors are: microbiological quality of input raw materials, properties of used raw materials (water activity, NaCl content, pH), production and packaging technology, storage temperature and hygiene of the production process (contact of food with production areas and production equipment, cross-contamination between raw materials) (Hoel et al. 2019).

Due to the fact that sushi in many cases contains raw fish or raw seafood and we include sushi in RTE foods, it is a very hygienically and at the same time technologically demanding food.

Fish meat is an excellent substrate for bacterial growth, mainly due to its high pH values *post mortem.* Contamination of fish meat can occur during technological steps such as filleting and slicing meat.

Sushi can be the source of a whole range of different pathogenic microorganisms. These are in particular *Vibrio parahaemolyticus, Vibrio cholerae, Staphylococcus aureus, Bacillus cereus, Escherichia coli, Salmonella* spp., *Listeria monocytogenes, Pseudomonas* spp. and *Aeromonas* spp. (Barralet et al. 2004, Jain et al. 2004, Muscolino et al. 2014, Neyts et al. 2000).

MATERIAL AND METHODS

A total of 90 samples were used for microbiological examination, which were taken in three sampling from restaurant facilities with the possibility of take away. These were samples of Maki and Nigiri sushi prepared with salmon (*Salmo salar*), tuna (*Thunnus albacares*) or shrimp (*Penaeus vannamei*). Samples of wasabi paste and pickled ginger were also part of the analysis.

Microbiological examination included examination for the number of *Enterobacteriaceae* bacteria (ČSN ISO 16649-2), number of coliform bacteria (ČSN ISO 4832), *Escherichia coli* (ČSN ISO 16649-2), TVC - total viable count (ČSN EN ISO 4833), number of lactic acid bacteria (ČSN ISO 15214 (560117)), number of psychrotrophic bacteria (ČSN ISO 17410), *Pseudomonas* spp. (ČSN EN ISO 13720), *Vibrio* spp. (ČSN P ISO / TS 21872-1 (560651)), *Salmonella* spp. (ČSN EN ISO 6579), *Listeria monocytogenes* (ČSN EN ISO 11290-1), *Escherichia coli* O157 (ČSN EN ISO 16654) and coagulase-positive staphylococci (ČSN EN ISO 6888-1).

Statistical analysis was performed using Statistica version 7.1 (StatSoft, Czech Republic). Two-factor ANOVA (type of sushi, type of filling) and post hoc Fisher's LSD test were used. A P value <0.05 was considered statistically significant.

RESULTS AND DISCUSSION

European Commission Regulation No. 2073/2005 on microbiological criteria for foodstuffs sets requirements for food intended for direct consumption, in other words for RTE food. This Regulation requires the absence of *Salmonella* spp. in 25 g of sample. It also states the amount of *Listeria monocytogenes.* The amount of *Listeria monocytogenes* in a sample of RTE food placed on the market is a maximum of 100 CFU/g.

Due to the raw materials which are used for sushi production and the sushi production technology, which includes a large amount of manual work, sushi is a suitable food for contamination, survival and development not only of pathogenic microorganisms, but also of many other bacteria. This study was prepared as the first study in the Czech Republic dealing with the microbiological nature of sushi.

All 90 examined samples were negative for the presence of pathogenic bacteria. The samples were free of the microorganisms *L. monocytogenes, Salmonella* spp., *E. coli* O157 and *Vibrio* spp. and *Staphylococcus aureus* (all staphylococcal colonies tested were coagulase negative). The investigated sushi therefore complied with the requirements of European legislation.

The same results for *L. monocytogenes* and *Salmonella* spp. achieved Muscolino et al. (2014) in his study. Muscolino et al. (2014) analyzed 50 samples (38 sushi, 12 sashimi) from restaurants and take aways. Ramires et al. (2019), who studied commercially prepared sushi, also obtained negative results for the presence of *Salmonella* spp., but one sample was positive for *E. coli* O157: H7.

Enterobacteriaceae is a family comprising a large number of different bacterial genera. These are gram-negative, aerobic or facultatively anaerobic bacteria that colonize the gastrointestinal tract. This family causes a wide range of infections in humans and animals (Paterson 2012). Coliform bacteria and *E. coli* are also included in the *Enterobacteriaceae* family (Rajkowski et al. 2013). A wide range of the number of these bacteria was found in the samples (below the detection limit up to 3.91 ± 1.16 log CFU/g) (Table 1–3). The highest proportion of these bacteria was detected in Nigiri sushi. This was followed by Maki sushi, ginger and then wasabi.

When determining the total number of microorganisms, i.e all bacteria, yeasts and fungi, they were found to be highest in wasabi paste and Nigiri samples, while ginger and Maki samples

showed lower level of contamination. In the determination of lactic acid bacteria, the highest amount was detected in the samples of wasabi paste, as in the case of total viable count. This was followed by samples of Nigiri sushi with tuna and ginger. Wasabi is well known for its antimicrobial effect caused by the presence of allyl isothiocyanate. However, it is known that the effect of this substance decreases significantly in aqueous solutions, where it is degraded by nucleophilic molecules (Li et al. 2015). Wasabi paste is most often prepared from powder by resuscitation in water. The preparation of a larger amount of paste at once and its long-term storage can thus lead to a relatively high amount of bacteria in this delicacy.

In order for RTE foods, including sushi, to fall into a suitable food category from a microbiological point of view, most national recommendations state a limit of 6 or 7 log CFU/g (Hoel et al. 2015). Czech standard Rules of good hygienic and manufacturing practice – Microbiological criteria for foodstuffs (ČSN 56 9609) do not specify a limit for sushi. An example is the British Health Protection Agency (2009), which considers a value below 6 CFU/g to be satisfactory for sushi in the case of total number of microorganisms, and considers a range of 6–7 log CFU/g to be a borderline value. For lactic acid bacteria, it considers values above 8 log CFU/g to be unsatisfactory. The stated limits are only recommended, not binding for manufacturers and sellers. Although the average values in our case met the stated recommended limits (Table 1–3), the values found were very variable and the limits for total viable count were exceeded for several specific samples. Specifically, there were 2 samples of Nigiri (7.4%), 2 samples of wasabi (11.1%) and one sample of ginger (5.6%). In addition, lactic acid bacteria counts above 8 log CFU/g were determined for one wasabi sample. Overall, 6 out of 90 samples (6.7%) were unsatisfactory. If we take into account the stricter limit (6 log CFU/g for total number of microorganisms), a total of 21 samples (23.3%) would be unsatisfactory. In a study by Hoel et al. (2015), however, even 48% of non-compliant samples were found, and in the case of this Norwegian study, industrially produced sushi was marketed, where a clear effect of non-compliance with the cold chain during distribution was found. In a German study comparing the quality of samples of industrially produced sushi with sushi from restaurants, the largest average total viable counts were found for Maki vegetarian samples (7.4 log CFU/g). As in our case, the greatest microbiological load was found for sushi with tuna (6.8 log CFU/g) in sushi with animal raw material. The results of the mentioned study prove that an important source of bacteria in sushi may not be only raw materials of animal origin, but also raw materials derived from plant sources (Atanassova et al. 2008). In terms of animal raw material, this and our study also confirmed that Nigiri samples with a higher proportion of animal component show a higher level of contamination than Maki samples, which suggests that this component of sushi is the main carrier of microbial contamination.

Table 1 Microbiological profile of Maki sushi prepared from salmon, tuna and shrimp (mean ± SD in log CFU/g)

	Maki			
	Salmon (N=9)	Tuna (N=9)	Shrimp (N=9)	P - level
ENT	3.70 ± 0.57^{a}	1.23 ± 0.41^{b}	1.04 ± 0.30^{b}	< 0.001
COLIF	3.16 ± 0.96^{a}	0.67 ± 0.56^{b}	0.25 ± 0.39^{b}	< 0.001
E. coli	0.15 ± 0.29^{a}	0.07 ± 0.22^{a}	not detected	< 0.001
TVC	4.77 ± 0.44^{a}	4.24 ± 0.33^{a}	4.00 ± 0.35^{a}	< 0.001
LAB	3.96 ± 0.58^{a}	3.09 ± 0.60^{b}	3.46 ± 0.54^{ab}	< 0.001
PSY	4.61 ± 0.27^{a}	4.38 ± 0.59^{a}	4.09 ± 0.78^{a}	< 0.001
PSEUDO	2.36 ± 1.05^{a}	1.68 ± 0.75^{b}	1.00 ± 0.00^{c}	< 0.001

ENT – Enterobacteriaceae, COLIF – coliform bacteria, TVC – Total Viable Count, LAB – Lacitc acid bacteria, PSY – psychrotrophic microorganisms, PSEUDO – Pseudomonass spp., a-c – statistically significant differences between samples

Due to the ability of some types of bacteria, which are called psychrotrophic, to grow at low temperatures, including refrigerator temperatures, these bacteria were also included in the microbiological examination of sushi. The highest numbers of psychrotrophic microorganisms

were found in Nigiri sushi. The difference in the proportion of psychrotrophic microorganisms between sushi such as Nigiri, Maki and wasabi paste was not statistically significant.

Pseudomonads are among the psychrotrophic bacteria. In the case of an Italian study by Muscolino et al. (2014) found a wide range in the proportion of pseudomonads in individual samples (3.26–8.00 log CFU/g). When determining pseudomonads, in our case the values also ranged in a wide range (undetected up to 4.64 log CFU/g).

In terms of the animal raw material used, the Maki type was clearly the most microbiologically loaded with salmon samples; however, this trend was less pronounced for the Nigiri type, and overall, in the case of determining the total viable count, lactic acid bacteria and psychrotrophic bacteria, no statistically significant difference was found between the use of individual animal raw materials.

Table 2 Microbiological profile of Nigiri sushi prepared from salmon, tuna and shrimp (mean ± SD in log CFU/g)

	Nigiri			
	Salmon (N=9)	Tuna (N=9)	Shrimp (N=9)	P - level
ENT	3.77 ± 0.52^{a}	3.91 ± 1.16^{a}	2.71 ± 0.68^{b}	< 0.001
COLIF	2.80 ± 0.27^{a}	3.66 ± 1.12^{b}	1.77 ± 0.65^{c}	< 0.001
E. coli	1.17 ± 0.18^{a}	0.49 ± 0.48^{b}	0.50 ± 0.48^{b}	< 0.001
TVC	5.28 ± 1.05^{a}	5.65 ± 1.38^{a}	5.52 ± 1.20^{a}	< 0.001
LAB	4.17 ± 0.59^{a}	5.42 ± 0.70^{b}	4.67 ± 0.92^{a}	< 0.001
PSY	5.06 ± 0.72^{a}	4.63 ± 0.83^{a}	4.80 ± 1.04^{a}	< 0.001
PSEUDO	4.18 ± 0.39^{a}	3.69 ± 0.39^{a}	2.16 ± 0.83^{b}	< 0.001

ENT – Enterobacteriaceae, COLIF – coliform bacteria, TVC – Total Viable Count, LAB – Lacitc acid bacteria, PSY – psychrotrophic microorganisms, PSEUDO – Pseudomonass spp. a-c – statistically significant differences between samples

Table 3 Microbiological profile of Maki, Nigiri pickled ginger and wasabi paste (mean ± SD in log CFU/g)

	Maki	Nigiri	Ginger (N=18)	Wasabi (N=18)	P - level
ENT	1.99 ± 1.30^{b}	3.46 ± 0.93^{a}	0.28 ± 0.36^{c}	0.26 ± 0.33^{c}	< 0.001
COLIF	1.35 ± 1.44^{b}	2.75 ± 1.06^{a}	0.11 ± 0.25^{c}	0.15 ± 0.28^{c}	< 0.001
E. coli	0.10 ± 0.26^{b}	0.74 ± 0.49^{a}	not detected	not detected	< 0.001
TVC	4.33 ± 0.48^{b}	5.47 ± 1.13^{a}	4.74 ± 1.26^{b}	5.53 ± 1.66^{a}	< 0.001
LAB	3.51 ± 0.64^{d}	4.75 ± 0.86^{c}	5.00 ± 0.92^{b}	6.68 ± 1.13^{a}	< 0.001
PSY	4.36 ± 0.58^{a}	4.84 ± 0.81^{a}	3.10 ± 1.46^{b}	4.43 ± 2.07^{a}	< 0.001
PSEUDO	1.67 ± 0.88^{a}	3.33 ± 1.06^{a}	not detected	not detected	< 0.001

ENT - Enterobacteriaceae, COLIF - coliform bacteria, TVC - Total Viable Count, LAB - Lacitc acid bacteria, PSY - psychrotrophic microorganisms, PSEUDO - Pseudomonass spp., a-d - statistically significant differences between samples

CONCLUSION

Due to the growing popularity of sushi consumption throughout Europe and the fact that sushi has become a trendy food, public health authorities have a difficult task in ensuring the safety of this food. It is necessary to take care of increased hygienic caution and vigilance in the production and distribution of not only sushi, but all foods intended for direct consumption. As part of the results of microbiological analysis of 90 samples of sushi, wasabi paste and pickled ginger from restaurant facilities, the presence of pathogenic bacteria was not detected in the samples. The average total number of microorganisms values of the samples complied with the recommended limits (<6 CFU/g and <7 CFU/g, respectively). The recommended limit of 7 CFU/g was exceeded in the case of only 5 specific samples. In the case of a stricter limit of 6 CFU/g, there were 21 non – compliant samples.

The variability of the average values of the results can be caused and largely influenced by the hygiene of production, training and experience of people preparing sushi. The differences between the animal component used were not clearly conclusive, but the results of the study confirmed a higher contamination of Nigiri compared to Maki, which may be due to the higher proportion of animal raw material in Nigiri sushi. A surprising finding was the high level of wasabi paste contamination.

ACKNOWLEDGEMENT
This work was created within the implementation of the project QK1810212 Rapid, complex and multiplex methods for simultaneous detection of food-borne pathogens in food of animal and plant origin.

REFERENCES

Atanassova, V. et al. 2008. Microbiological Quality of Sushi from Sushi Bars and Retailers. Journal of Food Protection, 71(4): 860–864.

Barralet, J. et al. 2004. Outbreak of Salmonella Singapore associated with eating sushi. Communicable Diseases Intelligence, 28(4): 527–528.

Health Protection Agency. 2009. Guidelines for Assessing the Microbiological Safety of Ready-to-Eat Foods. Health Protection Agency [online], 1(1): 1–33. Avaible at: https://assets.publishing.service.gov.uk/government/uploads/system/uploads/attachment_data/file/363146/Guidelines_for_assessing_the_microbiological_safety_of_ready-to-eat_foods_on_the_market.pdf [2020-08-10]

Hoel, S. et al. 2015. Assessment of microbiological quality of retail fresh sushi from selected sources in Norway. Journal of Food Protection, 78(5): 977–982.

Hoel, S. et al. 2019. The significance of mesophilic Aeromonas spp. In minimally processed ready-to-eat seafood. Microorganisms, 7(3): 91.

Jain, S. et al. 2004. An outbreak of enterotoxigenic Escherichia coli associated with sushi restaurants in Nevada, 2004. Clinical Infectious Diseases, 47(1): 1–7.

Li, Y. et al. 2015. Enhancement of aqueous stability of allyl isothiocyanate using nanoemulsions prepared by an emulsion inversion point method. Journal of Colloid and Interface Science, 438(1): 130–137.

Muscolino, D. et al. 2014. Hygienic-sanitary evaluation of sushi and sashimi sold in Messina and Catania, Italy. Italian Journal of Food Safety, 3(2): 1701.

Neyts, K. et al. 2000. Incidence and identification of mesophilic Aeromonas spp. from retail foods. Letters in Applied Microbiology, 31(5): 359–363.

Paterson, D. 2011. Infections due to other members of the enterobacteriaceae, including management of multidrug-resistant strains. 24th ed., Philadelphia, PA: Elsevier Saunders.

Rajkowski, K. T. et al. 2013. Catfish Special Edition: Microbial Quality of Catfish Nuggets. Journal of Food Processing and Technology, S11: 007.

Ramires, T. et al. 2019. First report of Escherichia coli O157:H7 in ready-to-eat sushi. Journal of Applied Microbiology, 128: 301–309.

Tirloni, E. et al. 2017. What happens to the microflora of retail sushi in the warm season? Journal of Food and Nutrition Research, 5(2): 95–100.

Effects of flavouring methods on the colour of olive oil

Tereza Kacalova, Alzbeta Jarosova, Tereza Brettfeldova
Department of Food Technology
Mendel University in Brno
Zemedelska 1, 613 00 Brno
CZECH REPUBLIC

xkacalo1@mendelu.cz

Abstract: Olive oil flavouring is a traditional practice in the Mediterranean gastronomy. The aim of this work is to compare the effects of various flavouring techniques on the oil colour. Rosemary was used in three flavouring methods: infusion by fresh herbs, infusion by dried herbs and the addition of essential oils into olive oil. Samples were stored for three months and colour was analysed. In particular, sensorial tests by trained panels were conducted. Colour was measured by a colorimeter using the CIELab colour space system. The obtained results evidenced that infusion by fresh rosemary had the biggest effect on the colour. Colour sensorial tests showed that flavouring by fresh herbs significantly changed colour and increased turbidity of the oil. Panellists perceived colour change from yellow to yellow-green colour and noticed a higher level of turbidity in this flavouring method. Sensorial tests also analysed the acceptance of turbidity; flavouring by essential oil had the highest score in this attribute noting that less turbid flavoured results were more acceptable. The change of colour was characterised by CIELab Colour Space and the change of colour was expressed by ΔE* value. The highest value was measured in fresh herb flavoured oils which correlates with sensorial analysis.

Key Words: flavoured oil, olive oil, sensorial analyse, CIEL*a*b* colour determination, rosemary

INTRODUCTION

Olive oil is a key ingredient in the Mediterranean diet. It is appreciated not only for its sensorial properties, taste and aroma, but also for its nutritional characteristics and health benefits. Olive oil has high oleic acid content and its monosaturated fatty acid composition with its content of phenolic compounds (chlorophyll, carotenoids) have protective effects against cancer, coronary heart disease and inhibit oxidative stress. Phephenolic compounds have potent antioxidant properties (Owen et al. 2000).

The olive is the fruit of the olive tree (*Olea europaea* L.) and its cultivation dates back to biblical times. The olive oil from Lebanese orchards (Figure 1) which was used for experimental trial has even older history dating back to the days the Phoenicians ruled these lands and spread the olive tree across the Mediterranean Sea through both trade and conquest.

Aromatization of olive oil is also well known in the Mediterranean gastronomy where the most common aromatic plants and spices used for the infusion are rosemary, oregano, basil, lemon, garlic, thyme, or chilli. The essential oils produced from these plants give unique flavour, antioxidant and antimicrobial properties (Gutierrez et al. 2008). The ancient tradition of macerating aromatic herbs in the oil is gaining popularity in recent years, where the aroma type and concentration which change the sensory characteristics, have a direct impact on the shelf life and nutritional value of the oil. Several methods of flavouring olive oil are known: infusion of spices, ultrasound maceration and malaxation of olives with spices (Akçar and Gümüşkesen 2011). In the present experiment rosemary was used as the primary herb; The aim of this experimental trial was to compare and evaluate the impact of the three flavouring methods (fresh, dried herb infusion and essential oil addition) on colour after 3 months of storing.

MATERIAL AND METHODS

Samples

A total of 24 oil samples were prepared; Extra virgin olive oil was obtained from the harvest of 2018/2019 (Lebanese Genco Olive Oil, Baassir, Lebanon), variety Ayrouni from North Lebanon and six samples of each flavouring method (by fresh herb, dried herb and essential oil) and unflavoured oil as control were completed (see Table 1).

Figure 1 Lebanese olive orchards

Table 1 Overview of unflavoured and rosemary-flavoured samples preparation

Flavour	Unflavoured	Rosemary		
		Fresh	Dried	Essential Oil
Code	N	RCE	RSU	RSI
Number	6	6	6	6

Herbs and aromatic plants are a natural source of microbial contamination; one of the most dangerous microorganisms occurring in infused oil is Clostridium botulinum. While keeping in mind that olive oil provides anaerobic low-acid condition necessary for C. botulinum growth and the production of its toxin it is important to note that visual and organoleptic clues do not provide adequate results about their potential growth (Nummer et al. 2011). A preservation acidification treatment for flavoured oil was conducted to monitor this journey.

Rosemary (*Salvia rosmarinus*) purchased from the gardening store (Gardening store U Masku, Brno) was washed and woody stems were removed. Next, Rosemary was acidified in 3% citric acid solution (1:10 ratio by weight) for 24 h. The content was poured into a colander to remove the acidified rosemary from the acidulate. Subsequently, 250 ml of distilled water was poured over to rinse off residual citric acid solution (Abo et al. 2014).

In the next step, part of the acidified matter was dried at 35–40 °C for 8 hours (constant weight) in an air flow drier. As a result, the dry matter of the rosemary consisted of 31.10% of the mix. This is where rosemary oil was prepared by adding 3.54 ± 0.04 g of fresh acidified rosemary (equivalent to 3g of herb before acidification, 2%), 0.87 ± 0.01 g dried rosemary, and 75 µl of essential oil (Zanaromi) in 150 ml olive oil. The samples were stored in 150 ml transparent glass bottles in a dark cool area at 20 ± 1 °C.

Sensorial analyses

The oil was submitted to a panel test that was composed of 6 trained students (Sensorial Analysis of Olive Oil Standard, IOC). The evaluation of the samples was carried out under a methodology described in the Commission Regulation (EEC) No 2568/91. Profile sheets were also modified to include attributes related to flavoured oil (Varva et al. 2016).

Colour parameters

Food appearance is the first sensation perceived by customers and a tool of acceptance or rejection of a food product. Colour has an important influence on food quality perception and can be corelated with quality attributes or defects. Colour was measured at colorimeter using CIELab colour space (Pankaj et al. 2013).

Colour of oils expressed as L* (lightness), b* (yellowness) and a* (redness) were measured (Escolar et al. 2002). The oil was detected in a plastic cuvette and recorded in units of L* (L* = 0 = black, L* = 100 = white), a* (+a* = red, -a* = green) and b* (+b* = yellow, -b* = blue). The measurements were repeated in triplicates and for to continue the comparison, the parameter of ΔE* was calculated using the following equation: $\Delta E* = \sqrt{(\Delta L*)^2 + (\Delta a*)^2 + (\Delta b*)^2}$. The obtained value reflects the colour difference, which is very important to evaluate the relationship between instrumental and visual analyses. Values ΔE* 3 or greater indicate colour differences perceptible to the human eye (Gordillo et al. 2011).

Statistical analyses

Each type of flavoured and unflavoured oil was replicated six times. The obtained data were subjected to one-way ANOVA and the Turkey test was used. A result was considered as statistically significant for p–value less than 0.05. Mean comparison, median and standard deviation were calculated using analysis software system (StatSoft, Inc., 2013, STATISTICA (data), version 12., statsoft.com.).

RESULTS AND DISCUSSION

Sensorial analyses

The panel judgment on flavoured oils shed light on the change of colour, turbidity and its acceptability; The results showed that the colour significantly changed from yellow to a yellow green colour in the RCE samples. In addition, the RCE flavouring method significantly increased turbidity of the oil comparing to RSI samples. In general, the RSI samples were by far the most acceptable. It was easy to note that there was a reverse correlation between the acceptance of the oil and the increase of turbidity as this trend was observed through experiments (Popov-Raljic et al. 2007). Medians of each main appearance attributes are mentioned below (Table 2).

Table 2 Overview of sensorial analyses results of unflavoured and rosemary-flavoured olive oil samples

Attribute	Unflavoured	Rosemary		
		Fresh	Dry	Essential Oil
Code	N	RCE	RSU	RSI
Turbidity acceptance	9.8	9.1	9.7	9.9
Turbidity	0.6	3.5	1.0	0.6
Colour	1.4	4.9	1.4	1.4

The sensory profiles of N and RSI oil largely overlapped. The main difference in sensorial attributes was observed in RCE samples as displayed in Figure 2.

CIELab Colour Differences

The instrumental part of the experiment was conducted by colorimeter using CEILab colour space and the colour characteristics of analysed flavoured oil samples are summarized in Table 3.

Figure 2 Visualisation of sensorial differences between unflavoured and rosemary-flavoured olive oil samples

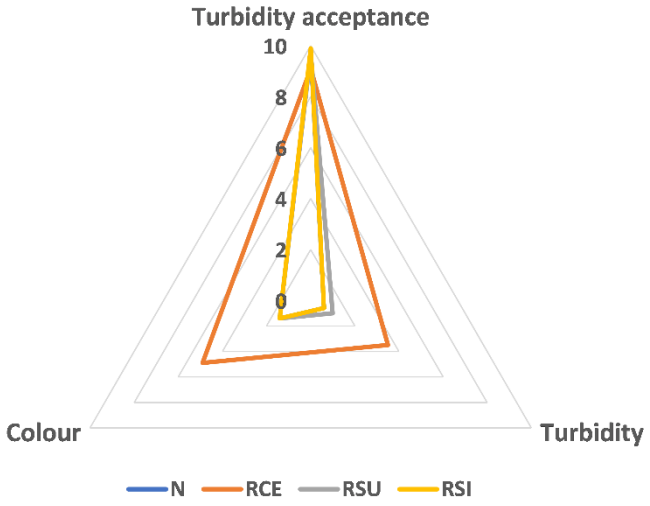

Legend: N – Unflavoured oil, RCE –Rosemary - fresh, RSU –Rosemary - dried, RSI – Rosemary – essential oil

Table 3 Overview of unflavoured and rosemary-flavoured olive oil colour characterisation described by ΔL, Δa*, Δb* and ΔE**

Flavour	Unflavoured	Rosemary		
		Fresh	Dry	Essential Oil
Code	N	RCE	RSU	RSI
Δ L*	0.000	-5.339	-0.295	-0.086
Δ a*	0.000	0.862	0.476	0.049
Δ b*	0.000	4.137	1.557	0.301
Δ E*	0.000	6.809	1.654	0.317

*Figure 3 Colour differences between rosemary-flavoured olive oil samples compared to unflavoured olive oil described as ΔE*value*

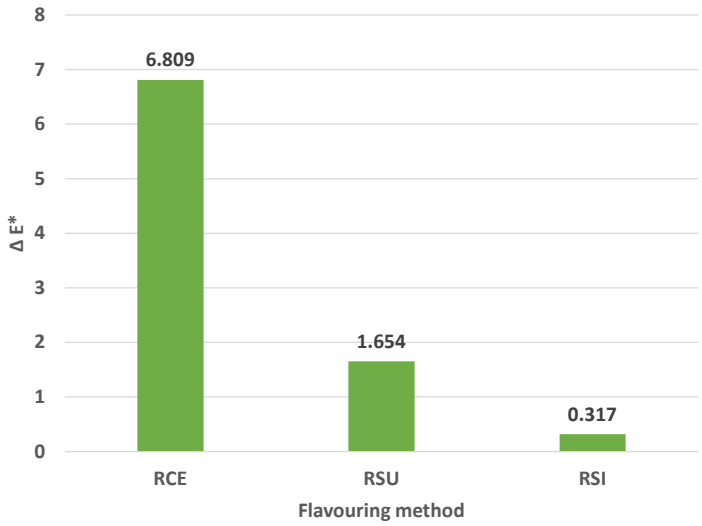

Legend: RCE –Rosemary - fresh, RSU – Rosemary - dried, RSI – Rosemary – essential oil

According to the results obtained by the instrumental measurement we can conclude that there was a significant difference in the L* value (lightness). A relationship between the L* and turbidity was clearly observed in the RCE samples. A Decrease of L* value entailed an increase in the turbidity (Gordillo et al. 2011); It was clear to see that while the amount of the reflected light increased, the light

transmitted through the sample decreases. The Value ΔL* obtained from the sample RCE was -5.339 which show the oil was darker compared to unflavoured oil.

The Value of Δb* (yellowness) was 4.137 where the colour change was significantly higher from other samples, however, this was not reflected in the sensorial test. It was then noticed that the effect of the turbidity (L*) had a greater effect on final colour perception.
The highest colour difference was observed in the RCE sample; The value of ΔE* was 6.809 and the colour change was perceptible to the human eye as the sensorial test confirms. A schematic representation of ΔE* values of flavoured oils are shown in Figure 3.

CONCLUSION

This study reports the obtained data of interaction between olive oil flavouring methods and its colour. It focuses on the sensorial (visual) and instrumental measurement of colour attributes of flavoured oil. The overall findings showed that flavouring method significantly influences the colour and the greatest effect on colour from all three methods used had fresh rosemary flavouring. In particular, colour changed from yellow to yellow-green and the oil was more turbid. On the other hand, turbidity was negatively correlated to acceptance; the most acceptable oil was the one flavoured by essential oil as the oil was not significantly different from unflavoured oil in terms of turbidity. The colour difference (ΔE*) calculated between the flavoured oil samples revealed the difference in colour visually perceived by human eye.

Keeping in mind that the results obtained show that the rosemary flavouring by essential oils were the most acceptable and at the same time observing the fact that colour is one of the most important factors influencing customers' perception to food products, further experimentation and testing is required to confirm which method is best one to be used. In order to get both the best results in term of food safety and value, and at the same time maintain an overall high rate of consumer acceptance.

ACKNOWLEDGEMENTS

The research was supported by Mendel University in Brno. I am grateful to Lebanese Genco Olive Oil for having provided the extra virgin olive oil for the experiment.

REFERENCES

Abo, B. et al. 2014. Acidification of Garlic and Herbs for Consumer Preparation of Infused Oils. Food Protection Trends [Online], 34(4): 247–257. Available at: https://www.foodprotection.org/files/food-protection-trends/Jul-Aug-14-Abo.pdf. [2020-08-11].

Akçar, H.H., Gumuskesen, A.S. 2011. Sensory evaluation of flavoured extra virgin olive oil. GIDA – The Journal of Food [Online], 36: 249–254. Available at: https://www.researchgate.net/publication/285777397_Sensory_evaluation_of_flavoured_extra_virgin_olive_oil. [2020-08-11].

Escolar, D. et al. 2002. An efficient method for a numerical description of virgin olive oil color with only two absorbance measurements. Journal of the American Oil Chemists´Society [Online], 8: 769–774. Available at: https://aocs.onlinelibrary.wiley.com/doi/epdf/10.1007/s11746-002-0557-8. [2020-09-09].

EU Commission Regulation (EEC). 1991. No 2568/91, Characteristics of olive oil and olive-residue oil and on the relevant methods of analysis. In: OJ. L248, 5.9.1991, p. 1. Also available at: https://eur-lex.europa.eu/legal-content/en/ALL/?uri=CELEX%3A31991R2568. [2020-09-09].

Gordillo, B. et al. 2011. Influence of Turbidity Grade on Color and Appearance of Virgin Olive Oil. Journal of the American Oil Chemists' Society [Online], 88(9): 1317–1327. Available at: https://doi.org/10.1007/s11746-011-1787-y. [2020-09-17].

Gutierrez, J. et al. 2008. The antimicrobial efficacy of plant essential oil combinations and interactions with food ingredients: the possible role of antioxidants. International Journal of Food Microbiology [Online], 124(1): 91–97. Available at: https://linkinghub.elsevier.com/retrieve/pii/S0168160508001177. [2020-08-12].

International Olive Council. 2018. Sensory Analysis of Olive Oil Standard: Guide for the selection, training and quality control of virgin olive oil tasters-qualifications of tasters, panel leaders and trainers. COI/T.20/DOC. NO 14/REV. 5. 5. Madrid – Spain: IOC.

Nummer, B.A. et al. 2011. Current Food Safety Issues of Home-prepared Vegetables and Herbs Stored in Oil. Food Protection Trends [Online], 31(6): 336–342. Available at: https://www.foodprotection.org/files/food-protection-trends/Jun-11-Nummer.pdf. [2020-08-11].

Owen, R.W. et al. 2000. Olive-oil consumption and health: The Possible Role of Antioxidants. The Lancet Oncology [Online], 1(2): 107–112. Available at: https://linkinghub.elsevier.com/retrieve/pii/S1470204500000152. [2020-08-12].

Pankaj, B.P. et al. 2013. Colour Measurement and Analysis in Fresh and Processed Foods: A Review. Food and Bioprocess Technology [Online], 6(1): 36–60. Available at: http://link.springer.com/10.1007/s11947-012-0867-9. [2020-08-11].

Popov-Raljic, J. et al. 2007. Colour and sensory properties of the mixed edible vegetable oils. Romanian Biotechnological Letters [Online], 12(2): 3189–3194. Available at: https://e-repository.org/rbl/vol.12/iss.2/9.pdf. [2020-09-17].

Varva, G. et al. 2016. Effect of infusion of spices into the oil vs. combined malaxation of olive paste and spices on quality of naturally flavoured virgin olive oils. Food Chemistry [Online], 202(7): 221–228. Available at: https://linkinghub.elsevier.com/retrieve/pii/S0308814616301510. [2020-08-11].

The effect of the cocoa solids content on the rheological behaviour of chocolate

Veronika Kourilova[1], Renata Dufkova[1], Ludek Hrivna[1], Vojtech Kumbar[2]
[1]Department of Food Technology
[2]Department of Technology and Automobile Transport
Mendel University in Brno
Zemedelska 1, 613 00 Brno
CZECH REPUBLIC

veronika.kourilova@mendelu.cz

Abstract: The rheological properties of chocolate were determined on three chocolate samples from the same commercial manufacturer, with a minimum cocoa solids content of 50%, 78% and 99%. The change in the shear stress at an increasing shear strain rate was determined from 0.01/s to 100/s at a sample temperature of 40 °C. The flow properties were measured using an RST rheometer (Brookfield, USA) with a cone-plate spindle arrangement (RCT-50-2) including a sample temperature duplicator. The measured values were modelled using suitable mathematical models, namely the Casson, Bingham, and Herschel-Bulkley flow models. The Casson and Herschel-Bulkley flow models seemed to be the most suitable, as evidenced by the value of the coefficient of determination R^2, which ranged from 0.9934–0.9994.

Key Words: chocolate, cocoa solids, Casson model, Herschel-Bulkley model, shear stress, shear strain rate

INTRODUCTION

To evaluate chocolate, it is important to know which raw materials with which quality were used in the production. It is also important to know their amount in relation to the total weight of the product. The chemical composition and physical properties related to the sensory analysis also depend on the share of the raw materials (Dostálová et al. 2014). For each type of chocolate, there is a certain minimum amount that the manufacturer must follow in order to be able to call it chocolate. All the limits applicable to the dry matter are set by Decree 76/2003 Coll. and are also mentioned in Directive 2000/36/EC. Dark chocolate means a product containing at least 18% by weight of cocoa butter, 14% fat-free cocoa solids and the total cocoa solids content should be at least 35%.

Chocolate has a wide range of physicochemical properties. These are organoleptic, physical and rheological properties. The rheological properties of chocolate (plastic viscosity and yield strength) are mainly influenced by the content of the formulation ingredients (cocoa butter, cocoa, emulsifiers and sugar) and chocolate production technology (particle size distribution, temperature, constriction time, temperance, thixotropy and vibration) (Fernandes et al. 2013, Afoakwa et al. 2009, Becket 2008). Chocolate in a liquid state is a complex polydisperse system, which is formed from sugar, cocoa or milk components in a continuous fat phase (Čopíková 1999, Becket 1999). The relationships between all the components in the polydisperse system have a significant effect on the microstructure of the resulting chocolate mass, which is reflected in the rheological and textural properties of the product (Glicerina et al. 2016). Due to its solids content and viscosity, chocolate does not behave like a real liquid, but behaves like a typical non-Newtonian (plastic) liquid. Chocolate has an obvious flow limit, which means that a given voltage must be applied to it to start its flow. The rheological relationships concerning the behaviour of chocolate were described by Casson, so we can find, in the literature, the notion that chocolate is a Casson's (plastic) liquid (Čopíková 1999, Becket 1999). The higher the shear strain rate, the lower the viscosity – the chocolate becomes more fluid. This behaviour is attributed to the disintegration of the internal structure or the disintegration of the polydisperse chocolate system (Juszczak et al. 2004).

The selection of a suitable mathematical flow model is very important for the analysis of the rheological behaviour of chocolate. The flow model in the basic shear diagram describes

the rheological data, such as the shear strain rate versus the shear stress. Furthermore, it is important to determine how the sizes of the model parameters are affected by the state variables (temperature, structure, composition) and to establish widely applicable relationships, which can be called functional models (Kumbár et al. 2018).

MATERIAL AND METHODS

Three chocolate samples were used in the practical measurements. These were chocolates of the same commercial manufacturer (LINDT & SPRÜNGLI GMBH Germany) with a cocoa content of at least 50%, 78% and 99%, their characteristics are given in Table 1. Chocolate samples were stored for 10 days at 6 °C and 70% relative humidity. All chocolate samples had 9 months to minimum shelf life. For all the samples, the change in the shear stress was measured as a function of the change in the shear strain rate at 40 °C.

Table 1 The characteristics of the used chocolates (data provided by the manufacturer LINDT & SPRÜNGLI GMBH Germany 2020)

Chocolate with a minimum cocoa solids content of	Ingredients	Nutritional information per 100 g				
		Energy value	Fats Of which are saturated fatty acids	Carbohydrates Of which are sugars	Protein	Salt
50%	cocoa mass, sugar, concentrated butter, cocoa butter and vanilla	2302 kJ 533 kcal	36 g 22 g	48 g 45 g	5.6 g	0.04 g
78%	cocoa mass, cocoa butter, sugar, low-fat cocoa powder, anhydrous milk fat	2384 kJ 576 kcal	46 g 29 g	24 g 17 g	10 g	0.05 g
99%	cocoa mass, low-fat cocoa powder, cocoa butter, sugar	2433 kJ 590 kcal	51 g 31 g	8 g 1 g	15 g	0.01 g

The flow properties were measured using an RST rheometer (Brookfield, USA) with a cone-plate spindle arrangement (RCT-50-2) including a sample temperature duplicator. To evaluate the experimental data, the specialised software Rheo 3000 (Brookfield, USA) was used, which allows one to programme the measuring cycles, to obtain and process the data, including the insertion of suitable mathematical models and the statistical evaluation. The obtained flow curves were modelled using three mathematical flow models, which can be used to obtain the flow limit values, namely: Herschel-Bulkley, Bingham and Casson flow models.

The chocolate samples were first dissolved at 36 °C on a heated RTS rheometer plate, then the plate was pressed against the rotating cone and the whole mechanism was tightened thoroughly. The temperature was then raised to 40 °C at which the measurement took place. Each measurement lasted 1 minute; the speed of the rotating cone increased from 0.01/s to 100/s.

RESULTS AND DISCUSSION

Table 2 shows the obtained values of the flow limit, viscosity (for the Bingham and Casson models), consistency and flow indices (for the Herschel-Bulkley model) and the coefficients of determination of the three used flow models.

For the Herschel-Bulkley model:

$$\tau = \tau_0 + K\dot{\gamma}^n,$$

where τ is the shear stress, τ_0 is the value of the stress at the flow limit, K is the consistency index, $\dot{\gamma}$ is the shear strain rate and n is the flow index. If $\tau < \tau_0$, the Herschel-Bulkley fluid behaves as a solid, otherwise it behaves as a liquid. If $n < 1$, it is a thinning fluid with an increasing shear rate (Kumbár

et al. 2018). Fluid thinning is a typical behaviour for non-Newtonian fluids whose viscosity decreases with the rate of the shear deformation (Bair and McCabe 2007). If $n > 1$, then the fluid solidifies with an increasing shear rate. The viscosity increases with an increasing shear strain rate, which is a typical example of non-Newtonian dilatant fluids (Painter and Coleman 1997). If $n = 1$ and $\tau_0 = 0$, it is a Newtonian fluid (Kumbár et al. 2018).

The equation for the Bingham model is given in the form:

$$\tau = \tau_0 + \eta_B \dot{\gamma},$$

where η_B is the Bingham plastic viscosity. If $\tau < \tau_0$, then the fluid is grouped into a structure that has a certain stiffness and resists deformation movements. The substance, therefore, flows like a solid body. As soon as the τ in the Bingham fluid exceeds the critical value τ_0, the fluid begins to flow fully and its behaviour in this region exhibits linear Newtonian properties (Rao 2014).

Casson's model is used in the form:

$$\sqrt{\tau} = \sqrt{\tau_0} + \sqrt{\eta_c \dot{\gamma}},$$

where η_c is the Casson viscosity value. Casson's model is based on the structure and is used to characterise the number of food dispersions (Rao 2014). The International Office of Cocoa and Chocolate has adopted Casson's model as the official method for interpreting the flow properties of chocolate (Servais et al. 2007).

Table 2 The regression coefficients of the flow models

Chocolate with a minimum cocoa solids content of	Herschel-Bulkley model				Bingham model			Casson model		
	τ_0	K	n	R^2	τ_0	η_B	R^2	τ_0	η_c	R^2
%	Pa	Pa/s^n	-	-	Pa	Pa/s	-	Pa	Pa/s	-
50	14.0713	3.5031	0.8318	0.9944	15.1589	1.7251	0.9727	10.1931	0.9841	0.9951
78	5.9529	1.1392	0.9298	0.9993	4.9011	0.8715	0.9821	3.6089	0.5168	0.9934
99	11.5055	6.2585	0.9087	0.9994	14.6267	4.2273	0.9967	6.4432	3.1586	0.9988

The higher cocoa butter content of the product results in a decrease in the flow and viscosity limits (Servais et al. 2007). The higher values of the flow limit indicate a coarser microstructure (Glicerina et al. 2016), which, in our case, could have caused a higher sugar content in the chocolate samples (see Table 1).

The Herschel-Bulkley and Casson flow models were used for the graphical processing, which proved to be the most suitable, as evidenced by the values of the coefficients of determination R^2 (Table 2).

Figure 1 The flow curves (according to the Herschel-Bulkley model) at 40 °C for the three types of chocolate

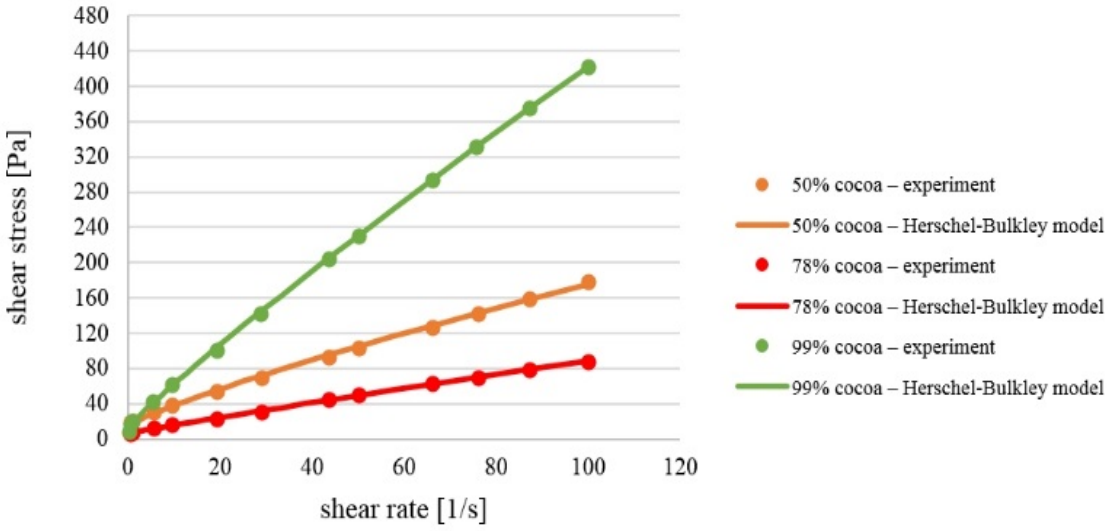

Figure 2 The flow curves (according to Casson's model) at 40 °C for the three types of chocolate

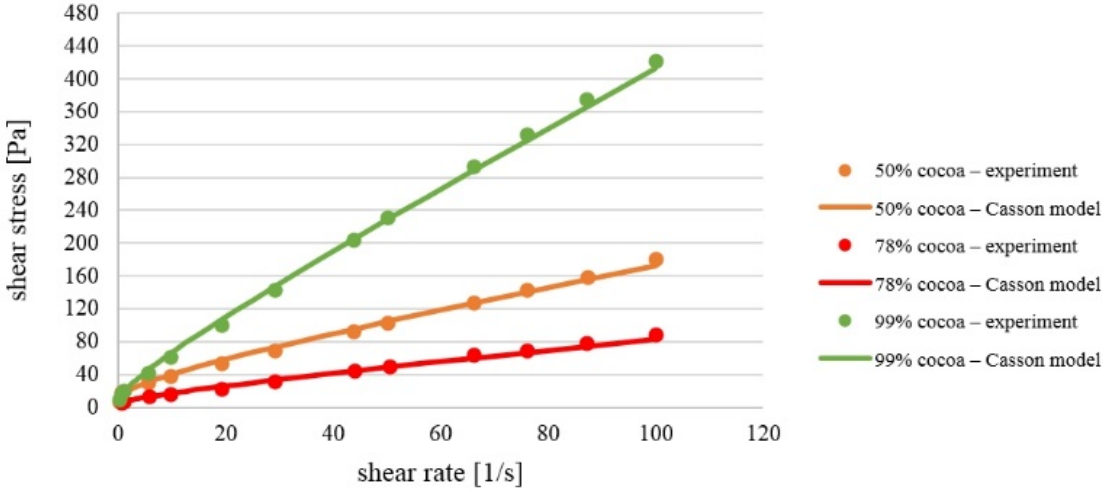

The highest value in the shear stress at a shear strain rate of 100/s at 40 °C was measured for the chocolate with a minimum cocoa content of 99%, namely 422.97 Pa. On the contrary, the lowest value was shown by chocolate with a minimum cocoa content of 78%, namely 88.13 Pa.

The measured experimental values were interpolated by the Herschel-Bulkley flow model (see Figure 1). The value of the coefficient of determination R^2 for this model ranged from 0.9944 to 0.9994. In Figure 2, the values are interpolated by the Casson model. The value of the coefficient of determination R^2 in this model ranged from 0.9934 to 0.9988. The high values of the coefficients of determination indicate the suitability of using both flow models (see Table 2).

Table 3 compares the shear stresses of all three chocolate samples at the selected shear strain rates of 1, 50 and 100/s and a temperature of 40 °C.

Table 3 The comparison of the shear stress values at the selected shear strain rate

Cocoa content	Shear rate	Shear stress	Shear rate	Shear stress	Shear rate	Shear stress
%	1/s	Pa	1/s	Pa	1/s	Pa
50	1	20.45	50	103.69	100	179.91
78	1	7.25	50	49.36	100	88.13
99	1	19.89	50	230.97	100	422.97

Due to the shear deformation rate, the shear stress of the individual chocolate samples also changed. The higher the shear strain rate, the higher the shear stress.

The lowest shear stress at a shear strain rate of 1/s was measured for the chocolate with a min. content of 78%, namely 7.25 Pa. On the contrary, the highest value of the shear stress was shown by the chocolate with a min. cocoa content of 50%, namely 20.45 Pa, which is 182% higher. At a shear strain rate of 50/s, the chocolate with the min. cocoa content of 78% had the lowest value of shear stress (49.36 Pa), while the highest value of shear stress was obtained in the chocolate sample with the min. cocoa content of 99% (230.97 Pa), whose shear stress is higher by 368%. The chocolate with the min. cocoa content of 78% again had the lowest value of the shear stress at a shear strain rate of 100/s (88.13 Pa). On the other hand, the highest shear stress of 422.97 Pa was measured for the chocolate sample with the min. cocoa content of 99%. This shear stress value was 380% higher.

At all three selected shear deformation rates, the lowest values in the shear stress were shown by the chocolate with a min. cocoa content of 78%. This phenomenon was apparently due to the composition of the chocolate, which, unlike the other chocolates, contained anhydrous milk fat. The addition of the milk powder affects the rheological properties of the chocolate, especially the low values of the shear stress (Lucisano et al. 2006).

CONCLUSION

The flow properties of chocolate are very important for many steps of its technological production and processing, for example, for transportation by pipeline, filling into moulds, storage, mixing, etc. The shear stress was measured dependent on the shear strain rate at 40 °C for dark chocolates with a min. cocoa content of 50%, 78% and 99%. The samples of these chocolates were selected due to the high and different cocoa contents, which are popular with consumers today. It was always an almost linear increase in the shear stress. The higher the shear strain rate was applied to the samples, the higher the shear stress.

The value of the coefficient of determination R^2 was equal to or higher than 0.9934 in both flow models (Casson and Herschel-Bulkley), by which the experimentally measured values were interpolated, which indicates the suitability of using these flow models.

The results can be used both to study this issue and to solve technological problems and improve the production process or storage conditions.

ACKNOWLEDGEMENTS

The research was financially supported by the Internal Grant Agency of the Faculty of AgriSciences no. AF-IGA2020-TP006 “Modelling of rheological properties of liquid and semi-liquid food raw materials and foods showing non-Newtonian behaviour”.

REFERENCES

Afoakwa, E.O. et al. 2009. Comparison of rheological models for determining dark chocolate viscosity. International Journal of Food Science and Technology [Online], 44(1): 162–167. Available at: https://ifst.onlinelibrary.wiley.com/doi/full/10.1111/j.1365-2621.2008.01710.x. [2020-08-16].

Bair, S.S., McCabe, C. 2007. High-pressure rheology for quantitative elastohydrodynamics. 2nd ed., Boston: Elsevier.

Becket, S.T. 1999. Industrial Chocolate Manufacture And Use. 3rd ed., Oxford: Blackwell Science.

Becket, S.T. 2008. The Science of Chocolate. 2nd ed., Cambridge: The Royal Society of Chemistry.

Česká Republika. 2003. Vyhláška č. 76/2003 Sb., kterou se stanoví požadavky pro přírodní sladidla, med, cukrovinky, kakaový prášek a směsí kakaa s cukrem, čokoládu a čokoládové bonbony. In: Sbírka zákonů České republiky. 32: 2470–2487. Available at: https://www.zakonyprolidi.cz/cs/2003-76. [2020-08-26].

Čopíková, J. 1999. Technologie čokolády a cukrovinek. 1st ed., Praha: VŠCHT.

Dostálová, J. et al. 2014. Potravinářské zbožíznalství: technologie potravin. 1st ed., Ostrava: Keypublishing.

Fernandes, V. et al. 2013. Thermal, structural and rheological characteristics of dark chocolate with different compositions. Journal of Food Engineering [Online], 116(1): 97–108. Available at: https://www.sciencedirect.com/science/article/pii/S0260877412005869. [2020-08-11].

Glicerina, V. et al. 2016. Microstructural and rheological characteristics of dark, milk and white chocolate. Journal of Food Engineering [Online], 169(1): 165–171. Available at: https://www.sciencedirect.com/science/article/pii/S0260877415003647. [2020-08-09].

Juszczak, L. et al. 2004. Rheological properties of commercial mustards. Journal of Food Engineering [Online], 63(1): 209–271. Available at: https://www.sciencedirect.com/science/article/pii/S0260877403003029. [2020-08-20].

Kumbár, V. et al. 2018. Rheological behaviour of chocolate at different temperatures. Potravinárstvo [Online], 12(1): 123–128. Available at: https://potravinarstvo.com/journal1/index.php/potravinarstvo/article/view/876. [2020-08-10].

Lucisano, M. et al. 2006. Influence of formulation and processing variables on ball mill refining of milk chocolate. European Food Research Technology [Online], 223(1): 797–802. Available at: https://link.springer.com/article/10.1007/s00217-006-0272-6. [2020-08-07].

Painter, P.C., Coleman, M.M. 1997. Fundamentals of polymer science: an introductory text. 2nd ed., Lancaster: Technomic Pub.

Rao, M.A. 2014. Flow and Functional Models for Rheological Properties of Fluid Foods. In Rheology of Fluid, Semisolid, and Solid Foods. Boston, USA: Springer, pp. 27–61.

Servais, C. et al. 2007. Determination of chocolate viscosity. Journal of Texture Studies [Online], 34(5–6): 467–497. Available at: https://onlinelibrary.wiley.com/doi/pdf/10.1111/j.1745-4603.2003.tb01077.x. [2020-08-17].

Effect of milk chocolate production technology and storage conditions on its stability

Veronika Kourilova, Renata Dufkova, Ludek Hrivna, Sarka Nedomova
Department of Food Technology
Mendel University in Brno
Zemedelska 1, 613 00 Brno
CZECH REPUBLIC

veronika.kourilova@mendelu.cz

Abstract: The effect of production technology, packaging method, temperature and storage regime was observed on the dynamics of textural changes in milk chocolate. Half of the products were retempered immediately after the production (at 23 °C for 24 hours). The individual samples were packed in foil or vacuum. The products were stored for six months in three temperature regimes (at -18 °C, 20 °C and above 25 °C). The hardness was detected every two months. The textural properties of the products were measured using a texturometer, using a rod-shaped probe. A conclusive positive effect of retemperation was found out on the hardness of milk chocolate due to more stable fat modification and minimal fat migration ($P \leq 0.05$). Also, higher storage temperatures and storage regime proved a conclusive effect on higher hardness of the products ($P \leq 0.05$).

Key Words: milk chocolate, retemperation, packaging, storage regime, storage time, chocolate texture

INTRODUCTION

Various chocolate types differing in the composition of dry matter content, cocoa, milk fat and cocoa butter can exist (Fernandes et al. 2013). Milk chocolate must contain at least 2.5% of fat-free cocoa solids, up to 25% of total cocoa solids, up to 3.5% of milk fat, up to 25% of the total fat (the sum of cocoa butter and milk fat content) and up to 14% of milk solids according to Decree 76/2003 Coll. The chocolate quality proves a completely homogeneous structure, fine melting taste, hard consistency, conch-shaped fracture and shiny surface. The chocolate quality is influenced not only by raw materials and recipes but above all by the individual technological processes. The quality deterioration and various product defects can be caused by non-compliance with production procedures, by storage or transport conditions (Čopíková 1999, Afoakwa 2010).

Knowledge of the mechanical chocolate properties is important for determining the response to various forces. The durability of chocolate products during the production, transport and storage process play an important role in chocolate products. The product resistance to falls and compressive loads during the product layering especially in the storage conditions and transport are necessary to ensure. The hardness of chocolate and its products should be monitored because of the product texture which is closely related to the sensory evaluation (Full et al. 1996). These chocolate properties depend on its structure. Chocolate is characterized by high fat content in the composition. The product mechanical properties are closely associated with the crystallization network of cocoa butter (Narine and Marangoni 1999). The hardness of the chocolate depends on the suitable tempering and thus the creation for a stable crystallization network of cocoa butter. Chocolate should prove a firm and hard structure with an adequate crunch during breaking the chocolate bar, a shiny surface and easy melting in the mouth with a homogeneous consistency. The texture defects can occur without meeting the above mentioned requirements (Afoakwa et al. 2008). Typical defects of chocolate and its products include sugar and fat bloom. Particularly, fat bloom proves a significant effect on the product textural properties (Bui and Coad 2014).

The mechanical properties of chocolate and the penetration pressure test are the most often used for the description. Another suitable test can also be the three-point bend testing. The determination of the hardness by the penetration test is based on the evaluation of the force in newtons by which the penetration probe penetrates into the centre of the product (Machálková 2019).

MATERIALS AND METHODS

Table 1 shows the exact composition of the milk chocolate mass provided by Nestlé Czechia Ltd. (Zora plant).

Table 1 Chocolate composition

Ingredients	Cocoa liquor std.	Sugar	Cocoa butter	Lecithin	Vanilla extract	Full-cream milk	Fat CBE	Milk fat	Dried whey	Lactose
Content - recipe [%]	11.65	51.01	14.30	0.60	0.01	14.40	4.75	1.15	1.10	1.10

Legend: CBE – Cocoa Butter Equivalent

The production took place under standard conditions of the manufacturer using the Selmi ONE tempering machine, produced in Italy. A heating temperature of 46 °C and a working temperature of 29 °C were chosen for tempering the chocolate mass. The chocolate samples (up to 100 g/product) were produced. The chocolate was cooled at 12 °C for 20 minutes after pouring into a mold and removing air on a vibrating plate followed by knocking out of the mold and half of the products were retempered at 23 °C for 24 hours and the other half of the products were returned to the warehouse (at 12 °C). The retempered products were returned to the warehouse after 24 hours. In each case, half of the retempered and unretempered products were packed in aluminium foil and the other half in PE packaging with the subsequent vacuuming. A Henkelman Boxer 35 packaging machine (The Netherland) was used for the vacuuming. After packaging, the products were divided and stored in three storage regimes with different temperatures up to -18 °C, 20 °C and more than 25 °C. The chocolate samples were taken every two months to determine the textural properties during the six months of storage.

The universal device known as Tira Test (type of 27025), produced in Germany, was used for the measuring hardness of the samples. A penetration test with a rod-shaped probe was used to test the chocolate products. The chosen criteria for the pressure penetration test of the chocolate products were stated as straight tip (type of attachment) up to 3 mm (probe diameter) and the test speed up to 100 mm/min. The hardness of chocolate products was properly measured by the equilibration (for 24 hours) to room temperature.

The obtained data were processed in MS Excel. The statistical evaluation was performed in STATISTICA 12.0 software using a multi-factor analysis of variance known as ANOVA (the tests at significance level $p < 0.05$).

RESULTS AND DISCUSSION

The effect of storage conditions and the production technology on changes in the textural properties of milk chocolate packed in foil are shown in Figure 1. The highest hardness of chocolate was characterized at the third sampling i.e. after 6 months of storage. The samples of unretempered chocolate, stored at the lowest temperature, were detected as the only exceptions. The temperature was crucial in terms of the textural product properties. The most stable texture proved the samples stored at the room temperature up to 20 °C at the end of the experiment. The hardness of the chocolate was increased during the storage. The effect of retemperation also showed a positive influence contributing to the higher hardness of chocolate in the most samples at the last sampling. According to Mohos (2010), the retemperation of chocolates apparently contributed to the crystal formation of more stable fat modification and thus a minimal fat migration to the product surface. The beneficial effect of retemperation on the texture of products was also reported by Ruban et al. (2016).

The highest hardness of products was observed in the third sampling (see Figure 2) in the most cases as can be seen from the evaluation of chocolates packaged in vacuum. The strongest texture was determined for the products of the unretempered chocolate stored at the highest temperature. The retempered chocolate proved this effect at 20 °C. The retemperation showed a favourable effect only on the vacuumed products at lower storage temperatures compared to the products packed in foil. The unretempered products were characterized by a firmer texture at temperatures above 25 °C.

Generally, the hardness of chocolate products can be significantly affected by the storage temperature (see Figure 3) as can be seen from the obtained results. The products, stored at a temperature higher than 25 °C, achieved the highest hardness values on the other hand the chocolates proved the lowest hardness stored at -18 °C. The favourable role of temperature above 25 °C can be explained mainly by the fact that getting closer to the retemperated temperature may promote the formation to a stable modification of cocoa butter crystals. This fact could contribute to higher product hardness. The conditions were not created for fat migration causing softening and higher stickiness of chocolate since the temperatures were close to 25 °C throughout the storage period as reported by Ali et al. (2001). If we focus on the evaluation, the effect of retemperation regardless of the other evaluated factors (Figure 4) has not proved a positive influence on hardness. The minimal differences between retempered and unretempered chocolate were detected on average as well as the packaging effect on this parameter (Figure 5). However, this result was not applied to the measured values in a time series. A favourable effect of retemperation was increased with the storage time reflected in the overall evaluation of the effect on the sampling date on the hardness of chocolate (Figure 6). The increase was detected about 3.3 N on average. This fact did not confirm the conclusions of Aguilera et al. (2004), who found out the chocolate softening after the prolonged storage caused by the fat migration to the product surface. This conclusion indicated that the temperatures of our storage conditions did not achieve the extreme level and rather suited to longer-term storage.

Figure 1 Effect of sampling date, temperature and production technology on the hardness of products packed in aluminium foil

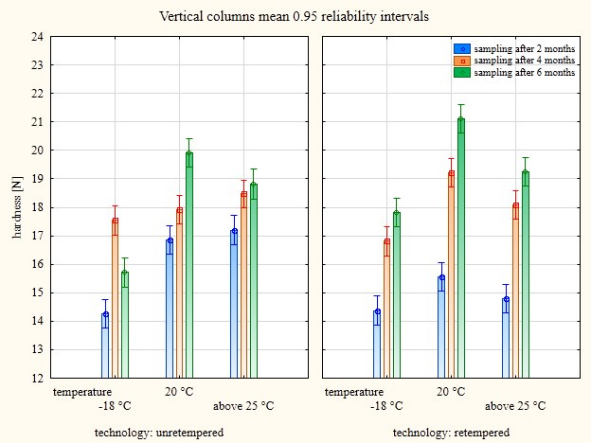

Figure 2 Effect of sampling date, temperature and production technology on the hardness of products packaged in vacuum

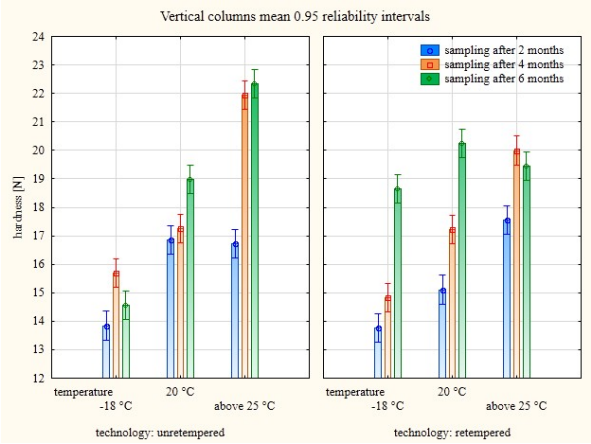

Figure 3 Effect of temperature on the hardness of stored products

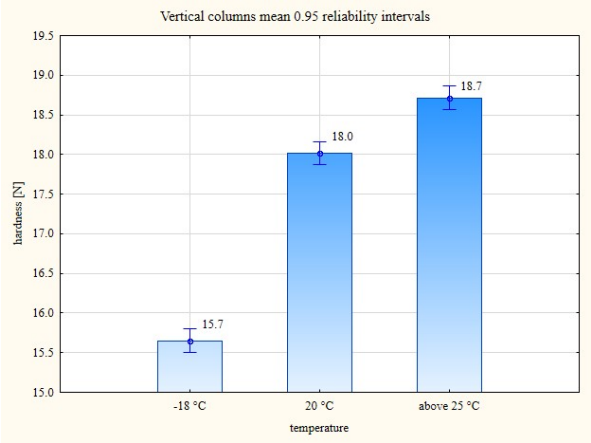

Figure 4 Effect of technology on the hardness of stored products

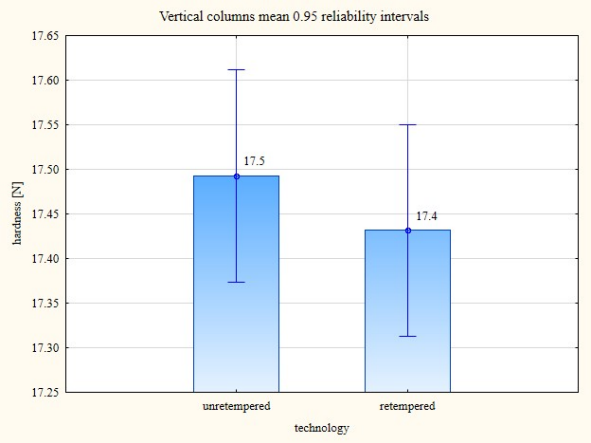

Figure 5 Effect of packaging on the hardness of stored products

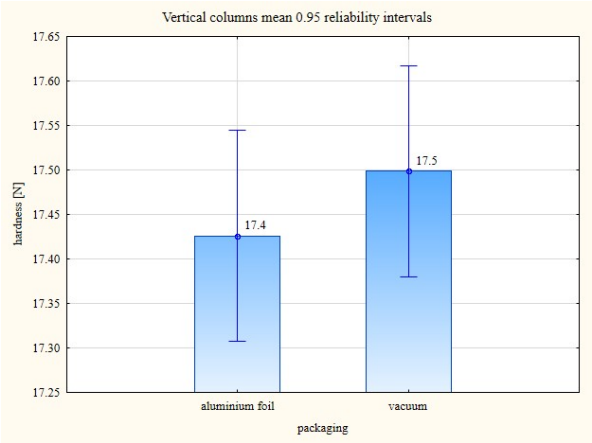

Figure 6 Effect of sampling on the hardness of stored products

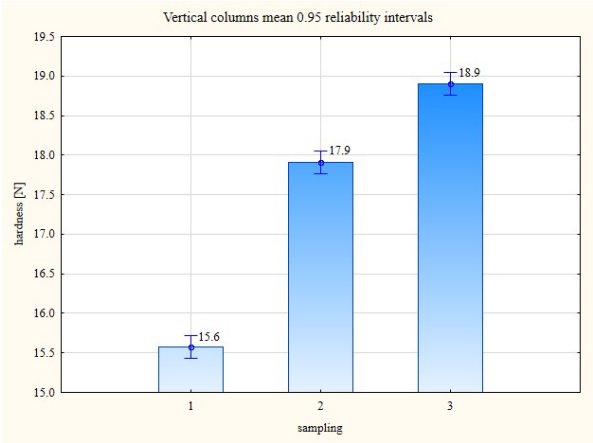

CONCLUSION

The hardness of chocolate is a suitable indicator of the appropriate tempering and the stability of the formed crystalline fat network. The aim of the retemperation was to support the completion of the perfect structure of the cocoa butter crystalline network and thus to increase the stability as expected. The samples were determined by hardness based on the evaluation of the force in newtons FH [N] by which the penetrating body penetrated into the centre of the chocolate product.

Higher storage temperatures and the storage length significantly affected the hardness of the product in a positive direction. The storage temperature of 20 °C as well as the retemperation proved a positive effect on higher hardness of the products packed in the foil. In the case of vacuum-packed products, the beneficial effect of retemperation was recorded only at lower storage temperatures. The unretempered products showed a stronger texture at the storage temperatures above 25 °C.

ACKNOWLEDGEMENTS

The research was financially supported by the Internal Grant Agency AF-IGA2020-IP049.

REFERENCES

Afoakwa, E.O. et al. 2008. Effects of particle size distribution and composition on rheological properties of dark chocolate. European Food Research and Technology [Online], 226(6): 1259–1268. Available at: https://www.academia.edu/24854080/Effects_of_particle_size_distribution_and_composition_on_rheological_properties_of_dark_chocolate. [2020-08-03].

Afoakwa, E. 2010. Chocolate Science and Technology. 1st ed., Chichester, United Kingdom: Wiley-Blackwell.

Aguilera, J.M. et al. 2004. Fat migration in chocolate: Diffusion or capillary flow in a particulate solid? – A hypothesis paper. Journal of Food Science [Online], 69(7): 167–174. Available at: https://www.academia.edu/12696860/Fat_Migration_in_Chocolate_Diffusion_or_Capillary_Flow_in_a_Particulate_Solid_A_Hypothesis_Paper. [2020-08-20].

Ali, A. et al. 2001. Effect of storage temperature on texture, polymorphic structure, bloom formation and sensory attributes of filled dark chocolate. Food Chemistry [Online], 72(4): 491–497. Available at: https://www.sciencedirect.com/science/article/pii/S0308814600002715. [2020-08-18].

Bui, L.T.T., Coad, R. 2014. Military ration chocolate: The effect of simulated tropical storage on sensory quality, structure and bloom formation. Food Chemistry [Online], 160(1): 365–370. Available at: https://coek.info/pdf-military-ration-chocolate-the-effect-of-simulated-tropical-storage-on-sensory-qu.html. [2020-08-15].

Česká republika. 2003. Vyhláška č. 76/2003 Sb., kterou se stanoví požadavky pro přírodní sladidla, med, cukrovinky, kakaový prášek a směsí kakaa s cukrem, čokoládu a čokoládové bonbony. In: Sbírka zákonů České republiky. 32: 2470–2487. Available at: https://www.zakonyprolidi.cz/cs/2003-76. [2020-08-31].

Čopíková, J. 1999. Technologie čokolády a cukrovinek. 1st ed., Praha: VŠCHT.

Fernandes, V. et al. 2013. Thermal, structural and rheological characteristics of dark chocolate with different compositions. Journal of Food Engineering [Online], 116(1): 97–108. Available at: https://www.sciencedirect.com/science/article/pii/S0260877412005869. [2020-08-20].

Full, N.A. et al. 1996. Physical and sensory properties of milk chocolate formulated with anhydrous milk fat fractions. Journal of Food Science [Online], 61(5): 1068–1084. Available at: https://onlinelibrary.wiley.com/doi/abs/10.1111/j.1365-2621.1996.tb10934.x. [2020-08-08].

Machálková, L. 2019. Vliv podmínek skladování a způsobu výroby čokoládových cukrovinek na vznik a vývoj tukového a cukerného výkvětu. PhD dissertation (in Czech), Mendel University in Brno.

Mohos, F. 2010. Confectionery and Chocolate Engineering: Principles and Applications. 1st ed., Chichester, U.K.: Wiley-Blackwell.

Narine, S.S., Marangoni, A.G. 1999. Mechanical and structural model of fractal networks of fat crystals at low deformations. Physical review E [Online], 60(1): 6991–7000. Available at: https://www.researchgate.net/publication/11397030_Mechanical_and_structural_model_of_fractal_networks_of_fat_crystal_at_low_deformations. [2020-08-19].

Ruban, A. et al. 2016. Effect of Storage Regime on Texture and Other Sensory Properties of Chocolate. In Proceedings of International PhD Students Conference MendelNet 2016 [Online]. Brno, Czech Republic, 9 November, Brno: Mendel University in Brno, Faculty of AgriSciences, pp. 645–650. Available at: https://mnet.mendelu.cz/mendelnet2016/mnet_2016_full.pdf. [2020-08-31].

The effect of the homogenization process on the viscoelastic properties of processed cheese sauce with furcellaran addition

Vendula Kurova[1], Richardos Nikolaos Salek[1], Nela Svajdova[1], Robert Gal[1], Frantisek Bunka[2]
[1]Department of Food Technology
Tomas Bata University in Zlin
nam. T.G. Masaryka 5555, 760 01 Zlin
[2]Food Research Laboratory, Department of Logistics
University of Defence
Kounicova 65, 662 10 Brno
CZECH REPUBLIC

v_kurova@utb.cz

Abstract: The present work examined the impact of the homogenization (two- and one-stage) and various furcellaran levels (0.25; 0.50; 0.75 and 1.00% w/w) addition on the viscoelastic properties of the processed cheese sauce (PCS), whereas the measurement was carried out 24 hours after the PCS manufacture. The gradual increase of furcellaran concentration significantly affected the viscoelastic properties which was indicated by an increase in the storage modulus (G´) and loss modulus (G´´). Homogenization elevated the complex modulus (G^*) values of the PCS produced with relatively low-furcellaran content (0.25% w/w), indicating an increase in the stiffness of the samples. However, the PCS samples with greater furcellaran levels were less rigid with the application of homogenization and increasing homogenization degree.

Key Words: casein-based structure, processing parameters, hydrocolloids, rheology, viscoelasticity

INTRODUCTION

Processed cheese sauce (**PCS**) could be described as novel dairy product characterized by various benefits, such as a relatively long-shelf life, low price (in comparison to other cheese products), simple use and a possibility of an addition of health-promoting components. However, there are not known any standards or legislative regulations that restrict PCS raw material composition. Therefore, a wide spectrum of ingredients [e.g. natural cheese, processed cheese (**PC**), cheese powder, milk and whey powders, butter, vegetable fats] and food additives [e.g. emulsifying salts (**ES**), hydrocolloids, flavor enhancers] could be applied to the PCS in order to obtain a smooth and stable product. Likewise, the production protocols of different PCS types could vary. Generally, the manufacture could be described as continuous mixing and stirring of the ingredients at elevated temperatures (85–110 °C) under a partial vacuum until a desired homogeneous emulsion-based product is formed (Shalaby et al. 2017, Salek et al. 2019, Szafrańska and Sołowiej 2020).

Moreover, homogenization can be included in the production process of PCS as an optional step, which can affect its functional properties (as a processing parameter), such as consistency, stability, smoothness, flavor and color (Szafrańska and Sołowiej 2020). The principle of PCS homogenization is to exposed the hot molten mass to higher pressure (usually 5 to 20 MPa) in order to promote the formation of a finer fat emulsion. Moreover, for dairy products with a relatively high dry matter content (compared to milk; such as PC or PCS), the two-stage homogenization could be applied. In addition, the application of homogenization can prevent occurrence of coarse particles (e.g. lumps of proteins or undissolved ES) and ensures further mixing of the individual components of the developed melt. On the other hand, the inclusion of the homogenization to the production process is a relatively expensive matter (Lopez et al. 2015, Mohammadi and Fadaei 2018).

Furthermore, hydrocolloids are a wide group of the long chain polymers (proteins and polysaccharides) which are commonly applied in the food industry as thickening, gelling, stabilizing or emulsifying agents (Saha and Bhattacharya 2010). Furcellaran is an anionic sulphated galactan

(obtained from red algae *Furcellaria lumbricalis*), which is ordinarily considered as a κ-carrageenan type. The basic structure of furcellaran and κ-carrageenan consists of repeating units of galactose and 3,6-anhydrogalactose units (sulphated and non-sulphated), which are joined by alternating α-(1,3) and β-(1,4) glycosidic links. However, the main difference lies in the lower sulphate content of furcellaran (one sulfate group per three to four monomeric units) (Imeson 2009, Robal et al. 2017).

However, in the literature, there is a lack of information of homogenization impact on the PC and PCS properties. This study was focused on the evaluation of the impact of homogenization on the viscoelastic PCS properties manufactured with different furcellaran levels (0.25–1.00% w/w). In addition, a second objective was to describe the effect of one- and two-stage homogenization on the PCS viscoelastic behavior.

MATERIAL AND METHODS

Manufacture and materials

The model PCS samples were prepared with 0.25; 0.50; 0.75 and 1.00% w/w furcellaran and 2.27% w/w ES addition, whereas all model samples were designed to have a dry matter (**DM**) content 30% w/w and fat in dry matter (**FDM**) content 66% w/w. After PCS manufacture, the hot molten mass was divided into three groups; the (i) of which was not subjected to homogenization (**NH**); the (ii) was subjected to one-stage homogenization (20 MPa; **H20**); and the (iii) was subjected to two-stage homogenization (20 MPa/10 MPa; **H30**). Moreover, control samples were produced (**CS**; without furcellaran addition). For the PCS preparation, the following ingredients were utilized: Edam cheese (AGRICOL s.r.o., Czech Republic; DM 50% w/w, FDM 30% w/w, 7 week maturity); butter (Sachsenmilch Leppersdorf, GmbH, Germany; DM 84% w/w, fat content 82% w/w); ES [Fosfa a.s., Czech Republic; Na_2HPO_4, NaH_2PO_4, $Na_4P_2O_7$ and sodium salt of polyphosphate (number of phosphate units ≈ 20), in a ratio of 2.6:3.0:2.2:2.2)] furcellaran (Estgel 1000; Est-Agar AS, Estonia); a mixture of monoacylglycerols and diacylglycerols (Brenntag CR s.r.o., Czech Republic) and water. The device Stephan UMC-5 (Stephan Machinery GmbH, Germany) with an indirect heating system was employed for the PCS manufacture, whereas the PCS was melted for 1 minute at 90 °C (total melting time was 12 min) at 3000 rpm. For PCS samples homogenization [at two homogenization regimes; (i) one stage: 20 MPa; and (ii) two-stage 20 MPa and 10 MPa, respectively] the PandaPLUS (GEA Niro Soavi, Italy) was used. For greater clarity, the scheme of the produced samples is shown in Figure 1. Thereafter, the hot PCS molten mass was transferred into polypropylene pots, which was closed with aluminum lids. The model samples were cooled down and stored for 24 hours at 6 ± 2 °C. The PCS model samples were produced in triplicate.

Figure 1 Overview of the composition of PCS samples manufactured

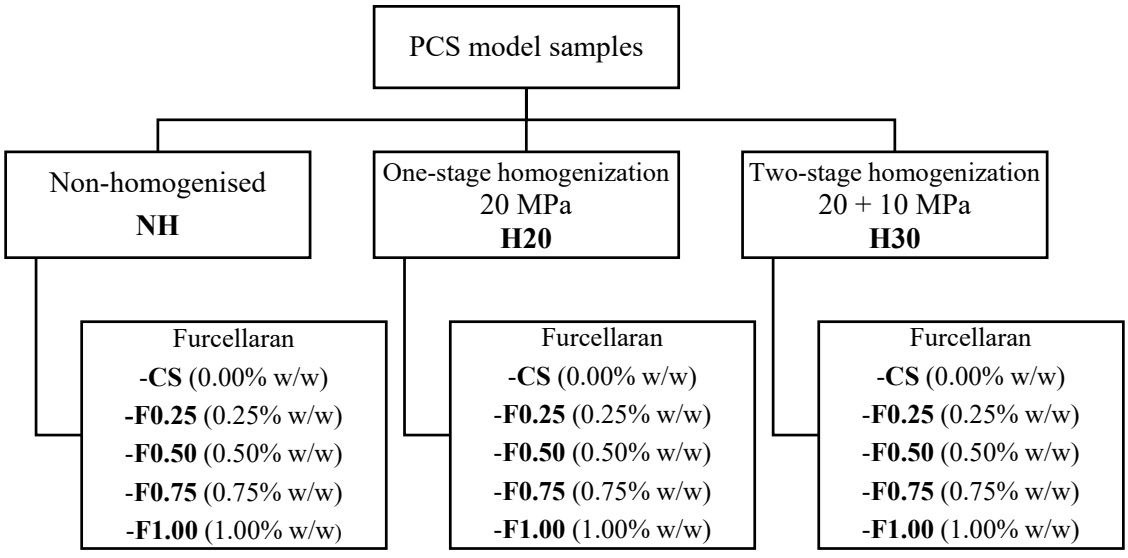

Basic chemical analysis

The basic chemical analysis consisted of the determination of DM content and pH of the PCS samples. The DM content was determined according to ISO 5534 (2004). For pH measurement (at 22 ± 2 °C), a puncture pen-type pH meter pHSpear (Eutech Instruments, Malaysia) with a glass tip electrode was used. All the measurements were performed at least three times for each model sample (n = 9; 3 repetitions × 3 batches).

Dynamic oscillatory rheology

Viscoelastic properties of PCS model samples were determined by a dynamic oscillatory shear rheometer Rheostress 1 (Haake, Germany) with plate-plate geometry (35 mm diameter, 1 mm gap). The storage modulus (**G′**; Pa; describing the elastic response) and the loss modulus (**G′′**; Pa; describing the viscous response) were measured. Moreover, complex modulus (G^*; Pa) and tangent of phase shift angle (**tanδ**; unitless) were calculated according to the equation (i) and (ii), respectively. All measurements were performed in the oscillation frequency range of 0.1–10.0 Hz (at 20.0 ± 0.1 °C). The shear stress amplitude (20 Pa) was within the linear viscoelastic region. The presented data are the mean value from three measurements of each PCS sample (n = 9). Moreover, the reference frequency of 1 Hz was chosen for tan δ and G^* data presentation.

$$\text{(i)} \quad G^* = \sqrt{(G')^2 + (G'')^2}$$

$$\text{(ii)} \quad tan\,\delta = G''/G'$$

Statistical analysis

For the evaluation of data obtained, Kruskal-Wallis and Wilcoxon tests were used (the selected significance level was 0.05).

RESULTS AND DISCUSSION

Evaluation of basic chemical analysis of the PCS samples

The DM content of all the model PCS samples ranged from 30.56 to 31.04% w/w, which met the specified requirements and assured the comparability of the PCS samples ($P \geq 0.05$). Furthermore, the pH values of model samples were in the range of 5.95–6.11. The growing furcellaran concentration (0.25–1.00% w/w) slightly increased the pH values of PCS samples; nevertheless, the changes were not significant ($P \geq 0.05$). Likewise, the effect of homogenization (and homogenization regime; H20, H30) was not demonstrated as well, the pH values were equal or slightly higher ($P \geq 0.05$) than those of NH samples (with the same furcellaran concentration).

Viscoelastic properties of the PCS samples

The G′ and G′′ development of the PCS samples tested (which varied in the furcellaran levels and homogenization regimes used) concerning the frequency (0.1−10.0 Hz) is presented in Figure 2. Generally, in the all model PCS samples tested, the elastic component of behavior predominated over the viscous response (G′ > G′′; in the whole range of tested frequencies); the PCS structure thus corresponds to a solid type structure rather than liquid and could be described as gel (Cunha et al. 2013).

Furthermore, the elevated concentration of furcellaran (0.25; 0.50; 0.75 and 1.00% w/w) progressively increased ($P \leq 0.05$; regardless the homogenization regime) the G′ and G′′ values in the whole range of frequency observed (0.1–10.0 Hz; Figure 2), which indicates the growing PCS rigidity. Moreover, according to Černíková et al. (2008), the creation of a denser network structure within the PCS matrix has occurred due to the more intense interaction between the chains of the hydrocolloid. The G′ and G′′ values of the homogenized (both H20 and H30) CS and samples produced with relatively low furcellaran addition (0.25% w/w) were significantly ($P < 0.05$) higher in comparison with the NH samples. If compared the homogenized (H20 and H30) products with each other, the higher ($P \leq 0.05$) G′ and G′′ curves were observed in case of those which was two-stage-homogenized ($P \leq 0.05$; at constant furcellaran levels). The latter phenomena can be explained by the reduction of particles (especially fat globules) during homogenization and also by the formation of a more intensive protein network (by the proteins newly covered the reduced fat droplets surface;

Mohammadi and Fadaei 2018). However, for PCS samples produced with relatively higher furcellaran content (0.50; 0.75 and 1.00% w/w), the opposite trend was observed; the G´ and G´´ values of homogenized (both H20 and H30) samples were even lower ($P < 0.05$) than those made without homogenization (NH). In terms of comparing different types of homogenization, the lowest values ($P < 0.05$) were measured after two-stage homogenization for those PCS (compared to H20). Furthermore, in the case of samples with 0.50% furcellaran content, the G´ and G´´ values were comparable in the range of measured frequencies (0.1 – 10.0 Hz; $P \geq 0.5$) for H30 samples and lower ($P \leq 0.05$) for H20 samples.

Table 1 Complex modulus (G; kPa) of PCS samples with different furcellaran levels) subjected to different homogenization regimes measured at reference frequency of 1 Hz*

Homogenization regime	G^*(kPa)[1]				
	Furcellaran concentration (% w/w)				
	0	0.25	0.50	0.75	1.00
NH	0.60 ± 0.02^{Aa}	1.32 ± 0.05^{Ba}	3.74 ± 0.01^{Cb}	7.64 ± 0.08^{Dc}	12.77 ± 0.11^{Ec}
H20	1.24 ± 0.03^{Ab}	2.26 ± 0.10^{Bb}	3.38 ± 0.04^{Ca}	6.00 ± 0.01^{Db}	8.55 ± 0.07^{Eb}
H30	1.32 ± 0.02^{Ab}	2.79 ± 0.02^{Bc}	3.78 ± 0.04^{Cb}	5.56 ± 0.03^{Da}	7.60 ± 0.02^{Ea}

Legend: NH – non-homogenized, H20 – one-stage homogenization; H30 – two-stage homogenization; [1]results are given as the mean ± standard deviation; $^{A–E}$ distinct superscripts in the row indicate the significant difference ($P < 0.05$); $^{a–c}$ distinct superscripts in the column indicate the significant difference ($P < 0.05$)

The G^* (Table 1) and tan δ (Table 2; for a reference frequency of 1 Hz) data were in an accordance with the above-mentioned trends. The increasing furcellaran content (0.25–1.00% w/w) and homogenization applied (H20 and H30; for CS and F0.25 samples) led to the increase ($P < 0.05$) in G^* and the decrease ($P \geq 0.05$, statistically insignificant) in tan δ, whereas, the greatest G^*values were observed ($P \leq 0.05$) for two-homogenized samples. Nevertheless, G^* of the homogenized (H20 and H30) products with relatively higher furcellaran concertation (0.75 and 1.00% w/w) declined ($P > 0.05$) in NH samples comparison (at a constant furcellaran level). The development of G^* for F0.50 samples were dependant on homogenization type (see Table 1). However, the differences in tan δ values were not significant ($P \geq 0.05$; Table 2). Thus, changes in the viscoelastic properties of PCS due to homogenization were affected by the concentration of furcellaran, which may be due to the disruption of the furcellaran chains (occurring in the greater quantities) by the homogenization pressure, and thus possible less effective impact on the ability to form a gel and increase the PCS firmness.

These findings provide a better insight of the use of various homogenization regimes in PCS manufacture. Moreover, applications of furcellaran (permitted to be used as a food additive in the European Union under the code E407 together with carrageenans) to dairy products in order to control their properties was described, since application of this carrageenan type has not yet been discussed in the available literature.

Table 2 Tangent of phase shift angle (tan δ; unitless) of PCS samples with different furcellaran levels subjected to different homogenization regimes measured at reference frequency of 1 Hz

Homogenization regime	tan δ[1]				
	Furcellaran concentration (% w/w)				
	0	0.25	0.50	0.75	1.00
NH	0.30 ± 0.01^{Aa}	0.25 ± 0.01^{Ba}	0.23 ± 0.02^{Ba}	0.23 ± 0.03^{Ba}	0.23 ± 0.02^{Ba}
H20	0.26 ± 0.04^{Aa}	0.24 ± 0.03^{Aa}	0.23 ± 0.02^{Aa}	0.22 ± 0.04^{Aa}	0.22 ± 0.03^{Aa}
H30	0.27 ± 0.03^{Aa}	0.24 ± 0.04^{Aa}	0.24 ± 0.04^{Aa}	0.22 ± 0.02^{Aa}	0.22 ± 0.03^{Aa}

Legend: NH – non-homogenized, H20 – one-stage homogenization; H30 – two-stage homogenization; [1]results are given as the mean ± standard deviation; $^{A–E}$ distinct superscripts in the row indicate the significant difference ($P < 0.05$); $^{a–c}$ distinct superscripts in the column indicate the significant difference ($P < 0.05$)

Figure 2 Development of the storage (G´, Pa; full symbols) and loss (G´´, Pa; open symbols) modulus in a relation to the frequency (0.1–10.0 Hz) of PCS samples manufactured with various levels of furcellaran (control sample – ●○; 0.25% w/w – ■□; 0.50% w/w – ▼▽ in parts A, C and E; and 0.75% w/w – ▲△; 1.00% w/w – ★☆in parts B, D and F). Produced with no homogenization applied (parts A, B) and with one-stage (20 MPa; parts B, C); and two-stage (20/10 MPa; parts E, F) homogenization applied.

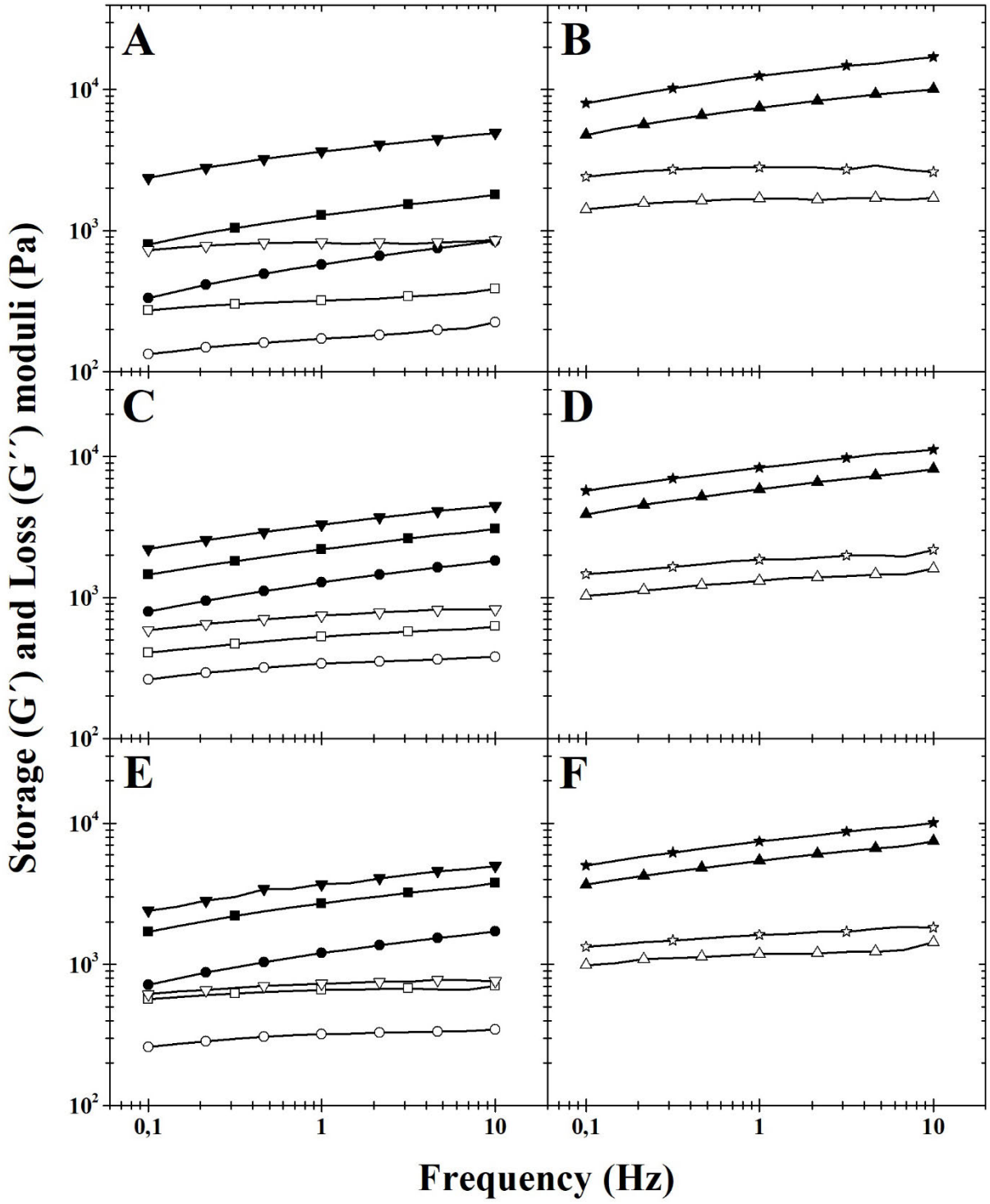

CONCLUSION

The various homogenization regimes affected the viscoelastic properties of PCS depending on the furcellaran content. The greatest influence was observed for the increasing addition of furcellaran

(0.25–1.00% w/w), which significantly increased the stiffness of all PCS samples. However, the homogenization process was only suitable for effectively increasing of furcellaran-free or low-content (0.25% w/w) samples firmness. In this case, two-stage homogenization was the most effective. On the other hand, at higher furcellaran concertation (0.50; 0.75 and 1.00% w/w), the effect of homogenization on the increase of PCS rigidity was not observed. The PCS showed lower firmness in the following order: two-stage homogenized < one-stage homogenized < non-homogenized. Nevertheless, further analyzes will be necessary in the future to understand the processes within the homogenization of processed cheese sauce and processed cheese.

ACKNOWLEDGEMENTS

The research was financially supported by the internal grant agency of Tomas Bata University in Zlín, Czech Republic (IGA/FT/2020/006).

REFERENCES

Černíková, M. et al. 2008. Effect of carrageenan type on viscoelastic properties of processed cheese. Food Hydrocolloids, 22(6): 1054–1061.

Cunha, C.R. et al. 2013. Effect of the type of fat on rheology, functional properties and sensory acceptance of spreadable cheese analogue. International Journal of Dairy Technology, 66(1): 54–62.

ISO 5534:2004. Cheese and processed cheese – Determination of the total solids content (reference method). Geneva: International Organization for Standardization.

Imeson, A.P. 2009. Carrageenan and furcellaran. In Handbook of hydrocolloids, 2nd edition. Cambridge: Woodhead Publishing Limited, pp. 164–185.

Lopez, C. et al. 2015. Organization of lipids in milks, infant milk formulas and various dairy products: role of technological processes and potential impacts. Dairy Science & Technology, 95(6): 863–893.

Mohammadi, A., Fadaei V. 2018.The effect of homogenization on texture of reduced dry matter processed cheese. Food Science and Technology 38(1): 190–195.

Robal, M. et al. 2017. Monocationic salts of carrageenans: Preparation and physico-chemical properties. Food Hydrocolloids, 63: 656–667.

Saha, D., Bhattacharya, S. 2010. Hydrocolloids as thickening and gelling agents in food: a critical review. Journal of Food Science and Technology, 47(6): 587–597.

Salek, R.N. et al. 2019. Evaluation of various emulsifying salts addition on selected properties of processed cheese sauce with the use of mechanical vibration damping and rheological methods. LWT, 107: 178–184.

Shalaby, S.M. et al.: 2017. Preparation of a novel processed cheese sauce flavored with essential oils. International Journal of Dairy Science, 12(3): 161–169.

Szafrańska, J.O., Sołowiej, B.G. 2020. Cheese sauces: Characteristics of ingredients, manufacturing methods, microbiological and sensory aspects. Journal of Food Process Engineering, 43(4):e13364.

Preparation of gelatine from poultry bones residue

Jakub Martinek[1], Robert Gal[2], Pavel Mokrejs[1], Jana Pavlackova[3]
[1]Department of Polymer Engineering
[2]Department of Food Technology
[3]Department of Fat, Surfactant and Cosmetics Technology
Tomas Bata University in Zlin
Vavreckova 275, 760 01 Zlin
CZECH REPUBLIC

j_martinek@utb.cz

Abstract: Poultry bone residue is formed as a by-product during the processing of poultry meat into mechanically deboned poultry meat. This product is very rich in collagen, yet unfortunately it is not widely used in current food practice. The bone residue can be used for the production of gelatine and other collagen hydrolysates with different molecular weights and can thus find application in the food industry, medicine, pharmacy or cosmetics. The main aim of this work is to determine optimal conditions for the preparation of gelatine by proteolytic enzyme (Protamex) with emphasis on high extraction efficiency and high gel strength of gelatine. Gelatine extraction was preceded by separation of soluble proteins, albumins (water), globulins (0.2 mol/l NaCl solution) and glutelins (0.03 mol/l NaOH solution). Defatting was performed using the enzyme Lipolase and acetone. Collagen was treated with Protamex endoprotease and gelatine was extracted with hot water. The influence of the treatment time with the enzyme Protamex (72 to 216 hours) and its amount used (0.0% to 2.4%) on the extraction efficiency and gel strength was studied. Other experimental conditions were extraction temperature (90 °C and 98 °C) and extraction time (0.5 to 4 hours). The extraction efficiency of the examined samples ranged from 6.0% to 31.6% and the gel strength of gelatine ranged from 87 to 357 Bloom. Depending on the strength of the gel, the gelatine produced in this way can find application in the food industry, especially as a substance modifying texture and mechanical properties, but also, for example in the preparation of biodegradable packaging materials, or in medicine (collagen films), cosmetics or pharmacy.

Key Words: mechanically deboned meat, poultry, by-products, gelatine, enzyme processing

INTRODUCTION

According to the Czech Statistical Office, the consumption of poultry meat per capita in the Czech Republic is growing every year. In 2018, it was almost 30 kg of poultry meat. And the long-term trend indicates that this value will continue to increase (Czech Statistical Office 2020). However, as meat consumption increases, so does the amount of by-products. These are mainly entrails, heads, runners, blood, skin, feathers and bones. However, some of the above cannot be further used for food production. (Seong et al. 2015).

Mechanical separation of meat is performed on separators. In addition to the meat itself, the mechanically separated meat contains bone marrow, parts of connective tissue and small bone fragments. After the separation of the meat, the by-product remains in the form of the rest of the bones, cartilage and tendons, which is also the subject of our experiment. Although it is a raw material rich in protein (mainly collagen), most of it is burned and only to a lesser extent is used as part of compound feed. (Míková 2013, Pipek 1998).

Partial hydrolysis of collagen produces gelatine, which has the ability to form gels. Most common methods for preparing gelatine are acidic and basic hydrolysis. However, this work deals with the determination of optimal conditions for more gentle enzymatic hydrolysis of collagen by the endoprotease Protamex. In addition to the amount of gelatine, the quality of the gel is also affected by its pH and temperature and possibly other additives. The Bloom unit is used to numerically express the strength of the gel. The stronger the gel, the higher the Bloom value and vice versa. (Ahmed et al. 2016).

The aims of this work

Our department has long been engaged in the processing of poultry by-products into collagen and subsequently into gelatine and other its hydrolysates. This contribution is another way of dealing with hitherto underused poultry by-products. The aim of this work was to focus on the possibility of extracting collagen from the remains of bones, cartilage and tendons, which arise as a by-product (not yet used) in the production of mechanically deboned poultry meat (MDPM) using Protamex enzyme and to evaluate the quality of the obtained material depending on the amount of enzyme and processing time.

The gel strength and the yield of gelatine of the resulting product were determined, and optimal extraction conditions were established based on them. The assumption was that as the enzyme increased, the yield of gelatine increased, but the gel strength decreased. The same development was expected at the time of enzyme treatment, i.e. the more time the more gelatine, but with lower strength.

MATERIAL AND METHODS

Bone residue were provided by Raciola s.r.o. Uherský Brod producing MDPM. These are residues (parts of bones and cartilage) that remain from the production of MDPM. The residue was delivered ground in a size of approximately 3 mm and stored in a freezer. It was thawed before the experiments. Bone residue composition: dry matter 38.15±0.57%, ash 28.59±4.62%, collagen 79.85±0.40% and 26.00±1.46% fat.

The methodology of the work was based on factor experiments, in this case 2^2. In this work, factor experiments consisted of two limit and one central experiment. The settings were as follows: Factor A amount of proteolytic enzyme Protamex at 0.6% and 2.4%, central 1.5% and Factor B processing time 72 and 216 hours, central 144 hours. The calculation of the amount of enzyme was based on the dry matter of the defatted bone residue. The extraction conditions of the first gelatine fraction were determined as follows: extraction time 90 minutes and extraction temperature 80 °C. For the extraction of the second fraction, the conditions were determined: extraction temperature at 90 and 98 °C and extraction time at 0.5; 1; 1.5 and 4 hours.

Appliances, tools and chemicals

WTB Binder dryer, shaker LT2 and 3, pH meter WTW 526, Kern 770 electronic analytical laboratory scale, Kern 440–47 electronic laboratory scale, Schott Garate GMBH heating plate with magnetic stirrer, Schott cooker, muffle furnace Nabertherm, refrigerator, mixer Eta, stopwatch, gas burner, desiccator, Sevens - LFRA analyzator, thermostat Thermo Hauke, Thermo spektronick Helios ε;

0.2M NaCl, 0.03M NaOH, enzyme Lipolase (lipase with *Thermomyces lanuginosus* produced by submerged fermentation of genetically modified micro-organism *Aspergillus oryzae*; declared activity of 100 KLU/g; K = Kilo, LU = Lipase unit), acetone, enzyme Protamex (*Bacillus* protease complex developed by the company Novozymes for hydrolysis of food proteins; declared activity 1.5 AU/g), chloroform, ethanol.

Statistical analysis

The results of the experiments were processed in software MiniTab 19.2020.1. The static significance of the investigated process factors within the monitored limits was evaluated using P values for the 95% confidence level. Factors that reach values lower than $\alpha = 0.05$ affect the evaluated variables with a probability of 95%. With decreasing value of P, the influence of selected factors on the sample increases.

Processing of mechanically deboned meat into gelatine

The processing of the bone residue into gelatine is shown in Figure 1. Separation of soluble proteins (albumins, globulins and glutelins) was performed according to the procedure from a previously published work, only with minor modifications (Du 2013). The material was defatted with 5% Lipolase enzyme, 1 : 10 water was added to the mixture. The raw material was shaken at room temperature for 3 days in four cycles of 7, 17, 7 and 17 hours. The remaining material was dried for 4 days at 35–40 °C. The remaining fat was removed by shaking the mixture for 8 hours with acetone in a ratio

of 1 : 9 and shaking for 8 hours at room temperature. Then the solvent was changed and shaking was performed again for 8 hours. The tissue was then spread on a plate and left in a fume hood to evaporate the remaining solvent. The raw material was mixed with distilled water in a ratio of 1 : 10 and the pH was adjusted to 6.5–7.0. Then the proteolytic enzyme Protamex (Factor A) was added and the mixture was shaken for the time of processing Factor B according to Table 1. For the first 4–6 hours, the raw material was shaken at room temperature and the pH was continuously adjusted to 6.5–7.0. After filtration, the crude was washed with cold water to remove as much enzyme as possible, followed by shaking for 10 minutes with an excess of 0.03 M NaOH solution.

The washed material was mixed with distilled water in a ratio of 1 : 8, and gelatine was extracted from the mixture after heating at 80 °C for 90 minutes. The gelatine solution of the first fraction separated from the solid tissue residue was brought to a boil for 5 minutes and dried at 45 °C for about 2 days. The solid tissue residue after extraction of the first fraction of gelatine was poured mixed with distilled water in a ratio of 1 : 7. The second fraction was extracted with constant stirring according to the conditions listed in Table 1. The gelatine solution of the second fraction was boiled, boiled for 5 minutes and dried at 45 °C for 2 days.

Figure 1 Processing of bone residue into gelatine

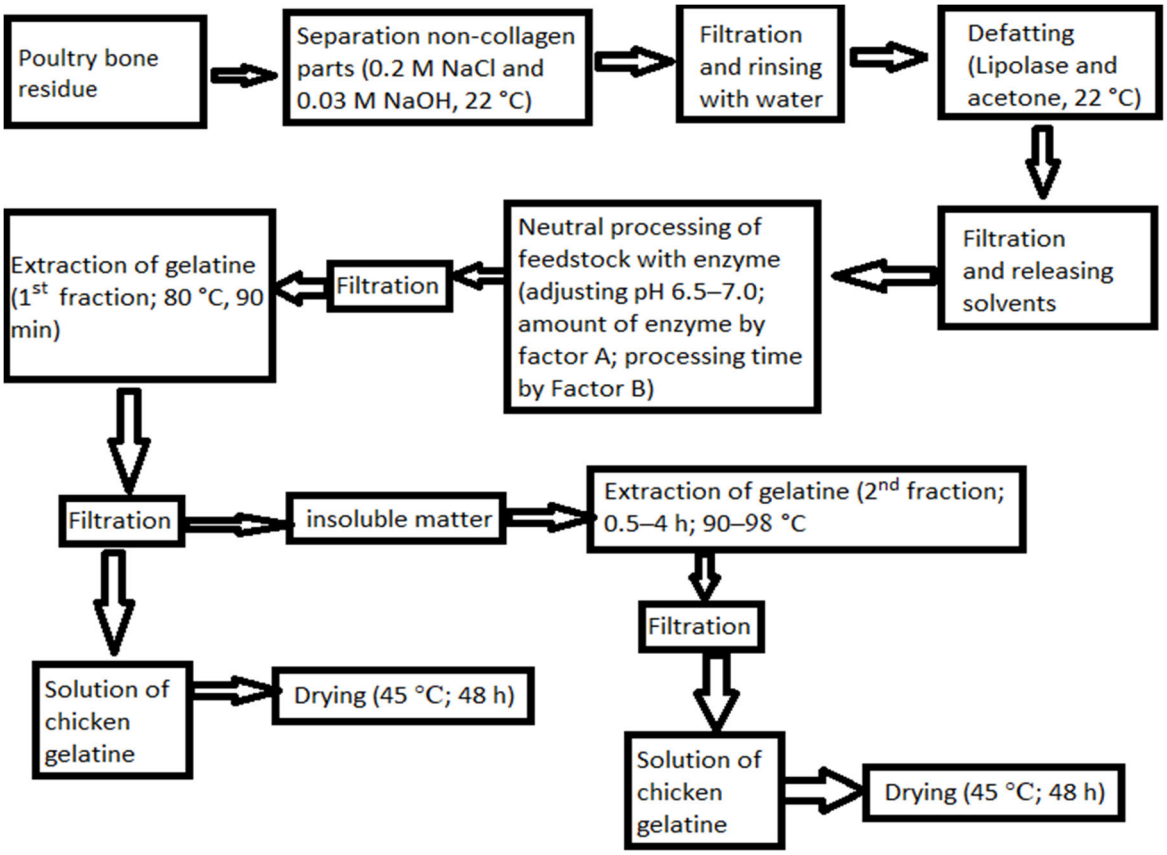

Calculation of yield of gelatine

The extraction efficiency was determined for all samples and was determined according to the following formula:

$$\eta = \frac{L}{m} \times 100\%$$

η is the total yield (%), m is weight of dry matter of bones residue after enzyme treatment, L is weight of gelatine and hydrolysate.

Measuring of gelatine gel strength

The strength of the gel was determined according to the official procedure of the American Institute for Gelatin Production. The strength is measured on a gel formed from a 6.67% solution of gelatine prepared according to the prescribed conditions by measuring the force (mass) required

to compress the prescribed area of the sample surface to a distance of 4 mm (Standard Testing Methods for Edible Gelatine 2013).

RESULTS AND DISCUSSION

An overview of performed experiments with technological conditions and characterization of produced gelatines is given in Table 1.

Table 1 Schedule of experiments including technological conditions, process characterization and characterization of prepared gelatines

	Factor A Addition of enzyme (%)	Factor B Processing time (h)	Extraction temperature of the 2nd fraction (°C)	Extraction time of the 2nd fraction (h)	Yield of gelatine (hydrolysate) η (%)	Gelatine gel strength F (Bloom)
1	0.6	72	90	0.5	26.7	266
2	0.6	216	90	1.5	21.4	202
3	2.4	72	90	4	31.6	140
4	2.4	216	98	1	28.8	87
5	1.5	144	98	4	31.3	173
6	0.0	144	98	4	6.0	357

Yield of gelatine

The gelatine extraction efficiency equation was: $\eta = 28.13 + 2.028\ A - 0.04259\ B + 0{,}009645\ A \times B + 4.175\ Ct\ Pt$

The highest yield would be obtained using a larger amount of enzyme and a shorter time as shown in Figure 2. It was assumed that with increasing processing time and amount of enzyme, the yield itself should increase, but values obtained did not confirm this assumption. The reason for achieving this result may be, for example, a larger number of bones, and the resulting larger number of undecomposed fractions in individual samples. The measurement was performed only once. With a larger number of repetitions, and thus a reduction in any error, the measurement result itself would rather look different.

Figure 2 Yield of gelatine depending on the amount of enzyme and the processing time

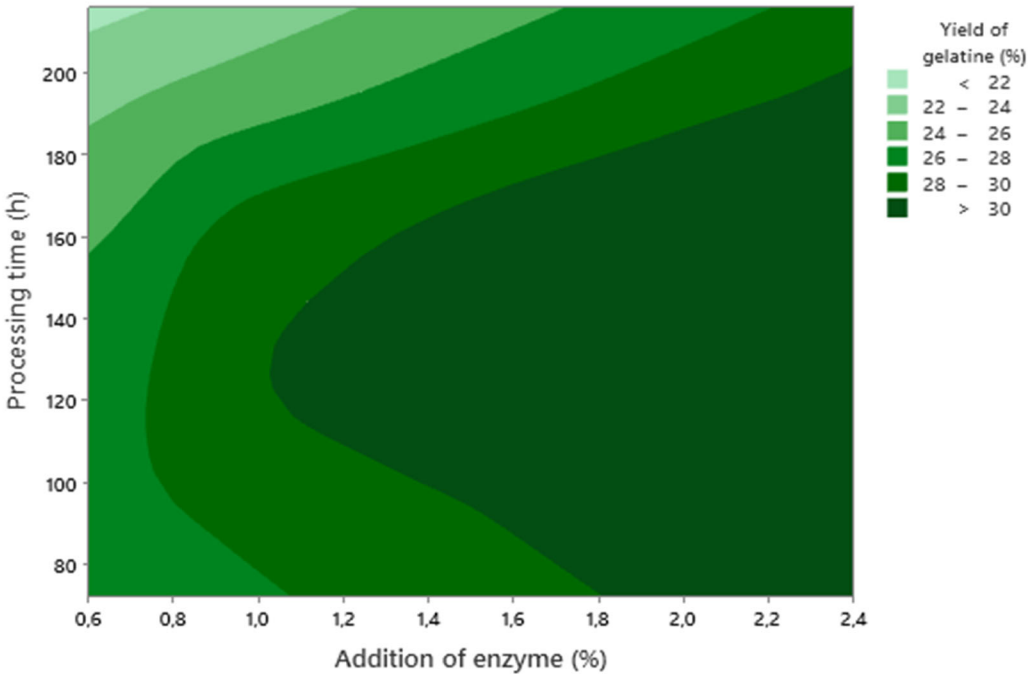

Gelatine gel strength

The gelatine gel strength equation was: F = 341.8 – 73.06 A – 0.4699 B + 0.04244 A x B–0.7500 Ct Pt.

The strength of the gel decreases with increasing amount of enzyme used as shown in Figure 3. The processing time also affects the strength of the gel. However, the significance of this factor is lower than the amount of enzyme used. As the time for which the tissue has been treated with the enzyme increases, the strength of the resulting gel decreases. The resulting gel thus achieves the highest strength with a small amount of enzyme and a short processing time. On the contrary, with the highest amount of enzyme and the longest time, the strength was the lowest. From the point of view of the highest gel strength, a processing time of 72 hours and an enzyme amount of 0.6% appear to be the optimal conditions.

Figure 3 The gel strength depending on the amount of enzyme and the processing time

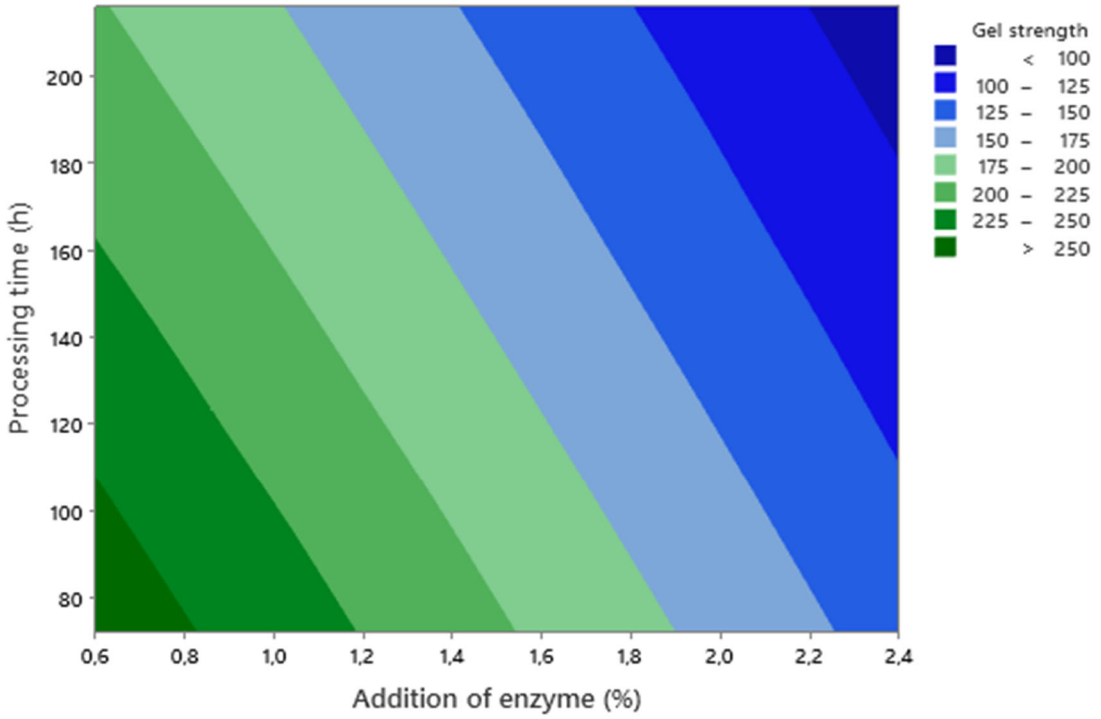

Almeida and da Silva Lannes prepared gelatine from chicken legs. The rinsed raw material was soaked in 4% acetic acid for 16 hours and extracted hot with distilled water at 55 °C for 6 hours. In this way, they managed to obtain a maximum of 7.83% gelatine and the highest value of gel strength was 294 Bloom (Almeida and da Silva Lannes 2013). Chakka et al. extracted gelatine from chicken legs using different food acids (acetic acid, citric acid and lactic acid) in different concentrations. The raw material was ground after rinsing with water and left in 0.5M NaOH solution for 20 hours. Then 1.5%, 3.0%, 4.5% acid solution was added for 18 hours. Gelatine extraction took 20 minutes at 55 °C. The highest efficiency was achieved with a 4.5% lactic acid solution (14.47%). The lowest efficiency of 6.59% was recorded using a 1.5% acetic acid solution. In contrast, this acetic acid solution gave the highest gel strength (204 Bloom), the strongest citric acid gel was obtained using its 4.5 solution (166 Bloom) and with lactic acid the highest gel strength was 164 Bloom at 1.5% contraction (Chakka et al. 2017).

CONCLUSION

The aim of the work was to verify the possibilities production of gelatine from bone residue and to find suitable conditions. As optimal conditions, such a combination of the processing time and the amount of enzyme which, when processing the bones from the separation, will provide the maximum extraction efficiency in combination with the greatest gel strength. The highest processing

efficiency was determined in this work using 2.4% enzyme and 72 hours of processing, its value was 31.6%. For the highest gel strength, the smallest possible amount of enzyme and the shortest possible processing time would be best. In this work, the best gel strength was a blank (without enzyme addition), which was 357 Bloom. The experiment with the following conditions had the lowest strength: 2.4% enzyme and 216 hours of treatment, its value was 87 Bloom. As the amount of enzyme increases, the extraction efficiency increases, but the gel strength decreases. As the processing time increases, both the extraction efficiency and the gel strength decrease. Thus, the assumption considered when planning the experiment was confirmed for the gel strength, however, the effect of the processing time on the gel strength and the extraction efficiency had a different trend than expected. It follows from the above that it is more appropriate to choose shorter processing times with the enzyme and to choose its amount depending on whether we require a high yield or a smaller amount of gelatine produced, but with higher gel strength. If the right conditions are chosen, the gelatine thus prepared in the gel strength can be equal to gelatine produced from pig, bovine and bones. Gelatine with a gel strength of 100 to 150 Bloom can be used for the production of confectionery, such as chewing gum, caramels, toffees, liquorice, gums, wine gums or meringues, or it can be used in dairy products such as cream, whipped cream or puddings. The strength of 250 Bloom gel is used in the production of jelly, marshmallows or butter spreads.

ACKNOWLEDGEMENTS

The research was financially supported by the Internal Grant Agency of the Faculty of Technology, Tomas Bata University in Zlin, ref. IGA/UTB/FT/2020/002.

REFERENCES

Ahmed, J. et al. 2016. Advances in Food Rheology and its Application. 1st ed., USA: Woodhead Publishing.

Almeida, P.F., Da Silva Lannes, S.C. 2013. Extraction and Physicochemical Characterization of Gelatin from Chicken By-Product. Journal of Food Process Engineering [On-line], 36(6): 824–833. Available at: https://onlinelibrary-wiley-com.proxy.k.utb.cz/doi/abs/10.1111/jfpe.12051. [2020–07–11].

Chakka, A.K. et al. 2017. Poultry Processing Waste as an Alternative Source for Mammalian Gelatin: Extraction and Characterization of Gelatin from Chicken Feet Using Food Grade Acids. Waste and Biomass Valorization [Online], 8(8): 2583–2593. Available at: https://link.springer.com/article/10.1007/s12649-016-9756-1. [2020–07–26].

Czech Statistical Office. 2019. Food consumption - 2018 [Online]. Available at: https://www.czso.cz/csu/czso/spotreba-potravin-2018. [2020–06–18].

Du, L. et al. 2013. Physicochemical and functional properties of gelatins extracted from turkey and chicken heads. Poultry Science, 92(9): 2463–2474.

Míková, K. 2013. Strojně oddělené drůbeží maso. Výživa a potraviny [Online], 68(3): 42–43. Available at: https://www.bezpecnostpotra-vin.cz/strojne-oddelene-drubezi-maso.aspx. [2020–08–07].

Pipek, P. 1998. Základy Technologie masa. 1st ed., Vyškov: Vysoká vojenská škola pozemního vojska ve Vyškově.

Seong, P.N. et al. 2015. Characterization of Chicken By-products by Mean of Proximate and Nutritional Compositions. Korean Journal for Food Science of Animal Resources, 35(2): 179–188.

Standard Testing Methods for Edible Gelatine. 2013. Gelatine Manufacturers Institute of America [Online]. Available at: http://www.gelatine_gmia.com/. [2020–07–23].

Influence of extraction time and temperature on the yield, gel strength and viscosity of chicken skin gelatine

Petr Mrazek[1], Robert Gal[2], Pavel Mokrejs[1], Jana Orsavova[3], Dagmar Janacova[4]
[1]Department of Polymer Engineering
[2]Department of Food Technology
[3]Language Centre
[4]Department of Automation and Control Engineering
Tomas Bata University in Zlin
Vavreckova 275, 760 01 Zlin
CZECH REPUBLIC

p_mrazek@utb.cz

Abstract: With an increasing consumption of poultry meat, the proportion of poultry by-products that can account for up to 33% of the overall output has also been growing. Such by-products include legs, heads, bones, and skins, and may serve as an excellent raw material for preparation of collagen-based products, such as gelatines with a wide range of applications, particularly in the food industry. Gelatine is derived from collagen, an abundant protein in animal tissues. Traditionally, it is produced by pre-treatment and subsequent extraction of collagen-rich materials, such as pork or bovine skins in distilled water at elevated temperature. Technological conditions during the process of extraction can substantially influenced the structure of prepared gelatine and thus its quality as well as the efficiency of the whole process. In this study, series of experiments employing factorial design were performed in which chicken skin gelatines (CSG) were prepared at different extraction conditions (varying temperature and time), and the effect on the gel strength and viscosity of CSG as well as the yield of the extraction process were observed. The yield of CSG ranged between 14.1 and 19.8%; the highest yield was obtained when using a longer extraction time and the highest extraction temperature. The CSG gel strength was determined from 126 to 190 Bloom with the highest value achieved within the application of a shorter extraction time and the lowest extraction temperature. The viscosity of CSG solution was established in the range from 2.06 to 4.40 mPa.s and the highest value was identified within a longer extraction time and the highest extraction temperature. Prepared CSG show a great potential for various applications especially in the food industry.

Keywords: collagen, factorial design, food gelatine, poultry by-products

INTRODUCTION

Gelatine is a water-soluble biopolymer produced by controlled hydrolysis causing partial denaturation of collagen, protein found in animal tissues, particularly in skins, tendons and bones of mammals, birds or fish. Collagen is a water-insoluble fibrous protein and possesses a crucial importance in maintaining integrity of biological structures; provides skin protection by inhibiting the absorption of toxins or pathogens; has various tissue functions, such as cell survival, proliferation and differentiation (Niu et al. 2013). Most commonly, gelatine is extracted after acidic or alkaline pre-treatment from two kinds of raw material: pigskins and cowhides (more than 98% of the production) (Khiari et al. 2017). However, pork gelatine consumption is prohibited in Judaism and Islam and beef gelatine is only allowed providing that it was prepared according to the religious requirements. What is more, Hindus are not allowed to consume cow-derived products at all. Therefore, alternative sources of gelatine, such as poultry or fish by-products, are highly desirable for the production of halal gelatine. Considering fish gelatine, one of the drawbacks is its characteristic fishy odour and the fact it does not sufficiently meet desired application parameters. On the other hand, poultry gelatine appears to be a promising commodity. Generally, due to its unique chemical and physical characteristics, gelatine is widely used in many technological applications both in food and non-food industries including stabilization, gelation, texturization, emulsification, sedimentation, clarification, thickening, film-formation, encapsulation, biodegradability, adhesiveness and biomaterial based packaging (Karim

and Bhat 2009). Regarding the food industry, gelatine is used, for example, as an agent increasing viscosity of aqueous systems or improving elasticity and consistency of food products. In confectionery, it provides chewing, texture or foam stabilization; ensures emulsification, gelling and stability in baked goods, or facilitates water binding in meat products (Sarabia et al. 2000). Factors influencing physicochemical properties of gelatine, such as gel strength or viscosity, include the type of tissue, age and species of animal as well as the type of the pre-treatment method or extraction conditions used in the process (Gomez-Guillen and Montero 2001). Increased extraction temperature and prolonged extraction time during gelatine production generally enhance the yield of the process; however, it may be accompanied by deterioration of gelling properties (Kittiphattanabawon et al. 2016). Therefore, the investigation of different processing parameters of the preparation of poultry gelatine is crucial.

The work aims to continue in the previous research of the processing chicken skin into gelatine (Mrázek et al. 2019) and to assess effects of the extraction parameters (temperature and time) on the yield and quality (represented by gel strength and viscosity) of chicken skin gelatines (CSG). The scientific hypothesis assumes that the increase of the extraction temperature and time results in the growth of the yield of CSG; nevertheless, also in the deterioration of its quality.

MATERIALS AND METHODS

Chicken skins were purchased from Raciola ltd., Uherský Brod, Czech Republic.

Appliances, tools and chemicals

Stevens LFRA Texture Analyser (Leonard Farnell and Co ltd., England), SPAR Mixer SP 100AD-B meat mincer (TH Industry RD, Taiwan), A 10 labortechnik analytical mill (IKA-Werke, Germany), Ubelohde kapillary viscometer (Schott, Germany), thermometer Thermo Haake C 10 (Thermo Fisher Scientific, USA). NaCl, NaOH, petroleum ether, ethanol (Verkon, Czech Republic); all of analytical grade. Enzyme Polarzyme 6.0 T – serine endoprotease (Novozymes, Denmark) with declared enzyme activity of 6 KPPU/g (kilo protease unit/g).

Preparation of chicken skin gelatine (CSG) samples

Initially, the raw material (chicken skin) was cleaned, pigments and non-collagenous proteins were removed and defatted according to the procedure described by Mrázek et al. (2019). Then, 25 g of such prepared raw material were mixed with distilled water at a ratio of 1:20 (w/v), the enzyme (Polarzyme 6.0T) was added in the amount of 0.2% (w/w – based on the dry matter of the raw material), pH was adjusted to 7.5 ± 0.3 to set the optimal enzyme conditions and the mixture was pre-treated by the enzyme on a shaker for 20 h. After that, water was separated from the pre-treated mixture which was then rinsed with distilled water and placed into a beaker. Subsequently, distilled water was added in the amount of 1:20 (w/v) and the mixture was heated to the required temperature to perform the extraction for a specified time (Table 1). The obtained gelatine solution was filtrated and reheated at 100 °C for 5 min. Reheating was necessary to deactivate possible residual enzyme. Then, the gelatine solution was dried in a thin layer in a forced air oven for approximately 24 h resulting in a chicken skin gelatine (CSG) film. Eight experiments with four different extraction temperatures (50, 60, 70 and 80 °C) and two different extraction times (30 min and 120 min) were performed employing combined factorial design (two-level and multi-level) to establish the influence of individual technological factors on the yield and quality of prepared CSG. Minitab 18 was used to design experiments and evaluate the results. The examined factors included: factor A – chicken skin gelatine (CSG) extraction temperature: 50, 60, 70 and 80 °C; factor B – CSG extraction time: the minimum of 30 min and maximum of 120 min. The evaluated variables were as follows: the yield of CSG, CSG gel strength and viscosity.

Yield of chicken skin gelatine

The yield of chicken skin gelatine (CSG) extraction (ξ) was calculated using the formula:

$$\xi = \frac{m_1}{m_0} \cdot 100\ (\%)$$

where m_1 is weight of dried CSG (g) and m_0 is weight of dried chicken skin (g) after separation of pigments, fats and non-collagenous proteins.

Chicken skin gelatine gel strength

CSG gel strength was determined according to the method described at GMIA – Standard Testing Methods for Edible Gelatine (GMIA, 2019) as follows: 7.5 g of CSG was mixed with 105 ml of distilled water in a standard Bloom vessel, allowed to swell at room temperature from 1 to 3 h and then heated in a water bath at 65 °C. 6.67% gelatine solution was obtained, cooled at room temperature and placed into a refrigerator for 16–18 h to form gelatine gel. The temperature was set to 10 °C. After that, gelatine gel strength was measured using the texture analyser. Gel strength is defined as a force (weight in g) required to depress a plunger by penetration speed of 1 mm/s on the surface of the gelatine gel sample to the distance of 4 mm. The analyses were repeated three times and arithmetic mean with the standard deviation was used to express the results.

Viscosity of chicken skin gelatine

Viscosity of CSG solution was established according to GMIA (2019): 6.67% gelatine solution was prepared following the same method as mentioned above and transferred into the viscosity pipette, placed inside the thermometer and the temperature of 60.00 ± 0.05 °C was set. Time required for 100 ml of gelatine solution to pass through the capillary tube of the pipette was measured and kinematic viscosity of the gelatine sample was calculated according to the formula:

$$\eta = \left(k \cdot t - \frac{B}{t}\right) \cdot \rho$$

where η is dynamic viscosity (mPa.s); k is viscosity constant (0.5); t is arithmetic mean of measured flow times (s); B is correction constant for kinetic energy (2.8) and ρ is chicken skin gelatine solution density (g/cm^3). Density of CSG solution was 1.003 g/cm^3 ± 0.005 determined by pycnometric method. The analyses were repeated three times and arithmetic mean with the standard deviations was used to express the results.

Statistical analysis

Statistical analysis were calculated using Minitab 18 (Fujitsu Ltd., Japan); one-way ANOVA at the significance level of *p* 0.05.

RESULTS AND DISCUSSION

Results of all experiments and extraction conditions are shown in Table 1. The yield of chicken skin gelatine (CSG) was in the range from 14.1 to 19.8%, with the highest yield obtained in experiment no. 8. CSG gel strength ranged from 126 to 182 Bloom with the highest value achieved in experiment no. 1. The viscosity of CSG solution varied between 2.06 and 4.40 mPa.s with the highest value recorded in experiment no. 8.

Table 1 The schedule and results of all experiments

Exp. No.	Extraction temperature (°C)	Extraction time (min)	Yield of CSG (%)	CSG Gel strength (Bloom ± SD)	Viscosity of CSG (mPa.s ± SD)
1	50	30	16.8	190 ± 3.1	2.06 ± 0.21
2	60	30	17.5	187 ± 2.9	2.18 ± 0.31
3	70	30	14.1	163 ± 2.8	3.38 ± 0.27
4	80	30	15.0	162 ± 2.5	3.54 ± 0.25
5	50	120	17.1	182 ± 3.1	2.53 ± 0.21
6	60	120	18.1	145 ± 2.7	3.01 ± 0.29
7	70	120	19.3	129 ± 2.9	3.91 ± 0.28
8	80	120	19.8	126 ± 3.0	4.40 ± 0.35

Yield of chicken skin gelatine

Figure 1 Effect of extraction temperature and time on the yield of chicken skin gelatine (contour plot)

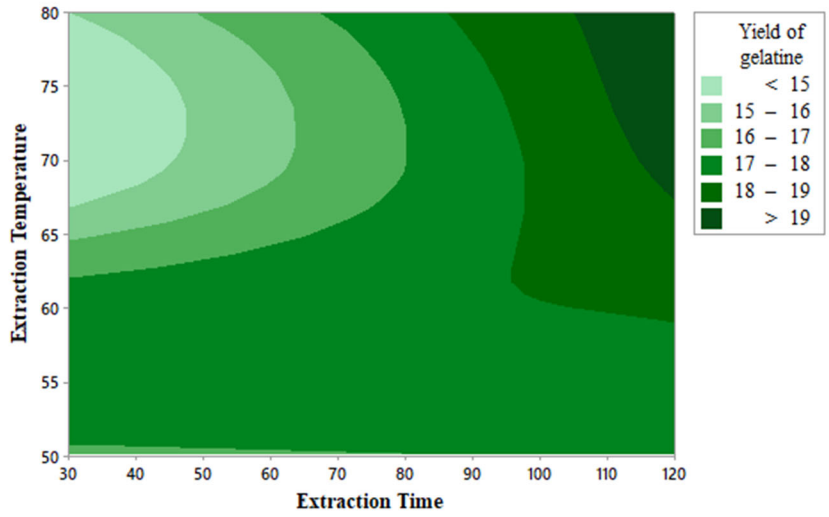

Figure 1 shows the effect of extraction temperature and time on the yield of chicken skin gelatine (CSG) extraction. In accordance with the hypothesis, the highest yield was obtained applying the highest extraction temperature and the longest extraction time since the most severe conditions cause more collagen molecules to be extracted. In contrast, the lowest yield was achieved using the shortest extraction time and highest extraction temperature. As can be seen, there is no noticeable increase in the yield of CSG at low extraction temperatures. The effect of extraction temperature on the CSG yield was not statistically significant ($p = 0.932$); similarly, the effect of extraction time ($p = 0.130$) was not statistically significant either. Sarbon et al. (2013) reported the yield of chicken skin gelatine of 16.1%, which is comparable with the result of experiment no. 1 in this study. Du et al. (2013) established a yield of gelatine extracted from poultry heads of 38%, which is significantly higher value than that achieved in this study, possibly due to a much longer extraction time (overnight).

Chicken skin gelatine gel strength

Figure 2 Effect of extraction temperature and time on the chicken skin gelatine gel strength

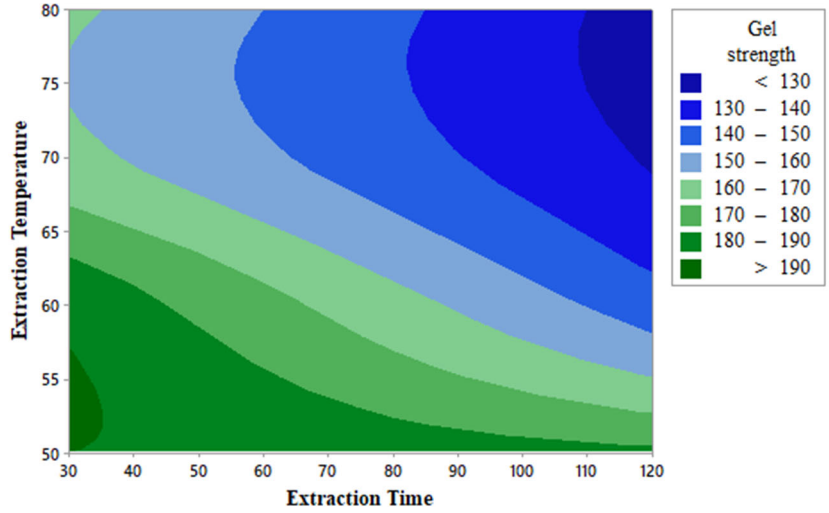

The strength of a gelatine gel (also the Bloom value) is a decisive factor in determining the quality of gelatine and therefore, directly affecting the price of gelatine. According to the Bloom value, gelatine is classified into low (<150 Bloom), medium (150–220) and high gel strength gelatine (220–300) (Johnston-Bank 1983). Gelatines prepared in experiments no. 1 to 5 meet the criterion for medium gel

strength gelatines. Figure 2 represents the effect of extraction conditions on the chicken skin gelatine (CSG) gel strength. As shown, the highest gel strength was obtained using the lowest extraction temperature and shortest extraction time, and conversely, the lowest strength using the highest extraction temperature and longest extraction time, which is consistent with the hypothesis. Mild extraction conditions seem to allow the extraction of higher molecular weight collagen chains resulting in the formation of stronger gel. Figure 2 also shows that both longer extraction time and higher temperature negatively affect the CSG gel strength. However, the influence of extraction temperature on the CSG gel strength was not statistically significant ($p = 0.074$) while the effect of extraction time was significant ($p = 0.028$). In the scientific literature, the gel strength of poultry gelatine was published in a wide range from 80 up to 526 Bloom. For comparison, the strength of beef or pork gelatines is between 200 and 240 (Widyasari and Rawdkuen 2014). Sarbon et al. (2013) stated the strength of CSG of 355 Bloom, which is considerably more than in this study. The difference may be the consequence of different extraction conditions (45 °C overnight). The gel strength of 80 Bloom of chicken thighs gelatine has been reported by Widyasari and Rawdkuen (2014) which, on the other hand, is less than in this study. The difference could be caused by different type of the raw material used.

Viscosity of chicken skin gelatine

Figure 3 Effect of extraction temperature and time on the viscosity of chicken skin gelatine solution

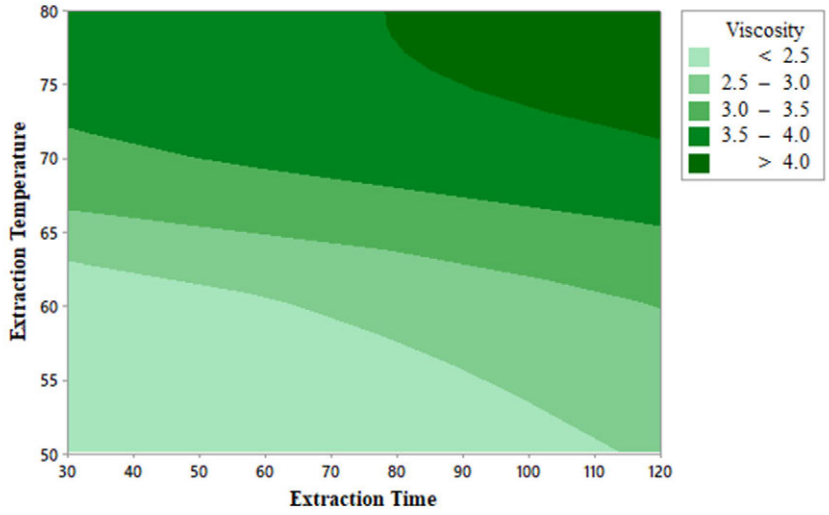

Viscosity of gelatine solution is the second most important parameter of gelatine. Figure 3 depicts the effect of extraction conditions on the viscosity of chicken skin gelatine (CSG) solution. As can be seen, mild extraction conditions cause a lower viscosity while an increased extraction temperature and prolonged extraction time result in a growing viscosity. This trend is in a true contrast to what was observed in the case of CSG gel strength, possibly due to better arrangement of higher molecular weight collagen chains resulting in less flow resistance. The effect of extraction temperature on viscosity of CSG was statistically significant ($p = 0.003$) as well as the effect of extraction time ($p = 0.007$). Sompie and Triasih (2018) determined the viscosity of CSG of 6.52 mPa.s, which is more than in this study. Bichukale et al. (2018) reported the viscosity of poultry skin and bone in the range of 3.83–9.10 mPa.s with the lowest values comparable with the results of experiments no. 4 and 7 in this study. The high viscosity of gelatine is desirable, for example, in the stabilization of food, pharmaceutical or photographic emulsions. In contrast, in the case of shaped products containing gelatine, e.g. in the confectionery, low-viscosity gelatine is preferred in order to avoid the tailing effect (Schrieber and Gareis 2007). The viscosity of commercial food grade gelatines ranges from 2.5 to 5.5 mPa.s and the viscosity recorded in 6 out of 8 experiments in this study was within this range.

CONCLUSION

Samples of chicken skin gelatines (CSG) were prepared using factorial design of experiments, and the influence of two key technological factors: extraction temperature (50, 60, 70 and 80 °C) and extraction time (30 and 120 min) on the CSG yield, gel strength and viscosity were investigated. The results showed that using the highest extraction temperature (80 °C) and the longest extraction time (120 min) resulted in the highest yield of CSG (19.8%). CSG prepared under these conditions performed the highest viscosity (4.40 mPa.s). In contrast, CSG prepared applying the lowest extraction temperature (50 °C) and shorter extraction time (30 min) performed the highest CSG gel strength (190 Bloom). Both increasing temperature and time during CSG extraction show a positive influence on its yield as well as on its viscosity, however, they negatively affect the gel strength. Therefore, the scientific hypothesis has been confirmed considering the CSG yield as well as gel strength; however, it has been refuted regarding viscosity. This research has shown that technological conditions of CSG extraction affect the final product, particularly its viscosity.

ACKNOWLEDGEMENTS

This research was financially supported by the Internal Grant Agency of the Faculty of Technology, Tomas Bata University in Zlín, ref. IGA/FT/2020/002.

REFERENCES

Bichukale, A.D. et al. 2018. Functional properties of gelatin extracted from poultry skin and bone Waste. International Journal of Pure & Applied Bioscience, 6(4): 87–101.

Du, L. et al. 2013. Physicochemical and functional properties of gelatines extracted from turkey and chicken heads. Poultry Science, 92: 2463–2474.

GMIA - Standard Testing Methods for Edible Gelatin. 2019.

Gomez-Guillen, M.C., Montero, P. 2001. Extraction of gelatin from megrim (Lepidorhombus boscii) skins with several organic acids. Journal of Food Science, 66: 213–216.

Johnston-Bank, F.A. 1983. From tannery to table: an account of gelatin production. Journal of the Society of Leather Technologists and Chemists, 68: 141–145.

Karim, A. Bhat, R. 2009. Fish gelatin: properties, challenges, and prospects as an alternative to mammalian gelatins. Food Hydrocolloids, 23: 563–576.

Khiari, Z. et al. 2017. Valorization of fish by-products: rheological, textural and microstructural properties of mackerel skin gelatines. Journal of Material Cycles and Waste Management, 19: 180–191.

Kittiphattanabawon, P. et al. 2016. Gelatin from clown featherback skin: extraction conditions. LWT Food Science and Technology, 66: 186–192.

Mrázek, P. et al. 2019. Chicken skin gelatine as an alternative to pork and beef gelatines. Potravinarstvo Slovak Journal of Food Sciences, 13(1): 224–233.

Niu, L. et al. 2013. Characterization of tilapia (Oreochromis niloticus) skin gelatine extracted with alkaline and different acid pre-treatments. Food Hydrocolloid, 33: 336–341.

Sarabia, A.I. et al. 2000. The effect of added salts on the viscoelastic properties of fish skin gelatin. Food Chemicals, 70(1):71–76.

Sarbon, N.M. et al. 2013: Preparation and characterisation of chicken skin gelatin as an alternative to mammalian gelatin. Food Hydrocolloids, 30: 143–151.

Schrieber, R., Gareis, H. 2007. Gelatine handbook: theory and industrial practice. Weinheim: Wiley VCH-Verl, pp. 348.

Sompie, M., Triasih, A. 2018. Effect of extraction temperature on characteristics of chicken legskin. In Proceedings of IOP Conference Series: Earth and Environmental Science 2017 Semarang, Indonesia, 26–27 September, 12089.

Widyasari, R., Rawdkuen, S. 2014: Extraction and characterization of gelatin from chicken feet by acid and ultrasound assisted extraction. Food Applied Bioscience Journal, 2: 85–97.

Sensory evaluation of hen's eggs with the addition of organic and inorganic selenium to the diet of laying hens

Sylvie Ondrusikova[1], Sarka Nedomova[1], Ondrej Stastnik[2], Leos Pavlata[2], Eva Mrkvicova[2]
[1]Department of Food Technology
[2]Department of Animal Nutrition and Forage Production
Mendel University in Brno
Zemedelska 1, 613 00 Brno
CZECH REPUBLIC

ondrusikova.sylva@seznam.cz

Abstract: The aim of this work was to monitor the sensory descriptors of boiled eggs from laying hens, which were given a basic feed mixture supplemented with organic and inorganic selenium. Sensory evaluation of eggs was performed at 41 weeks of laying, when 40 evaluators participated in the evaluation. A sensory questionnaire had ten descriptors were scored on unstructured 100 mm line scales and four descriptors related to defects or deviations were evaluated verbally. The questionnaires therefore contained these descriptors: shell peelability, albumen colour, yolk colour, albumen texture, yolk texture, albumen aroma, albumen aroma defects (yeast, sweet, sulfuric, buttery, rancid, or other), yolk aroma, yolk aroma defects (yeast, sweet, sulfuric, buttery, rancid, or other), albumen taste, albumen taste defects (yeast, sweet, sulfuric, buttery, astringent, metallic, rancid, or other), yolk taste, yolk taste defects (yeast, sweet, sulfuric, buttery, astringent, metallic, rancid, or other), overall impression. The peelability of the shell and the structure of the albumen are sensory parameters when we found a statistically significant difference. The other descriptors were without statistically significant differences. However, this result is considered positive, because in the case of a negative sensory manifestation, it can be taken up by humans in a bound form in the of hen's eggs.

Key Words: hen eggs, functional food, selenomethionine, sodium selenite, sensory analysis

INTRODUCTION

Hen eggs make up a significant part of consumers' diets, mainly due to their nutritional composition, as they are a source of high-quality protein, low in calories, but a rich source of vitamins, minerals, a are cheap and affordable raw material and can be consumed without religious and ideological differences (Pilarczyk et al. 2019). The nutritional properties are one of the factors that can be influenced in eggs by the composition of the feed mixture given to laying hens. Compound feeds can be modified with a number of ingredients, whether based on fat, minerals or antioxidants, and thus can affect not only the nutritional properties but also the quality parameters of eggs (Zduńczyk et al. 2013). In recent years, there has been a significant increase in the use of selenium supplements in the feed mixtures of laying hens (Borilova et al. 2020). The inorganic form of selenium in the form of sodium selenite and the organic form – selenomethionine are used for the modification of feed mixtures (Bityutskyy et al. 2019). Modification of compound feeds with selenium has proven to be very positive in many respects, as selenium is one of the fourteen trace elements necessary for animal health (Sayiner and Karagul 2017). Selenium is also an essential component of the enzyme glutathione peroxidase (GSH-Px) and in metabolism it is involved in the regulatory processes of hormones such as androgens, insulin, but also thyroid hormones (Li et al. 2019). However, selenium not only affects the health of laying hens, but also productivity, fatty acid composition, but also has a positive effect on the quality parameters of eggs (Čobanová et al. 2011), which is closely related to the nutritional composition and intake of selenium, as an essential element of human nutrition (Surai 2006). Because selenium is an essential microelement, the human body obtains it only through diet, where it plays a role in the correlation between selenium content and protein. Deficiency of this microelement in human nutrition correlates with an increased risk of some types of cancer and can lead to disruption of bone and tooth mineralization or participate in cardiomyopathy (Li et al. 2019). The human body is able

to absorb up to 80% of organic selenium from eggs. Rich sources of selenium are brazil nuts, viscera and seafoods. When using feed with the addition of selenium, the selenium content is reflected in the egg components, and thus nutritional enrichment in origin the so-called functional food (Čobanová et al. 2011, Buckiuniene et al. 2018). We can often also find the term enriched eggs, which means that a special feed was used for fattening laying hens, which increases the nutritional value of eggs compared to regular ones. Most often in the market network we can find eggs enriched with omega-3 fatty acids, iodine, but also selenium.

The aim of this study was to compare and sensory evaluate the eggs of laying hens fed mixtures with the addition of organic and inorganic selenium and to determine the extent to which selenium can affect the sensory descriptors.

MATERIAL AND METHODS

Animal and diet

Eggs of Lohmann Brown-Classic hybrids were used for sensory analysis, where the experiment was performed on 84 laying hens using a conventional deep litter system with wood shavings as a bedding material. The experiment was started at 33 weeks of age of laying hens and lasted until 41 weeks of age. Laboratory temperature, humidity and light regime were controlled according to Lohmann laying hen production recommendations (Lohmann Tierzucht 2020). The lighting system was set to a 16-hour and 8-hour dark light cycle. Laying hens were divided into three equal groups, with the first group being the control, in which the laying hens were fed with the mixture without the addition of selenium (selenium was contained only with the natural content in feed). The first experimental group of laying hens was fed a feed mixture with the addition of an organic selenium source (Sel-Plex – *Saccharomyces cerevisiae* CNCM I-3060) and the second experimental group of laying hens was fed with a mixture with the addition of an inorganic selenium source (Sodium selenite – Na_2SeO_3). In both experimental groups, selenium was supplied with its natural content in the feed (Table 1), but selenium was also added to give a total content of 0.31 mg/kg.

Table 1 Composition of diets

Components	Control	Organic Se	Inorganic Se
Maize [%]	33.339	33.339	33.339
Soybean meal [%]	31.000	31.000	31.000
Wheat [%]	19.000	19.000	19.000
Limestone grit [%]	5.400	5.400	5.400
Rapeseed oil [%]	4.000	4.000	4.000
Premix* [%]	3.000	3.000	3.000
Limestone milled [%]	2.500	2.500	2.500
Monocalcium phosphate [%]	1.300	1.300	1.300
Sodium chloride [%]	0.300	0.300	0.300
DL-Methionine [%]	0.160	0.160	0.160
L-Threonine [%]	0.001	0.001	0.001
Sel-Plex [%]	0.000	0.010	0.000
Sodium selenit [%]	0.000	0.000	0.001

*Legend: *Premix contains (per kg): L-Lysine 13 g; DL-Methionine 45 g; Calcium 295 g; Phosphorus 67 g; Sodium 46 g; Copper 300 mg; Iron 2,300 mg; Zinc 1,800 mg; Manganese 2,400 mg; Iodine 30 mg; Retinol 330,000 IU (international units); Calciferol 100,000 IU; Tocopherol 500 mg; Phylloquinone 40 mg; Thiamine 40 mg; Riboflavin 120 mg; Pyridoxin 54 mg; Cobalamin 400 ug; Biotin 3 mg; Niacinamid 420 mg; Folic acid 30 mg; Calcium pantothenate 250 mg; Cholin chloride 6,000 mg*

Three isocaloric and isonitrogenous diets were formulated according to the recommended nutrient content for Lohmann Brown-Classic hens (Lohmann Tierzucht 2020). The chemical composition of the diets was determined for dry matter, crude protein, crude fat, crude fiber and ash according to EC Commission Regulation (Commission Regulation (EC) 152/2009). The chemical composition of the diet is shown in Table 2. The health status of the laying hens was monitored daily and laying hens had free access to water and feed throughout the experiment.

Table 2 Chemical analysis of diets

Components	Control	Organic Se	Inorganic Se
Dry matter [%]	100.00	100.00	100.00
ME_N [MJ/kg]	11.47	11.47	11.47
Crude protein [%]	20.76	20.80	20.80
Ether extract [%]	6.27	6.50	6.34
Crude fibre [%]	2.21	1.55	1.97
Crude ash [%]	16.41	16.39	16.93
Ca [%]	4.57	4.57	4.57
P [%]	0.67	0.67	0.67
Se [mg/kg]	0.09	0.31	0.31

Legend: ME_N – Apparent metabolizable energy

Sensory analysis

Sensory analysis of boiled eggs was performed on eggs at 41 weeks of age of laying hens. Eggs were hand collected the day before sensory evaluation and stored at a non-fluctuating temperature at 4 °C overnight. The eggs were warmed to laboratory temperature (22 °C) for 3 hours and boiled in a water bath at 96 °C for 8 minutes. After heat treatment, was the egg immediately cooled in a water bath with a temperature of 15 °C, dried and sensory evaluation was performed immediately. The average weight of hen's eggs with addition was 60.63 ± 2 g. Sensory evaluation was performed at the Department of Food Technology of Mendel University in a laboratory designed for sensory evaluation according to ČSN EN ISO 8589:2007 (560036) and was attended by 40 evaluators. Each of the evaluators was given 1 egg from the group, ie 3 randomly selected eggs, which were marked with a randomly selected code. Pure water was provided as a taste neutralizer. The evaluators were given a questionnaire where ten descriptors were scored on unstructured 100 mm line scales and four descriptors related to defects or deviations were evaluated verbally in case of occurrence of any of the possibilities or other notices were added. In the questionnaire was the following descriptors: shell peelability (0 = poor, 100 = easy), albumen colour (0 = atypical, 100 = typical, white), yolk colour (0 = light, atypical, 100 = deep, intense), albumen texture (0 = very soft, brittle, 100 = very stiff, firm), yolk texture (0 = very soft, brittle, 100 = very stiff, firm), albumen aroma (0 = unpleasant, 100 = pleasant), albumen aroma defects (yeast, sweet, sulfuric, buttery, rancid, or other), yolk aroma (0 = unpleasant, 100 = pleasant), yolk aroma defects (yeast, sweet, sulfuric, buttery, rancid, or other), albumen taste (0 = unpleasant, 100 = pleasant), albumen taste defects (yeast, sweet, sulfuric, buttery, astringent, metallic, rancid, or other), yolk taste (0 = unpleasant, 100 = pleasant), yolk taste defects (yeast, sweet, sulfuric, buttery, astringent, metallic, rancid, or other), overall impression (0 = poor, 100 = excellent).

Statistical analysis

Statistical analysis of differences was based on Statistica12 (TIBCO, CA, USA), specifically single-factor ANOVA – Duncan's test. The statistically significant difference was considered to be a result whose probability value reached $p < 0.05$.

RESULTS AND DISCUSSION

Ten descriptors were sensory evaluated in boiled hens' eggs from laying hens fed mixtures with the addition of organic and inorganic selenium (Table 3). The same sensory evaluation was performed on eggs without the addition of selenium, where these eggs served as a control group. Shell peelability is one of two descriptors where a statistically significant difference has been demonstrated.

The values of shell peelability ranged from 32.38 (control) to 53.78 (inorganic selenium). Eggs derived from laying hens with the addition of inorganic selenium showed a statistically significant difference compared to the control group and the group with the addition of selenium in organic form. The ease of peeling eggs is also attributed to the age of the eggs, when in all our groups the eggs were fresh. Since shell peelability is one of the descriptors that can be easily influenced by the human factor, that is, dexterity, no deeper interest has been attributed to this result. Studies of sensory analysis of boiled eggs and the addition of selenium usually do not provide a shell peelability descriptor.

Sensory analysis of fresh eggs in the evaluation of yolk and albumen colour did not show a statistically significant difference due to the addition of selenium to the feed mixture of laying hens. The same results were obtained in study by Konca et al. (2019), where the addition heat-treated hempseed did not affect the sensory parameters of the colour.

The values of albumen texture ranged from 51.70 (organic) to 63.73 (inorganic selenium). This is one of the reasons why sensory, ie subjective evaluation could show a statistically significant difference between individual groups. If we take into account the results of sensory evaluation, it can be said that the addition of selenium in inorganic form to feed mixtures of laying hens had a positive effect on the texture of egg albumen, the addition of selenium in organic form, which worsened it. Fasiangova et al. (2017) shows, that the addition of selenium in organic form has a positive effect on the qualitative parameters of eggs, more precisely on Haugh units, whose value increases. However, inorganic selenium is more widely saved in egg albumen, where it can also play an important role and positively influence quality parameters, as demonstrated by our results in albumen texture. Buckiuniene et al. (2018) combined in their study the addition of inorganic and organic selenium together with the addition of sunflower and rapeseed oil, where this feed mixture fed to laying hens did not show a negative effect on the textural properties of boiled eggs in sensory evaluation.

The aroma and taste of either egg albumen or yolk can affect the oxidative processes that occur in eggs. Similar to our experimental findings of egg aroma and taste shows results Konca et al. (2019), when the addition heat-treated hempseed of additives to feed mixture laying hens was not statistically confirmed for taste or aroma parameters.

For the parameter of overall impression, the sample with the addition of organic selenium was evaluated the best and the worst was the control sample. The values ranged from 71.55 to 77.50, but the differences were not assessed as statistically significant.

Fasiangova et al. (2017) state that by adding selenium to the feed mixtures of laying hens, there are also changes in eggs, where selenium contributes to the reduction of lipid and protein oxidation, which can lead to a longer storage time. This idea could be the subject of further research.

Table 3 Sensory descriptors evaluated in hens' boiled eggs divided into groups according to the type of addition of selenium to compound feed

Descriptors	Control	Organic Se	Inorganic Se
Shell peelability	$32.38^{a} \pm 23.55$	$36.88^{a} \pm 25.35$	$53.78^{b} \pm 32.06$
Albumen color	$85.08^{a} \pm 13.26$	$84.73^{a} \pm 15.13$	$83.78^{a} \pm 14.94$
Yolk color	$34.51^{a} \pm 17.53$	$36.63^{a} \pm 18.38$	$36.78^{a} \pm 18.14$
Albumen texture	$57.33^{a, b} \pm 24.17$	$51.70^{a} \pm 23.99$	$63.73^{b} \pm 20.02$
Yolk texture	$44.38^{a} \pm 21.87$	$47.92^{a} \pm 23.06$	$48.85^{a} \pm 22.29$
Albumen aroma	$74.38^{a} \pm 21.72$	$79.25^{a} \pm 17.82$	$77.75^{a} \pm 20.65$
Yolk aroma	$77.95^{a} \pm 19.06$	$83.70^{a} \pm 13.98$	$82.85^{a} \pm 15.84$
Albumen taste	$77.00^{a} \pm 20.63$	$82.50^{a} \pm 16.23$	$82.08^{a} \pm 16.32$
Yolk taste	$78.20^{a} \pm 19.06$	$78.95^{a} \pm 18.43$	$80.25^{a} \pm 16.82$
Overall impression	$71.55^{a} \pm 21.92$	$77.50^{a} \pm 15.36$	$75.85^{a} \pm 18.74$

Legend: $^{a, b}$ – different superscripts in a line indicate a statistically significant difference at $p < 0.05$

The sensory questionnaires were expanded by 4 descriptors, where the evaluators could verbally express defects and deviations in the taste and smell of egg white and yolk. The results of this extension are shown in Table 4. Due to the rare occurrence of these deviations, no statistical evaluation was performed. Among the most common variations in smell and taste was sweet, which was more often associated with yolk, but was mentioned at least once for each parameter. Other variations were buttery and sulfuric, which are rather typical substances due to the fat content of the yolk and sulfuric in the eggs, as well as astringent, metallic, salty, sour, bitter, poultry and plant. In two cases, the aroma of egg albumen also showed a yeast aroma, but not only in the organic form of the addition of selenium, which could be expected, but also in the control group, so this observation was not given significant weight.

Table 4 Sensory descriptors evaluated some deviations of hens' boiled eggs divided into groups according to the type of addition of selenium to compound feed

Descriptors	Control	Organic	Inorganic
Albumen aroma defects	sweet	sweet	sweet
	yeast	yeast	buttery
	sulfuric	sulfuric	sulfuric
Yolk aroma defects	sweet	sulfuric	sweet
	buttery	buttery	buttery
	poultry	poultry	sulfuric
		plant	
Albumen taste defects	sweet	sweet	sweet
	astringent	buttery	buttery
		sulfuric	sulfuric
		metallic	astringent
		salt	
Yolk taste defects	sweet	sweet	sweet
	buttery	sulfuric	yeast
	astringent	buttery	sulfuric
	bitter	bitter	astringent
	sour	salt	metallic
	salt		

CONCLUSION

The effect on sensory properties of boiled eggs from hens fed with different addition of selenium was followed. The results of our study show a statistically significant difference that was found in the descriptor of shell peelability and albumen texture. The peelability of the shell is a descriptor that is strongly influenced by the human factor, so no relevance is given to this result. The other descriptors were without significant statistical differences, where this result is taken positively, because the human population suffers from a lack of selenium intake and due to the fact that it does not manifest itself in a negative direction in sensory evaluation, we can receive it in eggs from laying hens, which was enriched feed mixture with this essential element.

ACKNOWLEDGEMENTS

The research was financially supported by the Internal Grant Agency of Faculty of AgriSciences no. AF-IGA2020-TP012 „The influence of feeding selected phytoaditives on meat quality of broiler chickens“.

REFERENCES

Bityutskyy, V. et al. 2019. Effects of Different Dietary Selenium Sources Including Probiotics Mixture on Growth Performance, Feed Utilization and Serum Biochemical Profile of Quails. In Modern Development Paths of Agricultural Production. Cham: Springer, pp. 623–632.

Borilova, G. et al. 2020. Effects of selenium feed supplements on functional properties of eggs. Journal of Food Science and Technology, 57(1): 32–40.

Buckiuniene, V. et al. 2018. Effect of sunflower and rapeseed oil, organic and inorganic selenium and vitamin e in the diet on yolk fatty acids profile, malondialdehydes concentration and sensory quality of laying hens eggs. Veterinarija IR Zootechnika, 76(98).

Commission regulation (EC) 152/2009. Laying down the methods of sampling and analysis for the official control of feed. Brussels: The commission of the European Communities.

ČSN EN ISO 8589:2007 (560036). Senzorická analýza: Obecné pokyny pro uspořádání senzorického pracoviště. 2. Praha: Český normalizační institut.

Čobanová, K. et al. 2011. Effects of dietary form of selenium on its distribution in eggs. Biological Trace Element Research, 144(1–3): 736–746.

Fasiangova, M. et al. 2017. The effect of dietary Se supplementation on the Se status and physico-chemical properties of eggs–a review. Czech Journal of Food Sciences, 35(4): 275–284.

Konca, Y. et al. 2019. Effects of heat-treated hempseed supplementation on performance, egg quality, sensory evaluation and antioxidant activity of laying hens. British Poultry Science, 60(1): 39–46.

Li, L. et al. 2019. Effects of dietary supplementation of selenium enriched yeast on egg selenium content and egg production of north china hens. Pakistan Journal of Zoology, 51: 49–55.

Lohmann Tierzucht. 2020. Management guide. Available at: http://www.ltz.de/en/e-guide/new_e-guide/HTML/

Pilarczyk, B. et al. 2019. Eggs as a source of selenium in the human diet. Journal of Food Composition and Analysis, 78: 19–23.

Sayiner, S., Karagul, H. 2017. Blood selenium and vitamin E levels in Heifers: Regional and seasonal differences in Northern Cyprus. Pakistan Journal of Zoology, 49(2): 669–676.

Surai, P.F. 2006. Selenium in nutrition and health. Nottingham: Nottingham University Press.

Zduńczyk, Z. et al. 2013. The effect of dietary vitamin E and selenium supplements on the fatty acid profile and quality traits of eggs. Archives of Animal Breeding, 56(1): 719–732.

Relationship between pH values and electrical conductivity, their usability in chicken breast meat evaluation as marker post mortal quality

Oleksandra Ovchynnikova[1], Lucie Grossova[1], Nikol Snupikova[1], Ondrej Stastnik[2], Miroslav Juzl[1]
[1]Department of Food Technology
[2]Department of Animal Nutrition and Forage Production
Mendel University in Brno
Zemedelska 1, 613 00 Brno
CZECH REPUBLIC
xovchynn@mendelu.cz

Abstract: The meat quality parameters measured in carcass production at slaughterhouses tend to be essential for the control of its overall quality. In this experiment, two different groups of poultry, commercial broilers Ross 308 (n=24) and Lohmann Brown-Classic hens (n=24) in 3 independent batches (A, B, C) were used for pH and electric conductivity (EC) measurement at different times (45 and 180 minutes) after slaughter. Experiment was based on monitoring the dependence and applicability of pH and electric conductivity methods. There was found statistical difference ($P < 0.05$) between pH values and electrical conductivity between broilers and hens after slaughter. Differences were confirmed in both two times of measuring (45 and 180 min), which allows the use of both of them, without the risk of delay in control process of poultry in slaughterhouse. There was no statistical difference ($P > 0.05$) between pH values and electrical conductivity between independent batches, this showed the independence of these markers on the selected external factor. The last hypothesis of the experiment, that there is no difference ($P > 0.05$) between the first and second measurement of pH and electrical conductivity between groups and batches, was confirmed. Averagely strong negative relationship was determined between pH and EC in times 45 and 180 minutes, only in broiler group ($r = -0.61^*, -0.74$). Correlation increased in time, so using of a later measurement time (180 minutes) for pH or electrical conductivity is possible, and even more advantageous.

Key Words: pectoralis major, sensor, impedance, water holding capacity, carcass, hens, broiler

INTRODUCTION

Despite the fact that chicken meat is a food commonly and intensively consumed worldwide, very few investigations have been aimed at characterizing chicken muscle and post mortal processes and, in most of these studies, chickens are mainly regarded as animal models (D'Alessandro and Zolla 2013). The main factors determining poultry meat quality include appearance, texture, juiciness, wateriness, firmness, tenderness, odour and flavour. There are the most important and perceptible meat features that influence the initial and final quality judgment by consumers before and after purchasing a meat and meat product. The quantifiable properties of chicken meat such as water holding capacity, shear force, drip and cook loss, pH, shelf life and others are indispensable for processors involved in the manufacture of value added those products (Mir et al. 2017).

The applicability of a particular method should be considered due to the usability of the results. In that case, a closer research of the use of the method in laboratory as well as operational conditions within the process control is needed (Zia et al. 2020). One of the important method is pH measuring (Glamoclija et al. 2015). The importance of pH as an indicator of poultry meat quality has been extensively studied, which is more useful for measuring breast (pectoral muscle) than for thigh muscles. Most studies report that low pH values of poultry meat are associated with lower meat water holding capacity, as in PSE (pale, soft, exudative) pork meat (Li et al. 2020). Sandercockl et al. (2001) reported that low pH values of breast muscle show lower losses of meat juice by dripping, which may lead to higher meat water holding capacity. In some experiments (Li et al. 2020, Siekmann et al. 2018, Mueller et al. 2020) the relationship between higher pH values in the pectoral muscle and lower loss

of meat juice (drip loss) are described, which is related to higher meat water holding capacity. After animal slaughter, biochemical changes, causing the conversion of muscle to meat, determine overall meat quality. The water content increase in meat, enhancing tenderness, juiciness, firmness, and appearance, affect the quality and economical value of meat. *Post mortem* carcass temperature has profound effect on *rigor mortis* and the physicochemical changes observed in PSE muscles. It is attributed to *post mortem* glycolysis, temperature, and pH (Mir et al. 2017). PSE meat is defined by various criteria, depending on the authors, what time after slaughter and what limit they set for their experiment. For pH values is pH_1 defined as first time (15, 30, 45 or 60 min) and pH_{ult} values as time, when the pH values no longer change (24, 48 hours).

In poultry, values of a shorter time interval are used (pH_1 in range 15-45 min), compared to pork (pH_1 in 45–60 min, pH_{ult} in 24 hours) or beef (pH_{ult} in 48 hours) (Glamoclija et al. 2015, Mir et al. 2017). Parameter pHult ($pH \geq 6.2$) are linked to the DFD meat (dark, firm, dry), which is a problem of animal exhaustion before slaughter and is related to welfare. The main disadvantage of pH and electric conductivity methods, however, is the destructiveness of the measurement, ie. muscle failure when punctured by electrodes. And this causes the sample to be discarded for sale, used in processing plants for sausage production, this is particularly the case for poultry. The applicability of methods for assessing meat quality is summarized in detail by various authors. In the review of Zia et al. (2020), they described the examples of such an evaluation. Although it is not possible to meet all the requirements, there is great interest in the development of fast, non-destructive and non-contact scanning technology (Beibei et al. 2017).

The electric conductivity (EC) of meat, as well as pH method, is influenced by many factors. As it has been reviewed, animal management, transportation and the slaughter process itself at the abattoir level significantly influence the conversion of muscle to meat, its tenderness and ultimately meat quality (D'Alessandro and Zolla 2013). The pH values of poultry meat range from 5.2 to 7.0 (Beibei et al. 2017). Conductivity measurements (in µS/cm or mS/cm) of food systems are of high interest because they are related with food characteristics such as free water and salt content (García-Breijo et al. 2008). Fischer et al. (2002) described pork meat samples with electrical conductivity EC > 5.0 mS/cm as PSE meat. Conductivity measuring devices are very similar to a pH meter, with the same advantages or disadvantages, they have been used more in the past, where PSE meat was examined in more details (Mitchell and de Alwis 1989). Compared to that, electrical impedance has a potential to detect the chilling stage of storage so as to control quality traits in porcine meat (Leng et al. 2020). According to literature (Janisch et al. 2011, Qu et al. 2017, Zheng et al. 2020), the relationship between the pH and electric conductivity should be conclusive and negative (with high correlation coefficient). The aims of the study were to investigate how the trend to different groups of poultry (broilers, hens) in combination with independent factor, and study of relationships between pH and electrical conductivity.

MATERIAL AND METHODS

Material

The animal procedures were reviewed and approved by the Animal Care Committee of Mendel University in Brno and by the Ministry of Education, Youth and Sports (MSMT- 22771/2019-3). The trial was performed with two different groups of poultry. Commercial broilers (n=84) Ross 308 (R308 Bro) and Lohmann Brown-Classic hens (n=84) (LBC Hens) was divided into 3 batches (A, B, C). Differences between the batches are due to the feed additives in the last phase of the feeding. Experiment was based on monitoring the dependence and applicability of pH and electric conductivity methods. Therefore, all three batches were considered as independent unchanging groups, which aimed to simulate the independence of the groups as in slaughterhouse during carcass processing. A conventional deep litter system was used with wood shavings as the bedding material. Room temperature, humidity and lighting regime were controlled according to the requirements for the Lohmann hens and Ross 308 broilers standard breeds. The health status of animals was evaluated daily and live weight was measured regularly during the trial. Poultry had free access to feed and water. At the end of the experiment, all animals were weighed, and 8 birds were randomly selected from each batch and slaughtered by decapitation.

Measurement of pH and electric conductivity

The main physical traits of *pectoralis major* were evaluated. Values of pH and electrical conductivity (mS/cm) as the main quality markers of meat, were determined by the electrode puncture into the pectoral muscle and were measured in three batches of two different groups of poultry (n=8). The pH_1 values were measured in 45 and 180 minutes *post mortem* with a pH portable meter Knick PORTAVO 907 multi pH (Knick, Berlin, Germany) at the laboratory, after its calibration (buffers for pH7 and pH4). Electric conductivity was measured (mS/cm) with a Fleischtester LF 191/F (WTW, Weilheim, Germany) using a special device for calibration on KCl buffer (c = 0.01 mol/l). Each muscle sample was measured by a puncture with pH probe (left breast) and electric conductivity probe (right breast) in two different places (measure 1 and measure 2).

Statistical analysis

Statistical analysis was performed using STATISTICA 12 CZ software (StatSoft, Prague, Czech Republic). All data were expressed as the mean ± standard error of the mean and were compared by one-way ANOVA. Significant difference was determined with using probability test (Tukey's HSD test) on level $P \leq 0.05$, and both methods were subjected to Pearson correlation coefficients.

Hypothesis No. 1 of the experiment: there is no statistical difference ($P > 0.05$) between pH values and electrical conductivity between broilers and hens after slaughter.

Hypothesis No. 2 of the experiment: at there is no statistical difference ($P > 0.05$) between pH values and electrical conductivity between batches.

Hypothesis No. 3 of the experiment: there is no difference ($P > 0.05$) in the pH and electrical conductivity measurement in the time 45 or 180 minutes after slaughter.

Hypothesis No. 4 of the experiment: there is no difference ($P > 0.05$) between the first and second measurement of pH and electrical conductivity between groups and batches.

RESULTS AND DISCUSSION

The results measured for different groups of animals (hens and broilers) and within independent groups of samples (different batches - A, B, C) are shown in Table 1. Between batches there were no differences ($P > 0.05$) in both groups.

Table 1 The pH and electric conductivity values (mean ± SD) as meat quality parameters measured at different times (45 and 180 minutes) post mortem in groups of broilers (R308 Bro) and hens (LBC Hens)

Parameter	R308 Bro			LBC Hens			All groups (n=48)
	Batch A (n=8)	Batch B (n=8)	Batch C (n=8)	Batch A (n=8)	Batch B (n=8)	Batch C (n=8)	
pH_{45}	6.10±0.09^{a}	6.13±0.09^{a}	6.22±0.05^{a}	6.58±0.12^{b}	6.63±0.14^{b}	6.59±0.15^{b}	6.37±0.05
pH_{180}	5.74±0.06^{a}	5.81±0.06^{a}	5.85±0.04^{a}	6.11±0.09^{b}	6.20±0.11^{b}	6.15±0.09^{b}	5.98±0.04
ΔpH^2	0.17±0.06^{b}	0.11±0.02^{a}	0.15±0.04^{b}	0.26±0.06^{c}	0.21±0.06^{c}	0.25±0.10^{c}	0.19±0.03
EC_{45} (mS/cm)	2.89±0.25^{a}	2.92±0.28^{a}	2.41±0.27^{a}	1.75±0.21^{b}	1.73±0.13^{b}	1.77±0.08^{b}	2.24±0.11
EC_{180} (mS/cm)	4.29±0.38^{a}	4.49±0.52^{a}	3.55±0.39^{a}	3.35±0.42^{b}	3.19±0.26^{b}	2.89±0.26^{c}	3.63±0.17
ΔEC^2 $(mS/cm)^2$	2.25±0.58^{a}	3.39±0.97^{b}	1.58±0.47^{a}	3.33±1.46^{b}	2.46±0.70^{a}	1.86±0.97^{a}	2.48±0.37

Legend: R308 Bro - commercial broilers Ross 308 (n=24), LBC - Hens Lohmann Brown-Classic hens (n=24); SD – standard deviation of mean, ΔpH^2 and ΔEC^2 show quadratic difference between measurements at 45 and 180 minutes; ^{a,b,c} - different superscript in the row show statistically significant difference ($P < 0.05$)

The pH values showed lower variability, than the electrical conductivity values in both groups of animals. The hypothesis of independence between pH values and electrical conductivity between broilers and hens after slaughter was rejected ($P < 0.05$). Significantly higher ($P < 0.05$) pH values

(Figure 1) in different measuring times (45 and 180 minutes, respectively) were recorded in hens (6.59 ± 0.07, and 6.15 ± 0.05 resp.) than in broilers (6.15 ± 0.04, and 5.8 ± 0.03 resp.). As one of the few works in which there is electric conductivity as carcass/meat quality method, experiment of Janisch et al. (2011) reported pH_{ult} values between 5.91 and 5.93, depending on different broiler production lines. There are higher values for electrical conductivity, as well as higher variability (6.13 to 8.13 mS/cm) depending on the production group of broilers given by the genetic factor (Siekmann et al. 2018, Mueller et al. 2020).

Figure 1 Expression of pH and electric conductivity in different groups of animals (R308 Bro) and hens (LBC Hens) during measurement times 45 and 180 minutes (x ± SD)

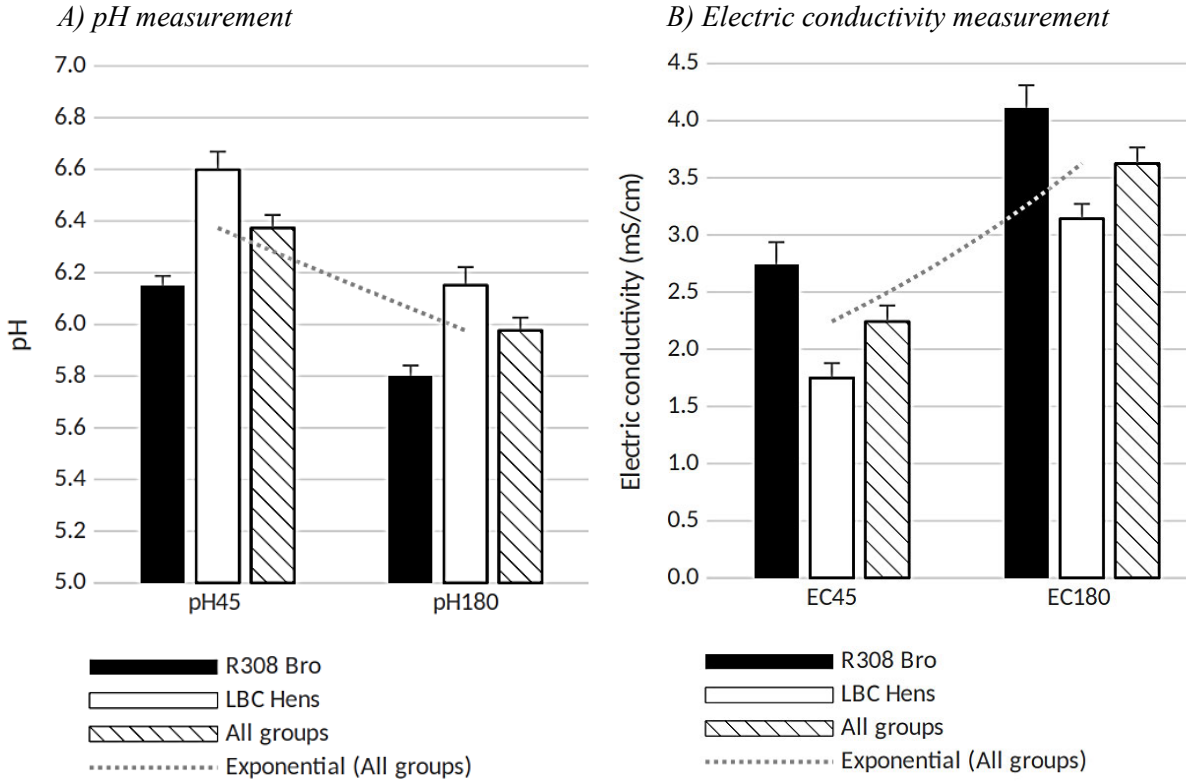

Legend: R308 Bro – commercial broilers Ross 308 (n=24), LBC – Hens Lohmann Brown-Classic hens (n=24); error bars are expressed by SD

Pearson correlation between groups is counted and presented in Table 2.

Table 2 Pearson correlation between pH and electric conductivity measured at different times (45 and 180 minutes) post mortem in groups of broilers (R308 Bro) and hens (LBC Hens)

	R308 Bro (n=24)			LBC Hens (n=24)		
	pH_{180}	EC_{45} (mS/cm)	EC_{180} (mS/cm)	pH_{180}	EC_{45} (mS/cm)	EC_{180} (mS/cm)
pH_{45}	0.67*	-0.61*	-0.81*	0.82*	-0.12	-0.46*
pH_{180}		-0.72*	-0.74*		0.00	-0.32
EC_{45} (mS/cm)			0.83*			0.45*

*Legend: R308 Bro – commercial broilers Ross 308 (n=24), LBC – Hens Lohmann Brown-Classic hens (n=24); SD – standard deviation of mean, ΔpH^2 and ΔEC^2 show quadratic difference between measurements at 45 and 180 minutes; *– superscript show statistically significant difference ($P < 0.05$)*

There were detected differences in both methods´ measurement between groups in measurement times, and it is not necessary to measure ultimate pH and electrical conductivity at 24 *post mortem* (Janisch et al. 2011). On the other hand, measurement at 24 hours *post mortem* is not suitable for poultry for operational reasons in slaughter lines, as is the case for quality control of pig carcasses (Qu et al. 2017). The results presented in this experiment (Tables 1 and 2, and Figure 1), confirmed

the possibility of using measurements of both methods (pH and electric conductivity) and at both times for broilers during operating conditions (Mir et al. 2017).

The first and third hypotheses of this experiment were rejected ($P < 0.05$) and the second and fourth were confirmed ($P > 0.05$). Nevertheless, parameters such as pH, electrical conductivity, and others (WHC; loss of meat juice by dripping, cook loss), texture (strength), colour (L*, a*, b*, C*, h°) and results obtained chemically (dry matter, protein, fat content) or microbiological quality (CFU, presence of typical groups of micro-organisms) cannot be relevantly and practically used by the average consumer (Mueller et al. 2020). Their role in the meat quality assessment is crucial for the possibility of controlling procedures and processes or controlling batches of animals delivered to slaughterhouses (Mir et al. 2017).

CONCLUSION

Parameters such as pH, electrical conductivity, could be relevantly and practically used by the producers and in control process at slaughterhouses for chicken meat quality. Better Differences were confirmed in both two times of pH and electric conductivity measurement. There were no differences between pH values and electrical conductivity between independent batches, this showed the independence of these markers on the selected external factor. The last hypothesis of the experiment, that there is no difference between the first and second measurement of pH and electrical conductivity between groups and batches, was confirmed. In broiler´s group, strong negative correlation was determined between pH and EC in times 45 and 180 minutes. Correlation increased in time, so using of a later measurement time for pH or electrical conductivity is possible, and even more advantageous.

ACKNOWLEDGEMENTS

The research was financially supported by the Internal Grant Agency of Faculty of AgriSciences Mendel University in Brno No. AF-IGA2020-TP012.

REFERENCES

Beibei, J. et al. 2017. Prediction of pH of fresh chicken breast fillets by VNIR hyperspectral imaging. Journal of Foof Engineering [Online], 208: 17–45. Available at: https://www.sciencedirect.com/science/article/pii/S0260877417301188. [2020-31-08].

D'Alessandro, A., Zolla, L. 2013. Meat Science: From proteomics to integrated omics towards system biology. Journal of Proteomics [Online], 78: 558–577. Available at: https://doi.org/10.1016/j.jprot.2012.10.023. [2020-09-01].

Fischer, K. et al. 2002. Variation of pork quality with ultimate pH out of the ordinary. Fleischwirtschaft, 82: 118–121.

García-Breijo, E. et al. 2008. Development of a puncture electronic device for electrical conductivity measurements throughout meat salting. Sensors and Actuators A: Physical [Online], 148(1): 63–67. Available at: https://doi.org/10.1016/j.sna.2008.07.013. [2020-09-01].

Glamoclija, N. et al. 2015. The Effect of Breed Line and Age on Measurements of pH-value as Meat Quality Parameter in Breast Muscles (m. Pectoralis Major) of Broiler Chickens. Procedia Food Science [Online], 5: 89–92. Available at: https://www.sciencedirect.com/science/article/pii/S2211601X15001133. [2020-08-31].

Janisch, S. et al. 2011. Color values and other meat quality characteristics of breast muscles collected from 3 broiler genetic lines slaughtered at 2 ages. Poultry Science [Online], 90(8): 1774–1781. Available at: https://doi.org/10.3382/ps.2010-01073. [2020-09-01].

Leng, Y. et al. 2020. Electrical impedance estimation for pork tissues during chilled storage, Meat Science [Online], 161: 108014. Available at: https://doi.org/10.1016/j.meatsci.2019.108014. [2020-09-01].

Li, J. et al. 2020. Effects of Slaughter Age on Muscle Characteristics and Meat Quality Traits of Da-Heng Meat Type Birds. Animals [Online], 10(1): 69. Avialable at: https://www.mdpi.com/2076-2615/10/1/69. [2020-08-31].

Mir, N.A. et al. 2017. Determinants of broiler chicken meat quality and factors affecting them: a review. Journal of Food Science and Technology [Online], 54(10): 2997–3009. Available at: https://doi.org/10.1007/s13197-017-2789-z. [2020-09-01].

Mitchell, F.R.G., de Alwis A.A.P. 1989. Electrical conductivity meter for food samples. Journal of Physics E: Scientific Instruments [Online], 22, 8: 554–556. Available at: https://iopscience.iop.org/article/10.1088/0022-3735/22/8/004/meta. [2020-09-01].

Mueller, L. et al. 2020. Growth, carcass, and meat quality of 2 dual-purpose chickens and a layer hybrid grown for 67 or 84 D compared with slow-growing broilers. Journal of Applied Poultry Research [Online], 29(1): 185–196. Available at: https://doi.org/10.1016/j.japr.2019.10.005. [2020-09-01].

Qu, D. et al. 2017. Development of class model based on blood biochemical parameters as a diagnostic tool of PSE meat. Meat Science [Online], 128: 24–29. Available at: https://doi.org/10.1016/j.meatsci.2017.01.012. [2020-09-01].

Sandercockl, D.A. et al. 2001. Acute heat stress-induced alterations in blood acid-base status and skeletal muscle membrane integrity in broiler chickens at two ages: Implications for meat quality. Poultry Science [On-line], 80(4): 418–425. Available at: https://www.sciencedirect.com/science/article/pii/S0032579119411061. [2020-08-31].

Siekmann, L. et al. 2018. Carcass Quality, Meat Quality and Sensory Properties of the Dual-Purpose Chicken Lohmann Dual. Foods [Online], 7: 156. Available at: https://www.mdpi.com/2304-8158/7/10/156. [2020-08-31].

Zheng, A. et al. 2020. Stress Associated with Simulated Transport, Changes Serum Biochemistry, Postmortem Muscle Metabolism, and Meat Quality of Broilers. Animals [Online], 10: 1442. Available at: https://www.mdpi.com/2076-2615/10/8/1442. [2020-09-01].

Zia, Q. et al. 2020. Current analytical methods for porcine identification in meat and meat products. Food Chemistry [Online], 324: 126664. Available at: https://doi.org/10.1016/j.foodchem.2020.126664. [2020-09-01].

Potential use of cod liver oil in a pig diet: effects on the chemical, physical and sensory parameters of a bologna sausage

Marketa Piechowiczova, Tomas Komprda, Milena Matejovicova, Miroslav Juzl, Sarka Nedomova, Vendula Popelkova, Pavla Vymazalova, Sylvie Ondrusikova
Department of Food Technology
Mendel University in Brno
Zemedelska 1, 613 00 Brno
CZECH REPUBLIC

xpiechow@mendelu.cz

Abstract: The aim of the study was to substantially increase PUFA n-3 content in bologna sausage based on meat of pigs fed a diet fortified with 8% fish oil. The control group of pigs was fed a standard feed ration without any added oils. The addition of oil into the feed ration did not cause increasing the fat level in bologna sausage. Fatty acid profile was affected significantly. The amount of these acids: C16:0, C18:0 and C18:2n-6 was significantly lower ($p < 0.05$) for the experimental group. On the other hand, the amount of following acids: C20:5n-3, C22:5n-3 and C22:6n-3 was higher ($p < 0.05$). Overall, the content of SFA decreased and the PUFA n-6/PUFA n-3 ratio was significantly lower ($p < 0.05$). The addition of fish oil into the diet did not affect the oxidative stability of the product ($p > 0.05$). Results of an instrumental and sensory analysis have shown a significant difference ($p < 0.05$) between both groups, when the experimental group was evaluated as harder and less juicy. Colour changes was recorded for redness (a*) parameter, the experimental group shown higher values ($p < 0.05$). The addition of fish oil did not affect ($p > 0.05$) the flavour, nor the odour of the product.

Key Words: meat products, fish oil, fatty acids, EPA, DHA, functional food

INTRODUCTION

On the one hand, meat and meat products are an important source of proteins, some vitamins, and minerals, on the other hand, they are criticized as a significant source of fat with an unsuitable lipid profile. According to FAO (2010) the daily recommended fat intake should be between 30–35% of overall energy intake, 10% of it should be SFA, TFA up to 1%, PUFA 6–11% and the rest should consist of MUFA. The recommendations are also specified for the EPA and DHA intake, where AI (adequate intake) is 0.25 g/day. According to Simopoulos (2002), a diet with high content of PUFA n-6 supports the development of cancer and other cardiovascular, inflammatory, and autoimmune diseases. The n-6/ n-3 ratio in a western diet is 15.0–16.7 (Simopoulos 2002), however, Elvevoll and James (2000) recommend the ratio around 4.0–10.0. Wood et al. (2008) state that the n-6/ n-3 ratio is around 7.6 for pork meat with adipose tissue and 7.2 for lean meat. From this reason, there is an effort to improve the fatty acid profile in meat products. Peréz-Palacios et al. (2019) summarize improving options of the fatty acid profile for meat products as: enrichment of meat through a fodder, enrichment of meat products by a direct addition of PUFA, PUFA emulsification or microencapsulation. Vegetable oil (linseed oil, chia oil, perilla oil), fish oil or algae oil are most used as PUFA sources. However, according to USDA (2010), vegetable sources of PUFA n-3 are less significant than oils acquired from sea sources. Wood et al. (2008) summarize knowledge of meat quality with respect to the fatty acids composition that had been affected by a fodder. The fatty acid composition affects mainly the meat texture, its oxidative stability, taste, and colour. In most cases, according to Peréz-Palacios et al. (2019), when the diet of pigs was enriched by oils rich in PUFA, there was a problem with subsequent oxidation and sensory quality of meat products, mainly regarding dried meat products. The aim of the study was to substantially increase PUFA n-3 content in bologna sausage based on meat of pigs fed a diet fortified with 8% fish oil.; concurrently we presumed that the expected decrease of oxidative stability will not damagingly affect the sensory acceptance of the products.

MATERIAL AND METHODS

Material

12 hybrid-breed sows were used for the experiment: 50% Landrace x 50% Large White (Bioprodukt Knapovec, Ústí nad Orlicí, Czech Republic). In the age of 12 weeks, these sows were divided into two groups of 6 pieces. For the following 30 days, the C group (control group) was fed a standard compound feed (De Heus, Marefy, Czech Republic), the F group (experimental group) was fed the same feed compound with 8% addition (w/w) of fish oil (pharmaceutical cod liver oil. The analysis of fatty acids of used fish oil is shown in the Table 1. The experiment was conducted in compliance with the Czech National Council Act No. 246/1992 Coll. to protect animals from cruelty (amendment to the Act 255/2017 Coll.) After fattening, slaughter was performed, and the meat was processed in pilot plants (CZ 22067) at Department of Food Technology within Mendel University in Brno.

Table 1 Fatty acid profile of used cod liver oil (Jecoris aselli oleum)

Fatty acid	Content [wt %]	Fatty acid	Content [wt %]	Fatty acid	Content [wt %]	Fatty acid	Content [wt %]
14:0	4.6	18:2n-6	3.3	20:5n-3	10.4	MUFA	45.7
16:0	11.1	18:3n-6	0.8	22:4n-6	1.1	PUFA	34.7
16:1	10.4	18:3n-3	1.6	22:5n-3	1.9	n-6	7.2
17:0	1.0	20:1	15.8	22:6n-3	13.6	n-3	27.5
18:0	2.9	20:2n-6	1.0	22:6n-3	13.6	n-6/n-3	0.18
18:1n-9	19.5	20:4n-6	1.0	SFA	19.6		

6 sows were chosen to produce bologna sausage, three of each group. The other sows were used for the production of other meat products. Lean and fatty meat was used; no other meat (like beef) was added to the product. 10 kg of bologna sausage was produced from each individual piece. This amount was divided to three parts for the analysis and each part was analysed twice (n = 9; except the sensory analysis). The bologna sausage were produced using 4.3 kg of the lean meat, 3.7 kg of the fatty meat, 0.194 kg of the nitrite salting mixture, 1.75 kg of water (in the form of ice), 0.126 kg of the spicing mixture (Combi-Bologna Sausage; Masoprofit, Czech Republic) consisting of phosphates, antioxidant (ascorbic acid), ground black pepper and white pepper. The whole mixture was ground up using a vacuum cutter (Seydelmann, Stuttgart, Germany) into the form of the meat emulsion, filled into the polyamide casing (diameter of 60 mm) by a filler (HTS 150; Germany) and heat-treated at 85 °C for 10 min in a smoker (Bastramat, Arnsberg, Germany). The bologna sausage were vacuum-packed immediately after production and stored at 2 °C.

Chemical analysis and oxidative stability

The dry matter, protein, fat and salt content were specified. For total amount of protein was used the Kjeldahl method, the total fat content was analysed by Soxhlet extraction, the salt content was determined by Mohr method and the dry matter content was analysed gravimetrically (AOAC 2005).

Furthermore, the fatty acid profile was specified. The analysis was performed according to Komprda et al. (2017) with some modifications. The gas chromatograph Agilent 6890 with an autosampler (Agient Technologies, Wilmington, USA) was used for the separation of fatty acids methyl esters (FAMEs). A capillary chamber with dimensions of 20 m x 0.18 mm x 0.15 µm, ZB FAST FAME brand (Phenomenex, Torrance, California, USA) was used. The temperature of an injector was 250 °C. A gas ionization detector (temperature of 260 °C) was used for detection. The temperature programme was as follows: the start temperature was 80 °C, held for two minutes; 10 °C/min until 160 °C; 3 °C /min until 185 °C; 30 °C/min until 240 °C, held for two minutes. The carrier gas flow (N2) was 0.5 ml/min a split ratio 1:100. The NU-CHECK 455 – 16 FAME (NU-CHECK Prep, Inc., Elysian, Minnesota, USA) was used as an external standard for FAME identification.

The oxidative stability of the product was specified according to Jezek et al. (2019). The extent of lipid oxidation was specified by the determination of thiobarbituric acid reactive substances

(TBARS). The TBARS values were obtained by multiplication of optical density by the factor of 7.8. Oxidative products were quantified as equivalents of malondialdehyde (MDA, mg/kg).

Instrumental measurement

Sample colour was analysed pursuant to the CIELAB system (ISO/CIE 2019). Colour parameters were evaluated: L* (axis from black to white), a* (axis from green to red) and b* (axis from blue to yellow). The specifications were obtained using a spectrophotometer Minolta® CM-3500d (Konica Minolta, Osaka, Japan) in the D65 lighting mode, a slit of 8 mm, SCE. Colour was measured on 2 cm slices that was taken from the central part of the product. Samples were measured within 5 minutes of their cutting.

The hardness of sausage was measured by TIRATEST 27025 (TIRA GmbH, Germany). The cylindrical slices of the bologna sausage (height 2 cm) were used for determination of hardness by the MORS knife with a crosshead speed of 10 mm/min and penetration to 10 mm. The hardness was also measured by the compression using 50% compression rate with a crosshead speed of 50 mm/min using the cylindrical samples with a diameter of 1 cm and height of 1 cm. In the both method the hardness of the bologna sausage samples was measured in the edge and the centre.

Sensory analysis

The evaluation was ongoing under ČSN ISO 6658 (560050) condition (ÚNMZ, 2010). Samples were assessed by a 12-member trained panel consisting of researchers. For sensory analysis was selected 100mm non-structured line scale with a description of anchored points, where 0 is the sign for minimum (not perceived) and 100 for maximum perception. For the descriptors “saltiness”, “intensity of colour” and “hardness”, 50 was considered as the optimum value. Each sample was coded with a randomly selected three-digit number. Unsalted rolls and room temperature water were served as neutralizers. Two slices (1.0–1.5 mm thick) of each samples of the bologna sausage were served at room temperature on the white porcelain plate. The slices were taken from the central part of the product. On the beginning of the evaluation, sausage was assessed as a whole piece (acceptability of the overall appearance). Other descriptors were assessed in the cut (intensity of colour, appearance, and odour). The intensity of strength on the bite, juiciness, saltiness and overall taste acceptability were also evaluated.

Statistical analysis

Data were tested for normality by Shapiro–Wilk test. The differences between samples were analysed by either a Mann-Whitney U test or an analysis of variance (one-way ANOVA), including Tukey´s test ($p < 0.05$). STATISTICA 12 (StatSoft, USA) was used for statistical evaluation.

RESULTS AND DISCUSSION

Results of chemical analysis are stated in the Table 2. Even though the F group was fed the food with added oil, no significant differences ($p > 0.05$) in fat content were observed between the F group and the C group. Comparing to the control, fish oil in the food increased the protein content in bologna sausage ($p < 0.05$). Besides proteins, also NaCL content increased. Bryhni et al. (2002) also added fish oil to a compound feed but they did not state fundamental chemical parameters within their study. When adding fish oil into a meat product, the fat content in meat is obviously increasing in proportion to the dose of added oil (Cáceres et al. 2008); a consumer can perceive this as a negative factor.

The influence of fish oil in a pig fodder on the fatty acid content in bologna sausage was proven for some fatty acids (Table 3). Contents of myristic acid 16:0, stearic acid 18:0 and linoleic acid 18:2n-6 were reduced. On the contrary, the increase was recorded for EPA C20:5n-3 (twelve times higher), DPA C22:5n-3 (almost five times higher) and DHA C22:6n-3 (more than twelve times higher). The n-6/n-3 ratio decreased significantly ($p < 0.05$) to 2.57, this value corresponds with the recommendations according to Elvevoll and James (2000). Overall content of SFA ($p < 0.05$) also decreased, the content of MUFA was not affected by the addition of fish oil into a fodder ($p > 0.05$). Bryhni et al. (2002) confirm the increasing amount of DPA in sausages, the DHA level was not increased because of the low dose of added fish oil (0.2%, 0.4%). The amount of EPA was not monitored. According to Cáceres et al. (2008), direct addition of fish oil into bologna sausage increased the amount of MUFA and PUFA, furthermore, the n-6/n-3 ratio decreased to 2.54 for 6% of batch.

Table 2 Basic chemical analysis of bologna sausage according to different diets

Parameter	C ($\overline{x}$ ± SEM) [g/100g]	F ($\overline{x}$ ± SEM) [g/100g]
Protein	13.02 ± 0.45 [b]	14.47 ± 0.50 [a]
Fat	9.30 ± 2.03	7.07 ± 3.01
Dry matter	27.70 ± 2.04	27.69 ± 3.03
NaCl	2.10 ± 0.03 [b]	2.25 ± 0.02 [a]

Legend: C – standard diet, F – diet with 8% of fish oil; Values with different superscripts in the same rows means there are significant differences ($p < 0.05$).

Table 3 Fatty acid profile of bologna sausage according to different diets

Fatty acid	C ($\overline{x}$ ± SEM) [mg/100g]	F ($\overline{x}$ ± SEM) [mg/100g]	Fatty acid	C ($\overline{x}$ ± SEM) [mg/100g]	F ($\overline{x}$ ± SEM) [mg/100g]
C14:0	100.1 ± 10.1	86.4 ± 12.0	C20:4n-6	30.9 ± 4.1	14.8 ± 2.9
C16:0	1837.2 ± 181.9 [a]	1144.5 ± 175.0 [b]	C20:5n-3	5.0 ± 0.1 [b]	60.4 ± 5.4 [a]
C16:1	187.0 ± 21.5	167.2 ± 20.7	C22:4n-6	8.9 ± 0.7	8.9 ± 0.9
C17:0	34.4 ± 2.8	28.4 ± 5.3	C22:5n-3	10.2 ± 0.9 [b]	46.2 ± 5.1 [a]
C18:0	986.1 ± 81.9 [a]	549.6 ± 85.9 [b]	C22:6n-3	5.3 ± 0.5 [b]	108.1 ± 13.7 [a]
C18:1n-9	3197.4 ± 336.6	2018.9 ± 319.8	SFA	2957.8 ± 276.1 [a]	1809.0 ± 271.5 [b]
C18:2n-6	992.0 ± 76.1 [a]	620.1 ± 90.2 [b]	MUFA	3366.3 ± 357.9	2186.1 ± 340.3
C18:3n-6	11.1 ± 1.4	10.6 ± 1.3	PUFA n-6	1100.2 ± 86.2 [a]	686.0 ± 97.8 [b]
C18:3n-3	65.9 ± 5.5	50.1 ± 7.6	PUFA n-3	82.2 ± 7.1 [b]	264.8 ± 35.0 [a]
C20:2n-6	48.4 ± 3.9 [a]	25.6 ± 3.8 [b]	n-6/n-3	13.45 ± 0.23 [a]	2.57 ± 0.07 [b]
C20:3n-6	9.0 ± 0.8	6.1 ± 0.7			

Legend: C – standard diet, F – diet with 8% of fish oil; Values with different superscripts in the same rows means there are significant differences ($p < 0.05$).

The results in the Table 4 shows that oxidative stability of bologna sausage was not significantly different when comparing with the control ($p > 0.05$). The limitation of oxidative acceptability is 2.5 mg of MDA/kg (Zhang et al. 2019), the results of the oxidative stability did not affect the sensory analysis though. Bryhni et al. (2002) state that, in their case, results of the sensory analysis evaluating the oxidative stability was inconsistent.

Table 4 Oxidative stability of bologna sausage according to different diets

Parameter	C ($\overline{x}$ ± SEM) [MDA, mg/kg]	F ($\overline{x}$ ± SEM) [MDA, mg/kg]
Oxidative stability	2.18 ± 0.13	2.67 ± 0.23

Legend: C – standard diet, F – diet with 8% of fish oil; Values with different superscripts in the same rows means there are significant differences ($p < 0.05$).

When measuring the texture of bologna sausage (Table 5), it was observed that the addition of fish oil into a pig fodder increases hardness (in the both method - by MORS knife and by compression). A significant difference ($p < 0.05$) between the C and the F group was observed both in the centre and in the edge part of the product. The texture may change for direct addition depending on other used raw materials, Cáceres et al. (2008) used caseinates that increased the hardness of the product.

Results of the colour measurement of bologna sausage are stated in the Table 6. A statistically significant difference was proven ($p < 0.05$) in redness parameter (a*). In this case, the control group has a lower value of a*. When directly adding fish oil, the lightness of the product increases proportionally to the amount of added oil; a* value decreases (Cáceres et al. 2008). Vossen et al. (2017) did not observed any difference in colour parameters directly after slicing samples of dried hams made of pigs fed an algae oil.

Table 5 Instrumental measurement of texture of bologna sausage according to different diets

Parameter		C ($\overline{x}$ ± SEM) [N]	F ($\overline{x}$ ± SEM) [N]
Edge	Hardness: MORS knife	2.30 ± 0.16 ^{b}	3.87 ± 0.21 ^{a}
	Hardness: compression	23.60 ± 1.18 ^{b}	31.75 ± 1.98 ^{a}
Centre	Hardness: MORS knife	2.23 ± 0.15 ^{b}	3.93 ± 0.28 ^{a}
	Hardness: compression	26.16 ± 1.32 ^{b}	36.10 ± 1.40 ^{a}

Legend: C – standard diet, F – diet with 8% of fish oil; Values with different superscripts in the same rows means there are significant differences ($p < 0.05$).

Table 6 Instrumental measurement of bologna sausage colour according to different diets

Parameter	C ($\overline{x}$ ± SEM)	F ($\overline{x}$ ± SEM)
L*	67.7 ± 0.59	67.2 ± 0.71
a*	7.6 ± 0.28 ^{a}	7.9 ± 0.16 ^{b}
b*	9.7 ± 0.18	9.5 ± 0.17

Legend: C – standard diet, F – diet with 8% of fish oil; Values with different superscripts in the same rows means there are significant differences ($p < 0.05$).

Results of the sensory analysis of the bologna sausage are stated in the Table 7. A statistically significant difference was proven ($p < 0.05$) in the descriptors: strength on the bite (hardness), juiciness and saltiness. The results of the strength on the bite correspond to the instrumental measurement of hardness. The F group was evaluated worse than the control group in the descriptor: juiciness and hardness ($p < 0.05$). The flavour and odour of the F group and the C group were practically the same ($p > 0.05$). The evaluators didn't notice any off-flavours or oxidative changes. Vossen et al. (2017) reported neither fishy odour nor fishy flavour in dry-cured hams produced from pork of pigs fed a diet enriched with algae. However, LC-PUFA n-3 content was lower in the diet (1.2 g of algae/100 g feed). Bryhni et al. (2002) report that a small amount (0.4%) of fish oil in the feed did not affect the flavour or odour, but interacted with other PUFAs to produce a stale odour. The bologna sausages with direct addition of fish oil was generally acceptable for evaluators in all doses of 1–6% (Cáceres et al. 2008).

Table 7 Sensory analysis of bologna sausage according to different diets

Descriptor	C ($\overline{x}$ ± SEM)	F ($\overline{x}$ ± SEM)
Overall appearance (hedonic)	84.1 ± 4.2	89.3 ± 3.1
Cross-section colour (intensity, from dark to light)	74.6 ± 5.6	70.7 ± 7.3
Cross-section appearance (hedonic)	72.1 ± 6.2	73.5 ± 5.5
Odour (hedonic)	81.7 ± 4.2	78.1 ± 4.6
Strength on the bite (intensity, from soft to hard)	52.0 ± 6.8 ^{b}	64.3 ± 6.3 ^{a}
Juiciness (intensity, from dry to juicy)	73.2 ± 4.9 ^{a}	63.1 ± 6.6 ^{b}
Saltiness (intensity, from unsalted to over-salted)	51.3 ± 3.2 ^{b}	55.9 ± 2.9 ^{a}
Flavour (hedonic)	75.8 ± 6.2	75.6 ± 6.7

Legend: C – sausage produced from pork meat of pigs fed a standard diet, F – sausage produced from pork meat of pigs fed a standard diet with 8% of fish oil; Values with different superscripts in the same rows means there are significant differences ($p < 0.05$).

CONCLUSIONS

Generally, it can be said that bologna sausage made of meat of pigs fed the food enriched by fish oil (8%) was very positively perceived by evaluators within the sensory analysis. Despite the higher level of malondialdehyde, no significant differences in the odour or flavour between the control and experimental group were recorded. The texture of the product was rated less positively but the improvement in nutritional value of bologna sausage, in which the SFA content decreased significantly, should be noted. The n-6/n-3 ratio decreased as well, while the content of EPA and DHA

increased. In conclusion, it should be noted that the DHA content was so high that a health claim can be made: DHA contributes to maintain normal brain, vision and heart function (European Union, 2010).

ACKNOWLEDGEMENTS
The research was financially supported by the Internal Grant Agency of the Mendel University in Brno (project No. AF-IGA2019-TP006).

REFERENCES

AOAC 2005. Official method of analysis. 18th ed., AOAC, Washington DC.
Bryhni, E.A. et al. 2002. Polyunsaturated fat and fish oil in diets for growing-finishing pigs: effects on fatty acid composition and meat, fat, and sausage quality. Meat Science [Online], 62(1): 1–8. Available at: https://doi.org/10.1016/S0309-1740(01)00211-X. [2020-18-09].
Cáceres, E. et al. 2008. Effect of pre-emulsified fish oil: as source of PUFA n-3 on microstructure and sensory properties of mortadella, a Spanish bologna-type sausage. Meat Science [Online], 80(2): 183–193. Available at: https://doi.org/10.1016/j.meatsci.2007.11.018. [2020-18-09].
Česká Republika. 2017. Zákon č. 255/2017, kterým se mění zákon č. 246/1992 Sb., na ochranu zvířat proti týrání, ve znění pozdějších předpisů. In: Sbírka zákonů České republiky.
Elvevoll, E.O., James, D.G. 2000. Potential benefits of fish for maternal, foetal and neonatal nutrition: A review of the literature. Food, Nutrition and Agriculture [Online], 27: 28–39. Available at: http://www.fao.org/3/x8576m/x8576m04.pdf. [2020-18-09].
European Union. 2010. Regulation (EU) No 116/2010 amending Regulation (EC) No 1924/2006 of the European Parliament and of the Council of 9 February 2010 with regard to the list of nutrition claims. In: Official Journal of the European Union. 37: 16–18.
FAO 2010. Fats and Fatty Acids in Human Nutrition. Report of an Expert Consultation. FAO Food and nutrition paper.
ISO/CIE 11664-4 2019. Colorimetry – Part 4: CIE 1976 L*a*b* colour space. International Commission on Illumination, Paris, France.
Jezek, F. et al. 2019. Comparison of oxidation status and antioxidant capacity of meat from surgically castrated and immunocastrated pigs, entire males and sows. Acta Veterinaria Brno [Online], 88(1): 113–119. Available at: https://actavet.vfu.cz/88/1/0113/. [2020-18-09].
Komprda, T. et al. 2017. Effect of dietary fish oil on fatty acid deposition and expression of cholesterol homeostasis controlling genes in the liver and plasma lipid profile: comparison of two animal models. Journal of Animal Physiology and Animal Nutrition, 101(6): 1093–1102.
Peréz-Palacios, T. et al. 2019. Strategies for Enrichment in ω−3 Fatty Acids Aiming for Healthier Meat Products. Food Reviews International [Online], 35(5): 485–503. Available at: https://doi.org/10.1080/87559129.2019.1584817. [2020-18-09].
Simopoulos, A.P. 2002. The importance of the ratio of omega-6/omega-3 essential fatty acids. Biomed Pharmacother [Online], 56: 365–379. Available at: https://doi.org/10.1016/S0753-3322(02)00253-6. [2020-18-09].
USDA 2010. Dietary Guidelines for Americans. US Government Printing Office, Washington.
ÚNMZ. 2010. Senzorická analýza: Metodologie, Všeobecné pokyny. ČSN ISO 6658 (560050). Praha: Úřad pro technickou normalizaci, metrologii a státní zkušebnictví.
Vossen, E. et al. 2017. Production of docosahexaenoic acid (DHA) enriched loin and dry cured ham from pigs fed algae: Nutritional and sensory quality. European Journal of Lipid Science and Technology [Online], 119(5): 1600144. Available at: https://doi.org/10.1002/ejlt.201600144. [2020-18-09].
Wood, J.D. et al. 2008. Fat deposition, fatty acid composition and meat quality: A review. Meat Science [Online], 78(4): 343–358. Available at: https://doi.org/10.1016/j.meatsci.2007.07.019. [2020-18-09].
Zhang, Y. et al. 2019. Understanding beef flavour and overall liking traits using two different methods for determination of thiobarbituric acid reactive substance (TBARS). Meat Science, [Online], 149: 114–119. Available at: https://doi.org/10.1016/j.meatsci.2018.11.018. [2020-18-09].

The use of chicken collagen hydrolyzate as a functional polymer in cosmetics

Aneta Polastikova[1], Jana Pavlackova[2], Robert Gal[3], Pavel Mokrejs[1], Jana Orsavova[4]
[1]Department of Polymer Engineering
[2]Department of Fat, Surfactant and Cosmetics Technology
[3]Department of Food Technology
[4]Language Centre
Tomas Bata University in Zlin
Vavreckova 275, 760 01 Zlin
CZECH REPUBLIC

a_polastikova@ft.utb.cz

Abstract: The food industry generates a wide range of animal by-products including collagen-rich by-products from the poultry processing, such as chicken stomachs which may be hydrolytically treated by food endoprotease to obtain collagen hydrolyzate with the possible applications in the food and cosmetic industry. The skin aging process is an inevitable biological process influenced by both external and internal aspects. These factors perform a synergistic effect on the overall skin condition and can cause a number of skin changes, such as dryness and deep wrinkles. This study aims to test the effects of a gel formulation enriched with 1.0% hydrolyzate on the properties of the skin in the temple area in the first, fourth and eighth week of a regular twice daily application (morning and evening). Skin hydration, measured corneometrically, and transepidermal water loss from the skin, determined tewametrically, were monitored and subsequently evaluated. An increase of the skin hydration of 1.9% and 3.7% was established in the 4th week in the right and left temple area, respectively, and 11.1% and 9.1% in the 8th week. Compared to control (skin untreated with tested formulation), the skin hydration rose in total by 13.0% and 12.8% in the right and left temple area, respectively. Considering transepidermal water loss, the skin barrier properties improved as well. A decrease of 11.0% and 9.2% was recorded in the 4th week in the right and left temple area, respectively, and 17.0% and 16.2% in the 8th week. In total, compared to control, a reduction of transepidermal water loss was established to 28.0% and 25.4% in the right and left temple area, respectively. As the results show, the longer the formulation is applied, the better results are obtained. Since the formulation positively affects the skin condition and quality, the application in the cosmetic industry is very promising.

Key Words: hydration, collagen hydrolyzate, chicken stomachs, transepidermal water loss, by-products

INTRODUCTION

The slaughter of livestock produces meat as the main edible product and also edible or inedible by-products, such as the liver, kidneys, heart, stomach, skin and blood. Some of these by-products are not intended for direct consumption; however, as their nutritional value is truly considerable, it is advantageous to manage them properly and processed them further. Mostly, they are applied in the production of compound feed for livestock and used as fertilizers or fuels. Since these by-products contain significant amounts of collagen, to use them in the production of hydrolysates and gelatin with a very wide range of applications in almost all industries has been thoroughly investigated (Barbut 2015). Even though the extraction and application of hydrolysates and gelatins from chicken tissues employing enzymatic processing of the raw material have been examined at this university department for a long time, only the application in the food and pharmaceutical industry has been in focus for the time being (Mokrejš et al. 2019).

The skin is an organ comprising up to 16.0% of the total body weight. The skin area of an adult person ranges from 1.5 to 2.0 m^2. It consists of three layers: the epidermis containing several layers of epithelial cells and participating in mechanical resistance, the dermis forming a ligament of collagen and elastic fibers and the sensory terminals embedded, and the hypodermis, which is formed by the

ligament attached to muscles or the skeleton. As it also contains fat cells, this layer has an insulating function (Langmeier 2009). The skin aging process is a complex and continuous process affected by both internal factors, such as heredity, alcohol consumption, smoking and lifestyle, and external influences including moisture, laundry and cleaning products and the type of clothing (Makrantonaki et al. 2014). Skin aging can be either intrinsic (internal) or extrinsic (external). Intrinsic skin aging is inevitable caused by a lower production of elastin and collagen resulting in the decline of the number of cells and reduced skin elasticity. Typical manifestations of this type of aging include dryness, weakness, skin irritation and commencing fine wrinkles. On the other hand, extrinsic skin aging or photoaging is initiated by external negative factors, of which UV radiation has the greatest influence. UV radiation prevents the formation of new collagen cells and can also degrade elastic fibers. Typical manifestations of this aging are deep wrinkles, excessive pigmentation and very dry skin (Poljšak et al. 2012). Wrinkles in the facial area are the most characteristic morphological changes observed on the skin surface. With age, mechanical properties deteriorate and the amount of collagen and elastin in the skin decrease which results in skin weakening and the formation of wrinkles in the dermis layer. A long-term and local application of variety of cosmetic products is used to suppress the aging process of the skin and to enhance the skin appearance and condition (Lee et al. 2015). Collagen is a highly soluble animal fibrous protein with the structure of three polypeptide chains arranged in a triple helix forming the main building block of most connective tissues. It is known for its contribution to the cosmetic and medical industries, where it is used as an anti-wrinkle product and plays a role as a humectant (Sahana and Rekha 2018). Skin hydration is a key factor affecting both mechanical and physical skin properties. Dry skin is a common dermatological problem that can be mitigated by using moisturizers. Hydration prevents an excessive water evaporation from the skin thus allowing inside rehydration of the skin (Spada et al. 2018). Transepidermal water loss (TEWL) expresses the water loss from the skin surface through external diffusion. It also indicates the skin barrier function directly influencing the skin quality as it enables to increase water content in the skin and to restrict TEWL (Mündlein et al. 2008).

In gel cosmetic formulations, bovine or porcine hydrolyzate is most often encountered, as it is commercially available. To our best knowledge, the application of poultry collagen hydrolysates in such formulations has not been examined and published yet. Therefore, the aim of the work was to test the effects of collagen hydrolyzate from chicken stomachs after the addition to a cosmetic formulation in a gel form on skin properties in the temple area, specifically hydration and transepidermal water loss. Scientific hypothesis: application of a cosmetic gel formulation with 1% chicken collagen hydrolyzate increases skin hydration and reduces transepidermal water loss from the skin.

MATERIALS AND METHODS

Chicken stomachs were first minced in a meat mincer and rinsed in water. Then, they were treated in 0.2 M NaCl for 1.5 h and 0.03 M NaOH for 24 h. After being dried at 35.0 ± 0.2 °C for 36 h, they were degreased with a mixture of petroleum ether and ethanol (1 : 1) in a ratio of 1 : 9 (200 g stomachs and 1800 ml solvent mixture) for 51 h. After 7, 24 and 31 h, the solvent mixture was replaced and finally, the mixture was filtered through a sieve. Collagen hydrolyzate was prepared from the defatted tissue by neutral processing. In the first phase, the tissue was mixed with water in a ratio of 1 : 10 (50 g stomachs and 500 ml water) and after 30 min, the pH of the swollen stomachs was adjusted to 6.5 ± 0.2 by the addition of ice-cold CH_3COOH or with 10% NaOH solution. Subsequently, 0.2% Polarzyme 6.0 T proteolytic enzyme was added and the mixture was being shaken for 30 h at room temperature. In the second phase, the mixture was mixed with water in a ratio of 1 : 8 (50 g of stomachs and 400 ml of water) and the tissue was heated to 65.0 ± 0.5 °C and maintained at this temperature for 45 min. In the third phase, the mixture was filtered hot through a sieve provided with three layers of PA fabric. The resulting hydrolyzate solution was dried in a thin film at 45.0 ± 0.2 °C for 48 h. The dried film was ground to a very fine powder, which was then inserted to the cosmetic formulation as a carbopol gel. Chicken collagen hydrolyzate of a concentration of 1.0% and Mw = 1500 Da (5 g of hydrolyzate and 500 g of carbopol gel) was added to the gel.

The methodology was based on testing the effectiveness of a gel cosmetic formulation with the addition of 1% chicken collagen hydrolyzate applied to the probands' right and left temple area. The selection of probands as well as the testing procedure strictly followed the International ethical

guidelines for biomedical research involving human subjects (Council for International Organizations of Medical Sciences 2002). As the effects of the gel formulation on the suppression of eye wrinkles was investigated, only elder women participated in the testing.

Appliances, tools and chemicals

MPA 10 station with individual probes (Courage & Khaza, Germany), tewameter TM 300 (Courage & Khaza, Germany), corneometer CM 825 (Courage & Khaza, Germany), analytical scale (Kern & Sohn, Germany), stirrer RZR 2020 (Ika, Germany), P-22/82 meat mincer Braher (Braher, Spain), LT2 shaker (Kavalier, Czech Republic), pH meter WTW 526 (WTW, Czech Republic), WTB Binder E-28-TB1 drier (Binder, Germany), Memmert ULP 400 drier (Memmert, Germany), heating board Schott Gerate GMBH with a stirrer (Schott, Czech Republic), mortar, PA fabric, metal sieve, laboratory glassware, plastic utensils, pulp, scissors. Enzyme Protamex (*Bacillus* protease complex developed for the hydrolysis of food proteins with a declared activity of 1.5 AU/g), distilled water, petroleum ether and ethanol, ice-cold CH_3COOH, 10% and 0.03 M NaOH, 0.2 M NaCl, Jarisch solution, Bioderma Sensibio H_2O make-up remover, carbopol gel.

Statistical analysis

The results were processed and statistically evaluated in Microsoft Excel (2010). From the obtained data, the arithmetic mean $\bar{x}$ and the standard deviation s were calculated according to the following equations (1) and (2).

$$\bar{x} = \frac{1}{N}\sum_{i=1}^{N} x_i \qquad s = \sqrt{\frac{1}{N}\sum_{i=1}^{N}(x_i - \bar{x})^2} \qquad (1)\ and\ (2)$$

Where: $\bar{x}$ – arithmetic mean, N – number of measurements, x_i – measurement value, s – standard deviation

Organization and principle of measurement

The investigated group consisted of a total of 10 probands aged 50 ± 9 years. The practical measurement examining the effectiveness of the gel in the right and left temple area was performed in February, March and April 2020. It was always executed after a month of the gel application in the same laboratory at 21 ± 2 °C and relative humidity of 38 ± 2%. Before commencing the experiment, the probands were acquainted with the organization of the measurements, signed an informed consent and filled in a questionnaire about their health condition. Prior to the measurement itself, the probands rested in the laboratory for 20 min and the tested skin area was cleaned with Bioderma make-up remover and Jasrisch solution to remove impurities. The probands received a vial of gel and were instructed to apply it in a thin layer each morning and evening to cleansed skin in the right and left temple area for eight weeks. They were asked not to use any other cosmetic products that could affect the results during the application of the gel formulation with 1% collagen hydrolyzate. The gel was stored in the refrigerator at all times and control measurements were performed in the fourth and eighth week.

Principle of measuring skin hydration. Initially, the examined right and left temple areas were cleaned and then the level of their hydration was measured by the CM 825 corneometer probe. Five hydration values were recorded on both sides. The highest and lowest values were omitted and the arithmetic mean and standard deviation were calculated from the three values without these extreme values. It is a quick and easy method to determine skin hydration using the CM 825 corneometer probe gently pressed to the measured area. The recorded value is immediately displayed on a computer monitor connected to the MPA station. The skin hydration scale classifies skin three types to the extremely dry (< 30 c.u.), dry (30–45 c.u.) and normal (> 45 c.u.) (the Corneometer CM 825: Technical charges 2013).

Principle of measuring transepidermal water loss from the skin (TEWL). Transepidermal water loss was determined immediately after examining skin hydration. The measurement was performed using the TM 300 tewameter probe in both the right and left temple areas. A total of 15 values were recorded on each side. The arithmetic mean and standard deviation were calculated using only ten values as the first five were omitted before the temperatures of the probe and skin balanced. The tewameter TM 300 with an open chamber is a device used to measure the amount of evaporated

moisture. Its probe is attached to the examined skin area and after pressing the button, the measurement is started; then after pressing the button again, the measurement is finished. The recorded values are immediately displayed on a computer monitor connected to the MPA station. The scale of TEWL values classifies the skin condition to very good (0–10 g/m^2/h), good (10–15 g/m^2/h), normal (15–25 g/m^2/h), tight (25–30 g/m^2/h) and critical (> 30 g/m^2/h) (the Tewameter TM 300: Technical charges 2013).

RESULTS AND DISCUSSION

Skin hydration

The average values of skin hydration in the right and left temple area in particular weeks of the application are shown in Table 1. Table 2 presents the average values including standard deviations.

Table 1 The average values of skin hydration in the right and left temple area in particular weeks of the application

Proband	Hydration – right side(c.u.)			Hydration – left side(c.u.)		
	Week			Week		
	1st	4th	8th	1st	4th	8th
1	49.5	67.0	97.2	49.6	72.1	92.6
2	60.7	43.9	59.2	63.1	31.6	51.4
3	48.6	37.7	49.1	42.7	32.5	47.2
4	59.7	81.9	40.7	57.8	88.5	40.2
5	48.4	48.7	57.6	43.2	47.6	60.1
6	71.9	76.9	78.4	79.8	82.4	84.9
7	56.8	44.2	78.2	54.5	43.8	73.5
8	48.1	49.4	51.4	46.4	51.4	59.4
9	51.3	54.2	58.7	51.3	57.5	58.2
10	45.1	39.9	37.6	41.4	37.6	33.4

Table 2 The average values of skin hydration in the right and left temple area in particular weeks of the application including standard deviations

Hydration ± Standard deviation(c.u.)		
Week	Right side	Left side
1st	53 ± 3	53 ± 3
4th	54 ± 3	55 ± 4
8th	60 ± 4	60 ± 4

As can be seen in Table 1, probands' skin was sufficiently hydrated already in the initial state and it was in a normal condition. Table 2 provides a comparison of the total increase in hydration in the right and left temple area. As far as the right temple area is concerned, the skin hydration increased by 1 c.u. in the 4th week and 6 c.u. in the 8th week. In total, the hydration rose by 7 c.u. In the left temple area, the hydration was enhanced by 2 c.u. in the 4th week and 5 c.u. in the 8th week. The overall skin hydration reached the increase of 7 c.u. compared to the initial condition. Considering the skin hydration trends in the individual probands, the greatest enhancement was observed in proband 1 with the hydration increase of 17.5 c.u. in the 4th week and 30.2 c.u. in the 8th week which responds to the total rise of 96.4% in the right and 86.7% in the left temple area. Proband 7 also shows a significant hydration growth in the 8th week with the values of 37.7% in the right and 34.9% in the left temple area. However, in the 4th week this proband showed a decrease of hydration in both right and left temple areas, from 56.8 c.u. to 44.2 c.u. and from 54.5 c.u. to 43.8 c.u., respectively. The highest hydration values in the 4th week were observed in proband 4 with the increase of 37.2% in the right and 53.1% in the left temple area. Nevertheless, in the 8th week the significant decrease of 50.3% and 45.4%, respectively, was recorded. Proband 10 was the only one suffering from the skin disease, psoriasis, and showed no positive hydrating effects. What is more, a decrease in hydration in both the 4th and 8th week of measurement was determined, 16.7% and 11.2% in the right and left temple area in total, respectively.

Jansen et al. (2019) measured skin hydration in various face areas: temple, cheeks, upper jaw, chin and forehead. The study included a short-term and long-term application (1 hour and 3 weeks) of a moisturizer within 21 probands aged 20 to 60 years with dry or extremely dry skin. It has been found

that the application of collagen agent in the irritated face areas enhanced the hydration. Interestingly, hydration in the chin and forehead area, the so-called T-zone, reached lower values after 3 weeks compared to other face areas where the hydrating effect was much more effective (Jansen et al. 2019).

Transepidermal water loss (TEWL)

The average values of TEWL in the right and left temple area in particular weeks of the application are depicted in Table 3. Table 4 displays the average values including standard deviations.

Table 3 The average values of transepidermal water loss in the right and left temple area in particular weeks of the application

Proband	TEWL – right side(g/m^2/h)			TEWL – left side(g/m^2/h)		
	Week			Week		
	1st	4th	8th	1st	4th	8th
1	17.9	13.9	12.8	16.3	14.5	14.1
2	18.3	22.2	14.2	16.5	22.3	13.7
3	4.9	6.1	4.2	4.6	6.4	3.9
4	19.7	7.8	9.3	19.1	8.3	9.8
5	16.9	18.1	13.9	14.9	16.4	9.5
6	21.6	24.8	17.5	18.5	24.2	17.9
7	23.6	23.5	20.4	24.3	22.1	21.3
8	11.6	9.1	7.0	11.7	10.4	8.2
9	20.1	13.9	13.0	20.2	12.3	11.1
10	17.2	12.0	14.8	16.4	10.6	13.7

Table 4 The average values of transepidermal water loss in the right and left temple area in particular weeks of the application including standard deviations

TEWL ± Standard deviation(g/m^2/h)		
Week	Week	Week
1st	17.2 ± 0.6	16.3 ± 0.6
4th	15.3 ± 0.8	14.8 ± 0.7
8th	12.7 ± 0.5	12.4 ± 0.5

As Table 3 shows, the values of TEWL in the initial state were acceptable and the skin condition was very good, good or normal. Table 4 compares the total change of TEWL in the right and left temple areas. In the right temple area, TEWL decreased by 1.9 g/m^2/h in the 4th week and 2.6 g/m^2/h in the 8th week. In total, TEWL decreased by 4.5 g/m^2/h compared to the initial condition. Considering the left temple area, the decrease in TEWL was 1.5 g/m^2/h in the 4th week and 2.4 g/m^2/h in the 8th week. Compared to the initial condition, TEWL decreased by 3.9 g/m^2/h in total. The best TEWL values prior the application of the gel formulation were achieved within proband 3 showing a decrease in TEWL by 14.2% and 15.2% in the 8th week. However, in the week 4 there was an undesirable increase in TEWL from 4.9 to 6.1 g/m^2/h and from 4.6 to 6.4 g/m^2/h in the right and left temple area, respectively. The biggest decline in the 8th week was observed within proband 4 with the values of 52.3% in the right and 51.3% in the left temple area. In contrast, the lowest decrease was achieved within proband 7 who performed also the highest TEWL values of 13.6% in the right and 12.3% in the left temple area. Generally, it has been proved that the average TEWL values decreased in both the 4th and 8th weeks and thus the skin barrier enhanced. In the 4th week, a decrease of TEWL of 11.0% and 9.2% was monitored in the right and left temple area, respectively; and in the 8th week, a decline of 17.0% and 16.2% in the right and left temple area, respectively. In total, TEWL decreased by 28.0% and 25.4% in the right and left temple area when compared to the initial condition.

Samad and Sikarwar (2016) determined TEWL values in the neck and forehead areas and tested the effect of the cream for several weeks. Some probands were exposed to heavy metals and chemicals at work, and differences in the average TEWL values occurred already in the first six weeks. During the three weeks of exposure, the average TEWL values grew five times. Afterwards, no significant changes were recorded and the values remained almost the same. The increase in TEWL may be the result of the workers' exposure to sulfuric acid and further heavy metals (Samad and Sikarwar 2016).

CONCLUSION

Chicken stomachs were processed, dried and defatted in the first phase. In the second phase, collagen hydrolyzate was prepared from the tissue by treatment in water with 0.2% of the proteolytic

enzyme Polarzyme 6.0 T followed by the extraction in hot water. In the third phase, the resulting hydrolyzate solution was dried and the film was ground to a fine powder. Subsequently, 1% collagen powder was added to the cosmetic formulation in the form of carbopol gel. As the results show, the application of a gel formulation containing 1% chicken collagen hydrolyzate increases the skin hydration and reduces transepidermal water loss. They have also confirmed that the longer the formulation is applied, the better hydration and TEWL values are. When monitoring the effect of the formulation on the hydration in the right and left temple area, a significant hydrating effect was observed in both the 4th and 8th weeks. In sum, hydration increased by 13.0% and 12.8% in the right and left temple area, respectively. A positive effect has been also reflected by TEWL values decreasing during the eight-week application. The overall decline in TEWL was 28.0% and 25.4% in the right and left temple area, respectively. The obtained results of skin hydration and TEWL have proved that a longer and regular twice daily application of the gel cosmetic formulation enhances the hydrating effects and barrier properties of the skin. Chicken collagen hydrolyzate has been shown to have the same effects as a functional polymer and could be applied in cosmetic gel formulations due to its positive hydrating properties. Thus, chicken hydrolyzate may be considered as a suitable alternative to porcine and bovine collagen commonly used in cosmetics.

ACKNOWLEDGEMENTS

This research was financially supported by the Internal Grant Agency of the Faculty of Technology, Tomas Bata University in Zlín, ref. IGA/UTB/FT/2020/002.

REFERENCES

Barbut, S. 2015. The Science of Poultry and Meat Processing. 1st ed., Guelph: University of Guelph.

The Council for International Organisations of Medical Sciences. 2016. International Ethical Guidelines for Biomedical Research Involving Human Subjects. Geneva: Copyright.

Jansen, V.R. et al. 2019. Measurement of Transepidermal Water Loss, Stratum Corneum Hydration and Skin Surface pH in Occupational Settings: A review. Skin Research and Technology, 25(5): 595–605.

Langmeier, M. 2009. Základy lékařské fyziologie. 1st ed., Praha: Grada.

Lee, H.Y. et al. 2015. Antioxidant, Collagen Synthesis Activity in vitro and Clinical Test on Anti-Wrinkle Activity of Formulated Cream Containing Veronica Officinalis Extract. Journal of Cosmetics, Dermatological Sciences and Application, 5(1): 45–51.

Makrantonaki, E. et al. 2014. Genetics and Skin Aging. Dermato-Endocrinology, 4(3): 280–284.

Mokrejš, P. et al. 2019. Biotechnological Preparation of Gelatines From Chicken Feet. Polymers [Online], 11(6): 1060. Available at: https://doi.org/10.3390/polym11061060. [2020-08-10].

Mündlein, M. et al. 2008. Comparison of Transepidermal Water Loss (TEWL) Measurements with Two Novel Sensors Based on Different Sensing Principles. Sensors and Actuators a: Physical, 142(1): 67–72.

Poljšak, B. et al. 2012. Intrinsic Skin Aging: The Role of Oxidative Stress. Acta Dermatovenerol Alpina Pannonica et Adriatica, 2: 33–36.

Sahana, T.G., Rekha, P.D. 2018. Biopolymers: Applications in Wound Healing and Skin Tissue Engineering. Molecular Biology Reports, 45(6): 2857–2867.

Samad, N., Sikarwar, A. 2016. Collagen: New Dimension in Cosmetic and Healthcare. International Journal of Biochemistry Research and Review, 14(3): 1–8.

Spada, F.T.M. et al. 2018. Skin Hydration is Significantly Increased by a Cream Formulated to Mimic the Skin's Own Natural Moisturizing Systems. Clinical, Cosmetic and Investigational Dermatology, 11: 491–497.

The Corneometer CM 825: Technical charges. 2013. Available at: https://www.courage-khazaka.de/en/scientific-products/all-products/16-wissenschaftliche-produkte/alle-produkte/183-corneometer-e. [2020-06-16].

The Tewameter TM 300: Technical charges. 2013. Available at: https://www.courage-khazaka.de/en/16-wissenschaftliche-produkte/alle-produkte/172-tewameter-e. [2020-06-16].

The nature of virgin fruit seed oils and their oxidative stability after three months of storage

Aneta Sinkova, Vladimir Masan, Lukas Vastik, Pavla Bukovska
Department of Horticultural Machinery
Mendel University in Brno
Zemedelska 1, 613 00 Brno
CZECH REPUBLIC

xsinkova@mendelu.cz

Abstract: The main aim of this work is to define pressed fruits oils of varieties of apricot (*Prunus armeniaca*), peach (*Prunus persica*) and plum (*Prunus domestica*) cultivated in Czechia and Slovak Republic. Correct parameters definition of these oils may lead to a right use as a raw material for new, valuable, secondary, or final products. The second aim was to analyze oxidative stability of oils after three months of storage based on physicochemical properties. Obtained results clearly indicated that the cold pressed oils without refining may have higher levels of oxidation already in a very early stage of storage, only after three months. Despite that, these oils, after pressing and three months of storage, met legislative limits. A significant positive correlation between peroxide value, acid value, saponification value and three months of oil storage and negative correlation of iodine value was found. These findings may be useful for European oil producers.

Key Words: fruit seed oil, physicochemical properties, screw press, cold pressed oils

INTRODUCTION

Many of studied varieties are important cultivated fruit species. A significant part of harvested fruits that are being processed, results in discarding of seeds which then causes many industrial residues. These seeds might be used, potentially and after minimal treatment, in food or cosmetic industry and therefore could minimize not only food waste but also biowaste produced within the food industry.

Nowadays, fruit seed oils have won recognition all over the world. Oils rich in unsaturated fatty acids and antioxidants, with its unique taste and pharmacological properties are highly recommended for consumption as protection and prevention against cancer, hypertension and other civilization diseases (Kris-Etherton et al. 2002).

After closer examination of some oils, the following was found out. The apricot oil, for example, is already being used as a part of other cosmetics products. Kernels from seeds or oils are used in a food industry marginally, as they consist of amygdalin, which is harmful to humans in larger quantities (Gupta et al. 2012). The oil yield from the apricot kernels ranged from 28–43% (Özcan et al. 2015).

Peach kernel can be considered as an important source of rawoil for the food and nutraceutical supplement industries. Peach kernels have 39–49% lipid content and with the extraction it is possible to obtain, with different solvents, up to 25–42% of oil (Özcan et al. 2015, Ashraf et al. 2011, Wu et al. 2011). The oil is nutritionally attractive for use in food industry due to its composition of fatty acid such as linoleic, palmitic and stearic and antioxidants such as tocopherols. This oil has been widely used in cosmetics industry, because it is a light, penetrating oil, and it absorbs easily (El Saadany et al. 1994).

The oil content of plum kernels varies from 24% to 30% (Özcan et al. 2015). The plum seed oil might be used in food products, but it is more likely to be used in cosmetics.

The quality of any oil is indicated by some physicochemical properties represented by iodine, peroxide and saponification value, free fatty acid and many others. While iodine value represents unsaturation and saponification value represents a measure of the fatty acid content. These properties provide an indication of both the nutritive and physical quality of oil. For healthy consumption, the unsaturated oils are better, even when they are susceptible for rancidity (Kris-Etherton et al. 2002).

The preservation of some studied oils has been minimally precisely quantified, yet. Oxidative stability is very important, especially with regard to storage capacity of micro and small producers. The most important is the time from production (mostly at the grower) to the purchase of oil by the processor or directly by the producer of food or cosmetics. Small growers often collect oil gradually over two or three months. Only after the purchase by the processors, oil is treated professionally. Therefore, this study focused on the first three months from the time when oil was pressed.

Different standards are used in different parts of the world. In Europe, which is the target area of this article, the guideline of FAO is used. For example, the guideline of FAO sets the limit and quality parameters for edible oils (FAO 2001). The qualitative parameters of oils may decrease upon improper extraction process, handling or storage. The oils rancidity may lead to food quality degradation, undesirable aroma, off-flavors, etc. and may pose health risks as oils break down into constituent fatty acids and decomposition of glyceride due to oxidation (Kris-Etherton et al. 2002).

The main objective of this study was to evaluate the quality of seed oils obtained from fruit grown in Czechia and Slovak Republic through the physicochemical properties, extracted by the screw press.

MATERIAL AND METHODS

Samples

The samples of oils used for this study are the oils from plant varieties in mild climate zone of Europe, specifically Czechia and Slovak Republic. The seeds from which the oils were produced were apricot (‘Veľkopavlovická – common Czech variety), peach (‘Redhaven’ – originally from US, currently one of the most grown in Czech and Slovak) and plum (‘Bystrická’ – common Slovak variety) obtained from 3 companies, OVOSAD, Ltd., Myjava, Slovakia, Plantex, Ltd., Veselé, Slovakia, Faculty of Horticulture, Mendel University in Brno, Lednice, Czech Republic.

While in many other publications and studies the oils from plant varieties were from the tropical climate zone, such as Mediterranean, Southwest Asia, India, and so on.

Seeds were harvested from fruit during the autumn of 2019 and then prepared accordingly. All seeds have been cleaned and separated from impurities, in particular skin and pulp. The hard seeds were cracked to obtain the kernel. The seed samples were air-dried in a box dryer (Lab-Line Instruments Inc., Melrose Park, IL) at 22 °C to reduce the moisture to permanent moisture level at 5%.

The seed samples were prepared for extraction of screw press after drying. The extraction by mechanical screw press is one of methods used for production of cold pressed oils – not virgin oils (FAO 2001). The oil obtained by this method has the highest quality. Samples of fruit oils were pressed in the laboratories of Mendel University in Brno, on the screw press type UNO FM 3F (Farmet Company, Malá Skalice, Czech Republic). This type of press is used mostly by small growers, for pressing different oil seeds and producing small batch of oils. The pressing conditions were the same for all samples to minimize external effects on the resulting oil quality. Before screw pressing experiments, the press head was pre-heated at the desired temperature for 20 minutes using a temperature-regulated heating ring. Pressing experiments were conducted without external heating (cold pressing). During pressing, seeds were fed into the press on demand by gravity through the hopper and seeds level was maintained constant to ensure constant press performance. The optimal screw rotation speeds were chosen within the press characteristics in order to achieve a correct expression and to avoid press overload. Seeds of all species were pressed at the same speed of 40 rpm. A nozzle with 6 mm diameter was used. Kernels or oils were just mechanically extracted and filtered; they were not refined. Nor any kind of solvent was used.

The first half production of these raw oils was prepared for determining the initial physicochemical parameters. The other half of the production was bottled and stored for three months in conventional fridges at 7 °C, with no air and light access.

Analytical methods

Water content of kernels was determined after harvesting in lab oven Memmert UN30 (Memmert GmbH + Co. KG, Schwabach, Germany) by dehydration at 103 °C according to ISO 665:2020 Oilseeds – Determination of moisture and volatile matter content. Analysis was made of 5 g grinded sample,

weighted with an accuracy of 0.1 mg. Results are indicated as the ratio of water loss per gram of dried sample.

Ash content was determined by ISO 749:1977 Oilseed residues - Determination of total ash. The pre-weighed dried residue material was burnt in muffle furnace Lack LMH (LAC, Ltd., Židlochovice, Czech Republic) at 550 °C and the loss of mass was calculated.

Density of oil was determined pycnometrically according to ISO 6883:2017 Animal and vegetable fats and oils - Determination of conventional mass per volume (litre weight in air).

The value of acid, iodine, peroxide and saponification as well as free fatty acid of pressed oils were determined by using methods by Ashraf et al. (2011) and methods AOCS (2017a–e).

Acid value is the mass of potassium hydroxide in milligrams which is required to neutralize 1 g of oil. It is a measure of amount of carboxylic acids in oil. The oil sample (5 g) was neutralized with 100 ml ethanol and was titrated with KOH by using phenolphthalein as an indicator. The acid value was calculated by using the standard procedure.

The value of free fatty acid was calculated by the following method. To 2 g of oil, 25 ml of neutral ethanol was added, and the resulting solution was titrated against KOH using phenolphthalein as an indicator.

Iodine value of an oil is the amount of iodine in grams which is consumed by 100 g of the given oil. It is a measure of degree of unsaturated fatty acids in oil. The oil sample (0.25 g) was taken in iodine flask, to which 15 ml of carbon tetrachloride and 25 ml of Wij's solution were added. After keeping the solution in dark for one hour, 15 ml of 10% KOH and 100 ml of distilled water was added. The liberated iodine was titrated against 0.1 N $Na_2S_2O_3$ solution, using freshly prepared starch solution as an indicator. The titration was continued till the disappearance of blue colour. Similar process was carried out for the blank. The iodine value was calculated by using the standard procedure.

The saponification value of an oil represents the number of milligrams of potassium hydroxide or sodium hydroxide required to hydrolyse 1 g of oil and is a measure of the average molecular mass of fatty acids found in the given oil. The oil (3 g) was mixed with 25 ml of 0.5 N KOH in a flask. Equal volume of solution was added into another flask for blank titration. Both the flasks were refluxed for two hours, allowed to cool to room temperature, and titrated against HCl solution using phenolphthalein as indicator. The saponification value was calculated.

Hydroperoxides are reacted with iodide ions to form iodine and the PV is determined by titration of the liberated iodine with thiosulphate using starch as an indicator. PV is expressed as millimoles of active oxygen lipids per kilogram.

Statistics

The extractions and all analyses were carried out at least in triplicate and data were expressed as means ± standard deviation. Tukey's honestly significant difference (HSD) tests were conducted to determine the differences among samples which means that the statistical significance was declared at $p \leq 0.05$. The differences were analysed only within the specific parameter not between the different parameters. Next, correlations were calculated between the initial physicochemical properties and after three months of storage with the statistical significance at $p \leq 0.05$. These statistical evaluation methods were applied using the computer software package "Statistica 12.0" (StatSoft Inc., USA).

RESULTS AND DISCUSSION

The proximate analysis of the kernels and oils produced is shown in Table 1. Peach kernel moisture is higher compared to other samples, which is probably thanks to applied technologies for growing - producers, two weeks before harvesting the peaches, irrigate much more so the peaches gain weight and kernels gain moisture.

The following compacts were obtained while pressing the oils: apricot 236, peach 189, plum 261 g of oil from 1 kg of seeds. Chamli et al. (2017) report a slightly higher compactness for plum and apricot. For peaches, it even states 505 g of oil. Özcan et al. (2015) report the amount of pressed oil for plum, apricot and peach in the range of 185–395 g, which are again slightly higher values of compactness compared to those obtained in the experiment.

Table 1 Analysis of fruit oil-bearing material and oils – Initial values

Sample	Kernel moisture (% dry basis ±SD)	Press performance (% dry basis ±SD)	Density of oil (kg/m^3±SD)	Ash (%)
Apricot	7.35 ± 0.7^b	23.62 ± 1.3^b	0.92 ± 0.0^a	2.51 ± 0.1^b
Peach	10.27 ± 1.4^a	18.94 ± 1.2^a	0.92 ± 0.0^a	1.12 ± 0.1^a
Plum	6.75 ± 0.8^b	26.14 ± 1.6^b	0.92 ± 0.0^a	1.44 ± 0.1^a

Legend: Values are mean ± SD, n = 3; In each column, ab mean values of different letters are significantly different at P<0.05.

In general, the results obtained during the study are quiet variable as variety of different fruit species and fruit seeds were studied. Furthermore, the produced oils were yellow which had partial impact on the indication during the titration. On the other hand, all of the oils had similar yellow tone so in the end the color did not seem to cause significant problem. Finally, differences were found when comparing individual samples (at the beginning of the process, during it as well as at the end of oil pressing). Also, for these reasons, the standard deviations for individual repetitions are larger. However, results show common features of fruit seed oils as well as common modifications resulting from the aging of oils.

As shown in Table 2, the peroxide value was initially the highest in plum (1.37 mmol (1/2 O2)/kg oil), but after three months, the value was highest in apricot (9.67 mmol (1/2 O2)/kg oil). The significant growth of peroxide value in apricot oil suggests that after some period of time when the peroxide value slowly and steadily increases, suddenly, a steep increase of peroxide value clearly shows that the oil has gone badly in its quality (Kris-Etherton et al. 2002). The smallest increase of peroxide value was identified in plum oil (from 1.37 to 5.73 mmol (1/2 O2)/kg oil).

Table 2 Physicochemical properties of fruit oils

Storage	Sample	Peroxide value (mmol (1/2 O2)/kg)	Acid value (mg of KOH/g oil)	Free fatty acid (%)	Saponification value (mg of KOH/g oil)	Iodine value (g of I/100 g of oil)
Initial values	Apricot	1.25 ± 0.4^a	2.77 ± 0.2^f	1.46 ± 0.4^c	193.0 ± 2.7^b	105.1 ± 2.9^b
	Peach	0.94 ± 0.5^a	0.21 ± 0.0^{bc}	0.15 ± 0.1^b	190.3 ± 1.5^{bc}	105.1 ± 4.1^b
	Plum	1.37 ± 0.7^a	0.28 ± 0.0^{cd}	0.11 ± 0.0^b	190.3 ± 5.7^{bc}	102.4 ± 4.9^b
After storage	Apricot	9.67 ± 1.1^{bc}	3.27 ± 0.0^g	1.67 ± 0.1^c	352.2 ± 5.0^a	54.8 ± 0.3^a
	Peach	8.93 ± 0.6^c	0.58 ± 0.0^e	0.28 ± 0.0^b	350.2 ± 2.8^a	53.5 ± 0.5^a
	Plum	5.73 ± 0.5^d	0.39 ± 0.0^d	0.20 ± 0.0^b	342.0 ± 1.0^a	54.7 ± 0.3^a

Legend: Values are mean ± SD, n = 3; In each column, ab mean values of different letters are significantly different at P<0.05.

Özcan et al. (2015) state the peroxide value 1.5 in plums, 1.4 in apricots and 1.5 mmol (1/2 O2)/kg oil in peaches. There are also the older data from author El Saadany et al. (1994) who stated the peroxide value 0.7 mmol (1/2 O2)/kg oil in peaches. When comparing this data with those obtained during our study, ours are a bit higher. On the other hand, authors hardly identify whether the oils were refined or not. In general, the limit values are higher when it comes to virgin (unrefined) oils. According to our findings, fruit seed oils reached these limits after three months of storage (Bell and Gillatt 1994).

The acid and peroxide values are according to Wu et al. (2011) good indicators for the oil stability. Cold pressed and virgin oils have limit to 4.0 mg KOH/g oil (FAO 2001). So again, we can declare that these oils, after pressing and three months of storage, met this limit.

The high oxidative stability of plum seeds oil was confirmed by Savic et al. (2020), of apricot by Gupta et al. (2012) and of peach by Ashraf et al. (2011).

Our results of acid values indicate a large scale of values in individual oils, form 0.210 in peach to 2.77 mg of KOH/g oil in apricot oil. In overall, it is possible to trace down differences between peach and plum seed oils and apricot oil, both in acid value and free fatty acid value. Acid value and free fatty acid value in apricot oil were significantly higher, compared with other studied oils.

In comparison to the results of the acid value which Wu et al. (2011) report in peaches, we find the value accurate, although the range is quite wide, from 0.08 to 0.9 mg KOH/g oil. In contrast, Özcan

et al. (2015) report double the values of free fatty acid in apricots (3.1%) and significantly higher values for other plum oils 3.4% and peaches 1.3%. Also, much higher values of free fatty acids in peaches are reported by Ashraf et al. (2011) (from 1.3 to 1.4%). From the results obtained and in the comparison of other authors, the great inconsistency of results and their variability is obvious. These claims are also supported by the mutual evaluation of oils regarding the peroxide value, but in acid value and free fatty acid they would meet them with a significant margin. Therefore, it is necessary to look at the overall quality of oils, not only at the selected factor, which is also highlighted by Kris-Etherton et al. (2002). In order to avoid misinterpreting, it is necessary to know the history of the sample.

These results of saponification value are comparable to data previously reported in research of Özcan et al. (2015) and Ashraf et al. (2011). Although, some differences might be found in this case as well. For example, El Saadany et al. (1994) declares a saponification value of 186 and Wu et al. (2011) even 154.3–165.7 mg of KOH/g oil in peaches. But the interesting fact is that after three months of storage the differences have settled and no significant differences in saponification value could be identified anymore for any oils.

The iodine value can be considered as a reference value for the quality of oil production, as its value decreases after heating, and causes the difference between cold pressed oils and virgin oils. Since the oils in the study were all produced by the same equipment and under the same conditions, the assumption that there were no differences was confirmed. Indirectly, it is also possible to confirm the opinions and views of some authors (Wu et al. 2011). After three months of storage, the differences in values were minimized again and there is no more significant difference between them.

Free fatty acid of apricot and peach oils showed no significant correlation within three months of storage (Table 3). When comparing the values with Table 2, the trend of increasing average values is also evident for these two species. However, when peroxide value, acid value and saponification value were considered, a significant positive correlation ($P<0.05$) within three months of storage was found. Similarly, to this, there was significant correlation between iodine value and storage but in a negative way.

Table 3 Correlation of the development of changes in physicochemical properties of fruit oils after three months of storage

Sample	Peroxide value	Acid value	Free fatty acid	Saponification value	Iodine value
Apricot	0.99*	0.92*	0.08	0.99*	-0.99*
Peach	0.99*	0.99*	0.81	0.99*	-0.99*
Plum	0.98*	0.95*	0.94*	0.99*	-0.99*

*Legend: * indicates statistical significant correlation (P<0.05).*

CONCLUSION

As mentioned in the review, several authors were dealing with quality characteristics of oils, but none of them were dealing with oils specifically produced in Europe. The differences in physical properties of fruit seed oils found in studies and literature were probably due to environmental conditions in conjunction with the varieties of species. These findings may be useful for European oil producers.

Acid value and free fatty acid in apricot oil were significantly higher, compared with the other oils in study. Fruit oils seem to have the different values in most parameters and showed also a considerable variability after three months of storage. In this case, it's difficult to identify a development trend of evaluated parameters.

Obtained results clearly indicated that the cold pressed oils without refining have significantly different studied parameters and higher levels of oxidation in a very early stage of storage, only after three months. The results of present study provide useful information for raw oils used in cosmetics and food industry and might be also beneficial when it comes to answering bio waste questions. For further support of these results, it would be highly beneficial to carry out similar study only with more samples and oils from Mediterranean.

ACKNOWLEDGEMENTS
This research was funded by "IGA-ZF/2020-AP005 "Evaluation of possibilities of utilization of by-products from fruit processing within the system of waste-free technologies" and "CZ.02.1.01/0.0/0.0/16_017/0002334 Research Infrastructure for Young Scientists, co-financed by Operational Programme Research, Development and Education".

REFERENCES

AOCS. 2017a. Free Fatty Acids in Crude and Refined Fats and Oils. Official Method Ca 5a-40 Revised 2017. Urbana, IL, USA: American Oil Chemists' Society.

AOCS. 2017b. Iodine Value of Fats and Oils, Cyclohexane-Acetic Acid Method. Official Method Cd 1d-92 Revised 2017. Urbana, IL, USA: American Oil Chemists' Society.

AOCS. 2017c. Saponification Value of Fats and Oils. Official Method Cd 3-25 Revised 2017. Urbana, IL, USA: American Oil Chemists' Society.

AOCS. 2017d. Acid Value of Fats and Oils. Official Method Cd 3d-63 Revised 2017. Urbana, IL, USA: American Oil Chemists' Society.

AOCS. 2017e. Peroxide Value, Acetic Acid, Isooctane Method. Official Method Cd 8b-90 Revised 2017. Urbana, IL, USA: American Oil Chemists' Society.

Ashraf, C.M. et al. 2011. Nutritional and physicochemical studies on fruit pulp, seed and shell of indigenous Prunus persica. Journal of Medicinal Plants Research [Online], 5(16): 3917–3921. Available at: https://academicjournals.org/journal/JMPR/article-full-text-pdf/A44B7C222542. [2020-09-17].

Bell, J.R., Gillatt, P.N. 1994. Standards to ensure the authenticity of edible oils and fats. Food, Nutrition and Agriculture [Online], 11: 29–35. Available at: http://www.fao.org/3/T4660T/t4660t0e.htm. [2020-09-17].

Chamli, D. et al. 2017. Chemical characterization and thermal properties of kernel oils from Tunisian peach and nectarine varieties of Prunus persica. Grasas y Aceites [Online], 68(3): e211. Available at: https://doi.org/10.3989/gya.0111171. [2020-09-17].

El Saadany, R.M.A. et al. 1994. Characterization of lipids extracted from peach kernels. Acta Horticulturae [Online], 368: 123–131. Available at: https://doi.org/10.17660/ActaHortic.1994.368.13. [2020-09-17].

FAO. 2001. Codex Alimentarius, fats and oils from vegetable sources. CODEX STAN 19-1981, Rev. 2 – 1999. Rome, Italy: Food and Agriculture Organization, World Health Organization.

Gupta, A. et al. 2012. Studies on physico-chemical characteristics and fatty acid composition of wild apricot (Prunus armeniaca Linn.) kernel oil. Indian Journal of Natural Products and Resources [Online], 3(3): 366–370. Available at: http://nopr.niscair.res.in/handle/123456789/14818. [2020-09-17].

Kris-Etherton, P.M. et al. 2002. Bioactive compounds in foods: their role in the prevention of cardiovascular disease and cancer. The American Journal of Medicine [Online], 113(9): 71–88. Available at: https://doi.org/10.1016/S0002-9343(01)00995-0. [2020-09-17].

Özcan, M.M. et al. 2015. A research on evaluation of some fruit kernels and/or seeds as a raw material of vegetable oil industry. Quality Assurance and Safety of Crops & Foods [Online], 7(2): 187–191. Available at: https://doi.org/10.3920/QAS2013.0319. [2020-09-17].

Savic, I. et al. 2020. Physico-Chemical Properties and Oxidative Stability of Fixed Oil from Plum Seeds (Prunus domestica Linn.). Biomolecules [Online], 10(2): 294. Available at: https://doi.org/10.3390/biom10020294. [2020-09-17].

Wu, H. et al. 2011. Essential oil extracted from peach (Prunus persica) kernel and its physicochemical and antioxidant properties. LWT - Food Science and Technology [Online], 44(10): 2032–2039. Available at: https://doi.org/10.1016/j.lwt.2011.05.012. [2020-09-17].

PLANT BIOLOGY

Plant species suitable for landfills recultivation

Martin Cerny, Erika Hurajova, Leos Kadlcek, Jan Winkler
Department of Plant Biology
Mendel University in Brno
Zemedelska 1, 613 00 Brno
CZECH REPUBLIC

xcerny@mendelu.cz

Abstract: Creating new ecosystems and supporting the occurrence of many plant species is the potential of reclaimed landfills. The paper aim is to analyze the species composition of the meadow (semi-natural habitat) and the reclaimed part of the landfill in 2010, 2011, and 2012. The area is located in Zdounky, belonging to the Kroměříž District in the Zlín Region of the Czech Republic. The evaluation of the species' coverage found at the selected habitats was carried out by Canonical Correspondence Analysis (CCA). During the observation, 67 plant species were found. In the species composition of the vegetation of the semi-natural habitat, there were local plant species that could be used for the landfill recultivation, such as *Arrhenatherum elatius, Festuca rubra,* and *Lolium perenne*. When restoring and reclaiming landfills, it is therefore essential to choose suitable plant species that are the basis of the ecosystem in the region.

Key Words: vegetation, landfill, recultivation, ecosystem

INTRODUCTION

The past five decades have seen unprecedented loss and degradation of landscapes on Earth resulting in both an irreversible decline of biodiversity and the rise of novel ecosystems containing combinations and relative abundances of species that have not occurred previously (Hobbs et al. 2006, Millennium Ecosystem Assessment 2005).

Restoration of landfill caps is generally considered problematic because of low soil structure (most often from imported soils from various sources), coarse substrate, and a high concentration of landfill gas (Athy 2006, Handel et al. 1997). After the final covering, the landfill areas have physical and chemical characteristics typical of strongly stressed environments: reducing conditions, low soil water content and low nutrient levels (Lisk 1991).

In Northern Europe, studies have indicated suitable methodologies for soil retrieval, environment renaturalization, and restoration to public use (Maurice et al. 1995). As a result, most knowledge of the potential plant species for environmental recovery is focused on those that are inappropriate for the drier climate. Theoretically, restoration practice should try to create appropriate conditions in the locality for the development of required types of plant communities over time (Depuit 1982) in order to replicate the highest levels of vegetative structure of communities, their functional attributes and ecosystem processes (Funk et al. 2008, Martin et al. 2005). However, the degree to which restored ecosystems, such as those on a capped landfill, replicate analogous systems' characteristics needs to be determined. Thus, for successful habitat restoration, knowledge of the vegetation community is crucial (Depuit 1982, Gilman et al. 1985, Wheater and Cullen 1997).

The aim of the paper is to analyze the species composition of the meadow (undisturbed habitat) and the reclaimed part of the landfill (disturbed habitat). Based on the results, identify local plant species suitable as part of the renewed vegetation in the reclaimed parts of the landfill.

MATERIAL AND METHODS

Characteristics of the area

The study was carried out in the cadastral area of Zdounky-Nětčice. It is a sanitary landfill built into a multi-layer composite bottom liner, a leachate and landfill gas collection system, and a final cover system. As for the maintenance, the landfill is included in the S-category – other waste, sub-category

S-OO3. The specified landfill area is 70 700 m^2. The total volume of this landfill is 907 000 m^3. Stage I, with an area of 19 200 m^2, has been built together with parts of phase II (5 500 m^2) and stage III (7 500 m^3). This landfill receives waste (category of other waste) from approx. 75 000 residents. The amount of waste stored annually is approx. 40 000 tons, of which 50% comes from the communal sphere. The landfill sector of subcategory S-OO1 has not yet been opened. The sector will be intended for the disposal of waste (other waste categories) with a low content of organic biodegradable substances.

The area belongs to the Kojetín region in Central Moravia (Czech Republic). The region forms a wide alluvial plain with regulated rivers. Biota has an azonal character and is dominated by agrocenoses, preserved floodplain forests, remnants of meadows and ponds with abundant fauna. According to Quitt (1971), the whole area is sitting in the warm zone T2 (the long-term average annual precipitation is 564 mm, the long-term average temperature is 8.6 °C).

Evaluation of vegetation and statistical processing

Three habitats were selected on the land with the recultivated part of the landfill, which differ in terms of the time when the reclamation was carried out. The first measurements took place at the site where the landfill was reclaimed in 2012. At the second measurement site, the landfill was reclaimed in 2011 and at the third measurement site, the landfill was reclaimed in 2010. The recultivation process involves covering the waste with a rubber film to prevent contact between the waste and the reclamation layers. Next, the approximately 1.5 m thick soil was transferred to a rubber foil. It was the original soil that was removed from the landfill. Last but not least, Festulolium was planted on this soil. The whole area is cut regularly. The fourth habitat was a meadow. It is semi-natural habitat, which is part of the landfill area and is regularly mowed twice a year. All habitats are in the area of the monitored landfill.

The evaluation of the vegetation was carried out using the phytosociological relevés of size 20 m^2. The coverage was estimated as a percentage. The monitoring took place in July 2020, 5 phytosociological relevés were recorded at each. The origin of individual plant species, names and invasive status of the plants were taken from the database of the Czech flora and vegetation Pladias (Pladias 2020).

The evaluation of the coverage of the species found at the selected habitats with different waste was carried out by means of multivariate analyses of ecological data. Then, a Canonical Correspondence Analysis (CCA) was used. Data of species covers were transformed using of square-root.

RESULTS AND DISCUSSION

Results of vegetation monitoring

Based on monitoring, 67 plant species were found. There were a total of 13 species of grasses, 10 species of legumes and 44 species of herbs. Table 1 shows the average cover of plant species found in the monitored habitats.

The gradient length calculated by DCA was 4.13. The canonical correspondence analysis CCA was chosen for further calculation. The spatial arrangement of individual plant species in the monitored variants is determined by CCA analysis. This analysis is then graphically displayed by an ordination diagram (Figure 1).

The CCA analysis results are significant at the significance level $\alpha = 0.001$ for all canonical axes. The found plant species can be divided into several groups based on CCA analysis.

The first group of species was represented mainly in the reclamation of the landfill, which took place in 2010. Species as *Erigeron annuus, Euphorbia esula, Linaria vulgaris, Medicago lupulina, Phragmites australis, Potentilla anserina, Rubus* sp., *Securigera varia, Stachys palustris, Symphytum officinale* and *Tussilago farfara* dominated in there.

The second group of species occurred mainly in the landfill, which recultivation took place in 2011. Occurring species were: *Allium oleraceum, Bromus japonicas, Calystegia sepium, Campanula rapunculoides, Cirsium vulgare, Convolvulus arvensis, Dactylis glomerata, Elytrigia repens, Festulolium, Galium album, Lactuca serriola, Melilotus officinalis, Phleum pratense, Reseda lutea,*

Silene vulgaris, Sisymbrium loeselii, Taraxacum sect. *Taraxacum, Tragopogon orientalis* and *Tripleurospermum inodorum.*

The third group are species identified in the landfill, which recultivation took place in 2012. Occurring species were: *Chelidonium majus, Dipsacus fullonum, Festuca pratensis, Sonchus oleraceus, Urtica dioica* and *Vicia cracca*.

The fourth group of species was found within the meadow – semi-natural habitat. Such species include: *Agrostis capillaris, Centaurea jacea, Lolium perenne, Lotus corniculatus, Pastinaca sativa, Pilosella officinarum, Plantago lanceolata, Salvia pratensis, Salvia verticillata, Sanguisorba officinalis* and *Trifolium repens.*

The fifth group of species was more in the landfill, which took place in 2010 and the meadow – semi-natural habitat. Plant species: *Achillea millefolium* aggr., *Arrhenatherum elatius, Artemisia vulgaris, Astragalus glycyphyllos*, *Calamagrostis epigejos*, *Carduus acanthoides, Cirsium arvense, Cornus sanguinea, Daucus carota, Falcaria vulgaris, Festuca rubra, Hypericum perforatum, Lathyrus pratensis, Picris hieracioides, Poa pratensis, Rosa canina, Silene latifolia, Tanacetum vulgare* and *Trifolium aureum.* These species can be used in recultivated areas and they also belong to flora sites.

Table 1 Average cover of found plant species in monitored habitats

Species	Abbreviations	Recultivation 2012	Recultivation 2011	Recultivation 2010	Meadow
Achillea millefolium aggr.	*Ach mill*	0.0	0.0	1.6	1.6
Agrostis capillaris	*Agr capi*	0.0	0.0	0.0	6.4
Allium oleraceum	*All oler*	0.0	0.3	0.0	0.0
Arrhenatherum elatius	*Arr elat*	23.0	23.8	36.4	34.0
Artemisia vulgaris	*Art vulg*	0.0	1.0	1.0	1.8
Astragalus glycyphyllos	*Ast glyc*	1.4	0.0	0.0	3.6
Bromus japonicus	*Bro japo*	0.6	0.4	0.0	0.0
Calamagrostis epigejos	*Cal epig*	12.4	6.9	6.1	9.0
Calystegia sepium	*Cal sepi*	0.0	1.1	0.6	0.0
Campanula rapunculoides	*Cam rapu*	0.0	0.1	0.0	0.0
Carduus acanthoides	*Car acan*	3.4	2.9	2.1	2.6
Centaurea jacea	*Cen jace*	0.0	0.0	0.0	2.0
Cirsium arvense	*Cir arve*	3.1	2.0	10.1	6.0
Cirsium vulgare	*Cir vulg*	1.6	0.0	0.0	0.0
Convolvulus arvensis	*Con arve*	1.6	1.5	1.1	0.0
Cornus sanguinea	*Cor sang*	0.0	0.0	0.3	1.0
Dactylis glomerata	*Dac glom*	4.1	6.5	0.0	3.0
Daucus carota	*Dau caro*	0.0	0.6	1.1	2.8
Dipsacus fullonum	*Dip full*	2.3	0.6	0.0	0.0
Elytrigia repens	*Ely repe*	11.8	5.4	0.6	4.0
Erigeron annuus	*Eri annu*	0.0	0.0	0.4	0.0
Euphorbia esula	*Eup esul*	0.0	0.1	0.6	0.0
Falcaria vulgaris	*Fal vulg*	0.0	0.6	0.0	0.8
Festuca pratensis	*Fes prat*	3.1	0.0	0.0	0.0
Festuca rubra	*Fes rubr*	1.3	1.5	2.5	8.0
x *Festulolium*	*xFestuloli*	23.1	24.6	8.4	0.0
Galium album	*Gal albu*	17.1	9.8	1.3	0.0
Hypericum perforatum	*Hyp perf*	0.8	1.8	3.5	1.8
Chelidonium majus	*Che maju*	0.1	0.0	0.0	0.0

Table 1 Average cover of found plant species in monitored habitats – continue

Species	Abbreviations	Recultivation 2012	Recultivation 2011	Recultivation 2010	Meadow
Lathyrus pratensis	*Lat prat*	0.0	1.3	7.8	3.6
Lathyrus tuberosus	*Lat tube*	12.1	15.0	28.5	5.0
Linaria vulgaris	*Lin vulg*	0.0	0.0	0.9	0.0
Lolium perenne	*Lol pere*	0.0	0.0	0.0	3.6
Lotus corniculatus	*Lot corn*	0.0	0.0	0.0	1.6
Lactuca serriola	*Lac serr*	1.0	0.0	0.0	0.0
Medicago lupulina	*Med lupu*	0.0	0.0	0.1	0.0
Melilotus officinalis	*Mel offi*	0.0	1.3	0.0	0.0
Pastinaca sativa	*Pas sati*	0.0	0.0	0.0	1.0
Phleum pratense	*Phl prat*	4.4	4.1	0.0	3.0
Phragmites australis	*Phr aust*	0.0	0.0	1.8	0.0
Picris hieracioides	*Pic hier*	0.0	0.0	0.6	0.2
Pilosella officinarum	*Pil offi*	0.0	0.0	0.0	1.6
Plantago lanceolata	*Pla lanc*	0.0	0.0	0.0	1.4
Poa pratensis	*Poa prat*	1.3	2.5	0.0	2.0
Potentilla anserina	*Pot anse*	0.0	0.0	0.1	0.0
Reseda lutea	*Res lute*	0.0	0.4	0.0	0.0
Rosa canina	*Ros cani*	0.0	0.1	1.3	0.6
Rubus sp.	*Rub sp.*	0.6	0.1	5.4	0.0
Salvia pratensis	*Sal prat*	0.0	0.0	0.0	4.2
Salvia verticillata	*Sal vert*	0.0	0.0	0.0	3.0
Sanguisorba officinalis	*San offi*	0.0	0.0	0.0	0.6
Securigera varia	*Sec vari*	0.0	10.4	15.0	0.0
Silene latifolia	*Sil lati*	0.0	0.9	0.0	3.0
Silene vulgaris	*Sil vulg*	0.0	0.3	0.0	0.0
Sisymbrium loeselii	*Sis loes*	0.5	1.0	0.0	0.0
Sonchus oleraceus	*Son oler*	0.1	0.0	0.0	0.0
Stachys palustris	*Sta palu*	0.0	0.0	0.3	0.0
Symphytum officinale	*Sym offi*	0.6	2.3	7.0	0.0
Tanacetum vulgare	*Tan vulg*	0.1	0.0	0.6	2.0
Taraxacum sect. *Taraxacum*	*Tar sect*	0.0	0.3	0.0	0.0
Tragopogon orientalis	*Tra orie*	2.5	3.3	1.9	0.0
Trifolium aureum	*Tri aure*	0.0	0.3	0.0	1.2
Trifolium repens	*Tri repe*	0.0	0.0	0.0	1.0
Tripleurospermum inodorum	*Tri inod*	0.0	1.1	0.3	0.0
Tussilago farfara	*Tus farf*	0.0	0.0	1.1	0.0
Urtica dioica	*Urt dioi*	0.6	0.0	0.0	0.0
Vicia cracca	*Vic crac*	1.5	0.0	0.0	0.0

Plant community structure and its dynamics are influenced by several local habitat quality factors combined with the effects of the regional species pool, dispersal limitation, and the presence of habitats nearby (Poschlod et al. 2005). Succession combined with management on newly created sites may lead to the formation of semi-natural grassland which may be further enhanced by the introduction of seed or plant material or by natural colonization if sources from the seed bank or neighbouring habitats are present (Ejrnæs et al. 2008, Morris et al. 2006).

From our results, it is clear that there are local plant species in the species composition of the vegetation of the semi-natural habitat, suitable for landfill recultivation. Such grass species include *Arrhenatherum elatius, Festuca rubra* and *Lolium perenne.* Among legumes, we can find the following species: *Astragalus glycyphyllos*, *Lotus corniculatus* and *Trifolium repens*. Of Herbs, these are the following species *Daucus carota*, *Pastinaca sativa*, *Salvia pratensis*, *S. verticillata* and *Silene latifolia*.

The presence of local plant species in the reclaimed landfill will enable faster restoration and creation of a new ecosystem and the effective integration of the recultivated landfill into the surrounding landscape. Some species are able to colonize the reclaimed landfill without human intervention, such as *Achillea millefolium* aggr., *Daucus carota, Hypericum perforatum* and *Lathyrus pratensis*. However, the succession of phytocenosis of a reclaimed landfill is a dynamic process. In order to formulate certain trends, multi-annual observations are needed.

Figure 1 Ordination diagram showing the relationship between monitored habitats and found plant species; result of CCA analysis

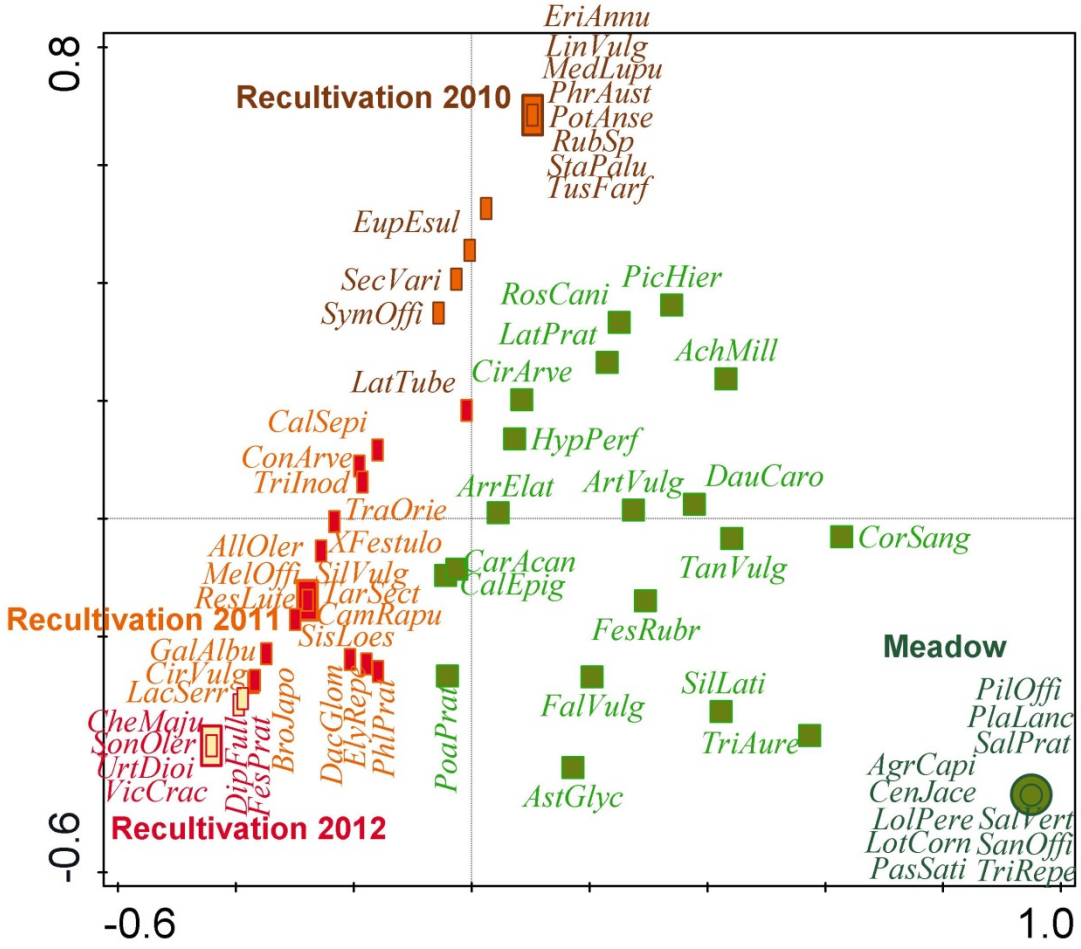

Legend: Recultivation 2010 – part of the landfill reclaimed in 2010; Recultivation 2011 – part of the landfill reclaimed in 2011; Recultivation 2012 – part of the landfill reclaimed in 2012; Meadow – the habitat with meadow

CONCLUSION

Reclaimed landfills have the potential to support the emergence of many plant species and could create new ecosystems. Therefore, it is crucial to choose suitable plant species based on the ecosystem in the region when restoring and reclamation landfills. The data collected in this work will provide a basis for future botanical monitoring and subsequent reclamation of other parts of the landfill in this region.

The results also show that botanical monitoring of the surrounding areas is necessary during recultivation, which must be the basis for choosing a suitable mixture of plants. The use of local plant species guarantees quick regeneration and integration of the new ecosystem into the surrounding landscape.

ACKNOWLEDGEMENTS

This work was created with the financial support of project IGA AF-IGA2020-IP004 Study of synantropic vegetation of municipal waste dumps.

REFERENCES

Athy, E.R. et al. 2006. Effects of mulch on seedlings and soil on a closed landfill. Restoration Ecology, 14(2): 233–241.

Depuit, J.E. 1982. Potential topsoiling strategies for enhancement of vegetation diversity on mined lands. Minerals and the Environmental, 6(3): 115–120.

Ejrnæs, R. et al. 2008. When has an abandoned field become a semi-natural grassland or heathland? Environmental Management, 42(4): 707–716.

Funk, J.L. et al. 2008. Restoration through reassembly: Plant traits and invasion resistance. Trends in Ecology & Evolution., 23(12): 695–703.

Gilman, E.F. et al. 1985. Standardized procedures for planting vegetation on completed sanitary landfills. Waste Management and Research, 3(1): 65–80.

Handel, S.N. et al. 1997. Restoration of woody plants to capped landfills: Root dynamics in an engineered soil. Restoration Ecology, 5(2): 178–186.

Hobbs, R.J. et al. 2006. Novel ecosystems: Theoretical and management aspects of the new ecological world order. Global Ecology and Biogeography, 15(1): 1–7.

Lisk, D.J. 1991. Environmental effects of landfill. The Science of the Total Environment, 100(2): 415–468.

Martin, L.M. et al. 2005. An assessment of grassland restoration success using species diversity components. Journal of Applied Ecology, 42(2): 327–336.

Maurice, C. et al. 1995. Vegetation as a biological indicator for landfill gas emissions: initial investigations. In Proceedings of Sardinia ’95, Fifth International Landfill symposium. S. Margherita di Pula, Italy, 2–6 October. Cagliari: Environmental Sanitary Engineering Centre, pp. 685–698.

Millennium Ecosystem Assessment. 2005. Millennium ecosystem assessment synthesis report. [Online]. Available at: http://www.maweb.org. [2020-05-12].

Morris, R.K.A. et al. 2006. The creation of compensatory habitat—Can it secure sustainable development? Journal for Nature Conservation, 14(10): 106–116.

Pladias. 2020. Database of the Czech flora and vegetation. [Online]. Available at: https://www.pladias.cz/en/. [2020-05-12].

Poschlod, P. et al. 2005. Plant dispersal potential and its relation to species frequency and coexistence. In Vegetation ecology. Oxford: Blackwell, pp. 147–171.

Quitt, E. 1971. Klimatické oblasti Československa. Studia geographica, Praha: Academia.

Wheater, C.P., Cullen, W.R. 1997. The flora and invertebrate fauna of abandoned limestone quarries in Derbyshire, United Kingdom. Restoration Ecology, 5(1): 77–84.

Genetic analysis of selected genes active in chickpea seed dormancy and germination testing

Veronika Sedlakova[1], Pavel Hanacek[1], Marie Grulichova[1], Petr Smykal[2]
[1]Department of Plant Biology
Mendel University in Brno
Zemedelska 1, 613 00 Brno
[2]Department of Botany
Palacký University Olomouc
Slechtitelu 27, 783 71 Olomouc
CZECH REPUBLIC

veronika.sedlakova@mendelu.cz

Abstract: The most important event in the plant life cycle is transition from seed to seedling. Germination is an irreversible process and therefore correct timing is required. Several dormancy mechanisms exist among plants. Physical dormancy can be observed in legumes. Recombinant inbred lines derived from crossing of cultivated and wild parents of chickpea serve as a good model to clarify seed dormancy loss during crop domestication and its genetic basis. Restriction analysis was carried out using the cleaving of amplified polymorphic sequences method. For 6 candidate loci located on intervals of chromosome 1 and 5 were determined possible primer combinations with products that showed variability over non-coding regions. Polymorphic restriction recognition sites were found and restriction mapping was done with parental genotypes. Testing of optimal conditions for restriction analysis and primer combinations for population mapping are still ongoing process. In addition, the presence of physical dormancy in seeds was observed during germination testing. Two parental genotypes and population of 51 inbred lines were evaluated over 7 days' period. Final germination percentage ranged from 20–100% and divided population into dormant and non-dormant group.

Key Words: chickpea, seed coat, germination, physical dormancy, hardseededness

INTRODUCTION

Chickpea (*Cicer arietinum* L.) is the second most important food legume crop (after beans) that is widely grown in arid and semi-arid regions all over the world in about 57 countries, with India as the largest producer. Chickpea seeds are rich source of protein (20–30%) with considerable amount of essential amino acids (e.g. lysine, tyrosine, glutamic acid and histidine), carbohydrates (40%), minerals (e.g. phosphorus, calcium, magnesium, iron and zinc) and vitamins (e.g. β-carotene) (Kudapa et al. 2018). Therefore, chickpea is essential for human nutrition both in developing and developed countries. Planet Earth is currently inhabited by approximately 7.8 billion people of which 2 billion experience micronutrient deficiency (Varshney et al. 2019) and by 2050 is projected almost 50% increase. Ongoing climate change and global warming pose vast challenges for plant breeders to maintain and enhance yield of more high quality crop food for growing human population using increasingly limited land and water resources (Merga and Haji 2019).

Chickpea was domesticated in the Fertile Crescent with many others so-called founder crops and it is also its place of origin (Kafadar et al. 2018). Both wild and cultivated chickpea are annual diploid (2n=16) and self-pollinating plants (Wang et al. 2019). Cultivated chickpea differs from its wild relatives in several traits, e.g. in its erect plant growth habit, pod dehiscence, seed coat texture and reduced seed dormancy. These are considered as 'domestication syndrome' traits, which were favoured by farmers during crop domestication process (Penmetsa et al. 2016). Seed dormancy is defined as a condition in which intact viable seeds are incapable to germinate even under favourable environmental conditions. Seed dormancy has two main functions: 1) to synchronize germination with optimal environmental conditions for plant survival; 2) to distribute seed germination in time, when possible disaster (e.g. frost, dry, herbivores) doesn't lead to the death of all individuals. Germination determines the beginning of plant growth in both natural and agricultural ecosystems.

Seeds of wild plants are often dormant and will germinate only after exposure to certain environmental conditions. In contrast, crop seeds germinate immediately after water imbibition.

There exist several seed dormancy classes and mechanisms. Underdeveloped embryo which requires more time to grow and germinate belongs to morphological dormancy. Predominant form of dormancy is physiological dormancy and comprise of abscisic acid (ABA) and gibberellins (GAs) metabolism. Furthermore, there exist morpho-physiological and combinational dormancies. In contrast to those very well studied categories, there is physical dormancy (often called hardseededness) that can be observed in legumes and at least 16 more plant families and is characteristic by water-impermeable seed coat generated by occurrence of phenolics- and suberin-impregnated layers of palisade cells (Baskin et al. 2000).

The aim of this study was to perform genetic analyses of selected genes that could be active in chickpea seed dormancy. Population of recombinant inbred lines was mapped with use of several molecular biology methods. Moreover, imbibition and germination testing were performed as a part of dormancy analysis.

MATERIAL AND METHODS

Plant material

Two parental genotypes were chosen for analysis – non-dormant cultivated chickpea (*Cicer arietinum* L., ICC 4958) and dormant wild chickpea (*Cicer reticulatum* L., PI 489777). Furthermore 119 F8 recombinant inbred lines (RILs) derived from the cross of these two parental genotypes (Faculty of Science, Palacký University Olomouc, Smykal).

Ten seeds of each of the parental genotypes and 119 RILs were placed onto filter paper wetted with tap water and fungicide (Maxim XL035 FS) to prevent fungal growth and let at room temperature in the dark. Germinated seeds were cultivated in substrate (Substrate for sowing and plantlets, Gramoflore, Germany) in a climatic chamber at 24/19 °C day/night temperatures under a 16/8 h day/night cycle photoperiod and light intensity 150 µmol m^{-2} s^{-1}. In case seeds didn't imbibe after 10 days, scarification was performed. After 7 days, young leaf samples were taken, lyophilized and stored in the freezer at -70 °C until genetic analyses.

The second stage of plant cultivation has the same process of germination, except that germinated seeds were cultivated in 3.5 litres pots in the soil substrate (TS3, Klasmann, Germany) in a greenhouse with 15 h light regime and temperature 23–25 °C/day and 18–20 °C/night. Plants with no buds after 2 months of cultivation had to go through the process of vernalisation in the climatic chamber with photoperiod 13 h and temperature 13–15 °C for 7–10 days. Greenhouse plants were grown to maturity. Immature seeds were harvested at defined developmental stages (10–15–20–25 dpa, days post anthesis). Embryo and seed coat of seeds were mechanically separated and stored at -70 °C for further transcriptomic analysis (not included in this work). Mature seeds were air dried and stored at room temperature in the dry place for subsequent germination testing.

Genetic mapping

Genomic DNA was isolated from lyophilized leaves using the NucleoSpin Plant II Mini Kit (Macherey-Nagel, Germany) and from fresh leaves using Invisorb® Spin Plant Mini Kit (Stratec Molecular, Germany).

According to Kudapa et al. (2018) gene expression atlas of chickpea (*Cicer arietinum*) and online database http://knowpulse.usask.ca were chosen possible candidate genes in defined intervals on chromosome 1 and 5. Defined intervals are located on chromosomes of cultivated chickpea, while genetic mapping was done with RILs population, therefore possible translocations and differences were expected.

CAPS-PCR (Cleaved Amplified Polymorphic Sequences–Polymerase Chain Reaction) analysis was performed with selected genes in the mapped intervals. Pairs of specific primers for chosen markers were designed using Geneious Prime 2019.1 (Biomatters Ltd., New Zealand) to amplify 1200–1600 bp DNA fragments. Selection of suitable markers was done by PCR amplification and sequencing of parental genotypes PCR products of each marker. Differences in sequences between parental genotypes – SNPs (Single Nucleotide Polymorphism) were found and compared with possible

restriction endonuclease recognition sites. Digestion with selected restriction enzymes (EcoR I, Hha I, Mse I, Mbo I, Taq I) was performed. In case there weren't any restriction sites for SNP, dCAPS (Derived Cleaved Amplified Polymorphic Sequences) was performed. This method allows introducing new restriction enzyme recognition site by using primer(s) with mismatch(es) to the DNA. dCAPS primers were designed by dCAPS Finder 2.0. PCR with combination of specific and dCAPS primers was performed. To avoid non-specific products, two-step amplification was performed – semi-nested PCR. Electrophoretic separation of PCR products was performed in 1% agarose gel and separation of digestion products was performed in 2% agarose gel.

Germination and dormancy testing

Two parental and 51 RILs of F9 generation were subjected to analysis of seed germination. Ten seeds per line/parent with two or three replicas were incubated in Petri dishes with filter papers, wetted with 3 ml of tap water with addition of fungicide (Maxim XL035 FS) and incubated at 25 °C in incubator in the dark. At 24 h intervals were scored numbers of imbibed seeds and once the radicle breaks through seed coat, it was considered germinated. If the seed didn't swell even after 10 days, mechanical scarification with sandpaper was performed. Final germination percentage (FGP) and Mean germination time (MGT) were calculated over 7 days' period.

RESULTS AND DISCUSSION

CAPS-PCR analysis

Isolated genomic DNA of two parental genotypes (non-dormant cultivated chickpea – ICC 4958 and dormant wild chickpea – PI 489777) and population of recombinant inbred lines were analysed. There were chosen 6 candidate genes with possible relation with genetic basis of seed dormancy. Candidate loci's primers were designed to span over non-coding regions with expectation of higher variability and with primer sequences in coding regions. However, our data wasn't in accordance with Tabassum and Suman (2006) study, where they stated that non-coding regions generally contain about three times more SNPs than the coding regions. Low variability may be caused due to a smaller genome size or other genetic aspects. Low genetic diversity was also detected by Wang et al. (2019) in the study of RILs population of two cultivated chickpea accessions.

Within analysed intervals of chromosome 1 and 5 with low rate of polymorphism were most of the founded SNPs located on PI sequences. This finding was based on a comparison with cultivated chickpea reference sequence and sequence of ICC that we analysed. Numbers of founded SNPs and numbers of usable polymorphic restriction recognition sites for CAPS-PCR analysis are shown in Table 1. Usability of SNP depends on its polymorphism between parental genotypes and its presence in restriction site. In all 6 candidate loci on chromosome 1 and 5 intervals were found SNPs, but polymorphic restriction recognition sites were found only in 4 loci. Restriction recognition sites matched with restriction endonucleases EcoR I, Hha I, Mbo I, Mse I and Taq I. Ca_12643_7821 candidate locus' SNP founded between parental genotypes that is at the same time polymorphic in restriction recognition site for restriction endonuclease EcoR I (Figure 1). Some of the analysed loci have higher SNPs number, such as locus Ca_00502_4007 that has 9 SNPs of which 3 are polymorphic with 3 different restriction endonucleases. On the other hand, loci Ca_03899_3254 and Ca_12687_647 have SNPs but no polymorphic restriction site. Therefore, dCAPS primers were designed both for loci with no polymorphic sites and also as supplementary for those with polymorphic sites. Locus Ca_00502_4007 hence, in addition gained two more restriction sites with plus one restriction endonuclease. Semi-nested PCR was done and two-step amplification with specific and dCAPs primers reduced occurrence of non-specific products, which is in accordance with study by Hruba (2007), where they obtained clear PCR products with this extra step.

Restriction analyses were done for parental genotypes and preliminary results are shown in a Table 2. Only provable combination of specific or dCAPS primers that digest PCR products are published. Testing of optimal conditions of restriction analyses and of optimal specific/dCAPS primer pairs combinations are still ongoing process. Once the desired results have been achieved, the whole RILs population can be analysed.

Table 1 Candidate loci and restriction endonucleases

	Candidate locus	SNPs	Polymorphic RRS	Restriction endonuclease	dCAPS polymorphic RRS
C5	Ca_03899_3254	7	0	-	MboI
	Ca_03926_2983	3	1	Mbo I	Mbo I, Taq I
	Ca_12643_7821	11	2	EcoR I, Mbo I	Mbo I, Taq I
	Ca_12687_647	1	0	-	Hha I
C1	Ca_00470_5125	6	2	Mse I, Taq I	-
	Ca_00502_4007	9	3	Hha I, Mbo I, Mse I	Mbo I, Taq I

Legend: C5 – chromosome 5 interval, C1 – chromosome 1 interval, SNP – single nucleotide polymorphism, RRS – restriction recognition site, dCAPS – Derived Cleaved Amplified Polymorphic Sequences

Figure 1 Candidate locus Ca_12643_7821 – polymorphic restriction recognition site for EcoR I between two parental genotypes

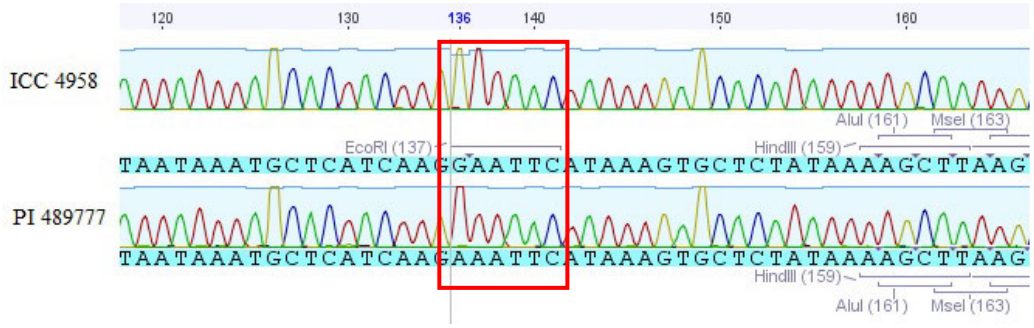

Legend: ICC – cultivated parent, PI – wild parent

Table 2 Preliminary data of restriction analysis

	Candidate locus	Primer combination	Restriction endonuclease	Restriction	
				ICC	PI
C5	Ca_03926_2983	26/2FdCAPS+26R	Taq I	N	R
		26.1F+26.1RdCAPS	Taq I	N	R
	Ca_12643_7821	43F+43R	EcoR I	R	N
	Ca_12687_647	87FdCAPS+87R	Hha I	N	R
C1	Ca_00502_4007	02F+02R	Hha I	N	R
		02.1FdCAPS+02.1R	Taq I	N	R
		02FdCAPS+02R	Mbo I	N	R

Legend: C5 – chromosome 5 interval, C1 – chromosome 1 interval, N – no restriction, R – restriction

Germination and dormancy testing

Imbibition and germination test were used to score a rate of seed dormancy. Two parental genotypes ICC, PI and population of 51 RILs of F9 generation were evaluated after 7 days. Primary interest of this work is study of physical dormancy (PY) caused by seed testa as a water impermeable barrier, that is a reason why number of imbibed seeds should be used as a measure of germination as it was used in pea analyses according to Hradilova et al. (2019). This intention has been abandoned, because of the fact, that after 7 days counting both ICC and PI plus another 41 RILs had 100% imbibition. Percentage of remaining 10 RILs didn't fall below 70%. All RILs imbibed quickly within 7 days. In contrast, 97 pea accessions analyses by Hradilova et al. (2019) were tested over period of 28 days and final percentage of germinated (imbibed) seeds ranged from 0–100%, that means some seeds didn't imbibe and germinate at all. Final germination percentage (FGP) was evaluated after 7 days of measurement and germinated seeds ranged from 20–100% (Figure 2). RILs data can be divided

into two groups – non-dormant group with further division into those that germinated very quickly (33 RILs germinating between 90–100% at 7 days) and those that germinated more slowly (13 RILs germinating between 60–89% at 7 days). Second is dormant group (5 RILs) germinating between 20–57% at 7 days. Cultivated parent ICC belongs to non-dormant group with 100% germinating at 7 days and Mean germination time 2.95. For comparison with non-dormant cultivated pea according to Hradilova et al. (2019), MGT is 3.4 and 100% imbibition within 24 h which coincide with imbibition data for cultivated chickpea. It was found out, that wild parent PI also germinate quickly and with 83% germinating at 7 days belong to non-dormant group, MGT is 4.76. These data doesn't correspond with previous dormancy testing (not published), where PI was dormant with 30% germinating at 7 days. This might be caused by limited number of seeds used in testing. A graphical representation of dormant and non-dormant RILs (Figure 2) would probably look different, as long as more RILs will be tested. Presumably due to the lack of light in the greenhouse and other environmental factors, relatively few seeds were harvested of the few RILs plants.

Figure 2 Final germination percentage divided RILs into two groups – dormant and non-dormant

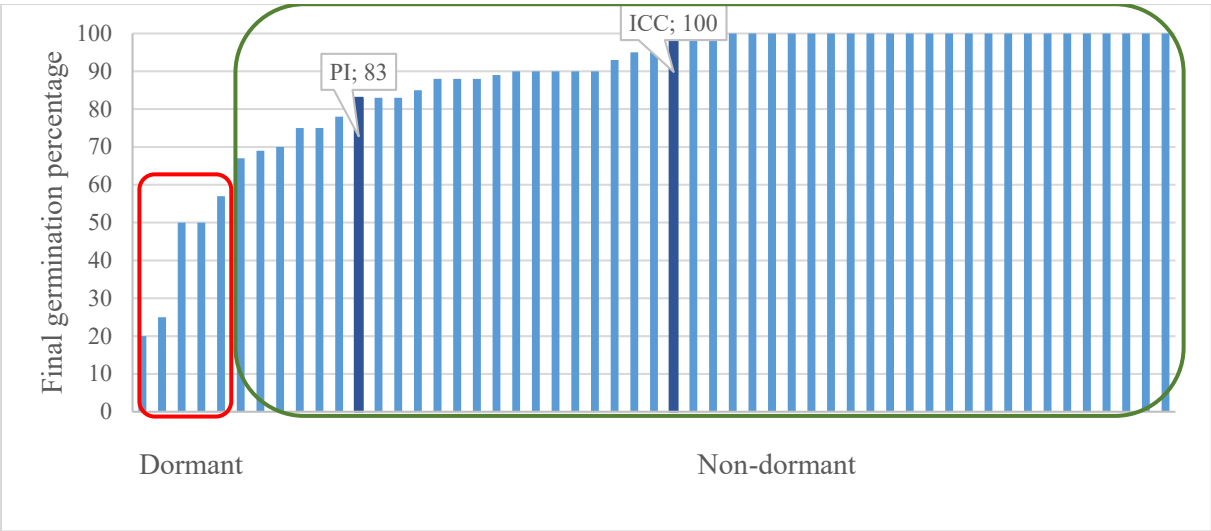

Legend: RILs – recombinant inbred lines, ICC – cultivated parent, PI – wild parent

CONCLUSION

In this study was performed genetic analysis of mapping population (RILs) of selected candidate genes active in chickpea seed dormancy that can be responsible for loss of dormancy during crop domestication. Several primer combinations of candidate loci were identified and CAPS-PCR analyses can be subsequently performed with the whole mapping population. Moreover, germination testing was accomplished and divided RILs into dormant and non-dormant group. Once the genetic mapping of population and dormancy testing is done, certain patterns and correlations can be observed.

ACKNOWLEDGEMENTS

The research was financially supported by the internal grant of Mendel University in Brno AF-IGA2020-IP011. Acknowledgements belong to Clarice J. Coyne (USDA-ARS Pullman, USA) and E.B. von Wettberg (UVM, USA) for providing seeds of parental genotypes and mapping population.

REFERENCES

Baskin, C.C. et al. 2000. Taxonomy, anatomy and evolution of physical dormancy in seeds. Plant Sciences Biology [Online], 15(1): 139–152. Available at: https://esj-journals.onlinelibrary.wiley.com/doi/full/10.1046/j.1442-1984.2000.00034.x. [2020-08-27].

Hradilova, I. et al. 2019. Variation in wild pea (*Pisum sativum* subsp. e*latius*) seed dormancy and its relationship to the environment and seed coat traits. PeerJ [Online], 7: e6263. Available at: https://peerj.com/articles/6263/. [2020-09-16].

Hruba, M. 2007. dCAPS method: Advantages, troubles, and solution. Plant Soil Environment [Online], 53(9): 417–420. Available at: https://www.agriculturejournals.cz/publicFiles/00334.pdf. [2020-09-17].

Kafadar, F.N. et al. 2018. Genetic and biochemical properties of *Cicer* spp reveal distinction between wild and cultivated chickpea genotypes. Legume Research, 42(1): 1–9.

Kudapa, H. et al. 2018. The RNA-Seq-based high resolution gene expression atlas of chickpea (*Cicer arietinum* L.) reveals dynamic spatio-temporal changes associated with growth and development. Plant, Cell & Environment [Online], 41(1): 2209–2225. Available at: https://onlinelibrary.wiley.com/doi/10.1111/pce.13210. [2020-08-27].

Merga, B., Haji, J. 2019. Economic importance of chickpea: Production, value, and world trade. Cogent Food & Agriculture [Online], 5(1): 1–12. Available at: https://www.cogentoa.com/article/10.1080/23311932.2019.1615718. [2020-08-27].

Penmetsa, R.V. et al. 2016. Multiple post-domestication origins of *kabuli* chickpea through allelic variation in a diversification-associated transcription factor. New Phytologist [Online], 211(1): 1440–1451. Available at https://nph.onlinelibrary.wiley.com/doi/full/10.1111/nph.14010. [2020-08-27].

Tabassum, J., Suman, L. 2006. Single nucleotide polymorphism (SNP)- Methods and applications in plant genetics: A review. Indian Journal of Biotechnology [Online], 5(1): 435–459. Available at: http://nopr.niscair.res.in/bitstream/123456789/5608/1/IJBT%205%284%29%20435-459.pdf. [2020-09-16].

Varshney, R.K. et al. 2019. Resequencing of 429 chickpea accessions from 45 countries provides insights into genome diversity, domestication and agronomic traits. Nature Genetics [Online], 51(1): 857–864. Available at https://www.nature.com/articles/s41588-019-0401-3. [2020-08-27].

Wang, R. et al. 2019. Co-localization of genomic regions associated with seed morphology and composition in a desi chickpea (*Cicer arietinum* L.) population varying in seed protein concentration. Theoretical and Applied Genetics [Online], 132(1): 1263–1281. Available at: https://link.springer.com/article/10.1007%2Fs00122-019-03277-5. [2020-08-27].

Growth, morphological and biochemical response of *Pisum sativum* roots to non-steroidal anti-inflammatory drug naproxen

Lucie Svobodnikova[1], Marie Kummerova[1], Stepan Zezulka[1], Petr Babula[2], Katarina Sendecka[3]
[1]Department of Experimental Biology
Masaryk University Brno
Kotlarska 2, 611 37 Brno
[2]Department of Physiology
Masaryk University Brno
Kamenice 753/5, 625 00 Brno
[3]Laboratory of Metabolomics and Isotope Analyses
Global Change Research Institute, AV
Belidla 986/4a, 603 00 Brno
CZECH REPUBLIC

svobodnikova@mail.muni.cz

Abstract: Non-steroidal anti-inflammatory drugs as an important group of emerging environmental contaminants in irrigation water and soils can influence biochemical and physiological processes essential for growth and development in plants as non-target organisms. Plants are able to take up, transport, transform, and accumulate drugs in the roots. Root biomass in ten-day old pea plants was lowered by 6% already under 0.1 mg/l naproxen (NPX) due to lowered number of lateral roots. Stimulation of the total root length by 30% under 0.5 mg/l was followed by its decline by 80% at 10 mg/l NPX as compared to control. Accumulated drug (up to 10 µg/g dry weight at 10 mg/l) in roots increased the amounts of hydrogen peroxide (by 33%), and superoxide (by 62%), which was reflected in elevated lipid peroxidation (by 32%). Antioxidant capacity reached its maximum at 0.5 mg/l but decreased at 10 mg/l NPX by approx. 30%. NPX was proved to cause changes at both cellular and tissue levels in roots, which was also reflected in their morphology. Higher environmental loading by drugs thus can influence even the root function.

Key words: drug, root growth, root system morphology, oxidative stress, antioxidant defence

INTRODUCTION

Drugs deserve the same attention as other pollutants because of their increasing entry into the environment and hazardous potential based on their possible high toxicity for non-target organisms (López-Pacheco et al. 2019) including plants (Ahmed et al. 2015, Bartrons and Peñuelas 2017). Obsolete or insufficient technologies for wastewater and sewage processing represent the main source of contamination by various mixtures of drugs and products of their transformation with possible synergistic or antagonist effects for both aquatic and terrestrial ecosystems (Bellver-Domingo et al. 2017). Nevertheless, to understand the combined effects, it is essential to assess each compound separately. Naproxen ((S)-(+)-2-(6-methoxy-2-naphthyl) propionic acid, NPX) is one of the most commonly used and currently monitored drugs throughout the world (López-Pacheco et al. 2019, Marsik et al. 2017).

Plants can play an essential and positive role in removing pollutants, including drugs, resulting from direct phytoremediation and indirectly enhancing sorption and biodegradation. Because plants are site-fixed, the plasticity of the root system represents one mechanism by which they can adapt to current environmental conditions. Root architecture results from complex and continuous *de novo* organogenic processes, consisting of activity of apical root meristem, cell differentiation, initiation and formation of lateral root primordia, and the emergence of lateral roots or processes of vascular bundle elements differentiation and maturation. These processes are initiated and regulated at the subcellular level not

only by endogenous signalling molecules like phytohormones or reactive oxygen species (ROS), but also influenced by various external stress factors.

Drugs are able to cause the overproduction of ROS, which is associated with the direct damage of various biomolecules and alterations in plant cell redox state. Changes in antioxidant capacity and amounts/activities of both enzymatic and non-enzymatic antioxidant mechanisms (Baxter et al. 2014, Farmer and Mueller 2013) are usually the first responses to environmental stress.

MATERIALS AND METHODS

Naproxen preparation

Naproxen sodium salt (NPX) was dissolved in a mixture of acetone and distilled water in ratio 1:9 (*v:v*) and added to a nutrient solution (pH 5.5 ± 0.1; Reid and York, 1958) to final concentrations simulating low environmentally realistic (0.1 and 0.5 mg/l; López-Pacheco et al. 2019) to higher (1 and 10 mg/l) loading.

Plant material and experimental design

The plant material used was pea (*Pisum sativum* L., cv. Zázrak z Kelvedonu). Five-day old seedlings were transplanted into cultivation vessels with a nutrient solution without (control; 0 mg/l) or with NPX and cultivated for 10 days. The cultivation was done under controlled conditions (23 ± 1 °C, relative air humidity 60%, photoperiod 14/10, and irradiation up to 300 µmol/m^2.s of photosynthetic active radiation – PAR provided by white metal-halid lamps, Kanlux, Czech Republic).

Growth and plant analysis

Dry weight was determined according to Zezulka et al. (2019). Root systems of five plants were acquired by a flatbed scanner and pictures were analysed using RootNav software (Pound et al. 2013) for determining the total length of root systems and the number of lateral roots.

Biochemical traits

Hydrogen peroxide, superoxide anion radical, and the content of total thiols were determined spectrophotometrically according to the methodology described in Zezulka et al. (2019). Lipid peroxidation was determined spectrophotometrically and expressed as malondialdehyde content (MDA) according to Zezulka et al. (2019). Total antioxidant capacity (TAC) was measured using Total Antioxidant Capacity Assay kit (Sigma-Aldrich, USA) and expressed in mmol of Trolox Equivalents according to manufacturer´s instructions.

Determination of NPX

After lyophilisation, the extraction of samples was performed according to Bartha et al. (2014) with HCl/acetonitrile (1:1, *v:v*) mixture into a volume of 4 mL. The extract was analysed by HLPC-HRMS (Dionex Ultimate 3000 with Hypersil Gold column (150mm × 2.1mm, 3µm)), and LTQ Orbitrap XL with HESI II source (all Thermo Fisher Scientific, USA) in negative polarity mode. The quantification of NPX was performed by external standard calibration.

Statistics

For statistical evaluation, the software STATISTICA (StatSoft, Inc.®, Tulsa, USA) was used. In all assessed parameters, the resulting data represent a mean over at least five repetitions. The significance of the difference was evaluated by the one-way analysis of variance after preceding verification of data normality and homogeneity of data variance (ANOVA, $P< 0.05$). The comparison of means was made by the Tukey HSD range test.

RESULTS AND DISCUSSION

Root system growth and morphology

The root biomass can be reliable external indicator of the internal affection of plant metabolism. Figure 1A presents that while the growth of pea roots, which were in direct contact with contamination, was limited already at 0.1 mg/l (dry weight lowered by 6% as compared to control), the above-ground

part of plants was reduced only by 10 mg/l NPX (by 15%). In contrast, reduced growth of roots in pea under diclofenac (DCF) and paracetamol (PCT) treatments (Zezulka et al. 2019) or in *Arabidopsis thaliana* treated by NPX (Landa et al. 2018) was found only under higher concentrations (from 5 mg/l and above). Remarkably, at 0.1 mg/l NPX, which can be found in the natural environment (López-Pacheco et al. 2019), the limited growth of roots expressed as a decrease (by 7%) in ratio of root and shoot dry weights (Root-to-Shoot Ratio, RSR, Figure 1A) did not affect the growth of shoot.

Figure 1 Dry weight (g) of roots and shoots and root-to-shoot dry weight ratio (RSR; A), total length of roots (cm), total number of lateral roots (B), and the naproxen content (µg/g dry weight) and bioconcentration factor (BCF, r.u.) (C) in Pisum sativum cultivated in nutrient solution with NPX (0, 0.1, 0.5, 1, and 10 mg/l). Data represent mean over five repetitions. Standard deviations are indicated by errors bars. Different letters above the neighbouring columns show statistically significant differences at P< 0.05 (ANOVA, Tukey HSD test).

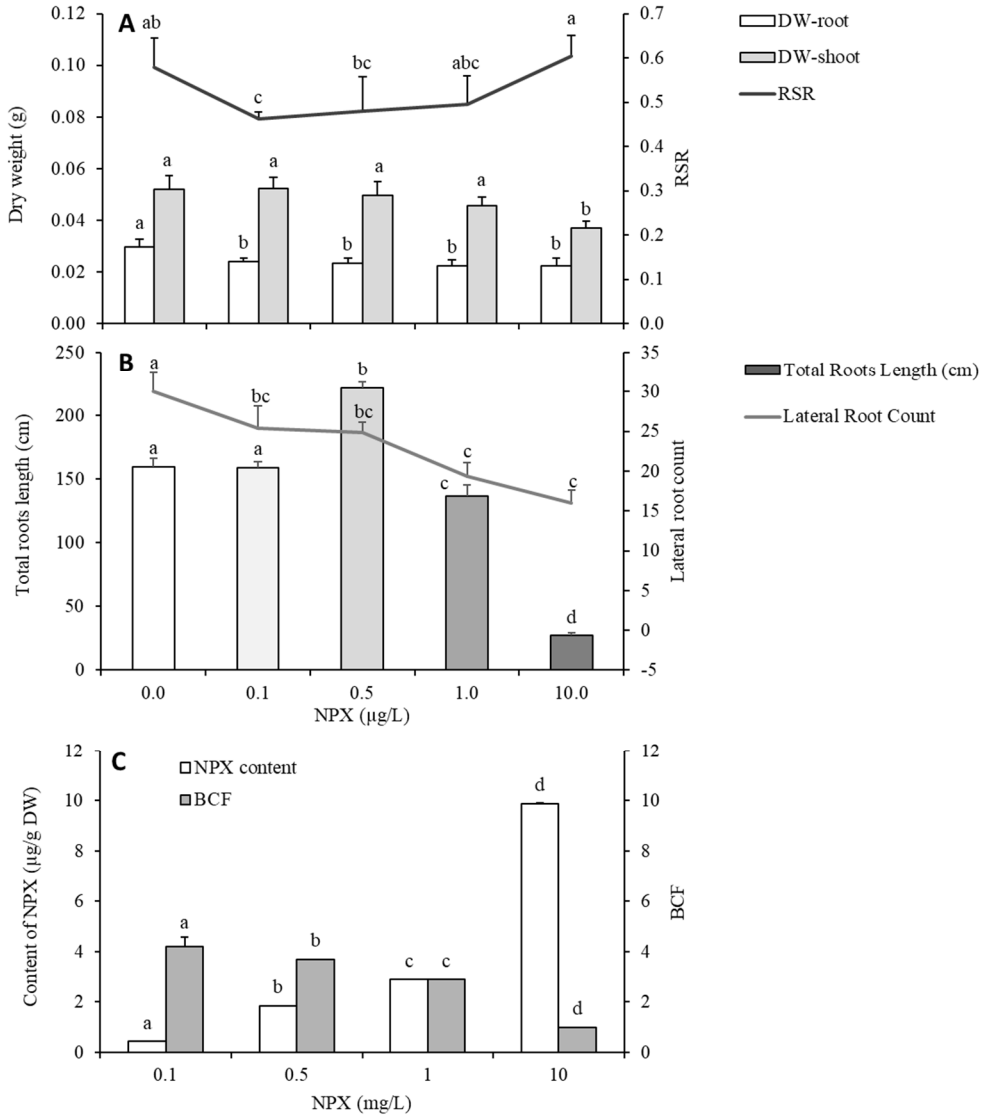

NPX affected the length of roots. Whereas the biggest total length of roots was found at 0.5 mg/l NPX (by 30% longer than in control), under 1 and especially 10 mg/l NPX its value decreased (by 6 and 80%, respectively; Figure 1B). This fact relates to changes in the number of lateral roots (Figure 1B) as is well visible even on root system photographs (Figure 2). The most adverse effect is evident in pea roots at 10 mg/l treatment simulating a high level of contamination, where mainly the lateral roots were the shortest (probably due to the inhibition in cell division as well as elongation) and their number was the lowest (by 36%) as compared to control and other NPX treatments.

Figure 2 Photos of root systems of Pisum sativum cultivated in nutrient solution with naproxen (NPX; 0, 0.1, and 10 mg/l). White bar = 5 cm.

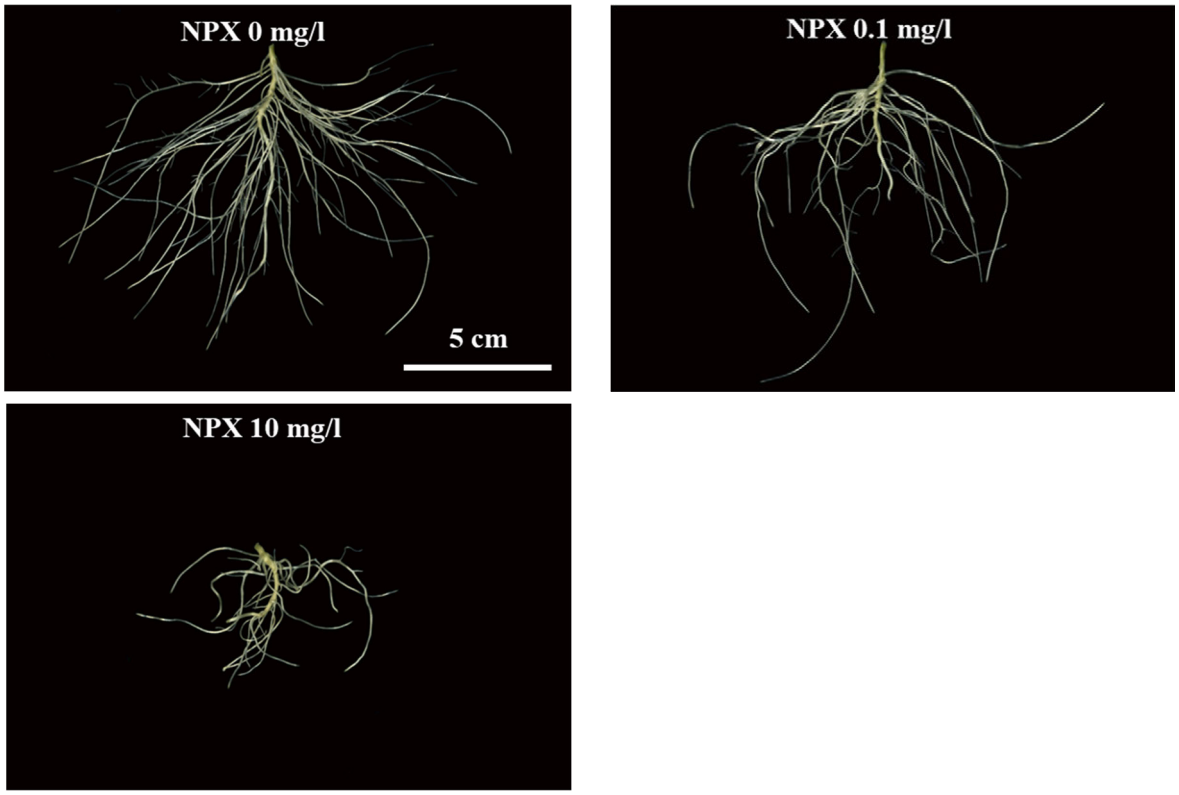

The occurrence of NPX in the environment and in root tissues (Figure 1C) reduced the number of lateral roots already from 0.1 mg/l NPX. This finding is in contrast with Bałdyga et al. (2005) or Kummerová et al. (2013), who found an increased formation of lateral roots when certain levels of the environmental loading by polycyclic aromatic hydrocarbons (PAHs) inhibited the primary root growth.

Content of NPX

The content of NPX detected in pea roots biomass and calculated bioconcentration factor (BCF; Figure 1C) demonstrated that the roots of plants accumulated certain amounts of NPX concerning contamination degree (nearly up to 10 µg/g DW at 10 mg/l NPX). Bioaccumulation is a non-linear process i.e., bioconcentration factors, indicating the ratio of compound content in fresh mass and its initial concentration in the cultivation medium, are generally high at low concentrations and decrease with increasing environmental loadings (Kummerová et al. 2016). Results given in Figure 1C have proved this fact as well, showing a nearly four-times higher BCF value found at 0.1 mg/l NPX compared to 10 mg/l.

Biochemical traits

Growth, developmental, structural, and morphological changes arise from alterations in biochemical processes running on various levels from subcellular to whole organs levels. Naproxen caused an increase in the production of reactive oxygen species (ROS), hydrogen peroxide (by 33%) and superoxide (by up to 62% as against control) at 10 mg/l (Figure 3A, B). Our results demonstrate that increased TAC at 0.1 and 0.5 mg/l NPX (by up to 42%) may to some extent eliminate the harmful effect of the overproduction of ROS, but at higher loads (1 and 10 mg/l) these antioxidant mechanisms including total thiols become deficient (TAC decreased by up to 26%, thiols by up to 14% as compared to control; Figure 3C, D). The occurrence of oxidative stress is confirmed even by the increase in content of MDA product (by 32%; Figure 4) probably because of the membrane lipid peroxidation as recorded even by Zezulka et al. (2019) for *P. sativum* and *Zea mays* under DCF and PCT treatments.

Figure 3 Content of hydrogen peroxide (H_2O_2; µmol/g FW; A), superoxide (O_2^-; %; B), total antioxidant capacity (mmol Trolox Equivalent/g FW; C), and total thiols (µmol/g FW; D) in Pisum sativum cultivated in nutrient solution with naproxen (NPX; 0, 0.1, 0.5, 1, and 10 mg/l). Statistical evaluation as given in Figure 1.

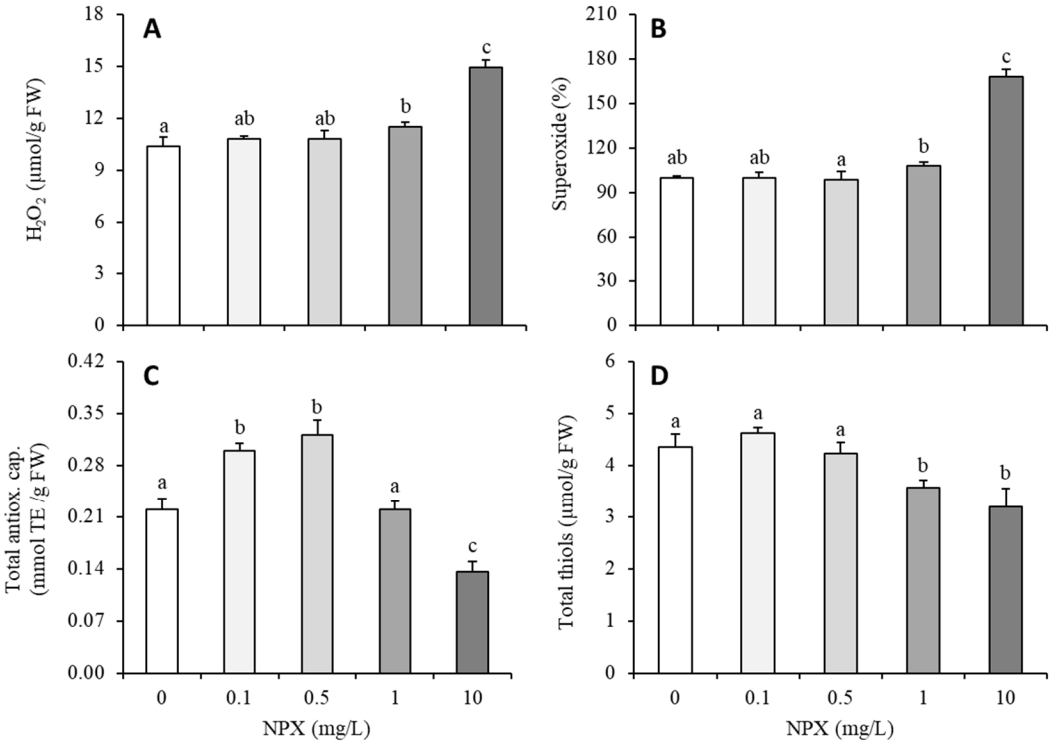

Figure 4 Content of malondialdehyde (MDA; nmol/g FW) in Pisum sativum cultivated in nutrient solution with naproxen (NPX; 0, 0.1, 0.5, 1, and 10 mg/l). Statistical evaluation as given in Figure 1.

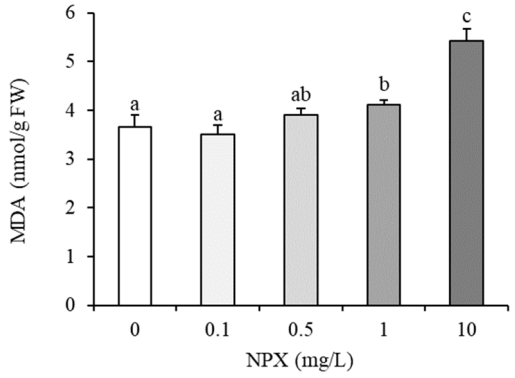

CONCLUSION

The understanding of the effect of drugs on biochemical and physiological processes is essential for explanation of changes in growth and development of plant growing in contaminated environment. As this study proves, enhanced formation of ROS, lipid peroxidation, and changes in antioxidant systems modulated the pea root growth in response to increasing NPX treatment. Furthermore, the documentation of morphological changes shows, that the alterations on subcellular level especially under high treatments express to the level of tissues and organs.

ACKNOWLEDGEMENT

This work was supported by the Czech Science Foundation (CZ) and FWF Der Wissenschaftsfonds (AT) joint project no. GF 17-33746L (I 3046- N28).

REFERENCES

Ahmed, M.B.M. et al. 2015. Distribution and accumulative pattern of tetracyclines and sulfonamides in edible vegetables of cucumber, tomato, and lettuce. Journal of Agricultural and Food Chemistry, 63(2): 398–405.

Bałdyga, B. et al. 2005. Pea plant response to anthracene present in soil. Polish Journal of Environmental Studies, 14(4): 397–401.

Bartha, B. et al. 2014. Uptake and metabolism of diclofenac in *Typha latifolia* – How plants cope with human pharmaceutical pollution. Plant Science, 227: 12–20.

Bartrons, M., Peñuelas, J. 2017. Pharmaceuticals and personal-care products in plants. Trends in Plant Science, 22(3): 194–203.

Baxter, A. et al. 2014. ROS as key players in plant stress signalling. Journal of Experimental Botany, 65(5): 1229–1240.

Bellver-Domingo, A. et al. 2017. Shadow prices of emerging pollutants in wastewater treatment plants: Quantification of environmental externalities. Journal of Environmental Management, 203: 439–447.

Farmer, E.E., Mueller, M.J. 2013. ROS-mediated lipid peroxidation and RES-activated signalling. Annual Review of Plant Biology, 64: 429–450.

Kummerová, M. et al. 2016. Possible ecological risk of two pharmaceuticals diclofenac and paracetamol demonstrated on a model plant *Lemna minor*. Journal of Hazardous Materials, 302: 351–361.

Kummerová, M. et al. 2013. Root response in *Pisum sativum* and *Zea mays* under fluoranthene stress: Morphological and anatomical traits. Chemosphere, 90(2): 665–673.

Landa, P. et al. 2018. Transcriptomic response of *Arabidopsis thaliana* roots to naproxen and praziquantel. Ecotoxicology and Environmental Safety, 166: 301–310.

López-Pacheco, I.Y. et al. 2019. Anthropogenic contaminants of high concern: Existence in water resources and their adverse effects. Science of The Total Environment, 690: 1068–1088.

Marsik, P. et al. 2017. Non-steroidal anti-inflammatory drugs in the watercourses of Elbe basin in Czech Republic. Chemosphere, 171: 97–105.

Pound, P.M. et al. 2013. RootNav: Navigating images of complex root architectures. Plant Physiology, 162(4): 1802–1814.

Reid, P.H., York, E.T. 1958. Effect of nutrient deficiencies on growth and fruiting characteristics of peanuts in sand culture. Agronomy Journal, 50(2): 63–67.

Zezulka, Š. et al. 2019. Sensitivity of physiological and biochemical endpoints in early ontogenetic stages of crops under diclofenac and paracetamol treatments. Environmental Science and Pollution Research, 26(4): 3965–3979.

ANIMAL BIOLOGY

Pathogens of bee brood present in the diet do not influence the immunity of nurse bees (*Apis mellifera*)

Silvie Dostalkova, Jiri Danihlik, Marek Petrivalsky
Department of Biochemistry
Palacky University Olomouc
Krizkovskeho 511/8, 779 00, Olomouc
CZECH REPUBLIC

silvie.dostalkova@upol.cz

Abstract: Honey bees are exposed to too many stress factors that can negatively influence their immune system. Bees of different age have different tasks in the hive and can be also influenced by diverse stress factors. Nurse bees are the very young bees (3–14 days old) and their function in the hive is mainly nursing and feeding the bee larvae. These bees live mainly inside the colony, where many microbial pathogens affecting the bee brood may occur. The aim of this work was to explore the effect of honey bee diet stored in the hive to the immunity of nurse bees. Our study was focused on spore forming microbial pathogens *Paenibacillus larvae* and *Ascosphaera apis*, due to the ability of spores persist in bee storages. In this study, 10–day old bees were exposed *in vitro* to a different type of feed composed of sucrose supplemented either with pollen, *P. larvae*, *A. apis* or a combination of pollen and pathogen. The relative gene expression of antimicrobial peptides (apidaecin, abaecin, hymenoptaecin, defensin-1) was studied to detect changes in humoral immunity. Gene expression of major royal jelly proteins was also detected. These proteins are related to royal jelly which is produced by nurse bees and used as feed to young larvae. Thus, the impact of pathogens on the production of these main larvae nutrients was studied. This study confirmed the role of antimicrobial peptides as inducible factors of humoral immunity and confirmed the close connection of immunity to the nutritional status of honey bees.

Key words: honey bee, immune system, antimicrobial peptides, major royal jelly proteins

INTRODUCTION

The Western honey bee, *Apis mellifera L.*, is one of the most important pollinators worldwide mainly due to its considerable contribution to agricultural production. Last decades increasing declines of bee populations are observed and correlated to a loss of natural habitats, malnutrition, exposure to toxins, climate changes, and mainly to diverse pests and pathogens (Steinhauer et al. 2018). One of the main drivers of colony losses is the mite *Varroa destructor*. Also, microbial pathogens have a significant impact on colony fitness, e.g. bacterium *Paenibacillus larvae* causing the American foulbrood or fungus *Ascosphaera apis* causing chalkbrood disease, both spores forming and predominant bee microbial pathogens (Fünfhaus et al. 2018, Aronstein and Murray 2010). Highly endangered is bee brood – larvae and pupae. The brood is sensitive to microbial infection, because of the weak immune system, life in high humidity environment at temperatures around 35 °C and missing cuticle at their bodies. They are fully dependent on adult bees. Larvae are fed by nurse bees that perform this particular task in the nest at age around 12 days. Larval food contaminated by spores often tends to infection of larvae and disease progression. Concerning the increase in honey bee colony losses and higher disease rates, there is a great focus on the impact of pathogens on the immune system.

As social insects, honey bees have immune system composed of two key levels (Evans et al. 2006). The first line of defence is ensured with social immunity based on behavioural cooperation among individuals in the colony. This is represented for example with the hygienic behaviour, meaning that adult workers identify infected larvae and remove them from the healthy brood (Spivak and Gilliam 2015). The second line of defence – individual immunity is a complex network of humoral and cellular reactions. Cellular reactions are secured by immune cells hemocytes and include a whole range of immune responses as coagulation, phagocytosis, nodule formation, and encapsulation of invading pathogen. Components of cellular immunity are constitutively produced and always present

in the hemolymph (Gillespie et al. 1997). On the other hand, humoral factors are inducible and produced mostly in response to specific invading pathogen after stimulation of recognition patterns. They are represented mainly with antimicrobial peptides (AmPs) and lysozymes (Laughton et al. 2011). Up to now, several AmPs (apidaecin, abaecin, defensin-1, hymenoptaecin) were detected in the hemolymph of *Apis mellifera* after immunostimulation, reviewed in Danihlík et al. (2016). Honey bee immunity is also highly influenced by the nutritional status of honey bees. Poor nutrition with missing pollen tends to downregulation of gene expression and production of AmPs (Danihlík et al. 2018).

Major royal jelly proteins (MRJPs) are the main proteins present in royal jelly (feed for queen larvae) and food jelly (feed for worker larvae) secreted by hypopharyngeal glands (HGs) of nurse bees (Schmitzová et al. 1998). Due to its presence in HGs it is generally assumed that they contribute mainly to proper larvae development. It was previously described that genome of *Apis mellifera* harbors nine transcripted *mrjp* genes named *mrjp1–9* (Dobritzsch et al. 2019). MRJP1–3 and MRJP5 are the predominant proteins in food jelly. Moreover, additional properties have also been described for MRJP1 and MRJP3. MRJP1 binds a pH-dependent fibrillary network with a peptide apisimin, giving the food jelly its special gelatinous consistency (Kurth et al. 2019). MRJP3 binds and stabilizes RNA in royal jelly which allows RNA to be shared and transmitted within bees and larvae through feeding, pointing out to its possible connection with the immune system (Maori et al. 2019).

The aim of this work was to determine the effect of pathogens that may occur in honey bee hive storages on the immune system of individual adult bees and thus influence the whole colony. Brood microbial pathogens *P. larvae* and *A. apis* were selected because of their ability to form spores, which can occur long-term in the hive, consequently in the bee storages. The study was also focused on the gene expression of MRJPs. We studied if the presence of pathogens in the diet influences their expression since this could influence the quality of jelly produced by individual workers in their HGs.

MATERIAL AND METHODS

In vitro maintenance of bees

Three frames with capped brood from the three individual colonies of *Apis mellifera carnica* were selected, placed in the cage, and transferred to a laboratory incubator (temperature 34.5 °C, humidity 80%). After 12 hours, newly emerged bees (up to 1 day) were collected and randomly divided into laboratory cages (approximately 20 bees per cage, 4 technical replicates per experimental group). Each cage received a different feed with the following composition: 50% sucrose + pollen, 50% sucrose containing *Paenibacillus larvae* (2.4×10^4 CFU), 50% sucrose containing *P. larvae* + pollen, 50% sucrose containing spores of *Ascosphaera apis* isolated from infected larvae, 50% sucrose containing *Ascosphaera apis* + pollen. Control groups received only 50% sucrose. Bees were maintained in the laboratory incubator (temperature 34.5 °C, 80% humidity) for 10 days. After 10 days bees were collected and frozen in liquid nitrogen.

RNA isolation and quantification of relative gene expression

Honey bee heads and abdomens (5 bee parts pooled in one sample) were homogenized in 2.5 ml of GITC buffer containing 1% ß-mercaptoethanol (Sigma Aldrich, USA) according to (Evans et al. 2015). Total RNA was extracted from 300 µl of homogenates in GITC buffer using the NucleoSpin RNA Plus kit according to the manufacturer´s instructions (Marchery-Nagel, Germany). Relative gene expression was determined from obtained RNA samples by using Luna® Universal One-Step RT-qPCR Kit (New England Biolabs, USA) according to the manufacturer´s instructions (annealing temperature 60 °C). RT-PCR was performed on CFX96 Touch Real-Time PCR Detection System (Bio-Rad, USA). Product quality was tested by measuring the melting curves of PCR products. The relative expression of genes of interest to housekeeping genes (*actin, EF-1 alpha*) was calculated according to Pfaffl (2001). For primer sequences see Table 1.

Statistical analysis

OriginPro 2019 software (OriginLab Corporations, Northampton, MA, USA) was used for the creation of plots and data analysis. Data were tested for normality by the Kolmogorov-Smirnov

test and the 2-way Analysis of Variance (ANOVA). 2-way ANOVA was used to test the significance of differences between the different treatments and measured parameters. Tests were performed at α=0.05 significance level with Bonferroni post hoc test. Each experimental group consisted of 10–12 samples.

Table 1 Primer sequences and the corresponding target gene names used for the quantification of relative gene expression

Target gene	Gene ID	Product size (bp)	Sequence 5′–3′	
			R	F
apidaecin type 14 (GOI)	GB13473	80	TTTTGCCTTAGC AATTCTTGTTG	GTAGGTCGAGTAG GCGGATCT
abaecin (GOI)	GB18323	72	CAGCATTCGCAT ACGTACCA	GACCAGGAAACG TTGGAAAC
defensin-1 (GOI)	GB41428	119	TGCGCTGCTAAC TGTCTCAG	AATGGCACTTAAC CGAAACG
hymenoptaecin (GOI)	GB51223	200	CTCTTCTGTGCC GTTGCATA	GCGTCTCCTGTCA TTCCATT
mrjp1 (GOI)	GB55205	230	TGGGTTCTGGAC TCAGGTCT	CCTTCACCTTTCTC GTCTGCTA
mrjp2 (GOI)	GB55212	234	GGGAGGGCTAG TGTCTTTGG	TTCGTCACGGGAC TAAGAGC
mrjp3 (GOI)	GB55204	319	TGGTTGTTGCTG GTGGTGTG	GAAGAGGTCCACC TTTGCCC
mrjp4 (GOI)	GB55206	274	TAGAGGTGGCGT TGTTCGAG	TAGAAGTCGTCCA CCGTTGC
mrjp5 (GOI)	GB55208	310	CTTGGTTGTTGC TGGTCGTG	CGTCCACCGTTGC CAATTTT
actin (HKG)	GB44311	155	TGCCAACACTGT CCTTTCTG	AGAATTGACCCAC CAATCCA
EF-1 alpha (HKG)	GB41358	153	GGAGATGCTGCC ATCGTTAT	CAGCAGCGTCCTT GAAAGTT

Legend: HKG = housekeeping gene; GOI = gene of interest

RESULTS AND DISCUSSION

Generally, the gene expression of AmPs was significantly influenced by diet fed to the individual groups (2-way ANOVA, df=3, F=39.238, p=8.718E-21). The interaction between experimental groups and gene expression of individual AmPs was significant (2-way ANOVA, df=15, F=6.274, p=3.265E-11). Specifically, the gene expression of *hymenoptaecin* was strongly upregulated in the groups fed without pollen compared to the other AmPs. On the contrary, *apidaecin* was upregulated after the addition of pollen to the feed (Figure 1). Interestingly, the expression of these two peptides showed the opposite pattern. Relative gene expression of *abaecin* and *defensin-1* was very low, independent of the experimental groups.

AmPs response to a pathogen was previously described in many studies focused on honey bees (Danihlík et al. 2016). It is obvious that intensive upregulation of gene expression occurs after immunostimulation or injury (Evans et al. 2006). Specifically, *apidaecin*, *abaecin*, *defensin-1* and *hymenoptaecin* were strongly upregulated after 24 hours post *P. larvae* injection. The upregulation of gene expression in response to pathogen was not statistically significant in our study. The elevated gene expression pattern of *apidaecin* in pollen fed groups could indicate the importance of a pollen diet for good nutritional status and immunocompetence of honey bees (Danihlík et al. 2018).

Low gene expression levels detected for other AmPs genes in our study can be explained by the different application of pathogens. To our knowledge, this is one of the few studies focused on orally infested bees, where bee brood pathogen is applied directly to the feed. Lourenço et al. (2009) observed immune activation after orally administered *Serratia marcescens*, but their study was focused more on storage proteins rather than immune activation. Lourenço et al. (2009) confirmed immune activation only by detecting the gene expression of *defensin-1* after 12 hours post infection. We did not determine the long-term effect of the presence of pathogens in bee food after 10–day exposure, which seemed to have no retentive effect on the humoral immunity of nurse bees. This confirms the generally accepted idea that AmPs are mainly produced as inducible factors immediately after infection or injury (Danihlík et al. 2016).

To determine a potential impact on the main nutritious proteins in food jelly, we measured the gene expression of MRJPs. The relative gene expression of *mrjps* differed significantly according to the used type of feed (2-way ANOVA, df=5, F=69.580, p=6.858E-48). Significantly increased gene expression of *mrjp3* and *mrjp1* was observed for groups where the pollen was added into feed (Figure 2).

Interestingly, no effect on all measured *mrjp* was observed within groups contained pathogen in feed (*A.apis* or *P. larvae*). The gene expression of *mrjp2*, *mrjp4*, *mrjp5* was not influenced at all among experimental groups. The expression of *mrjp* is well described for different bee parts and castes (Dobritzsch et al. 2019), but there is limited information about the expression of *mrjp* after immunization. Scharlaken et al. (2008) detected upregulated expression of *mrjp3* and *mrjp 4* eight hours after bacterial challenge with *Escherichia coli* injection. Our results suggest that *mrjp* gene expression is not influenced by the presence of pathogen spores in the bee diet. Moreover, here we present strong evidence that expression of *mrjp1* and *mrjp3* is influenced by the presence of pollen in the bee diet. Thus, we conclude that these MRJP are closely related to honey bee nutritional status.

Figure 1 Relative gene expression of AmP genes in experimental groups normalized to housekeeping genes

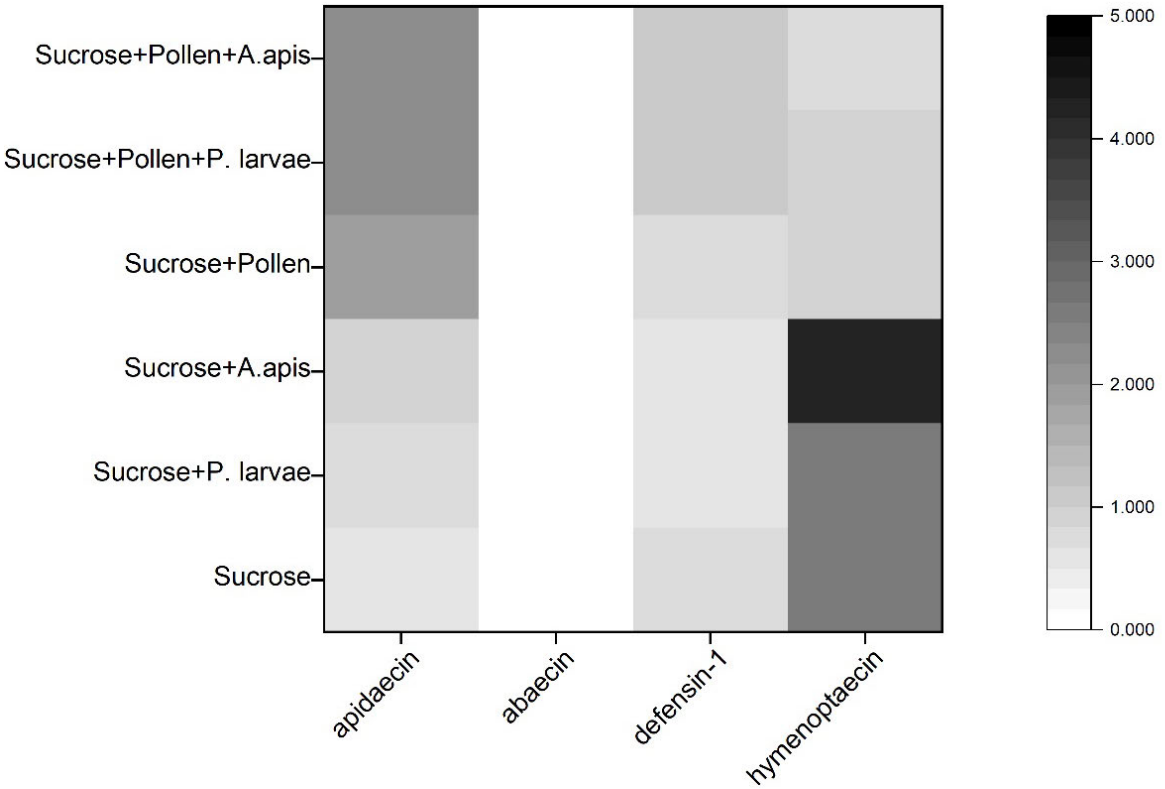

Legend: y axis – different type of feed, x axis – AmP genes. Individual rectangles represent the means of the value of relative gene expression for each experimental group. The scale next to the graph shows values from the lowest (white) to the highest (black)

Figure 2 Relative gene expression of mrjps in experimental groups normalized to housekeeping genes

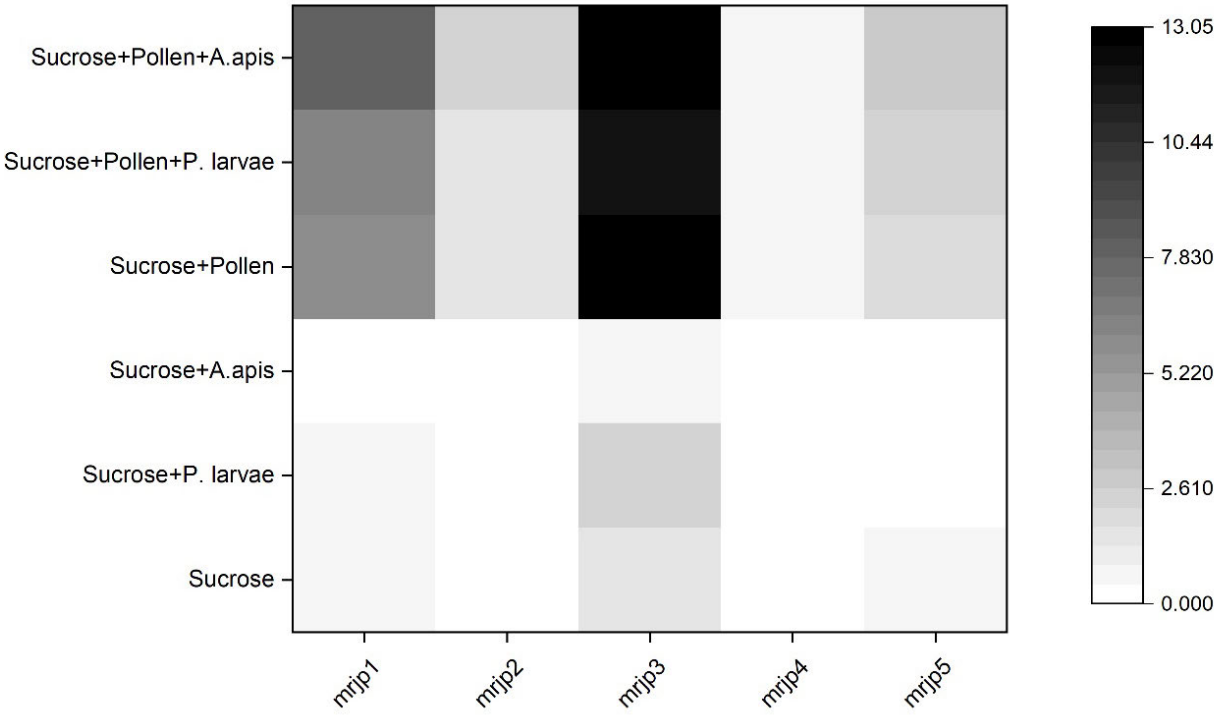

Legend: y axis – different type of feed, x axis – mrjp genes. Individual rectangles represent the means of the value of relative gene expression for each experimental group. The scale next to the graph shows values from the lowest (white) to the highest (black)

CONCLUSION

This is the first study describing the effect of spores of larval pathogens present in the bee diet on the humoral immunity of adult bees. *Apidaecin* and *hymenoptaecin* have an opposite pattern of relative gene expression based on pollen presented in the bee diet. Our findings brought evidence about variable stimulation of expression of AmPs concerning the nutritional status. The response of gene expression was the highest for *mrjp3* and *mrjp1*, on the other hand, *mrjp2*, *mrjp4*, and *mrjp5* did not respond at all. The presence of pollen in the honey bee diet enhanced *mrjp1* and *mrjp3* gene expression with a potential impact on the nutritional status of honey bee larvae.

ACKNOWLEDGEMENTS

We would like to thank Maria Skrabisova for primer design. This research was supported by Palacký University Internal Grant Agency (Project no. IGA_2020_013) and by The Ministry of Agriculture of the Czech Republic (QK1910286).

REFERENCES

Aronstein, K., Murray, K. 2010. Chalkbrood disease in honey bees. Journal of Invertebrate Pathology, 103: S20–S29.

Danihlík, J. et al. 2016. Antimicrobial peptides: a key component of honey bee innate immunity. Journal of Apicultural Research, 54(2): 123–136.

Danihlík, J. et al. 2018. Does the Pollen Diet Influence the Production and Expression of Antimicrobial Peptides in Individual Honey Bees? Insects, 9(3): 1–12.

Dobritzsch, D. et al. 2019. The rise and fall of major royal jelly proteins during a honeybee (*Apis mellifera*) workers' life. Ecology and Evolution, 9(15): 8771–8782.

Evans, J. et al. 2006. Immune pathways and defence mechanisms in honey bees *Apis mellifera*. Insect Molecular Biology, 15(5): 645–656.

Evans, J. et al. 2015. Standard methods for molecular research in *Apis mellifera*. Journal of Apicultural Research, 52(4): 1–54.

Fünfhaus, A. et al. 2018. Bacterial pathogens of bees. Current Opinion in Insect Science, 26: 89–96.

Gillespie J. et al. 1997. Biological mediators of insect immunity. Annual Review of Entomology, 42(1): 611–643.

Kurth, T. et al. 2019. Royal jelly in focus. Insectes Sociaux, 66(1): 81–89.

Laughton, A. et al. 2011. The ontogeny of immunity in the honey bee, *Apis mellifera L*. following an immune challenge. Journal of Insect Physiology, 57(7): 1023–1032.

Lourenço, A. et al. 2009. Trade-off between immune stimulation and expression of storage protein genes. Archives of Insect Biochemistry and Physiology, 71(2): 70–87.

Maori, E. et al. 2019. A Secreted RNA Binding Protein Forms RNA-Stabilizing Granules in the Honeybee Royal Jelly. Molecular Cell, 74(3): 598–608.

Pfaffl, M. 2001. A new mathematical model for relative quantification in real-time RT-PCR. Nucleic Acids Research, 29(9): 45e–45.

Scharlaken, B. et al. 2008. Differential gene expression in the honeybee head after a bacterial challenge. Developmental & Comparative Immunology, 32(8): 883–889.

Schmitzová, J. et al. 1998. A family of major royal jelly proteins of the honeybee *Apis mellifera* L. Cellular and Molecular Life Sciences CMLS, 54(9): 1020–1030.

Spivak, M., Gilliam, M. 2015. Hygienic behaviour of honey bees and its application for control of brood diseases and varroa. Bee World, 79(3): 124–134.

Steinhauer, N. et al. 2018. Drivers of colony losses. Current Opinion in Insect Science, 26: 142–148.

Optimization of mitochondrial DNA testing for biodiversity studies in invertebrates

Tamara Mifkova, Jan Wijacki, Tomas Bulawa, Tomas Urban
Department of Morphology, Physiology and Animal Genetics
Mendel University in Brno
Zemedelska 1, 613 00 Brno
CZECH REPUBLIC

xmifkova@mendelu.cz

Abstract: The aim of study was to verify usability of the mitochondrial genes cytochrome oxidase I (*COI*) and cytochrome B (*cyt B*) by the DNA barcoding method. We have demonstrated that these *COI* and *cyt B* gene fragments are suitable for species identification and whether these genes are further useful in biodiversity studies. This is a completely methodical study, which presents proven laboratory procedures that can be used for sample processing using molecular genetic methods.

Key Words: mitochondrial genes, *COI*, *cyt B*, biodiversity, invertebrates

INTRODUCTION

The mitochondrial genome occurs in the form of a non-nuclear ring molecule. The size of this molecule is variable, but most often it occurs in insects in the size of about 16 kbp (kilobase pair) (Alberts et al. 2007). The gene composition is stable and evolutionarily relatively conservative. However, mitochondrial DNA is more susceptible to mutations because it does not contain histones and other repair mechanisms as in nuclear DNA. Other influences that affect changes in the sequence of the mitochondrial genome include free radicals, which occur very close to this molecule, as they are radicals associated with cellular respiration, which are the mitochondria that provide (Druzhyna et al. 2008). In order to select suitable mt genes in biodiversity studies, it is necessary to realize how large intergenic and intragenic differences we want to investigate. It is obvious that not all mitochondrial genes are suitable for use in the identification of both higher and lower taxonomic levels. In general, sequences evolving faster (with a higher frequency of evolutionary nucleotide substitutions) are suitable for distinguishing lower taxonomic levels, and conservative sequences (with a lower frequency of changes) can be used for higher levels. Rapidly evolving sequences would not be suitable for higher levels because they accumulate substitutions at the same position and phylogenetically relevant information disappears.

This study should test the hypothesis that the mitochondrial COI and cytB genes are suitable for the DNA barcoding method in invertebrates. For the purposes of this study, a honeybee was chosen as a model organism. From the taxonomic point of view, it belongs to a very large taxonomic group, the superfamily of bees (Apoidea) numbering approximately> 16,000 species divided into 7 families (Michener 2000). The genus Bee (Apis) consists of 9 species, (including the honeybee) (Přidal 2011). These species can be divided into 3 basic groups (subgenuses) using phylogenetic analysis based on morphological features, nuclear and mitochondrial markers. The first group are bees nesting in cavities, to which the honeybee (Western) belongs. The second group is the group Megapis or giant bees, as the last group we determine Micrapis or dwarf bees (Han et al. 2012).

MATERIAL AND METHODS

For the purposes of optimization, 7 randomly selected samples from different localities and in different quality of the collected tissue were selected. For DNA isolation, the right leg of the third pair of forelegs is always used and must be thoroughly homogenized. Isolation is performed according to a standard protocol of NucleoSpin Tissue Genomic DNa kit (Macherey-Nagel GmbH & Co., Düren, Germany). The only change that is made by default is to reduce the amount of elution buffer from the recommended 100 µl to 50 µl. This procedure is performed if the tissue is demonstrably

to show a lower DNA yield and it is therefore more appropriate to have the resulting solution more concentrated. The quality of the isolated DNA then must be verified by agarose gel electrophoresis.

DNA amplification

The analyse fragments of the individual genes were amplified by PCR using specific primers (Table 1).

Table 1 Primer sequence

Gene	Primer	Sequence 5' - 3'	Length (bp)	% GC	PCR fragment (bp)	Author
COI	LCO1490	GGT CAA CAA ATC ATA AAG ATA TTG G	25	32.0	648	Folmer et al. 1994
	HCO2198	TAA ACT TCA GGG TGA CCA AAA AAT CA	26	34.6		Folmer et al. 1994
cytB	CYTB-f	TAT GTA CTA CCA TGA GGA CAA ATA TC	26	34.6	485	Feng-Yi Su et al. 2008
	CYTB-r	ATT ACA CCT CCT AAT TTA TTA GGA AT	26	26.9		Feng-Yi Su et al. 2008

The total volume of PCR reaction mix was 10.0 µl and consists of following reagencies (Table 2).

Table 2 Mastermixes for PCR amplification of COI and cytB genes

	COI	cytB
	µl	µl
H2O	3.5	3.6
Combi PPPmix	5.0	5.0
Forward primer	0.5	0.2
Reverse primer	0.5	0.2
DNA	0.5	1.0
Total	10.0	10.0

For DNA amplification was used thermal cycler ABI Veriti 96 Well (Applied Biosystems™, Foster City, CA, USA) and DNA was amplified according following protocols (Table 3).

Table 3 PCR amplification profiles for genes COI and cytB

	COI			cytB		
	°C	Time	Cycles	°C	Time	Cycles
Initial denaturation	95	3 min	1	95	4 min	1
Denaturation	95	40 s		95	20 s	
Annealing	50	40 s	40	52	30 s	32
Elongation	72	60 s		72	50 s	
Final extension	72	5 min	1	72	7 min	1
Cooling	4	∞		4	∞	

DNA sequencing and data analysis

For the sequencing analysis of our samples genetic analyser ABI PRISM 3500 (Applied Biosystems™, Foster City, CA, USA) was used and composition of reaction mix was: 7.09 µl PCR H_2O (Top-Bio, ltd., Prague, Czech Republic), 1.75 µl BigDye® Terminator v3.1 5× Sequencing Buffer, 0.5 µl BigDye® Terminator v3.1 Cycle Sequencing RR-100 (Thermo Fisher Scientific Inc., Waltham, USA), 0.16 µl primer and 0.5 µl PCR product. Total volume of reaction mix was 10.0 µl.

The temperature cycling profile was: 96 °C for 1 minute, 25 cycles of 96 °C for 10 s, 50 °C for 5 s, 60 °C for 4 min and finally were samples cooled for 4 °C. All samples were purified by BigDye® XTerminator™ Purification Kit (Thermo Fisher Scientific Inc., Waltham, USA). The sequencing analysis was performed in polymer POP-7 in 50cm length 8-channel capillary.

To evaluate the results, the Sequencing analysis software (Applied Biosystems™, Foster City, CA, USA) was used and sequences were aligned in SeqScape programme (Applied Biosystems™, Foster City, CA, USA). These results are also suitable for evaluation of evolutionary studies using e.g. MEGA 10 software.

RESULTS AND DISCUSSION

The results of DNA isolation using a tissue kit from Nagel macherey are very satisfactory. Fragments of genomic DNA are evident in the figure of 1.5% agarose electrophoresis. These large molecules are clearly visible at the top of the figure and have values of more than 10 kbs. Size is estimated using a weight standard (M1kb) from Thermo Fisher ranging from 1 kbs to 10 kbs. Smaller DNA molecules are also evident in the figure, which did not have a negative effect on further analyses. This phenomenon can be caused by degradation of genomic DNA during the isolation process. This result corresponds to the results of analyses comparing the quality of isolated DNA from fresh and archived insect tissues (Dean & Ballard, 2001). Electrophoresis was performed for 15 minutes at 130V and the carcinogenic visualization dye Goodview was used (E.coli s.r.o., Bratislava, Slovakia).

Figure 1 Verification of isolated DNA by gel electrophoresis

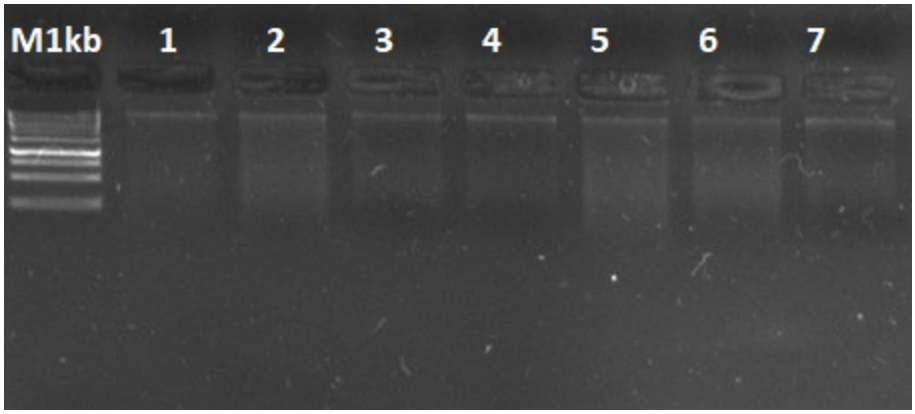

To verify the amplification resulting from the PCR reaction, 3% agarose electrophoresis was performed on both genes. It lasted 30 minutes at 130V. A marker in the fragment range of 100 bp (M100) was used as a size standard. The amplicons visible in Figure 2 and Figure 3 correspond in size, which confirms the correctness of the analysis performed for both genes.

Figure 2 Verification of COI gene amplification

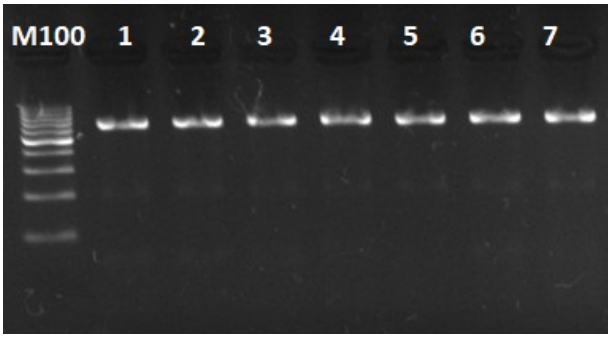

Figure 3 Verification of cytB gene amplification

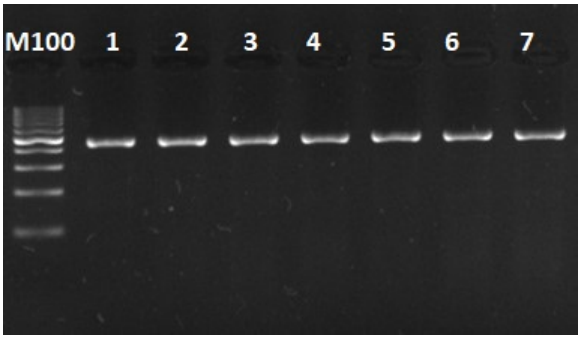

Since all previous analyses showed a suitable procedure and correctly processed material, in Figure 4 it is possible to see a quality result of sequencing analysis (electrophoretogram), which was analysed by capillary electrophoresis and the program for processing DNA sequences MEGA 10.

Figure 4 Electrophoretogram of DNA sequence

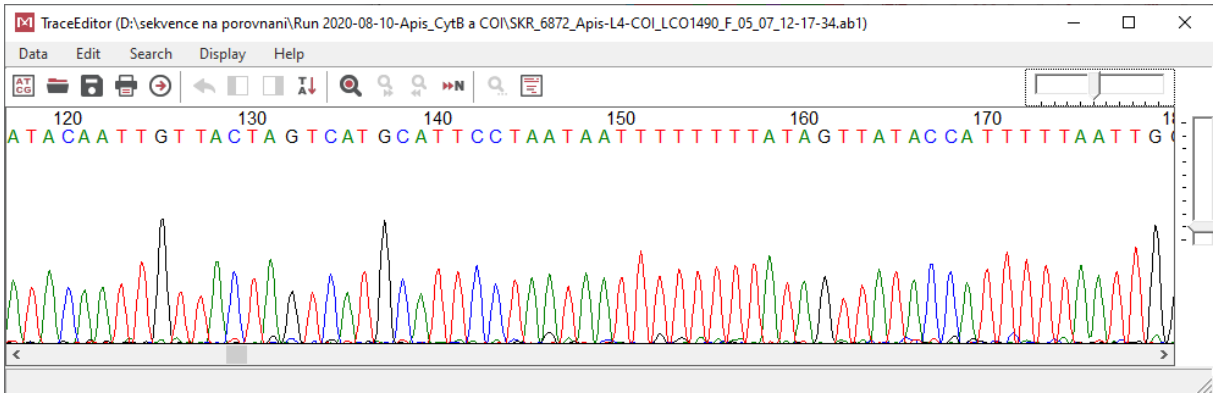

The results show that the above method of processing samples by molecular biology methods of cytochrome oxidase I and cytochrome b genes is suitable for providing high quality nucleotide sequences. These sequences can then be processed for various biodiversity studies. The knowledge gained during the elaboration of this methodology is applicable not only for representatives of bees, but also for other invertebrates within the intergenic areas of study.

ACKNOWLEDGEMENTS

The research was financially supported by the internal grant agency FA IP-2018/077.

REFERENCES

Alberts, B. et al. 2007. Molecular biology of the cell. 5th ed., New York: Garland Science.

Dean, M., Ballard, J. 2001. Factors affecting mitochondrial DNA quality from museum preserved Drosophila simulans. Entomologia Experimentalis et Applicata, 98(3): 279–283.

Druzhyna, N.M. et al. 2008. Mitochondrial DNA repair in aging and disease. Mechanisms of ageing and development, 129(7–8): 383–390.

Feng-Yi Su, K. et al. 2008. Morphology versus molecules: the phylogenetic relationships of Sepsidae (Diptera: Cyclorrhapha) based on morphology and DNA sequence data from ten genes. Cladistics, 24(6):902–916.

Folmer, O. et al. 1994. DNA primers for amplification of mitochondrial cytochrome c oxidase subunit I from diverse metazoan invertebrates. Molecular Marine Biology and Biotechnology, 3(5):294–299.

Han, F. et al. 2012. From where did the Western honeybee (Apis mellifera) originate? Ecology and Evolution, 2(8): 1949–1957.

Michener, C.D. 2000. The Bees of the World. Baltimore: Johns Hopkins Univ Press.

Přidal, A. 2011. Zootechnický význam klasifikace plemen včel rodu Apis. Moderní Včelař, 8(6): 177–179.

Effect of the digestive process of the Greater wax moth (*Galleria mellonella*) on the causative agents of American Foulbrood (*Paenibacillus larvae*)

Petr Mraz[1], Marian Hybl[3], Marek Kopecky[2], Jan Sipos[3], Stepan Ryba[4], Vladislav Curn[1]
[1]Department of Plant Production
[2]Department of Agroecosystems
University of South Bohemia in Ceske Budejovice
Studentska 1668, 370 05 Ceske Budejovice
[3]Department of Zoology, Fisheries, Hydrobiology and Apidology
Mendel University in Brno
Zemedelska 1, 613 00 Brno
[4]Biology Centre of Czech Academy of Sciences
Institute of Entomology
Branisovska 31, 370 05 Ceske Budejovice
CZECH REPUBLIC

mrazpe01@jcu.cz

Abstract: Both, greater wax moth (*Galleria mellonella*) and the causative agent of American Foulbrood (*Paenibacillus larvae*) cause considerable economic losses in beekeeping practice. Their life cycle is closely related to the honey bees, thus they can easily come into contact. The greater wax moth is exceptional for its ability to decompose beeswax. Therefore, it reduces also pathogen loads on old beeswax in nature. The aim of this study was to determine whether the greater wax moth is able to disrupt or destroy the very resistant spores of *P. larvae* in its digestive tract. In the laboratory experiment, the larvae of the greater wax moth were fed on wax foundation contaminated with *P. larvae* spores, either loosely or fixed in cages. After 2 days, their intestine was dissected and analysed by both, cultivation and molecular methods. The greatest amount of spores was found in the first parts of the intestine, fewer spores were found in the middle parts. No spores were detected in the back parts of the intestine. If the greater wax moth were able to destroy spores of the causative agent of American Foulbrood, there would be great potential for the development of a treatment that is still lacking. However, it is still not clear if the very efficient digestive tract of the greater wax moth is able to disrupt the spores or they are accumulated in the front part of the intestine.

Key Words: Honey bees, beekeeping pests, cultivation, digestive system, spores

INTRODUCTION

Pollinators, such as insects, birds, bats, and others, are very important for the sexual reproduction of many crops and wild plants. Bees are the main contributors to pollination and despite the great importance of solitary bees, the most numerous and also the most universal pollinator is the honey bee (*Apis mellifera*). Beekeeping, therefore, has a very close relationship with the environment and significantly contributes to strengthening the ecological stability of the landscape (Gallai et al. 2009). Honey bees are often the only way for farmers how to ensure sufficient pollination of crops if other pollinator species are rare or absent. Therefore, honey bees belong to one of the most important livestock (Klein et al. 2007, Morse and Calderon 2000).

However, despite the economic and environmental importance of bees, beekeeping is in decline throughout Europe (Biesmeijer et al. 2006). Increasing the application of agrochemicals to fields is a great risk, which significantly weakens bee colonies (Klein et al. 2017). Moreover, honey bee immunity is greatly influenced because of landscape changes, mainly manifested by malnutrition (Alaux et al. 2010, Hýbl et al. 2019). A combination of these negative factors makes bees more vulnerable to parasites and pathogens which resulted in a large decline of bees colonies every year.

One of the most economically serious diseases is American Foulbrood (AFB) which is caused by the bacteria *Paenibacillus larvae*. Once infected, the larva dies within 3 to 12 days. Adult bees cannot be infected, however, they can spread the disease (Genersch 2010). AFB spreads very easily both between hives and between localities (Lindström et al. 2008). The most common cause is the exchange of materials, bee robbing, or the sale of bee products that may be infected with this disease (Ashiralieva and Genersch 2006).

The greater wax moth is widespread and can be found in the beehive or on the old wax combs of the wild bees; therefore, it can easily come in contact with the bacteria causing AFB (Kwadha et al. 2017). It is considered a pest because its larvae feed mainly on older beeswax or combs with supplies of pollen. In nature, however, it plays an important role, namely the biological degradation of beeswax. It can even decompose very stable plastic materials (Billen et al. 2020, Bombelli et al. 2017), because their structures are similar to beeswax, both rich in long aliphatic chains (Kong et al. 2019). The process ensures the decomposition of very stable wax substances into simple components and their return back to the closed natural cycle. From this point of view, the larvae of the greater wax moth have a hygienic function in the landscape and also reduce the pathogen loads (Eillis et al. 2013). This raises the question of whether the larvae of the greater wax moth can deal with spores of *P. larvae*, which are commonly found in beeswax?

The aim of the work was to determine whether the greater wax moth is, thanks to its well-adapted digestive tract, able to disrupt the resistant layers of *P. larvae* spores and thus damage or destroy it.

MATERIAL AND METHODS

The larvae of greater wax moth (*Galleria mellonella*) were divided into 3 experimental groups. One of the test variants contained larvae, which were able to move freely inside the Petri dish (90 x 15 mm) on a wax foundation contaminated with spores of *P. larvae* (PK). For the second variant, small modified cages from mesh were prepared to prevent larval free movement (PR). The larvae were fixed inside the cages upside down and embedded in wax foundation contaminated with spores of *P. larvae* placed in a beaker (Figure 1). The fixed position ensured that the larvae were able to consume the contaminated wax but other parts of their body never came in contact with the spores. The spores had to go through the digestive system of larvae together with the food received. The last group consisted of larvae, which were able to move freely on the wax foundation without contamination (NK).

Figure 1 Larvae placed in cages

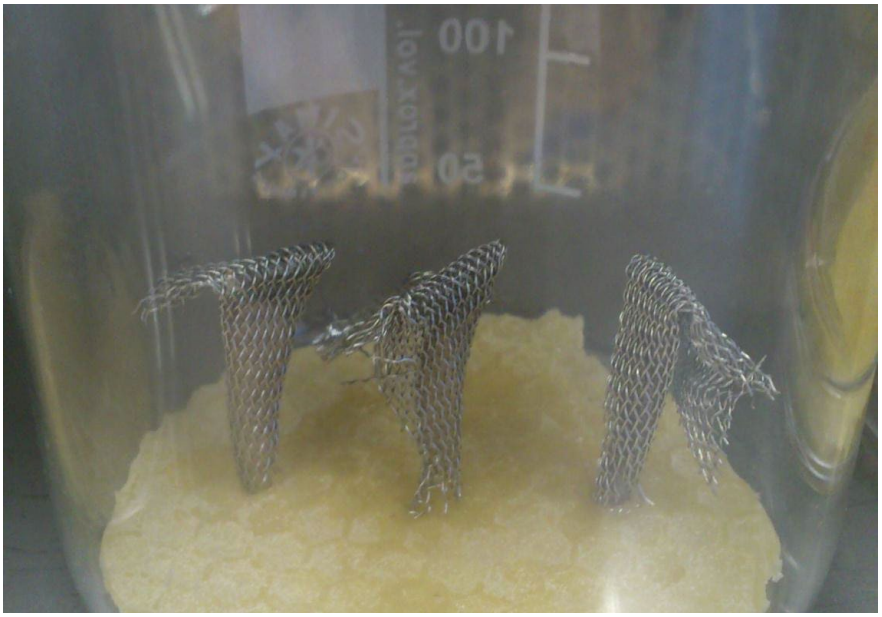

All of the larvae were fed for 2 days. Then, the larvae from the variants NK and PR were cut into 3 parts of the same size. The front part (1) consisted of a head and beginning of a digestive system.

The middle part (2) contained most of the digestive system and the back part (3) consisted of the end of digestive system and the Malpighian tubule system. From the last group of larvae (PK), the digestive system was dissected and divided into 3 parts in the same manner.

Spore extraction and inoculation

The sample amount of 0.1 g was diluted in 0.9 ml toluene and shaken for 1 hour. An amount of 0.2 ml of distilled water was added. The mixture was heated at 90 °C for 5 min to kill any undesirable bacteria. After cooling, 200 µl of the water phase was used for inoculation MYPGP agar and 100 µl of the water phase was used for the consequent PCR test (Ryba et al. 2009). All of the dishes were put in plastic bags to slightly increase CO_2 concentration and cultivated at 37 °C for 10 days. Growing colonies were assessed morphologically and identified by the peroxide test.

Molecular identification

The presence of spores was analysed also by PCR. Mixed samples from the PK and PR group were prepared. The whole DNA isolation procedure is according to the instructions of E.Z.N.A. Bacterial DNA Kit (2003). Genomic DNA of *P. larvae* was extracted and used as a template for PCR identification. The final volume was 50 µl including 1 µl of template DNA, 25 µl Master Mix, 20 µl of PCR Ultra H_2O and the specific ITS primers F3: TCCTGGCTCAGGACGAAC and B3: ACAGGTTGCCCCGTCTTT, 2 µl each at 10 µM. PCR was performed under the following conditions: initial template denaturation at 95 °C for 15 min; 35 cycles of 94 °C for 30 s, 58 °C for 30 s, and 72 °C for 1 min. PCR products were electrophoretically separated on 1.0% agarose gel and visualized by a UV transilluminator (INGENIUS, Trigon-plus, SYNGENE) (Ryba et al. 2009).

Statistical Analysis

The amount of viable spores between groups and part of intestine were statistically analysed by using repeated-measures nonparametric ANOVA (R Core Team 2020). Species groups and part of intestine were entered into the models as fixed effect, and each individual were entered as random effect. The post hoc comparison of the average of individual levels of fixed factors was compared by using the Tukey HSD test with Bonferroni corrected p-values.

RESULTS AND DISCUSSION

The number of viable spores in different experimental group and in each part of intestine differ significantly (ANOVA, $F_{(4,12)} = 59.323$, $p < 0.01$). As expected, the greater wax moth placed in an uncontaminated environment (NK) did not contain any *P. larvae* spores. The second variant which contained larvae placed in a contaminated environment (PK), was expected to have a high number of spores in all analysed parts. According to the cultivation tests, the front part contained a higher amount of spores. However, the middle part contained fewer spores (Tukey HSD, $p = 0.025$) and the back part did not even contain any spores. A slightly different situation occurred with the PR group. More spores were found in the middle part, less in the front part (Tukey HSD, $p = 0.019$) and the back part did not contain any spores (Figure 2). Overall, in the PK group, there were on average more than twice as many spores as in PR group in the front part of intestine. However, there were approximately equal numbers of viable spores in the middle intestines in both groups. That could be explained by the possible slow passage of spores through the digestive system of the greater wax moth. The spores are very small and can easily adhere to the surface of the intestine, which in addition has many folds (Kodrík 2004). The larvae in the PR group were fixed in small cages and could not move when they consumed all accessible diet. Therefore, their loads of spores were lower than in the PK group. In addition, more spores occurred in the middle part because many of the consumed spores passed through the front part. Due to the lack of accessible contaminated diet, no more spores were consumed. On the contrary, in the PK group, the intake of contaminated diet was unlimited and, therefore, more spores were accumulated in the front part. However, a very surprising result occurred in the back part where no spores were found. The absence of spores in the back part was confirmed also by the molecular analysis (Figure 3). Spores were either digested by the greater wax moth and intestinal microbiome enzymes (Cassone et al. 2020) or the passage through the intestine was very slow and spores were not able to reach the back part during the tested period of time.

Figure 2 Number of colonies in cultivation test

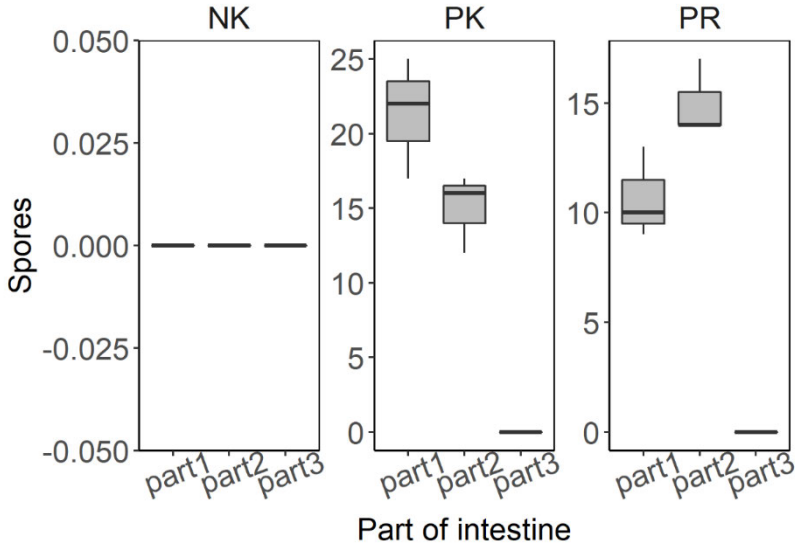

Insect infection via the oral route is prevented both, by the structure of the gut which has a lining of chitin and by the adverse conditions in the gut such as pH and digestive enzymes. Furthermore, the intestinal microflora significantly contributes to the reduction of incoming microorganisms (Wojda 2017).

The other issue is *G. mellonella* immunity which could eliminate the pathogen. As same as other insect species, the greater wax moth has only innate immunity. However, if *G. mellonella* has previously encountered the pathogen in small amounts, its resistance increases (Bergin et al. 2006). This phenomenon is unusual in insects (Wojda 2017). However, this should be of no significance in this case, as the larvae were in contact with *P. larvae* for the first time. In addition, this bacterium is closely specialized for honey bee larvae and *G. mellonella* is not a suitable host (Genersch 2010).

Figure 3 Result of molecular analysis (PCR)

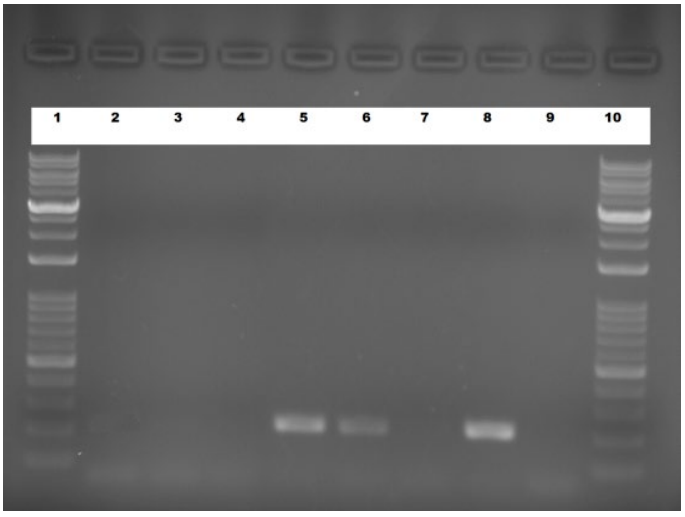

Legend: 1-Ladder 100bp, 2-NK first part of intestine, 3-NK second part of intestine, 4-NK third part of intestine, 5-PR+PK first part of intestine, 6- PR+PK second part of intestine, 7-PR+PK third part of intestine, 8-positive control, 9-negative control, 10-Ladder 100 bp

The greater wax moth immunity, development, and digestion efficiency is also influenced by the quality of food (Cassone et al. 2020, Kwadha et al. 2017). The natural diet is honey combs, honey, pollen and bee brood, but they can also be reared on artificial diets containing honey, wax and cereal products (Kwadha et al. 2017). In this case, the larvae were reared on artificial diet contained 660 g of corn bran, 330 g of wheat bran, 330 g of wheat flour, 330 g of powder milk, 165 g of dried yeast, 330 g of honey, 330 g of glycerine, 525 g of beeswax. Any negative side effect caused by the diet were not observed. Furthermore, an artificial diet can even support larval development and immunity

compared to natural diet (Jorjão et al. 2018). It is possible that naturally reared individuals can have different composition of microflora and thus the digestion efficiency between natural reared and artificial reared greater wax moth larvae can differ (Cassone et al. 2020).

CONCLUSIONS

The greater wax moth is known for its efficient digestive tract, which allows it to digest beeswax. At the same time, it significantly reduces the amount of bee pathogens, which occur mainly on old wax. On the other hand, spores of *P. larvae*, the causative agent of American Foulbrood, are very resistant. Therefore, the effect of the passage of *P. larvae* spores through the gastrointestinal tract of the greater wax moth was tested in this experiment. The main goal of the work was to determine the amount of spores and their germination after the passage. The results show that the most spores were in the front part of the intestine, the fewer spores were in the middle part and there were even no spores in the back part. However, it is not clear whether the spores in the digestive tract were digested or only accumulated in the anterior parts, which is full of folds and thus makes their passage more difficult. Therefore, further research is needed to clarify the details.

REFERENCES

Alaux, C. et al. 2010. Diet effects on honeybee immunocompetence. Biology Letters, 6(4): 562–565.

Ashiralieva, A., Genersch, E. 2006. Reclassifcation, genotypes and virulence of *Paenibacillus larvae*, the etiological agent of American foulbrood in honeybees - a review. Apidologie, 37(4): 411–420.

Bergin, D. et al. 2006. Pre-exposure to yeast protects larvae of *Galleria mellonella* from a subsequent lethal infection by *Candida albicans* and is mediated by the increased expression of antimicrobial peptides. Microbes Infect, 8: 2105–2112.

Biesmeijer, J.C. et al. 2006. Parallel declines in pollinators and insect pollinated plants in Britain and the Netherlands. Science, 313: 351–354.

Billen, P. et al. 2020. Technological application potential of polyethylene and polystyrene biodegradation by macro-organisms such as mealworms and wax moth larvae. Science of the Total Environment, 735: 1–10.

Bombelli, P. et al. 2017. Polyethylene bio-degradation by caterpillars of the wax moth *Galleria mellonella*. Current Biology, 27: 292–293.

Cassone, B.J. et al. 2020. Role of the intestinal microbiome in low-density polyethylene degradation by caterpillar larvae of the greater wax moth, *Galleria mellonella*. Proceedings of the Royal Society B. Biological Sciences, 287: 20200112.

Ellis, J.D. et al. 2013. Standard methods for wax moth research. Journal of Apicultural Research, 52(1): 1–17.

Gallai, N. et al. 2009. Economic valuation of the vulnerability of world agriculture confronted with pollinator decline. Ecologicals Economics, 68: 810–821.

Genersch, E. 2010. American Foulbrood in honeybees and its causative agent, *Paenibacillus larvae*. Journal of Invertebrate Pathology, 103: 10–19.

Hýbl, M. et al. 2019. Effects of phenolic bioactive substances on reducing mortality of bees (*Apis mellifera*) intoxicated by thiacloprid. In Proceedings of International PhD Students Conference MendelNet 2019 [Online]. Brno, Czech Republic, 6–7 November, Brno: Mendel University in Brno, Faculty of AgriSciences, pp. 131–135. Available at: https://mnet.mendelu.cz/mendelnet2019/mnet_2019_full.pdf

Jorjão, A.L. et al. 2018. From moths to caterpillars: Ideal conditions for *Galleria mellonella* rearing for in vivo microbiological studies. Virulence, 9(1): 383–389.

Klein, A.M. et al. 2007. Importance of pollinators in changing landscapes for world crops. Proceedings of the Royal Society B. Biological Sciences, 274: 303–313.

Klein, S. et al. 2017. Why bees are so vulnerable to environmental stressors. Trends in Ecology and Evolution, 32(4): 268–278.

Kodrík, D. 2004. Fyziologie hmyzu, učební texty. České Budějovice: Jihočeská univerzita.

Kong, H.G. et al. 2019. The *Galleria mellonella* hologenome supports microbiota-independent metabolism of long-chain hydrocarbon beeswax. Cell Reports, 26: 2451–2464.

Kwadha, C.A. et al. 2017. The Biology and Control of the Greater Wax Moth, *Galleria mellonella*. Insects, 8(61): 1–17.

Lindström, A. et al. 2008. Horizontal transmission of *Paenibacillus larvae* spores between honey bee (*Apis mellifera*) colonies through robbing. Apidologie, 39: 515–522.

Morse, R.A., Calderon, N.W. 2000. The value of honey bee pollination in the United States. Bee Culture, 128: 1–15.

Ryba, S. et al. 2009. A PCR method of detecting American Foulbrood (*Paenibacillus larvae*) in winter beehive wax debris. Veterinary Microbiology, 139: 193–196.

Survivability of sperm in insemination doses of Warmblood stallions using different types of extender

Katarina Souskova, Radek Filipcik, Ondrej Mamica, Tatana Havlickova
Department of Animal Breeding
Mendel University in Brno
Zemedelska 1, 613 00 Brno
CZECH REPUBLIC

katarina.souskova@mendelu.cz

Abstract: The aim of this study was to evaluate sperm motility and viability during storage using different types of extenders. Extender is one of the most important factors affecting survivability of sperm in insemination doses. In our study we evaluated sperm motility and viability of Warmblood stallions at 24, 48 and 72 hour intervals. Motility was measured by SCA® Sperm Class Analyzer and viability was determined by fluorescence microscopy. For experiment we used skimmed milk-based extender, extender based on caseins with addition of cholesterol and extender based on purified fraction of milk micellar proteins. Highest values of all evaluated parameters were observed in insemination doses with extender based on purified milk proteins 62.85% of motile sperm, 33.65% of progressive motile sperm and 72.87% of viable sperm.

Key Words: stallion, sperm, semen extender, SCA

INTRODUCTION

Artificial insemination with cooled storage insemination doses provides breeders a large number of benefits. That is why it is a widespread biotechnology (Aurich 2012, Rečková and Filipčík 2020). Its benefits include reducing the costs and stress associated with transport, expanding the genetic pool associated with the availability of stallions from remote regions or abroad, and reducing the risk of injury and the transmission of sexually transmitted diseases (Lane 2015). Short-term storage insemination doses show better indicators of fertilizing ability than long-term ones. For this reason, they are preferred if the transport time does not exceed 24 hours (Pagl et al. 2006). Evaluation of semen parameters provides important information of sperm survival (Věžník et al. 2007, Martečíková et al. 2010). A whole range of semen evaluations is available. The basic ones include motility, viability and morphological assay of sperm. Specialized methods are, for example, sperm acrosome assay (Věžník et al. 2007, Varner 2008, Rečková et al. 2015), DNA assay (Atroshchenko et al. 2019, Rečková et al. 2008, Varner 2008) and survival tests (Atroshchenko et al. 2019, Věžník et al. 2007). Sperm survival at insemination doses depends on factors such as ejaculate quality, percentage of seminal plasma (Jasko et al. 1992), cooling rate (Varner et al. 1988), storage temperature (Hernández-Avilés et al. 2020) and composition of an extender (Pagl et al. 2006). Diluents for cooled storage insemination doses have different compositions. The basic ones include milk-based extenders, which are practical and effectively preserve the fertilization ability of sperm. However, milk as a biological fluid with complex composition contains of large amount of substances, some of which have positive effects on sperm, but some may have negative effects on their survival (Batellier et al. 1997, Pagl et al. 2006). Fractionating of milk allowed the formation of a diluent containing purified fraction of milk micellar proteins. Such a diluent contains only substances that have demonstrably positive effect on sperm and therefore has an advantage for longer-survival of sperm at cooled storage insemination doses (Pagl et al. 2006). Recently, a diluent containing casein and cholesterol has been marketed, which also has a beneficial effect on maintaining the fertilization capacity of insemination dose (Novello et al. 2020).

Aim of this study was to evaluate the quality parameters of sperm in insemination doses of Warmblood stallions using three different extenders – skimmed milk-based extender, extender based on caseins with addition of cholesterol and extender based on purified fraction of milk micellar proteins. Selected qualitative parameters were sperm motility and viability, which were regularly evaluated during storage of insemination doses.

MATERIAL AND METHODS

For the experiment we used 9 Warmblood stallions aged 3 to 19 years housed in Stud farm Tlumačov. The stallions were breeds Oldenburg horse, Hanoverian horse, Holsteiner, Zangersheide, Czech Warmblood, Moravian Warmblood and Slovak Warmblood in Czech Republic. Collections of ejaculates were made during breeding season. The number of collections was 79.

For the experiment we used 3 different extenders. Extender I – prepared in Reproduction center of Stud farm Tlumačov based on skimmed milk. Extender II – BotuSemen Gold, Nidacon (Sweden) based on caseins with addition of cholesterol. Extender III – INRA 96, IMV (France) based on purified fractions of milk micellar proteins.

Collections of ejaculates took place in Stud farm Tlumačov. Right after collection, the sperm motility of native ejaculate was determined using the program SCA® Sperm Class Analyzer. A preparation for sperm viability assay was made. Three samples were then taken from the ejaculate and the same amount of each extender (I-III) was added to each sample. The samples were then transported to Mendel University Livestock Reproduction Laboratory under optimal conditions and stored at 4 °C. In the samples of insemination doses, sperm motility was evaluated by objective method in the time intervals of 24, 48 and 72 hours from dilution of an ejaculate. At the same time intervals, sperm viability was assessed by fluorescent microscopy and Hoechst 33258 dye. Data were evaluated using STATISTICA 12.0. Tukey´s HSD test was used for statistical evaluation.

RESULTS AND DISCUSSION

Mean values of motile, progressive motile and viable sperm were lowest in extender I based on skimmed milk and highest in extender III consists of purified fractions of milk micellar proteins.

Table 1 Mean values of motile, progressive motile and viable sperm using extenders I–III during storage of insemination doses

Extender	Sperm motility (%)	Progressive sperm motility (%)	Sperm viability (%)
I	44.63	17.75	64.48
II	61.40	31.17	64.73
III	62.85	33.65	72.87

Samples of insemination doses with extender I had statistically significant lower values of sperm motility (44.63%) and progressive motility (17.76%) than those of extender II (motility – 61.40%, progressive motility – 31.17%) and extender III (motility – 62.85%, progressive motility – 33.65%). Samples with extender III had statistically significant higher viability values (72.87%) than with extender I (64.48%) and extender II (64.73%).

*Table 2 Statistically significant differences in sperm motility, progressive sperm motility and viability using extenders I–III ($p < 0{,}001$ **)*

Qualitative parameter	Extender	I	II	III
Sperm motility	I	-	**	**
	II	**	-	-
	III	**	-	-
Progressive sperm motility	I	-	**	**
	II	**	-	-
	III	**	-	-
Sperm viability	I	-	-	**
	II	-	-	**
	III	**	**	-

Mean values of motile, progressive motile and viable sperm were highest in all monitored time intervals (24, 48 and 72 h) in extender III containing purified fractions of milk micellar proteins (INRA 96). For sperm survival, the second most suitable extender was extender II (BotuSemen Gold). Samples of insemination doses with extender II had the second highest values of sperm motility, progressive motility and viability, with the exception of the percentage of viable sperm during 24 hours storage, when extender I (skimmed milk-based extender) reached a higher value. However, with longer storage, extender II proved to be more effective in maintaining sperm viability than extender I.

Milk as a biological fluid has a complex composition. Some milk fractions can have a protective effects and some can have a detrimental effects on spermatozoa. Extenders containing only components with protective effects provide an opportunity to increase sperm survival in insemination doses (Batellier et al. 1997, Batellier et al. 2001, Pagl et al. 2006). Several authors achieved better results in maintaining survivability of spermatozoa in chemically defined extender INRA 96 compared to other diluents using in horse breeding industry (LeFrapper et al. 2010, Batellier et al. 1998, Batellier et al. 2001). LeFrapper et al. (2010) confirm that INRA 96 maintains fertility of sperm up to 72 hours. Novello et al. (2020) compared semen parameters of cooled stallion semen extended with INRA 96 and BotuSemen Gold. BotuSemen Gold extender displayed higher motility parameters in 48 hours storage. Thus further research is needed to compare these two extenders.

Figure 1 Mean values of motile, progressive motile and viable sperm using extenders I–III during storage for 24, 48 and 72 hours

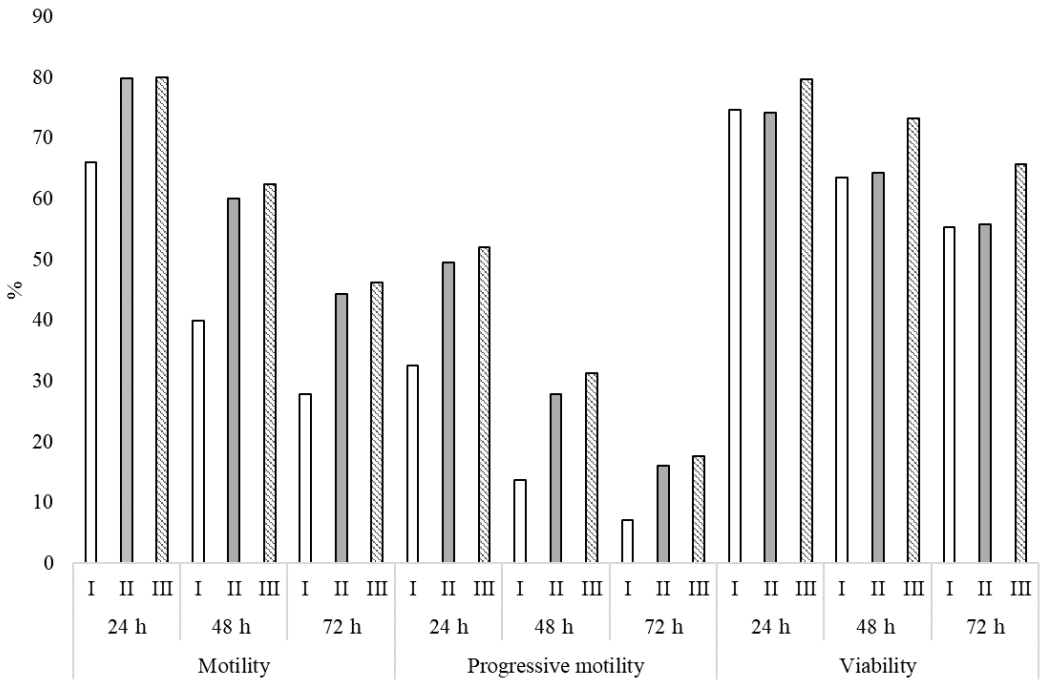

CONCLUSION

The results show that the most suitable extender in terms of maintaining sperm survival in insemination doses of Warmblood stallions is extender III containing purified fractions of milk micellar proteins. The second most suitable diluent is extender II containing casein and cholesterol. On average, the largest decrease in the monitored quality parameters was in samples with extender I containing skimmed milk.

ACKNOWLEDGEMENTS

Research was financially supported by the grant no. AF-IGA2020-IP066.

REFERENCES

Atroshchenko, M.M. et al. 2019. Reproductive Characteristics of Thawed Stallion Sperm. Animals [Online], 9(12): 1099. Available at: http://eds.b.ebscohost.com/eds/detail/detail?vid=3&sid=f71458f9-37de-4e0f-97fb-3cec412095f7%40pdc-v-sessmgr04&bdata=Jmxhbmc9Y3Mmc2l0ZT1lZHMtbGl2ZQ%3d%3d#AN=edselc.2-52.0-85076500932&db=edselc. [2020-09-01].

Aurich, J.E. 2012. Artificial Insemination in Horses – More than a Century of Practise and Research. Journal of Equine Veterinary Science [Online], 32(8): 458–463. Available at: https://www.sciencedirect.com/science/article/pii/S0737080612003310. [2020-08-25].

Batellier, F. et al. 1997. Effect of milk fractions on survival of equine spermatozoa. Theriogenology [Online], 48(3): 391–410. Available at: https://www.sciencedirect.com/science/article/pii/S0093691X97002501. [2020-08-25].

Batellier, F. et al. 1998. Delayed insemination is successful with a new extender for storing fresh equine semen at 15°C under aerobic conditions. Theriogenology [Online], 50(2): 229–236. Available at: https://www.sciencedirect.com/science/article/pii/S0093691X98001307?via%3Dihub. [2020-10-15].

Batellier, F. et al. 2001. Advances in cooled semen technology. Animal Reproduction Science [Online], 68(3–4): 181–190. Available at: https://www.sciencedirect.com/science/article/pii/S0378432001001555?via%3Dihub. [2020-10-15].

Hernández-Avilés, C. et al. 2020. Effects of glucose concentration in semen extender and storage temperature on stallion sperm quality following long-term cooled storage. Theriogenology [Online], 147(7): 1–9. Available at: https://www.sciencedirect.com/science/article/pii/S0093691X20301035. [2020-08-25].

Jasko, D.J. et al. 1992. Effect of seminal plasma and egg yolk on motion characteristics of cooled stallion spermatozoa. Theriogenology [Online], 37(6): 1241–1252. Available at: https://www.sciencedirect.com/science/article/pii/0093691X9290180Y. [2020-08-25].

Lane, C. 2015. Equine reproduction Part 1: Artificial insemination. Veterinary Nursing Journal [Online], 30(5): 146–149. Available at: https://www.tandfonline.com/doi/full/10.1080/17415349.2015.1028770. [2020-08-25].

LeFrapper, L. et al. 2010. Comparison of Various Extenders for Storage of Cooled Stallion Spermatozoa for 72 Hours. Journal of Equine Veterinary Science [Online], 30(4): 200–204. Available at: https://www.sciencedirect.com/science/article/pii/S0737080610000997. [2020-08-27].

Martečíková, S. et al. 2010. Effect of acrosome reaction progress in frozen-thawed boar spermatozoa on the efficiency of in vitro oocyte fertilization. Veterinární Medicína [Online], 55(9): 429–437. Available at: https://www.agriculturejournals.cz/web/vetmed.htm?volume=55&firstPage=429&type=publishedArticle. [2020-08-27].

Novello, G. et al. 2020. Stallion Semen Cooling Using Native Phosphocaseinate-based Extender and Sodium Caseinate Cholesterol-loaded Cyclodextrin-based Extender. Journal of Equine Veterinary Science [Online], 92(9): 103–104. Available at: https://www.sciencedirect.com/science/article/pii/S0737080620301957. [2020-08-25].

Pagl, R. et al. 2006. Comparison of an extender containing defined milk protein fractions with a skim milk-based extender for storage of equine semen at 5°C. Theriogenology [Online], 66(5): 1115–1122. Available at: https://www.sciencedirect.com/science/article/pii/S0093691X06001774. [2020-08-25].

Rečková, Z. et al. 2008. Evaluation of chromatin integrity of motile bovine spermatozoa capacitated in vitro. Zygote [Online], 16(3): 195–202. Available at: https://www.cambridge.org/core/journals/zygote/article/evaluation-of-chromatin-integrity-of-motile-bovine-spermatozoa-capacitated-in-vitro/1F21529EF2FF8240D936F1F2A82DFFD9. [2020-09-01].

Rečková, Z. et al. 2015. Relationship between acrosome integrity changes and in vitro fertilising ability of bovine spermatozoa. Veterinární medicína [Online], 60(9): 469–475. Available at: http://vri.cz/docs/vetmed/60-9-469.pdf. [2020-09-15].

Rečková, Z., Filipčík, R. 2020. An Analysis of Selected Aspects of Sperm Quality in Fresh and Cooled-Storage Stallion Semen. Iranian Journal of Applied Animal Science. [Online], 10(3): 405–408. Available at: http://ijas.iaurasht.ac.ir/article_675315_c1a9e1ab03a577c5ca5580877afaaa06.pdf. [2020-09-15].

Varner, D.D. 2008. Developments in stallion semen evaluation. Theriogenology [Online], 70(3): 448–462. Available at: https://www.sciencedirect.com/science/article/pii/S0093691X08002070. [2020-09-01].

Varner, D.D. et al. 1988. Effects of cooling rate and storage temperature on equine spermatozoal motility parameters. Theriogenology [Online], 29(5): 1043–1054. Available at: https://www.sciencedirect.com/science/article/pii/S0093691X88800281. [2020-08-25].

Věžník, Z. et al. 2007. The interrelationship between quality parameters of sperm before and after separation by gradient centrifugation. Veterinární Medicína [Online], 52(10): 423–429. Available at: https://www.agriculturejournals.cz/web/vetmed.htm?volume=52&firstPage=423&type=publishedArticle. [2020-08-25].

Study of selected signaling pathways genes that play an important role in bone metabolism in laying hens

Michala Steinerova[1], Cenek Horecky[1], Ales Knoll[1], Sarka Nedomova[2], Ales Pavlik[1]
[1]Department of Animal Morphology, Physiology and Genetics
[2]Department of Food Technology
Mendel University in Brno
Zemedelska 1, 613 00 Brno
CZECH REPUBLIC

xsteine5@node.mendelu.cz

Abstract: Due to the balanced activity of osteoclasts, the bone-reabsorbing cells, and osteoblasts, the bone-forming cells, bone remodeling is lifelong process, which can be influenced by number of factors. The key role in the control of osteoclastogenesis and osteoblastogenesis play signaling pathways. This work was primary focused on detection of single nucleotide polymorphisms in selected genes that are part of those signaling pathways that regulates skeletal development and homeostasis. The study of these genes is of great value for skeletal health and diseases in laying hens. The polymorphisms of five genes (*WISP1, SOST, TNFSF11, TNFRSF11A* and *TNFRSF11B*) was studied in order to survey their relationship with parameters of bones in hens of ISA Brown hybrids (bone breaking strength, length, width and bone mass). PCR and sequencing were used to determine the polymorphisms and each marker were tested in sixteen samples. No polymorphisms were found in selected gene regions in the experimental group of animals, which would show associations with the observed bone parameters of laying hens.

Key Words: polymorphism, osteoporosis, laying hens, bone, signaling pathways

INTRODUCTION

Osteoporosis, as a common degenerative disease, is characterized by reduced bone mass and microarchitectural deterioration of bone tissue (Guo et al. 2019). In the case of laying hens, this is a condition that involves the loss of structural bone during laying period (Whitehead and Fleming 2010).

Decisive in the regulation of how osteoclasts and osteoblasts control bone turnover are signaling pathways (Iñiguez-Ariza and Clarke 2015), while it has been largely proven that the RANK/RANKL/osteoprotegerin and Wnt signaling pathways play a key role in the control of osteoclastogenesis and osteoblastogenesis, respectively (Brunetti et al. 2019).

The Wnt signaling pathway has central roles in bone development, homeostasis, as well as bone repair and regeneration following injury (Houschyar et al. 2019). At the beginning of the skeletal development, it controls the formation of patterns before the skeletal elements are laid down. Also, abnormal Wnt signaling is associated with skeletal defects (Regard et al. 2012). In the case of the Wnt pathway, there are two pathways of signaling. The first is β-catenin-dependent canonical and the second is independent non-canonical pathways. Due to the action of this signaling pathway on osteoblast precursor cells, it promotes differentiation into mature osteoblasts. This is done through the β-catenin-dependent canonical pathway. Trough the same pathway, in mature osteoblasts, bone resorption is suppressed by regulating the receptor activator of NF-κB ligand (nuclear factor kB ligand) (RANKL)/osteoprotegerin (OPG) (Kobayashi et al. 2008). Within the components of the Wnt signaling pathway, WNT1-inducible-signaling pathway protein 1 (*WISP1*), also known as CCN4, has been found to be a novel target for modulating osteogenesis and improving bone strength (Ferrand et al. 2017). Sclerostin, a protein encoded by the SOST gene, is a potent antagonist of Wnt signaling. It is primarily expressed by mature osteocytes, binds to the Wnt co-receptors LRP 5/6 antagonizing downstream signaling, and interacts with another member of the LRP family, LRP4 (Delgado-Calle et al. 2017).

The RANK (receptor activator of NF-kB), RANKL (its ligand) and OPG (the decoy receptor of RANKL, osteoprotegerin) system is known for its roles in bone modeling, bone remodeling and osteoclasts maturation (Tobeiha et al. 2020). Critical to the formation, function, and survival of osteoclasts is a member of the TNF ligand superfamily RANKL, which exerts its functions by binding and activating its receptor RANK. It is expressed on the surface of osteoclastic precursors and mature osteoclasts (Kohli and Kohli 2011). OPG is a soluble member of the TNF receptor super family secreted by osteoblasts which, by competing with RANK for binding to RANKL, acts as a decoy receptor, thereby inhibiting osteoclastogenesis. RANKL/OPG balance changes characterized by excessive osteoclastic activity have been reported in a spectrum of skeletal diseases, including osteoporosis (Santini et al. 2011), whereas several related clinical conditions have been associated with mutations in the *TNFRSF11A* gene (RANK), *TNFSF11* gene (RANKL) and the *TNFRSF11B* gene (OPG) (Ralston and Uitterlinden 2010).

The aim of this study was to identify polymorphisms of selected genes and to determine if they show associations with bone mechanical parameters. Selected genes of this study are related to bone metabolism, therefore possible polymorphisms of these genes may be significant in that they affect protein production and consequently bone formation.

MATERIAL AND METHODS

The experiment was performed on ISA Brown hybrids, housed in enriched cages. Slaughter, using decapitation, occurred at an average age of 26 weeks, blood was taken immediately thereafter and subsequently stabilized with heparin. Isolated DNA samples were tested, wherein the isolation was performed using a commercially available DNA Lego kit (Top-Bio, Prague, Czech Republic) and sixteen samples from each marker were sequenced. Several parameters, as bone breaking strength, bone mass, length and width, were analyzed on femur. TIRATEST 27025 (TIRA Maschinenbau GmbH, Schalkau, Germany) is a universal testing machine with which it was evaluated and analyzed bone breaking strength. Bone dimensions was assessed using Vernier calipers. Using OLIGO v4.0 software (Molecular Biology Insights, Inc., Colorado Springs, CO, USA) according to sequences from GenBank database (http://www.ncbi.nlm.nih.gov/genbank/), own specific oligonucleotide primers were designed (Table 1).

Table 1 WISP1, SOST, TNFSF11, TNFRSF11A and TNFRSF11B primers

Gene	Primer sequence	Product size (bp)
WISP1 (exon 2)	Forward: 5'- TTATTCTTTGGTCTCCTTGTAGC-3' Reverse: 5'- TTGCCTTTCCTCATTCAGC-3'	579
WISP1 (exon 5)	Forward: 5'-CACACCTCTAGATCCGGACTGTAG-3' Reverse: 5'-CTGGCTGCTCTTAATGGATGG-3'	729
SOST (exon 1)	Forward: 5'-AACCCGACAACACGAGGAG-3' Reverse: 5'-CGATTCCTCCTCCATACCAAG-3'	604
TNFSF11 (exon 4 a 5)	Forward: 5'-TTATGGGATGTGTTCTTAGCAGTG-3' Reverse: 5'-GGTTTCAGGCCTCAATAGAGC-3'	581
TNFRSF11A (exon 1)	Forward: 5'-AATAGGATGCCAGAAGTTTGTGAC-3' Reverse: 5'-TCCTACGTACGTGCCTGAAGAC-3'	619
TNFRSF11A (exon 6)	Forward: 5'-TGTAGGAGCCACGACGAGC-3' Reverse: 5'-AAGGAGACACGAGGAAAGTTGG-3'	520
TNFRSF11B (exon 5)	Forward: 5'-TGGAAGGGACATGAAGGATC-3' Reverse: 5'-CTCCAAGAACACTGCAGAAGAC-3'	680

PCR was performed in solution with a final volume of 10 ml. The following PCR condition were employed: 94 °C for 3 min, 30 cycles at 94 °C for 1 min, 53, 55, 56 or 57 °C for 30 s; 72 °C for 1 min, 72 °C for 10 min, then maintained at 4 °C. Annealing temperature of 53 °C was used for *WISP1* exon 2, 55 °C for *WISP1* exon 5, *TNFSF11* exon 4 a 5, *TNFRSF11A* exon 1, *TNFRSF11A* exon 6, 56 °C for *SOST* exon 1 and 57 °C for *TNFRSF11B* exon 5. An ABI Veriti thermal cycler was used for the PCR reactions (Life Technologies, Applied Biosystems, Foster City, CA, USA). The products of the PCR reaction were visualized by 2.5% agarose gel electrophoresis followed by GoodView

staining (Ecoli, ltd., Bratislava, Slovak Republic) at 120 V for 30 min using TBE buffer. The 100 bp DNA ladder (M100) (Thermo Fisher Scientific Inc., Waltham, USA) was used as molecular size marker.

DNA sequencing of the PCR products was carried out using the BigDye® Terminator v3.1 Cycle Sequencing Kit (Applied Biosystems, Foster City, CA, USA), whereas conditions of cycle sequencing was 96 °C for 1 min, 25 cycles at 96 °C for 10 s, 50 °C for 5 s, 60 °C for 4 min, then maintained at 4 °C. An ABI PRISM 3500 DNA analyzer (Life Technologies, Applied Biosystems, Foster City, CA, USA) was used for sequencing. Sequence alignments were performed using SeqScape v2.7 (Life Technologies, Applied Biosystems, Foster City, CA, USA).

Obtained data were analyzed using Kruskal-Wallis test with genotype as an independent variable and bone breaking strength, bone length, width and bone mass as dependent variables. All statistical analyses were performed by STATISTICA 12 statistical software (StatSoft Inc., Tulsa, USA). The overall level of statistical significance was defined as $P<0.05$.

RESULTS AND DISCUSSION

Selected regions of studied genes were tested in sixteen samples for each marker. The *WISP1* gene is in laying hens located on chromosome 2, has 5 exons, whereas region of exon 2 and exon 5 were examined. The PCR products of *WISP1* exon 2 had size of 579 bp and products of *WISP* exon 5 had size of 729 bp. A total of 8 polymorphisms were detected in these regions and 2 polymorphisms were found in the exons (c.450A>C (exon 2), c.1133A>G (exon5)). The other polymorphisms were intronic (c.650+83C, c.1103-168C, c.1103-20T, c.1103-7G, c.1460+48C, c.1460+79G). The *SOST* gene has 2 exons and is located on chromosome 27. Exon 1 was tested. The PCR product had a size of 604 bp. Total of 2 exonic polymorphisms (c.164A>T, c.239G>T) and 5 intronic polymorphisms (c.254+9A, c.254+17A, c.254+40C, c.254+74G, c.254+85G) were found. The *TNFSF11* gene is located on chromosome 1 and has 6 exons, whereas region of exon 4 and exon 5 were examined. The PCR product had a size of 581 bp. All 6 polymorphisms (c.641T>A, c.651T>G, c.653T>A, c.661G>C, c.674C>A, c.679A>G) were found in exon 4. The *TNFRSF11A* gene has 10 exons and is located on chromosome 2. Region of exon 1 and exon 6 were tested. The PCR products of *TNFRSF11A* exon 1 had size of 619 bp and products of *TNFRSF11A* exon 6 had size of 520 bp. A total of 5 polymorphisms were detected in these regions, 3 polymorphisms were found in the exons (c.31G>A, c.57C>G, c.94C>G (exon 1) and the other polymorphisms were intronic (c.1-8G (exon 1), c.604+168C (exon 6)). The *TNFRSF11B* gene has 5 exons, it is also found on chromosome 2 and exon 5 was tested. The PCR product had a size of 680 bp. This gene showed non-specific amplification and was excluded from the analysis. The values of the femur breaking strength were from 39.47 to 271.67 N. The range of absolute values for bone width was between 6.93 and 8.82 mm, bone length 79.24 and 89.41 mm, bone mass 6.86 and 9.45 g. Within the *TNFRSF11A* gene, only one genotype was found in all the mentioned polymorphisms (*GA* genotype of c.31G>A polymorphism, *GC* genotypes of c.57C>G and c.94C>G polymorphisms, *GG* genotype of c.1-8G and *CT* genotype of c.604+168C polymorphisms). Also, for the c.450A>C polymorphism in the *WISP 1* gene was found only *CC* genotype. According to the distribution and position of the individual genotypes and alleles within the respective sequence and by giving all the statistically the same result, it can be concluded, that the polymorphisms of the *TNFRSF11* gene are linked, whereas this assumption would have to be substantiated by further, larger studies. No statistically significant difference was found in any of them (Table 2).

Table 2 P-values of TNFSF11 gene

Gene	SNP	Bone breaking strength	Length	Width	Bone mass
TNFSF11	c.641T>A, c.651T>G, c.653T>G c.661G>C, c.674C>A				
	P-value	*086.5*	*0.865*	*0.147*	*0.124*
	c.679A>G				
	P-value	*0.668*	*0.309*	*0.194*	*0.304*

The only statistically significant difference was found within the *WISP 1* gene and the bone length parameter, in the c.650 + 83C polymorphism (Table 3).

Table 3 Association of WISP 1 gene polymorphisms with selected bone parameters

Gene	SNP	Genotype (N)	Bone breaking strength	Length	Width	Bone mass
WISP 1	c.1133A>G	GG (7)	128.94	83.91	7.50	8.31
		GA (9)	126.58	86.34	7.11	8.80
		AA (0)	0.00	0.00	0.00	0.00
	P-value		*0.935*	*0.371*	*0.143*	*0.291*
	c.650+83C	AA (7)	108.56	86.84	8.02	9.13
		AC (9)	140.45	84.52	7.66	8.22
		CC (0)	0.00	0.00	0.00	0.00
	P-value		*0.827*	***0.049***	*0.824*	*0.723*
	c.1103-168C	CC (4)	186.10	85.50	7.50	8.17
		CT (6)	122.56	86.30	8.09	8.86
		TT (6)	106.05	85.31	7.60	8.38
	P-value		*0.47*	*0.727*	*0.431*	*0.505*
	c.1103-20T	CC (0)	0.00	0.00	0.00	0.00
		CT (9)	126.58	86.34	8.12	8.80
		TT (7)	128.94	83.91	7.50	8.31
	P-value		*0.935*	*0.371*	*0.143*	*0.291*
	c.1103-7G	AA (0)	0.00	0.00	0.00	0.00
		GA (9)	110.76	75.55	7.11	7.70
		GG (7)	107.45	69.93	6.25	6.93
	P-value		*0.935*	*0.371*	*0.143*	*0.291*
	c.1460+48C	CC (4)	186.10	85.50	7.50	8.17
		GC (7)	121.53	86.56	8.34	8.91
		GG (5)	124.08	85.42	7.65	9.13
	P-value		*0.535*	*0.798*	*0.246*	*0.501*
	c.1460+79G	AA (5)	124.08	85.42	7.69	9.13
		GA (7)	121.53	86.56	8.34	8.91
		GG (4)	186.10	85.50	7.50	8.17
	P-value		*0.535*	*0.798*	*0.246*	*0.501*

Legend: N – numbers of individuals of each genotype

No statistically significant difference was found within the polymorphisms of the *SOST* gene (Table 4).

The polymorphism of c.650 + 83C in *WISP 1* gene was significantly associated with bone length between *AA* ×*AC* genotypes. The *A* allele led to longer bone lengths than the *C* allele.

It is assumed that in the case of longer bone lengths, the increase in bone mass is due to an increase in length rather than bone density, so these bones could be more prone to fractures. However, this assumption is not substantiated by any study. Also, no study was found that would deal with the genes we studied in relation to bone length and strength.

Apart from the c.650 + 83C polymorphism in the *WISP 1* gene, the other studied polymorphisms, in this number of samples, did not show their effect on selected bone parameters. Despite this fact is still needed others, primarily more extensive studies.

One of the few studies that deals with the same issue, thus by testing polymorphisms of genes that are part of the signaling pathways that regulates skeletal development and homeostasis in laying hens, is study of Guo et al. (2017). In this study, bone quality was tested in a total of 1534 laying hens, revealing 9 single nucleotide polymorphisms (SNPs) that were associated with bone quality. Among the genes, in which these polymorphisms were found, were the *TNFSF11* and *SOST* genes, which are known for their association with osteoporosis in humans. It makes them appropriate candidate genes

for osteoporosis in chicken. Other studies that already focus mainly on other genes, but still concern osteoporosis in laying hens, are studies of Fornari et al. (2012) and Raymond et al. (2018).

Table 4 Association of SOST gene polymorphisms with selected bone parameters

Gene	SNP	Genotype	Bone breaking strength	Length	Width	Bone mass
SOST	c.164A>T	AA (5)	148.91	85.52	7.55	9.13
		AT (7)	129.17	85.94	7.97	8.58
		TT (4)	171.03	83.06	7.50	7.69
	P-value		*0.961*	*0.213*	*0.613*	*0.075*
	c.239G>T	GG (5)	148.91	85.52	7.55	9.13
		GT (4)	133.24	84.80	7.45	8.22
		TT (7)	151.84	84.90	7.99	8.26
	P-value		*0.99*	*0.793*	*0.425*	*0.115*
	c.254+9A	AA (9)	131.74	85.06	7.69	8.52
		AT (0)	0.00	0.00	0.00	0.00
		TT (7)	173.73	86.32	85.32	8.80
	P-value		*0.884*	*0.812*	*0.462*	*0.663*
	c.254+17A	AA (6)	133.30	84.84	7.86	8.28
		AT (5)	98.46	84.49	7.41	8.53
		TT (5)	175.37	86.15	7.71	9.07
	P-value		*0.565*	*0.275*	*0.634*	*0.290*
	c.254+40C	CC (6)	151.13	85.20	7.75	8.44
		CT (5)	69.53	83.60	7.08	9.29
		TT (5)	173.73	85.32	7.98	8.80
	P-value		*0.412*	*0.427*	*0.354*	*0.520*
	c.254+74G	GG (5)	171.74	83.44	7.43	7.86
		GT (4)	144.08	86.93	8.32	8.80
		TT (7)	127.08	85.28	7.57	8.93
	P-value		*0.566*	*0.096*	*0.239*	*0.213*
	c.254+85G	GG (8)	143.71	85.06	7.69	8.52
		GA (0)	0.00	0.00	0.00	0.00
		AA (8)	173.73	85.32	7.98	8.80
	P-value		*0.881*	*0.822*	*0.468*	*0.663*

Legend: N – numbers of individuals of each genotype

CONCLUSION

Bone weakness in laying hens caused by osteoporosis, which further leads to bone fractures, affects both animal welfare and the economic aspects of breeding. Skeleton problems in laying hens are becoming more common and if there is no reconsideration of the breeding, these problems can tend to get worse. Genetic factors are the basis for variability in bird susceptibility to osteoporosis and bone fractures. Studies of markers that could affect bone parameters, especially their strength, may contribute to the discovery of new findings that would be useful in breeding. Therefore, this work tried to focus on the search for single nucleotide polymorphisms that could affect the monitored bone indicators. No such polymorphism was found. Based on results, it would be advisable to extend the study to other regions of the genes that would be explored, optimize the partial methods, and the study could be extended to include new genes that are candidates and could help to deepen knowledge about osteoporosis of laying hens.

ACKNOWLEDGEMENTS

The research was financially supported by the Internal Grant Agency of the Faculty of AgriSciences, Mendel University in Brno (AF-IGA2020-IP053).

REFERENCES

Brunetti, G. et al. 2019. An update on the role of RANKL-RANK/osteoprotegerin and WNT-β-catenin signalling pathways in pediatric diseases. World Journal of Pediatrics, 15(1): 4–11.

Delgado-Calle, J. et al. 2017. Role and mechanism of action of Sclerostin in bone. Bone, 96: 29–37.

Ferrand, N. et al. 2017. WISP1/CCN4 inhibits adipocyte differentiation through repression of PPARγ activity. Scientific Reports [online], 7: 1749. Available at: https://www.nature.com/articles/s41598-017-01866-2. [2020-09-13].

Fornari, M.B. et al. 2012. Association of the A211G polymorphism in the bone sialoprotein gene with skeletal structure in a paternal broiler line. Poultry Science Journal [online]. Available at: https://pdfs.semanticscholar.org/109a/dd6f2fe28cde35f7821671ebe35b9307517e.pdf. [2019-08-18].

Guo, J. et al. 2017. Genetic architecture of bone quality variation in layer chickens revealed by a genome-wide association study. Scientific Reports, 7: 45317.

Guo, L. et al. 2019. Pathway and network analysis of genes related to osteoporosis. Molecular Medicine reports, 20(2): 985–994.

Houschyar, K.S. et al. 2019. Wnt pathway in bone repair and regeneration – What do we know so far. Frontiers in Cell and Developmental Biology [online], 6: 170. Available at: https://www.frontiersin.org/articles/10.3389/fcell.2018.00170/full. [2020-09-13].

Iñiguez-Ariza, N.M., Clarke, B.L. 2015. Bone biology, signalling pathways, and therapeutic targets for osteoporosis. Maturitas, 82: 245–255.

Kobayashi, Y. et al. 2008. Roles of Wnt signalling in bone formation and resorption. Japanese Dental Science Review, 44(1): 76–82.

Kohli, S.S., Kohli, V.S. 2011. Role of RANKL-RANK/osteoprotegerin molecular complex in bone remodelling and its immunopathologic implications. Indian Journal of Endocrinology and Metabolism, 15(3): 175–181.

Ralston, S.H., Uitterlinden, A.G. 2010. Genetics of osteoporosis. Endocrine Reviews, 31(5): 629–662.

Raymond, B. et al. 2018. Genome-wide association study for bone strength in laying hens. Animal Science, 96(7): 2525–2535.

Regard, J.B. et al. 2012. Wnt signaling in bone development and disease: Making stronger bone with Wnts. Cold Spring Harbor perspectives in biology, 4(12): a007997.

Santini, D. et al. 2011. Receptor activator of NF-kB (RANK) expression in primary tumors associates with bone metastasis occurrence in breast cancer patients. PLoS One, 6(4): e19234.

Tobeiha, M. et al. 2020. RANKL/RANK/OPG pathway: A mechanism involved in exercise-induced bone remodeling. BioMed Research International [online], 2020: 6910312. Available at: https://doi.org/10.1155/2020/6910312. [2020-10-14].

Whitehead, C.C., Fleming, R.H. 2000. Osteoporosis in cage layers. Poultry Science, 79(7): 1033–1041.

Bull sperm capacitation treatment and oocyte-sperm co-culture system affect *in vitro* bovine embryo development

Ivona Travnickova[1,2], Pavlina Hulinska[1], Zbysek Sladek[2], Marie Machatkova[1]
[1]Department of Genetics and Reproduction
Veterinary Research Institute
Hudcova 296/70, 621 00 Brno
[2]Department of Animal Morphology, Physiology and Genetics
Mendel University in Brno
Zemedelska 1, 613 00 Brno
CZECH REPUBLIC

xtravni2@mendelu.cz, travnickova@vri.cz

Abstract: The study was designed to define the effects of bull sperm treatment and co-culture system on *in vitro* embryo development. The mature oocytes were fertilized by sperm treated with heparin in standard co-culture (Exp.1) or by sperm treated with heparin supplemented either with PHE mix (penicillamine, hypotaurine, and epinephrine) or caffeine both in standard co-culture and in drops (Exp.2). A variability in the blastocyst rate was observed among bulls after fertilization of oocytes with heparin treated-sperm in standard co-culture. The significantly higher percentages of cleaved oocytes and developed blastocysts were derived from sperm treated with heparin-PHE in comparison with those treated with heparin-caffeine in drops (84.6 and 43.3 *vs.* 67.6 and 24.8, respectively). The significantly higher percentages of cleaved oocytes and developed blastocysts were recovered from sperm treated with heparin-PHE in drops than from those treated with heparin-caffeine in standard co-culture (85.9 and 47.1 *vs.* 73.3 and 25.6, respectively). We concluded, that the efficiency of *in vitro* bovine embryo development depends on sperm capacitation treatment and oocyte-sperm co-culture system.

Key Words: cattle, spermatozoa, stimulation agents, IVF outcomes

INTRODUCTION

The utilization of frozen-thawed sperm for *in vitro* fertilization (IVF) together with other reproductive techniques such as transvaginal oocyte aspiration (OPU), *in vitro* embryo production (IVP), cryopreservation and embryo transfer (ET) is an effective strategy for obtaining progeny from genetically valuable parents (Machatkova et al. 2008). However, the lower fertilizing capability of bull sperm under *in vitro* in comparison with *in vivo* conditions remains the key problem limiting the application of this biotechnology in cattle breeding (Rizos et al. 2002). One possibility for enhancing embryo yield for the majority of elite bulls is to optimize the IVF procedure in terms of sperm treatment and oocyte-sperm co-culture. When IVF conditions were specified for individual bulls, the embryo outcomes were comparable to those reached after cow superovulation and artificial insemination. A better understanding of the impact of the course of sperm capacitation and oocyte-sperm interaction on early embryonal development are necessary to improve the efficiency of *in vitro* embryo production in cattle.

The objective of this study was 1) to assessed the functional parameters of sperm of elite bulls and characterize their fertility in standard co-culture system 2) to specify the effect of the sperm capacitation treatment and oocyte-sperm co-culture on early embryo development.

MATERIAL AND METHODS

Oocyte collection and maturation

Slaughtered Holstein dairy cows, aged 4 to 6 years, with a checked ovarian cycle stage, were used as ovary donors. Only those with ovaries in the stagnation and regression phases, assessed by follicle and corpus luteum (CL) morphology, were selected for oocyte collection. The oocytes were collected

from 2 to 5 mm sized follicles by slicing of ovarian cortex. Only healthy cumulus-oocyte complexes with a homogenous ooplasm, surrounded by compact multiple layers of cumulus cells were selected and used in experiments.

They were matured in 500 µl of TCM-199 medium (Earle's salts), with 20 mM sodium pyruvate, 50 IU/ml penicillin, 50 µg/ml streptomycin, 5% oestrus cow serum (ECS; Sevapharma, Prague, Czech Republic) and gonadotropins (P.G. 600 15 IU/ml; Intervet, Boxmeer, Holland). Maturation took place in four-well plates (Nunclon Intermed, Roskilde, Denmark) under a humidified atmosphere of 5% CO_2 in air at 38.8 °C for 24 h (Knitlova et al. 2017).

Sperm isolation and capacitation

Frozen semen of elite Holstein bulls (A-E) was used. The straws were thawed in a water bath at 35 °C for 50 s using the standard protocol. After thawing, the motility, viability and integrity of acrosome of sperm were assessed subjectively by light microscopy, eosin-nigrosin and fluorescent FITC-PSA staining, respectively. Motile spermatozoa were isolated on a Percoll gradient (Reckova et al. 2008). Briefly, semen was gently layered on top of 1.5 ml 80% and 1.5 ml 40% Percoll in a modified SP-TALP medium and centrifuged at 440 × g for 15 min. The supernatant was discarded and the pellet containing sperm was washed twice for 4 min at 350 × g using SP-TALP medium and then IVF-TALP medium supplemented in Exp. 1 with heparin (10 µg/ml), in Exp. 2 either with heparin and PHE mix (2 mM penicillamine, 1 mM hypotaurine, and 250 µM epinephrine) or with heparin and caffeine (1 mM).

Oocyte fertilization and embryo culture

Sperm were added to 20–30 oocytes at a ratio of 8.000 sperm per oocyte. They were co-cultured either in a standard volume of IVF medium (500 µl) for 18 h or in drops (50 µl) for 1 h and after adding the remaining medium (450 µl) for another 17 h in 5% CO_2 in air at 38.8 °C. After that, the oocytes were completely denuded from cumulus cells and presumptive zygotes were transferred to a Buffalo rat liver cell line monolayer (BRL cell line, ATCC, Rockville, MD, USA) into Menezo B2 medium with 10% ECS. They were fertilized in a humidified atmosphere of 5% CO_2 in air at 38.8 °C for 7 days. The cleavage and blastocyst rates from the total number of co-cultured oocytes were calculated on Day 2 and Day 7, respectively, for each sperm treatment and co-culture system.

Statistical analysis

At least four replicates were carried out for each tested bull, sperm treatment and co-culture. All data were analysed by one-way ANOVA using SPSS version 11.5 for Windows (SPSS, INC. IL, USA). The significance of differences among the values was evaluated by the Chi-square test using the STATISTICA software system, version 10 (StatSoft, Inc. 2011). Differences at $P < 0.05$ were considered statistically significant.

RESULTS AND DISCUSSION

Experiment 1

Differences in motility, viability and acrosome integrity of sperm were found among breeding bulls A - E after semen thawing (Table 1).

Table 1 Functional parameters of sperm after bull semen thawing

Bulls	Motility / progressive motility [%]	Viability [%]	Acrosome integrity		
			Intact [%]	Reacted [%]	Without acrosome [%]
A	60 / 55	64.5	95.0	3.5	1.5
B	55 /45	72.5	94.5	3.0	2.5
C	50 / 40	61.5	93.5	5.5	1.0
D	60 / 50	67.5	92.0	4.5	3.5
E	65 / 60	74.0	92.0	8.0	0

Legend: The motility, viability and acrosome integrity were assessed subjectively by light microscopy, eosin-nigrosin and fluorescent FITC-PSA staining, respectively.

A significant variability in cleaved oocyte and developed blastocyst rates ($P < 0.05$) was also detected among bulls after the mature oocytes were co-cultured with heparin treated-sperm in standard culture (Table 2).

Table 2 Development of bovine embryos from oocytes fertilized by sperm treated with heparin in standard co-culture

Bulls	Oocytes fertilized (n)	Sperm treated with heparin	
		Embryo rate (%)	
		Cleaved	Blastocysts
A	342	87.3[a]	23.1[a]
B	353	85.1[a]	29.8[a]
C	360	68.9[a]	25.6[c]
D	358	88.3[a]	39.5[b]
E	342	80.4[a]	26.0[b]

Legend: [(a-c)] Values with different superscripts within the same column for cleaved oocytes and blastocysts are significantly different ($P < 0.05$). Sperm treated with 10 µg/ml heparin and co-cultured with oocytes in 500 µl volume.

Although various treatments have been investigated for bovine sperm, heparin is mostly used as a capacitation agent. The optimization of heparin level for each bull is recommended to enhance the IVF outcome for selected parent combinations (Lu and Seidel 2004, Xu et al. 2009, Barcelo-Fimbres et al. 2011). However, if the heparin level is tested during IVF, it is also necessary to change the sperm concentration in order to minimize polyspermy and adjust the optimal IVF conditions (Parrish 2014). To date, there has been very little information about *in vitro* embryo production from bovine sperm treated with further capacitation stimulants.

Experiment 2

To study the effect of another sperm treatment and co-culture system on embryo development, semen of bull E with an average motility and viability, and with the highest percentage of acrosome reacted sperm was selected. Significantly higher percentages of cleaved oocytes and developed blastocysts were obtained from sperm treated with heparin-PHE than those treated with heparin-caffeine in drops (Table 3).

Table 3 Development of bovine embryos from oocytes fertilized by sperm treated either with heparin and PHE or heparin and caffeine in drop co-culture

Development of embryos	Sperm treated with	
	Heparin-PHE	Heparin-caffeine
Oocytes inseminated (n)	104	105
Cleaved (%)	84.6[a]	67.6[b]
Blastocysts (%)	43.3[a]	24.8[b]

Legend: [(a-b)] Values with different superscripts within the same row are significantly different ($P < 0.05$). Sperm of bull E treated with a) 10 µg/ml heparin and 2 mM penicillamine, 1 mM hypotaurine, 250 µM epinephrine b) 10 µg/ml heparin and 1 mM caffeine and co-cultured with oocytes in 50 µl volume.

No significant differences in the percentage of cleaved oocytes and developed blastocysts were found for identically treated spermatozoa co-cultured either in standard co-culture or in drops. However, significantly higher percentages of cleaved oocytes and developed blastocysts ($P < 0.05$) were recovered from sperm treated with heparin-PHE in drops than from sperm treated with heparin-caffeine in a standard co-culture (Table 4).

It has also been confirmed previously that the presence of PHE during IVF improves the motility of sperm, their ability to undergo the acrosome reaction, penetrate mature oocytes and fertilize them (Leibfried and Bavister 1982, Meizel 1985). The supplementation of IVF medium with PHE has also been shown to enhance the cleavage rate and development of early embryos up to the blastocyst stage (Miller et al. 1994, Goncalves et al. 2014). In addition, it has been documented that the presence of PHE

in IVF medium shortens the time required for oocyte penetration and formation of pronuclei (Susko-Parrish et al. 1990).

Table 4 Development of bovine embryos from oocytes fertilized by sperm treated with heparin and PHE mix or heparin and caffeine in standard or drop co-culture

Development of embryos	Sperm treated with			
	Heparin-PHE	Heparin-caffeine	Heparin-PHE	Heparin-caffeine
	Standard co-culture		Drops	
Oocytes fertilized (n)	90	90	85	88
Cleaved (%)	$84.4^{a,b}$	$73.3^{a,c}$	85.9^{b}	60.2^{c}
Blastocysts (%)	$37.7^{a,b}$	25.6^{a}	$47.1^{b,c}$	25.0^{a}

Legend: [(a-c)] Values with different superscripts within the same row are significantly different ($P < 0.05$). Sperm of bull E treated with a) 10 µg/ml heparin and 2 mM penicillamine, 1 mM hypotaurine, 250 µM epinephrine b) 10 µg/ml heparin and 1 mM caffeine, and co-cultured with oocytes both in 500 µl and 50 µl volumes.

CONCLUSIONS

The present study confirmed that the efficiency of *in vitro* embryo development can be influenced by selection of sperm treatment and oocyte-sperm co-culture system. The treatment of bull sperm with heparin supplemented with PHE mix and tight contact between capacitated sperm and matured oocytes in drops for a short time improved the IVF outcome from specific bull compared with standard co-culture.

This study thus contributes to a better understanding of the behaviour patterns of bull sperm during *in vitro* fertilization.

ACKNOWLEDGEMENTS

The study was supported by Grant RO0518 of the Ministry of Agriculture of the Czech Republic.

REFERENCES

Barcelo-Fimbres, M. et al. 2011. *In vitro* fertilization using non-sexed and sexed bovine sperm: sperm concentration, sorter pressure, and bull effects. Reproduction in Domestic Animal, 46(3): 495–502.

Goncalves, F.S. et al. 2014. Heparin and penicillamine-hypotaurine-epinephrine (PHE) solution during bovine *in vitro* fertilization procedures impair the quality of spermatozoa but improve normal oocyte fecundation and early embryonic development. Vitro Cellular & Developmental Biology - Animal, 50(1): 39–47.

Knitlova, D. et al. 2017. Supplementation of L-carnitine during *in vitro* maturation improves embryo development from less competent bovine oocytes. Theriogenology, 102: 16–22.

Leibfried, M.L., Bavister, B.D. 1982. Effects of epinephrine and hypotaurine on in-vitro fertilization in the golden hamster. Journal of Reproduction and Fertility, 66(1): 87–93.

Lu, K.H., Seidel, G.E. 2004. Effects of heparin and sperm concentration on cleavage and blastocyst development rates of bovine oocytes inseminated with flow cytometrically-sorted sperm. Theriogenology, 62(5): 819–830.

Machatkova, M. et al. 2008. *In vitro* production of embryos from high performance cows and the development of frozen-thawed embryos after transfer: a field study. Veterinarni medicina, 53(7): 358–364.

Meizel, S. 1985. Molecules that initiate or help stimulate the acrosome reaction by their interaction with the mammalian sperm surface. American Journal of Anatomy, 174(3): 285–302.

Miller, G.F. et al. 1994. Addition of penicillamine, hypotaurine and epinephrine (PHE) or bovine oviductal epithelial cells (BOEC) alone or in combination to bovine *in vitro* fertilization medium increases the subsequent embryo cleavage rate. Theriogenology, 41(3): 689–696.

Parrish, J.J. 2014. Bovine *in vitro* fertilization: *in vitro* oocyte maturation and sperm capacitation with heparin. Theriogenology, 81(1): 67–73.

Reckova, Z. et al. 2008. Evaluation of chromantin integrity of motile bovine spermatozoa capacitated *in vitro*. Zygote, 16(3): 195–202.

Rizos, D. et al. 2002. Consequences of bovine oocyte maturation, fertilization or early embryo development *in vitro* versus *in vivo*: implications for blastocyst yield and blastocyst quality. Molecular Reproduction and Development, 61(2): 234–248.

Susko-Parrish, J.L. et al. 1990. The effect of penicillamine, hypotaurine, epinephrine and sodium metabisulfite, on bovine *in vitro* fertilization. Theriogenology, 33: 333.

Xu, J. et al. 2009. Optimizing IVF with sexed sperm in cattle. Theriogenology, 71(1): 39–47.

The use of molecular-genetic methods and bioinformatics tools to identify the representatives of the order Coleoptera occurring on decaying cadavers

Nicole Elizabeth Wrzecionkova, Jan Wijacki, Ales Knoll, Tamara Mifkova
Department of Morphology, Physiology and Animal Genetics
Mendel University in Brno
Zemedelska 1, 613 00 Brno
CZECH REPUBLIC

xzurkova@mendelu.cz

Abstract: The process of gradual settlement of the dead body by necrophagous insects plays an important role in forensic practice, especially when determining the time of death. This work deals with the decomposition of dead body of vertebrates by forensically important representatives from the order of Coleoptera in the Czech Republic. Experimental objects for our purposes were domestic pig and chicken. The research was realized from November 2017 to March 2019. During the study samples of larvae and adults were collected from the dead bodies and subsequently identified molecular-genetic methods. For research purposes was necessary to isolate the genomic DNA, amplify the fragment of cytochrome c oxidase I (*COI*) gene by the PCR method and sequencing this fragment DNA. The BLAST and BOLD databases showed the same outputs and based on the results the individuals were classified into individual families of the Coleoptera order.

Key Words: Coleoptera, forensic entomology, decomposition, dead body, DNA barcoding

INTRODUCTION

Forensic entomology is a discipline that uses knowledge of the development and succession of necrophagous insects on dead bodies (Stefan and Hladik 2012, Olesakova et al. 2018) and other invertebrates in the investigation of facts and verification of evidence in criminal and civil law. Through the identification of insects flying or finding on the decaying body (Hirt and Vorel 2016), it is possible to determine the time of death, the so-called postmortem interval (PMI) (Straus et al. 2017, Olesakova et al. 2018). The age of the larvae that hatched on the dead body indicates the minimum time since death (Erzinçlioglu 2008). The period in which insects occur on a dead body is typical of certain beetles or flies. The reason is the decomposition products that attract this insect (Hirt and Vorel 2016). Through new technologies, individuals can be accurately identified on the basis of DNA methods (Beran 2012).

DNA barcoding is a method that allows a large number of samples and species to be characterized with high accuracy in a short time (Cancian de Araujo et al. 2019). It is based on taxonomically specific differences in the nucleotide sequence (barcode) of the standard gene region. DNA barcoding requires only a small amount of a sample from an organism to identify, and therefore it is particularly useful for identifying small organisms, such as insects (Naaum et al. 2013). It allows to reliably distinguish visually very similar species, which were previously often confused on the basis of morphological features (Zaveska Drapkova 2012, Naaum et al. 2013) and identifies species in which morphological features important for morphological identification of species have been lost or removed (Naaum et al. 2013).

Beetles represent the second important group of insects colonizing dead bodies. However, these are less accurate indicators for determining the onset of colonization than flies (Straus et al. 2017). The reason is their later onset of the corpse. Beetles respond only to the release of putrefactive gases (Stefan and Hladik 2012, Straus et al. 2017), caused by bacterial decomposition. Representatives of beetles, unlike flies, do not lay eggs on the carcass immediately upon arrival, but only feed on it, which prolongs the time interval between death and laying, i.e. the beginning of developmental cycles. Despite the knowledge of succession waves, the exact calculation of the colonization time of beetles

is possible only thanks to the evaluation of the developmental cycles of individual representatives of this order (Straus et al. 2017).

The primary goal of this work was to identify forensically important species of the order Coleoptera occurring in the Czech Republic using molecular-genetic laboratory methods and their subsequent evaluation using bioinformatics tools BOLD and BLAST.

MATERIAL AND METHOD

Hypothesis 1: The size of cadavers occurring in one locality will not affect the species representation of the genus Coleoptera involved in the decomposition of bodies.

Hypothesis 2: The size of cadavers occurring in two geographically similar localities will not affect the species representation of the genus Coleoptera involved in the decomposition of bodies.

Samples and experiment locations

According to the original hypothesis, the second experimental body was to be located in the same locality and possible changes in the composition of the found representatives of the order Coleoptera were to be monitored, which was not possible within the logistics a year later. Both experimental bodies were left to decompose in the gardens near the houses. The first carcass was laid in the autumn of 2017 in the locality of Tišnov, which lies 270 metres above sea level and it was a medium-sized pig body (approx. 80 kg). The second cadaver (chicken) weighing 2 kg was laid a year later in the locality of Hodonín, which lies at an altitude of 281 metres above sea level.

The cadavers were monitored continuously, without the use of entomological traps. Collection was performed using entomological tweezers and closable tubes. As soon as possible, the insects were killed by frost. Samples treated in this way can be stored for a long time without losing significant value. However, the disadvantage is the worsened determination of eggs, larvae and pupae of individual representatives (Straus et al. 2017). The NucleoSpin Tissue genomic DNA kit from Macherey-Nagel GmbH & Co. (Düren, Germany) was used to isolate the DNA.

DNA amplification

To amplify the DNA segment were used ABI Verity 96 Well and GeneAmp 9700 automated cyclers from Life Technologies Corp., Carlsbad, USA with the following protocol: initial denaturation at 95 °C for 3 min; 40 cycles of denaturation at 95 °C for 30 s, annealing at 50 °C for 40 s and elongation at 72 °C for 100 s; final elongation at 72 °C for 5 min and holding at 4 °C.

DNA Sequencing and Data Analysis

The PCR products were purified according to the manufacturer's instructions MinElute PCR Purification Kit from Qiagen GmbH (Hilden, Germany). Then, according to the manufacturer's protocol, the sequencing reaction mixture was prepared using BigDye Terminator Cycle Sequencing Kit v3.1 from Life Technologies Corp. (Carlsbad, USA) with a final volume of 10 µl. The template was amplified using a GeneAmp®PCR System 9700 thermal cycler from Life Technologies (Carlsbad, USA), where the temperature cycle profile was 96 °C for 1 minute, 25 cycles of 96 °C for 10 s, 45 °C for 5 s, 60 °C for 4 minutes. The resulting sequencing mixture was purified by BigDye® XTerminatorTM Purification Kit from Life Technologies, Carlsbad, USA after amplification according to the manufacturer's protocol. Individual samples were analyzed by capillary electrophoresis and electrophoresis using ABI PRISM 3500 genetic analyzer from Applied Biosystems, Foster City, California, USA. All obtained data were processed using Chromas software (Technelysium Pty Ltd, South Brisbane, Australia). Species were identified using the bioinformatics databases BLAST and BOLD.

RESULTS AND DISCUSSION

Molecular-genetic identification of necrobionic beetles

Sequencing results were identified using BLAST and BOLD tools. these bioinformatics tools were used for comparison to evaluate the results of molecular-genetic identification of individuals.

Table 1 Comparison of the presence of identified species in domestic pig (Sus scrofa f. domestica) and in domestic chicken (Gallus gallus f. domestica)

Taxonomic name	*Sus scrofa*	*Gallus gallus*
Amara ovata Fabricius, 1792	yes	no
Brachinus crepitans Linné, 1758	yes	no
Harpalus distinguendus Duftschmid, 1812	yes	no
Harpalus rufipes De Geer, 1774	yes	no
Necrodes littoralis Linné, 1758	yes	yes
Nicrophorus fossor Erichson, 1837	yes	yes
Nicrophorus interruptus Stephens, 1830	yes	yes
Onthophagus coenobita Herbst, 1783	no	yes
Onthophagus ovatus Linné, 1767	yes	no
Poecilus cupreus Linné, 1758	yes	no
Pterostichus melanarius Illiger, 1798	yes	no
Saprinus planiusculus Motschulsky, 1849	no	yes
Saprinus semistriatus L.G. Scriba, 1790	no	yes
Thanatophilus rugosus Linné, 1758	yes	yes

A total of 14 species of the order Coleoptera were identified. Only 4 species occurred on both experimental cadavers - *Thanatophilus rugosus, Nicrophorus interruptus, Nicrophorus fossor, Necrodes littoralis*. The pig cadaver located at the Tišnov locality can be considered a more diverse stand. Although this result contradicts the original assumption of the more abundant diversity of this genus, all individuals found are among the species commonly found on the dead body (Byrd and Castner 2001).

The results confirmed the most common occurrence of forensically important species of the order Coleoptera in the family *Silphidae*. Other identified individuals, which may also occur near the dead body, included members from the family *Scarabaeidae* and *Histeridae*. Representatives of the family *Carabidae*, occurring among the samples, were taken as adults from the immediate vicinity of the dead body. Representatives of this family are characterized mainly by a predatory way of life, where they hunt various insects and their larvae, earthworms, mollusks, etc. However, there are also species that occur on corpses, where they feed on larvae and puparia of flies and eat the dead body only exceptionally. In our case, they are not a necrophagous individual. Thus, it is possible that these adults were attracted by the amount of necrophagous fauna found on the decomposing body and their capture was accidental. Of the expected forensically important family, *Staphylinidae, Dermestidae, Trogidae* and *Leiodidae* were not present among the samples taken. The time and weather conditions in which the experiments were based did not have to suit these representatives. Another factor was probably the small amount of samples taken from the experimental site.

CONCLUSION

The thesis dealt with entomological material obtained from established experiments in two localities of the South Moravian Region. The molecular-genetic method has proven to be very reliable, enabling accurate and reliable identification of necrophagous representatives. Two databases, BLAST and BOLD, were used to compare and check the identification. The outputs of these bioinformatics tools showed the same determination of most individuals.

Assessing of the first hypothesis in this research is not possible due to the impossibility of repeating the experiment at the same location and logistical complications. The second hypothesis was therefore established only after a change in the experimental conditions. The second hypothesis aimed to find out whether the composition of the Coleoptera order will change when the two selected localities are within the same region and only the size of the experimental cadaver will differ. From

the findings, it is clear, that this hypothesis was wrong. The body of the pig is more diverse in species, where 11 species of all found species were found. 7 species were found in the second locality. Of the 14 identified species of the order Coleptera, only in 4 cases did the found species match. In other cases, this agreement did not occur. From the point of view of sample processing using molecular biology, the work is processed adequately and if it were only a methodological study, it was completely sufficient. However, the work as a unit has methodological shortcomings that must be eliminated in future research.

ACKNOWLEDGEMENTS

I am especially grateful for the IGA FA project IP-2018/077, from which this research was funded. This work was created within the research infrastructure CEITEC – Central European Institute of Technology supported by the CEITEC 2020 project (LQ1601) with the financial support of the Ministry of Education, Youth and Sports of the Czech Republic under the National Sustainability Program (NPU II).

REFERENCES

Beran, M. 2012. Soudnělékařská identifikace. 1st ed., Praha: Karolinum.

Byrd, J.H., Castner, J. L. 2001. Forensic entomology: The utility of arthropods in legal investigations. Boca Raton: CRC Press.

Cancian de Araujo, B. et al. 2019. DNA barcoding data release for Coleoptera from the Gunung Halimun canopy fogging workpackage of the Indonesian Biodiversity Information System (IndoBioSys) project. Biodiversity Data Journal, 7: e31432.

Erzinçlioglu, Z. 2008. Forenzní metody vyšetřování. 1st ed., Praha: Fortuna Libri.

Hirt, M., Vorel, F. 2016. Soudní lékařství 1. díl. 1st ed., Praha: Grada Publishing.

Naaum, A.M. et al. 2013. DNA Barcoding as an Educational Tool: Case Studies in Insect Biodiversity and Seafood Identification. Teaching and Learning Innovations Journal, 16.

Olesakova, T. et al. 2018. Zvláštní případy užití forenzní entomologie v kriminalistické praxi. In Proceedings of the conference – Forensica. Olomouc, Czech Republic, 28–30 May. Brno: Tribut EU, pp. 31–32.

Stefan, J., Hladik, J. 2012. Soudní lékařství a jeho moderní trendy. 1st ed., Praha: Grada.

Straus, J. et al. 2017. Teorie, metody a metodologie kriminalistiky. Plzeň: Vydavatelství a nakladatelství Aleš Čeněk.

Zaveska Drapkova, L. 2012. Čárový kód života. Vesmír, 91(2): 96–99.

Novel method for morphometry analysis of bursa of Fabricius

Vladimir Zmrhal[1], Marketa Skoupa[2], Andrea Svoradova[1], Petr Slama[1], Martina Lichovnikova[2]
[1]Department of Animal Morphology, Physiology and Genetics
[2]Department of Animal Breeding
Mendel University in Brno
Zemedelska 1, 613 00 Brno
CZECH REPUBLIC

vladimir.zmrhal@mendelu.cz

Abstract: Morphological observation of bursa of Fabricius (BF) represent a valuable tool in evaluation of stress causative agents on poultry. The main goal of this study was to compare two methods for morphometry analysis of BF: standard hematoxylin/eosin (HE/EO) staining and immunofluorescence staining based on anti-basal cell cytokeratin antibody with DAPI background staining (CYT/DAPI). Chickens were divided into two groups (18 for HE/EO and 18 for CYT/DAPI). BF from 6 chickens from each group were taken in 7, 14 and 22 days of age. In every chicken, 40 randomly selected follicles were evaluated. In total, comparison of data from all days between groups didn´t show significant differences. However, age have a significant impact. In 14 days of age, size of the follicle and cortex were significantly higher in CYT/DAPI group ($P<0.05$). Additionally, in 22 days old chickens size of the medulla was significantly higher in HE/EO group. Cortex/medulla ratio at age 7 days was significantly higher in HE/EO ($P<0.05$), but in older chickens were significantly higher ($P<0.05$) in CYT/DAPI group. Immunofluorescence staining seems to be more exact method and should be used, if precise localization of cortico-medullary border is necessary. On the other hand, HE/EO staining is a better choice for quantitative analyses of higher number of samples.

Key Words: bursa of Fabricius, morphometry, broiler chicken, follicle, cytokeratin

INTRODUCTION

Bursa of Fabricius (BF) is a unique primary lymphoid organ in avian species which provides environment for development and proliferation of B cells. Due to indispensable role in antibody immune response, BF is a target organ for research in avian immunology and histology (Olah and Nagy 2013).

In birds, BF is connected with proctodeum of cloaca via bursal duct, so immune response is driven by antigens flowing from the intestine. Surface of the BF lumen is predominantly covered by interfollicular epithelium and only about 10% comprise follicle-associated epithelium FAE (Olah and Glick 1978). Cells of FAE samples antigens and transport them by pinocytosis to medulla of follicle. Antigenic particles are recognized by bursal secretory dendritic cells and through major histocompatibility complex II are presented to differentiating B cells (Nagy et al. 2016). Cell population of medulla comprise predominantly immature B cells, bursal secretory dendritic cells, and numbers of T cells and macrophages are negligible (Olah and Glick 1992). Before the hatch, basement membrane creates outer layer of the follicle. Around the time of hatching, cells migrate through the basement membrane to form a cortical region. Cortico-medullary border (CMB) is composed by cortico-medullary arch forming cells and blood capillaries, that are necessary for migration of B cells to the bloodstream (Olah et al. 2014). B cells after stimulation migrate through CMB and basal lamina and proliferate in cortex and subsequently leave out of the BF by blood capillaries (Chrzastek et al. 2011). Mesenchymal reticular cells create a skeleton of the cortex with B cells arranged in layers and some macrophages, lymphoblasts and plasma cells (Olah et al. 2014).

The follicle as a basic morphological and functional unit of BF have a fundamental role in acquiring a humoral immunity and peripheral lymphoid system development in young chickens. Normal development of BF follicles is a necessary for appropriate humoral immune response and defence capacity against pathogens (Merlot et al. 2008). It has been described negative effects of stressors and toxins on microarchitecture of bursal follicles, so the morphometry analysis of BF can

be a sensitive method to evaluate the effects of environment on chicken health (Sur and Celik 2003, Oznurlu et al. 2010). Until now, for morphometry analysis of bursal follicles was used only standard HE/EO staining (Korzeniowska et al. 2019, Madej et al. 2015, Muniz et al. 2006, Sultana et al. 2020) or Crossman's trichrome (Sur and Celik 2003, Oznurlu et al. 2010), but these methods are not accurate because CMB is not clearly visible. For this purpose, we propose a new method for morphometry analysis of BF based on immunofluorescence staining with anti-basal cell cytokeratin antibody (CYT) specifically binds to cortico-medullary arch forming cells with background staining with 4',6-diamidino-2-phenylindole dihydrochloride (DAPI). The main goal of this article is to compare new staining method of measurement of bursal follicles with standard HE/EO staining.

MATERIAL AND METHODS

Animals

In experiment were used 36 cockerels of Cobb 500 broiler chickens from same breeder flock. Chickens were kept in littered floor boxes under controlled environmental conditions according to guidelines for the hybrid. Feed was provided in tube feeders and water by nipple drinkers, both *ad libitum*. Starter was fed from 1 to 10 days of age and grower from 10 to 22 days of age. Due to BF acquirement, 12 chickens were sacrificed by cervical dislocation in age 7, 14, and 22 days (6 for HE/EO and 6 for CYT/DAPI staining). This relatively low number of animals was due to the fact that it was a preliminary experiment.

Sample processing and evaluation

The follicle and medulla areas of the BF were measured in transversal sections of 40 individual follicles from each chicken for both HE/EO and CYT/DAPI staining. All evaluated parameters were measured by same person. From obtained results, cortical area and cortex/medulla ratio were calculated.

Histological procedure and morphometry

BF were collected and fixed in 10% formaldehyde and processed in paraffin. Sections (4–5 μm thick) of each tissue were sliced from each block, mounted on glass slides, and stained with HE/EO. Morphometric analysis was performed with original magnification 100× on light microscope Olympus BX51 with PROMICAM 3-5CP digital camera (5Mpx SONY PREGIUS CMOUS USB 3.0). The follicle and medulla areas were measured by software Quick PHOTO MICRO 3.2 (PROMICRA).

Immunofluorescence staining

Samples of BF were fixed in 10% formaldehyde for 1 h. Then, the samples were also processed in paraffin and cut into 4 μm thick sections air dried and stained. Before staining, standard antigen retrieval protocol with citrate buffer (pH 6) was used, then the sections were incubated with 2.5% goat serum as a blocking buffer. For CMB localization was used Anti-Basal Cell Cytokeratin primary Antibody (Merck) and then for visualization was used Goat anti-Mouse IgG_1 Cross-Adsorbed Secondary Antibody, Alexa Fluor 594 (Invitrogen). Cell´s nucleus for visualization of follicles were stained with DAPI (Thermofisher). The slides were mounted with aqua polymount (PolySciences) and observed with fluorescent microscope Olympus BX51 with PROMICAM 3-5CP digital camera (5Mpx SONY PREGIUS CMOUS USB 3.0). Photos (magnification 100×) with CYT and DAPI staining were joint together by module Fluo+ and subsequently measured by Quick PHOTO MICRO 3.2 (PROMICRA).

Statistical analyses

The evaluated parameters in individual groups were characterized by the mean and the standard error of the mean. The Tukey-HSD test was used for subsequent testing of the significance of differences between means. Statistical evaluation was performed using Unistat 5.1 software (Unistat Ltd, UK).

RESULTS

In total, the mean values of follicle, medulla, cortex size and C/M ratio from all days were almost the same in both groups. However, several statistically significant differences were observed between groups in individual days of age (Table 1). Until 7 days of age, size of the follicle, cortex and medulla were not affected by staining. On the other hand, in 14 days of age, follicle and cortex size were

statistically significant higher (P<0.05) in CYT/DAPI group. On the contrary, size of the cortex and whole follicle were almost the same in both groups and medulla size was significantly higher in HE/EO group (P<0.05) in 22 days of age. In youngest chickens, cortex/medulla ratio was significantly higher (P<0.05) in HE/EO group, vice versa in older chickens were higher in CYT/DAPI group (P<0.05).

Figure 1 Cortico-medullary border in Cytokeratin/DAPI and Hematoxylin/Eosin stained BF

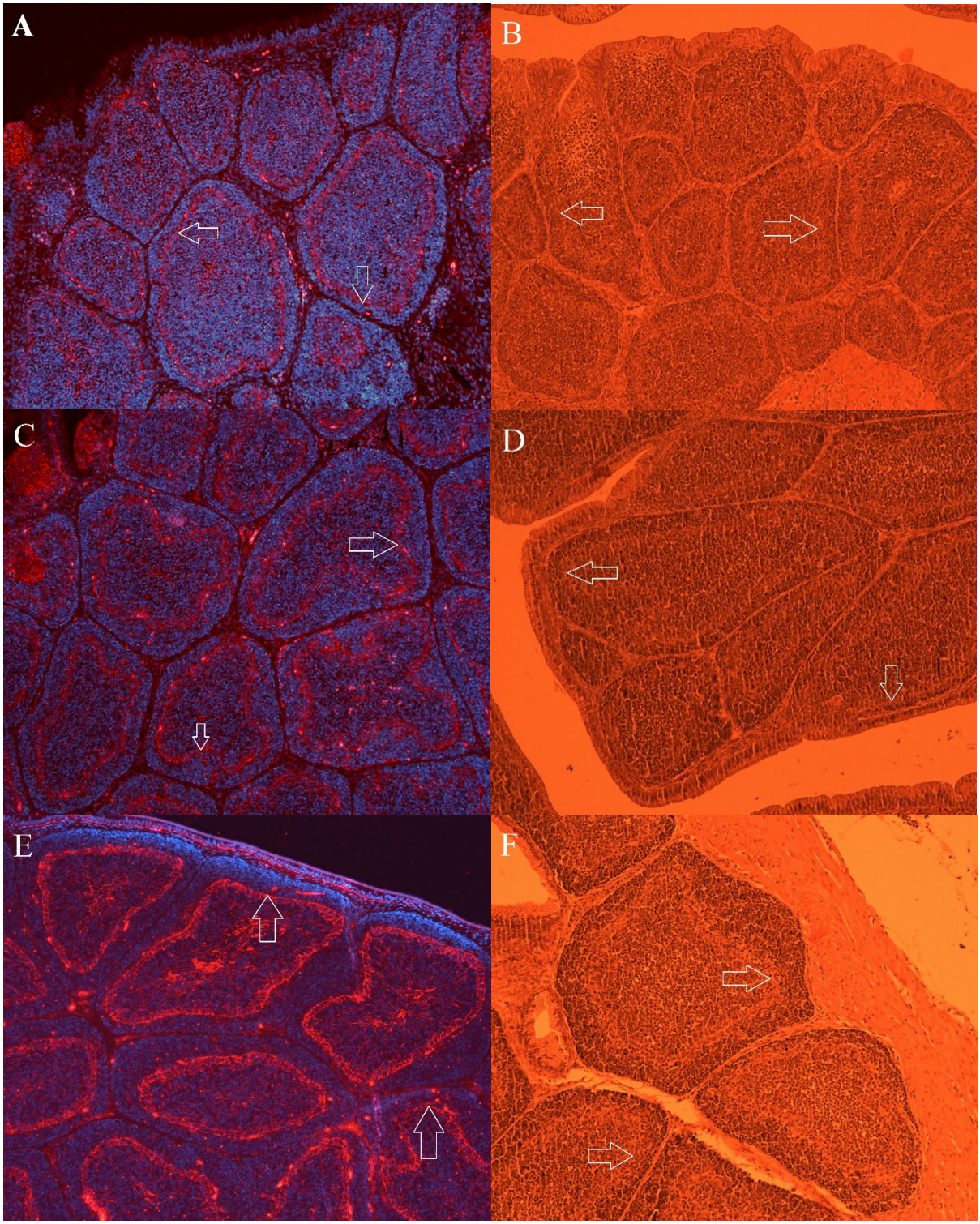

Legend: CMB marked by arrows, A, B: CYT/DAPI and HE/EO stained sections from 7 days old chickens, respectively; C, D: CYT/DAPI and HE/EO stained sections from 14 days old chickens, respectively; E, F: CYT/DAPI and HE/EO stained sections from 22 days old chickens, respectively

Table 1 The effect of staining on medulla, cortex and follicle size depending on age and in total

Parameter	Follicle ± SE	Medulla ± SE	Cortex ± SE	C/M ± SE
Age (days)		7		
HE/EO (μm^2)	36030^a ± 1277	18583^a ± 791	17447^a ± 566	1.014^a ± 0.027
CYT/DAPI (μm^2)	35872^a ± 1179	19904^a ± 771	15968^a ± 541	0.88^b ± 0.031
Age (days)		14		
HE/EO (μm^2)	65784^a ± 2585	36027^a ± 1715	29757^a ± 1035	0.932^a ± 0.031
CYT/DAPI (μm^2)	78333^b ± 2996	40465^a ± 1903	37868^b ± 1325	1.032^b ± 0.031
Age (days)		22		
HE/EO (μm^2)	125403^a ± 4070	67127^a ± 2694	58276^a ± 1703	0.974^a ± 0.034
CYT/DAPI (μm^2)	114442^a ± 4352	56684^b ± 2815	57759^a ± 2059	1.184^b ± 0.974
In total*				
HE/EO (μm^2)	75739^a ± 2568	40579^a ± 1522	35160^a ± 1135	0.973^a ± 0.018
CYT/DAPI (μm^2)	76216^a ± 2472	39018^a ± 1404	37198^a ± 1227	1.032^a ± 0.025

*Legend: HE/EO: hematoxylin/eosin; CYT: cytokeratin; *: means from all days and both groups; a, b: statistically significant differences (P<0.05)*

DISCUSSION

Morphometry analysis of lymphoid organs with combination of histopathological findings are the standard methods for evaluation of the stressors on poultry physiology. For this purpose, we compared standard HE/EO staining with new method based on immunofluorescence staining with cytokeratin primary antibody and DAPI. Immunofluorescence staining for morphometry analysis of BF have never been used, so it is not possible to compare this method with other studies. Main advantage of this immunofluorescence staining is an accurate localization of CMB to find border between cortex and medulla (Figure 1). Localization of CMB is a biggest disadvantage of standard HE/EO staining, where CMB is marked only lighter area around the cortico-medullary arch forming cells (Muniz et al. 2006).

After hatching, development of cortical region in follicles terminate the development of microarchitecture of BF (Nagy and Olah 2010). C/M ratio is an important parameter for development of BF and evaluation of distribution of B cells after hatch (Chrzastek et al. 2011). Thinner cortex means delay of B cells migration from medulla to cortex. This delay could be caused by lower stimulation of B cells by antigens. Conversely, widened cortex area could be a marker of higher B cells stimulation (Madej et al. 2015). Hence, C/M ratio could be a valuable complementary factor with distribution of B cells and antibody response to pathogens.

Especially in young birds, cortex is very thin and with HE/EO staining is CMB poorly visible which cause an inaccurate result. Therefore, we observed contradictory values of C/M ratio in 7 days old chickens with compared to older chickens. Cytokeratin expression in reticular epithelial cells increasing with age, therefore, in youngest chick's cytokeratin staining is weaker than in older chickens, but CMB in 7 days old chicks is still clearly visible (Sanchez-Refusta et al. 1996). In older chickens, some differences between groups are probably caused also by inaccurate localization of CMB in HE/EO staining. We believe that the significant differences between some values when taking at 14 and 22 days are caused by different techniques of sample visualization. The most important value is the C/M ratio which is statistically significantly different at all time points (7, 14, and 22 days) when comparing HE/EO and CYT/DAPI staining.

Our results indicate that staining method can influence the results, but further experiments are needed to confirm this hypothesis and to exclude the influence of the eventual individuality of the investigated animals. However, due to the number of follicles examined in each animal, an insignificant effect of the individual can be expected.

CONCLUSION

Based on result of study we recommend CYTO/DAPI staining, if precise results should be obtained, especially in young chicks until 14 days of age. HE/EO is a cheaper, easier and faster method so it is usable for evaluation of higher number of samples.

ACKNOWLEDGEMENTS
The research was financially supported by the Mendel University in Brno, grant number AF-IGA2020-IP040.

REFERENCES

Chrzastek, K. et al. 2011. The influence of antibiotics on B-cell number, percentage, and distribution in the bursa of Fabricius of newly hatched chicks. Poultry Science, 90(12): 2723–2729.

Korzeniowska, M. et al. 2019. Influence of Selenium on the Morphology of Immune System Organs in Healthy Broilers. Acta Veterinaria-Beograd, 69(4): 379–390.

Madej, J.P. et al. 2015. Effect of in ovo-delivered prebiotics and synbiotics on lymphoid-organs' morphology in chickens. Poultry Science, 94(6): 1209–1219.

Merlot, E. et al. 2008. Prenatal stress, fetal imprinting and immunity. Brain Behavior Immunity, 22: 42–51.

Muniz, E. et al. 2006. Histomorphology of bursa of Fabricius: Effects of stock densities on commercial broilers. Brazilian Journal of Poultry Science, 8(4): 217–220.

Nagy, N. et al. 2016. Avian dendritic cells: Phenotype and ontogeny in lymphoid organs. Developmental and Comparative Immunology, 58: 47–59.

Nagy, N., Olah, I. 2010. Experimental evidence for the ectodermal origin of the epithelial anlage of the chicken bursa of Fabricius. Development, 137: 3019–3023.

Olah, I., Glick, B. 1992. Follicle-associated epithelium and medullary epithelial tissue of the bursa of Fabricius are two different compartments. The Anatomical Record, 233(4): 577–587.

Olah, I. et al. 2014. Structure of the Avian Lymphoid System. In Avian Immunology. Elsevier, pp. 11–44.

Olah, I., Nagy, N. 2013. Retrospection to discovery of bursal function and recognition of avian dendritic cells; past and present. Developmental and Comparative Immunology, 41(3): 310–315.

Olah, I., Glick, B. 1978. The number and size of the follicular epithelium (FE) and follicles in the bursa of Fabricius. Poultry Science, 57: 1445–1450.

Oznurlu, Y. et al. 2010. Histochemical and histological evaluations of the effects of high incubation temperature on embryonic development of thymus and bursa of Fabricius in broiler chickens. British Poultry Science, 51(1): 43–51.

Sanchez-Refusta, F. et al. 1996. Age-related changes in the medullary reticular epithelial cells of the pigeon bursa of Fabricius. Anatomical Record, 246: 473–480.

Sultana, N. et al. 2020. Effects of Dexamethasone on the Morphometry and Biometry of Immune Organs of Broiler Chicken. International Journal of Morphology, 38(4): 1032–1038.

Sur, E., Celik, I. 2003. Effects of aflatoxin B 1 on the development of the bursa of Fabricius and blood lymphocyte acid phosphatase of the chicken. British Poultry Science, 44(4): 558–566.

TECHNIQUES AND TECHNOLOGY

Influence of DMLS method topology on mechanical properties of alloy AlSi10Mg

Jana Dvorakova[1], Karel Dvorak[2], Michal Cerny[3]
[1,3]Department of Technology and Automobile Transport
Mendel University in Brno
Zemedelska 1, 613 00 Brno
[2]Department of Technical Studies
College of Polytechnics Jihlava
Tolsteho 16, 586 01 Jihlava
CZECH REPUBLIC

xdvora15@mendelu.cz

Abstract: The application use of progressive methods of additive technologies for the production of functional machine parts requires verification of the mechanical characteristics of the material used. The text presents the results of research into the mechanical characteristics of the AlSi10Mg material for components made by 3D printing, using the DMLS method, representing the sintering of layers of powder material by a laser beam. The aim of the research is to verify mechanical characteristics in tension and torsion to determine values of allowable stress for components stressed by combinations of these loads with the emphasize put on the printing topology. The goal of the research is to compare the printing topology for the specific stress and to achieve a basis for printing topology optimization of real complex shapes. The difference in mechanical properties compared to the same components produced by machining methods from rolled semi-finished products is assumed. The advantage of 3D printing is fast preparation of production, when to produce a part it is necessary to have a properly prepared 3D digital CAD model. At the same time, it is possible to assume the influence of the production topology on the mechanical properties, consisting in the orientation of printing layers with respect to loading force. The obtained results are used in simulation tools to support calculations during design and in addition to the shape and dimensional characteristics of the part determine the appropriate orientation of the product during 3D printing.

Key Words: 3D model, computer aided design, computer aided engineering, direct metal laser sintering, topology optimization

INTRODUCTION

Additive technologies represent a wide portfolio of production methods, consisting in the application or transformation of a material into a solid unit with appropriate shape and dimensional characteristics (Dvořák and Zárybnická 2018, Takagishi and Umezu 2017). A wide portfolio of components in mechanical assemblies is made of metal-based materials. For specific components with reasonable strength requirements, it is advantageous to use aluminum alloys. The available additive method DMLS – Direct Metal Laser Sintering is the sintering of metal powder by a laser beam. The result is a layered compact structure with the required shape and dimensional characteristics. The advantage of additive methods is a rapid preparation of production technology using a 3D CAD model. The use of CAD - Computer Aided Design at the level of 3D models of parts and assemblies is the current industry development standard. Most of the proposed parts have a 3D model that can be used to prepare 3D printing (Camba et al. 2016), which results in a final part or a semi-finished product, including most shaped construction elements. For prototype production, where the main goal is the functional verification of the finished product, it is a time- and economically advantageous method. For serial or mass deployment, it is a method with low productivity with current technological possibilities. The optimal use of this method can be in small series production after cost evaluation in comparison with one of the classic production methods, consisting of machining, forming or casting. In order to achieve higher accuracy of selected structural elements, machining methods can be included in the subsequent postprocessing. Functional applications of machinery assemblies require the use

of components that are stressed by combinations of tension, compression, bending, and torsion, representing normal and tangential stresses due to internal forces according to the shape characteristics of the components. In most cases, these are combinations of these stresses. The material structure of components produced by the DMLS method is layered. The influence of the orientation of the layers on the strength of the material due to the stated load components can be assumed. The presented text presents the results of research into the mechanical characteristics of 3D printing material AlSi10Mg, produced by DMLS. Material testing is performed on test specimens with defined shape and dimensional characteristics. The material is tested for tensile and torsional strength. The aim is to determine the course of normal and tangential stress depending on the deformation under tensile and torsional loads. In addition to the separate limit characteristics, the combined stress limit is also determined. The obtained parameters can be used for the design and dimensioning of components for which production by the DMLS method and application use within assemblies of mechanisms and machinery is assumed. The obtained parameters, especially strength modules, are used in tools for calculations and simulations by the finite element method and used for calculations of deformations of stressed components at the level of digital models of virtual prototypes.

MATERIAL AND METHODS

Material AlSi10Mg

The tested material AlSi10Mg is a widely used aluminum alloy of the usual quality, usable for less stressed machine parts. The advantage is low specific weight and adequate mechanical properties as shown in Table 1. It is particularly advantageous for die casting machine bodies. It is characterized by good corrosion resistance and poorer machinability. Typical applications are, for example, thin-walled components for media transmission and complex design accessories. The DMLS method - Direct Metal Laser Sintering is a method of metal processing in which the powder material is sintered by a laser beam and a compact solid structure of the desired shape and dimensions is created (Chua 2010, Snyder et al. 2014). The signification AlSi10Mg describing the chemical composition of the alloy is used for both, the casting alloy and the metal powder used for DMLS, where the EN 1706:1998 signification is used only for casting alloy, therefore the material signification AlSi10Mg is further applied in this article to compare mechanical properties of the same material prepared by two different ways.

Table 1 Declared mechanical properties of AlSi10Mg (Stena 2020, EN 1676, EN 1706, Reinshaw 2020)

Parameter	Value	
	Casting material	DMLS printing material
Density	2.65 g/cm^3	2.68 g/cm^3
Tensile strength horizontal direction	240 MPa	442 MPa
Tensile strength vertical direction	240 MPa	417 MPa
Yield strength horizontal direction	200 MPa	264 MPa
Yield strength vertical direction	200 MPa	206 MPa
Elongation at Break horizontal direction	2%	9%
Elongation at Break vertical direction	2%	6%
Modulus of elasticity horizontal direction	70 GPa	71 GPa
Modulus of elasticity vertical direction	70 GPa	68 GPa

DMLS printing technology and parameters

The method consists in sintering the metal powder with a laser beam in layers. The layered structure presupposes the emergence of directionally different mechanical characteristics with respect to the orientation of the printing layers. Orientation is considered with respect to the coordinate system of the machine during production, for example, the horizontal orientation represents a horizontally placed bar during manufacture. The printing layers are horizontal with the axis of the body. Correct interpretation of the orientation of the printing layers is important, because if it is interpreted with respect

to the coordinate system of body loading, it can be interpreted rotated by 90 °. The orientation with respect to the coordinate system of the production equipment is chosen to correctly determine the production technology in practical applications. The layer thickness is 25 μm and the sintering temperature is 570 °C to 590 °C. The orientation of the product during printing with emphasis on the printing layers is in Fig.1.

Figure 1 Printing layers

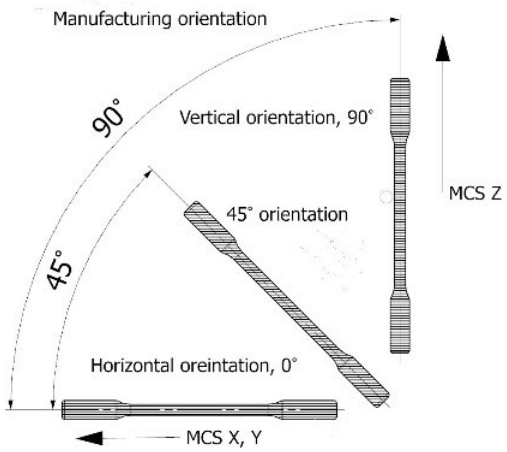

Sample printing is performed on a Renishaw AM400 machine. The use of a specific device and the declaration of the relevant parameters is important in the case of high reliability of the expected parameters. The product parameters of the DMLS technologies, declared in Table 1, are valid for the products implemented on the mentioned equipment. The material sheet lists the tensile characteristics for perpendicular orientations (horizontal and vertical). To refine the topological properties, a 45° orientation is also tested in the presented research. The material sheet does not state the properties in torsion. The torsional stress has a tangential character and the knowledge of the parameters makes it possible to determine the allowable stress for the combined tensile and torsional stresses at the same time. The determination of torsional characteristics is an important addition to the portfolio of parameters of mechanical properties of a specific form of material. In addition to mechanical properties, surface characteristics and achievable accuracy can also be considered for the design of practical applications of 3D printing products. The surface characteristics can be expected to be important for crack initiation in the case of cyclic stress which may be the focus of further research activities. The declared accuracy of 3D printing using the DMLS method is usually declared ISO 2768 c–K. The achievability of the mentioned parameters was verified by a previous measurement (Dvořák et al. 2019).

Tensile stress test

A characteristic mechanical property is tensile strength. The tensile strength is measured by uniaxial longitudinal loading of a standardized test specimen in the form of a rod with a circular cross-section. The parameters of the test sample are shown in the Figure 2.

Figure 2 Test sample parameters

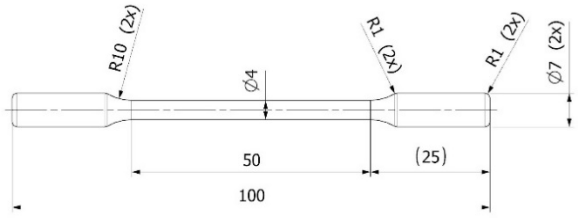

The combined test device Instron Electropuls 10000 is used to measure tensile parameters. The BlueHill Universal test software is used to record, display and evaluate the measured values. The procedures specified in the ISO standard 6892–1:2019 are applied to measure the tensile properties. Determination of the tensile characteristics of metallic materials. It is a standardized test. The force

values are read by a force gauge, the deformation values are read by a video extensometer. 10 samples prepared according to the ISO standard 6892–1:2019 are used for testing within each print orientation.

Torsional stress test

Torsional stress is characteristic of rotating components designed to transmit torque. At the same time, it represents a component of combined stress, often occurring in the mechanisms of machinery. The values of mechanical parameters in torsion are usually not declared in the basic material sheets and are often not even mentioned in research surveys. At the same time, the torsional characteristics cannot be considered secondary, due to the frequency of practical applications of combined stress. The torsional characteristics are determined on bodies in the form of rods with a circular cross-section, identical for measuring tensile properties. The combined Elektropuls 10000 device is used for the measurement and the Wave Matrix software is used for recording and displaying the results. The measured values are further evaluated via MS Excel. 10 samples are used for testing within each print orientation. The clamping of the samples is the same for both categories of tests. Photographs from testing with an example of a broken sample are presented in Figure 3.

Figure 3 Sample testing

RESULTS AND DISCUSSION

Influence of topology on tensile properties

The results of measuring tensile properties for defined print orientations are listed in Table 2 and shown in the graph of Figure 4 based on the average values of measured parameters. From the measured values, in comparison with the declared parameters, the topological dependence of the orientation of the printing layers on the ultimate strength and the yield strength is obvious. The difference is up to 25%, which can be considered significant to take into account in the design phase of a specifically stressed component. At the same time, based on the results obtained, the DMLS material can be considered comparable to the cast material from the yield strength point of view.

Table 2 Tensile properties according to topology in printing

Parameter	Value					
	Horizontal direction		45°		Vertical direction	
	Average	σ	Average	σ	Average	σ
Tensile strength	449 MPa	6.5	447 MPa	2.3	331 MPa	1.7
Yield strength	262 MPa	6.3	254 MPa	4.9	199 MPa	2.4
Elongation at Break	4.6%	0.26	4.7%	0,36	2.4%	0.43
Modulus of elasticity	69 GPa	2.1	67 GPa	2.2	61 GPa	1.65

A significant characteristic of the DMLS material is the lower ductility due to the inhomogeneity of the fibers of the internal material structure. The inclination of the tensile characteristics of the 45° orientation of the layers to the characteristics corresponding to the horizontal orientation can be considered as a significant factor. The course of the transition of characteristics cannot be considered as linear.

Figure 4: Tensile test strength

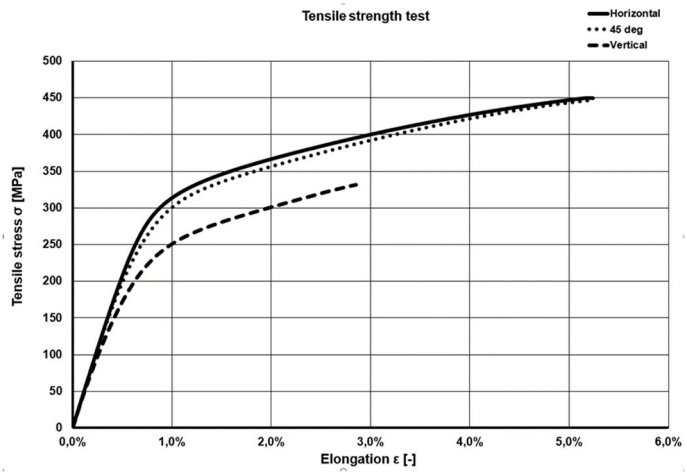

Influence of topology on property in torsion

Results of the measurement of torsional strength characteristics are given in Table 3 and graphically illustrated in Figure 5 based on the average values of measured parameters. Default values are not declared for the specified strength characteristic. The measured results can be considered as starting points for dimensioning components of practical applications in torsion. The difference in the achieved results corresponds similarly to the tensile characteristics of about 25%, which is again an important factor for determining the orientation under combined stress with possible consideration of the dominant load. The best torsional characteristics are evident in the vertical print orientation, ie. rotation of the printing layers relative to each other. The 45° orientation leans towards the horizontal orientation of the print layers, which is important information from the point of view of part design in the context of the respective load.

Table 3 Torsion properties according to topology in printing

Parameter	Value					
	Horizontal direction		45°		Vertical direction	
	Average	σ	Average	σ	Average	σ
Torsion strength	299 MPa	3.3	300 MPa	3.5	325 MPa	1.7
Torsion Yield strength	170 MPa	5	182 MPa	4.7	200 MPa	3.6
Rotation at Break	130°	13.6	126°	6.5	126°	3.4

Figure 5: Torsional strength

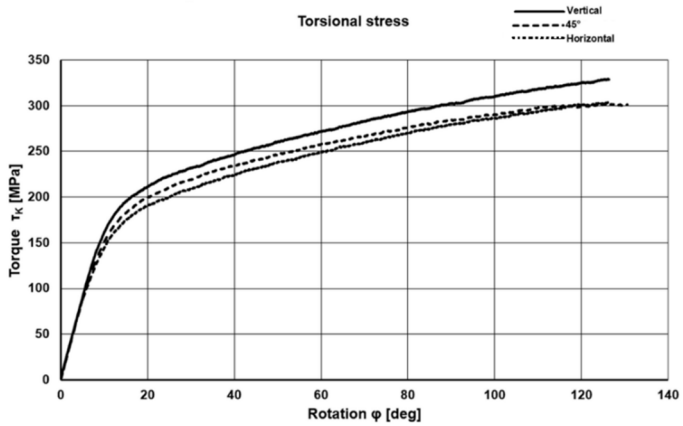

CONCLUSION

The research results show the importance of the topology of DMLS additive technology on the mechanical properties of the product. The values of mechanical properties, measured

by standardized methods, supplement the values tabulated so far for the initial formed or cast equivalent material. Determination of results for three different topologies, representing the orientation of the printing layers. The assumption of differences in mechanical properties for horizontal and vertical orientation has been proven. The influence of topology lying between perpendicular and vertical orientation can be considered an important factor. Practical applications of functional, mechanically stressed components usually involve loads of general directions. By analyzing the loading forces, it is possible to determine the most advantageous orientation of the product during printing. The possibility of general orientation is one of the characteristic attributes of the additive technology. In summary, the general rule is to orient the part in 3D printing in a horizontal position up to 45° for the direction of the predominant tensile stress and in a vertical position up to 45° from the vertical position for the predominant torsional stress vector. In the case of combined stress, it is a matter of finding the optimal printing orientation according to the vectors and the dominance of the respective components of the combined load. When designing a part produced by the DMLS method, it is advantageous to take into account the print orientation with respect to the functional properties of the part. The directions of maximum component stress found, for example, by CAE-FEM simulations, should correspond to the most advantageous directions found on basis of the presented measurement results. The advantage of additive technologies is the possibility of any orientation of the part during production. These findings can be used in topological optimization of the part, for example, by removing excess material in the unstressed structure of the part.

ACKNOWLEDGEMENTS

This research was supported by the College of Polytechnics, Jihlava, Czech Republic, under Grant "Research of parameters for topological optimization of 3D printed components".

REFERENCES

Camba, J.D. et al. 2016. Parametric CAD modeling: An analysis of strategies for design reusability. Computer-Aided Design, 74: 18–31.

Chua, C. 2010. Rapid prototyping: principles and applications. 3rd ed., World Scientific Pub Co, Inc.

Dvořák, K. et al. 2019. Quality Parameters of 3D Print Products by the DMLS Method. Manufacturing Technology, 19(2): 209–215.

Dvořák, K., Zárybnická, L. 2018. Influence of the 3D Model and Technological Parameters on the Mechanical Properties of Fused Deposition Modeling 3D Products. International Journal of Mechanical Engineering and Robotics Research, 7(4): 415–421.

European Committee for Standardization. 1996. Aluminium and aluminium alloys - Alloyet ingots for remelting. EN 1676: 1996. Brussels: European Committee for Standardization.

European Committee for Standardization. 1998. Aluminium and aluminium alloys - Casting - Chemical composition and mechanical properties. EN 1706:1998. Brussels: European Committee for Standardization.

International Organization for Standardization. 1989. General tolerances – Part 1: Tolerances for linear and angular dimensions without individual tolerance indications. ISO 2768–1:1989. Geneva, Switzerland: International Organization for Standardization.

International Organization for Standardization. 2019. Metallic materials – Tensile testing: Part 1: Method of test at room temperature. ISO 6892–1:2019. Geneva, Switzerland: International Organization for Standardization.

Reinshaw. 2020. Data sheets – Additive manufacturing [Online]. Available at: https://www.renishaw.com/media/pdf/en/0c48b4800c17480393f17ceaacb4ecdb.pdf. [2020-01-16].

Snyder, T.J. et al. 2014. 3D Systems' Technology Overview and New Applications in Manufacturing, Engineering, Science, and Education. 3D Printing and Additive Manufacturing [Online], 1(3): 169–176. Available at: http://www.liebertpub.com/doi/10.1089/3dp.2014.1502. [2020-01-18].

Stena Aluminium. 2020. Alloy Specifications EN AC-AlSi10Mg [Online]. Available at: https://www.stenaaluminium.com/aluminium-alloys-and-services/alloy-specifications. [2020-01-18].

Takagishi, K., Umezu, S. 2017. Development of the Improving Process for the 3D Printed Structure. Scientific Reports, 7: 39852. Available at https://www.nature.com/articles/srep39852. [2020-08-18].

Properties of the ecological energy carrier in the tractor's transmission–hydraulic system during the simulation of the operating load in laboratory conditions

Romana Janouskova, Matej Michalides, Peter Kozuch, Patricia Feriancova
Department of Transport and Handling
Slovak University of Agriculture in Nitra
Tr. A. Hlinku 2, 949 76 Nitra
SLOVAKIA

xjanouskova@uniag.sk

Abstract: The scientific paper deals with the assessment of the properties of the ecological energy carrier used in the agricultural tractors transmission–hydraulic system. Evaluated fluid is MOL Farm NH Ultra hydraulic–transmission fluid, tested on laboratory test rig, which can simulate operating conditions. The main results of this work include the evaluation of selected chemical elements of the fluid and the evaluation of the samples taken by ICP spectrometry at specified intervals.

Key Words: transmission-hydraulic fluids, laboratory research, physical properties, operating load simulation

INTRODUCTION

The laboratory research of the qualitative properties of the transmission–hydraulic fluid MOL Farm NH Ultra (Table 2) and its influence on the technical and operation properties of the QHD 17 hydraulic pump, as well as the design of laboratory test equipment of agricultural tractors hydraulic system is devoted to Hujo et al. (2019) and Jablonický et al. (2020). They focus on simulating the operating load of elements and fluids of the hydraulic systems. The basic precondition for the correct function and effective care of hydraulic fluids is a suitably chosen methodology for monitoring impurities in the fluid and a permanent comparison of the degree of contamination of the fluid and its impact on the operation of the equipment (Kopiláková et al. 2017, Kosiba et al. 2016). In order to optimize the testing time, accelerated liquid tests are used. After the test we analyze the physical properties and the impact of the used working fluid on the technical condition of the hydraulic pump with focusing and monitoring changes in friendly characteristics and pressure load of the hydraulic pump (Kučera et al. 2013). We reduce the time required to perform operational measurements through experimental set of pressure measurements with numerical simulation for engines in laboratory conditions (Puškár et al. 2015). For these reasons it is important to ensure the most accurate mechanical production of individual elements of the hydraulic system, where it is important to monitor the accuracy of CNC machine tools using new methods and trends in product development and planning. Equally important is also a multi–radial diagnostics of CNC machines (Košinár and Kuric 2011, Kuric et al. 2016). Also, production of the hydraulic fluids, which are used in hydraulic circuit of agricultural machinery, must be taken into account of environmental impact requirements (Simikic et al. 2014). The values of monitored flows and flow efficiency during measurement are used to create dynamic flow models in hydrostatic transducers. Main reason of this is to protect the environment from contamination (Puškár et al. 2019, Puškár et al. 2015).

MATERIAL AND METHODS

The measuring device was chosen for needs to prepare a simulation of the real operating load of the hydraulic pump and the working fluid during the test, in order to analyse the physical, chemical properties and also the effect of ecological liquid on the technical condition of the hydraulic pump after the tests. The test laboratory hydraulic equipment (Figure 1) makes it possible to carry out tests on the basis of signals recorded during in–service tests, where it is subsequently simulated by means of an electrohydraulic proportional valve (Hujo et al. 2019).

Figure 1 Hydraulic circuit diagram for testing hydrostatic transducers and hydraulic fluids (Hujo et al. 2019)

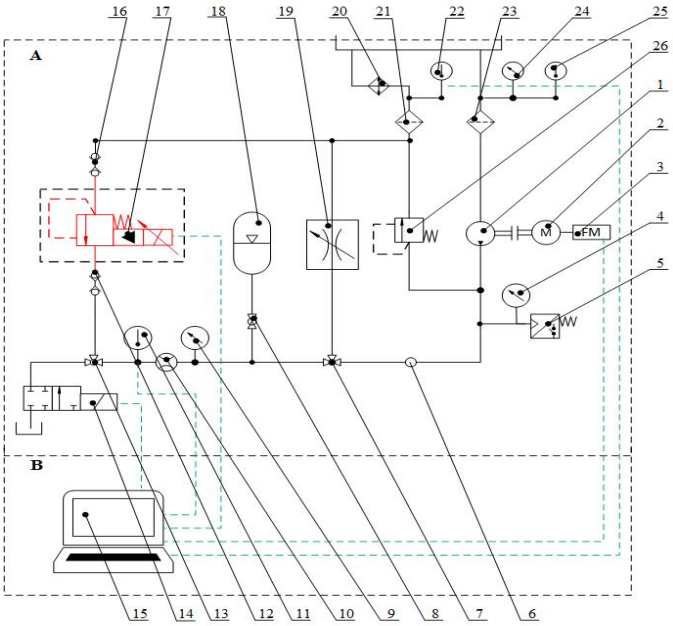

Legend: A – Hydraulic circuit; B – Control and evaluation circuit; 1 – hydraulic pump; 2 – electric motor; 3 – frequency converter; 4, 9, 24 – pressure sensors; 5 – pressure safety sensor; 6 – measuring point for evaluation of the liquid indicator; 7, 13 – three-way valves; 8 – ball valve; 10 – flow sensor; 11, 22, 25 – temperature sensors; 12, 16 – quick couplers; 14 – distributor; 15 – computer; 17 – electrohydraulic proportional valve; 18 – pressure accumulator; 19 – throttle valve with stabilization; 20 – cooler; 21, 23 – filters; 26 – pressure valve

The methodical sampling procedure will fallow the standard STN 65 6207 (Hydraulic oils and fluids. Sampling for the determination of the content of mechanical impurities) and will consist of these steps:

1. Taken sample has to represent the average composition of the hydraulic fluid in the hydraulic system.
2. The hydraulic test rig must be in operation for at least 20 minutes to mix and heat the test hydraulic fluid to specified operating temperature.
3. Approx. 500 ml of hydraulic fluid must be drained into the clean container and pour the same sample back into the hydraulic system of the test equipment.
4. After rinsing the sampling points, approx. 200 to 500 ml sample of tested hydraulic fluid has to be taken.

Table 1 Technical data of the lubricant and fluid analyser

Parameter	Specification
Application	Mineral and synthetic lubricants including gear and motor oils, hydraulic mixtures, turbines and biodiesel.
Output	Si, Al, Ti, Fe, Ni, Pb, Cu, Mo, Ag, Zn, V, TAN a TBN (mg.KOH/g), oxidation (abs/mm^2), water (number of particles/million), sulfation (abs/mm^2), glycol (% by weight), soot (% by weight), viscosity at 40 °C, 100 °C, particle counting > 4µm, solid abrasion > 4µm on the filter
Methodology	ASTM E 242 (IR), ASTM D7279 (visc.), ISO 21018–3 (particles counting)
Accuracy	≤±15% from the measured value
Sample volume	10 ml
Operating ambient temperature	0 °C to +40 °C
Relativity humidity	10% to 80%
Compliance with the standard	RoHS CE, FCC, CSA, IEC 61010–1:2001/EN 61010–1:2001, CE, cT cTÜVus, ICE 61010–1:2002

Equipment for evaluating samples of the tested hydraulic fluid

The integrated lubricant and oil analyzer is designed for measuring particle counting, filtration, elementary spectrometry with an ICP spectrometer and a viscometer. It used for testing the abrasion metals, contamination and the condition of the lubricants by measuring a small sample of the taken fluid (no solvents need to be used). Technical data of the equipment are given in Table 1.

Characteristic of the tested hydraulic fluid

Table 2 Basic properties of the tested hydraulic fluid Mol Farm NH Ultra

Properties	Unit	Value
Density at 15 °C	kg/m^3	875
Kinematic viscosity at 40 °C	mm^2/s	64.2
Kinematic viscosity at 100 °C	mm^2/s	10.9
Viscosity index	–	162
Pour point	°C	-36
Flash point in an open crucible	°C	210

RESULTS AND DISCUSSION

The tests were carried out in laboratory conditions with simulation of the operating load, to simulate the real condition under which hydraulic circuit of agricultural tractors operates. The test was focused on the assessment of the physical properties of the fluid and the values of abrasion metals, contaminants and additive elements were recorded by ICP spectrometry.

Evaluation of physical properties of the tested hydraulic fluid

The density signals the actual conditions of the fluid and especially its contamination by foreign substances. In Table 3, measured values of specific gravity are recorded, as a function of the number of hours worked. Density can be affected by the presence of the abrasive metals or impurities from the outside environment.

Table 3 Physical properties of the tested hydraulic fluid – according to ASTM D7042

Parameter	Unit	Sampling interval		
		0 h	125 h	375 h
Density at 40 °C	kg/m^3	860.70	860.65	860.60
Density at 100 °C	kg/m^3	827.00	826.20	826.00
Dynamic viscosity at 40 °C	mPa.s	49.00	47.10	46.56
Dynamic viscosity at 100 °C	mPa.s	8.42	7.99	7.85
Kinematic viscosity at 40 °C	mm^2/s	56.90	54.80	54.10
Kinematic viscosity at 100 °C	mm^2/s	10.20	9.71	9.54
Viscosity index	-	170.00	163.90	161.80
Acid number ASTM D664 A	mg.KOH/g	2.91	3.29	3.59
Water content DIN 51777	%	0.07	0.043	0.049

The value of the density of the tested fluid before the start of the tests is 827 kg/m^3, this value can be considered as a reference due to the fact, that manufacturer of the tested fluid does not proved this data at 100 °C (measurement were performed in an accredited laboratory Klüber). Following further sampling at well–defined intervals, slight decrease in density was observed at 125 and 375 hours compared to the start of the tests, which can be caused by to filtering of impurities. Samples taken after 125 and 375 hours showed the same value of density.

Kinematic viscosity is used to assess the condition of hydraulic fluid. Increase of this attribute can be caused mainly by oxidation products or impurities in the fluid, or decrease of this attribute, which is mainly caused by mechanical and thermal degradation of additional additives.

Evaluation of the TAN (total acid number) is an analysis to monitor oxidation by–products (mainly acids). Test itself can be used for the measurement, by which the acids in the fluid are neutralized by addition of potassium hydroxide (KOH). If the fluid oxidizes, organic acids are produced,

and the acid number start increased. The acid number reveals the damaged hydraulic fluid, in which the degradation processes took place and the antioxidant additives are depleted from the fluid. Evaluation of the fluid through TAN, the methodological procedure is carried out according to the ASTM D 644 standard. In the case of our testing, the samples were taken so that their weight when tested to determine the acid number was in the range of 4.5 to 5.5 g with a weighing accuracy of 0.02 g. The values correspond to a range of acid number from 1 to < 5 mg/g (Table 3).

Water content changes viscosity of the fluid, load–bearing capacity and lubricating film, thus deteriorating the lubricity, and increasing the wear of the functional pairs. The Figure 2 shows dependence of the water content in the tested transmission-hydraulic fluid on the number of hours worked.

Figure 2 Dependence of the water content in the tested transmission–hydraulic fluid on the number of hours worked

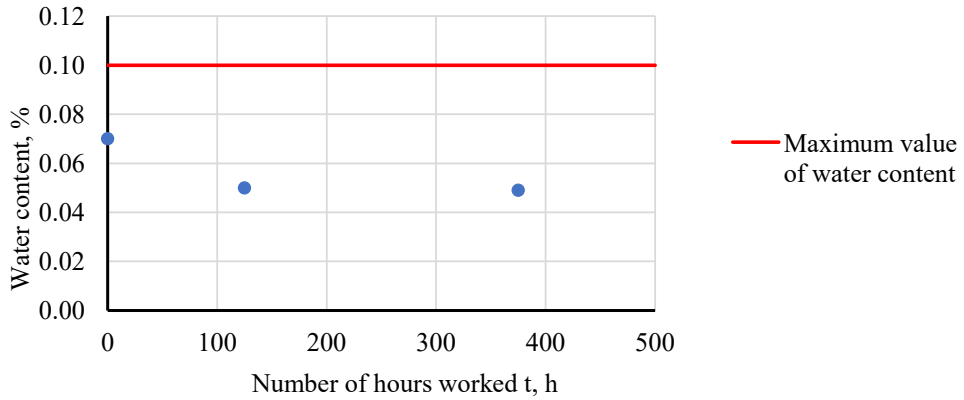

The maximum permissible value of the water content in hydraulic fluids is prescribed at the level of 0.1% and for transmission fluids the value is 0.3%. From analyses of MOL Farm NH Ultra, it is clear that the water content is within the permitted range (Table 3).

Table 4 ICP spectrometry results of tested fluid MOL Farm NH Ultra

ICP spectrometry: PN002, PN012, PN014					
	Chemically element	Unit	Sampling interval		
			0 h	125 h	375 h
Abrasive metals	Aluminium	mg/kg	<10	<10	<10
	Molybdenum*	mg/kg	<10	<10	<10
	Nickel	mg/kg	<10	<10	<10
	Chrome	mg/kg	<10	<10	<10
	Copper	mg/kg	<10	<10	<10
	Ferrum	mg/kg	<10	<10	<10
	Plumbum	mg/kg	<10	<10	<10
Contaminants	Zinc*	mg/kg	1450	1440	1470
	Silicium*	mg/kg	<10	<10	<10
	Natrium	mg/kg	<50	<50	<50
	Potassium	mg/kg	<10	<10	<10
Additives	Barium	mg/kg	<10	<10	<10
	Magnesium	mg/kg	15	12	13
	Phosphorus	mg/kg	1290	1300	1310
	Calcium	mg/kg	3650	3670	3710
Other important elements	Manganese	mg/kg	<10	<10	<10
	Sulphur	mg/kg	4650	4740	4780

*Legend: *the element can also be used as an additive*

Evaluation of the results of ICP spectrometry of the tested fluid, was focused on determining the concertation of important chemical elements. During operation, mechanical wear occurs in the hydraulic system and thus abrasion particles are formed, which is natural phenomenon that cannot

be avoided. Slightly small amounts of abrasive particles may also appear in the new fluid as part of the additives. However, if the size of those particles increases significantly, it may signal a malfunction of any part of the hydraulic system.

It is necessary to know the limit values of the amount of abrasive metals, when comes to evaluation of the tested transmission-hydraulic fluid MOL Farm NH Ultra. Standard D6595–0000 sets limit values for abrasive metals, which are given in Table 5.

Table 5 Range of abrasive metals in transmission–hydraulic fluid (ASTM D6596-00, 2011)

Element	Unit	Range	
		min	max
Aluminium	mg/kg	0.25	100
Molybdenum*	mg/kg	0.21	100
Nickel	mg/kg	0.35	100
Chrome	mg/kg	0.18	152
Cupper	mg/kg	0.47	100
Ferrum	mg/kg	4.8	210
Plumbum	mg/kg	0.43	101
Zinc*	mg/kg	5.3	1345

*Legend: * the element can also be used as an additive*

When comparing the results of ICP spectrometry (Table 4), which was performed by an accredited laboratory of Klüber, it can be argued that no increased incidence of abrasion parts was recorded in the tested liquid after 375 hours compared to the new sample. Limit values are given in Table 5. The findings show that the test fluid does not act aggressively on the components of the hydraulic system on which the service load was simulated (Figure 1).

CONCLUSION

Contamination of the working fluid causes accelerated wear of the hydraulic system, corrosion of steel surfaces, oxidation of the fluid, and can cause changes of its physical and chemical properties (Čorňák 2018). Pollution mainly affects ecological liquids, which accelerates their degradation process (Zastempowski 2013). Several authors (Tulík et al. 2017, Tkáč et al. 2017, 2018) deal with the evaluation of fluid during the operational test with subsequent analysis of polluting elements. Each transmission-hydraulic fluid is limited by its service life, and its properties are given by their physical–chemical composition. Impurities, depletion of additives and degeneration of the base fluid has main influence on the wear of the hydraulic fluid. Although impurities can be removed from to fluid, additives can be added to the fluid, however degradation of the base fluid is an irreversible process. The presented work is focused on the assessment of the qualitative properties of the MOL Farm NH Ultra fluid. In this work the data obtained during the tests were processed, which were carried out on a laboratory device, which allows to simulate changes in the physical properties of the fluid and its use does not affect the technical condition of the hydraulic circuit elements.

ACKNOWLEDGEMENTS

This work was supported by project VEGA 1/0155/18 „Applied research of the use of ecological energy carriers in agricultural, forestry and transport technology. “

This work was supported by project KEGA 028SPU–4/2019 „Practical utilization of design and testing knowledge of transmission systems of hydraulic mechanisms of mobile agricultural and forestry machinery.”

REFERENCES

Čorňák, S. 2018. Identification of Operating Fluids with Fingerprint Method Utilization. In Proceedings of 17th International Scientific Conference Engineering for Rural Development. Jelgava, Latvia, 23–25 May. Jelgava: Latvia University of Agriculture, pp. 2048–2053.

Hujo, L. et al. 2019. Laboratory Research of Transmission-Hydraulic Fluid. In Proceedings of 7th International Conference on Trends in Agricultural Engineering 2019. Prague, Czech Republic, 17–20 September. Prague: Czech University of Life Science Prague, pp. 183–188.

Jablonický, J. et al. 2020. Monitoring of Selected Physical and Chemical Parameters of Test Oil in the Wet Disc Brake System. Acta Technologica Agriculturae [Online], 23(1): 46–52. Available at: https://doi.org/10.2478/ata-2020-0008. [2020-02-20]

Kopiláková, J. et al. 2017. Evaluation of Hydraulic Resistance in Various Liquids and Temperature. Tribology in Industry [Online], 39 (1): 129–135. Available at: http://www.tribology.fink.rs/journals/2017/2017-1/14.pdf. [2020-08-20]

Kosiba, J. et al. 2016. Monitoring Oil Degradation During Operating Tests. Agronomy Research, 14(5): 1626–1634.

Košinár, I., Kuric, M. 2011. Monitoring CNC Machine Tool Accuracy. Postepy Nauki i Techniki, 6: 145–154.

Kučera, M. et al. 2013. Possibility of Hydraulic Fluids with a Low Environmental Impact Application in Agricultural and Transport Machinery. Journal of Central European Agricultural, 14(4): 1592–1601.

Kuric, I. et al. 2016. Analytical Intelligence Tools for Multicriterial of CNC Machines. Advances in Science and Technology Research Journal [Online], 10(32): 59–64. Available at: https://doi.org/10.12913/22998624/65105. [2019-12-01].

Puškár, M. et al. 2015. Numerical Simulation and Experimental Analysis of Acoustic Wave Influences on Brake Mean Effective Pressure in Thrust-Ejector Inlet Pipe of Combustion Engine. International Journal of Vehicles Design [Online], 67 (1): 63–67. Available at: https://doi.org/10.1504/IJVD.2015.066479. [2014-12-22].

Puškár, M. et al. 2019. Complex Analysis of Influence of Biodiesel and Its Mixture on Regulated and Unregulated Emissions of Motor Vehicles with the Aim to Protect Air Quality and Environment. Air Quality, Atmosphere and Health [Online], 12(7): 855–864. Available at: https://doi.org/10.1007/s11869-019-00704-w. [2019-05-02].

Simikic, M. et al. 2014. Power Delivery Efficiency of a Wheeled Tractor at Oblige Drawbar Force. Soil and Tillage Research, 141: 32–43.

Tkáč, Z. et al. 2017. Research of Biodegradable Fluid Impacts on Operation of Tractor Hydraulic System. Acta Technologica Agriculturae [Online], 20(2): 42–45. Available at: https://doi.org/10.1515/ata-2017-0008. [2017-06-23].

Tkáč, Z. et al. 2018. Experimental hydraulic device for the testing of hydraulic pumps and liquids. Tribology in Industry [Online], 40(1): 149–155. Available at: DOI: 10.24874/ti.2018.40.01.14. [2018-01-01].

Tulík, J. et al. 2017. Evaluation of New Biodegradable Fluid on the Basis of Accelerated Durability Test, FTIR and ICP Spectroscopy. Research in Agricultural Engineering [Online], 63(1): 1–9. Available at: https://doi.org/10.17221/6/2015-RAE. [2020-09-10]

Zastempowski, M. 2013. Test Stands with Energy Recovery System for Machines and Hydraulic Transmission. Journal of Research and Application in Agricultural in Agricultural Engineering, 58(2): 188–191.

Time series analysis of three-point hitch control by ploughing

Martin Kucin, Martin Fajman
Department of Technology and Automobile Transport
Mendel University in Brno
Zemedelska 1, 613 00 Brno
CZECH REPUBLIC

xkucin1@mendelu.cz

Abstract: The main goal of this contribution is to substantiate dissimilarities in operational characteristics between a conventional EHR control and a newly developed EHR regulation of agricultural tractor's three-point hitch. The dynamic time warping method (DTW) is used to solve this problem and for the representation of results, there are used plots with an alignment between time series points. The quantification of the dissimilarity between conventional EHR regulation control and the new one was measured by the total distance.

Key Words: time series analysis, DTW, EHR control, Python 3

INTRODUCTION

Nowadays time series data are being generated at an unprecedented scale and rate from almost every application domain, for example daily fluctuations of stock market, medical and biological experimental observation, sensors from industry, etc. Of course, as a consequence, there has been a dramatically increasing amount of interest in querying and mining such data in the last decades (Faloutsos et al. 1994, Han et al. 2012).

Time series are high dimensional data and working with them directly in raw format is very expensive in both terms of processing and storage costs. Because of this disadvantage, it is highly desirable to develop representation techniques, that can reduce the dimensionality of time series, while have to still preserve the fundamental characteristics of particular data set (Olofsson 2012). Two main goals of managing time series data are the effectiveness and efficiency of their analyses. For achieving them are used two key aspects: *representation methods* and *similarity measures* (Han et al. 2012). Unlike canonical or ordinal values are time series different, because the distance in between time series needs to be carefully defined to properly capture semantic and reflect the similarity or dissimilarity of such data (Han et al. 2012, Olofsson 2012).

To determine the distance measure, we can use several methods, which can be divided into the four main categories. The first is *lock-step measures*, these ones require both time series to be the equal length (n = m) and compare time point i of time series x with the same time point i of time series y. Another disadvantage is that limited in handling noise or time shifts. It should be noted that this technique can also be used for non-time series assignments; the only requirement is that all observations are numerical vectors of equal length (Mico and Oncina 1998). Into this category belong e.g.: *Manhattan Distance, Euclidean Distance* (Yi and Faloutsos 2000). To the first category fit also *Elastic measures*, these are more flexible than *lock-step measures* and allow one-to-many or one-to-one point matchings. This makes it possible for elastic distance measures to warp in time and be more robust when it comes to, for example, handling outliers. The disadvantage is that these measures generally come with an increase in time complexity (Vlachos et al. 2002). Into this category belongs e.g.: *Longest Common Subsequence (LCSS), Dynamic Time Warping (DTW)*.

The second category is *Feature-based distances*, these are often applied to obtain a reduction in both dimensionality and noise. Into this category typically belong *Discrete Fourier Transform (DFT), Discrete Wavelet Transform (DWT)*. The third category is *edit-based distances*, which expresses the dissimilarity of two time series based on the minimum number of operations that are needed to transform one series into the other series. Last, respectively fourth category is *Structure-based distances*, this one is used for measurements of dissimilarity, obtained by comparing higher-level structures that are obtained by modeling or compressing the time series (Roelofsen 2018).

We applied primarily DTW the method; therefore, we are going to describe this one method in detail only. Dynamic Time Warping warps two sequences x and y non-linearly in time to cope with time deformations and varying speeds in time-dependent data. According to Roelofsen (2018): *„When determining the DTW distance between two time series, first an (n × m) local cost matrix (LCM) is calculated, where element (i, j) contains the distance between x_i and y_j. This distance is usually defined as the quadratic difference".*

As the next step, the warping path is calculated as $max(n, m) \leq K \leq m + n - 1$. This path traverses the LCM under three constraints. The first constrain is „*Boundary Condition*", which means, that path has to start and end in the diagonal corners of the LCM. The second condition is „*Continuity*", which means only adjacent elements in the matrix are allowed for steps in the path. This includes diagonal adjacent elements. The last condition is „*Monotonicity*", which means that subsequent steps in the path have to be monotonically spaced in time. The total distance for the path is obtained by summing the individual elements (distances) of the LCM that the path traverse. To obtain the optimal DTW distance, it is required the path with minimal total distance. For obtaining the DTW distance, Keogh and Ratanamahatana (2004) recommend using summing the elements of the path with minimum cumulative distance.

In this contribution, the above-described methods and especially DTW was used for the analysis of field data of ploughing. The data were collected from tractors' sensors in a form of time series data in a frequency of 10 Hz. The main goal of the study was to compare the characteristics of two types of electro-hydraulic hitch control (EHR) tested by ploughing. It is important to reach optimal operational conditions for any primary soil tillage technologies, namely ploughing. It is because, despite various systems of reduced tillage without ploughing, mouldboard ploughing remains the most common way of primary soil tillage in the middle of Europe today. The percentage of ploughing of the arable land area in the Czech Republic was 70.4% in 2017 (Ministry of Agriculture of the CR 2018).

The main advantages of ploughing are well known in good soil loosening, easier seedbed preparation, which enables proper sowing and good weed control. On the other hand, main disadvantages of classical mouldboard ploughing represent relatively high energy expenses leading to costly technology. Therefore, a proper setup of tractor and plough together and optimal control of the operation is critical to reaching the advantages while reducing the disadvantages of this technology. A key issue is then an appropriate three-point-hitch control of the tractor. Nowadays, the vast majority of agricultural tractors are equipped with a conventional electro-hydraulic hitch control (EHR) developed from originally mechanical-hydraulic control (MHR) (Kovacev et al. 2008). Typically, the force control (regulation) the three-point-hitch is applied by ploughing when the regulation keeps a constant drawbar force while a ploughing depth varies significantly due to the EHR regulation processes. Often, the ploughing depth is higher than a preliminary set of minimal depth to keep the constant drawbar force. Thus, an undesired pull power is required, and the quality of the operation is not improved.

To improve the force regulation a new design of a regulator for the EHR was developed to reduce undesired pull power by ploughing under pre-set ploughing depth, to keep quality standards of the operation though maintain the advantages of the force control in overcoming unpredictable drawbar power demands; still, preserving all other agrotechnical requirements, namely the ploughing depth. There is a patent-pending for a way of such regulation and as well as for the text extent the details of the regulation are not deeper specified.

The goal of the contribution is to quantify a scope in a similarity/dissimilarity of operational characteristics of both types of the EHR regulation controls, conventional and the new one.

MATERIAL AND METHODS

The data for the analysis were obtained by a long term field trial focused on primary soil tillage, oriented to study the operation quality and characteristics of the ploughing at the Žabčice district, South Moravia, the Czech Republic in years 2018 and 2019. Middle-class power tractor (102 kW) and 5-mouldboard plough were used as a working set, the tractor was equipped with a measuring and control set by the NI (former National Instruments) formed by cRIO controller and chassis with modules for analog, digital, and force measurements. The measurement's software was self-

developed to gain the data for both types of the EHR control; and also, for the new-type regulation itself. More than 65 characteristics were measured in various frequencies, mean values were calculated directly in the cRIO controller and the data were saved in the *tdms* format (Technical Data Management Streaming, NI) in the frequency of 10 Hz. The regulation was always set to force regulation and the pre-set position of the three-point hitch (ploughing depth) was kept as similar as possible by all measurements. Repetition of the measurements was organized in the measuring sections marked in the field and the data collection for a specific measurement was triggered by the driver as the studied channels formed ca 330 samples.

To quantify the similarity of both EHR control types, the response of the regulation control in a form of the position of the three-point-hitch to actual drawbar force was studied. Therefore, for analysis in this contribution two data channels were selected in each examined tdms file – the primary one represents *actual force impacts* of the plough calculated as the mean value of the outputs the draft sensors situated in both lower links of three-point-hitch mountings. The secondary studied channel was the *actual position* of the upper links of the three-point-hitch. Both studied channels represent waveforms, i.e. the actual values have a timestamp; thus, they represent typically time series. Moreover, both channels are expressed as relative measures – the actual position is a percentage of the highest reachable position of the three-point hitch; the actual force impacts are presented as a share of the draft sensors output (signal) voltage and supply voltage; therefore, both channels are dimensionless quantities and no units will be presented in the results section.

A distance between the force impact signal and the position of three-point-hitch time series was introduced as the measure to quantify the similarity of the control types characteristics for both of the EHR controls individually. For measurement of the distance between time series was used programing language Python 3 (Van Rossum and Drake 2009) and library *dtw-python* (Giorgino 2009) which contains *Dynamic Time Warping (DTW) algorithm*.

For a proper comparison, the DTW requires normalization of the original data; thus, the z-normalization was used. The DTW algorithm was applied to 10 individual samples for conventional as well as for the new version of the EHR control from the field trials accomplished in 2018 and 2019. The LCM was determined and the total distance between the drawbar force and actual position time series was computed from the LCM path for each sample. As it is a typical presentation of results of the elastic measures of time series, the plots of the alignment between the datapoints were generated.

RESULTS AND DISCUSSIONS

Due to a limited extent of the text, selected plots – one for the conventional and one for the new EHR control are presented in the results section only.

Figure 1 represents a response of the conventional EHR force regulation control to actual force impacts by drawbar force. In the figure, the actual position is displayed by the blue curve and force impacts by the black curve; the same, the left Y-axis represents the scale for the force impacts normalized data and the right Y-axis represents the scale of the actual position of three-point hitch normalized data. Dotted lines express the alignment between points of both time series.

By the conventional EHR control, the principles of the force regulation are obvious (see Figure 1). The EHR control reacts to actual force impacts and the general shape of both curves is very similar. On the other hand, there is a time-offset remarkable (see the direction of the majority of the dotted lines), because it is expectable the reaction of the EHR control in shifting the position of the three-point hitch is slightly delayed by regulation processes. Therefore, the lock-step measures could not be used for such analysis. The result of the total distance by the DTW method for the conventional EHR control (and sample in Figure 1) was computed at the level of 113.

Figure 2 represents the new EHR control. The description of the plot is the same as for Figure 1.As it is visible in Figure 2, in general, the shape of both time series, namely by the actual position signal, is a bit different than in Figure 1. Still, the new EHR control keeps the principles of the force regulation – by an upper peak of the force impacts the EHR control shifts the position of the three-point hitch upwards; yet there is a notable time-shift. Nevertheless, the actual position upward shifts are not as high-level as by the conventional control, and the new control does not react

to every single (relatively insignificant) force impacts' alterations. Moreover, it is obvious, there is a lower boundary for the actual position; thus, it keeps the lower minimum level as it was pre-set for the ploughing depth. This dissimilarity of the studied channels is quantified by the DTW total distance at the level of 196.

Figure 1 Conventional EHR regulation control

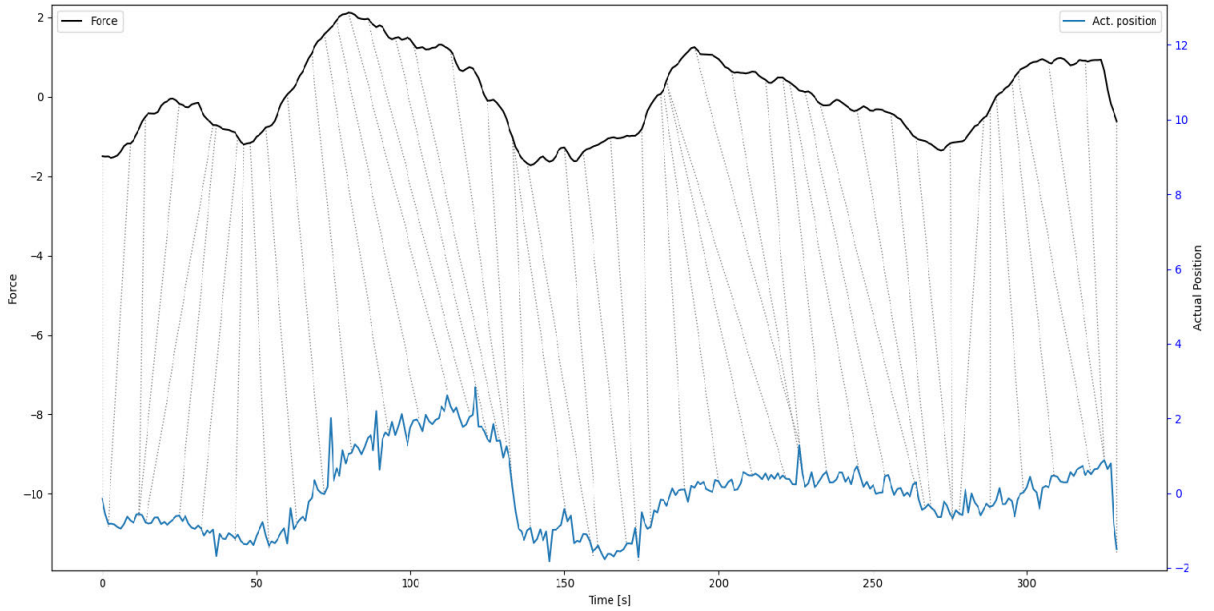

Figure 2 New EHR regulation control

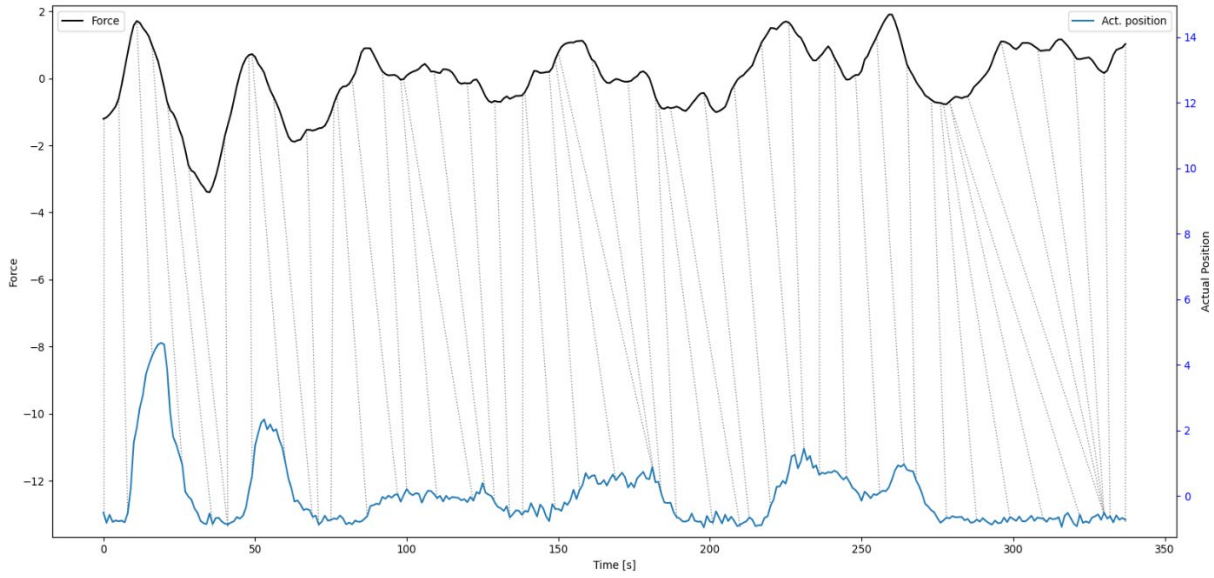

Comparing Figure 1 and Figure 2 and the total distance measures, we can conclude the conventional EHR regulation control performs with a higher level of dependency of the actual position to the actual force impacts than the newly developed one; while, by the new EHR control, the pre-set operational position of the three-point hitch links is kept for the longer time share meaning the ploughing depth is more constant. Similar results were obtained by the other 9 comparisons of non-presented samples. Potentially a statistical analysis (e.g. t-test) could be performed to deepen the contrasts; however, the original data were collected in different fields and time (years), i.e. under varying conditions. Therefore, such a statistical analysis would be factually incorrect.

Using the DTW algorithm in agriculture for this type of comparison is not typical. In our case it is an example of an application of advanced mathematical analyses into the agricultural sector; where, the operational data and their proper analyses become quite important. Other examples of the DTW

method were found for the mapping of rice cropping systems in Vietnam (Guan et al. 2016), crop's classification (Csillik et al. 2019) used namely by remote sensing; however, other applications of such methods seem to be quite rare in agriculture so far.

CONCLUSION

The goal of this contribution was to substantiate the hypothesis of a distinction between operational characteristics by the conventional EHR control and the new one developed. Thanks to the DTW method we were able to figure out that the new EHR regulation control performs a different way in terms of the reaction to actual force impacts than the conventional EHR control. It is confirmed by the total distance measure between these time series and contrasts between both EHR controls. According to field trials, we can also state the new EHR control retains the qualitative behavior for soil tillage.

ACKNOWLEDGMENTS

The research was financially supported by the AF-IGA2020-IP030.

REFERENCES

Csillik, O. et al. 2019. Object-Based Time-Constrained Dynamic Time Warping Classification of Crops Using Sentinel-2. Remote Sensing, 11(10): 1257–1283.

Faloutsos, C. et al. 1994. Fast subsequence matching in time-series databases. Acm Sigmod Record, 23(2): 419–429.

Giorgino, T. 2009. Computing and Visualizing Dynamic Time Warping Alignments in R: The dtw Package. Journal of Statistical Software, 31(7): 43746.

Guan, X.D. et al. 2016. Mapping Rice Cropping Systems in Vietnam Using an NDVI-Based Time-Series Similarity Measurement Based on DTW Distance. Remote Sensing, 8(1): 19.

Han, J. et al. 2012. Data Mining Concepts and Techniques third edition. 3rd ed. Waltham, USA: Morgan Kaufmann Publishers.

Keogh, E., Ratanamahatana, A. 2004. Everything you know about dynamic time warping is wrong. In 3rd Workshop on Mining Temporal and Sequential Data [Online]. Seattle, USA, 22 August, Seattle: Citesser, pp. 50–61. Available at: http://citeseerx.ist.psu.edu/viewdoc/download?doi=10.1.1.432.4253&rep=rep1&type=pdf#page=53. [2020-07-15].

Kovacev, I. et al. 2008. Impact of Electronic-Hydraulic Hitch Control on Rational Exploitation of Tractor in Ploughing. Strojarstvo, 50(5): 287–294.

Mico, L., Oncina, J. 1998. Comparison of fast nearest neighbour classifiers for handwritten character recognition. Pattern Recognition Letters[Online], 19(3–4): 351–356. Available at: https://www.sciencedirect.com/science/article/pii/S0167865598000075?via%3Dihub#SEC6. [2020-09-10].

Ministry of Agriculture of the Czech Republic. Situační a výhledová zpráva - půda. Praha, MZe, 2018. [Online], Available at: http://eagri.cz/public/web/file/611976/SVZ_Puda_11_2018.pdf. [2020-09-07].

Olofsson, P. 2012. Probability, statistics and stochastic processes. 2nd ed. New York, USA: Wiley Online Library.

Roelofsen, P. 2018. Time series clustering. Master thesis, Vrije Universiteit Amsterdam.

Van Rossum, V., Drake, F.L. 2009. Python 3 Reference Manual. 2nd ed., Scotts Valley, CA: CreateSpace.

Vlachos, M. et al. 2002. Discovering similar multidimensional trajectories. In Proceedings of 18th International Conference on Data Engineering. San Jose, USA, 26 February–1 March. Institute of Electrical and Electronics Engineers, pp. 673–684.

Yi, B., Faloutsos, C. 2000. Fast time sequence indexing for arbitrary Lp norms. In Proceedings of 26th International Conference on Very Large Data Bases [Online]. Cairo, Egypt, 10–14 September. San Francisco: Morgan Kaufmann Publishers Inc., pp. 385–394. Available at: http://www.vldb.org/conf/2000/P385.pdf. [2020-07-13].

Design of laboratory test hydraulic equipment for testing hydrostatic transducers and hydraulic fluids

Jozef Nosian, Romana Janouskova, Matej Michalides, Peter Kozuch
Department of Transport and Handling
Slovak University of Agriculture in Nitra
Tr. A. Hlinku 2, 949 76 Nitra
SLOVAK REPUBLIC

xnosian@uniag.sk

Abstract: The main goal of the presented article is the design of a laboratory test hydraulic equipment used to test the properties of hydrostatic transducers and hydraulic fluids. The proposed device allows testing of hydraulic elements and hydraulic fluids by simulating operating factors in laboratory conditions. Thanks to the possibility of testing hydrostatic transducers and hydraulic fluids in laboratory conditions using the designed laboratory hydraulic equipment described in the present article, repeatability of measurements is assured, and testing time is shortened. Laboratory test hydraulic equipment allows simultaneous testing of parameters of hydrostatic converters and hydraulic fluids by simulating the operation of an agricultural machine in laboratory conditions. The functionality of the proposed laboratory hydraulic equipment was verified by verification measurement of the basic parameters of hydrostatic transducers. The flow of the hydrostatic transducer UD–25 R at the specified rotation speed was recorded during the verification measurement. The subject test of the proposed laboratory hydraulic equipment took place in the Laboratory of the Slovak University of Agriculture in Nitra at the Faculty of Engineering. Based on the data obtained during the measurements, it was verified that the proposed laboratory equipment is suitable for testing hydraulic components and also for testing the properties of fluids used in hydraulic equipment.

Key Words: hydrostatic transducers, verification measurement, hydraulic equipment, flow, flow efficiency

INTRODUCTION

Hydraulic systems have become an important part of almost all types of machines and equipment today. Hydraulic systems and hydraulic equipment are often used in the agricultural and forestry industries. According to the authors Tkáč et al. (2017) a Simikič et al. (2014) machines which are used in agriculture and forestry are characterized by demanding operational hours and often work in dusty and humid environments. This has negative consequences on the proper functioning of hydraulic systems. Agricultural engineering requires continuous improvement of the service life and reliability of machinery (Tóth et al. 2019). The goal of hydraulic systems is to transfer energy and increase work efficiency. Current development and modernization in the field of hydraulic mechanisms is focused mainly on reducing energy consumption and increasing power that these machines can transmit. For these reasons, accurate engineering production of individual elements of the hydraulic circuit is important. It is important to monitor the accuracy of CNC machine tools using new methods and trends in product development and planning. Multimetric diagnostics of CNC machines is equally important as well (Košinár and Kuric 2011, Kuric et al. 2011). Also, in hydraulic systems, the development focuses on their ecological operation, which should ensure the lowest possible level of environmental contamination. That is why increasing demands are placed on the development of hydraulic systems. The article presents a design of hydraulic device used for testing hydrostatic transducers and hydraulic fluids. During the measurement itself, the hydrostatic transducer is removed from the agricultural machine and installed on the laboratory test equipment for measurement purposes. The device can test the properties of different types of hydraulic fluids as well as monitoring the parameters of hydrostatic transducers depending on the same or different conditions. The described laboratory test equipment can simultaneously test two types of hydrostatic transducers or two different

types of hydraulic fluids in the same or different conditions. Thanks to the proposed hydraulic equipment we are able to simulate operating parameters that occur in practice in agricultural and forestry machinery.

MATERIAL AND METHODS

When determining the good technical condition of hydrostatic transducers, it is important to know their flow and flow efficiency. During the verification measurement of the designed laboratory hydraulic equipment, flow of the hydrostatic transducer UD–25 R was monitored. The values of monitored flows and flow efficiency during the measurement are used to create dynamic flow models in hydrostatic transducers, which aim to protect the environment from contamination (Puškár et al. 2019). The proposed laboratory hydraulic equipment consists of two circuits, one primary and the other secondary, due to the possibility to test two hydrostatic transducers or two types of hydraulic fluids simultaneously and under the same conditions or different conditions. The flow measurement of the hydrostatic transducer were performed at the following rotation speeds:

- n_1= 250 rpm,
- n_2= 500 rpm,
- n_3= 750 rpm.

It is important to warm the working fluid to the required temperature before performing a verification measurement. Specifically, the operating temperature of the hydraulic fluid is 50 °C. The working fluid used in the proposed laboratory test facility is PARAMO HM 46. The author Kučera et al. (2016) claims that based on the analysis of the operating fluid, we can determine the technical condition of hydraulic elements located in hydraulic systems. The temperature of the working fluid used to monitor the parameters of the hydrostatic transducer located in the designed laboratory test equipment was determined according to the SAE J745 standard. Measurements were performed at each of the listed rotational speeds. Out of these measurements, three critical values were determined, compared and evaluated. Relationships for the determination of individual parts of the proposed laboratory test equipment for testing the operation of hydrostatic transducers and energy carriers:

- Hydrostatic transducer flow:

$$Q = \frac{V_g.n}{1{,}000}.\eta_{pr}, \text{ dm}^3\text{.rpm}, \quad (1)$$

where:

V_g – volume of hydrostatic transducer, dm^3,

n – speed of rotation hydrostatic transducer, rpm,

η_{pr} – flow efficiency of the hydrostatic transducer,

- Power of hydrostatic transducer:

$$P = \frac{V_g.n.p}{60.1{,}000.\eta_c}, \text{W}, \quad (2)$$

where:

p – pressure, MPa,

η_c – overall effectiveness,

- Inner diameter of the pipe:

$$d = \sqrt{\frac{4.Q}{\pi.w}}, mm, \quad (3)$$

where:

w – resistance to flow rate, m/s.

The above relations determined the basic parameters of the hydraulic elements located in the proposed laboratory hydraulic test equipment. Table 1 shows the technical parameters of the hydrostatic transducer UD–25 R, which flow was determined during the verification

measurement. Based on the data from Table 1, some elements of the proposed laboratory test equipment for testing hydrostatic transducers and hydraulic fluids were also dimensioned.

Table 1 Technical parameters of hydrostatic transducer UD–25 R

Parameter	Unit	Value
Rated speed	rpm	1500
Maximum/Minimum speed		3200/450
Maximal/Minimum pressure at the inlet	MPa	0.05/0.03
Nominal/Maximum outlet pressure		20/23
Geometric volume	dm^3	0.02546
Maximum/Minimum oil viscosity	mm^2/s	1200/10
Maximum/Minimum oil temperature	°C	80/-20

Figure 1 Kinematic scheme of hydraulic circuit

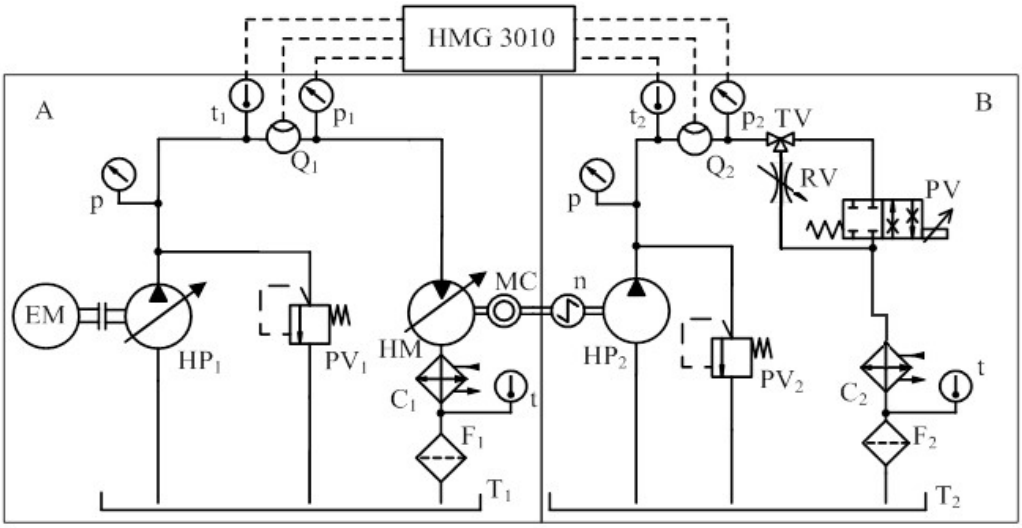

*Legend: **A** – primary hydraulic circuit, **B** – secondary hydraulic circuit, EM – electromotor, HP_1 – regulatory hydrostatic transducer, PV_1, PV_2 – pressure valve, HM – regulatory hydraulic motor, HP_2 – tested hydrostatic transducer, C_1, C_2 – cooler, t – temperature sensor for tanks,T_1, T_2 – tanks, F_1, F_2 – filters, p – pressure gauge, RV – reducing valve, TV – three-way valve, PV – proportional reducing valve, MC –mechanical coupling, n – rpm sensor, t_1, t_2 – ETS 4148-H-006-000 temperature sensors, Q_1, Q_2 – EVS 3108-H-0300-000 flow rate sensors, p_1, p_2 – HDA 4748-H-0400-000 pressure sensors, HMG 3010 – recording unit.*

The proposed laboratory test equipment consists of two hydraulic circuits. One circuit of the proposed laboratory equipment is primary while the other circuit is secondary, due to the possibility to continuously test two hydrostatic transducers or two types of hydraulic fluids simultaneously and under the same conditions. An asynchronous electric motor is used to propulsion the hydrostatic transducer in the primary circuit. The electric motor is connected to the hydrostatic transducers by means of a mechanical coupling. The mechanical coupling transmits mechanical energy, which the hydrostatic transducer converts into pressure energy in the primary hydraulic circuit of the laboratory equipment. The circuits also include a pressure valve, which is in the primary and secondary circuit and performs the function of a safety valve, thus protecting the circuit for high pressure. If the set pressure on the pressure valve is exceeded, the valve releases the hydraulic fluid back into the tank and thus prevents a hazardous condition. In both circuits there is a cooler, which serves to regulate the temperature of working fluids, in both circuits there is also a filter for filtering the working fluid. There are two tanks in the circuit, one tank for the primary circuit and the other tank for the secondary circuit. This allows simultaneous testing of the properties of two working fluids in the same but also different temperature conditions. A hydraulic motor is included in the primary circuit, which serves to convert pressure energy into mechanical energy and is connected to a hydrostatic converter in the secondary circuit via a mechanical coupling. In the secondary circuit of the proposed laboratory equipment, a three-way valve is included, which serves to control the flow of liquid and a throttle valve, which has the task of heating the liquid to the required operating temperature,

respectively creating a load in the hydraulic circuit. There is also a hydrostatic transducer UD–25 R in the secondary hydraulic circuit, the flow of which was monitored during the verification measurement on the designed device. There is also a proportional valve in the circuit, which is used to create a load and simulate operating pressures. In the hydraulic circuit there is a set of sensors for recording rotation speed, temperature, flow and pressure. These sensors are connected to the HYDAC HMG 3010 recording unit. Based on the settings of the HYDAC HMG 3010 meter, the flow of the hydrostatic transducer was monitored for one minute. The sampling was set to 0.100 ms on the meter and recorded 600 data on the flow of the hydrostatic transducer in one minute.

RESULTS AND DISCUSSION

Verification measurement of the proposed laboratory test equipment for measuring and testing hydrostatic transducers should determine whether the design is suitable for testing and measuring hydrostatic transducers. Before the verification measurement itself, it was necessary to calibrate the measuring instruments with verification of functionality. These actions are important in terms of the accuracy of the measurement itself and to eliminate the measurement error. Furthermore, it was necessary to verify and determine the functionality of all sensors used during the verification measurement, with connection to the HYDAC HMG 3010 recording unit and the functionality of the hydraulic circuit elements of the laboratory test equipment. During the verification measurement, the flow of the hydrostatic transducer UD–25 R was measured. According to the author Tulík et al. 2017, it was important to monitor the parameters of hydrostatic transducers in operating conditions. In the verification measurement of the proposed equipment, the first step was to heat the working fluid to an operating temperature of 50 °C. The authors Kosiba et al. (2016) and Kopiláková et al. (2017) dealt with the evaluation of hydraulic fluids depending on temperature and pressure. Both authors found that operating parameters, especially temperature and pressure, affect the working fluid and subsequent measurements. After heating the hydraulic fluid to the working temperature, the required rotation speed for the verification measurement of the hydrostatic transducer is set.

Table 2 Hydrostatic transducer flow values recorded during the verification measurement

Rotation speed, n, rpm	Arithmetic mean flow rate, Q, dm^3.rpm	Flow efficiency,η, –
250	5.694	0.8946
500	12.286	0.9651
750	18.747	0.9812

Table 3 Hydrostatic transducer flow values specified by the manufacturer

Rotation speed, rpm	Flow rate specified by the manufacturer, Q_H, dm^3.rpm
250	6.000
500	12.000
750	18.000

In Figure 2 and in Tables 2 and 3, it is possible to see the data from the verification measurement of the hydrostatic transducer UD–25 R on the proposed device and the flow data given by the manufacturer of the hydrostatic transducer in question. Based on the data from the verification measurement and the data from the manufacturer, it follows that as the rotation speed increases, the flow of the hydrostatic transducer gradually increases. The differences between the values recorded during the verification measurement and the values given by the manufacturer can be explained by the different measurement conditions. For example, the manufacturer states the flow of the hydrostatic transducer at an operating temperature of 45 °C, while the verification measurement was performed at an operating temperature of 50 °C as specified in the standard. Another difference versus the manufacturer was that the manufacturer used a different type of hydraulic fluid when measuring the flow of the hydrostatic transducer. The manufacturer used ISO Vg 46 liquid as the working medium in its flow measurement, and PARAMO HM 46 liquid was used as a working medium in the verification measurement on the designed device. Differences in measurements can therefore be caused by different hydraulic media. According to author Halenár et al. (2017) physical-chemical properties as well as fluid temperature affect the measurement results. Halenár et al. (2017) found in their work the flow of a hydrostatic transducer at a speed of 500 rpm, 7.64 dm^3.rpm and at a speed of 750 rpm found a flow

of 11.75 dm^3.rpm. The difference between the measurements by Halenár et al. (2017) and the measurement described in the article is that he used a hydrostatic transducer QHD-17R, which cyclically loaded with pressure. Author Tulík et al. (2017) in his article measured the flow of the hydrostatic transducer UD–25R, 34.77 dm^3.rpm. It detected this flow at a speed of 1500 rpm and at the same time permanently loaded the transducer with a pressure of 20 MPa. Both authors used a different type of hydraulic fluid in their measurements than the one used in the verification measurement described in the translated article.

Figure 2 Flow values recorded during the verification measurement and specified by the manufacturer

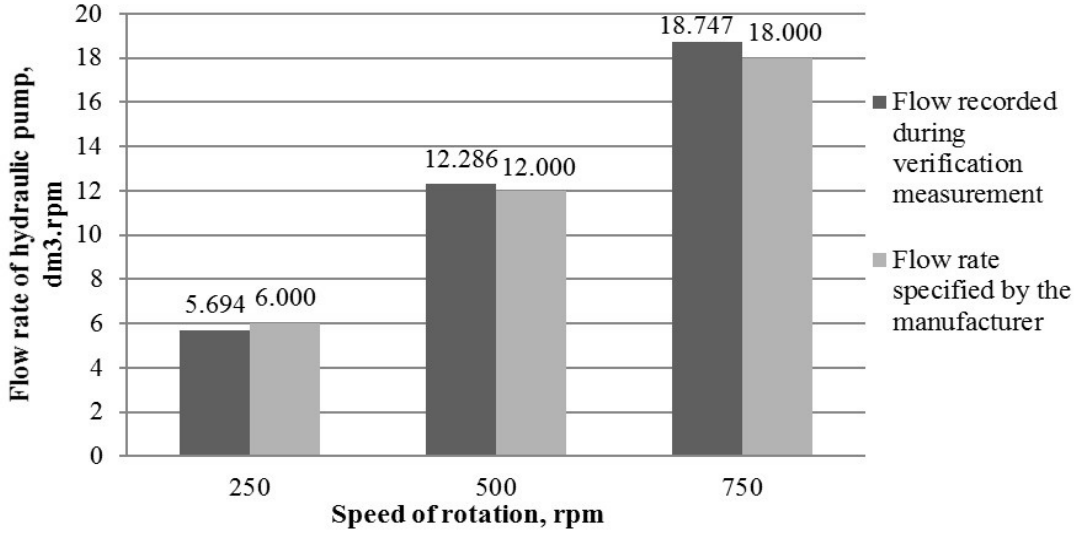

CONCLUSION

Hydraulic systems are widely used mainly in agricultural and forestry machinery. Therefore, there is a need to create a device that can effectively simulate the operating load even in laboratory conditions, while simultaneously testing various hydraulic fluids that are used in hydraulic circuits. The analysis of hydraulic fluids under operating conditions has already been dealt with by the authors Tkáč et al. (2017) and Čorňák (2018). According to author Zastempowski et al. (2013), the physico-chemical properties of hydraulic fluids are also affected by pollution, which results in degradation processes. The presented article deals with the design of a laboratory test equipment for measuring and testing hydrostatic transducers and hydraulic fluids. The design of laboratory test equipment for hydraulic systems of agricultural machines is addressed by Hujo et al. (2019) and Jablonický et al. (2020). From the point of view of hydraulic systems, the hydrostatic transducer is an input member of the hydraulic circuit. That is why it is important to monitor its condition with the possibility of testing in various conditions. The proposed laboratory test equipment allows to repeatedly simulate the operating conditions of agricultural and forestry machinery. Functionality of the proposed laboratory test equipment was verified by verification measurements, during which the flow of the hydrostatic transducer UD–25 R was monitored. Thanks to the proposed laboratory test equipment, it is possible to significantly shorten the testing of the parameters of hydrostatic transducers, as well as to shorten the testing of the properties of individual types of energy carriers used in hydraulic circuits.

ACKNOWLEDGEMENTS

This work was supported by project VEGA 1/0155/18 „Applied research of the use of ecological energy carriers in agricultural, forestry and transport technology“.

This work was supported by project KEGA 028SPU–4/2019 „Practical utilization of design and testing knowledge of transmission systems of hydraulic mechanisms of mobile agricultural and forestry machinery”.

This work was supported by project APVV SK-PL-18-0041 „The development of scientific cooperation in the study of the effects of biofuels in road transport, including environmental impact”.

REFERENCES

Čorňák, Š. 2018. Identification of Operating Fluids with Fingerprint Method Utilization. In Proceedings of 17th International Scientific Conference Engineering for Rural Development. Jelgava, Latvia, 23–25 May. Jelgava: Latvia University of Agriculture, pp. 2048–2053.

Halenár, M., Kuchar, P. 2017. Research of biodegradable fluid during operating test. In Proceedings of International PhD Students Conference MendelNet 2017 [Online]. Brno, Czech Republic, 8–9 November, Brno: Mendel University in Brno, Faculty of AgriSciences, pp. 784–788. Available at: https://mnet.mendelu.cz/mendelnet2017/mnet_2017_full.pdf

Hujo, Ľ. et al. 2019. Laboratory Research of Transmission-Hydraulic Fluid. In Proceedings of 7th International Conference on Trends in Agricultural Engineering 2019. Prague, Czech Republic, 17–20 September. Prague: Czech University of Life Sciences Prague, pp. 183–188.

Jablonický, J. et al. 2020. Monitoring of Selected Physical and Chemical Parameters of Test Oil in the Wet Disc Brake System. Acta Technologica Agriculturae [Online], 23(1): 46–52. Available at: https://doi.org/10.2478/ata-2020-0008. [2020-02-20].

Kopiláková, J. et al. 2017. Evaluation of Hydraulic Resistance in Various Liquids and Temperature. Tribology in Industry [Online], 39(1): 129–135. Available at: http://www.tribology.fink.rs/journals/2017/2017-1/2017-1-14.html. [2020-05-20].

Kosiba, J. et al. 2016. Monitoring Oil Degradation During Operating Tests. Agronomy Research, 14(5): 1626–1634.

Košinár, I., Kuric, M. 2011. Monitoring CNC Machine Tool Accuracy. Postepy Nauki i Techniki, 6: 145–154.

Kučera, M. et al. 2013. Possibility of Hydraulic Fluids with a Low Environmental Impact Application in Agricultural and Transport Machinery. Journal of Central European Agricultural, 14(4): 1592–1601.

Kuric, I. et al. 2011. Analytical Intelligence Tools for Multicriterial of CNC Machines. Advances in Science and Technology Research Journal [Online], 10(32): 59–64. Available at: https://doi.org/10.12913/22998624/65105. [2019-12-01].

Puškár, M. et al. 2019. Complex Analysis of Influence of Biodiesel and Its Mixture on Regulated and Unregulated Emissions of Motor Vehicles with the Aim to Protect Air Quality and Environment. Air Quality. Atmosphere and Health [Online], 12(7): 855–864. Available at: https://doi.org/10.1007/s11869-019-00704-w. [2019-05-02].

Simikič, M. et al. 2014. Power Delivery Efficiency of a Wheeled Tractor at Oblige Drawbar Force. Soil and Tillage Research, 141: 32–43.

Tkáč, Z. et al. 2017. Research of Biodegradable Fluid Impacts on Operation of Tractor Hydraulic System. Acta Technologica Agriculturae [Online], 20(2): 42–45. Available at: DOI: 10.1515/ata-2017-0008. [2017-06-23].

Tóth, F. et al. 2019. The possibilities of using ecological liquids in tribological gliding systems with a selected surface created by the radial welding technology. Acta Technologica Agriculturae, 22(4): 134–139.

Tulík, J. et al. 2017. Evaluation of New Biodegradable Fluid on the Basis of Accelerated Durability Test, FTIR and ICP Spectroscopy. Research in Agricultural Engineering [Online], 63(1): 1–9. Available at: https://doi.org/10.17221/6/2015-RAE. [2019-10-07].

Zastempowski, M. 2013. Test Stands with Energy Recovery System for Machines and Hydraulic Transmission. Journal of Research and Application in Agricultural Engineering, 58(2): 188–191.

Development of a new device for fire prevention in waste management facilities

Robert Rous[1], Dita Henek Dlabolova[2], Jan Chovanec[3], Tomas Ondracka[4]
[1,2]Department of Informatics
[3]Department of Agricultural, Food and Environmental Engineering
[4]Department of Chemistry and Biochemistry
Mendel University in Brno
Zemedelska 1, 613 00 Brno
CZECH REPUBLIC

robert.rous@mendelu.cz

Abstract: The design of a new experimental device for fire prevention is presented here together with data from the first experiment in real conditions. The experiment was held on a composting facility measuring the surface temperature of oil filtration clay together with environmental data (illuminance, relative air humidity, and ambient temperature). Surface temperature data were measured by MLX90640 IR temperature array (32 by 24 values) that gives the ability to use spatial information in measured data. Correlations between the surface temperature, the ambient temperature, and the illuminance are well visible from the results. The experiment showed it is possible to use this kind of sensor for temperature measurements and process the data afterward in the fire prevention cloud system.

Key Words: temperature measurement, IR array, fire safety, fire prevention, IoT, LoRa

INTRODUCTION

The amount of waste generated in the European Union by all economic activities and including household waste in 2016 was 2261 million tonnes (Eurostat 2020). European waste legislation imposes increasingly stringent operational requirements on processors. To meet the conditions and also to economize the waste management processes, facilities such as transhipment yards, collection yards, composting plants, sorting lines, etc. are operated. Uncontrolled burns or fires can occur at each of these locations throughout the processing stream.

Damage caused by waste fires is usually not located at the material losses. Waste can often have a negative value and the producer pays for its disposal. However, in the case of secondary raw materials, RDFs, compost or biogas, damage can also occur to the material itself or subsequently to the technology and equipment. As reported (Travnicek et al. 2018), 59 % of all accidents at biogas plants operations across the examined EU countries were related to some type of fire. Furthermore, there are mainly indirect costs, such as the departure of the fire brigades, the cost of water and fire extinguishers, processing facilities and equipment, etc. We can say with certainty that the uncontrolled burning results in environmental damage in the form of gaseous emissions as reported (Lemieux et al. 2004). The fire extinguishing itself can also bring an unintended environmental risk. As reported in (Mikalsen et al. 2020) water with foam extinguisher can contaminate a nearby pond or stream and have an acute toxic effect on aquatic animals.

One of the main fire causes in organic materials can be the so-called spontaneous combustion. A phenomenon in which the biological process at a controlled waste disposal site or a bio-waste pile in the composting plant produces such a high temperature, which allows burnout of decaying material. It is common for ripening compost to reach a temperature of around 80 °C. However, if the material contains an optimal amount of moisture that is sufficient to catalyse the oxidation process, but at the same time insufficient to cool the decaying material, temperatures can rise up to 200 °C (Coker 2019). If the process is oxygen-deficient, smouldering occurs, if oxygen is available, flame burning occurs.

While the manufacturing industry is moving towards new technologies in compliance with Industry 4.0 initiative and the Internet of Things since 2013 (Oztemel and Gursev 2018)

these progressive technologies affect associated industries such as waste management industry. Therefore, the main motivation was to design a system that would be able to predict potential fire hazard events in waste management facilities (especially landfills and compost facilities). Such commercial solutions already exist, i.e. PYROsmart® system by Orglmeister Infrarot-Systeme or TST Fire® by Termisk Systemteknik. They are all based on thermal cameras and computer vision processing. Use of IR thermographic measurement in early warning and fire prevention system is common (Pastor and Planas 2012) used it in remote sensing application to predict fire behaviour in wildfires, (Liu et al. 2015) used it for early detection of spontaneous combustion of sulphide ore stockpiles.

The here presented experimental equipment aims to apply the same principles therefore detecting changes in the temperature of the monitored material and preventing fire and consequent damage. The difference is in use of simpler (cheaper and low-power) IR temperature sensor than in thermal cam. The main goal of this paper is to evaluate the data from the experimental device (sensor module) in real conditions for future use.

MATERIAL AND METHODS

Characterization of experiment locality and experiment design

The experiment was held on Fertia composting plant in Náměšť nad Oslavou, Czech Republic and took 7 days from 28 August 2, 2020 to 3 September 2020.

The measurement was made using the experimental developed device (sensor module) which composes of several sensors and LoRa communication module for data transfer. The main part of the device is the MLX90640 sensor. This is an IR temperature array (32×24 values) sensor with a range from -40 °C to 300 °C. It has a typical target object temperature accuracy of 1 °C with precision across its full measurement scale. This sensor was used to measure the temperature of the monitored area. Ambient temperature and relative humidity were measured by SHTC3 sensor inside the sensor module and illuminance was measured by a VEML7700 sensor on the top of the sensor module. These sensors were connected to a microcontroller that performs all the sensor data readings, SD card data storage and LoRa communication. Simplified architecture of the whole measurement system is in Figure 1.

Figure 1 Simplified sensor module and communication architecture

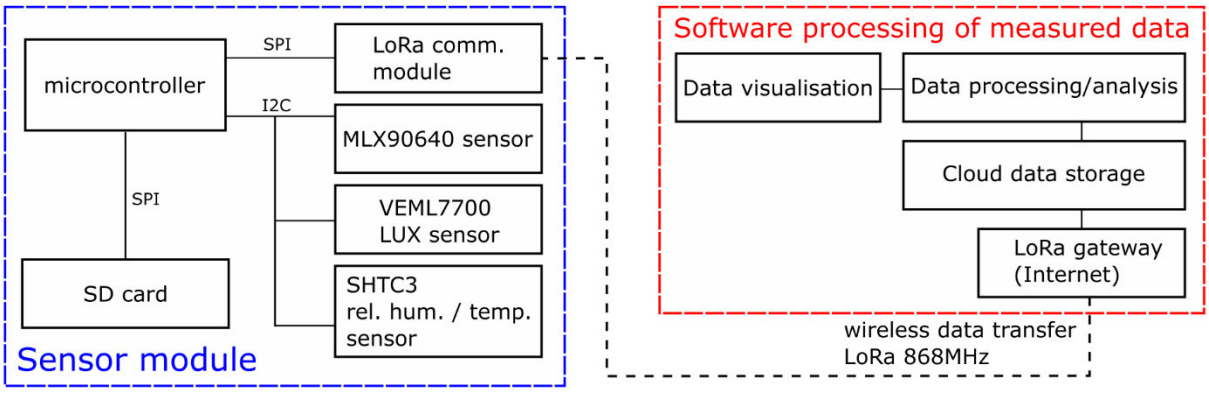

All the measured values were logged onto an SD card (1-minute interval) as raw unprocessed values for later data evaluation. The data reduction and outlier filtering of values are needed for the transmission via LoRa radio. The measured array of temperatures has to be reduced from 32 by 24 values down to 8 by 4 values using the mean value of each reduced subarray. Reduced values were then rounded to the nearest integer.

The monitored area was a pile of filter clay used in vegetable oil manufacturing. Data in this experiment were measured from one place with one sensor module. The sensor was placed 9 m from the pile and has a field of view of 55 ° horizontally by 35 ° vertically (see Figure 2).

Figure 2 Monitored area and sensor modules

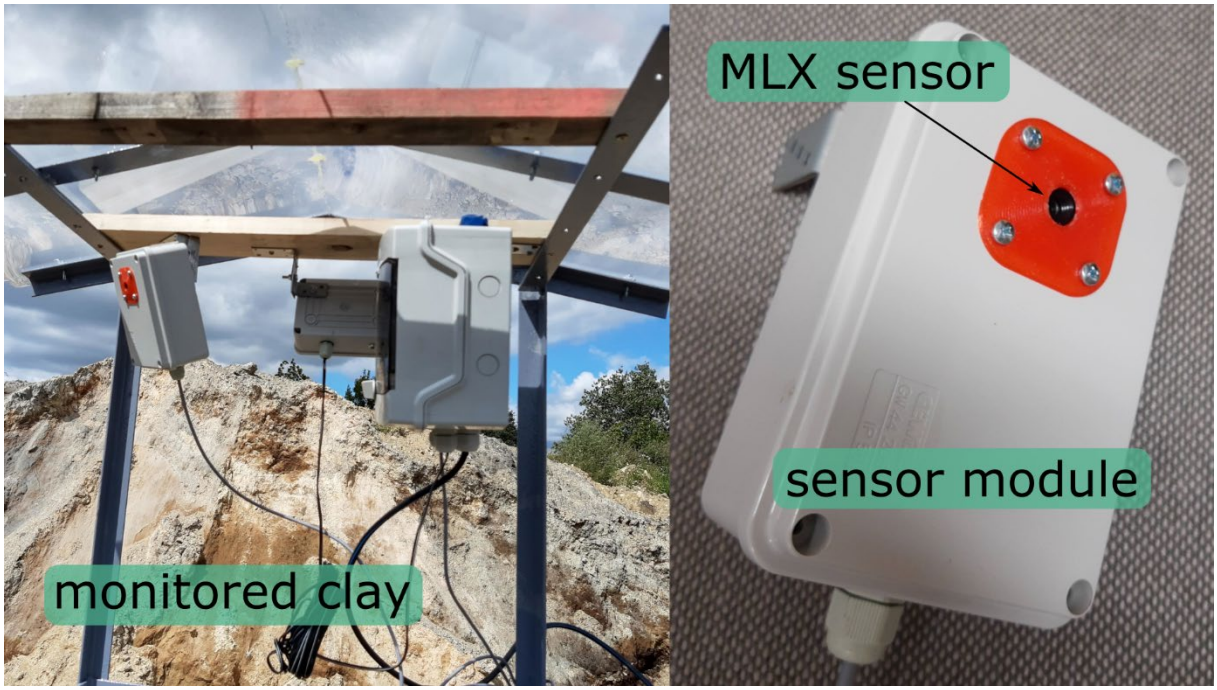

Data processing

Measured data were processed in Matlab 2020a. The first task was to filter outlier values using a *filloutliers()* function with a moving median window of 5 consecutive values (*filloutliers(data,'clip','movmedian',5)*). Normality of the temperature time series was then tested by Shapiro-Wilk test, Chi-square variance test and Kolmogorov-Smirnov tests. Correlation between datasets was determined using *corrcoef()* and *xcorr()* functions. The last part was a data reduction from 32 by 24 temperature values down to 8 by 6 values using *mean()* value of reduced subarray.

RESULTS AND DISCUSSION

Data evaluation

To be able to compare the measured data, we provide the weather data as they were measured by the Czech Hydrometeorological Institute (CHMI) for the given location and the given time period (see the Table 1.

Table 1 CHMI weather data – Náměšť nad Oslavou (CHMI 2020)

	Day 1	Day 2	Day 3	Day 4	Day 5	Day 6	Day 7
	28 August 2020	29 August 2020	30 August 2020	31 August 2020	1 September 2020	2 September 2020	3 September 2020
Rain [mm]	0	7.7	0.9	0.8	30.2	2.3	0
Sunshine [h/day]	10.8	1.1	0.8	-	0.6	6.7	9.4

All the data measured by the sensor module passed the normality test.

The Figure 3 depicts various correlations and a standard deviation of the mean temperature. There is a correlation between the illuminance and ambient temperature ($R=0.5789$, $p=0$), which is depicted on the top graph in the Figure 3. Then, there is a correlation between the illuminance and the mean surface temperature of the monitored area ($R=0.7044$, $p=0$). There is also a correlation between the ambient temperature and means surface temperature value ($R=0.8302$, $p=0$). These two correlations are visible when we combine the first and the third chart in the Figure 3. The maximum correlation

(*0.8226*) between the mean surface temperature and the illuminance is computed for a delay of 69 data points (hence minutes) using a cross-correlation function (*xcorr()* in Matlab).

Figure 3 Various types of measured data from 28 August 2020 to 3 September 2020 and their mutual relationships

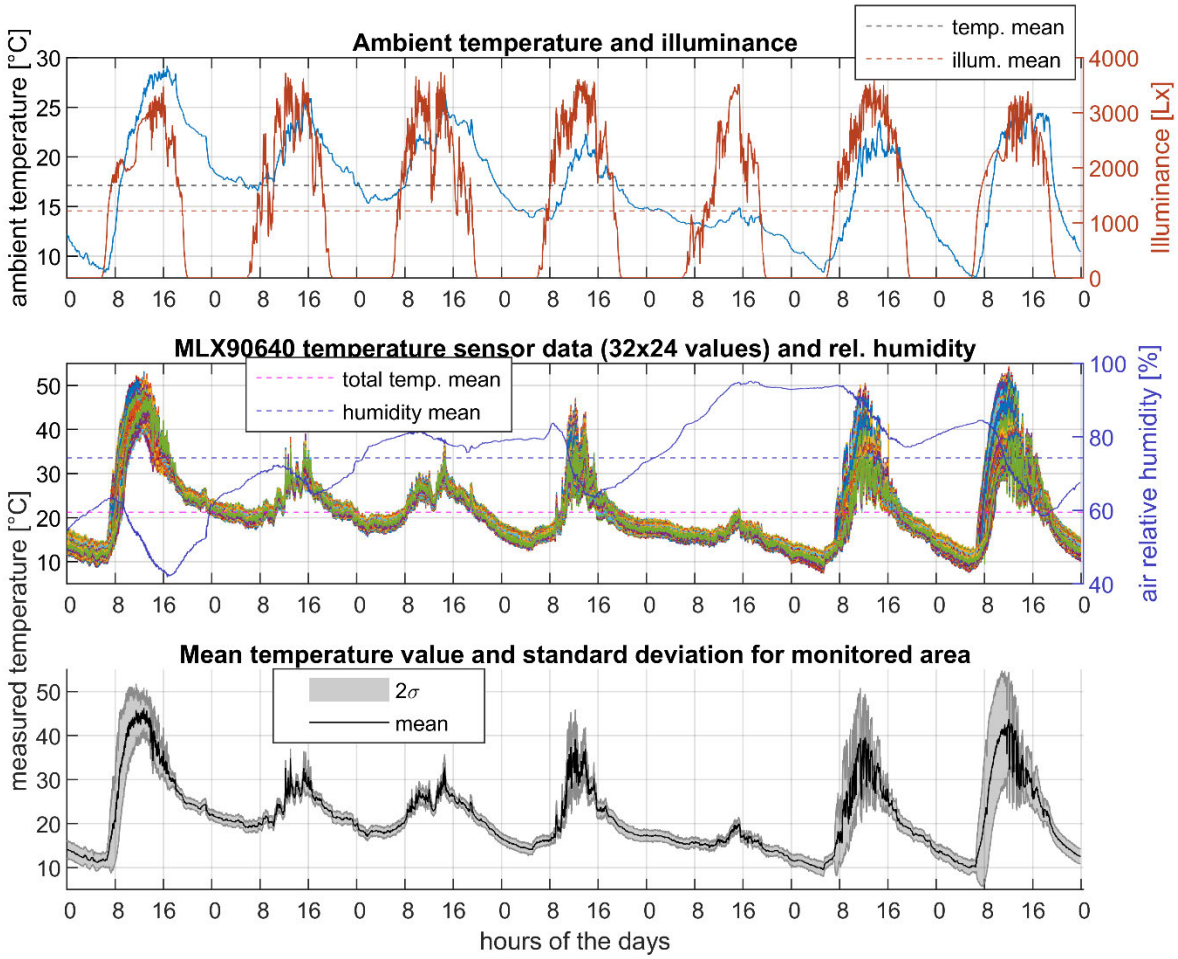

When the daily rainfall from the Table 1 is projected to the middle graph in the Figure 3, the effect of the rain on the monitored surface temperature can be seen on multiple days. After the rain on the 29 August – 7.7 mm, there is a drop in the temperature on the same day and on the following day (August 30). And after the rainy 1 September – 30.2 mm, there also a drop for the following days. On 1 September, the maximal monitored temperature is lower than a total mean value of measured temperature (dashed line in the graph). Days with a drop of temperature are also the days with a sunshine amount lower than 10 h/day.

Temperature variance interpretation – finding possible accidents

Detection of a potential fire hazard event relies on finding rising trends in the data. Using the standard deviation (see Figure 3) we can see there is a difference in the first (28 August) and the seventh day (3 September, boundary range of 2σ). This indicates there is a part of the array with a higher temperature than the rest. This is even easier to evaluate in combination with the homogenous monitored material. The big differences of the temperature among the particular spots of the array indicate the potential non-standard behaviour of the observed material, which might result into a potential fire.

The largest difference in the surface temperature in the measured data was on the seventh day (3 September) at 8:48 a.m. The temperature range is 22.0 °C (16.0–38.0 °C) and it is visible in the second and third graph of the Figure 3. The Figure 4 provides a more detailed view on this particular time period – the whole day of the 3 September. The visualisation in the Figure 4(C) shows the temperature distribution in the monitored area at 8:48 a.m. The Figure 4(A) shows a clear gap

between measured temperatures that is much more visible than in original non-reduced data (Figure 3). The left part in the temperature visualisation (from the morning to the early afternoon) has a higher temperature than the right part (from the late afternoon to the midnight). When taken into account the effect of the rain on the fifth day (1 September) the steep rise of the temperature is most probably caused by the wetness of the material. The overall shape of the temperature profile of the sixth day was similar to the first day (day without rain) so this does not indicate any unusual behaviour in the material. The same applies to the maximum daily temperature which was not significantly higher than on any of previous days.

Figure 4 Detailed view on the surface temperature for the seventh day (3 September)

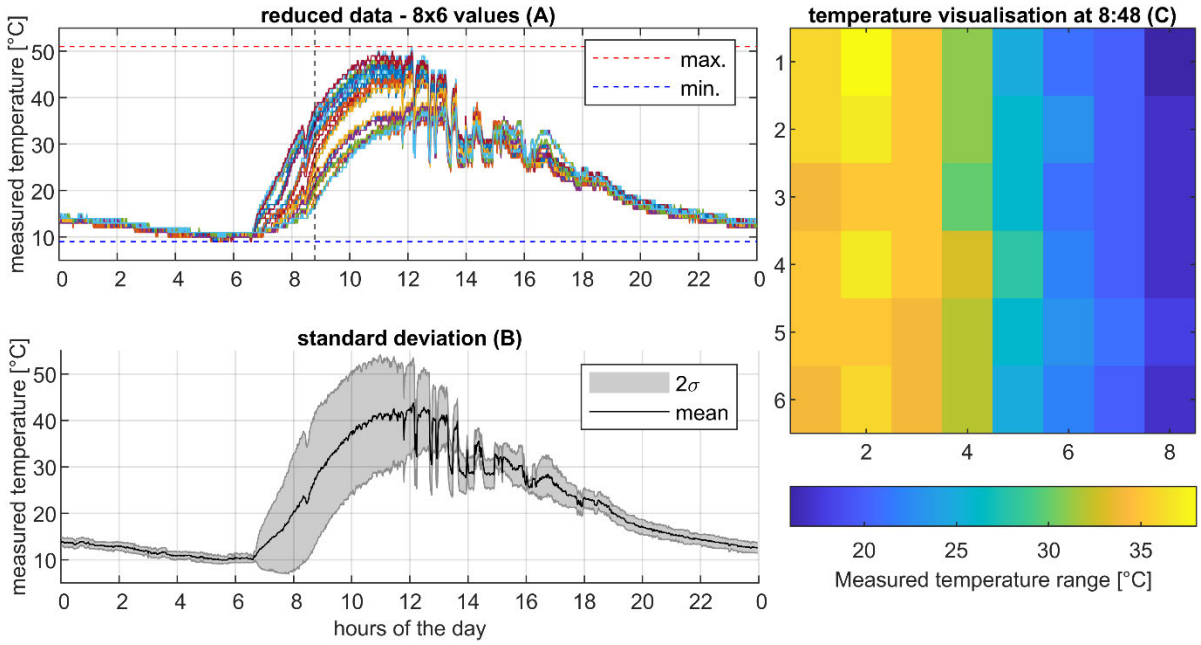

While there was no unwanted accident recorded during a duration of this experiment the measured data show it is possible to monitor a certain area with this type of measurement. Data evaluation also shows it is possible to use this type of measurement in different weather conditions and therefore differentiate between an effect of weather on the temperature or sensing a potential fire hazard event.

CONCLUSION

The experiment used an MLX90640 IR temperature array to measure the surface temperature of waste material, namely filter clay. The experiment aimed to validate the given approach in practice, the mutual correlations between the surface temperature, the ambient temperature and the illuminance are well visible from the results. When the measured surface temperature and the standard deviation are compared with the ambient temperature and the weather data (precipitation) measured by the CHMI in the given area, it is well visible that the higher standard deviation of the surface temperature relates with the usual weather conditions which increase the danger of spontaneous ignition – high temperature and illumination (day 1) and days after the rain (day 7). Even though the experiment was taken in a very short period of time (one week only), these preliminary results are promising for further research.

This experiment was a part of an ongoing research project and the future work will aim to gather more data for the software part of the system. This will allow finding clear decision borders in the data to evaluate potential fire hazard and to predict it.

ACKNOWLEDGEMENTS

The research was financially supported by the Technology Agency of the Czech Republic. Project identification number – TJ02000346.

REFERENCES

Buggeln, R., Rynk, R. 2002. Self-Heating In Yard Trimmings: Conditions Leading To Spontaneous Combustion. Compost Science & Utilization, 10 (2): 162–182.

CHMI, 2020. Portál ČHMÚ : Aktuální situace : Aktuální stav počasí : Česká republika : Stanice : Profesionální stanice : Přehled stanic : Náměšť nad Oslavou. [Online]. Available at: https://portal.chmi.cz/aktualni-situace/aktualni-stav-pocasi/ceska-republika/stanice/profesionalni-stanice/prehled-stanic/namest-nad-oslavou. [4. 9. 2020].

Coker, C. 2019. Managing compost and mulch fires. BioCycle, 60 (1): 26–28.

EUROSTAT. 2020. Waste statistics [Online]. Available at: https://ec.europa.eu/eurostat/statistics-explained/pdfscache/1183.pdf. [2020-09-15].

Lemieux, P. et al. 2004. Emissions of organic air toxics from open burning: a comprehensive review. Progress in Energy and Combustion Science [Online], 30 (1): 1–32. Available at: https://doi.org/10.1016/j.pecs.2003.08.001. [2020-09-15].

Liu, H., et al. 2015. Early detection of spontaneous combustion disaster of sulphide ore stockpiles. Tehnicki Vjesnik, 22 (6): 1579-1587

Mikalsen, R et al. 2020. Fires in waste facilities: Challenges and solutions from a Scandinavian perspective. Fire Safety Journal [Online], In Press. Available at: https://doi.org/10.1016/j.firesaf.2020.103023. [2020-09-15].

Oztemel, E., Gursev, S. 2018. Literature review of Industry 4.0 and related technologies. Journal of Intelligent Manufacturing [Online], 31: 127–182. Available at: https://doi.org/10.1007/s10845-018-1433-8. [2020-09-15].

Pastor, E., Planas, E. 2012. Infrared imagery on wildfire research. Some examples of sound capabilities and applications. In Proceedings of 3rd International Conference on Image Processing Theory, Tools and Applications (IPTA). Istanbul. Turkey, 15–18 October. Istanbul: IEEE, pp. 31–36.

Travnicek, P., et al. 2018. Quantitative analyses of biogas plant accidents in Europe. Renewable Energy [Online], 122 (1): 89–97. Available at: https://doi.org/10.1016/j.renene.2018.01.077. [2020-09-15].

Influence of phase structures on cutting surface quality and cutting tool degradation

Radim Smak, Jiri Votava, Adam Polcar
Department of Technology and Automobile Transport
Mendel University in Brno
Zemedelska 1, 613 00 Brno
CZECH REPUBLIC

xsmak@node.mendelu.cz

Abstract: Material cutting is a primary operation in most industries. Properly prepared semi-finished product is a prerequisite for easier production processes automation, such as machining on CNC machines, precision forging and others. The current production digitization and automation trend – Industry 4.0 directly requires the most accurate semi-finished products possible. The purpose of this article is to analyse the cutted materials microstructure and evaluate the effect of hardness and microstructure on the saw blade wear. The hardness of the samples will be measured by the Vickers method according to ČSN EN ISO 6507. The microhardness measurement will be performed using a Hannemann microhardness tester according to ČSN EN ISO 6507-1. These methods make it possible to predict the saw blade life based on the material hardness and phase structures.

Key Words: surface roughness, steel, saw bands, wear resistance, hardness

INTRODUCTION

Cutting of technical materials can be divided into two basic groups: the conventional machining technological processes, which is represented mainly in general engineering, and the unconventional machining methods which are represented mainly in the field of precision manufacturing (Sarwar et al. 2018). In a conventional material cutting, due to mechanical forces, chips are removed from the base material and thus a cutting gap is formed.

The unconventional machining methods are based on the physical and chemical principle of the base material disruption. It is a force-free action on the machined material. With these technologies, we can not talk about the formation of classic chips, which are created during machining with a cutting tool. These methods include technologies such as laser, plasma or electron beam cutting. Today, these technologies are used for difficult-to-machine materials cutting mainly, which conventional machines are not able to work with (Cao et al. 2018). The considerable unconventional cutting development can be also observed in the field of complex semi-finished products machining. These methods can also achieve highly irregular surfaces (external and internal). Especially using automation systems which are based on electronic data from the CAD system. These systems are capable to create a semi-finished product for the future workpiece with maximum accuracy and defined tolerances of shape or position (BARCAL 1989).

The unconventional technologies disadvantage is the considerable financial demands of machinery and their narrowly specialized production profile. These technologies are especially suitable for large-scale production with the maximum machine use. Cutting material for simple semi-finished products, a conventional machining using band saws will always be at the forefront due to flexibility and low financial demands.

MATERIAL AND METHODS

The research consists of two parts, the first part is focused on the surface roughness analysis, which is the result of the material cutting using a band saw. The second part deals with the machined

surface surroundings microstructure analysis and describes the influence of structural phases and the Widmanstätten layer on the cutting band wear.

The machined surface is prepared using a Bomar 160.120 band saw with the possibility of the belt speed modulation. For research purposes, round bar samples with a diameter of 35 mm were prepared and the belt cutting speed was set at 50 m/min. Selected saw bands had 12 teeth per inch with a rake angle of 10 °. The pressing force was set at 10 N. This force is constant when cutting all samples. The material was chosen based on the tested material heat treatment requirement. It is therefore S 235 JRG1 and C45 steel. The C45 steel was subjected to a heat treatment to increase the hardness, which simulated creating a heat affected area, for example, from laser cutting. Based on the performed tests, it is then possible to predict the cutting saw bands service life, or to recommend the cutted material hardness limit, when it is necessary to use another cutting technology. To determine the tested materials mechanical properties, the following tests were performed:

1. The tested material and saw belt hardness was measured according to ČSN EN ISO 6507.
2. The transverse and longitudinal surface roughness Ra was monitored on the prepared samples.
3. According to metallographic cuts, the given material basic structure was determined.
4. When cutting samples with the selected hardness, the saw belts wear was determined.

Tested materials characteristic

Material cutting using a band saw is one of the technologies designed primarily for metallurgical semi-finished products preparing, where an advantageous price to performance ratio is achieved. However, hard materials or hard structural phases contained in the cutted material can be problematic. The reason is the combination of mechanical and physical properties that increase the contact forces between the tool and the workpiece and increase the process temperature (Sales et al. 2020). For this research, the C 45 steel was selected, because it can be quenched to high hardness values so aggravated machining conditions can be simulated.

S 235 JRG1 is a usual quality structural steel intended primarily for welding. When cutting by laser or plasma, there is a risk of the Widmanstätten structure formation, which fundamentally affects the machinability of steel. The chemical composition of used steel is given in Table 1.

C45 is a structural steel intended for tempering and surface hardening. This material is suitable for large and medium forgings. Hardened steel is suitable for shafts of mining machines, turbochargers, augers, etc. The weldability of this steel is difficult because the carbon equivalent. The C45 steel chemical composition is given in Table 1.

Table 1 Chemical composition of used steels

Steel	Chemical composition [%]					Transformation tepm. [°C]			
	C	Mn	Si	P_{max}	S_{max}	Ac_1	Ac_3	Ar_1	Ar_3
S 235 JRG1	0.17	-	-	0.045	0.045	720	870	830	750
C45	0.45	0.5	0.17	-	-	720	780	725	685

The C45 steel heat treatment was performed in an MP 05 – 1.1 laboratory furnace. The heat treatment process took place without a protective atmosphere with the access of air. The process parameters are shown in Table 2.

Table 2 Heat treatment of C45 steel

Hardening			Tempering	
Austenitization [°C]	Emdurance [min]	Cooling	Temperature [°C]	Cooling
840	30	water	530	air

RESULTS AND DISCUSSION

Hardness and roughness

The universal Vickers method was used to analyze the tested materials and the cutting belt hardness. Indentor with an angle of 136 ° and the loading force 294 N (30 kp) was used. According to the hardness the load delay was determined to 15 s. The measured values are given in Table 3.

Table 3 Hardness of the samples

Material	Average [HV_{30}]	Standard deviation [HV_{30}]	Var. coefficient [%]
S 235 JRG1	185.4	4.3	2.3
C45	236.0	4.0	1.7
C45 heat-treated	300.6	4.5	1.5
Saw band	363.8	4.5	1.2

The surface roughness was measured with a Mitutoyo SJ-201 tester. It is a tactile profiler designed for measuring the arithmetic average roughness Ra. Ten measurements were performeded on each sample. The values were graphically processed, see Figure 1.

Figure 1 Processed sample roughness

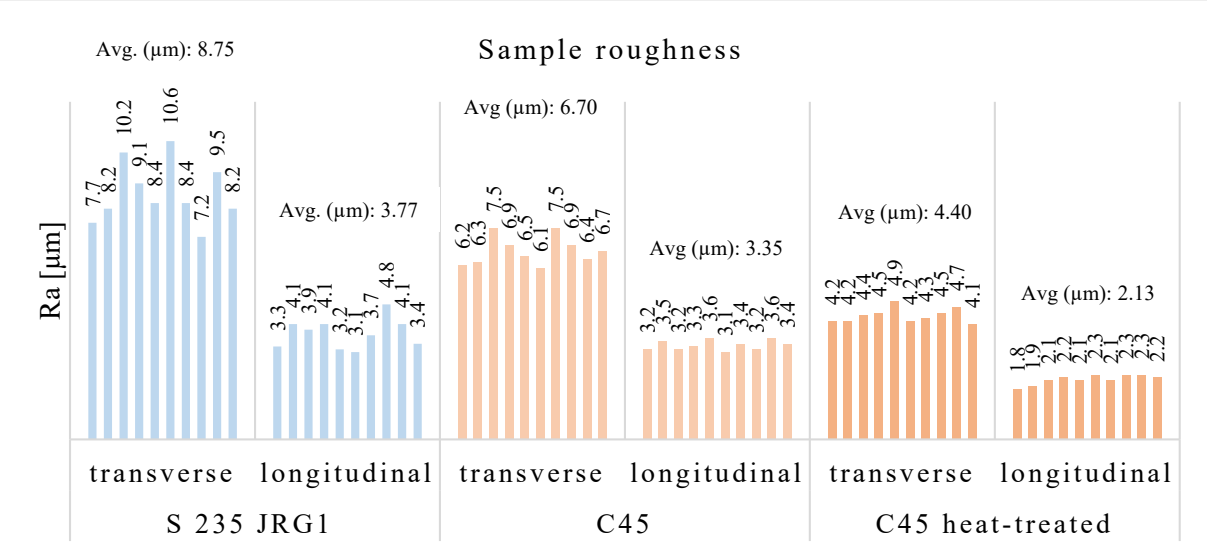

The roughness measurement results show that lower roughness values in the cutting direction are always achieved. The difference between the roughnesses is approximately 50%. The cutted material hardness has a significant effect on the machined surface quality too. With increasing hardness, the machined surface roughness decreases in both directions by approximately 35%. In contrast, research conducted by (Hlaváčová et al. 2020) shows that higher surface roughness values are achieved when cutting hardened steel c45 with an abrasive water jet (compared to conventional machining). The resulting surface roughness could be even reduced by adjusting the cutting conditions. By the cutting speed reducing, lower surface roughness values are achieved. (Sattar et al. 2019)

Internal structure of samples

The metallographic cuts of used steels were prepared. Due to its chemical composition, the S 235 JRG1 steel structure is mainly ferritic with pearlitic formations at the ferritic grains interface. The C45 steel initially had a ferritic-pearlitic structure with pearlite distributed at the grain boundaries. After heat treatment, this steel has a mostly sorbitic structure with dissolved martensite and residual austenite (see Figure 2). The occurrence of these hard structural phases significantly affects the cutting belt service life as well as all cutting tools (Votava et al. 2013). These phases are created either as a result of the required heat treatment or as an undesired heat-affected layer during the material

separation by flame or laser. When cutting steel with a flame or laser, the Widmanstätten structure can form around the cut, which leads to an increase of hardness and a decrease of toughness around the cut (Bhadeshia 2001). The Widmanstätten structure danger is manifested mainly in the field of a semi-finished products production for automated machining. There is usualy a requirement to cut off the area created by previous laser cutting. The saw blade works in the immediate vicinity of this area. Table 4 shows the microhardness of the area where the Widmanstätten structure occurs in S 235 JRG1 steel, see Figure 3. The microhardness of free carbides or ledeburite in cast iron is given as another example of cutting condition aggravation.

Figure 2 Hardened C45 steel structure

Figure 3 Widmanstätten structure

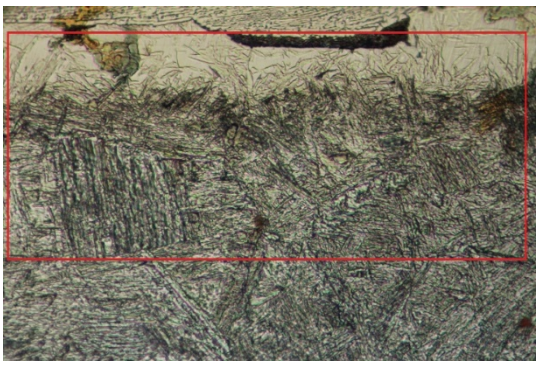

Saw belt wear

The cutting belt wear was measured in each case after making ten cuts from a round bar made of the selected material and hardness. The measurement was performed on a laboratory microscope with an integrated scale. The flat surface length which is created on the saw tooth blade was chosen as the cutting belt wear parameter. To ensure the highest possible quality of results, each belt was divided into four individual sections. Five teeth were selected from each section, on which the worn areas was measured. Statistical results are shown in Table 4.

Table 4 Saw belt wear

Type of material	Average microhardness [$HV_{0.1}$]	Structural phase	Average macrohardness [HV_{30}]	Average length [mm]	Standard deviation [mm]	Var. coefficient [%]
C45	230	pearlite	200	0.1028	0.0986	0.0097
	260	pearlite	225	0.1554	0.1723	0.0297
	366	Sorbite + ferrite	250	0.1954	0.2023	0.0409
	480	Sorbite	275	0.2554	0.2241	0.0502
	517	Sorbite	300	0.3994	0.3004	0.0902
	805	Sorbite + martensite	350	0.7468	0.1319	0.0174
Widmanstätten structure	489	-	-	-	-	-
Free carbides	942	-	-	-	-	-
Ledeburite	1221	-	-	-	-	-

Figure 4 shows the dependence of the teeth wear on the hardness of cutted C45 steel. The model was supplemented with Working-Hotelling confidence bands. The Fisher-Snedecor test was used for testing of model statistical signification. It was found that both model and all its parameters are statistically significant (95% significant level). The model calculating and tests were performed by the QC.Expert 3.3 software. The measured results show that with the increasing cutted material hardness, the teeth wear increases exponentially. Saw belt with a hardness of approximately HV_{30} 360 can cut the materials with a hardness of HV_{30} 250 well. The wear of the teeth after ten cuts

does not exceed 0.15 mm. In the case of samples with a hardness approaching HV_{30} 300, there is already considerable tooth edge wear and some teeth are also broken out (Figure 6). For samples which are close to the belt hardness, the teeth are unacceptably worn and mostly broken. Research realised by Suyama et al. 2020 shows that as the workpiece hardness increases, the tool edge abrasive wear gradually predominates. Abrasive wear is a serious problem not only in mechanical engineering, but also in the agricultural sector during tillage. Due to abrasive wear, the cutting tool geometry changes, which increases the cut energy intensity. Figures 5 and 6 show the new and the worn belt comparison. (Votava 2015).

Figure 4 Belt wear depending on cutted steel hardness

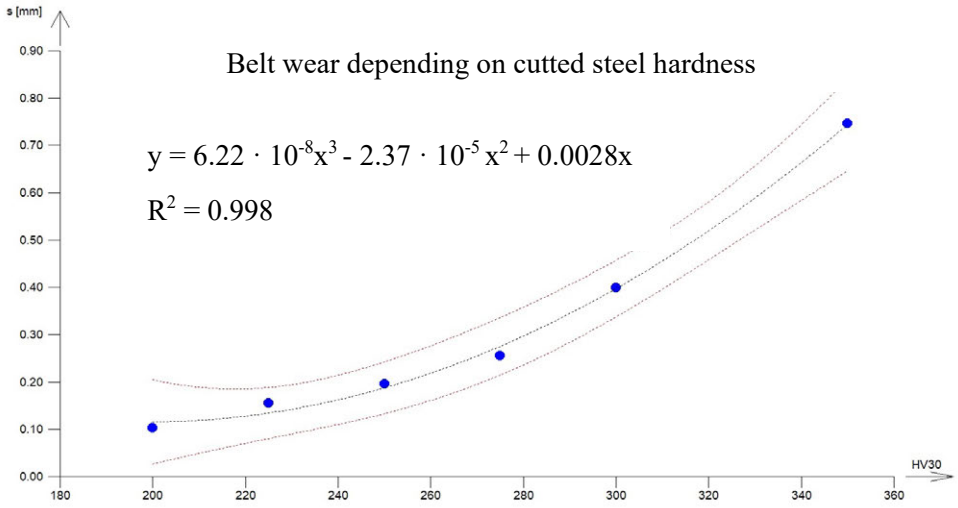

Figure 5 Brand new belt

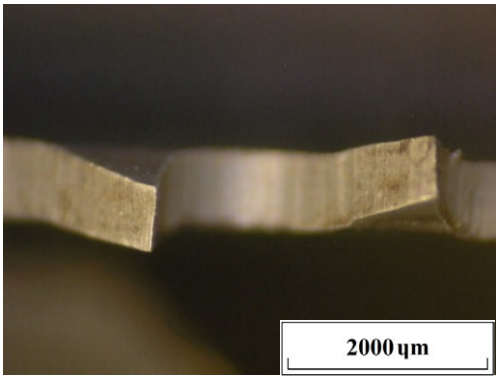

Figure 6 Worn belt, HV_{30} 300 sample

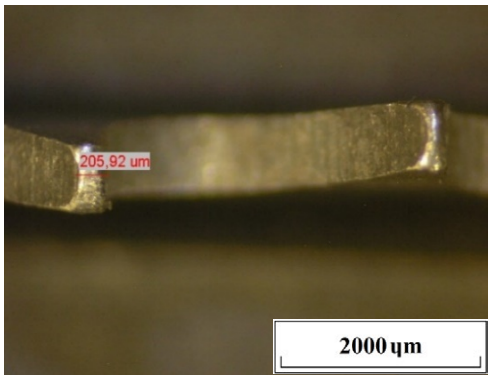

The machined surface analysis is common to the entire area of machining. Sales et al. 2020 shows the unsuitable process fluid presence as a reason for frequent tooth breakage. Especially at low cutting speeds, there is a demand for excellent process fluids penetration properties, which reduce friction and process temperature. At higher cutting speeds, the process fluid cooling properties prove to be the most important.

CONCLUSION

Material cutting is one of the basic technologies of engineering production. The trend is to increase the speed and quality of production. Conventional cutting of metallurgical semi-finished products using band saws allows the use of a favorable ratio between the processing price and the output quality. Depending on the semi-finished product size, the deviation tolerance varies in the order of tenths of a millimeter. Therefore considerable attention must be paid to the quality and the machined surface roughness. Based on the experimental measurements, a very good machined surface quality can be reached in common structural steels. According to the cutting belts optical evaluation, the rapid

cutting tool wear during the cutting of steels with a presence of harder structural phases is evident. A major problem can arise with steels, which have a higher percentage of carbon. A hard structural phase formed near the laser cutting surface rapidly increases the belt wear. Even the heat affected layer depth is small, the cutting belt is unable to withstand these hard structural phases for a long time. This assumption was confirmed in the experimental part. When cutting material with saw belt, it is necessary to select optimal cutting conditions and evaluate the individual materials which may be processed.

ACKNOWLEDGEMENT
This research was created with the contribution of the project ZETOR (EG15_019/0004799 – ZETOR TRACTORS a.s.) – Optimal aggregation of machines with a tractor.

REFERENCES

Barcal, J. 1989. Nekonvenční metody obrábění. 1st ed., Praha: ČVUT.

Bhadeshia, H.K.D.H. 2001. Bainite in steels: theory and practice. 3rd ed., London: IOM Com.

Cao, X. et al. 2020. A study on the laser-assisted milling of 13-8 stainless steel for optimal machining. Optics & Laser Technology [Online], 132: 106473. Available at: https://linkinghub.elsevier.com/retrieve/pii/S0030399220311063. [2020-08-22].

Hlaváčová, I. et al. 2020. Influence of Steel Structure on Machinability by Abrasive Water Jet. Materials [Online], 13(19): 4424. Available at: https://www.mdpi.com/1996-1944/13/19/4424. [2020-11-07].

Sales, W. et al. 2020. A review of surface integrity in machining of hardened steels. Journal of Manufacturing Processes [Online], 58: 136–162. Available at: https://linkinghub.elsevier.com/retrieve/pii/S1526612520304667. [2020-08-15].

Sarwar, M. et al. 2016. Forces, wear modes, and mechanisms in bandsawing steel workpieces. Proceedings of the Institution of Mechanical Engineers, Part B. Journal of Engineering Manufacture [Online], 224(11): 1655–1662. Available at: http://journals.sagepub.com/doi/10.1243/09544054JEM1872. [2020-08-05].

Sattar, H. et al. 2019. The Experimental Study on the Machining Conditions of Heat Treated Medium Carbon Steel using Ceramic Cutting Tool. International Journal of Mechanical and Production Engineering Research and Development [Online], 9(4): 1143-1150. Available at: http://www.tjprc.org/publishpapers/2-67-1563537026-118.IJMPERDAUG2019118.pdf. [2020-11-07].

Suyama, D. et al. 2020. Influence of tool vibrations on tool wear mechanisms in internal turning of hardened steel. Journal of the Brazilian Society of Mechanical Sciences and Engineering [Online], 42(7): 370. Available at: http://link.springer.com/10.1007/s40430-020-02452-w. [2020-09-02].

ÚNMZ. 2018. Kovové materiály – Zkouška tvrdosti podle Vickerse. Část 1: Zkušební metoda. ČSN EN ISO 6507-1. Praha: Úřad pro technickou normalizaci, metrologii a státní zkušebnictví.

ÚNMZ. 2015. Kovové materiály – Zkouška tvrdosti podle Vickerse. ČSN EN ISO 6507. Praha: Úřad pro technickou normalizaci, metrologii a státní zkušebnictví.

Votava, J. et al. 2015. Aplikace tvrdokovových nástřiků u nožového segmentu ořezávacího ústrojí sklízečů cukrové řepy. Listy cukrovarnické a řepařské [Online], 131(11): 341–346. Available at: http://www.cukr-listy.cz/on_line/2015/PDF/341-346.pdf. [2020-08-18].

Votava, J. 2015. Influence of edge radius of sintered-carbide tip on roughness of machined surface. Acta Universitatis Agriculturae et Silviculturae Mendelianae Brunensis, 61(5): 1497–1504.

Determination of Young's modulus of samples made from waste materials

Ladislav Smutny[1], Martin Sotnar[1], Omar Al-Shantir[2], Jan Marecek[1]
[1]Department of Agricultural, Food and Environmental Engineering
Mendel University in Brno
Zemedelska 1, 613 00 Brno
CZECH REPUBLIC
[2]Department of Physics
Constantine the Philosopher University in Nitra
Tr. A. Hlinku 1, 949 74 Nitra
SLOVAKIA

martin.sotnar@mendelu.cz

Abstract: The article is focused on the testing of the impulsion excitation technique for determination of Young's modulus of rectangular bar samples made from recycled waste materials. Usage of this type of substances, especially the mixture of PVC and glass, could lead to poor quality samples. Therefore, the determination of Young's modulus and also the logarithmic decrement could be tricky. For the testing of the possibility of measuring these parameters, the impulse excitation technique was used on such material. The in homogeneities occurred due to not fully filled PVC in the pores.

Key Words: waste materials, impulse excitation technique, Young's modulus

INTRODUCTION

The amount of waste from human activities is growing worldwide. Polyvinyl chloride (PVC) is one of the most commonly used thermoplastics. Approximately 35 million tons of this material is consumed annually in the industry (La Mantia 1996). Disposal of PVC waste has been a matter of recent years (Garcia 2007). Landfilling is one way to dispose of this waste, but given the chlorine content and other potential threats to the environment, it is advisable to look for other ways to dispose of this waste (La Mantia 1996). One option is to recycle this waste into specific products (Burat et al. 2009).

Waste glass is a potentially recyclable component of waste, but a large part of this waste ends up in landfills. All glass products have a limited lifespan (Zheng 2013). By recycling this waste, it is possible to reduce the consumption of these materials. In 2013, the Americans recycled about 27% of waste glass (Mohajerani et al. 2017). Many technologies for the production of recycled glass are difficult to sort this waste. For this reason, it is not possible to constantly increase the recycled amount (Kadirgamar 2014). In the European Union, 73% of glass packaging was recycled in 2015.

Construction is one of the industries that can use this waste (Mohajerani et al. 2017). For these purposes, several studies have already been carried out on the use of construction waste, such as bricks, concrete, asphalt concrete, and others (Ukwatta et al. 2016).

The volume of construction products is growing worldwide. It is assumed that by 2030 there will be an increase in construction output by 85% (Roy 2019). It can therefore be assumed that the demand for recyclable materials in this sector will also increase.

To be able to use these waste materials in construction, it is necessary to know their basic characteristics, which include Young's modulus of elasticity (E).

Therefore, this study is devoted to verifying the applicability of the method of measuring the young's modulus of elasticity according to ASTM E 1876-01 on samples from recycled waste. As is mentioned in this standard (see chapter 5.1) this technique could be applied on homogeneous, isotropic samples. The aim of this study was to verify the limit of determination of Young's modulus, in the case of inhomogeneous, non-isotropic samples. This goal will be achieved by the comparison of the obtained Fast Fourier Transformation spectra of samples with different porosity.

MATERIAL AND METHODS

Samples for testing the young's modulus of elasticity were made from waste materials. These materials were sorted from municipal waste. It was 30% of a mixture of crushed PET bottles and 70% of crushed container glass of various grain sizes. From this mixture, two groups of samples were made. Figure 1 shows the surface of the sample from each group used in this study. The properties of the input materials for the production of samples (grain size, specific weight, porosity, etc.) and the production technology are the know-how of the company that supplied the samples (see acknowledgements). Sample from group 1 was made, that the PVC fills the pores in the sample, and group 2 is the sample with the visible glass shards. Note that the sample preparation was performed by heating and melting at the temperature~150 °C and pressing to the required size 10×10×150mm. From each group, 8 samples for determination Young's modulus were made.

Figure 1 The image of the surface of the samples

Legend: 1 – Sample with the admixture of glass with larger grain size, 2 – sample with admixture glass with a smaller grain size

Apparatus:

The apparatus for the determination of Young's modulus of the rectangular bar is shown in Figure 2. This apparatus consists of an impactor (1), sample (2), support system (3), the microphone and signal amplifier (4) and computer (5). l is the length of the sample.

Figure 2 The apparatus for the determination of the Young's modulus

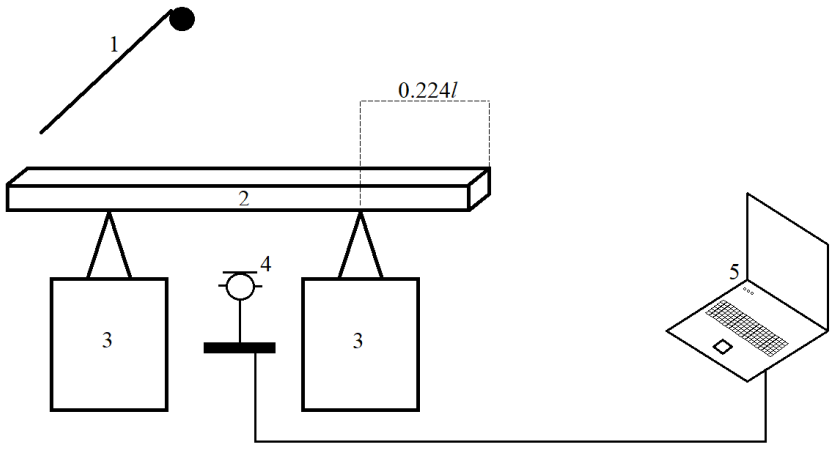

Mathematical background:

Using the aforementioned apparatus, the experimentally obtained frequency spectrum is analyzed by the fast Fourier transform (FFT) and the resonant frequency (f_r). Then, in case of rectangular bar, the Young's modulus can be calculated, according to the ASTM E 1876-01 as

$$E = 0.9465 \frac{m f_r^2}{b} \frac{L^3}{a^3} T_1,$$

where m is the mass, b is width, a is the thickness and L is the length of the sample. T_1 is the correction factor is the form

$$T_1 = 1 + 6.585(1 + 0.0752\mu + 0.8109\mu^2)\left(\frac{a}{L}\right)^2 - 0.868\left(\frac{a}{L}\right)^4 - \left[\frac{8.340(1 + 0.2023\mu + 2173\mu^2)\left(\frac{a}{L}\right)^4}{1 + 6338(1 + 0.1408\mu + 1.536\mu^2)\left(\frac{a}{L}\right)^2}\right],$$

where μ is the Poisson's ratio.

The uncertainties of these measurements were calculated based on the following equation:

$$\bar{s} = \sqrt{\left(\frac{\partial E}{\partial a}\right)^2 (\Delta a)^2 + \left(\frac{\partial E}{\partial b}\right)(\Delta b)^2 + \left(\frac{\partial E}{\partial L}\right)^2 (\Delta L)^2 + \left(\frac{\partial E}{\partial f_r}\right)^2 (\Delta f_r)^2}$$

where:

$$\frac{\partial E}{\partial a} = -2.8395\frac{m f_r^2}{b}\frac{L^3}{a^4}T_1$$
$$\frac{\partial E}{\partial b} = -0.9465\frac{m f_r^2}{b^2}\frac{L^3}{a^3}T_1$$
$$\frac{\partial E}{\partial L} = 2.8395\frac{m f_r^2}{b}\frac{L^2}{a^3}T_1$$
$$\frac{\partial E}{\partial f_r} = 1.893\frac{m f_r}{b}\frac{L^3}{a^3}T_1$$

The same apparatus could be also used to determine the logarithmic decrement δ according to the following equation (Inman 2008):

$$\delta = \frac{\pi(f_2 - f_1)}{\sqrt{3}}$$

where the f_1 and f_2 are described in Figure 3.

Figure 3 Determination of the logarithmic decrement from the half-width of the resonant peak. Figure taken from (Húlan et al. 2014).

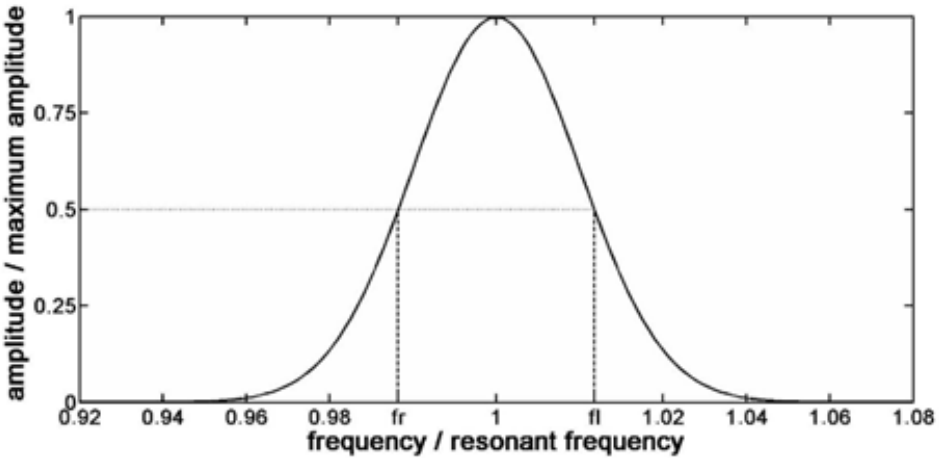

RESULTS AND DISCUSSION

As was previously mentioned, the samples with the same size of glass shards were used, where the only difference between them was the homogenization process during production. The surface of the two samples from each group is shown in Figure 1.

Figure 4 Recorded evolution of vibrations after excitation

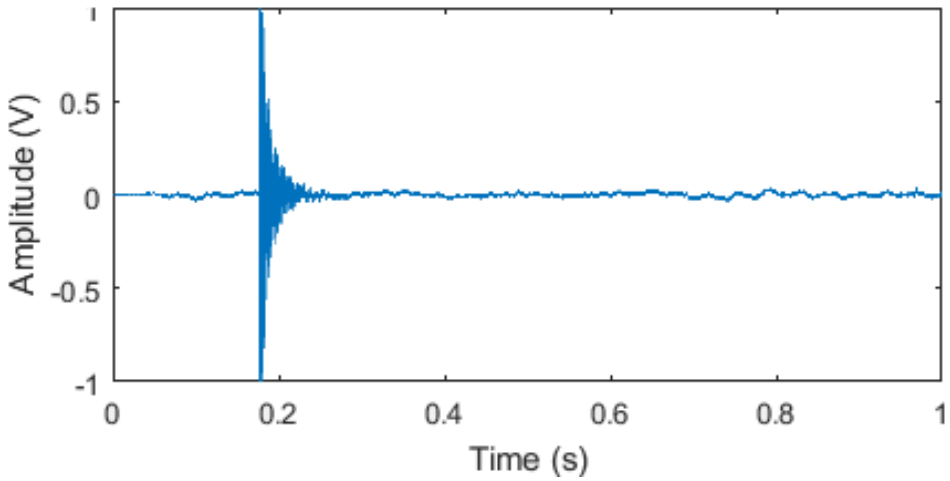

Using the apparatus described in the previous section, the evolution of the vibration after excitation was recorded (see Figure 4). Then, using the FFT the resonant frequency was determined. The results show, that in the sample where the PVC not fully filled the pores (Figure 5), the resonant frequency determination could be problematic from the FFT spectrum, and thus the value of E could not be calculated. If the resonant peak was determined, the determination of the logarithmic decrement from the half-width of the resonant peak can be still the problem due to the several peak overlay.

Figure 5 The FFT spectrumof the sample PVC not fully filled the pores between glass shards

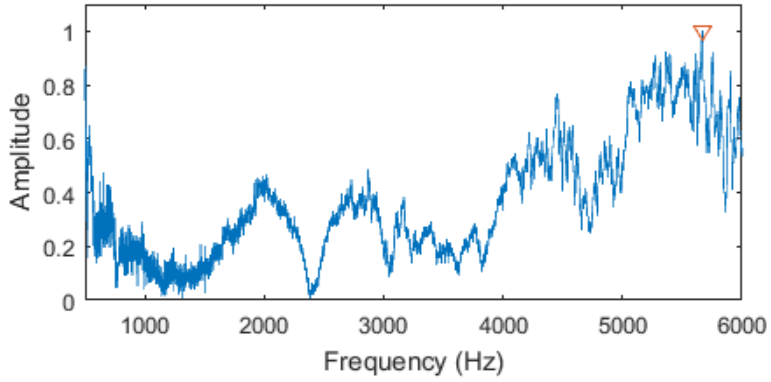

Figure 6 The FFT spectrumof the homogeneous sample

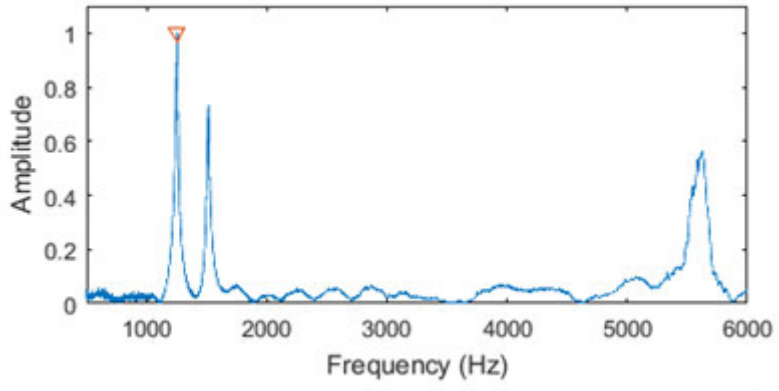

The different situation is in the case of the samples from the second group (see Figure 6), where the resonant peak could be determined. Also the noise in the FFT spectrum, in comparison with the significantly non-homogeneous sample, is minimal. The determined value of resonant frequency, in this case, is $f_r = (1506 \pm 3)$ Hz. Using this value together with dimensions of the sample, the calculated value of Young's modulus $E = (6.23 \pm 0.5)$ GPa and $\delta = 0.045 \pm 0.005$. It can be also concluded that the glass content leads to the higher value of Young's modulus, where for the rigid PVC its value

is ~3.4 GPa (Titow 1984). In (Müssing et al. 2006) measured the young's modulus of elasticity of various mixtures of waste plastics from end-of-life vehicles according to DIN EN 61. The resulting values show different variability with a value of (0.02–0.07) GPa. Only some samples here reach the values of factory products without the use of waste materials. Further analyzes showed a value of Young's modulus of elasticity of (0.42–0.46) GPa in various mixtures of plant fibers with thermoplastic starch (Wollerdorfer and Bader 1998). Therefore, it can be concluded, that the Young's modulus of elasticity in materials using waste shows considerable differences, so it is necessary to test different mixtures and ratios to describe the properties of these materials.

It is worth to noting, that the value of E is similar as in the case of traditional ceramics which is usually used material for bricks (Húlan et al. 2019). This comparison is important from the technological point of view, where the producer of samples which were used in this study, presented this material as building materials.

Based on these results, it can be concluded, that the particle size of the glass shards is not the limiting factor. On the other hand, it depends on the homogeneity and ability of the PVC to fills the pores.

CONCLUSION

In this study, the applicability of impulse excitation technique on the poor quality samples made from the waste materials was studied. The Young's modulus and the value of logarithmic decrement were calculated based on the frequency spectrum, which was analyzed by the fast Fourier transform. The results show, that this technique can be used on such mixtures, however, there is the limit in the case when the PVC is not fully filled in the pores. Another important factor, as expected, is homogeneity, where even if the bigger glass shards are used, the E and δ could be determined in a more homogeneous sample.

ACKNOWLEDGEMENTS

The authors would like to thank Jakub Jón and the staff of VIA ALTA Company for providing the samples.

REFERENCES

ASTM. 2006. Standard Test Method for Dynamic Young's Modulus, Shear Modulus, and Poisson's Ratio by Impulse Excitation of Vibration. ASTM E1876-01. West Conshohocken: ASTM International.

Burat, F. et al. 2009. Selective separation of virgin and post-consumer polymers (PET and PVC) by flotation method. Waste Management, 29: 1807–1813.

Garcia, D. et al. 2007. Compatibility of recycled PVC/ABS blends effect of previous degradation. Polymer Engineering Sciences, 47(6): 789–796.

Húlan, T. et al. 2014. Determination of the logarithmic decrement of poor quality samples. 15th International scientific conference of PhD. students, young scientists and pedagogues. Faculty of Natural Sciences, Constantine the Philosopher University in Nitra.

Húlan, T. et al. 2019. Development of Young's modulus of natural illitic clay during heating and cooling stage of firing. Clay Minerals, 54(3): 229–233.

Inman, D.J. 2008. Engineering Vibrations. Upper Saddle, NJ: Pearson Education, Inc. 53.

Kadirgamar, K. 2014. The applications of recycled crushed glass in civil construction in the Northern Territory. Charles Darwin University. Bachelor thesis.

La Mantia, F.P. 1996. Recycling of PVC and mixed plastic waste. Toronto: Chemical Technique Publishing.

Mohajerani, A. et al. 2017. Practical recycling applications of crushed waste glass in construction materials: A review. Construction and Building Materials, 156: 443–467.

Müssing, J. et al. 2006. Exterior components based on renewable resources produced with SMC technology-Considering a bus component as example. Industrial Crops and Products, 24(2): 132–145.

Roy, M. 2019. Using Construction and Demolition Waste as Construction Materials for New Buildings. In Encyclopedia of Renewable and Sustainable Materials. Netherlands: Elsevier, pp. 330–344.

Titow, M.V. 1984. PVC Technology. Netherlands: Elsevier Applied Science Publishers Ltd.

Ukwatta, A. et al. 2016. Variation in physical and mechanical properties of fired-clay bricks incorporating ETP biosolids. Journal of Cleaner Production, 119: 76–85.

Wollerdorfer, M., Bader, H. 1998. Influence of natural fibres on the mechanical properties of biodegradable polymers. Industrial Crops and Products, 8(2): 105–112.

Zheng, K. 2013. Recycled glass concrete. In Eco-Efficient Concrete. Cambridge: Woodhead Publishing, pp. 241–270.

Mathematical models for temperature dependent viscosity of biobutanol and gasoline blends

Daniel Trost[1], Adam Polcar[1], Petr Dostal[1], Josef Jelinek[2], Jiri Cupera[1], Vojtech Kumbar[1]
[1]Department of Technology and Automobile Transport
Mendel University in Brno
Zemedelska 1, 613 00 Brno
[2]Department of Combat and Special Vehicles
University of Defence in Brno
Sumavska 4, 662 10 Brno
CZECH REPUBLIC

xtrost@mendelu.cz

Abstract: Butanol is a potential alternative fuel for compensating the running out of fossil based liquid fuels. Biobutanol is butanol produced from renewable sources by fermentation of simple sugars. It could by produced locally, in each region of usage. Hence a local production and no need of an international fuel transportation, this method could be more ecological, and it also could bring significant savings. Butanol can be easily mixed with petrol, at any percentage and used as a fuel. A dynamic viscosity of biobutanol and gasoline blends where investigated in this paper. Various temperature (from -10 °C up to 40 °C) and various ratios between biobutanol and gasoline (0, 5, 10, 85, 100 vol. %) were tested. In the experiment four various models for viscosity of fuels were tested and compared. It was found, the Vogel model has the best result, according to the coefficient of determination R^2.

Key Words: mathematical models, viscosity, biobutanol, gasoline, temperature

INTRODUCTION

For a many years there has been an effort to find a suitable replacement for a fossil fuel. One of the possible option is a fuel production, from renewable sources, ideally directly at the place of its consumption. This possibility, can be accomplish by a biobutanol production, which is also mentioned by Jin et al. (2011).

Biobutanol can be produced similarly to bioethanol, it is by fermentation of directly fermentable simple sugars, called the ABE (Acetone-Butanol-Ethanol) process Qureshi et al. (2001), under the action of the microorganism Clostridium acetobutylicum. Traditional raw materials for the production of biobutanol are starch crops (cereals, maize, potatoes) and molasses from sugar cane or sugar beet Garcia et al. (2011).

However, the viscosity of biobutanol differs from a gasoline viscosity, and therefore there is a need to test the biobutanol/gasoline blends at various temperature. This topic has also been processed by Alptekin and Canakci (2008) and Mao et al. (2017). The viscosity is an important because of propel metering the volume of fuel injected into the combustion chamber. Thus, a detailed knowledge of the viscosity properties has an effect on the engine performance, consumption and other properties of internal combustion engines, as was stated in the experiment by Mao et al. (2017).

Available mathematical viscosity models can be used to describe the viscosity behaviour of fuel blends. The models describe changes in viscosity at different component ratios. A similar topic was published in the work by Peleg et al. (2017). However, there are many models and they differ significantly according to their area of use. In this work, four mathematical models used to model the temperature dependence of the viscosity of liquid fuel blends, were selected and compared. These models can be used for practical purposes, for example to determine and predict a dynamic viscosity according to the concentration and temperature of biobutanol/gasoline blends.

MATERIALS AND METHODS

In this experiment was followed the same procedure, which was already used for gasoline-etanol and diesel-butanol blends in paper by (Alptekin and Canakci 2008) and Kumbár et al. (2015). Fuel blends B0, B5, B10, B85 a B100 were prepared from gasoline BA 95 and BA 98 (Unipetrol, Czech Republic) and biobutanolu (Penta, Czech Republic), the name is according to the volume ratio of biobutanol in the blend (e.g. B85 contains 85 vol. % biobutanol and 15 vol. % gasoline).

The fuel mixtures were cooled down to -10 ˚C and the dynamic viscosity was measured every 5 ˚C up to 40 ˚C to determine the viscosity properties of the mixtures over the entire operating temperature range. Dynamic viscosity was measured with a DV2T rotary viscometer (Brookfield, USA).

In this paper four various mathematical models, for temperature dependence of viscosity, were used. Part of those models were also used by Peleg et al. (2017) and Trávníček et al. (2013). Used models and their equations:

Exponential: $\eta = \eta_0 \cdot e^{-b \cdot T}$ (1)

where, η is dynamic viscosity [Pa · s], η_0 is reference value of dynamic viscosity [mPa · s], b is a coefficient [K-1] and T is the absolute temperature [K].

Arrhenius: $\eta = \eta_0 \cdot e^{\frac{E_a}{R \cdot T}}$ (2)

where, η is dynamic viscosity [Pa · s], η_0 is reference value of dynamic viscosity [mPa · s], R is the gas constant and Ea is the Arrhenius activation energy respectively [K] and T is the absolute temperature [K].

Newton: $\eta = \eta_0 \cdot e^{\frac{b}{T}}$ (3)

where, η is dynamic viscosity [Pa · s], η_0 is reference value of dynamic viscosity [mPa · s], b is a coefficient [K] and T is the absolute temperature [K].

Vogel: $\eta = \eta_0 \cdot e^{\frac{b}{c+T}}$ (4)

where, η is dynamic viscosity [Pa · s], η_0 is reference value of dynamic viscosity [mPa · s], b and c are coefficients [K] and T is the absolute temperature [K].

RESULTS AND DISCUSSION

In the following chapter, the data obtained from the experiment are recorded in the tables. Results of measuring for BA 95 are in Table 1, results for BA 98 are in Table 2. All the obtained results were processed by MATLAB 2018b (MathWorks, USA).

Table 1 Values of dynamic viscosity of BA 95 and its blends (mean ± standard deviation, N = 20)

Temperature [°C]	Temperature [K]	Dynamic viscosity BA 95 [mPa · s]				
		B0	B5	B10	B85	B100
-10	263.15	0.72 ± 0.025	0.73 ± 0.021	0.83 ± 0.010	5.12 ± 0.026	7.34 ± 0.025
-5	268.15	0.70 ± 0.018	0.71 ± 0.023	0.78 ± 0.010	4.50 ± 0.023	6.71 ± 0.027
0	273.15	0.64 ± 0.035	0.66 ± 0.014	0.73 ± 0.017	3.88 ± 0.017	5.69 ± 0.025
5	278.15	0.61 ± 0.035	0.63 ± 0.019	0.69 ± 0.015	3.45 ± 0.017	5.11 ± 0.031
10	283.15	0.60 ± 0.018	0.63 ± 0.015	0.64 ± 0.012	3.05 ± 0.017	4.38 ± 0.016
15	288.15	0.61 ± 0.032	0.62 ± 0.013	0.64 ± 0.010	2.75 ± 0.015	3.76 ± 0.012
20	293.15	0.59 ± 0.025	0.62 ± 0.016	0.64 ± 0.014	2.47 ± 0.007	3.32 ± 0.010
25	298.15	0.58 ± 0.031	0.62 ± 0.015	0.64 ± 0.010	2.21 ± 0.011	2.88 ± 0.010
30	303.15	0.57 ± 0.024	0.60 ± 0.015	0.63 ± 0.012	1.97 ± 0.010	2.53 ± 0.009
35	308.15	0.56 ± 0.021	0.58 ± 0.021	0.62 ± 0.010	1.79 ± 0.010	2.21 ± 0.010
40	313.15	0.54 ± 0.018	0.57 ± 0.015	0.61 ± 0.013	1.61 ± 0.012	1.95 ± 0.010

It can be seen from the tables above, that the viscosity of the mixtures decreases with increasing temperature. Furthermore, that blends with a higher biobutanol content have a higher viscosity and also that BA 98 gasoline has a lower viscosity than BA 95, similarly to bioethanol and gasoline blends (Kumbár et al. 2015).

Table 2 Values of dynamic viscosity of BA 98 and its blends (mean ± standard deviation, N = 20)

Temperature [°C]	Temperature [K]	Dynamic viscosity BA 98 [mPa · s]				
		B0	B5	B10	B85	B100
-10	263.15	0.69 ± 0.027	0.70 ± 0.010	0.77 ± 0.011	4.89 ± 0.019	7.34 ± 0.025
-5	268.15	0.65 ± 0.029	0.68 ± 0.010	0.74 ± 0.010	4.39 ± 0.016	6.71 ± 0.027
0	273.15	0.62 ± 0.030	0.65 ± 0.008	0.69 ± 0.006	3.81 ± 0.011	5.69 ± 0.025
5	278.15	0.60 ± 0.029	0.65 ± 0.007	0.65 ± 0.007	3.28 ± 0.010	5.11 ± 0.031
10	283.15	0.61 ± 0.031	0.65 ± 0.008	0.63 ± 0.009	2.92 ± 0.010	4.38 ± 0.016
15	288.15	0.57 ± 0.030	0.65 ± 0.004	0.63 ± 0.010	2.62 ± 0.013	3.76 ± 0.012
20	293.15	0.55 ± 0.022	0.65 ± 0.008	0.64 ± 0.010	2.31 ± 0.012	3.32 ± 0.010
25	298.15	0.54 ± 0.026	0.63 ± 0.007	0.64 ± 0.010	2.09 ± 0.010	2.88 ± 0.010
30	303.15	0.53 ± 0.035	0.63 ± 0.006	0.63 ± 0.006	1.88 ± 0.011	2.53 ± 0.009
35	308.15	0.53 ± 0.028	0.61 ± 0.008	0.63 ± 0.004	1.69 ± 0.010	2.21 ± 0.010
40	313.15	0.52 ± 0.018	0.60 ± 0.009	0.62 ± 0.010	1.50 ± 0.008	1.95 ± 0.010

Below this text, follow Tables 3–6 with coefficients for all four models. The coefficients of the models are valid for thermodynamic temperature (Kelvin unit).

Table 3 Coefficients of exponential model and values of coefficients and statistical indicators

Exponential	η_0 [mPa · s]	b [K^{-1}]	R^2	SSE
B0-95	2.785	-0.005277	0.8904	0.003453
B5-95	2.291	-0.004474	0.8800	0.002957
B10-95	3.753	-0.005958	0.8234	0.009255
B85-95	2.785	-0.005277	0.8904	0.003453
B0-98	2.855	-0.005526	0.9412	0.001755
B5-98	1.318	-0.002481	0.8729	0.001026
B10-98	2.040	-0.003918	0.7008	0.007626
B85-98	2 926	-0.024320	0.9974	0.033080
B100 (butanol)	1.141e+04	-0.028090	0.9971	0.088950

Table 4 Coefficients of Arrhenius model and values of coefficient of determination

Arrhenius	η_0 [mPa · s]	b [K^{-1}]	R^2	SSE
B0-95	0.132900	3 634	0.9101	0.002831
B5-95	0.173500	3 085	0.8994	0.002481
B10-95	0.119400	4 134	0.8563	0.007531
B85-95	0.003794	1.576e+04	0.9996	0.005149
B0-98	0.118700	3 793	0.9566	0.001295
B5-98	0.316800	1 698	0.8742	0.001015
B10-98	0.208800	2 747	0.7397	0.006637
B85-98	0.003084	1.615e+04	0.9989	0.013940
B100 (butanol)	0.001479	1.856e+04	0.9997	0.010480

Table 5 Coefficients of Newton model and values of coefficient of determination

Newton	η_0 [mPa · s]	b [K^{-1}]	R^2	SSE
B0-95	0.132900	437.1	0.9101	0.002831
B5-95	0.173500	371	0.8994	0.002481
B10-95	0.119400	497.3	0.8563	0.007531
B85-95	0.003794	1 896	0.9996	0.005149
B0-98	0.118700	456.2	0.9566	0.001295
B5-98	0.316800	204.3	0.8742	0.001015
B10-98	0.208800	330.4	0.7397	0.006637
B85-98	0.003084	1 942	0.9989	0.013940
B100 (butanol)	0.001479	2 233	0.9997	0.010480

Table 6 Coefficients of Vogel model and values of coefficient of determination

Vogel 95	η_0 [mPa · s]	b [K]	c [K]	R^2	SSE
B0-95	0.4717000	12.590*	-233.80	0.9572	0.0013480
B5-95	0.5130000	9.758*	-235.90	0.9493	0.0012490
B10-95	0.5412000	8.194	-244.40	0.9700	0.0015740
B85-95	0.0079680*	1 500	-31.16*	0.9996	0.0047340
B0-98	0.4019000	25.060*	-216.50	0.9782	0.0006507
B5-98	0.0008957*	2 703*	50.67*	0.9989	0.0133100
B10-98	0.5850000	3.513*	-250.80	0.9321	0.0147100
B85-98	0.0008959*	2 703*	50.66*	0.9989	0.0133100
B100 (butanol)	0.0037680*	1 737	-33.16*	0.9997	0.0093950

*Legend: *coefficient is not statistically significant*

Tables show that despite the occurrence of several statistically insignificant coefficients, the above-used mathematical models for interpolation of the temperature dependence of dynamic viscosity is the most accurate Vogel model, according to the highest average value (0.97836) of the coefficient of determination R^2. In a row next are Newton and Arrhenius models, which have identical R^2 value (0.92342) and the exponential model has the lowest accuracy, according to the results of the average value R^2 (0.89907).

In the following section are provided graphs of the mathematical models for selected blends.

Figure 1 Mathematic models for BA 95

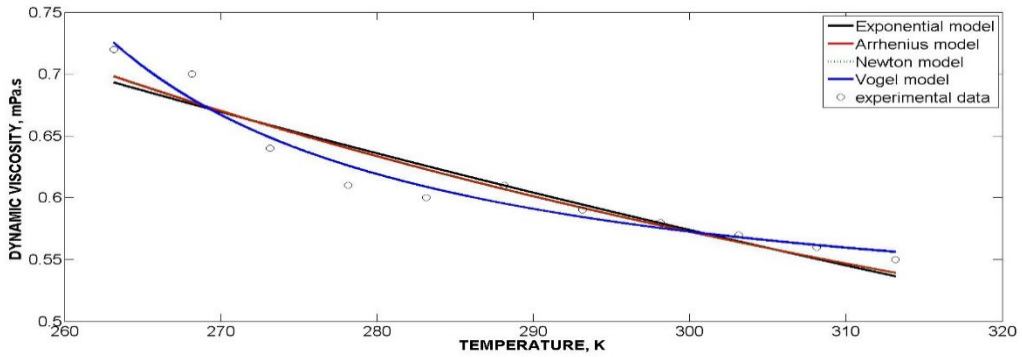

Figure 2 Mathematic models for BA 98

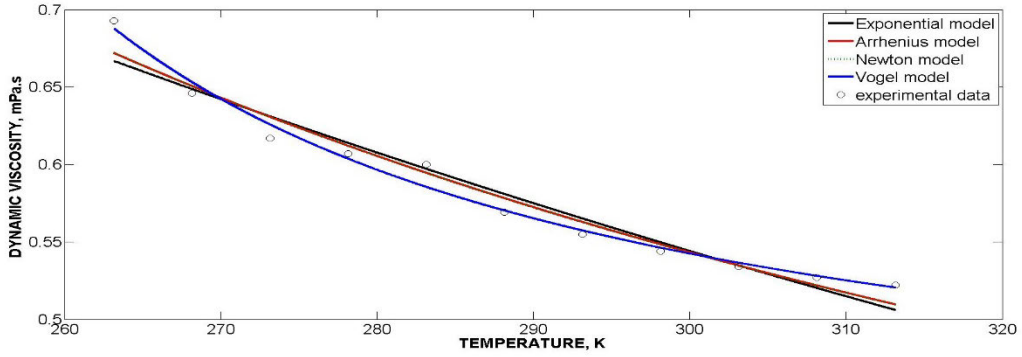

The graphs show nonlinear dynamic viscosity decrease with increasing temperature of mixtures. Also, with a higher content of biobutanol in the mixture the decrease is more significant. The dependence of viscosity on temperature is most significant for pure biobutanol and then for the blend B85 containing 85 vol. % of biobutanol for both tested gasolines. It can be stated that all used mathematical models were chosen appropriately, because the coefficient of determination R^2 was ≥0.899.

The issue of viscosity of biobutanol/gasoline blends is also described by Brandão et al. (2018) with similar results. Alptekin and Canakci (2008) also found nonlinear viscosity behaviour of biofuels but they used polynomial 2nd degree function, which is inaccurate in extrapolation. Mao et al. (2017) states that the low viscosity of gasoline may lead to potential reliability threats to a fuel system.

One of the results of our paper is the fact that the addition of biobutanol in gasoline increases the final viscosity.

Figure 3 Mathematic models for butanol B100

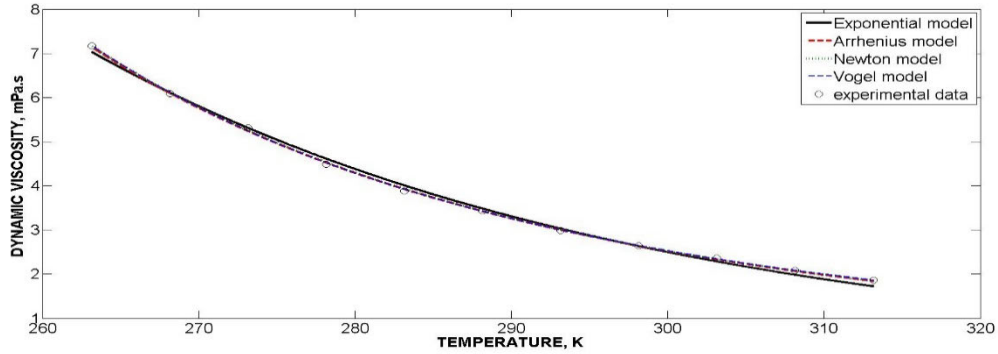

Figure 4 Exponential model for BA 95 and biobutanol blends

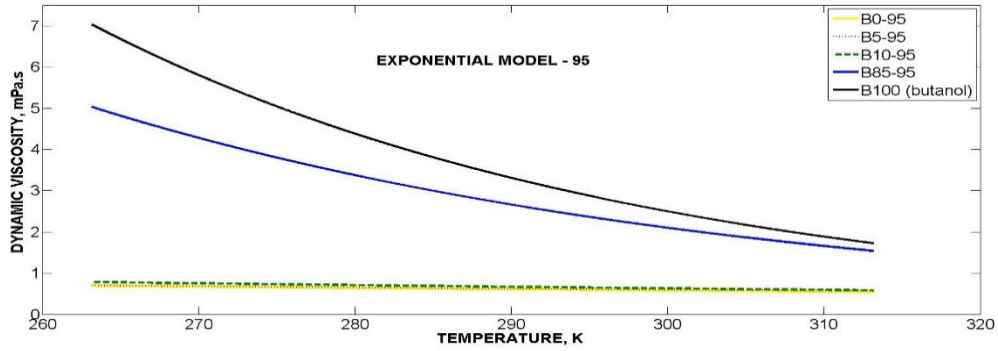

Figure 5 Exponential model for BA 98 and biobutanol blends

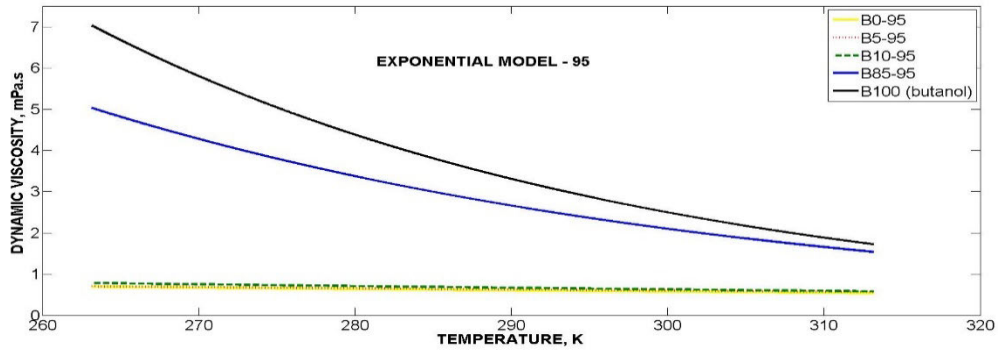

CONCLUSION

In this paper, four mathematical models for viscosity modelling were compared. Blends of two various gasolines and biobutanol were measured. The results show that all four models are convenient for modelling butanol/gasoline blends, furthermore the best results were obtained by Vogel model, according to the highest average value (0.97836) of the coefficient of determination R^2.

- The viscosity of biobutanol/gasoline blends decreases with increasing temperature.
- Biobutanol/gasoline blends with a higher biobutanol content have a higher viscosity.
- Dynamic viscosity of tested blends with contend up to 10 vol. % of biobutanol is almost the same to dynamic viscosity of BA 95 a BA 98 gasolines without bio-component.
- Gasoline BA 98 has lower dynamic viscosity then gasoline BA 95.
- Arrhenius and Newton model is applicable only for non-negative values of functional dependence. The Kelvin temperature scale must be used for these models. In the case of use Celsius temperature scale is exponential model the most versatile one.

The results obtained in this experiment are applicable in industrial practice. For example, our data could be used to set the car's control unit, which would be able to evaluate the exact amount of fuel needed for injection into the combustion chamber, thanks to using the obtained models coefficients. All of that according to the current amount of bio-component and temperature of blends, which affects the fuel viscosity. The similar intention was also considered by Marri et al. (2017).

ACKNOWLEDGEMENTS

The research was financially supported by the Internal Grant Agency of Faculty of AgriSciences no. AF-IGA-2020-IP060 "Influence of bioethanol on viscosity properties of gasoline".

REFERENCES

Alptekin, E., Canakci, M. 2008. Determination of the density and the viscosities of biodiesel–diesel fuel blends. Renewable Energy, 33(12): 2623–2630. Available at: https://www.sciencedirect.com/science/article/pii/S0960148108000773. [2020-09-24].

Brandão, L.F.P. et al. 2018. Alternative butanol/gasoline and butanol/diesel fuel blends: An analysis of the interdependence between physical-chemical properties by a multivariate principal component analysis model. Energy and Environment, 31(5): 733–754. Available at: https://journals.sagepub.com/doi/abs/10.1177/0958305X18776539. [2020-09-24].

Garcia, V. et al. 2011. Challenges in biobutanol production: How to improve the efficiency? Renewable and Sustainable Energy Reviews, 15(2): 964–980. Available at: https://www.academia.edu/15437942/Challenges_in_biobutanol_production_How_to_improve_the_efficiency. [2020-09-24].

Jin, C. et al. 2011. Progress in the production and application of n-Butanol as a biofuel. Renewable and Sustainable Energy Reviews, 15: 4080–4106. Available at: https://www.sciencedirect.com/science/article/pii/S1364032111002310. [2020-09-24].

Kumbár, V. et al. 2015. Physical and Mechanical Properties of Bioethanol and Gasoline Blends. Listy cukrovarnické a řepařské, 131: 112–116. Available at: http://www.cukr-listy.cz/on_line/2015/PDF/112-116.pdf. [2020-09-24].

Marri, V.B. et al. 2017. Butanol and pentanol: The promising biofuels for CI engines – A review. Renewable and Sustainable Energy Reviews, 78: 1068–1088. Available at: https://www.sciencedirect.com/science/article/pii/S1364032117306688. [2020-09-24].

Mao, B. et al. 2017. Effects of Gasoline Viscosity and Injection Pressure on the Performance and Emissions of a Multi-Cylinder Partially Premixed Combustion Engine. The Proceedings of the International symposium on diagnostics and modeling of combustion in internal combustion engines, 2017.9. C309.

Peleg, M. 2017. Temperature–viscosity models reassessed. Critical Reviews in Food Science and Nutrition, 58(15): 2663–2672. Available at: https://www.tandfonline.com/doi/full/10.1080/10408398.2017.1325836. [2020-09-24].

Qureshi, N. et al. 2001. Acetone butanol ethanol (ABE) recovery by pervaporation using silicalite-silicone composite membrane from fed-batch reactor of Clostridium acetobutylicum. Journal of Membrane Science, 187: 93–102. Available at: https://experts.nebraska.edu/en/publications/acetone-butanol-ethanol-abe-recovery-by-pervaporation-using-silic. [2020-09-24].

Trávníček, P. et al. 2013: Selected physical properties of liquid biofuels. Research in Agricultural Engineering, 59(4): 121–127. Available at: https://www.agriculturejournals.cz/publicFiles/14_2013-RAE.pdf. [2020-09-24].

Evaluation of energy potential in compost with proportion of grape marc

Patrik Zatloukal, Alice Cizkova, Pavel Zemanek, Vladimir Masan
Department of Horticultural Machinery
Mendel University in Brno
Zemedelska 1, 613 00 Brno
CZECH REPUBLIC

xzatlo13@mendelu.cz

Abstract: Rising interest in the use of energy biomass is leading to the search for new renewable energy sources, which can also include compost. According to current knowledge, compost is primarily an organic fertilizer, but it can also be used as a solid biofuel with good energy potential. For the needs of experimental measurements focused on calorimetric calorific values, 3 variants of mature compost were used. Two variants consists from a mixture of horticultural waste in combination with 25 and 50% grape pomace content. Changes in the calorific value of compost were determined with reference to the particle size distribution and also with regard to the humidity, which was set in the laboratory at 0, 15, 30 and 45%. The desired humidity was achieved by adding the required amount of deionized water to the dried compost. The obtained results show that grape pomace, as an input raw material added to compost bins, together with moisture, can significantly affect the resulting calorific value of compost. In the case of dried variants of compost with a proportion of grape pomace, it was at the level of 9.08–11.06 MJ/kg. In the control variant at the level of 6.18 MJ/kg, with increasing humidity, the calorific value decreases significantly. The reason for the higher calorific value in compost with a content of grape pomace is the presence of grape seeds with a part of oily components, which remain undecomposed during the composting process.

Key Words: compost, grape pomace, horticultural waste, calorific value, heating value

INTRODUCTION

Reduction of greenhouse gas emissions and utilisation of organic waste as material and for energy, as a partial substitute for fossil fuels, are currently the top priorities in the field of handling of biodegradable waste. The limited amount of fossil fuels and the increasing consumption of energy forces us to seek alternative sources of energy and new ways of exploiting these resources. Biomass energy is one potential substitute for fossil fuels. Biomass is a product of sunlight and photosynthesis, which makes it a renewable resource (Larson et al. 2015). Compost can be classified by its origin into agricultural and industrial. Agricultural compost is used to enrich soil with organic material generated in an agricultural enterprise. The source of organic material may be waste from agricultural production (straw, chaff), inorganic substances (soil, sediments from wastewater treatment plants) or microbial substrate (liquid manure, slurry). Industrial composts are processed at central composting facilities and the resulting substrate is intended for sale as a stabilized organic fertilizer. Very strict limits restrict the current potential for use of compost in agriculture and land reclamation. It is for these reasons that novel ways of utilising compost are being searched for and tested (Abdullah and Wu 2009, Wu et al. 2010). One of the areas in which compost could be profitably utilized is the energy industry. Compost can be used as a renewable source of heat – i.e. as an alternative fuel. The utilization of compost for generating energy is still in its infancy in the Czech Republic (Raclavská et al. 2011). Experience from other countries indicates that using compost to generate energy depends on a number of factors. They are mainly the composition of the compost, its moisture content and its particle size (Hettiarachchi et al. 2019). Results to date indicate that the net calorific value of compost ranges from 8 to 12 MJ/kg (Narra et al. 2010). This article therefore aims at providing more information about potential uses of composts from horticultural waste.

Its objective is to determine the net calorific values of horticultural waste composts with varied moisture content produced by means of windrow composting.

MATERIAL AND METHODS

Description of the composts and its properties

Mature compost with a varied content of input raw materials, consisting mainly of grape pomace, vegetable waste, straw, sawdust and cut grass, as given in Table 1, was used for the purpose of the experimental measurements. The compost was produced by means of windrow composting, the total duration of the composting process was 14 weeks with subsequent maturation in a heap for a period of 8 months.

Compost samples were collected in compliance with ČSN 465735 Industrial composts. A sample with a total weight of 5 kg was collected from each sample. The gross samples were reduced by quartering under laboratory conditions to representative samples with a weight of 1 kg.

After the samples were desiccated at 105 °C, they underwent a sieve analysis, which was carried out using vibratory sieve shakers AS 200 from (Retsch GmbH, Germany). Sieves of the following aperture diameters were used: 8.0–5.6– 4.0–2.8–2.0–1.4–1.0–0.5–0.25–0.125 and less than 0.125 mm. The mass % of individual particle sizes was determined.

Individual size fractions were milled and subsequently prepared for the calorimetric measurements. The moisture content of the samples was modified under laboratory conditions so that the target moisture content (in mass %) was achieved. Moisture content was set at the level of 0, 15, 30 and 45% for the individual samples and particle sizes. The amount of the water added was determined according to the formula (1):

$$V = (C \times S)/(1-C), \text{ (ml)} \quad (1)$$

Where:

V is the volume of water added to the dry samples (ml);

C is the target moisture content that is to be achieved (mass %);

S is the weight of the desiccated substrate to which the water is added (g).

The moisture content in the samples was always modified before the calorimetric measurements in order to minimize changes to moisture content. The values were determined for each sample twice.

Table 1 Raw material composition of piles

Sample	% of weight when added to the compost pile				
	Grape pomace	Vegetable waste	Straw	Sawdust	Cut grass
Var. 1	-	60	13	3	24
Var. 2	25	46	12	3	14
Var. 3	50	26	10	4	10

Calorimetric assessment

The net calorific value at a constant volume or under a constant pressure was calculated based on the gross calorific value of the analysed samples by ISO 1928:2009. The moisture and hydrogen content of the analysed sample must be known in order to perform the calculation at a constant volume. Determination of hydrogen content was performed using instrumental methods according to ČSN EN 15104. A 6400 Automatic Isoperibol Calorimeter (Parr Instrument Company, Illinois, USA) was used for the assessment of the gross calorific value and an Ohaus Adventurer Pro AV264C Analytical Balance (Mettler-Toledo International Inc, Ohio, USA) was used for exact assessment of the weight of the combusted sample. Determination of the gross calorific value and the subsequent use of this value to calculate the net calorific value of solid biofuels is necessary in order to assess the suitability of the sample for combustion. The established gross calorific values were used to calculate the net calorific values according to the formula below (2) in compliance with the ČSN EN 14918:

$$Q^r{}_i = Q^r{}_s - \gamma.(W_t^r + 8.94.H_t^r), \text{ (MJ/kg)} \quad (2)$$

Where:

Q^r_i – net calorific value of the evaluated sample (MJ/kg);

Q^r_s – gross calorific value of the original sample (MJ/kg);

γ – ratio of evaporation of 1% H_2O, MJ/kg, at temperature 25°C, γ = 0.02442 MJ/kg;

8.94 – hydrogen to water conversion ratio of (–);

W^r_t – total water content in the original sample (%);

H^r_t – total hydrogen content in the original sample (%).

Calorimetric assessment

A statistical analysis was performed using the software package "Statistics 12.0" (StatSoft Inc., Tulsa, Oklahoma, USA). Analysis of variance was conducted, and the results were compared using Tukey's range test at a significance level of α = 0.05.

RESULTS AND DISCUSSION

Combustion is a widespread technology used for processing solid communal waste, including compost, the goal of which is to generate energy while minimizing the volume and mass of waste. A particularly important aspect of combustion is the net calorific value. The net calorific value represents the amount of thermal energy released by complete combustion of a weight unit of the fuel, whereas the water contained in the combustion products stays in the form of water vapour. It is assumed that its heat cannot be utilized and it is released in gaseous form together with the combustion products.

Table 2 gives the results of the sieve analyses, which indicate statistically significant differences in the mass percentages of particles in the analysed samples of compost in relation to individual particle sizes. Jevič et al. (2013) state that the particle size texture of the compost plays an important role in relation to the content of combustible substances. They state that particle size of less than 0.16 mm, the content of combustible substances of which falls to below 50%, and particles of less than 0.045 mm, in which the content falls to less than 30%, are problematic as regards the net calorific value.

Table 2 Raw material composition of piles

Particle size (mm)	Percentage of particle sizes in individual classes (mass %)		
	Var. 1	Var. 2	Var. 3
8.000	9.13 ± 0.01^c	3.48 ± 0.01^b	1.98 ± 0.01^a
5.600	3.61 ± 0.02^c	2.26 ± 0.04^b	1.66 ± 0.00^a
4.000	3.76 ± 0.04^c	2.85 ± 0.05^b	2.27 ± 0.04^a
2.800	6.32 ± 0.01^a	17.54 ± 0.01^b	21.64 ± 0.01^c
2.000	6.20 ± 0.03^a	10.26 ± 0.02^c	8.03 ± 0.01^b
1.400	9.28 ± 0.01^b	10.56 ± 0.01^c	8.00 ± 0.03^a
1.000	8.95 ± 0.06^b	9.58 ± 0.03^c	8.59 ± 0.12^a
0.500	21.25 ± 0.03^c	14.35 ± 0.08^a	18.58 ± 0.03^b
0.250	16.24 ± 0.01^c	11.67 ± 0.02^a	12.61 ± 0.01^b
0.125	7.11 ± 0.01^b	7.35 ± 0.01^c	6.25 ± 0.05^a
<0.125	8.15 ± 0.00^a	10.10 ± 0.06^b	10.40 ± 0.03^c

Legend: Data are expressed as means ± standard deviation, different letters in the same lines represent significant difference (P < 0.05).

Tables 3 to 5 give the mean net calorific values of the assessed compost samples for individually assessed particle sizes and moisture content values. The values show a general trend of falling net calorific value with the decreasing size of particles (Baydar et al. 2007). The greatest net calorific value (16.43–18.42 MJ/kg) was achieved by compost with added pomace (var. 2 and var. 3) in particle sizes of 2–2.8 mm. This is related to the oil content of the seeds and their overall size. E.g. Ohnishi et al. (1990) states that the seeds contain 10–20% of oil. Baydar and Akkurt (2001) state that oils make

up 5–20% of the dry mass of the seeds. Berndes et al. (2003) state that the net calorific value of plant materials can be increased by the addition of energetically more valuable components, such as resins or oils.

The length of the seeds usually ranges between 3 and 6 mm, and the seeds remain un-decomposed during the composting process. With regard to their size, the whole seeds are caught by sieves with an aperture size of 2.8 mm, seed fragments are caught by sieves with an aperture size of 2.0 mm.

Table 3 Net calorific value of type 1 compost in relation to particle size and moisture content

Particle size (mm)	Mean net calorific values (MJ/kg) at a particular moisture content (%)			
	0	15	30	45
8.000	9.67 ± 0.01	9.13 ± 0.01	8.47 ± 0.01	8.10 ± 0.01
5.600	7.22 ± 0.01	7.54 ± 0.00	6.73 ± 0.01	5.11 ± 0.04
4.000	5.65 ± 0.15	5.25 ± 0.02	4.88 ± 0.11	5.55 ± 0.01
2.800	5.21 ± 0.01	5.62 ± 0.05	5.25 ± 0.05	4.88 ± 0.06
2.000	6.75 ± 0.02	6.13 ± 0.03	6.21 ± 0.03	5.39 ± 0.01
1.400	5.44 ± 0.03	5.52 ± 0.06	5.08 ± 0.00	4.49 ± 0.03
1.000	5.62 ± 0.01	4.82 ± 0.02	4.70 ± 0.01	4.84 ± 0.01
0.500	7.27 ± 0.01	7.11 ± 0.01	6.53 ± 0.01	6.13 ± 0.01
0.250	5.04 ± 0.04	4.67 ± 0.02	3.60 ± 0.03	3.49 ± 0.12
0.125	5.02 ± 0.02	3.84 ± 0.05	4.03 ± 0.01	3.85 ± 0.21
<0.125	5.12 ± 0.06	4.29 ± 0.01	4.44 ± 0.06	4.00 ± 0.07

Legend: Data are expressed as means ± standard deviation.

Table 4 Net calorific value of type 2 compost in relation to particle size and moisture content

Particle size (mm)	Mean net calorific values (MJ/kg) at a particular moisture content (%)			
	0	15	30	45
8.000	10.51 ± 0.01	11.22 ± 0.01	10.23 ± 0.02	8.61 ± 0.01
5.600	11.38 ± 0.08	11.17 ± 0.06	10.37 ± 0.02	8.37 ± 0.05
4.000	9.57 ± 0.02	9.54 ± 0.03	8.58 ± 0.11	7.63 ± 0.04
2.800	16.43 ± 0.04	16.08 ± 0.09	14.53 ± 0.01	12.25 ± 0.02
2.000	16.04 ± 0.04	15.93 ± 0.03	13.16 ± 0.02	12.24 ± 0.03
1.400	6.70 ± 0.01	6.64 ± 0.01	5.62 ± 0.09	6.03 ± 0.04
1.000	6.54 ± 0.01	5.26 ± 0.01	5.56 ± 0.03	5.90 ± 0.01
0.500	6.39 ± 0.03	5.39 ± 0.12	5.16 ± 0.03	5.39 ± 0.08
0.250	5.38 ± 0.00	4.41 ± 0.06	4.23 ± 0.01	5.38 ± 0.11
0.125	5.48 ± 0.15	4.40 ± 0.00	3.99 ± 0.01	5.48 ± 0.05
<0.125	5.44 ± 0.01	3.96 ± 0.04	3.34 ± 0.01	5.44 ± 0.04

Legend: Data are expressed as means ± standard deviation.

Table 6 gives the results of statistical comparison of mean net calorific values of mature compost depending on the moisture content. It is evident from the results that the net calorific value of all three samples of compost decreases as moisture content increases. On the whole, the composts with added pomace show higher net calorific values compared to the compost without added pomace (var. 1).

It is generally true that if a solid waste fuel is to be used for generating energy, it must have a net calorific value higher than 6.0 MJ/kg. The desired value can be achieved by the addition of a material with a higher heating capacity (e.g. plastic material), or by desiccating the material using waste heat (Eurostat Statistics Explained 2018). Both samples of compost with added pomace meet this requirement, even with a higher moisture content. However, the net calorific value of compost in general is lower than that of standard solid biofuels, e.g. those based on wood chips or agricultural products.

The net calorific value of these normally ranges above 15 MJ/kg (for pellets and briquettes) and usually does not fall below 10 MJ/kg. Souček (2014) also states that the reason for the low net calorific value of compost is the higher moisture and ash content, i.e. superfluous components without calorific value.

Table 5 Net calorific value of type 3 compost in relation to particle size and moisture content

Particle size (mm)	Mean net calorific values (MJ/kg) at a particular moisture content (%)			
	0	15	30	45
8.000	12.94 ± 0.01	12.57 ± 0.03	12.20 ± 0.01	12.20 ± 0.13
5.600	11.99 ± 0.04	11.62 ± 0.01	11.25 ± 0.07	11.25 ± 0.03
4.000	10.75 ± 0.01	10.38 ± 0.11	10.01 ± 0.01	10.01 ± 0.25
2.800	18.32 ± 0.02	17.95 ± 0.01	17.58 ± 0.04	14.58 ± 0.01
2.000	18.07 ± 0.01	17.70 ± 0.03	17.33 ± 0.04	14.33 ± 0.04
1.400	9.63 ± 0.00	9.26 ± 0.01	8.89 ± 0.01	8.89 ± 0.14
1.000	8.92 ± 0.04	8.55 ± 0.02	8.19 ± 0.03	8.19 ± 0.03
0.500	8.80 ± 0.14	8.43 ± 0.01	8.06 ± 0.01	6.06 ± 0.02
0.250	7.38 ± 0.11	7.01 ± 0.03	6.64 ± 0.01	4.64 ± 0.06
0.125	7.46 ± 0.03	7.09 ± 0.13	6.72 ± 0.05	4.72 ± 0.01
<0.125	7.43 ± 0.06	7.07 ± 0.03	6.70 ± 0.06	2.70 ± 0.01

Legend: Data are expressed as means ± standard deviation.

Table 6 Net calorific value of type 3 compost in relation to particle size and moisture content

Particle size (mm)	Mean net calorific values (MJ/kg) at a particular moisture content (%)			
	0	15	30	45
Var. 1	6.18 ± 0.04^{b}	5.81 ± 0.03^{b}	5.45 ± 0.03^{a}	5.07 ± 0.05^{a}
Var. 2	9.08 ± 0.04^{a}	8.55 ± 0.03^{a}	7.70 ± 0.03^{a}	7.52 ± 0.04^{a}
Var. 3	11.06 ± 0.04^{a}	10.69 ± 0.04^{a}	10.32 ± 0.03^{b}	8.88 ± 0.07^{b}

Legend: Data are expressed as means ± standard deviation, different letters in the same columns represent significant difference ($P < 0.05$).

CONCLUSION

This experimental evaluation focused on determining the net calorific value of compost made from horticultural waste, with varied moisture content. Three samples of compost, containing 0, 25 and 50 percent of pomace respectively, were tested. The moisture content of the samples was modified under laboratory conditions so that the target moisture contents of 0, 15, 30 and 45% of the mass were achieved. The results clearly show that the material composition is an important factor influencing the net calorific value of the compost. The highest net calorific value – on the level of 16.43–18.42 MJ/kg was achieved by composts with added pomace (var. 2 and var. 3). This is due to the oils contained in the seeds which are an integral part of pomace and which have a greater heating capacity. The highest net calorific values in all the compost samples that were examined were achieved by samples in their moisture-free state. The values fell by 18–20% as the moisture content increased. If it were to be used in the energy industry, it would be desirable to naturally air-dry the compost or to dry it using other technological processes, such as briquetting or pressing.

ACKNOWLEDGEMENTS

This paper was finalized and supported by the project IGA-ZF/2020–AP002 “Possibilities of using compost for energy purposes and production of shaped fuels” and by the project CZ.02.1.01/0.0/0.0/16_017/0002334 Research Infrastructure for Young Scientists, co-financed by Operational Programme Research, Development and Education.

REFERENCES

Abdullah, H., Wu, H. 2009. Biochar as a Fuel: 1. Properties and Grindability of Biochars Produced from the Pyrolysis of Mallee Wood under Slow-Heating Conditions. Energy and Fuels [Online], 23(8): 4174–4181. Available at: https://doi.org/10.1021/ef900494t. [2020-09-15].

Baydar N.G. et al. 2007. Characterization of grape seed and pomace oil extracts. Grasasy Y Aceites [Online], 58: 29–33. Available at: https://doi.org/10.3989/gya.2007.v58.i1.5. [2020-09-15].

Baydar, N.G., Akkurt, M. 2001. Oil content and oil quality properties of some grape seeds. Turkish Journal of Agriculture & Forestry [Online], 25: 163–168. Available at: https://citeseerx.ist.psu.edu/viewdoc/download?doi=10.1.1.827.349&rep=rep1&type=pdf. [2020-09-15].

Berndes, G. et al. 2003. The contribution of biomass in the future global energy supply: a review of 17 studies. Biomass and Bioenergy [Online], 25(1): 1–28. Available at: https://doi.org/10.1016/S0961-9534(02)00185-X. [2020-09-15].

ČSN. 1996. Průmyslové komposty. ČSN 46 5735 (465735). Praha: Český normalizační institut.

Eurostat Statistics Explained. 2018. Municipal waste statistics. [Online]. Available at: https://ec.europa.eu/eurostat/statistics-explained/index.php/Municipal_waste_statistics. [2020-09-15].

Hettiarachchi, L. et al. 2019. Effects of compost particle size, moisture content and binding agents on co-compost pellet properties. International Journal of Agricultural and Biological Engineering [Online], 12(4): 184–191. Available at: https://doi.org/10.25165/j.ijabe.20191204.4354. [2020-09-15].

ISO. 2009. Solid mineral fuels - Determination of gross calorific value by the bomb calorimetric method and calculation of net calorific value. ISO 1928:2009. Geneva: International Organization for Standardization.

Jevič, P. et al. 2013. Možnosti energetického využití kompostu a separátů z anaerobního zpracování biomasy (in Czech). Expertní neveřejná výzkumná zpráva č. 538-2013-17253-A/6/13. Praha: VUZT, 44 s.

Larsson, S. et al. 2015. Cassava Stem Powder as an Additive in Biomass Fuel Pellet Production. Energy and Fuels [Online], 29(9): 5902–5908. Available at: https://doi.org/10.1021/acs.energyfuels.5b01418. [2020-09-15].

Narra, S. et al. 2010. Increasing the Calorific Value of Rye Straw Pellets with Biogenous and Fossil Fuel Additives. Energy and Fuels [Online], 24(9): 5228–5234. Available at: https://doi.org/10.1021/ef100823b. [2020-09-15].

Ohnishi M. et al. 1990. Chemical composition of lipids, especially triacylglycerol, in grape seeds. Agricultural and Biological Chemistry, 54: 1035–1042.

Raclavská, H. et al. 2011. Conditions for energy generation as an alternative approach to compost utilization. Environmental Technology [Online], 32(4): 407–417. Available at: https://doi.org/10.1080/09593330.2010.501089. [2020-09-15].

Souček, J. 2014. Jak využít teplo ukryté v kompostu (in Czech). Alternativní energie, 1: 33–35.

ÚNMZ. 2010. Tuhá biopaliva - Stanovení spalného tepla a výhřevnosti. ČSN EN 14918 (838214). Praha: Úřad pro technickou normalizaci, metrologii a státní zkušebnictví.

ÚNMZ. 2011. Tuhá biopaliva - Stanovení obsahu celkového uhlíku, vodíku a dusíku - Instrumentální metody. ČSN EN 15104 (838216). Praha: Úřad pro technickou normalizaci, metrologii a státní zkušebnictví.

Wu, H. et al. 2010. Bioslurry as a Fuel. 1. Viability of a Bioslurry-Based Bioenergy Supply Chain for Mallee Biomass in Western Australia. Energy and Fuels [Online], 24(10): 5652–5659. Available at: https://doi.org/10.1021/ef1008105. [2020-09-15].

Drawbar pull increase of off-road car with special driving wheels

Tomas Zubcak[1], Katarina Kollarova[2], Eva Matejkova[3]
[1]Department of Transport and Handling
[2]Information and Coordination Centre of Research
[3]Department of Statistics and Operations Research
Slovak University of Agriculture in Nitra
Tr. A. Hlinku 2, 949 76 Nitra
SLOVAK REPUBLIC

zubcak.uniag@gmail.com

Abstract: The goal of this paper was to analyze a possibility of improving a tractive performance of an off-road car with new design of special driving wheels with spikes. Design of the special driving wheels uses the spikes segments placed in tire-tread pattern similar to snow chain. An inactive position of the spike segments allows transportation of a car on roads using standard tyres. An active position is designed for operation under terrain conditions. The article presents comparison of the active special driving wheels with the standard tyres without the special driving wheels. The experiments were realised on a mowed grass field at soil moisture of 24.8%. Comparing the active special driving wheels with standard tyres without the special driving wheels, the increase in drawbar pull reached value of 39.5% at wheel slip of 10%. The results showed improvement of drawbar properties of the off-road car under real terrain conditions.

Key Words: driving wheels, slip, tyre-soil interaction, tyre-tread pattern

INTRODUCTION

A relatively large part of vehicle power is wasted at tyre-soil interface. This fact is very important in case of off-road cars and agricultural tractors operating out of roadways. Besides the parameters of tyre-tread pattern, a tyre inflation pressure, wheel load, tyre width and diameter of unloaded tyre affects the tractive performance of driving wheels due to the change of contact area between driving wheels and ground. Poor drawbar efficiency due to a wheel slip wastes an energy of a vehicle engine, increases a fuel consumption (Uhrinová et al. 2013) makes worse emissions in exhaust gases (Králik et al. 2016) and a soil compaction in case of off-road vehicles and agricultural tractors (Malý et al. 2015).

Many researchers designed and tested various concepts of special driving wheels with lugs or spikes (Yang et al. 2014, Gasparetto et al. 1992). The objectives of this study were to design special driving wheels with spikes and test an off-road car tractive performance.

MATERIAL AND METHODS

Principle of special driving wheels

The aim of this article is a design and test of new special driving wheels with spikes for tyres of the off-road car. An off-road tyre has a relatively large space between the segments of a tyre-tread pattern and allows placing the spikes within them to improve the drawbar properties of the car. The principle of the special driving wheels is based on works presented by Abrahám et al. (2015), Abrahám et al. (2018), Majdan et al. (2018) and Abrahám, R. et al. (2019). The principle of the special driving wheels is shown in Figure 1. Eight spike segments (2) with three spikes are placed in riffles of the tyre-tread pattern (1). All segments can rotate to change the spike position. During the transportation on roads the spikes do not exceeds the tyre-tread pattern and do not interfere the road (Figure 1b). During the worse adhesive conditions, control lever (3) turns the spike segments to the active position where the spikes exceeds the tyre-tread pattern and improve drawbar properties of driving wheels. The carry wire rope (4) keep the contact between the spike segments and tyre during the driving wheels rotation and tyre deformation. The control wire rope (5) with the control levers (3) allow to control the spike position.

Figure 1 Principle of the special driving wheels for off-road tyres: a) the main parts, b) inactive position of spikes, c) active position of spikes

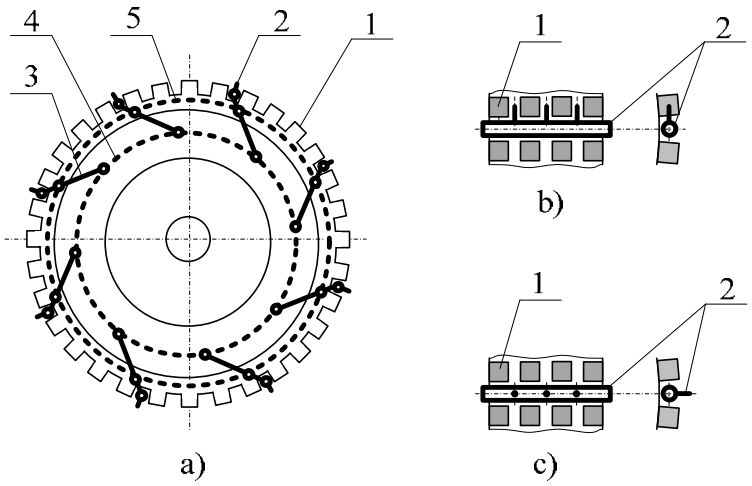

Test of the off-road car tractive performance

Figure 2 shows the measurement of drawbar parameters of the off-road car Daihatsu Eroza type (2) with special driving wheels (7) according to the OECD test code 2 and standard STN ISO 789-9:2002, which were adapted for the testing of this car type performed in field conditions. The standard rear driving wheels of the car was replaced by the prototypes of the special wheels. The force sensor (3) was connected between the load tractor Zetor 25 type (1) and the off-road car through a steel chain (4).

Figure 2 Measurement system for drawbar parameters of off-road car with special driving wheels

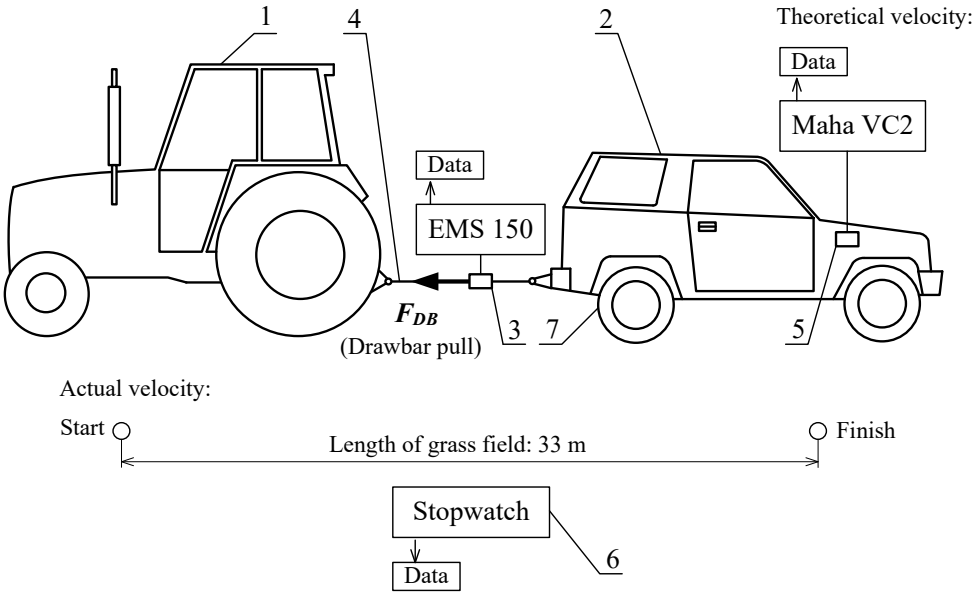

Legend: 1 – load tractor, 2 – off-road car, 3 – force sensor, 4 – steel chain, 5 – rotation speed sensor, 6 – stopwatch, 7 – special driving wheels.

To state the drawbar parameters of the car, the drawbar pull F_{DB}, actual V_a and theoretical velocity Vt were measured and recorded. The force sensor (3) EMS 150 type (Emsyst s. r. o., Slovak Republic) with a rated capacity of 20,000 N and with an accuracy of 0.5% of full scale, was used to measure the drawbar pull. A rotation speed sensor (5) VC2 type (Maha GmbH, Germany) with a 300 to 9,999 min^{-1} measuring range and 10 min-1 resolution measured the car engine speed. A stopwatch (6) with 0.01 s resolution was used for measuring the time between the start and the end of the measurements. A Hydac model HMG 3010 (Hydac GmbH, Germany) portable 12-bit data acquisition system with accuracy of 0.1% of full scale was used, with a 100 Hz sampling frequency. The special driving wheels was equipped with the tyres Pneu Ovada Maxi Cross 195/80 R15 type (Vraník s. r. o., Czech Republic).

Table 1 Specifications of the off-road vehicle and the load tractor

Vehicle type		Off-road car (Daihatsu Feroza)	Load tractor (Zetor 25)
Curb mass		1,220 kg	2,600 kg
Engine	Specification	Petrol, four-stroke	Diesel, four-stroke
	Number of cylinders	4	3
	Displacement	1,590 cm^3	2,590 cm^3
	Max. torque / rotation speed	126 N m / 3,500 rpm	160 N m / 2,200 rpm

The load tractor loaded the car during the measurement procedure using the resistance of gearbox in neutral, 1st, 2nd, 3rd and 4th reverse gears in combination with the three positions of the handbrake. The off-road car was loaded to the maximum load level until the car engine was overload and the rotation speed began to decrease. In this point, the measurements were finished. During the experiments, the off-road car was operated at maximum engine torque at 3,500 rpm in 1st gear, low range (gear ratio u_1 is 33.75).

Wheel slip δ, an important parameter to evaluate the tractive performance of wheeled car (Majdan et al. 2016), is given by expression:

$$\delta = 1 - \frac{V_a}{V_t} = 1 - \frac{V_a}{\omega r} \quad (1)$$

Where V_a – actual forward velocity of the car, m s^{-1}
V_t – theoretical velocity of the car, m s^{-1}
ω – angular velocity of wheel, rad s^{-1}
r – wheel radius, m.

Theoretical velocity V_t was calculated according to measurement of engine rotation speed as follows:

$$V_t = \frac{2\,\pi\,r\,n_m}{u_1} \quad (2)$$

Where n_m – the actual rotation speed of vehicle engine, rpm
u_1 – gear ratio.

Bashford and Kocher (1999) use the Gauss-Newton method of nonlinear regression to estimate the regression coefficients C_1 and C_2 to model relationship between net traction ratio and wheel slip. This method and statistical program (SAS EG 7.1) were used to express the functional relationship between drawbar pull and wheel slip according to Eq. (3).

$$F_{DB} = [C_1 \times \{1 - exp\,(-C_2 \times \delta)\}] \times W \quad (3)$$

Where C_1, C_2 – regression coefficients,
δ – wheel slip,
W – car weight, N.

The measurements were realised in October 2018. The off-road car with special driving wheels was tested on mowed gras field at soil moisture of 24.8% (STN ISO 11465). The soil type Cambisol (World Reference Base for Soil Resources) is typical for mountainous country (Middle Slovakia Region, Žarnovica district) where the tests were performed.

RESULTS AND DISCUSSION

Design and construction of special driving wheels

The special driving wheels (Figure 3) were designed at the Faculty of Engineering of the Slovak University of Agriculture in Nitra and mounted on the tyres body of the rear wheels.

During the transportation on roads, the vehicle uses inactive special driving wheels. The spikes do not exceed the tyre-tread pattern and do not interfere with the road. At worse adhesive conditions, all spikes segments are turned to the active position where the spikes exceed the tyre-tread pattern and improve the tractive performance of the vehicle.

The steel carry wire rope (2) connects eight spikes segments (1) and holds them in the tyre-tread pattern. The steel control wire rope (3) allows changing the active and inactive position of the spike segments (1). Spikes are made from steel bars having hexagonal cross-section. Using the pivots (4)

with threads, washers, and nuts, both wire ropes are fixed to the spike segments. All pivots (4) can turn in hoops of the spike segments. The change of the spike segments position (active or inactive) is mechanically controlled. To change the spike segments position, the safety nut (7) has to be released and next the nut (6) turned using fork wrench. It releases the fix connection of the supporting frame (8) and allows moving the control wire rope (3) and turning the spike segments (1). The shape of oscillating link (9) terminates position of the spikes in the active and the inactive position. The safety nut (7) fix the active or the inactive position. The central carrier bar (5) with the central pin is placed to the wheel rim to set a correct central position. All the parts of special driving wheels are designed and manufactured from common profiles of standard structural steel grade S355JR.

The special driving wheels were developed to fully replace the standard tyre under terrain. Yang et al. (2014) developed actively actuated lugged wheels to increase the drawbar pull of a vehicle. The actively actuated lugged wheels achieved the increase in drawbar pull but their planetary gear does not allow changing the lugged wheel to the smooth wheels in the case of transportation on a hard surface. Gasparetto et al. (1992) presented the design of steel lugged wheels for agricultural machinery on rice fields, sour and peaty soil. All the wheels mentioned above do not allow the transportation on solid surfaces. On the other hand, the design of the special driving wheels allows transportation on roads without the interactions between the spikes and ground because they do not exceed the tyre diameter in the inactive position. Abrahám et al. (2014) presented the special wheels with auto-extensible blades. These lug wheels are mounted besides the tractor driving wheels to improve the tractor drawbar properties by means of steel blades. The special driving wheels with spikes are simplifier construction and do not change the tractor width in comparison with lug wheels mentioned above.

Figure 3 Design of the special driving wheels: a) active position, b) oscillating link in inactive position, c) spike segment

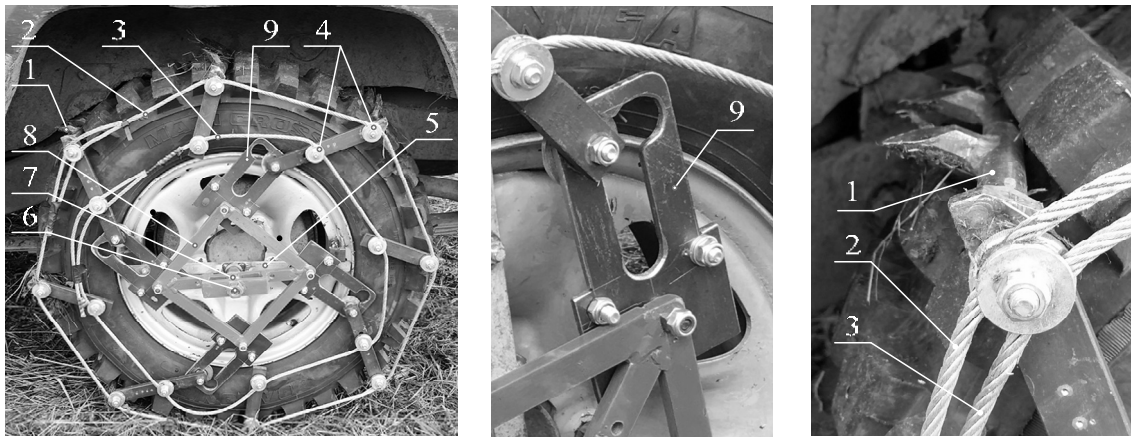

a) b) c)

Drawbar pull vs. slip

The model of drawbar pull as a function of wheel slip were calculated according to Eq. (3) and compared with the experimental data in the case of the tyres without the special driving wheels and the active special driving wheels (Figure 4). Considering the measured data and using the regression analysis, the nonlinear regression coefficients of the off-road car with the tyres without the special driving wheels ($C_1 = 0.679$ and $C_2 = 6.061$) and the active ($C_1 = 0.744$ and $C_2 = 8.653$) special driving wheels were stated to model drawbar pull as a function of slip. In case of the standard tyres, the coefficient of determination R^2 is 0.906, P-value is $4.73\ 10^{-8}$ (< 0.05) and $RMSE$ is 2.47. In case of the special driving wheels the coefficient of determination R^2 is 0.873, P-value is $3.43\ 10^{-7}$ (< 0.05) and $RMSE$ is 2.69. The descriptive statistic of regression models indicates a significant regression effect so that the models well fit with the experimental data. Comparing the models of drawbar pull as function of wheel slip, the special driving wheels improved the traction properties of the off-road car, as shown in Figure 5.

Figure 4 Drawbar pull as a function of wheel slip: a) active special driving wheels, b) standard tyres without special driving wheels

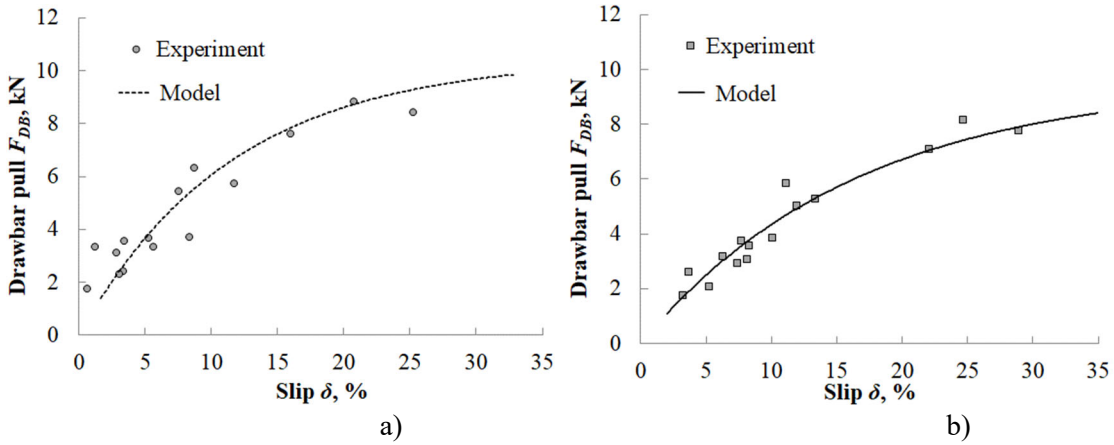

Figure 5 Comparison of drawbar pull of off-road car with and without special driving wheels

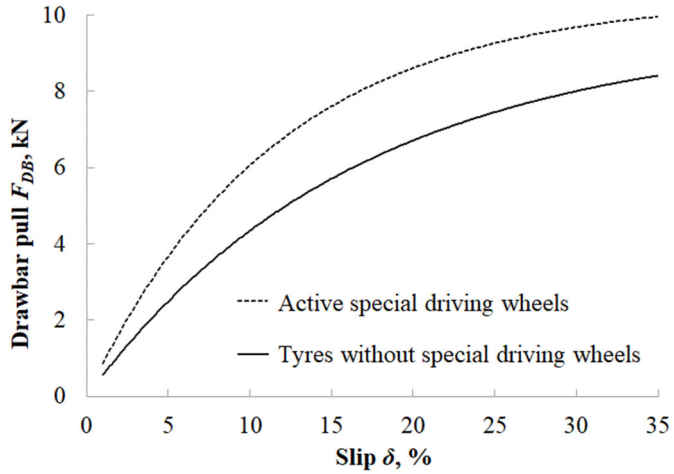

Increase in drawbar pull

Considering the drawbar pull at the relevant slip, the drawbar properties of the off-road car with the active special driving wheels were compared with the tyres without the special driving wheels (Table 2). The highest drawbar pull increase of 39.5% (Table 2) occurred at the wheel slip of 10%. The higher slips due to higher load levels caused lower increase in the drawbar pulls of the car. The highest increase in the drawbar pull at low slip is caused by the better function of the steel spikes penetrating raw ground. Using a rubber track, Rasool and Raheman (2018) increased the drawbar pull of wheeled walking tractor about 93% at slip of 15%.

Table 2 Comparison of active special driving wheels and tyres without special driving wheels

δ, %	F_{DB}, N		Increase, %	δ, %	F_{DB}, N		Increase, %
	Active special wheels	Standard tyres			Active special wheels	Standard tyres	
10	6,061	4,344	39.5	24	9,155	7,326	25
12	6,761	4,939	36.9	26	9,364	7,581	23.5
14	7,350	5,467	34.4	28	9,539	7,807	22.2
16	7,846	5,934	32.2	30	9,687	8,007	21
18	8,262	6,347	30.2	32	9,811	8,184	19.9
20	8,613	6,714	28.3	34	9,915	8,341	18.9
22	8,907	7,039	26.5	36	10,003	8,480	18

CONCLUSIONS

The drawbar properties of the off-road car with special driving wheels were evaluated and compared with standard tyres without the special driving wheels. s tractive performance. The tractive performance of the off-road car was analysed based on experiments under real operation conditions. Experimental data was used to model the drawbar pull as a function of the wheel slip. The active special driving wheels were compared with standard tyres without the special driving wheels. The increase in drawbar pull reached highest value 39.5% at the wheel slip of 10%. The next research will be aimed at automatization of spike extension and influence of the special driving wheels on fuel consumption because the increase in drawbar pull improves this factor.

ACKNOWLEDGEMENTS

The research was financially supported by the project VEGA No. 1/0724/19 of the Ministry of Education of the Slovak Republic "Research, Design and Application of Special Driving Wheels for Drawbar Properties Improvement and Elimination of Soil Damage under Operation of Cars and Tractors".

REFERENCES

Abrahám, R. et al. 2014. Increase in Tractor Drawbar Pull Using Special Wheels. Agronomy Research, 12(1): 7–16.

Abrahám, R. et al. 2015.Výsuvné hrotové zariadenie na zlepšenie záberových vlastností kolies. 7347. PUV 11-2015. Available at: http://skpatents.com/6-u7347-vysuvne-hrotove-zariadenie-na-zlepsenie-zaberovych-vlastnosti-kolies.html.

Abrahám, R. et al. 2018. Comparison of Consumption of Tractor at Three Different Driving Wheels on Grass Surface. Agronomy Research, 16(3): 621–633.

Abrahám, R. et al. 2019. Special Tractor Driving Wheels with Two Modification of Spikes Inclination Angle. Agronomy Research, 17(2): 333–342.

Bashford, L.L., Kocher, M.F. 1999. Belts vs. tires, belts vs. belts, tires vs. tires. Applied Engineering in Agriculture, 15(3): 175–181.

Gasparetto, E. et al. 1992. The rolling resistance of narrow steel wheels in Italian paddy fields. Journal of Agricultural Engineering Research, 52: 91–100.

Králik, M. et al. 2016. Monitoring of selected emissions of internal combustion engine. Research in Agricultural Engineering, 62(Special Issue): 66–70.

Majdan, R. et al. 2018. Drawbar Parameters of Tractor with Prototypes of Driving Wheels and Standard Tyres. Acta Technologica Agriculturae, 21(2): 63–68.

Majdan, R. et al. 2016. Teória a konštrukcia traktorov: teoretické, výpočtové riešenie kolesových traktorov, pojazdové ústrojenstvo, motor, hydraulický systém a elektrické príslušenstvo. 1st ed., Nitra: Slovak University of Agriculture.

Malý, V. et al. 2015. Laboratory test of the soil compaction. Acta Universitatis Agriculturae et Silviculturae Mendelianae Brunensis, 63(1): 77–85.

Rasool, S., Raheman, H. 2018. Improving the tractive performance of walking tractors using rubber tracks. Biosystems Engineering 167: 51–62.

STN ISO 11465: 2001. Soil Quality – Determination of Dry Matter and Water Content on a Mass Basis – Gravimetric Method.

STN ISO 789-9: 1993. Agricultural Tractors. Test procedures. Part 9: Power Tests for Drawbar. Slovak Office of Standards, Metrology and Testing.

Uhrinová, D. et al. 2013. Research of limited and unlimited emission effect on the environment during the burning of alternative fuels in agricultural tractors. Journal of Central European Agriculture, 14(4): 1402–1414.

Yang, Y. et al. 2014. Drawbar Pull of a Wheel with an Actively Actuated Lug on Sandy Terrain. Journal of Terramechanics, 56: 17–24.

APPLIED CHEMISTRY AND BIOCHEMISTRY

Workflow for targeted and semi-targeted quantitation of polar metabolites in *Solanum tuberosum* leaf via a high-resolution orbitrap GC-MS and Skyline, a freely-available open-source tool

Miroslav Berka[1], Simona Mensikova[1], Marie Greplova[2], Veronika Berkova[1], Bretislav Brzobohaty[1], Martin Cerny[1]
[1]Department of Molecular Biology and Radiobiology
Mendel University in Brno
Zemedelska 1, 613 00 Brno
[2]Potato Research Institute, Ltd.
Dobrovskeho 2366, 580 01 Havlickuv Brod
CZECH REPUBLIC

miroslavberka94@gmail.com

Abstract: In the post genomics era, metabolomics analyses provide a highly useful tool for analysing molecular mechanisms in plants. In contrast to transcriptomics or proteomics, small molecules are identical among diverse species, and a single metabolomics workflow can be easily adapted. Recently, a high-end orbitrap instrument has been introduced into the field of GC metabolomics, but the vendor-provided software does not meet the high-throughput standard. Here, we describe the novel workflow and demonstrate its efficiency in the analysis of *Solanum tuberosum* leaf metabolites.

Key Words: metabolomics, *Solanum tuberosum*, Skyline, quantitation

INTRODUCTION

Gas chromatography mass spectrometry (GC-MS) is fast, reliable and a high-throughput method for an effective analysis of metabolites in plant tissue. In contrast to its liquid chromatography (LC-MS) counterpart, it usually provides a higher chromatographic separation power and peak capacity. Further, the GC-based separation has highly reproducible cross-sample retention times, facilitating a robust quantitation and comparison of large cohorts of samples (e.g. Gowda and Djukovic 2014). On the other hand, the GC-MS is limited to volatile and thermally stable compounds, restricting its use to relatively small compounds (<650 Da). The set of accessible metabolites is thus limited predominantly to short-chain alcohols, acids, esters and hydrocarbons, and chemical derivatization is often mandatory before the analysis (Fiehn 2016).

Skyline is a freely-available and open-source application originally developed for proteomics analyses by the team around Brendan MacLean at MacCoss Labat the University of Washington in Seattle (MacLean et al, 2010). Skyline supports Selected Reaction Monitoring (SRM), Multiple Reaction Monitoring (MRM), Parallel Reaction Monitoring (PRM), Data Independent Acquisition (DIA/SWATH) and Data Dependent Acquisition (DDA) with MS1 quantitative methods. Despite its origin in targeted proteomics, Skyline has been developed into a versatile tool suitable for any LC-MS-based analysis and adjustable virtually for any high-resolution MS data.

Recently, an orbitrap-based GC-MS system has been introduced to the filed, effectively extending the capabilities of GC-MS metabolomics by increasing mass precision up to four decimal places and resolution to 120,000. Here, we describe Skyline-based data processing workflow for GC-MS-orbitrap-plant metabolomics.

MATERIAL AND METHODS

Plant material

S. tuberosum cv. Keřkovské rohlíčky plants were cultivated on Murashige-Skoog medium supplemented with 30 g of sucrose per litre and 7 g agar per litre in culture chamber at 22 °C with a long

day photoperiod (60 µmol/m^2/s). After four weeks, leaf tissue was collected and flash-frozen in liquid nitrogen.

Metabolite extraction, measurement and identification

Polar metabolites were extracted as described previously with few modifications (e.g. Cerna et al. 2018). Briefly, frozen tissue was homogenized in liquid nitrogen and aliquots corresponding to ca 50 mg were extracted with 1 ml methanol/methyl tert-butyl ether/water (1:3:1) overnight. For hormonal analysis, the extraction buffer was spiked with labeled phytohormone standards (Olchemim, CZ). Next, samples were mixed with 500 µl methanol:water (1:3), centrifuged, and 50 µl of polar phase was dried down and resubstituted in 20 µl of methoxyamine hydrochloride in pyridine (40 mg per 1 ml). After 90 min at 30 °C, samples were silylated with 80 µl of N-Methyl-N-(trimethylsilyl)trifluoroacetamide (MSTFA) for 30 min at 37 °C and spin down for 5 min. The clarified liquid was transferred into glass inserts (ca 60 µl) and put in GC vials for analysis.

The Q Exactive GC Orbitrap GC-MS/MS (Thermo) was operated with the following settings: split mode 1:5; helium flow 1.2 ml/min; injector temperature 250 °C; temperature gradient 70 °C for 5 min, ramp 70–320 °C at 9 °C/min; MS transfer line temperature 250 °C; ion source temperature 250 °C; ionization mode EI; resolution 60 000; full MS scan range 50 to 550 m/z; AGC target 1e6, maximum inject time 200 µs, data type - centroid. Data were collected by Thermo Xcalibur and metabolites were identified by TraceFinder using the default workflow for GC-MS analysis and a combination of NIST2014, GC-Orbitrap Metabolomics Library and inhouse library. Skyline 20.1 was employed for quantitative analyses.

RESULTS AND DISCUSSION

Sorting m/z features for the Skyline transition list construction

The leaf tissue of *S. tuberosum* was homogenized and metabolites were extracted as described in the Material and Methods. Next, metabolites were derivatized and analysed by GC-MS. The resulting raw files were imported into TraceFinder and searched for metabolites. Identified metabolites fulfilling identification criteria (score above 75, retention time ΔRI limit 5%) were exported into the NIST library file. The exported library was composed of spectra in the .msp file format, which is an ASCII text format long used with the NIST/EPA/NIH Mass Spectral Library of electron ionization spectra (https://www.nist.gov). Individual metabolite annotation is followed by the list of assigned peaks. Thus, the msp file contained multiple lines that had to be removed, filtered and rearranged prior the export to Skyline, as exemplified in Figure 1.

First, each peak was associated with the corresponding metabolite name (column "Compound" in Table 1B). This can be done e.g. in Google spreadsheet or Excel. The msp file was imported (the resulting import contained only a single column). Three columns were inserted (left), the command "**=IF(COUNTIF(D2,"*Name*")=1,D2,A1)**" was inserted into the cell **A2** and the formula was filled down in the column **A**. Name of the first metabolite (cell **D1**) was copy-pasted into the cell **A1**. The cell **B1** is set to **1** and the formula "**=IF(D2=A2,B1+1,B1)**" was inserted into the cell **B2** and filled down in the column **B**. Finally, to provide the final annotation, formula "**=B1&"_"&A1**" was inserted into the cell **C1**, filled down and columns **B** and **C** were copied and pasted back "as value".

Next, the peak had to be sorted because only the ten most intensive peaks were intended for the analysis. The peak m/z and intensity was first separated into two columns. This was achieved by copy-pasting the column **D** into **E** and **F,** selecting command "Find and replace" and replacing with blanks " *" and "* " for column **E** and **F**, respectively. Next, m/z of a lower specificity that were shared between multiple metabolites were removed. The row **1** was selected and filter set on (commands "Data", "Filter"). Values in the column **E** were filtered for the following common spectral "contaminants" and the corresponding rows were removed from the sheet (73.046–73.048, 75.025–75.026, 147.065–147.066, 149.044–149.046, 207.031–207.033). Note that this list can be easily extended to include identified experiment-specific contaminants, as indicated in Figure 2. Next, the table was sorted by columns **C** (A to Z) and **F** (Z to A). Finally, the cell **A1** value was set to **0** and the formula "**=IF(C2=C1,A1+1,0)**" was inserted into the cell **A2** and filled down. Values in the column **A** were then filtered for numbers above **18** and the corresponding rows were removed.

Annotation of retention times, precursor mass and charges

The present version of Skyline does not provide native support for GC-MS data. However, the electron impact ionization products can be imported as product ions of unknown precursors. Thus, one column was inserted right of column **C**, and the following formula was inserted in **D1** and filled down in the column **D**: "**=1000+A1**". Precursor and product ion charges were set to **1** (columns **E** and **G**). The retention time values were extracted from the TraceFinder output, employing the **VLOOKUP** function and matching retention indices and compound names. The retention time window is set to 0.2 min, i.e. 12 s.

Figure 1 Filtering of the exported msp file

The structure of the exported msp file

Name:Mannose 5TMS 1MOX isomer 1
Retention_index:SemiStdNP=1890
Formula:C22H55NO6Si5
CAS#:128705-67-9
Instrument_type:Q Exactive GC Orbitrap
Instrument:Exactive Series slot #0063
Sample_inlet:GC
Ionization:EI
Spectrum_type:in-source
Num Peaks:162
58.023361 5
59.031204 12
67.017868 1
72.039009 2
…

The structure of the final file suitable for Skyline

Compound	Precursor	Precursor charge	Product	Product charge	Retention time	Retention time window
83_ Mannose 5TMS 1MOX isomer 1	1083	1	129.073196	1	20.7	0.2
83_ Mannose 5TMS 1MOX isomer 1	1083	1	157.067993	1	20.7	0.2
83_ Mannose 5TMS 1MOX isomer 1	1083	1	217.107651	1	20.7	0.2
…	…	…	…	…	…	…

Importing transition list into Skyline

For the best performance, Skyline was operated in the small molecule mode with the following settings: Transition Settings – Instrument – Min m/z 30, max m/z 1,500 (or higher if the list of targeted compounds is larger than 500), Method match tolerance 0.001 m/z; MS/MS filtering centroided with 2 ppm mass accuracy. The retention time filtering was set to "include all matching scans" for the first imported sample. Next, Insert Transition List dialogue was opened, columns were modified to match the prepared transition list, and the transition list was copy-pasted (Figure 3).

Retention time alignment and export of quantitative data

The first imported file was set as a reference sample, and all targeted metabolites were inspected, and boarders of the retention time windows manually adjusted (if necessary). Once completed, the Retention time filtering in the Transition Settings menu was changed to "Use only scans within 0.5 minutes of predicted RT". This triggered a new option during the import of results dialogue, allowing the selection of the reference retention time. The correct peak alignment was evaluated via "Retention times Replicate Comparison" (Figure 4). Finally, the results were exported via a customized document grid view (Figure 5).

Figure 2 Selection of persistent ions. Average chromatogram and the corresponding extracted chromatograms for selected three ions.

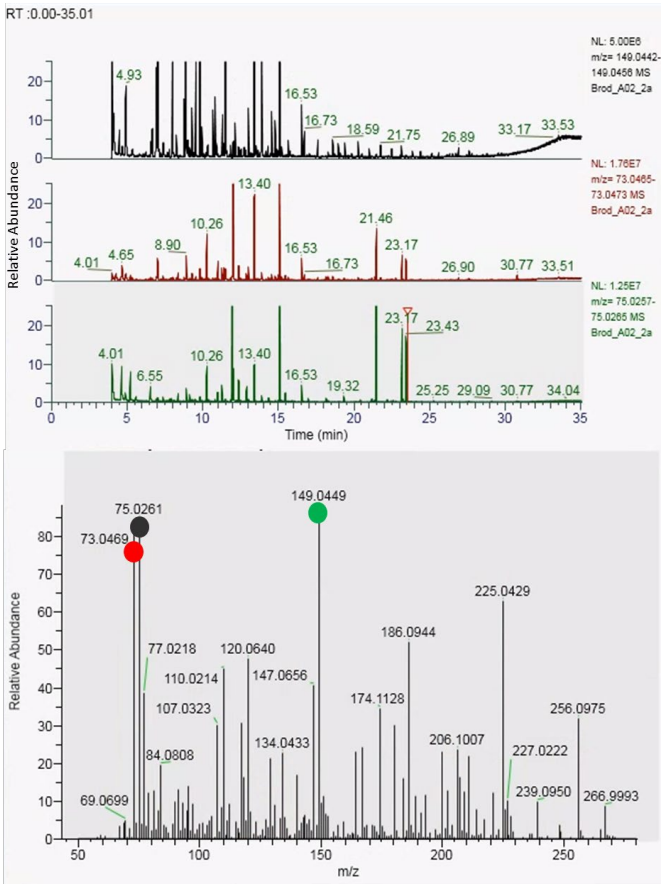

Figure 3 Inserting the transition list into Skyline

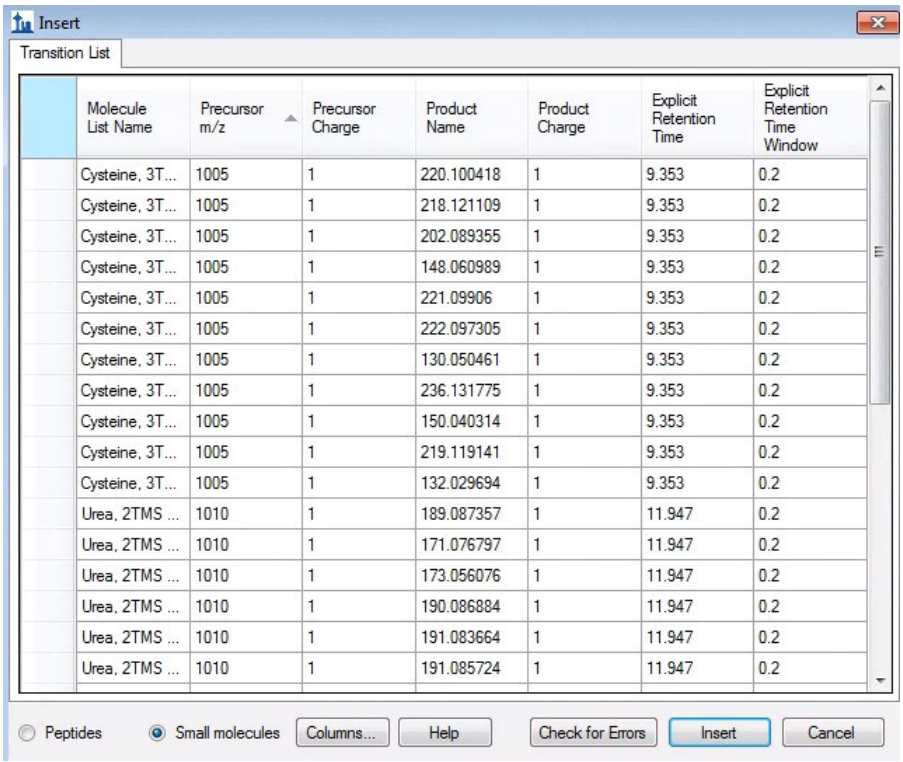

Figure 4 Creating customized view for exporting quantified metabolite peak areas

A) Selection of the result grid fields

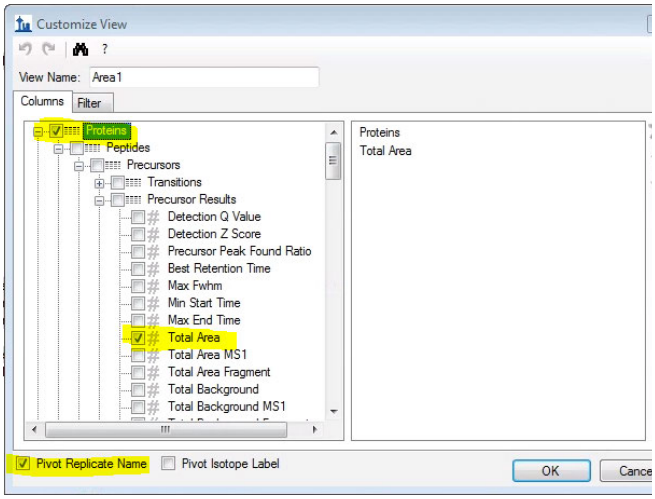

B) Summary of the metabolite quantitation

Document Grid: Area1

Views | 1 of 117 | Export... | Find:

Protein	02 Total Area	03 Total Area	04 Total Area
002_Propanoic_...	16369878	7905360	17445154
003_Lactic Acid_...	58655148	44987576	50958116
004_Glycolic aci...	10877324	4762185	10292342
005_L-Valine, T...	11466972	21166332	12487706
006_L-Alanine, 2...	356278976	642387456	651021568
007_Hydroxylami...	192653280	234523552	204951696
009_Oxalic acid_...	56274388	51085648	54279384
010_2-Pyrrolidin...	115770	19172692	28369252
011_L-Leucine,_...	19123816	11649125	15444953
012_L-Proline, T...	13431902	70160872	26003752
013_L-Isoleucin...	12442530	10224311	8445937
014_Malonic aci...	28633230	12476415	29297528
016_Valine, 2TMS	249718000	431603712	393787328
017_Ethylmaloni...	2794815	2309274	3042943
019_Benzoic Aci...	3931695	4118902	3965259

Figure 5 Metabolomics analysis of 72 samples

A) Example of extracted ion chromatogram

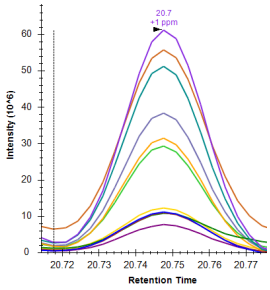

B) Mass error distribution for the whole dataset

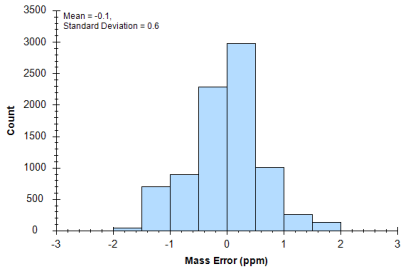

C) Separation of 136 identified and quantified metabolites

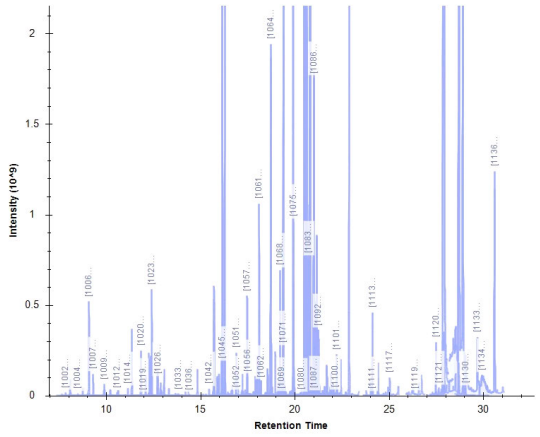

D) Retention times – Replicate comparison

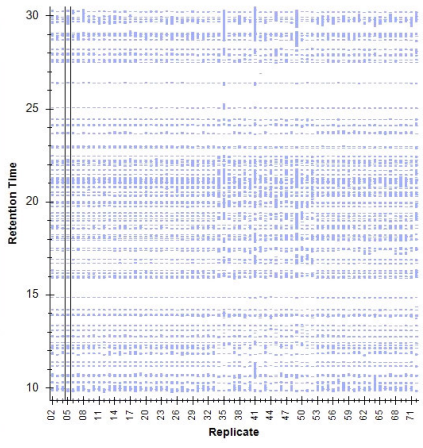

Evaluation of the method

GC-MS is one of the method of choice for metabolomics and there are multiple commercial and open-source software solutions for GC-MS data processing and analyses (e.g. Spicer et al. 2016). However, to our knowledge, none of these is as user-friendly and efficient as Skyline for targeted extraction of metabolomics data. In contrast to alternatives, the Skyline workflow utilizes high accuracy and high resolution of orbitrap data (Figure 5B). The workflow is rapid and the presented data analysis

of >100 metabolites in 72 samples was completed within few hours with the most time demanding step being the retention time matching of the reference sample.

Next, the Skyline workflow was adapted for a targeted analysis of plant hormones. Phytohormones represent an integral part of the plant signalling networks and therefore play multiple roles during the plants life. The plant matrix was spiked with 24 pmol of deuterated salicylic acid 2-hydroxy[$^{2}H_{4}$]benzoic acid, derivatized and analysed in five technical replicates. As illustrated in Figure 5, quantification of endogenous salicylic acid was highly reproducible.

Figure 6 Targeted analysis of salicylic acid. Extracted ion chromatogram and the inset showing the reproducibility of five technical replicates.

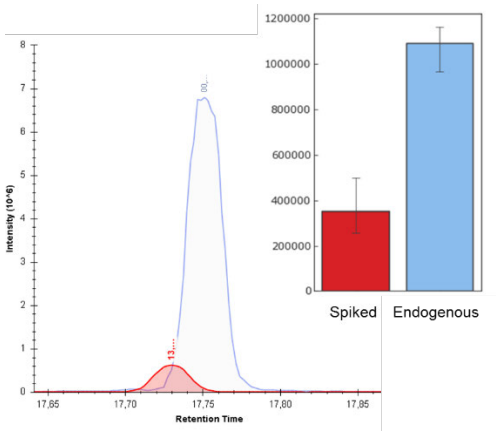

CONCLUSION

We have developed a GC-MS metabolomics workflow for targeted and semi-targeted analysis of metabolites and demonstrated that this Skyline-based method is suitable for large-scale studies.

ACKNOWLEDGEMENTS

The research was financially supported by the project NAZV QK1910045 Identification of metabolites correlating with quantitative resistance to *Phytophthora infestans*, and internal grant project AF-IGA2020-IP048.

REFERENCES

Cerna, H. et al. 2017. Proteomics offers insight to the mechanism behind Pisum sativum L. response to pea seed-borne mosaic virus (PSbMV). Journal of Proteomics, 153: 78–88.

Fiehn, O. 2016. Metabolomics by gas chromatography–mass spectrometry: Combined targeted and untargeted profiling. Current Protocols in Molecular Biology, 114(1): 30–4.

Gowda, G.N., Djukovic, D. 2014. Overview of mass spectrometry-based metabolomics: opportunities and challenges. In Mass Spectrometry in Metabolomics. New York: Humana Press, 3–12.

MacLean, B. et al. 2010. Skyline: an open source document editor for creating and analyzing targeted proteomics experiments. Bioinformatics, 26(7): 966–968.

Spicer, R. et al. 2017. Navigating freely-available software tools for metabolomics analysis. Metabolomics, 13(9): 106.

Bacterial growth and biofilm formation on titanium materials with specific surface treatment

Tatiana Fialova[1], Katerina Vrchovecka[2], Monika Pavkova-Goldbergova[2], Kristyna Dolezelikova[1], Ludmila Kosaristanova[1], Pavel Svec[1], Kristyna Smerkova[1]
[1]Department of Chemistry and Biochemistry
Mendel University in Brno
Zemedelska 1, 613 00 Brno
[2]Department of Patophysiology
Masaryk University
Kamenice 753/5, 625 00 Brno
CZECH REPUBLIC

tatiana.fialova.fialova@gmail.com

Abstract: Implant-related bone and tissue infections are one of the most serious post-operative complications. Bacteria adherent to the surface of the implants often form biofilm. This matrix is able to protect the bacteria against disinfection, antibiotic treatment, immune and inflammatory system of the host. Titanium is the most widely used material for the implant production. Modification of titanium can have a significant effect on bacterial adhesion by changing physical and chemical properties of the surface. The investigated samples were modified with a layer of titanium nanotubes by anodic oxidation. Nanotubes with a diameter of 30–120 nm were formed on the surface. Antimicrobial activity of the samples was examined by fluorescence microscopy, scanning electron microscopy (SEM) and the plate count method. The results show inhibition of bacterial colonisation up to 27%.

Key Words: titanium nanotubes, implant infection, biofilm, *Staphylococcus aureus*, fluorescence microscopy

INTRODUCTION

Each year, millions of medical implants are used. Despite many advances in biomaterial science, up to 5% of implants become colonized by bacteria. The implants can be infected at the time of surgery by surgical instruments, gloves and other devices. Contamination can come also from patients skin and from air (Bhardwaj and Webster 2017, Damiati et al. 2018, Feng et al. 2020, Lee et al. 2019). Bacterial implant infections are becoming an important problem requiring expensive treatment, long term hospitalization and often even multiple surgery. They can cause tissue inflammation, subsequent bone recession and even osteolysis and osteomyelitis (Damiati et al. 2018, Lee et al. 2019, Wang et al. 2016).

Infectious bacteria are divided into two main groups based on the composition of their cell wall. Gram positive and gram negative. The cell wall of the gram positive bacteria consists of 15–80 nm thick layer of peptidoglycan. Gram negative bacteria have the peptidoglycan layer only 1–2 nm thick (Bartlet et al. 2018). Thicker wall of the Gram positive bacteria can act like a barrier to protect the cells against lysis and determine their shape. The most often occurring gram positive bacteria on implants are *Staphylococcus aureus* and *Staphylococcus epidermidis*. Gram negative representatives are *Pseudomonas aeruginosa* and *Klebsiella pneumoniae* (Damiati et al. 2018, Popham 2013).

Attachment of bacteria to a surface occurs by several mechanisms, including hydrophobic and electrostatic interactions. Bacterial attachment to biological implants is dangerous and often leads to infection and biofilm formation (Banerjee et al. 2011). Biofilm can be simply described as a structured consortium of bacterial cells encompassed in a self-produced matrix. Depending on bacterial species, strain and environmental conditions, the matrix of biofilm consists of various substances such as exopolysaccharides, proteins, teichoic acids and extracellular DNA. Biofilms have the ability to resist antibiotic treatment, disinfection agents, phagocytosis and other parts of the immune

and inflammatory defence system of the host. Antibiotic resistance of biofilm bacteria can grow 1 000× stronger than that of unattached bacteria (Peng et al. 2013, Arciola et al. 2012).

Titanium (Ti) and its alloys are routinely used in dental and orthopaedic implants due to their chemical and mechanical properties: high strength to weight ratio, high yield and fatigue strength, corrosion resistance and biocompatibility (Damiati et al. 2018, Peng et al. 2013). Nevertheless, pristine Titanium is not able to induce or stimulate cell behaviour due to its bio inertness. This can eventually cause poor integration with surrounding bone tissues and may lead to implantation failure and even tissue necrosis. Untreated titanium is not able to show any significant antibacterial activity, itself it can not resist infection (Feng et al. 2020, Li et al. 2019). Various modifications of the surface of Titanium medical devices are promising goal to improve the quality of medical implants (Peng et al. 2013, Mansoorianfar et al. 2020).

Titanium nanotubes (TiNTs) are the material which shows out good biocompatibility and physiochemical properties. Simultaneously, this material can decrease bacterial attachment via high surface roughness and decreased water contact angles. Due to combination of this qualities, medicinal application of TiNTs has received increasing attention (Li et al. 2019, Peng et al. 2013, Ercan et al. 2011).

The aim of this study is to determine and compare the bacterial growth and biofilm formation of gram positive *Staphylococcus aureus* and gram negative *Pseudomonas aeruginosa* on Titanium materials with TiNTs surface layer by fluorescence microscopy, scanning electron microscopy and plate count method.

MATERIAL AND METHODS

Tested samples characterization

The tested material was prepared and delivered by the Institute of Pathological Physiology, Faculty of Medicine, Masaryk University. The surface of the titanium was modified by anodic oxidation. Nanotubular structures with a diameter of 30–120 nm are formed on the surface. Two types of samples were available: larger diameter titanium nanotubes 1 (TiNT1) and smaller diameter titanium nanotubes 2 (TiNT2). As a control, clear titanium (Ti) was used.

Bacterial inoculum preparation

For antimicrobial testing, bacterial strains from Czech Collection of Microorganisms (CCM) were used: gram negative *Pseudomonas aeruginosa* (CCM 3955) and gram positive *Staphylococcus aureus* (CCM 4223). The bacteria were cultivated on 5% Columbia blood agar (Labmediaservis, Czech Republic) overnight at 37 °C. The bacterial inoculum was prepared by diluting the bacterial colony to cell density 0.5 Mc Farland in Mueller Hinton broth (MH) (Sigma-Aldrich, USA) and then diluted 100× to reach approximate cell count 1–5 × 10^6 CFU/ml.

Fluorescence microscopy

Size of the samples for microscopy was approximate 1 cm^2. The samples were placed into sterile 12-well plate and to each well, 3 ml of bacterial inoculum was added. The plate was incubated at 37 °C for 3 h. After, the bacterial inoculum was removed, replaced with clear MH medium to preserve only the cells attached to the surface. The samples were incubated overnight and after incubation, they were washed with phosphate buffered saline (PBS) (Sigma-Aldrich, USA) and left to dry. To stain the cells attached on the surface, LIVE/DEAD BacLight Bacterial Viability and Counting Kit (Invitrogen, Germany) was used. The kit contains green fluorescent dye SYTO 9 for staining all the cells and red dye Propidium Iodide for staining dead cells. As a staining solution, 1.5 µl of each dye was mixed together with 1 ml of PBS saline. The samples were treated with 20 µl of prepared staining solution and incubated for a short time in the dark. After incubation, they were observed by OLYMPUS IX71 inverted fluorescence microscope (Olympus, USA) at magnification 200×.

Scanning electron microscopy

Preparation of the samples was similar to fluorescence microscopy. After incubation with bacteria, the samples were rinsed with PBS saline and observed by TESCAN MAIA3 microscope with CRYO mode (Tescan, Czech Republic).

Plate count method

For plate count method, only *S. aureus* was used. A drop of bacterial inoculum was applied on the sample surface. The samples were divided into 2 series. The first series of the samples was washed immediately with PBS saline to reach the blank value 0 h and the second series was incubated at 37 °C for 24 hours (value 24 h). After, the samples were washed with PBS saline. Resulting solution was after appropriate dilution inoculated at prepared Petri dishes with MH agar (Sigma-Aldrich, USA). The Petri dishes were incubated at 37 °C 24 h. Bacterial colonies grown on the dishes were counted and determined as colony forming units CFU/ml of inoculum. The experiment was executed in triplicates.

RESULTS AND DISCUSSION

Fluorescence microscopy

The surface of examined samples was left to overgrow with bacteria, rinsed with sterile saline and treated with LIVE/DEAD Counting Kit. The green dye SYTO 9 penetrates the membrane of bacterial cells and create green fluorescence by staining DNA. The red dye Propidium Iodide only enters dead cells with damaged membrane. With high bacterial surface coverage, these dyes can overlap. On the samples with *S. aureus* (Figure 1), there is visible difference in the amount of bacteria attached and growing on the surface. The bacterial colonisation on control Ti appears visibly higher than on TiNT1 and TiNT2 nanotubes. The bacteria on pristine Ti form a continuous coating and aggregates. On the TiNT1 samples, inhibition of bacterial colonisation is visible and the continuous layer appears disrupted. There is present also large proportion of dead cells. TiNT2 samples also show visible inhibition of bacterial colonisation. Bacteria here form small individual clusters. The ratio of dead cells appears lower than on TiNT1 samples. The biofilm is visible in the pictures as a green mist caused by presence of extracellular DNA interacting with SYTO 9 green dye. The highest visible biofilm formation in *S. aureus* is present on TiNT2 samples. High biofilm production serves as a defence of cells in unfavourable environment (Peng et al. 2013, Arciola et al. 2012). *P. aeruginosa* samples (Figure 2) also show a decreased bacterial growth and attachment on TiNT1 and TiNT2 compared to the control Ti. It is possible to observe a high coverage of bacteria on the control Ti samples, which form numerous clusters. The proportion of dead cells stained red appears to be fairly low here. TiNT1 exhibits visibly lower bacterial colonisation and biofilm formation here appears to be the highest of the samples used. On TiNT1 is also visible the highest bacterial cell mortality. The *P. aeruginosa* cells on TiNT2 material form isolated scattered clusters. Almost all the clusters imaged contain a large number of dead red stained cells. In untreated, bacterial-free controls, it is visibly confirmed that the dyes do not react with the material itself. Only small interactions, probably caused by small impurities, are visible. The results are in agreement with previous studies (Peng et al. 2013, Bartlet et al. 2018).

Scanning electron microscopy

The bacteria attached on the surface were observed by SEM TESCAN MAIA3 microscope with CRYO mode (Figure 4). This method showed the morphology of the cells and its possible changes caused by TiNTs. On the control Ti, the bacterial colonisation of *S. aureus* and also *P. aeruginosa* is very high. Bacterial cells surrounded by biofilm structures cover the entire visible surface of the examined Ti samples. In *P. aeruginosa*, the quality of the photograph is reduced due to the slimy consistency of the biofilm. On the TiNT1 samples, the colonisation appears visibly lower. The surface with nanotubes is clearly visible. The morphology of *S. aureus* remained unchanged, the cells appear in clusters retaining their typical cocci shape. In *P. aeruginosa* cells, certain lytic effect is visible, the structure and shape of the cells appear to be disrupted. On TiNT2 samples, the bacterial colonisation also appears lower. S. aureus cells retain their morphological properties even in these samples. However, *P. aeruginosa* shows considerable lysis, the cells are disrupted and their contents are absorbed into the surface of the nanotubes. The size of the nanotubes is likely to affect their ability to disrupt the bacterial membrane. Smaller nanotubes are sharper and therefore their lytic potential is larger. These results are consistent with previous studies (Peng et al. 2013, Bartlet et al. 2018). In contrast, in the study by Ercan et al. 2011, this relationship was not statistically proven.

Figure 1 Fluorescence microscopy of S. aureus, Ti, TiNT1, TiNT2 - Live/dead assay, magnification 200×

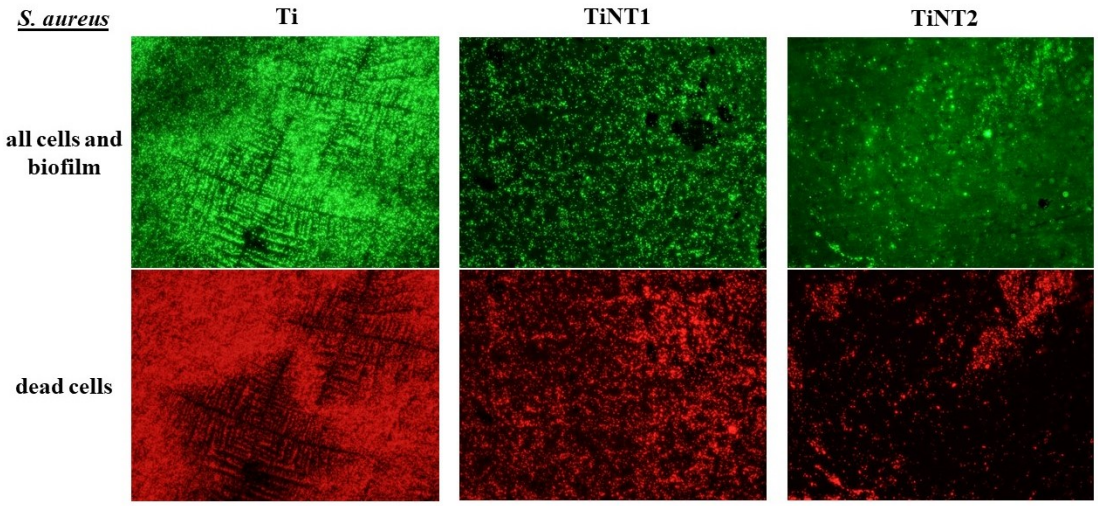

Figure 2 Fluorescence microscopy of P. aeruginosa, Ti, TiNT1, TiNT2 - Live/dead assay, magnification 200×

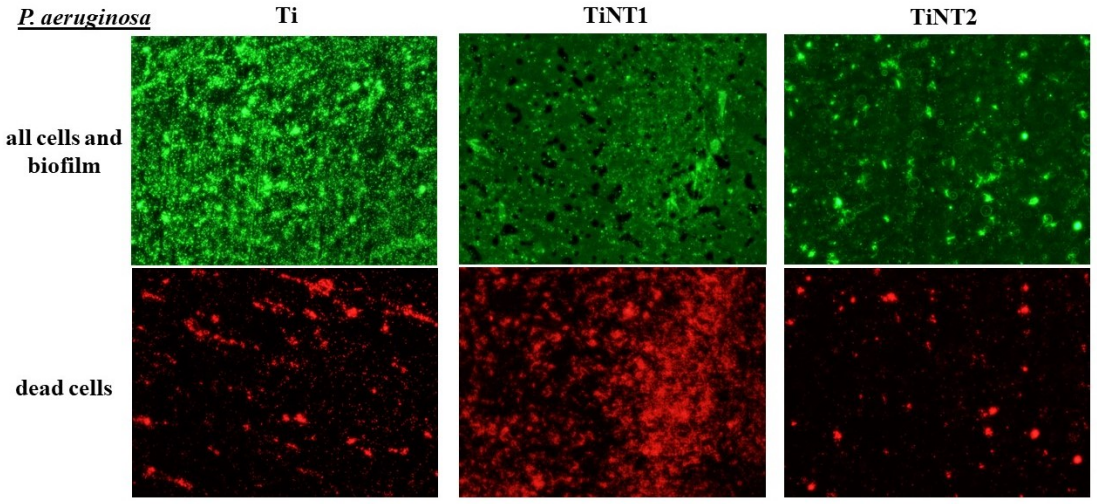

Figure 3 Fluorescence microscopy of untreated samples Ti, TiNT1, TiNT2- Live/dead assay, magnification 200×

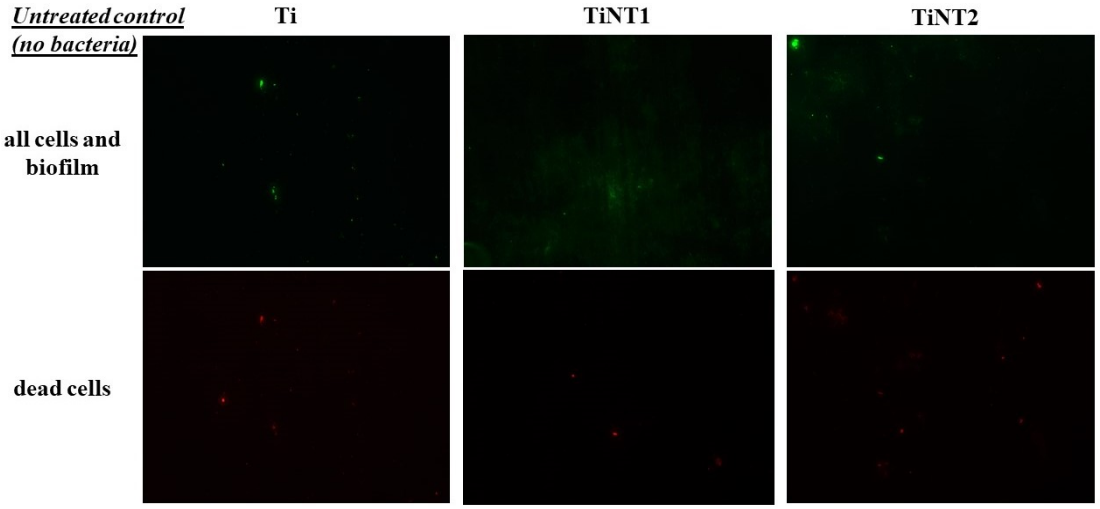

Figure 4 Scanning electron microscopy of bacteria on Ti, TiNT1, TiNT2

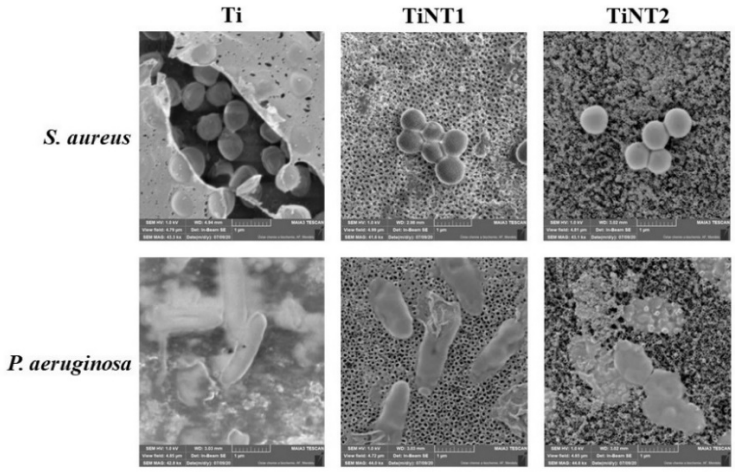

Plate count method

The results of the plate count method (Figure 5) show the increase of *S. aureus* bacterial cells on the surface of the monitored samples after 24 h of incubation and the percentage of inhibition compared to the control. The bacterial counts were expressed as CFU/ml inoculum added. As expected, antibacterial activity of titanium nanotubes was confirmed in both samples. Inhibition of TiNT1 was found to be 18.5% and of TiNT2 up to 27.09%. Compared to previous studies (Bhardwaj et al. 2017, Podporska-Carroll et al. 2015), which present more than 99% inhibition, this result is not as significant. Antibacterial titanium nanotubes are a promising material for further modifications. Studies (Spriano et al. 2018, Uhm et al. 2016, Li et al. 2016, Feng et al. 2020, Lee et al. 2019) investigate the antibacterial potential of titanium nanotubes enriched with other nanoparticles, such as Ag, Zn, Cu, antibiotics or organic antimicrobial compounds.

Figure 5 Plate count method – S. aureus growth on Ti, TiNT1, TiNT2 (CFU/ml) and % of inhibition

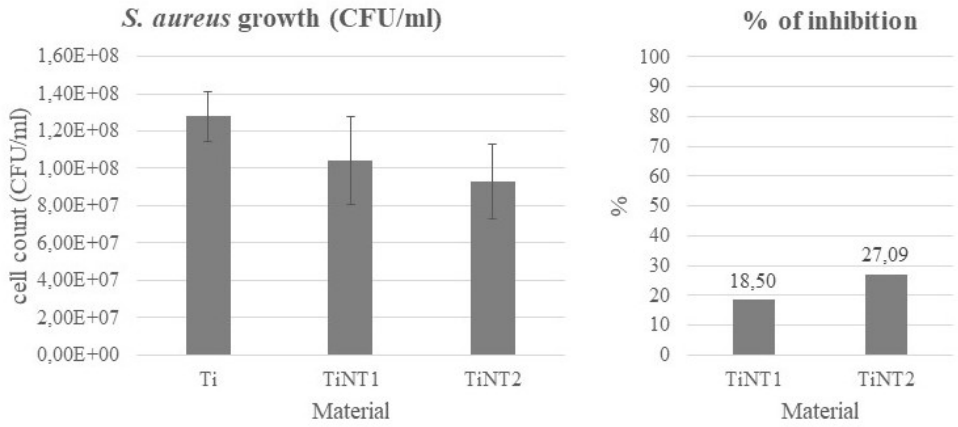

CONCLUSION

Bacterial infections of surgical implants are one of the most serious postoperative complications. Modification of the titanium surfaces of these devices with titanium nanotubes is one of the promising methods to reduce these infections. Titanium nanotubes are able to significantly reduce bacterial colonization of such treated surfaces. This study monitored the bacterial colonization of *S. aureus* and *P. aeruginosa* on titanium material coated with Titanium nanotubes 30–120 nm in diameter prepared by anodic oxidation compared to control titanium. Fluorescence microscopy showed visible decrease of bacterial colonisation on the surface treated with Ti nanotubes. Biofilm formation visible in fluorescence microscope pictures appears higher on both TiNTs compared to the control. SEM microscopy showed certain lytic effect on *P. aeruginosa* cells, morphological changes

and disruption of their membrane. Plate count method showed inhibition of *S. aureus* growth up to 27%. The material treated with titanium nanotubes thus appears to be a promising subject for further research for medical applications.

ACKNOWLEDGEMENTS
The research was financially supported by the internal grant agency of the Mendel University in Brno, project number AF-IGA2020-IP029 and GAČR MUNI project number GA20-11321S.

REFERENCES

Arciola, C.R. et al. 2012. Biofilm formation in Staphylococcus implant infections. A review of molecular mechanisms and implications for biofilm-resistant materials. Biomaterials, 33: 5967–82.

Banerjee, I. et al. 2011. Antifouling Coatings: Recent Developments in the Design of Surfaces That Prevent Fouling by Proteins. Bacteria, and Marine Organisms, 23: 690–718.

Bartlet, K. et al. 2018. Antibacterial activity on superhydrophobic titania nanotube arrays. Colloids and Surfaces B: Biointerfaces, 166: 179–86.

Bhardwaj, G., Webster, T.J. 2017. Reduced bacterial growth and increased osteoblast proliferation on titanium with a nanophase TiO_2 surface treatment. International Journal of Nanomedicine, 12: 363–69.

Damiati, L. et al. 2018. Impact of surface topography and coating on osteogenesis and bacterial attachment on titanium implants. Journal of Tissue Engineering, 9: 2041731418790694.

Ercan, B. et al. 2011. Diameter of titanium nanotubes influences anti-bacterial efficacy. Nanotechnology, 22: 295102.

Feng, W. et al. 2020. Rapid inactivation of multidrug-resistant bacteria and enhancement of osteoinduction via titania nanotubes grafted with polyguanidines. Journal of Materials Science & Technology. In Press.

Lee, J.S. et al. 2019. Facile preparation of mussel-inspired antibiotic-decorated titanium surfaces with enhanced antibacterial activity for implant applications. Applied Surface Science, 496: 143675.

Li, Y. et al. 2019. Enhanced antibacterial properties of orthopedic implants by titanium nanotube surface modification: a review of current techniques. International Journal of Nanomedicine, 14: 7217–36.

Li, G. et al. 2016. Antibacterial and Microstructure Properties of Titanium Surfaces Modified with Ag-Incorporated Nanotube Arrays. Journal of Materials Research, 19: 735–740.

Mansoorianfar, M. et al. 2020. Scalable fabrication of tunable titanium nanotubes via sonoelectrochemical process for biomedical applications. Ultrasonics Sonochemistry, 64: 104783.

Peng, Z. et al. 2013. Dual effects and mechanism of TiO_2 nanotube arrays in reducing bacterial colonization and enhancing C3H10T1/2 cell adhesion. International Journal of Nanomedicine, 8: 3093–105.

Podporska-Carrol, J. et al. 2015. Antimicrobial properties of highly efficient photocatalytic TiO_2 nanotubes. Applied Catalysis B: Environmental, 176–177: 70–75.

Popham, D.L. 2013. Visualizing the production and arrangement of peptidoglycan in Gram-positive cells. Molecular Microbiology, 88: 645–49.

Spirano, S. et al 2018. A critical review of multifunctional titanium surfaces: New frontiers for improving osseointegration and host response, avoiding bacteria contamination. Acta Biomaterialia, 79: 1–22.

Uhm, S. et al. 2016. Long-Term Antibacterial Performance and Bioactivity of Plasma-Engineered Ag-NPs/TiO2 Nanotubes for Bio-Implants. Journal of Biomedical Nanotechnology, 12: 1890–1906.

Wang, J. et al. 2016. Antibacterial Surface Design of Titanium-Based Biomaterials for Enhanced Bacteria-Killing and Cell-Assisting Functions Against Periprosthetic Joint Infection. ACS Applied Materials & Interfaces, 8: 11162–78.

Antimicrobial activity of PLGA nanoparticles

Ludmila Kosaristanova[1], Pavla Vymazalova[2], Vendula Popelkova[2], Tomas Komprda[2]
[1]Department of Chemistry and Biochemistry
[2]Department of Food Technology
Mendel University in Brno
Zemedelska 1, 613 00 Brno
CZECH REPUBLIC

lidka.kosaristanova@gmail.com

Abstract: Nowadays, one of the major problems in the world is occurring antimicrobial resistance of bacteria. Nanoencapsulation offers great potential in overcoming of antibiotics resistance using natural compounds for delivery. PLGA nanoparticles with entrapped mupirocin and fish oil have promising potential for nanodelivery system. Mupirocin is effective in inhibition of major grampositive bacteria. Fish oil has anti-inflammatory and regenerating effects in the healing process of the skin due to the content of long-chain n-3 polyunsaturated fatty acids (PUFAs). Expectedly, no antimicrobial effect was observed by PLGA with encapsulated fish oil unlike PLGA with encapsulated mupirocin. Unfortunately, the antimicrobial activity of mupirocin alone was significant compared to encapsulated mupirocin. Despite the following results, PLGA nanoparticles should be further studied and their production improved for other purposes.

Key Words: nanoparticles, antimicrobial activity, mupirocin, PLGA

INTRODUCTION

Using a broad spectrum of antibiotics has led to the emergence of multidrug resistant (MDR) microorganisms. These consequences intensified the public health problems such as bacterial infections with the consequent spreading in the population (Gómez-Sequeda et al. 2020). However, ways to overcome antibiotic resistance are increasingly being developed. Nanoencapsulation offers great potential in natural compounds delivery. That protects them from degradation, improves their aqueous solubility, and delivers active compounds to the action site (Silva et al. 2014). PLGA (Poly) (D, L-lactic-co-glycolide) is a biodegradable polymer synthesized by ring-opening polymerization or polycondensation reaction of lactic and glycolic acids. Recent studies presented, that submicron and nanosomic particles of PLGA demonstrate better infiltration capability. These compounds are also appearing to be good suitable transporter for nanoparticles. PLGA based drug delivery systems can be easily formed into any shape and size, such as particles, fibres, scaffolds, films, and coatings, and they can be used to incorporate and deliver a wide range of synthetic and natural drug (Kemme and Heinzel-Wieland 2018, Fan et al. 2020).

Nanodelivery system is available for capture and delivery of different kind natural compounds and antibiotics. Fish oil (FO) is a potent nutraceutical composed of long-chain n-3 polyunsaturated fatty acids (PUFAs), e.g., eicosapentaenoic acid (EPA) and docosahexaenoic acid (DHA). These acids offer important immunomodulating and anti-inflammatory properties mostly because their capacity of activating of peroxisome proliferator-activated receptors (PPARs) and decreasing nuclear factor (NF)-κB pathway (Giustina et al. 2020). Fish oil has been used as a dietary supplement for many years for its beneficial effects. The presented studies show that fish oil has favourably effects in other branches. Supplementation with the n-3 polyunsaturated fatty acids (PUFA) eicosapentaenoic acid (EPA) and docosahexaenoic acid (DHA) have shown promise as therapeutic agents in a number of inflammatory skin conditions, altering the lipid profile of the skin and production of bioactive lipids such as are eicosanoids, docosanoids and endocannabinoids. Fish oil is also primarily known for its healing and regenerating effects (Kendall et al. 2017). Besides, some studies have suggested that fish oil may also be beneficial in the treatment of skin cancer (Rehman and Zulfakar 2017).

The increasing incidence of infections caused by antibiotic-resistant strains such as *methicillin-resistant S. aureus* (MRSA) and *Staphylococcus aureus*, calls for exploration of new approaches to treat

these infections. Mupirocin, previously known as pseudomonic acid A, is an isoleucyl–adenylate analogy naturally produced by *Pseudomonas fluorescens* that inhibits bacterial protein synthesis by preventing the attachment of isoleucine to its cognate tRNA. It is an antibiotic with a unique mode of action that is active against MRSA, but its clinical use is restricted to topical administration because of its limited plasma stability and rapid degradation to inactive metabolites (Goldmann et al. 2019). This agent lacks cross-resistance to current antibiotics, but it is also unstable in vivo and thus not well-suited for systemic use in humans. However, mupirocin-based ointments have proven effective for the treatment of *S. aureus* skin and wound infections and have also recently emerged as the standard of care for presurgical nasal decolonization (Blanchard et al. 2016, Kwiatkowski et al. 2019). Other beneficial effects have been studied with Mupirocin nanofibers like as a new potential for proper application of scaffolds as a wound dressing (Amajuoyi et al. 2020).

MATERIAL AND METHODS

Material

The tested samples were poly (D, L-lactide-co-glycolide) (PLGA) with entrapped antibiotics mupirocin (MUP) and with poly (vinyl alcohol) (PVA). The next samples were poly (D, L-lactide-co-glycolide) (PLGA) with encapsulated fish oil (FO) and with poly (vinyl alcohol) (PVA). The last one were poly (D, L-lactide-co-glycolide) (PLGA) empty with poly (vinyl alcohol) (PVA). Every sample was dissolved in MiliQ water and sonicated for 5 minutes (40 KHz). These samples were obtained from Department of Food Technology, Mendel University in Brno.

Cultivation of tested bacterial strains

S. aureus (CCM 4223) methicillin-resistant *S. aureus* (MRSA) (CCM 7110) and *Escherichia coli* (CCM 3954) were obtained from the Czech Collection of Microorganisms, Faculty of Science, and Masaryk University in Brno, Czech Republic. The bacteria were cultured on 5% Columbia blood agar (LMS, Czech Republic) at 37 °C overnight.

Disk diffusion method

Bacterial cultures were diluted in saline to cell density 0.5 Mc Farland. Bacterial suspension was taken by a sterile cotton swab and inoculated on Petri dish with Muller Hinton agar (Sigma Aldrich, USA) by streaking. The surface of the medium was dried for 3–5 minutes. On Petri dishes with bacterial cultures, control antibiotics disks and cellulose disks with samples were applied. As a control, amoxicillin was used for *E. coli*, penicillin for *S. aureus* and vancomycin for MRSA. Samples (10 µl) were inoculated on cellulose disks. These Petri dishes were incubated at 37 °C for 24 hours. Every sample was prepared in duplicates.

Growth curve

Bacterial strains were diluted in 2× Mueller Hinton broth to 0.5 Mc Farland and then diluted 100× to cell density 1–2 × 10^6 CFU/ml. After that diluted strains of bacteria were placed in 100-well microplate and mixed with different concentrations of PLGA nanoparticles. The growth curve of bacteria was measured by Bioscreen C MBR (Dynex, Czech Republic). The absorbance reads at 620 nm were monitored at time zero, and then at 30 min intervals for 24 h at 37 °C. Every sample was prepared in duplicates.

Plate count method

Bacterial strains were diluted in 2× Mueller Hinton broth to 0.5 Mc Farland and then diluted 100× to cell density 1–2 × 10^6 CFU/ml. Samples of PLGA nanoparticles were diluted in different concentrations according to inhibition concentrations from the growth curves. Solution of PLGA nanoparticles and inoculum of bacteria were mixed in a ratio 1:1. Positive control was prepared by 500 µl of bacterial inoculum and 500 µl of Mili Q water. Samples with control were rotated in incubator at 37 °C 6 hours. After were diluted in saline and 100 µl of each sample was applied on Petri dish with Plate count agar (LMS, Czech Republic). Petri dishes were incubated at 37 °C for 24 hours. Samples were rotated in incubator at 37 °C for another 12 hours. Then they were diluted again in saline and 100 µl of each sample was applied on Petri dish with Plate count agar. Petri dishes were incubated at 37 °C for 24 hours. Every sample was prepared in duplicates.

RESULTS AND DISCUSSION

Disk diffusion method

For disk diffusion method were prepared three bacterial strains which are *S. aureus*, *E. coli* and MRSA. For antimicrobial assessment were diluted PLGA with mupirocin in concentration 1 mg/ml. The next sample was PLGA with fish oil and separate fish oil, both of them in concentration 1 mg/ml. The last one was PLGA empty in concentration 1 mg/ml and 0.5 mg/ml. None of the samples showed an antimicrobial effect against the above bacterial strains even in comparison with the control antibiotic disks. Antimicrobial activity of PLGA with mupirocin against *E. coli* has not been reported because antibiotic mupirocin is effective against grampositive bacteria. Therefore, *E. coli* was discarded for further testing. None antimicrobial activity of PLGA with fish oil was expected because fish oil rather promotes healing and helps regenerate skin which has been experimentally confirmed.

Growth curve and plate count method

Bacterial growth in the time was continually observed by determination of growth curves of *S. aureus* and MRSA. The tested samples were PLGA with mupirocin and separate mupirocin, PLGA with fish oil and PLGA empty. The samples were diluted to concentration of 1 mg/ml and then a half-dilution concentration series was performed.

Figure 1 Representation of the growth curves of MRSA and S. aureus with separate Mupirocin at the different concentrations

A) Mupirocin with S. aureus

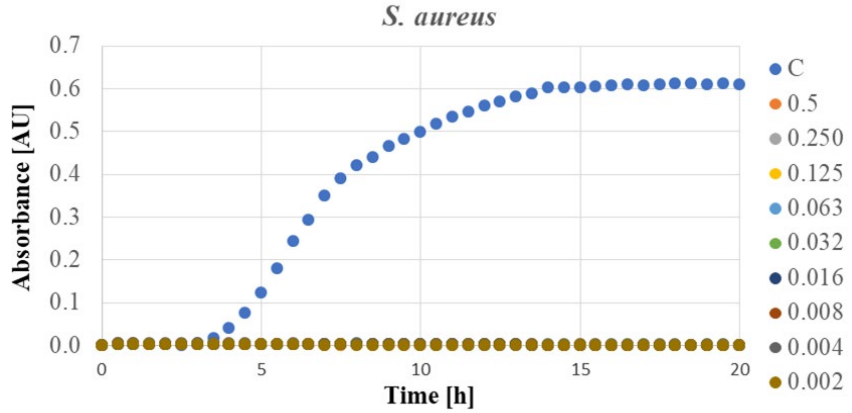

B) Mupirocin with MRSA

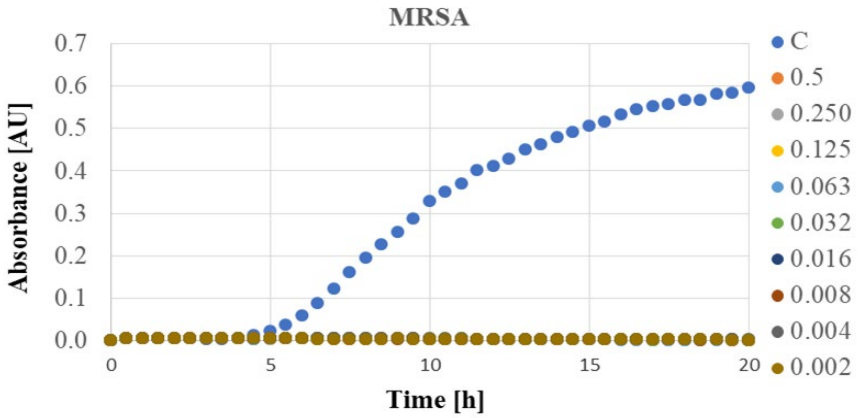

C) PLGA + Mupirocin with S. aureus

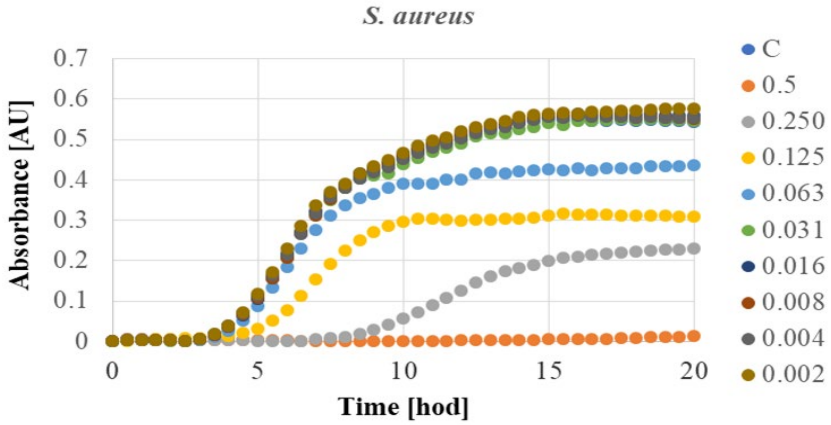

D) PLGA + Mupirocin with MRSA

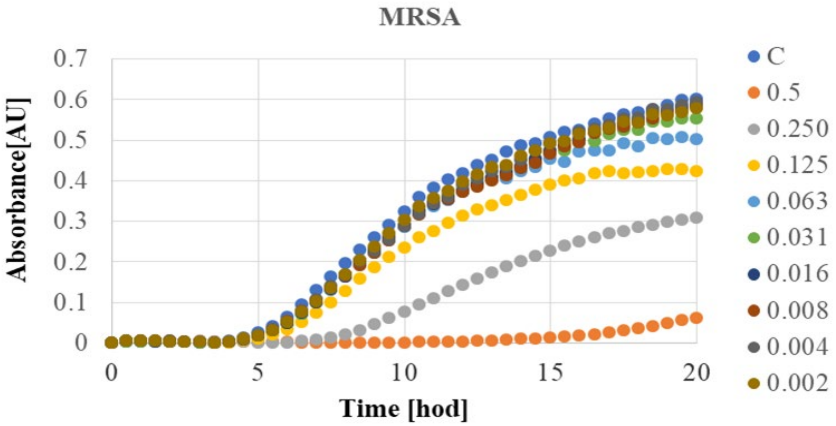

Legend: C – Control, Concentrations – 0.5 mg/ml, 0.250 mg/ml, 0.125 mg/ml, 0.063 mg/ml, 0.031 mg/ ml, 0.016 mg/ml, 0.008 mg/ml, 0.004 mg/ml, 0.002 mg/ml for. These concentrations were used for all samples.

PLGA empty and with fish oil showed no antimicrobial activity against both bacterial strains. But positive influence had PLGA with mupirocin against *S. aureus* and MRSA.

Based on the growth curves, the plate count method was performed. Concentrations that showed an inhibitory effect on the growth curves were used (c = 0.5 mg/ml, 0.250 mg/ml, 0.125 mg/ml). A separate mupirocin was used for comparison at the same concentration as PLGA nanoparticles. For both bacteria, colony counts decreased significantly at concentrations 0.5 mg/ml after 6 and 18 hours but in other concentrations, colony counts began to increase. However, separate mupirocin showed an inhibitory effect against both bacteria at all concentrations used after 6 and 12 hours. The reason why colony counts were gradually increased at lower concentrations may be the low concentration of encapsulated mupirocin in PLGA nanoparticles. The loading of PLGA nanoparticles with entrapped mupirocin purified by dialysis was 2.34 µg MUP /mg powder. Load capacity was calculated based on the amount of MUP in NPS (µg) divided by the amount of powder (mg). The low concentration of PLGA with encapsulated mupirocin may also the reason why the inhibitory effect was observed in the growth curves only at higher concentrations compared to the separate mupirocin against the above bacteria.

CONCLUSION

Antimicrobial activity was not observed with PLGA with fish oil and PLGA empty. None antimicrobial activity of PLGA with fish oil was expected because fish oil rather promotes healing and helps regenerate skin. PLGA with entrapped mupirocin showed better antimicrobial effects but was not as significant compared to control and separate mupirocin. The low concentration of encapsulated mupirocin could cause a low inhibitory effect.

ACKNOWLEDGEMENTS
The research was financially supported by the international grant agency of the Mendel University in Brno. Number of project is AF-IGA-2019-TP006.

REFERENCES

Amajuoyi, J. N. et al. 2020. Development of electrospun keratin/coenzyme Q10/poly vinyl alcohol nanofibrous scaffold containing mupirocin as potential dressing for infected wounds. Future Journal of Pharmaceutical Sciences, 6(1): 25.

Blanchard, C. L. et al. 2016. Neomycin Sulfate Improves the Antimicrobial Activity of Mupirocin-Based Antibacterial Ointments. Antimicrobial Agents and Chemotherapy, 60(2): 862-872.

Fan, W. et al. 2020. Quaternary ammonium silane, calcium and phosphorus-loaded PLGA submicron particles against Enterococcus faecalis infection of teeth: An in vitro and in vivo study. Materials Science and Engineering, C 111: 110856.

Giustina, A. D. et al. 2020. Lipoic Acid and Fish Oil Combination Potentiates Neuroinflammation and Oxidative Stress Regulation and Prevents Cognitive Decline of Rats After Sepsis. Molecular Neurobiology.

Goldmann, O. A. et al. 2019. Liposomal mupirocin holds promise for systemic treatment of invasive Staphylococcus aureus infections. Journal of Controlled Release, 316: 292-301.

Gómez-Sequeda, N. et al. 2020. Potent and Specific Antibacterial Activity against Escherichia coli O157:H7 and Methicillin Resistant Staphylococcus aureus (MRSA) of G17 and G19 Peptides Encapsulated into Poly-Lactic-Co-Glycolic Acid (PLGA) Nanoparticles. Antibiotics, 9(7): 384.

Kemme, M., Heinzel-Wieland, R. 2018. Quantitative Assessment of Antimicrobial Activity of PLGA Films Loaded with 4-Hexylresorcinol. Journal of Functional Biomaterials, 9(1): 4.

Kendall, A. C. et al. 2017. Lipid functions in skin: Differential effects of n-3 polyunsaturated fatty acids on cutaneous ceramides, in a human skin organ culture model. Biochimica et Biophysica Acta (BBA) - Biomembranes 1859, (9, Part B): 1679-1689.

Kwiatkowski, P. et al. 2019. The Influence of Essential Oil Compounds on Antibacterial Activity of Mupirocin-Susceptible and Induced Low-Level Mupirocin-Resistant MRSA Strains. Molecules, 24(17): 3105.

Rehman, K., Zulfakar M. H. 2017. Novel Fish Oil-based Bigel System for Controlled Drug Delivery and its Influence on Immunomodulatory Activity of Imiquimod Against Skin Cancer. Pharmaceutical Research, 34(1): 36-48.

Silva, L. M. et al. 2014. Delivery of phytochemicals of tropical fruit by-products using poly (dl-lactide-co-glycolide) (PLGA) nanoparticles: Synthesis, characterization, and antimicrobial activity. Food Chemistry, 165: 362-370.

Optimization of cryosection thickness of *Danio rerio* for MALDI-MSI

Zaneta Koudelkova[1], Tomas Do[1], Roman Guran[1,3], Jan Priborsky[1], Eva Postulkova[2], Marija Radojcic[2], Radovan Kopp[2], Jan Mares[2], Ondrej Zitka[1,3]
[1]Department of Chemistry and Biochemistry
[2]Department of Zoology, Fisheries, Hydrobiology and Apiculture
Mendel University in Brno
Zemedelska 1, 613 00 Brno
[3]Central European Institute of Technology
Brno University of Technology
Purkynova 123, 612 00 Brno
CZECH REPUBLIC

xkoudel9@mendelu.cz

Abstract: Matrix-assisted laser desorption/ionization mass spectrometry imaging (MALDI MSI) is semi-quantitative, relatively fast method which is able to measure a wide range of compounds and detect their molecular weights. In recent years it was used for determination and localization of plenty of biomarkers. The aim of this experiment is comparison of different thicknesses of sections used for MALDI MSI using Zebrafish (*Danio rerio*) as a model sample and determine the most suitable thickness for imaging of whole fish in further researches regarding the effects of the different types of nanoparticles in aquatic environment. This knowledge could improve accuracy and efficiency of imaging of the selected biomarkers. Thicknesses 15 µm, 20 µm and 25 µm of sections were used in this optimization. Their comparison was based on chosen peaks with the highest intensities (*m/z* 616.441 Da and 1480.481 Da) in the two specific regions of tissue sections (organ and organ-free areas).

Key Words: mass spectrometry imaging, zebrafish, cryosection

INTRODUCTION

Danio rerio (Zebrafish) is a small size freshwater fish belonging to the family of *Cyprinidae*. The typical habitat is clear stagnant water, for example rice paddies and canals in southeast Asia, of wide range temperature about 6 °C to 38 °C. Its diet consists of zooplankton, phytoplankton and insects (Spence et al. 2007). Zebrafish embryos and adults are frequently used as a vertebrate model organism for environmental toxicology, pharmacological and genetic testing (Figueroa et al. 2020, Segner 2009).

The quality of cryosections and their analysis can be affected by embedding medium and matrix application. Embedding prevents crushing of delicate structures and preserves structure of the sample. Zebrafish body contains a swim bladder filled with air. Frozen bladder is of a fragile structure, when it gets crushed during sectioning it can dislocate other organ structures (Nelson et al. 2013).

The principle of matrix-assisted laser desorption/ionization mass spectrometry imaging (MALDI MSI) is based on laser desorption of analytes with matrix after the effect of short laser pulses in ion source mass spectrometer, most often in the UV range. MALDI techniques enable detection of high molecular weight substances such as peptides, proteins and lipids and display their spatial distribution in tissues. Therefore, MALDI MSI is suitable for biological analysis and study of biomarkers (Duenas et al. 2017). MALDI is most often used in combination with the mass analyser time-of-light (TOF). This method has high sensitivity and it is capable of detection of relatively wide range of compounds. Combination of these advantages of the method is useful for drug development, observation of their reactions and formed compounds, as well as their localization (Rohner et al. 2005). Sections of thickness of about 5–20 µm placed on a glass slide covered by conductive surface are often used for imaging (Guráň et al. 2016). MALDI was used in recent years for some toxicological studies

of pesticides (Liu et al. 2020) or biomedicine antioxidants (Shi et al. 2020) using zebrafish as a model organism.

In the present study, we have focused on determining the most suitable thickness for MALDI MSI analysis of whole-body of Zebrafish tissue. Zebrafish was chosen as model organism because in further research we will focus on toxicological effects of the different types of nanoparticles in aquatic environment. The obtained results from this study will help us in future experiments to set up the optimal conditions in MALDI MSI analysis of selected biomarkers in Zebrafish.

MATERIAL AND METHODS

Materials and collection zebrafish samples

α-Cyano-4-hydroxycinnamic acid (HCCA), carboxymethylcellulose (CMC), gelatine and all the solvents (HPLC grade) used were purchased from Sigma-Aldrich (MO, USA), unless otherwise noted. Conductive indium-tin oxide (ITO) one-side coated glass slides were purchased from Bruker Daltonik GmbH (Germany).

Zebrafish samples originate in Mendel University in Brno (File number: 17OZ4655/2020-18134, Ref. number: 40774/2020-MZE-18134, Registration number: CZ 602760090). While working with animals, all forms of suffering are minimized and only professionally qualified people work with animals. The experiment was performed in compliance with the Act No. 246/1992 Coll. of the Czech National Council on the protection of animals against cruelty and the Decree No 419/2012 Coll. Ministry of Agriculture on the protection of experimental animals.

Preparation of tissues for mass spectrometry

Danio rerio used as a model organism in this experiment was 12 months old and its length was 25–30 mm. Fish were placed in the experimental tanks (25x15x15 cm) in a room with a stable air temperature 23±2 °C. The volume of the fish tanks was 3 litres. Hydrochemical parameters of water such as temperature, pH, amount of dissolved oxygen and conductivity were monitored during the experiment. Fish were killed and frozen in dry ice and 95% ethanol bath.

The frozen fish was embedded into a medium. As an embedding medium was used 2% carboxymethylcellulose (CMC) and 10% gelatine mixture, according to Nelson et al. (2013). Frozen fish were kept on dry ice until sectioning. Cryosections of zebrafish of 15, 20 and 25 µm thickness were prepared by Slee MTC Manual Bench Top Cryostat (Slee, Germany). Indium-Tin Oxide (ITO) coated glass slides with cryosections were stored in -80 °C.

ITO glass slides with cryosections were desiccated in vacuum for 20 minutes. Then the slides were placed in a chamber with ethanol (twice in 70% ethanol for 2 minutes, once 100% ethanol for 1 minute). Before the scanning and matrix spraying, slides were desiccated in vacuum once again for 10 minutes. After desiccation, glass slides were scanned by an Epson Perfection V500 Office scanner (Epson Europe B.V., Netherlands) at resolution of 3200 DPI. Before scanning, positions of tissues on slides were pointed by three guide signs using white pencil corrector to label them. ImagePrep™ standard programs (Bruker Daltonik GmbH, Germany) were used to spray α-Cyano-4-hydroxycinnamic acid (HCCA) in concentration of 7 mg/ml in acetontrile/water (50:50, v/v) with 0.2% trifluoroacetic acid (TFA), that was used as a matrix for imaging, on ITO glass slides. Matrix mixture was vortexed and ultrasonicated using Bandelin 152 Sonorex Digital 10P ultrasonic bath (Bandelin electronic GmbH, Berlin, Germany) for 2 minutes at 50% of intensity at a room temperature before spraying. For MSI analysis ITO slides were mounted into the MTP Slide Adapter II. The sample preparation for imaging is described in Figure 1.

MALDI imaging

MSI was performed on a MALDI-TOF mass spectrometer Bruker ultrafleXtreme (Bruker Daltonik GmbH, Bremen, Germany). A total sample set consisted of 9 ITO glass slides. Each ITO glass slide contains one tissue section of Zebrafish. Three tissue sections per different thickness were used. Each section came from the one Zebrafish individual. Adapter with two glass slides was inserted into the spectrometer. Scanned images of tissues were loaded into FlexImaging 3.0 software (Bruker Daltonik GmbH, Germany) to determine the location of sections by white guide signs. Regions

of acquisition were pointed by the mouse pointer in FlexImaging and 50 µm raster were selected. External calibration was performed using an antibiotic calibration standard mixture (ACS) which contains four small peptides in an *m/z* range of 100–1000 Da. Location of each *m/z* values, detected by intensity of each scan over the acquired mass range, was mapped and images were generated in using SCiLS Lab 2014b software (SCiLS – Bruker Daltonik GmbH, Germany). MALDI MSI was performed in reflector positive mode in the *m/z* range 0–1000 Da. The laser power was set to 65%. A total of 500 spectra were summed for each spot using a random walk raster pattern, with no evaluation criteria. The MSI data from FlexImaging were imported into the SCiLS Lab software to processing (Guran et al. 2017).

Figure 1 Scheme of zebrafish sample preparation for MALDI MSI

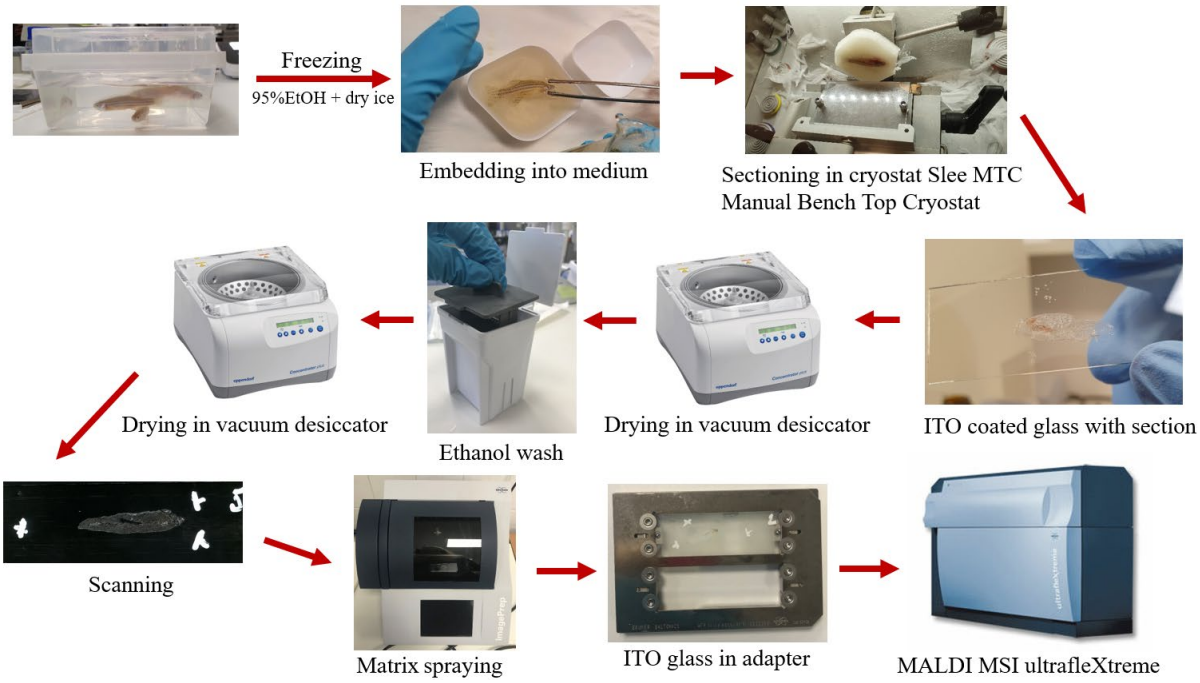

RESULTS AND DISCUSSION

Cryosections of various thicknesses were analysed by MALDI MSI and data from imaging were imported into SCiLS Lab software. The intensities of the selected peaks were compared to determine the suitable thickness of cryosection of the whole-body of *Danio rerio* for a future study. For the study were chosen these thicknesses cryosections of zebrafish: 15, 20 and 25 µm. In the previous optimization, thinner sections were used. However, this often resulted in tearing of sections so they were not as eligible as the thicker ones, therefore they were not included in this study.

In SCiLS Lab, a "find peaks" function was used to find a significant peak via an algorithm. The peak at *m/z* 616.441 Da was chosen from the area of organs and the peak at *m/z* 1480.481 Da from the organ-free area. These chosen peaks represent the peaks with the highest intensity in above mentioned areas. It was not identified what compounds these peaks represent, but for this study it is not necessarily important. According to studies, peak at *m/z* 616.441 Da probably represents haem molecule (Li et al. 1993, Gorchein et al. 2012). Selected peaks were used for generating MSI images (Figure 2) and box plots (Figure 3) and were used for comparison of thicknesses. In Figure 2 is shown only one tissue section for each thickness.

The data acquired from the imaging were statistically tested using Wilcoxon test. Obtained data for peaks 616.441 Da and 1480.481 Da varied significantly ($p < 0.001$) among tissues with various thickness. Only the peak at m/z 616.441 Da between thicknesses 15 µm and 20 µm was not revealed as significantly different ($p \geq 0.05$).

According to box plots, the peak at m/z 1480.481 Da has the highest median intensity in 15 µm section thickness which corresponds with previous optimization experiments (Nelson et al. 2013, Stutts

et al. 2020). However, for the peak at m/z 616.441 Da was the highest intensity in 25 µm thickness of the section, but dissimilarity between intensities of peak at m/z 616.441 Da of the tested thickness values was minor although statistically significant with exception between above mentioned thicknesses 15 µm and 20 µm. Based on these results, for MALDI MSI analysis of organ-free area is the most suitable thickness of cryosections 15 µm and for organ area 25 µm. The different results were probably caused by different tissue structure of organs and muscles. Furthermore, the difference in the peak intensity may be given not only by different thickness but also by different composition of neighbouring sections within one fish that was used for preparation of cryosections, but using the one Zebrafish individual is better for concluding the thickness because differences caused by neighbouring section are smaller that would be differences between various Zebrafish individuals. In addition, MALDI MSI is a semi-quantitative method, thus the obtained results do not provide exact quantitative information as acquired results for example by other methods of mass spectrometry but for purpose of this optimization MALDI MSI provides information that are sufficient for monitoring selected parameters.

Figure 2 Ion images of selected peaks (m/z 616.441 Da and 1480.481 Da) of compared thicknesses of Zebrafish cryosections

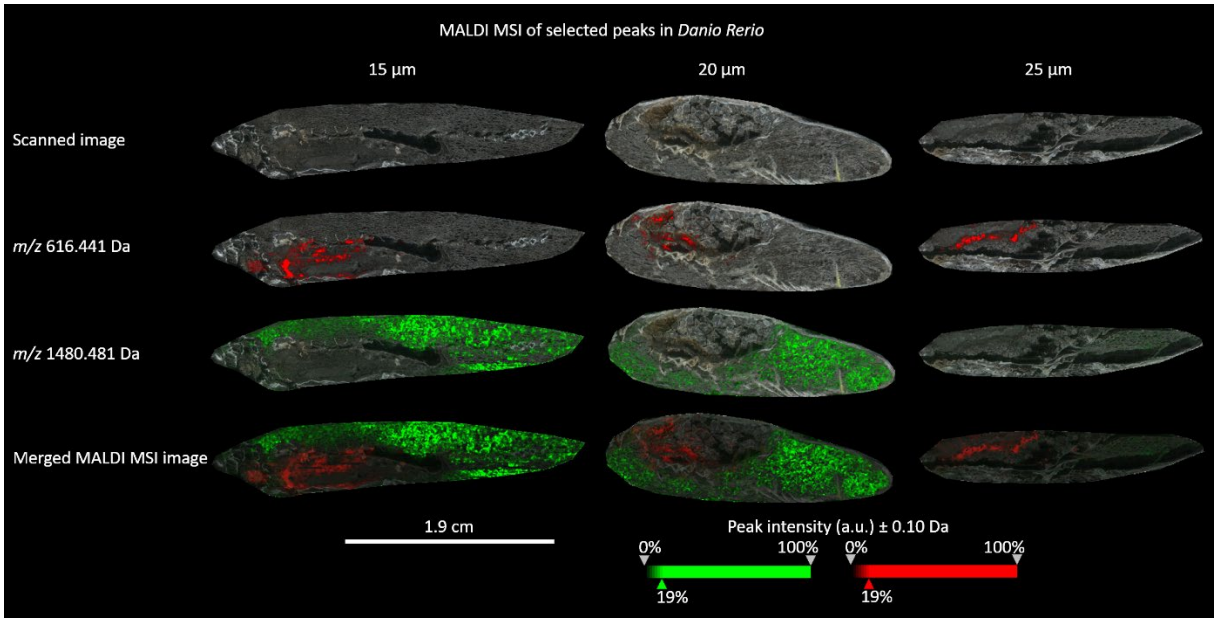

Figure 3 Intensity box plots of (A) 616.441 Da and (B) 1480.481 Da of compared thicknesses

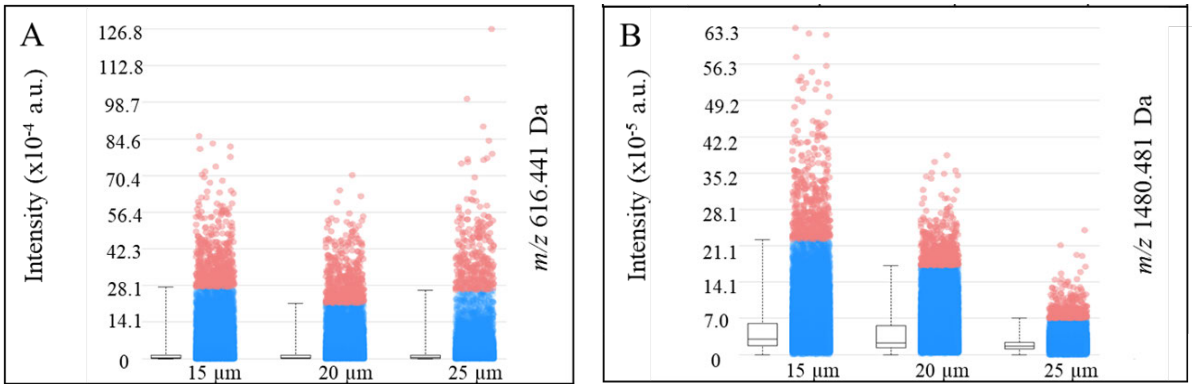

As the sorting of Zebrafish into parts with organ and non-organ parts would be economically demanding and in terms of preparation it is complicated, and could lead to damaging tissue, it is desirable to determine one or range of optimal thickness. According to previous experiments and our results, the suitable thickness of whole Zebrafish sections for MALDI MSI is determined in range from 15 to 20 µm, despite the optimal thickness in the area with organs was 25 µm. This conclusion was

based on the fact, that the differences of intensities of the selected peak for organ area among the different thicknesses were not as distinctive in contrast with intensities of the selected peak for organ-free area.

CONCLUSION

It was concluded that there are different optimal thicknesses for measurements in organ and non-organ areas. Optimal thickness for organ areas is 25 µm and for non-organ areas 15 µm. However, from the economical point of view, measuring these areas separately is not very efficient, so thicknesses ranging from 15 to 20 µm are determined as suitable for sections of whole fish. Within optimization of MALDI method will be needed to determine the most suitable MALDI matrix which will be used for MALDI MSI of selected biomarkers in Zebrafish sections. These results will be used in further research focusing on effects of different types of nanoparticles in aquatic organisms. In this future study MALDI MSI will be supported with proteomic analysis by LC-MS including optimization of the Zebrafish homogenization/extraction for preparation of samples for LC-MS analysis.

ACKNOWLEDGEMENTS

The financial supports received from IGA TP (AF-IGA-2018-tym005) and CEITEC 2020 (LQ1601) are gratefully acknowledged. This study was supported also by the project PROFISH CZ.02.1.01/0.0/0.0/16_019/0000869, the project is financed by European Regional Development Fund in the Operational Programme Research, Development and Education and The Czech Ministry of Education, Youth and Sports.

REFERENCES

Duenas, M.E. et al. 2017. 3D MALDI Mass Spectrometry Imaging of a Single Cell: Spatial Mapping of Lipids in the Embryonic Development of Zebrafish. Scientific Reports, 7: 14946.

Figueroa, D. et al. 2020. Toxicity and differential oxidative stress effects on zebrafish larvae following exposure to toxins from the okadaic acid group. Journal of Toxicology and Environmental Health, Part A, Current Issues, 83(15-16): 573–588.

Gorchein, A. et al. 2012. Isolation and characterization of free haem from the shell gland of quail and hen. Biomedical Chromatography, 26(3): 355–357.

Guran, R. et al. 2017. MALDI MSI of MeLiM melanoma: Searching for differences in protein profiles. Plos One, 12(12): e0189305.

Guráň, R. et al. 2016. MALDI zobrazovací hmotnostní spektrometrie pro studium fyziologických pochodů v nádorech. Chemické listy, 110(2): 106–111.

Li, Y.T. et al. 1993. Studies on heme-binding in myoglobin, hemoglobin and cytochrome-c by ion-spray mass spectrometry. Journal of the American Society for Mass Spectrometry, 4(8): 631–637.

Liu, W.J. et al. 2020. Phospholipid imaging of zebrafish exposed to fipronil using atmospheric pressure matrix-assisted laser desorption ionization mass spectrometry. Talanta, 209: 120357.

Nelson, K.A. et al. 2013. Optimization of whole-body zebrafish sectioning methods for mass spectrometry imaging. Journal of Biomolecular Techniques, 24(3): 119–127.

Rohner, T.C. et al. 2005. MALDI mass spectrometric imaging of biological tissue sections. Mechanisms of Ageing and Development, 126(1): 177–185.

Spence, R. et al. 2007. The behaviour and ecology of the zebrafish, Danio rerio. Biological Reviews, 83(1): 13–34.

Segner, H. 2009. Zebrafish (Danio rerio) as a model organism for investigating endocrine disruption. Comparative Biochemistry and Physiology C-Toxicology & Pharmacology, 149(2): 187–195.

Shi, Q. et al. 2020. Visualization of the tissue distribution of fullerenols in zebrafish (Danio rerio) using imaging mass spectrometry. Analytical and Bioanalytical Chemistry, 412: 7649–7658.

Stutts, W.L. et al. 2020. Methods for Cryosectioning and Mass Spectrometry Imaging of Whole-Body Zebrafish. Journal of the American Society for Mass Spectrometry, 31(4): 768–772.

Monitoring the disassembly process of human ferritins as tools for cancer nanotherapy

Zdenek Kratochvil[1, 2], Paulina Takacsova[1, 2], Marketa Charousova[1, 2]
[1]Department of Chemistry and Biochemistry
Mendel University in Brno
Zemedelska 1, 613 00 Brno
[2]Central European Institute of Technology
Brno University of Technology
Purkynova 123, 612 00 Brno
CZECH REPUBLIC

zdenek.kratochvil@mendelu.cz

Abstract: Ferritin is a protein able to disassemble and reassemble its structure composed of 24 subunits under specific pH conditions. Within this research work, the disassembly process of two recombinant human ferritins containing heavy (21 kDa, HsaH) and light subunits (19 kDa, HsaL) was monitored using native polyacrylamide gel electrophoresis (PAGE) and real-time record of ferritin size change. HsaH was proved to disassemble into smaller subunits at decreasing pH while both partial and complete disassembly occurred. On the contrary, only partially disassembling HsaL formed large aggregates, which hinders its potential application as a nanocarrier.

Key Words: ferritin, disassembly, pH conditions, nanoparticle size, nanotherapy

INTRODUCTION

Since ferritin is a molecule naturally found in human body and possesses many unique properties, it can be considered as a promising nanocarrier employed in targeted cancer treatment (Dostalova et al. 2015). Natural horse spleen ferritin was the first ferritin of which structural properties were tested (Banyard et al. 1978). One of those properties is its capability of partial disassembly at certain pH and reassembly when pH conditions revert to initial state (Dominguez-Vera and Colacio 2003). This can be used in order to entrap cytostatics or other bioactive agents to moderate undesirable effects on healthy cells. However, if the pH is more extreme, ferritin disassembles completely and irreversibly (Mihee et al. 2011).

This study focuses on determination of pH values at which partial and complete disassembly of two types of human ferritins occurs and how these pH conditions affect the size of ferritin nanoparticles in real time.

MATERIAL AND METHODS

To study partial and complete disassembly, recombinant human ferritins composed of either 24 heavy subunits (21 kDa, HsaH) or 24 light subunits (19 kDa, HsaL) were diluted in buffers with different pH values and then separated on 6% native polyacrylamide gels at 200 V for 28 min at 4 °C. Afterwards, gels were stained with Coomassie Blue in order to detect appropriate bands of separated ferritins subunits and assembled ferritin nanoparticles. The second part of this experiment was focused on monitoring the impact of disassembly on ferritin size after change of pH value in real time. Temporal kinetics of ferritin size changes was recorded by VASCO KIN™ using dynamic light scattering with sparse bayesian learning model. Particular pH values for individual measurements were chosen with regard to the results obtained from native PAGE.

RESULTS

At low pH values, partial disassembly of HsaH was observed in range of 2.0–3.5 while complete disassembly occurred in range of 1.0–1.5 (see Figure 1A). Alkaline environment then caused partial

disassembly between pH 10.0 and 12.5 and complete disassembly at pH 13.0. Results from VASCO KINTM suggest that after pH decrease to 1.5–3.5, HsaH ferritins split into smaller subunits rapidly whereas for pH decrease to 4.0, the size of HsaH nanoparticles remained constant for almost 5 min and only then the released subunits started to appear (see Figure 1B).

Figure 1 Examination of HsaH disassembly by native PAGE (A), temporal kinetics of HsaH ferritin size change after pH decrease (B)

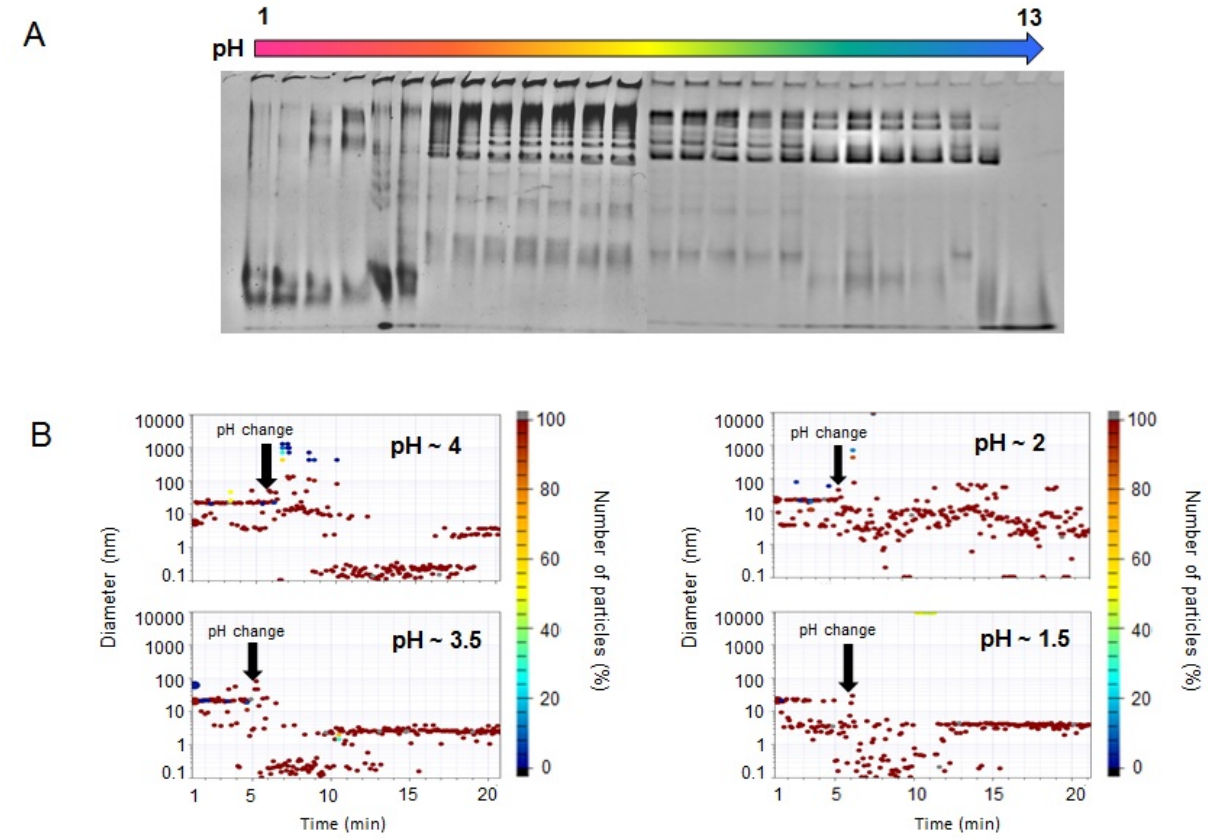

HsaL disassembled only partially in the pH range of 1.0–3.0 and at pH 13.0 and no complete disassembly was observed in any of the tested conditions (see Figure 2A). In contrast to HsaH, the size of HsaL ferritins changed immediately upon pH reduction but instead of released subunits, an increase of HsaL ferritins size was achieved due to aggregation of these subunits (see Figure 2B).

DISCUSSION

Differences in the disassembly between HsaL and HsaH ferritins were observed in this work. Only partial disassembly of HsaL occurred at correspondent pH, while complete disassembly of HsaH was found in extreme values of pH. Even then, HsaH turned out to be a more promising and reliable option for its potential use as a nanocarrier, because its disassembly into smaller subunits due to pH reduction was confirmed, which allows for physical entrapment of drugs for cancer nanotherapy. On the other hand, HsaL formed large aggregates that might prevent this kind of entrapment. However, this finding differs from results of the studies (Mihee et al. 2011, Stuehn et al. 2019) where the disassembly process of ferritin from equine spleen (EcaLH) composed of substantially higher number of light subunits over the heavy ones was investigated. By means of small-angle X-ray scattering (SAXS) and atomic force microscopy (AFM), respectively, the authors noticed ferritin disassembly into subunits when pH was reduced. Such dissimilarity compared to HsaL could be explained by diverse change in tertiary structure of two types of ferritin after pH adjustment and, thus, by different nature of their subunits.

Figure 2 Examination of HsaL disassembly by native PAGE (A), temporal kinetics of HsaL ferritin size change after pH decrease (B)

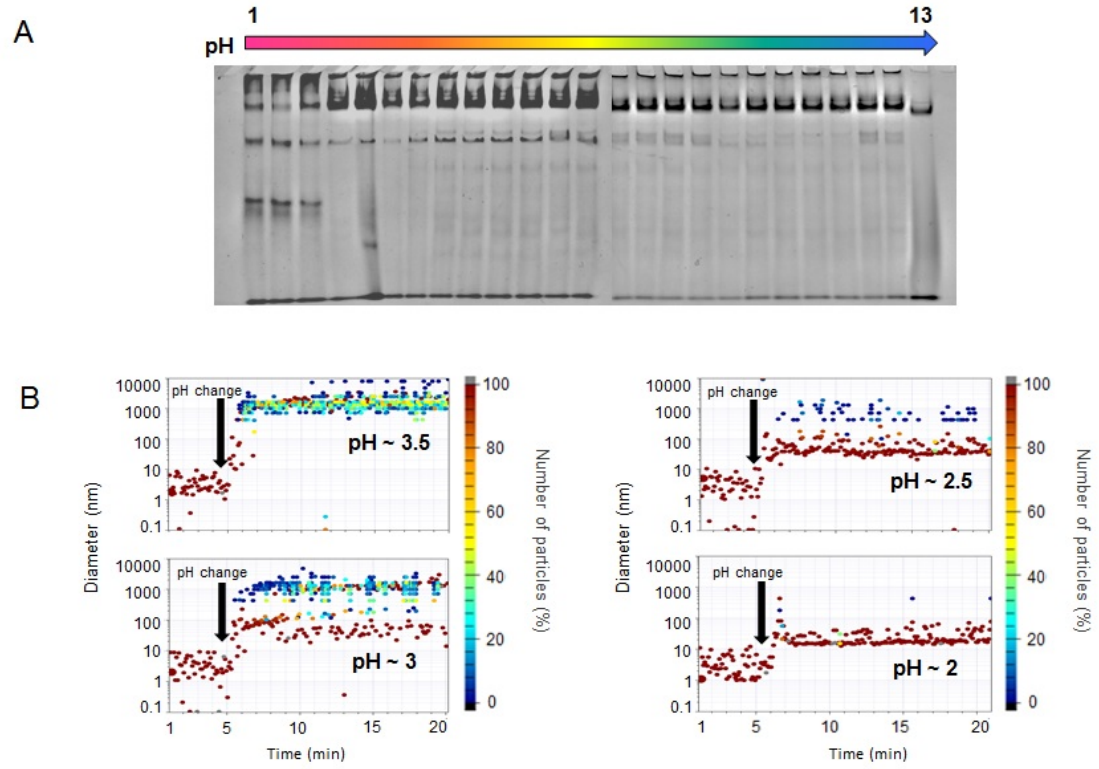

CONCLUSION

This study revealed novel information about structural behaviour of two different types of human ferritin at various pH conditions. In connection with their natural presence in human body, the results achieved within this work can be regarded as a significant contribution to the area of the potential use of ferritins as nanocarriers in the nanomedicine field.

ACKNOWLEDGEMENTS

The authors gratefully acknowledge financial support from the Grant Agency of the Czech Republic (GACR 19-13628S). VASCO KIN™ (Cordouan Technologies, Pessac, France) was kindly lent by Pragolab, s. r. o. (Prague, Czech Republic).

REFERENCES

Banyard, S.H. et al. 1978. Electron density map of apoferritin at 2.8-Å resolution. Nature, 271: 282–284.

Dominguez-Vera, J.M. and Colacio E. 2003. Nanoparticles of Prussian Blue Ferritin: A New Route for Obtaining Nanomaterials. Inorganic Chemistry, 42(22): 6983–6985.

Dostalova, S. et al. 2015. Apoferritin: protein nanocarrier for targeted delivery. In Nano Based Drug Delivery. Zagreb: IAPC Publishing, pp. 217–233.

Mihee, K. et al. 2011. pH-Dependent Structures of Ferritin and Apoferritin in Solution: Disassembly and Reassembly. Biomacromolecules, 12(5): 1629–1640.

Stuehn, L. et al. 2019. pH-depended protein shell dis- and reassembly of ferritin nanoparticles revealed by atomic force microscopy. Scientific Reports 9: 9.

Optimization of assay for total protein in the haemolymph of the honeybee (*Apis mellifera* L.)

Jan Musila[1], Zuzana Lackova[2,3], Ales Vladek[1], Antonin Pridal[1], Ondrej Zitka[2,3,4]
[1]Department of Zoology, Fisheries, Hydrobiology and Apidology
[2]Department of Chemistry and Biochemistry
Mendel University in Brno
Zemedelska 1, 613 00 Brno
[3]Central European Institute of Technology
Brno University of Technology
Purkynova 123, 612 00 Brno
[4]CEITEC – Central European Institute of Technology
Mendel University in Brno
Zemedelska 1, 61300 Brno
CZECH REPUBLIC

xmusila@mendelu.cz

Abstract: Protein levels in honeybee is a credible marker of a bee physiological status. Bradford's method is suitable for quantification of the total protein in the haemolymph. Two types of diluents, different diluting ratios and impact of storage were compared. Average decrease of the total protein content after one week storage of samples was lower in samples diluted in the phosphate buffer pH 7 in comparison with ones diluted with MilliQ water. The haemolymph samples dissolved in the phosphate buffer showed significantly higher yield and lower variability of the total protein content compared to the variability obtained by dissolving the haemolymph in MilliQ water. These results indicate that 200× dilution in the phosphate buffer (pH = 7) seems to be optimized for determination of the total protein in the bee haemolymph.

Key Words: haemolymph, *Apis mellifera*, total protein, Bradford's method, low volume sample

INTRODUCTION

Many proteins circulating in the haemolymph are created in the fat body (Lensky and Rakover 1983). The highest rate of protein synthesis in workers corresponds with the highest protein levels in the haemolymph (Crailsheim 1990). Quantity of the haemolymph protein is dependent on many factors: physiological status of a worker bee: "hive/forager" or "summer/winter" (Fluri et al. 1982), nutrition (Bitondi and Simões 1996, Cremonz et al. 1998, De Jong et al. 2009) and the hygienic abilities of the colony (Lazarov and Zhelyazkova 2018).

Inappropriate protein availability reduces bee longevity, brood rearing and honey production (Crailsheim 1990). Therefore, the total protein in the haemolymph is an important physiological parameter in the honeybee. The quantification protein for extra low volume samples was proposed by Bradford (1976). This spectrophotometric assay is very reproducible and rapid based on the dye binding process. The method is generally well evaluated and currently recommended as the protocol also for the bee haemolymph (Hartfelder et al. 2013).

The object of this contribution is optimization of the Bradford's method for our lab conditions due to our concurrent experiments on the winter bees. We compared different dilution and types of diluents for the haemolymph assay and also try to find the impact of type of storage on repeatability of measurements, i.e. very likely the stability of protein in the diluent until the test performing.

MATERIAL AND METHODS

Chemicals

Phosphate buffer (pH = 7) was prepared by mixing di-Sodium hydrogen phosphate anhydrous (11.876 g/l) and Sodium phosphate monobasic monohydrate (9.078 g/l). MilliQ water (demineralized water) was produced on a Milli Q RG (Millipore, Mass., USA). All chemicals were purchased from Sigma-Aldrich (St. Louis, USA).

Haemolymph collection

Workers were sampled on brood of the same colony and after that kept for a few minutes at 4 °C to immobilize them. The haemolymph sample from each worker was collected in volume 1 µl with using micro-capillary pipette by incision between 3rd and 4th abdominal tergites. The collected haemolymph was put into 1.5 ml Eppendorf tube with addition of tested diluents (MilliQ water of phosphate buffer pH7) with dilution 20×, 30×, 40×, 50×, 100×, 200×, 300×, 400× and 500×. Thus we obtained 2×9 samples from 18 workers applicated for presentation of results in Figures 1–3.

There were collected also paired samples for comparison results depended on applicated diluent in optimized dilution (n = 6, Figure 4). The haemolymph from the same bee in volume 3 µl was put into 0.5 ml Eppendorf and stirred up. Immediately after, always the 1 µl of the haemolymph was 200× diluted in the MilliQ water and the phosphate buffer (pH = 7) and analysed. Thus, six bees were paired-sampled.

Total protein quantification by method Bradford's assay

Bovine serum albumin (BSA) was used as a standard and was used for the validation of the method. Calibration curve was measured within the range from 0.50 to 0.03 mg/ml. Validation of the method using the BSA standard always took place before each determination (the standard was always prepared fresh). Ready-to-use protein reagent Dry Reagent Concentration (BIO-RAD, California, USA) was purchased. This reagent was diluted 1:4 with MilliQ water before analysis (the reagent was always prepared fresh). Determination procedure: 10 µl of the sample was pipetted into a 96 well microtiter plate Nunc Immuno (Fisher Scientific, Pardubice, Czech Republic). Subsequently, 200 µl of diluted protein reagent was added to 10 µl of the sample. Followed by incubation for 5 min at room temperature and absorbance measurement at 595 nm using instrument Infinite M200Pro (Tecan, Männedorf, Switzerland). Samples were measured immediately after the haemolymph collection and eventually some of them again after the one week storage in the freezer (-18 °C). Each sample has been analysed three-times (triplet).

Statistical evaluation

Values in graphs represent mean ± standard deviations (SD). Statistical significance of differences between average values were analysed with the Student's t-test. Values of the total protein in fresh and stored samples of haemolymph were compared to find the minimal differences (Figure 3 red oval). Statistical significance of differences in the paired samples were tested by paired t-test. The accuracy of the assay was estimated from average coefficient of variation (v_x) (Figure 4B).

RESULTS AND DISCUSSION

The results obtained in presented study are from two experiments i) influence of dilution and ii) testing of stability in storage in freezer.

The reason application of the dilutions is that haemolymph is very complex sample which may result in masking the real concentration of determined analyte. Therefore it is important to find the optimal dilution ratio which is in the same time in the linear dynamic range of the calibration curve of the assay method. The total protein in samples measured immediately after the collection of haemolymph with the phosphate buffer pH = 7 was higher than with MilliQ water (Figure 1 and 2).

Differences in the total protein content on dependence of used diluent was noted after the 1 week storage of samples in the freezer (-18 °C) (Figure 1A, 2A). The values of the total protein content in samples diluted with MilliQ water differed after 1 week significantly (p = 0.003) and decreased in average 5.7 µg/µl unlike the samples diluted in the phosphate buffer where the decrease was insignificant (p = 0.665) and only 1.9 µg/µl. The decrease values of the total protein after 1 week

of storage differed significantly in dependence of the used diluent (p = 0.0002). The BSA calibration curve in phosphate buffer (Figure 2B) provides a better standard response due to a more stable reaction with Bradford's reagent than the BSA calibration curve in water (Figure 1B). This phenomenon can be caused by the buffer provides free ions in higher concentrations, and these can better stabilise the counter ions in the structure of protein by surrounding them. This prevents any change in secondary and ternary structure of bigger proteins. This statement was confirmed by other results, where samples of haemolymph dissolved in phosphate buffer were much more stable than samples of haemolymph dissolved in water.

*Figure 1 (**A**) Total protein content in the samples of a bee haemolymph diluted 20–500× in MilliQ water (determination immediately after the collection and after the one week storage in the freezer). (**B**) The calibration curve of BSA in MilliQ water in range 0.50 to 0.03 mg/ml.*

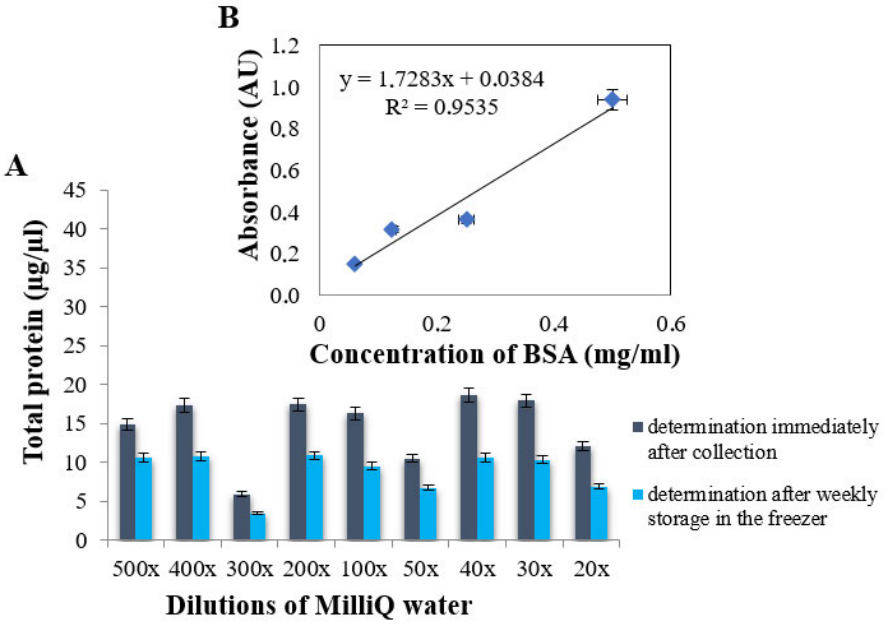

*Figure 2 (**A**) Total protein content in the samples of a bee haemolymph diluted 20–500× in phosphate buffer (pH=7) (determination immediately after the collection and after the one week storage in the freezer). (**B**) The calibration curve of BSA in phosphate buffer (pH=7) in range 0.50 to 0.03 mg/ml.*

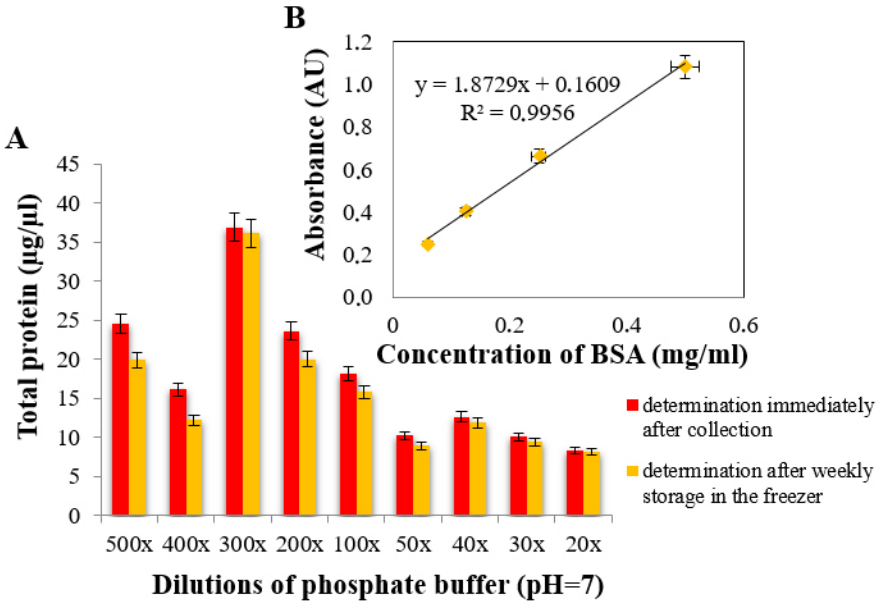

An expression of these differences as a percentage is depicted in Figure 3. The haemolymph samples diluted in MilliQ water showed in average a 39% decrease and ones dissolved in the phosphate buffer only 11%. This difference was statistically significant ($p < 0.001$). These comparisons confirm that the samples of haemolymph diluted in the phosphate buffer were more stable than in MilliQ water.

In the case of different sample dilutions, the 200× dilution of both tested diluents was evaluated as optimal. It may seem that a 300x dilution may be optimal, however higher or lower dilutions than 200× were no longer evaluated as optimal due to the extent of the detection limit and the determination of the Infinite M200Pro instrument used. Using 300x dilution would not ensure accuracy and reproducibility of results. Coincidentally, two different bees with extreme protein content were sampled for this dilution, therefore, these markedly different values (both diluents) from the other results are not decisive from the point of view of the dilution optimization.

Figure 3 Comparison of the decrease in the total protein after the one week storage in the freezer for samples dissolved in the MilliQ water and the phosphate buffer (pH = 7); the red oval = optimal dilution.

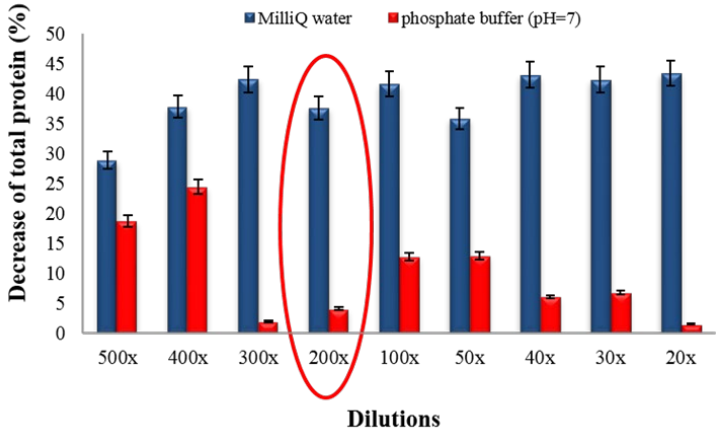

*Figure 4 The paired samples (n = 6) diluted 200× in the MilliQ water and the phosphate buffer (pH = 7); (**A**) the total protein content in the haemolymph; (**B**) average coefficient of variation of the total protein (t-test; p = 0.0006).*

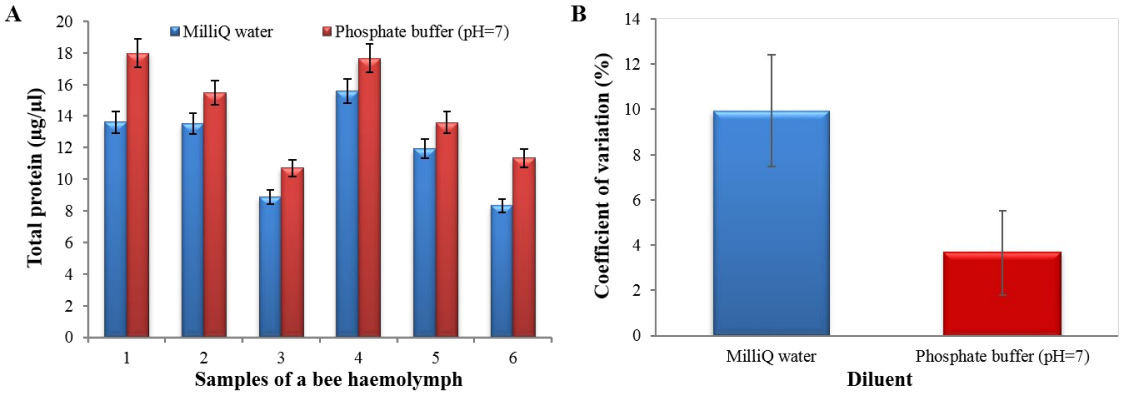

The optimal dilution at 200× was subsequently used in the paired samples (n = 6) for testing of the diluent impact (Figure 4). All haemolymph samples dissolved in the phosphate buffer showed higher yield of protein than from samples diluted in MilliQ water (Figure 4A). The total protein content in the MilliQ water's samples ($x = 11.98$ µg/µl) was significantly (paired t-test; $p < 0.001$) lower by 2.48 µg/µl in average in comparison with the phosphate buffer's samples ($x = 14.45$ µg/µl). The coefficient of variation among three determination (triplets) was significantly ($p = 0.0006$) lower by $v_x = 6.28\%$ in average for phosphate buffer's samples (Figure 4B).

The results confirmed that the phosphate buffer (pH = 7) and the sample dilution 200× were optimal for determination of the total protein in the bee haemolymph due to better protein yield by Bradford's assay. An optimal dilution or diluent have not yet been recommended and are absent also in the protocol by Hartfelder et al. (2013). The protein stability in aqueous solution in our case of experiment means that the all parts of the structure of protein, which consists of the ionisable side chains of aminoacids, which are not currently used in this time for intramolecular moieties, have the same level of chemical charge all the time without any change. Therefore, the reported concentration level by the assay method is the same. The buffer condition provides free ions in higher concentrations, and these can better stabilise the counter ions in the structure of protein by surrounding them. This prevents any change in secondary and ternary structure of bigger proteins, and therefore the assay method reports the same concentration in the same. Contrary, in the water conditions structure of protein may change in the time because the concentration of counter-ions which surrounds the protein structure decrease, and therefore protein founds better conformation which may result from change of structure – folding. After that the reported concentration by the Bradford assay method will be lower because of decrease of count of interaction between the CBB agents with the structure of protein which have to be determined. The works reported the difference between used buffers end the ionic strength which affects the total protein determination when the Bradford´s method is used have been published in some different types of the samples (Aoyama 2006, Sathe et al. 2009, Silverio et al. 2012).

The physiological status of a bee is dependent on the level of juvenile hormone (JH) in the haemolymph (Robinson 1992). Long-living workers (e.g.: winter generation) show the low JH level in the haemolymph which is associated with 2-4times higher level of the total protein in the haemolymph in comparison with summer bees, i.e. short-living bees (Fluri et al. 1982). The quantification of the total protein in the haemolymph is an easy practicable method (Hartfelder et al. 2013) in comparison with the JH quantification (Huang et al. 1995). Therefore, the results can slightly contribute to the refinement of research in the honeybee physiology (e.g.: division of the labour or development of the winter bees).

On the other hand, when any other specific protein could be considered and studied as a marker it is absolutely necessary to recalculate its concentration on total protein. Such approach is common in laboratory analysis for higher animals and plants, but it is much more complicated to transfer it for tiny samples as in case of bees.

CONCLUSION

The results confirm that determination of the total protein in a bee haemolymph is optimized with dilution 200× in the phosphate buffer (pH = 7). This study indicate that sample of haemolymph in the phosphate buffer and stored in -18 °C can be analysed one week later due to insignificant decrease of the total protein content. These findings could thus contribute to the methodical area of assaying the haemolymph parameters in bees.

ACKNOWLEDGEMENTS

The research was financially supported from the donations by elitbau, Ltd. and Konica Minolta Business Solution Czech, Ltd. The research team has been supported by the project CEITEC 2020 (LQ1601) with financial support from the Ministry of Education, Youth and Sports of the Czech Republic under the National Sustainability Programme II and by EFRR "Multidisciplinary research to increase application potential of nanomaterials in agricultural" (No. CZ.02.1.01/0.0/0.0/16_025/ 0007314).

REFERENCES

Aoyama, M. 2006. Properties of neutral phosphate buffer extractable organic matter in soils revealed using size exclusion chromatography and fractionation with polyvinylpyrrolidone. Soil Science and Plant Nutrition, 52(3): 378–386.

Bitondi, M.M.G., Simões, Z.L.P. 1996. The relationship between level of pollen in the diet, vitellogenin and juvenile hormone titres in Africanized *Apis mellifera* workers. Journal of Apicultural research, 35: 27–36.

Bradford, M.M. 1976. A rapid and sensitive method for the quantitation of microgram quantities of protein utilizing the principle of protein-dye binding. Analytical Biochemistry, 72(1–2): 248–254.

Crailsheim, K. 1990. The protein balance of the honey bee worker. Apidologie 21(5): 417–429.

Cremonz, T.M. et al. 1998. Quantification of hemolymph proteins as a fast method for testing protein diets for honey bees (Hymenoptera: Apidae). Journal of Economic Entomology, 91(6): 1284–1289.

De Jong, D. et al. 2009. Pollen substitutes increase honey bee haemolymph protein levels as much as or more than does pollen. Journal of Apicultural Research, 48(1): 34–37.

Fluri, P. et al. 1982. Changes in weight of the pharyngeal gland and haemolymph titres of juvenile hormone, protein and vitellogenin in worker honey bees. Journal of Insect Physiology, 28(1): 61–68.

Hartfelder, K. et al. 2013. Standard methods for physiology and biochemistry research in *Apis mellifera*. Journal of Apicultural Research, 52(1): 1–48.

Huang Z. et al. 1995. Seasonal changes in juvenile hormone titers and rates of biosynthesis in honey bees. Journal of Comparative Physiology, 165(1): 18–28.

Lazarov, S., Zhelyazkova, I. 2018. Hygienic behaviour of bee colonies and total protein content in the haemolymph of worker bees (*Apis mellifera* L.). Bulgarian Journal of Agricultural Science, 24(Suppl. 1): 156–161.

Lensky, Y., Rakover, Y. 1983. Separate protein body compartments of the worker honeybee (*Apis mellifera* L.). Comparative Biochemistry and Physiology Part B: Comparative Biochemistry, 75(4): 607–615.

Robinson, G.E. 1992. Regulation of division of labor in insect societies. Annual Review of Entomology, 37: 637–665.

Sathe, S.K. et al. 2009. Solubilization and Electrophoretic Characterization of Select Edible Nut Seed Proteins. Journal of Agricultural and Food Chemistry, 57(17): 7846–7856.

Silverio, S.C. et al. 2012. Interference of some aqueous two-phase system phase-forming components in protein determination by the Bradford method. Analytical Biochemistry, 421(2): 719–724.

Construction of experimental device suitable for the separation of heavy metals from wastewater

Tomas Ondracka[1, 3], Lenka Koukalova[1], Eva Kulovana[3], Tomas Koutny[2], Jiri Kois[3], Jan Pospichal[1], Jakub John[3]
[1]Department of Chemistry and Biochemistry
[2]Department of Agricultural, Food and Environmental Engineering
Mendel University in Brno
Zemedelska 1, 613 00 Brno
[3]VIA ALTA a.s.
Nadrazni 377, 675 21 Okrisky
CZECH REPUBLIC

xondrac3@mendelu.cz

Abstract: In addition to new technologies and materials, global development and industrialization have left many hazardous substances, including heavy metals released into the environment and inclusion in the substance and food chain. The level of these persistent toxic metals, not only in water, affects individuals, populations and entire ecosystems and is concentrated at the top of the food pyramid, i.e. in humans, where they cause serious health disorders. The removal of heavy metal ions can be accomplished by many methods, such as chemical precipitation, ion exchange, and electrochemical removal. This study aimed to design a unique prototype of the device that combines existing knowledge about electrochemical methods and the nature of wastewater. Several heavy metal ions were tested (copper, nickel, lead, cadmium, zinc). Based on the test of separation of heavy metal ions, the action of an electric field and the measurement of key parameters, the correct functionality of the prototype device was confirmed. The model case was demonstrated on zinc ions. The concentration of zinc ions at the specified parameters of the device, halved after 4 hours of electrolysis. Other heavy metal ions showed similar trend. The device is therefore able to remove selected risk elements from wastewater.

Key Words: wastewater, heavy metals, electrochemical methods, electrolysis

INTRODUCTION

The huge amount of not only industrial wastewater discharged into watercourses has a serious impact on the environment, all living organisms, including human lives. Metal ions, which are toxic to organisms even in the case of small concentrations (Hg, Cd, Pb), as well as metals, which are essential (Ni, Cu, Zn) but also toxic at higher concentrations, are dissolved in wastewater. Once these toxic substances enter the food chain, they accumulate in the bodies of top predators, including the human body. High concentration of heavy metal ions causes serious health disorders, both acute and chronic in nature, depending on the amount of the element in the body.

Heavy metals have toxic or other negative properties in relation to the environment and interaction with living matter. These properties are primarily toxicity, carcinogenic, mutagenic and teratogenic effects. These are caused by the high affinity of heavy metals for the thiol group, which causes the inhibition of some enzymes in the human body and the breakdown of the body's metabolic functions. Other heavy metals, although in trace amounts beneficial to the body (copper, zinc), cause environmental damage, copper at a dose of 0.09 mg/kg/day (Chutanni et al. 1965) and zinc at a dose of 0.81 mg/kg/day (Milne et al. 2001) cause disorders of the nervous system, have toxic effects on aquatic organisms or are also carcinogens. Due to the persistence of these heavy metals, i.e. the non-degradability by natural processes and the use of these metals in many industries, there is a constant concentration in the environment and also more frequent exposure to humans (Sarkar 2002).

The removal of heavy metal ions can be accomplished by many methods, such as chemical precipitation, ion exchange, and electrochemical removal. Previous work has suggested that the most widely used process in industrial wastewater treatment is the chemical precipitation method. During this

process, insoluble precipitates are separated from the water by filtration or sedimentation, and the treated water can be reused or discharged after decantation (Tran et al. 2017).

Electrochemical methods can be used to treat wastewater. They make it possible to obtain valuable products through relatively simple technological cleaning schemes without the use of expensive and rare chemical reagents. Electrochemical wastewater treatment is based on the processes of anodic oxidation and cathodic reduction, electro flocculation, electrocoagulation and electrolysis (Trokhymenko et al. 2020).

This study aimed to design a unique prototype of a device that combines existing knowledge about electrochemical methods and the nature of wastewater. The device works on the principle of electrolysis. It expects that the facility will be suitable for the removal of hazardous substances from wastewater or sewage sludge.

MATERIAL AND METHODS

Construction of device

First, the initial design of the device was designed concerning to the operating parameters and economics, which was directly proportional to the size of the device. The size of the device was determined based on the calculation of the migration of ions in the electric field, while one of the limit parameters was the operating temperature concerning the material of the device and also about the safety of the applied voltage. The design of the device before production is shown in Figure 1, where the arrangement of individual chambers, the location of membranes and electrodes can be seen. The final form of the device is shown in Figure 2.

Figure 1 Section of the laboratory device

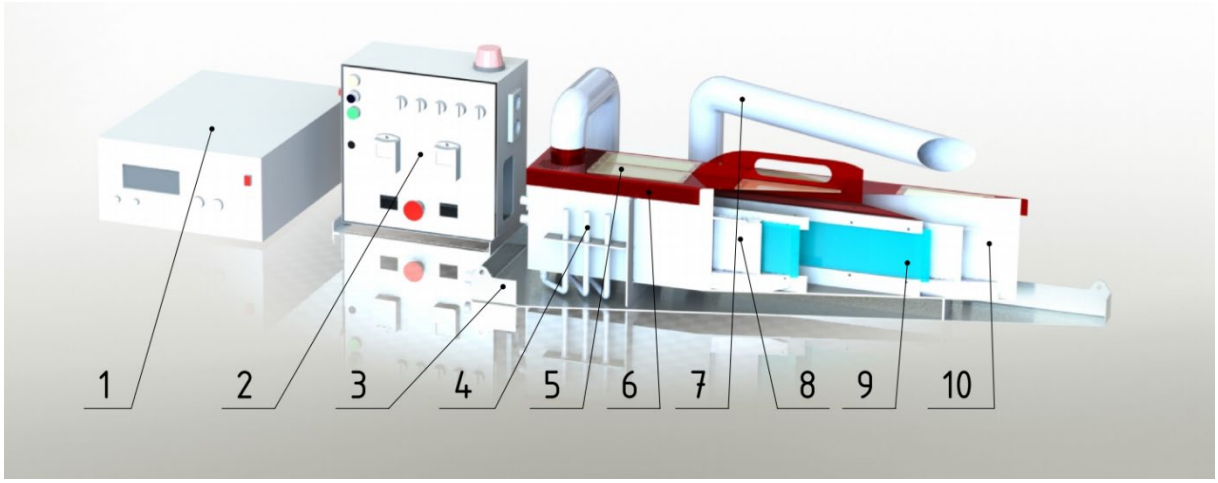

Legend: 1 – voltage source, 2 – switchboard, 3 – collecting vessel, 4 – watermark, 5 – inspection window, 6 – safety cover, 7 – ventilation system, 8 – electrode, 9 – membrane, 10 – device body

The device was designed so that it can be operated in discontinuous mode, especially for research purposes and in continuous mode for testing in pilot mode and with concerning the possibility of adjusting the input voltage while maintaining the thermal optimum of the device. The body of the device had to be made of durable material, both about temperature and aggressive environments, in the end a cheaper variant (polyethylene PE) was chosen, which met these conditions (Teflon version, was too expensive). Likewise, a more economical version had to be chosen for the electrodes, which were eventually made of titanium. The separation of the individual chambers was realized by ion-exchange membranes to order to prevent the mixing of the individual zones due to the hydrodynamic flow and then the diffusion. The switchboard was designed with several safety features. The device was tested for functionality and safety in basic tests. The trough was equipped with a collecting vessel in case of damage to the device or due to leakage of liquids due to leaks. The switchboard itself was tested for dangerous contact voltage, it was equipped with a current protector in case of the possibility of electric shock. The live trough is covered by a grounded cover, which is connected to safety elements that do not allow the circuit to close while the device is open. The laboratory apparatus is equipped with

several other safety elements, such as temperature sensors controlling the overheating of the apparatus, measuring elements for the analysis itself, such as a flow conductivity meter, voltmeter and ammeter. The upper cover of the device was made of sheet metal equipped with outlets for ventilation device due to the formation of gases during the process, also holes are cut into the cover, which are fitted with plexiglass to monitor processes inside the device, both as a visual inspection and for laboratory purposes. The ion can be monitored in the form of a dye (i.e. cationic dye ferroin), so that the dynamics and rate of ion migration can be observed, but also, for example, diffusion and other accompanying phenomena. The design of the device allows the setting of the distance between the electrodes and the water column, where the ratio applies especially between the working current and the distance of the electrodes.

Figure 2 The final form of laboratory device

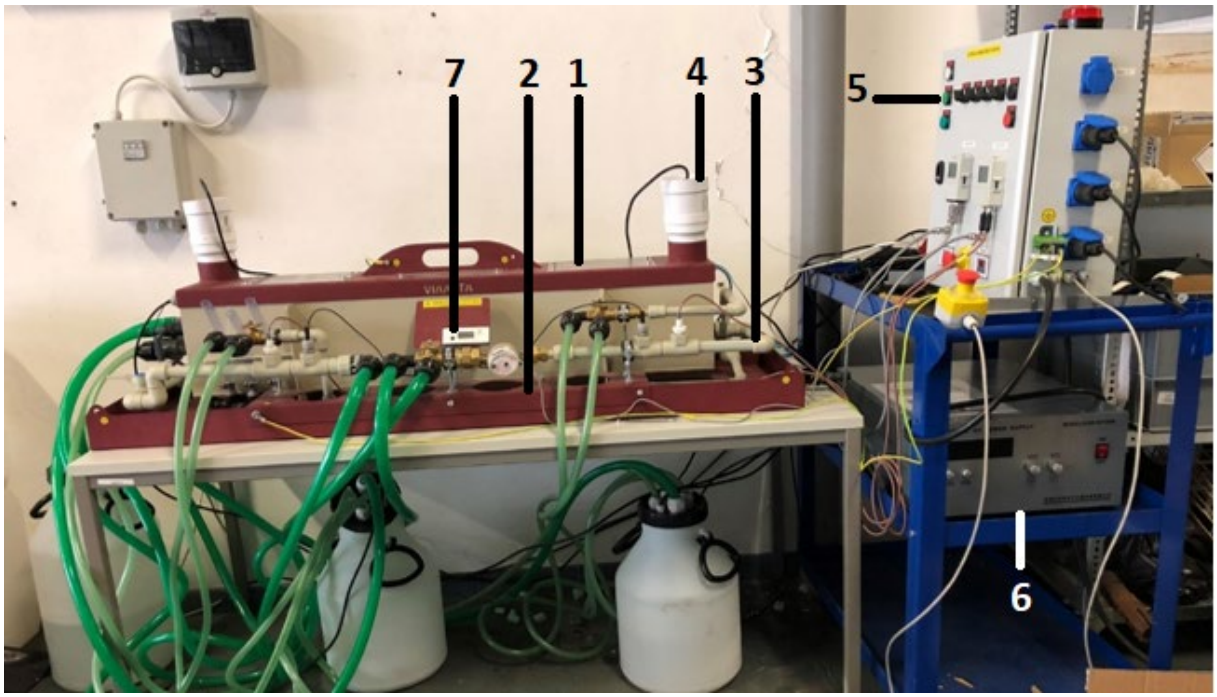

Legend: 1 – device, 2 – collecting vessel, 3 – water supply, 4 – ventilator, 5 – switchboard, 6 – voltage source, 7 – conductivity meter

Device testing and sampling methodology

During the test of the device, these parameters in individual chambers were monitored during the separation: conductivity, water temperature and pH, as well as the temperature of the electrodes, voltage and current during the separation at a given time. For these purposes, the installed measuring elements were used, as well as a manual pH meter and a conductometer. The distance between the electrodes was set at 10 cm. The device was filled with 10 cm of ordinary drinking water in height, using a flow meter, the total amount of water in the trough was determined to be 15.7 l. A model non-toxic metal in the form of zinc chloride $ZnCl_2$ was added to the water, the pH of water was 7.8–8.0. The measurements were performed at an interval of half an hour at the beginning of the separation and then after 1 hour. The measurement was always carried out by taking samples from individual chambers before start-up, measuring pH, temperature and conductivity, setting the limit temperature on the safety thermostat after covering the device, so that when this temperature is exceeded, the power supply is disconnected. The device ventilation has been switched on, a constant voltage has been set and the process has started. At the beginning, the value of the current at a given time was written. After the specified time has elapsed, the state of the flowing current has been recorded and the device has been disconnected. This was again followed by a measurement and sampling process. Zinc ions were selected as a model case. Other heavy metal ions were similarly tested (copper, nickel, lead, cadmium).

Isotachophoretic analysis of zinc ions

All experiments were performed using a commercially available isotachophoretic instrument (CS Isotachophoretic analyzer, Labeco, Slovak Republic). The operating electrolytes used for individual analyses were: 0.01 M ammonium acetate $NH_4CH_3CO_2$ as leading electrolyte and 0.01 M acetic acid

CH_3COOH as terminating electrolyte. All chemicals were obtained from Sigma-Aldrich and were analytical grade. All experiments on the analyzer were performed at a set current of 300 µA.

RESULTS AND DISCUSSION

Device test using zinc ion separation

The dependence of conductivity on electrolysis time in the main, cationic and anionic troughs was shown in Figure 3. In the main trough, the conductivity decreased with increasing electrolysis time, while in the cationic and anionic trough it increased. This is caused by the migration of positive and negative ions to their oppositely charged poles on the electrodes. The conductivity increased more markedly in the anionic trough, after about 60 minutes of electrolysis it was higher than in the main trough and reached a maximum in 360 minutes. On the other hand, in the cationic trough the conductivity increased more slowly, after about 180 minutes of electrolysis the conductivity was the same as in the main trough and reached a maximum at 360 minutes when the conductivity was slightly higher than in the main trough. This was due to the higher proportion of negatively charged ions in the water.

Figure 3 The dependence of conductivity on electrolysis time in the main, cationic and anionic troughs

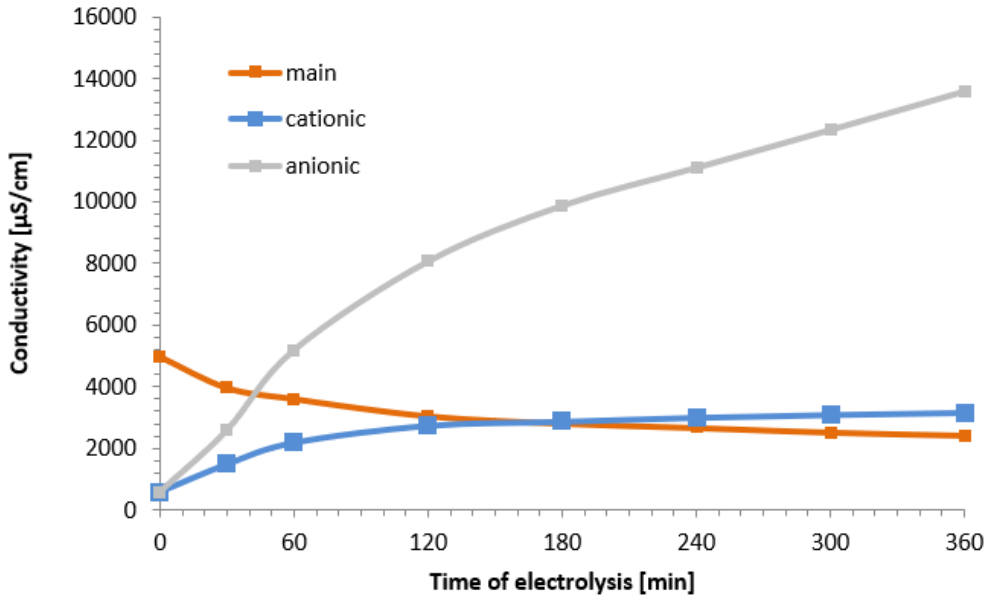

The temperature rose sharply within 60 minutes and then dropped slightly in all troughs. The highest temperature was measured at 28 °C, which was within the safe temperature range of the device, and as the ions in the main chamber decreased, the current and with it the temperature decreased. The electrolysis time and working temperature have a very close relationshhip due to the effects of the current density on the process (Tran et al. 2017).

In the anionic trough, the pH rose sharply within 30 minutes, while in the main and cationic trough it decreased. After 60 min, the pH was almost unchanged (constant). It is obvious that the device works properly, ions migrated to the electrodes, where there was a concentration, which resulted in increased conductivity, both at the anode and cathode, and at the same time a decrease in the concentration of ions in the main through. The final pH state was 12.02 at the cathode, 1.43 at the anode and 2.75 at the main though, which confirms the functionality of the device.

The electrolysis time of 60 minutes was decisive for our device, as in the 2017 study (Tran et al. 2017). On the other hand, in the 2017 study the optimal pH of industrial wastewater was 7.0, voltage applied was 15 V and heavy metal ion removal efficiency was 35 %.

The removal of heavy metals from wastewater was also investigated on a laboratory scale (AlJaberi 2018, Rajemahadik et al. 2013). Both study dealt with electrocoagulation method and with electrolysis time to 30 minutes.

Zinc ion concentration determining by isotachphoresis

The isotachophoregram of zinc samples from the main through was shown in Figure 4. Zinc concentrations were obtained from isotachophoregrams by CLARITY software. In the main though zinc concentration decreased exponentially with electrolysis time (Figure 5). After 60 minutes 30 % of zinc was removed from the main though. In the 2017 study (Tran et al. 2017), metal ions removal after 60 minutes was 35 %, which was probably achieved by adjusting the initial pH of the wastewater. The difference between the measured amount of separated metals could also be caused by ion exchange membranes, which could sorb part of the zinc, as well as the formation of complexes in the cathode part of the device. Another difference was the use of four times higher separation voltage. The zinc concentration halved in 4 hours (240 minutes). The opposite trend could be observed in the cationic though, where the concentration increased linearly with the time of electrolysis. Measuring the concentration of metal ions in the anode space is irrelevant for this experiment.

Figure 4 Isotachophoregram of zinc samples from the main through

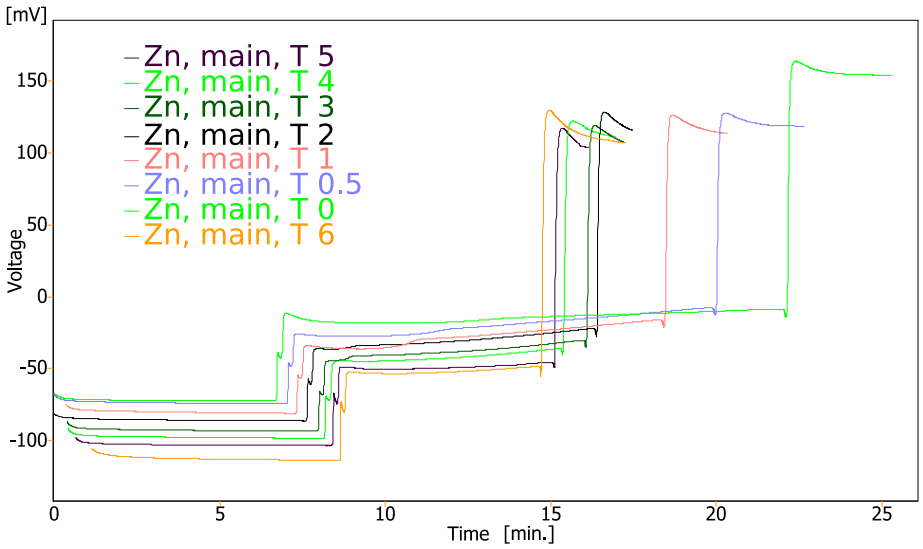

Legend: T 0 – concentration at the beginning of the test, T 0.5 – concentration after 0.5 hour of the test, T 1 – concentration after 1 hour of the test, T 2 – concentration after 2 hour of the test, T 3 – concentration after 3 hour of the test, T 4 – concentration after 4 hour of the test, T 5 – concentration after 5 hour of the test, T 6 – concentration after 6 hour of the test

Figure 5 Dependence of zinc concentration time on time of electrolysis in main, cationic and anionic though

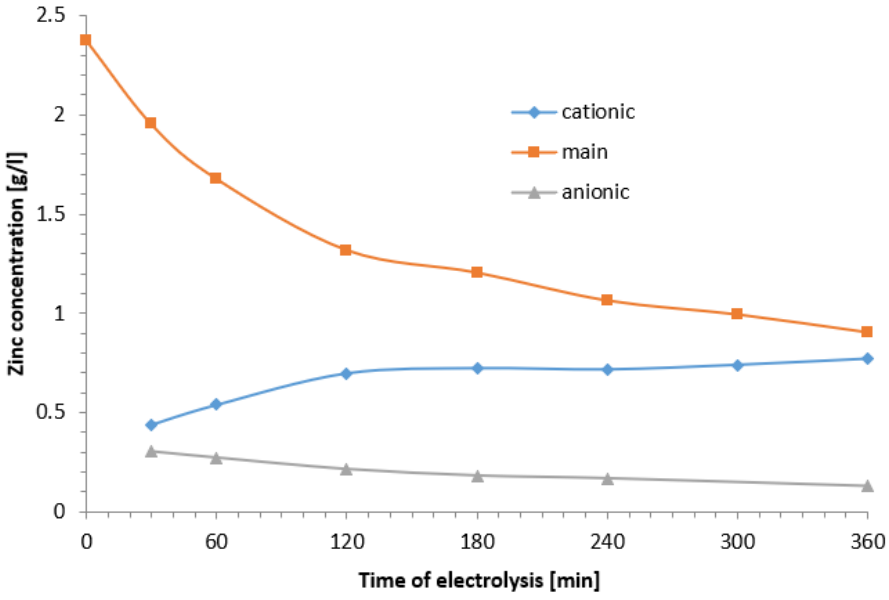

CONCLUSION

Heavy metals can be removed from wastewater using electrochemical methods. A unique device working on the principle of electrolysis was built. The zinc concentration halved after 4 hours of electrolysis. The device is therefore able to remove selected risk elements from wastewater and prevent their release into the environment. With the help of zinc ion separation, the correct functionality of the device was tested and confirmed, data and operational experience were obtained, thanks to which the device can be further tested, improved and efforts will be made to develop a functional industrial prototype.

ACKNOWLEDGEMENTS

The research was financially supported by the Technology Agency of the Czech Republic in the Zeta programme and project TJ02000304 entitled Removal of selected hazardous substances and elements from sewage sludge.

REFERENCES

AlJaberi, F.Y. 2018. Studies of autocatalytic electrocoagulation reactor for lead removal from simulated wastewater. Journal of Environmental Chemical Engineering, 6: 6069–6078.

Chutanni, H.K. et al. 1965. Acute copper suphate poisoning. American Journal of Medicine, 39: 849–854.

Milne, D.B. et al. 2001. Low dietary zinc alters indices of copper function and status in postmenopausal women. Nutrition, 17: 701–8.

Rajemahadik, C.F. et al. 2013. Efficient Removal of Heavy Metals from Electroplating Wastewater using Electrocoagulation. International Journal of Scientific and Research Publication, 3: 1–5.

Sarkar, B. 2002. Heavy metals in the environment. New York: Marcel Decker.

Tran, T.K. et al. 2017. Electrochemical Treatment of Heavy Metal-containing Wastewater with the Removal of COD and Heavy Metals Ions. Journal of the Chinese Chemical Society, 64: 493–502.

Trokhymenko, G. et al. 2020. Study of the Process of Electro Evolution of Copper Ions from Waste Regeneration Solutions. Journal of Ecological Engineering, 21: 29–38.

Behaviour of pesticides during the denitrification process

Kristina Panikova[1], Zuzana Bilkova[2], Jitka Mala[1]
[1]Institute of Chemistry
Brno University of Technology
Žižkova 17, 602 00 Brno
[2]RECETOX
Masaryk University
Kamenice 753/5, Pavilion A29, 625 00 Brno
CZECH REPUBLIC

kristina.panikova@vutbr.cz

Abstract: The presence of pesticides has been proven in many groundwater bodies worldwide. However, information about their behaviour and fate in anoxic conditions is lacking. The aim of this paper is to study the behaviour of selected pesticides during the process of denitrification. Laboratory batch tests were performed with terbuthylazine, atrazine, and tebuconazole. Poplar wood shavings were used as a carbon source for denitrification. The effect of pesticides on the denitrification process was evaluated from their inhibition of the denitrification rate. Abiotic and biotic losses were measured with high-performance liquid chromatography. No toxic effect on denitrification was observed. Biotic loss was found with terbuthylazine and atrazine. The highest abiotic loss was observed with tebuconazole.

Key Words: biodegradation, adsorption, wood shavings, terbuthylazine, atrazine, tebuconazole

INTRODUCTION

Pesticides rank among the most hazardous environmental pollutants due to their stability, mobility, high accumulative and persistent nature, and long-term effects on living organisms (Nasiri et al. 2020). The presence of pesticides in ecosystems has adverse effects which vary with the contaminant concentration, amount, and exposure time (Rice et al. 2007). However, current systems of agricultural management rely on the use of pesticides, meaning that about 3.6×10^6 t/y are applied worldwide (Food and Agriculture Organization of the United Nations. 2020). It was estimated that 10% of all pesticides applied to the soil reach non-target areas (Schulz 2004). In water, these compounds may metamorphose to produce substances with even greater toxicity (Nasiri et al. 2020). In 2018, metabolites of chloridazon, alachlor, metazachlor, metolachlor, acetochlor, atrazine, and dimethachlor were found in more than 5% of samples of groundwater in the Czech Republic (Kodeš 2019).

Pesticides from agricultural areas can be transported to groundwater together with nitrates, which are other typical pollutants found in agricultural run-offs. Nitrates undergo denitrification under anoxic conditions in subsurface regions. Similar conditions also prevail in denitrifying woodchip bioreactors, a passive treatment technology for the removal of nitrates from agricultural outflows (Weigelhofer and Hein 2015).

Atrazine (ATR) is a herbicide and its metabolites can persist in water and soil for decades (Jablonowski et al. 2011).

Due to the prohibition of atrazine in the European Union, terbuthylazine (TER) has gradually come to be employed as a replacement herbicide. It is considered to be the most persistent triazine herbicide in surface environments (Gikas et al. 2018).

Tebuconazole (TEB) is a systemic fungicide used against a variety of diseases affecting cereals and maize, and which controls numerous pathogens. It is highly adsorbed by soils and mainly concentrated in the topsoil layer (Herrero-Hernández et al. 2011).

Unfortunately, there is no standardized test available to predict the fate of chemical substances during denitrification. The aim of this work was to investigate the behaviour of three selected pesticides during the process of denitrification using the authors' own laboratory incubation test developed for this purpose (Pániková and Malá 2019).

MATERIALS AND METHODS

Chemicals and organic carrier

All of the analytical standards (atrazine, terbuthylazine and tebuconazole from the PESTANAL® product line) were obtained from Sigma-Aldrich (Germany) at ≥ 98% purity. Each stock solution was prepared in analytical grade methanol at a concentration of 1000 mg/l. The analytical standards were stored in the dark at 4 °C.

With respect to the employed denitrifying woodchip bioreactors, wood shavings were used as a bacterial carrier and a source of organic carbon. The wood shavings were from poplar trees; they were sieved at the 1.0–1.5 cm fraction. Argon gas (purity 99.996%) was purchased from Linde Gas (Czech Republic).

The laboratory batch testing of denitrification

The denitrification process was simulated in 2-litre bottles as a laboratory batch test. The principle behind the test is clear from Table 1.

Table 1 Overview of the sample types

Sample	Composition of liquid medium, solution in deionised water (DIW)	Description
1	KNO_3 (30 mg/l NO_3-N), $NaHCO_3$ (3 g/l for ATR and TER, 0.5 g/l for TEB), methanol (0.1 ml/l)	Denitrification in progress.
2	KNO_3 (30 mg/l NO_3-N), $NaHCO_3$ (3 g/l for ATR and TER, 0.5 g/l for TEB), the tested pesticide (100 µg/l; solution in 0.1 ml/l of methanol)	Denitrification and biodegradation in progress.
3	KNO_3 (30 mg/l NO_3-N), $NaHCO_3$ (3 g/l for ATR and TER, 0.5 g/l for TEB), the tested pesticide (100 µg/l; solution in 0.1 ml/l of methanol), $HgCl_2$ (6.5 mg/l, inhibitor)	Biological processes are stopped.

At the beginning of the test, each bottle contained 25 g of poplar wood shavings and 2000 ml of liquid phase containing $NaHCO_3$ and KNO_3 (see Table 1). The bottles were aerated with argon until the concentration of dissolved oxygen (DO) dropped below 0.5 mg/l. The bottles were closed and incubated at $T = 20 \pm 0.5$ °C in the dark. After 48 hours, 25 ml samples of liquid phase were taken from every bottle and concentrations of NO_X-N, pH, and DO were analysed. The bottles were divided into three groups (see Table 1) and the reagents were added. After mixing, 10 ml of liquid phase was taken from samples 2 and 3. These solutions were analysed for the initial concentration of pesticide. The bottles were closed and incubated at $T = 20 \pm 0.5$ °C in the dark. Each sample had two replicates.

The test was terminated after seven days. Immediately after opening, liquid phase from samples 2 and 3 was collected for analysis of the tested pesticide. The remaining liquid phase was filtered through filter paper for qualitative analysis KA2, and concentrations of NO_X-N, pH, DO and COD were measured in the supernatant.

Analytical methods

The laboratory analyses were performed as follows: DO and pH with a Hach HQ40D multi meter, COD via the semi-micro method with potassium dichromate and photometric evaluation, and NO_X-N (NO_3-N+ NO_2-N) via the UV absorption method with a Hach optical Nitratax plus sc Sensor.

Pesticides were extracted from the water samples using solid phase extraction (SPE) cartridges. The cartridges (Oasis HLB, 6 ml, 0.5 g HLB sorbent material) (Waters, Milford, MA, USA) were activated with 7.5 ml of methanol:acetone (3:2)(Sigma-Aldrich, Steinheim, Germany) and washed with 7.5 ml of mili-q water. A 10 ml water sample and 100 µl of internal standard (IS) metolachlor

(c= 1 ug/ml) were passed through the SPE cartridge. Afterwards, the SPE columns were washed with 7.5 ml of deionised water. The cartridges were then air-dried for 5 minutes and the adsorbed pesticide was eluted with 10 ml of methanol:acetone (3:2).

High-performance liquid chromatography (HPLC) analysis was performed using an Agilent 1200 chromatographic system (Agilent, Santa Clara, CA, USA) equipped with an Agilent Triple Quad 6410 mass spectrometer (Agilent, Santa Clara, CA, USA). The LC conditions were as follows: ACE 3 C18 chromatographic column of 150 mm length x 2.2 mm internal diameter and 3 µm particle size, with integrated guard column of 20 mm length x 2.2 mm internal diameter and 3 µm particle size (ACE, Scotland, UK). The column temperature was maintained at 30 °C. The mobile phase consisted of 0.1% formic acid (98% Sigma-Aldrich, Germany) in water and acetonitrile. The flow of the mobile phase was 0.3 ml/min during all the analyses. The resulting retention period was 10.4. The mean water recoveries of pesticides were 98%, and the limit of quantification (LOQ) achieved in the water samples was 1 µg/l.

Evaluation of the data

The effect of pesticides on the denitrification process was evaluated from their inhibition of the denitrification rate, which was calculated as the amount of NO_X-N removed per time unit. The effect of the tested substance was evaluated from the difference between the denitrification rates of samples 1 and 2.

The loss of the tested substance due to adsorption was assessed from the decrease in its concentration in sample 3. The decrease in the tested substance due to biodegradation was assessed by comparing the decrease in concentrations of the tested substance in samples 2 (biotic loss + abiotic loss) and 3 (abiotic loss).

RESULTS AND DISCUSSION

During the tests, organic substances of an acidic character were released from the wood shavings. The dose of 3 g/l of $NaHCO_3$ had a sufficient buffering capacity to preserve the pH at a level beneficial to the denitrification process. At the end of the test, the measured pH values were 7.97 ± 0.23 in the case of TER. When ATR was tested, the pH values increased to 8.97 ± 0.07. Therefore, in the case of TEB the dose of $NaHCO_3$ was reduced to 0.5 g/l, which caused pH to drop to 7.52 ± 0.11. pH values between 7.5 and 8.0 are more appropriate for denitrification than those measured during the ATR test (Paul 2007). The COD values at the end of the tests ranged from 160 to 393 mg/l. This amount of COD is sufficient to support denitrification (Lahdhiri et al. 2017). In the analysed samples without the added inhibitor (sample 1 and 2), DO values lower than 0.5 mg/l were measured after seven days.

Table 2 Overview of average denitrification rates

Sample	Average denitrification rate mg/l/d		
	TER	ATR	TEB
1	2.71	2.44	1.30
2	2.72	2.33	1.54

The denitrification process with TER (sample 2) ran at almost the same denitrification rate as in the sample without TER (sample 1), being 2.72 mg/l/d and 2.71 mg/l/d, respectively. During the test with ATR, the denitrification rate was 2.44 mg/l/d (sample 1). With the addition of ATR (sample 2), the rate was slightly reduced to 2.33 mg/l/d. This does not contradict the findings from the literature that denitrification rates were not inhibited by atrazine concentrations of 5 mg/l (Ilhan et al. 2011). In the case of TEB, the results were different from ATR and TER, i.e. rates of 1.30 mg/l/d (sample 1) and 1.54 mg/l/d (sample 2). The denitrification process can be promoted by a dose of tebuconazole. Cycoń et al. (2006) observed significant stimulation of the abundance of cultivable denitrifying bacteria in soil by tebuconazole at dose rates >2.7 mg/kg. The tests have shown that all tested pesticides had negligible effect on the denitrification rates in a seven-day test at the concentration of 0.1 mg/l.

Figure 1 presents individual processes occurring during the batch tests. The abiotic loss was dominant for all tested pesticides. The mean abiotic loss for TER was 9.8%, for ATR 26.9%,

and for TEB 80.0%. It can be assumed that the prevailing mechanism of abiotic loss was the sorption of pesticides on the wood shavings (Ilhan et al. 2011). The sorption of triazine pesticides TER and ATR was similar, while the sorption of TEB was much higher. This difference may be due to the different chemical structure and properties of these compounds. These results were in accordance with reports by Fenner et al. (2013) and Čadková et al. (2013). According to Fenner et al. (2013), the degradation of pesticides involves both biotic and abiotic processes. The transformation processes a given pesticide undergoes are determined by its structural affinity to specific types of transformation, and the environmental conditions it is exposed to as a result of its distribution and transport behaviour. Čadková et al. (2013) observed high adsorption of tebuconazole in soils with high contents of organic matter.

Figure 1 Fate of pesticides during denitrification after seven days

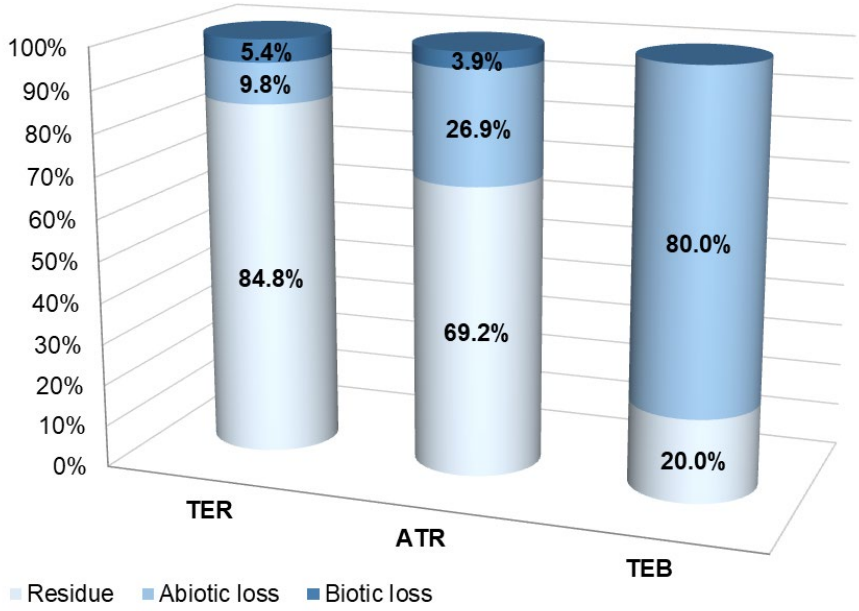

The highest biotic loss was observed for TER, namely 5.4%. This value is slightly higher than would be expected from the results of Navarro et al. (2004), who indicated that the dissipation half-life of TER in groundwater lies in the range from 263 to 366 d. In the case of ATR, a biotic loss of 3.9% was measured in our experiments. This is in accordance with the results of Douglass et al. (2014), who observed a half-life of 35–40 d for ATR. With TEB in liquid solution, no biotic loss was measured in our experiments. This finding was surprising considering the results of Caldas et al. (2010), who reported a half-life of TEB in groundwater that was in the range from 7 to 28 d.

The highest value of residue was measured in the case of TER, namely 84.8%, whereas the lowest was for TEB, 20.0%. From the point of view of the removal of pesticides from water, e.g. from agricultural drainage, the low residue in TEB in water is very positive. These results also correspond with the half-lives of the pesticides: the half-life of TER in groundwater is 263 to 366 d, while for TEB it is 7–28 d. The higher the half-life, the higher the residue value, and vice versa.

When assessing these results, it is necessary to take into account the fact that pesticides are very stable substances and 7 days is a very short time for their decomposition. It is possible that for some substances, decomposition would continue at an increased rate after the initial lag phase. Therefore, after the necessary adaptation of the methodology, the experiments will continue with a longer reaction time.

CONCLUSION

Behaviour of three pesticides (terbuthylazine, atrazine, and tebuconazole) during the denitrification process was assessed using a seven-day laboratory batch test developed

for this purpose. At a concentration of 0.1 mg/l, terbuthylazine did not affect the denitrification rate, atrazine caused its 4.5% inhibition, while tebuconazole its 15.6% stimulation. Tebuconazole did not undergo biochemical degradation. Atrazine and terbuthylazine showed biotic losses of 3.9% and 4.5% respectively. The dominant process involved in the decrease in concentration of the pesticides in aqueous phase was the abiotic loss: tebuconazole 80%, atrazine 26.9%, and terbuthylazine 9.8%.

In future, the methodology will be used to test other micropollutants and, moreover, will be further developed to allow longer test durations.

ACKNOWLEDGEMENTS

The research was financially supported by the Brno University of Technology Junior Specific Research Project FAST-J-20-6395 Degradation of pesticides in the denitrification bioreactors.

REFERENCES

Caldas, S.S. et al. 2010. Pesticide residue determination in groundwater using solid-phase extraction and high-performance liquid chromatography with diode array detector and liquid chromatography-tandem mass spectrometry. Journal of the Brazilian Chemical Society [Online], 21(4): 642–650. Available at: http://www.scielo.br/scielo.php?script=sci_arttext&pid=S0103-50532010000400009&lng=en&nrm=iso&tlng=en. [2020-09-07].

Cycoń, M. et al. 2006. Microbiological characteristics of a sandy loam soil exposed to tebuconazole and λ-cyhalothrin under laboratory conditions. Ecotoxicology [Online], 15(8): 639–646. Available at: http://link.springer.com/10.1007/s10646-006-0099-8. [2020-09-07].

Čadková, E. et al. 2013. Tebuconazole Sorption in Contrasting Soil Types. Soil and Sediment Contamination: An International Journal [Online], 22(4): 404–414. Available at: http://www.tandfonline.com/doi/abs/10.1080/15320383.2013.733448. [2020-09-07].

Douglass, J.F. et al. 2014. Mineralization of atrazine in the river water intake and sediments of a constructed flow-through wetland. Ecological Engineering [Online], 72: 35–39. Available at: https://linkinghub.elsevier.com/retrieve/pii/S0925857414003978. [2020-09-07].

Fenner, K. et al. 2013. Evaluating Pesticide Degradation in the Environment: Blind Spots and Emerging Opportunities. Science [Online], 341(6147): 752–758. Available at: https://www.sciencemag.org/lookup/doi/10.1126/science.1236281. [2020-09-07].

Food and Agriculture Organization of the United Nations. 2020. Pesticides Use [Online]. Available at: http://www.fao.org/faostat/en/#data/RP. [2020-09-07].

Gikas, G.D. et al. 2018. Low-cost approaches for the removal of terbuthylazine from agricultural wastewater: Constructed wetlands and biopurification system. Chemical Engineering Journal [Online], 335: 647–656. Available at: https://linkinghub.elsevier.com/retrieve/pii/S1385894717319435. [2020-09-07].

Herrero-Hernández, E. et al. 2011. Field-scale dissipation of tebuconazole in a vineyard soil amended with spent mushroom substrate and its potential environmental impact. Ecotoxicology and Environmental Safety [Online], 74(6): 1480–1488. Available at: https://linkinghub.elsevier.com/retrieve/pii/S0147651311001072. [2020-09-07].

Ilhan, Z.E. et al. 2011. Dissipation of Atrazine, Enrofloxacin, and Sulfamethazine in Wood Chip Bioreactors and Impact on Denitrification. Journal of Environmental Quality [Online], 40(6): 1816–1823. Available at: http://doi.wiley.com/10.2134/jeq2011.0082. [2020-09-07].

Jablonowski, N.D. et al. 2011. Still present after all these years: persistence plus potential toxicity raise questions about the use of atrazine. Environmental Science and Pollution Research [Online], 18(2): 328–331. Available at: http://link.springer.com/10.1007/s11356-010-0431-y. [2020-09-07].

Kodeš, V. 2019. Problematika pesticidů v ochraně vod – jaká data máme k dispozici a co nám říkají? In Sborník přednášek a posterových sdělení z 13. bienální konference a výstavy VODA 2019. Poděbrady, Czech Republic, 18–19 September. Brno: CzWA service s.r.o., pp. 18–25.

Lahdhiri, A. et al. 2017. Minimum COD needs for denitrification: From biological models to experimental set-up. DESALINATION AND WATER TREATMENT [Online], 61: 326–334. Available at: https://www.researchgate.net/publication/313374524_Minimum_COD_needs_for_denitrification_From_biological_models_to_experimental_set-up. [2020-09-07].

Nasiri, M. et al. 2020. Sample preparation and extraction methods for pesticides in aquatic environments: A review. TrAC Trends in Analytical Chemistry [Online], 123: 115772. Available at: https://linkinghub.elsevier.com/retrieve/pii/S0165993619305813. [2020-09-07].

Navarro, S. et al. 2004. Persistence of four s-triazine herbicides in river, sea and groundwater samples exposed to sunlight and darkness under laboratory conditions. Science of The Total Environment [Online], 329(1–3): 87–97. Available at: https://linkinghub.elsevier.com/retrieve/pii/S0048969704001901. [2020-09-07].

Pániková, K., Malá, J. 2019. Chování terbuthylazinu za denitrifikačních podmínek. In Sborník přednášek a posterových sdělení z 13. bienální konference a výstavy VODA 2019. Poděbrady, Czech Republic, 18–19 September. Brno: CzWA service s.r.o., pp. 465–468.

Paul, E.A. 2007. Soil microbiology, ecology, and biochemistry. 3rd ed., Boston: Academic Press.

Rice, P.J. et al. 2007. Advances in Pesticide Environmental Fate and Exposure Assessments. Journal of Agricultural and Food Chemistry [Online], 55(14): 5367–5376. Available at: https://pubs.acs.org/doi/10.1021/jf063764s. [2020-09-07].

Schulz, R. 2004. Field Studies on Exposure, Effects, and Risk Mitigation of Aquatic Nonpoint-Source Insecticide Pollution: A Review. Journal of Environmental Quality, 33(2): 419–448 [Online], Available at: https://www.agronomy.org/publications/jeq/abstracts/33/2/419. [2020-09-07].

Weigelhofer, G., Hein, T. 2015. Efficiency and detrimental side effects of denitrifying bioreactors for nitrate reduction in drainage water. Environmental Science and Pollution Research [Online], 22(17): 13534–13545. Available at: http://link.springer.com/10.1007/s11356-015-4634-0. [2020-09-07].

Identification of volatile compounds associated with sepsis progression by mass spectrometry

Kristyna Pavelicova, Kristyna Zemankova, Lucie P. Vanickova, Marketa Vaculovicova
Department of Chemistry and Biochemistry
Mendel University in Brno
Zemedelska 1, 613 00 Brno
CZECH REPUBLIC

xpavelic@node.mendelu.cz

Abstract: Herein, SPME−GC×GC−TOFMS method was used to optimize the parameters of the method and correct conditions for sample processing which will allow to develop a method for the identification of VOCs (mainly alcohol, ketones and hydrocarbons) sepsis biomarkers. The correct conditions for processing the samples (the incubation – heating/collection of samples, the selection of SPME fiber for sample collection and the addition of NaCl) were established. Moreover, in this work, the GC−MS (Pegasus 4D−C) method was used. Parameters of the chromatography and mass spectrometry methods GCxGC−TOFMS were tested and optimized (temperature of the secondary oven, modulator temperature, modulator period, cool time etc.). Altogether, about 5 methods with different settings were compared. Finally, the best combination of the optimized sample conditions and optimized method was developed. The heating and collection of the sample 30min/30min by the DVB/CAR/PDMS fiber in the addition of NaCl (200 mg/ml) were chosen. Moreover, one of the 5 optimized GCxGC−TOFMS method was selected. The optimized method will be used for analyses of monocyte from serum samples.

Key Words: mass spectrometry, gas chromatography, SPME, sepsis

INTRODUCTION

In spite of intensive research, development of sepsis remains one of the main causes of global mortality (Armstrong et al. 2017). Sepsis in humans often follows the body's attempt to thwart infectious agents such as bacteria and viruses. It is associated with changes in the function of monocytes that alter the content of volatile metabolites in the blood. Complex deregulation of the immune system during sepsis occurs in the phases described as early inflammatory status and late immunosuppressive phase (Figure 1).

Figure 1 Immunologic response in sepsis over time (Hotchkiss et al. 2009)

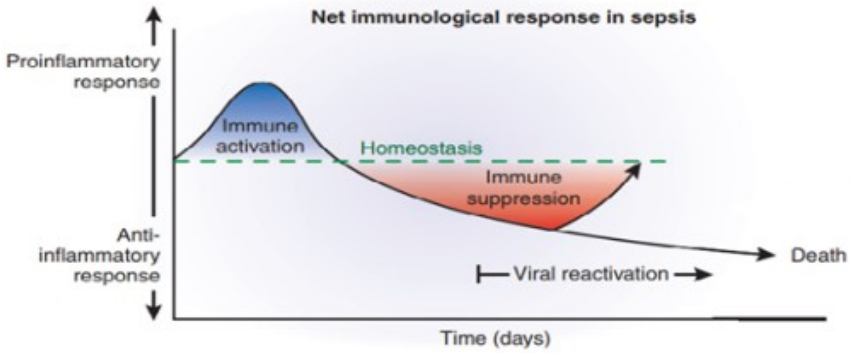

Early sepsis is often associated with the onset of immunosuppression, which may endanger the body's ability to cope with the infection (Hotchkiss et al. 2009). To limit organ dysfunction and reduce mortality, early recognition is paramount. Because there is a general need to find new the screening methods for searching of novel markers in sepsis, development of the new method is necessary. New predictable and reliable markers would be very useful in situations where sepsis develops in patients undergoing surgery or bone marrow transplantation. Early prediction of sepsis and its differentiation from the systemic inflammatory response of the organism is a key factor

in successful therapy and survival of the patient. Volatile organic compounds (VOCs) can be intermediate of metabolic pathways and their levels in biological samples, may provide a better understanding of diseases in addition to potential methods for diagnosis (Boomer et al. 2011, Aggio et al. 2016). Although several VOCs from various tissues (e.g. hepatocellular carcinoma (Amal et al. 2012) or human B-cell (Filipiak et al. 2016)) have been proposed as suitable biomarkers, the biochemical background of these metabolites from human monocytes has rarely been investigated. In this project, the SPME−GCxGC−TOFMS method was used. This effective technique will allow the identification of new VOCs sepsis biomarkers from human monocytes that will help with the future development of new diagnostic and therapeutic approaches.

MATERIAL AND METHODS

Materials and reagents

Sodium chloride was obtained from Sigma−Aldrich (St. Louis, MO, USA), the SPME holders for manual sampling, SPME fibers, 1.5 ml glass vials with septum were purchased from Supleco (Bellefonte, PA, USA). Primary peripheral blood monocytes were isolated from fresh buffy coats collected from four healthy donors (Department of Transfusion & Tissue Medicine of the Brno University Hospital, Brno, Czech Republic).

Optimization of SPME technique

The correct conditions for processing the samples of cells were established. The individual samples of monocytes were heated in a water bath at 37 °C in the glass vials sealed with the teflon septum and monocyte VOCs were collected on a fiber using the Solid Phase Micro Extraction (SPME). The selection of SPME fiber coating, incubation conditions and salting−out effect were optimized. The SPME fibers used for the method optimization were conditioned according to the manufacturer's instructions. Four different SPME fibers (gray, black, red and light blue) coatings were tested. Firstly, the sample vial was conditioned for 30 min at 37 °C, and then VOCs were obtained followed by fiber exposure to the headspace for 30 min at 37 °C. Different conditions for the SPME incubation were tested (sample heating/VOC collection: 30min/30min, 15min/15min, 30min/15min and 15min/30min). In addition, recovery of VOCs from samples with/without NaCl was tested (after the addition of 200 mg/ml NaCl).

GC−MS analyses

The GC×GC−TOFMS analyses of human monocyte VOCs were carried out with a LECO Pegasus 4D instrument (LECO Corp., St. Joseph, MI). A Rtx-5Sil MS column (RESTEK, USA; 30 m × 0.25 mm × 0.25 µm film thickness) and a BPX-50 column (SGE Inc., Austin, TX; 1.18 m × 0.1 mm × 0.1 µm film thickness) were used for GC in the first and second dimensions, respectively. Helium was used as a carrier gas at a constant flow of 1 ml/min. The temperatures of the GC×GC−TOFMS instrument were set at 250 °C at the injector, 270 °C at the transfer line, and 250 °C at the ion source. Parameters of the chromatography and mass spectrometric methods GC×GC−TOFMS were tested and optimized (temperature of the secondary oven, modulator temperature, modulator period, cool time etc.). Altogether, five methods with different settings were compared. The mass spectrometer was operated in the electron ionization mode (EI, 70 eV).

RESULTS AND DISCUSSION

Solid Phase Microextraction (SPME) is a technique used for the extraction of VOCs on a fiber that is attached to a needle and it has many advantages, such as sample extraction time minimization and the potential automation for this technique. The combination of headspace SPME with gas chromatography equipped with mass spectrometry (GC−MS) is profitable due to the good sensitivity of VOCs. The method is able to determine the molecules which are released into the headspace above the sampled to SPME fiber (Doležal et al. 2017, Alshehri et al. 2020). Therefore, this technique was selected for future detection of sepsis biomarkers.

As previously published for the analysis of the volatile metabolic signature of breast cells (HMEC) and breast cancer cell lines, the use of headspace associated with SPME has already been

developed (Silva et al. 2017). The individual samples of monocytes will be heated in a water bath at 37 °C and monocyte volatiles will be collected on a fiber using the SPME technique. The scheme of this process is shown in the Figure 2. Incubation conditions were optimized at different times (heating/collection: 30min/30min, 15min/15min, 30min/15min and 15min/30min). Subsequently, the best combinations (heating/collection: 30min/30min) were selected.

The coating of each fiber was shown to determine qualitative and quantitative differences in cells volatile profiles obtained by the SPME technique. Comparison of the VOC profiles collected on the SPME fibers with four different coatings clearly showed that gray fiber (DVB/CAR/PDMS) captured the broadest range of compounds (such as ketones, acids, ethers, aromatic compounds, etc.). On the other hand, as seen in Figure 4, the gray fiber expressed the lowest amount of negative interference (Figure 4a). In addition, the sensitivity of SPME can be increased by salting out effect. The salt is often used for the extraction of VOCs due to the 'salting out' effect, which increases the amount of analytes into the headspace and, subsequently, into the fibre coating (Monteiro et al. 2014). The salt effect on adsorption of cell volatile organic compounds was investigated in this study.

Figure 2 Scheme of the SPME sampling process

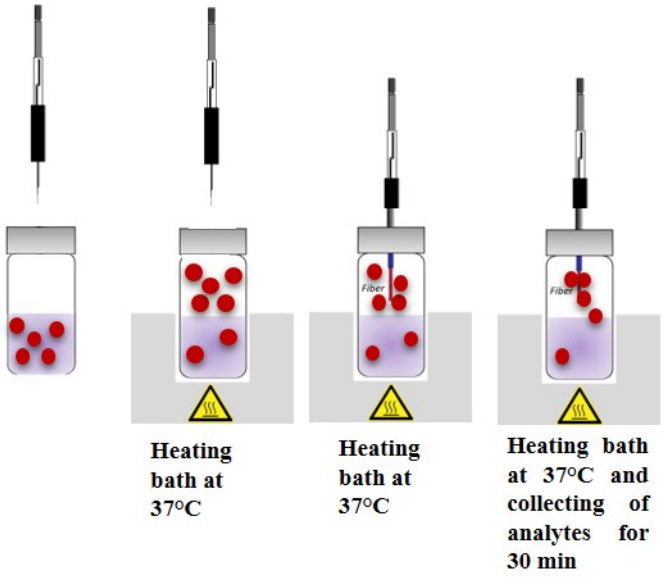

Finally, recovery of volatiles from samples with/without NaCl was tested (after the addition of 200 mg/ml NaCl). As shown in the Figure 3a, after addition of NaCl solution to the sample a significant increase of sensitivity was observed and more complex volatile mixture was detected by GCxGC−TOFMS technique.

Figure 3 3D chromatograms of VOCs adsorbed on gray SPME fiber (a) afters addition of NaCl, (b) before addition of NaCl in the monocyte sample

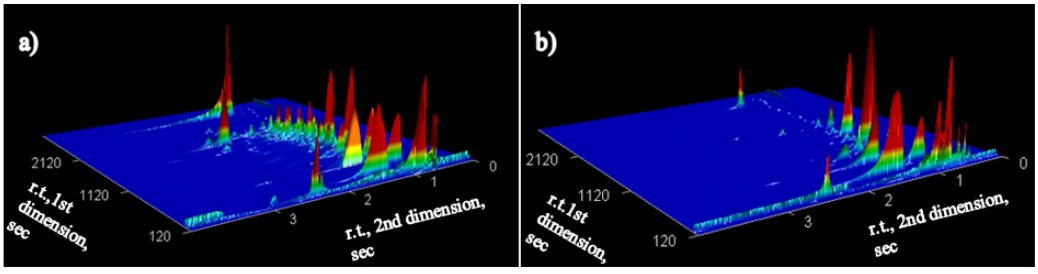

The GC-MS technique has previously successfully used for analysis of volatiles from cells (Amal et al. 2012, Silva et al. 2017). For this reason, in this study, a several GCxGC−TOFMS methods were optimized. Temperature plays an important role in the separation in the GCxGC system and a program with a gradual increase in temperature is necessary for the separation of volatile substances. For this reason, the final temperature program on the primary GC oven was as follows:

40 °C for 5 min, then 40−100 at 2 °C/min, and finally 100−280 at 15 °C/min with a hold for 5 min at 280 °C. The program in the secondary oven was 5 °C or 15 °C higher than in the primary one and was operated in a ramping mode. The optimized modulation period, the hot−puls duration, and the cool time between the stages were set at 4, 0.6, and 1.4 s, respectively.

Figure 4 3D chromatograms of monocyte VOCs collected on four different SPME fibers: gray (a), black (b), red (c) and light blue (d)

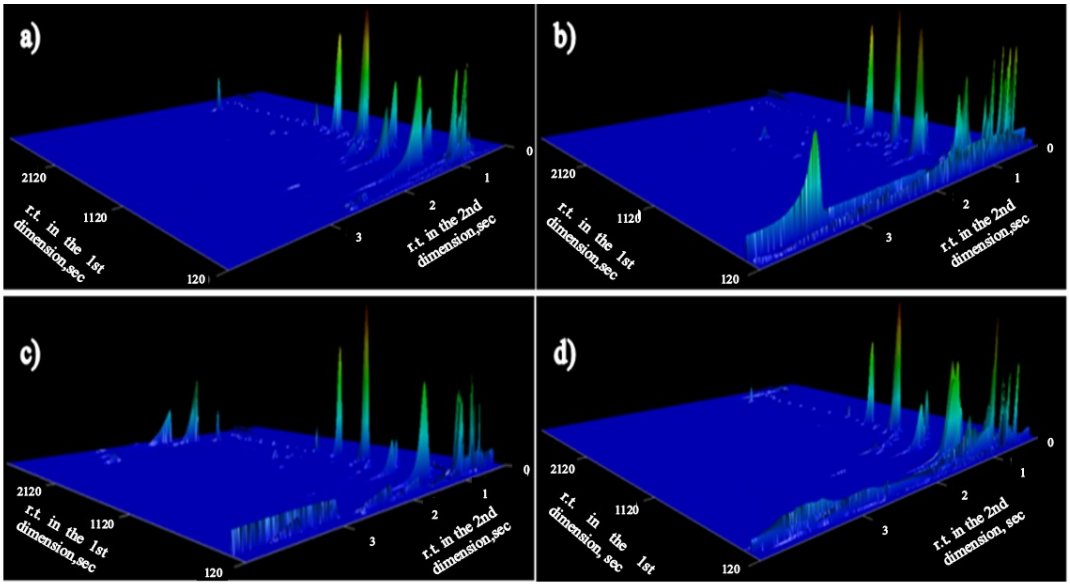

CONCLUSION

Although a large number of sepsis markers have been discovered over the past two decades, diagnostic accuracy remains unclear. Previous studies have intensified efforts to identify effective diagnostic and prognostic markers that can help in assessing the severity of the pathological condition. However, major markers for early prognosis of serious sepsis development are still missing. New predictable and reliable markers would be very useful in situations where sepsis develops in patients undergoing surgery or bone marrow transplantation. Early prediction of sepsis and its differentiation from the systemic inflammatory response of the organism is a key factor in successful therapy and survival of the patient. For this reason, we optimized GCxGC−TOFMS method and the ideal sample conditions for the SPME technique. The best combination of incubation conditions (heating/collection: 30min/30min, the DVB/CAR/PDMS fiber and the addition of NaCl) and optimized GC-TOFMS method was chosen. The optimizing method will be used for VOCs detection, in particular for alcohol, ketones, hydrocarbons etc. from human cells in the future research.

ACKNOWLEDGEMENTS

The research was financially supported by IGA grant, no. IP_058/2020.

REFERENCES

Aggio, R.B. et al. 2016. Freeze-drying: an alternative method for the analysis of volatile organic compounds in the headspace of urine samples using solid phase micro-extraction coupled to gas chromatography - mass spectrometry. Chemistry Central Journal, 10: 9–9.

Alshehri, Y.M. et al. 2020. HS-SPME-GC-MS as an alternative method for NDMA analysis in ranitidine products. Journal of Pharmaceutical and Biomedical Analysis, 191: 113582.

Amal, H. et al. 2012. The scent fingerprint of hepatocarcinoma: in-vitro metastasis prediction with volatile organic compounds (VOCs). International Journal of Nanomedicine, 7: 4135–4146.

Armstrong, B.A. et al. 2017. Sepsis and Septic Shock Strategies. Surgical Clinics, 97(6): 1339–1379.

Boomer, J.S. et al. 2011. Immunosuppression in patients who die of sepsis and multiple organ failure. Jama, 306(23): 2594–2605.

Doležal, P. et al. 2017. Qualitative analyses of less-volatile organic molecules from female skin scents by comprehensive two dimensional gas chromatography–time of flight mass spectrometry. Journal of Chromatography A, 1505: 77–86.

Filipiak, W. et al. 2016. A Compendium of Volatile Organic Compounds (VOCs) Released By Human Cell Lines. Current Medicinal Chemistry, 23(20): 2112–2131.

Hotchkiss, R.S. et al. 2009. The sepsis seesaw: tilting toward immunosuppression. Nature Medicine, 15(5): 496–497.

Monteiro, M. et al. 2014. Analysis of volatile human urinary metabolome by solid-phase microextraction in combination with gas chromatography–mass spectrometry for biomarker discovery: Application in a pilot study to discriminate patients with renal cell carcinoma. European Journal of Cancer, 50(11): 1993–2002.

Silva, C.L. et al. 2017. Volatile metabolomic signature of human breast cancer cell lines. Scientific Reports, 7: 43969.

Optimization of Metafectene-mediated transfection of metallothionein down-regulating siRNA in triple-negative breast cancer cells

Frantisek Petrlak, Hana Subrtova, Veronika Smidova
Department of Chemistry and Biochemistry
Mendel University in Brno
Zemedelska 1, 613 00 Brno
CZECH REPUBLIC

xpetrlak@mendelu.cz

Abstract: Small interfering RNA (siRNA) has become an important instrument for studying gene functions. These double strand RNA oligonucleotides are characterized by targeted mRNA degradation after introduction of specific sequence RNA. Efficiency of siRNA is the basis of gene silencing and gene therapy. In this case, we optimized siRNA transfection to achieve down regulation of gene expression. Then, we validated this optimization on specific sub isoform of metallothionein, *MT-1X*, into triple-negative breast carcinoma cell lines. In this project, we focused on achieving results with the best possible targeted gene suppression with high viability of cells and high transfection effectivity.

Key Words: metallothioneins, siRNA, transfection, qPCR, *MT-1X*

INTRODUCTION

Breast cancer (BCa) is the second most common cancer disease worldwide and the fifth most common cause of cancer death. In this contribution, we focused on triple-negative BCa. These types of BCa lack expression of receptor proteins for important hormones (human epidermal growth factor receptor 2, estrogen, progesterone receptor) and do not respond to hormonal or targeted therapies. Consequently, these tumors are associated with poor prognosis compared to other subtypes (Hutchinson 2010, Siegel et al. 2016).

Shift in understanding cancer biology can improve clinical care for cancer patients and lead the development of new treatment options. Recent studies show that small intracellular proteins called metallothioneins (MTs) can play a very important role in carcinogenesis, and the expression of their different sub isoforms could be helpful for prognostic and therapeutic purposes. In humans, four isoforms of MTs are known (MT1, MT2, MT3 and MT4), coding for multiple sub isoforms of MT-1 (MT-1A, -B, -E, -F, -G, H, J, -K, -L, -M, -X); and one isoform of MT-2A, MT-3, and MT-4. Although there is a high chemical and structural similarity among the isoforms, individual MTs are specifically involved in various processes, and their expression is dependent on various process and tissues. They consist of high number of cysteines, which are responsible for heavy metal-binding, antioxidant balance, and free radical scavenging. MTs influence levels of metals, cytokines, and stress factors in the cell. Additionally to detoxification and transport of heavy metals and stabilization of redox conditions in the cells, MTs regulate the expression of genes and the activity of numerous proteins, either by direct interaction, redox activities of thiol groups, or heavy metal administration (Zalewska et al. 2014, Heger et al. 2016).

MTs participate in the process of carcinogenesis and play critical roles in tumor growth, progression, metastasis, and drug resistance. MTs have also been shown to inhibit apoptosis in tumor cells. MTs can act as zinc donors for transcription factors and tumor suppressors, such as P53 to influence cell growth. P53 is a zinc-binding transcription factor that can inhibit cell cycle progression and induce apoptosis in response to DNA damage. MTs can remove zinc ions from P53 protein molecules, thus leading to changes in the spatial structure of P53, resulting in its inactivation, and thus in uncontrolled cell proliferation (von Bülow et al. 2005, Li and Maret 2008, Kaltenberg et al. 2010, Babula et al. 2012).

Silencing of these sub isoforms could be very helpful in understanding tumor growth and the efficiency cancer therapy. In this study we optimized transfections of siRNA for sub isoform *MT-1X* with hight transfection effectivity and viability in various breast cancer cell lines.

MATERIAL AND METHODS

Cells

Two different model human breast cancer cell lines were used (MDA-MB-231 and MDA-MB-468).

The cell lines were cultured in RPMI-1640 medium (Sigma–Aldrich, St. Louis, MO, USA) with 10% fetal bovine serum and supplemented by two antibiotics – penicillin (100 U/ml) and streptomycin (0.1 mg/ml). All cell lines were maintained inside the incubator Galaxy 170 R (Eppendorf, Hamburg, Germany) at 37 °C with 5% CO_2.

Transfection

For experiments, 50 000 cells were seeded into each well of a 24-well culture plate (VWR International, Pennsylvania, USA). Before transfection, the cells were incubated for 24 hours at 37 °C. After incubation, breast cancer cells were transfected by siRNA silencing duplex (*MT1X*, Sigma-Aldrich, MO, USA) diluted in Metafectene SI buffer (Bionix, Ontario, Canada) in transfection medium. For optimization, control siRNA MISSION® siRNA Fluorescent Universal Control #1, Cyanine 5 (Sigma-Aldrich, MO, USA) was used. Each well-plate contained a control sample without siRNA. After 24 h, medium was replaced by fresh medium and maintained for 48 h.

The optimization conditions differed in the concentration of siRNA transfectants (50 nM, 100 nM, 200 nM) and the time of incubation with siRNA (24 h, 48 h, 72 h). Transfection of siRNA was initiated after cells reached 50–60% confluence.

The transfected cells in the appropriate time period were counted by Countess FL (Thermo Fisher Scientific, MA, USA) and images were taken with fluorescent microscope EVOS FL Cell Imaging System (Thermo Fisher Scientific).

RNA isolation and transcription

Cells were harvested 48 hours after transfection. RNA isolation was performed according to the manufacturer's instructions using RNeasy Mini Kit (Qiagen, Hilden, Germany). Before reverse transcription, RNA quality was evaluated by bleach gel. Synthesis of cDNA was performed with Transcriptor First Strand cDNA Kit (Roche, Basel, Switzerland) with a total yield of 1000 ng in Mastercycler Realplex4 Thermocycler (Eppendorf, Hamburg, Germany).

Quantitative PCR

Gene expression analysis and quantification of knockdown of gene expression was performed in real-time thermal cycler qTOWER3 (Analytik Jena, Jena, Germany) with Luna® Universal qPCR Master Mix (New England Biolabs, MA, USA). Each 20 µl reaction mix contained 25 ng cDNA and set of primer with the final concentration of 0.25 µM. Relative gene expression between cells transfected with control siRNA and siRNA targeting *MT-1X* was normalized to reference gene (*ACTB*).

RESULTS AND DISCUSSION

Optimizing siRNA delivery into cells

First, we have optimized the transfection efficiency using non-coding Cy5-labelled siRNA through fluorescence microscopy. In this step, treatments differed in time points (24h, 48 h, and 72 h), volume of Metafectene SI (1.5 µl, 2 µl, and 2.5 µl) and concentration of siRNA (50 nM, 100 nM, and 200 nM). The results in figure 1 show the morphology of cells and the efficacy of transfection after 48 hours. Figure 1 (A) shows the best variant, the cells treated with 1.5 µl Metafectene SI and 100 nM concentration of siRNA. In this case, more than 90% of the healthy cells were successfully transfected by siRNA. In figure 1 (B), different concentrations were used. At higher concentrations of reagents, cells lost their natural morphological structure and showed higher mortality rates. Taken

together, volume optimization of Metafectene SI has been shown to be very crucial, particularly due to its cytotoxicity originating from its cationic nature.

Figure 1 Transfection efficiency siRNA analyzed by fluorescence microscopy (four cell lines, magnification 40×, scale 200 µm)

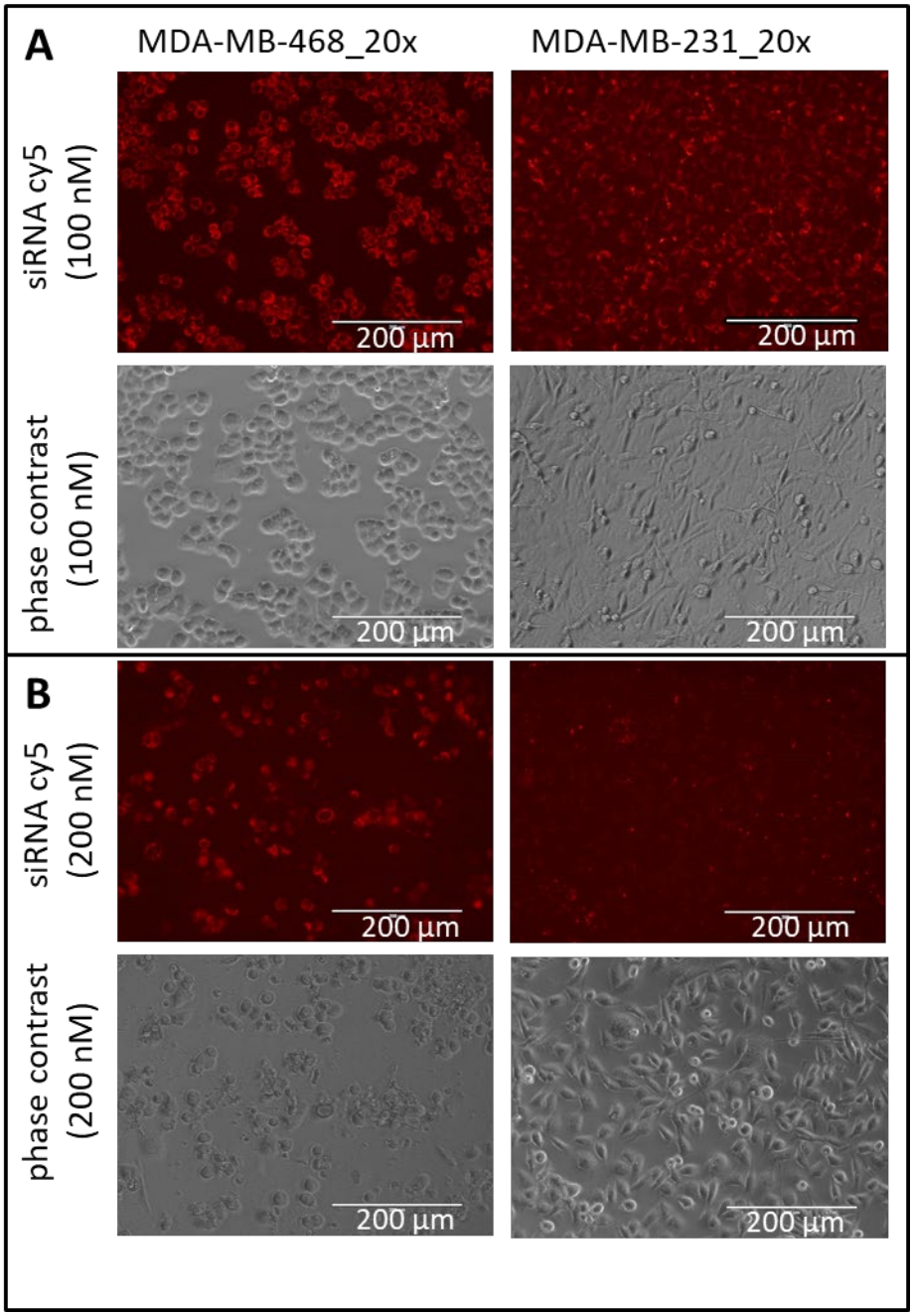

After optimization of transfection efficiency, we evaluated the efficacy of down-regulation of *MT-1X.* Using quantitative PCR, it was found that upon transfection (48 h post-transfection), *MT-1X* was markedly down-regulated in both tested triple-negative cell lines. Therefore, it can be concluded that optimized protocol is efficient and siRNA silencing duplex has pronounced activity is thus useful for follow-up experiments.

In the follow-up experiments, we will focus on the consequences of siRNA-mediated MT-1X knockdown, particularly on the bypass mechanisms of other MT sub isoforms evolving due to down-regulation of MT-1X expression and also on consequences related to the cancerogenesis that has been previously linked to MTs (Liu et al. 2018)

Figure 2 Validation of MT-1X knockdown in two cell lines. Results are shown as ΔCt normalized to ACTB

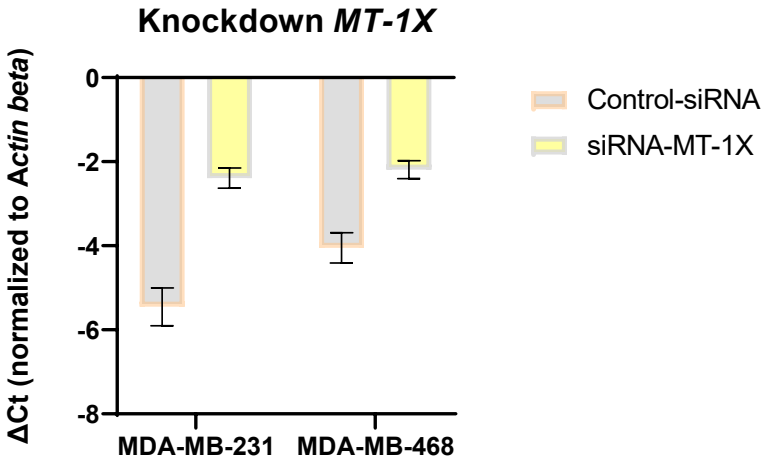

CONCLUSION

In this study, we optimized the transfection of siRNA with high transfection efficiency, and importantly, high cell viability in two representative cell lines derived from triple-negative breast cancer. Noteworthy, we achieved a profound knockdown of expression of *MT-1X* sub isoform. We show that for a successful transfection, all inputs of the reaction require throughout optimization to achieve as high transfection efficiency as possible with retaining a high viability of cells for follow-up experiments. This pipeline will be further employed for detailed understanding of a role of *MT-1X* in breast cancerogenesis, which has not yet been elucidated.

ACKNOWLEDGEMENTS

The research was financially supported by the Internal Grant Agency of Mendel University in Brno, (project No. AF-IGA2020-IP020) and The Czech Science Foundation (project no. 19-13766J).

REFERENCES

Babula, P. et al. 2012. Mammalian metallothioneins: properties and functions. Metallomics, 4(8): 739–750.

Heger, Z. et al. 2016. Metallothionein as a scavenger of free radicals-new cardioprotective therapeutic agent or initiator of tumor chemoresistance? Current Drug Targets, 17(12): 1438–1451.

Hutchinson, L. 2010. Challenges, controversies, breakthroughs. Nature Reviews Clinical Oncology, 7(12): 669–670.

Kaltenberg, J. et al. 2010. Zinc signals promote IL-2-dependent proliferation of T cells. European Journal of Immunology, 40(5): 1496–1503.

Li, Y., Maret, W. 2008. Human metallothionein metallomics. Journal of Analytical Atomic Spectrometry, 23(8): 1055–1062.

Liu, Z. et al. 2018. Metallothionein 1 family profiling identifies MT1X as a tumor suppressor involved in the progression and metastastatic capacity of hepatocellular carcinoma. Molecular Carcinogenesis, 57(11): 1435–1444.

Siegel, R. L. et al. 2016. Cancer statistics, 2016. CA: A Cancer Journal For Clinicians, 66(1): 7–30.

von Bülow, V. et al. 2005. Zinc-mediated inhibition of cyclic nucleotide phosphodiesterase activity and expression suppresses TNF-α and IL-1β production in monocytes by elevation of guanosine 3′, 5′-cyclic monophosphate. The Journal of Immunology, 175(7): 4697–4705.

Zalewska, M. et al. 2014. The role of metallothionein interactions with other proteins. Proteomics, 14(11): 1343–1356.

Synthesis of poly(lactic-co-glycolic) acid nanoparticles with incorporated fish oil

Vendula Popelkova[1], Pavla Vymazalova[2], Tomas Komprda[3], Cristina Sabliov[2], Carlos E. Astete[2]
[1]Department of Food Technology
Mendel University in Brno
Zemedelska 1, 613 00 Brno
CZECH REPUBLIC
[2]Department of Biological and Agricultural Engineering
Louisiana State University
141 E.B.Doran Building, LSU Baton Rouge, LA 70803
USA

vendula.popelkova@mendelu.cz

Abstract: Wound healing remains one of the most common and economically demanding health problems in the world. Omega-3 polyunsaturated fatty acids (present in fish oil) are valued for their anti-inflammatory property, which is significant in wound healing process. The main aim of this experiment was to develop organic nanoparticles (NPs) made from PLGA poly(lactic-co-glycolic acid) with incorporated fish oil (FO). The PLGA NPs with entrapped fish oil PLGA(FO) NPs synthesized by emulsion evaporation measured 233.3 nm in diameter. Value of PDI was evaluated as 0.351 a.u indicating a polydisperse sample, and the particles were very negatively charged, with a zeta potential of -68.1 mV. Particles were spherical as confirmed by TEM. The initial loading capacity was 22.4 g of FO/mg powder. The entrapment efficiency (*EE* %) was 22.47 %. The ability of nanodelivered FO on wound healing will be evaluated next.

Key Words: fish oil, PLGA, wound healing, nanoparticles, omega-3

INTRODUCTION

Despite intensive research in skin tissue engineering, the treatment of skin lesions remains a major challenge for healthcare professionals (Miguel et al. 2019). The development of biomaterials with the potential of accelerate wound healing is currently an excellent challenge for many industries (Chen et al. 2019). In the USA more than 100 million wounds per year are reported, including burns, surgical incisions, diabetic ulcers, ostomies or bedsores. Especially chronic wounds can be the result of prolonged inflammation including excessive polymorphonuclear leukocyte activity (Chereddy et al. 2014). The ultimate goal of wound healing is fast recovery and minimum scarring (Tian et al. 2007).

Wound healing is a normal biological process in the human body (Gillitzer and Goebeler 2001) involving four overlapping, highly programmed phases (hemostasis, inflammation, proliferation and remodeling) (Gercek et al. 2007). The first (hemostasis phase) takes seconds to hours and includes vasoconstriction, platelet aggregation, complement activation and thrombus formation. The following phase, the inflammatory phase takes hours to days. It includes phagocytosis, macrophages activation, neutrophil infiltration and lymphocyte infiltration. The proliferative phase encompasses fibroplasia, angiogenesis, reepithelialization and matrix deposition and it takes days to weeks. The last phase is the remodeling phase. It takes the longest time (week to months). This phase can be characterized as follows: remodeling of extra cellular matrix, epithelialization, increase tensile strength and formation of scar (Rajendar et al. 2018). For a successful wound healing process all phases must happen in the proper sequence and at the appropriate time. Many factors can affect the process of healing. These factors include: age, sex hormones, stress, oxygenation, diabetes, obesity, alcohol, nutrition, smoking or medications (Guo and Dipietro 2010).

Studies suggest that omega-3 polyunsaturated fatty acids (eicosapentaenoic and docosahaenoic fatty acids) generate bioactive lipid mediators and reduce inflammation and recruitment

of polymorphonuclear leukocytes (Mcdaniel et al. 2011). Today, a high percentage of the population is aware of the benefits of omega-3 polyunsaturated fatty acids (Solomando et al. 2020). These polyunsaturated fatty acids can be found in fish oil (Azizi et al. 2019) and can be used to expedite wound healing. EPA and DHA play significant role in prevention and treatment of other diseases, such as cardiovascular diseases, immune response disorders, hypertension, arthritis and some kind of cancer (breast, colon or prostate) (Soltani and Madadlou 2015). DHA and EPA are prone to oxidation and various efforts were made to develop novel delivery systems with the goal of increasing their stability and delay their release for enhanced efficacy (include reference).

In this study, PLGA poly(lactic-co-glycolic acid) was chosen as a suitable matrix for entrapment of FO in the form of NPs. PLGA is a biodegradable and biocompatible polymer commonly and mostly used in biomedical applications (Danhier et al. 2012). PLGA is good choice for wound healing application, because this kind of polymer supplies lactate that accelerates neovascularization and promotes proces of wound healing (Chereddy et al. 2014). In addition to PLGA, the polyester group of synthetic polymers further includes: poly(lactic acid) (PLA), poly(glycolic acid) (PGA) and it also belongs poly(ε-caprolactone) (PCL). However PLGA has been FDA (Food and Drug Administration) especially approved for human therapy (Astete and Sabliov 2006). PLGA is also approved by the European Medicines Agency (EMA) for sustained release, which provides an excellent opportunity to develop controlled and targeted drug use systems (Partikel et al. 2019).

MATERIAL AND METHODS

Chemicals and materials

DCM (dichlormethane), anhydrous, ≥99.8%, was purchased Sigma-Aldrich (St. Louis, MO, USA), Fish oil (Cold liver oil) was purchased from Sigma-Aldrich (St. Louis, MO, USA), PLGA poly(lactic-co-glycolic acid) with Mw 38,000–54,000 g/mol and lactide:glycolide (50:50) was purchased from Sigma-Aldrich (St. Louis, MO, USA), Hexane (95%) was purchased from JT Baker (JT Baker Chemical Co., Phillipsburg, NJ), PVA (Polyvinyl alkohol), 98–99% hydrolyzed, with Mw 31,000–50,000 g/mol from Sigma-Aldrich (St. Louis, MO, USA), Trechalose dihydrate (≥99.0%) with Mw 378,33 g/mol from Sigma-Aldrich (St. Louis, MO, USA). Nanopure water (Nanopure Diamond), 0.2 µm Barnsted D3750 Hollow Fiber Filter (Barnsted International, Dubuque, IA, USA).

Synthesis of NPs

NPs were synthesized by emulsion evaporation as follows. An organic phase was prepared from mixing 440 mg PLGA, 10 ml DCM and 200 mg fish oil. The aqueous phase consisted of 10 ml DCM (dichlormethane) and 2% PVA solution. The organic phase was added to the aqueous phase under mixing (220 RPM). The emulsion was microfluidized in four passes using a M 110P Microfluidizer (Microfluidics, MA) at 30 kpsi. Then, evaporation was performed to remove the solvent using by rotoevaporator, R-124 Rotovap (Buchi Inc., New Castle, DE) for 45 minutes under 800 mm methylene chloride of vacuum. The NPs were dialyzed for two days (25 °C) to remove excess PVA using 300 kDa Spectra/ POR CE membrane (Spectrum Rancho, CA, USA). The samples were mixed with 100 mg of trechalose (1:1, w/w), frozen for 30 minutes in freezer. Then was used freeze-dryed process (2.5 plus freezone) (Labconco Corporation, MO, USA) for two days. The NP powder was stored under dark, refrigerated conditions (under -20 °C) until further analysis. Empty NPs were prepared similarly without the addition of FO to be used as a control.

Size and Zeta Potential

The size distribution (PI, polydispersity index) and zeta potential of the NPs were evaluated by light dynamic scattering (DLS) using a Malvern Zetasizer Nano ZS (Malvern Instruments Ltd., Worcestershire, U.K.). PI was calculed pursuant a cumulative analysis as a dimensionless number ranging (from 0 to 1). Values greater than 0.7 indicate a very broad size distribution of particles. When is PI smaller than 0.1 the sample can be considered as a monodisperse. A volume of 0.1 ml of sample was mixed with 2 ml of distilled water and then 1 ml sample was placed in the cuvette and measured.

Morphology of NPs with fish oil by TEM

The morphology of PLGA(FO) NPs was studied by TEM (transmission electron microscopy). The PLGA(FO) NPs suspension was prepared at 5 mg/ml. One droplet (3 µl) of sample was placed on a 300 mesh with a carbon filmed grid (EMS: CF300-cu). The excess of liquid was removed by using filter paper. After 2 minutes of drying the sample was imaged (JEOL JEM-1400 transmission electron microscope), (JEOL USA Inc., Peabody, MA). The grid was stained with 2% UA (uranyl acetate) for 1 minutes. UA was used as a contrast agent.

Loading capacity measurement (release profile)

The evaluation of release profile was performed as follows. The freeze-dryed sample was resuspended in deionized water at 15 mg/ml NPs under sonication for 5 minutes (Branson 3510, USA). The sample (15 ml) was placed in a dialysis tube (12.000–14.000 Da kept at 37 °C). It was placed into a shaking incubator (C25KC incubator shaker, New Brunswick Scientific, NJ, USA). A volume of 200 µl sample was removed at each time point, 1800 µl of hexane was added, and the sample was shaken (5 minutes) and centrifuged for 30 minutes (Allegra 64R centrifuge, Beckman Coulter, Inc., CA, USA). Absorbance was measured at 320 nm by measured by a UV/Vis spectrophotometer (GENESIS 6, Thermo Electron Scientific Instruments LLC, WI, USA) to determine the amount of fish oil in the sample. The measurements were performed in triplicate. The loading capacity (%) was calculated as follows:

$$LC = \frac{\text{Amount of fish oil in NPs (µg)}}{\text{Total amount of NPs (mg)}}$$

Entrapment efficiency (*EE*) was calculated as follows:

$$EE\ (\%) = \frac{\text{Experimental drug loading (mg)}}{\text{Nominal drug loading (mg)}} \times 100$$

RESULTS AND DISCUSSION

Size, PDI and zeta potential

The diameter of the PLGA-FO NPs was 233.3 ± 23.3 nm. PDI was evaluated as 0.351 a.u indicating a polydisperse sample, and zeta potential was -68.1 mV (Table 1). The difference in zeta potential values for empty NPs and PLGA-FO NPs suggests that fish oil content may affect these value. The Zeta potential is really sensitive to even small changes in the surface character of NPs. Therefore, the addition of fish oil as an additional ingredient could significantly affect the value of the zeta potential. It can be assumed that even a small amount of fish oil adhering to the surface of NPs together with PVA can affect the zeta potential.

Table 1 Characterization of NPs with fish oil including size, PDI and zeta potential

Sample	Size (nm)	PDI (a.u[b])	Zeta potential (mV)
PLGA-FO NPs	233.3 ± 23.3	0.351 ± 0.016	-68.10 ± 1.04
Empty NPs	190.7 ± 1.0	0.218 ± 0.018	-4.95 ± 13.5

Morphology of NPs with fish oil by Transmission Electron Microscopy (TEM)

The morphology of NPs with FO were studied by TEM using JEOL 100-CX TEM by 200 nm and 500 nm (Figure 1).

Figure 1 TEM images by 200 nm and 500 nm of A) PLGA NPs(FO), B) empty PLGA NPs

A)

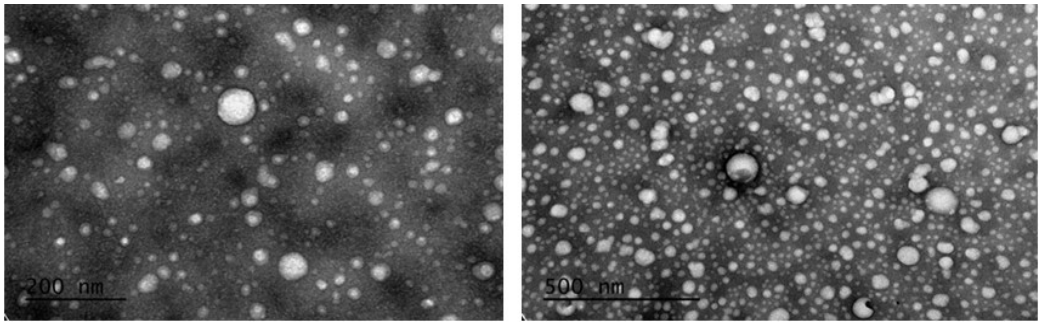

B)

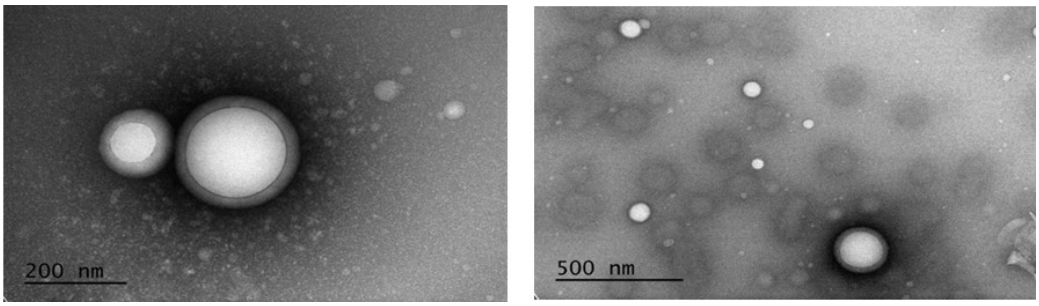

Loading capacity measurement (release) and entrapment efficiency (*EE* %)

The value of loading was 22.4 µg of fish oil/mg powder. Entrapment efficiency (*EE* %) for the standard amount of FO was calculated like 22.47% (Figure 2). Release profile was evaluated over time (hours), for 96 hours (37 °C). Each measurement was performed three times.

Figure 2 Release profile

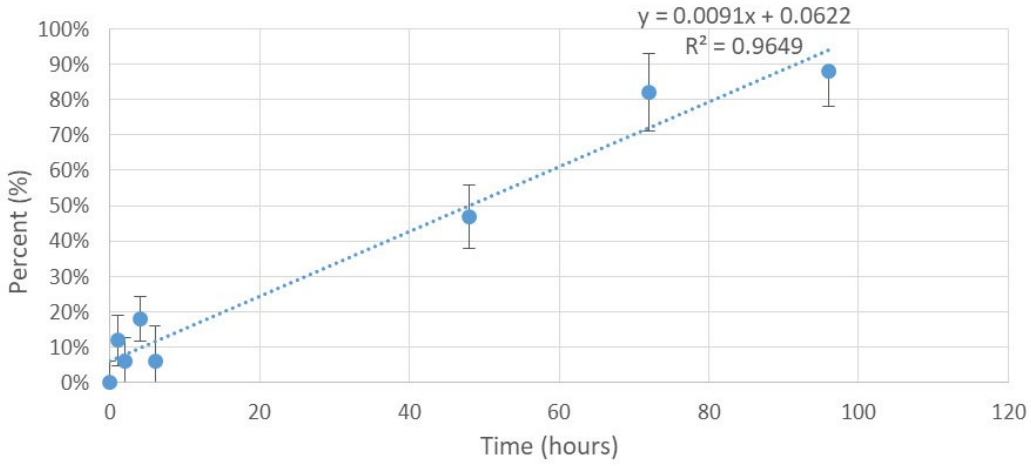

CONCLUSION

In this PLGA-FO NPs were synthesized and characterized. The results showed that NPs were measured in size (~ 200 nm) and negatively charged. Fish oil was successfully entrapped in the PLGA at 22.4 µg of fish oil/mg powder. The next expected and planned step of the research is to test cytotoxicity of the PLGA-FO NPs and to test their efficacy in wound healing *in vivo*.

ACKNOWLEDGEMENTS

The research was financially supported by the Internal Grant Agency of Mendel University in Brno, project No. AF-IGA2019-TP006.

REFERENCES

Astete, C.E., Sabliov, C.M. 2006. Synthesis and characterization of PLGA nanoparticles. Journal of Biomaterials Science, Polymer Edition, 17(3): 247–289.

Azizi, M. et al. 2019. Study of the Physicochemical Properties of Fish Oil Solid Lipid Nanoparticle in the Presence of Palmitic Acid and Quercetin. Journal of Agricultural and Food Chemistry, 67(2): 671–679.

Chen, J. et al. 2019. Fish collagen surgical compress repairing characteristics on wound healing process in vivo. Marine Drugs, 17(1): 33.

Chereddy, K.K. et al. 2014. PLGA nanoparticles loaded with host defense peptide LL37 promote wound healing. Journal of Controlled Release, 194: 1381–147.

Danhier, F. et al. 2012. PLGA-based nanoparticles: an overview of biomedical applications. Journal of Controlled Release, 161(2): 5051–522.

Gercek, A. et al. 2007. Effects of parenteral fish-oil emulsion (Omegaven) on cutaneous wound healing in rats treated with dexamethasone. Journal of Parenteral and Enteral Nutrition, 31(3): 1611–166.

Gillitzer, R., Goebeler, M. 2001. Chemokines in cutaneous wound healing. Journal of Leukocyte Biology, 69(4): 5131–521.

Guo, S., Dipietro, L.A. 2010. Factors affecting wound healing. Journal of Dental Research, 89(3): 2191–229.

Mcdaniel, J.C. et al. 2011. Fish oil supplementation alters levels of lipid mediators of inflammation in microenvironment of acute human wounds. Wound Repair and Regeneration, 19(2): 1891–200.

Miguel, S.P. et al. 2019. An overview of electrospun membranes loaded with bioactive molecules for improving the wound healing process. European Journal of Pharmaceutics and Biopharmaceutics, 139: 1–22.

Partikel, K. et al. 2019. Effect of nanoparticle size and PEGylation on the protein corona of PLGA nanoparticles. European Journal of Pharmaceutics and Biopharmaceutics, 141: 70–80.

Rajendran, N.K. et al. 2018. A review on nanoparticle based treatment for wound healing. Journal of Drug Delivery Science and Technology, 44: 4211–430.

Solomando, J.C. et al. 2020. Improvement of encapsulation and stability of EPA and DHA from monolayered and multilayered emulsions by high-pressure homogenization. Journal of Food Processing and Preservation, 44(1): e14290.

Soltani, S., Madadlou. A. 2015. Gelation characteristics of the sugar beet pectin solution charged with fish oil-loaded zein nanoparticles. Food Hydrocolloids, 43: 6641–669.

Tian, J. et al. 2007. Topical delivery of silver nanoparticles promotes wound healing. ChemMedChem: Chemistry Enabling Drug Discovery, 2(1): 1291–36.

Tyrosine kinase inhibitors differentially deregulate expression of metallothionein sub/isoforms in triple-negative breast cancer cells

Veronika Smidova, Frantisek Petrlak, Hana Subrtova
Department of Chemistry and Biochemistry
Mendel University in Brno
Zemedelska 1, 613 00 Brno
CZECH REPUBLIC

xvilimo1@mendelu.cz

Abstract: Metallothionein (MT) expression has been tied to drug resistance in cancer cells. The MT isoforms have also been investigated in connection to tyrosine kinase inhibitor (TKI) treatment – especially with sorafenib. Our work is focused on three different TKIs – vandetanib, lenvatinib and cabozantinib. Our aim was to investigate the effect of these TKIs on the expression of MT isoforms in breast cancer cell lines. We performed gene expression analysis of seven MT isoforms after TKI treatment. The analysis revealed that each TKI had a different impact on each cell line. Cabozantinib seemed to induce the biggest response of MT expression out of the three inhibitors, with fold change of *MT1F* and *MT1G* reaching 1.68 and 1.62, respectively, in MDA-MB-468 after 24h treatment. Lenvatinib, on the other hand, downregulated *MT1X* in the same cell line after 72h 0.48-fold. Similarly to MDA-MB-468, cabozantinib treatment upregulated *MT1E* and *MT1X* in MDA-MB-231 after 72h treatment, with 1.68 and 1.87-fold difference, respectively.

Key Words: gene expression, metallothionein, triple-negative breast cancer, tyrosine kinase inhibitors

INTRODUCTION

Tyrosine kinase inhibitors (TKIs) are small molecule drugs that bind to tyrosine kinases – receptor or free enzymes capable of phosphorylation of their substrate. This phosphorylation is a way to transduce signal through molecular pathways that control cell proliferation, cell survival, cell motility and more. Therefore, TKs are very important in cancer biology in general, and dysregulation of TK signalling can even be the cause of neoplastic growth (Tridente 2017). Unfortunately, cancer is adaptive in its nature, and therefore the emergence of resistance to TKIs is almost certain to occur after 10 to 13 months of therapy (Paz-Ares et al. 2010).

Metallothioneins (MTs), a group of low-molecular-weight intracellular proteins, have high cysteine and high metal content. They exhibit strong sequence homology between isoforms and have metal binding and redox abilities. In the human genome, seventeen MT genes have been identified, which are all located on chromosome 16 (Coyle et al. 2002). Ten of these isoforms are translated into proteins and play a significant role in protection against oxidative stress, apoptosis or DNA damage, which puts them into an important position in regard to cancer and drug resistance (Cherian et al. 2003). It was reported that MT1G inhibits glutathione (GSH) depletion, which is a key factor in cell death called ferroptosis (Sun et al. 2016). Without GSH, glutathione peroxidase 4 is deactivated, which leads to the accumulation of lipid-based reactive oxygen species and subsequently to ferroptosis (Su et al. 2020).

TKIs, like sorafenib (Sun et al. 2016) and neratinib (Nagpal et al. 2019) were found to induce ferroptosis in cancer cells. The goal of our study was to investigate the effect of three TKIs – vandetanib, lenvatinib and cabozantinib – on MT expression and subsequent connection with chemoresistance to these TKIs, which might include the inhibition of ferroptosis.

MATERIAL AND METHODS

Cell culture and reagents

Triple-negative breast cancer cell lines MDA-MB-231 and MDA-MB-468 were cultured in media RPMI-1640 (Sigma–Aldrich, St. Louis, MO, USA) with 10% fetal bovine serum and 1% antibiotic

(100 U/ml penicillin and streptomycin). The culture conditions were maintained at 5% CO_2 in a humidified incubator with ambient temperature of 37 °C. Media was changed every three to four days and cells were passaged as needed, at 90% confluency at the latest.

TKIs, namely vandetanib, lenvatinib and cabozantinib were purchased from LC Laboratories (Woburn, MA, USA). For use, each inhibitor was weighed out and dissolved in dimethyl sulfoxide (DMSO) to a stock concentration of 10 µM.

RNA isolation

Cells were plated in 12-well plates in the density of 1×10^5 cells per well. Cells were incubated overnight to attach and recover. After that, cells were treated with TKIs and DMSO as a control. DMSO concentration was 0.16% in each well. Concentration of TKIs for MDA-MB-231 and MDA-MB-468, respectively, were as follows: vandetanib – 7 µM and 5 µM; lenvatinib – 15 µM and 16 µM; cabozantinib – 9 µM for both cell lines. These values were decided based on 72h IC_{50} values determined previously.

After 24 h and 72 h, cells were washed with PBS, lysed and scraped. Total RNA was isolated with RNeasy Mini Kit (QIAGEN, Hilden, Germany), according to the manufacturer's protocol. RNA concentration was measured spectrophotometrically in plate reader Infinite 200 PRO (Tecan Life Sciences, Männedorf, Switzerland) at 260/280 nm wavelength. Additionally, absorbance spectrum for each RNA sample was measured from 230 nm to 500 nm. RNA integrity and purity was examined by means of bleach gel agarose electrophoresis, with 1% bleach 1% agarose gel run at 90 V for 35 min.

Reverse transcription

1000 ng of RNA was transcribed into cDNA by Transcriptor First Strand cDNA Synthesis Kit (Roche, Basel, Switzerland) using random hexamer primers, following the manufacturer's protocol. Produced cDNA was then diluted 12.5 times with ultra-pure water to a final concentration of 4 ng/µl.

Gene expression analysis

Expression of specific mRNA was examined by real-time PCR analysis using Luna® Universal qPCR Master Mix (New England Biolabs, MA, USA) with gene-specific primers (Sigma–Aldrich, St. Louis, MO, USA) on qTOWER³ G (Analytik Jena, Jena, Germany). The expression of MT isoforms 1A, 1E, 1F, 1G, 1X, 2A and 3 were monitored. Cycler conditions were as follows: 95 °C for 5 min, followed by 45 cycles of 20 s at 95 °C and 30 s at 60 °C. Melting curve analysis was performed at the end. The expression values were normalized to the expression of housekeeping gene *GAPDH*. The relative abundance of mRNA was quantified using the comparative $2^{-\Delta\Delta Ct}$ method, and data was analysed with unpaired Student's *t*-test in GraphPad Software (San Diego, California, USA).

RESULTS AND DISCUSSION

Sample from cell line MDA-MB-231 treated with cabozantinib for 24 h had insufficient RNA concentration. Therefore, it was excluded from further investigation. Other samples showed sufficient RNA concentration and reasonable absorbance curves, showing purity of a satisfactory level (Figure 1A). Bleach gel showed intact 28S and 18S subunits of rRNA. Samples from 72 h treatment had a slightly visible band in the upper part above 28S subunit. This suggests slight genomic DNA contamination, which, however, was not problematic due to our primers being designed to span an exon–exon junction.

Gene expression analysis revealed interesting changes that happened in reaction to TKI treatment. Each cell line had different reaction to the treatment, which is understandable, because each cell line has a unique gene expression profile. For example, MDA-MB-231 has naturally low expression of *MT1F* and *MT1G* subisoforms – as shown in the data from our previous experiments of basal *MT* gene expression (Figure 2); therefore, we were not able to detect them. MDA-MB-468, on the other hand, has a low expression of the *MT1A* isoform (Figure 2). *MT3* expression in breast cancer cell lines is commonly low (Figure 2); however, we were interested to see, whether there would be any effect of TKI treatment on *MT3* expression.

Figure 1 RNA isolation results – A. absorbance scan, B. bleach gel

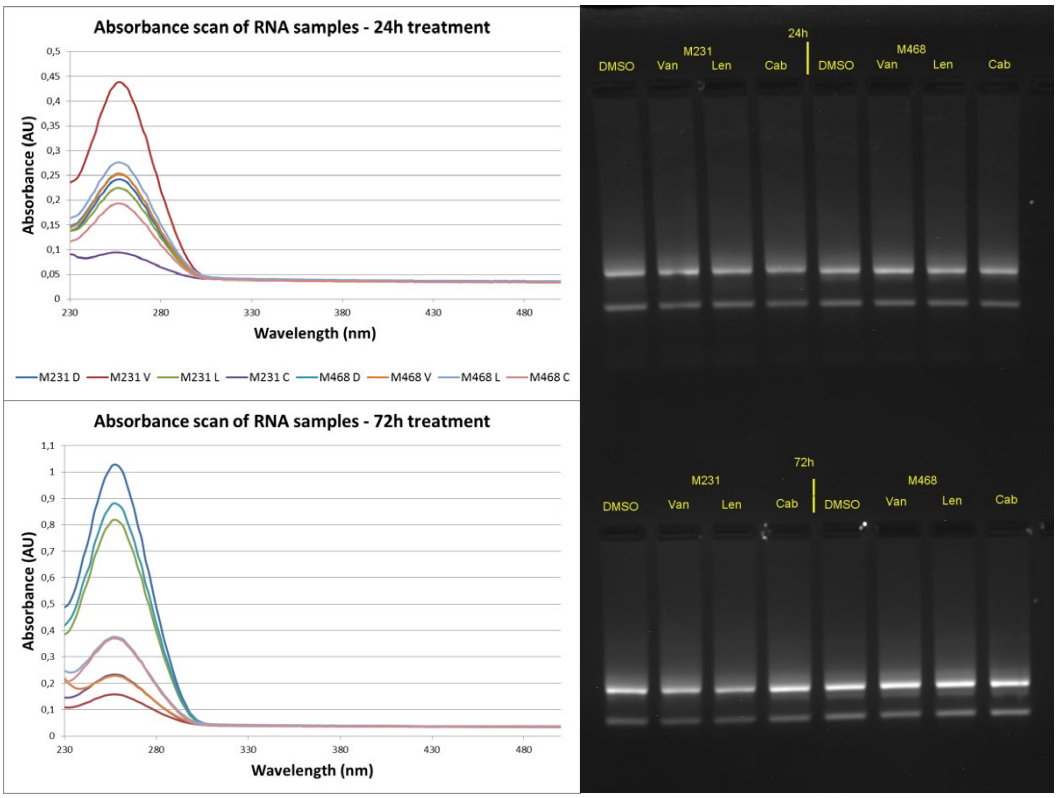

Legend for figure 1B: DMSO – dimethyl sulfoxide; Cab – cabozantinib; Len – lenvatinib; M231 – MDA-MB-231; M468 – MDA-MB-468; Van – vandetanib

Figure 2 Basal gene expression of MT isoforms in chosen breast cancer cell lines (n = 3)

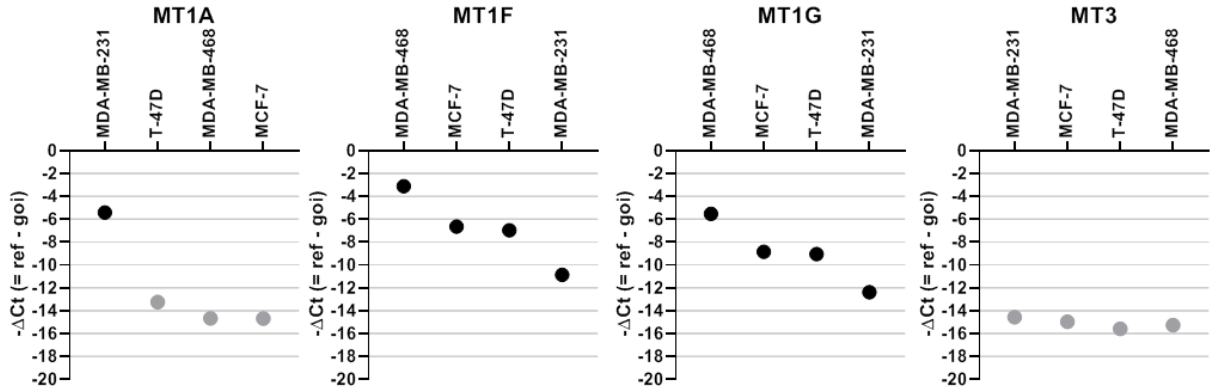

Legend: goi – gene of interest; ref – reference gene; grey colour – expression not detected, below cut-off, or primer dimers

Vandetanib treatment (Figure 3A) induced downregulation in *MT1A* and *MT2A* isoforms in both cell lines. *MT1X* was also slightly downregulated in MDA-MB-468. In MDA-MB-231, vandetanib did not induce expression of *MT1F* or *MT1G*; however, the expression of *MT1E* and *MT1X* were elevated. In MDA-MB-468, *MT1F* and *MT1G* expression did increase – although the treatment effect was most prominent at 24 h, and after 72 h it decreased.

Lenvatinib treatment (Figure 3B) had mostly down-regulatory effect on MDA-MB-468 cells. Especially 72-hour-long treatment had a major attenuating effect on *MT1E* and *MT1X* subisoforms. As for MDA-MB-231, *MT2A* isoform was downregulated, and *MT1A* and MT1E were slightly upregulated.

Cabozantinib treatment (Figure 3C) acted suppressive mainly on MT1X isoform of MDA-MB-468 after 72 h. The same cell line showed major upregulation of *MT1F* and *MT1G*, and slight upregulation of *MT1E* – both after 24 h. MDA-MB-231 had significant increase in expression of *MT1E* and *MT1X* after 72 h.

Figure 3 Analysis of MT isoform gene expression after treatment with vandetanib, lenvatinib and cabozantinib (n = 2)

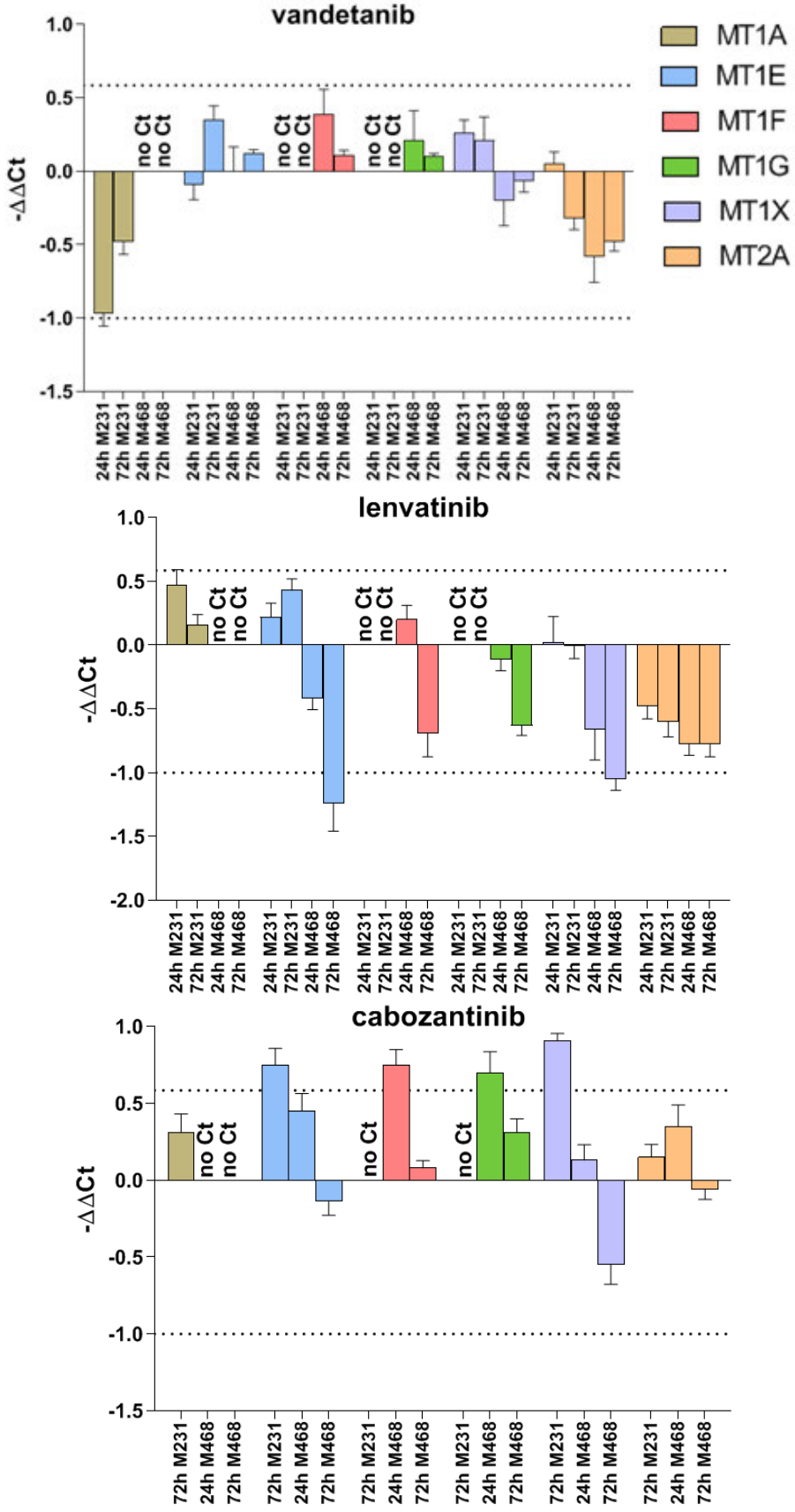

Legend: - ΔΔCt = -(ΔCt(treatment) - ΔCt(control)); ΔCt = Ct(gene of interest) - Ct(reference gene)

In a study of Sun et al. (2016), similar work was conducted on hepatocellular carcinoma (HCC) cell line. They treated the cells with sorafenib and monitored mRNA expression of MT isoforms. Significant increase in *MT1G* expression was induced by sorafenib treatment. Then, they treated with a variety of TKIs – however, none that were used in our experiment –, but no other TKI induced *MT1G* to the same level as sorafenib. Our results show increase of *MT1G* expression, as well as slight increase in *MT2A* expression after 24h of cabozantinib treatment in MDA-MB-468 cell line. This might correlate with Sun's findings that sorafenib is playing a key role in the induction of ferroptosis in HCC cells, while *MT1G* is expressed in order to regulate ferroptosis. Houessinon et al. (2016) treated HCC cells with two times higher concentration of sorafenib than Sun et al. and found increased expression of multiple MT isoforms – *MT1B*, *MT1G*, *MT1E*, *MT1L*, *MT1M* and *MT1H*. We also detected induction of *MT1E* in cabozantinib treated MDA-MB-468 cells; however, additionally the *MT1F* was also increased.

CONCLUSION

Vandetanib and lenvatinib did not induce substantial expression of MT isoforms. In the case of lenvatinib, most isoforms were downregulated. Therefore, we conclude that MTs might not be involved in the cell's response to the treatment with these two inhibitors. Cabozantinib, on the other hand, induced the expression of some MT isoforms; namely *MT1G* and *MT1F* in MDA-MB-468 cell line, and *MT1E* and *MT1X* in MDA-MB-231 cell line. These results hint the importance of MT in molecular mechanisms responding to TKI treatment, and further investigation of their role in modulating ferroptosis is necessary.

ACKNOWLEDGEMENTS

The research was financially supported by the grant AF-IGA2020-IP012 and The Czech Science Foundation (project no. 18-10251S).

REFERENCES

Cherian, M.G. et al. 2003. Metallothioneins in human tumors and potential roles in carcinogenesis. Mutation Research/Fundamental and Molecular Mechanisms of Mutagenesis, 533(1–2): 201–9.

Coyle, P. et al. 2002. Metallothionein: The multipurpose protein. Cellular and Molecular Life Sciences, 59: 627–647.

Houessinon, A. et al. 2016. Metallothionein-1 as a biomarker of altered redox metabolism in hepatocellular carcinoma cells exposed to sorafenib. Molecular Cancer, 15(1): 38.

Nagpal, A. et al. 2019. Neoadjuvant neratinib promotes ferroptosis and inhibits brain metastasis in a novel syngeneic model of spontaneous HER^{2+ve} breast cancer metastasis. Breast Cancer Research, 21(1): 94.

Paz-Ares, L. et al. 2010. Clinical outcomes in non-small-cell lung cancer patients with EGFR mutations: pooled analysis. Journal of Cellular and Molecular Medicine, 14(1–2): 51–69.

Su, Y. et al. 2020. Ferroptosis, a novel pharmacological mechanism of anti-cancer drugs. Cancer Letters, 483:127–136.

Sun, X. et al. 2016. Metallothionein-1G facilitates sorafenib resistance through inhibition of ferroptosis. Hepatology, 64: 488–500.

Tridente, G. 2017. Adverse Events and Oncotargeted Kinase Inhibitors. 1st ed., Cambridge, Massachusetts: Academic Press.

Comparative analysis of metallothionein expression profile in hepatocellular carcinoma cell lines

Hana Subrtova[1], Zbynek Splichal[1, 2], Veronika Smidova[1], Frantisek Petrlak[1]
[1]Department of Chemistry and Biochemistry
Mendel University in Brno
Zemedelska 1, 613 00 Brno
[2]Central European Institute of Technology
Brno University of Technology
Purkynova 123, 616 00 Brno
CZECH REPUBLIC

hanasub7@gmail.com

Abstract: Metallothioneins (MTs) are small cysteine-rich family of proteins which affect many fundamental cellular processes. MTs have been also intensively studied for their role in a carcinogenesis and also for their participation in a development of chemo-resistant phenotypes. The aim of this project was to investigate expression profiles of individual MT (sub)isoforms in two different types of liver tumour cell lines (Huh7, BCLC-3). These expression profiles, obtained by quantitative real-time PCR (qPCR), could subsequently be used to develop new biomarkers of hepatocellular carcinoma, which are still much needed. In our research, we found significant differences in the expression of three MT (sub)isoforms, namely MT1A with mean ΔCt -0.93 in BCLC3 and -4.94 in Huh7, MT1B with mean ΔCt -11.20 in BCLC3 and -7.47 in Huh7, and MT1H with mean ΔCt -15.91 in BCLC3 and -9.85 in Huh7. From these two selected liver tumour cell lines, BCLC3 is more resistant to many different types of chemotherapeutics.

Key Words: metallothionein, hepatocellular carcinoma, liver cancer, biomarkers

INTRODUCTION

Metallothioneins (MTs) belong to the family of low molecular weight (6–7 kDa) intracellular proteins with high cysteine content (Coyle et al. 2002, Ling et al. 2016). By binding heavy metals (especially cadmium), MTs protect cells against their toxicity and also defend cells from oxidative stress by scavenging free radicals. Moreover, MTs are involved in many basic biological processes, like cell growth and proliferation, via of binding essential metals, like zinc and copper (Si and Lang 2018, Albrecht et al. 2008). Recently, more and more studies indicate the participation of metallothioneins in the process of carcinogenesis, where they may play a key role in growth, progression, metastatic potential or chemo-resistance of tumours.

Four main isoforms of MTs have been described in humans (MT1, MT2, MT3, MT4), and all of them are localized on chromosome 16 (16q13). One of these isoforms – MT1– additionally includes another 8 functional (sub)isoforms, which are MT1A, MT1B, MT1E, MT1F, MT1G, MT1H, MT1M and MT1X (Pedersen et al. 2009, Krizkova et al. 2018). MT1 and MT2A isoforms are expressed in various types of tissue, especially in liver and kidney, while MT3 is expressed mainly in brain and MT4 in stratified epithelium (Si and Lang 2018, Krizkova et al. 2018).

This study was focused on mRNA expression of individual MT (sub)isoforms in hepatocellular carcinoma, which is the most prevalent type of liver tumour. Liver cancer is the sixth most commonly diagnosed cancer and fourth leading cause of death worldwide for both sexes (Bray et al. 2018). Early diagnosis of HCC remains essential but very challenging step complicated by liver inflammation and cirrhosis. That is why it is necessary to find new biomarkers for detection of HCC in its early stage (Fu et al. 2017). MTs are intensively investigated as one of new possible HCC biomarkers.

MATERIAL AND METHODS

Chemicals

All used chemicals were purchased from Sigma-Aldrich (St. Louis, Missouri, USA), unless noted otherwise.

Cell lines and cultivation

In this experiment, two different human hepatoma cell lines (Huh-7 and BCLC-3) that were a generous gift from Maria Luz Martinez-Chantar (CIC bioGUNE, Derio, Spain) were used. The first cell line, Huh-7, is a cancer cell line derived from a liver tumour of a 57-year-old man. The second cell line, BCLC-3 is a cancer cell line originally derived from hepatocellular carcinoma of a 67-year-old man with hepatitis C infection.

Cultivation of Huh-7 cells was performed in DMEM medium with 10% fetal bovine serum (FBS) and a mixture of antibiotics – penicillin (100 U/ml) and streptomycin (0.1 mg/ml). BCLC-3 cells were cultured in DMEM/F12 medium supplemented by 10% FBS, 1% non-essential amino acids and two types of antibiotics – penicillin (100 U/ml) and streptomycin (0.1 mg/ml). Cells with the density of 3×10^5 cells/well were maintained in sterile 6-well plate at 37 °C with 5% CO_2 for one day and then were harvested.

RNA isolation

Harvested cells were used for RNA isolation. Isolation was performed by RNeasy Mini Kit from QIAGEN (Hilde, Germany) according to the manufacturer's instructions. Concentration and purity of isolated RNA was measured spectrophotometrically by Infinite® M200 PRO from Tecan (Männedorf, Switzerland). RNA integrity was verified using a bleach gel (Aranda et al. 2012).

Reverse transcription

Synthesis of cDNA was achieved with The First Strand cDNA Synthesis Kit from Roche (Basel, Switzerland). A total 2 µg of isolated RNA was transcribed using Oligo(dT)18 primers. After reverse transcription, cDNA was diluted in 380 µl of ultra-pure H_2O (RNase and DNase free) to a final concentration of 5 ng/µl.

Gene expression analysis

Analysis of gene expression was done by qPCR method using qTOWER³ touch from Analytik Jena (Jena, Germany). For each reaction, 9 µl of Luna® Universal qPCR Master Mix (New England Biolabs, Ipswich, Massachusetts, USA) with 250 nM (0.5 µl of 10 µM stock solution) of forward and reverse primer was mixed, and finally 10 µl of cDNA (50 ng per reaction) was added. The qPCR program was carried out as follows: initial denaturation at 95 °C for 5 minutes and subsequent 45 cycles of denaturation at 95 °C for 20 s and extension at 60 °C for 30 s. Threshold cycle (CT) was determined by qPCRsoft 4.0 from Analytik Jena (Jena, Germany) with automatic baseline corrections. HMBS (hydroxymethylbilane synthase) was chosen as a reference gene for the normalization of metallothionein gene expression (ΔCT = CT HMBS - CT MT).

Verification of qPCR products

The amplification specificity and control of primer-dimer formation was analysed by gel electrophoresis. 1 g of agarose was dissolved in 50 ml 1x TAE buffer. 10 µl of amplified products and 2 µl of 100 bp DNA Ladder from New England Biolabs (Ipswich, Massachusetts, USA) were separated in prepared 2% agarose gel for 60 min at 90 V. Final gel with separated products was photographed by Azure c600 from Azure Biosystems (Dublin, California, USA).

High resolution melting curve analysis (MCA) after amplification of PCR products was done by qTOWER³ touch from Analytik Jena (Jena, Germany) as second step of verification of qPCR products. Third step of verification of qPCR products was performed by Sanger sequencing of purified qPCR products, which was done by SEQme s.r.o. (Dobris, Czech Republic).

Evaluation of PCR efficiency

Amplified products were purified by QIAquick PCR Purification Kit from QIAGEN (Hilde, Germany) according to the manufacturer's instructions. Purified products were than 100x diluted,

and these dilutions were used as starting concentrations. From these starting concentrations, seven series of 10-log dilution were made, and each part of dilution series was used for single qPCR reaction with diverse sets of primers. In the case of MT2A primers, seven series of 2-log dilution of cDNA reverse transcribed from HUH-7 RNA (started amount was 50 ng per reaction) instead of 10-log dilution series from purified qPCR products was used for qPCR reaction. From all measured C_T values, calibration curve for each set of primers was then calculated. From the slope of calibration curve, PCR efficiency was calculated.

PCR efficiency was evaluated also by LinRegPCR program (AMC, Amsterdam, Netherlands). Fluorescence data without baseline corrections was exported from software for qTOWER³ touch after end of qPCR. This data was then processed by LinRegPCR program, which performs a baseline correction on each sample separately, determines a window-of-linearity and then uses linear regression analysis to fit a straight line through the PCR data set. Subsequently, the mean PCR efficiency per amplicon group (same pair of primers) was calculated.

Statistics

Data are presented as mean of ΔC_T and standard deviation (mean±SD) from three biological replicates. Comparison of MT expression between two hepatoma cell lines was performed by unpaired Student's t-test in GraphPad Prism from GraphPad Software (San Diego, California, USA). P values less than 0.05 ($p < 0.05$) were considered as significant.

RESULTS AND DISCUSSION

Verification of qPCR products

Verification of qPCR products was done by three different methods. Specificity of qPCR was checked by MCA and also by Sanger sequencing. It was proved by both of these methods that only required products were amplified from all used sets of primers. Verification of the size of amplified products was done by agarose gel electrophoresis. Sizes of separated products from qPCR were compared to correct amplicon sizes listed in the table in Figure 1B. As we can see on the gel in Figure 1A, there were no unspecific products amplified in the qPCR reaction, and the sizes listed in the table correspond to the sizes of the products in the gel.

Figure 1 Verification of qPCR products – A. Separated products in 2% agarose gel, B. Table with correct sizes of amplified products

A

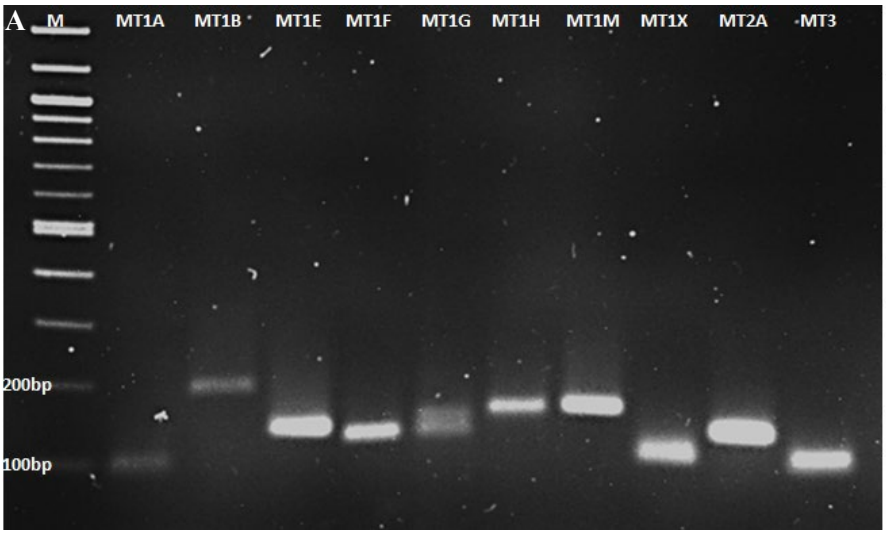

B

Gene	Amplicon length (bp)
MT1A	97
MT1B	187
MT1E	136
MT1F	128
MT1G	128/131
MT1H	153
MT1M	157
MT1X	104
MT2A	133
MT3	97

Legend: M – 100bp DNA ladder

Evaluation of PCR efficiency

Table 1 summarizes the results from the evaluation of PCR efficiency by both used methods. Optimal PCR efficiency should be between 90–110% and our results of almost all used sets of primers, except of MT1M, were in this range. In the case of MT1M, a little lower efficiency was found in contrast to other examined (sub)isoform primers – exactly 86.15%, however evaluation of efficiency from

fluorescence data by LinRegPCR program shown great efficiency for all sets of primers even for MT1M exactly 100.5%. In the end, high quality of all designed PCR reactions was obtained and therefore these setups were used for next analysis.

Table 1 Final values of PCR efficiency

Gene	Slope	PCR efficiency	LinRegPCR efficiency
MT1A	-3.1344	108.47%	102.5%
MT1B	-3.4975	93.16%	99%
MT1E	-3.372	97.95%	99%
MT1F	-3.3071	100.62%	101%
MT1G	-3.4066	96.58%	108%
MT1H	-3.421	96.03%	102%
MT1M	-3.7057	86.15%	100.5%
MT1X	-3.329	99.71%	98.5%
MT2A	-3.2389	103.59%	105.5%
MT3	-3.432	95.60%	98.5%

Comparison of basal gene expression of metallothioneins

Main goal of this study was to compare the expression of individual MT (sub)isoforms between two different types of human hepatoma cell lines (shown in Figure 2) – Huh-7 and BCLC-3. BCLC-3 is a cell line more resistant to many diverse types of chemotherapeutics (Ramos et al. 2016). Statistical significant difference ($p < 0.05$) was observed in the expression of MT1A. In Huh-7 cell line, we found lower expression of MT1A in comparison with the second cell line, BCLC-3. MT1A was described previously as a gene with low expression in hepatocellular carcinoma (Liu et al. 2018). In resistant BCLC-3, significantly ($p < 0.05$) lower expression of MT1B was observed, which is also known as a low expressed gene in liver cancer (Si and Lang 2018). Similar trend was observed in the expression of MT1H, but this result wasn't evaluated as statistically significant. MT1H was previously identified as one of the potential biomarkers to predict recurrence in hepatocellular carcinoma (Wang and Gribskov 2019). In other (sub)isoforms no statistical significant differences were observed. Our findings expand knowledge about MT expression in liver cancer and also suggest three (sub)isoforms of MT – namely MT1A, MT1B, MT1H – as possible biomarkers for chemo-resistance development in hepatocellular carcinoma.

Figure 2 Basal expressions of metallothionein genes in HUH7 and BCLC-3 hepatoma cell lines

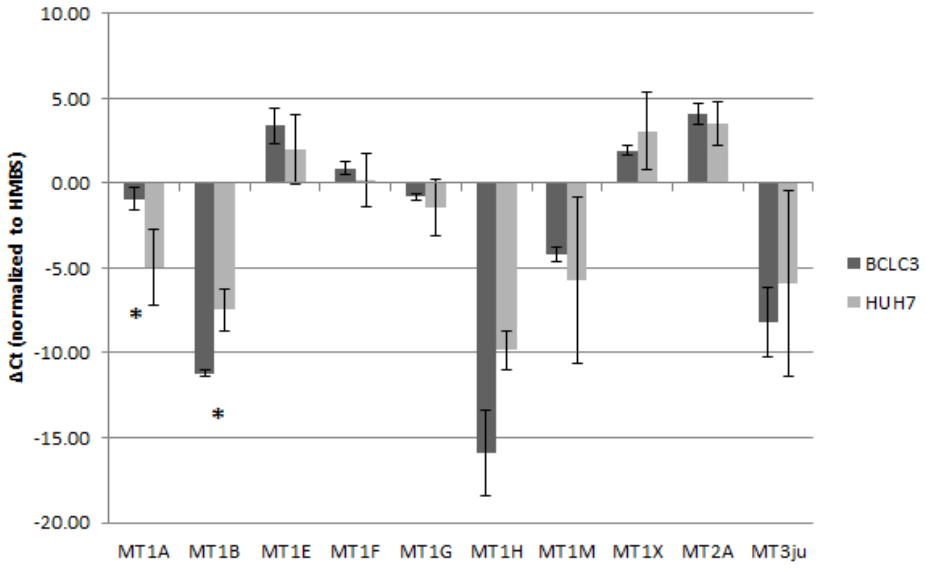

*Legend: Data presented as mean±SD of ΔCT from three biological replicates (n = 3); * – statistically significant difference p < 0.05*

CONCLUSION

Our investigation was focused on MT expression in hepatocellular carcinoma. We observed that in BCLC-3, which is the more resistant cell line, significantly higher expression of MT1A and lower expression of MT1B and MT1H were present compared to the second examined cell line, Huh-7. These results could be useful for future research of chemo-resistance development and search for new biomarkers in hepatocellular carcinoma, which is one the most commonly diagnosed cancers worldwide.

ACKNOWLEDGEMENTS

The research was financially supported by the Mendel University in Brno (project no. AF-IGA2020-IP026) and The Czech Science Foundation (project no. 19-13766J).

REFERENCES

Albrecht, A. et al. 2008. Basal and metal-induced expression of metallothionein isoform 1 and 2 genes in the RWPE-1 human prostate epithelial cell line. Journal of Applied Toxicology, 28: 283–293.

Aranda, P.S. et al. 2012. Bleach gel: a simple agarose gel for analyzing RNA quality. Electrophoresis, 33: 366–369.

Bray, F. et al. 2018. Global cancer statistics 2018: GLOBOCAN estimates of incidence and mortality worldwide for 36 cancers in 185 countries. CA: A Cancer Journal for Clinicians, 68: 394–424.

Coyle, P. et al. 2002. Metallothionein: the multipurpose protein. Cellular and Molecular Life Sciences CMLS, 59: 627–647.

Fu, C.-L. et al. 2017. Metallothionein 1M suppresses tumorigenesis in hepatocellular carcinoma. Oncotarget, 8: 33037–33046.

Krizkova, S. et al. 2018. An insight into the complex roles of metallothioneins in malignant diseases with emphasis on (sub)isoforms/isoforms and epigenetics phenomena. Pharmacology & Therapeutics, 183: 90–117.

Ling, X.-B. et al. 2016. Mammalian Metallothionein-2A and Oxidative Stress. International Journal of Molecular Sciences, 17: 1483.

Liu, Z. et al. 2018. Metallothionein 1 family profiling identifies MT1X as a tumor suppressor involved in the progression and metastastatic capacity of hepatocellular carcinoma. Molecular Carcinogenesis, 57: 1435–1444.

Pedersen, M.Ø. et al. 2009. The role of metallothionein in oncogenesis and cancer prognosis. Progress in Histochemistry and Cytochemistry, 44: 29–64.

Ramos, D.F. et al. 2016. Targeting of MIR-518D Reduces Chemoresistance in Hepatocellular Carcinoma Cell Lines. Journal of Hepatology, 64: S561.

Si, M., Lang, J. 2018. The roles of metallothioneins in carcinogenesis. Journal of Hematology & Oncology, 11: 107.

Wang, S., Gribskov, M. 2019. Transcriptome analysis identifies metallothionein as biomarkers to predict recurrence in hepatocellular cacinoma. Molecular Genetics & Genomic Medicine, 7: e693.

Palladium-loaded PLGA-chitosan NPs as efficient catalysts for bioorthogonal chemistry

Paulina Takacsova[1], Vladimir Pekarik[2]
[1]Department of Chemistry and Biochemistry
Mendel University in Brno
Zemedelska 1, 61300 Brno
[2]Department of Physiology
Masaryk University
Kamenice 753/5, 625 00 Brno
CZECH REPUBLIC

takacsovapaulina@gmail.com

Abstract: Bioorthogonal chemistry offers a wide range of reactions, which can be performed in the intracellular platform. Among the wide range of uses, bioorthogonal reactions can be employed for the controlled pro-drug activation *in situ*. Palladium compounds can be exploited as activation agents in the bioorthogonal reactions. However, their properties such as toxicity, poor cellular uptake and inactivation by biogenic thiols hinder their catalytic activity on the cellular level. In our study, we have prepared polymeric palladium-loaded poly(D,L-lactide-*co*-glycolide) (PLGA)-chitosan nanoparticles (NPs). The coating of these two polymers with chitosan has ensured cellular uptake and the gradual release of palladium compounds inside the cell. Their catalytic activity was demonstrated by the conversion of a fluorescent probe made of chemically modified 8-hydroxypyrene-1,3,6-trisulfonic acid trisodium salt propargyl ether (HPTS-PE).

Key Words: PLGA-chitosan NPs, bioorthogonal chemistry, palladium-mediated catalysis, fluorescent probe activation, nanomedicine

INTRODUCTION

Bioorthogonal chemistry employs specific catalysts to perform bond-forming or cleavage reaction under physiological conditions, thus allowing to interfere with the reactions in biological systems (Li and Chen 2016). In our study, we employed palladium catalyst bis[tri(2-furyl)phosphine] palladium(II) dichloride ($Pd(TFP)_2Cl_2$). Its catalytic activity was confirmed by depropargylation reaction of propargyl-ether modified pyranine fluorescent probe.

Among other, high specificity towards the modified compound, a wide range of catalyzed reaction and the broad spectrum of coordination ligands predestines palladium compounds to be a useful tool in bioorthogonal chemistry (Chankeshwara et al. 2014). The reaction can be mediated by the Pd^0 species (Unciti-Broceta et al. 2012), but also ligand-coordinated Pd^{2+} species (Li et al. 2011, Ma et al. 2014, Martinez-Calvo et al. 2018). The usage of palladium compounds as a promising catalyst for bioorthogonal therapy has been shown previously (Bray et al. 2018, Rubio-Ruiz et al. 2016, Weiss et al. 2014).

However, the intracellular environment provides many obstacles, which are mostly caused by thiol poisoning of the catalyst. Thiols groups, which are irreversibly coordinated to palladium central atoms and therefore inhibit its catalytic activity frequently occur in the biological environment as a part of peptide and protein compounds (Chankeshwara et al. 2014), free amino acids or redox maintaining system such as glutathione. In order to limit access of thiol compounds to the catalyst we have used encapsulation into NPs consisting of PLGA core coated with chitosan polymer. This formulation provides several benefits, such as reduced cytotoxicity, improved cellular uptake and controlled release of the encapsulated agent (Wang et al. 2013).

MATERIAL AND METHODS

PLGA-chitosan NPs preparation

70 µL of organic phase containing PLGA (40 µL of 50 mg/mL dissolved in acetonitrile) and TMP-BODIPY (1 µL of 32 mM dissolved in 30 µL of dimethylformamide) was added into 1000 µL of aqueous phase consisted of low molecular weight chitosan (0.1%), PVA (1%) dissolved in 0.5% acetic acid. The mixture was vortexed at maximum speed to form NPs and incubated for 10 minutes. From this mixture, 400 µL was further processed. The residual cargo and polymers were then separated from NPs using centrifugation (9425 x g, 15 minutes). The obtained pellet was resuspended in cryoprotectant sucrose solution (250 mM) to the final volume of 100 µL. The nanoparticle suspension was then cleared of aggregates using second centrifugation (94 x g, 5 minutes).

In the case of palladium-loaded PLGA-chitosan NPs, the same method for particle preparation was used. The palladium catalyst $Pd(TFP)_2Cl_2$ was added into organic phase (30 µL of 25 mM dissolved in DMF) instead of the fluorescent dye TMP-BODIPY. As a negative control, the PLGA-chitosan NPs without palladium catalyst were synthesized. The harvested NPs pellet was resuspended in 200 µL of sucrose solution.

The raw particle size, morphology and aggregates formed from residual polymers were observed under the microscope (Olympus IX53) on phase-contrast after individual steps in NPs preparation. After vortexing, 10 µL of NPs was resuspended in 100 µL water in a 96-well plate, after second centrifugation, 5 µL of NPs was resuspended in 100 µL water in a 96-well plate. The images of Pd-PLGA-chitosan NPs were obtained using SEM MAIA 3 equipped with a field emission gun from TESCAN Company (TESCAN Ltd. Brno, Czech Republic, EU).

Cellular uptake of TMP-BODIPY-PLGA-chitosan NPs

For all experiments, non-malignant mammalian cell line HEK 293T was used. Cells were incubated in complete medium (DMEM/F12 supplemented with 10% FBS, 100 U/mL penicillin, 100 µg/mL streptomycin) in a humidified incubator with 5% CO_2. Particle aggregates and cells images were taken using fluorescent microscope Olympus IX53. Cells are imaged using phase-contrast microscopy and fluorescent microscopy with green filter (excitation wavelength = 460–495 nm, emission wavelength = 510 nm, fluorescent lamp intensity = 12, exposition time = 800 ms).

Cells were seeded in a 24-well plate at 50% confluence and allowed to attach for 4 hours. Then, the medium was replaced with 500 µL of medium containing 5 µL of TMP-BODIPY-PLGA-chitosan NPs. Before taking the pictures after 17 h incubation, the media were replaced with 500 µL of fresh complete media.

Cell-free fluorescent probe precursor activation using Pd-PLGA-chitosan NPs

A mixture of fluorescent sensor 8-hydroxypyrene-1,3,6-trisulfonic acid propargyl ether (HPTS-PE) (50 µM) in 200 µL of complete cell media was added into 3 µL of palladium-loaded PLGA-chitosan NPs or $Pd(TFP)_2Cl_2$ catalyst (50 µM). The suspension was placed in a 96-well plate and the fluorescent probe depropargylation was measured at the beginning of the reaction, and after 24, 72 hours and 6 days as fluorescence on TECAN reader (excitation wavelength = 450 nm, emission wavelength = 515 nm).

Pd-PLGA-chitosan NPs intracellular catalytic activity evaluation

Cells were seeded in a 6-well plate at 50% confluence and allowed to attach for 4 hours. Then, the old medium was replaced with 2 mL of complete cultivation medium containing 50 µL of Pd-PLGA-chitosan NPs. As a negative control, 50 µL PLGA-chitosan NPs without catalyst was used. After overnight incubation, cells were split into a 24-well plate to 50% confluence and allowed to attach for 6 hours. Afterwards, cells were treated with 500 µL of media containing HPTS-PE (50 µM) and Hoechst 33258 (4 µg/mL). After overnight incubation, images of fluorescence were taken. Cells were imaged using a phase contrast microscopy and fluorescent microscopy with blue light emission filter (Hoechst nuclear staining) (excitation wavelength = 360–370 nm, emission wavelength =

420–460 nm, fluorescent lamp intensity = 25, exposition time = 20 ms) and with green filter (excitation wavelength = 460–495 nm, emission wavelength = 510 nm, fluorescent lamp intensity = 25, exposition time = 500 ms).

RESULTS AND DISCUSSION

The aim of our study was to prepare the palladium-loaded PLGA-chitosan NPs (Pd-PLGA-chitosan NPs), which would be able to catalyze a deprotection reaction in cells under physiological conditions.

In the first part of our research, we have focused on the tuning of the PLGA-chitosan NPs formulation. For the optimization process, the fluorescent dye TMP-BODIPY was encapsulated to facilitate the visualization of NPs and cellular uptake. The process of optimization of the PLGA-chitosan NPs consisted of the testing of the correct ratio of the particles-forming polymers PLGA, chitosan, and polyvinylalcohol (PVA) stabilizer. Hydrophobic PLGA polymer provides a gradual release of the encapsulated compound inside the cells and interacts with the hydrophobic fluorescent dye or hydrophobic organometallic palladium catalyst. Poly-cationic polymer chitosan serves as a particle coating and its positive charge also improves the cellular uptake. The PVA stabilizer prevents particles from aggregation.

During the synthesis of PLGA-chitosan NPs, different amounts of each component, as well as different emulsification technologies (sonication and vortexing) were tested. The main problem during the NPs preparation turned out to be the formation of aggregates induced by the presence of chitosan polymer in reaction mixture. To control the production of aggregates in NPs suspension, we made microscopic observation (phase contrast) of macro-aggregate formation. The key steps leading to aggregates-free suspension were the acidic pH of aqueous phase that ensured a more soluble form of chitosan polymer, the emulsification method using vortexing and the centrifugation of the NPs suspension at low speed to remove the largest aggregates. The comparison between the suspensions after vortexing (A) and after the second centrifugation, when the final product was reached (D) is shown in Figure 1. The formation of NPs in range below 500 nm has been confirmed by SEM (Figure 1g).

Figure 1 Microscopic observation of PLGA-chitosan NPs

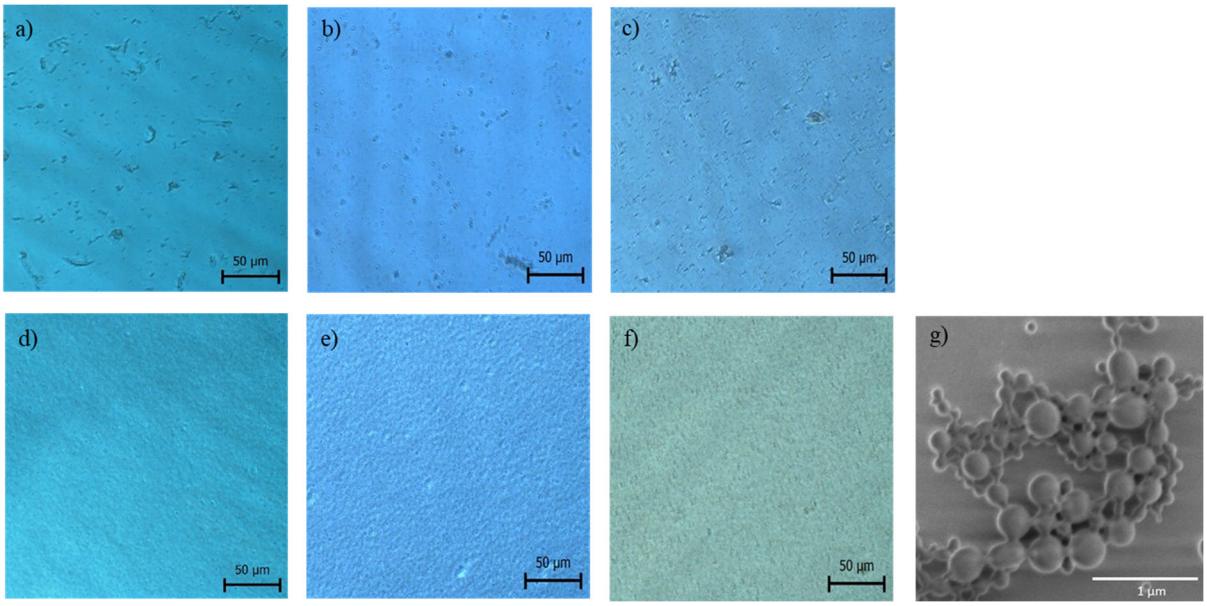

Legend: Phase contrast microscopy of PLGA-chitosan NPs (a-f). Samples a), b) and c) show the NPs after vortexing. Samples d), e) and f) show the final NPs after the second centrifugation leading to removal of chitosan aggregates. Samples a) and d) contained TMP-BODIPY-PLGA-chitosan NPs, samples b) and e) contained PLGA-chitosan NPs without any encapsulated compound and c) and f) contained Pd-PLGA-chitosan NPs. Scanning electron microscopy analysis of Pd-PLGA-chitosan NPs (g).

After the NPs preparation, their cellular uptake into non-malignant HEK cells has been tested. NPs with the encapsulated fluorescent dye were incubated with cells overnight. After incubation,

the cell media were changed to remove non-internalized NPs. Figure 2 shows that TMP-BODIPY-PLGA-chitosan NPs have been effectively internalized by HEK cells. Since TMP-BODIPY is completely insoluble in water, the green fluorescence indicates inclusion of the dye in the NPs.

Figure 2 Cellular uptakes of TMP-BODIPY-loaded PLGA-chitosan NPs

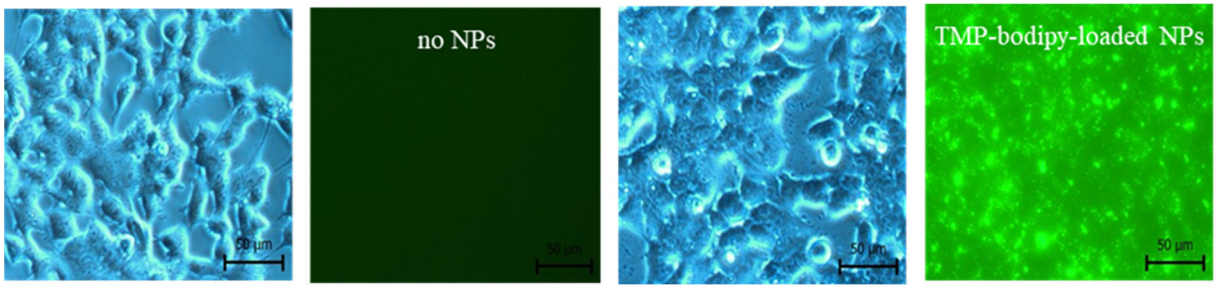

Legend: Cellular uptake of TMP-BODIPY-loaded PLGA-Chitosan NPs after 17 h hours of incubation.

After confirmation of model NPs cellular uptake, we prepared NPs with the palladium catalyst $Pd(TFP)_2Cl_2$ using the same method. As a negative control, PLGA-chitosan NPs without a catalyst were prepared (see Figure 1b, c, e, f).

Figure 3 Fluorescence emission intensity in samples evaluating cell-free precursor fluorescent probe activation in complete cell media

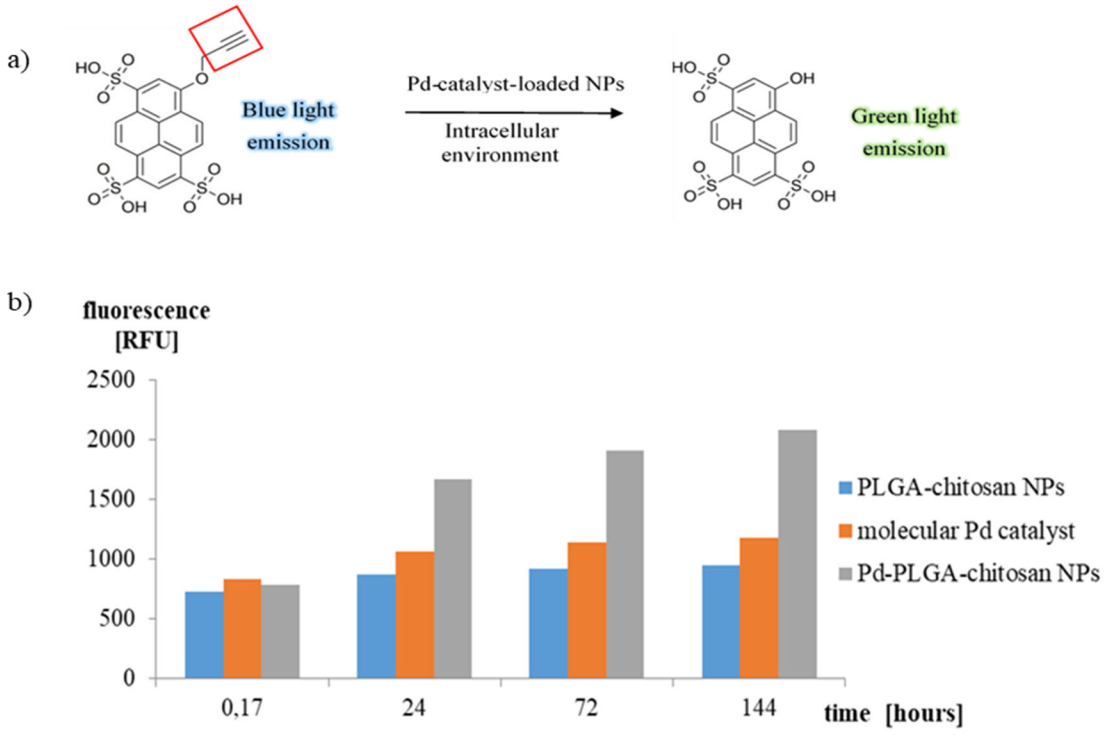

Legend: a) Pd-catalyst-mediated HPTS-PE precursor fluorescent probe activation reaction. b) Probe activation in cell-free conditions. Sample "PLGA-chitosan NPs" did not contain any palladium catalyst, sample "molecular Pd catalyst" contained non-encapsulated $Pd(TFP)_2Cl_2$ catalyst and sample "Pd-PLGA-chitosan NPs" contained $Pd(TFP)_2Cl_2$ catalyst encapsulated in PLGA-chitosan polymer.

Pd-PLGA-chitosan NPs were tested for the ability to deprotect palladium sensitive probe HPTS-PE. The cleavage of the propargylic group is exclusively mediated by palladium catalyst (see Figure 3a). At first, *in vitro* test was conducted. The encapsulated and free palladium catalysts were incubated in complete cell medium supplemented with FBS. The catalytic activity was evaluated as an increase in fluorescence of deprotected HPTS within 6 days. Figure 3b shows that the palladium catalyst gradually activates the HPTS-PE probe, upon release from the NPs. On the contrary,

$Pd(TFP)_2Cl_2$ alone has almost no catalytic activity. In the presence of proteins and biogenic thiols, palladium compounds suffer from "thiol poisoning" which precludes palladium catalytic activity. In our study, the reaction mixture was supplied with fetal bovine serum, to resemble the biological environment rich in thiol-group-containing compounds. The encapsulation protected the catalyst from its immediate inactivation, which encouraged us to evaluate the NPs catalytic activity in cellular system. There are reports using palladium with thiol ligands for catalytic purposes, however, these reactions are executed at high temperatures or in organic solvents where the thiol dissociation from active metal center is facilitated by the conditions. In physiological conditions, the thiol poisoning is a real concern.

Figure 4 Microscopic observation of HPTS-PE fluorescent probe activation inside cells using fluorescent microscope

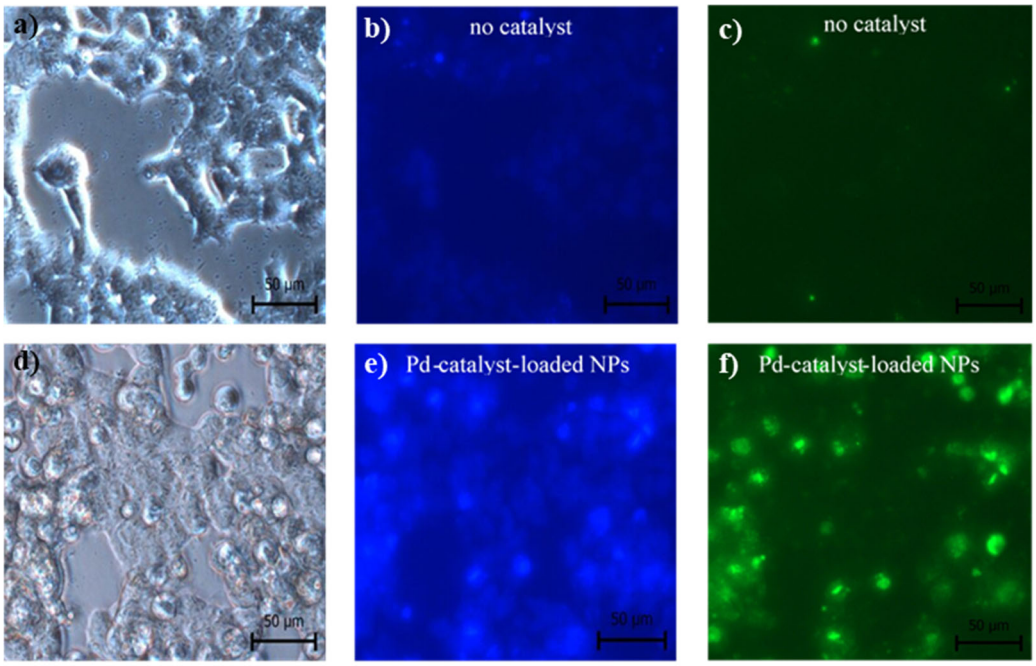

Legend: Intracellular HPTS-PE fluorescent probe activation. Cells were incubated with negative control PLGA NPs (a, b, c) or Pd-catalyst-loaded NPs overnight (d, e, f). The next day, Hoechst33258 and the probe were added and incubated overnight.

At first, cells were incubated with Pd-PLGA-chitosan NPs. The NPs with Pd catalyst slightly inhibit cells growth. Cells treated with NPs were seeded at the same confluence. Cells were treated with the probe overnight. The activation was detected as green fluorescence emission. The results in Figure 4 show that in cell culture treated with Pd-PLGA-chitosan NPs, the fluorescent probe was activated. To the contrary, the negative control cell culture containing PLGA-chitosan NPs without Pd catalyst did not exhibit any catalytic activity. The blue signal is derived from Hoechst 33258 dye, which was added to all samples as nuclei marker.

In summary, we have developed an efficient method for the PLGA-chitosan NPs preparation, which is more user friendly compared to commonly used solvent-evaporation emulsification methods employing long solvent evaporation (de Castro et al. 2020). Some bioorthogonal chemistry approaches rely on the pre-activation of a protected compound in extracellular space (Martinez-Calvo et al. 2018, Weiss et al. 2014). This approach might not be useful in many applications. The benefit of the encapsulation into PLGA-chitosan polymeric NPs is the ability to catalyze the reactions inside the cells. Owing to the incorporation of the Pd catalyst to the polymer network the catalyst retains its activity during prolonged incubation in the cellular environment. Therefore, these particles are promising nanocarrier of bioactive catalysts for potential bioorthogonal therapies.

CONCLUSIONS

We have prepared non-toxic Pd-PLGA-chitosan NPs. The NPs are effectively internalized into cells and their catalytic activity is preserved during two-day incubation in the cellular environment as documented by activation of fluorescent probe. These are key properties, which are needed from the catalyst employed in bioorthogonal pro-drug activation.

ACKNOWLEDGEMENTS
The research was financially supported by the IGA individual project AF-IGA2020-IP039.

REFERENCES

Bray, T.L. et al. 2018. Bright Insights into Palladium-Triggered Local Chemotherapy. Chemical Science, 9: 7354–7361.

Chankeshwara, S.V. et al. 2014. Palladium-Mediated Chemistry in Living Cells. Current Opinion in Chemical Biology, 21: 128–135.

de Castro, K.C. et al. 2020. Drug-Loaded Polymeric NPs: A Review. International Journal of Polymeric Materials and Polymeric Biomaterials, 13.

Li, J., Chen, P.R. 2016. Development and Application of Bond Cleavage Reactions in Bioorthogonal Chemistry. Nature Chemical Biology, 12: 129–137.

Li, N. et al. 2011. Copper-Free Sonogashira Cross-Coupling for Functionalization of Alkyne-Encoded Proteins in Aqueous Medium and in Bacterial Cells. Journal of the American Chemical Society, 133: 15316–15319.

Ma, X.J. et al. 2014. N-Heterocyclic Carbene-Stabilized Palladium Complexes as Organometallic Catalysts for Bioorthogonal Cross-Coupling Reactions. Journal of Organic Chemistry, 79: 8652–8658.

Martinez-Calvo, M. et al. 2018. Intracellular Deprotection Reactions Mediated by Palladium Complexes Equipped with Designed Phosphine Ligands. Acs Catalysis, 8: 6055–6061.

Rubio-Ruiz, B. et al. 2016. Efficient Palladium-Triggered Release of Vorinostat from a Bioorthogonal Precursor. Journal of Medicinal Chemistry, 59: 9974–9980.

Unciti-Broceta, A. et al. 2012. Synthesis of Polystyrene Microspheres and Functionalization with Pd-0 NPs to Perform Bioorthogonal Organometallic Chemistry in Living Cells. Nature Protocols, 7: 1207–1218.

Wang, Y.C. et al. 2013. Chitosan-Modified PLGA NPs with Versatile Surface for Improved Drug Delivery. Aaps Pharmscitech, 14: 585–592.

Weiss, J.T. et al. 2014. Development and Bioorthogonal Activation of Palladium-Labile Prodrugs of Gemcitabine. Journal of Medicinal Chemistry, 57: 5395–5404.

Development of electrochemical biosensor for direct histamine detection by using selective peptides as biorecognition element

Veronika Vanova[1], Vedran Milosavljevic[1,2], David Hynek[1,2], Lukas Richtera[1,2], Vojtech Adam[1,2]
[1]Department of Chemistry and Biochemistry
Mendel University in Brno
Zemedelska 1, 613 00 Brno
[2]Central European Institute of Technology
Brno University of Technology
Purkynova 123, 612 00 Brno
CZECH REPUBLIC

veronika.vanova@mendelu.cz

Abstract: The level of histamine (HIS) in different food sources is critical as an indicator of food quality and safety. In this context, the proper monitoring of HIS in food is necessary. Electrochemical biosensors, with the possibility of fast, sensitive, and portable technology, represent a new promising approach for direct detection of HIS. Moreover, peptides as biorecognition elements are promising due to their unique properties such as good stability, specific and selective binding to various biomolecules. In this study, the fabrication and optimization of an electrochemical biosensor for direct detection of HIS based-on peptides as recognition elements, is presented. The specific HIS binding peptides (HBP) were immobilized via a sulphonamide bond on 1-amino-2-naphthol-4-sulfonic acid (ANSA), which was electrodeposited on a glassy carbon electrode (GCE). Furthermore, the optimization of the surface coverage with the peptide probe as well as the effect of the pH conditions for HIS binding was investigated. The measured concentrations were from 10 nM (10^{-8} M) to 1 mM (10^{-3} M) and LOD was calculated as 6.53 nM and LOQ as 21.75 mM.

Key Words: histamine, peptide, biorecognition element, electrochemical biosensor, electrochemistry

INTRODUCTION

Histamine (HIS), with its heterocyclic amine structure, belongs to a group of alkaloids that are responsible for various physiological effects in the human organisms. HIS is synthesized from L-histidine by L-histidine decarboxylase and then stored in the granules of mast cells and basophils, the main sources of HIS in the human body (Tanaka et al. 2004). Moreover, HIS plays key roles as a neurotransmitter, hormone mediator, and is involved in the inflammation process and immunity system (Nieto-Alamilla et al. 2016). HIS is essential in human metabolism, but on the other hand, it can be harmful to the organism if it occurs in food at higher levels (Rocha et al. 2016). The digestion of HIS in the human body is mainly secured by enzymes diamine oxidase (DAO). The activity of these enzymes greatly affects the toxic effect of HIS. However, in higher concentrations of HIS in food, the enzymatic system might not be able to eliminate all intake of HIS, and then the poisoning of the organism can occur. HIS is produced as a result of the metabolic activity of microorganisms in food and beverages (Taylor and Eitenmiller 1986). Therefore, HIS can be found mainly in foodstuffs that are rich in proteins, such as fish and meat, as well as in food produced by the fermentation processes such as wine and beer. If there is a higher level of HIS intake in the body, it can be toxic for the organism. Thus, the determination of HIS is an important indicator of freshness or spoilage of food as well as a quality indicator (Papageorgiou et al. 2018).

Comparing with the traditional approaches for HIS detection such as HPLC and ELISA (Önal 2007), several new alternative approaches are currently being investigated (Horemans et al. 2010, Jiang et al. 2015). One of such approaches uses electrochemical biosensors for direct HIS detection (Butwong et al. 2019) with the advantages of quicker, portable technology and high sensitivity benefit.

In this study, a novel electrochemical biosensor for HIS detection is described, which is using short synthetic peptides as biorecognition elements. The specific amino acid sequence, various binding groups, and flexible conformation structure create the unique abilities of peptides such as high specificity and selectivity to the target molecule. Furthermore, they are well known because of their high stability and good catalytic activity with multiple binding groups (Karimzadeh et al. 2018).

Thus, in this study, the peptide with sequence selective for HIS binding was used as a biorecognition layer. For peptide probe immobilization, electropolymerization of the ANSA layer was done. ANSA is characteristic of the possibility of binding with the –NH group via a sulphonamide coupling reaction (Hermanson 2013). HIS selectively binds to the HIS binding peptide (HBP) via hydrogen and ion-strength interaction which are strongly dependent on pH condition. Therefore, this work will mainly focus on the modification and optimization of the biosensor.

MATERIAL AND METHODS

Reagents

Electrodes polishing was provided by Water Based Diamond suspension (0.50 µm) and Alumina Slurries (0.05 µm; 0.30 µm; 1.00 µm) purchased from Electron Microscopy Science, Hatfield, United Kingdom. For electrodes washing ethanol absolute, acetone (≥99.5%) (VWR chemicals, Randor, Pennsylvania, USA) and MilliQ water, 18.20 MΩ/cm, were used.

The other chemicals used in this study were purchased from Sigma-Aldrich (St. Louis, MO, USA) if it is not stated otherwise. 10 mM 1-amino-2-naphthol-4-sulfonic acid (ANSA) was diluted in Phosphate buffered saline (PBS) (pH 7, 25 mM) (Table 1.). 40 mM phosphorus pentachloride (PCl_5) was dissolved in acetone.

HBP probe with sequence CSLESLESLESLE was synthetized by Fmoc solid phase synthesis, closely described at (Mazumdar et al. 2020), by using Liberty Blue peptide synthesizer (CEM, Matthews, NC, USA).

Table 1 Buffers composition

Buffer	Compounds
Phosphate buffered saline	20.00 g NaCl, 0.5 g KCl, 3.6 g Na_2HPO_4, 0.6 g KH_2PO_4 were diluted into 1000 ml of MilliQ water.
Britton-Robinson buffer (B-R)	For B-R at pH 1.81: 1.15 ml of acetic acid, 1.36 ml of H_3PO_4 and 1.24 g of boric acid was added into 500 ml of MilliQ water. For B-R at pH 4: 2.6 ml of 0.2 M NaOH was added into 10 ml of B-R pH 1.81 stock solution. For B-R at 6 pH 4.5 ml of NaOH was added into 10 ml of B-R pH 1.81 stock solution. For B-R at 7 pH 5.4 ml of NaOH was added into 10 ml of B-R pH 1.81 stock solution. For B-R at 8 pH 6.2 ml of NaOH was added into 10 ml of B-R pH 1.81 stock solution (Reynolds III et al. 2013).
Measuring electrolyte solution	5 mM Potassium hexacyanoferrate(II) trihydrate $K_4[Fe(CN)_6]$ and 5 mM Potassium hexacyanoferrate(III) $K_3[Fe(CN)_6]$ in 0.1 M KCl.

Biosensor preparation

The GCE was mechanically cleaned stepwise with 1.00 µm, 0.30 µm, 0.05 µm alumina slurry, and diamond suspension each for 90 s. Between each step, the residual powder was removed by electrodes sonication in acetone, ethanol, and MilliQ water for 3 min in each. Subsequently, the electrochemical cleaning was followed. The three electrodes (working, counter, and reference) were immersed in 0.5 M H_2SO_4 and the CV carrying out potential cycles between −1.2 and +1.2 V and a scan rate of 50 mV/s until the characteristic voltammogram of clean GCE was obtained. After that, working electrodes were washed with MilliQ and dried under argon gas.

The electrodeposition of ANSA was done by immersing electrodes in 4 ml of the solution of ANSA in PBS. The deposition was carried out by CV with a potential set up between +1.5 and −0.5 V and with scan rate 20 mV/s. The deposition was running eight cycles until the steady CV voltammogram was formed. In the following step, the exchange of the sulfonic group from ANSA into the sulfonyl group was done by incubation of 40 mM PCl_5 in acetone for 30 min (Wang et al. 2013). After obtaining the sulfonylated ANSA the peptide probe was applied on the electrode surface by dropping 10 µl of peptide probe (50 µM) diluted in MilliQ and then dried at 40 °C for 40 min. Before measuring the biosensor with peptide, the probe was washed with PBS and MilliQ water in each for 1 min.

HIS binding was carried out in B-R buffer in various pH ranges. HIS at exact concentration was diluted in B-R and subsequently incubated with peptide attached to the electrode for 1 hour. After that, the electrode was slightly washed and measured by Electrical impedance spectroscopy (EIS), Square wave voltammetry (SWV), and Cyclic voltammetry (CV).

Electrochemical measurement

All electrochemical measurements were performed by Autolab PGSTAT302N and processed with NOVA 2.1.4 software (Metrohm, Herisau, Switzerland). Three electrode connection was used for each electrochemical measurement, where GCE electrode act as working electrode (BASI, West Lafayette, USA), platinum wire as the counter electrode and 3 M Ag/AgCl as the reference electrode (Metrohm, Herisau, Switzerland). All electrochemical measurements were undertaken in measuring electrolyte solution (Table 1).

SWV experiments were performed at potential starting from −0.5 V and ending at +1.0 V, step potential was set up at 0.001 V, modulation amplitude at 0.02 V and Frequency 25 Hz. CV was running in the potential scan range +0.6 V and +0.2 V and scan rate 50 mV/s. EIS was conducted using open circuit potential, frequencies in range of 0.01 Hz to 10 kHz, DC potential was set at 0.23 V and amplitude of 5 mV.

RESULTS AND DISCUSSION

Modification of the electrode

The monitoring of step-by-step electrode modification was recorded by CV measurement. For each modification step, a characteristic voltammogram was obtained (Figure 1). The yellow curve corresponds to the bare electrode where a pair of typical redox peaks for GCE occurred. The peaks are corresponding to the electrochemical process of electron exchange of $[Fe(CN)_6]^{3-/4-}$ redox couple.

In the first step of electrode modification, the electropolymerization of ANSA was done by CV (Figure 1; red curve). It is clear that the redox peaks visibly decreased, with a layer of ANSA on the electrode surface, which can be explained by the fact, that electron transfer of $[Fe(CN)_6]^{3-/4-}$ was blocked by the ANSA. There are two possible reasons of why a blockage of electron transfer occurs. One is that ANSA is a physical barrier for electron transfer between electrode and electrolyte and the second can be due to electrostatic repulsion (Tabanlıgil Calam and Yılmaz 2020).

Figure 1 CV voltammograms of each step of the GCE modification

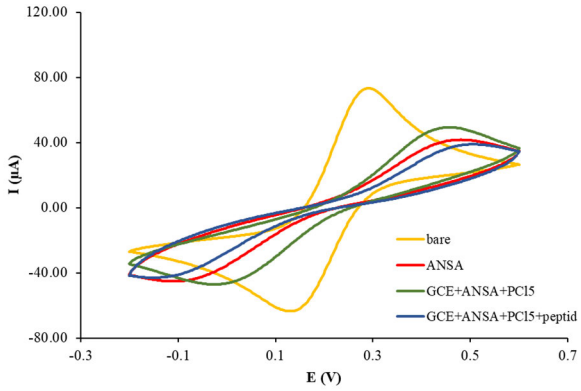

For conjugation of the peptide with sulfonic acid, the sulfonyl chloride derivate pre-step must be done. The derivate is prepared by reaction of the sulfonic acid with PCl_5 in acetone solution (Figure 2)

(Hermanson, 2013). In this step, transfer of sulfonic group from ANSA into the sulfonyl group reaction was done by the incubation of electrode with PCl_5, the redox peaks of CV appreciably increased (Figure 1; green curve). Explanation of this can be that sulphuric acid groups were negatively charged and after binding with Cl, it turns into a neutral sulfonyl group, which allows better diffusion of electrons to the electrode surface (Wang et al. 2013).

Therefore, a sulfonated electrode was coupled with a peptide probe by dropping 10 µl of peptide (50 µM) and dried in an oven at 40 °C for 40 min. In this modification step, the height of the redox peaks decreased dramatically because the peptide does not have a conductive character, thus it is blocking charge transfer between electrode and electrolyte.

Optimization of peptide probe coverage

For obtaining the best sensitivity of the biosensor, the electrode surface coverage with the peptide probe must be optimized. The higher surface loading density of a biorecognition element was desired to maximize the number of available analyte binding sites. For this reason, it is necessary to cover all binding sites of the ANSA with a peptide probe to achieve higher density surface coverage. However, steric hindrance must be taken under the account as well. In this study, different concentrations of the peptide probe were applied on the electrode surface to investigate how much peptide can be caught on the electrode surface. Various concentrations (10.0 µM, 25.0 µM, 50.0 µM, 100.0 µM; 500.0 µM) of the HBP were applied on the GCE modified with ANSA and PCl_5. The peptide probe was dropped on the modified electrode at exact concentration and subsequently dried in oven for 40 min at 40 °C. After the washing step the measurement by EIS was following (Figure 2).

The results show that the best electrode surface coverage was obtained at 50 µM concentration of the HBP, which was assumed according the largest Nyquist semicircle, which indicate the lowest charge transfer resistance. Peptides are usually not electrochemically active, thus they act more as an isolator, which means the more peptide is on the electrode the larger diameter of Nyquist semicircle will occur. The lowest concentrations of the peptide (10 µM and 25 µM) had clearly smaller diameter of semicircle, which indicate the not fully covered electrode surface. On the other hand, in the higher concentrations of peptide, decreasing of semicircle diameter was occurred as well. It happened possibly because of saturated electrode surface.

Figure 2 Influence of the various peptide concentrations on EIS records. A – Nyquist plots from measurement of various peptide concentrations. B – dependence of peptide probe concentrations on the diameter of the semicircle. The error bars are represented by standard 5% error of measurements (n=3).

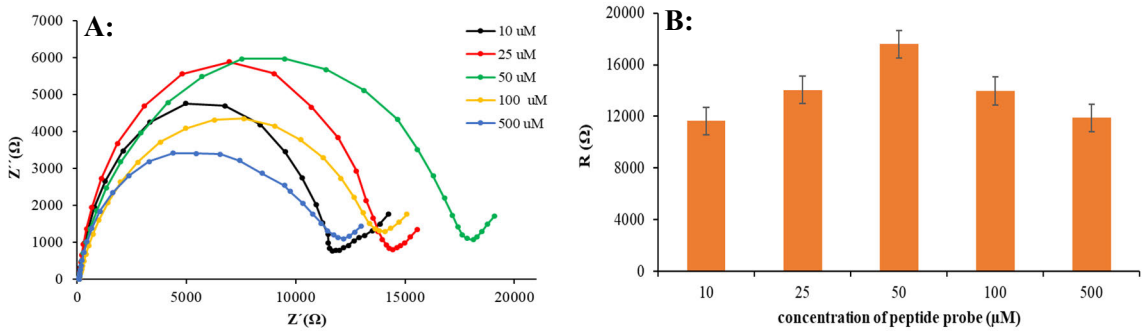

Histamine binding buffer optimization

In this section, the optimization of different binding buffers for HIS is discussed. Because different pH values of peptide and HIS indicate the protonated and deprotonated state of these molecules, various pH conditions were tested. HIS is mainly presented in the single protonated state which corresponds to 6.9 to 10.4 pH range (Jiang et al. 2015). Moreover, HBP is also affected by different pH conditions where its protonated state is ranging at pH 6.0 to 7.0. Peptide-HIS binding is presented based on specific hydrogen and ion-dipole interaction. Therefore, this formation is strongly dependent on the optimal pH condition.

Here we report the measurement focusing on optimization of the right condition for peptide-HIS binding in different buffers. The peptide-modified electrode was incubated in 1 mM solution of HIS in B-R buffer at pH 4; 6; 7; 8 and MilliQ water. The results show the best binding efficiency by using

B-R pH 7, which was observed by EIS measurement (Figure 3). At pH 6–7, the Nyquist semicircle is the smallest, which indicates the higher charge transfer resistance. The more HIS is caught on the electrode surface the higher charge transfer will occur. At this condition, HIS is in the single protonated state and shows the best binding response with HBP, which is also in a protonated state. The good results were also presented in MilliQ water, which represents conditions between pH 6–7. However, the stability of the peptide-HIS linkage was unstable.

In acidic conditions, HIS is almost fully protonated, while peptide is deprotonated in acidic pH. For this reason, only a weak hydrogen bond can occur between peptide and HIS. This statement was verified by EIS measurement at B-R pH 4 (Figure 3), where the charge transfer resistance is the lowest, thus the diameter of the Nyquist semicircle is the highest, which is caused by only a small amount of HIS bonded to the peptide.

At alkaline pH, HIS starts to a deprotonated, and only a small amount of hydrogen bonding can be originated, which is visible on the increasing diameter of the Nyquist plot in Figure 3A.

Figure 3 Optimization of pH conditions for HIS binding. A – EIS records of 1 mM HIS in different pH buffers. B – dependence of pH conditions on the diameter of the semicircle. The error bars are represented by standard 5% error of measurements (n=6).

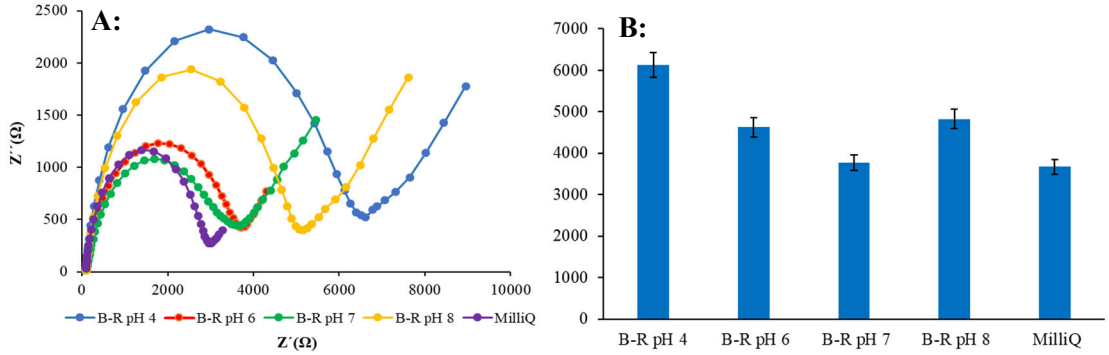

Calibration curve

Biosensor ability for HIS detection was measured in different concentrations by SWV (Figure 4). This study was aimed to investigate if the charge transfer is increasing with an increasing amount of the HIS. Concentrations of HIS are reported as log *c* (M) for displaying their linear dependence. Calibration curve (Figure 4) presents the concentration from 10 nM (10^{-8} M) to 1 mM (10^{-3} M). LOD and LOQ values were counting true the regression equation. The LOD was calculated as 6.53 nM and the LOQ as 21.75 nM (Table 2). The results show that the biosensor is sensitive enough for HIS values, which are ranging in food from µM to mM concentrations. (Wang at al. 2013).

Figure 4 Calibration curve for HIS detection.

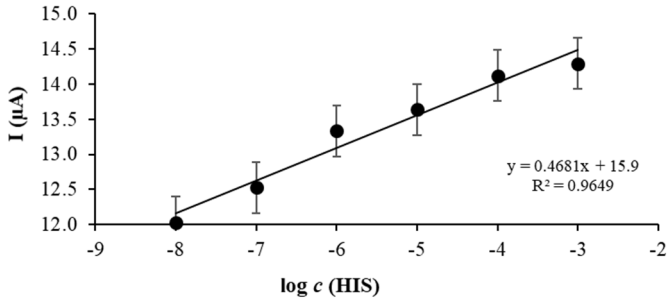

Table 2 Analytical table

Sample	Regression Equation	Linear dynamic range log *c* (M)	R^2	LOD (nM)	LOQ (nM)	RSD (%)
histamine	y = 0.4681x + 15.9	–8 to – 3	0.9649	6.53	21.75	10.80

CONCLUSION

To summarize the issue up, the electrochemical biosensor with HBP as a recognition element for direct HIS detection was designed. In this study, the step-by-step modification and optimization of the biosensor are presented. Moreover, it was demonstrated that a wide range of HIS concentrations is possible to detect with the suggested biosensor. Thus, the biosensor is prepared for the next experiments and testing with real samples, such as wine or other fermented beverages.

ACKNOWLEDGEMENTS

The research was financially supported by the IGA MENDELU AF-IGA2020- IP009.

REFERENCES

Butwong, N. et al. 2019. Electrochemical sensing of histamine using a glassy carbon electrode modified with multiwalled carbon nanotubes decorated with Ag-Ag_2O nanoparticles. Microchimica Acta, 186(11): 714.

Hermanson, G.T. 2013. The reactions of bioconjugation. In Bioconjugate techniques. Elsevier, pp. 229–258.

Horemans, F. et al. 2010. MIP-based sensor platforms for the detection of histamine in the nano- and micromolar range in aqueous media. Sensors and Actuators B: Chemical, 148(2): 392–398.

Jiang, S. et al. 2015. Surface plasmon resonance sensor based on molecularly imprinted polymer film for detection of histamine. Sensors and Actuators B: Chemical, 221(1): 15–21.

Karimzadeh, A. et al 2018. Peptide based biosensors. TrAC Trends in Analytical Chemistry, 107(1): 1–20.

Mazumdar, A. et al. 2020. Peptide-Carbon Quantum Dots conjugate, Derived from Human Retinoic Acid Receptor Responder Protein 2, against Antibiotic-Resistant Gram Positive and Gram Negative Pathogenic Bacteria. Nanomaterials, 10(2): 325.

Nieto-Alamilla, G. et al. 2016. The histamine H3 receptor: structure, pharmacology, and function. Molecular Pharmacology, 90(5): 649–673.

Önal, A. 2007. A review: Current analytical methods for the determination of biogenic amines in foods. Food Chemistry, 103(4): 1475–1486.

Papageorgiou, M. et al. 2018. Literature update of analytical methods for biogenic amines determination in food and beverages. TrAC Trends in Analytical Chemistry, 98: 128–142.

Reynolds III, J.E. et al. 2013. Spectral and redox properties of the GFP synthetic chromophores as a function of pH in buffered media. Chemical Communications, 49(71): 7788–7790.

Rocha, S.M. et al. 2016. Histamine induces microglia activation and dopaminergic neuronal toxicity via H1 receptor activation. Journal of Neuroinflammation, 13(1): 1–16.

Tabanlıgil Calam, T., Yılmaz, E.B. 2020. Electrochemical determination of 8-hydroxyquinoline in a cosmetic product on a glassy carbon electrode modified with 1-amino-2-naphthol-4-sulphonic acid. Instrumentation Science & Technology, 1–20.

Tanaka, S. et al. 2004. Expression of L-histidine decarboxylase in granules of elicited mouse polymorphonuclear leukocytes. European Journal of Immunology, 34(5): 1472–1482.

Taylor, S. L., Eitenmiller, R. R. 1986. Histamine food poisoning: toxicology and clinical aspects. CRC Critical Reviews in Toxicology, 17(2): 91–128.

Wang, Q., et al. 2013. A sensitive DNA biosensor based on a facile sulfamide coupling reaction for capture probe immobilization. Analytica Chimica Acta, 788(1): 158–164.

Molecularly imprinted polymers as a recognition element for pesticide detection

Milada Vodova, Lukas Nejdl, Jaroslava Bezdekova, Kristyna Pavelicova, Kristyna Zemankova, Navid Assi, Eliska Sedlackova, Marketa Luklova, Marketa Vaculovicova
Department of Chemistry and Biochemistry
Mendel University in Brno
Zemedelska 1, 613 00 Brno
CZECH REPUBLIC

xcvodova@vutbr.cz

Abstract: The molecular imprinting technique is very popular due to the high selectivity, chemical stability, mechanical strength, and the formation of specific binding sites. In this work, we focus on the detection of cypermethrin using an innovative fluorescence method (UV-fingerprinting) after analyte elution from molecularly imprinted polymers (MIPs) in real pesticide sample with the trade name Bandit 40 WP. MIPs were prepared from dopamine. All steps (washing, binding kinetics, analyte elution, and fluorescence detection) necessary for isolation and quantification of cypermethrin were optimized. The results clearly showed that MIPs and UV-fingerprinting are a promising method for pesticides monitoring in real sample of Bandit 40 WP. The detection limit (LOD) of 780 ng/ml was calculated with the coefficient of determination $R^2 = 0.99$.

Key Words: pesticides, fluorescence spectroscopy, fingerprinting, molecularly imprinting polymer, UV irradiation

INTRODUCTION

In the first half of the 20th century, public interest in environmental protection increased, including concerns about the use of chemicals (pesticides) on agricultural land in intensive agriculture. Chemicals have an adverse effect on individual components of the environment (disruption of the natural nutrient cycle), ecosystems and ecosystem services. There are also some risks associated with contamination of drinking water sources that have a proved effect on human health (Li et al. 2014). As the population continues to grow, the food consumption increases which leads to intensive use of agricultural soil and utilization of chemicals. Conventional agriculture is currently dependent on the use of pesticides to ensure a sufficient yield of crops (Abu-Qare and Duncan 2002). In last few years, an increase in amount of pesticides used is estimated to be even more than 10% each year (Aktar et al. 2009) in some developing countries.

There is a growing number of registered active substances (pesticides) in the world used for killing weeds; animal pests; for control of plant diseases; for plant protection or for protection of stockpile stocks, technical products, houses, animals and humans. Most countries have a legal limitations for concentrations of the active ingredient (Temminghoff et al. 2004). Improper handling of commercial pesticides can lead to chronic diseases and even to death (Aktar et al. 2009). For example, Grandjean and Landrigan have shown that pesticides are found in the environment and they also affect children's development (Grandjean and Landrigan 2006, Grandjean and Landrigan 2014). Some pathological manifestations are associated with impaired memory and attention, learning disabilities, autism, decreased IQ, hyperactivity, or attention deficit united hyperactivity disorder (ADHD) (Rauh and Margolis 2016).

The current analysis of pesticides is mainly performed using instrumental methods that are time consuming and expensive, most often liquid chromatography with mass spectrometric (MS) detection or gas chromatography with MS detection is used (Khan and Rahman 2017). In many cases, the sample must be treated before analysis (e.g. extraction, isolation and/or separation). For these reasons, it is necessary to look for new alternatives that could speed up the analysis of commercial pesticides.

Therefore, a new spectroscopic method (so-called UV-fingerprint) was tested for the analysis of pesticides in combination with MIPs, which guarantee the required specificity (Vodova et al. 2019).

The UV-fingerprint method is based on the natural spectral properties of the sample in the ultraviolet and in the visible region (230–600 nm) before irradiation and after irradiation with an external UV source (λ_{em} = 254 nm). UV radiation causes spectral changes of the sample based on photooxidation of molecules, photodissociation or photofragmentation. The changes caused by UV irradiation are unique to the sample and create a so-called UV-fingerprint, thanks to which the sample can be identified (Vodova et al. 2019). The MIPs improve quantification of the pesticide active ingredient in complex mixtures.

In this work, the preparation of MIP for specific binding of cypermethrin from a real pesticide sample with the trade name Bandit 40 WP was optimized. After elution of cypermethrin from MIPs, quantitative analysis was performed using the UV-fingerprint spectral method.

MATERIAL AND METHODS

Chemicals

Dimethyl sulfoxide, cypermethrin, dopamine hydrochloride, TRIZMA base were purchased from Sigma-Aldrich (St. Louis, MO, USA) in ACS purity, Bandit 40 WP was purchased from Transchem s.r.o. (Amstelveen, Holland) with the active ingredient cypermethrin 400 g/kg.

Fluorimetric analysis

Fluorescence was measured on a Tecan Infinite 200 M PRO (TECAN, Switzerland). 50 µl of the sample was analyzed in a 96 well CoStar flat bottom microtiter plate (Corning, USA). Excitation scanning at a fixed λ_{em} = 400, 450 and 500 nm was recorded on the instrument. The microtiter plate was then placed in a UV transilluminator (Vilber Lourmat, Marne-la-Vallee Cedex, France) with λ_{em} = 254 nm and with area 20 x 20 cm, illuminated by six emitting tubes with a power of 15 W (each). The samples were irradiated for 10 minutes. All measurements were performed at a standard laboratory temperature of 25 °C.

Analysis procedure

The preparation of MIPs selective for the active substance cypermethrin consists of several steps, which are shown in Figure 1. In the first step, the template (cypermethrin) is mixed with functional monomer (dopamine) and specific binding interactions are formed between both components. In the second step, the functional monomer is polymerized with the imprinted molecule to form molecularly imprinted layers. In the next step, the template is removed from the polymer matrix. Next, the MIPs are ready to be used for interaction with the sample containing the analyte. The analyte is selectively extracted from the sample by MIP surface and after elution analyzed by spectrometer. Finally, the extracted analyte is irradiated in a UV transilluminator for 10 minutes UV and analyzed again on a spectrometer.

Figure 1 Schematic representation of the experiment

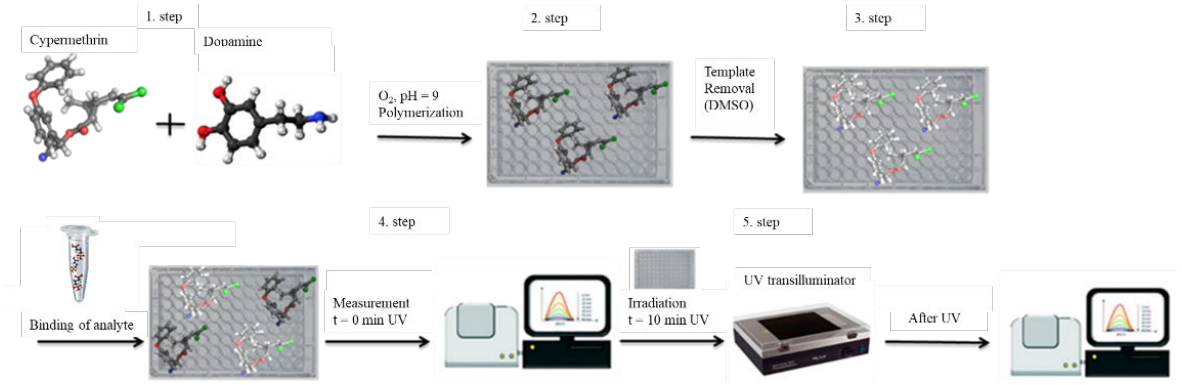

RESULTS AND DISCUSSION

Selected pesticides

But the problem arose in the quantification of the active substance in complex mixture, when the resulting excitation spectrum is affected by other ingredients, such as formulation components (solvents, carriers, surfactants, stabilizers, colorants, additives improving the applicability, safety and pesticides effects of the whole mixture), safeners (increasing product safety), synergents (to support the activity of the active substance) and adjuvants (improving the physicochemical and biological properties of the product). A scheme of the basic ingredients contained in a commercially available pesticide solution is shown in Figure 2. For these reasons, MIPs were used to provide the required selectivity prior to UV-fingerprint quantification.

Figure 2 Scheme of basic components contained in a commercially available pesticide (Unfortunately, in this case, the manufacturer only states the active substance, not other components)

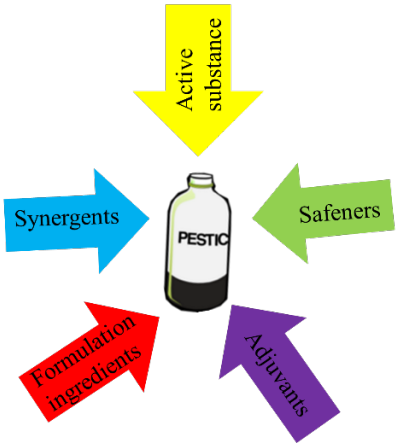

Optimization of UV-fingerprint method

In this part of the work, we dealt with the fluorescent properties of cypermethrin after exposure to UV radiation. The time required for irradiation of the sample was studied and sensitively of the method this active substance can be quantified from the sample. Figure 3A shows a typical spectrum of cypermethrin before and after UV exposure. Next, the sample was irradiated with a UV source in 2minute intervals. Figure 3B shows that the maximum fluorescence intensity was recorded after 10 min of UV exposure. Finally, the effect of concentration on fluorescence intensity was studied, as seen in Figure 3C. From this dependence (calibration curve) the detection limit (LOD) of 780 ng/ml was calculated with the coefficient of determination R^2 = 0.99. The LOD indicates that it is sufficient to detect cypermethrin in a real sample.

Figure 3 Optimization steps for quantitative analysis of cypermethrin, when, is A) the typical spectrum of cypermethrin before irradiation at 0 min UV and after 10 min UV irradiation, for a concentration of 0.125 mg/ml, B) best time to irradiate cypermethrin at a concentration of 0.125 mg/ml and C) calibration series of cypermethrin for concentrations from 1.95 µg/ml to 0.125 mg/ml

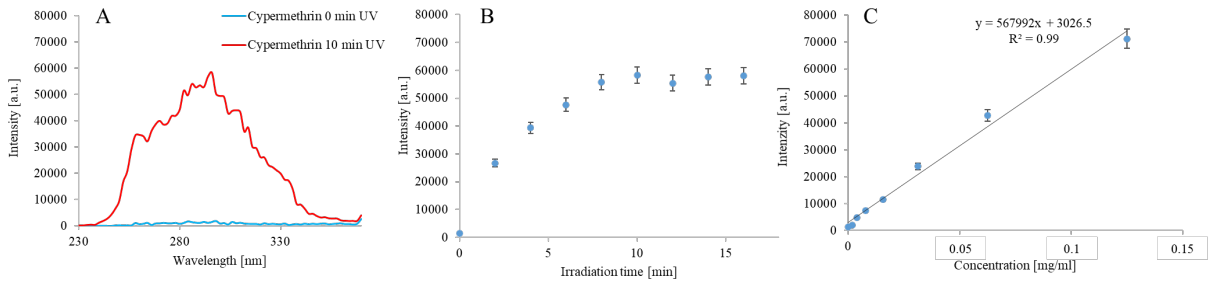

Optimization of MIPs and NIPs for a specific binding of cypermethrin

Optimization of washing is one of the most important steps for template removal, where the template is washed out of the polymer layer to form cavities, typical molecular-selective recognition sites (Batlokwa et al. 2011). Three different washing solutions were used to remove the template:

99.8% DMSO, DMSO: distilled water (1:1 v:v) and distilled water. The data obtained are shown in Figure 4A. The most suitable washing solution was 99.8% DMSO, which allowed for washing of 88.7% of the template from the polymer layer. Other solutions showed lower washing efficiency, which could be caused by different solubility of cypermethrin in these solvents.

To verify the binding properties, an experiment was performed at different initial concentrations of cypermethrin in the range 0.125–1 mg/ml. The binding capacity of MIPs to NIPs was then compared. Figure 4B shows data a calibration series before and after UV irradiation. As shown, the intensity of MIPs – 0 min UV and MIPs – 10 min UV for a concentration of 1 mg/ml. The intensity of MIPs-10 min UV was 9-fold higher than for MIPs 0 min UV. It is also apparent that the fluorescence response of cypermethrin increases with increasing concentration after irradiation in a UV transilluminator. With increasing cypermethrin concentrations, there is an undesirable increase in non-selective interactions in NIPs.

Isolation of cypermethrin from a commercially available pesticide (Bandit 40 WP) was performed using optimized MIP and the active substance was detected by UV-fingerprint. Figure 4C shows the signal obtained for the specific isolation of cypermethrin from a sample, the shape of which corresponds to a standard substance. Using the calibration curve equation, the concentration was found to be 0.074 mg/ml. After conversion to sample weight, it was ascertained that the measured concentration of cypermethrin (0.074 mg/ml) agrees with the declared concentration on the package within a 6% measurement error.

Figure 4 Optimization steps for MIPs analysis A) Optimization of the selection of a suitable washing solvent compared to the concentration of the imprinted molecule (cypermethrin), B) Calibration series of cypermethrin bound to MIPs and NIPs at 0 min UV and 10 min UV, C) Isolated cypermethrin from an commercially available pesticide compared to a cypermethrin standard at a concentration of 0.074 mg/ml

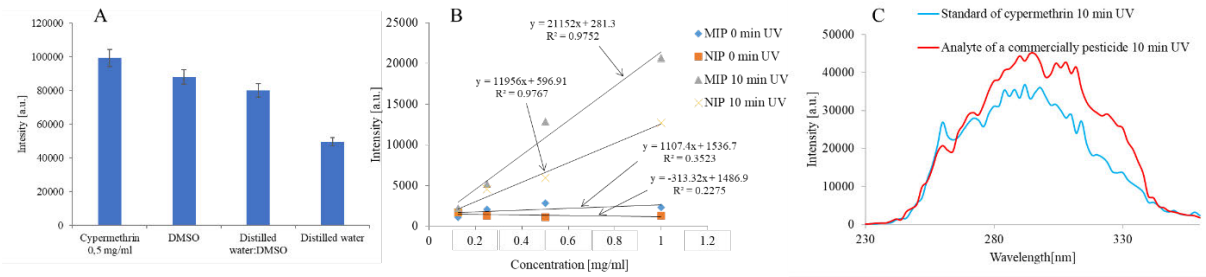

CONCLUSION

In this work, the suitability of combining the UV-fingerprint method with MIPs for qualitative and quantitative analysis was demonstrated. In the first part it was necessary to optimize the method of UV-fingerprints. When the best time for irradiation of the sample in the UV transilluminator was found (10 minutes) the calibration dependence with the coefficient of determination $R^2 = 0.99$ was prepared. These optimizations were then used for MIPs separation. MIPs were first prepared from cypermethrin and dopamine and allowed to polymerize in a microtiter plate. The MIPs thus prepared were subsequently optimized. The first optimization was to evaluate the best washing solution to remove the template, which was DMSO removing 99.8% of the template.

Isolation of the active substance from a commercially available pesticide under the trade name Bandit 40 WP was successfully performed. Cypermethrin was successfully isolated by MIPs and subsequently quantified by the UV-fingerprint method at a concentration of 0.074 mg/ml. The main benefits these methods are mainly instrumental simplicity, short analysis time.

ACKNOWLEDGEMENTS

The research was founded by Internal Grant Agency of Mendel University in Brno IGA MENDELU 2019_TP_009.

REFERENCES

Abu-Qare, A.W., Duncan, H.J. 2002. Herbicide safeners: uses, limitations, metabolism, and mechanisms of action. Chemosphere, 48(9): 965–974.

Aktar, M.W. et al. 2009. Impact of pesticides use in agriculture: their benefits and hazards. Interdisciplinary Toxicology, 2(1): 1–12.

Batlokwa, B.S. et al. 2011. Optimal Template Removal from Molecularly Imprinted Polymers by Pressurized Hot Water Extraction. Chromatographia, 73(5): 589–593.

Grandjean, P., Landrigan, P.J. 2006. Developmental neurotoxicity of industrial chemicals. Lancet, 368(9553): 2167–2178.

Grandjean, P., Landrigan, P.J. 2014. Neurobehavioural effects of developmental toxicity. Lancet Neurology, 13(3): 330–338.

Khan, M. S., Rahman, M.S. 2017. Pesticide Residue in Foods. 1st ed., Cham, Germany: Springer.

Li, Y.B. et al. 2014. Chiral fungicide triadimefon and triadimenol: Stereoselective transformation in greenhouse crops and soil, and toxicity to Daphnia magna. Journal of Hazardous Materials, 265(30): 115–123.

Rauh, V.A., Margolis, A.E. 2016. Research Review: Environmental exposures, neurodevelopment, and child mental health - new paradigms for the study of brain and behavioral effects. Journal of Child Psychology and Psychiatry, 57(7): 775–793.

Temminghoff, E.J.M. et al. 2004. Plant Analysis Procedures. 2nd ed., Dordrecht, Netherlands: Springer.

Vodova, M. et al. 2019. UV-Fingerprinting as a tool for monitoring of pesticides. In Proceedings of International PhD Students Conference MendelNet 2019 [Online]. Brno, Czech Republic, 6 November, Brno: Mendel University in Brno, Faculty of AgriSciences, pp. 687–689. Available at: https://mendelnet.cz/pdfs/mnt/2019/01/132.pdf.

Synthesis of PLGA nanoparticles with entrapped antibiotic mupirocin

Pavla Vymazalova[1], Vendula Popelkova[1], Tomas Komprda[1], Cristina Sabliov[2], Carlos E. Astete[2]
[1]Department of Food Technology
Mendel University in Brno
Zemedelska 1, 613 00 Brno
CZECH REPUBLIC
[2]Department of Biological and Agricultural Engineering
Louisiana State University
141 E.B.Doran Building, LSU Baton Rouge, LA 70803
USA

pavla.vymazalova@mendelu.cz

Abstract: Infections caused by resistant strains of bacteria have reached a critical level calling for increasingly effective delivery system of drugs to prevent and treat these infections. PLGA nanoparticles (NP) with mupirocin encapsulated could be good for better and quicker wound healing process. The aim of the experiment is to develop PLGA NPs with entrapped mupirocin and determine basic characteristic of it. Mupirocin is effective antibiotic in the fight against mentioned infection. For synthesis of these NPs was used emulsion evaporation method. Characterization of prepared NPs consisted of measuring size (141.1 ± 9.3 nm), zeta potential (-21.9 ± 4.6 mV) and morphology by method TEM. Also, we did a release profile of mupirocin from NPs. Loading capacity was calculated as 2.34 µg and entrapped efficiency as 22.4%.

Key Words: PLGA, nanoparticles, synthesis, mupirocin, healing process

INTRODUCTION

Recent studies on improving the healing process of acute and chronic wounds have sought to develop innovative and effective wound dressing materials that could accelerate healing or prevent frequent complications (Rajendran et al. 2018). One such complication is infection with resistant strains of bacteria or sepsis, which could slow or worsen the healing process. The aim of many studies is to deliver the highest concentration of antibiotic directly to the site of action, thereby increasing its efficacy (Vashishth and Kaushik 2017). This can be achieved by nanodelivery systems such as PLGA NPs. The advantages of nanodelivery systems include protection of the drug from degradation and targeted controlled drug release (Shah et al. 2015, Pavitra et al. 2019, Ma and Mumper 2013).

Several types of nanodelivery systems were developed. One of these systems is liposome. Liposomes are frequently used to entrap hydrophilic or hydrophobic antibiotics, have good permeability through cell membranes, low toxicity, and are shown to enhance antimicrobial activity of antibiotic (Schiffelers et al. 2001, Yang et al. 2009). Other nanodelivery system is nanoemulsion. Advantages of this system are biodegradability, biocompatibility, ease of preparation and physical stability can be very useful for delivery of antibiotics (Santos-Magalhaes et al. 2000). Alternatively, polymeric NPs with entrapped or covalently attached drug have been developed to improve stability of the delivery system during storage relative to the other delivery systems (Lockman et al. 2002, Misra and Sahoo 2012). Polymeric NPs can protect the drug against degradation in the body and they have improved body or tissue tolerance (Müller et al. 2000, Kalhapure et al. 2015).

Mupirocin (MUP) was isolated in 1971 from *Pseudomonas fluorescens* (Fuller et al., 1971) and was proven to be effective in treating skin infections, especially impetigo, burns, folliculitis and foot ulcers (Perumal et al. 2014). MUP is a hydrophobic topical antibiotic used in the form of topical ointments to treat these conditions. This antibiotic has documented antimicrobial activity against

resistant strain bacteria *Staphyloccocus aureus* (Mahalakshmi and Sankar, 2020). MUP inhibits bacterial protein synthesis by specific and reverse binding to isoleucine tRNA synthetase. This causes isoleucine not to be incorporated into the emerging proteins (Okur et al. 2019, Rode et al. 1989). After intravenous or oral administration, mupirocin is metabolized to an inactive form (monic acid) and excreted into the kidneys (Alcantara et al. 2019).

The goal of the study was to synthesis PLGA NPs with entrapped mupirocin. PLGA polymer was chosen because it is good polymer for encapsulating hydrophobic drugs and is widely used in the pharmaceutical industry. Basic characteristics such as morphology, size, size distribution, surface charge, and release kinetics were determined. Ultimately, these NPs will be incorporated in dressings and their efficacy in wound healing will be assessed *in vivo*.

MATERIAL AND METHODS

Chemicals and materials

Poly(lactic-co-glycolic acid), mupirocin (MUP), polyvinyl alcohol (PVA), trehalose dihydrate obtained from Sigma-Aldrich (St. Louis, MO, USA). Ethyl acetate and acetonitrile were obtained from EMD Chemicals Inc. (Gibbstown, NJ, USA). Nanopure water obtained using Nanopure Diamond and 0.2 µm Barnsted D3750 Hollow Fiber Filter (Barnsted International, Dubuque, IA, USA).

Synthesis of PLGA NPs with entrapped mupirocin

Synthesis of NPs was achieved by emulsion evaporation method. Aqueous solution of 2% PVA was prepared while stirring (400 RPM) at 60 °C. Then 7 ml ethyl acetate was added to the aqueous phase. An organic phase was formed by dissolving 220 mg of PLGA and 11 mg MUP in 5 ml of ethyl acetate under stirring (220 RPM). The organic phase was added to the aqueous phase drop wise and the formed emulsion was microfluidized (Microfluidizer M110P, Microfluidics, MA) 4 times at 30,000 psi in an ice bath. Next, ethyl acetate was evaporated on Rotovap (R-124 rotary evaporator Buchi Inc., New Castle, DE) for 60 min under vacuum (40 mmHg) and stirring at 60 RPM. NPs were purified by dialysis with a 300 kDa Spectra/ POR CE membrane (Spectrum Rancho, CA, USA) in water to remove free PVA. After two days of dialysis, 650 mg trechalose (1:1 w/w) was added to the NPs suspension prior to freeze-drying. The sample was freeze-dryed with Labconco (2.5 plus freezone, Labconco Corporation, MO, USA) for two days. Finally, the sample was stored at -20 °C for further analysis. Empty NPs were prepared by the same protocol without added mupirocin in the organic phase.

Characterization of PLGA-MUP NPs

Morphology

Morphology of loaded and empty NPs was determined by Transmission Electron Microscopy (TEM) assessed using a JEOL JEM-1400 transmission electron microscope (JEOL USA Inc., Peabody, MA, USA). The lyophilized sample was re-suspended in water at a concentration of 5 mg/ml and sonicated in a water bath for 5 minutes. One droplet (3 µl) of sample was placed on the glow discharged 300 mesh carbon film grid (TEM-CF300-cu) obtained from Sigma-Aldrich (St. Louis, MO, USA). After 2 minutes, a filter paper was used to remove excess liquid and 2% UA (uranyl acetate) was added as a contrast agent.

Size and zeta potential

Lyophilized samples were dissolved in water at a concentration of 0.25 mg/ml, placed into disposable capillary cell (Malvern Panalytical Inc., Westborough, MA, USA) and the size and zeta potential was measured by DLS using the Malvern Zetasizer Nano ZS (Malvern Instruments Inc., Southborough, MA, USA).

Release of mupirocin from NPs

Lyophilized NPs were dissolved in water at a concentration of 5 mg/ml. Then, 15 ml of the suspension was placed into a dialysis tube (Spectra/por Dialysis membrane, Mw 300 kD) and suspended in water. The sample was stored at 37 °C and at 95 rpm in an incubator shaker C25 KC (New Brunswick Scientific Inc., Edison, NJ, USA). At each time interval (0, 2, 4, 6, 24, 48, 72 hours) 0.2 ml sample was taken out of the dialysis tube, mixed with acetonitrile (ACN) at 8:2 ACN: water v/v

and was placed in vortex for 30 minutes shaking. After that, the sample was centrifuged with Allegra 64R centrifuge (Beckman Coulter) at 20 000 rpm for 20 min at 10 °C. Supernatant was removed and the MUP measured by UV spectrometry at 210 nm by UV-Vis spectrophotometer (Genesys 6, ThermoFisher Scientific, Waltham, MA). The MUP concentration was determined based on a standard curve made under the same conditions.

RESULTS AND DISCUSSION

The empty and loaded NPs were smaller than 200 nm and were negatively charged, with loaded NPs more negatively charged (-21.9 ± 4.6 mV) than empty NPs (-4.95 ± 13.5 mV). Both types of particles were polydispersed as indicated by the high PDI (Table 1) and the TEM images (Figure 1).

Table 1 Size and zeta potential

Sample	Size (nm)	Zeta potential (mV)	PDI
Control (empty NPs)	190.7 ± 19	-4.95 ± 3.5	0.218 ± 0.018
Loaded NPs	141.1 ± 9.3	-21.9 ± 4.6	0.336 ± 0.013

Morphology

Entrapped NPs had a spherical shape. There are no differences between the morphology of entrapped NPs (B) and control (empty) NPs (A) and both types of particles were polydisperse.

Figure 1 TEM pictures of PLGA NP*s with PVA (A) empty NPs, (B) with entrapped Mupirocin*

A) B)

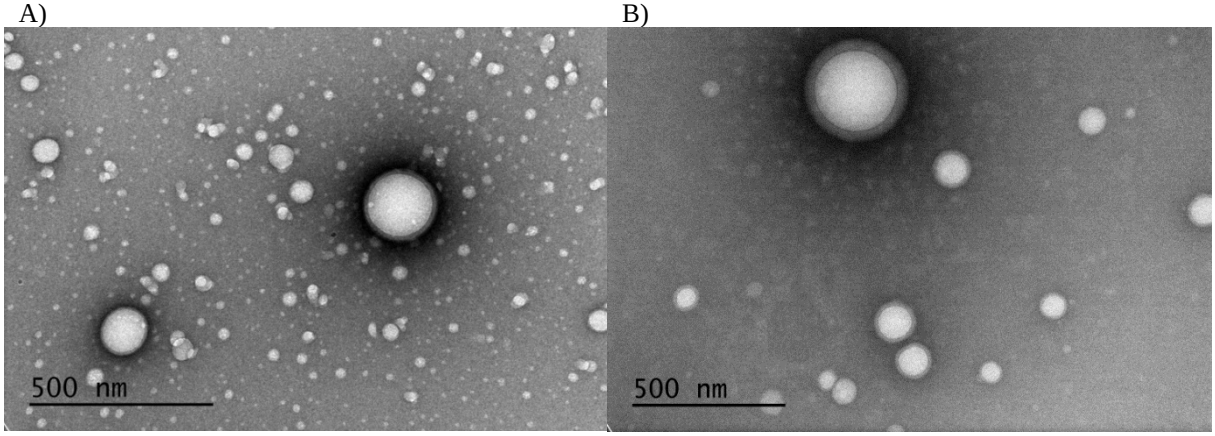

Loading capacity (LC)

The loading capacity was calculated using the equation:

$$LC = \frac{\text{amount of MUP in NPs (µg)}}{\text{amount of powder NPs (mg)}}$$

Loading of NPs with entrapped mupirocin purified by dialysis was 2.34 µg MUP/mg powder.

Entrapped efficiency (EE)

Entrapped efficiency was calculated using the equation:

$$EE(\%) = \frac{\text{amount of MUP in the system on start (µg)} - \text{free MUP}}{\text{amount of MUP in the system on start (µg)}} \times 100$$

Entrapment efficiency was found to be 22.4% for entrapped NPs purified by dialysis.

Release study

Release profile was measured over a period of 72 hours by UV spectrometry. Most of MUP (x%) was released in 24 hours and 100% was released in 48 hours (Figure 2).

Figure 2 Release study of mupirocin over time

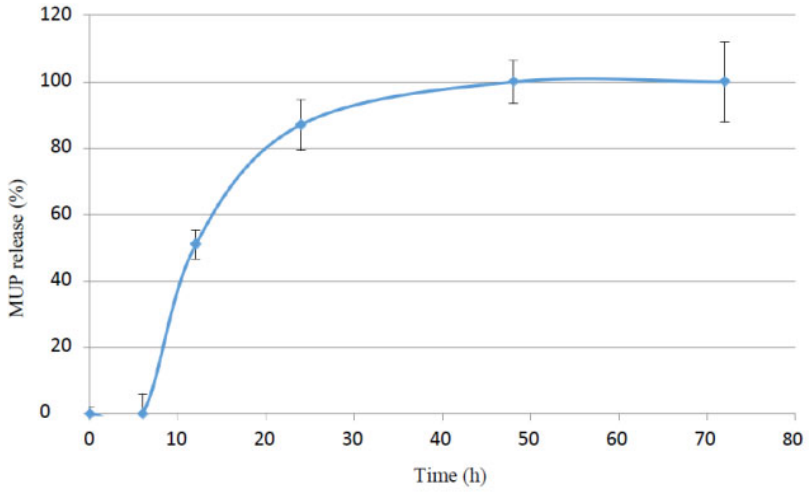

CONCLUSION

PLGA NPs with entrapped MUP were synthesized by emulsion evaporation method in the presence of PVA as a surfactant. According to the results of the study, these NPs are small, negatively charged and can be efficiently loaded with MUP. The controlled release of this antibiotic over two days could prove beneficial in wound healing. Next step of this research consists of testing the NP cytotoxicity *in-vitro* and their antibiotic efficacy *in vivo* as measured by wound healing in postoperative conditions.

ACKNOWLEDGEMENTS

The research was financially supported by the internal grant agency of the Mendel University in Brno. Number of project is AF-IGA2019-TP006.

REFERENCES

Alcantara, K.P. et al. 2019. Development, characterization and pharmacokinetics of mupirocin-loaded nanostructured lipid carriers (NLCs) for intravascular administration. International Journal of Pharmaceutics, 118–705.

Fuller, A.T. et al. 1971. Pseudomonic acid: an antibiotic produced by Pseudomonas fluorescens. Nature, 234: 416–417.

Kalhapure, R.S. et al. 2015. Nanoengineered drug delivery systems for enhancing antibiotic therapy. Journal of Pharmaceutical Sciences, 104(3): 872–905.

Lockman, P.R. at al. 2002. Nanoparticle technology for drug delivery across the blood-brain barrier. Drug Development and Industrial Pharmacy, 28(1): 1–13.

Ma, P., Mumper, R.J. 2013. Paclitaxel nano-delivery systems: a comprehensive review. Journal of Nanomedicine & Nanotechnology, 4(2): 100–164.

Mahalakshmi, S., Sankar, V. 2020. *In-vitro* antibacterial effect of mupirocin in combination with three essential oils against *Staphylococcus aureus*. International Journal of Pharmaceutical Sciences and Research, 11(2): 705–709.

Misra, R., Sahoo, S.K. 2012. Antibacterial activity of doxycycline-loaded nanoparticles. Methods in Enzymology, 509: 61–85.

Müller, R.H. at al. 2000. Solid lipid nanoparticles (SLN) for controlled drug delivery–a review of the state of the art. European Journal of Pharmaceutics and Biopharmaceutics, 50(1): 161–177.

Okur, N.Ü. et al. 2019. An alternative approach to wound healing field; new composite films from natural polymers for mupirocin dermal delivery. Saudi Pharmaceutical Journal, 27(5): 738–752.

Pavitra, E. et al. 2019. Engineered nanoparticles for imaging and drug delivery in colorectal cancer. Seminars in Cancer Biology. (In press)

Perumal, S. et al. 2014. Sol-gel processed mupirocin silica microspheres loaded collagen scaffold: A synergistic bio-composite for wound healing. European Journal of Pharmaceutical Sciences, 52: 26–33.

Rajendran, N.K. et al. 2018. A review on nanoparticle based treatment for wound healing. Journal of Drug Delivery Science and Technology, 44: 421–430.

Rode, H. et al. 1989. Efficacy of mupirocin in methicillin-resistant Staphylococcus aureus burn wound infection. Antimicrobial Agents and Chemotherapy, 33(8): 1358–1361.

Santos-Magalhaes, N.S. et al. 2000. Colloidal carriers for benzathine penicillin G: nanoemulsions and nanocapsules. International Journal of Pharmaceutics, 208(1): 71–80.

Schiffelers, R. et al. 2001. Liposome-encapsulated aminoglycosides in pre-clinical and clinical studies. Journal of Antimicrobial Chemotherapy, 48(3): 333–344.

Shah, M. et al. 2015. Green synthesis of metallic nanoparticles via biological entities. Materials, 8(11): 7278–7308.

Vashishth, V., Kaushik, D. 2017. Mupirocin amalgamated inorganic nanoparticles for augmenting drug delivery in resistant microbial strains. World Journal of Pharmacy and Pharmaceutical Sciences, 6(11): 1214–1229.

Yang, D. et al. 2009. The antimicrobial activity of liposomal lauric acids against Propionibacterium acnes. Biomaterials, 30(30): 6035–6040.

In vitro anti-microbial activity of titanium dioxide nanoparticles

Almotasem Bellah Younis[1,2], Ludmila Kosaristanova[1], Kristyna Dolezelikova[1], Kristyna Smerkova[1,2]
[1]Department of Chemistry and Biochemistry
Mendel University in Brno
Zemedelska 1, 613 00 Brno
[2]Central European Institute of Technology
Purkynova 123, 612 00 Brno
CZECH REPUBLIC

xyounis@mendelu.cz

Abstract: Titanium dioxide (TiO_2) has wide applications in various fields including cosmetics, pharmaceuticals, textile and waste water treatment due to its many properties such as photocatalytic activity and stability. In the present study, the synthesis of TiO_2 nanoparticles (NPs) was achieved by hydrolysis condensation method where a liquid phase of TiO_2 was obtained. TiO_2 NPs were characterized by X-ray Diffraction (XRD), UV-Visible spectrometry, Scanning Electron Microscopy (SEM). The photocatalytic activity of TiO_2 NPs was examined by monitoring the degradation of methylene blue dye in water when treated with TiO_2 NPs. TiO_2 NPs were found to be highly photocatalytic achieving 90% degradation ratio after 80 min. In this study antimicrobial activity test was carried out for TiO_2 NPs against selected Gram-positive/negative bacteria both in the presence or absence of UV exposure. TiO_2 NPs expressed a significant effect on microbial growth only on high concentrations exceeding 1 mg/ml.

Key Words: titanium dioxide, nanoparticles, antimicrobial activity, ultraviolet

INTRODUCTION

In recent years, microorganisms acquired resistance to the commonly used antibiotics, and thus diseases caused by these strains were getting troublesome to treat. Titanium dioxide (TiO_2) nanoparticles (NPs) are significantly known for their non-toxic property, high functionality toward biomaterials and chemical stability (Kaseem et al. 2019). TiO_2 has three crystal structures: anatase, rutile and brookite which have different characteristics and applications. Commonly used TiO_2 are considered as one of semiconductor metals which can also be utilized as a photocatalytic antimicrobial material (Kang et al. 2019).

According to what is known from band energy theory, the disconnected band structure of semiconductors is constituted of low energy valence bands filled with electrons, high-energy conduction bands, and band gaps. The values of band gap of TiO_2 are 3.0 and 3.2 eV for rutile and anatase phases. There are two characters to understand the mechanism of TiO_2 NPs: firstly, ability to degrade biopolymeric compounds (such as polysaccharides and proteins) and secondly, alteration of the surface properties of the objects to hydrophilic state when TiO_2 is on the surface. TiO_2 is more likely to oxidize when it is exposed to ultraviolet (UV), particularly in a wavelength lower than 385 nm. As a result, TiO_2 can produce reactive oxygen species (ROS) (Azizi-Lalabadi et al. 2019). The production of ROS (*e.g.*, hydrogen peroxides, superoxide radicals, and hydroxyl radicals) is initiated immediately after UV exposure (Kang et al. 2019). These active species destroy the outer membrane of the bacteria, namely phospholipids, proteins, and lipopolysaccharides, and finally damage the bacteria (Nosaka and Nosaka, 2017). Despite all these features, there are still some limitations; for instance, ROS are highly reactive and have very short lifetimes (2 μs for $^1O_2$, 200 μs for $OH^{\bullet}$, and from 5 s to hundreds of seconds for $O_2^{\bullet-}$), and their composition and concentration change almost constantly during photo catalysis (Wang et al. 2014).

MATERIALS AND METHODS

Chemicals

All chemicals and solvents were supplied by Sigma-Aldrich (St. Louis, MO, USA), in ACS purity, used without further purification.

Synthesis of TiO_2

TiO_2 biphasic NPs were synthesized via hydrolysis condensation method and were obtained as liquid phase of TiO_2 dispersion.

Dynamic light scattering (DLS)

Particle size distribution was performed with the Zeta sizer Nano (Malvern Instruments, Malvern, UK). Size distribution was determined by the DLS measured three times.

X-Ray diffraction (XRD)

XRD analysis was carried out using an X-ray diffractometer (SmartLab, Rigaku, Japan). The air-dried NPs were coated onto an XRD grid and diffracted intensities were documented from 20 to 90 of 2θ angles with a scan speed of 2°/min at 40 kV and 30 mA.

Scanning electron microscopy (SEM)

NPs powder was coated onto a coverslip and the morphology of the synthesized NP powder was studied using SEM imaging (ZEISS Sigma Scanning Electron Microscope, 10 kV accelerating voltage).

Photocatalytic activity

Photocatalytic activity was studied by a modified method (Periyat et al. 2008). Two millilitres of 25 mg/ml TiO_2 NP solution was dispersed in 50 ml of 1.0×10^{-5} M methylene blue solution. Prior to the UV exposure, the suspension was kept in the dark for 30 min. Then the suspension was exposed to 312 mJ/s of UV radiation (GS Gene Linker UV Chamber, Bio-Rad). Photo degradation was monitored at 5 min time intervals by withdrawing 3 ml aliquots of the TiO_2 NPs added to methylene blue solution. Absorbance was taken using a UV-Visible spectrophotometer. Percentage of photo degradation was plotted against exposure time.

In vitro bacterial culture

In vitro antibacterial effect of TiO_2 NPs was evaluated by minimum inhibitory concentration (MIC) and disc diffusion method. *Staphylococcus aureus* (CCM 4223) and *Escherichia coli* (CCM 3954) (Czech Collection of Microorganisms, Brno, Czech Republic) were cultured on Muller-Hinton (MH) agar (Oxoid, Hampshire, UK) overnight at 37 °C.

Effect of UV irradiation on antimicrobial potential of TiO_2 NPs

To evaluate the effect of UV light exposure on antimicrobial activity of TiO_2 NPs, separate stocks were prepared using 10 mg TiO_2. NPs were dissolved in distilled ACS water and exposed to UV light (UV-C light – wavelength 254 nm) for 0, 30, 60, and 100 min for usage in antibacterial assay. UV transparent glass vials were used for that purpose, whereas for the purpose of disc diffusion method, different approaches were carried out, as every dish was irradiated separately via exposure of UV light for 10, 15, 20 and 30 min.

Antibiotic susceptibility test (Disk Diffusion method)

Antibiotic susceptibility test was carried out by disc diffusion method. MH agar media was poured in 90 mm Petri dishes and incubated at 37 °C overnight to check sterility. The bacterial suspension was adjusted to an optical density OD_{600nm} = 0.1 AU (10^6 CFU/ml). Bacterial suspension was inoculated on each plate by spread-plate method and then antibiotic sensitivity discs were placed on the surface of the medium. After that, TiO_2 NPs samples (1–0.5 mg/ml) were added from two stocks into each disc and incubated for 24 h at 37 °C and the antibacterial sensitivity was measured as the zone of inhibition in mm diameter, for the purpose of activation of TiO_2 UV light was applied within a time interval of 10 min reaching, adjusted.

Determination of the minimum inhibitory concentration (MIC)

The MIC of the bacterial strains was determined as concentration minimum of NPs which inhibits the growth of 90% bacterial population after incubation time of 18 to 24 h at 37 °C. Approximately 100 µl of distilled ACS water were added to each well of a micro titre plate containing 96 wells, and 200 µl of the stock aqueous suspension of NPs (10 mg/ml) were added to the second row wells of each from which series of geometric dilution common ratio of 2 were made. Approximately 100 µl of the bacterial suspension of 0.5 McFarland standard 100 folds dilute cell were added to each well, and the microtitre plate was incubated at 37 °C for 24 h in the dark, while shaking.

RESULTS AND DISCUSSION

TiO_2 NPs synthesis and characterization

In this experiment, biphasic TiO_2 NPs hydrolysis condensation synthesis was obtained in liquid phase of TiO_2 dispersion and was determine the particle size distribution performed. The TiO_2 NPs particle size distribution in one particle fraction exhibited a mean size of about 250 nm (Figure 1A). X-ray scattering study showed that nearly 48.90% of mass of the particles was attributed to Ti atoms (Table 1). Oxygen and carbon atoms masses contributed to 28.95% and 22.15%, respectively. It is possible that the carbon was added during the synthesis procedure. Based on SEM imaging (Figure 1B), NPs are possibly agglomerates of smaller TiO_2 particles that are possibly electrostatically stabilized and may be mechanically disrupted.

Figure 1 Characterization of TiO_2 NPs

A) Dynamic light scattering

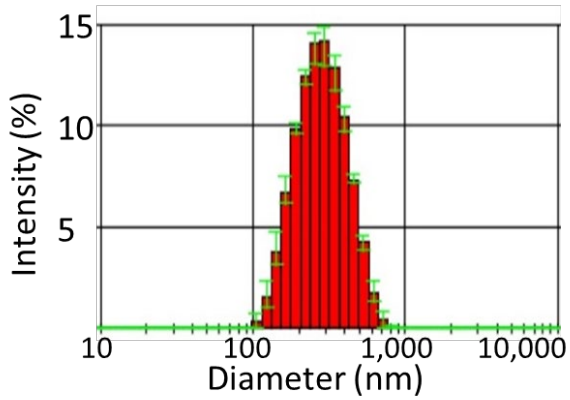

B) Scanning electron microscopy

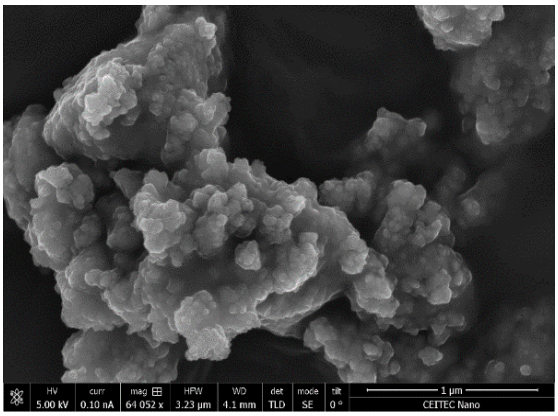

C) Photocatalytic activity

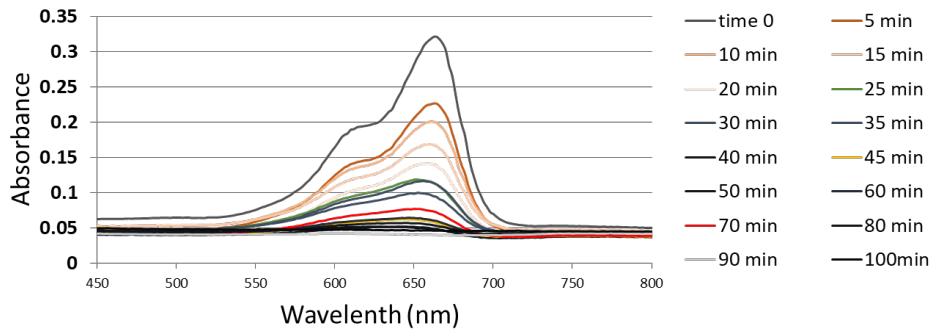

The photocatalytic activity of synthesized TiO_2 NPs was determined by observing the changes in methylene blue concentration using UV-Visible spectroscopy after TiO_2 NP treatment and UV exposure (Figure 1C). TiO_2 NPs started to decolorize methylene blue dye within 10 min

and nearly all visible color was removed after 80 min. Fifty percent of the maximum peak absorbance (dye reduction) was observed within 20 min of exposure for both TiO_2 NP samples. This was confirmed by the reduction of the intensity of the characteristic peak position of untreated methylene blue with time (Figure 1C).

Table 1 Atomic composition via X-ray scattering

Atoms	Atomic conc. (%)	Error (%)	Mass conc. (%)	Error (%)
O 1s	38.71	0.83	28.95	0.69
Ti 2p	21.85	0.58	48.90	0.85
C 1s	39.44	0.92	22.15	0.67

TiO_2 NPs antimicrobial activity

The MIC results for *S. aureus* were collected after 24 h of incubation (Figure 2A–B). The findings indicated that the TiO_2 of concentration over 1 mg/ml had antimicrobial activity when it was applied against *S. aureus* with higher selectivity than *E. coli* (data not shown), the results showed a stronger activity of higher concentration of TiO_2 with the absence of the UV light, on the other hand, the same method was carried out against the same strain of bacteria *S. aureus* but with the presence of the UV light as mentioned above in the material and methods, with less activity of the NPs (Figure 2A–B).

The disc diffusion procedure was conducted to assess the antimicrobial activity of NPs. Results showed no significant activity of TiO_2 NPs at two different concentrations. Inhibition zone diameter indicated that TiO_2 NPs had no antimicrobial effect against bacteria in the presence of UV light (Figure 2C).

Figure 2 Antimicrobial activity of TiO_2 NPs in Staphylococcus aureus

A) MIC test without UV

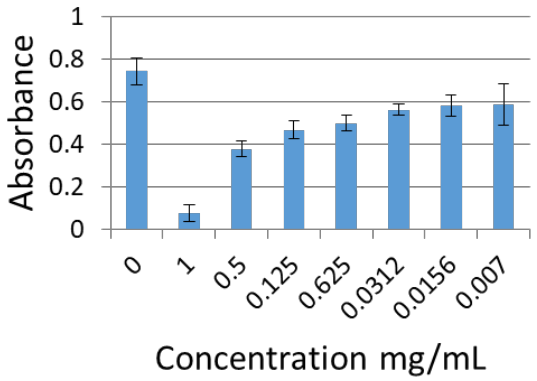

B) MIC test after 100 min UV exposure

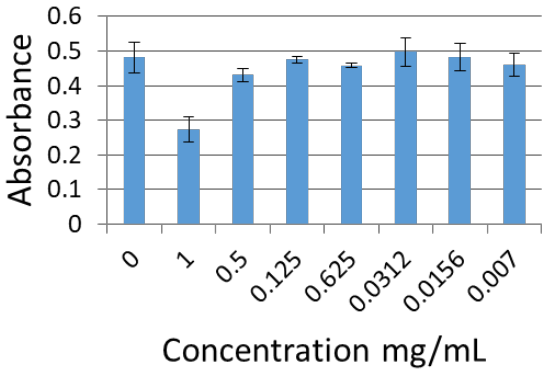

C) Disc diffusion test

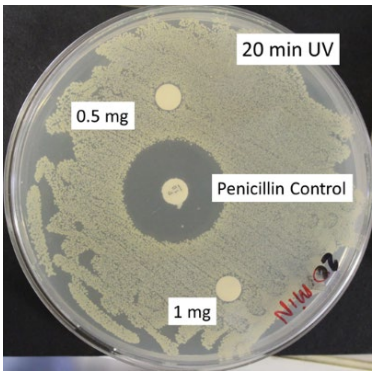

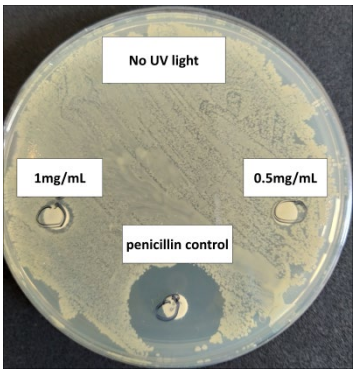

CONCLUSION

In this work, we have studied the potential of TiO_2 NPs activation by UV light to inhibit the growth of *S. aureus*. NPs were found to have a mean particle size of 250 nm, while SEM showed them to be formed in agglumerates. We have found that large amount of the atomic masses as estimated by XRS was attributed to Ti (~48.90%) while oxygen and carbon atomic masses were relativily similar. TiO_2 NPs started to decolorize methylene blue dye within 10 min and nearly all visible color was removed after 80 min. TiO_2 of concentration over 1 mg/ml had antimicrobial activity when it was applied against *S. aureus* as indicated by MIC, however disc diffusion method did not show any significant antimicrobial role.

Future work will involve modification of the particles to adjust the methodology of UV activation of TiO_2 NPs by using visible light. Such modification may include forming composites or coating or any other method that can expand the band gap.

ACKNOWLEDGEMENTS

The research was financially supported by Internal Grant Agency of Mendel University in Brno (AF-IGA2020-IP068 Almotasem Bellah Younis project).

REFERENCES

Azizi-Lalabadi, M. et al. 2019. Antimicrobial activity of Titanium dioxide and Zinc oxide nanoparticles supported in 4A zeolite and evaluation the morphological characteristic. Scientific Reports, 9(1): 17439.

Kang, X.L. et al. 2019. Titanium Dioxide: From Engineering to Applications. Catalysts, 9(2): 191.

Kaseem, M. et al. 2019. Review of Recent Advances in Polylactic Acid/TiO_2 Composites. Materials, 12(22): 3659.

Nosaka, Y., Nosaka, A.Y. 2017. Generation and Detection of Reactive Oxygen Species in Photocatalysis. Chemical Reviews, 117(17): 11302–11336.

Periyat, P. et al. 2008. High temperature stable mesoporous anatase TiO_2 photocatalyst achieved by silica addition. Applied Catalysis A: General, 349(1): 13–19.

Wang, D. et al. 2014. Online Detection of Reactive Oxygen Species in Ultraviolet (UV)-Irradiated Nano-TiO_2 Suspensions by Continuous Flow Chemiluminescence. Analytical Chemistry, 86(21): 10535–10539.

MALDI MSI of MeLiM melanoma: search for prognostic miomarker in skin cancer

Kristyna Zemankova, Kristyna Pavelicova, Jaroslava Bezdekova, Lucie Vanickova, Marketa Vaculovicova
Department of Chemistry and Biochemistry
Mendel University in Brno
Zemedelska 1, 613 00 Brno
CZECH REPUBLIC

zemankova.kristyna@seznam.cz

Abstract: Skin is the body's largest organ served as a physical and chemical barrier against negative factors. These stresses may accumulate in the body and results in skin carcinogenesis. Melanoma is one of the most aggressive forms of cancer. The search of suitable biomarkers for tumor growth is very important. Metallothionein is the cysteine rich metalloprotein belong to the potential markers for tumor disease development. The spatial imaging of this protein in tumor tissues will lead to better understanding of the processes leading to carcinogenesis. Present project proposes to combine two mass-spectrometric methods for the detection and quantification of essential metals together with metal binding proteins.

Key Words: melanoma, metallothionein, biomarker, MALDI MSI, cancer

INTRODUCTION

Malignant melanoma is one of the most aggressive and deadly forms of cancer, being responsible for 1.2% of all cancer deaths in the European Union. It is characterized by early metastasis and poor prognosis, and its incidence is increasing each year (Faller et al. 2010). If melanoma is diagnosed and treated in its early stages, it can be cured but if the diagnosis becomes late, melanoma can grow deeper into the skin and spread to other parts of the body and then it can be hazardous as it is difficult to treat (Jain et al. 2015).

Causal factor for cancerous growth develops is DNA damage. When erroneous DNA repair triggers to mutations or chromosomal aberrations affecting oncogenes and tumor suppressor genes, cells undergo malignant transformation resulting in cancer development (Torgovnick and Schumacher 2015).

Metallothioneins (MTs) are a family of low molecular weight (6 to 7 kDa), cysteine-rich proteins that play a vital role in metal ion homeostasis and detoxification (Si and Lang 2018). Generally, it is ubiquitous group of proteins with high affinity for heavy metal ions, e.g. zinc, copper and cadmium (Weinlich et al. 2003). Metallothionein expression is induced by carcinogenic effects include the generation of reactive oxygen species, oxidative DNA damage, genomic instability, inhibition of DNA repair and others (Slusser et al. 2015). For well-timed therapy and increase the chance to survival of melanoma are important histopathological and clinical parameters and the identification of potential biomarkers (Krizkova et al. 2016).

This work, proposes to combination of two mass spectrometric methods, namely matrix-assisted laser desorption combined with mass spectrometric imaging (MALDI MSI) and laser ablation inductively coupled plasma connected with mass spectrometric detection (LA-ICP-MS) in order to create a map of the MT distribution in the melanoma tissue. This information is essential for further development of effective and timely diagnostic tools for melanoma.

MATERIALS AND METHODS

Materials

2,5-dihydroxybenzoic acid (DHB), sinapinic acid and all solvents (HPLC grade) used were purchased from Sigma-Aldrich (MO, USA), unless otherwise noted. Peptide and protein calibration standards were purchased from Bruker Daltonik GmbH (Germany).

Sample collection and preparation

Two groups of the MeLiM minipigs (both 10 weeks old) with progressing melanoma and animals with spontaneously regressing melanoma were used in this project. The multiple skin melanomas allow for tissue samples to be taken repeatedly (2–3 times) from the same animal. This enabled observation of changes in the study parameters during melanoma progression and/or melanoma spontaneous regression and comparison of these processes.

The preparation of serial cryosections for the MALDI MSI were prepared by a Leica CM 1850-Cryostat (Leica, Germany). The formalin-fixed and paraffin-embedded MeLiM minipigs tissue sections were mounted onto ITO glass slides and stored at -80 °C. Prior to analysis, it was necessary to warm up the slides and desiccated under vacuum for 15 min. Thereafter, the slides were washed in a Coplin jar with ethanol (twice in 70% ethanol for 2 min and once in 100% ethanol for 2 min). The matrix application samples were dried under vacuum for 15 min, and the positions of the tissue slices were marked with three guide marks using a white pencil corrector. Afterwards, the glass slides were scanned by an Epson Perfection V500 Office scanner (Epson Europe B.V., Netherlands) at a resolution of 2400 DPI.

Matrix application

MALDI matrix was sprayed onto ITO glass slides using ImagePrepTM standard programs (Bruker Daltonik GmbH, Germany). Three different organic matrix solutions were tested, namely sinapinic acid and 2,5-dihydroxybenzoic acid, with DHB diluted in 1% trifluoroacetic acid (TFA) being considered the optimal solution, since less background was produced in the final spectrum.

MALDI MSI analysis

MeliM minipigs tissue samples were analysed using MALDI-TOF-MS (ultrafleXtreme instrument, Bruker Daltonik GmbH, Bremen Germany). The scanned images of tissue slices were loaded into FlexImaging 3.0 software (Bruker Daltonik GmbH, Germany), and a MALDI adapter with two ITO glass slides was loaded into the mass spectrometer. The position of the MALDI adapter was adjusted according to the white guide marks on the ITO glass slides. External calibration was performed using a peptide and protein standard mixture in the range of m/z 1–20 kDa. A total of 500 spectra were summed for each spot using the Random Walk raster pattern, with no evaluation criteria. Images were generated and visualized using SCiLS Lab 2014b software (SCiLS– Bruker Daltonik GmbH, Germany). Different numbers of laser shots per raster spot – 300, 500, 1000 and 1200 laser shot per raster spot – were tested.

LA-ICP-MS analysis

LA-ICP-MS imaging experiments were performed using a setup consisting of the laser ablation system UP213 (NewWave Research, USA) emitting laser radiation with a wavelength of 213 nm. The ablated material was washed away using He (1.0 L/min) from the ablation chamber (Supercell). Ar flow (0.6 L/min) was admixed into a flow of helium with the sample aerosol behind the ablation cell. Hence, the total gas flow was 1.6 L/min. This mixture was fed into a quadrupole ICP-(Q)MS spectrometer Agilent 7500CE (Agilent Technologies, Japan) equipped with a collision-reaction cell (CRC) for suppressing possible polyatomic interferences. The CRC was utilized in collision mode with a He (99.000%) flow rate of 2mL/min.

RESULTS AND DISCUSSION

Fresh frozen melanoma tissue sections from two MeLiM minipigs were analysed using MALDI MSI (Figure 1), and the resulting data were compared with data from matching healthy skin tissues stored under the same conditions. The samples were processed using a solvent washing step prior to peptide/protein MSI analysis. The MSI data were then imported into SCiLS Lab software for post-processing and generation of protein profiles. As optimal MALDI matrix for MT analysis, DHB was determined and therefore it was used in all MALDI MSI experiments in this work. The optimal number of laser shots per raster spots was found to be at least 500, and the optimal raster spot dimension was 50×50 μm.

Figure 1 Schematic experimental workflow of the MALDI MSI experiment

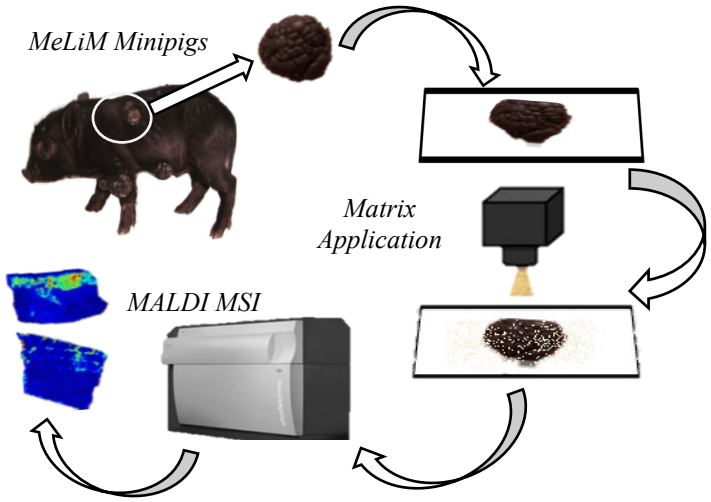

Two relevant *m/z* ions of pig metallothionein-1A peptides were detected, namely CAQGCICK and SCCSCCPAGCAR, of which the expression levels varied significantly among the studied MeLiM tissues. These two ion peaks were used to create mass ion images/maps and visualize the differences between tumor and healthy skin specimens (Figure 2).

Furthermore, the mass ion peaks at m/z 3044, 6011, 6140 and 10180 were overexpressed in melanoma compared with healthy skin tissue. More specifically, m/z 6140 was expressed at significantly higher levels in normally growing melanoma regions than in regions with early and late spontaneous regression.

Figure 2 Scan and MSI images of ion peak at m/z 825.334 (Metallothionein-1A peptide sequence: CAQGCICK) and at m/z 1160.37 (Metallothionein-1A peptide sequence: SCCSCCPAGCAR) of MeLiM cryosection tissues of A) healthy skin tissue, B) melanoma progression and C) melanoma spontaneous regression.

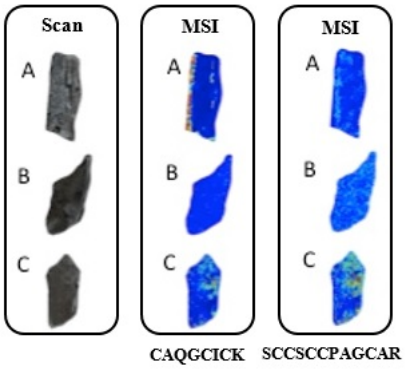

Metal detection in MT by LA-ICP-MS

MALDI-TOF-MS is not a method of choice if precise quantification is needed (Benk and Roesli 2012). Therefore, a mass spectrometric method more suitable for quantitative analysis (LA-ICP-MS) was employed for quantitation of levels of metal ions present in MT.

In MeLiM tissue cryosections, the Zn and Fe levels were elevated in the majority of melanoma sections in comparison with healthy skin (Figure 3). As a type of physiological defence, cells can over-express Zn-containing antioxidant molecules or transport and accumulate them from adjacent tissues. Furthermore, a content of Cu and Ca declines as a result of advancing spontaneous regression, due to destruction of melanoma cells by anti-tumor immune reaction. Expression of metal and Ca-binding proteins might be directly linked to the changes of elements described here. This hypothesis was further exanimated applying nanoLC-MS and MALDI MSI techniques that confirmed the identification of the proteins (metal and Ca-binding) and their spatial distribution in the MeLiM tissues, respectively.

Figure 3 LA-ICP-MS mapping of four elements Zn and Fe in histologically characterised MeLiM tissues of A) skin, B) spontaneous regression, and C) melanoma progression. On the left side are presented the optical images of the tissue and sections of histological images.

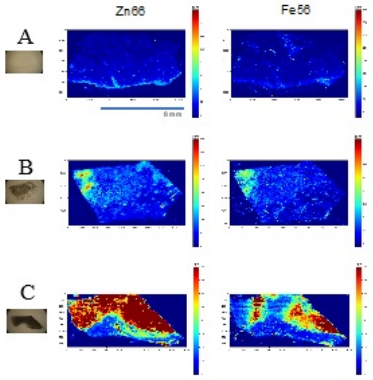

CONCLUSION

In this work, signals of pig metallothionein-1A peptides were detected. Protein profiles visualize differences between the melanoma and healthy skin tissues. In particular, peptides with m/z 3044, 6011, 6140 and 10180 were detected in melanoma. Furthermore, LA-ICP-MS analyses served for metal quantification in MT. More specifically, the ^{66}Zn and ^{56}Fe levels were elevated in the majority of melanomas in comparison with healthy skin. The combination of these two mass spectrometric methods (MALDI MSI and LA-ICP-MS) enable the get information which are essential for further development of effective and timely diagnostic tools for melanoma detection.

ACKNOWLEDGEMENTS

The research was financially supported by AF-IGA20120-IP059.

REFERENCES

Benk, A.S., and Roesli C. 2012. Label-free quantification using MALDI mass spectrometry: considerations and perspectives. Analytical and Bioanalytical Chemistry, 404: 1039–1056.

Faller, W.J. et al. 2010. Metallothionein 1E is methylated in malignant melanoma and increases sensitivity to cisplatin-induced apoptosis. Melanoma Research, 20: 392–400.

Jain, S. et al. 2015. Computer Aided Melanoma Skin Cancer Detection Using Image Processing. Procedia Computer Science, 48: 735–740.

Krizkova, S. et al. 2016. Microarray analysis of metallothioneins in human diseases—A review. Journal of Pharmaceutical and Biomedical Analysis, 117: 464–473.

Si, M., Lang, J. 2018. The roles of metallothioneins in carcinogenesis. Journal of Hematology and Oncology, 11: 107.

Slusser, A. et al. 2015. Metallothionein isoform 3 expression in human skin, related cancers and human skin derived cell cultures. Toxicology Letters, 232: 141–148.

Torgovnick, A., Schumacher, B. 2015. DNA repair mechanisms in cancer development and therapy. Frontiers in Genetics, 6: 157.

Weinlich, G. et al. 2003. Metallothionein-overexpression as a prognostic factor for progression and survival in melanoma. A prospective study on 520 patients. The British Journal of Dermatology, 149: 535–41.

Optimized assembly of functionalized-neuroblastoma targeting EcLHFRT nanocarriers

Hana Zivotska[1], Katerina Kapołkova[2]
[1]Department of Chemistry and Biochemistry
[2]Department of Animal Morphology, Physiology and Genetics
Mendel University in Brno
Zemedelska 1, 613 00 Brno
CZECH REPUBLIC

hanazivotska1@seznam.cz

Abstract: Biomimetic peptide ligands designed by using computational biology and *in silico* chemistry can bring crucial results related to their possible application in targeted anticancer therapy, more specifically in the field of active targeting of malignant neuroblastoma cell lines by modified apoferritin nanocarriers (EcLHFRT) with encapsulated cytotoxic drug. Using the high-performance throughput computing technology, unique peptides (CpTrkA, CpNGF, CpNT4) were designed and synthesized in this work. These peptides showed high affinity *in silico* to tropomyosin receptor kinases (TrkA, TrkB, TrkC), which are expressed on membranes of neuroblastoma cells. The main aim of this work was detailed characterization of prepared EcLHFRT nanocarriers through which we evaluated the size, stability and hemolytic properties of EcLHFRT with unmodified or modified surface insomuch as mentioned parameters are key for the further research in neuroblastoma nanomedicine. The prepared EcLHFRT nanocarriers possessed optimal size (<50 nm) and stability (ζ~ -20 mV) and in contrast to free cytotoxic drug, they did not cause any hemolysis.

Key Words: EcLHFRT, biomimetic peptide ligands, tropomyosin receptor kinases, neuroblastoma

INTRODUCTION

Neuroblastoma is one of the highly metastatic types of cancer and also one of the most mortal tumors in children younger than 5 years of age. Current treatment by chemotherapy is frequently non-effective and uncertain due to extreme cytotoxicity for non-malignant cells and the development of drug chemoresistance of cancer cells (Nakagawara et al. 2018). Active targeting in neuroblastoma therapy seems to be a promising solution for future treatment of this serious disease. In order to attain the active targeting of specific cancer cells, a variety of ligands (in our case peptides) are being utilized. In general, peptides as targeting ligands exhibit ideal properties thanks to their small size, good potency, and biocompatibility (Tesauro et al. 2019, Yoo et al. 2019). In our laboratory, the designed peptides were tested *in silico* by molecular docking, dynamics, and mechanics. The peptides with the highest affinity and the lowest binding energy (CpTRkA, CpNGF, and CpNT4) were synthesized using standard F-moc synthesis. These peptides were derived directly from known ligands to tropomyosin receptor kinases expressed by cancer cells, especially by neuroblastoma cells.

In this experimental work, active targeting was achieved by surface peptide modifications of ferritin nanocarrier, organic biocompatible protein responsible for the storage and transfer of iron ions. When the iron ions are removed, FRT creates a structure of hollow cage of 460 kDa called apoferritn (EcLHFRT). It is isolated from the equine spleen and composed of 2 heavy subunits (21 kDa) and 22 light (19 kDa) subunits with an outer diameter of 12.5 nm and an inner diameter of 8 nm. EcLHFRT posseses the properties of an ideal nanocarrier for application in nanomedicine because one of the most significant attribute of nanocarrier is its size. The nanocarrier must be less than 100 nm to exhibit increased permeability and enter the tumor matter through tumor blood vessels with an irregular shape. On the other hand, nanocarrier must be greater than 10 nm, so that it is not removed from the organism by renal clearance (Dostalova et al. 2017, Sergeev et al. 2018). The other advantage of EcLHFRT is its ability of easy decomposition and recomposition of EcLHFRT structure, which is controlled only by the change in the pH of surrounding environment (decomposition in pH 3.5; recomposition in pH 6.5). This capability was used for the process of encapsulation of cytotoxic

compound ellipticine, which effectively inhibits growth of most cancer cells (Cascajo-Castresana et al. 2020). The problem is that ellipticine is also highly toxic for non-malignant cells and it has serious mutagenic and genotoxic side effects. However, by encapsulation of ellipticine into suitable nanocarrier, the mentioned negative effects could be reduced or removed while increasing the specificity of this experimental drug (Stiborova et al. 2011). The surface modification of the EcLHFRT nanocarriers by peptides derived from tropomyosin receptor kinases and their ligands could increase the selectivity of encapsulated ellipticine for target neuroblastoma cells. This could reduce serious negative side effects on off-target cells in human body and enhance the efficiency of anticancer treatment.

At first it was important to optimize the process of decomposition and recomposition of EcLHFRT, process of ellipticine encapsulation and modification of EcLHFRT by peptides. Optimized and synthesized surface-modified nanocarriers were characterized through spectrometry (encapsulation efficiency of ellipticine), native gel electrophoresis (degree of recomposition), Doppler microelectrophoresis (ζ-potential), and dynamic light scattering (size). The impact of free or encapsulated ellipticine in EcLHFRT on red blood cells was studied by hemolytic assay.

MATERIAL AND METHODS

Chemicals

All chemicals of ACS purity were obtained from Sigma-Aldrich (St. Louis, MO, USA).

Ellipticine encapsulation into EcLHFRT without DMSO and surface modification with tropomyosin receptor kinases-derived peptides

200 µL of cytotoxic compound ellipticine (disbanded in 1 M HCl and deionized water in ratio 1 : 95) with concentration of 1 mg/mL was mixed with 20 µL of equine spleen EcLHFRT (with concentration of 50 mg/mL) and 100 µL of deionized water and cautiously blended for 15 min at 20 °C and 100 g to decompose the structure of EcLHFRT in pH 3.5. 1.35 µL of 1 M NaOH was added to attain the recomposition of EcLHFRT structure in pH 6.5, and all samples were blended for 15 min at 20 °C and 100 g (creating the EcLHFRT-ellipticine complex). To remove non-encapsulated ellipticine, supernatant exchange was performed 3× for 15 min at 4 °C and 6000 g. 25 µL of AuNPs (prepared by mixing 2 mL of 1% trisodium citrate with 10 mL of 1 mM gold(III) chloride hydrate and blended on Orbital Shaker for 72 h at 20 °C) was added to the samples and cautiously blended for 14 h at 20 °C and 100 g (creating the complex of EcLHFRT-ellipticine-Au). Next, 2.8 µL of peptides [CpTrkA (seq. CVSFPASVQLHTAV), CpNGF (seq. CSSSHPIFHRGEFSV), CpNT4 (seq. CGVSETAPASRRGELAV)] in a concentration of 1.25 mg/mL were added to the samples and they were incubated for 1 h at 45 °C and 90 g. To strain out unbound peptides, supernatant exchange was performed 1× for 15 min at 4 °C and 6000 g (creating the EcLHFRT-ellipticine-Au-peptide complex).

Ellipticine encapsulation into EcLHFRT with DMSO and surface modification with tropomyosin receptor kinases-derived peptides

Samples with DMSO were prepared similar to samples without DMSO. DMSO was used to precipitate the peptides on the surface of EcLHFRT, rather than bind the peptides to AuNPs through cysteine. Two conditions in the procedure were different. First, in the third step of centrifugation, EcLHFRT-ellipticine was resuspended in 25% DMSO (261.7 µL of Mili-Q and 87.25 µL of 100% DMSO). Second, 2.8 µL of peptides (CpTrkA, CpNGF CpNT4) in a concentration of 1.25 mg/mL were added to the samples and they were incubated for 1 h at 24 °C and 90 g.

Characterization of non-targeted and targeted nanocarriers

The encapsulation efficiency of ellipticine in non-targeted EcLHFRT-ellipticine and targeted EcLHFRT-ellipticine-peptide was assayed by UV-Vis spectrometry with Tecan Infinite 200 PRO (Männedorf, Switzerland) based on absorbance value measured at wavelength of 420 nm.

The average size of non-targeted and targeted nanocarriers were determined by dynamic light scattering (Malvern Instruments Ltd., Worcestershire, UK). Individual nanocarriers were diluted in ratio 1 : 200 and measured in cuvettes ZEN0040 in hexaplicates with the refractive index of sample 1.45 (equivalent for protein which forms the majority of the nanocarriers) and the refractive index of the dispersion 1.333 at 20 °C. The ζ-potential of non-targeted and targeted nanocarriers were assayed

using Doppler microelectrophoresis (Malvern Instruments Ltd., Worcestershire, UK). Individual nanocarriers were diluted in ratio 1 : 20 and measured in cuvettes DTS1070 in triplicates.

Hemotoxicity of non-targeted and targeted nanocarriers

Hemolytic assay was carried out to evaluate the impact of free and encapsulated ellipticine in non-targeted and targeted nanocarriers in the environment of human fresh blood. Firstly, fresh blood was centrifuged for 10 min at 600 g to remove blood plasma. The remaining red blood cells were repeatedly cleaned by 150 mM sodium chloride and centrifuged for 10 min at 600 g, until the supernatant was fully limpid. Purified red blood cells were diluted by warmed PBS and 150 µL of this suspension was added to 150 µL of various concentrations of individual nanocarriers. Individual sample of 0.2% Triton X-100 was chosen as a positive control and negative control was PBS. All samples were incubated in a thermoblock for 1 h at 37 °C while shaking at 70 g, then centrifuged for 10 min at 600 g. The last step, absorbance of the sample supernatant was assayed using UV-Vis spectrometry at wavelength of 540 nm. From obtained values, the degree of hemolysis was determined for various concentrations of individual nanocarriers.

RESULTS AND DISCUSSION

The average size of empty EcLHFRT before the process of ellipticine encapsulation was 11.7 nm, process of encapsulation without using DMSO increased it to 13.5 nm (EcLHFRT-ellipticine-CpTrkA), 15.7 nm (EcLHFRT-ellipticine-CpNT4) or to 43.8 nm (EcLHFRT-ellipticine). The process of encapsulation with using DMSO produced complexes of 32.7 nm (EcLHFRT-ellipticine-CpTrkA), 37.8 nm (EcLHFRT-ellipticine-CpNGF), 21.0 nm (EcLHFRT-ellipticine-CpNT4) or 24.4 nm (EcLHFRT-ellipticine). The standard deviations (SD) are not shown as the software for Zetasizer Nano ZS incorrectly assumes Gaussian distributions of the nanoparticle size so the SD would not be correct. The results showed that process of ellipticine encapsulation caused changes in size of prepared nanocarriers. The changes in the size of mentioned nanocarriers could have been induced by an insufficient recomposition, causing aggregation of free EcLHFRT subunits of the structure of EcLHFRT (Kim et al. 2011) possibly even by molecules of ellipticine attached to the outside surface of EcLHFRT, as has been shown in the past for molecules of doxorubicin and tyrosine kinase inhibitors (Dostalova et al. 2017). However, for nanomedicine applications, the biggest measured size (43.8 nm) is still sufficient. Only targeted nanocarrier with CpNGF peptide (without DMSO) had the same size before and after the process of encapsulation. As shown in Table 1 and 2, within non-targeted and targeted nanocarriers, similar values of ζ-potential in Ringer's solution (0.2 g/L $NaHCO_3$, 0.25 g/L $CaCl_2$, 0.42 g/L KCl and 6.5 g/L of NaCl, pH 7.4), were established. Although the standard guidelines for relating ζ-potential with colloidal stability say, that highly stable nanoparticles possess ζ-potential >30 mV and the values shown for EcLHFRT nanocarriers would identify them as only moderately (20-30 mV) or relatively (10-20 mV) stable, the reality is that the ζ-potential does not reflect the entirety of nanoparticle stability. It only provides information on the electrostatic repulsive forces without any insight on the van der Waals attractive forces. As other nanoparticle dispersions have been known to possess lower ζ-potential and still be stable (Bhattacharjee 2016) and as s major iron-detoxyfying protein, FRT is naturally present in plasma (Sergeev et al. 2018), an environment that Ringer's solution is known to simulate, our results show that the stability of EcLHFRT nanocarriers prepared in this work is similar to that of native EcLHFRT. The average encapsulation efficiency of ellipticine in prepared nanocarriers without DMSO was 60%; in nanocarriers with DMSO it was 43%. Comparison of yields of encapsulated ellipticine in all prepared nanocarriers (Figure 1) showed that nanocarriers without using DMSO exhibit a higher encapsulation efficiency after surface modification.

Table 1 Size, ζ-potential and efficiency of ellipticine in EcLHFRT without DMSO

Nanocarrier	Average size (nm)	Average ζ-potential (mV)	Average efficiency of ellipticine (%)
EcLHFRT	11.7	-20.3	–
EcLHFRT-Elli	43.8	-21.6	69.7
EcLHFRT-Elli-CpTrkA	15.7	-20.5	62.5
EcLHFRT-Elli-CpNGF	11.7	-17.4	69.1
EcLHFRT-Elli-CpNT4	13.5	-17.7	58.0

Table 2 Size, ζ-potential and efficiency of ellipticine in EcLHFRT with DMSO

Nanocarrier	Average size (nm)	Average ζ-potential (mV)	Average efficiency of ellipticine (%)
EcLHFRT	11.7	-20.3	–
EcLHFRT-Elli	24.4	-21.8	42.6
EcLHFRT-Elli-CpTrkA	32.7	-20.8	44.0
EcLHFRT-Elli-CpNGF	37.8	-21.9	45.2
EcLHFRT-Elli-CpNT4	21.0	-19.9	45.2

Figure 1 The changes in efficiency of encapsulated ellipticine in prepared nanocarriers before and after surface modification

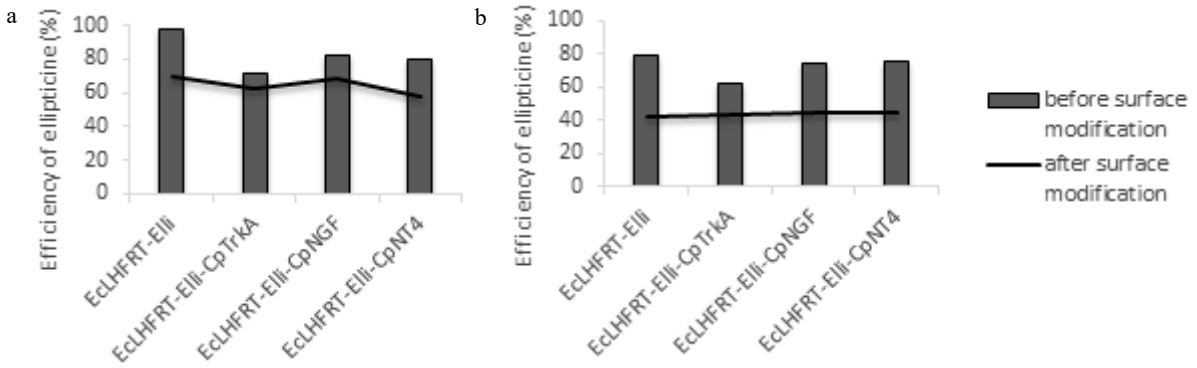

Legend: a – EcLHFRT without DMSO, b – EcLHFRT with DMSO

To evaluate the degree of recomposition of individual EcLHFRT nanocarriers, native gel electrophoresis (Figure 2) was carried out. Non-targeted and targeted nanocarriers (number 3–6 on gel) looked the same as the original empty EcLHFRT (number 2), that did not undergo the decomposition process. The results prove that the changes in size were not caused by incomplete recomposition of EcLHFRT nanocarriers.

Figure 2 The composition of individual EcLHFRT visualized by 6% native gel

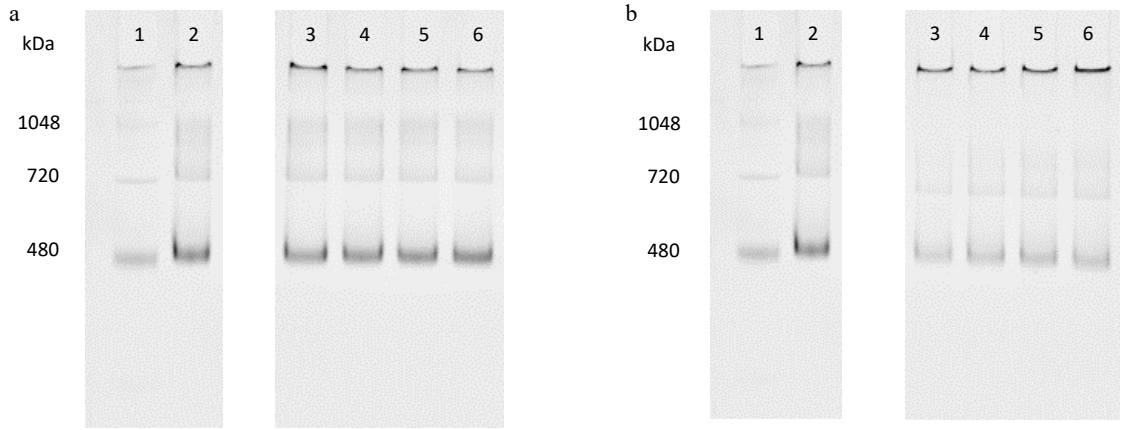

Legend: a – EcLHFRT without DMSO, b – EcLHFRT with DMSO; 1 – Marker, 2– EcLHFRT, 3 – EcLHFRT-ellipticine, 4 – EcLHFRT-ellipticine-CpTRkA, 5 – EcLHFRT-ellipticine-CpNGF, 6 – EcLHFRT-ellipticine-CpNT4

Hemolytic assay (Figure 3 and 4) showed that all prepared non-targeted and also targeted nanocarriers with encapsulated cytotoxic compound ellipticine did not exhibit hemolytic effect on red blood cells. On the other hand, free ellipticine induced hemolysis of 2.2% red blood cells at its highest concentration used. This negative cytotoxic feature of ellipticine was entirely suppressed through its encapsulation into non-targeted or targeted nanocarriers.

Figure 3 Hemolytic assay of free and encapsulated ellipticine in EcLHFRT without DMSO

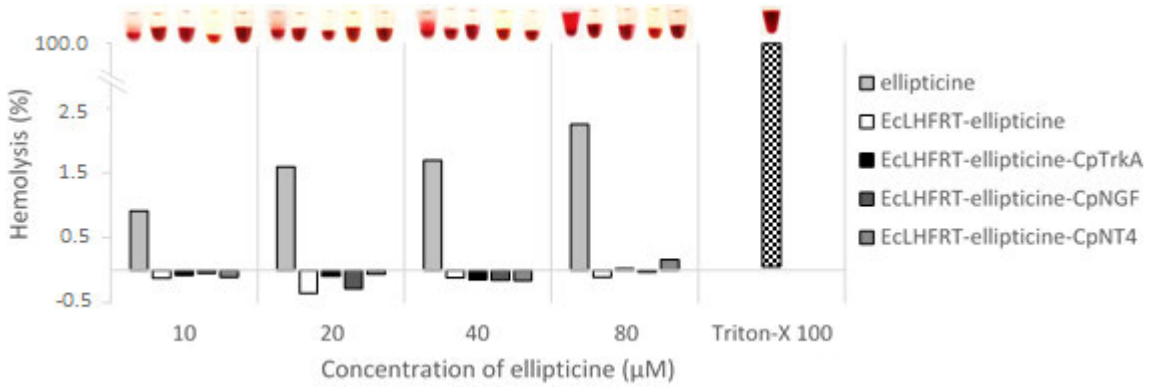

Figure 4 Hemolytic assay of free and encapsulated ellipticine in EcLHFRT with DMSO

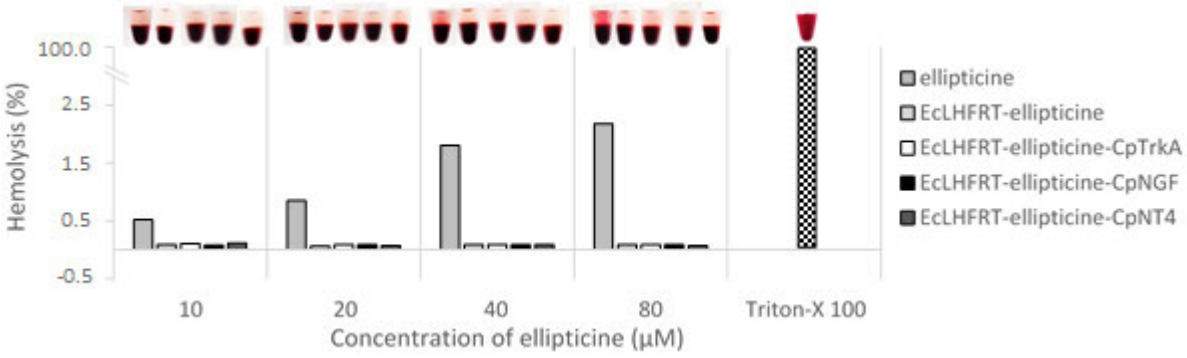

CONCLUSION

The main goal of this experimental work was to evaluate basic characterization properties of prepared EcLHFRT nanocarriers with unmodified or modified surface by peptides derived from tropomyosin receptor kinases. We prepared 8 types of EcLHFRT with suitable size (11–45 nm), ideal value of ζ-potential (-20 mV) and high encapsulation efficiency of cytotoxic compound ellipticine (42–60%). As a result of hemolytic assay we found that process of ellipticine encapsulation into EcLHFRT nanocarrier with unmodified or modified surface led to elimination of its cytotoxic properties on human blood, because only free ellipticine caused hemolysis.

The process of synthesis of nanocarriers was successfully optimized, which is crucial for further nanomedicine research in the *in vitro* conditions, mainly for testing of active targeting to target cells by biomimetic peptide-based ligands.

ACKNOWLEDGEMENTS

The authors gratefully acknowledge financial support from the Grant Agency of the Czech Republic (GACR 17-12816S), by grant no. AF-IGA2020-IP023.

REFERENCES

Cascajo-Castresana, M. et al. 2020. Protein aggregates nucleate ice: the example of apoferritin. Atmospheric Chemistry and Physics, 20: 3291–3315.

Bhattacharjee, S. 2016. DLS and zeta potential – What they are and what they are not? Journal of Controlled Release, 235(10): 337–351.

Dostalova, S. et al. 2017. Apoferritin as an ubiquitous nanocarrier with excellent shelf life. International Journal of Nanomedicine, 12: 2265–2278.

Kim, M. et al. 2011. pH-Dependent Structures of Ferritin and Apoferritin in Solution: Disassembly and Reassembly. Biomacromolecules, 12(5): 1629–1640.

Nakagawara, A. et al. 2018. Neuroblastoma. Japanese Journal of Clinical Oncology, 48(3): 214–241.

Sergeev, Y.V. et al. 2018. Apoferritin is maintaining the native conformation of citrate synthase in vitro. Journal of Analytical and Pharmaceutical Research, 7(6): 680–684.

Stiborova, M. et al. 2011. Ellipticine cytotoxicity to cancer cell lines - a comparative study. Interdisciplinary Toxicology, 4(2): 98–105.

Sweegers, M.G. et al. 2020. Ferritin measurement IN Donors—Effectiveness of iron Monitoring to diminish iron deficiency and low haemoglobin in whole blood donors (FIND'EM): study protocol for a stepped wedge cluster randomised trial. Trials, 21(1): 823.

Tesauro, D. et al. 2019. Peptide-Based Drug-Delivery Systems in Biotechnological Applications: Recent Advances and Perspectives. Molecules, 24(2): 351.

Yoo, J. et al. 2019. Active Targeting Strategies Using Biological Ligands for Nanoparticle Drug Delivery Systems. Cancers, 11(5): 640.

AUTHORS INDEX

ADAM Vojtech 578
ADAMCOVA Dana 266
AL-SHANTIR Omar 480
ALBA-MEJIA Jhonny Edison 38
ANTONIC Bojan 227
ANTOSOVKY Jiri 68
ASSI Navid 584
ASTETE Carlos E 557, 589
BABICA Ondrej 81, 127
BABULA Petr 396
BAHOLET Daria 86, 133
BALAZS Attila 200
BAUER Josef 290
BEDNAROVA Ivana 97
BENO Filip 290
BERKA Miroslav 505
BERKOVA Veronika 505
BEZDEK Jan 200
BEZDEKOVA Jaroslava 584, 599
BILKOVA Zuzana 542
BLAHOVA Jana 190, 195
BLSAKOVA Lucia 296
BRETTFELDOVA Tereza 318
BRUDNAKOVA Michaela 91
BRYCHTA Jiri 232
BRZOBOHATY Bretislav 505
BUKOVSKA Pavla 377
BULAWA Tomas 409
BUNKA Frantisek 335
BURG Patrik 74, 237
CERNY Martin 32, 384, 505
CERNY Michal 445
CHAROUSOVA Marketa 527
CHLADEK Gustav 107, 175
CHOVANEC Jan 468
CIZKOVA Alice 237, 492

CUPERA Jiri 486
CURN Vladislav 413
DANIHLIK Jiri 403
DO Tomas 522
DOLEZAL Petr 159
DOLEZELIKOVA Kristyna 511, 594
DORDEVIC Dani 227
DOSTAL Petr 486
DOSTALKOVA Silvie 403
DOSTALOVA Marie 301
DUFFKOVA Renata 26
DUFKOVA Renata 15, 307, 324, 330
DVORAK Karel 445
DVORAKOVA Denisa 205
DVORAKOVA Jana 445
ELBL Jakub 44
ELZNER Petr 21
FAJMAN Martin 457
FALDYNA Martin 190
FALTA Daniel 107
FERIANCOVA Patricia 451
FIALOVA Tatiana 511
FILIPCIK Radek 142, 419
FOLTYN Marian 178
FRANTOVA Nicole 21
FURMANCIKOVA Petra 97, 313
FUZIK Tibor 81, 127
GAL Robert 335, 341, 347, 371
GREGOR Tomas 296
GREPLOVA Marie 505
GRONDELOVA Aneta 97
GROSSOVA Lucie 359
GRULICHOVA Marie 390
GURAN Roman 522
HADAS Zdenek 122
HAJKOVA Lenka 232
HANACEK Pavel 390
HAVLICKOVA Tatana 419

HENEK DLABOLOVA Dita 468
HIC Pavel 74
HODKOVICOVA Nikola 190
HOLKOVA Ludmila 21
HOLLEROVA Aneta 190
HORAKOVA Lucie 102
HORECKY Cenek 424
HORNIACEK Igor 26
HOSEK Martin 142
HRIVNA Ludek 15, 307, 324, 330
HRUDOVA Eva 50
HULANKOVA Radka 313
HULEJOVA Petra 211
HULINSKA Pavlina 430
HURAJOVA Erika 32, 384
HYBL Marian 216, 413
HYNEK David 578
JANACOVA Dagmar 347
JANCIKOVA Simona 227
JANDAK Jiri 283
JANOUSKOVA Romana 451, 462
JAROSOVA Alzbeta 318
JELINEK Josef 486
JENIK David 107
JIROUSEK Martin 261
JISKROVA Iva 116
JOHN Jakub 536
JOVANOVIC Ivana 38
JUZL Miroslav 359, 365
KACALOVA Tereza 318
KADLCEK Leos 384
KAPOLKOVA Katerina 603
KLEM Karel 64
KLOFAC Daniel 68
KNOLL Ales 424, 435
KOIS Jiri 536
KOLLAROVA Katarina 498
KOMPRDA Tomas 365, 517, 557, 589

KONKOL Damian 111
KOPEC Tomas 107
KOPECKY Marek 413
KOPECKY Tomas 200
KOPP Radovan 522
KORANDOVA Romana 290
KORCZYNSKI Mariusz 111
KOSARISTANOVA Ludmila 511, 517, 594
KOSULIC Ondrej 211
KOUDELKOVA Zaneta 522
KOUKALOVA Lenka 536
KOURILOVA Veronika 15, 307, 324, 330
KOUTNY Tomas 536
KOVACIK Peter 55
KOZUCH Peter 451, 462
KRASOWSKA Anna 111
KRATOCHVIL Zdenek 527
KUBIKOVA Zuzana 116
KUBISTOVA Barbora 116
KUCERA Josef 243, 249
KUCIN Martin 457
KULOVANA Eva 536
KUMBAR Vojtech 183, 296, 301, 307, 324, 486
KUMMEROVA Marie 396
KUROVA Vendula 335
LACKOVA Zuzana 127, 530
LICHOVNIKOVA Martina 147, 155, 178, 439
LONDYNOVA Marketa 151
LUJKA Jan 122
LUKAS Vojtech 26, 44
LUKASZEWICZ Marcin 111
LUKLOVA Marketa 584
MACHATKOVA Marie 430
MACO Roman 15
MALA Jitka 542
MAMICA Ondrej 419
MARECEK Jan 480
MARES Jan 195, 522

MARTINEK Jakub 341
MARTINEZ BARROSO Petra 255
MASAN Vladimir 74, 377, 492
MATEJKOVA Eva 498
MATEJOVICOVA Milena 365
MEDKOVA Denisa 195
MENSIKOVA Simona 505
MEZERA Jiri 44
MICHALIDES Matej 451, 462
MIFKOVA Tamara 409, 435
MIKUSOVA Dominika 68
MILOSAVLJEVIC Vedran 578
MOKREJS Pavel 341, 347, 371
MRAZ Petr 216, 413
MRAZEK Petr 347
MRKVICOVA Eva 86, 102, 133, 137, 159, 165, 170, 183, 353
MUSILA Jan 81, 127, 151, 530
NAVRATILOVA Pavlina 97
NECASOVA Aneta 50, 59
NECASOVA Daniela 97
NEDOMOVA Sarka 86, 301, 330, 353, 365, 424
NEJDL Lukas 584
NEUDERT Lubomir 26, 44
NEUPAUER Jakub 55
NEVRKLA Pavel 122
NOSIAN Jozef 462
NOVOTNY Jakub 86, 133, 137, 165, 170, 183
ONDRACKA Tomas 468, 536
ONDRUSIKOVA Sylvie 86, 301, 353, 365
OPAVSKA Tereza 178
OPPELTOVA Petra 277
ORSAVOVA Jana 347, 371
OULEHLA Jan 261
OVCHYNNIKOVA Oleksandra 359
PANIKOVA Kristina 542
PAVELICOVA Kristyna 548, 584, 599
PAVKOVA-GOLDBERGOVA Monika 511
PAVLACKOVA Jana 341, 371

PAVLATA Leos 86, 102, 133, 137, 159, 165, 170, 183, 353
PAVLIK Ales 424
PEKARIK Vladimir 572
PESAN Vojtech 142
PESANOVA TESAROVA Martina 147
PETRIVALSKY Marek 403
PETRLAK Frantisek 553, 562, 567
PIECHOWICZOVA Marketa 365
PLEVKA Pavel 81, 127, 151
PODHRAZSKA Jana 232, 243, 249
POHUNEK Vaclav 290
POLASTIKOVA Aneta 371
POLCAR Adam 474, 486
POPELKOVA Vendula 365, 517, 557, 589
POSPICHAL Jan 536
POSTULKOVA Eva 195, 522
PRAZANOVA Zaneta 50, 59
PRIBORSKY Jan 522
PRIDAL Antonin 81, 127, 151, 530
PROUZA Jan 127, 151
RABEK Michal 21, 159
RADOJCIC Marija 522
RADSETOULALOVA Iva 155
RICHTERA Lukas 578
RICHTR Premysl 290
RIHACEK Michal 159
ROUS Robert 468
ROZTOCILOVA Andrea 86, 133, 137, 165, 170, 183
RYBA Stepan 413
SABLIOV Cristina 557, 589
SALEK Richardos Nikolaos 335
SEDLACKOVA Eliska 584
SEDLAKOVA Veronika 390
SEFROVA Hana 59
SEHONOVA Pavla 195
SEIDENGLANZ Marek 50
SENDECKA Katarina 396
SIMOR Jan 64

SINKOVA Aneta 377
SIPOS Jan 205, 211, 216, 222, 413
SKARPA Petr 68
SKLENAR Jiri 175
SKOLNIKOVA Marie 68
SKOPALOVA Gabriela 222
SKOUPA Marketa 178, 439
SLADEK Libor 175
SLADEK Zbysek 430
SLAMA Petr 439
SMAK Radim 474
SMERKOVA Kristyna 511, 594
SMIDOVA Veronika 553, 562, 567
SMUTNA Pavlina 21
SMUTNY Ladislav 480
SMUTNY Vladimir 26, 44, 159
SMYKAL Petr 390
SNUPIKOVA Nikol 15, 359
SOBOTKOVA Eva 91
SOTNAR Martin 480
SOURKOVA Marketa 266
SOUSKOVA Katarina 419
SPLICHAL Zbynek 567
STASTKOVA Zora 97
STASTNA Milada 271
STASTNIK Ondrej 86, 102, 133, 137, 159, 165, 170, 183, 301, 353, 359
STEINEROVA Michala 424
STREDA Tomas 38, 249
SUBRTOVA Hana 553, 562, 567
SUCHOMEL Josef 205, 222
SVAJDOVA Nela 335
SVEC Pavel 511
SVOBODNIKOVA Lucie 396
SVOBODOVA Zdenka 195
SVORADOVA Andrea 439
SZMIGIEL Ida 111
SZTURC Jan 249
TAKACSOVA Paulina 527, 572

TESIKOVA Karolina ... 227
TRAVNICKOVA Ivona ... 430
TREMLOVA Bohuslava ... 227
TROST Daniel ... 486
TUZOVA Kristyna ... 271
ULRICH Ondrej ... 277
UMLASKOVA Barbora ... 137
URBAN Tomas ... 409
VACULOVICOVA Marketa ... 548, 584, 599
VAIDOVA Michaela ... 237
VANICKOVA Lucie P. ... 548, 599
VANOVA Veronika ... 578
VASTIK Lukas ... 74, 377
VAVERKOVA Magdalena Daria ... 255, 266
VECERA Milan ... 175
VLADEK Ales ... 530
VODOVA Milada ... 584
VOTAVA Jiri ... 474
VRCHOVECKA Katerina ... 511
VYKYDALOVA Lucie ... 32
VYMAZALOVA Pavla ... 365, 517, 557, 589
WIJACKI Jan ... 409, 435
WINKLER Jan ... 32, 384
WRZECIONKOVA Nicole Elizabeth ... 435
YOUNIS Almotasem Bellah ... 594
ZACHOVALOVA Marketa ... 283
ZALESAKOVA Dana ... 183
ZATLOUKAL Patrik ... 237, 492
ZEMANEK Pavel ... 492
ZEMANKOVA Kristyna ... 548, 584, 599
ZEZULKA Stepan ... 396
ZITKA Ondrej ... 127, 522, 530
ZIVOTSKA Hana ... 603
ZLOCH Jan ... 266
ZMRHAL Vladimir ... 439
ZUBCAK Tomas ... 498

Name of publication:	MendelNet 2020 *Proceedings of 27th International PhD Students Conference*
Editors:	Assoc. Prof. Ing. Radim Cerkal, Ph.D. Ing. Natálie Březinová Belcredi, Ph.D. Ing. Lenka Prokešová
Publisher:	Mendel University in Brno Zemědělská 1665/1 613 00 Brno Czech Republic
Year of publication:	2020
Number of pages:	616
ISBN:	978-80-7509-765-1

Contributions are published in original version, without any language correction.